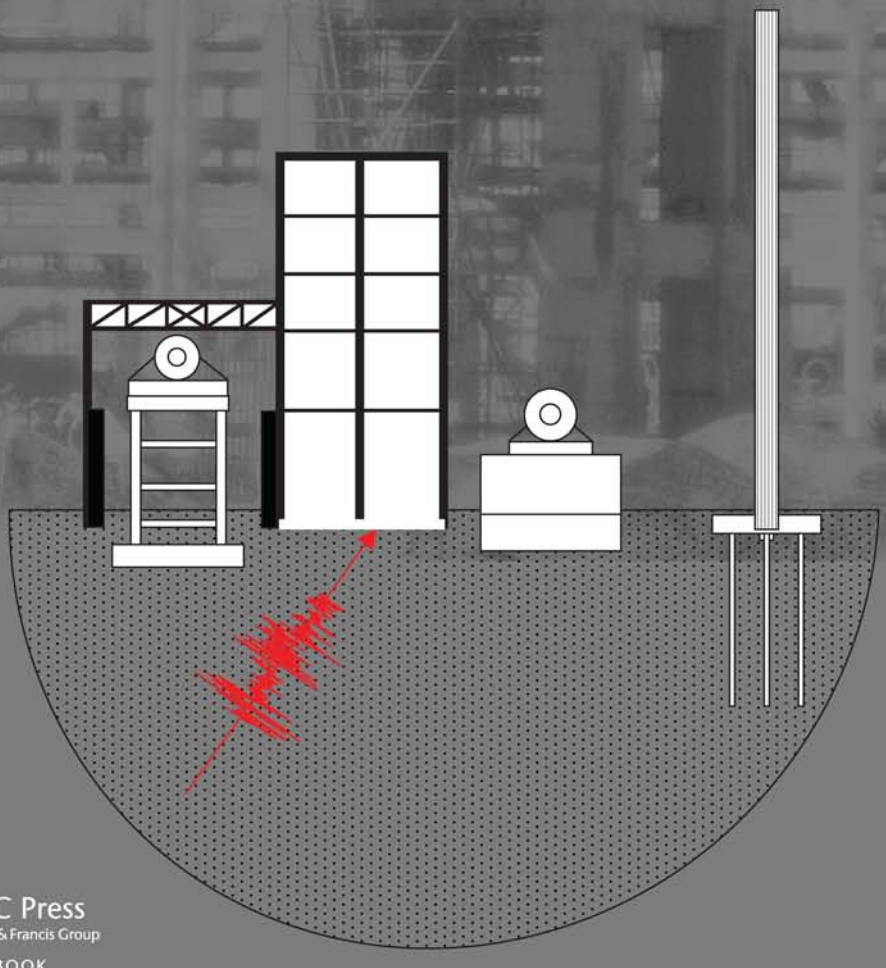
DYNAMICS OF STRUCTURE AND FOUNDATION

A UNIFIED APPROACH

Indrajit Chowdhury & Shambhu P. Dasgupta

1. FUNDAMENTALS



CRC Press
Taylor & Francis Group
A BALKEMA BOOK

Dynamics of Structure and Foundation – A Unified Approach

1. Fundamentals

Dynamics of Structure and Foundation – A Unified Approach

1. Fundamentals

Indrajit Chowdhury

Petrofac International Ltd
Sharjah, United Arab Emirates

Shambhu P. Dasgupta

Department of Civil Engineering
Indian Institute of Technology
Kharagpur, India



CRC Press
Taylor & Francis Group
Boca Raton London New York Leiden

CRC Press is an imprint of the
Taylor & Francis Group, an **informa** business

A BALKEMA BOOK

Also available:
Dynamics of Structure and Foundation – A Unified Approach
1. Fundamentals

Indrajit Chowdhury & Shambhu P. Dasgupta 2009, CRC Press/Balkema

ISBN: 978-0-415-47145-9 (Hbk)
ISBN: 978-0-203-88527-7 (eBook)

CRC Press/Balkema is an imprint of the Taylor & Francis Group, an informa business

© 2009 Taylor & Francis Group, London, UK

Typeset by Vikatan Publishing Solutions (P) Ltd, Chennai, India.
Printed and bound in Great Britain by Antony Rowe (a CPI Group company), Chippenham, Wiltshire.

All rights reserved. No part of this publication or the information contained herein may be reproduced, stored in a retrieval system, or transmitted in any form or by any means, electronic, mechanical, by photocopying, recording or otherwise, without written prior permission from the publisher.

Although all care is taken to ensure integrity and the quality of this publication and the information herein, no responsibility is assumed by the publishers nor the author for any damage to the property or persons as a result of operation or use of this publication and/or the information contained herein.

Published by: CRC Press/Balkema
P.O. Box 447, 2300 AK Leiden, The Netherlands
e-mail: Pub.NL@taylorandfrancis.com
www.crcpress.com – www.taylorandfrancis.co.uk – www.balkema.nl

Library of Congress Cataloging-in-Publication Data
Applied for

ISBN: 978-0-415-49223-2 (Hbk)
ISBN: 978-0-203-87922-1 (eBook)

Contents

Preface xv

1 Introduction **1**

1.1 Why this book 1
1.2 Why the topic of dynamics? 2
1.3 The demography of the book 4

2 Theory of elasticity and numerical methods in engineering **9**

2.1 Mechanics of continua: Stress and strain 9
2.2 Concept of strain 9
2.2.1 Displacement field 9
2.2.2 Concept of small domain 10
2.2.3 Body undergoing small deformation 13
2.2.4 Strain tensor 15
2.2.5 Derivative of a vector fixed in a moving reference 18
2.2.6 Physical interpretation of strain tensor 24
2.2.7 Cubical dilatation 27
2.2.8 Transformation of strains 29
2.2.9 Equations of compatibility 34
2.3 Stresses 37
2.3.1 Concept of stress 37
2.3.2 Principal stresses and strains, invariants 42
2.3.3 Cauchy's stress quadric and Mohr diagram 44
2.3.4 Plane stress conditions 48
2.3.5 Plane strain conditions 49
2.3.6 Octahedral stresses and strains 50
2.3.7 Spherical and deviatoric stress components 51
2.4 Constitutive relations 52

2.5 Equations of equilibrium 59
2.5.1 Some useful expressions 59
2.5.2 Differential equations at a point (general) 60
2.5.3 Differential equations at a point (in terms of stresses) 60
2.5.4 Differential equations at a point (in terms of displacements) 61
2.5.5 General solution 62
2.5.6 Two-dimensional cases 62
2.6 Theorems of elasticity 65
2.6.1 Principles of superposition 65
2.6.2 Strain energy 66
2.6.3 Virtual work 70
2.7 Mechanics of homogeneous isotropic elastic bodies 79
2.7.1 Material derivative of volume integral 82
2.7.2 The equations of continuity 83
2.7.3 The equations of motion 83
2.7.4 Moment of momentum 85
2.7.5 Basic equation of motion of an elastic body 86
2.7.6 Various strain measures 87
2.7.7 Solution of the three-dimensional equation 88
2.7.8 Static solutions with no body forces 90
2.8 Some basics 92
2.8.1 Summary of governing equations/relations 92
2.8.2 Lame's equations [combining all equations, governing differential equation in terms of u, v, w] 93
2.9 Some classical solutions of elastostatics 94
2.9.1 Kelvin (1848) problem – A single force acting in the interior of an infinite solid. (Malvern 1969, Fung 1965) 94
2.9.2 Boussinesq (1878) problem – A normal force acting on the surface of a semi-infinite solid 95
2.9.3 Cerruti (1882) problem – A tangential force acting on the surface of a semi-infinite solid (Mindlin 1936, Love 1944), [*same as Boussinesq's problem, only the load acting on the surface is horizontal*] 96
2.9.4 Mindlin's (1936) solution 97
2.9.5 Theories of Elastodynamics 102
2.10 Numerical methods in engineering: *Basics and applications* 102
2.10.1 Introduction 102

2.10.2 Approximate methods applied to boundary value problems 106
2.11 The Finite Difference Method (FDM) 115
2.11.1 Application to ordinary differential equations (ode) 119
2.11.2 Application to partial differential equations 130
2.11.3 Laplace and Biharmonic equations 147
2.11.4 Irregular meshes or grids 154
2.11.5 Laplace operator with irregular mesh 155
2.11.6 Bi-harmonic equations with irregular meshes 156
2.11.7 Refined finite difference analysis 157
2.11.8 Free edged plates with different boundary conditions 159
2.11.9 Finite difference in polar co-ordinate 161
2.11.10 Finite difference solution for initial value problem 163
2.11.11 Finite difference solution for initial-boundary value problem 163
2.11.12 Finite difference application in dynamics 165
2.12 The finite element method 167
2.12.1 The finite element club and its members 167
2.12.2 Brief history on the development of finite element method 168
2.12.3 The basic philosophy 171
2.12.4 Displacement based derivation of stiffness matrix 172
2.12.5 Plane strain CST element 182
2.12.6 Why constant strain and how effective is the element? 182
2.12.7 Why convergence improve with refined meshes 183
2.12.8 The constitutional laws which bound the developers 183
2.12.9 The rule of polynomial – the entry rule to developers club 184
2.12.10 How do we select the polynomial function correctly? 186
2.12.11 The law of convergence – the three commandments 187
2.12.12 Non-conforming elements an exception to the law 189
2.12.13 Natural coordinates: the gateway to numerical analysis through computer 189

2.12.14 Numerical integration technique used for FEM 191
2.12.15 Gauss quadrature scheme for numerical integration 191
2.12.16 Stiffness matrix for 4-nodded rectangular element under plane strain condition 194
2.12.17 Iso-parametric formulation for elements with arbitrary shape 199
2.12.18 Other form of isoparametric elements 210
2.12.19 Iso-parametric formulation of CST element 211
2.12.20 Condensation – The Houdini trick of vanishing nodes 214
2.12.21 Alternative method of deriving a quadrilateral element 217
2.12.22 The Reverse Logic – How correct it is? 219
2.12.23 Incompatible or Non-conforming element – Where two wrongs make one right 219
2.12.24 How tough is this lawbreaker? 225
2.12.25 Taylor's improved incompatible quadrilateral 225
2.12.26 Higher order finite elements – The second generation members of the FEM family 234
2.12.27 Lagrange's interpolation function – An extension to school co-ordinate geometry 238
2.12.28 Elements of Serendipidity family – named after Princes of Serendip 242
2.12.29 Other type of higher order elements 247
2.12.30 Plate element – the problem child of FEM family 248
2.12.31 Triangular plate element in bending – the Catch-22 element 249
2.12.32 DKT Plate element 252
2.12.33 Rectangular plate element in bending mode 254
2.12.34 Four-nodded quadrilateral plate element in bending 258
2.12.35 Three Dimensional Hexahedral Element – One last to bore you 263
2.12.36 Twenty-nodded hexahedral element 268
2.12.37 The patch and eigenvalue test – The performance warranty certificates 269
2.12.38 A retrospection on what we presented so far 275
2.12.39 The assemblers – the tailors who stitches the pieces to give final shape 275

2.12.40 Formulation of the global stiffness matrix 276
2.12.41 Transformation in space for 3D analysis 281
2.12.42 Members vertical in space – *a special case* 283
2.12.43 Global stiffness matrix and transformation of finite element continuum 291
2.12.44 Implementing the boundary condition 291
2.12.45 Formulating specified support displacement 293
2.12.46 Calculation of element stress and displacements 295
2.12.47 Solution of equilibrium equation 302
2.12.48 Gaussian elimination – The technique of back substitution 303
2.12.49 The LDL^T decomposition technique 304
2.12.50 Frontal wave solution – Iron's technique reflecting present consumer market 307
2.12.51 The World of Boris Galerkin – A look at finite element beyond stress analysis 310
2.12.52 Thermal analysis of composite wall in one dimension 312
2.12.53 The user domain-rookies, fakes, control freaks and clever Ivans 319
2.12.54 Finite element model of table top centrifugal compressor with dynamic soil-structure interaction 322
2.12.55 Static soil-structure interaction analysis of a pedestrian subway below ground 327

3 Basics of lumped parameter vibration 335

3.1 Introduction 335
3.2 Single-degree-of freedom 336
3.2.1 Free vibration: Undamped case 336
3.2.2 Forced vibration 351
3.2.3 Steady-state analysis: Mechanical impedance method 355
3.2.4 Q-values and their interpretation 356
3.2.5 Power absorption 360
3.2.6 Heavy damping 362
3.2.7 Frequency dependent loading 363
3.2.8 Dissipation of energy 371
3.2.9 Velocity squared damping 373
3.2.10 Solid damping 374
3.2.11 Analysis of friction forces (Coulomb friction, dry friction) 374

3.2.12 Response under impulsive loading 379
3.2.13 General solution for any arbitrary forcing system 380
3.2.14 Response spectra 385
3.2.15 Earthquake type of excitation 390
3.3 Stability of dynamic solutions 390
3.3.1 Phase planes and stability of solution 390
3.3.2 Basics of differential equation 391
3.3.3 Homogeneous Systems with Constant Coefficients, Phase Plane, Critical Points 393
3.3.4 Phase plane method for SDOF system 402
3.3.5 Self-excited oscillations 404
3.3.6 Autonomous system 404
3.3.7 State space method 404
3.3.8 State speed 405
3.3.9 Stability of the solution 407
3.4 Multiple-degrees-of-freedom systems 434
3.4.1 Free vibration: Undamped system 434
3.4.2 Steady-state analysis: Mechanical impedance method 435
3.4.3 Coupled translation and rotation 437
3.4.4 Forced vibration 439
3.4.5 Semi-definite systems 443
3.5 Nonlinear systems 449
3.5.1 Free vibrations 449
3.5.2 Forced vibrations 460
3.5.3 Large amplitudes in response: Order and chaos 463

4 An introduction to soil-structure systems under statical condition 469

4.1 Introduction 469
4.1.1 What we did twenty years ago... 469
4.1.2 The Present Scenario... 470
4.2 Soil-structure interaction 470
4.3 Static soil-structure interaction 470
4.4 Non uniform contact pressure 474
4.5 Various soil models–the tools in the toolkit... 477
4.5.1 Winkler springs 477
4.5.2 Estimation of sub-grade modulus 478
4.6 Evaluation of nodal springs 480
4.6.1 So the ground rule is... 481

4.7 Limitations/advantages of Winkler spring model 481
4.8 Finite element models 482
4.8.1 Plate element 483
4.9 Finite element analysis of plate with soil stiffness based on isotropic elastic half space theory 485
4.9.1 Displacement profile of soil under a foundation based on half space theory 485
4.10 Finite grid method/equivalent beam element, the unsung work horse 488
4.11 FEM application for problems of class 2D 490
4.12 Plane stress and plane strain condition 493
4.12.1 Plane stress condition 493
4.12.2 Plane strain condition 494
4.13 FEM model for the vertical cut problem 494
4.14 Infinite finite element a logical paradox... 496
4.15 Basis of formulation of the infinite element 497
4.15.1 What does it really mean? 497
4.15.2 Why did we transform the co-ordinate and what did we gain out of it? 499
4.16 Material property affecting the model 500
4.17 Relation between sub-grade modulus and modulus of elasticity 501
4.18 Selection of Poisson's ratio 502
4.19 Limitation and advantages of finite element method in static soil structure interaction problem 502

5 Concepts in structural and soil dynamics 505

5.1 Introduction 505
5.2 A brief history of dynamic analysis of structure and foundation in civil engineering 505
5.2.1 Basic concepts 508
5.2.2 Orthogonal transformation or the transformation basis 524
5.2.3 Direct integration technique, the alternate approach 548
5.2.4 Wilson-Theta method 557
5.3 Eigen value analysis 584
5.3.1 Some techniques for eigen value analysis 584
5.3.2 Standard Jacobi's technique 610
5.3.3 Generalized Jacobi technique 617
5.3.4 Dynamic analysis based on finite element method 623

5.4 Introduction to soil and elasto-dynamics 639
5.4.1 Development of soil dynamics to the present state of art 639
5.4.2 One-dimensional propagation of wave through an elastic medium 642
5.4.3 Three-dimensional propagation of waves in an infinite elastic medium 644
5.4.4 Propagation of waves in polar co-ordinates 657
5.4.5 Reflection/Refraction 659
5.4.6 Where does this all lead to? 671
5.4.7 Some background on integral transforms and other mathematical theorems 671
5.5 Halfspace elastodynamic solution 687
5.5.1 Lamb's solution for two-dimensional problem 687
5.5.2 Pekeris' solution for surface pulse 703
5.5.3 Pekeris' solution for buried pulse 712
5.5.4 Interpretation of Pekeris' solution 718
5.5.5 Chang's Solution to dynamic response for horizontal surface loading 719
5.6 Geotechnical earthquake analysis 722
5.6.1 Soil dynamics and earthquake 722
5.6.2 Waves induced by underground blast 739
5.7 Geotechnical analysis of machine foundations 740
5.7.1 Soil dynamics and machine foundation 740
5.7.2 Reissner's method 740
5.7.3 Sung and Quinlan's method 743
5.7.4 Bycroft's solution for dynamic response of foundation 744
5.7.5 Reissner and Sagoci's method of torsional oscillation 750
5.7.6 Hseih's method for dynamic response of foundation 751
5.7.7 Lysmer and Richart's model for dynamic response of foundation 752
5.7.8 Hall's analog for sliding and rocking vibration 756
5.7.9 Vibration of rectangular footings resting on elastic half-space 761
5.7.10 Rigid strip footing 765
5.7.11 Luco and Westmann solution for rigid strip footing 781

5.7.12 Dynamic response of circular footings 791
5.7.13 Vibration of an elastic half space under rectangular loading 805
5.8 Vibration of embedded footings 820
5.8.1 Embedment effect on foundation 820
5.8.2 Research carried out in India 829
5.8.3 Energy transmitted from a circular area 833
5.9 Finite element solution for foundation dynamics 834
5.9.1 Soil dynamics and finite element analysis 834
5.9.2 Use of structural boundary conditions 835
5.9.3 Use of spring or boundary elements 835
5.9.4 Use of transmitting/silent boundaries with finite elements 837
5.9.5 Standard viscous and Rayleigh boundary elements 838
5.9.6 Paraxial boundaries 841
5.9.7 Infinite finite elements 843
5.9.8 Epilogue 843

References 847

Subject index 855

Preface

The idea of writing this book first took its root, while I was working with Bechtel way back in 1996–97. The company was building a power plant in India and it was my first interaction with US engineers sitting across the table. The work was executed in an extremely congenial atmosphere, except for concerning one aspect, which amused me to no end. Whenever it came to any structures or foundations, related to dynamic analysis, I could very well sense the innate reluctance of my overseas colleagues, who were not so sure about the capability of the New Delhi office and the Indian Engineers on this topic. It surely took me by surprise, for, from 1970–1990, India has taken giant leaps in terms of technology. We have installed our own power plants ranging from 210 to 500 MW. We have indigenously built our own nuclear power plants, developed our own short and long range missiles ameliorating our defense, designed and built our own offshore facilities in Bombay, etc. Rummaging through literature, I was genuinely shocked to realize that though many Indian engineers, scientists and academician have contributed significantly in terms of national and international research papers, enriching this magnificent subject, yet nobody had written a book on dynamics that could compete in international market. Except for the book titled *A Handbook of Machine foundation* by Vaidyanathan and Srinivasalu there is hardly any long standing book prevalent in the national or international market, which has emerged out of India, pertaining to dynamics!

Dynamics *per se* is a funny subject. In spite of its firm existence in the realm of civil engineering for last 70 years or more, it is a topic that is still abhorred by many and loved by few. I believe this is mostly due to the terse and oblique way many academicians often teach the subject, without giving the requisite background.

I would not like to furnish any apologies (except for in very few cases) we have never tried to pose that we are smart (or elegant for that matter) and tried to show you the intricacies and subtle nuances of this mystic topic in almost a story-telling session.

If you are really interested in this subject, I do believe that reading this book would be a fun session for you; for we firmly believe that if you do not enjoy what you are reading, learning a topic is always difficult.

There are of course some background topics like elasticity, mechanical vibration, etc. that we have presented in a factual fashion, for we felt these are preparatory

background topics that you may or may not have (those of you who know this already can skip).

I sincerely wish you happy reading and expect, you would enjoy it as much as reading a Frederick Forsyth or an Agatha Christie novel, unraveling the majestic mystery of soil and structural dynamics.

In my long and arduous journey through this book I have been lucky to get immense support of many friends and colleagues without whose active cooperation I could never have finished this book.

I therefore take this opportunity to convey my profound thanks and gratitude to my company, *Petrofac International Limited, Sharjah*, without whose sustained and unflinching support I could have never completed this voluminous work. My Oliver Twist gang of Messrs. Anindya Roy, Hitesh Roy, Dr. J.P. Singh, M.N. Ravi, Mrs. Negar Sadeghpour owe hearty thanks for patiently going through many of my drafts. I immensely enjoyed their subtle as well as blunt criticism (at times) that often made me look at things as to how the reader would react. I was extremely lucky to have such a brilliant team, equipped with such brilliant technical minds. A very special thanks to Mr. Prabir Kumar Som, Dr. Nirmalya Bandopadhay, Prof. Bratish Sengupta (my ex-teacher) for going through the draft manuscript and giving many valuable suggestions for improvements in the presentation.

My sincere gratitude goes to .....

My Mother for, always having that unshakeable faith in my academic ability, though I was spending too much time (as a student) in the ground playing serious-level cricket. To my family, my wife Tinku, son Rohan and my giant Great Dane Timmy, for their infinite patience and standing by my self- imposed social seclusion, while working on this book.

I guess this section cannot end without mentioning Dr. Sambhu P. Dasgupta, present Head of Civil Engineering Department of Indian Institute of Technology (Kharagpur) and my co author. It all started in 1982–83 when he was my formal teacher in Dynamics and then went on to become my graduate thesis advisor. For an academician like Dr. Dasgupta it is "business as usual", as a number of students come and go like this every year. However, in our case the relationship jelled into something more than usual possible, because of our common and intense passion for dynamics and also perhaps due to our innate curiosity daring us to trespass beyond any line of specialization (geotechnical/structural engineering) and to look at it in totality. That jeans and T-shirt clad thin student 24 years ago, has of course changed to today's middle aged slightly pot bellied executive. While Dr. Dasgupta has also grayed sufficiently with time, but our relationship has become strengthier over the years. His guidance, support and advises on a number of technical and non-technical issues had always stood like an unwavering lighthouse in all my good and bad times for the last 25 years. Irrespective of my corporate commitments and his heavy academic and research load, whenever I posed him a problem or a solution from any corner of the globe, he would always make time to go through it carefully and give his considered opinion.

This has resulted in a number of innovative techniques we developed together, which now constitute many portions of this book.

Thus, when I thought of writing this book, I could think of nobody else but him to guide, support and work as a team with me in this venture. For whatever I did or for what has been my reputation in industry, is based on the philosophies he has rigourously taught me in those early days.

Indrajit Chowdhury(IC)
Sharjah, 7th November 2007

This book is intended to serve the purpose of a graduate-level text and a reference for practicing engineers. Our approach is to write to the students rather to the instructors using the book. Here we have made a long and detailed text that strives for the completeness and rigour on one hand and, on the other, we poise to distribute complete handouts for the designers in the field. In fact, there is no clash as such and we have tried to bridge the gap as far as possible.

The material in this book grew out of texts used for teaching the graduate students at Indian Institute of Technology, Kharagpur and my co-author's experiences at the Design Offices of Development Consultant at Kolkata, Bechtel Corporation, New Delhi, Siemens Corporation, New Delhi, Petrofac International at Sharjah.

Even the recruiters from industry under the present global scenario are now asking for people who are proficient in their area of expertise and candidates need now more-than-ever a sound, basic in-depth knowledge of solid mechanics, building carefully from that point onwards. Playing with softwares and 'canned' programs without this sound and carefully developed background are leading to the careers as technicians rather than as engineers.

I am grateful to my teachers, Professors N.S.V. Kameswara Rao, M.R. Madhav, M. Anandakrishnan, Navin. C. Nigam of the Indian Institute of Technology Kanpur, who have introduced and encouraged me to work in the area foundation dynamics and dynamic soil-structure interaction. This book is my offering to these teachers as a token of my gratitude for their gift of knowledge and inspiration. I recollect the excellent academic environment fostered by them in my student days at IIT, Kanpur.

I am grateful for the encouragement received from a number of colleagues and students during the preparation of the book. Early versions of most of the chapters of this book were distributed to my graduate students, and I gratefully acknowledge their assistance and encouragement.

I would finally like to express my tender appreciation to my wife Tapati who cheerfully devoted herself in the task of inspiring me in every way in finishing this lofty task and my daughter Satarupa a lot for instilling me with her deep affection. For their continued encouragement, smiling assistance in the various stages of writing the book will remain forever in my mind.

Numerical modeling of foundation dynamics and constitutive modeling have been the areas of my personal research over two decades and this book emphasizes these research areas. My association with Indrajit Chowdhury goes back to the 80s when he took up a problem on dynamic soil-structure interaction. With the dawn of the present millennium we were associated again in jointly venturing research in the area of dynamic soil structure interaction. It has been an enjoyable and challenging experience and the present book is the testimony of those long years of labour, dream and aspiration.

We would love to see that this book is being used by the students with utmost care and reverence, also after the course is over. We hope to see the unending beginning and that reading the book will stimulate a new impetus for them and for the future generation.

It is quite natural that some errors might have crept into the text of this volume; we shall appreciate if such errors are brought to our notice. Suggestions for improvement of the book are most welcome.

We greatly appreciate the kind of support extended to us by the staff of CRC Press (Taylor & Francis Group, A Balkema Book), The Netherlands.

Shambhu P. Dasgupta
I.I.T., Kharagpur, 9th November, 2007

Chapter 1

Introduction

1.1 WHY THIS BOOK

It is said that authorship of any kind is a tremendous boost to one's ego. Readers, who would care to go through these pages, can be rest assured that this book has not been written to gratify one's ego trip.

Reason for its birth has been our deep-rooted concern on the way profession of engineering and especially civil engineering is going – in terms of teaching and practice. Civil Engineering is perhaps the oldest profession amongst the realms of technology, which has been practiced by human being from the early dawn of civilization. It is also indeed a fact that umpteen numbers of books have been written addressing various topics on Civil and Structural engineering from the time of Galileo (1594) till date. So what made us write this book when many of the things mentioned herein may or may not be available in other literature?

The reason for its birth can be attributed as follows:

Civil engineering community in India, in spite of making a lot of progress, very few authors have addressed the topics that we have tried to cover under one platform.

Topics related to structural and soil dynamics that are taught in the universities or referred to in design offices are still dependent on very limited number of books[1], or code of practices (often outdated) or research papers not readily available to an average student/engineer.

Finally, in last two decades we have seen a very peculiar trend and that which has affected the profession globally, and could have a long lasting influence on it.

If we look around the world in terms of books published in civil engineering in the last two decades (1980–2000) it will be observed that unlike the period 1960–70 almost all books have been authored by academicians where practicing engineers rarely contributed!

Whatever could be the reason for this apathy from engineers in the industry the point remains that students coming out of engineering institutes, unlike 30 years ago are being exposed minimally to practice as prevalent in industry.

And this we believe is creating a serious gap in engineering education. Till such times practicing engineers are encouraged like in developed countries to participate in

1 Many of them are again out of print...

teaching we are fearful that engineering especially civil engineering will metamorphose into more an advance course in mathematical physics rather than a scientific art where theory is honed by intuitive practices and field realties.

Engineering is not only a maze of differential equations, tensors, matrix algebra, or developing software program. It is much beyond these, where all these mathematical techniques are mere tools in the hands of a capable engineer who can intuitively visualize the behavior of the structure and foundation he is going to design and check his intuitive deduction based on the above tools in hands and this makes it essential to synthesize theory and practice that becomes the hallmark of a complete engineer.

1.2 WHY THE TOPIC OF DYNAMICS?

Again why did we choose a topic as abstract as dynamics? When writing a book on Soil mechanics/Foundation engineering or say Reinforced Concrete design would surely have been a more profitable and less laborious a venture.

The motivation behind the same was that dynamics as a subject we have found carries a peculiar stigma, where it is either loved or pathologically abhorred by engineers in the industry and even in academics by many.

While its mathematical beauty fascinates and charm many an intellectual mind, the same thing others find it too intimidating and abstract which creates a mind block that the topic is far too theoretical, not worth professional attention and can well be taken care off by proper detailing be it a steel or a concrete structure[2].

The value of proper detailing can never be undermined. However, mathematical models far too simplified to avoid a little bit of mathematics can well result in moments and shear that could be out by 200% from reality. We can assure you that no amount of excellent detailing would save the structure if the moment and shear that are derived are unrealistic in the first place.

Having counseled many such anti-dynamists in last 25 years in industry and academics we have found the root cause for this aversion culminates from how the topic has been presented to him during his initiation to the subject. Our observation has been that:

- The apathy/mind block has developed due to the way it has been presented to many of them-which they found difficult to comprehend with instructor showing little or no sympathy to make it interesting or understandable.
- Compulsion to complete the coursework within inadequate time frame leaving the instructor with very little time to cite examples from real world to make things look easy and comprehensible – this has further complicated the issue.
- Tendency of some to make things look mathematically elegant thus unnecessarily resorting to complex mathematical presentation without preparing the students to comprehend the physical significance of the same in the first place.

2 Or at worst, use commercially available software as a black box and follow the results blindly.

- Finally lack of experience of some instructors in real world practices thus presenting the topic in an extremely theoretical fashion[3] does not make things easy at all.

The study of dynamics has thus become almost like the philosophy of *Tantra* – powerful yet fear evoking. Understood by few, while abhorred and misunderstood by most. And this what we have tried to eradicate here.

To unravel many unpopular myths the topic unjustifiably bears, trying to present the reader with its divine yet mysterious charm.

In our presentation of the subject we have not demarcated it into either structural dynamics or soil dynamics but has rather attributed it as a unified approach.

For we strongly feel that it is high time this barrier is broken between structural and geo-technical engineering. Without sounding prophetic, it is our strong conviction that structural and soil dynamics will ultimately merge into one unified topic of "Dynamic Soil Structure Interaction (DSSI)" and which as a subject will surely regain its importance and strength in years to come.

Research and development on DSSI got a strong impetus in the late 70 and 80s (in India)[4] but somehow lost the momentum in between.

The reason for its faltering to our perception could be attributed to the following:

1 Decline in development of Nuclear power plants in India from the late 80's due to the CTBT issues.
2 Reluctance of the geotechnical and structural engineers to sit together and look into the thing in totality and show the courage to digress beyond the boundary they have always been taught not to cross.

At the start of the 21st century if we look at the energy scenario of our country things surely do not look very promising. We have almost exhausted our reserve of first class coal which is an essential ingredient of a thermal power plant. Whatever balance coal we have the ash content is far too high and using the same to generate power would surely make it a serious environmental issue. With environmental scientists drawing a bleak picture of future due to global warming and green house effect, building thermal power plants with second grade coal compounded by expensive and tedious ash handling, and tough environmental legislation that one has to now abide by would indubitably make conventional fossil fuel power plants a less and less potential choice as an energy source in future.

3 It is sad to see some of these academicians adept with Laplace and Fourier transforms, Gaussian distribution of power spectrum but ask them to provide technical advice for a real life structure where money and human life is at stake, they would drop the same like a hot potato at first instance.

They live in their own Cinderella world where dynamics is a branch of theoretical physics they use conveniently to advance their academic career by publishing one paper after another (mostly having insignificant or no relevance to any real world engineering practice). It is unfortunate that many of these paper tigers having little practical experience and are the very people who dominate the engineering education scenario in our country today.

4 Like Finite Element Method burst into the scene in early 70s.

With ever spiraling cost of these two commodities in global market (presently touching $120 per barrel) running power plants with LPG or gas (combined cycle power plant) one would have to import the same and would surely not be a cost effective public utility venture – for the electric tariff to cover the cost would be far too expensive for a common man to bear.

Considering our geographical location utilization of alternate source of energy like hydel, solar or wind is only limited. Thus for mass generation of electricity which is essential for industrialization and economic development, nuclear power plant would thus surely play an important role in near future, where dynamic analysis/DSSI would again possibly be a crucial issue to ensure its safety adhering to the international norms for such power plants[5].

Leaving aside Nuclear power plants, there are number of other industrial plants like Petrochemical, Chemical, Mineral beneficiation plants that handles a number of hazardous items like methyl iso-cyanide, hydrogen sulfide, liquefied natural gas (highly inflammable) to name only a few. Leakage of these items even due to a moderate earthquake can create sufficient damage to environment that could take centuries to recover. Buildings (high rise or other wise) are getting destroyed inevitably in almost all strong motion earthquakes that take place around the world- killing millions of people and destroying properties worth billions of dollars. Thus irrespective of our reluctance to adapt the technology "dynamic analysis of structures and foundations" have become an important weapon in our arsenal to fight the awesome fury of the mother nature whose ways are still known little to us.

1.3 THE DEMOGRAPHY OF THE BOOK

The book has been divided into two volumes of which the present book is the Volume-1. This volume introduces the theoretical aspects of dynamic analysis. Volume-2 uses these background theories and applies them to different structures and foundations that are considered important and major infrastructures in civil engineering.

Volume-1 consists of five chapters of which three chapters (Chapters II, III and IV) are preparatory. It creates the background for your initiation to dynamics and soil-structure interaction as a subject of study.

Chapter II deals with Theory of Elasticity and Numerical Methods. Theory of elasticity as we know is mother of all stress analysis and is used by all stress engineers in their profession. It forms the backbone of all static and dynamic analysis in civil engineering. People wanting to develop a background on dynamics we presume already have some background on this. However just for quick recapitulation and reference the major results and concepts have been furnished in a heuristic form for ready reference.

Numerical methods, in last twenty years with the advent of digital computers have become one of the most powerful tool in the analytical arsenal of an engineer. We have observed, that many engineers beyond a level often find it difficult to cope with

5 Nobody would surely want a Charnobyl in hand. Considering the population density of India it is indeed a fearful prospect.

many a practical problem related to dynamics, simply because his background in numerical analysis is inadequate or insufficient. As such, we have dealt this in sufficient detail especially finite difference and finite element method (FEM) so that an engineer feels confident in handling a problem either static or dynamic in his research and professional work.

While penning this section we had to make some very careful choice as to what to put herein that gives the reader a broad overall picture, while at the same time ensure that he does not get lost into too much of mathematical intricacy of many higher order elements whose presentations are surely mathematically very elegant but has limited use. Since this book is not essentially a book on Finite Element method we have taken the liberty of presenting only those key elements that are most popular and has a high usage in practice. We sincerely hope that on going through this section many engineers would give up the habit of using a finite element software simply as a "black box" – a trend which is not only deplorable but could have a devastating consequence if left unabated.

Another point which few of the readers might find intriguing is that we have not presented any software in terms of finite element which is the generic trend in most of the memoirs available in the market.

Our motive is to make you understand the basics underlying the method, thus enabling you to use a number of commercially available FEM software available in the market efficiently as well as with confidence. We would much appreciate to have some feedback from you to evaluate if we could fulfill this aspiration of ours.

Chapter III deals with vibration of discrete systems and you might just wonder, why have we started with this topic here? Historically, civil engineers started tinkering around with bodies subjected to motion quite late (1950s) while mechanical and aerospace engineers started working on this area much ahead of them (1920). It started possibly from the time when Den Hartog (1924) began giving series of lectures to the Westinghouse Engineers who were designing Turbines and engines. Civil engineers when started developing the theory of structural dynamics in late 1950s they thus depended heavily on these theories of mechanical vibration to develop realistic model of structures based on lumped mass, springs and dashpots. It will be seen subsequently when we take up the theories of structural dynamics (in Chapter V) that the theories are same in many cases and so are many of the results. Thus we felt having some background on mechanical vibration will only enhance your knowledge data base and make subsequent understanding better when we take up the theory of structural dynamics in later chapter.

Chapter IV deals with some fundamental concepts of Static soil-structure interaction. Like in structural analysis as a prelude to dynamic analysis one must have a clear concept on behavior of structures under static load similarly for DSSI one must have a clear concept of how does the structure and soil behave in tandem under static loading. One of the major tool that is used for such coupled analysis (both static and dynamic problems) is obviously Numerical methods especially FEM and this is where lies the roots of many mistakes due to improper modeling. This we have discussed here in quite a detail trying to elaborate on some of the common mistakes people often make during the mathematical idealization. We sincerely hope that this will help you to come up with a reasonably correct mathematical model in many cases and enhance your skill as a FEM modeler.

This is relatively a short chapter yet it deals with a number of key problems conceptually that many engineers face in their work and often find them difficult if not confusing to handle.

Chapter V constitutes of basic theories pertaining to structural and soil dynamics.

We start this chapter with the theories of structural dynamics starting from a body having single degree of freedom to multi-degrees freedom – all possible mathematical models have been dealt herein with a number of solved problems to give you a better insight into the system. You will see in many cases as to how the models considered becomes similar to many we have considered in Chapter III under the heading of theory of mechanical vibration. One of the major stumbling blocks in the analysis of multi-degree freedom system has been to assume modal damping ratio to be constant for all modes[6]. An innovative solution has been suggested herein where the damping can be forced to vary with modes giving a more realistic output – we hope you will enjoy the technique.

Time history analysis (THA) is another area where many engineers squirm out of discomfort and would try their level best to restrict their analysis within the domain of modal analysis. Leaving aside the intense calculation THA calls for, the main reason for this apathy is again due to the far too concise treatment meted out to such an important topic in most of the books in dynamics. On this we have again cut no corners and have solved sufficient numbers of problems (including the damping effect) that you can even manage with only a calculator to make you comfortable with the issue.

All the concepts in this section is explained based on harmonic loading which makes the understanding and insight to the problem in hand easy to understand and yet may offend an earthquake specialist who might feel we have by passed such an important issue. However, such impression would be unjustified as dynamic analysis of structures subjected to earthquake has been dealt in sufficient detail in Volume-2 of this book where a complete chapter is dedicated to this very important topic.

The second part of the chapter deals with soil and elasto-dynamics. We agree and confess that it was the toughest section that we wrote and took considerable time and planning from our end as to what and how to present. To our experience soil and elasto-dynamics as a topic is though now a part of curriculum at post graduate level in many institutes- but is still given a very cursory treatment where the thrust is more on laboratory investigation rather than treating the mathematical issues[7]. Thus, no wonder that the soil dynamics is a topic which has remained a source of acute discomfort to many people in research and industry alike. We have tried to give it a most comprehensive treatment in starting with Lamb's (1904) solution to Pekeris (1955), Pekeris and Lifson (1957) and then slowly digressing into the formulations of Lysmer (1965), Holzohner (1969), Novak and Berdugo (1972) etc. The objective has been to give a step by step commentary as to how it developed from Lamb to where it is presently when dynamic finite element analysis with paraxial and viscous

6 Structural Engineers are forced to use this as there are no mathematical model available till date which caters to the progressive increment of damping ratio with each mode.

7 The book titled "Wave Motion in Elastic solid" – Karl Graff Dover publication or "Wave Propagation through Elastic media" – J.D. Achenbach; North Holland Publication, is still not a part of regular curriculum for students taking coursework in soil dynamics in many Engineering colleges!

boundaries are used to model infinite domain problem. In this process we have also shown how at one stage soil dynamics digressed into a new area of technology often termed as *geotechnical earthquake engineering* now a days.

At the very outset, we would like to pacify those readers who might get impatient with the pages of fearful looking integral equation that invariably generates due to wave propagation through an elastic medium under mixed boundary conditions that prevail in foundation dynamics – a topic often not addressed properly in many graduate courses.

But we can surely assure you that wrestling with a few fundamental theorems in advanced calculus and a referring to a decent mathematical handbook would suffice as they are surely not unconquerable. Even if the theoretical implications belies one's comprehension due to his lack of practice with such mathematics – the end results are sufficiently complete and clear for usage and programming – and these have very important applications.

One of the major reason based on which we went on to work out many of these formulations in such detail is because we have observed that many engineers who use these solutions in their day to day work in the design of machine foundation and earthquake analysis do it mechanically without a basis as to how some of them have evolved. It is heartbreaking to hear people believe Lysmer's or Wolf's spring which they have possibly used hundred times (if not more) "are derived based on experiment" and even "empirical"!

We would rather feel our effort has not gone in vain if we can eradicate such misconceptions through this book.

Chapter 2

Theory of elasticity and numerical methods in engineering

2.1 MECHANICS OF CONTINUA: STRESS AND STRAIN

Mechanics of continua constitutes the backbone of civil engineering analysis of elasto and dynamic problems. Irrespective of whether one is working in the area of structural or geotechnical engineering, all are based on the basic ideas of the theory of elasticity.

Considering that the book is basically focused on the dynamic analysis of structure and foundation, we presume that the reader already has some background on this topic. As such, essence of this section is not to elaborate on the fundamentals, but to present the basic equations of elasticity in a heuristic manner for ready reference, since many of these equation are often used for various analysis or calculating the stresses and strains that a body is induced to under static and dynamic loads.

2.2 CONCEPT OF STRAIN

In our colloquial world of communication when we see somebody is working very hard we often use sentences like "*Oh! Mr. X is going through a lot of strain.*" Or, "*Do not stress yourself by working so hard – it is not good for your health etc.*" If you carefully note these sentences you will observe that words like *work*, *stress* and *strain* are used in the same breathe. Though the words have been used in literary sense however in terms of physics this is absolutely correct for the phenomena are truly inter-related. Going back to our high school physics we can say that when a force F is applied to a body and it undergoes a deformation δ, we say the external work done is $\mathrm{F} \cdot \delta$. If the un-deformed length of the body in one dimension is L say, then the strain ε induced is $\varepsilon = \delta/\mathrm{L}$ and corresponding stress is expressed as $\sigma = \mathrm{E} \cdot \varepsilon$ where E is the Young's modulus of the body. The science of elasticity is nothing but study of these stresses and strains in one, two and three dimensions.

2.2.1 Displacement field

Consider a body Ω in a three dimensional Cartesian space (X, Y, Z) and let there be a point $P(x, y, z)$. The straight line joining OP is known as position vector, $\underline{r} = x\boldsymbol{i} + y\boldsymbol{j} + z\boldsymbol{k}$, where $\boldsymbol{i}$, $\boldsymbol{j}$, $\boldsymbol{k}$ are unit vectors along X, Y, and Z-axis. Let the body occupies a position Ω' as a result of straining and P now occupies the position

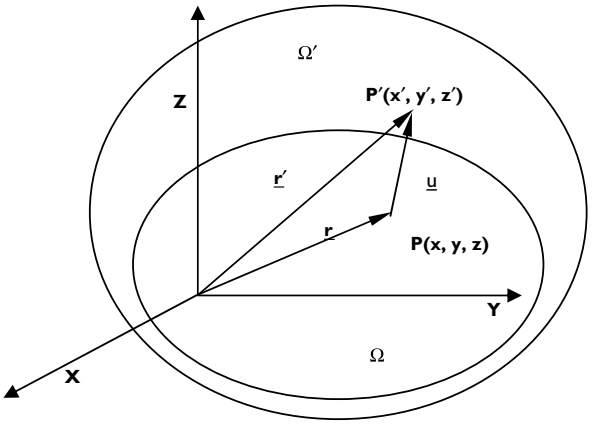


Figure 2.2.1 Definition of displacement field.

$P(x', y', z')$, having position vector, $\underline{r}' = x'\boldsymbol{i} + y'\boldsymbol{j} + z'\boldsymbol{k}$. The vector,

$$\underline{u} \triangleq u_x\boldsymbol{i} + u_y\boldsymbol{j} + u_z\boldsymbol{k} \tag{2.2.1}$$

is called a displacement vector [also written as, $u = u_x$, $v = u_y$, $w = u_z$, respectively in the x, y and z-direction]. Geometric definition of the displacement field $\underline{u}$ is shown in Figure 2.2.1. If we assume $\underline{u}$ to be a continuous function varying continuously from point to point, $\underline{u}$ will be called a vector field. Thus $\underline{u}$ is defined as displacement field and expressed as a function of coordinates of the *undeformed* geometry (x, y, z) and as such denoted by $\underline{u}\,(x, y, z)$. In Cartesian tensor form this may be written as

$$\underline{u} = u_i\varepsilon_i \tag{2.2.2}$$

Repetitive subscripts imply summation of indices, $i = 1, 2, 3$, denoting axes X, Y and Z respectively and ε_i are the unit vectors in i-th direction.

2.2.2 Concept of small domain

Consider a body, Ω, shown in Figure 2.2.2, undergoing deformation. Select two arbitrary points P and Q which forms a vector $\underline{A}$. In the deformed state; P changes to P' and Q to Q'. As a consequence, $\underline{A}$ is changed to $\underline{A}'$.

We may denote: $\delta\underline{A} \triangleq \underline{A}' - \underline{A}$
Again, we have

$$\underline{u}_P + \underline{A}' = \underline{A} + \underline{u}_Q \quad \rightarrow \quad \delta\underline{A} = \underline{A}' - \underline{A} = \underline{u}_Q - \underline{u}_P \tag{2.2.3}$$

The displacement field $\underline{u}$, we assume, always to be an analytic function [i.e. single-valued function having continuous first derivative]. We now assume Q to be a neighbouring point of P and, as such, expand $\underline{u}_Q$ around $\underline{u}_P$ in Taylor's series:

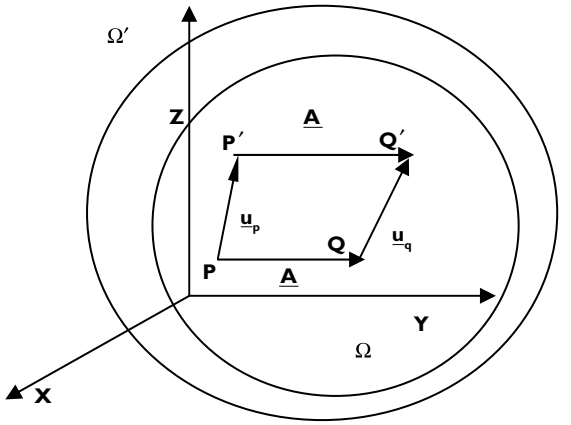


Figure 2.2.2 Small domain concept.

In general: If, $f = f(x, y, z)$, then $f(x + h, y + k, z + \ell)$

$$= \sum_{n=0}^{N-1} \frac{1}{n!} \left[h\frac{\partial}{\partial x} + k\frac{\partial}{\partial y} + \ell\frac{\partial}{\partial z} \right]^n f(x, y, z) + \frac{1}{N!} \left[h\frac{\partial}{\partial x} + k\frac{\partial}{\partial y} + \ell\frac{\partial}{\partial z} \right]^N$$

$$f(x + \theta h, y + \theta k, z + \theta \ell);\ 0 < \theta < 1.$$

---

using, $\Delta x = h$, $\Delta y = k$ and $\Delta z = \ell$,

$$\underline{u}_Q = \underline{u}_P + \Delta x \left(\frac{\partial \underline{u}}{\partial x} \right)_P + \Delta y \left(\frac{\partial \underline{u}}{\partial y} \right)_P + \Delta z \left(\frac{\partial \underline{u}}{\partial z} \right)_P + \cdots \tag{2.2.4}$$

Substituting,

$$\Delta x = A_1 = \left|\underline{A}\right| \cos(a, x) :\ \Delta y = A_2 = \left|\underline{A}\right| \cos(a, y) :$$
$$\Delta z = A_3 = \left|\underline{A}\right| \cos(a, z) \quad \text{and } n = 1;$$
$$\cos(a, x) = \text{direction cosine of a with } x, \text{ and so on } \ldots. \tag{2.2.5}$$

We have ➔ $\underline{u}_Q = \underline{u}_P + \left(\frac{\partial \underline{u}}{\partial x_j} \right) A_j + \text{higher order terms.}$ (2.2.6)

in which $j = 1, 2, 3$, i.e. the directions of x, y and z.

If the vector $\underline{A}$ is very small in magnitude, i.e. *we limit our attention to a very small domain about P*, the higher order terms in the Taylor's series can be neglected. Thus for small domain, we can write

$$\underline{u}_Q = \underline{u}_P + \left(\frac{\partial \underline{u}}{\partial x_j}\right)_P A_j \text{ – this is in tensor form.} \tag{2.2.7}$$

From Equation (2.2.3) we have, $\quad \delta\underline{A} = \left(\frac{\partial \underline{u}}{\partial x_j}\right)_P A_j \tag{2.2.8}$

and $\quad (\delta A)_i = \delta A_i \quad$ and $\quad \left(\frac{\partial \underline{u}}{\partial x_j}\right)_i = \frac{\partial u_i}{\partial x_j} \quad$ or $\delta A_i = \frac{\partial u_i}{\partial x_j} A_j \tag{2.2.9}$

Equation (2.2.9) represents the change in any vector $\underline{A}$ in a vanishingly small domain about a point (x, y, z).

Example 2.2.1

Let the displacement field be: $\underline{u} = (xyi + 3x^2z\,j + 4xz\,k) \times 10^{-2}$ m. A very small segment ΔP has direction cosines $a_{px} = 0.1$, $a_{py} = 0.7$ and $a_{pz} = 0.707$. This segment is directed away from (1, 1, 5). What is the new vector $\Delta P'$ after this displacement field has been imposed?

Solution:

$$\frac{\partial u_1}{\partial x} = \frac{\partial u_1}{\partial x_1} = 0.01y \qquad \frac{\partial u_1}{\partial y} = \frac{\partial u_1}{\partial x_2} = 0.01x \qquad \frac{\partial u_1}{\partial z} = \frac{\partial u_1}{\partial x_3} = 0.0$$

$$\frac{\partial u_2}{\partial x} = \frac{\partial u_2}{\partial x_1} = 0.06xz \qquad \frac{\partial u_2}{\partial y} = \frac{\partial u_2}{\partial x_2} = 0.0 \qquad \frac{\partial u_2}{\partial z} = \frac{\partial u_2}{\partial x_3} = 0.03x^2$$

$$\frac{\partial u_3}{\partial x} = \frac{\partial u_3}{\partial x_1} = 0.04z \qquad \frac{\partial u_3}{\partial y} = \frac{\partial u_3}{\partial x_2} = 0.0 \qquad \frac{\partial u_3}{\partial z} = \frac{\partial u_3}{\partial x_3} = 0.04x$$

Thus

$$\frac{\partial u_i}{\partial x_j} = \begin{bmatrix} 0.01y & 0.01x & 0 \\ 0.06xz & 0 & 0.03x^2 \\ 0.04z & 0 & 0.04x \end{bmatrix}$$

$$\rightarrow \quad \left(\frac{\partial u_i}{\partial x_j}\right)_{\text{at (1,1,5)}} = \begin{bmatrix} 0.01 & 0.01 & 0 \\ 0.30 & 0 & 0.03 \\ 0.20 & 0 & 0.04 \end{bmatrix}.$$

Now, $[\delta(\Delta p)]_1 = \left(\frac{\partial u_1}{\partial x_j}\right)_P (\Delta p)_j = \left(\frac{\partial u_1}{\partial x}\right)_P (\Delta p) a_{Px}$

$$+ \left(\frac{\partial u_1}{\partial y}\right)_P (\Delta p) a_{Py} + \left(\frac{\partial u_1}{\partial z}\right)_P (\Delta p) a_{Pz}$$

$$= \Delta P\,[0.01(0.1) + 0.01(0.7) + 0(0.707)] = 0.008\Delta P.$$

Similarly, $[\delta(\Delta p)]_2 = \left(\frac{\partial u_2}{\partial x_j}\right)_P (\Delta p)_j = \left(\frac{\partial u_2}{\partial x}\right)_P (\Delta p) a_{Px}$

$$+ \left(\frac{\partial u_2}{\partial y}\right)_P (\Delta p) a_{Py} + \left(\frac{\partial u_2}{\partial z}\right)_P (\Delta p) a_{Pz}$$

$$= \Delta P\,[0.3(0.1) + 0(0.7) + 0.03(0.707)] = 0.05121\Delta P.$$

and, $[\delta(\Delta p)]_3 = \left(\frac{\partial u_3}{\partial x_j}\right)_P (\Delta p)_j = \left(\frac{\partial u_3}{\partial x}\right)_P (\Delta p) a_{Px}$

$$+ \left(\frac{\partial u_3}{\partial y}\right)_P (\Delta p) a_{Py} + \left(\frac{\partial u_3}{\partial z}\right)_P (\Delta p) a_{Pz}$$

$$= \Delta P\,[0.2(0.1) + 0(0.7) + 0.04(0.707)] = 0.04828\Delta P.$$

$$\rightarrow \quad \delta(\Delta P) = [0.008\boldsymbol{i} + 0.05121\boldsymbol{j} + 0.04828\boldsymbol{k}]\Delta P.$$

Hence, the new vector, $\Delta P'$ takes the form:

$$\begin{aligned}\Delta P' &= \Delta \underline{P} + \delta(\Delta \underline{P}) = (0.1\boldsymbol{i} + 0.7\boldsymbol{j} + 0.707\boldsymbol{k})\Delta P \\ &\quad + (0.008\boldsymbol{i} + 0.05121\boldsymbol{j} + 0.04828\boldsymbol{k})\Delta P \\ &= (0.108\boldsymbol{i} + 0.7512\boldsymbol{j} + 0.7552\boldsymbol{k})\Delta P \\ &= (0.094\boldsymbol{i} + 0.655\boldsymbol{j} + 0.659\boldsymbol{k})1.146\Delta P.\end{aligned}$$

2.2.3 Body undergoing small deformation

Consider a body Ω in a three-dimensional space (x, y, z) and subsequent deformed states are Ω' and Ω'' respectively under two deformation fields $\underline{u}^1$ and $\underline{u}^2$. This is shown in Figure 2.2.3.

At undeformed state, the vector $\underline{A}$ is at 'a' and, under subsequent deformations a moves to a', and finally to a''. In any small domain, the change of a vector $\underline{A}$ as a

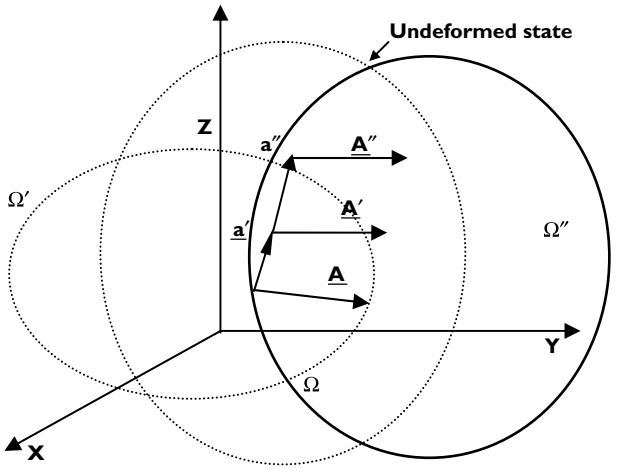


Figure 2.2.3 Small domain concept.

result of the first deformation field $\underline{u}^1$, using Equation (2.2.9) can be written (Shames 1975) as

$$\delta A_i = \left(\frac{\partial u_i^1}{\partial x_j}\right)_a A_j \tag{2.2.10}$$

in which $\left(\frac{\partial u_i^1}{\partial x_j}\right)_a$ is evaluated in the undeformed geometry at a.

$$\text{Thus for } A_i', \text{ we have} \quad A_i' = A_i + \left(\frac{\partial u_i^1}{\partial x_j}\right)_a A_j \tag{2.2.11}$$

For the deformation field, u_i^2

$$A_i'' = A_i' + \left(\frac{\partial u_i^2}{\partial x_k}\right)_{a'} A_k' \tag{2.2.12}$$

$$\text{Thus} \quad A_i'' = A_i + \left(\frac{\partial u_i^1}{\partial x_j}\right)_a A_j + \left(\frac{\partial u_i^2}{\partial x_k}\right)_{a'} A_k + \left(\frac{\partial u_i^2}{\partial x_k}\right)_{a'} \left(\frac{\partial u_k^1}{\partial x_j}\right)_a A_j \tag{2.2.13}$$

$$\text{That is} \quad A_i'' = A_i + \left[\left(\frac{\partial u_i^1}{\partial x_j}\right)_a + \left(\frac{\partial u_i^2}{\partial x_j}\right)_{a'}\right] A_j + \left(\frac{\partial u_i^2}{\partial x_k}\right)_{a'} \left(\frac{\partial u_k^1}{\partial x_k}\right)_a A_j \tag{2.2.14}$$

Now, express $\left(\partial u_i^2/\partial x_k\right)_{a'}$ about the position a by Taylor's series [we shall use Cartesian tensor notation for brevity]:

$$\left(\frac{\partial u_i^2}{\partial x_j}\right)_{a'} = \left(\frac{\partial u_i^2}{\partial x_j}\right)_a + \left[\frac{\partial}{\partial x_k}\left(\frac{\partial u_i^2}{\partial x_j}\right)\right]_a u_k^1 + \left[\frac{\partial^2}{\partial x_k \partial x_\ell}\left(\frac{\partial u_i^2}{\partial x_j}\right)\right]\frac{u_k^1 u_\ell^1}{2} + \cdots \tag{2.2.15}$$

We now impose small deformation restrictions by saying that u_i^1, u_i^2, $\left(\frac{\partial u_i^1}{\partial x_j}\right)_a$ and $\left(\frac{\partial u_i^2}{\partial x_j}\right)_{a'}$ to be very small and we retain, thus the first order term,

$$\text{i.e.} \quad \left(\frac{\partial u_i^2}{\partial x_j}\right)_{a'} = \left(\frac{\partial u_i^2}{\partial x_j}\right)_a \tag{2.2.16}$$

The above mentioned expression results in a conclusion that we can use the undeformed geometry for computing the effects of successive deformations.

Neglecting product of derivatives, we have

$$A_i'' - A_i = (\delta A_i)_{\text{total}} = \left(\frac{\partial u_i^1}{\partial x_j} + \frac{\partial u_i^2}{\partial x_j}\right) A_j \tag{2.2.17}$$

Finally

1 This results in the superposition principle for infinitesimal displacement.
2 Order of imposing infinitesimal displacements does not have an effect on the total deformation.

We can handle most of the engineering problems using the small deformation theory. Small domain view-point has nothing to do with large or small deformation; it can be used for the both. The use of small domain view-point and the small deformation restriction means that we shall be considering the deformation of small elements of a body undergoing small deformations.

2.2.4 Strain tensor

In a vanishingly small element undergoing small deformation, the changes of length and orientation of line segments were found in the preceding sections. Accordingly $\partial u_i/\partial x_j$ will be the key quantity in studying such deformation.

$$\text{We can express} \quad \frac{\partial u_i}{\partial x_j} = \frac{1}{2}\left(\frac{\partial u_i}{\partial x_j} + \frac{\partial u_j}{\partial x_i}\right) + \frac{1}{2}\left(\frac{\partial u_i}{\partial x_j} - \frac{\partial u_j}{\partial x_i}\right) = \varepsilon_{ij} + \omega_{ij} \tag{2.2.18}$$

$$\text{Thus} \quad \delta A_i = (\varepsilon_{ij} + \omega_{ij}) A_j \tag{2.2.19}$$

ε_{ij} → is a symmetrical matrix, called pure deformation, strain matrix, also the strain tensor,
ω_{ij} → is an antisymmetric matrix.

Description of ε_{ij} and ω_{ij} (Using: $u_1 = u_x$ – x-component of displacement vector $\underline{u}$ and so on . . .):

$$\varepsilon_{11} = \varepsilon_{xx} = \frac{\partial u_1}{\partial x_1} = \frac{\partial u_x}{\partial x} : \varepsilon_{22} = \varepsilon_{yy} = \frac{\partial u_2}{\partial x_2} = \frac{\partial u_y}{\partial y} : \varepsilon_{33} = \varepsilon_{zz} = \frac{\partial u_3}{\partial x_3} = \frac{\partial u_z}{\partial z}$$

$$\varepsilon_{12} = \varepsilon_{xy} = \varepsilon_{21} = \varepsilon_{yx} = \frac{1}{2}\,\gamma_{xy} = \frac{1}{2}\gamma_{yx} = \frac{1}{2}\left(\frac{\partial u_1}{\partial x_2} + \frac{\partial u_2}{\partial x_1}\right) = \frac{1}{2}\left(\frac{\partial u_x}{\partial y} + \frac{\partial u_y}{\partial x}\right)$$

$$\varepsilon_{13} = \varepsilon_{xz} = \varepsilon_{31} = \varepsilon_{zx} = \frac{1}{2}\,\gamma_{xz} = \frac{1}{2}\gamma_{zx} = \frac{1}{2}\left(\frac{\partial u_1}{\partial x_3} + \frac{\partial u_3}{\partial x_1}\right) = \frac{1}{2}\left(\frac{\partial u_x}{\partial z} + \frac{\partial u_z}{\partial x}\right)$$

$$\varepsilon_{23} = \varepsilon_{yz} = \varepsilon_{32} = \varepsilon_{zy} = \frac{1}{2}\,\gamma_{yz} = \frac{1}{2}\gamma_{zy} = \frac{1}{2}\left(\frac{\partial u_2}{\partial x_3} + \frac{\partial u_3}{\partial x_2}\right) = \frac{1}{2}\left(\frac{\partial u_y}{\partial z} + \frac{\partial u_z}{\partial y}\right)$$

$$\omega_{11} = \omega_{xx} = \frac{1}{2}\left(\frac{\partial u_1}{\partial x_1} - \frac{\partial u_1}{\partial x_1}\right) = \frac{1}{2}\left(\frac{\partial u_x}{\partial x} - \frac{\partial u_x}{\partial x}\right) = 0, \tag{2.2.20}$$

similarly $\omega_{22} = \omega_{yy} = \omega_{33} = \omega_{zz} = 0$ and,

$$\omega_{12} = \omega_{xy} = \frac{1}{2}\left(\frac{\partial u_1}{\partial x_2} - \frac{\partial u_2}{\partial x_1}\right) = \frac{1}{2}\left(\frac{\partial u_x}{\partial y} - \frac{\partial u_y}{\partial x}\right);$$

$$\omega_{21} = \omega_{yx} = \frac{1}{2}\left(\frac{\partial u_2}{\partial x_1} - \frac{\partial u_1}{\partial x_2}\right) = \frac{1}{2}\left(\frac{\partial u_y}{\partial x} - \frac{\partial u_x}{\partial y}\right)$$

$$\omega_{31} = \omega_{zx} = \frac{1}{2}\left(\frac{\partial u_3}{\partial x_1} - \frac{\partial u_1}{\partial x_3}\right) = \frac{1}{2}\left(\frac{\partial u_z}{\partial x} - \frac{\partial u_x}{\partial z}\right); \tag{2.2.21}$$

$$\omega_{13} = \omega_{xz} = \frac{1}{2}\left(\frac{\partial u_1}{\partial x_3} - \frac{\partial u_3}{\partial x_1}\right) = \frac{1}{2}\left(\frac{\partial u_x}{\partial z} - \frac{\partial u_z}{\partial x}\right)$$

$$\omega_{23} = \omega_{yz} = \frac{1}{2}\left(\frac{\partial u_2}{\partial x_3} - \frac{\partial u_3}{\partial x_2}\right) = \frac{1}{2}\left(\frac{\partial u_y}{\partial z} - \frac{\partial u_z}{\partial y}\right);$$

$$\omega_{32} = \omega_{xx} = \frac{1}{2}\left(\frac{\partial u_3}{\partial x_2} - \frac{\partial u_2}{\partial x_3}\right) = \frac{1}{2}\left(\frac{\partial u_z}{\partial y} - \frac{\partial u_y}{\partial z}\right)$$

Consider an element of a body at point P undergoing infinitesimal deformation as shown in Figure 2.2.4.

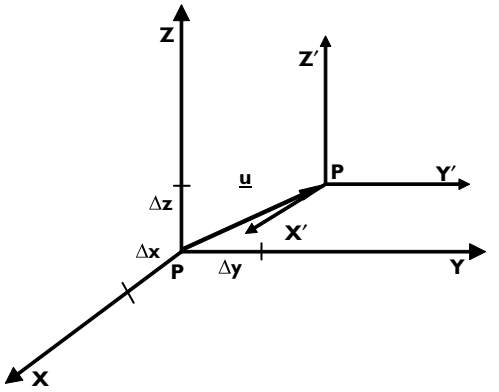


Figure 2.2.4 Translation.

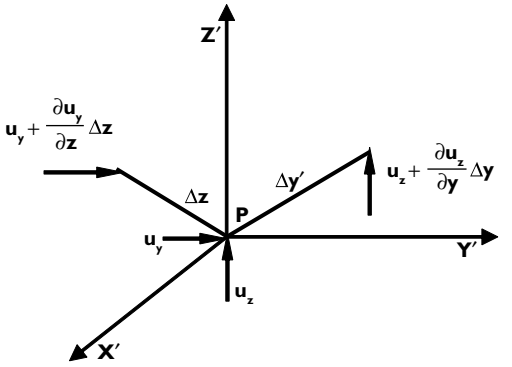


Figure 2.2.5 Translation as result of rotation in *y*-*z* plane.

As a result of deformation $P \to P'$: Translation of element is given by $\underline{u}(P)$. Now consider (X', Y', Z') frame in Figure 2.2.5.

Rotation about X or X' axis:

Due to change in $u_z = \dfrac{\partial u_z}{\partial y}$: due to change in $u_y = -\dfrac{\partial u_y}{\partial z}$.

$$\text{Total rotation about } x\text{-axis} = (\delta\phi)_x = \frac{\partial u_z}{\partial y} - \frac{\partial u_y}{\partial z} = \frac{\partial u_3}{\partial x_2} - \frac{\partial u_2}{\partial x_3} = 2\omega_{zy} = 2\omega_{32}. \tag{2.2.22}$$

$$\text{Similarly} \quad (\delta\phi)_y = \frac{\partial u_x}{\partial z} - \frac{\partial u_z}{\partial x} = \frac{\partial u_1}{\partial x_3} - \frac{\partial u_3}{\partial x_1} = 2\omega_{xz} = 2\omega_{13}. \tag{2.2.23}$$

$$(\delta\phi)_z = \frac{\partial u_x}{\partial y} - \frac{\partial u_y}{\partial x} = \frac{\partial u_1}{\partial x_2} - \frac{\partial u_2}{\partial x_1} = 2\omega_{xy} = 2\omega_{12.} \tag{2.2.24}$$

Now since u_x, u_y and u_z are analytic functions of (x, y, z), we can write

$$du_x = \frac{\partial u_x}{\partial x}dx + \frac{\partial u_x}{\partial y}dy + \frac{\partial u_x}{\partial z}dz : du_y = \frac{\partial u_y}{\partial x}dx + \frac{\partial u_y}{\partial y}dy + \frac{\partial u_y}{\partial z}dz;$$
$$du_z = \frac{\partial u_z}{\partial x}dx + \frac{\partial u_z}{\partial y}dy + \frac{\partial u_z}{\partial z}dz. \tag{2.2.25}$$

Specifying $\varepsilon_{xx} = \varepsilon_{yy} = \varepsilon_{zz} = \varepsilon_{xy} = \varepsilon_{yz} = \varepsilon_{zx} = 0$: that is no strain, from Equations (2.2.18) and (2.2.25)

$$du_x = \frac{\partial u_x}{\partial y}dy + \frac{\partial u_x}{\partial z}dz \tag{2.2.26}$$

Again, $\varepsilon_{xy} = 0 \rightarrow \frac{\partial u_x}{\partial y} = -\frac{\partial u_y}{\partial x}$: $\varepsilon_{zx} = 0 \rightarrow \frac{\partial u_x}{\partial z} = -\frac{\partial u_z}{\partial x}$

Hence $du_x = -\frac{\partial u_y}{\partial x}dy - \frac{\partial u_z}{\partial x}dz$ (2.2.27)

Adding Equations (2.2.26) and (2.2.27), we have

$$du_x = \frac{1}{2}\left(\frac{\partial u_x}{\partial z} - \frac{\partial u_z}{\partial x}\right)dz - \frac{1}{2}\left(\frac{\partial u_y}{\partial x} - \frac{\partial u_x}{\partial y}\right)dy \tag{2.2.28}$$

$\rightarrow du_x = \omega_{xz}dz - \omega_{xy}dy$

Similarly $du_y = \omega_{yx}dx - \omega_{yz}dz$ (2.2.29)

$du_z = \omega_{xy}dy - \omega_{zx}dx$

Thus ω_{ij} contributes to *rigid body rotation* to the deformation of a body undergoing infinitesimal deformation. ω_{ij} is also called the rotation matrix. From Equations (2.2.22), (2.2.23) and (2.2.24) one may write the rotation matrix as

$$\delta\underline{\phi} = \omega_{zy}\underline{i} + \omega_{xz}\underline{j} + +\omega_{yx}\underline{k} = \phi_x\underline{i} + \phi_y\underline{j} + \phi_z\underline{k} \tag{2.2.30}$$

➔ *Contribution of ω_{ij} to δA_i is the result of rigid body rotation.*

2.2.5 Derivative of a vector fixed in a moving reference

We know that if a body is rotating with an angular velocity ω and if a vector $\underline{V}$ is attached to the body at point P as shown in Figure 2.2.6.

Now $\omega d = |\underline{\omega}||\underline{r}| \sin\gamma =$ speed of P; and $\underline{V} = \frac{d\bar{r}}{dt} = \underline{\omega}\ X\ \underline{r}$

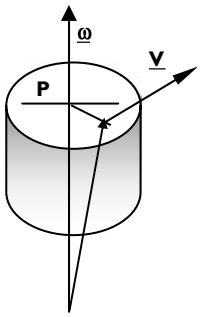


Figure 2.2.6a Real system.

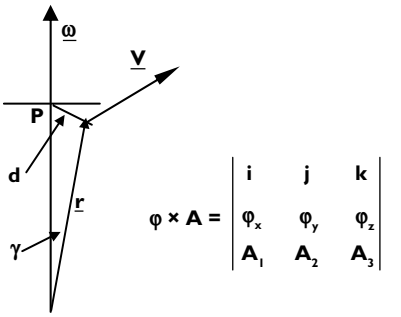


Figure 2.2.6b Ideal case.

Consider the following path s in (X, Y, Z) reference axes shown in Figure 2.2.7.

$$\frac{d\underline{r}}{dt} = \lim_{\Delta t \to 0} \frac{\Delta \underline{r}}{\Delta t} = \lim_{\Delta t \to 0} \frac{\Delta \underline{r}}{\Delta s} \frac{\Delta s}{\Delta t}$$

Now $\Delta \underline{r}$ approaches Δs as $\Delta t \to 0$

$$\rightarrow \frac{\Delta \underline{r}}{\Delta t} \to \varepsilon_t = \text{unit tangent vector to the trajectory.}$$

$$\text{Thus,} \quad \frac{d\underline{r}}{dt} = \frac{ds}{dt}\varepsilon_t. \tag{2.2.31}$$

Hence $d\underline{r}/dt$ leads to a vector having magnitude equal to the speed of the point and direction tangent to the trajectory.

If $\underline{r}(t) = x(t)\underline{i} + y(t)\underline{j} + z(t)\underline{k}$,

then $\frac{d\underline{r}}{dt} = \underline{V}(t) = \dot{x}(t)\underline{i} + \dot{y}(t)\underline{j} + \dot{z}(t)\underline{k}$ and $\frac{d^2\underline{r}}{dt^2} = \underline{a}(t) = \ddot{x}(t)\underline{i} + \ddot{y}(t)\underline{j} + \ddot{z}(t)\underline{k}$.

Again $\underline{V}(t) = \dfrac{ds}{dt}\varepsilon_t$

$$\therefore \frac{d\underline{V}}{dt} = \underline{a} = \frac{d^2s}{dt^2}\varepsilon_t + \frac{ds}{dt}\frac{d\varepsilon_t}{dt} = \frac{d^2s}{dt^2}\varepsilon_t + \frac{ds}{dt}\frac{d\varepsilon_t}{ds}\frac{ds}{dt} = \frac{d^2s}{dt^2}\varepsilon_t + \left(\frac{ds}{dt}\right)^2 \frac{d\varepsilon_t}{ds} \tag{2.2.32}$$

Again, $\frac{d\underline{\varepsilon}_t}{ds} = \lim_{\Delta s \to 0} \frac{\underline{\varepsilon}_t(s+\Delta s) - \underline{\varepsilon}_t(s)}{\Delta s}$ and this can be represented as shown in Figure 2.2.8

$$\therefore \frac{d\underline{\varepsilon}_t}{ds} = \lim_{\Delta s \to 0} \frac{\Delta \underline{\varepsilon}_t}{\Delta s} \text{ that is } \left|\Delta \underline{\varepsilon}_t\right| \approx |\varepsilon_t|\, \Delta\phi \; = \Delta\phi$$

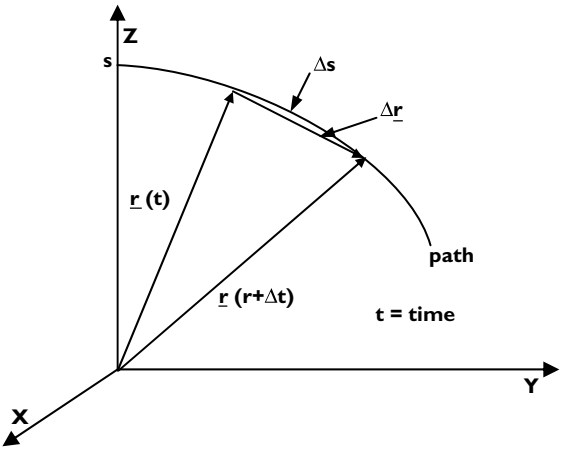


Figure 2.2.7 Derivative of a vector in moving references.

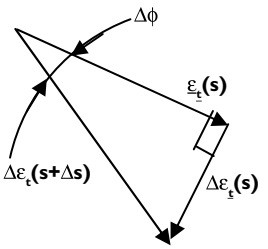


Figure 2.2.8

i.e. $|\Delta\varepsilon_t| \approx \dfrac{\Delta s}{R}$, as $\Delta\phi = \dfrac{\Delta s}{R}$, R = radius of curvature.

$$\rightarrow \quad \Delta\underline{\varepsilon}_t \approx \frac{\Delta s}{R}\underline{\varepsilon}_n, \quad \underline{\varepsilon}_n \text{ is unit normal vector to } \underline{\varepsilon}_t(s). \tag{2.2.33}$$

$$\text{Thus,} \quad \frac{d\underline{\varepsilon}_t}{ds} = \lim_{\Delta s\to 0}\left[\frac{(\Delta s/R)}{\Delta s}\underline{\varepsilon}_n\right] = \frac{\underline{\varepsilon}_n}{R}\underline{a} = \frac{d^2s}{dt^2}\underline{\varepsilon}_t + \frac{\left(ds/dt\right)^2}{R}\underline{\varepsilon}_n. \tag{2.2.34}$$

First term is tangent to the path and the second term is in the osculating plane (i.e. the plane formed by $\underline{\varepsilon}_t(s)$ and $\underline{\varepsilon}_t(s+\Delta s)$ in the limit as $\Delta s \to 0$) at right angles to the path and directly towards the centre of curvature.

Let we have two references X, Y, Z and x, y, z moving arbitrarily relative to one another. Let $XYZ \to xyz$ as shown in Figure 2.2.9.

Choosing 'O' as origin, translational velocity $\dot{R}$ equal to the velocity of the origin of xyz plus a rotational velocity $\underline{\omega}$ with an axis of rotation through 'O' fully describe the motion of xyz relative to XYZ.

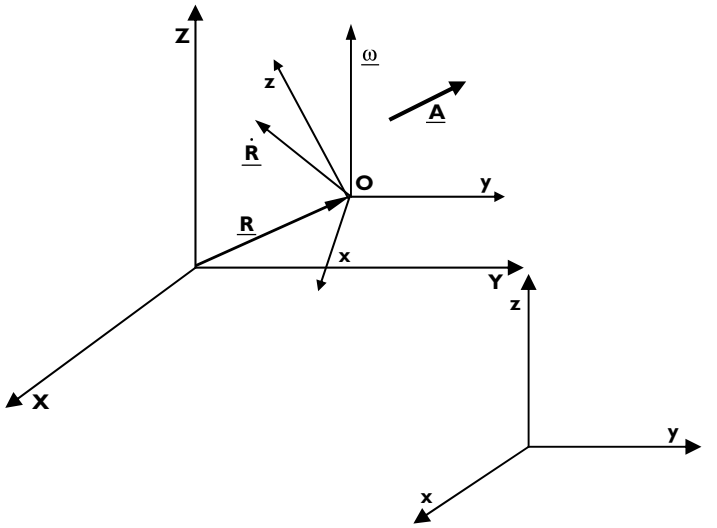


Figure 2.2.9

Let the vector $\underline{A}$ of fixed length and of fixed orientation as seen from xyz (i.e. $\underline{A}$ is fixed with respect to xyz). Thus, $(d\underline{A}/dt)_{xyz} = 0$. However, w.r.t. XYZ, $(d\underline{A}/dt)$ need not be zero.

To evaluate $\left(\frac{d\underline{A}}{dt}\right)_{XYZ}$ consider the following sequence [*Chasle's theorem*]:

1 The translation motion $\underline{R}$ for the whole system does not alter the direction of $\underline{A}$, as the magnitude of $\underline{A}$ is fixed there can be no change of $\underline{A}$ as a result of such motion.
2 A pure rotation contribution about an axis of rotation through 'O'. Ends of vector $\underline{A}$ forms circular arcs about the axis of rotation.

Let us resolve $\underline{A}$ into cylindrical components with the axis of rotation forming the axial direction $\underline{Z}$ (Figure 2.2.10).

Thus, $\underline{A} = A_{Z'}\,\underline{\varepsilon}_{Z'} + A_\phi\,\underline{\varepsilon}_\phi + A_r\underline{\varepsilon}_r$

As $\underline{A}$ rotates about Z' axis, $A_r = A_\phi = A_{Z'} = 0$. Also $\underline{\varepsilon}_{Z'} = 0$, as ends of the vector form circular arcs.

$$\rightarrow \left(\frac{d\underline{A}}{dt}\right)_{XYZ} = A_\phi\left(\frac{d\underline{\varepsilon}_\phi}{dt}\right)_{XYZ} + A_r\left(\frac{d\underline{\varepsilon}_r}{dt}\right)_{XYZ} = -A_\phi\,\omega\,\underline{\varepsilon}_r + A_r\,\omega\,\underline{\varepsilon}_\phi \quad (2.2.35)$$

$$\underline{\omega}\,X\,\underline{A} = \omega\,\underline{\varepsilon}_{Z'}\,X(A_{Z'}\underline{\varepsilon}_{Z'} + A_\phi\underline{\varepsilon}_\phi + A_r\underline{\varepsilon}_r) = -\omega\,A_\phi\underline{\varepsilon}_r + \omega\,A_r\underline{\varepsilon}_\phi$$

$$\rightarrow \left(\frac{d\underline{A}}{dt}\right)_{XYZ} = \underline{\omega} \times \underline{A}. \quad (2.2.36)$$

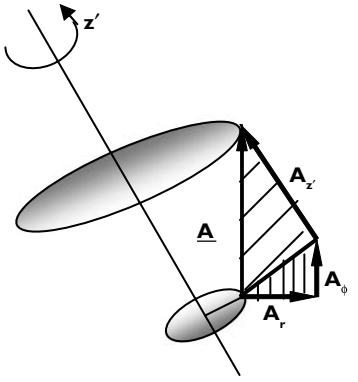


Figure 2.2.10

So $\dfrac{d\underline{A}}{dt} = \underline{\omega} \times \underline{A}$ that is $d\underline{A} = \underline{\omega}\, dt \times \underline{A}$ or $\delta\underline{A} = \delta\underline{\phi} \times \underline{A}$

i.e. $\delta A_i = (\delta\, \underline{\phi} \times \underline{A})_i = \delta\phi_y A_3 - \delta\phi_z A_2$ or $\delta A_1 = \omega_{13}A_3 - \omega_{21}A_2 = \omega_{11}A_1 + \omega_{12}A_2 + \omega_{13}A_3$, as $\omega_{11} = 0$ and $\omega_{12} = -\omega_{21}$, Equation (2.2.30) reduces to

$$\rightarrow \quad \delta A_i = \omega_{ij} A_j \tag{2.2.37}$$

So, ω_{ij} gives rigid body rotation contribution to the deformation of an element of the body undergoing infinitesimal deformation.

Example 2.2.2

A body has deformed under a displacement field $\underline{u}$ with its rectangular components

$$u_1 = u_x = 0.004x_1 + 0.001x_2 + 0.005x_3$$
$$u_2 = u_y = -0.005x_1 + 0.0003x_2$$
$$u_3 = u_z = 0.0001x_1 + 0.005x_2 - 0.006x_3$$

Compute strain and rotation components.

Solution:

$$\frac{\partial u_i}{\partial x_j} = \begin{bmatrix} .004 & .001 & .005 \\ -.005 & .0003 & 0 \\ .0001 & .005 & -.006 \end{bmatrix}$$

Strain components: $\varepsilon_{ij} = \frac{1}{2}\left[\frac{\partial u_i}{\partial x_j} + \frac{\partial u_j}{\partial x_i}\right]$

$\varepsilon_{11} = 0.004 : \varepsilon_{22} = 0.0003 : \varepsilon_{33} = -0.006 : \varepsilon_{12} = -0.002 : \varepsilon_{21} = -0.002 : \varepsilon_{23} = 0.0025 : \varepsilon_{32} = 0.0025 : \varepsilon_{31} = 0.00255 : \varepsilon_{13} = 0.00245.$

Rotation components: $\omega_{ij} = \frac{1}{2}\left[\frac{\partial u_i}{\partial x_j} - \frac{\partial u_j}{\partial x_i}\right]$

$\omega_{11} = \omega_{22} = \omega_{33} = 0$

$\omega_{12} = 0.003 : \omega_{21} = -0.003 : \omega_{13} = 0.00245 : \omega_{31} = -0.00245 : \omega_{23} = -0.0025 : \omega_{32} = 0.0025.$

Now, $(\delta\phi)_1 = \omega_{32} = 0.0025$ radian: $(\delta\phi)_2 = \omega_{13} = 0.00245$ radians: $(\delta\phi)_3 = \omega_{21} = -0.003$ radians.

The deformation here is *affine deformation* [$u_i = \lambda_{ij}x_j$; λ_{ij} = matrix of components].

The strain and rotation matrices are composed of constants. This means that each small element – of the body has same rotation and pure deformation as every other element – this is called homogeneous deformation.

Example 2.2.3

Show that $(\partial u_i/\partial x_j)$ can be uniquely decomposed into ε_{ij} and ω_{ij} [Equation (2.2.18)].

Solution:

Let $\frac{\partial u_i}{\partial x_j} = n_{ij} + p_{ij}$ (a)

and also $\frac{\partial u_i}{\partial x_j} = \varepsilon_{ij} + \omega_{ij}$ (b)

Subtract (b) from (a)

$(\varepsilon_{ij} - n_{ij}) + (\omega_{ij} - p_{ij}) = 0$ (c)

As $n_{ij} = n_{ji}$, symmetric and $p_{ij} = -p_{ji}$, skew-symmetric.
Transposing Equation (c) $(\varepsilon_{ji} - n_{ji}) + (\omega_{ji} - p_{ji}) = 0$ (d)
Adding (c) and (d)

$$n_{ij} + \varepsilon_{ji} - n_{ji} + \omega_{ij} - p_{ij} + \omega_{ji} - p_{ji} = 0 \quad \rightarrow \quad 2(\varepsilon_{ij} - n_{ij}) = 0 \quad \rightarrow \quad \varepsilon_{ij} = n_{ij}.$$

Similarly subtracting (c) from (d), it can be shown that $\omega_{ij} = p_{ij}$.

Example 2.2.4

A body has deformed so as to have the following deformation field:

$$u_1 = (3x_1^2 x_2 + 6)10^{-2}; \quad u_2 = (x_2^2 + 6x_1 x_3)10^{-2};$$
$$u_3 = (6x_3^2 + 2x_2 x_3 + 15)10^{-2}$$

What is the rotation of an element at position (1, 0, 2)?

Solution:

$$\frac{\partial u_i}{\partial x_j} = \begin{bmatrix} 6x_1x_2 & 3x_1^2 & 0 \\ 6x_3 & 2x_2 & 6x_1 \\ 0 & 2x_3 & 12x_3 + 2x_2 \end{bmatrix} \times 10^{-2} :$$

$$\left(\frac{\partial u_i}{\partial x_j}\right)_{(1,0,2)} = \begin{bmatrix} 0 & 3 & 0 \\ 12 & 0 & 6 \\ 0 & 4 & 24 \end{bmatrix} \times 10^{-2}$$

Hence, $\omega_{23} = 0.01 = -\delta\phi_1 : \omega_{13} = 0.0 = \delta\phi_2 : \omega_{21} = 0.045 = \delta\phi_3;$
$\therefore \ \delta\underline{\phi} = -0.01\underline{i} + 0.045\underline{k}.$

2.2.6 Physical interpretation of strain tensor

2.2.6.1 *Normal strains*

Consider a line segment Δx along x-axis, connecting P and Q. In the deformed state P goes to P' and Q to Q'. This is presented in Figure 2.2.11

Let the projection of $P'Q'$ in x-direction be $(P'\ Q')_x$ and it is computed in terms of Δx and displacement in x-direction of points P and Q.

$$(P'Q')_x = \Delta x + (u_x)_Q - (u_x)_P \tag{2.2.38}$$

Now, express $(u_x)_Q$ in Taylor's series around point P:

$$\left(P'Q'\right)_x = \Delta x + \left[(u_x)_P + \left(\frac{\partial u_x}{\partial x}\right)_P \Delta x + \cdots\right] - (u_x)_P \tag{2.2.39}$$

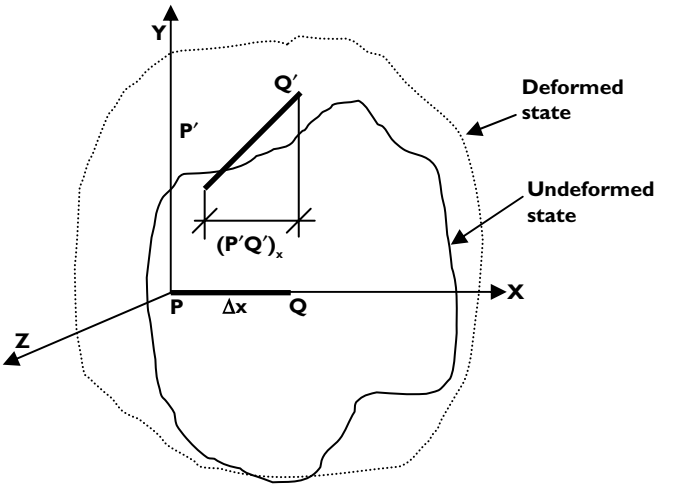


Figure 2.2.11 Normal strains.

or $\dfrac{(P'Q')_x - \Delta x}{\Delta x} = \left(\dfrac{\partial u_x}{\partial x}\right)_P + \cdots$ higher order terms containing Δx.

$$\text{Now,} \quad \lim_{\Delta x \to 0} \frac{(P'Q')_x - \Delta x}{\Delta x} = \left(\frac{\partial u_x}{\partial x}\right)_P \tag{2.2.40}$$

➔ This is the strain ε_{xx} or ε_{11} at point P.

We can use $(P'Q')_x = P'Q'$ for small deformations. Similar interpretations can be made for ε_{yy} and ε_{zz} (or ε_{22} and ε_{33}).

Thus ε_{pp} can be also be interpreted as merely the change in length of a segment originally in the pth coordinate direction per unit original length.

2.2.6.2 Shear strains

Consider line segments QP, PR along x and y-axis respectively as shown in Figure 2.2.12. In the deformed state these lines assume the form $Q'P'$ and $P'R'$.

We are interested in the projections $(P'Q')$ and $(P'R')$ on to x-plane as shown in Figure 2.2.13.

Hence, $\alpha =$ angle between the projection of $P'R'$ and y-direction; $u_x =$ displacement of P in x-direction.

Displacement of R in x-direction $= \left[u_x + \left(\frac{\partial u_x}{\partial y}\right)\Delta y + \cdots\right]$ ($\Delta x = \Delta z = 0$, for this expression).

Component of projected length of $P'R'$ in y-direction $= (P'R')_y = \Delta y + \left[\delta(\Delta y\underline{j})\right]_y$

[Refer to $\delta A_i = \frac{\partial u_i}{\partial x_j} A_j : A_i' = A_i + \delta A_i$ given earlier in Equation (2.2.9)].

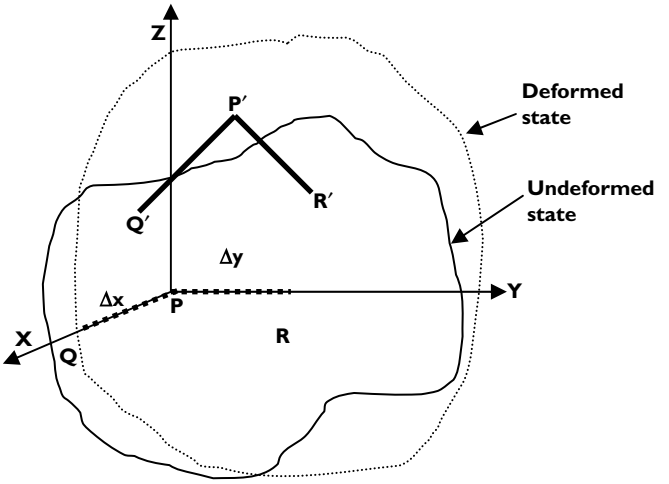


Figure 2.2.12 Shear strains.

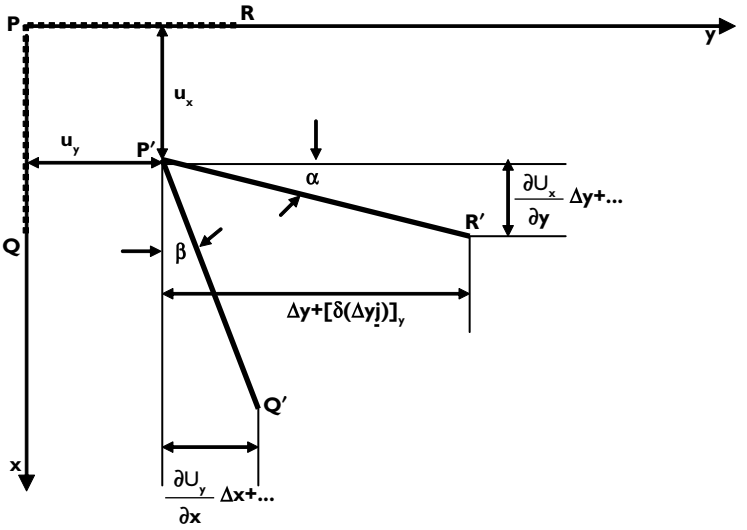


Figure 2.2.13 Projection of strains.

$$\therefore \tan\alpha = \frac{\frac{\partial u_x}{\partial y}\Delta y + \cdots\cdots\cdots}{\Delta y + [\delta\,(\Delta y\underline{j})]_y}$$

As $\Delta y \to 0$, higher order terms vanish, hence $\tan\alpha = \dfrac{\partial u_x}{\partial y}$.

When α is small $\alpha = \dfrac{\partial u_x}{\partial y}$

$$\text{Similarly,} \quad \beta = \frac{\partial u_y}{\partial x} \tag{2.2.41}$$

Sum of the angles $\alpha + \beta$ is the decrease in rightangle of the pair of infinitesimal line segments at P, when we project the deformed geometry onto the plane formed by the line segments in the undeformed geometry. For small deformation requirement, the change of right angle between the infinitesimal segment in the deformed geometry can be used in the place of the angle found by projecting the deformed geometry back onto the x-y plane.

$$\text{Thus} \quad \alpha + \beta = \frac{\partial u_x}{\partial y} + \frac{\partial u_y}{\partial x} = 2\varepsilon_{xy} \tag{2.2.42}$$

The strains shown in Equation (2.2.42) are called shear strains.

Similarly we can have y-z and z-x plane considerations to have

$$\frac{\partial u_y}{\partial z} + \frac{\partial u_z}{\partial y} = 2\varepsilon_{yz} \tag{2.2.43}$$

$$\text{and} \quad \frac{\partial u_x}{\partial z} + \frac{\partial u_z}{\partial x} = 2\varepsilon_{zx} \tag{2.2.44}$$

Sometimes, one uses γ_{ij} to represent the total decrease of the right angles between dx_i and dx_j i.e.

$$\gamma_{ij} = 2\ \varepsilon_{ij}. \tag{2.2.45}$$

2.2.7 Cubical dilatation

2.2.7.1 *Under normal strains alone*

Let us consider an infinitesimal three-dimensional rectangular parallelepiped shown in Figure 2.2.14, wherein only normal strains are non-zero.

We conclude that the rectangular parallelepiped remains rectangular during and after deformation. It should be pointed out that the element may also have rigid body rotation; as a result, the sides of the rectangular parallelepiped may not be parallel to the reference (undeformed state) coordinate axes after deformation.

Hence,

$$dx'_1 = dx_1 + \varepsilon_{11}dx_1 = (1 + \varepsilon_{11})dx_1,$$

$$\text{similarly} \quad dx'_2 = (1 + \varepsilon_{22})dx_2, \quad \text{and} \quad dx'_3 = (1 + \varepsilon_{33})\ dx_3 \tag{2.2.46}$$

Now $dx'_1dx'_2dx'_3 - dx_1dx_2dx_3 = dx_1dx_2dx_3(1 + \varepsilon_{11})(1 + \varepsilon_{22})(1 + \varepsilon_{33}) - dx_1dx_2\ dx_3 = [1 + \varepsilon_{11} + \varepsilon_{22} + \varepsilon_{33} +$ higher order strain products $-1]\ dx_1dx_2dx_3$

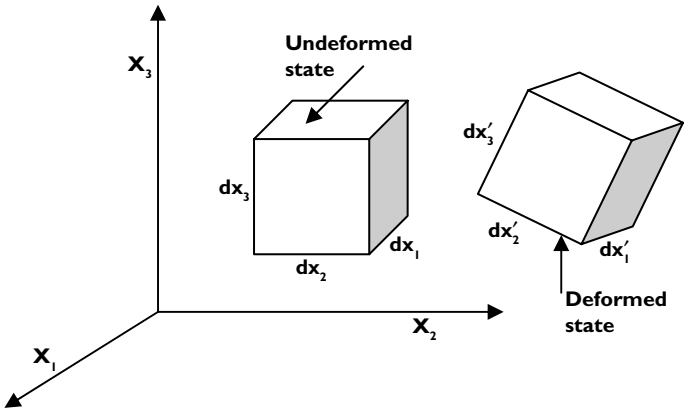


Figure 2.2.14 Cubical dilatation.

Ignoring products, we have

$$\frac{dx'_1 + dx'_2 + dx'_3 - dx_1 dx_2 dx_3}{dx_1 dx_2 dx_3} = \varepsilon_{11} + \varepsilon_{22} + \varepsilon_{33}$$

$$\frac{\text{Change in volume}}{\text{Original volume}} = \varepsilon_{11} + \varepsilon_{22} + \varepsilon_{33} = \text{Cubical dilatation.} \tag{2.2.47}$$

2.2.7.2 *Deformation under pure shear*

Consider an infinitesimal element subjected to pure shear strains. A rectangular parallelepiped in undeformed state will undergo a deformation where the sides remain the same (i.e. of same length) for the first order consideration and the original orthogonality between the sides is possibly destroyed. The sides may change from rectangles to a parallelepiped as shown in Figure 2.2.15.

$$\text{Change in volume} = L_1 L_2 L_3 - \underline{L'}_1 \cdot (\underline{L'}_2 \times \underline{L'}_3) \tag{2.2.48}$$

$$\text{We know,} \quad \underline{L'}_1 \,.\, (\underline{L'}_2 \times \underline{L'}_3) = L'_1\, L'_2\, L'_3 \cos[\underline{L'}_1, \underline{L'}_2 \times \underline{L'}_3] \sin(\underline{L'}_2,\ \underline{L'}_3)$$
$$= \text{scalar tripple product.}$$

Angle between $\underline{L'}_2$ and $\underline{L'}_3 = \pi/2 - 2\,\varepsilon_{23}$.

Since, the deformation is small, angle between L'_1 and $L'_2 \times L'_3$, will be of the same order of magnitude as ε_{23} and let, $2\varepsilon_{23} \sim 2\varepsilon_{12} \sim 2\varepsilon$.

$$\underline{L'}_1 \cdot (\underline{L'}_2 \times \underline{L'}_3) = L'_1\, L'_2\, L'_3 \cos\, 2\varepsilon \sin(\pi/2 - 2\varepsilon) = L'_1\, L'_2\, L'_3\, \cos\, 2\varepsilon\, \cos\, 2\varepsilon$$
$$= L'_1\, L'_2\, L'_3 \left(1 - \frac{4\varepsilon^2}{2!} + \cdots\right)\left(1 - \frac{4\varepsilon^2}{2!} + \cdots\right)$$
$$= L'_1\, L'_2\, L'_3, \text{ neglecting higher order terms.} \tag{2.2.49}$$

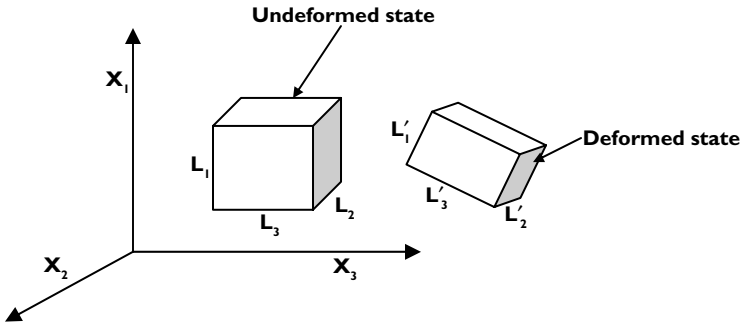


Figure 2.2.15 Straining under pure shear.

Hence for small deformation, change in volume = 0.

Thus, normal strains cause dilatation without changing mutual orthogonality of the sides while shear strains destroy orthogonality of the edges but do not affect the volume. So in a strain tensor (second order)

1 Diagonal terms → normal strains,
2 Off-diagonal terms → shear strains,
3 Trace of the matrix → cubical dilatation.

2.2.8 Transformation of strains

We shall show that the geometrical interpretations of strain terms form a second order tensor field.

2.2.8.1 Normal strains

Consider normal strains at a point P in Figure 2.2.16 in the direction, $\underline{n}$.

Displacement of point P in the $\underline{n}$ direction

$$(u_n)_P = (u_x)_P a_{nx} + (u_y)_P a_{ny} + (u_z)_P a_{nz} = (u_j)_P a_{nj} \tag{2.2.50}$$

Displacement of point Q in the $\underline{n}$ direction by Taylor series

$$(u_n)_Q = (u_n)_P + \left(\frac{\partial u_n}{\partial x_i}\right)_P \Delta x_i + \left(\frac{\partial^2 u_n}{\partial x_i \partial x_k}\right)_P \frac{\Delta x_i \Delta x_k}{2!} + \cdots$$

$$(u_n)_Q - (u_n)_P = \left(\frac{\partial u_n}{\partial x_i}\right)_P \Delta x_i + \left(\frac{\partial^2 u_n}{\partial x_i \partial x_k}\right)_P \frac{\Delta x_i \Delta x_k}{2!} + \cdots$$

Neglecting higher order terms and setting $\Delta n \to 0$

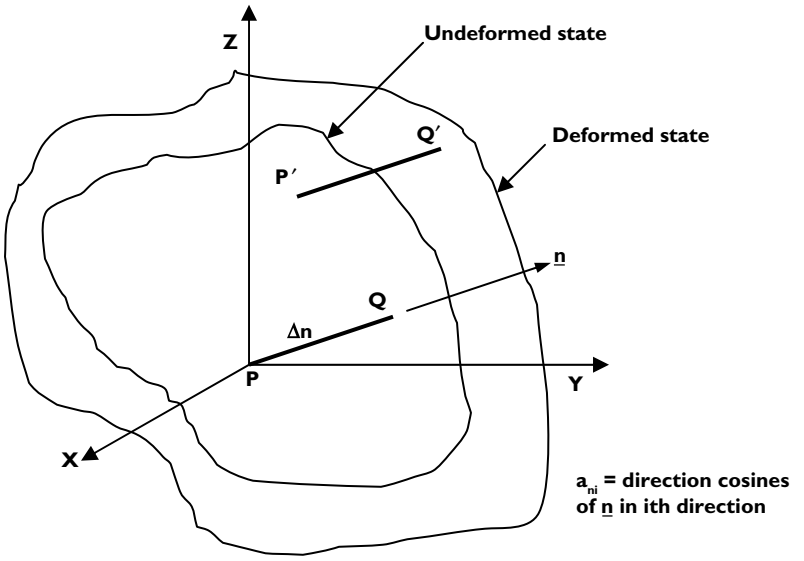


Figure 2.2.16 Transformation of normal strains.

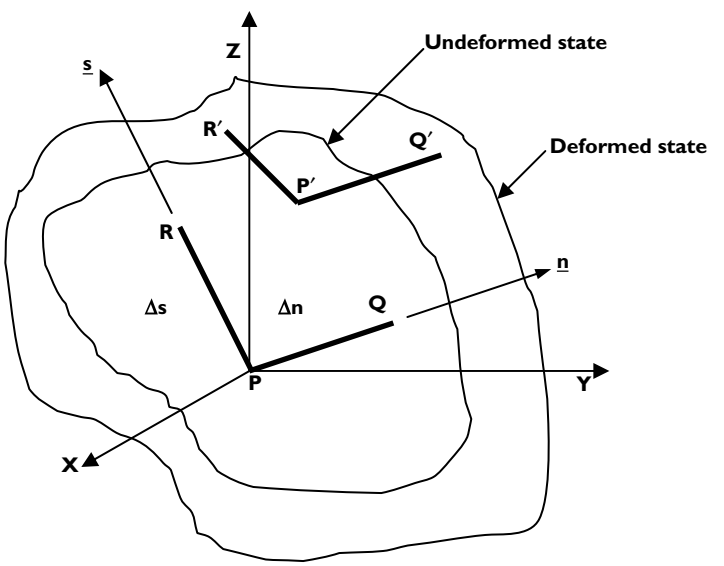


Figure 2.2.17 Transformation of shear strains.

$$\lim_{\Delta n \to 0} \frac{(u_n)_Q - (u_n)_P}{\Delta n} = \lim_{\Delta n \to 0} \left(\frac{\partial u_j}{\partial x_i} \right)_P \frac{\Delta x_i}{\Delta n} a_{nj}; \quad \text{As we have, } \frac{\Delta x_i}{\Delta n} = a_{ni}$$

$$\rightarrow \quad \varepsilon_{nn} = \frac{\partial u_j}{\partial x_i} a_{ni} a_{nj}, \text{ for any point } P. \tag{2.2.51}$$

Hence, we have

$$\varepsilon_{nn} = \frac{\partial u_1}{\partial x_1}a_{n1}^2 + \frac{\partial u_2}{\partial x_2}a_{n2}^2 + \frac{\partial u_3}{\partial x_3}a_{n3}^2 + \left(\frac{\partial u_1}{\partial x_2} + \frac{\partial u_2}{\partial x_1}\right)a_{n1}a_{n2} + \left(\frac{\partial u_1}{\partial x_3} + \frac{\partial u_3}{\partial x_1}\right)a_{n1}a_{n3} + \left(\frac{\partial u_2}{\partial x_3} + \frac{\partial u_3}{\partial x_2}\right)a_{n2}a_{n3}$$

or $\varepsilon_{nn} = \varepsilon_{xx}a_{nx}^2 + \varepsilon_{yy}a_{ny}^2 + \varepsilon_{zz}a_{nz}^2 + 2\left(\varepsilon_{xy}a_{nx}a_{ny} + \varepsilon_{yz}a_{ny}a_{nz} + \varepsilon_{zx}a_{nz}a_{nx}\right)$

That is $\rightarrow \varepsilon_{nn} = a_{ni}a_{nj}\varepsilon_{ij}$ (2.2.52)

2.2.8.2 *Shear strains*

Now consider shear strain terms

Shear strain: $\varepsilon_{ns} = \frac{1}{2}\left(\frac{\partial u_n}{\partial s} + \frac{\partial u_s}{\partial n}\right)$

We can express u_n and u_s in terms of displacements along the coordinate directions, n and s (Figure 2.2.17) i.e.

$$u_n = u_i a_{ni} : u_s = u_i a_{si}$$

Again $\varepsilon_{ns} = \frac{1}{2}\left(\frac{\partial u_i}{\partial s}a_{ni} + \frac{\partial u_i}{\partial n}a_{si}\right)$ (2.2.53)

And we may write: $\frac{\partial u_i}{\partial s} = \frac{\partial u_i}{\partial x_j}\frac{\partial x_j}{\partial s} = \frac{\partial u_i}{\partial x_j}a_{sj} : \frac{\partial u_i}{\partial n} = \frac{\partial u_i}{\partial x_k}\frac{\partial x_k}{\partial n} = \frac{\partial u_i}{\partial x_k}a_{nk}.$

$\rightarrow \varepsilon_{ns} = \frac{1}{2}\left[\frac{\partial u_i}{\partial x_j}a_{sj}a_{ni} + \frac{\partial u_i}{\partial x_k}a_{nk}a_{si}\right]$ (2.2.54)

In the second expression of the right hand side of Equation (2.2.55), i and k are dummy and can be replaced by j and i respectively

$\rightarrow \varepsilon_{ns} = a_{ni}a_{sj}\left(\frac{\partial u_i}{\partial x_j} + \frac{\partial u_j}{\partial x_i}\right) = a_{ni}a_{sj}\varepsilon_{ij}$ (2.2.55)

Equation (2.2.55) indicates that the strain at a point is a second order tensor. Physically this transformation may be interpreted as follows:

Suppose that all the six components of strain are known for the fixed coordinate axes x, y and z, we want to define six components of strain for the new orthogonal axes x', y' and z'.

With the help of a table of direction cosines

	x	y	z
x'	ℓ_1	m_1	n_1
y'	ℓ_2	m_2	n_2
z'	ℓ_3	m_3	n_3

From Equation (2.2.55), we may write

$$\begin{aligned}
\varepsilon_{x'} &= \ell_1^2\varepsilon_x + m_1^2\varepsilon_y + n_1^2\varepsilon_z + 2\ell_1 m_1\varepsilon_{xy} + 2m_1 n_1\varepsilon_{yz} + 2n_1\ell_1\varepsilon_{xz} \\
\varepsilon_{yx} &= \ell_2^2\varepsilon_x + m_2^2\varepsilon_y + n_2^2\varepsilon_z + 2\ell_2 m_2\varepsilon_{xy} + 2m_2 n_2\varepsilon_{yz} + 2n_2\ell_2\varepsilon_{xz} \\
\varepsilon_z &= \ell_3^2\varepsilon_x + m_3^2\varepsilon_y + n_3^2\varepsilon_z + 2\ell_3 m_3\varepsilon_{xy} + 2m_3 n_3\varepsilon_{yz} + 2n_3\ell_3\varepsilon_{xz} \\
2\varepsilon_{x'y'} &= 2\ell_1\ell_2\varepsilon_x + 2m_1 m_2\varepsilon_y + 2n_1 n_2\varepsilon_z + 2(\ell_1 m_2 + m_1\ell_2)\varepsilon_{xy} \\
&\quad + 2(m_1 n_2 + n_1 m_2)\varepsilon_{yz} + (n_1\ell_2 + \ell_1 n_2)\varepsilon_{xz} \qquad (2.2.56) \\
2\varepsilon_{y'z'} &= 2\ell_2\ell_3\varepsilon_x + 2m_2 m_3\varepsilon_y + 2n_2 n_3\varepsilon_z + 2(\ell_2 m_3 + m_2\ell_3)\varepsilon_{xy} \\
&\quad + 2(m_2 n_3 + n_2 m_3)\varepsilon_{yz} + (n_2\ell_3 + \ell_2 n_3)\varepsilon_{xz} \\
2\varepsilon_{z'x'} &= 2\ell_3\ell_1\varepsilon_x + 2m_3 m_1\varepsilon_y + 2n_3 n_1\varepsilon_z + 2(\ell_3 m_1 + m_3\ell_1)\varepsilon_{xy} \\
&\quad + 2(m_3 n_1 + n_3 m_1)\varepsilon_{yz} + (n_3\ell_1 + \ell_3 n_1)\varepsilon_{xz}
\end{aligned}$$

Thus it may be concluded that the strain components are the components of a symmetric tensor of order two.

Now we may introduce a strain surface, defined as:

Specify a constant k and lay off along each direction a quantity equal to the product of this constant and the quantity equal to the product of this constant and the inverse square root of the elongation in this direction.

$$r = \frac{k}{\sqrt{\varepsilon_r}} \qquad (2.2.57)$$

The coordinates of the end point of this segment with respect to the origin are given by $x = r\ell$; $y = rm$ and $z = r\,n$.

Now, we may get from Equation (2.2.56),

$$f(x, y, z) = \varepsilon_x x^2 + \varepsilon_y y^2 + \varepsilon_z z^2 + 2\varepsilon_{xy}xy + 2\varepsilon_{yz}yz + 2\varepsilon_{xz}xz = \pm k^2 \qquad (2.2.58)$$

The end points in Equation (2.2.58) lie on a second degree surface; the sign on the right hand side is chosen such that the surface is real. The strain surface will be ellipsoid if all the elements are stretched or compressed. In the other case, when the elements are compressed along some directions and stretched along some other direction, the surface is a hyperboloid of one or two sheets. The asymptotic cone, the boundary surface, corresponds to the directions along which the elongation is equal to zero. From the theory of quadratic form [Equation (2.2.58)], it follows

that it is always possible to choose such a system of coordinates that the quadratic form can be reduced to the basic form, i.e. the stress tensor is diagonal. Thus one can have

$$\varepsilon_x x^2 + \varepsilon_y y^2 + \varepsilon_z z^2 = \pm k^2 \tag{2.2.59}$$

The axes for which the basic form is attained called the principal axes of the strain tensor, and the shear strain along these axes vanish. Such surface is a second degree curve and the principal stresses have extremal values.

The directions of the principal axes may be obtained by using Lagrangian multiplier and extremal value of the quadratic form (Parton and Perlin 1984).

$$S(\ell, m, n) = \ell^2\varepsilon_x + m^2\varepsilon_y + n^2\varepsilon_z + 2\ell m\varepsilon_{xy} + 2mn\varepsilon_{yz} + 2m\ell\varepsilon_{zx} - \lambda(\ell^2 + m^2 + n^2) \tag{2.2.60}$$

Now,

$$\begin{aligned} &\frac{\partial S}{\partial \ell} = (\varepsilon_x - \lambda)\ell + \varepsilon_{xy}m + \varepsilon_{xz}n = 0; \quad \frac{\partial S}{\partial m} = (\varepsilon_y - \lambda)m + \varepsilon_{xy}\ell + \varepsilon_{yz}n = 0; \\ &\frac{\partial S}{\partial n} = (\varepsilon_z - \lambda)n + \varepsilon_{yz}m + \varepsilon_{xz}\ell = 0 \end{aligned} \tag{2.2.61}$$

System of the above homogeneous equations have solution only if

$$\begin{vmatrix} (\varepsilon_x - \lambda) & \varepsilon_{xy} & \varepsilon_{xz} \\ \varepsilon_{xy} & (\varepsilon_y - \lambda) & \varepsilon_{yz} \\ \varepsilon_{xz} & \varepsilon_{yz} & (\varepsilon_z - \lambda) \end{vmatrix} = 0, \text{ and this leads to } \lambda^3 - J_1\lambda^2 + J_2\lambda - J_3 = 0 \tag{2.2.62}$$

J_1, J_2 and J_3 are the strain invariants given by

$$\begin{aligned} J_1 &= \varepsilon_x + \varepsilon_y + \varepsilon_z \\ J_2 &= \begin{vmatrix} \varepsilon_x & \varepsilon_{xz} \\ \varepsilon_{xz} & \varepsilon_z \end{vmatrix} + \begin{vmatrix} \varepsilon_x & \varepsilon_{xy} \\ \varepsilon_{xy} & \varepsilon_y \end{vmatrix} + \begin{vmatrix} \varepsilon_y & \varepsilon_{yz} \\ \varepsilon_{yz} & \varepsilon_z \end{vmatrix} \\ &= \varepsilon_x\varepsilon_y + \varepsilon_y\varepsilon_z + \varepsilon_z\varepsilon_x - \varepsilon_{xy}^2 - \varepsilon_{yz}^2 - \varepsilon_{zx}^2 \\ J_3 &= \begin{vmatrix} \varepsilon_x & \varepsilon_{xy} & \varepsilon_{xz} \\ \varepsilon_{xy} & \varepsilon_y & \varepsilon_{yz} \\ \varepsilon_{xz} & \varepsilon_{uyz} & \varepsilon_z \end{vmatrix} = \varepsilon_x\varepsilon_y\varepsilon_z - \varepsilon_x\varepsilon_{yz}^2 - \varepsilon_y\varepsilon_{zx}^2 - \varepsilon_z\varepsilon_{xy}^2 + 2\varepsilon_{xy}\varepsilon_{yz}\varepsilon_{zx}. \end{aligned} \tag{2.2.63}$$

Roots of Equation (2.1.61) are the principal strains and substituting these strains ($\lambda_i,\ i = 1, 2, 3$) in Equation (2.2.62) along with the condition, $\ell_i^2 + m_i^2 + n_i^2 = 1$, one can obtain the direction cosines ℓ_i, m_i and n_i for particular value of λ_i.

It can be shown that the extremal shearing strain act on the surface elements passing through one of the principal axes and bisecting the angle between the remaining two. The magnitude of these shearing strains are equal to the difference between the values of the corresponding principal strains. In the direction normal to these planes the elongation is equal to half the sum of the principal strains.

2.2.9 Equations of compatibility

Consider the strain-displacement relationship:

$$\varepsilon_{ij} = \frac{1}{2}\left(\frac{\partial u_i}{\partial x_j} + \frac{\partial u_j}{\partial x_i}\right) \tag{2.2.64}$$

If a displacement field is specified, ε_{ij}'s can be found out. The reverse problem, i.e. if strain is specified, it is not so simple to find out the corresponding displacement field. This is more so since, we have here three functions of displacement field and u_i have to be obtained from six partial differential equations, Equation (2.2.64).

In order to ensure a single-valued, continuous solution for u_i, we must impose certain restrictions on the strain functions ε_{ij}. We know that the displacement field is single-valued and continuous, thus the restriction on ε_{ij} stem from these considerations lead to the compatibility equations.

2.2.9.1 Necessary condition of compatibility

We have the following differential equations:

$$\varepsilon_{xx} = \frac{\partial u_x}{\partial x}; \quad \varepsilon_{yy} = \frac{\partial u_y}{\partial y}; \quad \varepsilon_{zz} = \frac{\partial u_z}{\partial z}; \quad \gamma_{xy} = \left(\frac{\partial u_y}{\partial x} + \frac{\partial u_x}{\partial y}\right)$$

$$\gamma_{yz} = \left(\frac{\partial u_z}{\partial y} + \frac{\partial u_y}{\partial z}\right); \quad \gamma_{zx} = \left(\frac{\partial u_x}{\partial z} + \frac{\partial u_z}{\partial x}\right)$$

Differentiate ε_{xx} w.r.t. y twice and ε_{yy} w.r.t. x twice and add them

$$\frac{\partial^2 \varepsilon_{xx}}{\partial y^2} + \frac{\partial^2 \varepsilon_{yy}}{\partial x^2} = \frac{\partial^2}{\partial x \partial y}\left(\frac{\partial u_x}{\partial y} + \frac{\partial u_y}{\partial x}\right) = \frac{\partial^2 \gamma_{xy}}{\partial x \partial y} \tag{2.2.65}$$

Since all derivatives are continuous, one can interchange the order of partial differentiation.

Similarly one can have

$$\frac{\partial^2 \varepsilon_{yy}}{\partial z^2} + \frac{\partial^2 \varepsilon_{zz}}{\partial y^2} = \frac{\partial^2 \gamma_{yz}}{\partial y \partial z} \tag{2.2.66}$$

$$\frac{\partial^2 \varepsilon_{zz}}{\partial x^2} + \frac{\partial^2 \varepsilon_{xx}}{\partial x^2} = \frac{\partial^2 \gamma_{zx}}{\partial x \partial z} \tag{2.2.67}$$

Now differentiate ε_{xx} w.r.t. z and y: $$\frac{\partial^2 \varepsilon_{xx}}{\partial y \partial z} = \frac{\partial^3 u_x}{\partial y \partial z \partial x} \tag{2.2.67a}$$

Differentiate γ_{xy} w.r.t. x and z: $$\frac{\partial^2 \gamma_{xy}}{\partial x \partial z} = \frac{\partial^3 u_y}{\partial x^2 \partial z} + \frac{\partial^3 u_x}{\partial x \partial y \partial z} \tag{2.2.67b}$$

Differentiate γ_{yz} w.r.t. x twice: $$\frac{\partial^2 \gamma_{yz}}{\partial x^2} = \frac{\partial^3 u_z}{\partial x^2 \partial y} + \frac{\partial^3 u_y}{\partial x^2 \partial z} \tag{2.2.67c}$$

Differentiate γ_{zx} w.r.t. y and x: $$\frac{\partial^2 \gamma_{zx}}{\partial x \partial y} = \frac{\partial^3 u_x}{\partial x \partial y \partial z} + \frac{\partial^3 u_z}{\partial x^2 \partial y} \tag{2.2.67d}$$

Now (2.2.67b) + (2.2.67d) − (2.2.67c) can be expressed as

$$-\frac{\partial^2 \gamma_{yz}}{\partial x^2} + \frac{\partial^2 \gamma_{xy}}{\partial x \partial z} + \frac{\partial^2 \gamma_{zx}}{\partial x \partial y} = -\frac{\partial^3 u_z}{\partial x^2 \partial y} - \frac{\partial^3 u_y}{\partial x^2 \partial z} + \frac{\partial^3 u_y}{\partial x^2 \partial z} + \frac{\partial^3 u_x}{\partial x \partial y \partial z}$$

$$+ \frac{\partial^3 u_x}{\partial x \partial y \partial z} + \frac{\partial^3 u_z}{\partial x^2 \partial y} = 2\frac{\partial^2 \varepsilon_{xx}}{\partial y \partial z} \qquad \text{[from (2.2.67a)]}$$

That is $$2\frac{\partial^2 \varepsilon_{xx}}{\partial y \partial z} = \frac{\partial}{\partial x}\left[-\frac{\partial \gamma_{yz}}{\partial x} + \frac{\partial \gamma_{zx}}{\partial y} + \frac{\partial \gamma_{xy}}{\partial z}\right] \tag{2.2.68}$$

Similarly, $$2\frac{\partial^2 \varepsilon_{yy}}{\partial x \partial z} = \frac{\partial}{\partial y}\left[-\frac{\partial \gamma_{zx}}{\partial y} + \frac{\partial \gamma_{xy}}{\partial z} + \frac{\partial \gamma_{yz}}{\partial x}\right] \tag{2.2.69}$$

and $$2\frac{\partial^2 \varepsilon_{zz}}{\partial y \partial x} = \frac{\partial}{\partial z}\left[-\frac{\partial \gamma_{xy}}{\partial z} + \frac{\partial \gamma_{yz}}{\partial x} + \frac{\partial \gamma_{zx}}{\partial y}\right] \tag{2.2.70}$$

Equations (2.2.66) through (2.2.71) can be expressed as

$$\frac{\partial^2 \varepsilon_{ij}}{\partial x_k \partial x_\ell} + \frac{\partial^2 \varepsilon_{k\ell}}{\partial x_i \partial x_j} = \frac{\partial^2 \varepsilon_{ik}}{\partial x_j \partial x_\ell} + \frac{\partial^2 \varepsilon_{j\ell}}{\partial x_i \partial x_k} \tag{2.2.71}$$

This is the compatibility equation proposed by St. Venant. Six Equations (2.2.65)–(2.2.70) are a part of $3^4 = 81$ total equations given above. Note that one can have only six independent equations as obtained above out of total 81 equations.

Strain tensor must satisfy the preceding equations if the strain field is to correspond to a single-valued, continuous deformation.

2.2.9.2 Sufficient conditions for compatibility

2.2.9.2.1 Simply connected body

The one in which each and every closed path in a body can be continuously shrunk to a point without cutting a boundary. The path may be in anyway in the process of shrinking it to a point.

The path '*a*' can be shrunk to a point without cutting the outside boundary surface S_1 or the closed internal boundary surface S_2 which encloses a cavity inside the material. The path '*b*' cannot be shrunk to a point without cutting the boundary S_2 (Figure 2.2.18).

2.2.9.2.2 Multiply connected body

The one, where can exist one or more paths which cannot be shrunk to a point in the manner described earlier. Example is a ring, torus etc. shown in Figure 2.2.19.

The sufficient condition for the uniqueness of the strain-displacement relation is that the body should be simply connected. If the body is multiply connected, the six equations described earlier give only the necessary condition for compatibility.

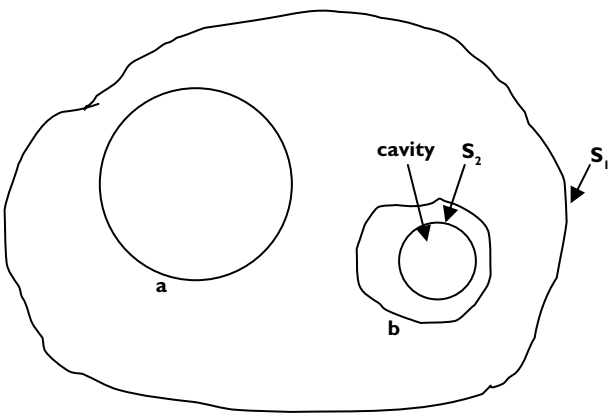


Figure 2.2.18 Simply connected domain.

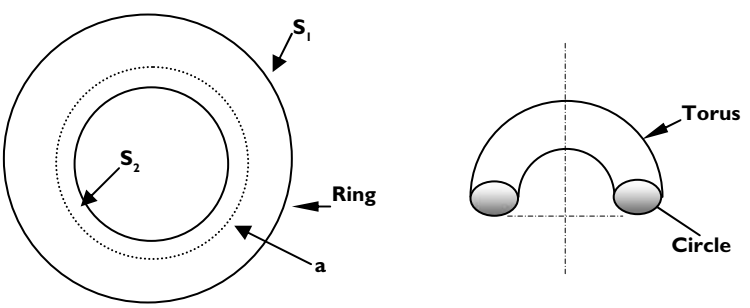


Figure 2.2.19 Multiply connected domain.

Example 2.2.5

1 Given:

$$\varepsilon_{ij} = \begin{bmatrix} .01 & -.02 & 0 \\ -.02 & .03 & -.01 \\ 0 & -.01 & 0 \end{bmatrix}$$

in the direction $\underline{n} = 0.0\ \underline{i} + 0.00\ \underline{j} + 0.8\ \underline{k}$; What is ε_{nn}?

2 In problem 1, a set of axes x', y', z' is chosen as follows

What is the strain tensor at the point of interest for this new reference in Figure 2.2.20?

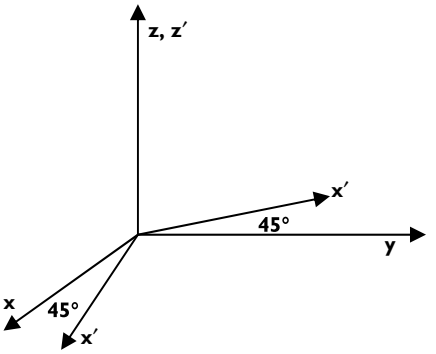


Figure 2.2.20

3 Given the following plane strain distribution:

$$\varepsilon_{xx} = 128\ x^2\ y; \quad \varepsilon_{yy} = 4\ y^2\ x^3 + 10^{-5} : \gamma_{xy} = 4\ xy + 10\ x^4.$$

Are the compatibility equations satisfied?

2.3 STRESSES

2.3.1 Concept of stress

The concept is well documented in textbooks and materials to be covered herein are just sufficient to formulate theorems presented in the subsequent sections. As in classical mechanics, we consider the force systems acting on a soil body in equilibrium are of two kinds: body forces which are spatially distributed on all elements of the body, and surface forces which are applied on the boundary of the body. Unit weights,

seepage force are body forces, they develop without the agency of physical contact. Surface forces on the other hand develop by virtue of the pressure between bodies. Dimensionally body force is force per unit volume whereas surface force is defined as a force per unit area of the surface.

If a normal force ΔF_n is transmitted across an area ΔA, shown in Figure 2.3.1 and consisting of mineral skeleton and water surface, reaction to ΔF_n may be thought of consisting of

$$(\Delta F_n)_{\text{soil mineral}} + (\Delta F_n)_{\text{pore water}} = \Delta F_n \tag{2.3.1}$$

Now stress at a point can be obtained by setting $\Delta A \to 0$, i.e. surface tractions may be written as

$$\sigma_n = \lim_{\Delta A \to 0} \frac{(\Delta F_n)_{\text{soil}}}{\Delta A} + \lim_{\Delta A \to 0} \frac{(\Delta F_n)_{\text{water}}}{\Delta A}$$

$$\tau_{nx} = \lim_{\Delta A \to 0} \frac{\Delta F_{nx}}{\Delta A}; \quad \tau_{ny} = \lim_{\Delta A \to 0} \frac{\Delta F_{ny}}{\Delta A}$$

$$\text{Thus} \quad \sigma_n = \bar{\sigma}_n + u \tag{2.3.2}$$

where $\bar{\sigma}_n$ = effective stress; u = pore water pressure; σ = total normal pressure.

This is the *von Karman notation* for normal and shear stresses, other one is simply τ_{ij} and indices change with the coordinate axes.

If pores are completely saturated, we have total head, $h = \frac{p_w}{\gamma_w} + z$, in which p_w = water pressure; z = elevation head.

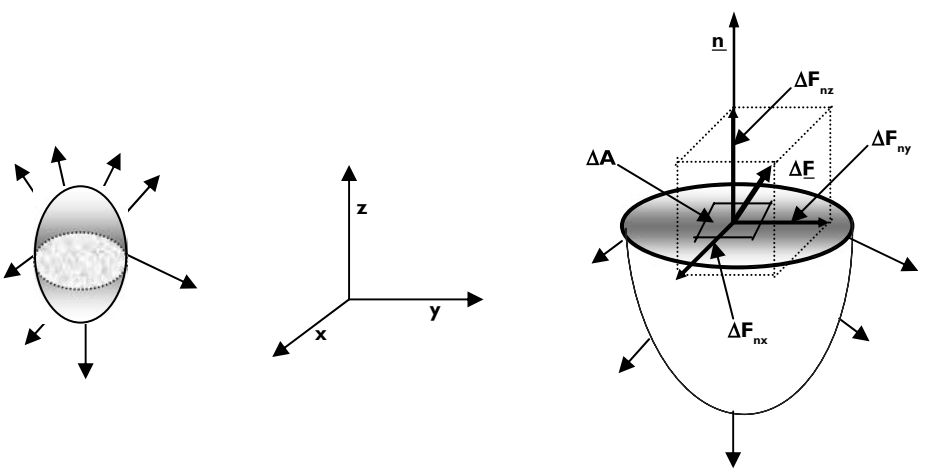


Figure 2.3.1 Concept of stress.

Thus, Equation (2.3.2) may be reduced to

$$\sigma_n = \bar{\sigma}_n + \gamma_w(h - z) \tag{2.3.3}$$

The defined positive normal and shear acting on the surfaces of an elemental cube at a point P within a soil mass are shown in Figure 2.3.2. This can be achieved through using the concept that when $\Delta x\, \Delta y\, \Delta z \to 0$, the situation converges to the stresses at P.

The stress tensor at a point is written as

$$[\sigma] = \begin{bmatrix} \sigma_x & \tau_{xy} & \tau_{xz} \\ \tau_{yx} & \sigma_y & \tau_{yz} \\ \tau_{zx} & \tau_{zy} & \sigma_z \end{bmatrix} = \sigma_{ij} = \tau_{ij} \tag{2.3.4}$$

Considering, the moment equilibrium at a point, stress tensor may be proved to be symmetric, i.e. $\sigma_{ij} = \sigma_{ji}$.

Stress at point is a second order tensor and as such all transformations related to tensor is applicable here as well.

2.3.1.1 Equilibrium equation in cartesian coordinates

Variation of effective stresses acting on the sides of a cubical element that contribute to its equilibrium in the y-direction is shown in Figure 2.2.3. The unit weight of soil is γ and acts in the negative z-direction and γ_w is the unit weight of water.

Summing up forces in y-direction, we get

$$\frac{\partial \tau_{xy}}{\partial x} + \frac{\partial \bar{\sigma}_y}{\partial y} + \frac{\partial \tau_{yz}}{\partial z} + \gamma_w \frac{\partial h}{\partial y} = 0$$

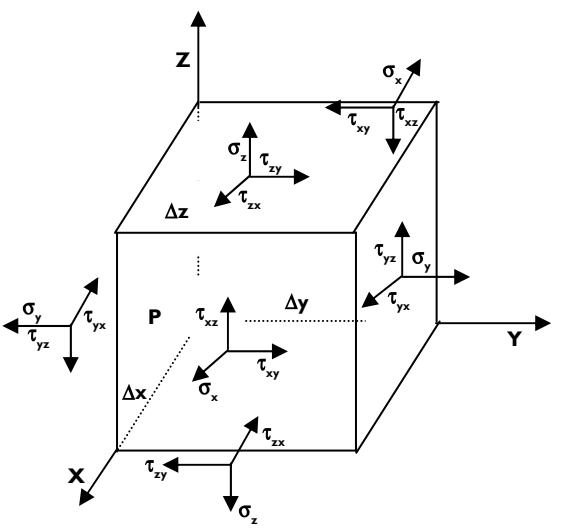


Figure 2.3.2 Positive stresses acting at a point *P*.

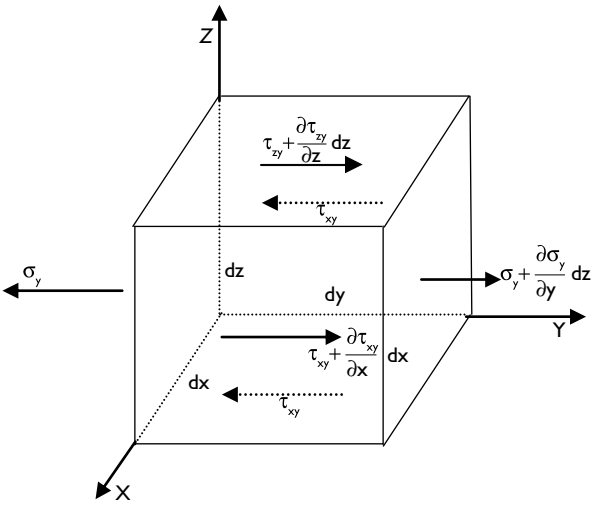


Figure 2.3.3 Equilibrating forces in the *Y*-direction.

Using similar arguments in the y and z directions, we can get the general equations of equilibrium at a point and they can be written as

$$\begin{aligned}
&\frac{\partial\bar{\sigma}_x}{\partial x}+\frac{\partial\tau_{xy}}{\partial y}+\frac{\partial\tau_{xz}}{\partial z}+\gamma_w\frac{\partial h}{\partial x}=0\\
&\frac{\partial\tau_{xy}}{\partial x}+\frac{\partial\bar{\sigma}_y}{\partial y}+\frac{\partial\tau_{yz}}{\partial z}+\gamma_w\frac{\partial h}{\partial y}=0\\
&\frac{\partial\tau_{xz}}{\partial x}+\frac{\partial\tau_{xy}}{\partial y}+\frac{\partial\bar{\sigma}_z}{\partial z}+\gamma_w\frac{\partial h}{\partial z}+\gamma-\gamma_w=0
\end{aligned}\tag{2.3.5}$$

where the body forces consists of seepage force (γ_w grad h) and buoyant unit weight $\gamma-\gamma_w$ in the z-direction.

2.3.1.2 Equilibrium equation in cylindrical coordinates (r, θ, z)

In foundation engineering cylindrical coordinates are often used for circular footings and problems related to axisymmetric situations. Diagram sketch of the situation is given in Figure 2.3.4.

Here $\tau_{r\theta}=\tau_{\theta r}$, $\tau_{rz}=\tau_{zr}$ and $\tau_{\theta z}=\tau_{z\theta}$, the equation of equilibrium can be written as

$$\begin{aligned}
&\frac{\partial\sigma_r}{\partial r}+\frac{1}{r}\frac{\partial\tau_{r\theta}}{\partial\theta}+\frac{\partial\tau_{zr}}{\partial z}+\frac{\sigma_r-\sigma_\theta}{r}=0\\
&\frac{\partial\tau_{r\theta}}{\partial r}+\frac{1}{r}\frac{\partial\sigma_\theta}{\partial\theta}+\frac{\partial\tau_{\theta z}}{\partial z}+\frac{2\tau_{r\theta}}{r}=0\\
&\frac{\partial\tau_{zr}}{\partial r}+\frac{1}{r}\frac{\partial\tau_{\theta z}}{\partial\theta}+\frac{\partial\sigma_z}{\partial z}+\frac{\tau_{zr}}{r}+\gamma=0
\end{aligned}\tag{2.3.6}$$

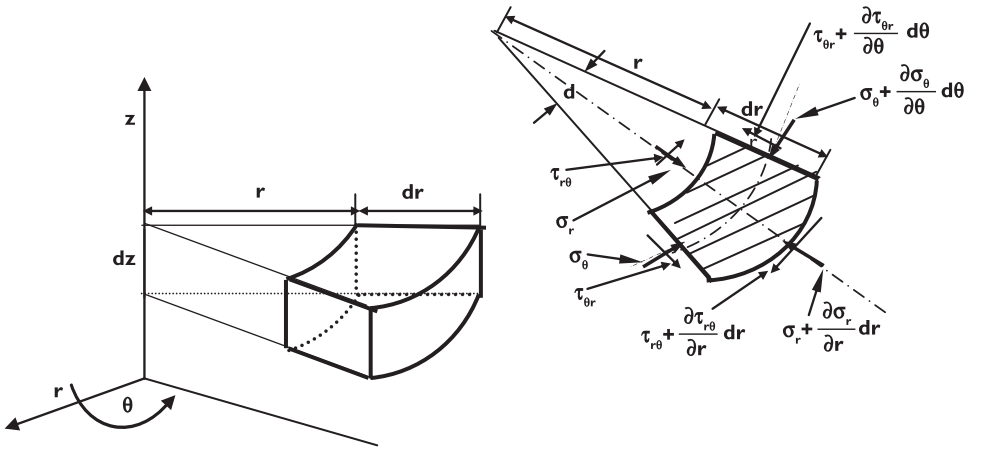


Figure 2.3.4 Axisymmetric configuration.

2.3.1.3 Traction

Figure 2.3.5 presents a tetrahedron formed by drawing three planes normal to the coordinate planes and a fourth plane with a direction normal $\underline{n}$ at a distance h from the point P, located at the origin.

In the limit as $h \to 0$ the tetrahedron will become of infinitesimal order with sides dx, dy and dz and all four planes will pass through the point P. The resultant stress $\underline{p}_n$ acting along $\underline{n}$ with components p_{nx}, p_{ny} and p_{nz}. In the limit as $h \to 0$, the equilibrium of all forces in the y-direction requires

$$\frac{1}{2}\sigma_y dxdz + \frac{1}{2}\tau_{xy} dydz + \frac{1}{2}\tau_{zy} dxdy = p_{ny} dA:$$

dA = area of the inclined surface.

It may be noticed that $\frac{1}{2}dydz = dA\cos(n,x)$, $\frac{1}{2}dxdz = dA\cos(n,y)$, and $\frac{1}{2}dxdy = dA\cos(n,z)$; $\cos(n,x)$, $\cos(n,y)$ and $\cos(n,z)$ are the direction cosines of $\underline{n}$ with x, y and z-directions.

Thus, we can write: $P_{ny} = \tau_{xy}\cos(n,x) + \sigma_y \cos(n,y) + \tau_{zy}\cos(n,z)$.

Hence, the surface traction on a surface having normal $\underline{n}$ can be written as

$$\begin{Bmatrix} \sigma_{nx} \\ \sigma_{ny} \\ \sigma_{nz} \end{Bmatrix} = \begin{bmatrix} \sigma_x & \tau_{xy} & \tau_{xz} \\ \tau_{xy} & \sigma_y & \tau_{yz} \\ \tau_{xz} & \tau_{yz} & \sigma_z \end{bmatrix} \begin{Bmatrix} \cos(n,x) \\ \cos(n,y) \\ \cos(n,z) \end{Bmatrix} \tag{2.3.7}$$

where $\cos(n,x)$ etc. are direction cosines of $\underline{n}$ with x-direction and so on.

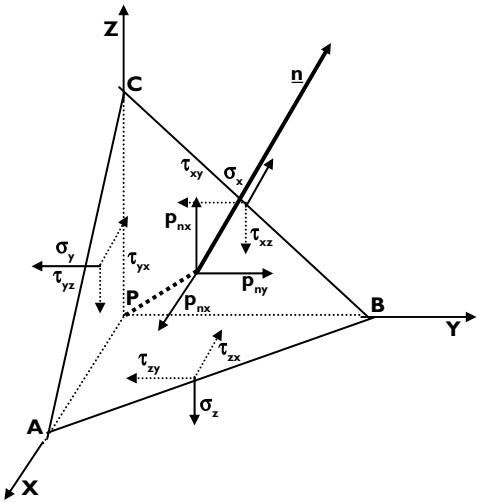


Figure 2.3.5 Stresses on an inclined plane.

Transformation of stresses from XYZ coordinate system to $X'Y'Z'$ coordinate system is given by:

$$\begin{bmatrix} \sigma_{x'} & \tau_{x'y'} & \tau_{x'z'} \\ \tau_{x'y'} & \sigma_{y'} & \tau_{y'z'} \\ \tau_{x'z'} & \tau_{y'z'} & \sigma_{z'} \end{bmatrix} = \begin{bmatrix} a_{11} & a_{12} & a_{13} \\ a_{21} & a_{22} & a_{23} \\ a_{31} & a_{32} & a_{33} \end{bmatrix} \begin{bmatrix} \sigma_x & \tau_{xy} & \tau_{xz} \\ \tau_{xy} & \sigma_y & \tau_{yz} \\ \tau_{xz} & \tau_{yz} & \sigma_z \end{bmatrix} \begin{bmatrix} a_{11} & a_{21} & a_{31} \\ a_{12} & a_{22} & a_{32} \\ a_{13} & a_{23} & a_{33} \end{bmatrix} \tag{2.3.8}$$

In tensor notation [similar to Equation (2.2.53)]:

$$\sigma_{mn} = a_{mk} a_{n\ell} \sigma_{k\ell} \tag{2.3.9}$$

indices $m, n, \ldots$ etc. have range, 1, 2, 3 implying X, Y and Z coordinate system respectively.

Direction cosine table:

	X	Y	Z	X	Y	Z
X'	a_{11}	a_{12}	a_{13}	$\cos(x', \mathrm{x})$	$\cos(x', \mathrm{y})$	$\cos(x', \mathrm{z})$
Y'	a_{21}	a_{22}	a_{23}	$\cos(y', \mathrm{x})$	$\cos(y', \mathrm{y})$	$\cos(y', \mathrm{z})$
Z'	a_{31}	a_{32}	a_{33}	$\cos(z', \mathrm{x})$	$\cos(z', \mathrm{y})$	$\cos(z', \mathrm{z})$

2.3.2 Principal stresses and strains, invariants

Stress and strain at a point, both are tensors of second order and, thus, both will follow similar law of transformation from one coordinate system to another.

A principal stress is defined as the normal stress on a plane on which there is no shear. The corresponding plane is the principal planer. If p is the directed normal on a principal plane and the normal stress (principal stress) is σ_p and Equation (2.3.6) can be written as

$$\begin{aligned}
(\sigma_x - \sigma_p)\cos(p,x) + \tau_{yx}\cos(p,y) + \tau_{xz}\cos(p,z) &= 0 \\
\tau_{yx}\cos(p,x) + (\sigma_y - \sigma_p)\cos(p,y) + \tau_{yz}\cos(p,z) &= 0 \\
\tau_{xz}\cos(p,x) + \tau_{yz}\cos(p,y) + (\sigma_z - \sigma_p)\cos(p,z) &= 0
\end{aligned} \tag{2.3.10}$$

in which σ_p and p are unknowns.

$$\text{Also, we have} \quad \cos^2(p,x) + \cos^2(p,y) + \cos^2(p,z) = 1 \tag{2.3.11}$$

From Equation (2.3.11) it is obvious that all direction cosines cannot be zero, hence for a nontrivial solution, one should have

$$\begin{vmatrix} \sigma_x - p & \tau_{xy} & \tau_{xz} \\ \tau_{xy} & \sigma_y - p & \tau_{yz} \\ \tau_{xz} & \tau_{yz} & \sigma_z - p \end{vmatrix} = 0. \tag{2.3.12}$$

Expanding the determinant, we get the characteristic equation [This is an eigen value problem, wherein σ_p are the eigen values and corresponding direction cosines are eigen vectors] as follows:

$$f(\sigma_p) = \sigma_p^3 - I_1 \quad \sigma_p^2 + I_2 \quad \sigma_p - I_3 = 0 \tag{2.3.13}$$

in which I_1, I_2 and I_3 given below are the stress invariants (i.e. invariant to coordinate transformation).

The invariants are:

$$\begin{aligned}
I_1 &= \sigma_x + \sigma_y + \sigma_z \\
I_2 &= \begin{vmatrix} \sigma_x & \tau_{xz} \\ \tau_{xz} & \sigma_z \end{vmatrix} + \begin{vmatrix} \sigma_x & \tau_{xy} \\ \tau_{xy} & \sigma_y \end{vmatrix} + \begin{vmatrix} \sigma_y & \tau_{yz} \\ \tau_{yz} & \sigma_z \end{vmatrix} \\
&= \sigma_x\sigma_y + \sigma_y\sigma_z + \sigma_z\sigma_x - \tau_{xy}^2 - \tau_{yz}^2 - \tau_{zx}^2 \\
I_3 &= \begin{vmatrix} \sigma_x & \tau_{xy} & \tau_{xz} \\ \tau_{xy} & \sigma_y & \tau_{yz} \\ \tau_{xz} & \tau_{yz} & \sigma_z \end{vmatrix} = \sigma_x\sigma_y\sigma_z - \sigma_x\tau_{yz}^2 - \sigma_y\tau_{zx}^2 - \sigma_z\tau_{xy}^2 + 2\tau_{xy}\tau_{yz}\tau_{zx}
\end{aligned} \tag{2.3.14}$$

If I's are nonzero and positive, Equation (2.3.13), according to Descarte's rule, should have three distinct roots. Once roots are known planes may be obtained from Equation (2.3.10). These principal planes can be shown to be mutually orthogonal.

First strain invariant say J_1 has an important physical meaning.

$$J_1 = \varepsilon_{xx} + \varepsilon_{yy} + \varepsilon_{zz} = \varepsilon_1 + \varepsilon_2 + \varepsilon_3 \tag{2.3.15}$$
$$= \text{sum of principal strains} = \text{cubical dilatation/volume dilatation.}$$

If products of strains are not neglected as in Equation (2.2.47), e, can be written as

$$e_{\text{large}} = \sqrt{1 + 2J_1 - 4J_2 + 8J_3} - 1 \tag{2.3.16}$$

J_1, J_2 and J_3 are strain invariants, given Equation (2.2.63).

2.3.3 Cauchy's stress quadric and Mohr diagram

Consider Equation (2.3.9), the stress given by

$$\sigma_{nn} = a_{nk} a_{n\ell} \sigma_{k\ell}$$

indicates normal stress at a point on a surface having normal direction $\underline{n}$.

Nature of variation of σ_{nn} as the orientation of $\underline{n}$ (as an axis) changes can be written as

$$\tau_{nn} = \sigma_n = \sigma_x \ell^2 + \sigma_y m^2 + \sigma_z n^2 + 2\tau_{xy} \ell m + 2\tau_{yz} mn + 2\tau_{zx} n\ell \tag{2.3.17}$$

It follows from Equation (2.3.17) that the stress components are the components of a symmetric tensor of rank two. Let us now introduce the concept of a certain surface, called the stress surface define in the following manner.

Set in the direction of $\underline{n}$ a vector whose length is r and say

$$r = \frac{k}{\sqrt{|\sigma_n|}}, \quad \text{where } k \text{ is a constant.} \tag{2.3.18}$$

Coordinates of the end of this vector, $x = \ell r$, $y = mr$ and $z = nr$.

$$\rightarrow \quad \sigma_n = \frac{k^2}{r^2}; \tag{2.3.19}$$

Implying that as the plane rotates about the point say '0', the end of the vector 'r' always lie on the surface of the second degree curve, that is

$$\rightarrow \quad \pm k^2 = \sigma_x x^2 + \sigma_y y^2 + \sigma_z z^2 + 2\tau_{xy} xy + 2\tau_{yz} yz + 2\tau_{zx} zx \tag{2.3.20}$$

+ve indicates tension and −ve, a compression.

When all three principal (we shall discuss them later) stresses have same sign, only one of the alternative sign is needed and the surface is an ellipsoid. When the principal stresses are not all of the same sign, both signs are needed and the surface consists of a hyperboloid of two surfaces, with a common asymptotic cone, which is the boundary surface, corresponding to the directions along which the stress is zero.

2.3.3.1 Mohr diagram

Take x, y, z as the directions 1, 2 and 3 as shown in Figure 2.3.6.
From Equation (2.3.6)

$$\text{We have,} \quad p_{n1} = \sigma_1 \cos(n,1); \quad p_{n2} = \sigma_2 \cos(n,2); \quad p_{n3} = \sigma_3 \cos(n,3) \tag{2.3.21}$$

The resultant is

$$\rightarrow \quad p_n^2 = p_{n1}^2 + p_{n2}^2 + p_{n3}^2 = \sigma_1^2 \cos^2(n,1) + \sigma_2^2 \cos^2(n,2) + \sigma_3^2 \cos^2(n,3)$$

$$\text{also} \quad p_n^2 = \sigma_n^2 + \tau_n^2 \tag{2.3.22}$$

Also we have,

$$\begin{Bmatrix} p_{n1} \\ p_{n2} \\ p_{n3} \end{Bmatrix} = \begin{bmatrix} \sigma_1 & 0 & 0 \\ 0 & \sigma_2 & 0 \\ 0 & 0 & \sigma_3 \end{bmatrix} \begin{Bmatrix} \cos(n,1) \\ \cos(n,2) \\ \cos(n,3) \end{Bmatrix}$$

Hence we may write

$$\begin{aligned} &\sigma_1^2 \cos^2(n,1) + \sigma_2^2 \cos^2(n,2) + \sigma_3^2 \cos^2(n,3) = \sigma_n^2 + \tau_n^2 \\ &\sigma_1 \cos^2(n,1) + \sigma_2 \cos^2(n,2) + \sigma_3 \cos^2(n,3) = \sigma_n \\ &\cos^2(n,1) + \cos^2(n,2) + \cos^2(n,3) = 1 \end{aligned} \tag{2.3.23}$$

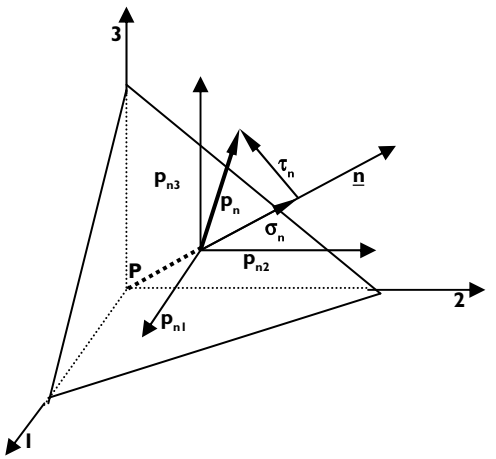


Figure 2.3.6 Development of Mohr diagram.

Assuming $\sigma_1 > \sigma_2 > \sigma_3$, solution of Equation (2.3.23) may be written as

$$\cos^2(n,1) = \frac{\tau_n^2 + (\sigma_n - \sigma_2)(\sigma_n - \sigma_3)}{(\sigma_1 - \sigma_2)(\sigma_1 - \sigma_3)};$$
$$\cos^2(n,2) = \frac{\tau_n^2 + (\sigma_n - \sigma_3)(\sigma_n - \sigma_1)}{(\sigma_2 - \sigma_3)(\sigma_2 - \sigma_1)}; \tag{2.3.24}$$
$$\cos^2(n,3) = \frac{\tau_n^2 + (\sigma_n - \sigma_1)(\sigma_n - \sigma_2)}{(\sigma_3 - \sigma_1)(\sigma_3 - \sigma_2)}.$$

Now, the cosines squared terms are never negative and as $\sigma_1 > \sigma_2 > \sigma_3$,

$$\tau_n^2 + (\sigma_n - \sigma_2)(\sigma_n - \sigma_3) \geq 0; \quad \tau_n^2 + (\sigma_n - \sigma_3)(\sigma_n - \sigma_1) \leq 0;$$
$$\tau_n^2 + (\sigma_n - \sigma_1)(\sigma_n - \sigma_3) \geq 0. \tag{2.3.25}$$

The first equation may be written as

$$\tau_n^2 + [\sigma_n^2 - \sigma_n(\sigma_2 + \sigma_3) + \sigma_2\sigma_3] \geq 0$$

$$\text{or,} \quad \tau_n^2 + \sigma_n^2 - 2\sigma_n\frac{(\sigma_2 + \sigma_3)}{2} + \left(\frac{\sigma_2 + \sigma_3}{2}\right)^2 \geq \frac{1}{4}\left[\left(\frac{\sigma_2}{2}\right)^2 - 4\sigma_2\sigma_3\right] = \left(\frac{\sigma_2 - \sigma_3}{2}\right)^2.$$

$$\tau_n^2 + \left[\sigma_n - \frac{(\sigma_2 + \sigma_3)}{2}\right]^2 \geq \left(\frac{\sigma_2 - \sigma_3}{2}\right)^2 \tag{2.3.26}$$

$$\tau_n^2 + \left[\sigma_n - \frac{(\sigma_1 + \sigma_3)}{2}\right]^2 \leq \left(\frac{\sigma_1 - \sigma_3}{2}\right)^2 \tag{2.3.27}$$

$$\tau_n^2 + \left[\sigma_n - \frac{(\sigma_1 + \sigma_2)}{2}\right]^2 \geq \left(\frac{\sigma_1 - \sigma_2}{2}\right)^2 \tag{2.3.28}$$

Choosing a (σ_n, τ_n) coordinate, we see that for the condition of equality of each of the above equations defines the locus of a circle. Equation (2.3.26) defines a circle with centre at $\sigma = (\sigma_2 + \sigma_3)/2$ with $(\sigma_2 - \sigma_3)/2$ as radius centred at '*a*' in Figure 2.3.7.

Similarly Equation (2.3.27) defines a circle with centre at $\sigma = (\sigma_1 + \sigma_3)/2$ with $(\sigma_1 - \sigma_3)/2$ as radius, centred at '*b*' and Equation (2.3.28) is a circle with centre at $\sigma = (\sigma_1 + \sigma_2)/2$ with $(\sigma_1 - \sigma_2)/2$ as radius, centred at '*c*' in Figure 2.3.7.

It is apparent from the Figure 2.3.7 that all stress conditions are confined within the interior of the outer circle and out side of the two circles drawned. Hence the maximum shear stress is given by

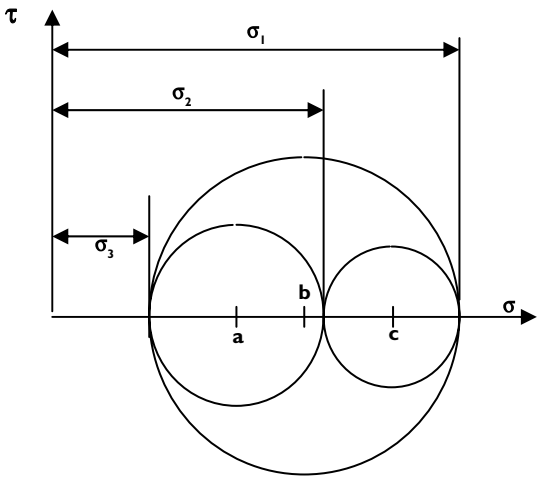


Figure 2.3.7 Mohr diagram.

$$\tau_{\max} = \frac{\sigma_1 - \sigma_3}{2}$$

corresponding normal stress is $\sigma = \dfrac{\sigma_1 + \sigma_3}{2}$. (2.3.29)

The direction cosines of the directed normal to the plane on which $\tau_{\max}$ acts are given by

$$\cos^2(n,1) = \frac{\left(\frac{\sigma_1 - \sigma_3}{2}\right)^2 + \left(\frac{\sigma_1 + \sigma_3}{2} - \sigma_2\right)\left(\frac{\sigma_1 + \sigma_3}{2} - \sigma_3\right)}{(\sigma_1 - \sigma_3)(\sigma_1 - \sigma_2)} = \frac{1}{2}$$

$$\cos^2(n,2) = \frac{\left(\frac{\sigma_1 - \sigma_3}{2}\right)^2 + \left(\frac{\sigma_1 + \sigma_3}{2} - \sigma_1\right)\left(\frac{\sigma_1 + \sigma_3}{2} - \sigma_3\right)}{(\sigma_2 - \sigma_3)(\sigma_2 - \sigma_1)} = 0 \qquad (2.3.30)$$

$$\cos^2(n,3) = \frac{\left(\frac{\sigma_1 - \sigma_3}{2}\right)^2 + \left(\frac{\sigma_1 + \sigma_3}{2} - \sigma_3\right)\left(\frac{\sigma_1 + \sigma_3}{2} - \sigma_3\right)}{(\sigma_3 - \sigma_1)(\sigma_3 - \sigma_2)} = \frac{1}{2}.$$

➔ Hence d.c.s are $\dfrac{1}{\pm\sqrt{2}} = 0; \dfrac{1}{\pm\sqrt{2}}$.

2.3.3.2 Spherical stress matrix

Here we have $\sigma_1 = \sigma_2 = \sigma_3 \rightarrow$ Mohr circle reduces to a point at a distance $= \sigma_h = \sigma_1 + \sigma_2 + \sigma_3$ on σ-axis.

2.3.3.3 *Deviatoric stress matrix*

It plots Mohr diagram the same way as the general stress matrix but with the τ-axis shifted by an amount, $\sigma_h = (\sigma_1 + \sigma_2 + \sigma_3)/3$. This is shown in Figure 2.3.8.

2.3.4 Plane stress conditions

Let us assume that stresses are confined to x-z plane. For this case, we have $\sigma_y = \tau_{xy} = \tau_{uz} = 0$. The stress tensor can be written as

$$\sigma_{ij} = \begin{bmatrix} \sigma_x & 0 & \tau_{xz} \\ 0 & 0 & 0 \\ \tau_{xz} & 0 & \sigma_z \end{bmatrix} \tag{2.3.31}$$

Characteristic equation can be written as

$$(\sigma_x - \sigma_n)(\sigma_z - \sigma_n) - \tau_{xz}^2 = 0 \tag{2.3.32}$$

Two principal stresses are:

$$\sigma_{1,2} = \frac{1}{2}(\sigma_x + \sigma_z) \pm \sqrt{\left(\frac{\sigma_x - \sigma_z}{2}\right)^2 + \tau_{xz}^2} \tag{2.3.33}$$

This is the equation of a circle with its centre on σ-axis at $\sigma = (\sigma_x + \sigma_z)/2$ and with a radius of $[(\sigma_x - \sigma_x)^2/4 + \tau_{xz}^2]^{1/2}$.

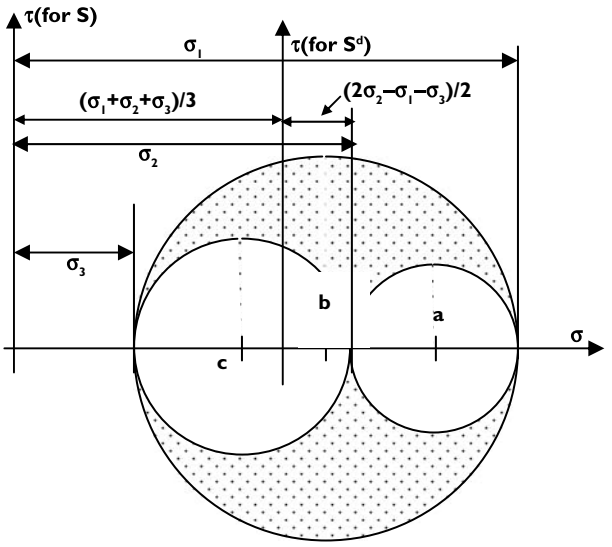


Figure 2.3.8 Mohr diagram – special cases.

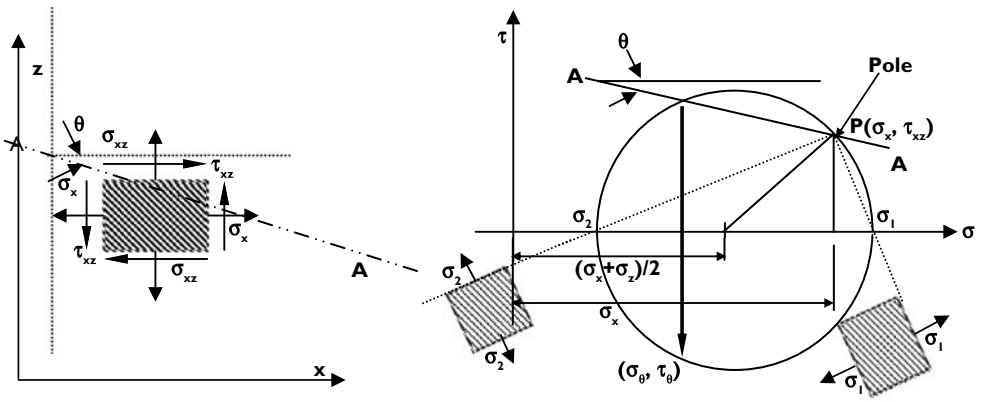


Figure 2.3.9 Construction of Mohr diagram.

Thus for plane stress, the stresses in any direction at a point in the plane under consideration lie on the circumference of a unique circle. This circle can also be drawn in parametric form, introducing the parameter 2θ, by equation

$$\sigma_\theta = \frac{(\sigma_x + \sigma_z)}{2} + \frac{(\sigma_x - \sigma_z)}{2}\cos 2\theta + \tau_{xz}\sin 2\theta;$$
$$\tau_\vartheta = \frac{(\sigma_x - \sigma_z)}{2}\sin 2\theta - \tau_{xz}\cos 2\theta \tag{2.3.34}$$

This equation can be plotted with respect to a plane stress (positive stress system) element shown in Figure 2.3.9.

Consider the stresses on the right side of the element and take it to be positive. Construction procedure is as follows: Draw σ(normal) and τ (shear) axes along x and z directions. Take the centre of Mohr circle at $(\sigma_x + \sigma_z)/2$ on the σ-axis. Draw pole with coordinates (σ_x, τ_{xz}). Join the pole with the centre and with the line joining centre to the pole is the radius of the Mohr circle. Draw the Mohr circle. Stresses on any plane *A-A* can be obtained from drawing a line parallel to *A-A* from the pole and dropping a vertical line from the point, the line *a-a* intersects the mohr circle. This is $(\sigma_\theta, \tau_\theta)$. Principal stresses are drawn by joining line from the pole to the points where the circle intersects the σ-axis. This is shown in Figure 2.3.9.

2.3.5 Plane strain conditions

For plane strain condition, again we consider xz-plane as the reference plane, $\tau_{xy} = \tau_{yz} = 0$ and the stress tensor can be written as

$$\begin{bmatrix} \sigma_x & 0 & \tau_{xz} \\ 0 & \sigma_y & 0 \\ \tau_{xz} & 0 & \sigma_z \end{bmatrix} \tag{2.3.35}$$

The characteristic equation may be written as

$$(\sigma_y - \sigma_n)[(\sigma_x - \sigma_n)(\sigma_z - \sigma_n) - \tau_{xz}^2] = 0 \tag{2.3.36}$$

This is the same equation we had for a plane stress situation. So all considerations we had for a plane stress situation is applicable to the plane strain condition as well. The third principal stress is σ_y, normal to xz-plane and this may be obtained from $\sigma_y = \nu(\sigma_x + \sigma_z)$.

2.3.6 Octahedral stresses and strains

Octahedral planes and octahedral stress and strains are of considerable importance in studying in elastic behaviour of materials like soils. In a material body we have here eight planes with direction cosines. Without any loss of generality we can consider Haig-Westergaard space as in Figure 2.3.10 (σ_1, σ_2, σ_3 – three principal stresses) instead of conventional Euclidean space (x, y, z). Thus, direction cosines relative to the principal axes are: $\cos(n,1) = \cos(n,2) = \cos(n,3) = \pm\frac{1}{\sqrt{3}}$.

Normal stress on the octahedral plane:

$$\sigma_{\text{oct}} = < \frac{1}{\sqrt{3}} \frac{1}{\sqrt{3}} \frac{1}{\sqrt{3}} > \begin{bmatrix} \sigma_1 & 0 & 0 \\ 0 & \sigma_2 & 0 \\ 0 & 0 & \sigma_3 \end{bmatrix} < \frac{1}{\sqrt{3}} \frac{1}{\sqrt{3}} \frac{1}{\sqrt{3}} >^T \tag{2.3.37}$$

$$\rightarrow \quad \sigma_{\text{oct}} = \frac{1}{3}(\sigma_1 + \sigma_2 + \sigma_3)$$

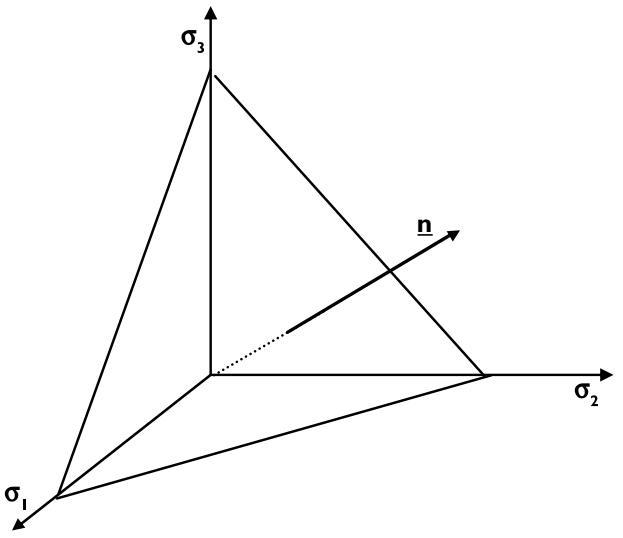


Figure 2.3.10 Haig-Westergaard space.

Shear stress:

$$\tau_{\text{oct}}^2 = \sigma_n^2 - \sigma_{\text{oct}}^2 = [\sigma_1 \cos(n,1)]^2 + [\sigma_2 \cos(n,2)]^2 + [\sigma_3 \cos(n,3)]^2 - \frac{1}{9}[\sigma_1 + \sigma_2 + \sigma_3]^2$$

$$\therefore \tau_{\text{oct}} = \frac{1}{3}\sqrt{(\sigma_1 - \sigma_2)^2 + (\sigma_2 - \sigma_3)^2 + (\sigma_3 - \sigma_1)^2} \tag{2.3.38}$$

In invariant form:

$$\sigma_{\text{oct}} = \frac{1}{3} I_1 : \ \tau_{\text{oct}}^2 = \frac{2}{9}[I_1^2 - 3I_2] \tag{2.3.39}$$

Similarly in terms of strains:

$$\varepsilon_{\text{oct}} = \frac{J_1}{3}; \quad \gamma_{\text{oct}} = \frac{2}{3}\sqrt{(\varepsilon_1 - \varepsilon_2)^2 + (\varepsilon_2 - \varepsilon_3)^2 + (\varepsilon_3 - \varepsilon_1)^2}$$

$$\gamma_{\text{oct}}^2 = \frac{8}{9}\left[J_1^2 - 3J_2\right] \tag{2.3.40}$$

2.3.7 Spherical and deviatoric stress components

Spherical-stress matrix is defined as

$$\sigma^s = \begin{bmatrix} \sigma_h & 0 & 0 \\ 0 & \sigma_h & 0 \\ 0 & 0 & \sigma_h \end{bmatrix} \text{ where, } \sigma_h = \text{hydrostatic compression} = \frac{\sigma_x + \sigma_y + \sigma_z}{3} \tag{2.3.41}$$

$$\text{Invariants are:} \quad I_1^s = I_1 : I_2^s = \frac{I_1^2}{3} : I_3^s = \frac{I_1^3}{27} \tag{2.3.42}$$

Deviatoric stress matrix is defined as

$$\sigma^d = [\sigma\,] - [\sigma^s] = \begin{bmatrix} \sigma_x - \sigma_h & \tau_{xy} & \tau_{xz} \\ \tau_{xy} & \sigma_y - \sigma_h & \tau_{yz} \\ \tau_{xz} & \tau_{yz} & \sigma_z - \sigma_h \end{bmatrix} \tag{2.3.43}$$

Invariants are:

$$I_1^d = 0 : I_2^d = I_2 - \frac{I_1^3}{3} = -\left(\frac{I_1^2}{3} - I_2\right) = -\frac{1}{3}(I_1^3 - 3I_2) = -\frac{1}{3} \times \frac{9}{2}\tau_{\text{oct}}^2 :$$

$$I_3^d = I_3 - \frac{I_1 I_2}{3} + \frac{2}{27} I_1^3; \quad \text{and} \quad \tau_{\text{oct}} = -\frac{2}{3} I_2^d$$

Similar expressions can be obtained for strains as well.

2.4 CONSTITUTIVE RELATIONS

In experiment with a cylindrical (a rod to be precise) specimen subjected to axial load, a linear stress-strain behaviour is exhibited for stresses sufficiently below the yield stress of the material.

$$\text{Thus} \quad \sigma_z = E\varepsilon_z \tag{2.4.1}$$

➔ This is *Hooke's law*.

We shall postulate that, in a more general state of stress, materials behave according to Equation (2.4.1), hence,

$$\begin{aligned}
\sigma_x &= c_{11}\,\varepsilon_x + c_{12}\,\varepsilon_y + c_{13}\,\varepsilon_z + c_{14}\,\gamma_{xy} + c_{15}\,\gamma_{yz} + c_{16}\,\gamma_{zx} \\
\sigma_y &= c_{21}\,\varepsilon_x + c_{22}\,\varepsilon_y + c_{23}\,\varepsilon_z + c_{24}\,\gamma_{xy} + c_{25}\,\gamma_{yz} + c_{26}\,\gamma_{zx} \\
\sigma_z &= c_{31}\,\varepsilon_x + c_{32}\,\varepsilon_y + c_{33}\,\varepsilon_z + c_{34}\,\gamma_{xy} + c_{35}\,\gamma_{yz} + c_{36}\,\gamma_{zx} \\
\gamma_{xy} &= c_{41}\,\varepsilon_x + c_{42}\,\varepsilon_y + c_{43}\,\varepsilon_z + c_{44}\,\gamma_{xy} + c_{45}\,\gamma_{yz} + c_{46}\,\gamma_{zx} \\
\gamma_{yz} &= c_{51}\,\varepsilon_x + c_{52}\,\varepsilon_y + c_{53}\,\varepsilon_z + c_{54}\,\gamma_{xy} + c_{55}\,\gamma_{yz} + c_{56}\,\gamma_{zx} \\
\gamma_{zx} &= c_{61}\,\varepsilon_x + c_{62}\,\varepsilon_y + c_{63}\,\varepsilon_z + c_{64}\,\gamma_{xy} + c_{65}\,\gamma_{yz} + c_{66}\,\gamma_{zx}
\end{aligned} \tag{2.4.2}$$

where c's are constants of proportionality.

So, we may write Equation (2.4.2) as (Harr 1969)

$$\underset{6\times 1}{\{\sigma\}} = \underset{6\times 6}{[C]} \quad \underset{6\times 1}{\{\varepsilon\}} \tag{2.4.3}$$

This is *generalized Hooke's law*.

We are saying that each stress component at a point is linearly proportional to all the strain components at that point.

Though not essential, let us assume that the material is *homogeneous*. We shall presently derive our equations for an *isotropic* material. It means that material property is direction independent. Now consider a few transformations using the isotropy of the material property. Basic transformation equation is

$$\sigma_{mn} = a_{mk}\; a_{n\ell}\; \sigma_{k\ell} \tag{2.4.4}$$

a) Consider a 180° rotation about z-axis (Figure 2.4.1a):

Direction cosines

	x	y	z
x'	-1	0	0
y'	0	-1	0
z'	0	0	1

In Equation (2.4.8): $m = x'$, $n = y'$, $k = x$ and $\ell = y$.

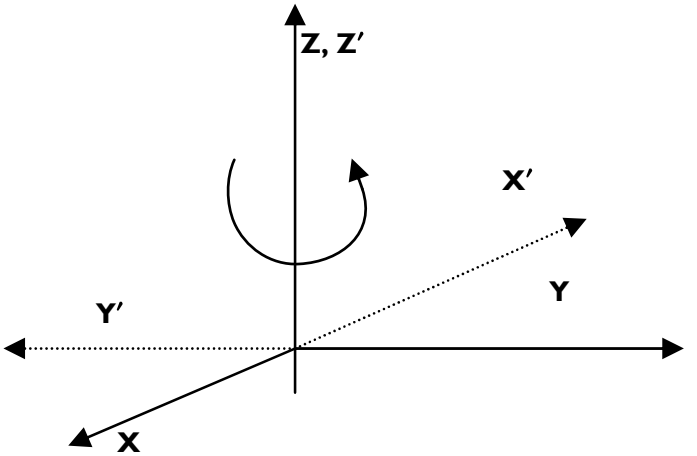


Figure 2.4.1a Rotation of axes.

Thus:

$$\begin{aligned}\tau_{x'y'} &= a_{x'x}(a_{y'x}\sigma_x + a_{y'y}\tau_{xy} + a_{y'z}\tau_{xz}) + a_{x'y}(a_{y'x}\tau_{yx} + a_{y'y}\sigma_y + a_{y'z}\tau_{yz}) \\ &\quad + a_{x'z}(a_{y'x}\tau_{xz} + a_{y'y}\tau_{yz} + a_{y'z}\sigma_z) \\ &= (-1)[0 + (-1)\tau_{xy} + 0] = \tau_{xy}.\end{aligned}$$

Hence, with transformation, we have

$$\sigma_{x'} = \sigma_x; \quad \tau_{x'y'} = \tau_{xy}; \quad \sigma_{y'} = \sigma_y; \quad \tau_{y'z'} = -\tau_{yz}; \quad \sigma_{z'} = \sigma_z; \quad \tau_{x'z'} = -\tau_{xz}.$$

Similarly

$$\varepsilon_{x'} = \varepsilon_x; \quad \gamma_{x'y'} = \gamma_{xy}; \quad \varepsilon_{y'} = \varepsilon_y; \quad \gamma_{y'z'} = -\gamma_{yz}; \quad \varepsilon_{z'} = \varepsilon_z; \quad \gamma_{x'z'} = -\gamma_{xz}.$$

Now, if c_{ij} is valid for some reference axis $X'Y'Z'$

$$\sigma_{x'} = c_{11}\varepsilon_{x'} + c_{12}\varepsilon_{y'} + c_{13}\varepsilon_{z'} + c_{14}\gamma_{x'y'} + c_{15}\gamma_{y'z'} + c_{16}\gamma_{z'x'} \text{ (Imposing isotropy)}$$

This equation can also be written as

$$\sigma_x = c_{11}\ \varepsilon_x + c_{12}\ \varepsilon_y + c_{13}\ \varepsilon_z + c_{14}\ \gamma_{xy} - c_{15}\gamma_{yz} - c_{16}\ \gamma_{zx} \tag{2.4.5}$$

From Equations (2.4.2) and (2.4.5): c_{15} and c_{16} are both positive and negative. This implies that $c_{15} = c_{16} = 0$.

Similarly considering other stresses, we may conclude that

$$c_{15} = c_{16} = c_{25} = c_{26} = c_{36} = c_{35} = c_{45} = c_{46} = c_{51} = c_{52} = c_{53} = c_{54} = c_{61} = c_{62} = c_{63} = c_{64} = 0.$$

➔ eliminates 16 constants.

This implies that the mechanical behaviour in X and X' and Y and Y' are symmetric.
➔ *Elastic symmetry about YZ and XZ planes.*

b) Consider a rotation of 180° about X-axis (Figure 2.4.1b).

Direction cosines

	x	y	z
x'	1	0	0
y'	0	−1	0
z'	0	0	−1

From Equation (2.3.8), we get

$$\sigma_{x'} = \sigma_x; \quad \sigma_{y'} = \sigma_y; \quad \sigma_{z'} = \sigma_z; \quad \tau_{x'y'} = -\tau_{xy}; \quad \tau_{y'z'} = \tau_{yz}; \quad \tau_{z'x'} = -\tau_{zx};$$
$$\varepsilon_{x'} = \varepsilon_x; \quad \varepsilon_{y'} = \varepsilon_y; \quad \varepsilon_{z'} = \varepsilon_z; \quad \gamma_{x'y'} = -\gamma_{xy}; \quad \gamma_{y'z'} = \gamma_{yz}; \quad \gamma_{z'x'} = -\gamma_{zx}.$$

Once again, $\sigma_{x'} = c_{11}\varepsilon_{x'} + c_{12}\varepsilon_{y'} + c_{13}\varepsilon_{z'} + c_{14}\gamma_{x'y'}$
Comparing with Equation (2.4.2), we get $c_{14} = 0$, and examining other stress components, we have

$$c_{24} = c_{34} = c_{41} = c_{42} = c_{43} = c_{56} = c_{65} = 0.$$

So, we got rid of 8 more constants and a total of $16 + 8 = 24$ constants.

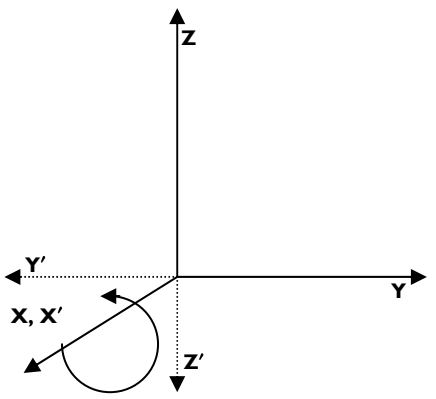


Figure 2.4.1b Rotation of axes.

This implies symmetry in mechanical behaviour in Z and Z' directions.

➔ *Elastic symmetry about XY plane.*

A material behaving, satisfying the conditions like symmetry about XY, YZ and ZX planes are known as *orthotropic* material. Corresponding constitutive matrix [C] in such case can be written as

$$[C] = \begin{bmatrix} c_{11} & c_{12} & c_{13} & 0 & 0 & 0 \\ c_{21} & c_{22} & c_{23} & 0 & 0 & 0 \\ c_{31} & c_{32} & c_{33} & 0 & 0 & 0 \\ 0 & 0 & 0 & c_{44} & 0 & 0 \\ 0 & 0 & 0 & 0 & c_{55} & 0 \\ 0 & 0 & 0 & 0 & 0 & c_{66} \end{bmatrix} \rightarrow \text{with 12 constants.}$$

c) Rotate the axis 'X' by 90° (Figure 2.4.1c):

Direction cosines

	x	y	z
x'	1	0	0
y'	0	0	1
z'	0	−1	0

Using Equation (2.3.8), we get

$$\sigma_{x'} = \sigma_x; \quad \sigma_{y'} = \sigma_z; \quad \sigma_{z'} = \sigma_y; \quad \tau_{x'y'} = \tau_{xz}; \quad \tau_{y'z'} = -\tau_{yz}; \quad \tau_{z'x'} = -\tau_{yx};$$

$$\varepsilon_{x'} = \varepsilon_x; \quad \varepsilon_{y'} = \varepsilon_z; \quad \varepsilon_{z'} = \varepsilon_y; \quad \gamma_{x'y'} = \gamma_{zx}; \quad \gamma_{y'z'} = -\gamma_{yz}; \quad \gamma_{z'x'} = -\gamma_{yx}.$$

Once again, $\sigma_{x'} = c_{11}\varepsilon_{x'} + c_{12}\varepsilon_{y'} + c_{13}\varepsilon_{z'}$

Comparing with Equation (2.4.2), one has $c_{12} = c_{13}$, while examining other stress components, we may write

$$c_{31} = c_{21}; \quad c_{22} = c_{33}; \quad c_{23} = c_{22} \quad \text{and} \quad c_{44} = c_{66}.$$

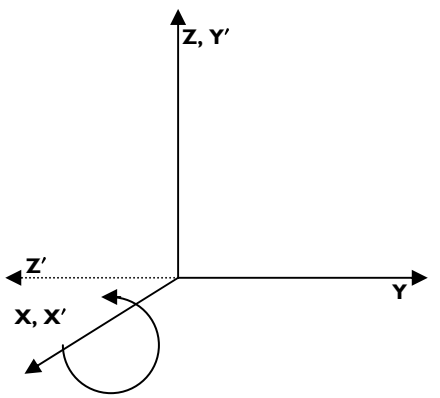


Figure 2.4.1c Rotation of axes.

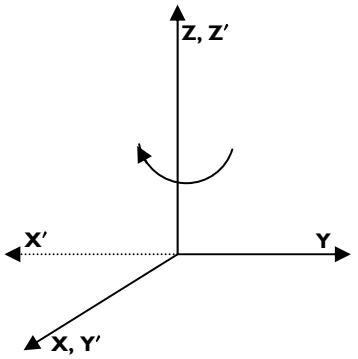


Figure 2.4.1d Rotation of axes.

d) Rotation of axis *Z* by 90° (Figure 2.4.1d):

Direction cosines

	x	y	z
x'	0	−1	0
y'	1	0	0
z'	0	0	1

This implies: $c_{12} = c_{23}; c_{31} = c_{32}; c_{11} = c_{22}$ and $c_{44} = c_{55}$.
Thus constitutive relation reduces to 3-constants.
Hence one can write

$$\begin{aligned} \sigma_x &= c_{11} \quad \varepsilon_x + c_{12}(\varepsilon_y + \varepsilon_z) \quad \tau_{xy} = c_{44} \quad \gamma_{xy} \\ \sigma_y &= c_{11} \quad \varepsilon_y + c_{12}(\varepsilon_z + \varepsilon_x) \quad \tau_{yz} = c_{44} \quad \gamma_{yz} \\ \sigma_z &= c_{11} \quad \varepsilon_z + c_{12}(\varepsilon_x + \varepsilon_y) \quad \tau_{zx} = c_{44} \quad \gamma_{zx} \end{aligned} \tag{2.4.6}$$

We assume
$c_{12} = \lambda$; Lame's constant
$c_{44} = \mu = G =$ shear modulus of elasticity.
λ and G are called Lame's constants.

e) Rotating the *XYZ* reference by 45° about *Z*-axis (Figure 2.4.1e):

Direction cosines

	x	y	z
x'	$1/\sqrt{2}$	$1/\sqrt{2}$	0
y'	$-1/\sqrt{2}$	$1/\sqrt{2}$	0
z'	0	0	1

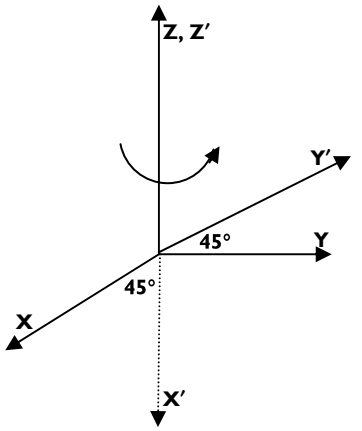


Figure 2.4.1e Rotation of axes.

Employing Equation (2.3.8)

$$\sigma_{x'} = \frac{1}{2}(\sigma_x + \sigma_y + 2\tau_{xy}); \quad \sigma_{y'} = \frac{1}{2}(\sigma_x + \sigma_y - 2\tau_{xy}); \quad \sigma_{z'} = \sigma_z;$$

$$\tau_{x'y'} = \frac{1}{2}(\sigma_y - \sigma_x); \quad \tau_{y'z'} = \left(\tau_{yz} - \tau_{zx}\right)/\sqrt{2}$$

Similar expressions can be made for $\varepsilon_{x'x'}, \varepsilon_{y'y'}, \ldots$.
From Equation (2.4.6), $\sigma_{x'} = c_{11}\varepsilon_{x'} + \lambda(\varepsilon_{x'} + \varepsilon_{z'})$
Thus

$$\frac{1}{2}(\sigma_x + \sigma_y + 2\tau_{xy}) = c_{11}(\varepsilon_x + \varepsilon_y + \gamma_{xy})/2 + \lambda\left[\frac{1}{2}(\varepsilon_x + \varepsilon_y - \gamma_{xy}) + \varepsilon_z\right]$$

Substituting the first, second and fourth expression of Equation (2.4.6) in the above expression, we have

$$\frac{1}{2}[c_{11}\varepsilon_x + \lambda\,(\varepsilon_y + \varepsilon_z) + c_{11}\varepsilon_y + \lambda\,(\varepsilon_x + \varepsilon_z) + 2G\gamma_{xy}]$$

$$= \frac{c_{11}}{2}(\varepsilon_x + \varepsilon_y + \gamma_{xy}) + \lambda\left[\frac{1}{2}(\varepsilon_x + \varepsilon_y - \gamma_{xy}) + \varepsilon_z\right]$$

Solving $\rightarrow$ $c_{11} = 2G + \lambda$ (2.4.7)

Hence, $\sigma_x = (2G + \lambda)\varepsilon_x + \lambda\,(\varepsilon_y + \varepsilon_z) : \sigma_y = (2G + \lambda)\varepsilon_y + \lambda\,(\varepsilon_z + \varepsilon_x) :$

$$\sigma_z = (2G + \lambda)\varepsilon_z + \lambda\,(\varepsilon_x + \varepsilon_y)$$

$$\tau_{xy} = G\gamma_{xy} : \tau_{yz} = G\gamma_{yz} : \tau_{zx} = G\gamma_{zx} \quad (2.4.8)$$

Any further rotation of axes (i.e. transformation) will not result in reduction of the number of independent moduli (constants).

Solving Equation (2.4.8) we may also obtain

$$\begin{aligned}
\varepsilon_x &= \frac{\lambda + G}{G(3\lambda + 2G)}\sigma_x - \frac{\lambda}{2G(3\lambda + 2G)}(\sigma_y + \sigma_z) \\
\varepsilon_y &= \frac{\lambda + G}{G(3\lambda + 2G)}\sigma_y - \frac{\lambda}{2G(3\lambda + 2G)}(\sigma_z + \sigma_x) \\
\varepsilon_z &= \frac{\lambda + G}{G(3\lambda + 2G)}\sigma_z - \frac{\lambda}{2G(3\lambda + 2G)}(\sigma_x + \sigma_y) \\
\gamma_{xy} &= \frac{\tau_{xy}}{G}; \quad \gamma_{yz} = \frac{\tau_{yz}}{G}; \quad \gamma_{zx} = \frac{\tau_{zx}}{G}
\end{aligned} \tag{2.4.9}$$

Proportionality of shearing stress and shearing strain indicates that the principal axes of stress tensor and strain tensor coincide. This is because the transformation matrix is the same for a transformation of coordinate axes in the case of stress tensor as well as strain tensor.

The Hooke's law in arbitrary curvilinear orthogonal coordinates α, β, γ is given as

$$\sigma_\alpha = 2G\left(\varepsilon_\alpha + \frac{\nu e}{1-2\nu}\right); \quad \sigma_{\alpha\beta} = G\gamma_{\alpha\beta}; \quad \varepsilon_\alpha = \frac{1}{2G}\left(\sigma_\alpha - \frac{\nu p}{1+\nu}\right) \tag{2.4.10}$$

in which, $p = \sigma_\alpha + \sigma_\beta + \sigma_\gamma$; $\quad e = \varepsilon_\alpha + \varepsilon_\beta + \varepsilon_\gamma$.

From a simple tensile test on a rod, we have $\sigma_x = 0 = \sigma_y$

This gives

$$\varepsilon_z = \frac{\lambda + G}{G(3\lambda + 2G)}\sigma_z \quad \rightarrow \quad E = \text{Young's modulus of elasticity} = \frac{G(3\lambda + 2G)}{\lambda + G}.$$

Also $\varepsilon_x = -\nu \quad \varepsilon_z = \varepsilon_y =$ due to Poisson effect.

$$\varepsilon_x = -\frac{\lambda}{2G(3\lambda + 2G)}\sigma_z = -\frac{\lambda}{2G(3\lambda + 2G)}\varepsilon_z E \quad \rightarrow \quad \frac{\nu}{E} = \frac{\lambda}{2G(3\lambda + 2G)} \tag{2.4.11}$$

Generalised Hooke's law, in terms of E and ν [Young's modulus and Poisson ratio] may be written as

$$\begin{aligned}
&\varepsilon_x = \frac{\sigma_x}{E} - \frac{\nu}{E}(\sigma_y + \sigma_z); \quad \varepsilon_y = \frac{\sigma_y}{E} - \frac{\nu}{E}(\sigma_z + \sigma_x); \quad \varepsilon_z = \frac{\sigma_z}{E} - \frac{\nu}{E}\left(\sigma_x + \sigma_y\right) \\
&\gamma_{xy} = \frac{\tau_{xy}}{G}; \quad \gamma_{yz} = \frac{\tau_{yz}}{G}; \quad \gamma_{zx} = \frac{\tau_{zx}}{G}
\end{aligned} \tag{2.4.12}$$

The Lame's parameter may be written as

$$\lambda = \frac{2G^2 - EG}{E - 3G} = \frac{2G^2\nu}{E - 2G\nu}; \quad G = \frac{E}{2(1+\nu)} \tag{2.4.13}$$

Also K = the bulk modulus of elasticity $= \lambda + (2/3)G = E/(1-2\nu)$.

During deformation, a certain amount of energy is stored in a body. The energy must be a positive quantity. From Equation (2.6.7), given later, we may conclude, $\lambda > 0$ and $G > 0$, and

$$\frac{\nu E}{(1+\nu)(1-2\nu)} > 0; \quad \frac{E}{2(1+\nu)} > 0 \quad \rightarrow \ (1+\nu) \geq 0 \text{ and } 1 - 2\nu \geq 0.$$

Hence, $-1 < \nu \leq 0.5$.

Using tensor notation, we may write

$$\varepsilon_{ij} = \frac{1+\nu}{E}\tau_{ij} - \frac{\nu}{E}\tau_{kk}\delta_{ij} \tag{2.4.14}$$

in which $\delta_{ij} = 1$, for $i = j$

$= 0$, for $i \neq j$

= Kronecker delta.

2.5 EQUATIONS OF EQUILIBRIUM

2.5.1 Some useful expressions

Stress-strain relations

$$\sigma_x = \lambda e + 2G\frac{\partial u_x}{\partial x} : \sigma_y = \lambda e + 2G\frac{\partial u_y}{\partial y} : \sigma_z = \lambda e + 2G\frac{\partial u_z}{\partial z}$$
$$\tau_{xy} = G\left[\frac{\partial u_x}{\partial y} + \frac{\partial u_y}{\partial x}\right] : \tau_{yz} = G\left[\frac{\partial u_y}{\partial z} + \frac{\partial u_z}{\partial y}\right] : \tau_{zx} = G\left[\frac{\partial u_z}{\partial x} + \frac{\partial u_x}{\partial z}\right] \tag{2.5.1}$$

Strain-stress relations

$$\varepsilon_x = \frac{1}{E}\left[\sigma_x - \nu(\sigma_y + \sigma_z)\right] : \varepsilon_y = \frac{1}{E}\left[\sigma_y - \nu(\sigma_z + \sigma_x)\right] : \varepsilon_z = \frac{1}{E}\left[\sigma_z - \nu(\sigma_x + \sigma_y)\right]$$
$$\gamma_{xy} = \frac{\tau_{xy}}{G} = 2\varepsilon_{xy} : \gamma_{yz} = \frac{\tau_{yz}}{G} = 2\varepsilon_{yz} : \gamma_{zx} = \frac{\tau_{zx}}{G} = 2\varepsilon_{zx} \tag{2.5.2}$$

in which $e = \varepsilon_x + \varepsilon_y + \varepsilon_z$ and E = Young's modulus of elasticity.

2.5.2 Differential equations at a point (general)

Differential equations of equilibrium at point is given by

$$\begin{aligned}
&\frac{\partial \sigma_x}{\partial x} + \frac{\partial \tau_{xy}}{\partial y} + \frac{\partial \tau_{xz}}{\partial z} + X = 0 \\
&\frac{\partial \tau_{xy}}{\partial x} + \frac{\partial \sigma_y}{\partial y} + \frac{\partial \tau_{yz}}{\partial z} + Y = 0 \\
&\frac{\partial \tau_{xz}}{\partial x} + \frac{\partial \tau_{yz}}{\partial y} + \frac{\partial \sigma_z}{\partial z} + Z = 0
\end{aligned} \tag{2.5.3}$$

in which X, Y and Z are the body forces respectively in the x, y and z directions.

Equation (2.5.3) contains six unknowns with three equations, hence it is statically indeterminate [cannot be solved with the three equations of equilibrium of statics at a point, i.e. $\Sigma F_{x_i} = 0;\ \Sigma F_{y_i} = 0;\ \Sigma F_{z_i} = 0$]. We have to make use of compatible displacement relations with constitutive equations to obtain other relations which make it solvable.

2.5.3 Differential equations at a point (in terms of stresses)

Differential equations of equilibrium at a point in terms of stresses [obtained using compatibility equations, Equations (2.2.65)–(2.2.71) and equations of equilibrium, Equation (2.3.5) and constitutive equation, Equation (2.4.8)] can be written as

$$\begin{aligned}
&\nabla^2 \sigma_x + \frac{1}{1+\nu}\frac{\partial^2 \theta}{\partial x^2} = -\frac{\nu}{1+\nu}\left[\frac{\partial X}{\partial x} + \frac{\partial Y}{\partial y} + \frac{\partial Z}{\partial z}\right] - 2\frac{\partial X}{\partial x} \\
&\nabla^2 \sigma_y + \frac{1}{1+\nu}\frac{\partial^2 \theta}{\partial y^2} = -\frac{\nu}{1+\nu}\left[\frac{\partial X}{\partial x} + \frac{\partial Y}{\partial y} + \frac{\partial Z}{\partial z}\right] - 2\frac{\partial Y}{\partial y} \\
&\nabla^2 \sigma_z + \frac{1}{1+\nu}\frac{\partial^2 \theta}{\partial z^2} = -\frac{\nu}{1+\nu}\left[\frac{\partial X}{\partial x} + \frac{\partial Y}{\partial y} + \frac{\partial Z}{\partial z}\right] - 2\frac{\partial Z}{\partial z} \\
&\nabla^2 \tau_{xy} + \frac{1}{1+\nu}\frac{\partial^2 \theta}{\partial x \partial y} = -\left(\frac{\partial X}{\partial y} + \frac{\partial Y}{\partial x}\right); \quad \nabla^2 \tau_{yz} + \frac{1}{1+\nu}\frac{\partial^2 \theta}{\partial y \partial z} = -\left(\frac{\partial Z}{\partial y} + \frac{\partial Y}{\partial z}\right) \\
&\nabla^2 \tau_{zx} + \frac{1}{1+\nu}\frac{\partial^2 \theta}{\partial z \partial x} = -\left(\frac{\partial Z}{\partial x} + \frac{\partial X}{\partial z}\right)
\end{aligned} \tag{2.5.4}$$

in which, ν = Poisson ratio; $\theta = \sigma_x + \sigma_y + \sigma_z$ and $\lambda = \dfrac{E\nu}{(1+\nu)(1-2\nu)}$, Lame's parameter.

2.5.4 Differential equations at a point (in terms of displacements)

Using Equations (2.5.1) and (2.5.3), we can write

$$(\lambda + G)\frac{\partial e}{\partial x} + G\nabla^2 u_x + X = 0; \quad (\lambda + G)\frac{\partial e}{\partial y} + G\nabla^2 u_y + Y = 0;$$
$$(\lambda + G)\frac{\partial e}{\partial z} + G\nabla^2 u_z + Z = 0 \tag{2.5.5}$$

without body forces/or constant body forces.

Differentiating first with respect to x; second with respect to y, third with respect to z of Equation (2.5.5) and adding them, we have

$$(\lambda + 2G)\nabla^2 e = 0, \quad \text{and } e = \text{volumetric strain.} \tag{2.5.6}$$

Thus, volumetric expansion satisfies the Laplace's equation

$$\frac{\partial^2 e}{\partial x^2} + \frac{\partial^2 e}{\partial y^2} + \frac{\partial^2 e}{\partial z^2} = 0 \tag{2.5.7}$$

Equation (2.5.6) or Equation (2.5.7) is to be solved with appropriate boundary conditions.

2.5.4.1 Boundary conditions

a) In terms of stresses:

$$\bar{p}_x = \sigma_x \ell + \tau_{xy} m + \tau_{xz} n; \quad \bar{p}_y = \tau_{xy}\ell + \sigma_y m + \tau_{yz} n; \quad \bar{p}_z = \tau_{xz}\ell + \tau_{yz} m + \sigma_z n \tag{2.5.8}$$

in which, $\bar{p}_x$, $\bar{p}_y$, $\bar{p}_z$ are the surface tractions prescribed on some surface say, ds having direction cosines ℓ, m and n in x, y and z directions respectively.

b) In terms of displacements:

$$\bar{p}_x = \lambda e\ell + G\left[\frac{\partial u_x}{\partial x}\ell + \frac{\partial u_x}{\partial y}m + \frac{\partial u_x}{\partial z}n\right] + G\left[\frac{\partial u_x}{\partial x}\ell + \frac{\partial u_y}{\partial x}m + \frac{\partial u_z}{\partial x}n\right]$$
$$\bar{p}_y = \lambda e\ell + G\left[\frac{\partial u_y}{\partial x}\ell + \frac{\partial u_y}{\partial y}m + \frac{\partial u_y}{\partial z}n\right] + G\left[\frac{\partial u_x}{\partial y}\ell + \frac{\partial u_y}{\partial y}m + \frac{\partial u_z}{\partial y}n\right] \tag{2.5.9}$$
$$\bar{p}_z = \lambda e\ell + G\left[\frac{\partial u_z}{\partial x}\ell + \frac{\partial u_z}{\partial y}m + \frac{\partial u_z}{\partial z}n\right] + G\left[\frac{\partial u_x}{\partial z}\ell + \frac{\partial u_y}{\partial z}m + \frac{\partial u_z}{\partial z}n\right]$$

2.5.5 General solution

Equilibrium equations Equation (2.5.5) are satisfied by solutions proposed by Papkovitch (1932) and Neubar (1934):

$$u_x = \alpha_1 - \bar{\alpha}\frac{\partial}{\partial x}[\alpha_0 + x\alpha_1 + y\alpha_2 + z\alpha_3]$$

$$u_y = \alpha_2 - \bar{\alpha}\frac{\partial}{\partial y}[\alpha_0 + x\alpha_1 + y\alpha_2 + z\alpha_3] \tag{2.5.10}$$

$$u_z = \alpha_3 - \bar{\alpha}\frac{\partial}{\partial z}[\alpha_0 + x\alpha_1 + y\alpha_2 + z\alpha_3]$$

in which, $4\bar{\alpha} = 1/(1-\nu)$, and $\alpha_0, \alpha_1, \alpha_2, \alpha_3$ are harmonic solutions of

$$\nabla^2\alpha_0 = 0 : \nabla^2\alpha_1 = 0 : \nabla^2\alpha_2 = 0 : \nabla^2\alpha_3 = 0 \tag{2.5.11}$$

and this is also true for $\alpha_0 = 0$.

This is the general solution of Equation (2.5.5).

2.5.6 Two-dimensional cases

Let the problem be confined to the xy-plane (Figure 2.5.1).

a) Differential equations of equilibrium [a particular case of Equation (2.5.3)]:

$$\frac{\partial\sigma_x}{\partial x} + \frac{\partial\tau_{xy}}{\partial y} + X = 0 \tag{2.5.12}$$

$$\frac{\partial\tau_{xy}}{\partial x} + \frac{\partial\sigma_y}{\partial y} + Y = 0 \tag{2.5.13}$$

If the body force is due to gravity and it acts in the negative y-direction, we have

$$\frac{\partial\sigma_x}{\partial x} + \frac{\partial\tau_{xy}}{\partial y} = 0 \tag{2.5.14}$$

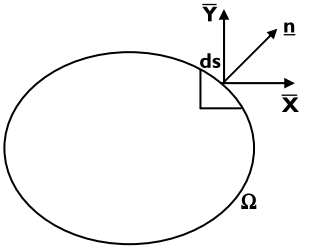


Figure 2.5.1

$$\frac{\partial \tau_{xy}}{\partial x} + \frac{\partial \sigma_y}{\partial y} - \rho g = 0 \tag{2.5.15}$$

b) Boundary conditions (Figure 2.5.1):
If ℓ and $\underline{m}$ are the d.c's of the normal $\underline{n}$ of the surface ds, we may write

$$\bar{X} = \ell\sigma_x + m\tau_{xy} \tag{2.5.16}$$

$$\bar{Y} = m\sigma_y + \ell\tau_{xy} \tag{2.5.17}$$

If the boundary is parallel to x-axis ($\underline{n}$ is in y-direction)

$$\ell = 0; \quad m = \pm 1 \tag{2.5.18}$$

If the boundary is parallel to y-axis ($\underline{n}$ is in x-direction)

$$\ell = \pm 1; \quad m = 0 \tag{2.5.19}$$

c) Compatibility equations
In terms of strains in two dimension

$$\frac{\partial^2 \varepsilon_x}{\partial y^2} = \frac{\partial^3 u}{\partial x \partial y^2} :: \frac{\partial^2 \varepsilon_y}{\partial x^2} = \frac{\partial^3 v}{\partial y \partial x^2} :: \frac{\partial^2 \gamma_{xy}}{\partial x \partial y} = \frac{\partial^3 u}{\partial x \partial y^2} + \frac{\partial^3 v}{\partial y \partial x^2}$$

$$\rightarrow \frac{\partial^2 \varepsilon_x}{\partial y^2} + \frac{\partial^2 \varepsilon_y}{\partial x^2} = \frac{\partial^2 \gamma_{xy}}{\partial x \partial y} \tag{2.5.20}$$

Equation (2.5.20) in terms of stresses:

$$\frac{\partial^2}{\partial x^2}\left(\sigma_y - \nu\,\sigma_x\right) + \frac{\partial^2}{\partial y^2}\left(\sigma_x - \nu\,\sigma_y\right) = 2(1+\nu)\frac{\partial^2 \tau_{xy}}{\partial x \partial y} \tag{2.5.21}$$

Differentiating Equation (2.5.14) with respect to x and (2.5.15) with respect to y and adding them

$$2\frac{\partial^2 \tau_{xy}}{\partial x \partial y} = -\left(\frac{\partial^2 \sigma_x}{\partial x^2} + \frac{\partial^2 \sigma_y}{\partial y^2}\right) \tag{2.5.22}$$

From Equations (2.5.21) and (2.5.22)

$$\left(\frac{\partial^2}{\partial x^2} + \frac{\partial^2}{\partial y^2}\right)(\sigma_x + \sigma_y) = 0 \tag{2.5.23}$$

➔ This is for *plane stress condition.*

For *plane strain condition*:

$$\varepsilon_z = 0 = \frac{\sigma_z}{E} - \frac{\nu}{E}(\sigma_x + \sigma_y) \quad \rightarrow \quad \sigma_z = \nu\,(\sigma_x + \sigma_y) \tag{2.5.24}$$

Hence,

$$\varepsilon_x = \frac{1-\nu^2}{E}\sigma_x - \frac{\nu\,(1+\nu)}{E}\sigma_y : \varepsilon_y = \frac{1-\nu^2}{E}\sigma_y - \frac{\nu\,(1+\nu)}{E}\sigma_x;$$
$$\gamma_{xy} = \frac{2(1+\nu)}{E}\tau_{xy} \tag{2.5.25}$$

Substituting Equation (2.5.25) in Equation (2.5.20), we get

$$(1-\nu)\left(\frac{\partial^2\sigma_x}{\partial y^2} + \frac{\partial^2\sigma_y}{\partial x^2}\right) - \nu\left(\frac{\partial^2\sigma_y}{\partial y^2} + \frac{\partial^2\sigma_x}{\partial x^2}\right) = 2\frac{\partial^2\tau_{xy}}{\partial x\partial y} = -\left(\frac{\partial^2\sigma_x}{\partial x^2} + \frac{\partial^2\sigma_y}{\partial y^2}\right)$$
$$\rightarrow \quad (1-\nu)\left\{\left(\frac{\partial^2\sigma_x}{\partial y^2} + \frac{\partial^2\sigma_y}{\partial x^2}\right) + \left(\frac{\partial^2\sigma_y}{\partial y^2} + \frac{\partial^2\sigma_x}{\partial x^2}\right)\right\} = 0 \tag{2.5.26}$$

Since $\nu \neq 1$, $\left(\frac{\partial^2}{\partial y^2} + \frac{\partial^2}{\partial x^2}\right)(\sigma_x + \sigma_y) = 0$; same as Equation (2.4.23).

All these calculations are valid for no-body forces or having a constant body force. Equation (2.5.26) is independent of material properties. This is the basis for using transparent materials in photoelastic experiments for studying stress distribution in real structural bodies. When we have body forces, it can be shown that, if $\bar{X}$ and $\bar{Y}$ are body forces, governing equations may be written as

$$\textit{Plane stress}: \left(\frac{\partial^2}{\partial x^2} + \frac{\partial^2}{\partial y^2}\right)(\sigma_x + \sigma_y) = -(1+\nu)\left(\frac{\partial\bar{X}}{\partial x} + \frac{\partial\bar{Y}}{\partial y}\right) \tag{2.5.27}$$

$$\textit{Plane strain}: \left(\frac{\partial^2}{\partial x^2} + \frac{\partial^2}{\partial y^2}\right)(\sigma_x + \sigma_y) = -\frac{1}{(1-\nu)}\left(\frac{\partial\bar{X}}{\partial x} + \frac{\partial\bar{Y}}{\partial y}\right) \tag{2.5.28}$$

Thus for gravity type of body forces, we have the governing equations of motion as

$$\frac{\partial\sigma_x}{\partial x} + \frac{\partial\tau_{xy}}{\partial y} = 0; \quad \frac{\partial\tau_{xy}}{\partial x} + \frac{\partial\sigma_y}{\partial y} - \rho g = 0$$

$$\left(\frac{\partial^2}{\partial x^2} + \frac{\partial^2}{\partial y^2}\right)(\sigma_x + \sigma_y) = 0 \tag{2.5.29}$$

2.6 THEOREMS OF ELASTICITY

2.6.1 Principles of superposition

If we want to solve an elasticity problem in terms of stress components [Equation (2.5.3)], we have to satisfy

1 Equations of equilibrium: 3-equations;
2 Compatibility conditions: 6-equations;
3 Boundary conditions.

Let $\sigma_x, \sigma_y, \ldots, \tau_{zx}$ are the stresses so determined for X, Y, Z body forces and $\bar{p}_x, \bar{p}_y, \bar{p}_z$ surface tractions.

Also let $\sigma_{x'}, \sigma_{y'}, \ldots, \tau_{z'x'}$ are the stresses determined for X', Y', Z' body forces and $\bar{p}_x, \bar{p}_y, \bar{p}_z$ surface traction.

➔ Both for the same solid.

Then the stress components:

$\sigma_{x'} + \sigma_x, \sigma_{x'} + \sigma_x, \ldots, \tau_{z'x'} + \tau_{zx}$ will represent stress due to $X' + X, Y' + Y$, and $Z' + Z$ body forces and $\bar{p}_{x'} + \bar{p}_x, \bar{p}_{y'} + \bar{p}_y$ and $\bar{p}_{z'} + \bar{p}_z$ surface tractions.

This holds good, as the governing differential equation, Equation (2.5.3) and boundary conditions are linear. As for example:

$$\begin{aligned}
&\frac{\partial \sigma_{x'}}{\partial x} + \frac{\partial \tau_{x'y'}}{\partial y} + \frac{\partial \tau_{x'z'}}{\partial z} + X' = 0 \\
&\frac{\partial \tau_{x'y'}}{\partial x} + \frac{\partial \sigma_{y'}}{\partial y} + \frac{\partial \tau_{y'z'}}{\partial z} + Y' = 0 \\
&\frac{\partial \tau_{x'z'}}{\partial x} + \frac{\partial \tau_{y'z'}}{\partial y} + \frac{\partial \sigma_{z'}}{\partial z} + Z' = 0
\end{aligned} \tag{2.6.1}$$

Adding Eqns. (2.5.3) and (2.6.1), we have

$$\begin{aligned}
&\frac{\partial (\sigma_{x'} + \sigma_x)}{\partial x} + \frac{\partial (\tau_{x'y'} + \tau_{xy})}{\partial y} + \frac{\partial (\tau_{x'z'} + \tau_{xz})}{\partial z} + (X' + X) = 0 \\
&\frac{\partial (\tau_{x'y'} + \tau_{xy})}{\partial x} + \frac{\partial (\sigma_{y'} + \sigma_y)}{\partial y} + \frac{\partial (\tau_{y'z'} + \tau_{yz})}{\partial z} + (Y' + Y) = 0 \\
&\frac{\partial (\tau_{x'z'} + \tau_{xz})}{\partial x} + \frac{\partial (\tau_{y'z'} + \tau_{yz})}{\partial y} + \frac{\partial (\sigma_{z'} + \sigma_z)}{\partial z} + (Z' + Z) = 0
\end{aligned} \tag{2.6.2}$$

Similarly boundary conditions are

$$\begin{aligned}
\bar{p}_{x'} + \bar{p}_x &= (\sigma_{x'} + \sigma_x)\ell + (\tau_{x'y'} + \tau_{xy})m + (\tau_{x'z'} + \tau_{xz})n \\
\bar{p}_{y'} + \bar{p}_y &= (\tau_{x'y'} + \tau_{xy})\ell + (\sigma_{y'} + \sigma_y)m + (\tau_{y'z'} + \tau_{yz})n \\
\bar{p}_{z'} + \bar{p}_z &= (\tau_{x'z'} + \tau_{xz})\ell + (\tau_{y'z'} + \tau_{yz})m + (\sigma_{z'} + \sigma_z)n
\end{aligned} \tag{2.6.3}$$

where we have not made any distinction between the position and form of element before and after loading i.e. we kept ℓ, m, n same in all the cases.

→ This is an instance of the principle of super position. Naturally this is valid for small deformations.

2.6.2 Strain energy

2.6.2.1 With no body forces

Consider an elemental cube with no body forces as shown in Figure 2.6.1:

With reference to Figure 2.6.2;

$$\text{Workdone} = \frac{1}{2}(\sigma_x\, dydz)\varepsilon_x\, dx :: \text{Work done on displacement } dx \text{ by } p = p\, dx$$

$$\rightarrow \quad dU = \frac{1}{2}\sigma_x\varepsilon_x\, dxdydz :: \text{Work done for displacement } x = \int_0^x \frac{p_x z}{x} dz = \frac{1}{2}p_x x. \tag{2.6.4}$$

Now, what happens to this work?

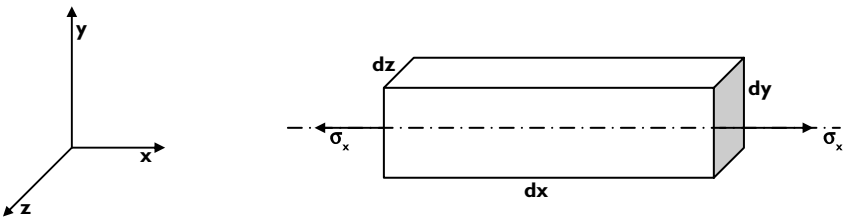


Figure 2.6.1

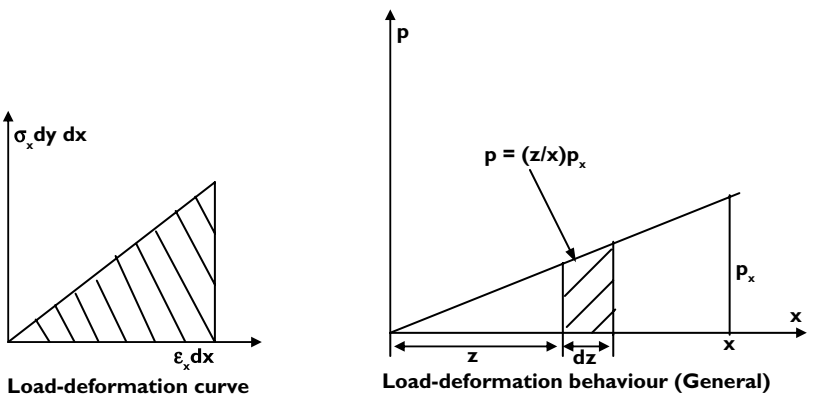


Figure 2.6.2 Development of strain energy.

An adiabatic compression causes a rise in temperature in a steel bar, but this rise of temperature is rather insignificant. However, the original temperature in steel can be restored if we take away heat and this change in temperature due to this will alter the strain, but only a very small fraction of the adiabatic strain. This must be the case, or else there would have been a very significant difference between adiabatic and isothermal moduli of elasticity. In fact we have

$$\frac{E_{\text{Adi}} - E_{\text{Iso}}}{E_{\text{Adi}}} \approx 0.26 \tag{2.6.5}$$

Thus, we can ignore such differences and conclude that the work done on an element, and stored in it, will be called *strain energy*. This element remains elastic and no kinetic energy is expected to be developed. Same consideration is applicable to all the six stress-components.

Conservation of energy requires that the work cannot depend on the order in which the forces are applied but only on the final configuration or else one can load in one sequence and unload in another leading to large amount of work. Hence a net amount of work would have been gained from the element in a complete cycle.

Hence,

$$dV = \frac{1}{2}[\sigma_x\varepsilon_x + \sigma_y\varepsilon_y + \sigma_z\varepsilon_z + \tau_{xy}\gamma_{xy} + \tau_{yz}\gamma_{yz} + \tau_{zx}\gamma_{zx}]dx\,dy\,dz. \tag{2.6.6}$$

2.6.2.2 *Strain energy for materials with body forces*

Consider an elemental cube having body forces as shown in Fig. 2.6.3. In comparison to its no-body force counterpart stress will vary through the body.

Force-flux on face 2: $\frac{1}{2}(\sigma_x u)_2 dydz$: Force-flux on face 1: $-\frac{1}{2}(\sigma_x u)_1 dydz$

Work done by the total force for the two faces $= \frac{1}{2}[(\sigma_x u)_2 - (\sigma_x u)_1]dydz$.

This can be written at a point as

$$\lim_{\Delta x \to 0}\left[\frac{(\sigma_x u_x)_2 - (\sigma_x u)_1}{\Delta x}\right]\Delta x dydz = \frac{1}{2}\frac{\partial(\sigma_x u)}{\partial x}dxdydz$$

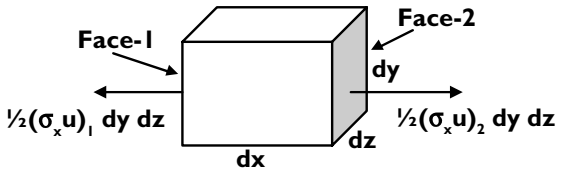


Figure 2.6.3 Elemental cube with body forces.

Similarly work done by shear forces can be written as

$$\frac{1}{2}\frac{\partial}{\partial x}(\tau_{xy}v + \tau_{xz}w)dxdydz.$$

Considering all such forces and adding all resulting works done, we have

$$\frac{1}{2}\left[\frac{\partial}{\partial x}(\sigma_x u + \tau_{xy}v + \tau_{xz}w) + \frac{\partial}{\partial y}(\sigma_y v + \tau_{yz}w + \tau_{xy}u) + \frac{\partial}{\partial z}(\sigma_z w + \tau_{yz}v + \tau_{xz}u)\right] dxdydz$$

Work done by the body forces $= \frac{1}{2}[Xu + Yv + Zw]\,dxdydz.$
$\therefore$ Total work done on the element

$$= \frac{1}{2}\left[\sigma_x\frac{\partial u}{\partial x} + \sigma_y\frac{\partial v}{\partial y} + \sigma_z\frac{\partial w}{\partial z} + \tau_{xy}\left(\frac{\partial v}{\partial x} + \frac{\partial u}{\partial y}\right) + \tau_{yz}\left(\frac{\partial v}{\partial z} + \frac{\partial w}{\partial y}\right) + \tau_{zx}\left(\frac{\partial w}{\partial x} + \frac{\partial u}{\partial z}\right)\right] dxdydz + \frac{1}{2}\left[u\left(\frac{\partial \sigma_x}{\partial x} + \frac{\partial \tau_{xy}}{\partial y} + \frac{\partial \tau_{xz}}{\partial z} + X\right) + v\left(\frac{\partial \tau_{xy}}{\partial x} + \frac{\partial \sigma_y}{\partial y} + \frac{\partial \tau_{yz}}{\partial z} + Y\right) + w\left(\frac{\partial \tau_{xz}}{\partial x} + \frac{\partial \tau_{yz}}{\partial y} + \frac{\partial \sigma_z}{\partial z} + Z\right)\right] dxdydz.$$

Imposing equilibrium equation, Equation (2.5.3), we get

$$dV = \frac{1}{2}[\sigma_x\varepsilon_x + \sigma_y\varepsilon_y + \sigma_z\varepsilon_z + \tau_{xy}\gamma_{xy} + \tau_{yz}\gamma_{yz} + \tau_{zx}\gamma_{zx}]dxdydz$$

➔ Same for both with or without body forces.
Strain energy density is defined as

$$V_0 = \frac{1}{2}[\sigma_x\varepsilon_x + \sigma_y\varepsilon_y + \sigma_z\varepsilon_z + \tau_{xy}\gamma_{xy} + \tau_{yz}\gamma_{yz} + \tau_{zx}\gamma_{zx}] \tag{2.6.7}$$

→ This is also simply defined as *strain energy*.

2.6.2.3 Strain energy in terms of strains

Strain energy density can be expressed in terms of strains by using Equation (2.5.1) as

$$V_0 = \frac{1}{2}\lambda e^2 + G(\varepsilon_x^2 + \varepsilon_y^2 + \varepsilon_z^2) + \frac{G}{2}(\gamma_{xy}^2 + \gamma_{yz}^2 + \gamma_{zx}^2) \tag{2.6.8}$$

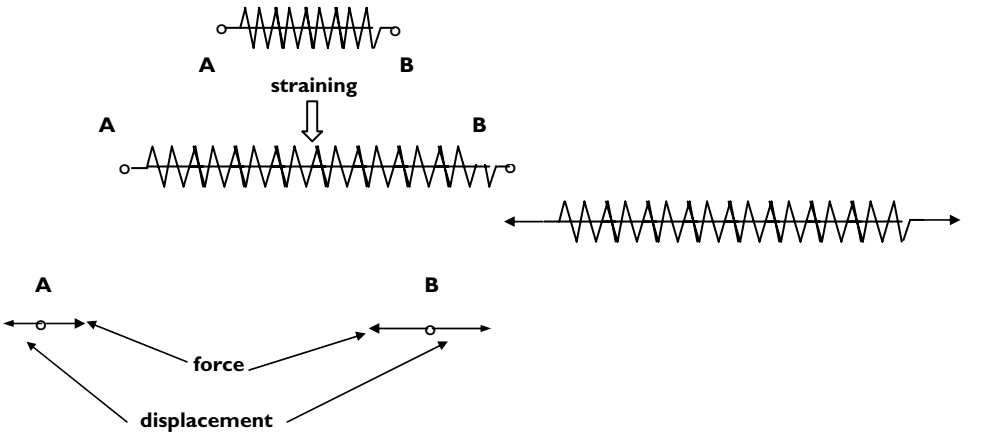


Figure 2.6.4 Strain energy concept.

Some interesting findings

$$\frac{\partial V_0}{\partial \varepsilon_x} = \lambda e + 2G\varepsilon_x = \sigma_x \text{ and it is true for other strain components.} \tag{2.6.9}$$

$$\frac{\partial V}{\partial \sigma_x} = \frac{\sigma_x}{E} - \frac{\nu}{E}(\sigma_y + \sigma_x) = \varepsilon_x \text{ and it is true for other stress components as well.} \tag{2.6.10}$$

Total strain energy of a body is given by, $V = \int_V V_0 \, dxdydz$.

The effect or influence of strain energy can be studied as follows:

Consider two mass points in the body, A and B and follow the sequence of free body diagrams shown in Figure 2.6.4.

Thus work done by the particle (mass point) is $= -V =$ negative of strain energy.

2.6.2.4 *Yielding of material in terms of energy*

An isotropic material can sustain very large hydrostatic pressure without yielding. We may, now, split the energy into two parts, one due to change in volume and the other as a result of distortion and consider the second part in determining the strength of the material. In this regard, consider the deviatoric part of the stress tensor given in Equation (2.3.22). Change in volume is entirely due to σ_h i.e. Strain energy due to change in volume

$$= \frac{1}{2} e\sigma_h = \frac{3(1-2\nu)}{2E}\sigma_h^2 = \frac{1-2\nu}{6E}(\sigma_x + \sigma_y + \sigma_z)^2 \tag{2.6.11}$$

Subtracting Equation (2.6.11) from the total strain energy density and using the identity:

$$xy + yz + zx = -\frac{1}{2}[(x-y)^2 + (y-z)^2 + (z-x)^2], \text{we have}$$

$$V_0 - \frac{1-2\nu}{6E}(\sigma_x + \sigma_y + \sigma_z)^2 = \frac{1+\nu}{6E}[(\sigma_x - \sigma_y)^2 + (\sigma_y - \sigma_y)^2 + (\sigma_z - \sigma_x)^2] + \frac{1}{2G}[\tau_{xy}^2 + \tau_{yz}^2 + \tau_{zx}^2] = V_0^{\text{distortion}} \tag{2.6.12}$$

In a particular case, when only, $\sigma_x \neq 0$ and all other stress components are absent, we have,

$$V_0^{\text{distortion}} = \frac{1+\nu}{6E}(2\sigma_x)^2 = \frac{1+\nu}{3E}\sigma_x^2 \tag{2.6.13}$$

$$\text{Similarly when only, } \tau_{xy} \neq 0, \text{we have } V_0^{\text{distortion}} = \frac{1}{2G}\tau_{xy}^2 \tag{2.6.14}$$

If we assume that a material fails when a level of distortional energy reaches a definite level, the ratio of stresses are given by

$$\tau_{xy} = \frac{1}{\sqrt{3}}\sigma_x \tag{2.6.15}$$

Experiments with steel verify this statement.

2.6.3 Virtual work

2.6.3.1 For particles/mass points

Definition: If a particle is in equilibrium, the total work of all the forces on the particle in any virtual displacement vanishes.

If $\delta u, \delta v$ and δw are the components of virtual displacements and ΣF_x, ΣF_y and ΣF_z are the sums of projections of forces in x, y and z directions, respectively on the particle, the principle stated above results in

$$\delta u \sum F_x = 0; \quad \delta v \sum F_y = 0; \quad \delta w \sum F_z = 0. \tag{2.6.16}$$

These conditions are satisfied for any virtual displacement, if

$$\sum F_x = 0; \quad \sum F_y = 0; \quad \sum F_z = 0. \tag{2.6.17}$$

2.6.3.2 *Virtual strains*

Virtual strains may be defined as

$$\delta\varepsilon_x = \frac{\partial \delta u}{\partial x}; \quad \delta\varepsilon_y = \frac{\partial \delta v}{\partial y}; \quad \delta\varepsilon_z = \frac{\partial \delta w}{\partial z};$$

$$\delta\gamma_{xy} = \left(\frac{\partial \delta v}{\partial x} + \frac{\partial \delta u}{\partial y}\right); \quad \delta\gamma_{yz} = \left(\frac{\partial \delta v}{\partial z} + \frac{\partial \delta w}{\partial y}\right); \quad \delta\gamma_{zx} = \left(\frac{\partial \delta w}{\partial x} + \frac{\partial \delta u}{\partial z}\right) \tag{2.6.18}$$

and associated virtual work is given by

$$(\sigma_x \delta\varepsilon_x + \sigma_x \delta\varepsilon_y + \sigma_x \delta\varepsilon_z + \tau_{xy}\delta\gamma_{xy} + \tau_{yz}\delta\gamma_{yz} + \tau_{zx}\delta\gamma_{zx})dxdydz \tag{2.6.19}$$

The work done by mutual forces on particles, as mentioned earlier

$$= -\int_V \delta V_0 dxdydz \tag{2.6.20}$$

Thus, the total virtual work:

$$\int_S [\bar{p}_x \delta u + \bar{p}_y \delta v + \bar{p}_z \delta w]dS + \int_V [X\delta u + Y\delta v + Z\delta w]dV - \int_V \delta V_0 dV = 0 \tag{2.6.21}$$

Since during deformation, in the equation above, the forces and actual stresses were held constant, we may write

$$\delta\left[\int_V V_0 dV - \int_S (\bar{p}_x u + \bar{p}_y v + \bar{p}_x w)dS - \int_V (Xu + Yv + Zw)\, dV\right] = 0 \tag{2.6.22}$$

in which,
the first term indicates → Potential energy of deformation (strain energy);
the second term indicates → Potential energy of surface forces;
the third term indicates → Potential energy of body forces.
That is,

$$\delta\,[\text{Total potential energy of the system}] = 0 \tag{2.6.23}$$

The virtual displacement and corresponding virtual work imply the use of arbitrary multiplier represented by δu, δv and δw with the equation of equilibrium [Equation (2.5.3)]. We may regard them as *variations of the actual displacement u, v and w*.

Thus, Equation (2.6.21) infers that the actual displacement u, v and w under the given external forces and given mode of support are such that the first order variation of the total potential energy is zero [Equation (2.6.22)] for any virtual displacement or *the potential energy is stationary*.

2.6.3.3 Stability of equilibrium

a) Physical argument:
Consider a conservative system. The system is subjected to an impulsive disturbance followed by actual variations of the equilibrium displacement.

Now, we have, Potential energy + Kinetic energy = constant.

On departing from the equilibrium configuration, two possibilities may occur

1 P.E. increases : increases from a value which is minimum
K.E. decreases → as PE + KE = constant.
2 P.E. decreases : decreases from a value which is maximum
K.E. increases → as PE + KE = constant.

This is depicted in Figure 2.6.5.

Thus, *the stability implies that the potential energy is the minimum in the equilibrium position*. The maximum potential energy implies an unstable configuration.
In the usage above, we have assumed that in the motion following the disturbance:

1 The body and surface forces go with the material elements on which they act in the equilibrium configuration,
2 The body and surface forces remain unchanged in magnitude and direction.

b) Mathematical arguments
Consider the strain energy per unit volume under plane stress condition. The following an impulsive disturbance, after a while, the equilibrium strain components increase by $\delta\varepsilon_x$, $\delta\varepsilon_y$ and $\delta\gamma_{xy}$. Under equilibrium configuration

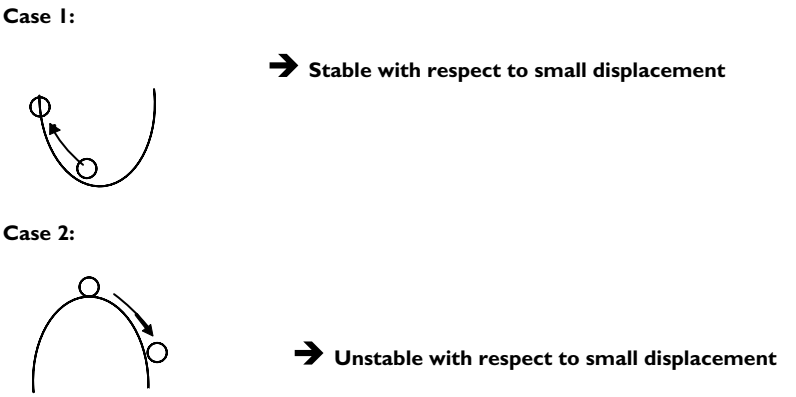


Figure 2.6.5

$$V_0 = \frac{E}{2(1-\nu^2)}[\varepsilon_x^2 + \varepsilon_y^2 + 2\nu\varepsilon_x\varepsilon_y] + \frac{G}{2}\gamma_{xy}^2 \tag{2.6.24}$$

Changed new value, following the disturbance is

$$V_0' = \frac{E}{2(1-\nu^2)}[(\varepsilon_x + \delta\varepsilon_x)^2 + (\varepsilon_y + \delta\varepsilon_y)^2 + 2\nu(\varepsilon_x + \delta\varepsilon_x)(\varepsilon_y + \delta\varepsilon_y)] + \frac{G}{2}(\gamma_{xy} + \delta\gamma_{xy})^2 \tag{2.6.25}$$

Subtracting the *equilibrium value* from V_0'

$$\underbrace{\frac{E}{2(1-\nu^2)}[2\varepsilon_x\delta\varepsilon_x + 2\nu(\varepsilon_x\delta\varepsilon_y + \varepsilon_y\delta\varepsilon_x) + 2\varepsilon_y\delta\varepsilon_y] + \frac{G}{2}2\gamma_{xy}\delta\gamma_{xy}}_{\text{I}} + \underbrace{\frac{E}{2(1-\nu^2)}[(\delta\varepsilon_x)^2 + (\delta\varepsilon_y)^2 + 2\nu(\delta\varepsilon_x)(\delta\varepsilon_y)] + \frac{G}{2}(\delta\gamma_{xy})^2}_{\text{II}} \tag{2.6.26}$$

I—first order increment corresponding to $(\delta V_0 dxdydz)$

II—second order increment may be written as : $[\delta\varepsilon_x + \nu\delta\varepsilon_x]^2 + (1-\nu^2)(\delta\varepsilon_x)^2$

➔ This is always positive.

In Equation (2.6.25), the first order increment vanishes since actual displacement δu, δv and δw can be taken as actual displacements. The second order increment is always positive. Hence, we have the stability in the sense defined earlier. The conclusion we made is, however, depend on Hooke's law. For nonlinear materials increments higher than second order would be necessary.

2.6.3.4 *Castigliano's Theorem*

Consider stresses in a body under equilibrium. We know that the developed stresses should satisfy the following:

a 3-partial differential equations [Equation (1.4.3)]
b boundary conditions.

These are however, not sufficient for determining stress components having six independent quantities. We may, thus, find many stress distributions satisfying a) and b).

Castigliano's theorem distinguishes the true distribution from all other statically possible stress distributions satisfying Equation (2.5.3).

The variation of strain energy, corresponding to variation of stress components which preserve equilibrium is given by

$$\delta V = \int_S (u\delta\bar{p}_x + v\delta\bar{p}_y + w\delta\bar{p}_z)dS \tag{2.6.27}$$

The true stresses are those which satisfy Equation (2.6.27). These variations are certainly mathematical and not physical. The physical stress variations by varying the boundary loading are subjected to more restrictions than those of equations of equilibrium.

Mathematically,

$$V = \frac{1-2\nu}{6E}(\sigma_x+\sigma_y+\sigma_z)^2 + \frac{1+\nu}{6E}[(\sigma_x-\sigma_y)^2+(\sigma_y-\sigma_z)^2+(\sigma_z-\sigma_x)^2] + \frac{1}{2G}[\tau_{xy}^2+\tau_{yz}^2+\tau_{zx}^2] \tag{2.6.28}$$

is a function of six independent variables and strain energy has a variation whenever any of these six variable, individually or in any combination change, no matter how.

Example 2.6.1

a A prismatic bar, as shown in Figure 2.6.6, is subjected to an axial force, F.
Stress = σ_x = F/A, uniform over the cross-section along the length.

$$V = \int_V \frac{1}{2E}(\sigma_x)^2\,dV = \frac{1}{2E}\int_0^{\ell}\left(\frac{F}{A}\right)^2 A\,dx = \frac{F^2\ell}{2AE}$$

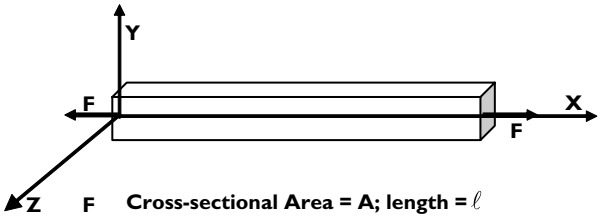


Figure 2.6.6

b An elongation Δ_x is imposed on the bar.
We have $\varepsilon_x = \frac{\Delta_x}{\ell}$; $\varepsilon_y = -\nu\frac{\Delta_x}{\ell}$; $\varepsilon_z = -\nu\frac{\Delta_x}{\ell}$; $\gamma_{xy} = \gamma_{yz} = \gamma_{zx} = 0$.

$$\therefore V = \int_V \left[\frac{1}{2}\lambda e^2 + G(\varepsilon_x^2+\varepsilon_y^2+\varepsilon_z^2) + \frac{G}{2}(\gamma_{xy}^2+\gamma_{yz}^2+\gamma_{zx}^2)\right]dV$$

$$= \int_V \left[\frac{1}{2}\lambda e^2 + G\left\{\frac{\Delta_x^2}{\ell^2}(1+2\nu^2)\right\} + 0\right]dV = \frac{EA}{2\ell}\Delta_x^2.$$

Example 2.6.2

A beam loaded as shown in Figure 2.6.7:

Normal stress: $\sigma_x = -\dfrac{M_z y}{I_z}$ **: Shear stress :** $\tau_{xy} = \dfrac{V_y Q_y}{bI_z}$

Strain energy :

$$V_\sigma = \int_V \frac{M_z^2 y^2}{2EI_z^2} dV = \int_0^\ell \left[\frac{M_z^2}{2EI_z^2} \int_A y^2 dA \right] dx = \int_0^\ell \frac{M_z^2}{2EI_z} dx$$

$$V_\tau = \int_V \frac{1}{2G} \left[\frac{V_y Q_y}{bI_z} \right]^2 dxdydz = \frac{1}{2GI_z^2} \left[\int_A \frac{Q_y^2}{b^2} dA \right] \left[\int_0^\ell V_y^2 dx \right]$$

V_σ and V_τ will be evaluated using the variations of M_z, V_y, and Q_y.

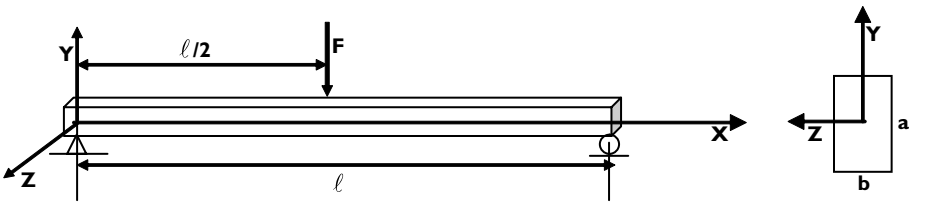


Figure 2.6.7

Solution:

For a particular case, if we assume: $\ell = 4$ m; $F = 100$ kN, $E = 200$ GPa, $G = 100$ GPa, $a = b = 100$ mm.

$$V_\sigma = \int_0^{\ell/2} \frac{\left(\frac{F}{2}x\right)^2}{2EI_z} dx + \int_{\ell/2}^{\ell} \frac{\left[\frac{Fx}{2} - F(x - \ell/2)\right]^2}{2EI_z} dx = \frac{F^2\ell^3}{96EI_z} = 4 \text{ kN} - \text{m}.$$

$$V_\tau = \frac{1}{2GI_z^2} \left(\frac{b^3}{4} \int_{-a/2}^{a/2} \left[\frac{a^2}{4} - y^2 \right]^2 dy \right) \left(\int_0^\ell \frac{F^2}{4} dx \right)$$

$$= \frac{3F^2\ell}{20\ \text{Gab}} = 0.006 \text{ kN} - \text{m}$$

Hence, $V_\sigma \gg V_\tau$.

So we ignore V_τ. In our normal calculation with beam for its flexural dominance.

Example 2.6.3

a) A rod subjected to torsion M_x.

$$V = \frac{1}{2G}\int_V \tau_{xy}^2 dV = \frac{1}{2G}\int_V \left(\frac{M_x r}{I_P}\right)^2 dV = \frac{M_x^2 \ell}{2GI_P},$$

where I_P = polar moment of area.

b) The bar(shaft) is subjected to a angle of twist Δ_ϕ over a length ℓ.

$$\gamma = \frac{M_x r}{GI_P} = \frac{\Delta_\phi GI_P}{\ell}\frac{r}{GI_P} = \frac{\Delta_\phi r}{\ell} \quad \rightarrow V = \int_V \frac{G}{2}\left(\frac{\Delta_\phi r}{\ell}\right)^2 dV = \Delta_\phi^2 \frac{GI_P}{2\ell}.$$

2.6.3.5 *Uniqueness of elasticity solutions*

From the given surface and body forces, let us suppose that we have found two sets of solutions given by

$$\begin{aligned} &\text{I} \quad \sigma_x', \sigma_y', \sigma_z', \ldots, \tau_{zx}'; \quad \text{with } \bar{p}_x, \bar{p}_y, \bar{p}_z, X, Y, Z \\ &\text{II} \quad \sigma_x'', \sigma_y'', \sigma_z'', \ldots, \tau_{zx}''; \quad \text{with } \bar{p}_x, \bar{p}_y, \bar{p}_z, X, Y, Z \end{aligned} \tag{2.6.29}$$

Stresses must satisfy Equation (2.5.3) and hence

$$\frac{\partial \sigma_x'}{\partial x} + \frac{\partial \tau_{xy}'}{\partial y} + \frac{\partial \tau_{xz}'}{\partial z} + X = 0; \quad \frac{\partial \tau_{xy}'}{\partial x} + \frac{\partial \sigma_y'}{\partial y} + \frac{\partial \tau_{yz}'}{\partial z} + Y = 0;$$

$$\frac{\partial \tau_{xz}'}{\partial x} + \frac{\partial \tau_{yz}'}{\partial y} + \frac{\partial \sigma_z'}{\partial z} + Z = 0$$

with,

$$\bar{p}_x = \sigma_x' \ell + \tau_{xy}' m + \tau_{xz}' n; \quad \bar{p}_y = \tau_{xy}' \ell + \sigma_y' m + \tau_{yz}' n; \quad \bar{p}_z = \tau_{xz}' \ell + \tau_{yz}' m + \sigma_z' n \tag{2.6.30}$$

$$\frac{\partial \sigma''_x}{\partial x} + \frac{\partial \tau''_{xy}}{\partial y} + \frac{\partial \tau''_{xz}}{\partial z} + X = 0; \quad \frac{\partial \tau''_{xy}}{\partial x} + \frac{\partial \sigma''_y}{\partial y} + \frac{\partial \tau''_{yz}}{\partial z} + Y = 0;$$

$$\frac{\partial \tau''_{xz}}{\partial x} + \frac{\partial \tau''_{yz}}{\partial y} + \frac{\partial \sigma''_z}{\partial z} + Z = 0$$

with

$$\bar{p}_x = \sigma''_x \ell + \tau''_{xy} m + \tau''_{xz} n; \quad \bar{p}_y = \tau''_{xy} \ell + \sigma''_y m + \tau''_{yz} n; \quad \bar{p}_z = \tau''_{xz} \ell + \tau''_{yz} m + \sigma''_z n \tag{2.6.31}$$

Subtracting (2.6.31) from (2.6.30), we have

$$\begin{aligned}
&\frac{\partial(\sigma'_x - \sigma''_x)}{\partial x} + \frac{\partial(\tau'_{xy} - \tau''_{xy})}{\partial y} + \frac{\partial(\tau'_{xz} - \tau''_{xz})}{\partial z} + X = 0; \\
&\frac{\partial(\tau'_{xy} - \tau''_{xy})}{\partial x} + \frac{\partial(\sigma'_y - \sigma''_y)}{\partial y} + \frac{\partial(\tau'_{yz} - \tau''_{yz})}{\partial z} + Y = 0 \\
&\frac{\partial(\tau'_{xz} - \tau''_{xz})}{\partial x} + \frac{\partial(\tau'_{yz} - \tau''_{yz})}{\partial y} + \frac{\partial(\sigma'_z - \sigma''_z)}{\partial z} + Z = 0
\end{aligned} \tag{2.6.32}$$

Surface tractions

$$\begin{aligned}
&(\sigma'_x - \sigma''_x)\ell + (\tau'_{xy} - \tau''_{xy})m + (\tau'_{xz} - \tau''_{xz})n = 0 \\
&(\tau'_{xy} - \tau''_{xy})\ell + (\sigma'_y - \sigma''_y)m + (\tau'_{yz} - \tau''_{yz})n = 0 \\
&(\tau'_{xz} - \tau''_{xz})\ell + (\tau'_{yz} - \tau''_{yz})m + (\sigma'_z - \sigma''_z)n = 0
\end{aligned} \tag{2.6.33}$$

➔ all external stresses vanish.

So, we obtain a solution in Equation (2.6.32) without any surface traction and body forces.

Conditions of equilibrium is also satisfied by the corresponding strain components i.e. $(\varepsilon'_x - \varepsilon''_x), (\varepsilon'_y - \varepsilon''_y), \ldots, (\gamma'_{xz} - \gamma''_{xz})$. Work done by zero surface and body forces are also zero and it follows from Equation (2.6.23) that $\int_V V_0 dV$ should vanish. Thus, it implies that $\int_V V_0 dV = 0$. Now, V_0 is positive for all states of strain and the integral can vanish only if V_0 vanishes at all points of the body. This requires that each component $(\varepsilon'_x - \varepsilon''_x), (\varepsilon'_y - \varepsilon''_y), \ldots$, and $(\gamma'_{xz} - \gamma''_{xz})$ should be zero.

So these two states of stresses are not possible and the solution is unique.

2.6.3.6 Reciprocal theorem (Maxwell-Betti's Theorem)

Assume an elastic body subjected to two systems of forces:

1 Surface forces: $\bar{p}'_x, \bar{p}'_y, \bar{p}'_z$
  Body forces: X', Y', Z'

Resulting in: $u', v', w', \varepsilon'_x, \varepsilon'_y, \ldots, \sigma'_x, \sigma'_y, \ldots, \tau'_{xz}$.

2 Surface forces: $\bar{p}''_x, \bar{p}''_y, \bar{p}''_z$
Body forces : X'', Y'', Z''
Results in :: u'', v'', w'', $\varepsilon''_x, \varepsilon''_y, \ldots, \sigma''_x, \sigma''_y, \ldots, \tau''_{xz}$.

If we define

$$\int_S [\bar{p}'_x u'' + \bar{p}'_y v'' + \bar{p}'_z w'']dS + \int_V [X'u'' + Y'v'' + Z'w'']dw = E_2^1 \tag{2.6.34}$$

$' \rightarrow$ designates system I: $'' \rightarrow$ designate system II.

and $$\int_S [\bar{p}''_x u' + \bar{p}''_y v' + \bar{p}''_z w']dS + \int_V [x''u' + y''v' + z''w']dw = E_1^2 \tag{2.6.35}$$

The reciprocal theorem states that $E_2^1 = E_1^2$ (2.6.36)

Physically the theorem may be stated as the "*work of the first state of forces on displacement of the second state ($E_{\underline{2}}^{\underline{1}}$) is same as the work of the second state of forces on displacement of the first state ($E_{\underline{1}}^{\underline{2}}$)*".

Example 2.6.4

Consider a prismatic bar of cross-section (hxh) and length ℓ is laterally loaded as shown in Figure 2.6.8. Find the elongation of the bar [A = cross-sectional area].

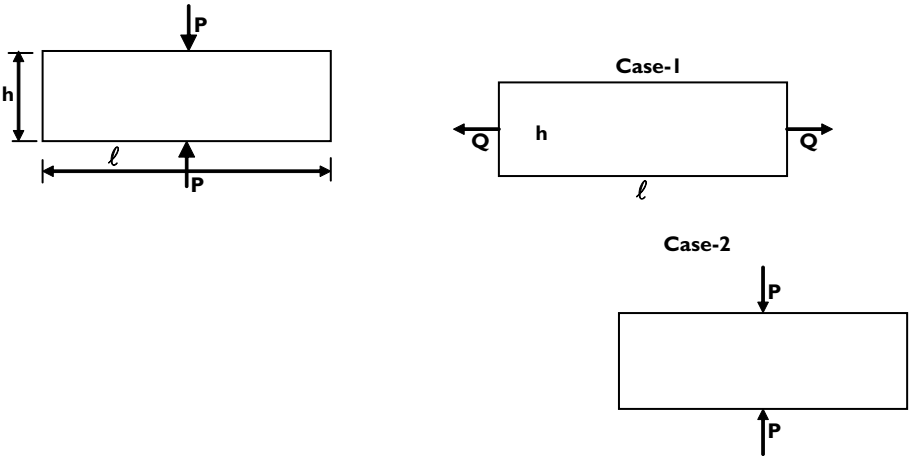


Figure 2.6.8

***Case 1*:** Lateral contraction, $\delta_1 = \dfrac{\nu Q h}{AE}$;
***Case 2*:** Lateral elongation $= \delta_2$, say.
From Reciprocal theorem, we have, $P\delta_1 = Q\delta_2$. ➔ $\delta_2 = \dfrac{\nu P h}{AE}$.
This is independent of the shape of cross-section.

2.7 MECHANICS OF HOMOGENEOUS ISOTROPIC ELASTIC BODIES

Soil medium is idealized as an elastic half space and an analytical solution is obtained for the problem of dynamic load acting on the surface of a homogeneous and isotropic continuum.

An elastic body returns to its unique natural state when all external loads are removed. All stresses, strains and particle displacements are measured from this natural state and have zero values at its natural state. A deformed body is described in two different ways, namely, the material description and the spatial description. The instantaneous geometric location of a particle is taken as a material point or simply point. A body is composed of particles. The particles in a body can be labeled through a Cartesian frame of reference and identify the coordinates (ξ_1, ξ_2, ξ_3) of the particles at a time $t = 0$. At a later time the particle moves to another point whose coordinates are (x_1, x_2, x_3), referred to the same coordinate system. The relation:

$$x_i = \bar{x}_i(\xi_1, \xi_2, \xi_3, t), \quad i = 1, 2, 3: \tag{2.7.1}$$

connects the configuration of the body at different instants of time.

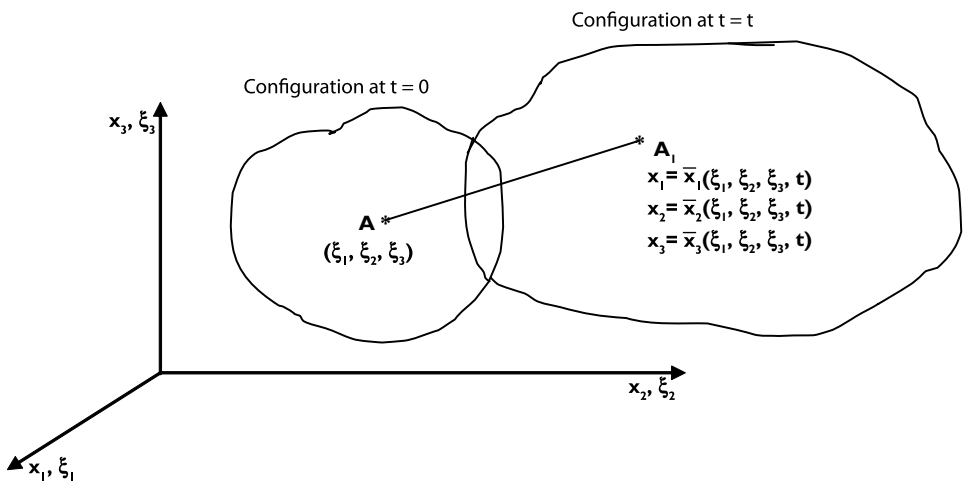


Figure 2.7.1 Particle Labels at different times.

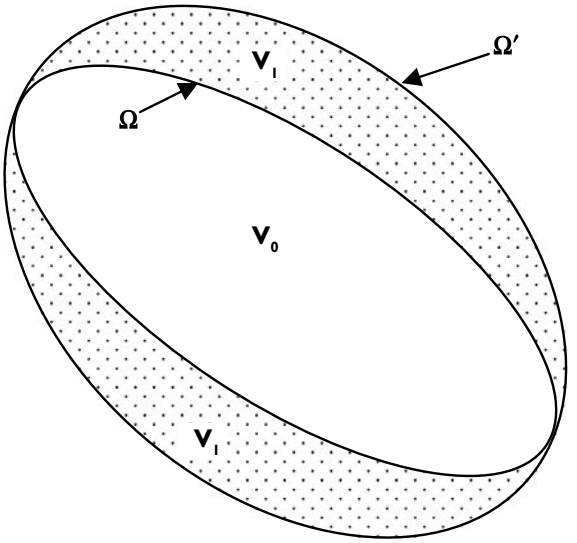


Figure 2.7.2 Continuous change of the boundary of a region.

The function, mentioned in Equation (2.7.1), $\bar{x}_i$ are single-valued continuous function whose Jacobean does not vanish.

Bodies have a basic property that they have mass. In classical mechanics, mass is assumed to be conserved, that is the mass of a material body is the same at all times. In continuum mechanics, the mass is an absolutely continuous function of volume. It is assumed that a positive quantity, ρ, called density, can be obtained at every point in the body as

$$\rho(\bar{X}) = \lim_{k\to\infty} \frac{\text{mass of } V_k}{\text{volume of } V_k} \tag{2.7.2}$$

where V_k is a suitably chosen infinite sequence of particle sets shrinking down upon the point $\bar{X}$, (x_1, x_2, x_3). At time $t = 0$, the density at the point $\bar{\xi} \equiv (\xi_1, \xi_2, \xi_3)$ is defined by $\rho_0(\bar{\xi})$.

Conservation of mass is expressed by

$$\int \rho(\bar{X}) dx_1 dx_2 dx_3 = \int \rho(\bar{\xi}) d\xi_1 d\xi_2 d\xi_3, \tag{2.7.3}$$

where integrals extend over the same particles.

$$\text{Now, as} \quad \int \rho(\bar{X}) dx_1 dx_2 dx_3 = \int \rho(\bar{X}) \left| \frac{\partial x_i}{\partial \xi_j} \right| d\xi_1 d\xi_2 d\xi_3 \tag{2.7.4}$$

and this relation must hold for all bodies, one can write

$$\rho_0(\bar{\xi}) = \rho(\bar{X}) \left| \frac{\partial x_i}{\partial \xi_j} \right|; \quad \rho(\bar{X}) = \rho_0(\bar{\xi}) \left| \frac{\partial \xi_i}{\partial x_j} \right|,$$

where $\left| \frac{\partial \xi_i}{\partial x_j} \right|$ denotes the determinant of $\left[\frac{\partial \xi_i}{\partial x_j} \right]$.

These equations relate the density in different configurations of the body to the transformation that leads from one configuration to another.

For a particle (ξ_1, ξ_2, ξ_3), with trajectory $x_i = \bar{x}_i(\xi_1, \xi_2, \xi_3, t)$, the velocity is $v_i(\bar{\xi}, t) = \frac{\partial \bar{x}_i}{\partial t}$ and acceleration is given by $\dot{v}_i(\bar{\xi}, t) = \frac{\partial^2 \bar{x}_i(\bar{\xi}, t)}{\partial t^2} = \frac{\partial v_i(\bar{\xi}, t)}{\partial t}$, $\bar{\xi}$ is (ξ_1, ξ_2, ξ_3) and is held constant.

A description of mechanical evolution which uses (ξ_1, ξ_2, ξ_3), and t as independent variable is called a *material description*. If the location (x_1, x_2, x_3) and t are taken as independent variables the description is called *spatial description*. This is convenient because measurements in many kinds of materials are more directly interpreted in terms of what happened at a certain place, rather than following the particles. These two methods of description, though both are due to Euler, are commonly known as the *Lagrangian* and the *Eulerian* description, respectively. The variables a_1, a_2, a_3 and t are usually called the *Lagrangian variables*, whereas x_1, x_2, x_3 and t are called *Eulerian variables. For a given particle, it is convenient to speak of* (ξ_1, ξ_2, ξ_3) *as the Lagrangian coordinates of the particle at* (x_1, x_2, x_3).

The instantaneous motion of a body can be described by its velocity vector field v_i (x_1, x_2, x_3, t) in spatial description and associated with the instantaneous location of each particle. The acceleration of the particle is obtained from Taylor's series expansion. A particle located at (x_1, x_2, x_3) at time t is moved to a point with coordinates $x_i + v_i$ dt at the time $t + dt$ i.e.

$$\begin{aligned} \dot{v}_i(\bar{X}, t)dt &= v_i(x_j + v_j dt, t + dt) - v_i(\bar{X}, t) \\ &= v_i + \frac{\partial v_i}{\partial t}dt + \frac{\partial v_i(\bar{X}, t)}{\partial x_j} v_j dt - v_i = \frac{\partial v_i(\bar{X}, t)}{\partial t} + v_j \frac{\partial v_i(\bar{X}, t)}{\partial x_j} \end{aligned} \tag{2.7.5}$$

where $\bar{X}$ stands for the variables x_1, x_2, x_3 and every quantity in this expression is evaluated at $(\bar{X}, t)$.

The first term can be interpreted as the time dependence of the velocity field whereas the second term is the contribution of the motion of the particle in the instantaneous velocity field. Accordingly these terms are called the *local* and the *convective* parts of the acceleration, respectively.

Equation (2.7.5) is applicable to any function $f(x_1, x_2, x_3, t)$ that is attributed to the moving particles, e.g. the temperature. An important term, *the material derivative* is denoted by a dot or the symbol D/Dt. That is

$$f \equiv \frac{Df}{Dt} \equiv \left[\frac{\partial f}{\partial t} \right]_{x=\text{const.}} + v_1 \frac{\partial f}{\partial x_1} + v_2 \frac{\partial f}{\partial x_2} + v_3 \frac{\partial f}{\partial x_3} \equiv \left[\frac{\partial f}{\partial t} \right]_{\xi=\text{const.}} \tag{2.7.6}$$

in which $\bar{\xi} = (\xi_1, \xi_2, \xi_3)$ is the Lagrangian coordinate of the particle, which is located at $\bar{X}$ at any time t and connected by: $x_i = \bar{x}_i(\xi_1, \xi_2, \xi_3, t)$.

2.7.1 Material derivative of volume integral

If $A(\bar{X}, t)$ denotes a property of the continuum and the integral $I = \int_{\text{Volume}} A(\bar{X}, t)dV$ is evaluated at an instant of time t, one would like to know how fast the body itself sees the value I changing. That is the value of DI/Dt.

Particles at x_i at time t will have the coordinates $x_i = x_i + v_i dt$ at the time $t + dt$. The boundary Ω of the body at t will have moved at time $t + dt$ to a neighbourhood surface Ω' bounding the volume V'.

The material derivative of I is given by

$$\frac{DI}{Dt} = \lim_{dt \to 0} \frac{1}{dt} \left[\int_V A(X', t + dt)dV' - \int_V A(X, t)dV \right] \tag{2.7.7}$$

The r.h.s. of Equation (2.7.7) contains two contributions, one over the region V_0, which is common to V and V' and the other over the region V_1 where V differs from V'. The first one can be written as $\int_{V_0} \frac{\partial A}{\partial t} dt dV$.

The second one comes from the value of A on the boundary multiplied by the volume swept by the particles on the boundary in the time interval dt. If n_i is the unit vector along the exterior normal of S, and since the displacement of a particle on the boundary is $n_i dt$, the volume swept by particles occupying an element of area dS on the boundary S is $dV = v_i n_i dS dt$. The contribution of this element to DI/Dt is $(A v_i n_i dS)$. n is the unit outer normal vector to S with components n_1, n_2, and n_3. The total contribution is given by integration over S, i.e.

$$\frac{D}{Dt} \int_V A dV = \int_V \frac{\partial A}{\partial t} dV + \int_S A v_i n_i dS \tag{2.7.8}$$

Using Gauss' theorem and Equation (2.6.6)

$$\begin{aligned} \frac{D}{Dt} \int_V A dV &= \int_V \frac{\partial A}{\partial t} dV + \int_V \frac{\partial}{\partial x_j} (A v_j) dV \\ &= \int_V \left[\frac{\partial A}{\partial t} + v_j \frac{\partial A}{\partial x_j} + A \frac{\partial v_j}{\partial x_j} \right] dV = \int_V \left[\frac{DA}{Dt} + A \frac{\partial v_j}{\partial x_j} \right] dV \end{aligned} \tag{2.7.9}$$

The above spatial integration is, in general, non-commutative.

2.7.2 The equations of continuity

The mass contained in a region V at a time t is given by

$$m = \int_V \rho dV \tag{2.7.10}$$

in which $\rho = \rho(\overline{X}, t)$ is the density field of the continuum. Conservation of mass demands that $Dm/Dt = 0$. If A is replaced by ρ and as the result must hold for any arbitrary V, the integrand in Equations (2.7.8) and (2.7.9) must vanish. Thus an alternative form of the conservation of mass can be written as

$$\int_V \frac{\partial \rho}{\partial t} dV + \int_S \rho v_j n_j dS = 0, \quad \text{or,} \ \frac{\partial \rho}{\partial t} + \frac{\partial \rho v_j}{\partial x_j} = 0, \quad \text{or,} \ \frac{D\rho}{Dt} + \rho \frac{\partial v_i}{\partial x_j} = 0 \tag{2.7.11}$$

These equations are called the equations of continuity. The first expression in Equation (2.6.11) is useful when the differentiability of ρv_j cannot be assumed. In statics, all the equations in Equation (2.7.11) are identically satisfied.

2.7.3 The equations of motion

Euler extended Newton's 'laws of motion' for particles to all kinds of bodies. If the inertial frame is referred by a coordinate system, x_1, x_2, x_3, the space occupied by a material body at any time, t, is denoted by $V(t)$, the position vector of a particle with respect to the origin of the coordinate system is $\boldsymbol{r}$ and $\boldsymbol{v}$ is the velocity vector of the particle at point (x_1, x_2, x_3) the linear momentum of the body in the configuration V is given by

$$\bar{M} = \int_V \rho v dV \quad \text{or } M_i = \int_V \rho v_i dV \tag{2.7.12}$$

and the moment of momentum is denoted by

$$\bar{M}m = \int_{V(t)} r \times v \rho dV \quad \text{or } Mm_i = \int_{V(t)} e_{ijk} x_j \rho v_k dV \tag{2.7.13}$$

Newton's laws for a continuum, as stated by Euler, is that the rate of change of linear momentum is equal to the applied force $\bar{F}$ acting on the body, i.e. $\frac{D\bar{M}}{Dt} = \bar{F}$ and the rate of change of moment of momentum is equal to the total applied torque $\bar{T}$, i.e. $\frac{D\bar{M}m}{Dt} = \bar{T}$. The torque is taken with respect to the same point as the origin of the position vector $\boldsymbol{r}$.

If the body is subjected to surface traction p_{nj} and body force per unit volume B_i, the resultant force is

$$F_i = \int_S p_{nj} dS + \int_V B_i dV \tag{2.7.14}$$

Using Cauchy's definition of surface traction, $p_{nj} = \sigma_{ji} n_j$ in which σ_{ji} is the stress field and n_j is the unit vector along the exterior normal to the boundary surface S of the volume V. Using this definition and transforming the surface to volume integral, using Gauss' theorem, $F_i = \int_V \left[\frac{\partial \sigma_{ij}}{\partial x_j} + B_i\right] dV$. Again, Newton's law states that $\frac{DM_i}{Dt} = F_i$.

From Equation (2.7.9) replacing A by (ρv_i),

$$\int_V \left[\frac{\partial \rho v_i}{\partial t} + \frac{\partial (\rho v_i v_j)}{\partial x_j}\right] dV = \int_V \left[\frac{\partial \sigma_{ij}}{\partial x_j} + B_i\right] dV \tag{2.7.15}$$

As the above equation holds for any arbitrary region V, the integrand on the two sides must be equal, i.e.

$$\frac{\partial \rho v_i}{\partial t} + \frac{\partial (\rho v_i v_j)}{\partial x_j} = \frac{\partial \sigma_{ij}}{\partial x_j} + B_i \tag{2.7.16}$$

Equation (2.7.16) can be written as

$$v_i \left[\frac{\partial \rho}{\partial t} + \frac{\partial (\rho v_j)}{\partial x_j}\right] + \rho \left[\frac{\partial v_i}{\partial t} + v_j \frac{\partial (\rho v_i)}{\partial x_j}\right] = \frac{\partial \sigma_{ij}}{\partial x_j} + B_i \tag{2.7.17}$$

The first expression vanishes by the equation of continuity while the other is the acceleration Dv_i/Dt. Thus

$$\rho \frac{Dv_i}{Dt} = \frac{\partial \sigma_{ij}}{\partial x_j} + B_i \tag{2.7.18}$$

➔ *This is Euler's equation of motion of a continuum.*

Static equations of equilibrium can be obtained by assuming all velocity components equal to zero. Euler's equation of motion in the integral form can be also written as

$$\int_V \frac{\partial \rho v_i}{\partial t} dV = \int_S \left[\sigma_{ij} - \rho v_i v_j\right] v_j dS + \int_V B_i dV \tag{2.7.19}$$

The corresponding static equal can be obtained by setting velocity components to be zero.

2.7.4 Moment of momentum

It is known that the law of balance of angular momentum to a particular case of static equilibrium leads to the conclusion that the stress tensor is symmetric. No additional restriction to the motion of a continuum is introduced in dynamics by the angular momentum postulate. At an instant of time t, a body occupying a regular region V of space with boundary S has the moment of momentum with respect to the origin is (Equation (2.7.13))

$$Mm_i = \int_V e_{ijk} x_j \rho \, v_k dV \tag{2.7.20}$$

If the body is having the body force B_i per unit volume and a surface traction p_{ni}, the resultant moment about the origin is

$$Mm_i = \int_V e_{ijk} x_j B_k dV + \int_S e_{ijk} x_j p_{nk} dS \tag{2.7.21}$$

Using Cauchy's formula $p_{ni} = \sigma_{ki} n_k$ in the last integral and transforming the result into a volume integral by Gauss' theorem

$$Mm_i = \int_V e_{ijk} x_j B_k dV + \int_V (e_{ijk} x_j \sigma_{\ell k})_\ell dV \tag{2.7.22}$$

Now, the Euler's law states that for any region V

$$\frac{DMm_i}{Dt} = M_i \tag{2.7.23}$$

Using Equation (2.7.21) in Equation (2.7.9)

$$e_{ijk} x_j \frac{\partial(\rho v_k)}{\partial t} + \frac{\partial(e_{ijk} x_j \rho v_k v_\ell)}{\partial x_\ell} = e_{ijk} x_j B_k + e_{ijk} (x_j \sigma_{\ell k})_{,\ell} \tag{2.7.24}$$

The second term in Equation (2.7.24) can be written as

$$e_{ijk} \rho v_k v_j + e_{ijk} x_j \frac{\partial(\rho v_\ell v_k)}{\partial x_\ell} = e_{ijk} x_j \frac{\partial(\rho v_\ell v_k)}{\partial x_\ell} \tag{2.7.25}$$

The last term in Equation (2.7.24) can be written as

$$e_{ijk}\sigma_{jk} + e_{ijk}x_j\sigma_{ik,\ell} \tag{2.7.26}$$

Thus Equation (2.7.24) can be rewritten as

$$e_{ijk}x_j\left[\frac{\partial(\rho v_k)}{\partial t} + \frac{\partial(\rho v_k v_\ell)}{\partial x_\ell} - B_k - \sigma_{\ell k,\ell}\right] - e_{ijk}\sigma_{jk} = 0 \tag{2.7.27}$$

Using Equation (2.7.15), the bracketed part of Equation (2.7.27) vanishes and hence it reduces to

$$e_{ijk}\ \sigma_{jk} = 0, \quad \text{i.e. } \sigma_{jk} = \sigma_{kj}. \tag{2.7.28}$$

$\Rightarrow$ *If the stress tensor is symmetric, the law of balance of moment of momentum is identically satisfied.*

The laws of conservation of energy further govern the motion of a continuum. In a problem, if the mechanical energy is of concern, the energy equation is the first integral of the equation of motion. If the interaction of thermal process and mechanical process is significant, then the equation of energy contains a thermal energy term and is an independent equation to be satisfied.

The equations of continuity and motion constitute four equations for ten unknown functions of time and position. These are the density, three velocities or displacements and the six independent stress components. Thus, further restrictions have to be introduced before the motions of a continuum can be determined. One such restriction comes from the mechanical property of the medium, in the form of stress-strain relationship, known as constitutive equations. A different approach is to determine the physical relations experimentally, characterizing a material through experimental results. In the theory of linear elasticity, the stress-strain relationship provides six additional equations relating the variables named above, making the motion of the continuum deterministic.

2.7.5 Basic equation of motion of an elastic body

As was mentioned in §2.5.1, for an isotropic linearly elastic material the stress and strain tensors may be related through

$$\sigma_{ij} = \lambda\,\varepsilon_{\alpha\beta}\delta_{\alpha\beta} + 2G\,\varepsilon_{ij} \quad \text{or } \varepsilon_{ij} = \frac{1+\nu}{E}\,\sigma_{ij} - \frac{\nu}{E}\,\sigma_{\alpha\beta}\,\delta_{\alpha\beta} \tag{2.7.29}$$

(repetitive symbols indicate sum and δ denotes kroneker delta with $\delta_{ij} = 1$, for $i = j$ or $\delta_{ij} = 0$ for $i \neq j$). λ and G are Lame's parameter: E, ν, G and K are Young's modulus

of elasticity, Poisson ratio, shear modulus and Bulk modulus of elasticity, respectively. These constants are related through:

$$\lambda = \frac{2G\nu}{1-2\nu} = K - \frac{2}{3}G = \frac{E\nu}{(1+\nu)(1-2\nu)};$$
$$G = \frac{\lambda(1-2\nu)}{2\nu} = \frac{3}{2}(K-\lambda) = \frac{E}{2(1+\nu)} = \frac{3KE}{9K-E}$$
$$E = \frac{\lambda(1+\nu)(1-2\nu)}{\nu} = 2G(1+\nu) = \frac{G(3\lambda+2G)}{\lambda+G}; \quad \nu = \frac{\lambda}{2(\lambda+G)} = \frac{3K-E}{6K};$$
$$K = \lambda + \frac{2}{3}G = \frac{E}{3(1-2\nu)}. \tag{2.7.30}$$

For a Poisson ratio, $\nu = 1/4$, $\lambda = G$; $\nu = 1/2$: $G = E/3$; $1/K = 0$, i.e. $\varepsilon_{\alpha\alpha} = 0$ (incompressible material).

2.7.6 Various strain measures

In spatial description the motion of a continuum is described by the instantaneous velocity field $v_i(x_1, x_2, x_3, t)$. For describing strains in the body, a displacement field $u_i(x_1, x_2, x_3, t)$ is specified which describes the displacement of particle at (x_1, x_2, x_3) at time t from its position in the natural state.

Strain measures for the displacement field are defined as follows:

The *Almansi strain tensor*:

$$\varepsilon_{ij} = \frac{1}{2}\left[\frac{\partial u_j}{\partial x_i} + \frac{\partial u_i}{\partial x_j} - \frac{\partial u_k}{\partial x_i}\frac{\partial u_k}{\partial x_j}\right] \tag{2.7.31}$$

The particle velocity can be obtained from the material derivative of the displacement

$$v_i = \frac{\partial u_i}{\partial t} + v_j \frac{\partial u_i}{\partial x_j} \tag{2.7.32}$$

The particle acceleration is obtained from the material derivative of the velocity

$$a_i = \frac{\partial v_i}{\partial t} + v_j \frac{\partial v_i}{\partial x_j} \tag{2.7.33}$$

We have nonlinear terms in above equations. We have to linearize these equations by confining ourselves to small displacements and small velocities and thus, neglecting nonlinear terms. In the linear theory we have

$$\varepsilon_{ij} = \frac{1}{2}\left[\frac{\partial u_j}{\partial x_i} + \frac{\partial u_i}{\partial x_j}\right], \quad v_i = \frac{\partial u_i}{\partial t} \quad \text{and} \quad a_i = \frac{\partial v_i}{\partial t}. \tag{2.7.34}$$

The motion of the body must obey the equation of continuity [Equation (2.7.11)] and the equation of motion [Equation (2.7.18)]. Also, the theory of linear elasticity is based on Hooke's law. For a homogeneous isotropic material we have

$$\sigma_{ij} = \lambda \varepsilon_{kk} \delta_{ij} + 2G\,\varepsilon_{ij} \tag{2.7.35}$$

and combining it with Equation (2.7.31) or Equation (2.7.11) with the linear form of Equation (2.7.33), we have 22 equations for 22 unknowns ρ, u_i, v_i, ε_{ij}, σ_{ij}. For infinitesimal displacement, one can substitute σ_{ij} of Equation (2.7.35) into Equation (2.7.18) and using Equation (2.7.34), Navier's equation is obtained as follows

$$\mu \nabla^2 u_i + (\lambda + G)\varepsilon_i + B_i = \rho \frac{\partial^2 u_i}{\partial t^2} \quad \text{or } G u_{i,jj} + (\lambda + G) u_{j,ji} + B_i = \rho \frac{\partial^2 u_i}{\partial t^2} \tag{2.7.36}$$

in which $\varepsilon = u_{j,j}$ and $\nabla^2 u_i = u_{i,jj}$.

If one writes x, y, z instead of x_1, x_2, x_3; u_1, u_2, u_3 is replaced by u, v, w; and B_1, B_2, B_3 is replaced by B_x, B_y, B_z, Love's equation similar to Equation (2.7.36) results and they are given as follows:

$$G\nabla^2 u + (\lambda + G)\frac{\partial e}{\partial x} + B_x = \rho \frac{\partial^2 u}{\partial t^2}; \quad G\nabla^2 v + (\lambda + G)\frac{\partial e}{\partial y} + B_y = \rho \frac{\partial^2 v}{\partial t^2};$$
$$G\nabla^2 w + (\lambda + G)\frac{\partial e}{\partial z} + B_z = \rho \frac{\partial^2 w}{\partial t^2} \tag{2.7.37}$$

in which $\nabla^2 = \frac{\partial^2}{\partial x^2} + \frac{\partial^2}{\partial y^2} + \frac{\partial^2}{\partial z^2}$ = Laplace operator; $e = \frac{\partial u}{\partial x} + \frac{\partial v}{\partial y} + \frac{\partial w}{\partial z} = \varepsilon_x + \varepsilon_y + \varepsilon_z$ = dilatation = divergence of displacement vector.

2.7.7 Solution of the three-dimensional equation

Equation (2.7.37) is the governing equation of three-dimensional motion for an isotropic, linear elastic solid. In an *unbounded* solid, only two types wave travel through the body.

The solution for the first type of wave can be obtained by differentiating each of the equation [Equation (2.7.37)] with respect to x, y, z and adding them to form

$$G\nabla^2 \left[\frac{\partial u}{\partial x} + \frac{\partial v}{\partial y} + \frac{\partial w}{\partial z}\right] + (\lambda + G)\left[\frac{\partial^2 e}{\partial x^2} + \frac{\partial^2 e}{\partial y^2} + \frac{\partial^2 e}{\partial z^2}\right] + \left[\frac{\partial B_x}{\partial x} + \frac{\partial B_y}{\partial y} + \frac{\partial B_z}{\partial z}\right]$$
$$= \rho \frac{\partial^2}{\partial t^2}\left[\frac{\partial u}{\partial x} + \frac{\partial v}{\partial y} + \frac{\partial w}{\partial z}\right] \tag{2.7.38}$$

$$\text{or} \quad (\lambda + 2G)\nabla^2 e + \left[\frac{\partial B_x}{\partial x} + \frac{\partial B_y}{\partial y} + \frac{\partial B_z}{\partial z}\right] = \rho \frac{\partial^2 e}{\partial t^2} \tag{2.7.39}$$

With no body forces the equation of motion reduces to

$$\frac{(\lambda + 2G)}{\rho}\nabla^2 e = \frac{\partial^2 e}{\partial t^2} \quad \text{or } V_P^2 \nabla^2 e = \frac{\partial^2 e}{\partial t^2} \tag{2.7.40}$$

e is the volumetric strain i.e. deformation without any shear strain or rotation. This wave equation represents an irrotational or dilatational wave and will propagate through the body at a velocity

$$V_P = \sqrt{\frac{\lambda + 2G}{\rho}} = \sqrt{\frac{2G(1-\nu)}{\rho(1-2\nu)}} \tag{2.7.41}$$

This type of wave is commonly called p-wave or primary wave. Equation (2.7.41) indicates that as ν approaches 0.5, the body is incompressible and V_P approaches infinity.

The second type of wave solution can be obtained by differentiating the first equation of Equation (2.7.37) with respect to y and the second with respect to x and then subtracting one from the other, i.e.

$$G\nabla^2\left[\frac{\partial u}{\partial y} - \frac{\partial v}{\partial x}\right] + \frac{\partial B_x}{\partial y} - \frac{\partial B_y}{\partial x} = \rho \frac{\partial^2}{\partial t^2}\left[\frac{\partial u}{\partial y} - \frac{\partial v}{\partial x}\right];$$

$$\text{or} \quad G\nabla^2 \Omega_z + \frac{\partial B_x}{\partial y} - \frac{\partial B_y}{\partial x} = \rho \frac{\partial^2}{\partial t^2}\Omega_z \tag{2.7.42}$$

Similarly other two equations can be obtained by differentiating the second and third equation of Equation (2.7.37) by z and y, and the third and first equation of Equation (2.7.37) by x and z and the subtracting one from the other

$$G\nabla^2\left[\frac{\partial v}{\partial z} - \frac{\partial w}{\partial y}\right] + \frac{\partial B_y}{\partial z} - \frac{\partial B_z}{\partial y} = \rho \frac{\partial^2}{\partial t^2}\left[\frac{\partial v}{\partial z} - \frac{\partial w}{\partial y}\right];$$

$$\text{or} \quad G\nabla^2 \Omega_x + \frac{\partial B_y}{\partial z} - \frac{\partial B_z}{\partial y} = \rho \frac{\partial^2}{\partial t^2}\Omega_x \tag{2.7.43}$$

$$G\nabla^2\left[\frac{\partial w}{\partial x}-\frac{\partial u}{\partial z}\right]+\frac{\partial B_z}{\partial x}-\frac{\partial B_x}{\partial z}=\rho\frac{\partial^2}{\partial t^2}\left[\frac{\partial w}{\partial x}-\frac{\partial u}{\partial z}\right];$$

$$\text{or}\quad G\nabla^2\Omega_y+\frac{\partial B_z}{\partial x}-\frac{\partial B_x}{\partial z}=\rho\frac{\partial^2}{\partial t^2}\Omega_y \tag{2.7.44}$$

in which

$$\Omega_x=\frac{1}{2}\left(\frac{\partial w}{\partial y}-\frac{\partial v}{\partial z}\right);\quad \Omega_y=\frac{1}{2}\left(\frac{\partial u}{\partial z}-\frac{\partial w}{\partial x}\right);$$
$$\Omega_z=\frac{1}{2}\left(\frac{\partial v}{\partial x}-\frac{\partial u}{\partial y}\right)\text{ are the rotation vectors.} \tag{2.7.45}$$

Equations with no body forces can be written as

$$\frac{G}{\rho}\nabla^2\Omega_x=\frac{\partial^2\Omega_x}{\partial t^2};\quad \frac{G}{\rho}\nabla^2\Omega_y=\frac{\partial^2\Omega_y}{\partial t^2};\quad \frac{G}{\rho}\nabla^2\Omega_z=\frac{\partial^2\Omega_z}{\partial t^2} \tag{2.7.46}$$

Equation (2.7.45) describes equivoluminal or distortional waves of rotations about x, y and z axes respectively. These waves will propagate through the solid at a velocity, $V_s=\sqrt{(G/\rho)}$ and is commonly known as *s*-wave or shear wave.

S-waves can be divided into two perpendicular components, SH-wave and SV-waves. While in SH-waves particle motion occurs in a horizontal plane, in SV-waves particle motion lies in a vertical plane. Thus, a given *s*-wave with arbitrary particle motion can be represented as the vector sum of its SH and SV components.

The above two types of waves, known as body waves, can exist in an unbounded elastic body. The ratio of the body wave velocities namely, V_P/V_S is a function of the Poisson ratio given as below

$$\frac{V_P}{V_S}=\sqrt{\frac{2-2\nu}{1-2\nu}} \tag{2.7.47}$$

For a typical Poisson ratio of 0.25, this ratio is $\sqrt{3}$.

2.7.8 Static solutions with no body forces

For such cases Equation (2.7.40) reduces to

$$\nabla^2 e\ =0 \tag{2.7.48}$$

A function satisfying Equation (2.7.48) is known as *harmonic function*. Thus dilation e is a harmonic function when body force vanishes. Also we have a relation that $(3\lambda+2\mu)e=(\sigma_x+\sigma_y+\sigma_z)/3=\sigma=$ mean stress and this implies

$$\nabla^2\sigma = 0 \tag{2.7.49}$$

Hence, the mean stress is also a harmonic function.

Again from Equation (2.7.37), with no body forces and using Laplacian, ∇^2

$$G\nabla^2\nabla^2 u + (\lambda + G)\frac{\partial}{\partial x}\nabla^2 e = 0; \quad G\nabla^2\nabla^2 v + (\lambda + G)\frac{\partial}{\partial y}\nabla^2 e = 0;$$

$$G\nabla^2\nabla^2 w + (\lambda + G)\frac{\partial}{\partial z}\nabla^2 e = 0$$

and making use of Equation (2.7.48)

$$\nabla^4 u = 0; \quad \nabla^4 v = 0; \quad \nabla^4 w = 0 \tag{2.7.50}$$

in which the biharmonic operator in rectangular Cartesian coordinates is given by

$$\nabla^4 = \frac{\partial^4}{\partial x^4} + \frac{\partial^4}{\partial y^4} + \frac{\partial^4}{\partial z^4} + 2\left[\frac{\partial^4}{\partial x^2\partial y^2} + \frac{\partial^4}{\partial y^2\partial z^2} + \frac{\partial^4}{\partial z^2\partial x^2}\right] \tag{2.7.51}$$

Equation (2.7.51) is called biharmonic equation and its solution is called a biharmonic function. Thus the displacement components are biharmonic.

Hence, an elastic body with no body forces each of the strain components and each of the stress components, being linear combination of the first derivative of displacement components, are all biharmonic.

Equation (2.7.37) is to be solved for appropriate boundary and initial conditions. The boundary conditions normally used are

1 Specified displacements: The displacement components u, v, and w are prescribed on the boundary.
2 Specified surface tractions: The surface traction components p_i is assigned on the boundary.

The boundary conditions such as the displacement are prescribed on a part of the boundary while the surface tractions are prescribed over another part of the boundary. Normally, the region occupied by the body is denoted by V, while the boundary surface of V is denoted by S. The surface is further divided into S_u and S_σ. Thus on S_σ the surface traction $p_i = \sigma_{ij}\, n_j$, is prescribed where n_j is the unit vector normal to the surface S_σ. By using constitutive equations this can be further reduced to satisfying the function $[\lambda u_{k,k}\delta_{ij} + G(u_{i,j} + u_{j,I})]n_j =$ the prescribed stress condition. Hence, over the entire surface, the boundary conditions are that either u_i or a combination of the first derivatives of u_i is prescribed.

In dynamic problems, however, a set of initial conditions on u_i or σ_{ij} must be given in the region V and on the surface S. We have already specified the condition under which unique solution exists in a boundary value problem mentioned in the preceding.

2.8 SOME BASICS

Elastic constants: E = Young's modulus; ν = Poisson ratio.

Lame's constants: $\lambda = \dfrac{\nu E}{(1+\nu)(1-2\nu)}$; G = shear modulus $= \dfrac{E}{2(1+\nu)}$

For a homogeneous, isotropic and elastic material elastic constants reduce to just two, E and ν. The relationship among the constants may be written as

$$E = \frac{G(3\lambda + 2G)}{\lambda + G}; \quad \nu = \frac{\lambda}{2(\lambda + G)}.$$

In general, we have:

State	No. of equations	Unknowns: Stresses = 6: $\{\sigma_{xx}, \sigma_{yy}, \sigma_{zz}, \tau_{xy}, \tau_{yz}, \tau_{zx}\}$
Equilibrium	3	
Compatibility	6	Displacements: $3\{u, v, w\}$
Stress-strain (constitutive relations)	6	
	Total = 15 equations.	Total = 9.

2.8.1 Summary of governing equations/relations

1 Equations of equilibrium: $\tau_{ji,j} + X_i = 0$

2

$$\frac{\partial \sigma_{xx}}{\partial x} + \frac{\partial \tau_{xy}}{\partial y} + \frac{\partial \tau_{xz}}{\partial z} + X = 0; \quad \frac{\partial \tau_{xy}}{\partial x} + \frac{\partial \sigma_{yy}}{\partial y} + \frac{\partial \tau_{yz}}{\partial z} + Y = 0;$$

$$\frac{\partial \tau_{xz}}{\partial x} + \frac{\partial \tau_{zy}}{\partial y} + \frac{\partial \sigma_{zz}}{\partial z} + Z = 0$$

➔ *6-unknowns and 3 equations: taking stress tensor as a symmetric one.*

3 Equations of stress and strain: $\varepsilon_{ij} = \dfrac{1+\nu}{E}\tau_{ij} - \dfrac{\nu}{E}\tau_{kk}\delta_{ij}$: $\sigma_{ij} = \lambda\, \varepsilon_{kk}\delta_{ij} + 2G\, \varepsilon_{ij}$

$$\varepsilon_{xx} = \frac{\sigma_{xx}}{E} - \frac{\nu}{E}(\sigma_{yy} + \sigma_{zz}) \; : \; \varepsilon_{yy} = \frac{\sigma_{yy}}{E} - \frac{\nu}{E}(\sigma_{zz} + \sigma_{xx}) :$$

$$\varepsilon_{zz} = \frac{\sigma_{zz}}{E} - \frac{\nu}{E}(\sigma_{xx} + \sigma_{yy})$$

$$\varepsilon_{xy} = \frac{\gamma_{xy}}{2} = \frac{1+\nu}{E}\tau_{xy} = \frac{\tau_{xy}}{2G}; \quad \varepsilon_{yz} = \frac{\gamma_{yz}}{2} = \frac{1+\nu}{E}\tau_{yz} = \frac{\tau_{yz}}{2G};$$

$$\varepsilon_{zx} = \frac{\gamma_{zx}}{2} = \frac{1+\nu}{E}\tau_{zx} = \frac{\tau_{zx}}{2G}.$$

➔ *6-unknowns and six equations.*

4 Strain-displacement relations: $\varepsilon_{ij} = \frac{1}{2}\left(u_{i,j} + u_{j,i}\right)$

$$\varepsilon_{xx} = \frac{\partial u}{\partial x}; \varepsilon_{yy} = \frac{\partial v}{\partial y}; \quad \varepsilon_{zz} = \frac{\partial w}{\partial z}; \quad \varepsilon_{xy} = \frac{1}{2}\left(\frac{\partial u}{\partial y} + \frac{\partial v}{\partial x}\right);$$

$$\varepsilon_{yz} = \frac{1}{2}\left(\frac{\partial v}{\partial z} + \frac{\partial w}{\partial y}\right); \quad \varepsilon_{zx} = \frac{1}{2}\left(\frac{\partial w}{\partial x} + \frac{\partial u}{\partial z}\right).$$

5 Equations of compatibility: $\varepsilon_{ij,kl} + \varepsilon_{kl,ij} - \varepsilon_{ik,jl} - \varepsilon_{jl,ik} = 0$

$$\frac{\partial^2 \varepsilon_{xx}}{\partial y \partial z} = \frac{\partial}{\partial x}\left(-\frac{\partial \varepsilon_{yz}}{\partial x} + \frac{\partial \varepsilon_{zx}}{\partial y} + \frac{\partial \varepsilon_{xy}}{\partial z}\right); \quad \frac{\partial^2 \varepsilon_{yy}}{\partial z \partial x} = \frac{\partial}{\partial y}\left(-\frac{\partial \varepsilon_{zx}}{\partial y} + \frac{\partial \varepsilon_{xy}}{\partial z} + \frac{\partial \varepsilon_{yz}}{\partial x}\right);$$

$$\frac{\partial^2 \varepsilon_{zz}}{\partial x \partial y} = \frac{\partial}{\partial z}\left(-\frac{\partial \varepsilon_{xy}}{\partial z} + \frac{\partial \varepsilon_{zy}}{\partial x} + \frac{\partial \varepsilon_{zx}}{\partial y}\right); \quad 2\frac{\partial^2 \varepsilon_{xy}}{\partial x \partial y} = \frac{\partial^2 \varepsilon_{xx}}{\partial y^2} + \frac{\partial^2 \varepsilon_{yy}}{\partial x^2};$$

$$2\frac{\partial^2 \varepsilon_{yz}}{\partial y \partial z} = \frac{\partial^2 \varepsilon_{yy}}{\partial z^2} + \frac{\partial^2 \varepsilon_{zz}}{\partial y^2}; \quad 2\frac{\partial^2 \varepsilon_{zx}}{\partial z \partial x} = \frac{\partial^2 \varepsilon_{zz}}{\partial x^2} + \frac{\partial^2 \varepsilon_{xx}}{\partial z^2}.$$

➔ *6-equations and 6-unknowns.*

2.8.2 Lame's equations [combining all equations, governing differential equation in terms of u, v, w]

Before going in for the equations, let us spend some time in the derivation of them.

We have $\frac{\partial \tau_{ij}}{\partial x_j} + X_i = 0$ (2.8.1)

and $\tau_{ij} = \lambda\, \varepsilon_{kk}\, \delta_{ij} + 2\mu\, \varepsilon_{ij}$ (2.8.2)

Using linearised theory, i.e. $\varepsilon_{ij} = \frac{1}{2}(u_{i,j} + u_{j,i})$ (2.8.3)

and substituting (2.8.2) in (2.8.1), we

$$\lambda \varepsilon_{kk,j}\delta_{ij} + \lambda\, \varepsilon_{kk}\delta_{ij,j} + 2G\, \varepsilon_{ij,j} + X_i = 0$$

$$\lambda \varepsilon_{kk,i} + G\nabla^2 u_i = 0$$

i.e. $2\lambda\, \varepsilon_{kk,i} = \lambda\,(u_{k,ki} + u_{k,ki}) = 2\lambda\, u_{k,ki}$

We have, $2G\, \varepsilon_{ij,j} = G\,(u_{i,jj} + u_{j,ij})$

i.e. $\lambda\, u_{k,ki} + G\, u_{i,jj} + G\, u_{i,ij} + X_i = G\, u_{i,jj} + (\lambda + G)\, u_{j,ji} + X_i = 0$

$$G\nabla^2 u_i + (\lambda + G)\frac{\Delta}{\partial x_i} + X_i = 0 \tag{2.8.4}$$

Hence,

$$(\lambda + G)\frac{\partial \Delta}{\partial x} + G\nabla^2 u + F_x = 0; \quad (\lambda + G)\frac{\partial \Delta}{\partial y} + G\nabla^2 v + F_y = 0;$$
$$(\lambda + G)\frac{\partial \Delta}{\partial z} + G\nabla^2 w + F_z = 0 \tag{2.8.5}$$

where, Δ = dilatation = $\frac{\partial u}{\partial x} + \frac{\partial v}{\partial y} + \frac{\partial w}{\partial z}$; u, v, $w \rightarrow$ displacement components; F_x, $F_{y,}$, F_z body forces per unit volume in x, y, and z-directions.

2.9 SOME CLASSICAL SOLUTIONS OF ELASTOSTATICS

2.9.1 Kelvin (1848) problem – A single force acting in the interior of an infinite solid. (Malvern 1969, Fung 1965)

Let a force P is applied at the origin in the interior of an infinite solid and acting in the z-direction as shown in Figure 2.9.1. The boundary conditions are:

a) At infinity, all stresses vanish; b) At the origin, the stress singularity is equivalent to a concentrated force of magnitude $2P$ in the z-direction.

Using

$$R = \sqrt{x^2 + y^2 + z^2} = \sqrt{r^2 + z^2}; \quad Z = BR; \quad B = \frac{P}{8\pi(1-\nu)}; \quad \nu = \text{Poisson ratio}, \tag{2.9.1}$$

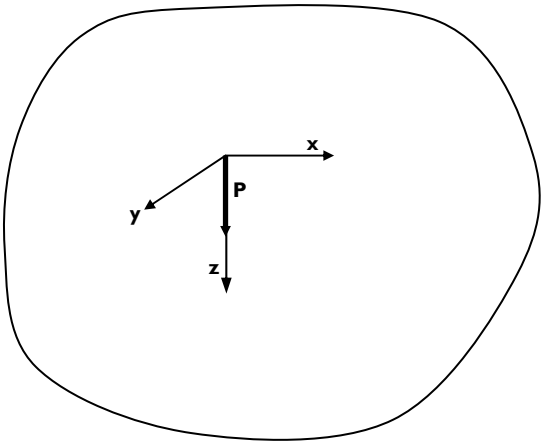


Figure 2.9.1 Kelvin problem.

Stresses in (r, z, θ) system, with radial symmetry, may be written as

$$\sigma_r = B\left[\frac{(1-2\nu)z}{R^3} - \frac{3r^2z}{R^5}\right]; \quad \sigma_z = -B\left[\frac{(1-2\nu)z}{R^3} + \frac{3z^3}{R^5}\right]$$

$$\sigma_\theta = \frac{(1-2\nu)Bz}{R^3}; \quad \tau_{rz} = -B\left[\frac{(1-2\nu)r}{R^3} + \frac{3rz^2}{R^5}\right]; \quad \tau_{z\theta} = \tau_{r\theta} = 0. \tag{2.9.2}$$

$$u_r = \left[\frac{P}{16\pi G(1-\nu)}\right]\frac{rz}{R^3}; \quad u_z = \left[\frac{P}{16\pi G(1-\nu)}\right]\left[\frac{(3-4\nu)}{R} + \frac{z^2}{R^3}\right]; \quad u_\theta = 0. \tag{2.9.3}$$

When the Poisson ratio is 0.5, the stresses become

$$\sigma_r = \frac{-3Pr^2z}{4\pi R^5}; \quad \sigma_z = \frac{-3Pz^3}{4\pi R^5}; \quad \tau_{rz} = \frac{-3Prz^2}{4\pi R^5}; \quad \sigma_\theta = \tau_{r\theta} = \tau_{z\theta} = 0. \tag{2.9.4}$$

and $$u_r = \left[\frac{P}{8\pi G}\right]\left[\frac{rz}{R^3}\right]; \quad u_z = \left[\frac{P}{8\pi G}\right]\left[\frac{1}{R} - \frac{z^2}{R^3}\right]; \quad u_\theta = 0. \tag{2.9.5}$$

2.9.2 Boussinesq (1878) problem – A normal force acting on the surface of a semi-infinite solid

Let us consider a normal force P acting at the origin, O, of the elastic half space as shown below:

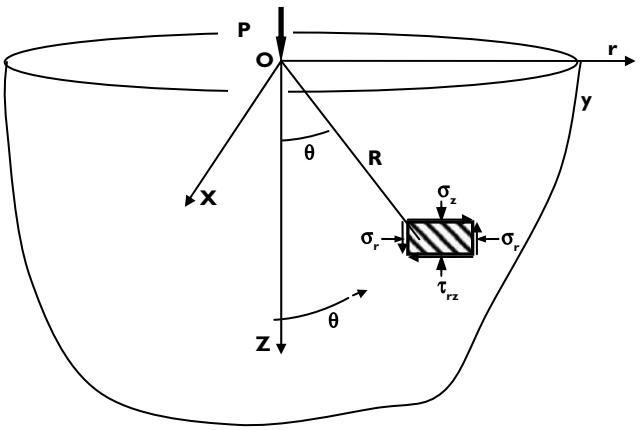


Figure 2.9.2 Concentrated force acting at and normal to the half space.

Using $R^2 = r^2 + z^2 = x^2 + y^2 + z^2$, we can have (2.9.6)

$$\text{Stresses:} \quad \sigma_z = \frac{3P}{2\pi}\frac{z^3}{R^5}; \quad \sigma_r = \frac{P}{2\pi}\left[\frac{3zr^2}{R^5} - \frac{(1-2\nu)}{R(R+z)}\right];$$

$$\sigma_\theta = \frac{P(1-2\nu)}{2\pi}\left[\frac{1}{R(R+z)} - \frac{z}{R^3}\right]; \quad \tau_{rz} = \frac{3P}{2\pi}\frac{z^2 r}{R^5}. \tag{2.9.7}$$

Displacements

$$u = \frac{P(1+\nu)}{2\pi E}\left[\frac{xz}{R^3} - \frac{(1-2\nu)x}{R(R+z)}\right]; \quad v = \frac{P(1+\nu)}{2\pi E}\left[\frac{yz}{R^3} - \frac{(1-2\nu)y}{R(R+z)}\right];$$

$$w = \frac{P(1+\nu)}{2\pi E}\left[\frac{z^2}{R^3} - \frac{(1-\nu)}{R}\right]. \tag{2.9.8}$$

E is the Young's modulus of elasticity and ν is the Poisson ratio of the half space.

It is interesting to note that the vertical normal and shear stresses are independent of the elastic constants, however the assumption of linear elasticity is assumed.

In civil engineering practice, the following expressions are usually used for Boussinesq solution

$$\sigma_z = K\frac{P}{z^2}, \quad \text{where } K = \frac{3}{2\pi}\left[1 + \left(\frac{r}{z}\right)^2\right]^{-5/2} \tag{2.9.9}$$

2.9.3 Cerruti (1882) problem – A tangential force acting on the surface of a semi-infinite solid (Mindlin 1936, Love 1944), [*same as Boussinesq's problem, only the load acting on the surface is horizontal*]

For a concentrated force acting parallel to the boundary surface solution is given by

$$\sigma_z = \frac{3P}{2\pi}\frac{xz^2}{R^5}; \quad \sigma_x = \frac{Px}{2\pi}\left[\frac{(1-2\nu)}{R^3} - \frac{3x^2}{R^5} - \frac{(1-2\nu)}{R(R+z)^2}\left\{3 - \frac{x^2(3R+z)}{R^2(R+z)}\right\}\right]$$

$$\sigma_y = \frac{Px}{2\pi}\left[\frac{(1-2\nu)}{R^3} - \frac{3y^2}{R^5} - \frac{(1-2\nu)}{R(R+z)^2}\left\{1 - \frac{y^2(3R+z)}{R^2(R+z)}\right\}\right]; \tag{2.9.10}$$

$$\tau_{yz} = -\frac{3Pxyz}{2\pi R^5}; \quad \tau_{zx} = -\frac{3Px^2 z}{2\pi R^5};$$

$$\tau_{xy} = -\frac{Py}{2\pi}\left[\frac{3x^2}{R^5} + \frac{(1-2\nu)}{R(R+z)^2}\left\{1 - \frac{x^3(3R+z)}{R^2(R+z)}\right\}\right]$$

$$u = \frac{P}{4\pi GR}\left[1 + \frac{x^2}{R^2} + \frac{R(1-2\nu)}{z+R} - \frac{(1-2\nu)x^2}{(z+R)^2}\right]$$

$$v = \frac{Pxy}{4\pi GR^3}\left[1 - \frac{(1-2\nu)R^2}{(z+R)^2}\right]; \quad w = \frac{Pxz}{4\pi GR^3}\left[1 + \frac{(1-2\nu)R^2}{z(z+r)}\right]. \qquad (2.9.11)$$

2.9.4 Mindlin's (1936) solution

A force at any inclination is acting at a point in the interior of a semi-infinite body. Solution is given in two parts:

2.9.4.1 Force normal to the boundary

Geometrical description is given in Figure 2.9.3, with $R_1 = [r^2 + (z-c)^2]^{1/2}$, $R_2 = [r^2 + (z+c)^2]^{1/2}$ and $r = [x^2 + y^2]^{1/2}$, solution in (r, θ, z) coordinate system is given by

$$\sigma_z = \frac{P}{8\pi(1-\nu)}\left[-\frac{(1-2\nu)(z-c)}{R_1^3} + \frac{(1-2\nu)(z-c)}{R_2^3} - \frac{3(z-c)^3}{R_1^5}\right]$$
$$- \frac{P}{8\pi(1-\nu)}\left[\frac{3(3-4\nu)z(z+c)^2 - 3c(z+c)(5z-c)}{R_2^5} + \frac{30cz(z+c)^3}{R_2^7}\right] \qquad (2.9.12)$$

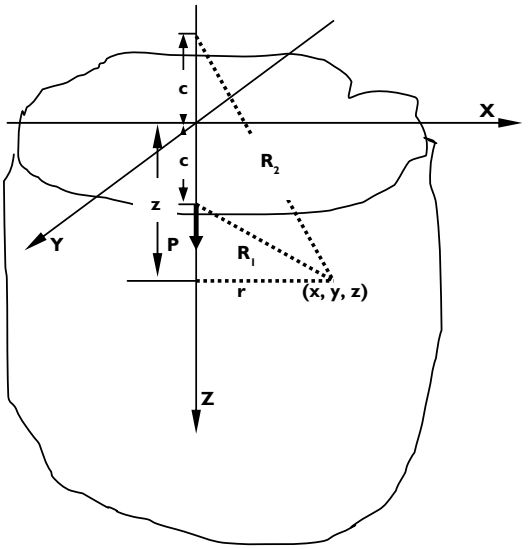


Figure 2.9.3 Concentrated force within mass normal to boundary.

$$w = \frac{P(1+\nu)}{16\pi E(1-\nu)}\left[\frac{3-4\nu}{R_1} + \frac{8(1-\nu)^2-(3-4\nu)}{R_2}\right] + \frac{P(1+\nu)}{16\pi E(1-\nu)}\left[\frac{(z-c)^2}{R_1^3} + \frac{(3-4\nu)(z+c)^2-2cz}{R_2^3} + \frac{6cz(z+c)^2}{R_2^5}\right] \tag{2.9.13}$$

$$u = \frac{Pr}{16\pi G(1-\nu)}\left[\frac{z-c}{R_1^3} + \frac{(3-4\nu)(z-c)}{R_2^3} - \frac{4(1-\nu)(1-2\nu)}{R_2(R_2+z+c)} + \frac{6cz(z+c)}{R_2^5}\right] \tag{2.9.14}$$

$$\sigma_r = \frac{P}{8\pi(1-\nu)}\left[\frac{(1-2\nu)(z-c)}{R_1^3} - \frac{(1-2\nu)(z+7c)}{R_2^3} + \frac{4(1-\nu)(1-2\nu)}{R_2(R_2+z+c)} - \frac{3r^2(z-c)}{R_1^5}\right] + \frac{P}{8\pi(1-\nu)}\left[\frac{6c(1-2\nu)(z+c)^2 - 6c^2(z+c) - 3(3-4\nu)r^2(z-c)}{R_2^5} - \frac{30cr^2z(z+c)}{R_2^7}\right] \tag{2.9.15}$$

$$\sigma_\theta = \frac{P(1-2\nu)}{8\pi(1-\nu)}\left[\frac{(z-c)}{R_1^3} + \frac{(3-4\nu)(z+c)-6c}{R_2^3} - \frac{4(1-\nu)}{R_2(R_2+z+c)} + \frac{6c(z+c)^2}{R_2^5} - \frac{6c^2(z+c)}{(1-2\nu)R_2^5}\right] \tag{2.9.16}$$

$$\tau_{rz} = \frac{Pr}{8\pi(1-\nu)}\left[-\frac{1-2\nu}{R_1^3} + \frac{1-2\nu}{R_2^3} - \frac{3(z-c)^2}{R_1^5} - \frac{3(3-4\nu)(z+c)z - 3c(3z+c)}{R_2^5} - \frac{30cz(z+c)^2}{R_2^7}\right] \tag{2.9.17}$$

When $c \to \infty$ all terms containing R_2 vanish and the solution becomes that for Kelvin Problem where he force is applied at $(0, 0, c)$ in the positive z-direction.

When $c \to 0$ the stresses and displacements correspond to Boussinesq Problem.

Stresses and displacements in rectangular coordinates (x, y, z) are:

$$\sigma_x = \frac{P}{8\pi(1-\nu)}\left[\frac{(1-2\nu)(z-c)}{R_1^3} - \frac{3x^2(z-c)}{R_1^5} + \frac{(1-2\nu)[3(z-c)-4\nu(z+c)]}{R_2^3}\right]$$
$$- \frac{P}{8\pi(1-\nu)}\left[\frac{3(3-4\nu)x^2(z-c) - 6c(z+c)[(1-2\nu)z - 2\nu c]}{R_2^5} + \frac{30cx^2z(z+c)}{R_2^7}\right]$$
$$- \frac{P}{8\pi(1-\nu)}\left[\frac{4(1-\nu)(1-2\nu)}{R_2(R_2+z+c)}\left\{1 - \frac{x^2}{R_2(R_2+z+c)} - \frac{x^2}{R_2^2}\right\}\right] \tag{2.9.18}$$

$$\sigma_y = \frac{P}{8\pi(1-\nu)}\left[\frac{(1-2\nu)(z-c)}{R_1^3} - \frac{3y^2(z-c)}{R_1^5} + \frac{(1-2\nu)[3(z-c)-4\nu(z+c)]}{R_2^3}\right]$$
$$- \frac{P}{8\pi(1-\nu)}\left[\frac{3(3-4\nu)y^2(z-c) - 6c(z+c)[(1-2\nu)z - 2\nu c]}{R_2^5} + \frac{30cy^2z(z+c)}{R_2^7}\right]$$
$$- \frac{P}{8\pi(1-\nu)}\left[\frac{4(1-\nu)(1-2\nu)}{R_2(R_2+z+c)}\left\{1 - \frac{y^2}{R_2(R_2+z+c)} - \frac{y^2}{R_2^2}\right\}\right] \tag{2.9.19}$$

$$\sigma_z = \frac{P}{8\pi(1-\nu)}\left[-\frac{(1-2\nu)(z-c)}{R_1^3} - \frac{3(z-c)^3}{R_1^5} + \frac{(1-2\nu)(z-c)]}{R_2^3}\right]$$
$$- \frac{P}{8\pi(1-\nu)}\left[\frac{3(3-4\nu)z(z+c)^2 - 3c(z+c)(5z-c)]}{R_2^5} + \frac{30cz(z+c)^3}{R_2^7}\right] \tag{2.9.20}$$

$$\tau_{yz} = \frac{Py}{8\pi(1-\nu)}\left[-\frac{(1-2\nu)}{R_1^3} + \frac{(1-2\nu)}{R_2^3} - \frac{3(z-c)^2}{R_1^5}\right.$$
$$\left. - \frac{3(3-4\nu)z(z+c) - 3c(3z+c)}{R_2^5} - \frac{30cz(z+c)^2}{R_2^7}\right] \tag{2.9.21}$$

$$\tau_{zx} = \frac{Px}{8\pi(1-\nu)}\left[-\frac{(1-2\nu)}{R_1^3} + \frac{(1-2\nu)}{R_2^3} - \frac{3(z-c)^2}{R_1^5}\right.$$
$$\left. - \frac{3(3-4\nu)z(z+c) - 3c(3z+c)}{R_2^5} - \frac{30cz(z+c)^2}{R_2^7}\right] \tag{2.9.22}$$

$$\tau_{xy} = \frac{Pxy}{8\pi(1-\nu)}\left[-\frac{3(z-c)}{R_1^5} - \frac{3(3-4\nu)(z-c)}{R_2^5}\right.$$
$$\left. + \frac{4(1-\nu)(1-2\nu)}{R_2^2(R_2+z+c)}\left\{\frac{1}{R_2+z+c} + \frac{1}{R_2}\right\} - \frac{30cz(z+c)}{R_2^7}\right] \tag{2.9.23}$$

Mindlin obtained a plane strain solution given by Melan, by using a uniform distribution of forces of magnitude p per unit length along a line through $(0, 0, c)$ parallel to the y-axis. If db is a small element of this line at a distance b from the z-axis, the stresses due to this uniform pressure p acting on db can be computed by substituting

pdb for P and $(y-b)$ for y in the above equations. If now we integrate these formulae with respect to b between the limits $-\infty$ to $+\infty$.

2.9.4.2 Force parallel to the boundary

Geometrical description is given in Figure 2.9.4

$$\sigma_x = \frac{Qx}{8\pi(1-\nu)}\left[-\frac{(1-2\nu)}{R_1^3}+\frac{(1-2\nu)(5-4\nu)}{R_2^3}-\frac{3x^2}{R_1^5}-\frac{3(3-4\nu)x^2}{R_2^5}\right]$$
$$-\frac{Qx}{8\pi(1-\nu)}\left[\frac{4(1-\nu)(1-2\nu)}{R_2(R_2+z+c)^2}\left\{3-\frac{x^2(3R_2+z+c)}{R_2^2(R_2+z+c)}\right\}\right.$$
$$\left.-\frac{6c}{R_2^5}\left\{3c+(3-2\nu)(z+c)+\frac{5zx^2}{R_2^2}\right\}\right]$$

$$\sigma_y = \frac{Qx}{8\pi(1-\nu)}\left[\frac{1-2\nu}{R_1^3}+\frac{(1-2\nu)(3-4\nu)}{R_2^3}-\frac{3y^2}{R_1^5}-\frac{3(3-4\nu)y^2}{R_2^5}\right]$$
$$-\frac{Qx}{8\pi(1-\nu)}\left[\frac{4(1-\nu)(1-2\nu)}{R_2(R_2+z+c)^2}\left\{1-\frac{y^2(3R_2+z+c)}{R_2^2(R_2+z+c)}\right\}\right.$$
$$\left.-\frac{6c}{R_2^5}\left\{c-(1-2\nu)(z+c)+\frac{5zy^2}{R_2^2}\right\}\right]$$

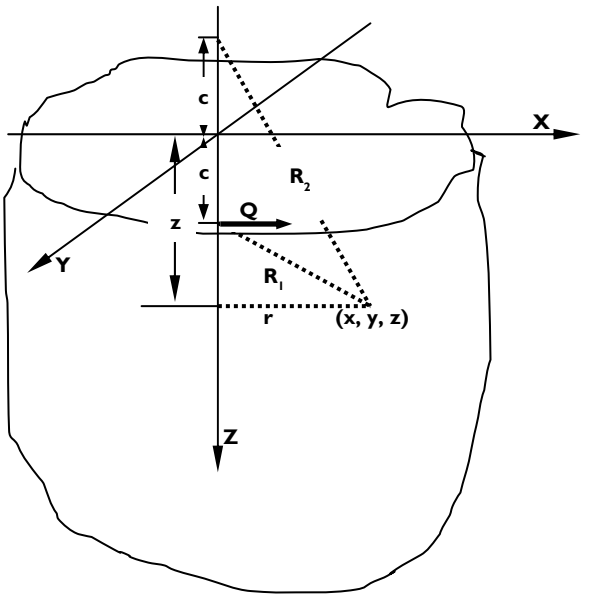


Figure 2.9.4 Concentrated force within mass parallel to boundary.

$$\sigma_z = \frac{Qx}{8\pi(1-\nu)}\left[\frac{1-2\nu}{R_1^3} - \frac{1-2\nu}{R_2^3} - \frac{3(z-c)^2}{R_1^5} - \frac{3(3-4\nu)(z+c)^2}{R_2^5}\right]$$
$$+ \frac{Qx}{8\pi(1-\nu)}\left[\frac{6c}{R_2^5}\left\{c + (1-2\nu)(z+c) + \frac{5z(z+c)^2}{R_2^2}\right\}\right]$$

$$\tau_{yz} = \frac{Pxy}{8\pi(1-\nu)}\left[-\frac{3(z-c)}{R_1^5} - \frac{3(3-4\nu)(z+c)}{R_2^5} + \frac{6c}{R_2^5}\left(1-2\nu+\frac{5z(z+c)}{R_2^2}\right)\right]$$

$$\tau_{zx} = \frac{P}{8\pi(1-\nu)}\left[-\frac{(1-2\nu)(z-c)}{R_1^3} + \frac{(1-2\nu)(z-c)}{R_2^3} - \frac{3x^2(z-c)}{R_1^5}\right.$$
$$\left. - \frac{3(3-4\nu)x^2(z+c)}{R_2^5}\right]$$
$$- \frac{P}{8\pi(1-\nu)}\left(\frac{6c}{R_2^5}\right)\left\{z(z+c) - (1-2\nu)x^2 - \frac{5x^2z(z+c)}{R_2^2}\right\}$$

$$\tau_{xy} = \frac{Py}{8\pi(1-\nu)}\left[-\frac{(1-2\nu)}{R_1^3} + \frac{(1-2\nu)}{R_2^3} - \frac{3x^2}{R_1^5} - \frac{3(3-4\nu)x^2}{R_2^5}\right]$$
$$- \frac{Py}{8\pi(1-\nu)}\left[\left(\frac{4(1-\nu)(1-2\nu)}{R_2(R_2+z+c)^2}\right)\left(1-\frac{x^2(3R_2+z+c)}{R_2^2}\right) - \frac{6cz}{R_2^5}\left(1-\frac{5x^2}{R_2^2}\right)\right]$$

(2.9.24)

$$u = \frac{Q}{16\pi G(1-\nu)}\left[\frac{3-4\nu}{R_1} + \frac{1}{R_2} + \frac{x^2}{R_1^3} + \frac{(3-4\nu)x^2}{R_2^3} + \frac{2cz}{R_2^3}\left(1-\frac{3x^2}{R_2^2}\right)\right]$$
$$+ \frac{Q}{16\pi G(1-\nu)}\left[\frac{4(1-\nu)(1-2\nu)}{R_2+z+c}\left(1-\frac{x^2}{R_2(R_2+z+c)}\right)\right]$$

$$v = \frac{Qxy}{16\pi G(1-\nu)}\left[\frac{1}{R_1^3} + \frac{3-4\nu}{R_2^3} - \frac{6cz}{R_2^5} - \frac{4(1-\nu)(1-2\nu)}{R_2(R_2+z+c)^2}\right]$$

$$w = \frac{Qx}{16\pi G(1-\nu)}\left[\frac{z-c}{R_1^3} + \frac{(3-4\nu)(z-c)}{R_2^3} - \frac{6cz(z+c)}{R_2^5} + \frac{4(1-\nu)(1-2\nu)}{R_2(R_2+z+c)}\right]$$

(2.9.25)

When $c \to \infty$ all terms in the above equations vanish and the solution becomes that for the Kelvin Problem with the force applied in the x-direction.

When $c \to 0$ the equations above give stresses and displacements for the Cerruti Problem.

2.9.5 Theories of Elastodynamics

Elastodynamics is the branch of science that deals with study of waves and time dependent force propagating through a continuum or an elastic media. This is a very important study related to the branch of engineering related to soil dynamics, seismology and geotechnical earthquake engineering. We will not furnish further details here for the topic has been dealt in detail in Chapter 5 (Vol. 1) under the heading of Basic concepts of soil and elastodynamics.

2.10 NUMERICAL METHODS IN ENGINEERING: *BASICS AND APPLICATIONS*

2.10.1 Introduction

In this section, we will discuss some of the important numerical methods applied to civil engineering problems for the solution of a variety of boundary value problems.

Though the basic focus in this book is towards dynamic response of structures and foundations, however we shall discuss a little on the static problems herein, without which we feel that you may find some of the concepts in subsequent chapters difficult.

A pre-requisite to this section is some background on

- *Theory of elasticity, calculus, and strength of materials.*
- *Basic matrix algebra.*
- *Little of programming background helps (not mandatory though).*
- *A lot of imagination, which we believe is the major constituent of being a creative engineer.*

On completion of this chapter, we expect you to

- *Understand the difference between various methods illustrated herein.*
- *Realize the limitations of each of the methods and appreciate the concept that "Garbage input would always give garbage output"*[1].
- *The stumbling blocks and cracks through which errors unknowingly creep in the analysis.*
- *How to attack various practical engineering problems, without overdoing it.*
- *Six digits after decimal in the output file and aesthetically pleasing colored stress contour does not necessarily give the requisite results.*

What is numerical method – *what is so special about it?*

First thing we would like to clarify about the numerical method is that it is an *approximate analysis* and the answers may have some errors in it.

There are problems where results obtained based on numerical methods would have zero error (i.e. it converges to the exact value) and there would be cases where there would be some finite errors in the solution but this error should be of acceptable level.

1 Software does not have the divine power to correct an ill-defined problem and come up with a correct answer.

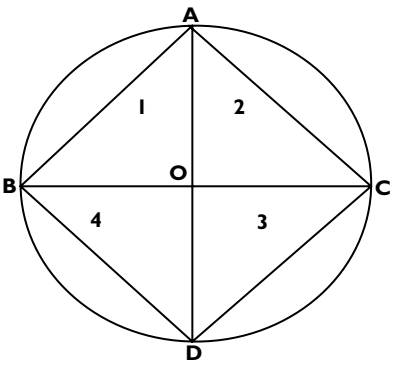


Figure 2.10.1 Circle approximated by four triangles.

We emphasize that, if there exists a closed form analytical solution to an engineering problem, then that would be invariably the most accurate answer and no further numerical analysis would be required.

But in real world this is hardly the case for in many day to day practical problems we come across situations where due to complicated boundary condition, heterogeneous material/ geometric property, complex loading etc. it becomes impossible to find an analytical solution to the problem. It is under these situations, numerical analysis comes to our aid in arriving at a solution, which is approximate (having some error in the result), however, the result should be acceptable for practical design purpose.

To further elucidate this, consider an elementary school problem by asking what is the area of a circle having radius r? Answer would be πr^2. This is clearly a closed form analytical solution to the problem that is exact.

Now suppose we put you in a time machine and take you back to sixth or seventh grade when you had no knowledge of calculus or area of a circle. Only thing you know is the area of a triangle (1/2 base X height) and you are asked to solve this problem – how would you do it?

If you are smart you would possibly attack the problem as shown in Figure 2.10.1.

You can argue that the area of the circle is approximately equal to the area of the four triangles AOB, AOC, BOD, DOC. This gives the total area of four triangle as $A = 4(1/2 \cdot r \cdot r) = 2r^2$ – *which is approximately equal to the area of the circle.*

Well, as a sixth grader, we feel you have not done too badly, for you have arrived at an answer, which is correct up to the order of 67%. The error in your result is because you could not take into account the curved portions outside the triangle.

We again put you back in the time machine and bring you to Class IX where you still do not know calculus but you know geometry and some trigonometry and pose you the same problem to solve[2].

2 We presume that as a IXth grader you would like to improve upon your VIth grade answer.

We increase the number of triangles from four to eight and follow the same logic as posed earlier, and state that the circle is approximately sum of the area of eight triangles as shown in Figure 2.10.2.

For one triangle (Figure 2.10.3) we have

$$\angle AOB = 45^\circ \quad \text{and} \quad \angle OBC = \angle OAC = 67.5^\circ \quad \text{and} \quad OA = OB = r.$$

Based on basic trigonometry we can say that $OC = OB \sin 67.5^\circ = r \sin 67.5^\circ$ and $BC = r \sin 22.5^\circ$ which implies $AB = 2r \sin 22.5^\circ$.

Thus area of the triangle $AOB = (1/2)2r \sin 22.5^\circ \cdot r \sin 67.5^\circ = r^2 \sin 22.5^\circ \sin 67.5^\circ$

Thus, sum of eight triangles gives the total area as $\Delta = 8r^2 \sin 22.5^\circ \sin 67.5^\circ = 2.83r^2$; which is an approximate area of the circle. The error in the answer now is $= [(\pi - 2.83)/\pi] \times 100 = 9.9\%$ a sure improvement to what you found in sixth grade.

Can we improve this result a bit more? Let us see how .....

We know that error in our result is the curved area out side the octagon is shown in Figure 2.10.4.

At the center of the curve the maximum ordinate value is

$$y = r - h = r(1 - \sin 67.5^\circ)$$

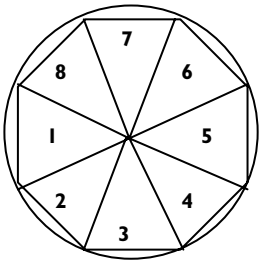


Figure 2.10.2 Circle approximated by an octagon.

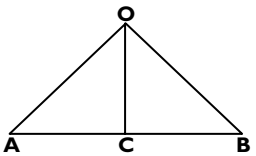


Figure 2.10.3 Area of one triangle.

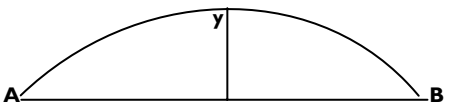


Figure 2.10.4 Curved area outside the octagon.

While at the end the value of the ordinate is zero, thus average value of ordinate is

$$y_{av} = r(1 - \sin 67.5^\circ)/2$$

Thus approximating the curved area by a rectangle the area of the rectangle is

$$\text{Area} = \frac{r}{2}(1 - \sin 67.5^\circ) \times 2r \sin 22.5^\circ = 0.02913r^2$$

Thus for the eight equivalent rectangle that we ignored initially the total area is $= 0.23304r^2$.

Adding this to previously obtained result of eight triangles, we have total area of the circle approximated as

$$\text{Area} \cong 2.83r^2 + 0.23304r^2 = 3.063r^2$$

Thus error to the exact result is $= [(\pi - 3.06)/\pi] \times 100 = 2.6\%$ only.

We will not pursue the matter further but would like to draw some important conclusions from the above exercise.

- The actual area of the circle is πr^2. This is an analytical solution and is exact.
- We solved the subsequent problem based on discretising the area into simpler shapes whose area is known to us and summing it up we approximately arrived at an answer that had some error in it.
- Based on the solution we could also notice that cruder were the elements more was the error as we increased the number of elements the errors progressively decreased (4 triangles versus 8 triangles).

It is possibly in this way by summing the area of known geometrical shapes inscribing a circle the Chinese[3] found out the value of $pi(\pi)$ correct to 3.1415927 and gave the famous postulation that "Area of a circle when divided by the square of its radius r is always a constant".

We will see later that a very similar philosophy is followed in mathematical modeling of systems when we analyze the same based on finite difference method (FDM) or finite element method (FEM).

In our real world of engineering, we often face differential equations (could be ordinary or partial) whose direct analytical solutions are not always possible due to various complexities in its boundary conditions. This is when we resort to approximate numerical solution, which is acceptable for practical use and has eased our life significantly. The impetus has grown strongly with the advent of digital computers, when solving large number of algebraic equations through a computer has become a routine affair.

3 Mathematician Teu Tzeng Tze (A.D. 429–500) determined $3.1415926 < \pi < 3.1514927$.

2.10.2 Approximate methods applied to boundary value problems

By posing the above title, we do neither mean to be mathematically elegant nor intend to be abstract in our presentation. Thus the first thing we explain is what is a boundary value problem?

Say that $a\frac{d^2y}{dx^2} + b = 0$ is a boundary value problem; we have surely done our duty to define it, but may not have perhaps cleared the concept to all. Since we presume that this book is being read by a civil engineer, we borrow an equation from strength of materials and pose

$$EI\frac{d^2y}{dx^2} + M_x = 0 \tag{2.10.1}$$

Is a boundary value problem, we believe that things have improved significantly in terms of our understanding.

The equation is solved for obtaining displacement expressions for beams whose solution will depend upon the end or boundary conditions like $y = 0$ at $x = 0$, $dy/dx = 0$ at $x = 0$ etc.

Since the solution is a function of the end or end–boundary conditions these are termed as the boundary value problems.

Other equations are also broadly classified as boundary value problems but are strictly not so. Let us consider the equation,

$$m\frac{d^2x}{dt^2} + c\frac{dx}{dt} + kx = P(t). \tag{2.10.2}$$

This is the equation of motion of lumped mass suspended from a spring and dashpot[4]. Those of you who are conversant with the theory of vibration would know that key to its solution lies in its initial conditions like at $t = 0$ $u = 0$ and at $t = 0$ $du/dt = v$ etc.

Since the solution is a function of the initial condition of the displacement and velocity vector at $t = 0$, *they are called initial value problem.* Let us now consider another partial differential equation,

$$G\frac{\partial^2 u}{\partial z^2} = \rho\frac{\partial^2 u}{\partial t^2}. \tag{2.10.3}$$

This is the equation of motion of wave propagation through an elastic media[5] in one dimension. Solution to such equation is a function of both the end condition like whether the boundary is free, constrained etc and also dependent on time like at $t = 0$ $u = u_0$ etc.

4 We will see in later chapter that this equation has an immense application in solution of problems related to structural dynamics.

5 This equation we will see later has a lot of application in soil dynamics and also to problems related to Earthquake engineering.

These types of equations are called initial-boundary value problem for they are dependent on both initial and end-boundary conditions.

In the following sections, we present some of the approximate solution methods that are used to solve boundary value problems.

2.10.2.1 Rayleigh-Ritz method

The method was originally proposed by Rayleigh. The method can be explained as follows:

If we have a differential equation whose boundary condition are known, then rather than solving the equation itself, the solution is started off with an assumed function. The function is so chosen that it satisfies the boundary conditions for the given differential equation. Thus instead of solving the differential equation applying the assumed function to a functional Πp a substitute approximate solution to the problem is obtained.

The accuracy of the solution increases as more and more number of higher order terms is considered in the assumed function.

To explain the above problem let us borrow a classroom-problem shown in Figure 2.10.5 and whose exact solution is known.

We consider a simply supported beam subjected to a uniformly distributed load w spanning over a length L.

To determine the deflection we write

$$EI\frac{d^2y}{dx^2} = -M_x \quad \text{or } EI\frac{d^2y}{dx^2} = -\frac{wL}{2}x + \frac{wx^2}{2} \tag{2.10.4}$$

which on integration gives,

$$EIy = -\frac{wL}{12}x^3 + \frac{wx^4}{24} + C_1x + C_2 \tag{2.10.5}$$

where C_1 and C_2 are integration constants and imposing the boundary conditions at $x = 0\ y = 0$, gives, $C_2 = 0$ and with $x = L, y = 0$ we have,

$$EIy = -\frac{wL}{12}x^3 + \frac{wx^4}{24} + \frac{wL^3}{24}x \tag{2.10.6}$$

At $x = L/2$ we have,

$$y_{L/2} = y_{\max} = \frac{5wL^4}{384EI} = 0.013021\frac{wL^4}{EI}. \tag{2.10.7}$$

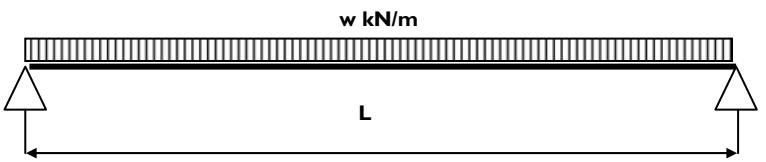


Figure 2.10.5 A simply supported beam under udl.

Thus based on above the general equation of displacement can be written as

$$y = y_{\max}\left[\frac{16}{5}\left(\frac{x}{L}\right)^4 - \frac{32}{5}\left(\frac{x}{L}\right)^3 + \frac{16}{5}\left(\frac{x}{L}\right)\right] \tag{2.10.8}$$

In the above expression, the value within the bracket describes the displacement function at various points in the beam with respect to the maximum displacement. *The shape function is exact as it was obtained based on the solution of the differential equation.*

Now suppose we do not want to solve the differential equation and yet arrive at a solution to the above problem. We assume a parabolic function say,

$$y = A\frac{x}{L}\left(1 - \frac{x}{L}\right). \tag{2.10.9}$$

It will be observed that the function satisfies the boundary condition that at $x = 0$, $y = 0$ and at $x = L, y = 0$.

The potential energy of the system is then given by

$$\Pi p = \frac{EI}{2}\int_0^L \left(\frac{d^2y}{dx^2}\right)^2 dx - w\int_0^L y dx \tag{2.10.10}$$

Substituting $y = A\left(\frac{x}{L} - \frac{x^2}{L^2}\right)$ and on integration we have $\Pi p = \frac{2EIA^2}{L^3} - \frac{wAL}{6}$.

For stationary value of the functional Πp $\frac{\partial \Pi_p}{\partial A} = 0$ and we may obtain

$$A = \frac{wL^4}{24EI}. \tag{2.10.11}$$

The approximate solution of the problem is given by

$$y = \frac{wL^4}{24EI}\left(\frac{x}{L} - \frac{x^2}{L^2}\right) \quad \rightarrow \quad y_{\max} = 0.010417\frac{wL^4}{EI}. \tag{2.10.12}$$

It shows that there is some error in the answer; however, this will be minimized if we take more terms. For instance if we consider the function as

$$y = A_1\frac{x}{L}\left(1 - \frac{x}{L}\right) + A_2\frac{x^2}{L^2}\left(1 - \frac{x}{L}\right) \tag{2.10.13}$$

The results would improve and we would get a better answer.

We now solve the same problem with a different function. Let,

$$y = A \sin \frac{\pi x}{L}. \tag{2.10.14}$$

Note that this function satisfies the boundary condition of $y = 0$ at $x = 0$ and $x = L$.

The potential energy is given by

$$\Pi p = \frac{EI}{2} \int_0^L \left(\frac{d^2 y}{dx^2} \right)^2 dx - w \int_0^L y dx \quad \text{i.e. } \Pi p = \frac{EIA^2 \pi^4}{4L^3} - \frac{2wAL}{\pi}. \tag{2.10.15}$$

Taking $\frac{\partial \Pi_p}{\partial A} = 0$, we have $A = \frac{4wL^4}{EI\pi^5}$

The displacement expression can now be stated as,

$$y = \frac{4}{\pi^5} \frac{wL^4}{EI} \sin \frac{\pi x}{L} \tag{2.10.16}$$

which gives $y_{\max} = 0.01307 \frac{wL^4}{EI}$ which is almost the exact answer.

The values are plotted in Figure 2.10.6 for your comparison. Reviewing the plot, you will see that while the parabolic one term approximation has some error in the solution, by assuming the shape function as a sinusoidal function we have arrived at almost an exact solution.

So, what was the magic in the sine function?

Pondering over it, we will see that there is nothing magical about it and the result is very logical. First, the sine function satisfies the boundary condition representing the

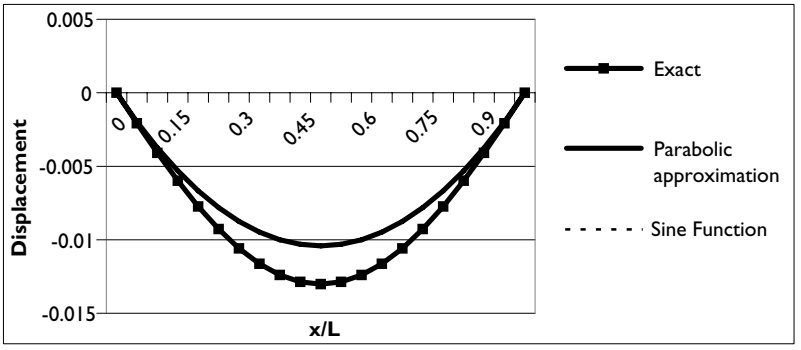


Figure 2.10.6 Displacement plot of a simply supported beam, Rayleigh-Ritz method.

differential equation, which makes it a compatible function. Moreover, the same sine function can be represented by an infinite series

$$\sin\frac{\pi x}{L} = \frac{\pi x}{L} - \frac{\pi^3 x^3}{L^3 3!} + \frac{\pi^5 x^5}{L^5 5!} - \frac{\pi^7 x^7}{L^7 7!} + \cdots\cdots\infty \tag{2.10.17}$$

Thus, when the sine function is integrated, we are in effect integrating an algebraic series of infinite order with no truncation error. Since sufficient number of terms is being considered in the algebraic series, the value almost converges to the exact value.

Instead of the sine function if we would have approximated the value of sine function as

$$\sin\frac{\pi x}{L} \cong \frac{\pi x}{L} - \frac{\pi^3 x^3}{L^3 3!} + \frac{\pi^5 x^5}{L^5 5!} - \frac{\pi^7 x^7}{L^7 7!} \tag{2.10.18}$$

Considering only the first four terms, we would have nonetheless arrived at a solution albeit with some errors.

Having stated the Rayleigh-Ritz method we proceed on to explain another method termed as *Weighted Residual Methods* (WRM) which is yet an important stepping stone for derivation of the shape functions of various elements which when combined with Rayliegh's method ultimately generate the stiffness of individual elements.

2.10.2.2 Weighted residual methods

While explaining the Rayleigh-Ritz Method earlier, we have stated to have a simplified solution of the differential equation by assuming a shape function, which satisfies the end boundary conditions, and solve for an alternative problem and arrive at an approximate solution. The accuracy of the result would depend on the choice of shape function and the number of terms considered in it. We can argue now that since the shape function assumed is not exact[6], the results would surely have some error prevalent in it. Applying the weighted residual method, we try to minimize this error in some way by averaging it out over the whole domain and arrive at a solution that is closer to the exact solution.

The method can be explained as follows:

Consider the beam element we had dealt earlier. The displacement equation is given by

$$EI\frac{d^2y}{dx^2} = -M_x; \quad EI\frac{d^3y}{dx^3} = -V_x \quad \text{and} \quad EI\frac{d^4y}{dx^4} = -w. \tag{2.10.19}$$

Now if we choose an approximate function

$$y = A_1\phi_1 + A_2\phi_2 + A_3\phi_3 + \cdots\cdots + A_n\phi_n \tag{2.10.20}$$

6 Since we did not arrive at it by solving the differential equation.

implying, $y = \sum_1^n A_j\phi_j$ which satisfies the boundary condition of the fourth order differential equation, then

$$EI\frac{d^4y}{dx^4} = \sum_1^n A_j\phi_j^{iv} \tag{2.10.21}$$

Since the function is approximate, we expect a residual error to remain in the answer and this is given by

$$R_e = \sum_1^n A_j\phi_j^{iv} + w \tag{2.10.22}$$

We now examine various methods available to minimize this residual error.

2.10.2.2.1 *Collocation method*

In this method, the residual error is forced to zero at a number of selected points that should be equal to the number of unknowns in the shape function equation (A1, A2, ... An).

Thus if the shape function has one unknown (A1), the collocation point is the one in which error is forced to zero. If there are two unknowns (A1, A2), collocation points are two where errors are forced to zero and so on.

Thus considering

$$R_e = \sum_1^n A_n\phi_n'''' + w = 0 \tag{2.10.23}$$

for n collocation points, we have n algebraic equations from which the coefficients are obtained.

To further elucidate the problem let us go back to the beam problem we solved earlier having an assumed shape function of $y = A\sin\frac{\pi x}{L}$.

$$\text{Thus,}\quad EI\frac{d^4y}{dx^4} = \frac{EIA\pi^4}{L^4}\sin\frac{\pi x}{L} \tag{2.10.24}$$

and the residual error can be expressed as

$$R_e = \sum_1^n A_n\phi_n^{iv}w = 0 \quad \text{or } \frac{EIA\pi^4}{L^4}\sin\frac{\pi x}{L} + w = 0. \tag{2.10.25}$$

Since number of constant is one (i.e. A), we force the error to zero at one point $x = L/2$.

This gives $\frac{EIA\pi^4}{L^4} + w = 0$ or $A = -\frac{wL^4}{\pi^4 EI}$, and the displacement function is now given by

$$y = -\frac{wL^4}{\pi^4 EI} \sin \frac{\pi x}{L} \tag{2.10.26}$$

We may notice two things; the function is differentiable four times and especially for the Collocation Method, experience is required as to where to choose the collocation points. If $x = L/3$ were taken, we would have got a different coefficient value.

2.10.2.2.2 Sub-domain method

In this method the error is averaged out over the sub-domain in which the integration is carried out by setting it to zero. The number of sub domain chosen should be equal to the number of unknown coefficients (A1, A2, . . . , An) in the shape function. For the given beam problem we have seen the residual error is given by

$$R_e = \frac{EIA\pi^4}{L^4} \sin \frac{\pi x}{L} + w \tag{2.10.27}$$

Since the unknown coefficient is only one (A) we integrate the residue over the whole domain 0–L that gives

$$\frac{EIA\pi^4}{L^4} \int_0^L \sin \frac{\pi x}{L} + \int_0^L w dx = 0 \tag{2.10.28}$$

This gives $\frac{EIA\pi^3}{L^3} [1 - \cos \pi] + wL = 0$ or $A = -\frac{wL^4}{2EI\pi^3}$, which gives the displacement function as

$$y = -\frac{wL^4}{2EI\pi^3} \sin \frac{\pi x}{L}. \tag{2.10.29}$$

2.10.2.2.3 Galerkin's method

In this Method, the residual error is minimized by multiplying the residual error by the assumed shape function itself and integrating it over the domain. Thus as per this method

$$\int_0^L R_e y dx = 0, \tag{2.10.30}$$

where y is the assumed shape function considered as the solution to the problem.

For the above beam problem

$$\int_0^L \left[\frac{EIA\pi^4}{L^4} \sin \frac{\pi x}{L} + w \right] \sin \frac{\pi x}{L} dx = 0$$

$$\text{or} \quad \frac{EIA\pi^4}{L^4} \int_0^L \sin^2 \frac{\pi x}{L} dx + w \int_0^L \sin \frac{\pi x}{L} dx = 0 \tag{2.10.31}$$

Equation (2.10.31), on integration and imposition of the limits, gives $A = -\frac{4wL^4}{\pi^5 EI}$ and

$$y = -\frac{4wL^4}{EI\pi^5} \sin \frac{\pi x}{L}. \tag{2.10.32}$$

2.10.2.2.4 Least square method

In this case, square of the error is integrated over the domain and to minimize this functional the same is differentiated with respect to the unknown coefficients. This minimizes the error.

Based on the beam problem we have

$$R_e = \frac{EIA\pi^4}{L^4} \sin \frac{\pi x}{L} + w \tag{2.10.33}$$

Squaring the above, we get

$$R_e^2 = \left[k^2 A^2 \sin^2 \frac{\pi x}{L} + w^2 + 2kAw \sin \frac{\pi x}{L} \right], \quad \text{where } k = \frac{EI\pi^4}{L^4}. \tag{2.10.34}$$

Integrating it over the domain 0–L we have

$$R_e^2 = \int_0^L \left[k^2 A^2 \sin^2 \frac{\pi x}{L} + w^2 + 2kAw \sin \frac{\pi x}{L} \right] dx. \tag{2.10.35}$$

$$\text{This gives,} \quad E_R = R_e^2 = \frac{k^2 A^2 L}{2} + w^2 L + \frac{2kAwL}{\pi}, \tag{2.10.36}$$

for minimizing this functional we set $\frac{\partial E_R}{\partial A} = 0$ which gives $A = -\frac{4wL^4}{\pi^5 EI}$.

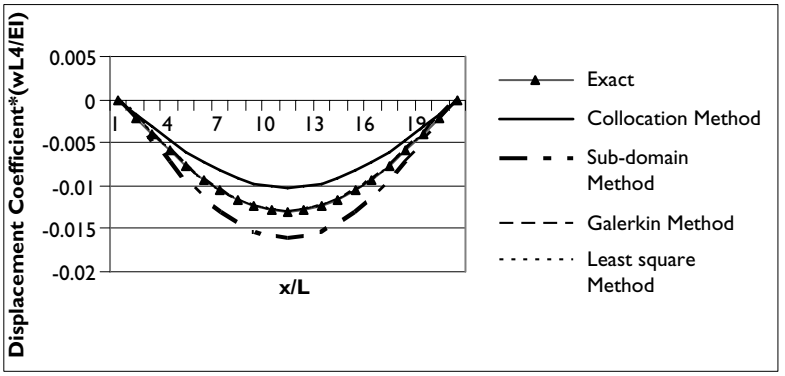


Figure 2.10.7 Displacement plot of simply supported beam based on various weighted residual methods.

Thus, the displacement equation is now given by

$$y = -\frac{4wL^4}{EI\pi^5} \sin \frac{\pi x}{L}. \tag{2.10.37}$$

We show in Figure 2.10.7, the comparative values of displacements based on the various methods for this particular case.

Based on the above, *one should not draw an immediate conclusion on the superiority of a particular method. It depends on the type of function chosen and the boundary condition as to which method would give the best result.*

The weighted residual method though is a powerful method for solution of differential equation yet suffers from one serious drawback. The choice of shape function there are no systematic way to arrive at an appropriate value. Especially for the case when the boundary conditions are complicated, engineers find it convenient to resort to finite difference method (FDM)[7] where though the computational efforts are more (than WRM) is far easier to cater to the complex boundary conditions.

The choice of appropriate boundary condition requires lot of judgment and if this selection is not correct, the solution could give unacceptable results.

From the above discussion, it can be concluded that provided we are in a position to develop a systematic generic approach to develop piecewise continuous function over a domain which is complete and compatible, the WRM can become a powerful tool in the hand of an analyst.

This is what we are going to study under the heading of Finite Element Method (FEM) later.

7 This we are going to take up in next section.

2.11 THE FINITE DIFFERENCE METHOD (FDM)

In the previous section, we had shown that the solution of differential equation based on assumed shape functions simplifies the analysis considerably. We had also mentioned that if selections of such shape functions were not appropriate the results achieved would be in error. Also mentioned was that there exists no generic laws to choose the shape function and choice remains a judgment in the hand of an analyst.

To circumvent this problem for systems with complex boundary conditions the application of finite difference method came into being. Here a differential equation having complex boundary conditions are broken into finite number of difference equations and ultimate solutions are obtained by solving a specific number of algebraic equations[8].

Now let us consider Figure 2.11.1. The figure shows the values of a function of x at finite intervals $h/2$. The differences $f(x+h)-f(x), f(x)-f(x-h)$ and $f(x+h/2)-f(x-h/2)$ and the differences between the values of the function at a finite interval h are called the *finite differences*.

The finite difference $f(x+h)-f(x)$ is called **the forward difference** at point j the finite difference $f(x)-f(x-h)$ is called the **backward difference** at point j and $f(x+h/2)-f(x-h/2)$ is called the **central difference** at point j.

The use of central difference generally results in smaller truncation error than when forward and backward difference equations and becomes the *subject for our subsequent discussion*.

The **first central difference** equation of the function at point j is defined as

$$\delta f(x) = f\left(x+\frac{h}{2}\right) - f\left(x-\frac{h}{2}\right) \tag{2.11.1}$$

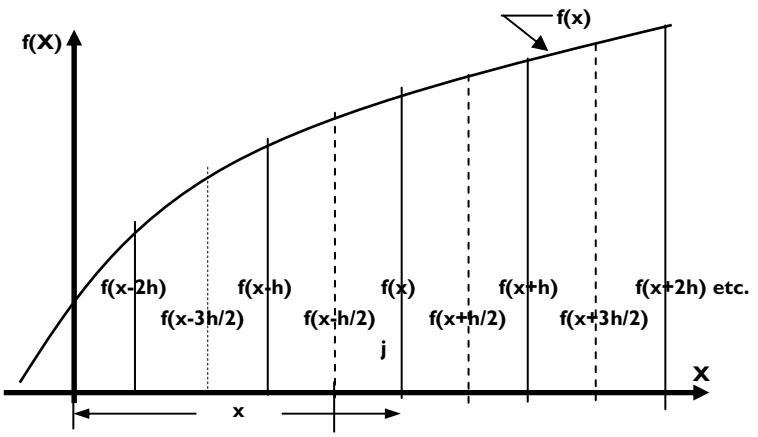


Figure 2.11.1 Variation of function of X for steps h/2.

8 This is usually solved by matrix method of solution of linear equations.

That is $\delta f(x)$ represents the difference between the value of the function at $(x + h/2)$ and that at $(x - h/2)$ where the symbol δ is called the **central difference operator.**

Like the differential operator, $D\left(\equiv \frac{d}{dx}\right)$, δ is a linear operator satisfying the formal laws of algebra.

The **second central difference** of the function at point j is the **difference** of the *first central difference.*

$$\delta^2 f(x) = \delta[\delta f(x)] \equiv [f(x+h) - f(x)] - [f(x) - f(x-h)]$$

$$= f(x+h) - 2f(x) + f(x-h)$$

$$\text{Similarly} \quad \delta^3 f(x) = \delta[\delta^2 f(x)] = f\left(x + \frac{3h}{2}\right) - 3f\left(x + \frac{h}{2}\right) + 3f\left(x - \frac{h}{2}\right) - f\left(x - \frac{3h}{2}\right)$$

And $\delta^4 f(x) = \delta[\delta^3 f(x)]$, this on expansion gives

$$\delta^4 f(x) = f(x+2h) - 4f(x+h) + 6f(x) - 4f(x-h) + f(x-2h)$$

$$\text{In general,} \quad \delta^n f(x) = \delta[\delta^{n-1} f(x)] = \delta^r[\delta^{n-r} f(x)] \tag{2.11.2}$$

The above can be expanded as

$$\delta^n f(x) = f\left(x + \frac{n}{2}h\right) - {}^nC_1 f\left(x + \frac{n}{2}h - h\right) + {}^nC_2 f\left(x + \frac{nh}{2} - 2h\right) - \cdots + {}^nC_r\left(x + \frac{n}{2}h - rh\right) + \cdots + (-1)^n f\left(x + \frac{n}{2}h - nh\right) \tag{2.11.3}$$

where ${}^nC_r = \frac{n!}{r!(n-r)!}$.

In the above first central difference formulation the term $f(x)$ is expressed in terms of the values of the function $(x + h/2)$ and $(x - h/2)$. Usually it is easier to work with values of function at full interval h rather then half intervals $h/2$. Thus rather than using first central difference, it is generally preferable to use the averaged first central difference, $\mu\delta f(x)$ defined by

$$\mu\delta f(x) = \frac{1}{2}\left[\delta f\left(x + \frac{h}{2}\right) + \delta f\left(x - \frac{h}{2}\right)\right] \quad \text{or,} \quad \mu\delta f(x) = \frac{1}{2}\left[f(x+h) - f(x-h)\right] \tag{2.11.4}$$

Next, we try to establish the relation between the finite difference and differential operator

- $\mu\delta f(x) \leftrightarrow hDf(x) \equiv f'(x)$
- $\delta f(x) \leftrightarrow hDf(x) \equiv f'(x)$
- $\delta^2 f(x) \leftrightarrow h^2D^2f(x) \equiv f''(x)$ (2.11.5)

Here $D \equiv d/dx$.
By Taylor's series, we know that

$$f(x+h) = f(x) + h\dot{f}(x) + \frac{h^2}{2!}\ddot{f}(x) + \frac{h^3}{3!}\dddot{f}(x) + \cdots\cdots \tag{2.11.6}$$

Thus expressing the above in terms of the differential operator D, we have

$$\begin{aligned} f(x+h) &= f(x) + hDf(x) + \frac{h^2D^2}{2!}f(x) + \frac{h^3D^3}{3!}f(x) + \cdots\cdots + \frac{h^nD^n}{n!}f(x) \\ &= \left[1 + \frac{hD}{1!} + \frac{h^2D^2}{2!} + \frac{h^3D^3}{3!} + \cdots\cdots + \frac{h^nD^n}{n!}\right] f(x) = e^{hD}f(x) \end{aligned} \tag{2.11.7}$$

i.e. *Taylor's expansion of* $f(x+h)$ *is given by the exponential series* e^{hD} *operating on* $f(x)$.

Thus $\quad f(x-h) = e^{-hD}f(x)$ (2.11.8)

Now $\quad \mu\delta f(x) = \frac{1}{2}[f(x+h) - f(x-h)] = \frac{1}{2}\left[e^{hD} - e^{-hD}\right]f(x) = \sinh(hD)f(x)$

$$\mu\delta f(x) = \left[hD + \frac{h^3D^3}{6} + \frac{h^5D^5}{120} + \cdots\cdots\right] f(x) \tag{2.11.9}$$

Neglecting $\frac{h^3D^3}{6}$, $\frac{h^5D^5}{120}$ as higher order terms, we have

$$\mu\delta f(x) = hDf(x). \tag{2.11.10}$$

$$Df(x) = \frac{1}{h}\mu\delta f(x) \quad \rightarrow \quad f'(x) = \frac{1}{2h}\left[f(x+h) - f(x-h)\right] \tag{2.11.11}$$

Again based on similar logic we have

$$f\left(x + \frac{h}{2}\right) = e^{hD/2}f(x) \quad \text{and} \quad f\left(x - \frac{h}{2}\right) = e^{-hD/2}f(x)$$

As $\delta f(x) = f\left(x + \frac{h}{2}\right) - f\left(x - \frac{h}{2}\right)$, we can represent it by

$$\delta f(x) = [e^{hD/2} - e^{-hD/2}]f(x) = 2\sinh\frac{hD}{2}f(x)$$

$$\rightarrow \quad \delta = 2\sinh\frac{hD}{2} = \left[hD + \frac{h^3D^3}{24} + \frac{h^5D^5}{1920} + \cdots\cdots\right] \tag{2.11.12}$$

$$\text{Also,} \quad \delta^2 = \delta\cdot\delta = \left[hD + \frac{h^3D^3}{24} + \frac{h^5D^5}{1920} + \cdots\cdots\right] \times \left[hD + \frac{h^3D^3}{24} + \frac{h^5D^5}{1920} + \cdots\cdots\right]$$

$$= [h^2D^2 + \text{Higher orders of } h \text{ and } D]$$

Ignoring the higher orders, we have $\delta^2 = h^2D^2 + \text{Errors}$

Thus we have, $D^2 = \frac{1}{h^2}\delta^2$ and $f''(x) = \frac{1}{h^2}[f(x+h) - 2f(x) + f(x-h)]$ and $\frac{d^2y}{dx^2}$ at point i

$$\text{can be expressed as} \quad \frac{d^2y_i}{dx^2} = \frac{1}{h^2}[y_{i+1} - 2y_i + y_{i-1}] \tag{2.11.13}$$

Similarly,

$$D^4f(x) = \frac{1}{h^4}\delta^2(\delta^2 f(x)) = \frac{1}{h^4}[f(x+2h) - 4f(x+h) + 6f(x) - 4f(x-h) + f(x-2h)]$$

and $\frac{d^4y}{dx^4}$ at point i can be expressed as

$$\frac{d^4y_i}{dx^4} = \frac{1}{h^4}[y_{i+2} - 4y_{i+1} + 6y_i - 4y_{i-1} + y_{i-2}] \tag{2.11.14}$$

The reader may check based on similar steps that

$$\frac{d^3y_i}{dx^3} = \frac{1}{h^3}[-y_{i+2} + y_{i+1} - 2y_{i-1} + y_{i-2}] \tag{2.11.15}$$

2.11.1 Application to ordinary differential equations (ode)

To apply the theory we start with the problem we had derived earlier a simple beam subject to a uniform distributed load over span L. The equation of equilibrium is a linear differential equation.

For the beam as shown below we try to find out the deflection and bending moment of the beam by finite difference method. As a first step we break up the beam into six segments, each of length $h = L/6$ by putting 5 internal nodes (1 to 5) as shown in Figure 2.11.2. You will observe that we had also taken 2 additional nodes (-1, and 7) along the beam axis. These nodes are often called *phantom nodes* (fictitious nodes). These are imaginary nodes, whose application will be seen subsequently while we perform the analysis.

From our basic knowledge of strength of material, we know that

$$EI\frac{d^2y}{dx^2} = M_x; \quad EI\frac{d^3y}{dx^3} = V_x \quad \text{and} \quad EI\frac{d^4y}{dx^4} = w \tag{2.11.16}$$

where w is the uniformly distributed load on the beam.

Based on finite difference derivation, vide Equation 2.11.14 we can write this as

$$\frac{d^4y}{dx^4} = \frac{1}{h^4}\left[y_{i+2} - 4y_{i+1} + 6y_i - 4y_{i-1} + y_{i-2}\right] = \frac{w}{EI} \tag{2.11.17}$$

Applying the above equation at node i we have

$$\begin{aligned}
&\text{At} \quad i = 1, \quad \frac{1}{h^4}\left[y_3 - 4y_2 + 6y_1 - 4y_0 + y_{-1}\right] = \frac{w}{EI};\\
&\text{At} \quad i = 2, \quad \frac{1}{h^4}\left[y_4 - 4y_3 + 6y_2 - 4y_1 + y_0\right] = \frac{w}{EI};\\
&\qquad i = 3, \quad \frac{1}{h^4}\left[y_5 - 4y_4 + 6y_3 - 4y_2 + y_1\right] = \frac{w}{EI};\\
&\qquad i = 4, \quad \frac{1}{h^4}\left[y_6 - 4y_5 + 6y_4 - 4y_3 + y_2\right] = \frac{w}{EI};\\
&\qquad i = 5, \quad \frac{1}{h^4}\left[y_7 - 4y_6 + 6y_5 - 4y_4 + y_3\right] = \frac{w}{EI}.
\end{aligned} \tag{2.11.18}$$

Now at the node 0 and 6, the deflections must be zero. Moreover, as the beam is simply supported the moment must be also zero at the nodes 0 and 6.

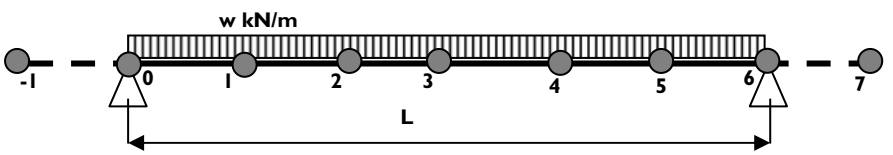


Figure 2.11.2 Simply supported beam with udl.

Considering $EI\frac{d^2y}{dx^2} = M_x$, we can write this in finite difference form as

$$\frac{d^2y}{dx^2} = \frac{1}{h^2}\left[y_{i+1} - 2y_i + y_{i-1}\right] = \frac{M}{EI} \tag{2.11.19}$$

For node $i = 0$, $\frac{1}{h^2}\left[y_{-1} - 2y_0 + y_1\right] = 0$, and for node $i = 6$, $\frac{1}{h^2}\left[y_5 - 2y_6 + y_7\right] = 0$. Since the beam is simply supported at node 0 and 6, we have

$$y_0 = y_6 = 0 \Rightarrow y_{-1} = -y_1 \quad \text{and} \quad y_5 = -y_7$$

Substituting these values, we have following five equations to be solved.

$$y_3 - 4y_2 + 5y_1 = \frac{wh^4}{EI}; \quad y_4 - 4y_3 + 6y_2 - 4y_1 = \frac{wh^4}{EI};$$
$$y_5 - 4y_4 + 6y_3 - 4y_2 + y_1 = \frac{wh^4}{EI}; \quad -4y_5 + 6y_4 - 4y_3 + y_2 = \frac{wh^4}{EI};$$
$$5y_5 - 4y_4 + y_3 = \frac{wh^4}{EI}.$$

Expressing the above five equations in the matrix form, we have

$$\begin{bmatrix} 5 & -4 & 1 & 0 & 0 \\ -4 & 6 & -4 & 1 & 0 \\ 1 & -4 & 6 & -4 & 1 \\ 0 & 1 & -4 & 6 & -4 \\ 0 & 0 & 1 & -4 & 5 \end{bmatrix} \begin{Bmatrix} y_1 \\ y_2 \\ y_3 \\ y_4 \\ y_5 \end{Bmatrix} = \begin{Bmatrix} 1 \\ 1 \\ 1 \\ 1 \\ 1 \end{Bmatrix} \frac{wh^4}{EI}$$

$$\rightarrow \quad [A]\,\{y\} = \{F\} \quad \rightarrow \quad \{y\} = [A]^{-1}\,\{F\}\,. \tag{2.11.20}$$

Inversion[9] of matrix A and multiplying with the column matrix on the right hand side gives

$$\begin{Bmatrix} y_1 \\ y_2 \\ y_3 \\ y_4 \\ y_5 \end{Bmatrix} = \begin{Bmatrix} 8.75 \\ 15 \\ 17.25 \\ 15 \\ 8.75 \end{Bmatrix} \frac{wL^4}{1296EI} \quad \text{which gives} \quad \begin{Bmatrix} y_1 \\ y_2 \\ y_3 \\ y_4 \\ y_5 \end{Bmatrix} = \begin{Bmatrix} 0.006752 \\ 0.011574 \\ 0.01331 \\ 0.011574 \\ 0.006752 \end{Bmatrix} \frac{wL^4}{EI} \tag{2.11.21}$$

9 This is quite straight forward exercise now a days and can very easily be done in Mathcad, Matlab or even Excel.

The bending moment may be now back calculated from the equation (2.11.13) as

$$\frac{d^2y}{dx^2} = \frac{M_x}{EI} = \frac{y_{i-1} - 2y_i + y_{i+1}}{h^2} \tag{2.11.22}$$

$$\begin{aligned}
\text{Thus, at node } -1, \quad & M_{x1} = \frac{36EI}{L^2}[y_0 - 2y_1 + y_2] = 0.06944wL^2; \\
\text{at node } 2, \quad & M_{x2} = \frac{36EI}{L^2}[y_1 - 2y_2 + y_3] = 0.11111wL^2; \\
\text{at node } 3, \quad & M_{x3} = \frac{36EI}{L^2}[y_2 - 2y_3 + y_4] = 0.125wL^2; \\
\text{at node } -4, \quad & M_{x4} = \frac{36EI}{L^2}[y_3 - 2y_4 + y_5] = 0.11111wL^2; \quad \text{and} \\
\text{at node } -5, \quad & M_{x5} = \frac{36EI}{L^2}[y_4 - 2y_5 + y_6] = 0.06944wL^2.
\end{aligned} \tag{2.11.23}$$

Having obtained the values of displacements and moments, we now compare them with the exact solution we have derived earlier.

From the curves in Figures 2.11.3 and 4, you will see that the values match quite well both for displacement and bending moments. However, if you look at the curves very carefully you will see that there exists a small error at points in between the nodes compared to the exact solution (though at selected points the values are almost exact[10]).

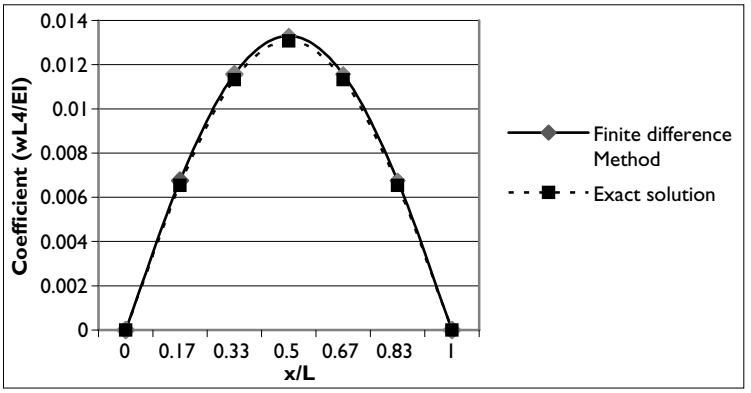


Figure 2.11.3 Comparison of displacements for a simply supported beam.

10 The values converge here in collocating sense.

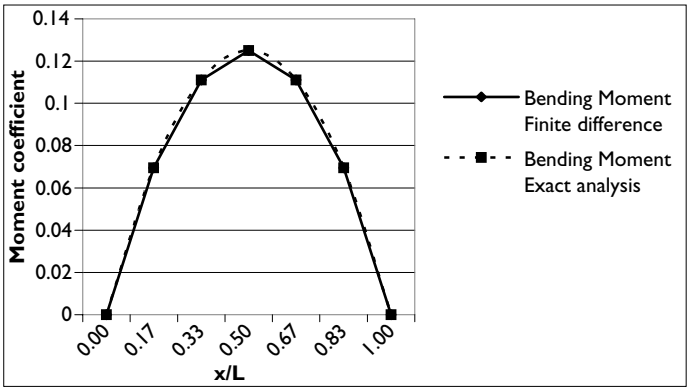


Figure 2.11.4 Comparison of bending moment for a simply supported beam.

This can still be minimized if we take more number of points in lieu of seven (five internal and two at support) like 10 or 15, this will reduce this error considerably[11], but of course at the expense of more computational effort since we have to solve for 10 or 15 unknown as the choice may be.

Having looked at the above example you might get an idea about the validity of the theory but still remain skeptical on its application and feel that this a typical theoretician's approach to solve a three line problem[12] in a round about way. A problem that can be solved by simple static equation, we have unnecessarily gone to the extent of forming five simultaneous equations[13] and solved the same to arrive at a solution which is theoretically not exact but however may be acceptable for design of the section! Without trying to defend our stand or put up any argument like- what do you do when you do moment distribution[14] of a continuous beam or a frame, we would simply ask you to solve the problem given below?

Shown in Figure 2.11.5 is a pile embedded in layered soil where each of the layers has its unique sub-grade modulus. We need to analyze the pile for a lateral load V acting at the top of pile cap of height D_p.

The differential equation of equilibrium is given by

$$EI\frac{d^4y}{dx^4} + kDy = w \tag{2.11.24}$$

11 Remember our circle problem at the outset where we had seen that more is the number of area less is the error.

12 $\Sigma V = 0$, $\Sigma H = 0$ and $\Sigma M = 0$.

13 Even suggesting you to take more equations.....

14 Is it exact? Ask yourself.....

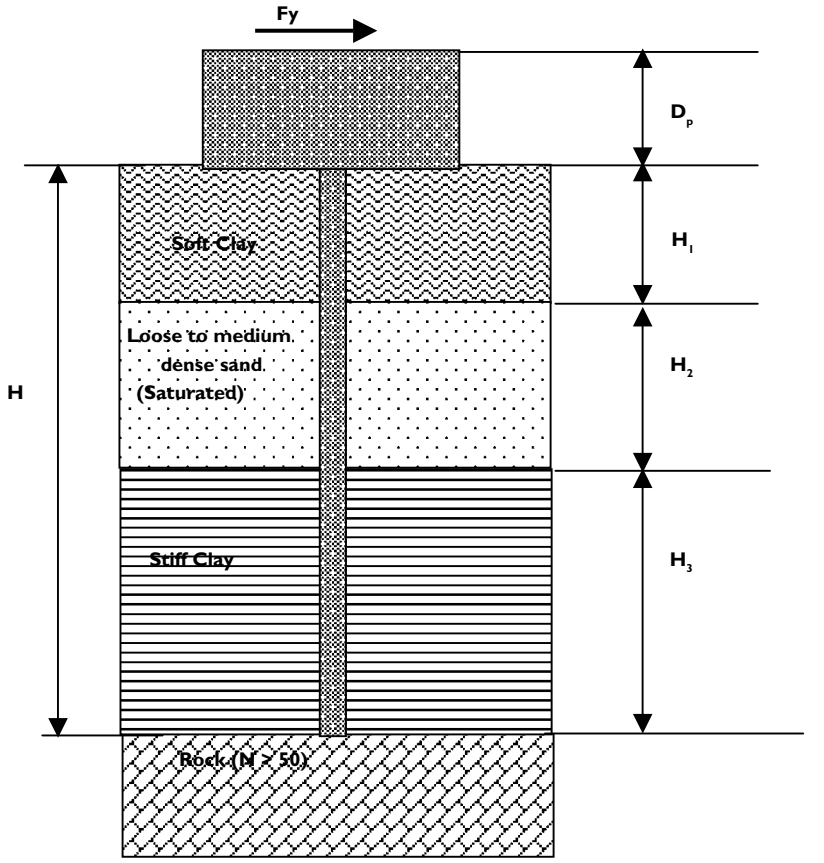


Figure 2.11.5 A pile subjected to lateral load in a layered soil medium.

where k is the sub-grade modulus (kN/m^3) of soil[15] and w (kN/m) is the lateral load acting on the pile and D its diameter.

To further help you on the matter we also provide you with the exact solution of the fourth order differential equation given by

$$y = e^{-\beta x}\left[C_1 \cos \beta x + C_2 \sin \beta x\right]; \quad \text{here } \beta = \sqrt[4]{kD/(4EI)} \tag{2.11.25}$$

where, $E =$ Young's modulus of soil in kN/m^2; I = moment of inertia of the pile section in m^4, and C_1 and C_2 = are integration constants whose values depend on the boundary condition of the piles.

15 Remember it varies for each layer of the soil.

If you try out this problem, you will find it very difficult to solve[16], unless you take a weighted average of the soil modulus along the depth and assume it to be a constant or take it as some continuous function of depth could be linear, parabolic etc.

If you do so then what are you doing? *You are trying to find an exact solution to a problem with only approximate idealized parameter*[17] *and your answer may not be realistic.*

Now let us presume, as shown in Figure 2.11.5, that this pile is being installed in an earthquake prone zone where the second layer of soil can liquefy under ground shaking (i.e. the stiffness of the soil layer tends to zero under ground shaking) and we would like to know how this will effect the pile behavior locally. Can you find a solution based on the exact equation?

You cannot, for your exact solution can only take sub-grade modulus averaged out over the entire depth-*thus averaging out a reduced (or semi zero) sub grade modulus for the soil layer 2 over the entire length of the pile you could be committing a greater error.*

Let us see now how finite difference helps us in solving this problem. This is a typical beam on elastic foundation problem. To explain the solution based on finite difference method we break up the pile/beam in 11 nodes (10 elements). The soil is represented by Winkler springs of magnitude kDh (unit kN/m). Here D is diameter of the pile and h is the length of each element segment as shown Figure 2.11.6. Since there are no lateral uniformly distributed load acting on the pile, thus at any point i the equation of equilibrium is given by

$$EI\frac{d^4y_i}{dx^4} + k_i y_i = 0 \tag{2.11.26}$$

where $k_i = k_s \cdot D \cdot h$, D = diameter of pile and h = distance between each node.

The finite difference equation can thus be expressed as

$$y_{i+2} - 4y_{i+1} + \left[6 + \frac{k_i h^4}{EI}\right] y_i - 4y_{i-1} + y_{i-2} = 0 \tag{2.11.27}$$

The above expression can be applied successively from nodes 2 to 10 to yield 9 equations. The equations will have displacement functions from node 1 to 11 as well as two phantom nodes 0 and 12.

At node 1 considering the expression $EI\frac{d^2y}{dx^2} = -M_x \rightarrow \frac{y_0 - 2y_1 + y_2}{h^2} = -\frac{M}{EI}$ which gives $y_0 = 2y_1 - y_2 - \frac{Mh^2}{EI}$.

Similarly applying moment equation at node 11 we have, $\frac{y_{10} - 2y_{11} + y_{12}}{h^2} = 0$ and this gives $y_{12} = 2y_{11} - y_{10}$. This takes care of the phantom nodes.

16 If not impossible.....

17 Error creeps herein anway!

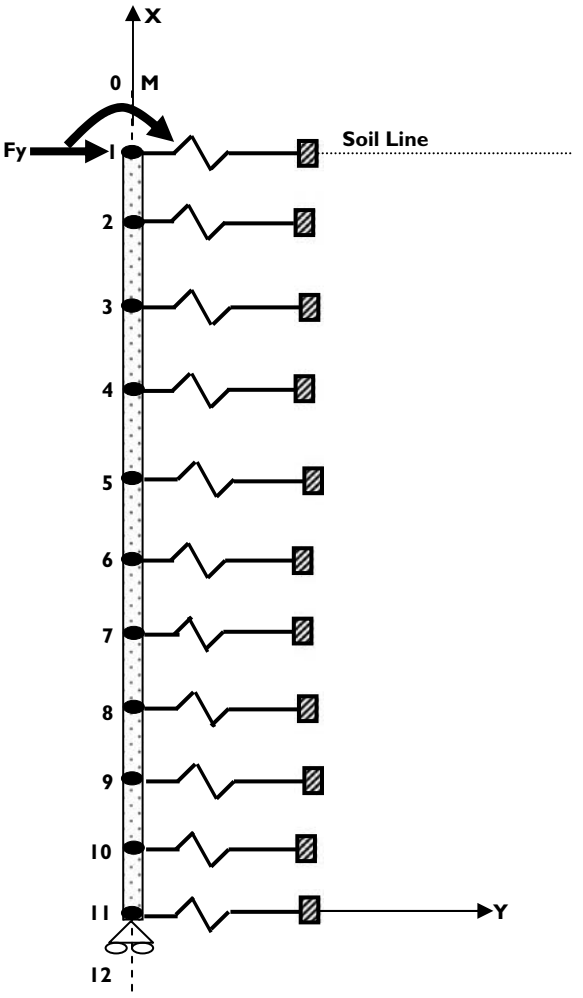


Figure 2.11.6 Mathematical model of pile with Winkler springs depicting the soil stiffness.

We substitute back the values of y_0 and y_{12} in expressions in the above nine equations derived earlier to eliminate y_0 and y_{12}. Thus, we are left with unknowns from y_1 to y_{11}. However, we have nine equations in total.

To get other two equations we take $\Sigma H = 0$ and $\Sigma M = 0$ which gives

$$k_1 y_1 + k_2 y_2 + k_3 y_3 + \cdots\cdots + k_{11} y_{11} = F_y$$
$$10k_1 y_1 h + 9k_2 y_2 h + 8k_3 y_3 h + \cdots\cdots + k_{10} y_{10} h = 10F_y h + M \qquad (2.11.28)$$

Thus expressing these 11 equations in matrix notation, we have the total formulation as follows

$$[A] =$$

$$\begin{bmatrix}
-2 & 5+\frac{k_2h^4}{EI} & -4 & 1 & 0 & 0 & 0 & 0 & 0 & 0 & 0 \\
1 & -4 & 6+\frac{k_3h^4}{EI} & -4 & 1 & 0 & 0 & 0 & 0 & 0 & 0 \\
0 & 1 & -4 & 6+\frac{k_4h^4}{EI} & -4 & 1 & 0 & 0 & 0 & 0 & 0 \\
0 & 0 & 1 & -4 & 6+\frac{k_5h4}{EI} & -4 & 1 & 0 & 0 & 0 & 0 \\
0 & 0 & 0 & 1 & -4 & 6+\frac{k_6h^4}{EI} & -4 & 1 & 0 & 0 & 0 \\
0 & 0 & 0 & 0 & 1 & -4 & 6+\frac{k_7h^4}{EI} & -4 & 1 & 0 & 0 \\
0 & 0 & 0 & 0 & 0 & 1 & -4 & 6+\frac{k_8h^4}{EI} & -4 & 1 & 0 \\
0 & 0 & 0 & 0 & 0 & 0 & 1 & -4 & 6+\frac{k_9h^4}{EI} & -4 & 1 \\
0 & 0 & 0 & 0 & 0 & 0 & 0 & 1 & -4 & 5+\frac{k_{10}h_4}{EI} & -2 \\
k_1 & k_2 & k_3 & k_4 & k_5 & k_6 & k_7 & k_8 & k_9 & k_{10} & k_{11} \\
10k_1 & 9k_2 & 8k_3 & 7k_4 & 6k_5 & 5k_6 & 4k_7 & 3k_8 & 2k_9 & k_{10} & 0
\end{bmatrix}$$

$$\{y\} = \langle y_1 \quad y_2 \quad y_3 \quad y_4 \quad y_5 \quad y_6 \quad y_7 \quad y_8 \quad y_9 \quad y_{10} \quad y_{11} \rangle^T \tag{2.11.29}$$

Here the term T stands for transpose of the matrix (i.e. the matrix is actually a column matrix).

The force matrix is given by

$$\{F\} = \left\langle \frac{Mh^2}{EI} \quad 0 \quad 0 \quad 0 \quad 0 \quad 0 \quad 0 \quad 0 \quad 0 \quad F_y\left(10F_y + \frac{M}{h}\right) \right\rangle^T \tag{2.11.30}$$

The matrix being of a modest size you can directly input them in excel, mat-lab or math-cad to arrive at solution to the problem.

We now show you an example of this and this we do with a real life data.

Example 2.11.1

A 20 meter long RCC pile of diameter 900 mm shown in Figure 2.11.7 is passing through three layers of soil whose sub grade modulus is as given hereafter.

The base shear acting at pile head (at top of pile cap) is 70 kN. Determine the deflection, shear, and moment in the pile section. Depth of pile cap is 1.2 meter. $E_{\text{conc}} = 2.85 \times 10^7$ **kN/m^2.**

Layer	*Soil type*	*Lateral sub-grade Modulus (kN/m^3)*
1	Soft clay	21000
2	Saturated loose to medium dense sand	110000
3	Stiff clay	190000

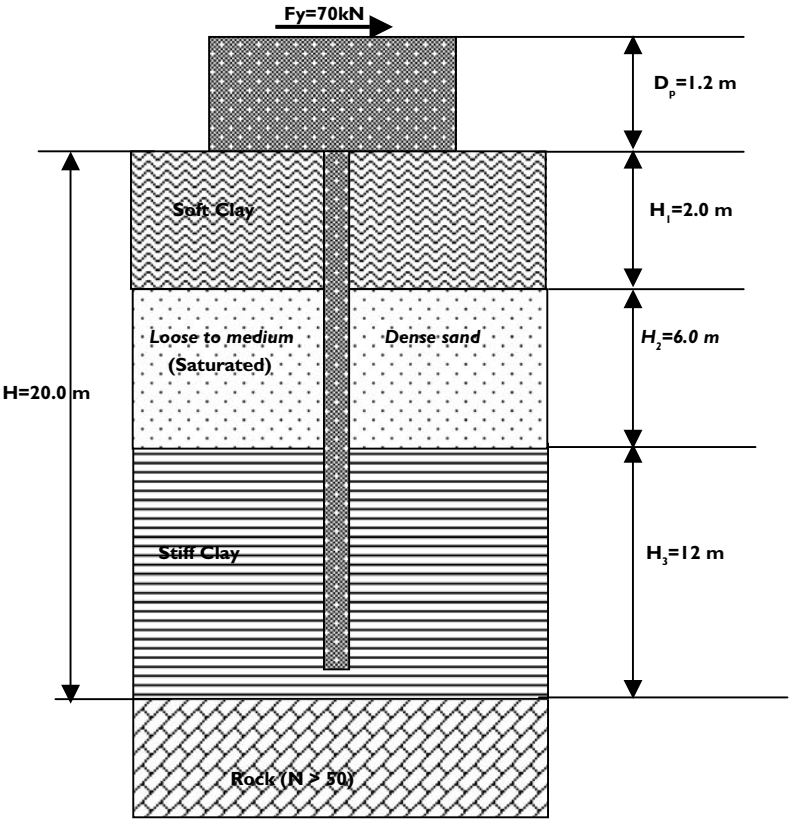


Figure 2.11.7 Pile and pile cap embedded in layered soil.

Solution:

We break up the pile in 11 numbers of nodes of each element length $h = 2.0$ meter and find out the contributing sub-grade Modulus as follows.

Soil layer (m)	*Sub grade Modulus*	*Node*	*Co-ordinate (meter)*	*Contributing soil Modulus (k_s)*	*Spring stiffness ($k_s \times D \times h$) kN/m*
0–2	21000	1	0	21000	18900
2–8	110000	2	2	65500	117900
8–20	190000	3	4	110000	198000
		4	6	110000	198000
		5	8	150000	270000
		6	10	190000	342000
		7	12	190000	342000
		8	14	190000	342000
		9	16	190000	342000
		10	18	190000	342000
		11	20	190000	17100

Based on above data the [*A*] matrix is formed as per Equation (2.11.29) and on inversion the displacement, moments and shear are obtained as shown Figs. 2.11.8, 9 and 10.

Node	*Displacement meter*	*Bending Moment (kN · m)*	*Shear force (kN)*	*Soil reaction (kN)*
1	1.82371×10^{-03}	84.000	35.532	34.468
2	4.60964×10^{-04}	201.279	−18.816	54.348
3	-2.46282×10^{-05}	101.168	−13.939	−4.876
4	-6.93414×10^{-05}	20.563	−0.210	−13.730
5	-2.44450×10^{-05}	−5.125	6.390	−6.600
6	-1.88081×10^{-06}	−4.411	7.034	−0.643
7	1.46008×10^{-06}	−1.125	6.534	0.499
8	-1.00815×10^{-07}	0.164	6.569	−0.034
9	-9.46315×10^{-07}	1.591	6.892	−0.324
10	5.14176×10^{-06}	4.312	5.134	1.758
11	3.00231×10^{-05}	0.000	0.000	5.134
				Total = 70 kN

The bending moments are obtained from the expression

$$M_i = EI\frac{y_{i-1} - 2y_i + y_{i+1}}{h^2}$$

applied at each successive node after calculation of y from the expression, $y = [A]^{-1}F$. The soil reaction is obtained as $R_i = k_i \times \delta_i$ [(Spring stiffness) × (deflection)], while shear is obtained by algebraic summation of the lateral shear and soil reaction.

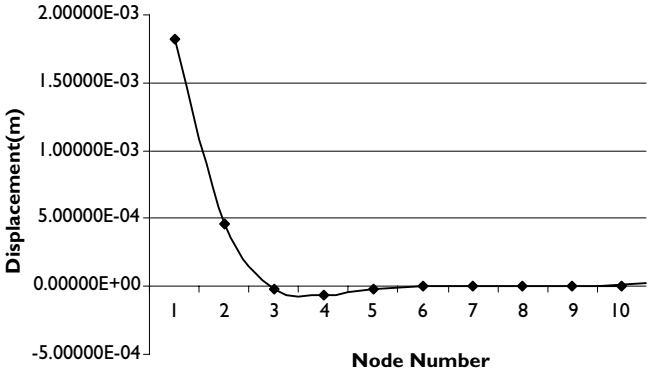


Figure 2.11.8 Displacement plot of pile.

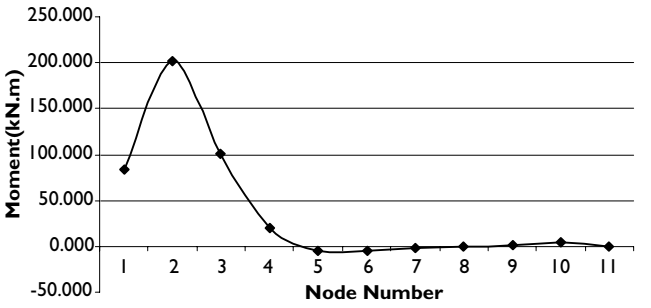


Figure 2.11.9 Bending Moment diagram for the pile.

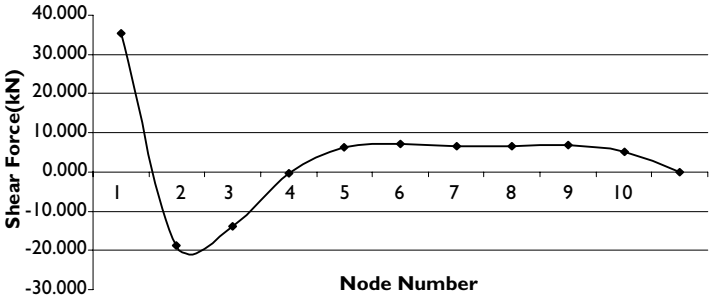


Figure 2.11.10 Shear force diagram for the pile.

To check the correctness of the formulation it should be checked that summation of soil reaction is equal to the applied shear (70 kN).

We hope now you realize that the method is surely not a theoretical conjecture[18] and can solve some very complex boundary problems with relative ease where for the sake of analytical solution we have to otherwise resort to oversimplification of the parameters that could land us with unrealistic results.

Another typical example of similar category is a combined footing resting on elastic base when the foundation slab cannot be assumed as rigid. A similar logic can be followed as considered for the lateral pile problem described above to derive the [*A*] matrix and rest of the steps will remain same (Bowles 1974). It is normally seen that about 10 to 15 nodes with at least two nodes on each of the overhang portions of the foundation is sufficient to provide a result good enough for practical application.

18 Mycroft Holmes syndrome.....

2.11.2 Application to partial differential equations

Since a second order pde is of particular interest in the field of wave propagation, heat conduction (consolidation), elasticity, vibrations, boundary layer theory, potential flow etc., we shall consider this type of equations for the development to this end.

Let $u = u(x, y)$, and a second order pde is given by

$$A(x,y)\frac{\partial^2 u}{\partial x^2} + B(x,y)\frac{\partial^2 u}{\partial x \partial y} + C(x,y)\frac{\partial^2 u}{\partial y^2} + f\left(x, y, u, \frac{\partial u}{\partial x}, \frac{\partial u}{\partial y}\right) = 0 \qquad (2.11.31)$$

This equation is linear in second order terms, but f may be linear or nonlinear. In the first case the equation is said to be linear and in the second case it is termed as quasi-linear.

Now, if

$B^2 - 4AC > 0$, it is called *hyperbolic equation*;
$B^2 - 4AC = 0$, it is termed as *parabolic equation*, *and*
$B^2 - 4AC < 0$, it is called an *elliptic equation*.

A, B and C are functions of independent variables. The differential equation may have different classification in the different regions of the domain in which the problem is defined. As for example, in a flow problem:

$$(1 - M^2)\frac{\partial^2 \phi}{\partial x^2} + \frac{\partial^2 \phi}{\partial y^2} = 0, \quad \text{where } M \text{ is called Mach Number.} \qquad (2.11.32)$$

Now, if

$M < 1$, the equation is elliptic (a sub-sonic flow)
$M > 1$, the equation is hyperbolic (a super-sonic flow).

The significance of this classification is intimately connected with the theory of characteristics. A pde is classified in terms of its characteristics, i.e. of the loci of possible discontinuities in the derivatives of a solution (Salvadori and Baron 1966). We call the equation hyperbolic at a point, if there are two real characteristic directions (wave propagation: $x \pm ct$); parabolic, if there is only one real characteristic direction, and elliptic if there are no real characteristic direction at that point.

a) Elliptic equations

It should satisfy $B^2 - 4AC < 0$, over the domain.

Functional values and derivatives should be specified on the *closed region*, R (Figure 2.11.11).

Example: 1. Laplace equation: 2. Poisson equation:

$$\frac{\partial^2 u}{\partial x^2} + \frac{\partial^2 u}{\partial y^2} = 0 \qquad \frac{\partial^2 u}{\partial x^2} + \frac{\partial^2 u}{\partial y^2} = f(x, y) \qquad (2.11.33)$$

Here $B = 0$, $C = 1$ and $A = 1 \rightarrow B^2 - 4AC < 0$.

Geomechanics example and boundary conditions (Figure 2.11.12)

When the boundary conditions are given as derivatives

Say the condition is: $a_1 \frac{\partial u}{\partial x} + a_2 \frac{\partial u}{\partial y} = 0$; consider the boundary shown below where 3–6 is the irregular boundary (Figure 2.11.13).

In the present case 2 and 6 are fictitious points. Using difference, at point '10' at the boundary: $a_1 \left[\frac{u_{11}-u_{10}}{h}\right] + a_2 \left[\frac{u_6-u_3}{h}\right] = 0$ – assuming the slope to be constant along, say, 3–6.

As we have, $u_{10} = u_3 + \frac{\alpha h}{h}(u_6 - u_3)$

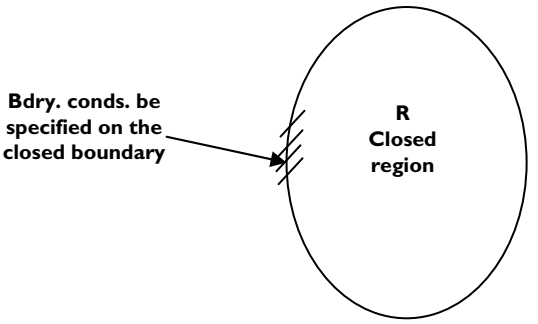


Figure 2.11.11

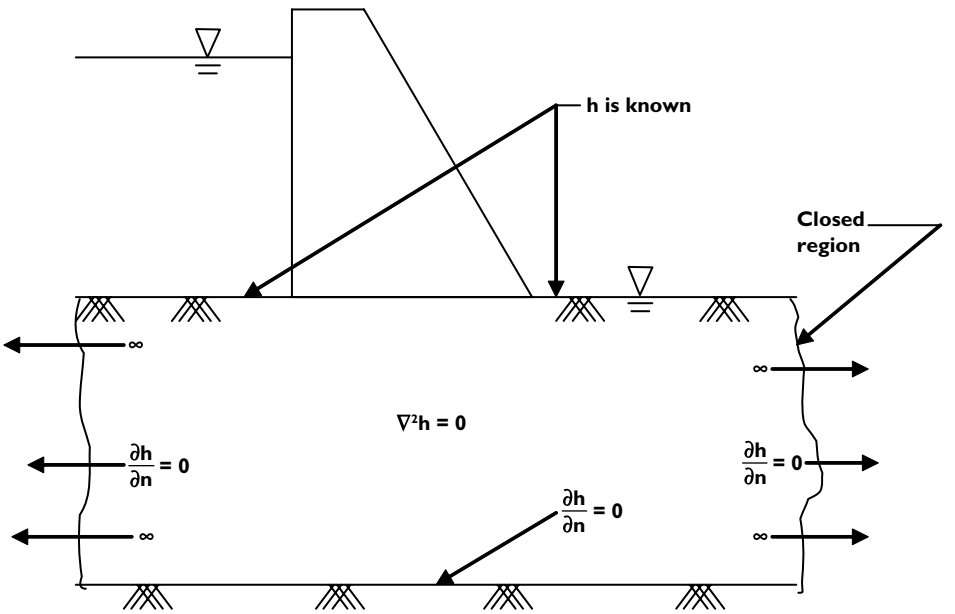


Figure 2.11.12

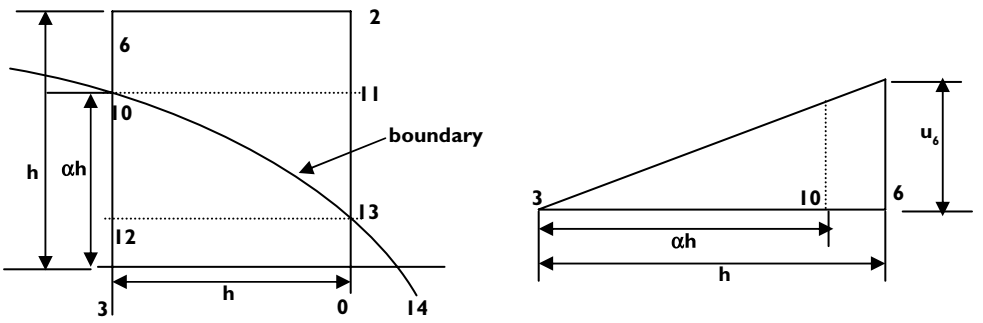


Figure 2.11.13

Thus,

$$a_1\left[\frac{\{u_0+\alpha(u_2-u_6)\}-\{u_3+\alpha(u_6-u_3)\}}{h}\right]+a_2\frac{(u_6-u_3)}{h}=0.$$

Seepage problem

$$k_x\frac{\partial^2 h}{\partial x^2}+k_y\frac{\partial^2 h}{\partial y^2}=0 \text{ – elliptic equation: } B^2-4AC<0. \tag{2.11.34}$$

In finite difference form:
Node '0' in Figure 2.10.14

$$\frac{k_x}{(\Delta x)^2}(h_1\ 2h_0+h_3)+\frac{k_x}{(\Delta y)^2}(h_2\ 2h_0+h_4)=0$$

$$\text{Let}\quad \frac{k_x}{(\Delta x)^2}=\frac{k_y}{(\Delta y)^2}\quad\rightarrow\quad \Delta x=\left(\sqrt{\frac{k_x}{k_y}}\right)\Delta y. \tag{2.11.35}$$

The difference equation, now, reduces to

$$h_1+h_2+h_3+h_4-4h_0=0 \tag{2.11.36}$$

Now, obtain such equations for all nodes.

Boundary conditions

1 Heads are given on the boundary,
2 Derivatives are given on part of the boundary, say S_2. For example impermeable boundary $\frac{\partial h}{\partial n}=0$, can be written as $c_1\frac{\partial h}{\partial x}+c_2\frac{\partial h}{\partial y}=0$, c_1 and c_2 are the direction cosines.
3 Combination of derivatives and the functional values.

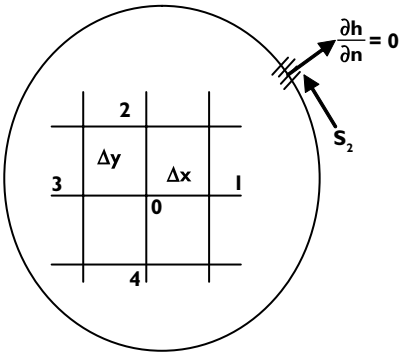


Figure 2.11.14

Problem 1. Dam on permeable base (Figure 2.11.15)

For steady state seepage

$$k_x \frac{\partial^2 h}{\partial x^2} + k_y \frac{\partial^2 h}{\partial y^2} = 0$$

$$\underset{\Rightarrow}{\text{transformed to}} \quad \frac{\partial^2 \bar{h}}{\partial x^2} + k_y \frac{\partial^2 \bar{h}}{\partial y^2} = 0, \quad \text{using } \Delta x = \left(\sqrt{\frac{k_x}{k_y}}\right) \Delta y \tag{2.11.37}$$

The region is bounded by – AB = head is specified; BC = no flow, *b.c.* is specified in terms of derivatives; CD = no flow, same as BC; DE = no flow, same as BC; EF = head is specified;

For fictitious boundary – FH = no flow, *b.c.* is specified in terms of derivatives; GH = no flow, same as FH; GA = no flow, same as FH.

➔ *Finite simulation of infinite region. The region is bounded by A and G meeting at* ∞ *and F and H also meeting at* ∞.

For the ith node:

$$h_{i+1} + h_{i+2} + h_{i+3} + h_{i+4} - 4h_i = 0 \quad \text{➔ in the domain.} \tag{2.11.38}$$

Writing down all such equations as for 'i' and implementing proper boundary conditions, we shall have

$$[A]\,\{h\} = \{g\} \tag{2.11.39}$$

and we have to solve for $\{h\}$.

Problem 2. Sheet-pile

Consider a sheet-pile as shown in Figure 2.11.16

Boundaries AB, BC, CD, DE, EH, HG and GA of Figure (a) are same as before. Same governing equation and hence the procedure will be the same.

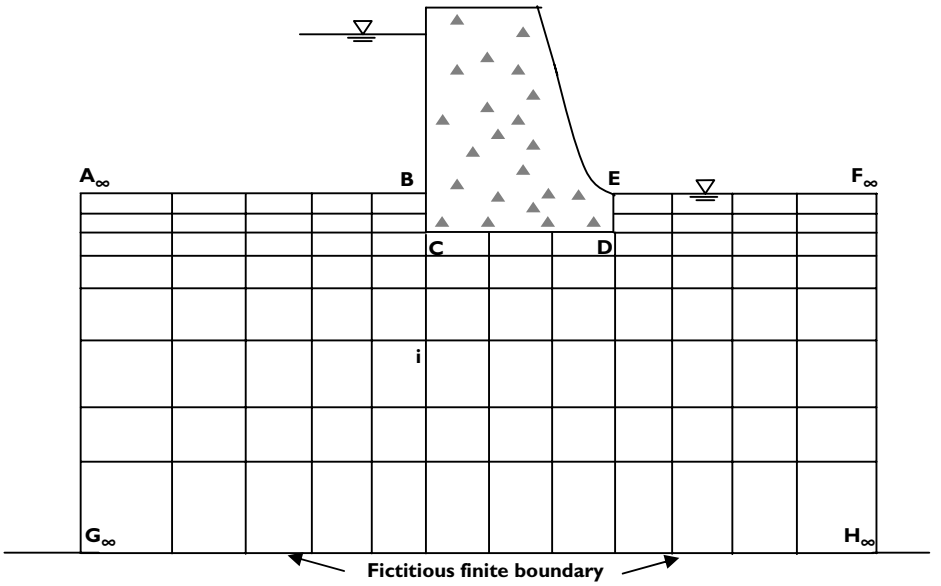


Figure 2.11.15

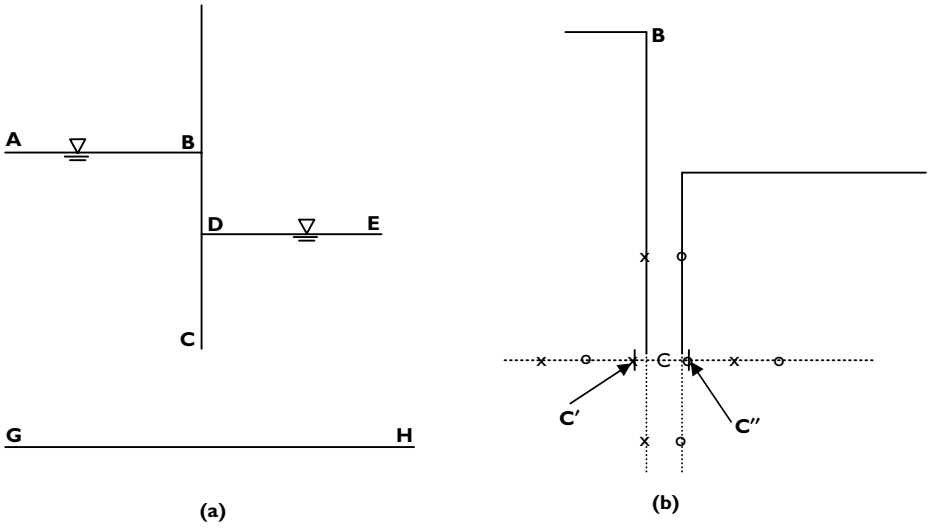


Figure 2.11.16

Problem will be with *BCD* as the point *C* is a singular point. Proceed as follows given in Figure (b).

$$h_C = \frac{(h_{c'} - h_{c''})}{2}. \tag{2.11.40}$$

Non-homogeneous soils

As such a layered soil (Figure 2.11.17) does not offer any difficulty in applying the procedures outlined in the preceding, however, problem arises when a point like 'o' as shown in the figure lies in the interface.

To tackle this problem, first consider the k_2-portion of the domain (Figure 2.11.18):

Case (a)

Imagine a coefficient such that if we multiply it with h_2 it will give a value h_2' which is a transformed value of h_2 for a homogeneous layer-2.

$$\text{So, we have:} \quad h_1 + h_3 + h_4 + h_2' - 4h_0 = 0. \tag{2.11.41}$$

Similarly,

$$h_1 + h_2 + h_3 + h_4' - 4h_0 = 0 \tag{2.11.42}$$

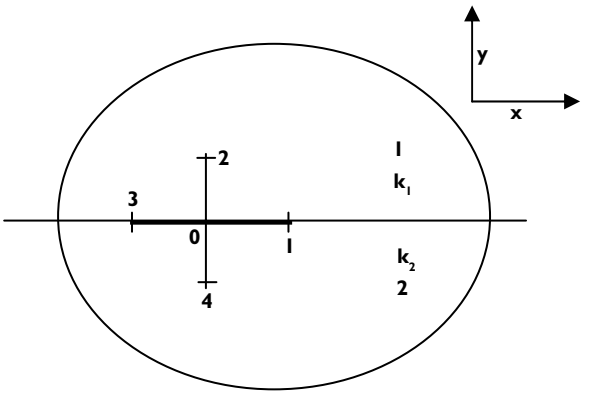


Figure 2.11.17

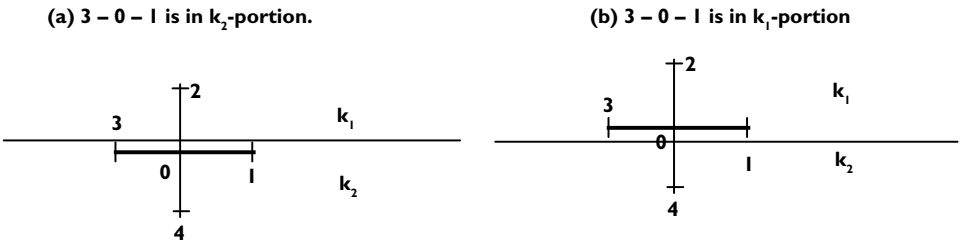


Figure 2.11.18

case (b)

Subtracting (2.11.42) from (2.11.41), we get, $h_2 - h'_2 + h'_4 - h_4 = 0$, from continuity of flow:

$$k_1 \left(\frac{\partial h}{\partial y}\right)_1 = k_2 \left(\frac{\partial h}{\partial y}\right)_2 \tag{2.11.43}$$

i.e. $k_1 \dfrac{(h_2 - h'_4)}{2\Delta y} = k_2 \dfrac{(h'_2 - h_4)}{2\Delta y} \quad \rightarrow \quad h'_2 = \dfrac{k_1}{k_2}(h_2 - h'_4) + h_4$

Solving we have: $h_1 + \dfrac{2k_1}{k_1 + k_2} h_2 + h_3 + \dfrac{2k_2}{k_1 + k_2} h_4 - 4h_0 = 0.$ (2.11.44)

When the interface is inclined, rotate the grid-line parallel to the interface.

b) Parabolic equations

It should satisfy $B^2 - 4AC = 0$, over the domain. Initial value of the function u(say) at some time t_0 is to be specified. The value of either the function or its derivatives, or a linear combination of both, on the boundary is the required boundary condition.

Example: Heat conduction problem/Consolidation equation (Figure 2.11.19). One dimensional consolidation is governed by the equation

$$C_v \frac{\partial^2 u}{\partial x^2} = \frac{\partial u}{\partial t} \tag{2.11.45}$$

Here, B = 0, C, $A = C_v$: $A = C_v$, C = 0; $C = C_v$, A = 0; B = 0, C = 0, $A = C_v$

➔ $B^2 - 4AC = 0$.

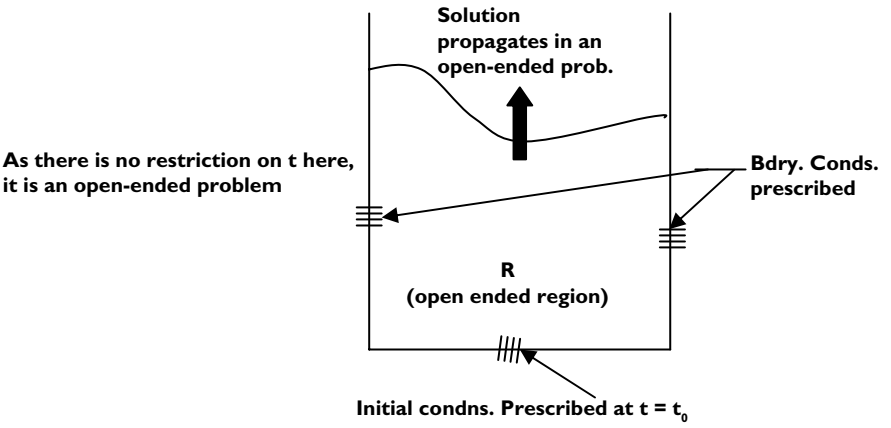


Figure 2.11.19

The solution space is given in Figure 2.11.20. For $\frac{\partial U}{\partial T}$, we cannot use central difference scheme as it involves a functional value at a negative T which does not carry any physical meaning. Hence, we use forward difference scheme for the right-hand-side of Equation (2.11.45), and central difference for the left-hand-side of Equation (2.11.45).

Consider a rectangular grid in the Z–T plane, shown in Figure 2.11.21, in which the quantity $U_{i,j}$ is defined as the pore pressure at the point $Z = Z_i$ at the time $T = T_j$. Let the grid spacing be $\Delta Z = h$ in space and $\Delta T = k$ in time. Equation (2.11.45) can be written as

$$U_{i+1,j} - 2U_{i,j} + U_{i-1,j} = \frac{h^2}{k}[U_{i,j+1} - U_{i,j}] \tag{2.11.46}$$

$$\text{or,} \quad U_{i,j+1} = \frac{k}{h^2}[U_{i+1,j} + U_{i-1,j} - 2U_{i,j}] + U_{i,j} \tag{2.11.47}$$

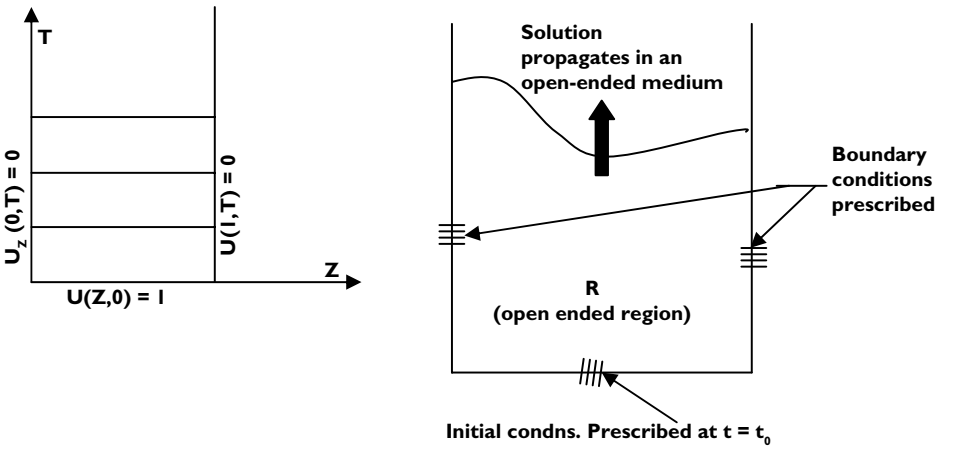


Figure 2.11.20

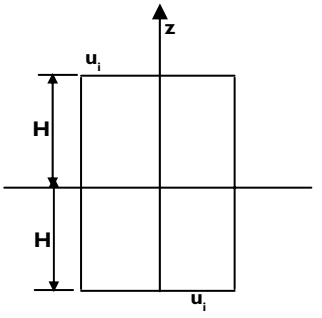


Figure 2.11.21

Equation (2.11.47) allows for the evaluation of $U_{i,j+1}$ in terms of the pore pressures at the points Z_i , Z_{i+1} and Z_{i-1} at the time T_j.

Since both k and h are dimensionless, the factor k/h^2 is also dimensionless and may be described as an operator on the prior values of U through which the new values can be computed. In any case, Equation (2.11.47) should be stable in operation.

Explicit and implicit schemes

Before we go in for the solution of Equation (2.11.47), let us discuss a few standard schemes, namely the explicit and implicit schemes of integration.

In the explicit scheme, we seek the approximate solution for U_{ij} at the time level T_{j+1} in terms of the known values of $U_{i,j}$ at the previous time level T_j. Explicit schemes can often be formulated in which some values of $U_{i,j}$ at time T_{j+1} are also known. The scheme, generally, involves a new value at one point only and permits step-by-step evaluation of $U_{i,j}$ directly. The scheme in Equation (2.11.47) is an explicit scheme.

If the expressions were written in terms of new values at the three points in Equation (2.11.47), namely $i, i+1$ and $i+2$, a similar equation could be formed at each point in turn, which would imply that a set of simultaneously generated set of difference equations could be set up whose solution would describe the excess pore pressure at the new time throughout the layer. The model equation would then be an implicit relation.

In the left-hand-side of simultaneous equation, the $U_{i,j}$ at T_{j+1} occur as unknowns, and the right-hand-side of the algebraic equations constitute the known values of $U_{i,j}$ at time level T_j. A general form of finite difference analogue of Equation (2.11.46) can be expressed as

$$\theta \left(\frac{\partial^2 U}{\partial Z^2}\right)_{i,j+1} + (1-\theta)\left(\frac{\partial^2 U}{\partial Z^2}\right)_{i,j} = \frac{U_{i,j+1} - U_{i,j}}{k} \tag{2.11.48}$$

$$\text{in which,} \quad \left(\frac{\partial^2 U}{\partial Z^2}\right)_{i,j} = \frac{1}{h^2}[u_{i-1,j} - 2U_{i,j} + U_{i+1,j}]. \tag{2.11.49}$$

Other notations are same as in Equation (2.11.48). The magnitude of θ can have different values. The simplest explicit scheme can be obtained by setting, $\theta = 0$ [same as Equation (2.11.48)]. An implicit scheme results if θ is adopted as unity. One commonly used implicit form is Crank-Nicolson scheme, which results when $\theta = \frac{1}{2}$.

The discretisation error in the foregoing simple explicit and implicit scheme is of the order of $O[k + h^2]$, whereas that for the Crank-Nicolson scheme is of the order of $O[k^2 + h^2]$.

Example 2.11.2

Refer to Equation (2.11.48)

Take $k/h^2 = \frac{1}{2}$; assuming, $h = \frac{1}{2} \rightarrow k = \frac{1}{8}$ with $U_Z(0, T) = 0$, no flow condition; $U(1, T) = 0$, final surface condition; $U(Z, 0) = 1, \forall Z, \rightarrow$ initial condition.

As soon as consolidation starts $U(1, T) = 0$. From Equation (2.11.48), and using Figure 2.11.22, we have

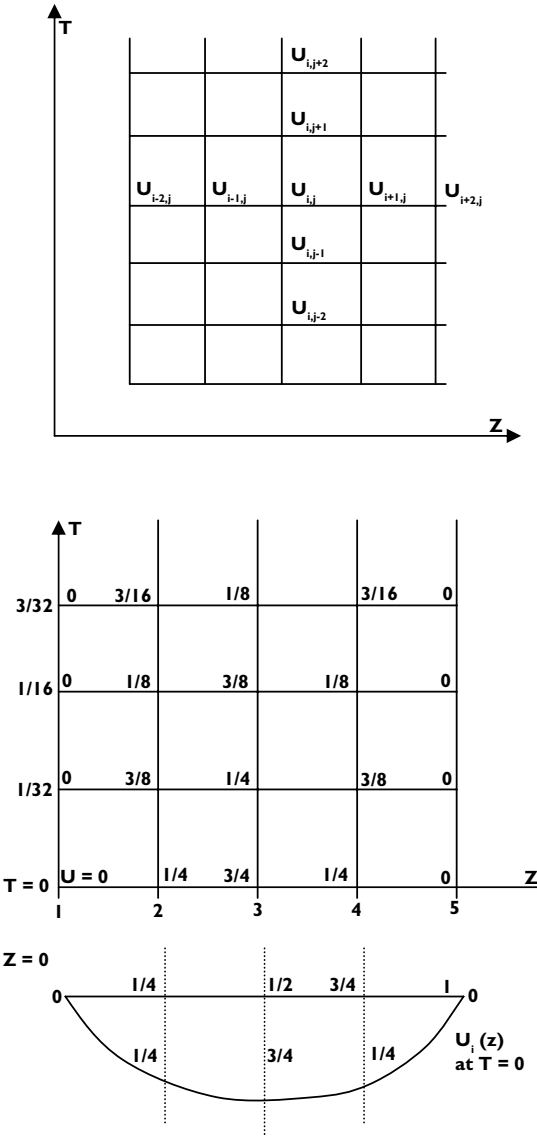


Figure 2.11.22

$$\rightarrow \quad U_{i,j+1} = \frac{1}{2}[U_{i+1,j} + U_{i-1,j}]. \tag{2.11.50}$$

Value of $U(Z,1) = 1; U(1,T) = 0 \rightarrow U(1,0) = \frac{1}{2}$

Hence, $U_{1,1} = 1; U_{2,1} = 1$ and $U_{3,1} = \frac{1}{2}$, and $U_{1,2} = \frac{1}{2}[U_{2,1} + U_{0,1}] = 2$.

Say, it is given that $U_Z(0,T) = C_1, \rightarrow C_1 = [U_{i+1,j} - U_{i-1,j}]/2h$

$\rightarrow U_{i-1,j} = -2C_1h + U_{i+1,j}$, and so on; when $C_1 = 0 \rightarrow U_{i-1,j} = U_{i+1,j}$.

If *bc* is given as

$$C_1U + C_2\frac{\partial U}{\partial Z} = C_3, \quad \text{we have, } C_1U_{i,j} + \frac{C_2}{2h}[U_{i+1,j} - U_{i-1,j}] = C_3;$$

Now proceed for the solution.

Example 2.11.3

Take $h = \frac{1}{4}$, assume $k = \frac{1}{32}$, $k/h^2 = \frac{1}{2}$.

bc: $U(0,T) = 0 : U(1,T) = 0;$

$U(Z,0) = U_i(z) : U_Z = 0.$

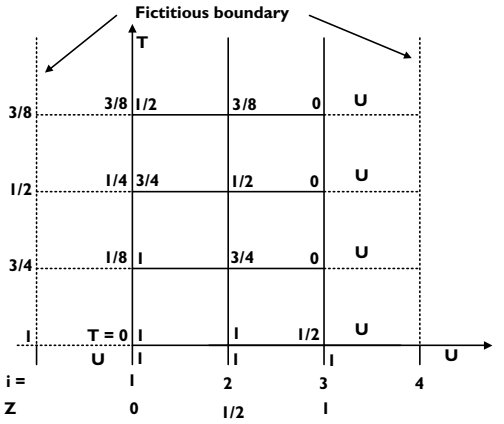


Figure 2.11.23

We have, from Figure 2.11.23, $U_{i,j+1} = \frac{1}{2}[U_{i+1,j} + U_{i-1,j}]$

***bc* gives**

$U_{i+1,j} = U_{i-1,j}$; from $U_Z(0, T) = 0$.

$$U_{2,2} = \frac{1}{2}[U_{3,1} + U_{1,1}] = \frac{3}{8}; \quad U_{3,2} = \frac{1}{2}[U_{4,1} + U_{2,1}]$$

$$= \frac{1}{4}U_{4,2} = \frac{1}{2}[U_{5,1} + U_{3,1}] = \frac{3}{8}, \text{ and so on.}$$

Some of the examples are shown in Figure 2.11.24.

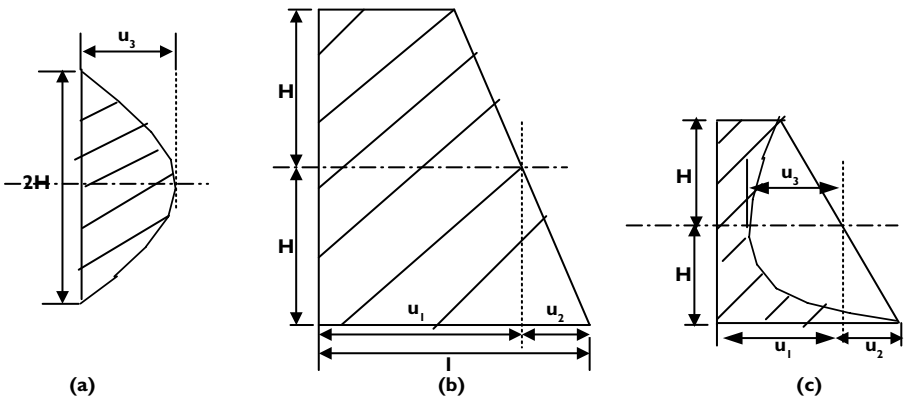


Figure 2.11.24

c) Hyperbolic equations

It should satisfy $B^2 - 4AC > 0$, over the domain (Figure 2.11.25). And,

i The initial values of the function u and of its first derivatives with respect to time (or one of the independent variable is given).
ii Either the value of the function, or its normal derivatives, or a linear combination of the function and its normal derivative on the boundary of the domain are the required boundary conditions.

Example: One dimensional wave propagation equation

$$\beta^2 \frac{\partial^2 u}{\partial x^2} = \frac{\partial^2 u}{\partial t^2} \tag{2.11.51}$$

$A = \beta^2, C = -1 \rightarrow B^2 - 4AC > 0.$

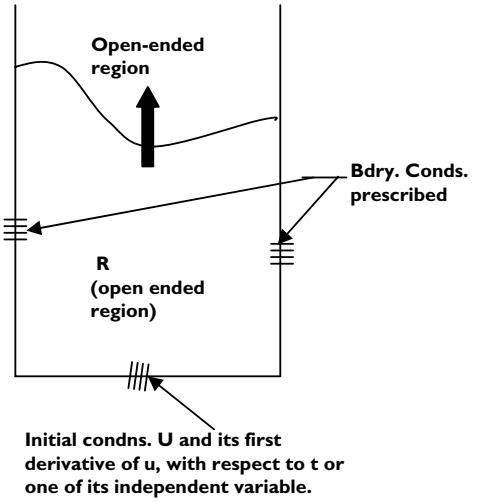


Figure 2.11.25

Equations of equilibrium in terms of displacements

$$(\lambda+\mu)\frac{\partial \Delta}{\partial x}+\mu\nabla^2 u=\rho\frac{\partial^2 u}{\partial t^2} \quad \text{with } v=0,\ w=0.$$

$$G\nabla^2 u=\rho\frac{\partial^2 u}{\partial t^2};\quad \text{with } C^2=\frac{G}{\rho} \quad \rightarrow \quad C^2\frac{\partial^2 u}{\partial x^2}=\frac{\partial^2 u}{\partial t^2}$$

This is a hyperbolic equation; $B^2-4AC>0$.
Boundary conditions (for Figure 2.11.25):

$$u(0,t)=0;\quad u(\ell,t)=0;\quad u(x,0)=f(x)[\text{say}] \quad \text{and}$$

$$\left|\frac{\partial u}{\partial t}\right|_{t=0}=u_t(x,0)=0\ [\text{say}]. \tag{2.11.52}$$

The hyperbolic Equation (2.11.51) together with the boundary conditions constitutes a boundary value problem in one-dimensional space-time. The problem is of the boundary value type for the space variation and initial value type for the time variable.

As in the case of parabolic and elliptic equations, finite differences may be used to solve this hyperbolic problem. Consider a rectangular grid in the $x-t$ plane indicated by $u_{i,j}$, the deflection at the point $x=x_i$ at a time $t=t_j$. Let the grid spacing be $\Delta x=h$ in space and $\Delta t=k$ in time. Using central difference operators of order $O(h^2)$ and $O(k^2)$ in space and time, respectively. Thus

$$\frac{\partial^2 u}{\partial x^2}=\frac{u_{i+1,j}-2u_{i,j}+u_{i-1,j}}{h^2}\ :\ \frac{\partial^2 u}{\partial t^2}=\frac{u_{i,j+1}-2u_{i,j}+u_{i,j-1}}{k^2} \tag{2.11.53}$$

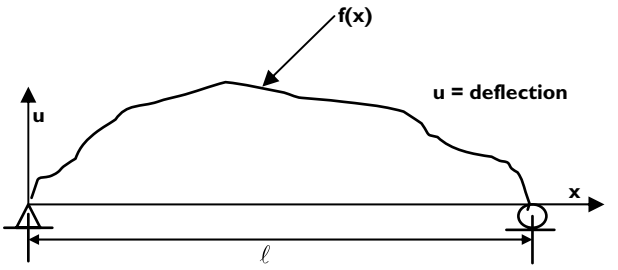


Figure 2.11.26

Thus, Equation (2.11.52) reduces to the following finite difference equation:

$$u_{i+1,j} - 2u_{i,j} + u_{i-1,j} = \frac{h^2}{C^2k^2}[u_{i,j+1} - 2u_{i,j} + u_{i,j-1}] \tag{2.11.54a}$$

Using, $\alpha^2 = C^2k^2/h^2$, we have

$$u_{i,j+1} = \alpha^2[u_{i+1,j} + u_{i-1,j}] + 2(1-\alpha^2)u_{i,j} - u_{i,j-1} \tag{2.11.54b}$$

And, when $\alpha = 1$, $\quad \rightarrow u_{i,j+1} = [u_{i+1,j} + u_{i-1,j}] - u_{i,j-1}$ (2.11.54c)

Considering the boundary and initial conditions as: $u_{0,j} = u_{N,j} = 0$; $u_{i,0} = f(x_i)$, using, $h = \ell/N$ and

$$u_t(x,0) = 0 = \frac{1}{2k}[u_{i,j+1} - u_{i,j-1}] = \frac{1}{2k}[u_{i,1} - u_{i,-1}],$$
$$\rightarrow u_{i,1} = u_{i,-1}$$

Example 2.11.4

Take $\alpha = 1, h = 1/4 \rightarrow k = h/C = 1/4C$.

Boundary conditions:

1 Left hand boundary

$$u_{i,j} + \frac{3}{2h}(u_{i+1,j} - u_{i-1,j}) = 4 \quad \Rightarrow \quad u_{i-1,j} = \frac{2h}{3}u_{i,j} + u_{i+1,j} - \frac{8}{3}h \tag{2.11.55}$$

2 Right hand boundary

$$2u_{i,j} + \frac{1}{2h}(u_{i+1,j} - u_{i-1,j}) = 1 \quad \Rightarrow \quad u_{i+1,j} = 2h + u_{i-1,j} + 4hu_{i+1,j} \tag{2.11.56}$$

3 Initial (time condition)

$$\frac{1}{2k}[u_{i,j+1} - u_{i,j-1}] = 1 \quad \Rightarrow \quad u_{i,j+1} = 2k + u_{i,j-1} \tag{2.11.57}$$

Governing equation (for $\alpha = 1$):

$$u_{i,j+1} = [u_{i+1,j} + u_{i-1,j}] - u_{i,j-1} \tag{2.11.58}$$

Also given $u_{i,0} = f(x_i)$ (2.11.59)

Solution problem shown in Figure 2.11.27.

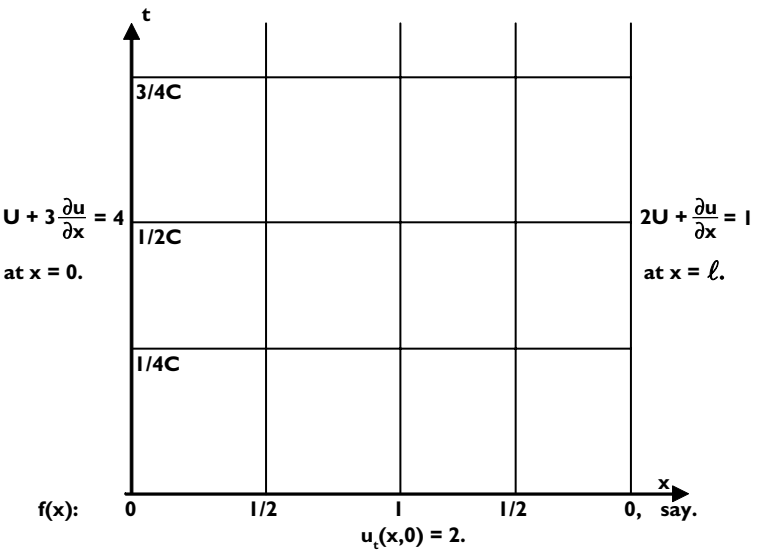


Figure 2.11.27

In Equation (2.11.58), $j = 0 \rightarrow u_{i,1} = (u_{i+1,0} + u_{i-1,0}) - u_{i,-1}$
In Equation (2.11.57), $u_{i,1} = 2k + u_{i,-1}$; $u_{i,1} = u_{i+1,0} + u_{i-1,0} - u_{i,1} + 2k$

$$\rightarrow \quad u_{i,1} = \frac{1}{2}(u_{i+1,0} + u_{i-1,0}) + k \tag{2.11.60}$$

Using, $\quad j = 1, \quad u_{i,2} = [u_{i+1,1} + u_{i-1,1}] - u_{i,0}$ (2.11.61)

$$j = 2, \quad u_{i,3} = [u_{i+1,2} + u_{i-1,2}] - u_{i,1} \tag{2.11.62}$$

Level $j = 1$:
We need $u_{i-1,0}$ values in Equation (2.11.58) so put $j = 0$ in Equation (2.11.55)

$$\rightarrow \; u_{i-1,0} = (2h/3)u_{i,0} + u_{i+1,0} - (8h/3)$$

From Equation (2.10.60): $\quad u_{i,1} = \dfrac{1}{2}\left(u_{i+1,0} + \dfrac{2h}{3}u_{i,0} + u_{i+1,0} - \dfrac{8h}{3}\right) + \dfrac{1}{4C}$

$$\rightarrow \; u_{i,1} = u_{i+1,0} + \frac{1}{12}u_{i,0} - \frac{1}{3} + \frac{1}{4C}, \quad i = 0, 1, 2, 3, \ldots.$$

For $i = 4$, use Equation (2.11.56):

$$u_{i+1,0} = \frac{1}{2} + u_{i-1,0} - u_{i,0}$$

$$u_{i,1} = \frac{1}{2}\left[\frac{1}{2} + u_{i-1,0} - u_{i,0} + u_{i-1,0}\right] + \frac{1}{4}C$$

$$\rightarrow u_{4,1} = \frac{1}{4} + u_{3,0} - \frac{1}{2}u_{4,0} + \frac{1}{4}C.$$

Boundary conditions:

Initial: $\quad u_t(x, 0) = 1 : u_{i,1} = 2k + u_{i,-1}, \text{ for } j = 0.$

Left-hand side boundary: $\quad u_{i,j} + (3/2h)(u_{i+1,j} - u_{i-1,j}) = 4$

$$\text{Or} \quad u_{i-1,j} = \frac{2h}{3}u_{i,j} + u_{i+1,j} - \frac{8h}{3} \tag{2.11.63}$$

Right-hand side boundary:

$$2u_{i,j} + \frac{1}{2h}(u_{i+1,j} - u_{i-1,j}) = 1 \tag{2.11.64}$$

$$\text{Or} \quad u_{i,1} = \frac{1}{2}(u_{i+1,0} + u_{i-1,0}) + k \tag{2.11.65}$$

Initial condition:

$$u_{i,0} = f(x_i)$$

$$u_{i,1} = \frac{1}{2}\left(u_{i+1,0} + u_{i-1,0}\right) + k$$

$$u_{i,2} = [u_{i+1,1} + u_{i-1,1}] - u_{i,0}; \quad [\text{for } j = 1, \text{ Equation (2.11.67)}]$$

For side nodes in Figure 2.11.28, use Eqns. (2.11.65) and (2.11.64).

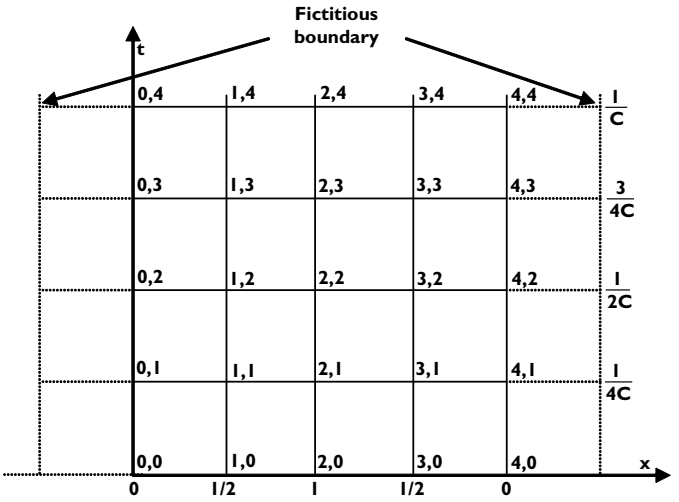


Figure 2.11.28

Stability of solution

1 If $\alpha > 1$, the solution is not stable and instability increases with increasing α.
2 When $\alpha = 1$, the solution is stable and the solutions for this problem are found to be identical with the exact solution.
3 When $\alpha < 1$, solution is stable but inaccuracy creeps in with decreasing α, as round-off error increases.
4 Optimal accuracy is obtained if the characteristic direction of the finite difference solution coincides with the characteristic directions of the hyperbolic pde.

The fact that an exact finite difference solution is obtained for the problem in question comes from the peculiar property of the wave equation, having two characteristics $(x + ct)$ and $(x - ct)$, which are straight lines. For more complicated hyperbolic equation, which, in general, has curved characteristics, optimal accuracy is obtained by using a curvilinear system of coordinates, corresponding as nearly as possible to the curvilinear characteristics of the pde rather than a fixed system of rectangular coordinates of the type used in the present presentation. In many problems of practical

interest, it has been found convenient to use the arcs of the curved characteristics as coordinates in the finite difference network for the hyperbolic type of pde.

2.11.3 Laplace and Biharmonic equations

In problems related to plates and slabs bi-harmonic equation of the type

$$\nabla^4\phi \Rightarrow \frac{\partial^4\phi}{\partial x^4} + 2\frac{\partial^4\phi}{\partial x^2\partial y^2} + \frac{\partial^4\phi}{\partial y^4} = \frac{w}{D} \tag{2.11.66}$$

is encountered routinely[19].

Solutions often become very complex for these PDEs when boundary conditions become varied and mixed[20]. With a little bit of intelligent manipulation, a number of them can be solved quite easily and with very good accuracy by applying the theory of finite difference.

We show hereafter the mathematical background behind application of the finite difference equations to PDEs.

We had shown earlier that $D^2 = \frac{1}{h^2}\delta^2$, thus

$$D_x^2[f(x)] = \frac{1}{h^2}\delta_x^2[f(x)] \quad \text{or } D_x^2[f(x)] = \frac{1}{h^2}[f(x+h) - 2f(x) + f(x-h)] \tag{2.11.67}$$

Now let us consider a mesh grid as shown in Figure 2.11.29.

For the mesh grid shown above for a typical point i we have

$$D_x^2[f(i)] = \frac{1}{h^2}\delta_x^2[f(i)] = \frac{1}{h^2}[f(3) - 2f(i) + f(1)] \quad \text{and}$$

$$D_y^2[f(i)] = \frac{1}{h^2}\delta_y^2[f(i)] = \frac{1}{h^2}[f(4) - 2f(i) + f(2)].$$

$$\text{Thus,} \quad \nabla^2 f(i) = \frac{\partial^2 f(i)}{\partial x^2} + \frac{\partial^2 f(i)}{\partial y^2} = \frac{1}{h^2}[f(1) + f(2) - 4f(i) + f(3) + f(4)]$$

The Laplace equation with respect to a nodal point i can be represented by format is shown Figure 2.11.30.

We had shown above that

$$D_x^2[f(i)] = \frac{1}{h^2}\delta_x^2[f(i)] = \frac{1}{h^2}[f(3) - 2f(i) + f(1)]$$

19 Here w is the load per meter square over plate and $D = Et^3/12(1-\nu^2)$ where E is Modulus of elasticity, t is the thickness, ν is Poisson's ratio.

20 Like fixed, free, simply supported etc.

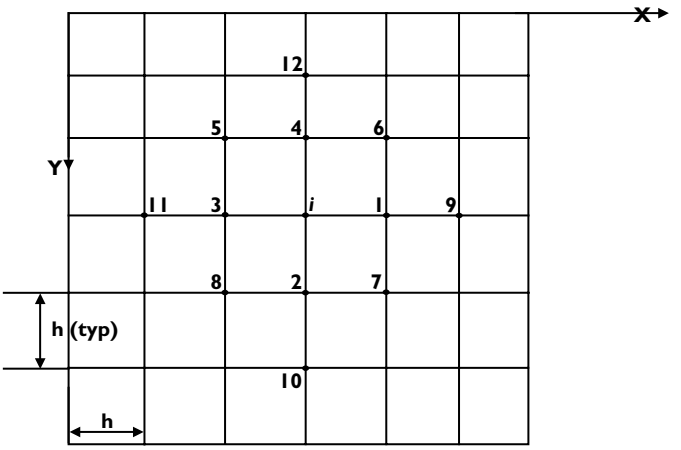
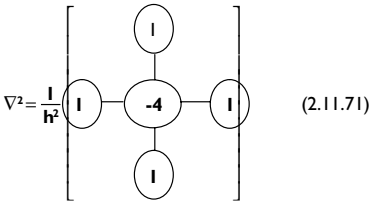


Figure 2.11.29 Typical mesh grids with nodal points.



(2.11.71)

Figure 2.11.30

$$\text{Thus,}\quad D_x^4[f(i)] = \frac{1}{h^4}\delta_x^2[f(3) - 2f(i) + f(1)]$$

$$= \frac{1}{h^4}[f(11) - 2f(3) + f(i) - 2[f(3) - 2f(i) + f(1)]$$

$$+ f(i) - 2f(1) + f(9)]$$

$$\text{Similarly}\quad D_y^4[f(i)] = \frac{1}{h^4}\delta_y^2[f(4) - 2f(i) + f(2)]$$

$$\frac{1}{h^4}[f(12) - 2f(4) + f(i) - 2[f(4) - 2f(i) + f(2)] + f(i) - 2f(2) + f(10)]$$

$$\text{Again,}\quad D_y^2 D_x^2[f(i)] = \frac{1}{h^4}\delta_y^2\delta_x^2[f(i)] = \frac{1}{h^4}\delta_y^2[f(3) - 2f(i) + f(1)]$$

$$\frac{1}{h^4}[f(5) - 2f(3) + f(8) - 2[f(4) - 2f(i) + f(2)] + f(6) - 2f(1) + f(7)]$$

Thus, for a point $f(i)$ adding up all the above terms the bi-harmonic operator $\nabla^4 f(i) \Rightarrow \left[\frac{\partial^4}{\partial x^4} + 2\frac{\partial^4}{\partial x^2 \partial y^2} + \frac{\partial^4}{\partial y^4}\right] f(i) = \frac{w}{D}$, can be represented as

$$20f(i) - 8[f(4) + f(2) + f(3) + f(1)] + 2[f(5) + f(6) + F(7) + f(8)]$$

$$+ f(9) + f(10) + f(11) + f(12) = \frac{wh^4}{D} \tag{2.11.68}$$

Above can be pictorially expressed as shown in Figure 2.11.31.

Having established the above, we now present some examples of the same. Like for ODE we started with a simple beam problem that we can compare with an exact solution for comparison before graduating to more complex problem (pile).

For the plate problem, also we first start with a simple case before we tackle a real life complex problem that requires more elaborate computational effort.

We first derive the deflection of a simple square plate having two sides fixed and two sides simply supported subjected to a load of intensity q kN/m^2. The results thus obtained, we compare with exact solution as provided in Timoshenko and Krieger (1958).

Shown in Figure 2.11.32 is a square plate/slab of span L having its two sides fixed and two sides simply supported we break it up into a 4 by 4 mesh ($h = L/4$) as shown above. The internal nodes (marked with black dots) are numbered.

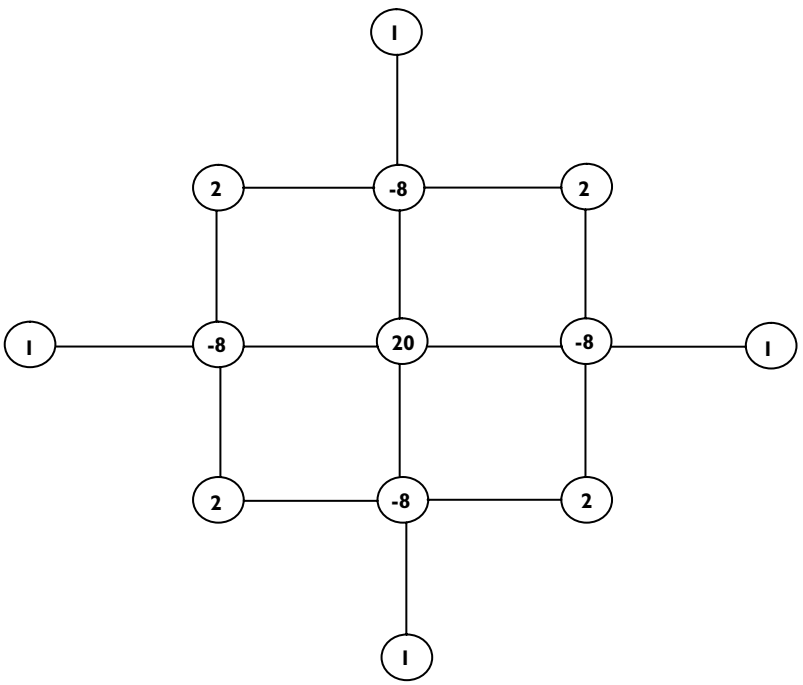


Figure 2.11.31 Nodal representation of plate equation by finite difference method.

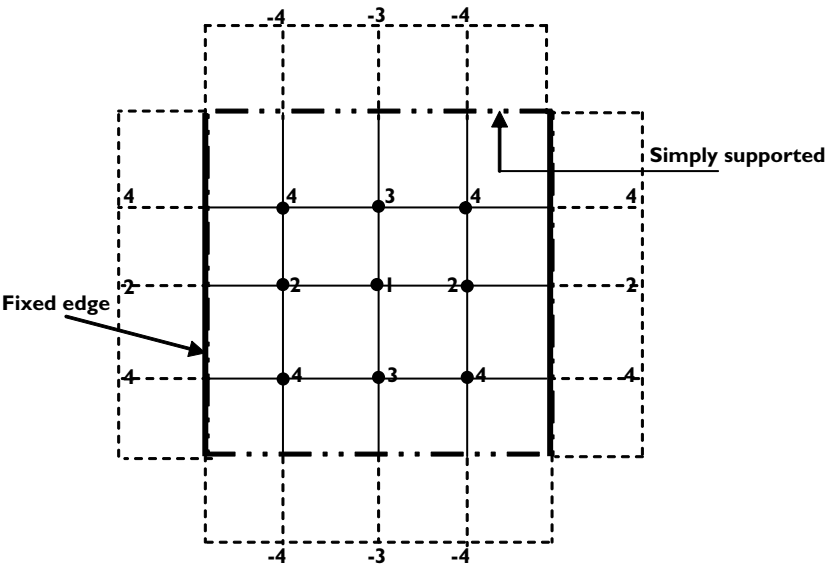


Figure 2.11.32 A square plate with two opposite sides fixed and other two sides simply supported.

Theoretically there being nine internal nodes there should have been nine equations. However, as the plate is square and we have uniform load, the displacements at the nodes will be symmetric. Taking advantage of this we see (Figure 2.11.32) nine displacement points are reduced to 4 unknowns.

At fixed edge (marked by dark lines) the rotation being zero with respect to the fixed edge we have

$$\frac{w_p - w_i}{2h} = 0 \quad \text{which gives } w_p = w_i$$

Here w_p are displacements at phantom nodes outside the slab and w_i are displacements at internal nodes while h is the width of meshing.

At simply supported edge as Bending moment $M = 0$ we have with respect to the edge nodes

$$M = \frac{w_p - 2w_e + w_i}{h^2} = 0, \quad \text{Here } w_e = \text{ the displacements at edge nodes.}$$

Since $w_e = 0$ at all edge points we have, $w_i = -w_p$.

Now applying the plate equation at node 1 we have

$$20w(1) - 8\,[2w(3) + 2w(2)] + 2\,[4w(4)] + 0 + 0 + 0 + 0 = \frac{qh^4}{D}$$

or $$20w(1) - 16w(2) - 16w(3) + 8w(4) = \frac{qh^4}{D}$$

Applying the plate difference equation successively at each nodes we develop the other three equations as,

$$-8w(1)+22w(2)+4w(3)-16w(4)=\frac{qh^4}{D}$$

$$-8w(1)+4w(2)+20w(3)-16w(4)=\frac{qh^4}{D}$$

and $$2w(1)-8w(2)-8w(3)+22w(4)=\frac{qh^4}{D} \tag{2.11.69}$$

The above can be expressed in the matrix form as

$$\begin{bmatrix} 20 & -16 & -16 & 8 \\ -8 & 22 & 4 & -16 \\ -8 & 4 & 20 & -16 \\ 2 & -8 & -8 & 22 \end{bmatrix} \begin{Bmatrix} w(1) \\ w(2) \\ w(3) \\ w(4) \end{Bmatrix} = \begin{Bmatrix} 1 \\ 1 \\ 1 \\ 1 \end{Bmatrix} \frac{qL^4}{256D}$$

The above on inversion and multiplication with the unit matrix gives

$$\begin{Bmatrix} w(1) \\ w(2) \\ w(3) \\ w(4) \end{Bmatrix} = \begin{Bmatrix} 0.002466 \\ 0.001619 \\ 0.001821 \\ 0.001204 \end{Bmatrix} \frac{qL^4}{D} \tag{2.11.70}$$

As per analytical method, exact value at node 1(w_{max}) is given by $0.001922qL^4/D$.

It is obvious there is some error in the answer (about 28%) the reason being the mesh size is *far too crude*. Once the mesh size is reduced (like half or one fourth of the present value) results would surely improve and the value will be much closer to the exact solution.

The above problem was only cited to give you a first hand feel of how plate problems are solved based on finite difference method. It is evident that for solution of practical plate problem much more refined meshes are required and the computational effort involved- surely calls for the solution to be carried out in a computer.

Having established the basis of solving the bi-harmonic equation we proceed to solve a practical problem as described hereafter.

Example 2.11.5

A control building roof slab is shown in Figure 2.11.33. There being transformers one west and south sides of building, the slab is monolithically fixed with blast proof RCC walls. The north and east sides are simply resting on 250 mm thick brick walls. The room being full of control equipment does not allow for any column to be built inside. Cable entries being from roof, does not allow any roof beams to be cast with roof slab. Thickness of slab is 250 mm

having 75 mm thick roof finish; Live load on slab is 2 kN/m^2. Analyze the slab for moment and deflection. Consider $E = 2.85 \times 10^7$ kN/m^2 and $\nu = 0.25$. Density of RCC = 25 kN/m^3. Roof finish = 24 kN/m^3.

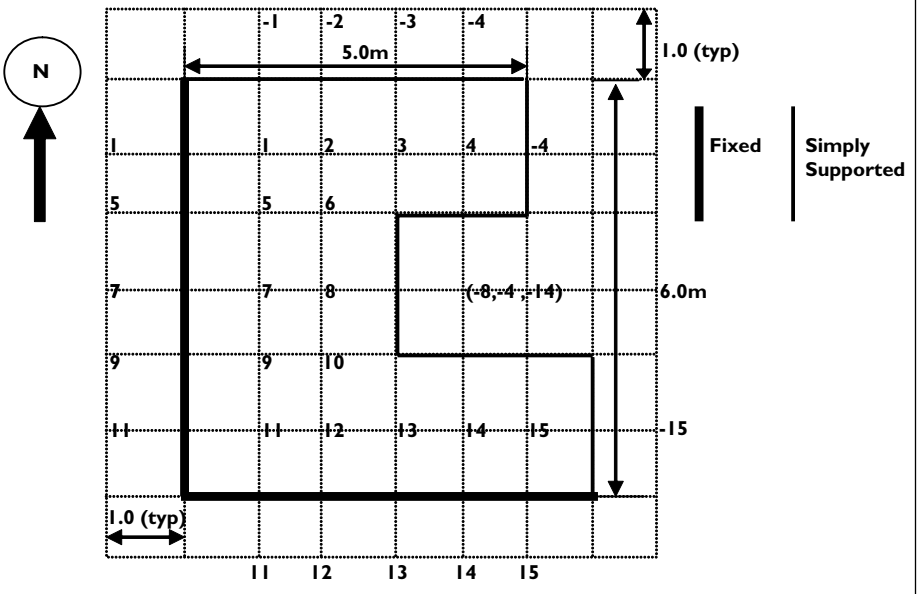


Figure 2.11.33 Plan view of control building.

Solution:

Observe it is a typical flat slab problem, where codal procedures cannot be applied. The slab being irregular in shape and having mixed boundary conditions coefficients furnished in codes cannot be applied. As such, the only alternative way to solve the problem is by numerical method.

Thickness of slab = 250 mm

Dead Load of slab = $0.25 \times 25 = 6.25$ kN/m^2; Wt. of 75 mm roof finish = $0.075 \times 24 = 1.8$ kN/m^2

Live load = 2 kN/m^2

Total Load intensity = $6.25 + 1.8 + 2 = 10.05$ kN/m^2

Like in the previously cited example of square plate at simply supported edge

$$M = \frac{w_p - 2w_e + w_i}{h^2} = 0 \quad \text{which gives } w_i = -w_p$$

For fixed end considering the rotation is zero at edge we have $\frac{w_p - w_i}{2h} = 0 \Rightarrow w_p = w_i$; The above conditions are marked in the mathematical model above.

Now applying the plate equation successively at each of the internal nodes we have

$$[A] = \begin{bmatrix}
20 & -8 & 1 & 0 & -8 & 2 & 1 & 0 & 0 & 0 & 0 & 0 & 0 & 0 & 0 \\
-8 & 19 & -8 & 1 & 2 & -8 & 0 & 1 & 0 & 0 & 0 & 0 & 0 & 0 & 0 \\
1 & -8 & 19 & -8 & 0 & 2 & 0 & 0 & 0 & 0 & 0 & 0 & 0 & 0 & 0 \\
0 & 1 & -8 & 17 & 0 & 0 & 0 & 0 & 0 & 0 & 0 & 0 & 0 & 0 & 0 \\
-8 & 2 & 0 & 0 & 21 & -8 & -8 & 2 & 1 & 0 & 0 & 0 & 0 & 0 & 0 \\
2 & -8 & 2 & 0 & -8 & 20 & 2 & -8 & 0 & 1 & 0 & 0 & 0 & 0 & 0 \\
1 & 0 & 0 & -8 & 2 & 21 & -8 & -8 & 2 & 1 & 0 & 0 & 0 & 0 & 0 \\
0 & 1 & 0 & 0 & 2 & -8 & -8 & 19 & 2 & -8 & 0 & 1 & 0 & 0 & 0 \\
0 & 0 & 0 & 0 & 1 & 0 & -8 & 2 & 19 & 0 & -8 & 2 & 0 & 0 & 0 \\
0 & 0 & 0 & 0 & 0 & 1 & 2 & -8 & -8 & 20 & 2 & -8 & 2 & 0 & 0 \\
0 & 0 & 0 & 0 & 0 & 0 & 1 & 0 & -8 & 2 & 21 & -8 & 1 & 0 & 0 \\
0 & 0 & 0 & 0 & 0 & 0 & 0 & 1 & 2 & -8 & -8 & 21 & -8 & 1 & 0 \\
0 & 0 & 0 & 0 & 0 & 0 & 0 & 0 & 0 & 2 & 1 & -8 & 21 & -8 & 1 \\
0 & 0 & 0 & 0 & 0 & 0 & 0 & 0 & 0 & 0 & 0 & 1 & -8 & 20 & -8 \\
0 & 0 & 0 & 0 & 0 & 0 & 0 & 0 & 0 & 0 & 0 & 0 & 1 & -8 & 19
\end{bmatrix}$$

and $\{w\} = \langle w_1\ w_2\ w_3\ w_4\ w_5\ w_6\ w_7\ w_8\ w_9\ w_{10}\ w_{11}\ w_{12}\ w_{13}\ w_{14}\ w_{15}\rangle^T$

Here, $q = 10.05$ kN/m^2; $h = 1.0$ m and

$$D = \frac{Et^3}{12(1-\nu^2)} = \frac{2.85 \times 10^7 \times (0.25)^3}{12(1-0.25^2)} = 39583 \text{ kN} \cdot \text{m}.$$

Thus $$\frac{qh^4}{D} = \frac{10.05 \times (1)^4}{39583} = 2.538968 \times 10^{-4} \text{ m}$$

Hence $$\{F\} = \frac{qh^4}{D}\langle 1\ 1\ 1\ 1\ 1\ 1\ 1\ 1\ 1\ 1\ 1\ 1\ 1\ 1\ 1\rangle^T$$

On inversion of the [*A*] matrix and multiplying it by the [*F*] matrix the deflections in mm are as shown in Figure 2.11.34.

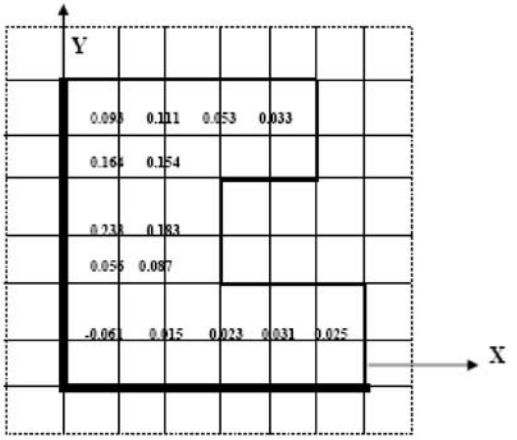


Figure 2.11.34 Displacement (mm) plot of nodes for the control building roof slab.

The Bending moment at left edge of node 1 is calculated hereafter for clarity.

The Moment in x direction is given by

$$M_x = D\left[\frac{\partial^2 w}{\partial x^2} + \nu\frac{\partial^2 w}{\partial y^2}\right] \quad \text{and}$$

$$M_y = D\left[\frac{\partial^2 w}{\partial y^2} + \nu\frac{\partial^2 w}{\partial x^2}\right]$$

$$= \frac{D}{h^2}[w_1 - 2w_{e1} + w_1] + \frac{D}{h^2}[0 - 2 \times 0 + 0] = \frac{D}{h^2}[2w_1]$$

$$= \frac{39583 \times 2 \times 0.093}{1000 \times 1^2} = 7.362 \text{ kN} \cdot \text{m} \quad \text{and so on. .....}$$

The formulas may now be successively applied at each of the edge and internal nodes to obtain Moments in x and y direction. Based on the above problem we hope you have now some idea on how to solve problems related to plate by finite difference method. We have also defined the boundary condition of a plate under two common end conditions that are encountered while solving a plate problem a) the end fixed b) simply supported. There are many cases however where the edge is free[21].

The boundary condition of this case is not difficult to derive. Since the edge is free, the moment and shear force at edge must be equal to zero. Thus if an edge is free and parallel to x axis or y axis, we have

$$M_y = \frac{\partial^2 w}{\partial y^2} + \nu\frac{\partial^2 w}{\partial x^2} = 0 \quad \text{and} \quad V_y = \frac{\partial^3 w}{\partial y^3} + (2 - \nu)\frac{\partial^3 w}{\partial y \partial x^2} = 0$$

Thus with reference to Figure 2.11.29, for free edge we have

$$\frac{[w_3 - 2w_i + w_1]}{h^2} + \nu\frac{[w_4 - 2w_i + w_2]}{h^2} = 0$$

a similar expression can be derived for the shear equation for pivotal point i.

We will leave the topic here for the time being and shall come back on this issue on a more generalized form later before we address some other important issues.

2.11.4 Irregular meshes or grids

Until now, we have derived expressions where for one-dimensional cases (beams) the spacing has been equal while for two-dimensional case the mesh grids have been regular (i.e. a square). However while solving practical engineering problems there could be

21 Raft or isolated footings are classic examples. Porticos before building would usually have one side of the slab free.

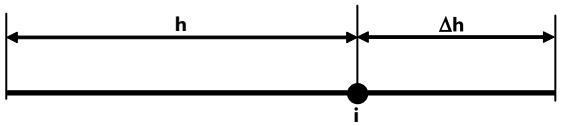


Figure 2.11.35 A nodal point *i* with uneven grid.

cases when one is forced to consider irregular grids to improve the accuracy of results while formulations derived earlier need to be modified for the same.

We present herein the cases when such situation arrives.

Shown in Figure 2.11.35 is a node point i with uneven grid at its two ends given by h and Δh.

By Taylor's series

$$f(x+\alpha h) = f(x) + \alpha h Df(x) + \frac{\alpha^2 h^2}{2!} D^2 f(x) + \frac{\alpha^3 h^3}{3!} D^3 f(x) + \cdots\cdots$$

and $$f(x-h) = f(x) - hDf(x) + \frac{h^2}{2!} D^2 f(x) - \frac{h^3}{3!} D^3 f(x) + \cdots\cdots$$

Eliminating $h^2 D^2 f(x)$ from the above equations and also ignoring the higher orders we have

$$Df(x) = \frac{1}{\alpha(1+\alpha)h}[f(x+\alpha h) - (1-\alpha^2)f(x) - \alpha^2 f(x-h)] + \text{error of order } h^2 \tag{2.11.71}$$

Similarly eliminating $hDf(x)$ we have

$$D^2 f(x) = \frac{2}{\alpha(1+\alpha)h^2}[f(x+\alpha h) - (1+\alpha)f(x) + \alpha f(x-h)] + \text{error of order } h \text{ for } \alpha^1 1 \tag{2.11.72}$$

2.11.5 Laplace operator with irregular mesh

For the above case at node point i the Laplace operator with irregular mesh shown in Figure 2.11.36 is expressed as

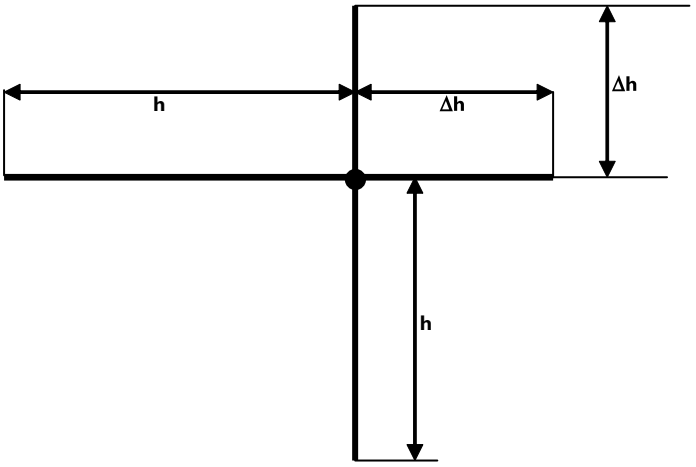


Figure 2.11.36 Irregular mesh at node point *i* in two dimension.

$$\nabla^2 = \frac{2}{\alpha\beta(1+\alpha)(1+\beta)h^2}\begin{bmatrix} & \alpha(1+\alpha) & \\ \alpha\beta(1+\beta) & -(1+\alpha)(1+\beta)(\alpha+\beta) & \beta(1+\beta) \\ & \alpha\beta(1+\alpha) & \end{bmatrix}$$

2.11.6 Bi-harmonic equations with irregular meshes

Shown in Figure 2.11.37, is a typical grid with irregular mesh having division of h in x direction and h in y direction. For the present case

$$\frac{1}{h^4}\delta x^4 f(i) = \frac{1}{h^4}[f(9) - 4f(1) + 6f(i) - 4f(3) + f(11)]$$

$$\frac{1}{\alpha^4 h^4}\delta y^4 f(i) = \frac{1}{\alpha^4 h^4}[f(10) - 4f(2) + 6f(i) - 4f(4) + f(12)]$$

and $$(\frac{1}{h^2}\delta_x^2)(\frac{1}{\alpha^2 h^2}\delta_y^2) = \frac{1}{h^2}\delta_x^2\frac{1}{\alpha^2 h^2}[f(2) - 2f(i) + f(4)]$$

$$= \frac{1}{\alpha^2 h^4}[\delta_x^2 f(2) - 2\delta_x^2 f(i) + \delta_x^2 f(4)]$$

$$= \frac{1}{\alpha^2 h^4}[(f(8) - 2f(2) + f(7)) - 2(f(3) - 2f(i) + f(1)) + (f(5) - 2f(4) + f(6))]$$

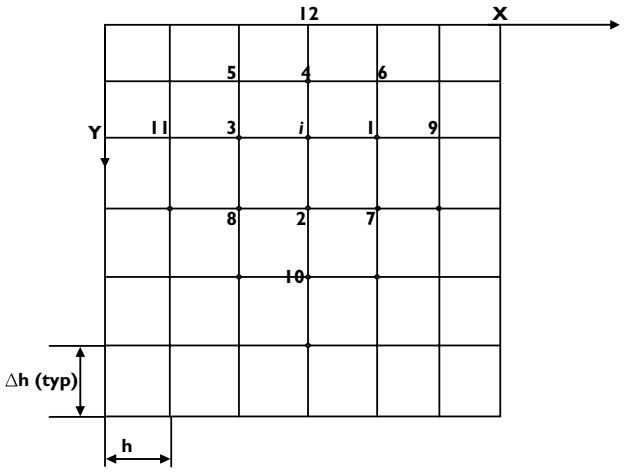


Figure 2.11.37 Typical rectangular mesh grids with nodal points.

Combining the above equations, we have

$$\Delta^4 = \frac{1}{\alpha^4 h^4}\begin{bmatrix} & & 1 & & \\ & 2\alpha^2 & -4\alpha^2-4 & 2\alpha^2 & \\ \alpha^4 & -4\alpha^4-4\alpha^2 & 6\alpha^4+8\alpha^2+6 & -4\alpha^4-4\alpha^2 & \alpha^4 \\ & 2\alpha^2 & -4\alpha^2-4 & 2\alpha^2 & \\ & & 1 & & \end{bmatrix}$$

+ error of order (h^2). (2.11.73)

2.11.7 Refined finite difference analysis

Until now formulations shown is for ordinary finite difference equations where error is of the order h^2, where h is the distance between the nodes.

When we apply ordinary finite difference equation to higher order derivatives and a large number of mesh points the solutions due to truncation, errors may converge to a wrong number or the convergence could be quite slow. One of the reasons for such slow convergence is that finite difference equations converge in collocating sense and

agree only in value with the exact function at mesh points and their derivatives do not match.

Additional source of errors could creep in due to the approximation of the boundary conditions and the use of coarse load averaging rules.

On the other hand using extremely fine meshes or nodes results in large number of simultaneous equations and could create round off errors in computer solutions having adverse effect on the accuracy and economy of the method. Consequently, when high accuracy in finite difference solution is required improved or refined finite difference equations should be used.

The basis of the above is presented hereafter.

Based on Taylor's series

$$f(x+h) = f(x) + \frac{hf'(x)}{1!} + \frac{h^2f''(x)}{2!} + \frac{h^3f'''(x)}{3!} + \frac{h^4f''''(x)}{4!} + \cdots\cdots \quad \text{and}$$

$$f(x-h) = f(x) - \frac{hf'(x)}{1!} + \frac{h^2f''(x)}{2!} - \frac{h^3f'''(x)}{3!} + \frac{h^4f''''(x)}{4!} - \cdots\cdots$$

Adding the above two equations we have

$$f(x+h) + f(x-h) = 2f(x) + \frac{2h^2f''(x)}{2!} + \frac{2h^4f^{iv}(x)}{4!} + \cdots\cdots$$

or $$f(x+h) - 2f(x) + f(x-h) = h^2f''(x) + \frac{h^4f^{iv}(x)}{12} + \cdots\cdots$$

or $$\delta_x^2 f(x) = h^2f''(x) + \frac{h^4f^{IV}(x)}{12} + \frac{h^6f^{VI}(x)}{360} + \cdots\cdots$$

or $$D_x^2 f(x) = f''(x) + \frac{h^2f^{IV}(x)}{12} + \frac{h^4f^{VI}(x)}{360}$$

or $$D_x^2 f(x) = f''(x) + \varepsilon_1 + \varepsilon_2 \quad \text{where } \varepsilon_1 \text{ and } \varepsilon_2 \text{ are errors of higher order.}$$

Since we want to reduce the error, we take

$$D_x^2 f(x) = f''(x) - \varepsilon_1 \quad \text{where } \varepsilon_1 = \frac{h^2f^{IV}(x)}{12}, \text{ thus}$$

$$D_x^2 f(x) = \frac{1}{h^2}[f(x+h) - 2f(x) + f(x-h)] - \frac{h^2}{12}$$

$$\times \frac{1}{h^4}[f(x+2h) - 4f(x+h) + 6f(x) - 4f(x-h) - f(x-2h)]$$

$$= \frac{1}{12h^2}[-f(x+2h) + 16f(x+h) - 30f(x) + 16f(x-h) - f(x-2h)]$$

Thus refined finite difference formulation for

$$\frac{d^2y_i}{dx^2} = \frac{1}{12h^2}[-y_{i+2} + 16y_{i+1} - 30y_i + 16y_{i-1} - y_{i-2}]$$

Based on similar derivation it can be shown that

$$\frac{dy_i}{dx} = \frac{1}{12h}[-y_{i+2} + 8y_{i+1} - 8y_{i-1} + y_{i-2}]$$

$$\frac{d^3y_i}{dx^3} = \frac{1}{8h^3}[-y_{i+3} + 8y_{i+2} - 13y_{i+1} + 13y_{i-1} - 8y_{i-2} + y_{i-3}] \quad \text{and}$$

$$\frac{d^4y_i}{dx^4} = \frac{1}{6h^4}[-y_{i+3} + 12y_{i+2} - 39y_{i+1} + 56y_i - 39y_{i-1} + 12y_{i-2} - y_{i-3}]$$

Based on identical procedures the Laplace equation based on improved finite difference is given by

$$\nabla^2 = \frac{1}{12h^2}\begin{bmatrix} & & -1 & & \\ & & 16 & & \\ -1 & 16 & \textcircled{-60} & 16 & -1 \\ & & 16 & & \\ & & -1 & & \end{bmatrix}$$

and the bi-harmonic equation for plate is given by

$$\nabla^4 = \frac{1}{6h^4}\begin{bmatrix} & & & -1 & & & \\ & & -1 & 14 & -1 & & \\ & -1 & 20 & -77 & 20 & -1 & \\ -1 & 14 & -77 & \textcircled{184} & -77 & 14 & -1 \\ & -1 & 20 & -77 & 20 & -1 & \\ & & -1 & 14 & -1 & & \\ & & & -1 & & & \end{bmatrix}$$

Here the node marked with a circle indicates the pivot point.

2.11.8 Free edged plates with different boundary conditions

We present here plates with different boundary conditions as shown in Figure 2.11.37 to 42 having irregular meshes when the node i could be a general interior node or node near or on the boundary (Ghali and Bathe 1970).

The values of symbols used are expressed in Table 2.11.1.

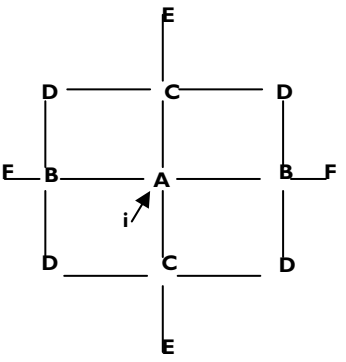


Figure 2.11.38 Internal Node.

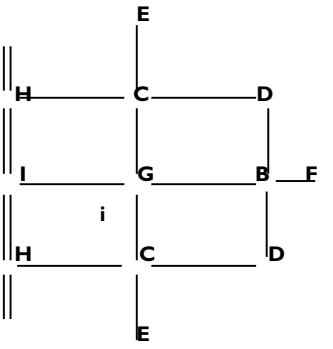


Figure 2.11.39 Internal Node with one edge free.

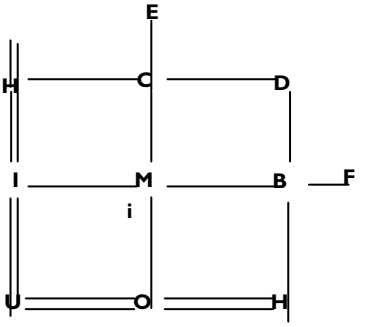


Figure 2.11.40 Internal node with both edge free.

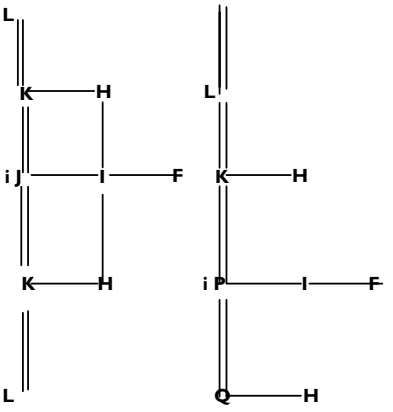


Figure 2.11.41 Node on one free edge.

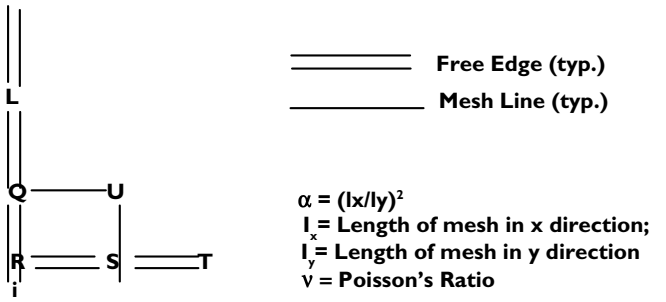


Figure 2.11.42 Corner node on free edge.

Table 2.11.1 Finite Difference coefficients for plates.

Sl. No.	*Symbol*	*Expression*
1	A	$6+6\alpha^2+8\alpha$
2	B	$-4(1+\alpha)$
3	C	$-4\alpha(1+\alpha)$
4	D	2α
5	E	α^2
6	F	1
7	G	$5+6\alpha^2+8\alpha$
8	H	$\alpha(2-\nu)$
9	I	$-2(2\alpha-\nu\alpha+1)$
10	J	$1+4\alpha(1-\nu)+3\alpha^2(1-\nu^2)$
11	K	$-2\alpha[1-\nu+\alpha(1-\nu^2)]$
12	L	$\alpha^2(1-\nu^2)/2$
13	M	$5+5\alpha^2+8\alpha$
15	O	$-2\alpha(2-\nu+\alpha)$
16	P	$1+4\alpha(1-\nu)+(5/2)\alpha^2(1-\nu^2)$
17	Q	$-2\alpha[1-\nu+(\alpha/2)(1-\nu^2)]$
18	R	$2\alpha(1-\nu)+(1/2)(1-\alpha^2)(1-\nu^2)$
19	S	$-2[\alpha(1-\nu)+(1/2)(1-\nu^2\|)]$
20	T	$(1/2)(1-\nu^2)$
21	U	$2\alpha(1-\nu)$

2.11.9 Finite difference in polar co-ordinate

There are cases when solving a problem in polar co-ordinate makes the solution much simpler to tackle than in Cartesian co-ordinate. For instance, circular plates with different types of loading or chimney rafts on elastic foundations are cases when treating the problem in polar co-ordinate (Figure 2.11.43) makes the problem easier to solve. In such cases, the finite difference equation in polar co-ordinate is as expressed hereafter.

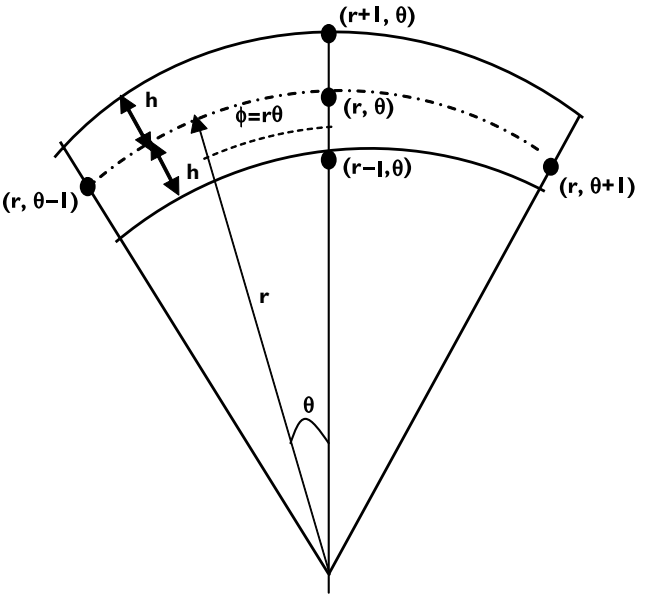


Figure 2.11.43 Nodes in polar co-ordinate.

In polar co-ordinate

$$\nabla^2 w = \frac{\partial^2 w}{\partial r^2} + \frac{1}{r}\frac{\partial w}{\partial r} + \frac{1}{r^2}\frac{\partial^2 w}{\partial \theta^2} \tag{2.11.74}$$

With respect to above Figure one may express it in finite difference form as

$$\frac{\partial w}{\partial r} = \frac{1}{2h}[w_{r+1,\theta} - w_{r-1,\theta}] \quad \text{and} \quad \frac{\partial^2 w}{\partial r^2} = \frac{1}{h^2}[w_{r+1,\theta} - 2w_{r,\theta} + w_{r-1,\theta}] \tag{2.11.75}$$

$$\frac{\partial^2 w}{\partial \theta^2} = \frac{1}{\phi^2}[w_{r,\theta+1} - 2w_{r,\theta} + w_{r,\theta-1}] \tag{2.11.76}$$

Hence $$\nabla^2 w = \frac{\partial^2 w}{\partial r^2} + \frac{1}{r}\frac{\partial w}{\partial r} + \frac{1}{r^2}\frac{\partial^2 w}{\partial \theta^2}$$

$$= \frac{1}{h^2}[w_{r+1,\theta} - 2w_{r,\theta} + w_{r-1,\theta}] + \frac{1}{2hr}[w_{r+1,\theta} - w_{r-1,\theta}]$$

$$+ \frac{1}{\phi^2 r^2}[w_{r,\theta+1} - 2w_{r,\theta} + w_{r,\theta-1}] \tag{2.11.77}$$

$$\text{or,} \quad h^2\nabla^2 w = \left[1+\frac{h}{2r}\right] w_{r+1,\theta-2} \left[1+\left(\frac{h}{\varphi r}\right)^2\right] w_{r,\theta} + \left[1-\frac{h}{2r}\right] w_{r-1,\theta} + \left(\frac{h}{\varphi r}\right)^2 w_{r,\theta+1} - \left(\frac{h}{\varphi r}\right)^2 w_{r,\theta-1} \tag{2.11.78}$$

and so on.....

2.11.10 Finite difference solution for initial value problem

We had explained earlier that the equation of vibration for lumped mass connected to by spring and dashpot is expressed as

$$m\frac{d^2x}{dt^2} + c\frac{dx}{dt} + kx = P(t) \tag{2.11.79}$$

Based on the initial condition it is possible to break it up in finite difference equation for solution of the problem. We will however not solve this problem here.

The same has been explained in detail in Chapter 5 (Vol. 1)[22], under the heading of Numerical Integration and Time history Analysis, wherein we have also described other implicit methods like Wilson Theta, Newmark beta etc.

2.11.11 Finite difference solution for initial-boundary value problem

Let us consider the equation

$$G\frac{\partial^2 u}{\partial z^2} = \rho\frac{\partial^2 u}{\partial t^2} \tag{2.11.80}$$

where G = dynamic shear modulus of the medium; and ρ = mass density of the medium.

Equation (2.11.80) is the equation of propagation of wave in an elastic medium. The above equation can be further expressed as

$$\frac{\partial^2 u}{\partial z^2} = \frac{1}{v_s^2}\frac{\partial^2 u}{\partial t^2} \tag{2.11.81}$$

where v_s = shear wave velocity of the medium.

In this case the meshing has to be done in z-t co-ordinate i.e. we break up equation in length steps of h and time step t as given in Figure 2.11.44.

22 Basic concepts in structural dynamics.

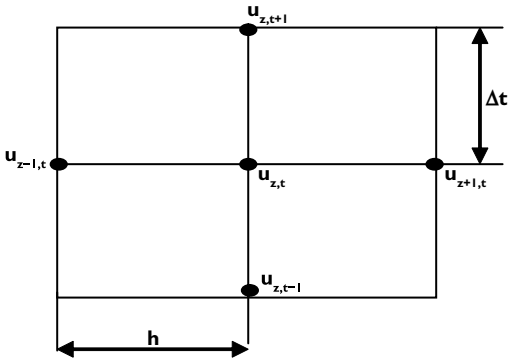


Figure 2.11.44 Meshing in *z-t* co-ordinate.

Based on finite difference theory expressed earlier we have

$$\frac{\partial^2 u}{\partial z^2} = \frac{1}{h^2}[u_{z-1,t} - 2u_{z,t} + u_{z-1,t}];$$

$$\frac{\partial^2 u}{\partial t^2} = \frac{1}{\Delta t^2}[u_{z,t-1} - 2u_{z,t} + u_{z,t+1}] \tag{2.11.82}$$

Substituting it in the PDE we have

$$\frac{1}{h^2}[u_{z-1,t} - 2u_{z,t} + u_{z+1,t}] = \frac{1}{v_s^2 \Delta t^2}[u_{z,t-1} - 2u_{z,t} + u_{z,t+1}]$$

$$\rightarrow \quad u_{z-1,t} - 2(1 - r^2)u_{z,t} + u_{z+1,t} - r^2 u_{z,t-1} - r^2 u_{z,t+1} = 0 \tag{2.11.83}$$

The above can be pictorially expressed as

$$\begin{bmatrix} & \boxed{-r^2} & \\ \boxed{1} & \boxed{-2(1-r^2)} & \boxed{1} \\ & \boxed{-r^2} & \end{bmatrix} \quad \text{where } r^2 = \frac{h^2}{v_s^2\ \Delta t^2} \tag{2.11.84}$$

In the above problem for $r \geq 1$ the results become unstable, while for $r \leq 1$ the computational effort is more and truncation error creeps in, the most optimum solution is arrived at for $r = 1$.

2.11.12 Finite difference application in dynamics

Finite difference equations may be effectively used in problems related to structural dynamics.

Especially for cases when the moment of inertia undergoes an abrupt change numerical analysis based on finite difference equation can be an effective tool to find out the natural frequencies of a system.

In this section, we elucidate the fundamental concepts only.

For a beam element the equation of vibration in transverse direction is expressed as

$$EI\frac{d^4y}{dx^4} = m\omega^2 y \tag{2.11.85}$$

Here E = Young's Modulus of the beam; I = Moment of inertia of the beam cross-section; m = mass per unit length; y = deflection; ω^2 = square of the natural frequency.

Based on finite difference the above equation can be expressed as

$$EI\frac{d^4y}{dx^4} = \frac{EI}{h^4}\left[y_{i+2} - 4y_{i+1} + 6y_i - 4y_{i-1} + y_{i-2}\right] = m\omega^2 y_i$$

or $$y_{i+2} - 4y_{i+1} + 6y_i - 4y_{i-1} + y_{i-2} = \frac{mh^4\omega^2}{EI}y_i$$

or $$y_{i+2} - 4y_{i+1} + 6y_i - 4y_{i-1} + y_{i-2} = \lambda y_i \quad \text{where } \lambda = \frac{mh^4\omega^2}{EI} \tag{2.11.86}$$

The above equation when applied with appropriate boundary condition gives the natural frequency of the system.

To further illustrate the matter let us consider a simply supported beam with self-weight m per unit length as shown in Figure 2.11.45.

As stated earlier the finite difference equation free vibration is given by the expression

$$y_{i+2} - 4y_{i+1} + 6y_i - 4y_{i-1} + y_{i-2} = \lambda y_i \tag{2.11.87}$$

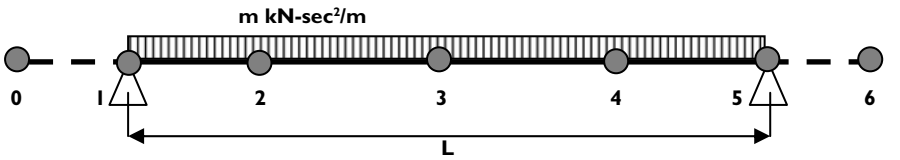


Figure 2.11.45 A simply supported beam with mass m as an udL.

Thus applying the above expression at node 2, 3 and 4 successively, we have

$$\begin{aligned} &y_4 - 4y_3 + 6y_2 - 4y_1 + y_0 = \lambda y_2 \\ &y_5 - 4y_4 + 6y_3 - 4y_2 + y_1 = \lambda y_3 \quad \text{and} \\ &y_6 - 4y_5 + 6y_4 - 4y_3 + y_2 = \lambda y_4. \end{aligned} \tag{2.11.88}$$

Since the beam is simply supported we have $y_1 = y_5 = 0$ and for the phantom nodes

$$y_0 = -y_2 \quad \text{and} \quad y_4 = -y_6\ ^{23}.$$

Substituting the above values in the above equations we have

$$y_4 - 4y_3 + 5y_2 = \lambda y_2 \quad -4y_4 + 6y_3 - 4y_2 = \lambda y_3 \quad \text{and} \quad 5y_4 - 4y_3 + y_2 = \lambda y_4$$

Expressing the above in matrix notation, we have

$$\begin{bmatrix} 5 & -4 & 1 \\ -4 & 6 & -4 \\ 1 & -4 & 5 \end{bmatrix} \begin{Bmatrix} y_2 \\ y_3 \\ y_4 \end{Bmatrix} = \lambda \begin{bmatrix} 1 & 0 & 0 \\ 0 & 1 & 0 \\ 0 & 0 & 1 \end{bmatrix} \begin{Bmatrix} y_2 \\ y_3 \\ y_4 \end{Bmatrix}$$

The above being a generalized eigen value problem can be further expressed as

$$\begin{bmatrix} 5-\lambda & -4 & 1 \\ -4 & 6-\lambda & -4 \\ 1 & -4 & 5-\lambda \end{bmatrix} \begin{Bmatrix} y_2 \\ y_3 \\ y_4 \end{Bmatrix} = 0$$

Expanding above gives a cubical equation in λ given by

$$\lambda^3 - 16\lambda^2 + 52\lambda - 16 = 0$$

This equation can very well be solved by Newton-Raphson method or other techniques like Stodola-Vinello's method etc can be used.

Solution of the above equation[24] gives the three roots as shown in Table 2.11.2.

It will be observed that there is some error in the frequencies with respect to exact value. The reason for this being that the number of nodes considered for analysis is crude/less. The results can surely be improved by taking more number of nodes or using refined finite difference formulation as shown earlier- of course at the expense of more computational effort.

23 The boundary conditions have been derived in detail for static problem of the beam earlier.
24 Refer to Section-5.2.6.: Techniques for eigen value solutions for further detail.

Table 2.11.2 First three fundamental frequency of a simply supported beam.

Mode	λ	λ *(finite difference)*	λ *(exact value)*
1	0.172	$6.63\sqrt{\frac{EI}{mL^4}}$	$9.86\sqrt{\frac{EI}{mL^4}}$
2	4.0	$32\sqrt{\frac{EI}{mL^4}}$	$39.47\sqrt{\frac{EI}{mL^4}}$
3	11.656	$54.63\sqrt{\frac{EI}{mL^4}}$	$88.8\sqrt{\frac{EI}{mL^4}}$

2.12 THE FINITE ELEMENT METHOD

The Finite Element Method (FEM) is a very powerful numerical method that has invaded the domain of engineering and science; arguably one of the finest contributions provided to engineering and science by aerospace and civil engineers. It has brought about a completely new dimension to the numerical solution of problems related to various disciplines.

Initially developed as a tool for stress analysis of the continuum, it was quickly established onto a solid mathematical foundation when people from all disciplines like civil, aerospace, mechanical, chemical, electrical engineering, geology and even people from medical professions are using the method almost routinely to seek solutions to problems they face in their respective professions.

Rapid development of FEM along with advancement in the computational capability of computer has brought this technology within the grasp of the majority of engineers and design offices where tasks that were thought to be impossible even twenty/thirty years ago are now executed almost routinely.

2.12.1 The finite element club and its members

People who work with this technology can usually be classified into three categories:

- **The developers** – these are mostly engineers and scientists who develop the finite elements for various uses[25]. They develop these elements for use in different stress analysis, field problems, tests their accuracy, robustness of the mathematical formulation used[26]. In other words, they are the people who develop the building blocks, which others use to analyze problems at macro level.
- **The assemblers** – these are the people, who collect all these elements developed by the "developers" (as mentioned above) and write general-purpose finite element software[27] to be used by various people. This is in fact is a formidable task, for

25 HCT triangular element-Developed by Hughes, Clough and Turner, 8-nodded iso-parametric elements developed by Irons and Zienkiewicz, Higher order 6-nodded triangular elements developed by Carlos Felippa to name a few.

26 For example patch test-of which we would talk later. . . .

27 ABAQUAS, ADINA, ANSYS, GTSRUDL, PAFEC, SAP 2000, STAAD PRO to name a few of them in alphabetical order.

team of engineers have worked for years developing these programs testing them, checking them and updating them from feedback furnished by the users[28].

- **The end users** – these are the people who would use the above software in their day-to-day work to develop mathematical models of structures or system. They would like to analyze and come up with the solution using them and interpreting the results thus obtained from these programs for further use-like designing the members/section or interpreting the behavior under a particular condition etc.

In this section, we would touch upon the functions of the first two categories as mentioned above, however our major focus would be on the application part (the end user category), which constitutes the major activity in today's design office[29].

2.12.2 Brief history on the development of finite element method

The name of Zienkiewicz, Irons and finite element method is almost synonymous. There is no question about contribution of this duo in establishing the technology to its present stature from an obscure abstract method understood by a few and applied by still fewer. For in blooming days of FEM, computer, the inseparable twin of FEM was something that was not accessible to everybody as it is today.

Historically, the possibility of the theory of finite element was first perhaps proposed by Courant (1943), Prager and Synge (1947) wherein they mentioned that in an elastic domain a constant strain field is equivalent to a regional descretization. The proposal did not receive much attention at that time for basis of such analysis called for a huge amount of computation which was deemed impossible then for IBM was yet to arrive with their business computing machines which were later named as simply computers[30].

By 1960's the aircraft industry was going through revolutionary changes. After the end of Second World War, the need was felt to ameliorate the defense by developing superior aircrafts[31]. Jet engine has already been invented and people realized using them would render the aircrafts with having greater speed and flexibility in comparison to the traditional propeller driven aircrafts.

During this time, the aircraft bodies-which were continuum (constituting of metal sheets or plates) were mostly analyzed for stress based on lattice analogy as developed by Hrennikoff (1941) and McHenry (1943). However, this technology was valid only for rectangular areas and could not be applied for non-rectangular shapes. On the other hand, fluid-dynamists working on the profile of these second generation aircrafts were coming up with weirdo shapes, which would make them aerodynamically more efficient. The stress analysis group who were analyzing these aircrafts was

28 It is said that NASTRAN the FEM package used by NASA for stress analysis of spacecraft took almost thirty years to be developed to its present stage today.

29 And where lies the nemesis of a number of errors giving a spectacular amount of garbage outputs.

30 The first commercially available computer was ENIAC –1 which came into being somewhere in late 1950 was a 4 ton giant required one complete building to house it and would invert a 17×17 matrix in roughly 12–17 hours. . . .

31 The Mosquitoes, Harriers and Luftwaffe's were fast fading into oblivion.

thus confronted with significant difficulty in arriving at an accurate answer to these irregular shapes as there was no technology in vogue.

In the summer of 1952–53, Ray. W. Clough[32] joining the Summer Faculty Program of Boeing Company faced this problem (Clough & Wilson 1999). He was working with Joe Turner then the Head of Structural dynamics group on combined torsion-flexural influence on swept back delta wings where experimental results matched poorly with structural analysis results produced by one-dimensional elements.

Their joint effort first developed the stiffness matrix for a triangular element under plane stress condition[33]. This significant historical work was reported much later wherein Clough (1991) magnanimously gave complete credit to Turner on this pioneering work, the term finite element was then yet to be born. Turner presented this Boeing pioneering work at the January 1954 meeting of the Institute of Aeronautical Science in New York; however the work was formally published two years later in September 1956 (Turner et al. 1956).

After his stint with Boeing Company, Clough went on a sabbatical leave to Norway, where he had some time to reflect on his work at Boeing Company with Turner. He also studied a series of papers published by Argyris from University of Stuttgart[34], wherein it was shown that, based on matrix transformation methods, most structural analysis methods can either be categorized as either force or a displacement method.

It was during this period Clough concluded that two dimensional elements connected to more then two nodes could be used to solve problems in continuum mechanics. For Turner's triangular elements the stress strain relationship within the element, displacement compatibility between adjacent elements and force equilibrium on an integral basis at a finite number of node points within the structure was satisfied. It was evident that satisfying these three fundamental boundary conditions proved convergence to exact elasticity solution, as the mesh size was refined.

By end of 1950's industry was going through a rapid growth and never ever in the history of mankind, stress-engineers were so much on demand in various fields. It was also the height of cold war when US defense department was contemplating to build buildings and bunkers that were resistant to nuclear explosion. 1952 Tehachapi Earthquake has devastated the west coast of USA bringing into light the inadequacy of the structural analytical tools available with civil engineers then. United States transportation system was undergoing radical changes, with construction of Rapid Mass Transportation Systems having long span bridges, girders and highways. Manned space program was one of the top national priorities[35]. Nuclear power plant was becoming a distinct possibility with conventional fossil fuel reserve fast depleting[36]. Offshore oil drilling in deep water and Alaskan pipeline required complete new technology to fulfill these requirements.

32 Emeritus Professor of Structural Engineering, University of California, Berkeley, USA.

33 Popularly known as Constant Strain Triangular (CST) Element.

34 These papers were later edited by Butterrworth Publication and published as a book titled "Energy Theorems in Structure".

35 The start of the star wars.....

36 Gulf Oil boom was yet to come....

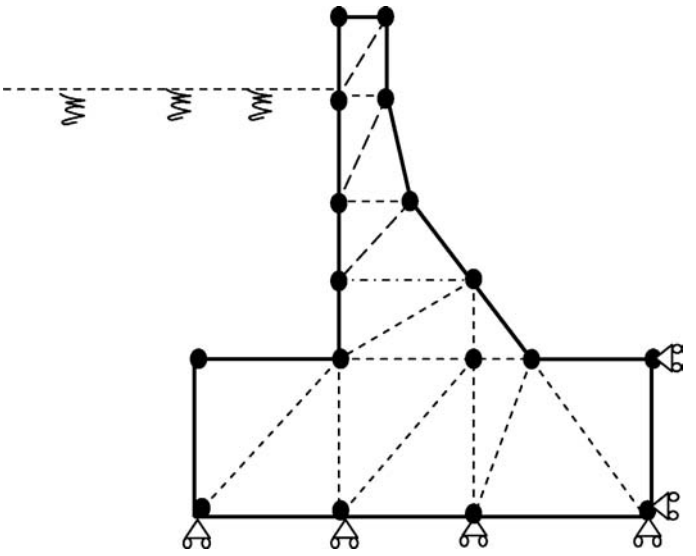


Figure 2.12.1 First generation finite element model used for analysis of gravity dams.

In many of these cases the major obstacle was the accurate stress analysis of complex continuum, as there was no comprehensive analytical tool available except a few with simple boundary conditions.

Clough wanted to test his convictions on how this theory worked on continuum with complex boundary conditions. On his return to Berkeley, he received a small grant from National Science Foundation to support research on computer analysis of structures.

Armed with an IBM 701 digital computer with 4k of 16 bit memory[37] he started to put this theory on test. Under Clough's guidance, Ari Adini a graduate student first came out with solutions of several plane stress problems using triangular elements. Since, all the matrices had to be hand computed before the final solution was obtained through computer, it was considerably time consuming and only a coarse mesh was possible. One of the first uses of such finite element application is as shown in Figure 2.12.1.

This approach was used to produce all examples in paper titled "**Finite Element Method in Plane Stress Analysis**" by Clough in 2nd ASCE Conference on Electronic Computations in September 1960 and the name **Finite Element Method** came into being.

After this, the method spread rapidly almost across the world and 1960–90 saw one of the most spectacular amounts of research carried out in this area almost at every corner of the world, covering most of the disciplines of technology.

37 The computer could solve only maximum 40 numbers of equations at a time.

When Clough presented the paper in 1960 in 2nd ASCE conference it attracted the attention of Zienkiewicz who was then in the faculty of North Western University USA. A few weeks after the presentation of the paper, Zienkiewicz invited Clough to give a lecture to his students on finite element method in his University. Zienkiewicz was then considered a leading expert in the application of finite difference method to continuum mechanics. People were excited, for they expected a stimulating debate amongst the two doyens on the relative merits of the two methods. However, after a few penetrating questions to Clough on finite element, Zienkiewicz became an instant convert to the method. Zienkiewicz later migrated to University of Wales at Swansea and founded the Department of Numerical Methods on Engineering. He brought about phenomenal originality in finite element research. He along with Bruce Irons established the finite element on a generic mathematical basis rather then only a tool for stress analysis for continuum and showed that it could be applied to many branch of engineering like rock mechanics, heat mass transfer, fluid dynamics, geo-technical engineering and many other areas of engineering and science. His first book on this topic (Zienkiewicz 1970) is still considered a landmark contribution which has gone a long way to popularize the topic among the present generation of engineers who have worked and are still working on this subject around the world.

2.12.3 The basic philosophy

Since the development was first based on matrix method of structural analysis, we follow the same path to explain the basic philosophy. This we believe would also be easier for a civil engineer to understand who are new to this topic.

Shown in Figure 2.12.2 is an arbitrary shaped body with an external load for which we would like to know the stress and displacement. The relationship between the load and the displacement is given by

$$\{P\} = [K]\{\delta\} \tag{2.12.1}$$

where $\{P\}$ = external load vector; $[K]$ = stiffness matrix of the body and $\{\delta\}$ = displacement vector of the body.

It is apparent that it would be difficult to derive the stiffness matrix of this body as the shape of the body is arbitrary. Now let us look at Figure 2.12.3 carefully.

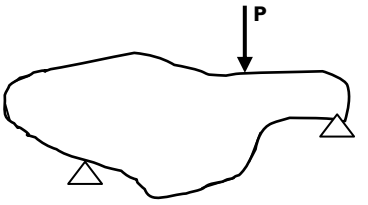


Figure 2.12.2 An arbitrary shaped body with external loads and supports.

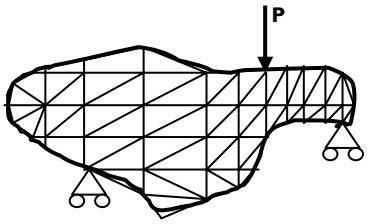


Figure 2.12.3 Arbitrary structure broken up into small finite shapes.

If we can break up the body into small parts of regular shape (could be triangle or quadrilateral) whose stiffness is known to us and if we assemble[38] the stiffness of all these elements in a manner such that it represents the body (could be approximately) then surely substituting it in the equation, $\{P\} = [K]\{\delta\}$, and we can have a solution

$$\{\delta\} = [K]^{-1}\{P\}. \tag{2.12.2}$$

This in essence is the basic philosophy of the FEM theory.

Does it look familiar to something?

Recall the problem of the area of circle we solved at the outset, now if you ponder over the matter it may be observed that both the philosophies are almost analogous.

In the circle problem, we presumed we do not know the area of the circle and approximated its value by summing the area of the triangle whose area is known to us. More is the number of triangular area we considered, the error reduced progressively. In FEM analysis also we will see that as we refine the mesh of elements taken the results converge towards an exact value.

We would like to re-emphasize at this point that FEM like finite difference method is also an approximate method. It can be shown that for a linear element finite element solution is exactly same as a central difference solution of the problem by using a finite difference technique. The accuracy of result (i.e. limiting the error to an acceptable level) depends on a number of factors like order of polynomial chosen to develop the element stiffness, refinement of mesh, using the appropriate finite element which correctly resembles the behavior of the structure, correct simulation of boundary condition etc.

2.12.4 Displacement based derivation of stiffness matrix

Before we enter the developers club it would be interesting to derive how stiffness matrix is developed for various elements in general term. We start with the

38 Here by the word assemblage we mean summing up all the stiffness in some sense so that it approximately represent the body.

displacement based formulation as this would be easier for a civil engineer to follow. The steps involved can be summarized as follows:

- For a particular element define displacement as a polynomial function expressed as $f = \alpha_1 + \alpha_2 x + \alpha_3 x^2 + \alpha_4 x^3 + \cdots\cdots \alpha_{n+1} x^n$. The shape functions should be chosen in such a fashion that number of constants $(\alpha_1, \alpha_2, \alpha_3 \ldots\ldots \alpha_{n+1}) =$ number of degrees of freedom for the element. Let this be expressed as $\{f\} = [M]\{\alpha\}$.
- Express the nodal parameters in terms of constants $\{\delta\} = [C]\{\alpha\}$. Here the nodal displacements and $[C]$ is obtained by introducing nodal co-ordinates in matrix $[M]$.
- Find the displacement polynomial constant relationship as $\{\alpha\} = [C]^{-1}\{\delta\}$ which gives

$$\{f\} = [M][C]^{-1}\{\delta\} \quad \text{or} \quad \{f\} = [N]\{\delta\} \tag{2.12.3}$$

  where $[N] = [M][C]^{-1}$ and is known as the interpolation shape function or simply shape function of the problem.
- Establish the strain displacement relationship. This is established by differentiating the shape function as appropriate to obtain

$$\{\varepsilon\} = [B]\{\delta\} \tag{2.12.4}$$

- Determine the stress-strain relationship as $\{\sigma\} = [D]\{\varepsilon\}$ which can then be expressed in terms of displacement as

$$\{\sigma\} = [D][B]\{\delta\}. \tag{2.12.5}$$

To obtain the stiffness matrix the easiest way is to impose an arbitrary virtual nodal displacement and to equate the internal and external work done by the various external force and internal stresses during that displacement.

Let such virtual displacement be expressed as $d\{\delta\}$ and this results in displacements and strain within the element equal to

$$d\{f\} = [N]\, d\{\delta\} \quad \text{and } d\{\varepsilon\} = [B]\, d\{\delta\}. \tag{2.12.6}$$

Now the work done by nodal force is equal to the sum of the products of the individual force components and corresponding displacement. Thus in matrix notation this can expressed as

$$W_e = d\{\delta\}^T\{P\},$$

where $W_e =$ external work done and $\{P\} =$ external load vectors.

The internal work done by the stress within the body is given by

$$W_i = \int d\{\varepsilon\}^T \{\sigma\}.dv \quad \text{or,} \quad W_i = \int d\{\delta\}^T [B]^T \{\sigma\} \cdot dv \tag{2.12.7}$$

Since, $\{\sigma\} = [D][B]\{\delta\}$, substituting the above we have

$$W_i = \int d\{\delta\}^T [B]^T [D][B]\{\delta\} \cdot dv \tag{2.12.8}$$

Since the internal and external work done must be equal we have, $W_e = W_i$ and

$$d\{\delta\}^T [P] = \int d\{\delta\}^T [B]^T [D]\ [B]\{\delta\} \cdot dv$$

$$\rightarrow \quad \{P\} = \int [B]^T [D]\ [B]\{\delta\} \cdot dv \tag{2.12.9}$$

Considering $\{P\} = [K]\{\delta\}$ where $[K]$ = stiffness matrix, we may write

$$[K]\{\delta\} = \int [B]^T [D][B]\{\delta\}\, dv$$

that finally results in

$$[K] = \int [B]^T [D][B] \cdot dv \tag{2.12.10}$$

We will now enter the developers club to see how the above formulation vide Equation 2.12.10 is used to derive element stiffness matrices of several finite element idealizations.

2.12.4.1 Element Stiffness Matrix of a 2D Beam Element

The beam element is strictly speaking a discrete element and not a continuum, as such cannot be theoretically termed as finite element. Nonetheless, we will derive the stiffness matrix based on the above theory to give you some mathematical background on how the above theory is applied to develop the element stiffness.

Let us consider a beam having degrees of freedom as shown in Figure 2.12.4. Since the total degrees of freedom is four we choose the displacement function as

$$f = \alpha_1 + \alpha_2 x + \alpha_3 x^2 + \alpha_4 x^3 \tag{2.12.11}$$

Now as $\{f\} = [M]\{\alpha\}$ we have

$$\{f\} = \langle 1 \quad x \quad x^2 \quad x^3 \rangle \langle \alpha_1 \quad \alpha_2 \quad \alpha_3 \quad \alpha_4 \rangle^T \tag{2.12.12}$$

Now, at $x = 0, \{f\} = \delta_1 = \alpha_1$ and again, at $x = L, \{f\} = \delta_2 = \alpha_1 + \alpha_2 L + \alpha_3 L^2 + \alpha_4 L^3$.

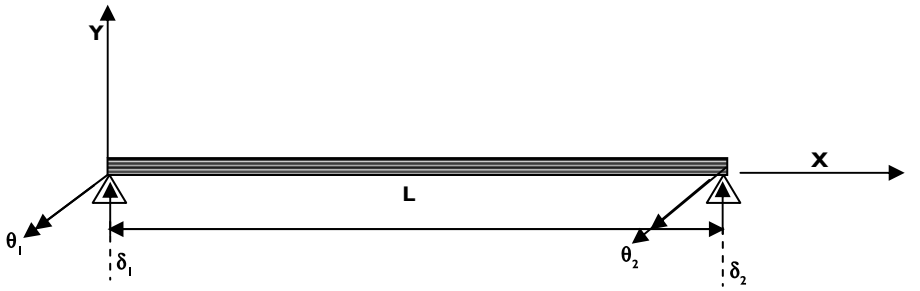


Figure 2.12.4 A beam element in 2D having two degrees of freedom per node.

At $x = 0$, $\frac{df}{dx} = \theta_1 = \alpha_2$ and at $x = L$, $\frac{df}{dx} = \theta_2 = \alpha_2 + 2\alpha_3 L + 3\,\alpha_4 L^2$.

The above can be expressed in matrix form as

$$\{f\} = \begin{bmatrix} 1 & 0 & 0 & 0 \\ 0 & 1 & 0 & 0 \\ 1 & L & L^2 & L^3 \\ 0 & 1 & 2L & 3L^2 \end{bmatrix} \begin{Bmatrix} \alpha_1 \\ \alpha_2 \\ \alpha_3 \\ \alpha_4 \end{Bmatrix} = \begin{Bmatrix} \delta_1 \\ \theta_1 \\ \delta_2 \\ \theta_2 \end{Bmatrix} \rightarrow \begin{Bmatrix} \alpha_1 \\ \alpha_2 \\ \alpha_3 \\ \alpha_4 \end{Bmatrix} = \begin{bmatrix} 1 & 0 & 0 & 0 \\ 0 & 1 & 0 & 0 \\ \frac{-3}{L^2} & \frac{-2}{L} & \frac{3}{L^2} & \frac{-1}{L} \\ \frac{2}{L^3} & \frac{1}{L^2} & \frac{-2}{L^3} & \frac{1}{L^2} \end{bmatrix} \begin{Bmatrix} \delta_1 \\ \theta_1 \\ \delta_2 \\ \theta_2 \end{Bmatrix}$$

i.e. $\{\alpha\} = [C]^{-1}\{\delta\}$ (2.12.13)

Considering $\{f\} = [M][C]^{-1}\{\delta\}$ we have

$$\{f\} = \left\langle 1 \quad x \quad x^2 \quad x^3 \right\rangle \begin{bmatrix} 1 & 0 & 0 & 0 \\ 0 & 1 & 0 & 0 \\ \frac{-3}{L^2} & \frac{-2}{L} & \frac{3}{L^2} & \frac{-1}{L} \\ \frac{2}{L^3} & \frac{1}{L^2} & \frac{-2}{L^3} & \frac{1}{L^2} \end{bmatrix} \begin{Bmatrix} \delta_1 \\ \theta_1 \\ \delta_2 \\ \theta_2 \end{Bmatrix}$$

$\rightarrow \quad \{f\} = [N][\delta]$ (2.12.14)

where $[N] = \langle 1 \quad x \quad x^2 \quad x^3 \rangle \begin{bmatrix} 1 & 0 & 0 & 0 \\ 0 & 1 & 0 & 0 \\ \frac{-3}{L^2} & \frac{-2}{L} & \frac{3}{L^2} & \frac{-1}{L} \\ \frac{2}{L^3} & \frac{1}{L^2} & \frac{-2}{L^3} & \frac{1}{L^2} \end{bmatrix}$

$$\rightarrow \quad [N] = \left\langle \left(1 - \frac{3x^2}{L^2} + \frac{2x^3}{L^3}\right)\left(x - \frac{2x^2}{L} + \frac{x^3}{L^2}\right)\left(\frac{3x^2}{L^2} - \frac{2x^3}{L^3}\right)\left(\frac{-x^2}{L} + \frac{x^3}{L^3}\right)\right\rangle$$

$$\text{Thus} \quad \{f\} = \left\langle \left(1 - \frac{3x^2}{L^2} + \frac{2x^3}{L^3}\right)\left(x - \frac{2x^2}{L} + \frac{x^3}{L^2}\right)\left(\frac{3x^2}{L^2} - \frac{2x^3}{L^3}\right)\left(\frac{-x^2}{L} + \frac{x^3}{L^3}\right)\right\rangle \begin{Bmatrix} \delta_1 \\ \theta_1 \\ \delta_2 \\ \theta_2 \end{Bmatrix} \tag{2.12.15}$$

For a beam element we know that $EI\frac{d^2f}{dx^2} = -M_x$ which is same as $\{\sigma\} = [D]\{\varepsilon\}$, where $\{\sigma\} = M_x, [D] = EI$ and $\{\varepsilon\} = \frac{d^2f}{dx^2} = [B]\{\delta\}$.

$$\text{Thus} \quad [\sigma] = EI\left\langle \left(\frac{6}{L^2} - \frac{12x}{L^3}\right)\left(\frac{4}{L} - \frac{6x}{L^2}\right)\left(\frac{-6}{L^2} + \frac{12x}{L^3}\right)\left(\frac{2}{L} - \frac{6x}{L^2}\right)\right\rangle \langle \delta_1\ \theta_1\ \delta_2\ \theta_2 \rangle^T$$

which gives

$$[B] = \left\langle \left(\frac{6}{L^2} - \frac{12x}{L^3}\right)\left(\frac{4}{L} - \frac{6x}{L^2}\right)\left(\frac{-6}{L^2} + \frac{12x}{L^3}\right)\left(\frac{2}{L} - \frac{6x}{L^2}\right)\right\rangle \tag{2.12.16}$$

as $[K] = \int [B]^T [D][B] \cdot dv$ for beam element we have $[K] = EI \int_0^L [B]^T [B]\, dx$

$$[K] = EI \begin{bmatrix} \frac{12}{L^3} & \frac{6}{L^2} & -\frac{12}{L^3} & \frac{6}{L^2} \\ \frac{6}{L^2} & \frac{4}{L} & -\frac{6}{L^2} & \frac{2}{L} \\ -\frac{12}{L^3} & -\frac{6}{L^2} & \frac{12}{L^3} & -\frac{6}{L^2} \\ \frac{6}{L^2} & \frac{2}{L} & -\frac{6}{L^2} & \frac{4}{L} \end{bmatrix} \tag{2.12.17}$$

which is the element stiffness matrix for the beam.

It will be observed that in this case the FEM approximation converges to the exact value as obtained usually by classical slope deflection method.

2.12.4.2 *Element stiffness matrix for 2D triangular element*

This is the first element that was put to use for analysis of continuum by FEM. As stated earlier, was developed by Turner et al. 1956 and is still in use. Though it has been found that rectangular and quadrilateral 2D elements developed subsequently gives superior results.

Prior to deriving the stiffness matrix of this triangular element we pose a simple problem to you for some clarification. Recall the simply supported beam in Figure 2.10.5, where we derived the deflection having udl of w kN/m.

Based on solution of differential equation we have,

$$y_{\max} = \frac{5wL^4}{384EI}, \quad M_{\max} = \frac{wL^2}{8}$$

and maximum stress at center span could be expressed as

$$\sigma_{\max} = \frac{3wL^2}{4BD^2},$$

where $B =$ width of the beam and D the overall depth.

Suppose, the beam under question looks as shown in Figure 2.12.5.

Now, are the answers we derived earlier are correct?

The reasons that the solution derived earlier may not be correct can be summarized as follows

- The cut-out (presumed reasonably large) will reduce the moment of inertia I considerably for which the deflection expected would be larger than a beam without any cutout.
- The beam based on dimension looks to be neither a prismatic beam nor a deep beam but something intermediate as such the differential expression $EI\frac{d^2y}{dx^2} = -M_x$ may not be valid in this case.
- The stress around the opening would be significantly larger than $\sigma_{\max} = (3wL^2)/(4BD^2)$ and cannot be ignored, for if this is too high cracks may be generated around the corners.

A simple problem, yet the solution is not easy. If you ponder further you will realize that neither there is a closed form analytical solution to this nor it can be solved by finite difference too!

Based on FEM method the problem may be solved as shown in Figure 2.12.6.

We break up the beam constituting of 65 nodes and 98 triangular elements (the node and element numbers are not shown picture clarity)[39]. Knowing the element stiffness matrix of a individual triangular element we assemble it to form the global stiffness of the above beam and then find out the displacement from the equation $\{P\} = [K]\{\delta\}$ and subsequently find out the stress developed. For problems such as these, finite element method is almost unrivalled.

Now, we will derive the element stiffness matrix of this triangular element under plane stress condition.

39 The model shown is only a conceptual one to give you an idea on how it should be solved and may not necessarily be a correct model in terms of number of elements and nodes taken to arrive at a solution with desired accuracy.

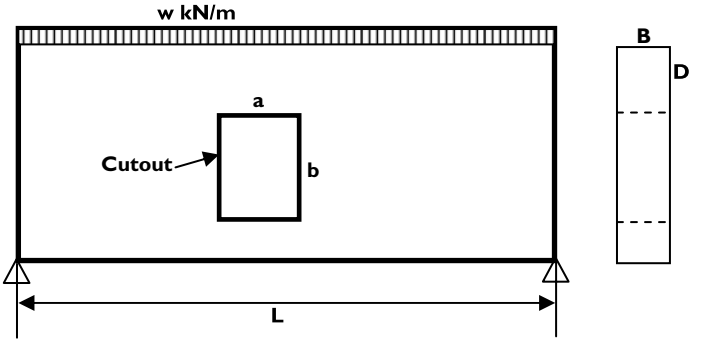


Figure 2.12.5 Beam with cutout in center span (scaled proportionally).

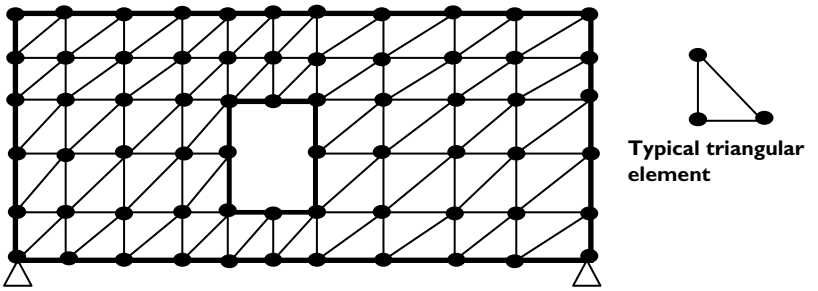


Figure 2.12.6 Finite element discretisation of beam with triangular elements.

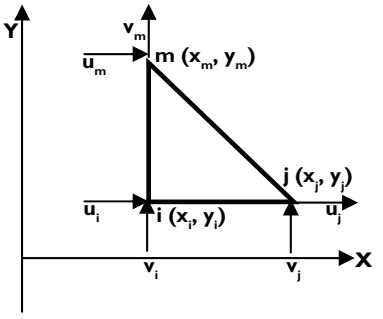


Figure 2.12.7 2D-triangular element with nodal degrees of freedom.

Shown in Figure 2.12.7 is a triangular plane stress element having nodes i, j and m. The co-ordinates of each node can be expressed as $(x_i, y_i), (x_j, y_j)$ and (x_m, y_m) respectively. Let the displacements at each node be expressed as $(u_i, v_i), (u_j, v_j)$, and (u_m, v_m).

The polynomial of the shape function can be chosen for this case as

$$u = \alpha_1 + \alpha_2 x + \alpha_3 y \quad \text{and} \quad v = \alpha_4 + \alpha_5 x + \alpha_6 y. \tag{2.12.18}$$

The displacement function can be expressed as

$$\{f\} = \begin{Bmatrix} u \\ v \end{Bmatrix} = \begin{bmatrix} 1 & x & y & 0 & 0 & 0 \\ 0 & 0 & 0 & 1 & x & y \end{bmatrix} \langle \alpha_1\ \alpha_2\ \alpha_3\ \alpha_4\ \alpha_5\ \alpha_6 \rangle^T$$

$$\rightarrow \quad \{f\} = [M]\{\alpha\} \tag{2.12.19}$$

With respect to the nodal co-ordinates, displacements can be expressed as

$$u_i = \alpha_1 + \alpha_2 x_i + \alpha_3 y_i; \quad u_j = \alpha_1 + \alpha_2 x_j + \alpha_3 y_j; \quad u_m = \alpha_1 + \alpha_2 x_m + \alpha_3 y_m. \tag{2.12.20}$$

Above in matrix notation can be expressed as

$$\begin{bmatrix} 1 & x_i & y_i \\ 1 & x_j & y_j \\ 1 & x_m & y_m \end{bmatrix} \begin{Bmatrix} \alpha_1 \\ \alpha_2 \\ \alpha_3 \end{Bmatrix} = \begin{Bmatrix} u_i \\ u_j \\ u_m \end{Bmatrix} \tag{2.12.21}$$

Inversion of the above gives

$$\begin{Bmatrix} \alpha_1 \\ \alpha_2 \\ \alpha_3 \end{Bmatrix} = \frac{1}{2\Delta} \begin{bmatrix} x_j y_m - x_m y_j & x_m y_i - x_i y_m & x_i y_j - x_j y_i \\ y_j - y_m & y_m - y_i & y_i - y_j \\ x_m - x_j & x_i - x_m & x_j - x_i \end{bmatrix} \begin{Bmatrix} u_i \\ u_j \\ u_m \end{Bmatrix} \quad \rightarrow \quad \{\alpha\} = [C]^{-1}\{\delta\} \tag{2.12.22}$$

where $\Delta = \frac{1}{2} \begin{vmatrix} 1 & x_i & y_i \\ 1 & x_j & y_j \\ 1 & x_m & y_m \end{vmatrix}$ is the area of the triangle.

Similarly, $\begin{bmatrix} 1 & x_i & y_i \\ 1 & x_j & y_j \\ 1 & x_m & y_m \end{bmatrix} \begin{Bmatrix} \alpha_4 \\ \alpha_5 \\ \alpha_6 \end{Bmatrix} = \begin{Bmatrix} v_i \\ v_j \\ v_m \end{Bmatrix}$

i.e. $\begin{Bmatrix} \alpha_4 \\ \alpha_5 \\ \alpha_6 \end{Bmatrix} = \frac{1}{2\Delta} \begin{bmatrix} x_j y_m - x_m y_j & x_m y_i - x_i y_m & x_i y_j - x_j y_i \\ y_j - y_m & y_m - y_i & y_i - y_j \\ x_m - x_j & x_i - x_m & x_j - x_i \end{bmatrix} \begin{Bmatrix} v_i \\ v_j \\ v_m \end{Bmatrix}$

The above can be expressed in a simplified form as

$$\begin{Bmatrix} \alpha_1 \\ \alpha_2 \\ \alpha_3 \end{Bmatrix} = \frac{1}{2\Delta} \begin{bmatrix} a_i & a_j & a_m \\ b_i & b_j & b_m \\ c_i & c_j & c_m \end{bmatrix} \begin{Bmatrix} u_i \\ u_j \\ u_m \end{Bmatrix} \quad \text{and} \quad \begin{Bmatrix} \alpha_4 \\ \alpha_5 \\ \alpha_6 \end{Bmatrix} = \frac{1}{2\Delta} \begin{bmatrix} a_i & a_j & a_m \\ b_i & b_j & b_m \\ c_i & c_j & c_m \end{bmatrix} \begin{Bmatrix} v_i \\ v_j \\ v_m \end{Bmatrix} \tag{2.12.23}$$

where $a_i = x_j y_m - x_m y_j, b_i = y_j - y_m, c_i = x_m - x_j$.

The polynomial constants for the full triangle can be expressed as

$$\begin{Bmatrix}\alpha_1\\ \alpha_2\\ \alpha_3\\ \alpha_4\\ \alpha_5\\ \alpha_6\end{Bmatrix} = \frac{1}{2\Delta}\begin{bmatrix} a_i & 0 & a_j & 0 & a_m & 0\\ b_i & 0 & b_j & 0 & b_m & 0\\ c_i & 0 & c_j & 0 & c_m & 0\\ 0 & a_i & 0 & a_j & 0 & a_m\\ 0 & b_i & 0 & b_j & 0 & b_m\\ 0 & c_i & 0 & c_j & 0 & c_m\end{bmatrix}\begin{Bmatrix}u_i\\ v_i\\ u_j\\ v_j\\ u_m\\ v_m\end{Bmatrix},$$

where $[M] = \begin{bmatrix}1 & x & y & 0 & 0 & 0\\ 0 & 0 & 0 & 1 & x & y\end{bmatrix}$.

Considering $[N] = [M]\,[C]^{-1}$, we have

$$[N] = \frac{1}{2\Delta}\begin{bmatrix}1 & x & y & 0 & 0 & 0\\ 0 & 0 & 0 & 1 & x & y\end{bmatrix}\begin{bmatrix} a_i & 0 & a_j & 0 & a_m & 0\\ b_i & 0 & b_j & 0 & b_m & 0\\ c_i & 0 & c_j & 0 & c_m & 0\\ 0 & a_i & 0 & a_j & 0 & a_m\\ 0 & b_i & 0 & b_j & 0 & b_m\\ 0 & c_i & 0 & c_j & 0 & c_m\end{bmatrix}$$

$$[N] = \frac{1}{2\Delta}\times\begin{bmatrix}d_{11} & 0 & d_{22} & 0 & d_{33} & 0\\ 0 & d_{11} & 0 & d_{22} & 0 & d_{33}\end{bmatrix} \tag{2.12.24}$$

in which,

$$d_{11} = a_i + b_i x + c_i y;\quad d_{22} = a_j + b_j x + c_j y;\quad d_{33} = a_m + b_m x + c_m y$$

The strain matrix for the triangle is given by

$$\{\varepsilon\} = \begin{Bmatrix}\varepsilon_x\\ \varepsilon_y\\ \gamma_{xy}\end{Bmatrix} = \begin{Bmatrix}\dfrac{\partial u}{\partial x}\\ \dfrac{\partial v}{\partial y}\\ \dfrac{\partial u}{\partial y}+\dfrac{\partial v}{\partial x}\end{Bmatrix} = \frac{1}{2\Delta}\begin{bmatrix} b_i & 0 & b_j & 0 & b_m & 0\\ 0 & c_i & 0 & c_j & 0 & c_m\\ c_i & b_i & c_j & b_j & c_m & b_m\end{bmatrix}\begin{Bmatrix}u_i\\ v_i\\ u_j\\ v_j\\ u_m\\ v_m\end{Bmatrix} = [B]\ \{\delta\} \tag{2.12.25}$$

which gives

$$[B] = \frac{1}{2\Delta}\begin{bmatrix} b_i & 0 & b_j & 0 & b_m & 0\\ 0 & c_i & 0 & c_j & 0 & c_m\\ c_i & b_i & c_j & b_j & c_m & b_m\end{bmatrix} \tag{2.12.26}$$

For plane stress case the elasticity matrix (Timoshenko and Goodier 1970) may be written as

$$[D] = \frac{E}{1-\nu^2}\begin{bmatrix} 1 & \nu & 0 \\ \nu & 1 & 0 \\ 0 & 0 & \dfrac{1-\nu}{2} \end{bmatrix} \tag{2.12.27}$$

The stiffness matrix, which is given by $[K] = \int [B]^T [D][B] dv$, for this particular case is expressed as simply expressed as $[K] = [B]^T [D] \cdot [B] \cdot \Delta \cdot t$, since it is independent of x and y; t is thickness in the z-direction.

The stiffness matrix can be finally expressed as

$$[K] = \frac{t}{4\Delta}\begin{bmatrix} b_i & 0 & c_i \\ 0 & c_i & b_i \\ b_j & 0 & c_j \\ 0 & c_j & b_j \\ b_m & 0 & c_m \\ 0 & c_m & b_m \end{bmatrix}\begin{bmatrix} D_1 & D_1D_2 & 0 \\ D_1D_2 & D_1 & 0 \\ 0 & 0 & D_{12} \end{bmatrix}\begin{bmatrix} b_i & 0 & b_j & 0 & b_m & 0 \\ 0 & c_i & 0 & c_j & 0 & c_m \\ c_i & b_i & c_j & b_j & c_m & b_m \end{bmatrix}$$

in which $D_1 = E/(1-\nu^2), D_2 = \nu$ and $D_{12} = D_1(1-D_2)/2$.

$$\text{or,} \quad [K] = \frac{t}{4\Delta}\begin{bmatrix} b_i & 0 & c_i \\ 0 & c_i & b_i \\ b_j & 0 & c_j \\ 0 & c_j & b_j \\ b_m & 0 & c_m \\ 0 & c_m & b_m \end{bmatrix}\begin{bmatrix} D_1 b_i & D_1D_2 c_i & D_1 b_j & D_1D_2 c_j & D_1 b_m & D_1D_2 c_m \\ D_1D_2 b_i & D_1 c_i & D_1D_2 b_j & D_1 c_j & D_1D_2 b_m & D_1 c_m \\ D_{12} c_i & D_{12} b_i & D_{12} c_j & D_{12} b_j & D_{12} c_m & D_{12} b_m \end{bmatrix} \tag{2.12.28}$$

or $[K] = \dfrac{t}{4\Delta}$

$D_1 b_i^2 + D_{12} c_i^2$					
$D_1D_2 b_i c_i + D_{12} b_i c_i$	$D_1 c_i^2 + D_{12} b_i^2$		Symmetric		
$D_1 b_i b_j + D_{12} c_i c_j$	$D_1D_2 b_i c_i + D_{12} b_i c_j$	$D_1 b_j^2 + D_{12} c_j^2$			
$D_1D_2 b_i c_j + D_{12} b_j c_i$	$D_1 c_i c_j + D_{12} b_i b_j$	$D_1D_2 b_j c_j + D_{12} b_j c_j$	$D_1 c_j^2 + D_{12} b_j^2$		
$D_1 b_i b_m + D_{12} c_i c_m$	$D_1D_2 b_m c_i + D_{12} b_i c_m$	$D_1 b_j b_m + D_{12} c_j c_m$	$D_1D_2 b_m c_j + D_{12} b_j c_m$	$D_1 b_m^2 + D_{12} c_m^2$	
$D_1D_2 b_i c_m + D_{12} b_m c_i$	$D_1 c_i c_m + D_{12} b_i b_m$	$D_1D_2 b_j c_m + D_{12} b_m c_j$	$D_1 c_j c_m + D_{12} b_j b_m$	$D_1D_2 b_m c_m + D_{12} b_m c_m$	$D_1 c_m^2 + D_{12} b_m^2$

2.12.5 Plane strain CST element

The steps involved in deriving the element stiffnes matrix is identical to the plane stress case as derived above(including the shape functions). The only difference is that the $[D]$ matrix in the equation $[K] = \int [B]^T [D] [B] \, dv$ is different.

For plane strain condition the $[D]$ matrix is given by

$$[D] = \frac{E(1-\nu)}{(1+\nu)(1-2\nu)} \begin{bmatrix} 1 & \frac{\nu}{1-\nu} & 0 \\ \frac{\nu}{1-\nu} & 1 & 0 \\ 0 & 0 & \frac{1-2\nu}{2(1-\nu)} \end{bmatrix},$$

this can be further expresssed as

$$[D] = \begin{bmatrix} D_1 & \text{Symmetrical} & \\ D_1 D_2 & D_1 & \\ 0 & 0 & D_{12} \end{bmatrix} \tag{2.12.29}$$

where, $D_1 = \frac{E(1-\nu)}{(1+\nu)(1-2\nu)}, D_2 = \frac{\nu}{(1-\nu)}, D_{12} = \frac{D_1(1-D_2)}{2}$,

This would give the same element stiffness matrix as derived above except that the matrix $[D]$ as mentioned herein is different.

2.12.6 Why constant strain and how effective is the element?

We have shown while deriving the element stiffness that the $[B]$ matrix vis a vis the strain matrix remains unchanged with repsect to x and y coordinate. In other words, irrespective of the orientation of the x and y coordinate the strain remains in-variant. It is for this property the element is named as constant strain triangle (CST).

In todays scenario, where in a commercially available software the option of various types of finite elements available in its library is multiple, many analyst frown on this element construing it as an inefficent element. For though the element is found to give reasonable result with displacements, their convergence in terms of stress value is poor. The results are also meaningful only when the mesh is sufficently refined[40]. Moreovoer since the shape of the polynomial is linear it does not have the capability to simulate rotation (d^2y/dx^2) and is found to give higher stiffnes then it actually should be.

If the material in use is nearly incompressible[41], the stress calculation can create lot of problems in the results. Nevertheless when the continuum consists of corners or one wants to change from one shape to the other where high stress gradient is not prevalent, the element still has a lot of use.

40 Meaning more computation, more storage data, and more inputs.
41 That is Poisson's ratio approaches 0.5.

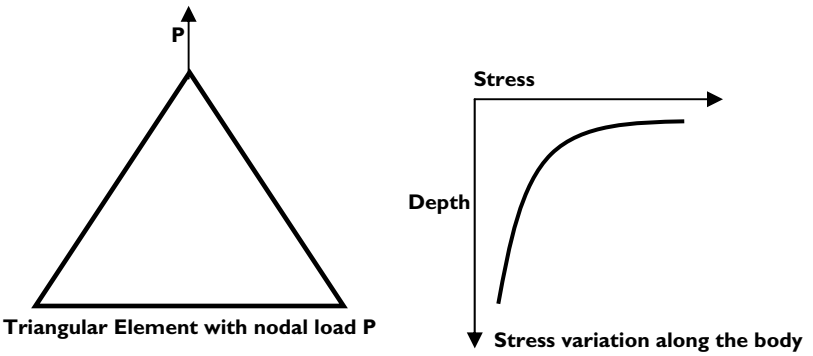


Figure 2.12.8 CST-element with variation of stress under point load.

2.12.7 Why convergence improve with refined meshes

We had mentioned ealier that output results improve with refinement of elements. The reason for the same can well be derived from engineering intuition rather then a formal mathematical proof. Shown in Figure 2.12.8 is a triangular element with a nodal load *P*. Theoretically speaking this is a point load and the point at which it is acting has an infinitesimally small area tending to zero giving infinite stress at that point.

As we progressively move inside the triangle the cross sectional area increases and after a certain distance stress vis a vis strain becomes finite. The variation of stress is as shown above.

Now suppose we progressively decrease the area of the triangle we can achieve a state that when the traingle is sufficiently small the strain within the body (and stress) becomes constant and truly represents a state of constant strain. Thus it is apparent that as the meshes are refined the triangle area diminish and tends towards a true constant strain for which the results improve due to convergence.

2.12.8 The Constitutional laws which bound the developers

Before we proceed further to derive element stiffness matrix of other elements we would like to explain a few things and rules first. This we believe would make the subsequent understanding better.

While discussing the CST element we came up with comments like "Analysts construe it is an inefficient element" or "the stress convergence is poor", this might make you wonder that if there is something called good or bad elements, or how do we know which results tend to converge and which do not? *Very pertinent questions, which we believe, you should always ask yourself when carrying out a finite element analysis (FEA).*

The finite element library available in the market is like a huge super bazaar, where choices are many (Kardestuncer and Norie 1987). Each of these elements available in the market has its own distinct merits and a few limitations too. There are indeed

elements available which are excellent, good, bad and even temperamental! (i.e. it gives very good results for certain geometry while produces poor results for others). *So, before putting an element into use, knowing its strength and weaknesses is strongly advisable.*

In order to assess this (what makes an element good or bad...) one needs to know a few basic rules that go into the development of finite elements.

2.12.9 The rule of polynomial – the entry rule to developers club

While generating the element stiffness matrix of the 2*D* beam and CST element we had shown that the starting point is developing a polynomial shape function.

While developing the beam element we had also stated that – *number of coefficients* $(\alpha_1, \alpha_2, \alpha_3, \ldots\ldots \alpha_v)$ *in a polynomial function must be equal to the total degrees of freedom for each element.*

Stop! and ponder for a while – *the above is actually a rule*. From where did this rule come? Is it by trial and error, intuition or is there a logical basis to it?

Recall the beam equation $EI\frac{d^2y}{dx^2} = -M_x$, and double differentiation of the above gives,

$$EI\frac{d^4y}{dx^4} = w, \tag{2.12.30}$$

where, w is the external load acting on the beam.

For no load acting on the beam, the above equation can be expressed as

$$\frac{d^4y}{dx^4} = 0 \tag{2.12.31}$$

From which we get on successive integration

$$y = \frac{C_1}{6}x^3 + \frac{C_2}{2}x^2 + C_3x + C_4, \tag{2.12.32}$$

where C_1, C_2, C_3, and C_4 are integration constants and are functions of nodal degrees of freedom for each element.

The above thus in generic term can be expressed as

$$y = \alpha_1 + \alpha_2 x + \alpha_3 x^2 + \alpha_4 x^3 \tag{2.12.33}$$

Thus it is observed that the above shape function equation correctly represents the degrees of freedoms for each element – and this is the logic from where the rule came into being[42].

42 Posing this query in an interview we have also heard answer to this as it is Zienkeiwics's first law!

Based on above for a line element having n degrees of freedom can be expressed in generalized co-ordinate as

$$u = \alpha_1 + \alpha_2 x + \alpha_3 x^2 + \alpha_4 x^3 + \cdots\cdots + \alpha_n x^{n-1} \tag{2.12.34}$$

Here greater the number of terms be included in the shape function more closer would be the result to the exact solution.

The above in matrix notation can be expressed as

$$\{u\} = [M]\{\alpha\} \tag{2.12.35}$$

where $[M] = \langle 1 \quad x \quad x^2 \quad x^3 \ldots\ldots x^{n-1} \rangle$ and $\{\alpha\}^T = \langle \alpha_1 \quad \alpha_2 \quad \alpha_3 \quad \alpha_4 \ldots\ldots \alpha_n \rangle$.

For two-dimensional element in generalized coordinate the shape function can be expressed as

$$u(x,y) = \alpha_1 + \alpha_2 x + \alpha_3 y + \alpha_4 x^2 + \alpha_5 xy + \alpha_6 y^2 \cdots\cdots + \alpha_p y^n$$

$$v(x,y) = \alpha_{p+1} + \alpha_{p+2} x + \alpha_{p+3} y + \alpha_{p+4} x^2 + \alpha_{p+5} xy + \alpha_{p+6} y^2 \cdots\cdots + \alpha_{2p} y^n$$

$$\text{and} \quad p = \sum_{i=1}^{n+1} i \tag{2.12.36}$$

The above in matrix notation can be expressed as

$$\{\delta_{x,y}\} = \begin{Bmatrix} u(x,y) \\ v(x,y) \end{Bmatrix} = [M]\{\alpha\} = \begin{bmatrix} \{M_1\}^T & \{0\}^T \\ \{0\}^T & \{M_1\}^T \end{bmatrix} \{\alpha\} \tag{2.12.37}$$

where $[M] = \langle 1 \quad x \quad y \quad x^2 \quad xy \ldots\ldots y^n \rangle; \{\alpha\}^T = \langle \alpha_1 \quad \alpha_2 \quad \alpha_3 \quad \alpha_4 \ldots\ldots \alpha_{2p} \rangle$.

Similarly, a three dimensional displacement function in generalized coordinate of nth order is given by

$$u(x,y,z) = \alpha_1 + \alpha_2 x + \alpha_3 y + \alpha_4 z + \alpha_5 xz + \cdots\cdots + \alpha_p z^n$$

$$v(x,y,z) = \alpha_{p+1} + \alpha_{p+2} x + \alpha_{p+3} y + \alpha_{p+4} z + \alpha_{p+5} xz + \cdots\cdots + \alpha_{2p} z^n$$

$$w(x,y,z) = \alpha_{2p+1} + \alpha_{2p+2} x + \alpha_{2p+3} y + \alpha_{2p+4} z + \alpha_{2p+5} xz + \cdots\cdots + \alpha_{3p} z^n \tag{2.12.38}$$

where $p = \sum_{i=1}^{n+1} i\,(n+2-i)$ and u, v, and w are the displacements along x, y and z directions.

Each of the above polynomial can be truncated to any degrees of freedom to give linear, bilinear quadratic … or higher order elements. For the CST element derived earlier we assumed the displacement as linear thus we chose the shape function as

$$u(x,y) = \alpha_1 + \alpha_2 x + \alpha_3 y \quad \text{and} \quad v(x,y) = \alpha_4 + \alpha_5 x + \alpha_6 y \tag{2.12.39}$$

If the shape function is assumed bilinear we can choose the polynomial function as

$$u(x,y) = \alpha_1 + \alpha_2 x + \alpha_3 y + \alpha_4 xy \quad \text{and} \quad v(x,y) = \alpha_5 + \alpha_6 x + \alpha_7 y + \alpha_8 xy \tag{2.12.40}$$

For a quadratic model we can write this as

$$\begin{aligned} u(x,y) &= \alpha_1 + \alpha_2 x + \alpha_3 y + \alpha_4 x^2 + \alpha_5 xy + \alpha_6 y^2 \\ v(x,y) &= \alpha_7 + \alpha_8 x + \alpha_9 y + \alpha_{10} x^2 + \alpha_{11} xy + \alpha_{12} y^2 \end{aligned} \tag{2.12.41}$$

and so on.....

2.12.10 How do we select the polynomial function correctly?

In the previous section we have given the generic form of shape functions in terms of generalized coordinate. This might tempt you to join the developers club and formulate a finite element of your own-just go ahead and do it[43].

However, for doing so the first criterion is to select the polynomial function in a fashion that it correctly predicts the behavior that you intend it to exhibit[44].

The first condition to this is to select the polynomial in such a fashion that it should be independent of the orientation of the local co-ordinate system. This property is otherwise known as *geometrical or spatial isotropy*.

This is usually achieved by using the Pascal hierarchical triangle and especially for two and three dimensional element it is to be ensured that the terms are chosen in such a fashion that the terms are not skewed towards one particular coordinate but has a balance in the expression. The 2D Pascal hierarchical triangle is a shown Figure 2.12.9.

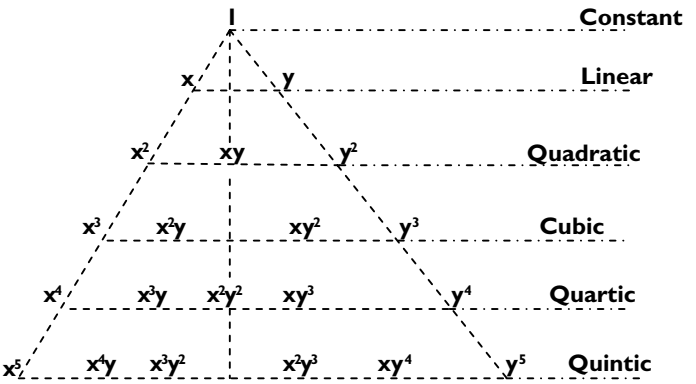


Figure 2.12.9 Pascal hierarchical triangle for 2D finite elements.

43 However while developing the same just make sure that it is not already available in the market-no point in re-inventing the wheel.

44 If this basic condition is not satisfied be sure that the results will put you in lot of problems.

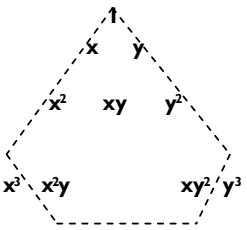


Figure 2.12.9a Pascal triangle for 2D elements.

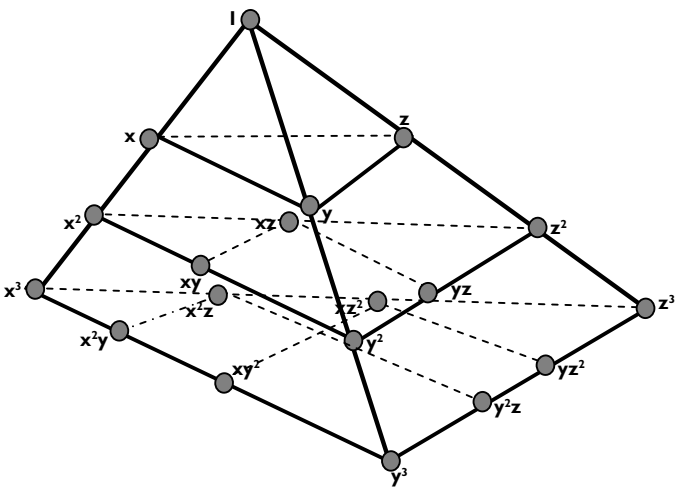


Figure 2.12.10 Pascal pyramid for 3D finite elements.

Thus for quadratic element the polynomial function shall be based on Figure 2.12.9a.

For three dimensional elements similarly we derive the polynomials based on pascal pyramid as given in Figure 2.12.10.

2.12.11 The law of convergence – the three commandments

We had stated at the outset that FEM is an approximate analysis where by there could be some error in the solution. This error is minimized by increasing the number of elements, when the result tend to converge to an exact value.

In many cases the stiffness matrix derived based on displacement formulation gives lower deflection than an exact solution (i.e. the stiffness derived is higher than the actual stiffness of the structure). As the finite element meshes are refined the approximate displacement approaches the exact solution as qualitatively shown in Figure 2.12.11[45].

45 This also known as monotonic convergence.

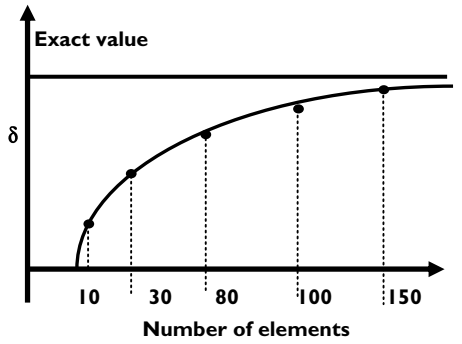


Figure 2.12.11 Monotonic convergence with increase in number of elements.

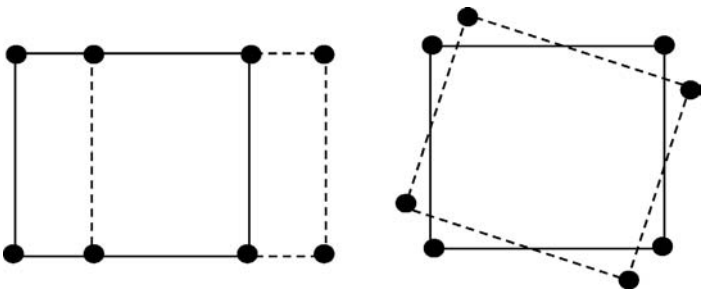


Figure 2.12.12 Rigid body deformation of a rectangular element in translational and rotational mode.

In order to ensure that the element do follow this behavior of monotonic convergence the following three laws must be conformed to.

1 *The displacement function must be continuous within an element and also must be compatible with adjacent element.*

The continuity of the function is basically satisfied by the chosen polynomial function which is inherently continuous, second condition implies that at common node of two elements the displacement must be same, in other words they should not deform without causing any openings, discontinuities or overlaps.

2 *The displacement modes must include rigid body mode of the element.*

A rigid body mode as we know is the most fundamental deformation an element can undergo. In this case the body moves physically without undergoing any stress or strain.

It is apparent from Figure 2.12.12 that all nodes in rigid body mode experience same displacement. One such combination should occur for both translation and rotation for an element.

For instance for the beam and CST element α_1 represent the rigid body displacement.

3 *The displacement must include a constant strain state of the element.*

The above law means that there should exist at least one mode for each of the combinations where all the points within the element can undergo a state of constant strain.

We had already explained earlier that as the mesh get finer and finer i.e as the elements approach an infinitesimal size, the strain approach a constant state and if this condition is not satisfied the results will not converge to a correct solution.

For the CST element the terms $\alpha_2 x$ and $\alpha_3 y$ represents this condition since

$$\varepsilon_x = \frac{\partial u}{\partial x} = \alpha_2 \quad \text{and} \quad \varepsilon_y = \frac{\partial v}{\partial y} = \alpha_3 \text{ are constants.}$$

In finite element procedure elements which satisfies the first law are called *compatible or conforming elements* while elements which obeys law (2) and (3) are called *complete elements*.

Generally an element stiffness matrix developed must be complete and conforming to converge to a correct result as meshes are progressively refined.

2.12.12 Non-conforming elements an exception to the law

Like all law have an exception[46] there is also an exception to the laws as posed above. Usually conforming elements have higher stiffness than the actual structure and deflection converges as a lower bound (Figure 2.12.11).

To circumvent this problem, elements have been developed where additional polynomial terms are taken beyond the conforming limit which makes it more flexible and for certain problems gives much better results even with a coarser mesh. Such type of elements are called the non-conforming elements as it violates the law(1) as described previously. This element gives great computational advantage over conforming elements where significant refinement are required especially in areas where there is a high stress gradient.

One must however be careful with such elements for at times their values become dependent on Poisson's ratio and gives poor result if the meshes undergo high distortion. Finally the bounded nature of the convergence is lost.

Inspite of the above demerits Non-conforming elements have been successfully used in many practical problems with excellents results. We will discuss more about this element at a later stage.

2.12.13 Natural coordinates: the gateway to numerical analysis through computer

We had derived earlier that the element stiffness matrix based on FEM is expressed as

$$[K] = \int [B]^T [D][B] dv. \tag{2.12.42}$$

46 Except possibly the natural law of creation where all living things born must one day perish without exception...

While deriving the beam and CST elements we had hand computed the stiffness matrix where all the matrix inversions and integrations were carried out manually and explicitly.

For many higher order elements and elements based on iso parametric formulation, such explicit integration or matrix inversion is not feasible, since the procedure becomes quite tedious and laborious.

Forgiving the inherent laziness prevalent in human nature and also considering, that computers are at hand we usually let computer carry out such inversions and integrations.

Since computer cannot carry out the integration $\int_0^{\xi} f(x)dx$ we usually resort to numerical integration to arrive at a solution to such integrals. It is in this case transferring the functions from generalized coordinate to natural co-ordinates gives us significant computational advantage and has great application in FEM[47].

To elaborate this further let us take an integral

$$I = \int_0^H \int_0^b \left[\sin \frac{\pi x}{2H} \sin \frac{3\pi x}{2H} + \cos \frac{\pi y}{2b} \cos \frac{3\pi y}{2b} \right] dxdy \quad \text{which can be expressed as}$$

$$\rightarrow \quad I = b \int_0^H \sin \frac{\pi x}{2H} \sin \frac{3\pi x}{2H} dx + H \int_0^b \cos \frac{\pi y}{2b} \cos \frac{3\pi y}{2b} dy \tag{2.12.43}$$

Considering $\int_0^n u \cdot v \cdot dx = u \int v \, dx \Big|_0^n - \int_0^n \left[\frac{du}{dx} \int v dx \right] dx$ we can carry out the explicit integration of each term above, which though is a bit tedious is still manageable.

Now suppose the integral happens to be say

$$I = \int_0^H \int_0^b \left[\sin \frac{\pi x}{2H} \sin \frac{3\pi x}{2H} + \cos \frac{\pi y}{2b} \cos \frac{3\pi y}{2b} \right]^2 dxdy \tag{2.12.44}$$

You are surely in for a tough time for it becomes inordinately difficult and laborious to carry out this integral analytically.

The only option then is to resort to numerical integration through computer. But there also we are faced with a difficulty as because the limits of the integral H and b are only symbolic that a computer cannot handle. *So what do we do here?*

We tackle the problem as mentioned hereafter.

47 Historically there is possibly some confusion as to who first applied this technique in deriving the stiffness of finite elements. Some believe it was Carlos Felippa who first used this technique to derive the higher order plane stress, plane strain and plate bending element – "Refined Finite Element Analysis of Linear and Non Linear Two Dimensional Structures", PhD Dissertation, Dept. of Civil Engineering University of California, Berkeley 1966.

While others feel it was B.M. Irons who first used this technique in deriving the element stiffness matrix based on iso-parametric formulation. We shall be grateful if somebody can let us know the exact information.

We convert the function x and y into another co-ordinate ξ and η where it becomes independent of H and b.

Here let $x = \frac{H(1+\xi)}{2}$ and $y = \frac{b(1+\eta)}{2}$ which gives $dx = \frac{Hd\xi}{2}$ and $dy = \frac{bd\eta}{2}$ moreover as $\xi \to 1; x \to H$ and $\xi \to -1; x \to 0$ similarly as $\eta \to 1; y \to b$ and $\eta \to -1; y \to 0$.

Based on above the integral can now be expressed as

$$I = \frac{bH}{4} \int_{-1}^{1} \int_{-1}^{1} \left[\sin \frac{\pi\,(1+\xi)}{4} \sin \frac{3\pi\,(1+\xi)}{4} + \cos \frac{\pi\,(1+\eta)}{4} \cos \frac{3\pi\,(1+\eta)}{4} \right]^{2} d\xi\, d\eta \tag{2.12.45}$$

Looking at the above integral, it is seen that we have converted the x-y coordinate of the integral into a natural coordinate $\xi - \eta$. The integral here is independent of the limits H and b, and got converted into a specific limit of 1 and -1. The internal parameters are also independent of H and b and poses no difficulty in carrying out a direct numerical integration.

This type of transformation has great application in derivation of element stiffness matrix in FEM which we will see subsequently.

2.12.14 Numerical integration technique used for FEM

Having stated above that numerical integration in natural coordinate are usually deployed for derivation of element stiffness matrix in FEM, it would be worthwhile to know what scheme to use for this, as options available are many.

Of all the methods available[48] it has been found that *Gauss Quadrature Formula* is particularly suitable and proves to be most efficient in performing numerical integration for expression like $[K] = \int [B]^T [D] [B]\, dv$. The method is briefly described as in the following.

2.12.15 Gauss quadrature scheme for numerical integration

Gauss was looking for an answer to the following problem. "If there exists an integral $\int_a^b f(x)dx$, whose value has to be evaluated from a given number of values $f(x)$, what selected values of absicca in general give most accurate result?"

Gauss observed that points on the absicca need not be equally spaced but they should be symmetrical about the midpoint of the interval of the integration.

Without going into the detail of derivation of the formula (Sastry 1987), the procedure for application of the same is as follows:

For one dimensional case: $$I = \int_{-1}^{1} f(\xi) d\xi = \sum_{i=1}^{n} W_i f_i, \tag{2.12.46}$$

where W_i = weighting function and f_i = Value of $f(\xi)$ at the Gauss-point i.

48 Trapezoidal, Romberg, Simpson rule, Newton Coates Method… etc.

For two dimensional case, integration by Gauss Quadrature is expressed as

$$I = \int_{-1}^{1} \left[\int_{-1}^{1} f(\xi, \eta) d\xi \right] d\eta \tag{2.12.47}$$

The integration is carried out by first evaluating the inner integral by keeping the outer integral constant and then finally evaluating the outer integral as shown hereafter.

$$I = \int_{-1}^{1} \left[\int_{-1}^{1} f(\xi, \eta)\, d\xi \right] d\eta = \int_{-1}^{1} [W_i f(\xi, \eta)] d\eta = W_i W_j f(\xi, \eta), \tag{2.12.48}$$

where W_i, W_j are weighted functions.

The sampling points and their weights for Gauss quadrature are as given in Table 2.12.1. In the expression for double integral it is assumed that there are n_j sampling points in the ξ-direction and n_i points in the η-direction. There are thus consequently $(n_i \times n_j)$ number of sampling points in all. Usually same number of sampling points are used in each direction so that $n_i = n_j$, but need not be an essential rule. Shown in Figure 2.12.13 are samples for (2×2) and (3×3) integration by Gauss quadrature scheme.

Table 2.11.3 Sampling points and their weights for Gaussian integration.

Number of points	*Position of point* (ξ_i)	*Weights* (W_i)
1	0	2
2	0.577340269	1
	−0.577340269	1
3	0	0.8888888
	0.774596669	0.5555555
	−0.77456669	0.5555555
4	0.86113631 1	0.347854845
	−0.86113631 1	0.347854845
	0.339981043	0.652145154
	−0.339981043	0.652145154

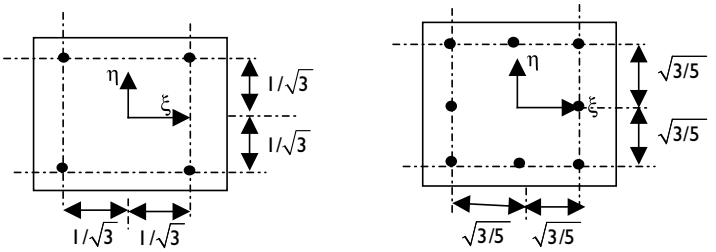


Figure 2.12.13 Gauss samples at two and three points respectively.

To elaborate further let us consider the integral

$$I = \int_{-1}^{1}\int_{-1}^{1} \frac{1+\xi^2}{4a}\frac{1-\eta^2}{4b}d\xi\, d\eta = \frac{1}{16ab}\int_{-1}^{1}\int_{-1}^{1}(1+\xi^2)(1-\eta^2)d\xi\, d\eta \tag{2.12.49}$$

Considering 2×2 integration values of sampling points at selected node are given Figure 2.12.14.

Here $W_i = W_j = 1.0$

$$f(\xi_1, \eta_1) = [\{1 + (-1/\sqrt{3})^2\}\{1 - (-1/\sqrt{3})^2\}] = (1 + 1/3)(1 - 1/3) = 8/9$$
$$f(\xi_1, \eta_2) = [\{1 + (1/\sqrt{3})^2\}\{1 - (-1/\sqrt{3})^2\}] = 8/9;$$
$$f(\xi_2, \eta_1) = [\{1 + (-1/\sqrt{3})^2\}\{1 - (1/\sqrt{3})^2\}] = 8/9 \quad \text{and}$$
$$f(\xi_2, \eta_2) = [\{1 + (1/\sqrt{3})^2\}\{1 - (1/\sqrt{3})^2\}] = 8/9.$$

Thus $$I = \frac{1}{16ab} W_i[f(\xi, \eta)]_{i\times j} W_j \tag{2.12.50}$$

$$I = \frac{1}{16ab}\langle 1 \quad 1\rangle \begin{bmatrix} f(\xi_2, \eta_1) & f(\xi_2, \eta_2) \\ f(\xi_1, \eta_1) & f(\xi_1, \eta_2) \end{bmatrix} \begin{Bmatrix} 1 \\ 1 \end{Bmatrix} \tag{2.12.51}$$

$$I = \frac{1}{16ab}[1 \quad 1] \begin{bmatrix} 8/9 & 8/9 \\ 8/9 & 8/9 \end{bmatrix} \begin{bmatrix} 1 \\ 1 \end{bmatrix} = \frac{2}{9ab} \tag{2.12.52}$$

By analytical solution we have, $$I = \frac{1}{16ab}\int_{-1}^{1}\int_{-1}^{1}(1+\xi^2)(1-\eta^2)d\xi\, d\eta \tag{2.12.53}$$

$$I = \frac{1}{16ab}\left[\int_{-1}^{1}(1+\xi^2)d\xi\right]\left[\int_{-1}^{1}(1-\eta^2)d\eta\right];$$

$$I = \frac{1}{16ab}\left[(\xi)_{-1}^{1} + \left(\frac{\xi^3}{3}\right)_{-1}^{1}\right]\left[(\eta)_{-1}^{1} - \left(\frac{\eta^3}{3}\right)_{-1}^{1}\right]$$

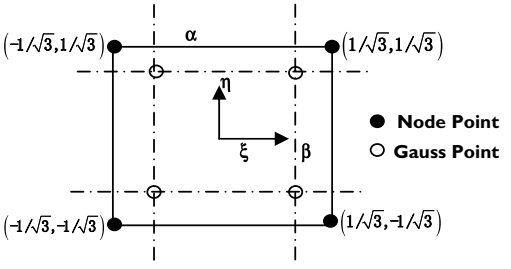


Figure 2.12.14 Gauss samples at two Gauss-points.

$$I = \frac{1}{16ab}\left[2+\frac{1}{3}+\frac{1}{3}\right]\left[2-\frac{1}{3}-\frac{1}{3}\right]; \quad I = \frac{1}{16ab}\left[\frac{8}{3}\right]\left[\frac{4}{3}\right] = \frac{2}{9ab},$$

— *the results matches exactly to two point Gauss quadrature integration.*

Going through the above example you might wonder as to what level of numerical integration should be used in evaluating the elemental properties?

For n integration points Gauss Quadrature procedure provides exact evaluation of integral of any polynomial function of degree $2n-1$ *or less.*

For example two point integration would give exact result for polynomial upto third order. It might instinctively be felt that the procedure should be carried out exactly or as close to exactly as possible – but however is always not good! The reason for this being use of excessive sampling points is computationally expensive and use of lower order (thus not exact) integration can be beneficial in practice as it tends to result in reduced stiffness which compensates the natural tendency of over stiffness of a structure for displacement based formulation. This is often termed as reduced integration technique.

However if a lower order integration is carried out for deriving the element stiffness does not necessarily ensure overstiffness for the whole body, as such bound condition discussed earlier no longer applies. This however is of not much consequence so long as the final results converge to correct value as the meshes are progressively refined.

2.12.16 Stiffness matrix for 4-nodded rectangular element under plane strain condition

Having established the natural co-ordinate and the numerical integration scheme we use these theories to develop the element stiffness matrix for a rectangular element under plane strain condition.

Shown in Figure 2.12.15 is a four-nodded rectangular element in generalized X-Y coordinate and natural ξ–η co-ordinate where the relation between the generalized and natural co-ordinate is given by

$$\xi = \frac{x}{a} \quad \text{and} \quad \eta = \frac{y}{b}$$

The rectangular element has two degrees of freedom for each node and is given by (u_j, v_j) where $j = 1, 2, 3, 4$.

Based on the law of polynomial as expressed earlier in generalized co-ordinate the same can be expressed for a four nodded element as

$$[\delta] = \alpha_1 + \alpha_2 x + \alpha_3 y + \alpha_4 xy \tag{2.12.54}$$

Thus in natural co-ordinate the same can be expressed as

$$u = \alpha_1 + \alpha_2\xi + \alpha_3\eta + \alpha_4\xi\eta \quad \text{and} \quad v = \alpha_5 + \alpha_6\xi + \alpha_7\eta + \alpha_8\xi\eta \tag{2.12.55}$$

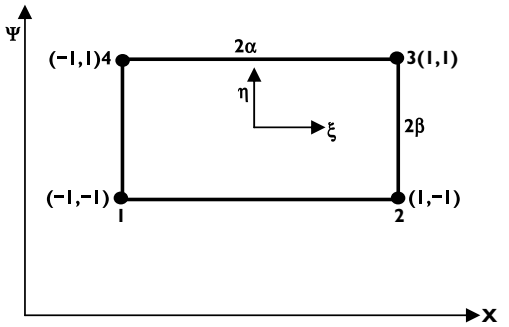


Figure 2.12.15 Rectangular element in natural coordinate.

Thus in natural co-ordinate for the rectangular element as shown above we have

$u_1 = \alpha_1 - \alpha_2 - \alpha_3 + \alpha_4; \quad u_2 = \alpha_1 + \alpha_2 - \alpha_3 - \alpha_4$

$u_3 = \alpha_1 + \alpha_2 + \alpha_3 + \alpha_4$ and $u_4 = \alpha_1 - \alpha_2 + \alpha_3 - \alpha_4$, which gives

$$\begin{Bmatrix} u_1 \\ u_2 \\ u_3 \\ u_4 \end{Bmatrix} = \begin{bmatrix} 1 & -1 & -1 & 1 \\ 1 & 1 & -1 & -1 \\ 1 & 1 & 1 & 1 \\ 1 & -1 & 1 & -1 \end{bmatrix} \begin{Bmatrix} \alpha_1 \\ \alpha_2 \\ \alpha_3 \\ \alpha_4 \end{Bmatrix} \quad \text{and} \quad \begin{Bmatrix} v_1 \\ v_2 \\ v_3 \\ v_4 \end{Bmatrix} = \begin{bmatrix} 1 & -1 & -1 & 1 \\ 1 & 1 & -1 & -1 \\ 1 & 1 & 1 & 1 \\ 1 & -1 & 1 & -1 \end{bmatrix} \begin{Bmatrix} \alpha_5 \\ \alpha_6 \\ \alpha_7 \\ \alpha_8 \end{Bmatrix} \tag{2.12.56}$$

Considering $\{f\} = [M]\{\alpha\}$ we have

$$\{f\} = \begin{bmatrix} 1 & \xi & \eta & \xi\eta & 0 & 0 & 0 & 0 \\ 0 & 0 & 0 & 0 & 1 & \xi & \eta & \xi\eta \end{bmatrix} \langle \alpha_1 \ \alpha_2 \ \alpha_3 \ \alpha_4 \ \alpha_5 \ \alpha_6 \ \alpha_7 \ \alpha_8 \rangle^T \tag{2.12.57}$$

Letting the computer do the donkey work we invert the 4×4 matrix to obtain

$$\begin{Bmatrix} \alpha_1 \\ \alpha_2 \\ \alpha_3 \\ \alpha_4 \end{Bmatrix} = \frac{1}{4} \begin{bmatrix} 1 & 1 & 1 & 1 \\ -1 & 1 & 1 & -1 \\ -1 & -1 & 1 & 1 \\ 1 & -1 & 1 & -1 \end{bmatrix} \begin{Bmatrix} u_1 \\ u_2 \\ u_3 \\ u_4 \end{Bmatrix} \quad \text{and}$$

$$\begin{Bmatrix} \alpha_5 \\ \alpha_6 \\ \alpha_7 \\ \alpha_8 \end{Bmatrix} = \frac{1}{4} \begin{bmatrix} 1 & 1 & 1 & 1 \\ -1 & 1 & 1 & -1 \\ -1 & -1 & 1 & 1 \\ 1 & -1 & 1 & -1 \end{bmatrix} \begin{Bmatrix} v_1 \\ v_2 \\ v_3 \\ v_4 \end{Bmatrix}$$

$$\begin{Bmatrix}\alpha_1\\ \alpha_2\\ \alpha_3\\ \alpha_4\\ \alpha_5\\ \alpha_6\\ \alpha_7\\ \alpha_8\end{Bmatrix} = \frac{1}{4}\begin{bmatrix}1 & 0 & 1 & 0 & 1 & 0 & 1 & 0\\ -1 & 0 & 1 & 0 & 1 & 0 & -1 & 0\\ -1 & 0 & -1 & 0 & 1 & 0 & 1 & 0\\ 1 & 0 & -1 & 0 & 1 & 0 & -1 & 0\\ 0 & 1 & 0 & 1 & 0 & 1 & 0 & 1\\ 0 & -1 & 0 & 1 & 0 & 1 & 0 & -1\\ 0 & -1 & 0 & -1 & 0 & 1 & 0 & 1\\ 0 & 1 & 0 & -1 & 0 & 1 & 0 & -1\end{bmatrix}\begin{Bmatrix}u_1\\ v_1\\ u_2\\ v_2\\ u_3\\ v_3\\ u_4\\ v_4\end{Bmatrix} \quad \text{or } [\alpha] = [C]^{-1}[\delta] \tag{2.12.58}$$

Again considering $[N] = [M][C]^{-1}$ we have

$$[N] = \frac{1}{4}\begin{bmatrix}1 & \xi & \eta & \xi\eta & 0 & 0 & 0 & 0\\ 0 & 0 & 0 & 0 & 1 & \xi & \eta & \xi\eta\end{bmatrix}\begin{bmatrix}1 & 0 & 1 & 0 & 1 & 0 & 1 & 0\\ -1 & 0 & 1 & 0 & 1 & 0 & -1 & 0\\ -1 & 0 & -1 & 0 & 1 & 0 & 1 & 0\\ 1 & 0 & -1 & 0 & 1 & 0 & -1 & 0\\ 0 & 1 & 0 & 1 & 0 & 1 & 0 & 1\\ 0 & -1 & 0 & 1 & 0 & 1 & 0 & -1\\ 0 & -1 & 0 & -1 & 0 & 1 & 0 & 1\\ 0 & 1 & 0 & -1 & 0 & 1 & 0 & -1\end{bmatrix}$$

The above on multiplication gives

$$[N] = \begin{bmatrix}N_1 & 0 & N_2 & 0 & N_3 & 0 & N_4 & 0\\ 0 & N_1 & 0 & N_2 & 0 & N_3 & 0 & N_4\end{bmatrix} \tag{2.12.59}$$

where

$$N_1 = \frac{(1-\xi)(1-\eta)}{4}, \quad N_2 = \frac{(1+\xi)(1-\eta)}{4}, \quad N_3 = \frac{(1+\xi)(1+\eta)}{4} \quad \text{and}$$

$$N_4 = \frac{(1-\xi)(1+\eta)}{4}.$$

The strain matrix is given by

$$\begin{Bmatrix}\varepsilon_x\\ \varepsilon_y\\ \gamma_{xy}\end{Bmatrix} = \begin{bmatrix}\frac{\partial N_1}{\partial x} & 0 & \frac{\partial N_2}{\partial x} & 0 & \frac{\partial N_3}{\partial x} & 0 & \frac{\partial N_4}{\partial x} & 0\\ 0 & \frac{\partial N_1}{\partial y} & 0 & \frac{\partial N_2}{\partial y} & 0 & \frac{\partial N_3}{\partial y} & 0 & \frac{\partial N_4}{\partial y}\\ \frac{\partial N_1}{\partial y} & \frac{\partial N_1}{\partial x} & \frac{\partial N_2}{\partial y} & \frac{\partial N_2}{\partial x} & \frac{\partial N_3}{\partial y} & \frac{\partial N_3}{\partial x} & \frac{\partial N_4}{\partial y} & \frac{\partial N_4}{\partial x}\end{bmatrix}\begin{Bmatrix}u_1\\ v_1\\ u_2\\ v_2\\ u_3\\ v_3\\ u_4\\ v_4\end{Bmatrix}$$

or $\{\varepsilon\} = [B]\{\delta\}$ (2.12.60)

Considering $\frac{\partial}{\partial x} = \frac{\partial}{\partial \xi} \times \frac{\partial \xi}{\partial x} = \frac{1}{a}\frac{\partial}{\partial \xi}$ and $\frac{\partial}{\partial y} = \frac{\partial}{\partial \eta} \times \frac{\partial \eta}{\partial y} = \frac{1}{b}\frac{\partial}{\partial \eta}$ gives,

$$\begin{Bmatrix} \varepsilon_x \\ \varepsilon_y \\ \gamma_{xy} \end{Bmatrix} = \begin{bmatrix} \frac{\eta-1}{4a} & 0 & \frac{1-\eta}{4a} & 0 & \frac{1+\eta}{4a} & 0 & -\frac{1+\eta}{4a} & 0 \\ 0 & \frac{\xi-1}{4b} & 0 & -\frac{1+\xi}{4b} & 0 & \frac{1+\xi}{4b} & 0 & \frac{1-\xi}{4b} \\ \frac{\xi-1}{4b} & \frac{\eta-1}{4a} & -\frac{1+\xi}{4b} & \frac{1-\eta}{4a} & \frac{1+\xi}{4b} & \frac{1+\eta}{4a} & \frac{1-\xi}{4b} & -\frac{1+\eta}{4a} \end{bmatrix} \begin{Bmatrix} u_1 \\ v_1 \\ u_2 \\ v_2 \\ u_3 \\ v_3 \\ u_4 \\ v_4 \end{Bmatrix}$$

Thus, $$[B] = \begin{bmatrix} \frac{\eta-1}{4a} & 0 & \frac{1-\eta}{4a} & 0 & \frac{1+\eta}{4a} & 0 & -\frac{1+\eta}{4a} & 0 \\ 0 & \frac{\xi-1}{4b} & 0 & -\frac{1+\xi}{4b} & 0 & \frac{1+\xi}{4b} & 0 & \frac{1-\xi}{4b} \\ \frac{\xi-1}{4b} & \frac{\eta-1}{4a} & -\frac{1+\xi}{4b} & \frac{1-\eta}{4a} & \frac{1+\xi}{4b} & \frac{1+\eta}{4a} & \frac{1-\xi}{4b} & -\frac{1+\eta}{4a} \end{bmatrix}$$

Considering the element stiffness matrix as $[K] = \iint_v \int [B]^T [D] [B] \, dv$ in this case as the condition is plane strain, we have

$$[D] = \frac{E(1-\nu)}{(1+\nu)(1-2\nu)} \begin{bmatrix} 1 & \frac{\nu}{1-\nu} & 0 \\ \frac{\nu}{1-\nu} & 1 & 0 \\ 0 & 0 & \frac{1-2\nu}{2(1-\nu)} \end{bmatrix}$$ which finally gives

$$[K] = \frac{\eta(1-\nu)}{(1+\nu)(1-2\nu)} \int_{-1}^{1}\int_{-1}^{1} \begin{bmatrix} (\eta-1)/4a & 0 & (\xi-1)/4b \\ 0 & (\xi-1)/4b & (\eta-1)/4a \\ (1-\eta)/4a & 0 & -(1+\xi)/4b \\ 0 & -(1+\xi)/4b & (1-\eta)/4a \\ (1+\eta)/4a & 0 & (1+\xi)/4b \\ 0 & (1+\xi)/4b & (1+\eta)/4a \\ -(1+\eta)/4a & 0 & (1-\xi)/4b \\ 0 & (1-\xi)/4b & -(1+\eta)/4a \end{bmatrix}$$

$$\times \begin{bmatrix} 1 & \frac{\nu}{1-\nu} & 0 \\ \frac{\nu}{1-\nu} & 1 & 0 \\ 0 & 0 & \frac{1-2\nu}{2(1-\nu)} \end{bmatrix}$$

$$\times \begin{bmatrix} \frac{\eta-1}{4a} & 0 & \frac{1-\eta}{4a} & 0 & \frac{1+\eta}{4a} & 0 & -\frac{1+\eta}{4a} & 0 \\ 0 & \frac{\xi-1}{4b} & 0 & -\frac{1+\xi}{4b} & 0 & \frac{1+\xi}{4b} & 0 & \frac{1-\xi}{4b} \\ \frac{\xi-1}{4b} & \frac{\eta-1}{4a} & -\frac{1+\xi}{4b} & \frac{1-\eta}{4a} & \frac{1+\xi}{4b} & \frac{1+\eta}{4a} & \frac{1-\xi}{4b} & -\frac{1+\eta}{4a} \end{bmatrix} d\xi \, d\eta \tag{2.12.61}$$

This gives the stiffness matrix for the four nodded rectangular element.

The integration is carried out for two point Gauss integration and this is carried out at each of the Gauss sampling point and since weighting function is 1.0 *for this case we simply add the four stiffnesses to get the global stiffness matrix*[49].

The 4-nodded rectangular element is considered a far more superior element than CST. It gives much better result than CST even when the meshes are not so refined especially when the aspect ratio (a/b is near or equal to 1). It is a very effective element which can be used to model soil under plane strain condition or deep beams under various nodal or distributed loads where flexural behavior is not predominant. *The behavior of this four-nodded rectangular element under pure flexure is not good.* The reason for the same is as explained below.

Figure 2.12.16 shows the actual and ideal behavior of the 4-nodded rectangular element. It is evident that the element cannot deform in ideal fashion under pure flexure. The reason for this is development of spurious shear strain energy that makes it much stiffer then it actually should be and lock the element especially when the aspect ratio is large.

It has been shown elsewhere (Cook et al. (1989) that for same displacement, ratio of M_1 and M_2 is given by

$$\frac{M_1}{M_2} = \frac{1}{1+\nu}\left[\frac{1}{1-\nu} + \frac{1}{2}\left(\frac{a}{b}\right)^2\right] \tag{2.12.62}$$

It is evident from above that for large aspect ratio for stress calculation the results would be highly erroneous. Even with aspect of ratio of one, which is considered ideal, the error is of the order of 48%. However, when a/b is 0.5 error is about 16%. Thus, if one uses this element at all for case where flexural behavior is dominating it would be preferable to use an aspect ratio less than 1.0 in direction of major stress gradient.

As shown in Figure 2.12.17, the parasitic shear that develops due to spurious shear strain, makes $M_1 > M_2$ and locks the meshes when the aspect ratio a/b is large.

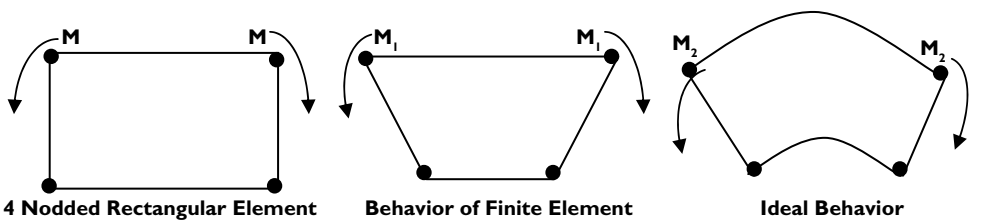


Figure 2.12.16 Deformation of 4-nodded finite element under actual and idealized mode.

49 This has been explained by a numerical example later.

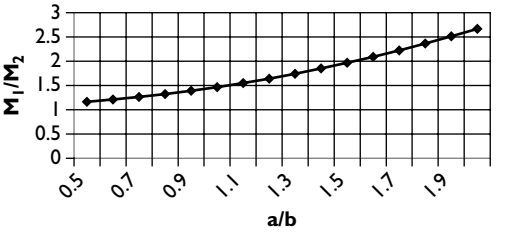


Figure 2.12.17 Variation of M_1/M_2 with aspect ratio a/b for $v = 0.25$.

2.12.17 Iso-parametric formulation for elements with arbitrary shape

Till now we had derived element stiffness matrix for elements that has regular shape like triangle rectangle etc. However, in practical engineering, in many cases we are faced with problems when the surfaces are curved.

Trying to model them based on finite element it was found that triangular and rectangular elements are always not very effective, and a shape which was much more general was necessary. This requirement led to the development of element shapes of arbitrary nature.

Before we get into the derivation of the same we reinforce our argument by a typical finite element model of a circular disc where three of its quadrants are modeled by three types of elements.

Figure 2.12.18 is self-explanatory, while modeling with the triangular element as we approach the center the triangles become highly distorted with high aspect ratio more over number of elements may have to be taken much more to come to a meaningful result.

The rectangular elements on the other hand cannot take into consideration the last portion that is semi-triangular and has to be further divided into further rectangles calling for further mesh refinement. On the contrary, a mixture of rectangular and quadrilateral element as is observed is best suited to cater to the situation where the mesh is uniform and stress interpretation becomes relatively easy due to the uniformity of the mesh. The iso-parametric elements come in different shapes as shown in Figure 2.12.19.

To understand the basis of iso-parametric formulation we derive the 4-nodded quadrilateral originally proposed by Taig (1961) and generalized by Irons (1966) for other elements (we would take up the curved elements when we discuss elements of higher order).

Rectangle as we know is nothing but a particular case of quadrilateral whose opposite sides are equal and angle subtended at each corner is 90 degrees. Naturally, the starting point for the derivation of the element stiffness matrix is the rectangular element that we had derived earlier.

This we call as *the parent element*. Now consider Figure 2.12.20:

Shown therein is a rectangular element in natural co-ordinate and an iso-parametric quadrilateral element in global co-ordinate. We will now derive the property of the quadrilateral element from the parent rectangular element by a process termed as mapping.

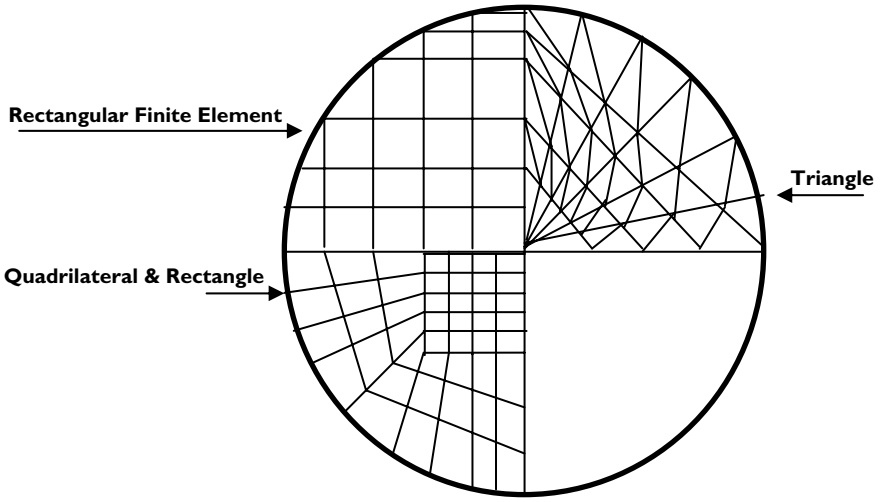


Figure 2.12.18 A circular disc modeled by various elements in each quadrant.

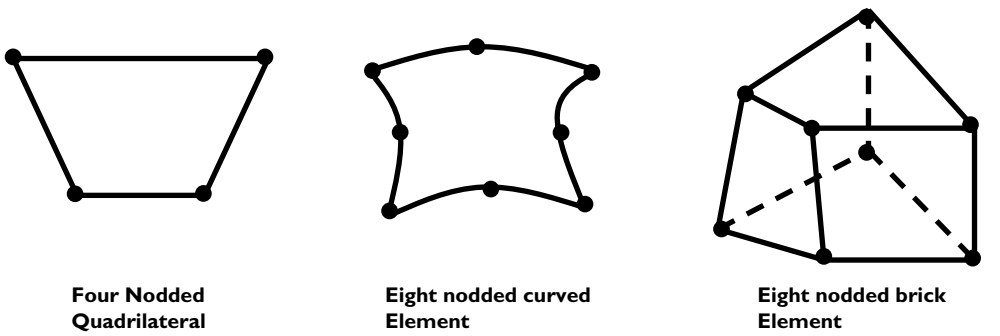


Figure 2.12.19 Different types of iso-parametric elements.

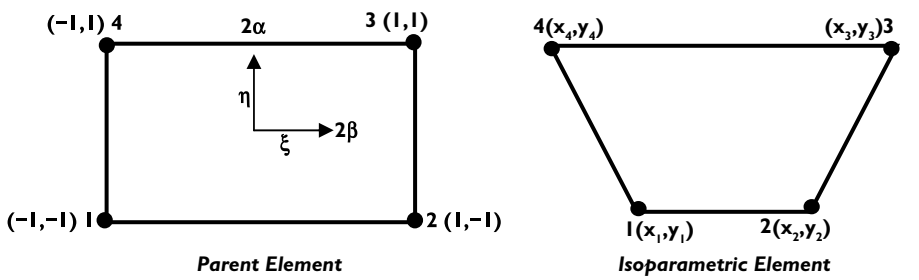


Figure 2.12.20 The parent element and the iso-parametric element.

The geometry of the quadrilateral element is described by

$$x = \sum_{i=1}^{4} G_i(x, y)x_i \quad \text{and} \quad y = \sum_{i=1}^{4} G_i(x, y)y_i \tag{2.12.63}$$

the term $G_i(x, y)$ can be assumed to be a geometric interpolation function and each such function is related to a particular node of the quadrilateral.

Now if we consider the parent element and the quadrilateral are geometrically equivalent then we can say that

$$(\xi_1, \eta_1) = (-1, -1) \Leftrightarrow (x_1, y_1) :: (\xi_2, \eta_2) = (1, -1) \Leftrightarrow (x_2, y_2)$$

$$(\xi_3, \eta_3) = (1, 1) \Leftrightarrow (x_3, y_3) \quad \text{and} \quad (\xi_4, \eta_4) = (-1, 1) \Leftrightarrow (x_4, y_4) \tag{2.12.64}$$

Here the symbol $\Leftrightarrow$ *signifies corresponds to or maps to.*

Now observing the equation shown for x and y it is evident that the geometric function $G_i(x, y)$ must be unity at node related to it and zero at all other nodes. This property is again same as the shape function we use to derive the nodal displacement thus the geometric expression for the global co-ordinate in terms of natural co-ordinate becomes

$$x = \sum_{i=1}^{4} N_i(\xi, \eta)x_i \quad \text{and} \quad y = \sum_{i=1}^{4} N_i(\xi, \eta)y_i \tag{2.12.65}$$

Since both geometric and nodal displacements are expressed by same interpolation function – these elements are called iso-parametric elements.

You might still have some misgivings in the geometric expression given above in terms of shape function which was almost put in intuitively.

To give you a more formal mathematical proof we take a specific example to explain this further.

Shown in Figure 2.12.21 is quadrilateral with nodes 1, 2, 3, 4 whose nodal coordinates are shown in the parenthesis. We derive the equation of line 2–3 based on mapping and co-ordinate geometry.

If the mapping formula is correct, it should give same result. Based on iso-parametric mapping we have

$$x = \frac{(1-\xi)(1-\eta)}{4}x_1 + \frac{(1+\xi)(1-\eta)}{4}x_2 + \frac{(1+\xi)(1+\eta)}{4}x_3$$

$$+ \frac{(1-\xi)(1+\eta)}{4}x_4 \quad \text{and}$$

$$y = \frac{(1-\xi)(1-\eta)}{4}y_1 + \frac{(1+\xi)(1-\eta)}{4}y_2 + \frac{(1+\xi)(1+\eta)}{4}y_3 + \frac{(1-\xi)(1+\eta)}{4}y_4$$

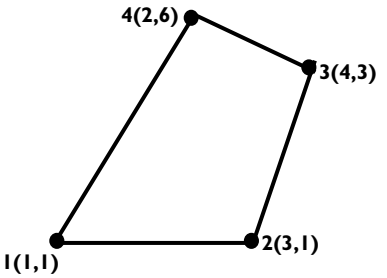


Figure 2.12.21 Four-nodded quadrilateral element with nodal coordinates.

Now substituting the value of the nodal coordinates we have

$$x = \frac{(1-\xi)(1-\eta)}{4}(1) + \frac{(1+\xi)(1-\eta)}{4}(3) + \frac{(1+\xi)(1+\eta)}{4}(4) + \frac{(1-\xi)(1+\eta)}{4}(2)$$

$$y = \frac{(1-\xi)(1-\eta)}{4}(1) + \frac{(1+\xi)(1-\eta)}{4}(1) + \frac{(1+\xi)(1+\eta)}{4}(3) + \frac{(1-\xi)(1+\eta)}{4}(6)$$

On the edge 2–3, $\xi = 1$, thus substituting this value in the above two equation we have

$$x = \frac{7+\eta}{2} \quad \text{and} \quad y = 2 + \eta$$

We thus have two equations

$$\eta = 2x - 7 \quad \text{and} \quad \eta = y - 2$$

eliminating η from the above two equation we have $y = 2x - 5$.

Based on coordinate geometry, at node 2 considering the equation of straight line as $y = mx + c$ and we have

At node-2 $1 = 3m + c$ :: A node-3 $3 = 4m + c$.

Solving the above two equation we have $m = 2$ and $c = -5$ which again gives

$$y = 2x - 5$$

which is the same as iso-parametric mapping.

To derive the element stiffness matrix for the quadrilateral element in Figure 2.12.20 we start with the strain matrix

$$\begin{Bmatrix} \varepsilon_x \\ \varepsilon_y \\ \gamma_{xy} \end{Bmatrix} = \begin{Bmatrix} \dfrac{\partial u}{\partial x} \\ \dfrac{\partial v}{\partial y} \\ \dfrac{\partial u}{\partial y} + \dfrac{\partial v}{\partial x} \end{Bmatrix}, \quad \text{where } u = \sum_{i=1}^{4} N_i(\xi, \eta) u_i \text{ and } v = \sum_{i=1}^{4} N_i(\xi, \eta) v_i \tag{2.12.66}$$

as u is a function of x and y so based on chain rule of differential calculus we can write

$$\frac{\partial u}{\partial \xi} = \frac{\partial u}{\partial x}\frac{\partial x}{\partial \xi} + \frac{\partial u}{\partial y}\frac{\partial y}{\partial \xi} \quad \text{and} \quad \frac{\partial u}{\partial \eta} = \frac{\partial u}{\partial x}\frac{\partial x}{\partial \eta} + \frac{\partial u}{\partial y}\frac{\partial y}{\partial \eta}$$

Above in matrix notation can be expressed as

$$\begin{Bmatrix} \dfrac{\partial u}{\partial \xi} \\ \dfrac{\partial u}{\partial \eta} \end{Bmatrix} = \begin{bmatrix} \dfrac{\partial x}{\partial \xi} & \dfrac{\partial y}{\partial \xi} \\ \dfrac{\partial x}{\partial \eta} & \dfrac{\partial y}{\partial \eta} \end{bmatrix} \begin{Bmatrix} \dfrac{\partial u}{\partial x} \\ \dfrac{\partial u}{\partial y} \end{Bmatrix} \tag{2.12.67}$$

The above mathematical expression is otherwise simply expressed as

$$\begin{Bmatrix} \dfrac{\partial u}{\partial \xi} \\ \dfrac{\partial u}{\partial \eta} \end{Bmatrix} = [J] \begin{Bmatrix} \dfrac{\partial u}{\partial x} \\ \dfrac{\partial u}{\partial y} \end{Bmatrix}$$

The matrix $[J]$ is known as the *Jacobian* matrix and is expressed as

$$[J] = \begin{bmatrix} J_{11} & J_{12} \\ J_{21} & J_{22} \end{bmatrix} = \begin{bmatrix} \dfrac{\partial x}{\partial \xi} & \dfrac{\partial y}{\partial \xi} \\ \dfrac{\partial x}{\partial \eta} & \dfrac{\partial y}{\partial \eta} \end{bmatrix}$$

Thus,

$$J_{11} = \frac{\partial x}{\partial \xi} = \frac{\partial}{\partial \xi}\sum_{i=1}^{4} N_i x_i = \frac{\partial}{\partial \xi}\left[\frac{(1-\xi)(1-\eta)}{4}x_1 + \frac{(1+\xi)(1-\eta)}{4}x_2\right]$$
$$+ \frac{\partial}{\partial \xi}\left[\frac{(1+\xi)(1+\eta)}{4}x_3 + \frac{(1-\xi)(1+\eta)}{4}x_4\right]$$

or $$J_{11} = \frac{1}{4}\left[(\eta-1)x_1 + (1-\eta)x_2 + (1+\eta)x_3 - (1+\eta)x_4\right]$$

Similarly

$$J_{12} = [(\eta - 1)\, y_1 + (1 - \eta)\, y_2 + (1 + \eta)\, y_3 - (1 + \eta)\, y_4]\,/4;$$
$$J_{21} = [(\xi - 1)\, x_1 - (1 + \xi)\, x_2 + (1 + \xi)\, x_3 + (1 - \xi)\, x_4]\,/4 \quad \text{and}$$
$$J_{22} = [(\xi - 1)\, y_1 - (1 + \xi)\, y_2 + (1 + \xi)\, y_3 + (1 - \xi)\, y_4]\,/4$$

This displacement relation in terms of Jacobian matrix can now be expressed as

$$\begin{Bmatrix} \dfrac{\partial u}{\partial x} \\ \dfrac{\partial u}{\partial y} \end{Bmatrix} = [J]^{-1} \begin{Bmatrix} \dfrac{\partial u}{\partial \xi} \\ \dfrac{\partial u}{\partial \eta} \end{Bmatrix}; \quad \text{which can be expanded to}$$

$$\begin{Bmatrix} \dfrac{\partial u}{\partial x} \\ \dfrac{\partial u}{\partial y} \end{Bmatrix} = \frac{1}{|J|} \begin{bmatrix} J_{22} & -J_{12} \\ -J_{21} & J_{11} \end{bmatrix} \begin{Bmatrix} \dfrac{\partial u}{\partial \xi} \\ \dfrac{\partial u}{\partial \eta} \end{Bmatrix} \tag{2.12.68}$$

where the term $|J|$ represents the determinant of the Jacobian Matrix.

Since the interpolation function remains same for the displacement v, proceeding in identical manner we have

$$\begin{Bmatrix} \dfrac{\partial v}{\partial x} \\ \dfrac{\partial v}{\partial y} \end{Bmatrix} = \frac{1}{|J|} \begin{bmatrix} J_{22} & -J_{12} \\ -J_{21} & J_{11} \end{bmatrix} \begin{Bmatrix} \dfrac{\partial v}{\partial \xi} \\ \dfrac{\partial v}{\partial \eta} \end{Bmatrix}$$

Thus, the strain matrix can now be expressed as

$$\begin{Bmatrix} \varepsilon_x \\ \varepsilon_y \\ \gamma_{xy} \end{Bmatrix} = \begin{Bmatrix} \dfrac{\partial u}{\partial x} \\ \dfrac{\partial v}{\partial y} \\ \dfrac{\partial u}{\partial y} + \dfrac{\partial v}{\partial x} \end{Bmatrix} = \frac{1}{|J|} \begin{bmatrix} J_{22} & -J_{12} & 0 & 0 \\ 0 & 0 & -J_{21} & J_{11} \\ -J_{21} & J_{11} & J_{22} & -J_{12} \end{bmatrix} \begin{Bmatrix} \dfrac{\partial u}{\partial \xi} \\ \dfrac{\partial u}{\partial \eta} \\ \dfrac{\partial v}{\partial \xi} \\ \dfrac{\partial v}{\partial \eta} \end{Bmatrix} \tag{2.12.69}$$

or $\begin{Bmatrix} \varepsilon_x \\ \varepsilon_y \\ \gamma_{xy} \end{Bmatrix} = [G] \left\langle \dfrac{\partial u}{\partial \xi} \quad \dfrac{\partial u}{\partial \eta} \quad \dfrac{\partial v}{\partial \xi} \quad \dfrac{\partial v}{\partial \xi} \right\rangle^T$ where $[G]$ is called the *geometric mapping matrix* and is identified as $[G] = \dfrac{1}{|J|} \begin{bmatrix} J_{22} & -J_{12} & 0 & 0 \\ 0 & 0 & -J_{21} & J_{11} \\ -J_{21} & J_{11} & J_{22} & -J_{12} \end{bmatrix}$ (2.12.70)

Since $u = \sum_{i=1}^{4} N_i(\xi,\eta)u_i;\ v = \sum_{i=1}^{4} N_i(\xi,\eta)v_i$ we have

$$\begin{Bmatrix} \frac{\partial u}{\partial \xi} \\ \frac{\partial u}{\partial \eta} \\ \frac{\partial v}{\partial \xi} \\ \frac{\partial v}{\partial \eta} \end{Bmatrix} = \begin{bmatrix} \frac{\partial N_1}{\partial \xi} & 0 & \frac{\partial N_2}{\partial \xi} & 0 & \frac{\partial N_3}{\partial \xi} & 0 & \frac{\partial N_4}{\partial \xi} & 0 \\ \frac{\partial N_1}{\partial \eta} & 0 & \frac{\partial N_2}{\partial \eta} & 0 & \frac{\partial N_3}{\partial \eta} & 0 & \frac{\partial N_4}{\partial \eta} & 0 \\ 0 & \frac{\partial N_1}{\partial \xi} & 0 & \frac{\partial N_2}{\partial \xi} & 0 & \frac{\partial N_3}{\partial \xi} & 0 & \frac{\partial N_4}{\partial \xi} \\ 0 & \frac{\partial N_1}{\partial \eta} & 0 & \frac{\partial N_2}{\partial \eta} & 0 & \frac{\partial N_3}{\partial \eta} & 0 & \frac{\partial N_4}{\partial \eta} \end{bmatrix} \begin{Bmatrix} u_1 \\ v_1 \\ u_2 \\ v_2 \\ u_3 \\ v_3 \\ u_4 \\ v_4 \end{Bmatrix}$$

Substituting this in strain equation one obtains

$$\begin{Bmatrix} \varepsilon_x \\ \varepsilon_y \\ \gamma_{xy} \end{Bmatrix} = \frac{1}{|J|} \begin{bmatrix} J_{22} & -J_{12} & 0 & 0 \\ 0 & 0 & -J_{21} & J_{11} \\ -J_{21} & J_{11} & J_{22} & -J_{12} \end{bmatrix} \times \begin{bmatrix} \frac{\partial N_1}{\partial \xi} & 0 & \frac{\partial N_2}{\partial \xi} & 0 & \frac{\partial N_3}{\partial \xi} & 0 & \frac{\partial N_4}{\partial \xi} & 0 \\ \frac{\partial N_1}{\partial \eta} & 0 & \frac{\partial N_2}{\partial \eta} & 0 & \frac{\partial N_3}{\partial \eta} & 0 & \frac{\partial N_4}{\partial \eta} & 0 \\ 0 & \frac{\partial N_1}{\partial \xi} & 0 & \frac{\partial N_2}{\partial \xi} & 0 & \frac{\partial N_3}{\partial \xi} & 0 & \frac{\partial N_4}{\partial \xi} \\ 0 & \frac{\partial N_1}{\partial \eta} & 0 & \frac{\partial N_2}{\partial \eta} & 0 & \frac{\partial N_3}{\partial \eta} & 0 & \frac{\partial N_4}{\partial \eta} \end{bmatrix} \begin{Bmatrix} u_1 \\ v_1 \\ u_2 \\ v_2 \\ u_3 \\ v_3 \\ u_4 \\ v_4 \end{Bmatrix}$$

$$\text{i.e.} \quad [B]\ \{\delta\} \tag{2.12.71}$$

The $[B]$ matrix can be explicitly expressed as

$$[B]^T = \frac{1}{4\,|J|} \times \begin{bmatrix} -J_{22}(1-\eta)+J_{12}(1-\xi) & 0 & J_{21}(1-\eta)-J_{11}(1-\xi) \\ 0 & J_{21}(1-\eta)-J_{11}(1-\xi) & -J_{22}(1-\eta)+J_{12}(1-\xi) \\ J_{22}(1-\eta)+J_{12}(1+\xi) & 0 & -J_{21}(1-\eta)-J_{11}(1+\xi) \\ 0 & -J_{21}(1-\eta)-J_{11}(1+\xi) & J_{22}(1-\eta)+J_{12}(1+\xi) \\ J_{22}(1+\eta)-J_{12}(1+\xi) & 0 & -J_{21}(1+\eta)+J_{11}(1+\xi) \\ 0 & -J_{21}(1+\eta)+J_{11}(1+\xi) & J_{22}(1+\eta)-J_{12}(1+\xi) \\ -J_{22}(1+\eta)-J_{12}(1-\xi) & 0 & J_{21}(1+\eta)+J_{11}(1-\xi) \\ 0 & J_{21}(1+\eta)+J_{11}(1-\xi) & -J_{22}(1+\eta)-J_{12}(1-\xi) \end{bmatrix} \tag{2.12.72}$$

Considering $[K]_e = \iiint [B]^T[D][B]\,dv$ for constant thickness t we can express it as $[K]_e = t \iint [B]^T [D]\,[B] dx \cdot dy$. It can be shown that, $dA = dx \cdot dy = |J|\, d\xi\, d\eta$, thus the element stiffness matrix for the quadrilateral can be expressed as

$$[K]_e = t \int_{-1}^{1} \int_{-1}^{1} [B]^T [D]\,[B]\,|J| d\xi \cdot d\eta \tag{2.12.73}$$

Time for a numeric example specifically to appease those engineers, who frown on spattering of del, zi and phi and would rather have hard Figures on hand to have a feel on the matter.

Fair enough, to elaborate the theory more clearly we solve following problem.

Example 2.12.1

Given in Figure 2.12.22, the quadrilateral element having nodal coordinates as shown in the parentheses determine the element stiffness based on iso-parametric formulation given thickness of the element is 200 mm and Young's modulus $E = 2 \times 10^8$ kN/m^2, and Poisson's ratio $\nu = 0.25$.

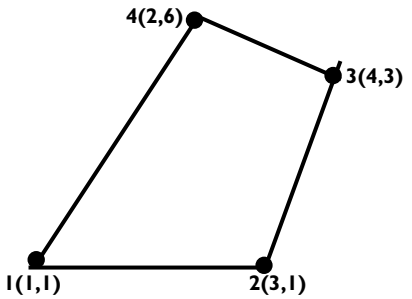


Figure 2.12.22 Four noded isoparametric quadrilateral.

Solution:

This is a plane stress case as such the matrix $[D]$ is given by

$$[D] = \frac{E}{1-\nu^2} \begin{bmatrix} 1 & \nu & 0 \\ \nu & 1 & 0 \\ 0 & 0 & \dfrac{1-\nu}{2} \end{bmatrix}$$

Substituting the value $E = 2 \times 10^8$ kN/m^2 and $\nu = 0.25$ we get

$$[D] = \begin{bmatrix} 2.33 & 0.533 & 0 \\ 0.533 & 0.533 & 0 \\ 0 & 0 & 0.80 \end{bmatrix} \times 10^8 \text{ kN/m}^2$$

For derivation of stiffness matrix we had shown in the theoretical derivation 2 point Gauss integration would suffice.

Considering

$$J_{11} = [(\eta - 1)x_1 + (1 - \eta)x_2 + (1 + \eta)x_3 - (1 + \eta)x_4]/4$$
$$J_{12} = [(\eta - 1)y_1 + (1 - \eta)y_2 + (1 + \eta)y_3 - (1 + \eta)y_4]/4$$
$$J_{21} = [(\xi - 1)x_1 - (1 + \xi)x_2 + (1 + \xi)x_3 + (1 - \xi)x_4]/4$$
$$J_{22} = [(\xi - 1)y_1 - (1 + \xi)y_2 + (1 + \xi)y_3 + (1 - \xi)y_4]/4 \quad \text{and}$$
$$|J| = J_{11}J_{22} - J_{12}J_{21}$$

Based on above the nodal coordinates and the Jacobian parameters are as derived hereafter

Node	x	y	ξ	η	J_{11}	J_{12}	J_{21}	J_{22}	Det-J
1	1	1	−0.57735027	−0.57735027	1	−0.3169	0.5	2.1830	2.341506351
2	3	1	0.57735027	−0.57735027	1	−0.3169	0.5	1.3169	1.475480947
3	4	3	0.57735027	0.57735027	1	−1.1830	0.5	1.3169	1.908493649
4	2	6	−0.57735027	0.57735027	1	−1.1830	0.5	2.1830	2.774519053

We will now determine the matrix $[B]$ and the stiffness $t[B]^T[D][B]|J|$ at each Gauss point at the 4 sample points calling them $k_{g1}, k_{g2}, k_{g3}, k_{g4}$ where

$$[B]^T = \frac{1}{4|J|} \times \begin{bmatrix} -J_{22}(1-\eta) + J_{12}(1-\xi) & 0 & J_{21}(1-\eta) - J_{11}(1-\xi) \\ 0 & J_{21}(1-\eta) - J_{11}(1-\xi) & -J_{22}(1-\eta) + J_{12}(1-\xi) \\ J_{22}(1-\eta) + J_{12}(1+\xi) & 0 & -J_{21}(1-\eta) - J_{11}(1+\xi) \\ 0 & -J_{21}(1-\eta) - J_{11}(1+\xi) & J_{22}(1-\eta) + J_{12}(1+\xi) \\ J_{22}(1+\eta) - J_{12}(1+\xi) & 0 & -J_{21}(1+\eta) + J_{11}(1+\xi) \\ 0 & -J_{21}(1+\eta) + J_{11}(1+\xi) & J_{22}(1+\eta) - J_{12}(1+\xi) \\ -J_{22}(1+\eta) - J_{12}(1-\xi) & 0 & J_{21}(1+\eta) + J_{11}(1-\xi) \\ 0 & J_{21}(1+\eta) + J_{11}(1-\xi) & -J_{22}(1+\eta) - J_{12}(1-\xi) \end{bmatrix}$$

For point 1 the gauss points are $(-1/\sqrt{3}, -1/\sqrt{3})$ for which[50]

$[B] =$

−0.42102	0	0.3533	0	0.112815	0	−0.0451	0
0	−0.0842	0	−0.1293	0	0.0225	0	0.1909
−0.0842	−0.4210	−0.1293	0.3533	0.0225	0.1128	0.1909	−0.0451

50 The dotted line shown in the following page is a match line, meaning the matrix extend beyond the line in the same sequence.

$$[k_{g1}] = t\,[B]^T\,[D]\,[B]\,|J|$$

$$[k_{g1}] = \left[\begin{array}{cccc|cccc}
1.80\times10+07 & 2.21\times10+06 & -1.45\times10+07 & 2.45\times10+05 & -4.82\times10+06 & -5.93\times10+05 & 1.30\times10+06 & -1.87\times10+06 \\
2.21\times10+06 & 7.35\times10+06 & 1.30\times10+06 & -4.49\times10+06 & -5.93\times10+05 & -1.97\times10+06 & -2.92\times10+06 & -8.95\times10+05 \\
-1.45\times10+07 & 1.30\times10+06 & 1.31\times10+07 & -2.85\times10+06 & 3.87\times10+06 & -3.48\times10+05 & -2.52\times10+06 & 1.90\times10+06 \\
2.45\times10+05 & -4.49\times10+06 & -2.85\times10+06 & 6.35\times10+06 & -6.57\times10+04 & 1.20\times10+06 & 2.67\times10+06 & -3.06\times10+06 \\
-4.82\times10+06 & -5.93\times10+05 & 3.87\times10+06 & -6.57\times10+04 & 1.29\times10+06 & 1.59\times10+05 & -3.47\times10+05 & 5.00\times10+05 \\
-5.93\times10+05 & -1.97\times10+06 & -3.48\times10+05 & 1.20\times10+06 & 1.59\times10+05 & 5.28\times10+05 & 7.82\times10+05 & 2.40\times10+05 \\
1.30\times10+06 & -2.92\times10+06 & -2.52\times10+06 & 2.67\times10+06 & -3.47\times10+05 & 7.82\times10+05 & 1.57\times10+06 & -5.38\times10+05 \\
-1.87\times10+06 & -8.95\times10+05 & 1.90\times10+06 & -3.06\times10+06 & 5.00\times10+05 & 2.40\times10+05 & -5.38\times10+05 & 3.72\times10+06
\end{array}\right]$$

For point 2 the gauss points are $1/\sqrt{3}, -1/\sqrt{3}$ for which,

$$[k_{g2}] = \left[\begin{array}{cccc|cccc}
1.46\times10+07 & -9.32\times10+05 & -1.24\times10+07 & 2.87\times10+06 & -5.58\times10+06 & -1.17\times10+06 & 3.31\times10+06 & -7.69\times10+05 \\
-9.32\times10+05 & 5.62\times10+06 & 3.92\times10+06 & -5.48\times10+06 & -1.94\times10+06 & -1.60\times10+06 & -1.05\times10+06 & 1.47\times10+06 \\
-1.24\times10+07 & 3.92\times10+06 & 1.23\times10+07 & -4.96\times10+06 & 3.39\times10+06 & -2.93\times10+05 & -3.28\times10+06 & 1.33\times10+06 \\
2.87\times10+06 & -5.48\times10+06 & -4.96\times10+06 & 1.01\times10+07 & 7.59\times10+05 & -1.89\times10+06 & 1.33\times10+06 & -2.70\times10+06 \\
-5.58\times10+06 & -1.94\times10+06 & 3.39\times10+06 & 7.59\times10+05 & 3.10\times10+06 & 1.38\times10+06 & -9.08\times10+05 & -2.03\times10+05 \\
-1.17\times10+06 & -1.60\times10+06 & -2.93\times10+05 & -1.89\times10+06 & 1.38\times10+06 & 2.99\times10+06 & 7.84\times10+04 & 5.07\times10+05 \\
3.31\times10+06 & -1.05\times10+06 & -3.28\times10+06 & 1.33\times10+06 & -9.08\times10+05 & 7.84\times10+04 & 8.80\times10+05 & -3.56\times10+05 \\
-7.69\times10+05 & 1.47\times10+06 & 1.33\times10+06 & -2.70\times10+06 & -2.03\times10+05 & 5.07\times10+05 & -3.56\times10+05 & 7.23\times10+05
\end{array}\right]$$

For point 3 the gauss points are $1/\sqrt{3}, 1/\sqrt{3}$ for which,

$$[k_{g3}] = \left[\begin{array}{cccc|cccc}
1.29\times10+06 & 1.59\times10+05 & -3.47\times10+05 & 5.00\times10+05 & -4.82\times10+06 & -5.93\times10+05 & 3.87\times10+06 & -6.57\times10+04 \\
1.59\times10+05 & 5.28\times10+05 & 7.82\times10+05 & 2.40\times10+05 & -5.93\times10+05 & -1.97\times10+06 & -3.48\times10+05 & 1.20\times10+06 \\
-3.47\times10+05 & 7.82\times10+05 & 1.57\times10+06 & -5.38\times10+05 & 1.30\times10+06 & -2.92\times10+06 & -2.52\times10+06 & 2.67\times10+06 \\
5.00\times10+05 & 2.40\times10+05 & -5.38\times10+05 & 3.72\times10+06 & -1.87\times10+06 & -8.95\times10+05 & 1.90\times10+06 & -3.06\times10+06 \\
-4.82\times10+06 & -5.93\times10+05 & 1.30\times10+06 & -1.87\times10+06 & 1.80\times10+07 & 2.21\times10+06 & -1.45\times10+07 & 2.45\times10+05 \\
-5.93\times10+05 & -1.97\times10+06 & -2.92\times10+06 & -8.95\times10+05 & 2.21\times10+06 & 7.35\times10+06 & 1.30\times10+06 & -4.49\times10+06 \\
3.87\times10+06 & -3.48\times10+05 & -2.52\times10+06 & 1.90\times10+06 & -1.45\times10+07 & 1.30\times10+06 & 1.31\times10+07 & -2.85\times10+06 \\
-6.57\times10+04 & 1.20\times10+06 & 2.67\times10+06 & -3.06\times10+06 & 2.45\times10+05 & -4.49\times10+06 & -2.85\times10+06 & 6.35\times10+06
\end{array}\right]$$

For point 4 the gauss points are $-1/\sqrt{3}, 1/\sqrt{3}$ for which,

$$[k_{g4}] = \left[\begin{array}{cccc|cccc}
3.10\times10+06 & 1.38\times10+06 & -9.08\times10+05 & -2.03\times10+05 & -5.58\times10+06 & -1.94\times10+06 & 3.39\times10+06 & 7.59\times10+05 \\
1.38\times10+06 & 2.99\times10+06 & 7.84\times10+04 & 5.07\times10+05 & -1.17\times10+06 & -1.60\times10+06 & -2.93\times10+05 & -1.89\times10+06 \\
-9.08\times10+05 & 7.84\times10+04 & 8.80\times10+05 & -3.56\times10+05 & 3.31\times10+06 & -1.05\times10+06 & -3.28\times10+06 & 1.33\times10+06 \\
-2.03\times10+05 & 5.07\times10+05 & -3.56\times10+05 & 7.23\times10+05 & -7.69\times10+05 & 1.47\times10+06 & 1.33\times10+06 & -2.70\times10+06 \\
-5.58\times10+06 & -1.17\times10+06 & 3.31\times10+06 & -7.69\times10+05 & 1.46\times10+07 & -9.32\times10+05 & -1.24\times10+07 & 2.87\times10+06 \\
-1.94\times10+06 & -1.60\times10+06 & -1.05\times10+06 & 1.47\times10+06 & -9.32\times10+05 & 5.62\times10+06 & 3.92\times10+06 & -5.48\times10+06 \\
3.39\times10+06 & -2.93\times10+05 & -3.28\times10+06 & 1.33\times10+06 & -1.24\times10+07 & 3.92\times10+06 & 1.23\times10+07 & -4.96\times10+06 \\
7.59\times10+05 & -1.89\times10+06 & 1.33\times10+06 & -2.70\times10+06 & 2.87\times10+06 & -5.48\times10+06 & -4.96\times10+06 & 1.01\times10+07
\end{array}\right]$$

The total stiffness matrix for element is now given by

$$[K]_e = \sum_{i=1}^{4} [k_{gi}] = [k_{g1}] + [k_{g2}] + [k_{g3}] + [k_{g4}]$$

or

$$[K]_e = \left[\begin{array}{cccc|cccc}
\mathbf{3.70 \times 10 + 07} & 2.82 \times 10 + 06 & -2.81 \times 10 + 07 & 3.41 \times 10 + 06 & -2.08 \times 10 + 07 & -4.29 \times 10 + 06 & 1.19 \times 10 + 07 & -1.94 \times 10 + 06 \\
2.82 \times 10 + 06 & \mathbf{1.65 \times 10 + 07} & 6.08 \times 10 + 06 & -9.22 \times 10 + 06 & -4.29 \times 10 + 06 & -7.15 \times 10 + 06 & -4.61 \times 10 + 06 & -1.16 \times 10 + 05 \\
-2.81 \times 10 + 07 & 6.08 \times 10 + 06 & \mathbf{2.78 \times 10 + 07} & -8.70 \times 10 + 06 & 1.19 \times 10 + 07 & -4.61 \times 10 + 06 & -1.16 \times 10 + 07 & 7.23 \times 10 + 06 \\
3.41 \times 10 + 06 & -9.22 \times 10 + 06 & -8.70 \times 10 + 06 & \mathbf{2.09 \times 10 + 07} & -1.94 \times 10 + 06 & -1.16 \times 10 + 05 & 7.23 \times 10 + 06 & -1.15 \times 10 + 07 \\
\hline
-2.08 \times 10 + 07 & -4.29 \times 10 + 06 & 1.19 \times 10 + 07 & -1.94 \times 10 + 06 & \mathbf{3.70 \times 10 + 07} & 2.82 \times 10 + 06 & -2.81 \times 10 + 07 & 3.41 \times 10 + 06 \\
-4.29 \times 10 + 06 & -7.15 \times 10 + 06 & -4.61 \times 10 + 06 & -1.16 \times 10 + 05 & 2.82 \times 10 + 06 & \mathbf{1.65 \times 10 + 07} & 6.08 \times 10 + 06 & -9.22 \times 10 + 06 \\
1.19 \times 10 + 07 & -4.61 \times 10 + 06 & -1.16 \times 10 + 07 & 7.23 \times 10 + 06 & -2.81 \times 10 + 07 & 6.08 \times 10 + 06 & \mathbf{2.78 \times 10 + 07} & -8.70 \times 10 + 06 \\
-1.94 \times 10 + 06 & -1.16 \times 10 + 05 & 7.23 \times 10 + 06 & -1.15 \times 10 + 07 & 3.41 \times 10 + 06 & -9.22 \times 10 + 06 & -8.70 \times 10 + 06 & \mathbf{2.09 \times 10 + 07}
\end{array}\right]$$

This matrix will always be symmetric having diagonal element (K_{ii}) as positive. The correctness can be established by sum of any particular row or column – that will be zero.

2.12.18 Other form of isoparametric elements

We had shown earlier that for isoparametric element the geometric function is given by

$$x = \sum_{i=1}^{4} G_i x_i \quad \text{and} \quad y = \sum_{i=1}^{4} G_i y_i \tag{2.12.74}$$

which when transferred to iso-parametric domain gets transferred to $x = \sum_{i=1}^{4} N_i x_i$ and $y = \sum_{i=1}^{4} N_i y_i$. Here the term G_i defines the geometric interpolation function for the element and the term N_i is the polynomial function which describes the displacement at the node.

When $G_i = N_i$ the element is called *iso-parametric*.

For $G_i < N_i$ the element is called *sub-parametric*, and for $G_i > N_i$, they are called *super-parametric* element. Though isoparametric elements are the most popular sometimes the other forms as mentioned above are also used.

2.12.19 Iso-parametric formulation of CST element

We had derived the element stiffness matrix of CST element explicitly based on generalized global co-ordinate. We will see through Figure 2.12.23 how this element can be derived also from the iso-parametric formulation. We are not re-inventing the wheel for this derivation has an important bearing subsequently for deriving the element stiffness of four-nodded quadrilateral by a different method that we will study later.

Since the element is in natural coordinate, we write $x = \sum_{i=1}^{3} N_i x_i$ and $y = \sum_{i=1}^{3} N_i y_i$.

The above expression can be expanded in natural coordinate as

$$x = (x_1 - x_3)\,\xi + (x_2 - x_3)\eta + x_3 \quad \text{and} \quad y = (y_1 - y_3)\,\xi + (y_2 - y_3)\eta + y_3 \tag{2.12.75}$$

We had shown earlier while deriving the stiffness matrix $[K]_e$ for the quadrilateral element that relation between global and natural co-ordinate is given by

$$\begin{Bmatrix} \frac{\partial u}{\partial \xi} \\ \frac{\partial u}{\partial \eta} \end{Bmatrix} = [J] \begin{Bmatrix} \frac{\partial u}{\partial x} \\ \frac{\partial u}{\partial y} \end{Bmatrix} \quad \text{where } [J] = \begin{bmatrix} J_{11} & J_{12} \\ J_{21} & J_{22} \end{bmatrix} = \begin{bmatrix} \frac{\partial x}{\partial \xi} & \frac{\partial y}{\partial \xi} \\ \frac{\partial x}{\partial \eta} & \frac{\partial y}{\partial \eta} \end{bmatrix}$$

Differentiating the expression of x and y furnished above we have

$$[J] = \begin{bmatrix} x_1 - x_3 & y_1 - y_3 \\ x_2 - x_3 & y_2 - y_3 \end{bmatrix}$$

Thus $[J]^{-1} = \frac{1}{|J|} \begin{bmatrix} y_2 - y_3 & -(y_1 - y_3) \\ -(x_2 - x_3) & x_1 - x_3 \end{bmatrix}$ and $|J| = (x_1 - x_3)(y_2 - y_3) - (y_1 - y_3)(x_2 - x_3)$

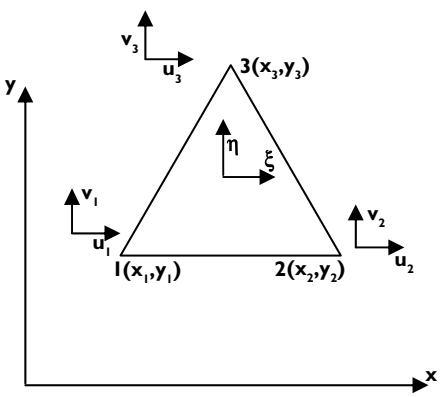


Figure 2.12.23 A CST element in global and natural coordinate.

Thus $$\begin{Bmatrix} \frac{\partial u}{\partial x} \\ \frac{\partial u}{\partial y} \end{Bmatrix} = [J]^{-1} \begin{Bmatrix} \frac{\partial u}{\partial \xi} \\ \frac{\partial u}{\partial \eta} \end{Bmatrix}; \quad \text{or} \quad \begin{Bmatrix} \frac{\partial u}{\partial x} \\ \frac{\partial u}{\partial y} \end{Bmatrix} = \frac{1}{|J|} \begin{bmatrix} y_2 - y_3 & -(y_1 - y_3) \\ -(x_2 - x_3) & x_1 - x_3 \end{bmatrix} \begin{Bmatrix} \frac{\partial u}{\partial \xi} \\ \frac{\partial u}{\partial \eta} \end{Bmatrix}.$$

This gives the relation between the global and natural coordinate. Similarly for other direction

$$\begin{Bmatrix} \frac{\partial v}{\partial x} \\ \frac{\partial v}{\partial y} \end{Bmatrix} = \frac{1}{|J|} \begin{bmatrix} y_2 - y_3 & -(y_1 - y_3) \\ -(x_2 - x_3) & x_1 - x_3 \end{bmatrix} \begin{Bmatrix} \frac{\partial v}{\partial \xi} \\ \frac{\partial v}{\partial \eta} \end{Bmatrix}$$

The strain matrix is given by

$$\begin{Bmatrix} \varepsilon_x \\ \varepsilon_y \\ \gamma_{xy} \end{Bmatrix} = \begin{Bmatrix} \frac{\partial u}{\partial x} \\ \frac{\partial v}{\partial y} \\ \frac{\partial u}{\partial y} + \frac{\partial v}{\partial x} \end{Bmatrix}$$

$$= \frac{1}{|J|} \begin{Bmatrix} (y_2 - y_3) \frac{\partial u}{\partial \xi} - (y_1 - y_3) \frac{\partial u}{\partial \eta} \\ -(x_2 - x_3) \frac{\partial v}{\partial \xi} + (x_1 - x_3) \frac{\partial v}{\partial \eta} \\ -(x_2 - x_3) \frac{\partial u}{\partial \xi} + (x_1 - x_3) \frac{\partial u}{\partial \eta} + (y_2 - y_3) \frac{\partial v}{\partial \xi} - (y_1 - y_3) \frac{\partial v}{\partial \eta} \end{Bmatrix} \tag{2.12.76}$$

Since the formulation is iso-parametric we can assume displacement functions as

$$u = (u_1 - u_3)\,\xi + (u_2 - u_3)\,\eta + u_3 \quad \text{and} \quad v = (v_1 - v_3)\,\xi + (v_2 - v_3)\,\eta + v_3 \tag{2.12.77}$$

Substituting the above values of u and v in strain matrix we have

$$\begin{Bmatrix} \varepsilon_x \\ \varepsilon_y \\ \gamma_{xy} \end{Bmatrix} = \frac{1}{|J|} \begin{Bmatrix} (y_2 - y_3)\,u_1 + (y_3 - y_1)\,u_2 + (y_1 - y_2)u_3 \\ (x_3 - x_2)\,v_1 + (x_1 - x_3)\,v_2 + (x_2 - x_1)\,v_3 \\ (x_3 - x_2)\,u_1 + (y_2 - y_3)v_1 + (x_1 - x_3)u_2 + (y_3 - y_1)v_2 \\ \quad +(x_2 - x_1)u_3 + (y_1 - y_2)v_3 \end{Bmatrix}$$

The above can be further expressed as

$$\begin{Bmatrix} \varepsilon_x \\ \varepsilon_y \\ \gamma_{xy} \end{Bmatrix} = \frac{1}{|J|} \begin{bmatrix} y_2 - y_3 & 0 & y_3 - y_1 & 0 & y_1 - y_2 & 0 \\ 0 & x_3 - x_2 & 0 & x_1 - x_3 & 0 & x_2 - x_1 \\ x_3 - x_2 & y_2 - y_3 & x_1 - x_3 & y_3 - y_1 & x_2 - x_1 & y_1 - y_2 \end{bmatrix} \begin{Bmatrix} u_1 \\ v_1 \\ u_2 \\ v_2 \\ u_3 \\ v_3 \end{Bmatrix}$$

i.e $\{\varepsilon\} = [B]\{\delta\}$ which gives

$$[B] = \frac{1}{|J|}\begin{bmatrix} y_2 - y_3 & 0 & y_3 - y_1 & 0 & y_1 - y_2 & 0 \\ 0 & x_3 - x_2 & 0 & x_1 - x_3 & 0 & x_2 - x_1 \\ x_3 - x_2 & y_2 - y_3 & x_1 - x_3 & y_3 - y_1 & x_2 - x_1 & y_1 - y_2 \end{bmatrix} \quad (2.12.78)$$

Considering $[K]_e = \iiint [B]^T [D][B]\, dv$ for constant thickness t we can express it as

$$[K]_e = A_e \times t \times [B]^T [D][B] \quad (2.12.79)$$

In this case as the element is independent of the orientation of the global axes x and y, Gauss integration is not required.

Example 2.12.2

For a plane stress triangular element as shown in Figure 2.12.24 calculate the element stiffness matrix based on isoparametric formulation. Consider E_{mat} = 2.85 x 10^8 kN/m^2 and ν = 0.25. The thickness of the element is 0.25 m.

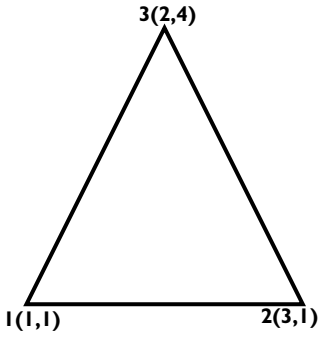


Figure 2.12.24

Solution:

The nodes and their coordinates are as shown hereafter in tabular form

Node Number	x_i	y_i
1	1	1
2	3	1
3	2	4

Thickness of triangle = 0.25 m; Area of triangle = 3.0 m^2

$$[D] = \frac{E}{1-\nu^2}\begin{bmatrix} 1 & \nu & 0 \\ \nu & 1 & 0 \\ 0 & 0 & \dfrac{1-\nu}{2} \end{bmatrix} = \begin{bmatrix} 2.99\times10^8 & 7.47\times10^7 & 0 \\ 7.47\times10^7 & 2.99\times10^8 & 0 \\ 0 & 0 & 1.12\times10^8 \end{bmatrix}$$

$|J| = (x_1 - x_3)(y_2 - y_3) - (y_1 - y_3)(x_2 - x_3)$ which gives $|J| = (1-2)(1-4) - (1-4)(3-2) = 6$

$$[B] = \frac{1}{|J|}\begin{bmatrix} y_2-y_3 & 0 & y_3-y_1 & 0 & y_1-y_2 & 0 \\ 0 & x_3-x_2 & 0 & x_1-x_3 & 0 & x_2-x_1 \\ x_3-x_2 & y_2-y_3 & x_1-x_3 & y_3-y_1 & x_2-x_1 & y_1-y_2 \end{bmatrix}$$

$$\text{or,}\quad [B] = \begin{bmatrix} -0.5 & 0 & 0.5 & 0 & 0 & 0 \\ 0 & -0.16667 & 0 & -0.16667 & 0 & 0.33333 \\ -0.16667 & -0.5 & -0.16667 & 0.5 & 0.3333 & 0 \end{bmatrix}$$

Considering the stiffness matrix as $[K]_e = A_e \times t \times [B]^T [D] [B]$ we have

$[K]_e =$

$5.83\times10^{+07}$	$1.17\times10^{+07}$	$-5.37\times10^{+07}$	$-2.33\times10^{+06}$	$-4.67\times10^{+06}$	$-9.33\times10^{+06}$
$1.17\times10^{+07}$	$2.72\times10^{+07}$	$2.33\times10^{+06}$	$-1.48\times10^{+07}$	$-1.40\times10^{+07}$	$-1.24\times10^{+07}$
$-5.37\times10^{+07}$	$2.33\times10^{+06}$	$5.83\times10^{+07}$	$-1.17\times10^{+07}$	$-4.67\times10^{+06}$	$9.33\times10^{+06}$
$-2.33\times10^{+06}$	$-1.48\times10^{+07}$	$-1.17\times10^{+07}$	$2.72\times10^{+07}$	$1.40\times10^{+07}$	$-1.24\times10^{+07}$
$-4.67\times10^{+06}$	$-1.40\times10^{+07}$	$-4.67\times10^{+06}$	$1.40\times10^{+07}$	$9.33\times10^{+06}$	$0.00\times10^{+00}$
$-9.33\times10^{+06}$	$-1.24\times10^{+07}$	$9.33\times10^{+06}$	$-1.24\times10^{+07}$	$0.00\times10^{+00}$	$2.49\times10^{+07}$

2.12.20 Condensation – The Houdini[51] trick of vanishing nodes

Many of you must have seen a magician perform on stage, vanishing before your eyes a number of objects like a rabbit, pigeon coins etc. It is of course an illusion, for the objects do not actually vanish and are very much there. The magician only creates an illusion that this is gone. Condensation technique is also something very similar to this. It is a vanishing or an elimination trick where the desired or an unwanted degree of freedom vanishes from the matrix reducing the size, though the effect of the eliminated degree of freedom is still retained in the original matrix.

This particular technique has great application in FEM and structural dynamics for developing compound element and as an eigen-value economizer respectively. Since

[51] Houdini was a great magician who pioneered the art of vanishing objects before the audience, which in technical term is called "Shuffling". In professional magician's circle the art of vanishing an object is popularly known as "Doing a Houdini".

the reduction is carried out over static equilibrium equation the method is also called "*Static Condensation Technique*" among finite element analysts.

Let us consider the static equilibrium condition in matrix notation

$$\begin{bmatrix} [K_{11}] & [K_{12}] \\ [K_{21}] & [K_{22}] \end{bmatrix} \begin{Bmatrix} \{u_1\} \\ \{u_2\} \end{Bmatrix} = \begin{Bmatrix} \{P_1\} \\ \{P_2\} \end{Bmatrix} \tag{2.12.80}$$

where $K_{11}, K_{12} \ldots\ldots K_{22}$ etc. are stiffness of the system where they could either be a number or a sub-matrix, u_1, u_2 are displacements which are either a number or a sub-matrix and P_1 and P_2 are nodal loads acting on u_1 and u_2.

We presume that for some reason we want to eliminate the u_2 degree of freedom from the matrix.

To eliminate u_2 we expand the above equilibrium equation to get

$$[K_{11}]\{u_1\} + [K_{12}]\{u_2\} = \{P_1\} \quad \text{and} \quad [K_{21}]\{u_1\} + [K_{22}]\{u_2\} = \{P_2\} \tag{2.12.81}$$

From the second equation we have

$$\{u_2\} = \frac{\{P_2\} - [K_{21}]\{u_1\}}{[K_{22}]} = [K_{22}]^{-1}\{\{P_2\} - [K_{21}]\{u_1\}\} \tag{2.12.82}$$

Substituting this in the first equation we have

$$[K_{11}][u_1] + [K_{12}]\{[K_{22}]^{-1}[[P_2] - [K_{21}][u_1]]\} = [P_1] \tag{2.12.83}$$

The above on simplification gives

$$[[K_{11}] - [K_{12}][K_{22}]^{-1}[K_{21}]]\{u_1\} = \{P_1\} - [K_{12}][K_{22}]^{-1}\{P_2\} \tag{2.12.84}$$

Considering $[K_c]$ and $\{P_c\}$ as condensed stiffness and load matrix we have

$$[K_c]\{u_1\} = \{P_c\} \tag{2.12.85}$$

where $[K_c] = [[K_{11}] - [K_{12}][K_{22}]^{-1}[K_{21}]]$ and $\{P_c\} = \{P_1\} - [K_{12}][K_{22}]^{-1}\{P_2\}$

Example 2.12.3

For a particular system the stiffness and load matrix are as given hereafter

$$[K] = \begin{bmatrix} 10 & -5 & 0 & 4 \\ -5 & 20 & 2 & 4 \\ 0 & 2 & 40 & 12 \\ 4 & 4 & 12 & 400 \end{bmatrix} \quad \text{and} \quad \{P\} = \begin{Bmatrix} 100 \\ 20 \\ 50 \\ -10 \end{Bmatrix}$$

The equilibrium equation is given by $[K]\{u\} = \{P\}$ where $\{u\}^T = \langle u_1\ u_2\ u_3\ u_4 \rangle$.

Eliminate u_4 from the system by static condensation and compare the values of u_1, u_2 and u_3 with the original matrix.

Solution:

Here considering $[K]\{u\} = \{P\}$ we have

$$\left[\begin{array}{cccc|c} 10 & -5 & 0 & | & 4 \\ -5 & 20 & 2 & | & 4 \\ 0 & 2 & 40 & | & 12 \\ \hline 4 & 4 & 12 & | & 400 \end{array}\right] \begin{Bmatrix} u_1 \\ u_2 \\ u_3 \\ u_4 \end{Bmatrix} = \begin{Bmatrix} 100 \\ 20 \\ 50 \\ -10 \end{Bmatrix}$$

Since we want to eliminate u_4 we partition the matrix as shown by dotted line representing the above matrix as

$$\begin{bmatrix} \{K_{11}\} & \{K_{12}\} \\ \{K_{21}\} & \{K_{22}\} \end{bmatrix}; \quad \text{where } [K_{11}] = \begin{bmatrix} 10 & -5 & 0 \\ -5 & 20 & 2 \\ 0 & 2 & 40 \end{bmatrix}, [K_{12}] = \begin{Bmatrix} 4 \\ 4 \\ 12 \end{Bmatrix},$$

$$[K_{21}] = \begin{bmatrix} 4 & 4 & 12 \end{bmatrix}, [K_{22}] = 400$$

Considering the expression

$$[K_c] = [[K_{11}] - [K_{12}]\,[K_{22}]^{-1}\,[K_{21}]], \quad \text{we have}$$

$$[K_c] = \begin{bmatrix} 10 & -5 & 0 \\ -5 & 20 & 2 \\ 0 & 2 & 40 \end{bmatrix} - \frac{1}{400} \begin{bmatrix} 4 \\ 4 \\ 12 \end{bmatrix} \begin{bmatrix} 4 & 4 & 12 \end{bmatrix}$$

$$= \begin{bmatrix} 9.96 & -5.04 & -0.12 \\ -5.4 & 19.96 & 1.88 \\ -0.12 & 1.88 & 39.64 \end{bmatrix}$$

The condensed load matrix is given by

$$\{P_c\} = \{P_1\} - [K_{12}]\,[K_{22}]^{-1}\,\{P_2\};$$

$$\{P_c\} = \begin{Bmatrix} 100 \\ 20 \\ 50 \end{Bmatrix} - \frac{-10}{400} \begin{Bmatrix} 4 \\ 4 \\ 12 \end{Bmatrix} = \begin{Bmatrix} 100.1 \\ 20.1 \\ 50.3 \end{Bmatrix}$$

Substituting the above values in the expression $[K_c]\{u_c\} = \{P_c\}$ and solving in math-cad we have

$$\begin{Bmatrix} u_1 \\ u_2 \\ u_3 \end{Bmatrix} = \begin{Bmatrix} 12.061032 \\ 3.947161 \\ 1.118231 \end{Bmatrix}$$ the original matrix gives the values as

$$\begin{Bmatrix} u_1 \\ u_2 \\ u_3 \\ u_4 \end{Bmatrix} = \begin{Bmatrix} 12.061032 \\ 3.947161 \\ 1.118231 \\ -0.218629 \end{Bmatrix}.$$

The results are found to be exactly matching in this case.

2.12.21 Alternative method of deriving a quadrilateral element

Element stiffness matrix of a quadrilateral element can also be derived from assemblage of four CST elements as shown in Figure 2.12.25.

In this case, after generating the element stiffness matrix for each of the four CST elements they are assembled to form the quadrilateral element as shown in the figure.

Since each of the CST elements has two degrees of freedom per node the global assemblage gives a matrix that has an order of 10×10. While that of a normal quadrilateral element is 8×8.

This is achieved by eliminating the node 5 (marked by a dotted circle in the figure) by means of static condensation. One of the CST elements is shown in Figure 2.12.26.

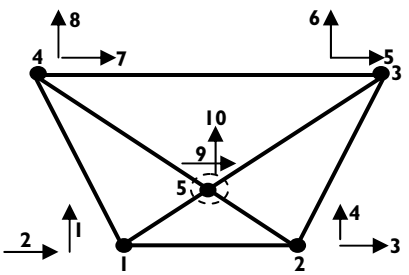


Figure 2.12.25 Four-nodded quadrilateral as an assemblage of four CST elements.

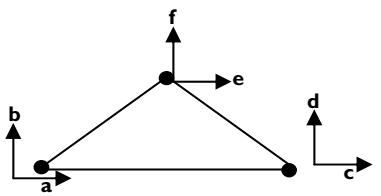


Figure 2.12.26 A CST element with local degrees of freedom.

Let the element stiffness matrix for an element i be expressed as

$$[K]_i = \begin{bmatrix} (K_{11})_i & (K_{12})_i & (K_{13})_i & (K_{14})_i & (K_{15})_i & (K_{16})_i \\ (K_{21})_i & (K_{22})_i & (K_{23})_i & (K_{24})_i & (K_{25})_i & (K_{26})_i \\ (K_{31})_i & (K_{32})_i & (K_{33})_i & (K_{34})_i & (K_{35})_i & (K_{36})_i \\ (K_{41})_i & (K_{42})_i & (K_{43})_i & (K_{44})_i & (K_{45})_i & (K_{46})_i \\ (K_{51})_i & (K_{52})_i & (K_{53})_i & (K_{54})_i & (K_{55})_i & (K_{56})_i \\ (K_{61})_i & (K_{62})_i & (K_{63})_i & (K_{64})_i & (K_{65})_i & (K_{66})_i \end{bmatrix} \tag{2.12.86}$$

Here the subscript i outside the parenthesis represents the element number. The local and global coordinate relations are as given hereafter

Element number	*Local coordinate*	*a*	*b*	*c*	*d*	e	*f*
1	Global coordinate	1	2	3	4	9	10
2	Global coordinate	3	4	5	6	9	10
3	Global coordinate	5	6	7	8	9	10
4	Global coordinate	1	2	7	8	9	10

Assembling the four elements we get the global matrix as shown hereafter

$$[\mathbf{K}]_G =$$

$$\begin{bmatrix} (K_{11})_1 + (K_{11})_4 & (K_{12})_1 + (K_{12})_4 & (K_{13})_1 & (K_{14})_1 \\ (K_{21})_1 + (K_{21})_4 & (K_{22})_1 + (K_{11})_2 + (K_{22})_4 & (K_{23})_1 + (K_{12})_2 & (K_{24})_1 \\ (K_{31})_1 & (K_{32})_1 + (K_{21})_2 & (K_{33})_1 + (K_{22})_2 & (K_{34})_1 \\ (K_{41})_1 & (K_{42})_1 & (K_{43})_1 & (K_{44})_1 \\ 0 & (K_{31})_2 & (K_{32})_2 & 0 \\ 0 & (K_{41})_2 & (K_{42})_2 & 0 \\ (K_{31})_4 & (K_{32})_4 & 0 & 0 \\ (K_{41})_4 & (K_{42})_4 & 0 & 0 \\ (K_{51})_1 + (K_{51})_4 & (K_{52})_1 + (K_{51})_2 + (K_{52})_4 & (K_{53})_1 + (K_{53})_2 & (K_{54})_1 \\ (K_{61})_1 + (K_{61})_4 & (K_{62})_1 + (K_{61})_2 + (K_{62})_4 & (K_{63})_1 + (K_{61})_2 & (K_{64})_1 \end{bmatrix}$$

$$\begin{bmatrix} 0 & 0 & (K_{13})_4 & (K_{14})_4 \\ (K_{13})_2 & (K_{14})_2 & (K_{23})_4 & (K_{24})_4 \\ (K_{23})_2 & (K_{24})_2 & 0 & 0 \\ 0 & 0 & 0 & 0 \\ (K_{33})_2 + (K_{11})_3 & (K_{34})_2 + (K_{12})_3 & (K_{13})_3 & (K_{14})_3 \\ (K_{43})_2 + (K_{21})_3 & (K_{44})_2 + (K_{22})_3 & (K_{23})_3 & (K_{24})_3 \\ (K_{31})_3 & (K_{32})_3 & (K_{33})_3 + (K_{33})_4 & (K_{34})_3 + (K_{34})_4 \\ (K_{41})_3 & (K_{42})_3 & (K_{43})_3 + (K_{43})_4 & (K_{44})_3 + (K_{44})_4 \\ (K_{53})_2 + (K_{51})_3 & (K_{54})_2 + (K_{52})_3 & (K_{53})_3 + (K_{53})_4 & (K_{54})_3 + (K_{54})_4 \\ (K_{63})_2 + (K_{61})_3 & (K_{64})_2 + (K_{62})_3 & (K_{63})_3 + (K_{63})_4 & (K_{64})_3 + (K_{64})_4 \end{bmatrix}$$

$$
\begin{array}{ll}
| \ (K_{15})_1 + (K_{15})_4 & (K_{16})_1 + (K_{16})_4 \\
| \ (K_{25})_1 + (K_{15})_2 + (K_{25})_4 & (K_{26})_1 + (K_{16})_2 + (K_{26})_4 \\
| \ (K_{35})_1 + (K_{35})_2 & (K_{36})_1 + (K_{36})_2 \\
| \ (K_{45})_1 & (K_{46})_1 \\
| \ (K_{35})_2 + (K_{15)3} & (K_{36})_2 + (K_{16})_3 \\
| \ (K_{45})_2 + (_{K25})_3 & (K_{46})_2 + (K_{26})_3 \\
| \ (K_{35})_3 + (K_{35})_4 & (K_{36})_3 + (K_{36})_4 \\
| \ (K_{45})_3 + (K_{45})_4 & (K_{46})_3 + (K_{46})_4 \\
| \ (K_{55})_1 + (K_{55})_2 + (K_{55})_3 + (K_{55})_4 & (K_{56})_1 + (K_{56})_2 + (K_{56})_3 + (K_{56})_4 \\
| \ (K_{65})_1 + (K_{65})_2 + (K_{65})_3 + (K_{65})_4 & (K_{66})_1 + (K_{66})_2 + (K_{66})_3 + (K_{66})_4
\end{array}
$$

The global displacement vector is given by

$$\{U\}^T = \langle u_1 \ u_2 \ u_3 \ u_4 \ u_5 \ u_6 \ u_7 \ u_8 \ u_9 \ u_{10} \rangle \tag{2.12.87}$$

Once the global matrix is formed the displacements u_9 *and* u_{10} *which are the displacements for the internal node needs to be condensed out*. This crunches the assembled 10×10 matrix to the desired 8×8 matrix for a four nodded quadrilateral element.

2.12.22 The Reverse Logic – How correct it is?

Many people believe that since a quadrilateral is an improved element over CST and because a quadrilateral element can be derived from assemblage of 4 CST the reverse is also true.

That is, a CST may be obtained from a quadrilateral (having nodes i, j, k, l) by defining $k = l$ and this will give an improved result. If an element is defined in such a fashion in any standard commercial FEM software it will not destabilize and would indeed give a stiffness matrix that is symmetric, but on comparison it has been found that in such degenerated element error induced is quite high and should be avoided as far as practicable.

2.12.23 Incompatible or Non-conforming element – Where two wrongs make one right[52]

It is unfortunate that many users who use FEM almost regularly do not appreciate the power of this element and how much effort can be reduced by judicious use of this.

We had stated earlier that Rectangular and Quadrilateral Elements though gives better results than CST are not so accurate under flexural load. However for cases such as shown in Figure 2.12.27, the flexural behavior of the system is inevitable.

52 Comment of Prof. G. Strang, Dept. of Mathematics-MIT, on reviewing Prof Ed Wilson's derivation of the maverick formulation.

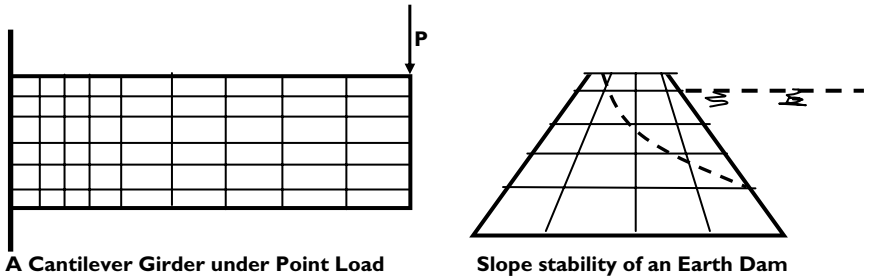


Figure 2.12.27 Systems where flexural behavior dominates.

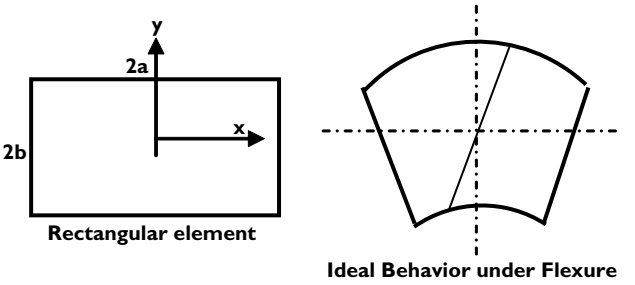


Figure 2.12.28 Rectangular element ideal deformation under flexure.

So, what do we do, if we want to do a FEM analysis? Shall we accept such erroneous result? Or abandon the use of such element for the problems as posed above, proclaiming FEM a failure?

The situation is not so bad as it seems for people especially not so conversant with non-conforming element would usually try to overcome this by

- Use of refined meshes in the area of high stress gradient.
- Use of higher order elements whose inherent polynomial function – the very backbone of stiffness matrix, are much better equipped to simulate this behavior.

The above solutions are not without its problem. For instance in the earth dam problem it is difficult to identify the area where the major stress will be induced (the critical slip circle), and one has to make a number of trial runs before arriving at a correct refined mesh zone – this means more effort, more time = "More Money".

While using higher order elements the number of nodes increases significantly resulting in more input effort and the model in hand, if it is big the cost of run can surely become quite expensive.

The third alternative is to improve the performance of the 4 nodded quadrilateral (Figure 2.12.28*) itself by inducing correction to it so that its flexural behavior gets better.* This was what was attempted by Wilson et al. (1973) and we would like to discuss it here.

Previously while introducing this element to you, we had just mentioned about its inadequacy against flexural behavior without trying to analyze – why it happens? Except mentioning the fact that parasitic shear locks the meshes.

In this section we would examine the behavior of this element a bit more carefully.

From our knowledge of strength of material we know that for a rectangular section under flexure

$$\sigma_x = \frac{E}{R}y, \quad \sigma_y = \tau_{xy} = 0, \tag{2.12.88}$$

where $R =$ radius of curvature of the beam; $y =$ distance of extreme fiber from the neutral axis and $E =$ modulus of elasticity.

The strain within the element is given by

$$\varepsilon_x = \frac{\partial u}{\partial x} = \frac{y}{R}; \quad \varepsilon_y = \frac{\partial v}{\partial y} = -\frac{\nu y}{R} \quad \text{and} \quad \gamma_{xy} = \frac{\partial u}{\partial y} + \frac{\partial v}{\partial x} = 0 \tag{2.12.89}$$

Integrating the strain expression in x direction we have

$$u = \frac{xy}{R} + C_1, \tag{2.12.90}$$

where C_1 is an integration constant.

Now since at the origin (i.e. the centroid of the section) we have at $x = 0$ $u = 0$, imposing this boundary condition we have $C_1 = 0$ which gives

$$u = \frac{xy}{R} \tag{2.12.91}$$

Similarly integrating the strain equation in y direction we have, $v = -\dfrac{\nu y^2}{2R} + C_2$.

Since $\gamma_{xy} = \dfrac{\partial u}{\partial y} + \dfrac{\partial v}{\partial x} = 0$ we have $\dfrac{\partial v}{\partial x} = -\dfrac{\partial u}{\partial y} = -\dfrac{x}{R}$ $\left[\because u = \dfrac{xy}{R}\right]$

Thus $v = -\frac{x^2}{2R} + C_3$. Hence, v can be expressed as $v = -\frac{x^2}{2R} - \frac{\nu y^2}{2R} + C_2 + C_3$.

$$\rightarrow \quad v = -\frac{x^2}{2R} - \frac{\nu y^2}{2R} + C_4, \tag{2.12.92}$$

where $C_4 = C_2 + C_3$

Since $v = 0$ across the cross section of the element, at four corners we have $v = 0$ at $x = \pm a$ and $y = \pm b \Rightarrow C_4 = \frac{a^2}{2R} + \frac{\nu b^2}{2R}$ which gives

$$v = \left(1 - \frac{x^2}{a^2}\right)\frac{a^2}{2R} + \left(1 - \frac{y^2}{b^2}\right)\frac{\nu b^2}{2R} \tag{2.12.93}$$

Now assuming, $\alpha_1 = \frac{1}{R}, \alpha_2 = \frac{a^2}{2R}$ and $\alpha_3 = \frac{b^2}{2R}$ we can write

$$u = \alpha_1 xy; \quad v = \alpha_2 \left(1 - \frac{x^2}{a^2}\right) + \alpha_3 \left(1 - \frac{y^2}{b^2}\right). \tag{2.12.94}$$

Thus looking at the displacement function it is seen that under flexural mode the polynomial function for the quadrilateral element simulates correctly the behavior in x direction. However, for y direction the absence of the quadratic term makes it stiffer as such is incapable of projecting the flexural behavior properly.

To simulate this behavior Wilson proposed to modify the displacement function as follows.

He proposed

$$\begin{aligned} u &= N_1 u_1 + N_2 u_2 + N_3 u_3 + N_4 u_4 + N_5 \alpha_1 + N_6 \alpha_2 \quad \text{and} \\ v &= N_1 v_1 + N_2 v_2 + N_3 v_3 + N_4 v_4 + N_5 \alpha_3 + N_6 \alpha_4 \end{aligned} \tag{2.12.95}$$

Here as derived earlier $N_1 = \frac{(1-\xi)(1-\eta)}{4}, N_2 = \frac{(1+\xi)(1-\eta)}{4}, N_3 = \frac{(1+\xi)(1+\eta)}{4}, N_4 = \frac{(1-\xi)(1+\eta)}{4}$ and $N_5 = (1-\xi^2), N_6 = (1-\eta^2)$ – the two missing terms which conforming elements do not cater to[53].

We had shown earlier while deriving the stiffness matrix $[K]_e$ for the conforming quadrilateral element that relation between global and natural co-ordinate is given by

$$\begin{Bmatrix} \frac{\partial u}{\partial \xi} \\ \frac{\partial u}{\partial \eta} \end{Bmatrix} = [J] \begin{Bmatrix} \frac{\partial u}{\partial x} \\ \frac{\partial u}{\partial y} \end{Bmatrix} \quad \text{where } [J] = \begin{bmatrix} J_{11} & J_{12} \\ J_{21} & J_{22} \end{bmatrix} = \begin{bmatrix} \frac{\partial x}{\partial \xi} & \frac{\partial y}{\partial \xi} \\ \frac{\partial x}{\partial \eta} & \frac{\partial y}{\partial \eta} \end{bmatrix} \tag{2.12.96}$$

Here

$$\begin{aligned} x &= \frac{(1-\xi)(1-\eta)}{4} x_1 + \frac{(1+\xi)(1-\eta)}{4} x_2 + \frac{(1+\xi)(1+\eta)}{4} x_3 \\ &\quad + \frac{(1-\xi)(1+\eta)}{4} x_4 \quad \text{and} \\ y &= \frac{(1-\xi)(1-\eta)}{4} y_1 + \frac{(1+\xi)(1-\eta)}{4} y_2 + \frac{(1+\xi)(1+\eta)}{4} y_3 \\ &\quad + \frac{(1-\xi)(1+\eta)}{4} y_4 \end{aligned} \tag{2.12.97}$$

53 The two wrongs that violate the compatibility law.

which gives

$$
\begin{aligned}
J_{11} &= \left[\frac{(\eta-1)}{4}x_1 + \frac{(1-\eta)}{4}x_2 + \frac{(1+\eta)}{4}x_3 - \frac{(1+\eta)}{4}x_4\right] \\
J_{12} &= \frac{1}{4}\left[(\eta-1)\,y_1 + (1-\eta)\,y_2 + (1+\eta)\,y_3 - (1+\eta)\,y_4\right] \\
J_{21} &= \frac{1}{4}\left[(\xi-1)\,x_1 - (1+\xi)\,x_2 + (1+\xi)\,x_3 + (1-\xi)\,x_4\right] \\
J_{22} &= \frac{1}{4}\left[(\xi-1)\,y_1 - (1+\xi)\,y_2 + (1+\xi)\,y_3 + (1-\xi)\,y_4\right]
\end{aligned}
\tag{2.12.98}
$$

This displacement relation in terms of the Jacobian matrix can now be expressed as $\begin{Bmatrix} \frac{\partial u}{\partial x} \\ \frac{\partial u}{\partial y} \end{Bmatrix} = [J]^{-1} \begin{Bmatrix} \frac{\partial u}{\partial \xi} \\ \frac{\partial u}{\partial \eta} \end{Bmatrix}$ which can be expanded to $\begin{Bmatrix} \frac{\partial u}{\partial x} \\ \frac{\partial u}{\partial y} \end{Bmatrix} = \frac{1}{|J|}\begin{bmatrix} J_{22} & -J_{12} \\ -J_{21} & J_{11} \end{bmatrix} \begin{Bmatrix} \frac{\partial u}{\partial \xi} \\ \frac{\partial u}{\partial \eta} \end{Bmatrix}$ where the term $|J|$ represents the determinant of the Jacobian.

Since the interpolation function remains same for the displacement v, proceeding in identical manner we have

$$
\begin{Bmatrix} \dfrac{\partial v}{\partial x} \\ \dfrac{\partial v}{\partial y} \end{Bmatrix} = \frac{1}{|J|}\begin{bmatrix} J_{22} & -J_{12} \\ -J_{21} & J_{11} \end{bmatrix} \begin{Bmatrix} \dfrac{\partial v}{\partial \xi} \\ \dfrac{\partial v}{\partial \eta} \end{Bmatrix}
$$

Thus, the strain matrix can now be expressed as

$$
\begin{Bmatrix} \varepsilon_x \\ \varepsilon_y \\ \gamma_{xy} \end{Bmatrix} = \begin{Bmatrix} \dfrac{\partial u}{\partial x} \\ \dfrac{\partial v}{\partial y} \\ \dfrac{\partial u}{\partial y} + \dfrac{\partial v}{\partial x} \end{Bmatrix} = \frac{1}{|J|}\begin{bmatrix} J_{22} & -J_{12} & 0 & 0 \\ 0 & 0 & -J_{21} & J_{11} \\ -J_{21} & J_{11} & J_{22} & -J_{12} \end{bmatrix} \left\langle \frac{\partial u}{\partial \xi} \;\; \frac{\partial u}{\partial \eta} \;\; \frac{\partial v}{\partial \xi} \;\; \frac{\partial v}{\partial \eta} \right\rangle^T
$$

or $\begin{Bmatrix} \varepsilon_x \\ \varepsilon_y \\ \gamma_{xy} \end{Bmatrix} = [G]\left\langle \frac{\partial u}{\partial \xi} \;\; \frac{\partial u}{\partial \eta} \;\; \frac{\partial v}{\partial \xi} \;\; \frac{\partial v}{\partial \eta} \right\rangle^T$ where $[G] = \frac{1}{|J|}\begin{bmatrix} J_{22} & -J_{12} & 0 & 0 \\ 0 & 0 & -J_{21} & J_{11} \\ -J_{21} & J_{11} & J_{22} & -J_{12} \end{bmatrix}$

Since $u = \sum_{i=1}^{6} N_i(\xi,\eta)u_i : v = \sum_{i=1}^{6} N_i(\xi,\eta)v_i$ we have

$$
\begin{aligned}
u &= N_1u_1 + N_2u_2 + N_3u_3 + N_4u_4 + N_5\alpha_1 + N_6\alpha_2 \\
v &= N_1v_1 + N_2v_2 + N_3v_3 + N_4v_4 + N_5\alpha_3 + N_6\alpha_4
\end{aligned}
\tag{2.12.99}
$$

This gives

$$\begin{Bmatrix} \frac{\partial u}{\partial \xi} \\ \frac{\partial u}{\partial \eta} \\ \frac{\partial v}{\partial \xi} \\ \frac{\partial v}{\partial \eta} \end{Bmatrix} = \begin{bmatrix} \frac{\partial N_1}{\partial \xi} & \frac{\partial N_2}{\partial \xi} & \frac{\partial N_3}{\partial \xi} & \frac{\partial N_4}{\partial \xi} & \frac{\partial N_5}{\partial \xi} & \frac{\partial N_6}{\partial \xi} & 0 & 0 & 0 & 0 & 0 & 0 \\ \frac{\partial N_1}{\partial \eta} & \frac{\partial N_2}{\partial \eta} & \frac{\partial N_3}{\partial \eta} & \frac{\partial N_4}{\partial \eta} & \frac{\partial N_5}{\partial \eta} & \frac{\partial N_6}{\partial \eta} & 0 & 0 & 0 & 0 & 0 & 0 \\ 0 & 0 & 0 & 0 & 0 & 0 & \frac{\partial N_1}{\partial \xi} & \frac{\partial N_2}{\partial \xi} & \frac{\partial N_3}{\partial \xi} & \frac{\partial N_4}{\partial \xi} & \frac{\partial N_5}{\partial \xi} & \frac{\partial N_6}{\partial \xi} \\ 0 & 0 & 0 & 0 & 0 & 0 & \frac{\partial N_1}{\partial \eta} & \frac{\partial N_2}{\partial \eta} & \frac{\partial N_3}{\partial \eta} & \frac{\partial N_4}{\partial \eta} & \frac{\partial N_5}{\partial \eta} & \frac{\partial N_6}{\partial \eta} \end{bmatrix} \times \langle u_1 \ u_2 \ u_3 \ u_4 \ \alpha_1 \ \alpha_2 \ v_1 \ v_2 \ v_3 \ v_4 \ \alpha_3 \ \alpha_4 \rangle^T$$

$$\begin{Bmatrix} \varepsilon_x \\ \varepsilon_y \\ \gamma_{xy} \end{Bmatrix} = [G]$$

$$\times \begin{bmatrix} \frac{\partial N_1}{\partial \xi} & \frac{\partial N_2}{\partial \xi} & \frac{\partial N_3}{\partial \xi} & \frac{\partial N_4}{\partial \xi} & \frac{\partial N_5}{\partial \xi} & \frac{\partial N_6}{\partial \xi} & 0 & 0 & 0 & 0 & 0 & 0 \\ \frac{\partial N_1}{\partial \eta} & \frac{\partial N_2}{\partial \eta} & \frac{\partial N_3}{\partial \eta} & \frac{\partial N_4}{\partial \eta} & \frac{\partial N_5}{\partial \eta} & \frac{\partial N_6}{\partial \eta} & 0 & 0 & 0 & 0 & 0 & 0 \\ 0 & 0 & 0 & 0 & 0 & 0 & \frac{\partial N_1}{\partial \xi} & \frac{\partial N_2}{\partial \xi} & \frac{\partial N_3}{\partial \xi} & \frac{\partial N_4}{\partial \xi} & \frac{\partial N_5}{\partial \xi} & \frac{\partial N_6}{\partial \xi} \\ 0 & 0 & 0 & 0 & 0 & 0 & \frac{\partial N_1}{\partial \eta} & \frac{\partial N_2}{\partial \eta} & \frac{\partial N_3}{\partial \eta} & \frac{\partial N_4}{\partial \eta} & \frac{\partial N_5}{\partial \eta} & \frac{\partial N_6}{\partial \eta} \end{bmatrix} \times \langle u_1 \ u_2 \ u_3 \ u_4 \ \alpha_1 \ \alpha_2 \ v_1 \ v_2 \ v_3 \ v_4 \ \alpha_3 \ \alpha_4 \rangle^T$$

$$\begin{Bmatrix} \varepsilon_x \\ \varepsilon_y \\ \gamma_{xy} \end{Bmatrix} = \frac{1}{|J|} \begin{bmatrix} J_{22} & -J_{12} & 0 & 0 \\ 0 & 0 & -J_{21} & J_{11} \\ -J_{21} & J_{11} & J_{22} & -J_{12} \end{bmatrix}$$

$$\times \frac{1}{4} \begin{bmatrix} \eta-1 & 1-\eta & 1+\eta & -(1+\eta) & -8\xi & 0 & 0 & 0 & 0 & 0 & 0 & 0 \\ \xi-1 & -(1+\xi) & 1+\xi & 1-\xi & 0 & -8\eta & 0 & 0 & 0 & 0 & 0 & 0 \\ 0 & 0 & 0 & 0 & 0 & 0 & \eta-1 & 1-\eta & 1+\eta & -(1+\eta) & -8\xi & 0 \\ 0 & 0 & 0 & 0 & 0 & 0 & \xi-1 & -(1+\xi) & 1+\xi & 1-\xi & 0 & -8\eta \end{bmatrix}$$

$$\times \langle u_1 \ u_2 \ u_3 \ u_4 \ \alpha_1 \ \alpha_2 \ v_1 \ v_2 \ v_3 \ v_4 \ \alpha_3 \ \alpha_4 \rangle^T$$

The above can be adjusted and written as

$$\begin{Bmatrix} \varepsilon_x \\ \varepsilon_y \\ \gamma_{xy} \end{Bmatrix} = \frac{1}{|J|} \begin{bmatrix} J_{22} & -J_{12} & 0 & 0 \\ 0 & 0 & -J_{21} & J_{11} \\ -J_{21} & J_{11} & J_{22} & -J_{12} \end{bmatrix}$$

$$\times \frac{1}{4} \begin{bmatrix} \eta-1 & 0 & (1-\eta) & 0 & (1+\eta) & 0 & -(1+\eta) & 0 & -8\xi & 0 & 0 & 0 \\ \xi-1 & 0 & -(1+\xi) & 0 & 1+\xi & 0 & 1-\xi & 0 & 0 & -8\eta & 0 & 0 \\ 0 & (\eta-1) & 0 & (1-\eta) & 0 & 1+\eta & 0 & -(1+\eta) & 0 & 0 & -8\xi & 0 \\ 0 & \xi-1 & 0 & -(1+\xi) & 0 & 1+\xi & 0 & 1-\xi & 0 & 0 & 0 & -8\eta \end{bmatrix}$$

$$\times \langle u_1 \ v_1 \ u_2 \ v_2 \ u_3 \ v_3 \ u_4 \ v_4 \ \alpha_1 \ \alpha_2 \ \alpha_3 \ \alpha_4 \rangle^T \tag{2.12.100}$$

$\{\varepsilon\} = [\ B]\{\delta\}$ which gives $[\ B] = \dfrac{1}{4\,|J|} \begin{bmatrix} J_{22} & -J_{12} & 0 & 0 \\ 0 & 0 & -J_{21} & J_{11} \\ -J_{21} & J_{11} & J_{22} & -J_{12} \end{bmatrix}$

$$\times \begin{bmatrix} \eta-1 & 0 & (1-\eta) & 0 & (1+\eta) & 0 & -(1+\eta) & 0 & -8\xi & 0 & 0 & 0 \\ \xi-1 & 0 & -(1+\xi) & 0 & 1+\xi & 0 & 1-\xi & 0 & 0 & -8\eta & 0 & 0 \\ 0 & (\eta-1) & 0 & (1-\eta) & 0 & 1+\eta & 0 & -(1+\eta) & 0 & 0 & -8\xi & 0 \\ 0 & \xi-1 & 0 & -(1+\xi) & 0 & 1+\xi & 0 & 1-\xi & 0 & 0 & 0 & -8\eta \end{bmatrix} \tag{2.12.101}$$

Considering $[K]_e = t \int_{-1}^{1} \int_{-1}^{1} [B]^T [D] [B] |J| \, d\xi \cdot d\eta$ we can now easily find out the stiffness matrix whose order would be (12×12).

From this matrix we eliminate the internal degrees of freedom $\alpha_1, \alpha_2, \alpha_3$ *&* α_4 *and crunch it to the desired* 8×8 *matrix.*

2.12.24 How tough is this lawbreaker?

In any democratic civilized society that enjoys freedom of speech and work – flaunting of constitutional law is construed as a criminal offence. The finite element developers club that has always functioned under a democratic framework[54] where members freely exchanged ideas, formulations[55], was no exception. Thus, when Wilson proposed the novel formulation violating the first law of compatibility, skeptics around were in abundance. Fortunately for us, he got away with the crime without being prosecuted and unlike the proceedings in a criminal court even got praised for it (Hughes 1974).

In-spite of violating the compatibility condition the element just worked fine giving excellent result under flexural load-*provided the shape of the mesh was a rectangle.* However, if the shape of the mesh was a generic quadrilateral, the stress results were not so good and under constant displacement condition even the rectangular elements were found to give erroneous results.

The element was thus only conditionally stable, and as mentioned earlier was perceived to be a *temperamental element.* This prompted Taylor[56] (1976) to revise and upgrade the element, so that the deficiencies mentioned above are eliminated. We present herein this improved element that has great practical application.

2.12.25 Taylor's improved incompatible quadrilateral

We had shown earlier that displacement function for incompatible element is given by

$$u = N_1 u_1 + N_2 u_2 + N_3 u_3 + N_4 u_4 + N_5 \alpha_1 + N_6 \alpha_2 \quad \text{and}$$

$$v = N_1 v_1 + N_2 v_2 + N_3 v_3 + N_4 v_4 + N_5 \alpha_3 + N_6 \alpha_4 \tag{2.12.102}$$

The global coordinates are expressed as

$$x = N_1 x_1 + N_2 x_2 + N_3 x_3 + N_4 x_4;$$

$$y = N_1 y_1 + N_2 y_2 + N_3 y_3 + N_4 y_4 \tag{2.12.103}$$

54 This was possibly one of the main reasons for the development of this subject to such a great height in such a short period of time.

55 Including pinching each others source code at times....

56 One of the member along with Prof. Ed.Wilson who proposed this model...

We express the displacement function in generic matrix notation as

$$\{\delta_t\} = [N]\{\delta\} + [\Lambda]\{\alpha\} \tag{2.12.104}$$

where $[\Lambda] = \begin{bmatrix} N_5 & N_6 & 0 & 0 \\ 0 & 0 & N_5 & N_6 \end{bmatrix}$ and $\{\alpha\}^T = \langle \alpha_1, \alpha_2, \alpha_3, \alpha_4 \rangle$

For conforming element considering, $\{\varepsilon\} = [B]\{\delta\}$, the strain equation for the present case can be written as

$$\{\varepsilon\} = [B]\{\delta\} + [\Lambda']\{\alpha\}, \tag{2.12.105}$$

where $[\Lambda']$ = differentiation of the function $[\Lambda]$ with respect to global x and y.

Again for conforming element the stiffness matrix is given by

$$[K]_e = \int\int\int [B]^T [D][B]\, dv,$$

for the present case, the stiffness matrix is given by

$$[K]_e = \int\int\int \begin{Bmatrix} [B]^T \\ [\Lambda']^T \end{Bmatrix} [D]\ [[B]\ [\Lambda']]\, dv \quad \text{or,}$$

$$[K]_e = \begin{bmatrix} \int\int\int [B]^T [D]\ [B]\, dv & \int\int\int [B]^T [D]\ [\Lambda']dv \\ \int\int\int [\Lambda']^T [D]\ [B]\, dv & \int\int\int [\Lambda']^T [D]\ [\Lambda]dv \end{bmatrix} \tag{2.12.106}$$

i.e. $\begin{bmatrix} [K_{\delta\delta}] & [K_{\delta\alpha}] \\ [K_{\alpha\delta}] & [K_{\alpha\alpha}] \end{bmatrix} = \begin{bmatrix} \int\int\int [B]^T [D]\ [B]\, dv & \int\int\int [B]^T [D]\ [\Lambda']dv \\ \int\int\int [\Lambda']^T [D]\ [B]\, dv & \int\int\int [\Lambda']^T [D]\ [\Lambda]dv \end{bmatrix}$

Considering the equilibrium equation, $[K]\{\delta\} = \{P\}$, we have

$$\begin{bmatrix} [K_{\delta\delta}] & [K_{\delta\alpha}] \\ [K_{\alpha\delta}] & [K_{\alpha\alpha}] \end{bmatrix} \begin{Bmatrix} \{\delta\} \\ \{\alpha\} \end{Bmatrix} = \begin{Bmatrix} \{P\} \\ \{0\} \end{Bmatrix} \tag{2.12.107}$$

where $[K_{\delta\delta}]$ represents the stiffness matrix corresponding to the displacement $\{\delta\}$, while $[K_{\alpha\alpha}]$ is the stiffness related to the nonconforming displacement $\{\alpha\}$ and $[K_{\delta\alpha}] = [K_{\alpha\delta}]$.

Let the displacement vector under constant deformation case be $\{\delta_c\}$. Under this condition the displacement vector related to the incompatible mode must not get activated. From second row of matrix equilibrium relation as stated above

we have

$$[K_{\alpha\delta}]\{\delta_c\} + [K_{\alpha\alpha}]\{\alpha\} = \{0\} \tag{2.12.108}$$

Since incompatible displacement shall remain inactive, hence $\{\alpha\} = \{0\}$, and it gives

$$[K_{\alpha\delta}]\{\delta_c\} = \{0\} \quad \rightarrow \quad \int\int\int [\Lambda']^T [D]\, [B]\{\delta_c\}\, dv = \{0\}. \tag{2.12.109}$$

Now considering $\{\varepsilon\} = [B]\{\delta\}$ we can express the above equation as,

$$\int\int\int [\Lambda']^T [D]\, \{\varepsilon_c\}\, dv = \{0\} \tag{2.12.110}$$

where $\{\varepsilon_c\}$ is constant strain $\rightarrow$ considering the displacement as constant.

As the material matrix, $[D]$ is also a constant we may write

$$\int\int\int [\Lambda']^T dv = [0]; \quad \text{or} \int\int\int [\Lambda']\, dv = [0]^T \tag{2.12.111}$$

Thus in terms of iso-parametric formulation we have

$$t\int_{-1}^{1}\int_{-1}^{1} [\Lambda']\ |J|\, d\xi\, d\eta = [0] \tag{2.12.112}$$

where, $[\Lambda'] = \frac{1}{4|J|}\begin{bmatrix} J_{22} & -J_{12} \\ -J_{21} & J_{11} \end{bmatrix}\begin{bmatrix} -8\xi & 0 & 0 & 0 \\ 0 & 0 & -8\eta & 0 \end{bmatrix} = \frac{1}{4}|J|\begin{bmatrix} 8J_{22}\xi & 0 & 8J_{12}\eta & 0 \\ 8J_{21}\xi & 0 & -8J_{11}\eta & 0 \end{bmatrix}$;

and t is the thickness in the normal direction of the plane.

Thus we can say that

$$t\int_{-1}^{1}\int_{-1}^{1} \begin{bmatrix} -8J_{22}\xi & 0 & 0 & 8J_{12}\eta \\ 8J_{21}\xi & 0 & 0 & -8J_{11}\eta \end{bmatrix} |J|\, d\xi\, d\eta = [0] \tag{2.12.113}$$

It is evident that the above integrals can only be zero when $\xi = \eta = 0$; *i.e. the integration is carried out at the centroid of the element, instead of the Gauss points.*

The Jacobian matrix evaluated at the centroid of the element is given by

$$[J] = \begin{bmatrix} J_{11} & J_{12} \\ J_{21} & J_{22} \end{bmatrix} = \frac{1}{4}\begin{bmatrix} -x_1 + x_2 + x_3 - x_4 & -y_1 + y_2 + y_3 - y_4 \\ -x_1 - x_2 + x_3 + x_4 & -y_1 - y_2 + y_3 + y_4 \end{bmatrix}$$

$$\rightarrow \quad [J]^{-1} = \frac{1}{4|J|}\begin{bmatrix} -y_1 - y_2 + y_3 + y_4 & y_1 - y_2 - y_3 + y_4 \\ x_1 + x_2 - x_3 - x_4 & -x_1 + x_2 + x_3 - x_4 \end{bmatrix};$$

$$|J| = J_{11} \times J_{22} - J_{12} \times J_{21}$$

Let the above be expressed as

$|J^c|^{-1} = \frac{1}{4}\begin{vmatrix} j^c_{22} & -j^c_{21} \\ -j^c_{12} & j^c_{11} \end{vmatrix}$ the Jacobean matrix at centroid and let

$|J^g|^{-1} = \frac{1}{4}\begin{vmatrix} j^g_{22} & -j^g_{21} \\ -j^g_{12} & j^g_{11} \end{vmatrix}$ the Jacobean matrix as expressed in Eqn (2.12.96) to (2.11.98).

Then $[B]$ Matrix is thus expressed as

$$[B] = \frac{1}{4}\left[\begin{array}{cccccc|cccccc} -j^g_{22}(1-\eta) & & j^g_{22}(1-\eta) & & j^g_{22}(1+\eta) & | & & -j^g_{22}(1+\eta) & & & & \\ +j^g_{12}(1-\xi) & 0 & +j^g_{12}(1-\xi) & 0 & -J^g_{12}(1+\xi) & | & 0 & +j^g_{11}(1-\xi) & 0 & -8j^c_{22}\xi & 8j^c_{12}\eta & 0 & 0 \\ & j^g_{21}(1-\eta) & & -j^g_{21}(1-\eta) & & | & -j^g_{21}(1-\eta) & & j^g_{21}(1+\eta) & & & & \\ 0 & -j^g_{11}(1-\xi) & 0 & -j^g_{11}(1+\xi) & 0 & | & +j^g_{11}(1+\xi) & 0 & +j^g_{11}(1-\xi) & 0 & 0 & 8j^c_{21}\xi & -8j^c_{11}\eta \\ j^g_{21}(1-\eta) & -j^g_{22}(1-\eta) & -j^g_{21}(1-\eta) & j^g_{22}(1-\eta) & -j^g_{21}(1+\eta) & | & j^g_{22}(1+\eta) & j^g_{21}(1+\eta) & -j^g_{22}(1+\eta) & & & & \\ -j^g_{11}(1-\xi) & +j^g_{12}(1-\xi) & -j^g_{11}(1+\xi) & +j^g_{12}(1+\xi) & +j^g_{11}(1+\xi) & | & -j^g_{12}(1+\xi) & +j^g_{11}(1-\xi) & -j^g_{12}(1-\xi) & -8j^c_{11}\xi & -8j^c_{11}\eta & -8j^c_{22}\xi & 8j^c_{12}\eta \end{array}\right] \tag{2.12.114}$$

It may be observed that for first 8 columns global Jacobean $[J]^g$ is used while for columns 9 to 12 Jacobean at centroid $[J]^c$ is used.

Considering, $[K]_e = t\int_{-1}^{1}\int_{-1}^{1}[B]^{\mathrm{T}}[\mathrm{D}][B]\,|J|\,d\xi \cdot d\eta$, we can now easily formulate the element stiffness matrix of order 12×12 from which we condense out the incompatible displacement functions $[\alpha]_{i=1}^{4}$ to formulate the desired stiffness matrix of order 8×8.

This element is stable and without the flaws as discussed earlier and is used in a number of commercially available FEM software.

Example 2.12.4

Given the quadrilateral element (Figure 2.12.29) having nodal coordinates as shown in the parentheses determine the element stiffness based on Taylor's incompatible formulation given thickness of the element is 200 mm and Young's modulus $E = 2 \times 10^8$ kN/m^2, and Poisson's ratio $\nu = 0.25$.

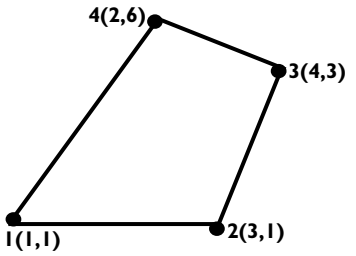


Figure 2.12.29 Four noded quadrilateral element.

Solution:

This is a plane stress case as such the matrix $[D]$ is given by

$$[D] = \frac{E}{1-\nu^2}\begin{bmatrix} 1 & \nu & 0 \\ \nu & 1 & 0 \\ 0 & 0 & \dfrac{1-\nu}{2} \end{bmatrix};$$

Substituting the value $E = 2 \times 10^8$ kN/m^2 and $\nu = 0.25$, we get

$$[D] = \begin{bmatrix} 2.33 & 0.533 & 0 \\ 0.533 & 0.533 & 0 \\ 0 & 0 & 0.80 \end{bmatrix} \times 10^8 \text{ kN/m}^2$$

For derivation of stiffness matrix at we had shown in the theoretical derivation 2 point Gauss integration suffice.

Here

$$[J^c] = \begin{bmatrix} J^c_{11} & J^c_{12} \\ J^c_{21} & J^c_{22} \end{bmatrix} = \frac{1}{4}\begin{bmatrix} -x_1 + x_2 + x_3 - x_4 & -y_1 + y_2 + y_3 - y_4 \\ -x_1 - x_2 + x_3 + x_4 & -y_1 - y_2 + y_3 + y_4 \end{bmatrix}$$

$$|J^c| = J^c_{11} \times J^c_{22} - J^c_{12} \times J^c_{21}$$

Based on above the nodal coordinates and the Jacobian parameters are as derived hereafter

For the element the global Jacobian $[J^g]$ elements are as given hereafter

Node	x	y	ξ	η	J_{11}	J_{12}	J_{21}	J_{22}	Det-J
1	1	1	−0.57735027	−0.57735027	−0.316987298	0.5	2.183012702	2.341506351	−0.316987298
2	3	1	0.57735027	−0.57735027	−0.316987298	0.5	1.316987298	1.475480947	−0.316987298
3	4	3	0.57735027	0.57735027	−1.183012702	0.5	1.316987298	1.908493649	−1.183012702
4	2	6	−0.57735027	0.57735027	−1.183012702	0.5	2.183012702	2.774519053	−1.183012702

The centroidal Jacobian element are given by $J^c_{11} = 1, J^c_{12} = -0.75, J^c_{21} = 0.5$, $J^c_{22} = 1.75$ and Det $J^c = 2.125$

We will now determine the matrix [B] and the stiffness $[B]^T [D] [B]$ at each Gauss point at the 4 sample points calling them $k_{g1}, k_{g2}, k_{g3}, k_{g4}$ where

$$[B] = \frac{1}{4}\begin{bmatrix} -j^g_{22}(1-\eta) & & j^g_{22}(1-\eta) & & j^g_{22}(1+\eta) & \\ +j^g_{12}(1-\xi) & 0 & +j^g_{12}(1-\xi) & 0 & -J^g_{12}(1+\xi) & \\ & j^g_{21}(1-\eta) & & -j^g_{21}(1-\eta) & & \\ 0 & -j^g_{11}(1-\xi) & 0 & -j^g_{11}(1+\xi) & 0 & \\ j^g_{21}(1-\eta) & -j^g_{22}(1-\eta) & -j^g_{21}(1-\eta) & j^g_{22}(1-\eta) & -j^g_{21}(1+\eta) & \\ -j^g_{11}(1-\xi) & +j^g_{12}(1-\xi) & -j^g_{11}(1+\xi) & +j^g_{12}(1+\xi) & +j^g_{11}(1+\xi) & \end{bmatrix}$$

$$\begin{bmatrix} & -j^g_{22}(1+\eta) & & & & & \\ 0 & +j^g_{11}(1-\xi) & 0 & -8j^c_{22}\xi & 8j^c_{12}\eta & 0 & 0 \\ -j^g_{21}(1-\eta) & & j^g_{21}(1+\eta) & & & & \\ +j^g_{11}(1+\xi) & 0 & +j^g_{11}(1-\xi) & 0 & 0 & 8j^c_{21}\xi & -8j^c_{11}\eta \\ j^g_{22}(1+\eta) & j^g_{21}(1+\eta) & -j^g_{22}(1+\eta) & & & & \\ -j^g_{12}(1+\xi) & +j^g_{11}(1-\xi) & -j^g_{12}(1-\xi) & -8j^c_{11}\xi & -8j^c_{11}\eta & -8j^c_{22}\xi & 8j^c_{12}\eta \end{bmatrix}$$

For point 1 the gauss points are $-\frac{1}{\sqrt{3}}, -\frac{1}{\sqrt{3}}$ for which

$[B] =$

−0.4210	0.0000	0.3143	0.0000	0.1436	0.0000	0.0699	0.0000	0.9509	−0.4075	0.0000	0.0000
0.0000	−0.0842	0.0000	−0.0391	0.0000	0.0226	0.0000	0.1910	0.0000	0.0000	0.2717	0.5434
−0.0842	−0.4210	−0.1293	0.3533	0.0226	0.1128	0.1910	−0.0451	0.5434	0.5434	0.9509	−0.4075

The stiffness matrix[57] for Gauss point 1 $\left[k_{g1}\right] = [B]^T [D] [B]$

$$\left[\begin{array}{cccccc|cccccc}
3.84E{+}07 & 4.73E{+}06 & -2.74E{+}07 & -1.50E{+}06 & -1.31E{+}07 & -1.27E{+}06 & -7.56E{+}06 & -3.98E{+}06 & -8.91E{+}07 & 3.29E{+}07 & -1.25E{+}07 & -9.45E{+}06 \\
4.73E{+}06 & 1.57E{+}07 & 2.95E{+}06 & -1.12E{+}07 & -1.40E{+}06 & -4.21E{+}06 & -6.75E{+}06 & -1.91E{+}06 & -2.26E{+}07 & -1.65E{+}07 & -3.69E{+}07 & 3.97E{+}06 \\
-2.74E{+}07 & 2.95E{+}06 & 2.24E{+}07 & -4.31E{+}06 & 9.39E{+}06 & -7.89E{+}05 & 2.71E{+}06 & 3.67E{+}06 & 5.81E{+}07 & -3.29E{+}07 & -5.29E{+}06 & 1.33E{+}07 \\
-1.50E{+}06 & -1.12E{+}07 & -4.31E{+}06 & 1.03E{+}07 & 3.39E{+}05 & 3.00E{+}06 & 5.25E{+}06 & -2.87E{+}06 & 1.34E{+}07 & 1.62E{+}07 & 2.46E{+}07 & -1.60E{+}07 \\
-1.31E{+}07 & -1.40E{+}06 & 9.39E{+}06 & 3.39E{+}05 & 4.44E{+}06 & 3.76E{+}05 & 2.49E{+}06 & 1.38E{+}06 & 3.01E{+}07 & -1.15E{+}07 & 3.80E{+}06 & 3.42E{+}06 \\
-1.27E{+}06 & -4.21E{+}06 & -7.89E{+}05 & 3.00E{+}06 & 3.76E{+}05 & 1.13E{+}06 & 1.81E{+}06 & 5.12E{+}05 & 6.05E{+}06 & 4.41E{+}06 & 9.89E{+}06 & -1.06E{+}06 \\
-7.56E{+}06 & -6.75E{+}06 & 2.71E{+}06 & 5.25E{+}06 & 2.49E{+}06 & 1.81E{+}06 & 3.96E{+}06 & 2.21E{+}04 & 2.25E{+}07 & 2.23E{+}06 & 1.55E{+}07 & -4.20E{+}06 \\
-3.98E{+}06 & -1.91E{+}06 & 3.67E{+}06 & -2.87E{+}06 & 1.38E{+}06 & 5.12E{+}05 & 2.21E{+}04 & 7.94E{+}06 & 7.72E{+}06 & -6.11E{+}06 & 7.63E{+}06 & 2.36E{+}07 \\
-8.91E{+}07 & -2.26E{+}07 & 5.81E{+}07 & 1.34E{+}07 & 3.01E{+}07 & 6.05E{+}06 & 2.25E{+}07 & 7.72E{+}06 & 2.17E{+}08 & -5.90E{+}07 & 5.51E{+}07 & 9.83E{+}06 \\
3.29E{+}07 & -1.65E{+}07 & -3.29E{+}07 & 1.62E{+}07 & -1.15E{+}07 & 4.41E{+}06 & 2.23E{+}06 & -6.11E{+}06 & -5.90E{+}07 & 5.90E{+}07 & 3.54E{+}07 & -2.95E{+}07 \\
-1.25E{+}07 & -3.69E{+}07 & -5.29E{+}06 & 2.46E{+}07 & 3.80E{+}06 & 9.89E{+}06 & 1.55E{+}07 & 7.63E{+}06 & 5.51E{+}07 & 3.54E{+}07 & 8.81E{+}07 & 4.87E{+}05 \\
-9.45E{+}06 & 3.97E{+}06 & 1.33E{+}07 & -1.60E{+}07 & 3.42E{+}06 & -1.06E{+}06 & -4.20E{+}06 & 2.36E{+}07 & 9.83E{+}06 & -2.95E{+}07 & 4.87E{+}05 & 7.63E{+}07
\end{array}\right]$$

For point 2 the gauss points are $(1/\sqrt{3}, -1/\sqrt{3})$ for which $[k_{g2}] =$

$$\left[\begin{array}{cccccc|cccccc}
3.03E{+}07 & -3.10E{+}06 & -2.83E{+}07 & -1.34E{+}06 & -2.77E{+}07 & -3.73E{+}06 & 2.35E{+}06 & -2.50E{+}06 & 7.33E{+}07 & 3.53E{+}07 & 1.01E{+}07 & -1.29E{+}07 \\
-3.10E{+}06 & 1.21E{+}07 & 1.31E{+}07 & -6.24E{+}06 & -5.74E{+}06 & -2.30E{+}06 & -3.29E{+}06 & 3.57E{+}06 & 1.31E{+}07 & -1.76E{+}07 & -3.21E{+}07 & 1.94E{+}07 \\
-2.83E{+}07 & 1.31E{+}07 & 3.60E{+}07 & -6.23E{+}06 & 1.80E{+}07 & -1.68E{+}06 & -5.04E{+}06 & 4.18E{+}06 & -4.94E{+}07 & -4.61E{+}07 & -3.53E{+}07 & 2.26E{+}07 \\
-1.34E{+}06 & -6.24E{+}06 & -6.23E{+}06 & 9.52E{+}06 & 7.52E{+}06 & 1.04E{+}07 & 2.14E{+}06 & 1.53E{+}06 & -1.84E{+}07 & 8.72E{+}06 & 1.26E{+}07 & 6.77E{+}06 \\
-2.77E{+}07 & -5.74E{+}06 & 1.80E{+}07 & 7.52E{+}06 & 3.22E{+}07 & 7.78E{+}06 & 2.38E{+}05 & 7.44E{+}05 & -8.34E{+}07 & -2.14E{+}07 & 1.24E{+}07 & 2.93E{+}06 \\
-3.73E{+}06 & -2.30E{+}06 & -1.68E{+}06 & 1.04E{+}07 & 7.78E{+}06 & 1.40E{+}07 & 1.26E{+}06 & 4.28E{+}06 & -1.95E{+}07 & 2.76E{+}06 & 2.06E{+}05 & 2.10E{+}07 \\
2.35E{+}06 & -3.29E{+}06 & -5.04E{+}06 & 2.14E{+}06 & 2.38E{+}05 & 1.26E{+}06 & 1.03E{+}06 & -7.45E{+}05 & -6.52E{+}04 & 6.64E{+}06 & 8.50E{+}06 & -4.16E{+}06 \\
-2.50E{+}06 & 3.57E{+}06 & 4.18E{+}06 & 1.53E{+}06 & 7.44E{+}05 & 4.28E{+}06 & -7.45E{+}05 & 2.87E{+}06 & -2.33E{+}06 & -5.45E{+}06 & -1.17E{+}07 & 1.48E{+}07 \\
7.33E{+}07 & 1.31E{+}07 & -4.94E{+}07 & -1.84E{+}07 & -8.34E{+}07 & -1.95E{+}07 & -6.52E{+}04 & -2.33E{+}06 & 2.17E{+}08 & 5.90E{+}07 & -2.76E{+}07 & -9.83E{+}06 \\
3.53E{+}07 & -1.76E{+}07 & -4.61E{+}07 & 8.72E{+}06 & -2.14E{+}07 & 2.76E{+}06 & 6.64E{+}06 & -5.45E{+}06 & 5.90E{+}07 & 5.90E{+}07 & 4.72E{+}07 & -2.95E{+}07 \\
1.01E{+}07 & -3.21E{+}07 & -3.53E{+}07 & 1.26E{+}07 & 1.24E{+}07 & 2.06E{+}05 & 8.50E{+}06 & -1.17E{+}07 & -2.76E{+}07 & 4.72E{+}07 & 8.81E{+}07 & -6.25E{+}07 \\
-1.29E{+}07 & 1.94E{+}07 & 2.26E{+}07 & 6.77E{+}06 & 2.93E{+}06 & 2.10E{+}07 & -4.16E{+}06 & 1.48E{+}07 & -9.83E{+}06 & -2.95E{+}07 & -6.25E{+}07 & 7.63E{+}07
\end{array}\right]$$

57 Here stiffness values are directly taken from computer output where E+06 mean 10^{+06}.

For point 3 the gauss points are $(1/\sqrt{3}, 1/\sqrt{3})$ for which $[k_{g3}] =$

$$\left[\begin{array}{cccccc|cccccc}
4.15E{+}06 & 5.11E{+}05 & 3.00E{+}05 & -9.40E{+}05 & -1.44E{+}07 & -1.91E{+}06 & 6.05E{+}06 & -7.13E{+}05 & 2.93E{+}07 & -1.08E{+}07 & 4.11E{+}06 & 3.11E{+}06 \\
5.11E{+}05 & 1.70E{+}06 & 2.58E{+}06 & 8.43E{+}05 & -1.85E{+}06 & -6.33E{+}06 & -1.44E{+}06 & 1.35E{+}06 & 7.42E{+}06 & 5.42E{+}06 & 1.21E{+}07 & -1.30E{+}06 \\
3.00E{+}05 & 2.58E{+}06 & 4.40E{+}06 & 3.29E{+}06 & -1.18E{+}06 & -9.64E{+}06 & -3.32E{+}06 & 3.94E{+}06 & 8.68E{+}06 & 1.08E{+}07 & 1.77E{+}07 & -7.85E{+}06 \\
-9.40E{+}05 & 8.43E{+}05 & 3.29E{+}06 & 9.18E{+}06 & 3.15E{+}06 & -3.14E{+}06 & -4.24E{+}06 & 8.89E{+}06 & -1.61E{+}06 & 1.13E{+}07 & 2.68E{+}06 & -2.63E{+}07 \\
-1.44E{+}07 & -1.85E{+}06 & -1.18E{+}06 & 3.15E{+}06 & 4.97E{+}07 & 6.91E{+}06 & -2.08E{+}07 & 2.34E{+}06 & -1.02E{+}08 & 3.71E{+}07 & -1.48E{+}07 & -1.05E{+}07 \\
-1.91E{+}06 & -6.33E{+}06 & -9.64E{+}06 & -3.14E{+}06 & 6.91E{+}06 & 2.36E{+}07 & 5.36E{+}06 & -5.04E{+}06 & -2.77E{+}07 & -2.02E{+}07 & -4.53E{+}07 & 4.87E{+}06 \\
6.05E{+}06 & -1.44E{+}06 & -3.32E{+}06 & -4.24E{+}06 & -2.08E{+}07 & 5.36E{+}06 & 1.20E{+}07 & -4.46E{+}06 & 3.71E{+}07 & -2.57E{+}07 & -8.93E{+}06 & 1.15E{+}07 \\
-7.13E{+}05 & 1.35E{+}06 & 3.94E{+}06 & 8.89E{+}06 & 2.34E{+}06 & -5.04E{+}06 & -4.46E{+}06 & 8.79E{+}06 & 9.40E{+}05 & 1.24E{+}07 & 6.52E{+}06 & -2.51E{+}07 \\
2.93E{+}07 & 7.42E{+}06 & 8.68E{+}06 & -1.61E{+}06 & -1.02E{+}08 & -2.77E{+}07 & 3.71E{+}07 & 9.40E{+}05 & 2.17E{+}08 & -5.90E{+}07 & 5.51E{+}07 & 9.83E{+}06 \\
-1.08E{+}07 & 5.42E{+}06 & 1.08E{+}07 & 1.13E{+}07 & 3.71E{+}07 & -2.02E{+}07 & -2.57E{+}07 & 1.24E{+}07 & -5.90E{+}07 & 5.90E{+}07 & 3.54E{+}07 & -2.95E{+}07 \\
4.11E{+}06 & 1.21E{+}07 & 1.77E{+}07 & 2.68E{+}06 & -1.48E{+}07 & -4.53E{+}07 & -8.93E{+}06 & 6.52E{+}06 & 5.51E{+}07 & 3.54E{+}07 & 8.81E{+}07 & 4.87E{+}05 \\
3.11E{+}06 & -1.30E{+}06 & -7.85E{+}06 & -2.63E{+}07 & -1.05E{+}07 & 4.87E{+}06 & 1.15E{+}07 & -2.51E{+}07 & 9.83E{+}06 & -2.95E{+}07 & 4.87E{+}05 & 7.63E{+}07
\end{array}\right]$$

For point 4 the gauss points are $(-1/\sqrt{3}, 1/\sqrt{3})$ for which $[k_{g4}] =$

$$\left[\begin{array}{cccccc|cccccc}
1.47E{+}07 & 4.12E{+}06 & 5.12E{+}06 & -6.30E{+}05 & -1.83E{+}07 & -3.06E{+}06 & 6.91E{+}06 & -1.46E{+}06 & -5.63E{+}07 & -1.65E{+}07 & 5.72E{+}06 & 3.26E{+}06 \\
4.12E{+}06 & 8.28E{+}06 & 1.71E{+}06 & -1.27E{+}06 & -1.62E{+}06 & -6.28E{+}06 & -3.18E{+}06 & -2.74E{+}06 & -1.72E{+}07 & 8.25E{+}06 & 1.20E{+}07 & 6.07E{+}06 \\
5.12E{+}06 & 1.71E{+}06 & 1.80E{+}06 & -2.60E{+}05 & -6.17E{+}06 & -1.47E{+}06 & 2.07E{+}06 & -3.16E{+}05 & -1.97E{+}07 & -4.91E{+}06 & 3.11E{+}06 & 5.99E{+}05 \\
-6.30E{+}05 & -1.27E{+}06 & -2.60E{+}05 & 1.93E{+}05 & 2.53E{+}05 & 9.49E{+}05 & 4.79E{+}05 & 4.33E{+}05 & 2.62E{+}06 & -1.24E{+}06 & -1.79E{+}06 & -9.65E{+}05 \\
-1.83E{+}07 & -1.62E{+}06 & -6.17E{+}06 & 2.53E{+}05 & 2.60E{+}07 & -1.55E{+}06 & -1.31E{+}07 & 4.33E{+}06 & 6.92E{+}07 & 3.17E{+}07 & 7.55E{+}06 & -1.12E{+}07 \\
-3.06E{+}06 & -6.28E{+}06 & -1.47E{+}06 & 9.49E{+}05 & -1.55E{+}06 & 1.03E{+}07 & 6.36E{+}06 & -5.54E{+}06 & 1.38E{+}07 & -1.62E{+}07 & -2.89E{+}07 & 1.54E{+}07 \\
6.91E{+}06 & -3.18E{+}06 & 2.07E{+}06 & 4.79E{+}05 & -1.31E{+}07 & 6.36E{+}06 & 9.67E{+}06 & -4.33E{+}06 & -2.48E{+}07 & -2.39E{+}07 & -1.87E{+}07 & 1.18E{+}07 \\
-1.46E{+}06 & -2.74E{+}06 & -3.16E{+}05 & 4.33E{+}05 & 4.33E{+}06 & -5.54E{+}06 & -4.33E{+}06 & 1.13E{+}07 & 4.63E{+}06 & 1.08E{+}07 & 2.32E{+}07 & -2.93E{+}07 \\
-5.63E{+}07 & -1.72E{+}07 & -1.97E{+}07 & 2.62E{+}06 & 6.92E{+}07 & 1.38E{+}07 & -2.48E{+}07 & 4.63E{+}06 & 2.17E{+}08 & 5.90E{+}07 & -2.76E{+}07 & -9.83E{+}06 \\
-1.65E{+}07 & 8.25E{+}06 & -4.91E{+}06 & -1.24E{+}06 & 3.17E{+}07 & -1.62E{+}07 & -2.39E{+}07 & 1.08E{+}07 & 5.90E{+}07 & 5.90E{+}07 & 4.72E{+}07 & -2.95E{+}07 \\
5.72E{+}06 & 1.20E{+}07 & 3.11E{+}06 & -1.79E{+}06 & 7.55E{+}06 & -2.89E{+}07 & -1.87E{+}07 & 2.32E{+}07 & -2.76E{+}07 & 4.72E{+}07 & 8.81E{+}07 & -6.25E{+}07 \\
3.26E{+}06 & 6.07E{+}06 & 5.99E{+}05 & -9.65E{+}05 & -1.12E{+}07 & 1.54E{+}07 & 1.18E{+}07 & -2.93E{+}07 & -9.83E{+}06 & -2.95E{+}07 & -6.25E{+}07 & 7.63E{+}07
\end{array}\right]$$

The total stiffness matrix for element is now given by

$$[K]_e = \sum_{i=1}^{4} [k_{gi}] = [k_{g1}] + [k_{g2}] + [k_{g3}] + [k_{g4}] \quad \text{or} \quad [K]_e =$$

$$\left[\begin{array}{cccccc|}
8.75E{+}07 & 6.26E{+}06 & -5.02E{+}07 & -4.42E{+}06 & -7.35E{+}07 & -9.96E{+}06 \\
6.26E{+}06 & 3.77E{+}07 & 2.03E{+}07 & -1.79E{+}07 & -1.06E{+}07 & -1.91E{+}07 \\
-5.02E{+}07 & 2.03E{+}07 & 6.46E{+}07 & -7.51E{+}06 & 2.00E{+}07 & -1.36E{+}07 \\
-4.42E{+}06 & -1.79E{+}07 & -7.51E{+}06 & 2.92E{+}07 & 1.13E{+}07 & 1.12E{+}07 \\
-7.35E{+}07 & -1.06E{+}07 & 2.00E{+}07 & 1.13E{+}07 & 1.12E{+}08 & 1.35E{+}07 \\
-9.96E{+}06 & -1.91E{+}07 & -1.36E{+}07 & 1.12E{+}07 & 1.35E{+}07 & 4.91E{+}07 \\
7.74E{+}06 & -1.47E{+}07 & -3.57E{+}06 & 3.62E{+}06 & -3.12E{+}07 & 1.48E{+}07 \\
-8.65E{+}06 & 2.68E{+}05 & 1.15E{+}07 & 7.99E{+}06 & 8.80E{+}06 & -5.79E{+}06 \\
-4.28E{+}07 & -1.92E{+}07 & -2.28E{+}06 & -4.00E{+}06 & -8.57E{+}07 & -2.74E{+}07 \\
4.09E{+}07 & -2.04E{+}07 & -7.31E{+}07 & 3.50E{+}07 & 3.60E{+}07 & -2.92E{+}07 \\
7.48E{+}06 & -4.49E{+}07 & -1.97E{+}07 & 3.81E{+}07 & 8.93E{+}06 & -6.41E{+}07 \\
-1.60E{+}07 & 2.81E{+}07 & 2.87E{+}07 & -3.66E{+}07 & -1.53E{+}07 & 4.02E{+}07
\end{array}\right.$$

$$\left.\begin{array}{cccccc}
7.74E{+}06 & -8.65E{+}06 & -4.28E{+}07 & 4.09E{+}07 & 7.48E{+}06 & -1.60E{+}07 \\
-1.47E{+}07 & 2.68E{+}05 & -1.92E{+}07 & -2.04E{+}07 & -4.49E{+}07 & 2.81E{+}07 \\
-3.57E{+}06 & 1.15E{+}07 & -2.28E{+}06 & -7.31E{+}07 & -1.97E{+}07 & 2.87E{+}07 \\
3.62E{+}06 & 7.99E{+}06 & -4.00E{+}06 & 3.50E{+}07 & 3.81E{+}07 & -3.66E{+}07 \\
-3.12E{+}07 & 8.80E{+}06 & -8.57E{+}07 & 3.60E{+}07 & 8.93E{+}06 & -1.53E{+}07 \\
1.48E{+}07 & -5.79E{+}06 & -2.74E{+}07 & -2.92E{+}07 & -6.41E{+}07 & 4.02E{+}07 \\
2.67E{+}07 & -9.51E{+}06 & 3.46E{+}07 & -4.08E{+}07 & -3.54E{+}06 & 1.49E{+}07 \\
-9.51E{+}06 & 3.09E{+}07 & 1.10E{+}07 & 1.17E{+}07 & 2.57E{+}07 & -1.61E{+}07 \\
3.46E{+}07 & 1.10E{+}07 & 8.66E{+}08 & 0.00E{+}00 & 5.51E{+}07 & 0.00E{+}00 \\
-4.08E{+}07 & 1.17E{+}07 & 0.00E{+}00 & 2.36E{+}08 & 1.65E{+}08 & -1.18E{+}08 \\
-3.54E{+}06 & 2.57E{+}07 & 5.51E{+}07 & 1.65E{+}08 & 3.52E{+}08 & -1.24E{+}08 \\
1.49E{+}07 & -1.61E{+}07 & 0.00E{+}00 & -1.18E{+}08 & -1.24E{+}08 & 3.05E{+}08
\end{array}\right]$$

The above matrix now needs to be subjected to static condensation to eliminate the $\alpha_1, \alpha_2, \alpha_3$, and α_4.

Here $[K]_{11} =$

8.75E+07	6.26E+06	−5.02E+07	−4.42E+06	−7.35E+07	−9.96E+06	7.74E+06	−8.65E+06
6.26E+06	3.77E+07	2.03E+07	−1.79E+07	−1.06E+07	−1.91E+07	−1.47E+07	2.68E+05
−5.02E+07	2.03E+07	6.46E+07	−7.51E+06	2.00E+07	−1.36E+07	−3.57E+06	1.15E+07
−4.42E+06	−1.79E+07	−7.51E+06	2.92E+07	1.13E+07	1.12E+07	3.62E+06	7.99E+06
−7.35E+07	−1.06E+07	2.00E+07	1.13E+07	1.12E+08	1.35E+07	−3.12E+07	8.80E+06
−9.96E+06	−1.91E+07	−1.36E+07	1.12E+07	1.35E+07	4.91E+07	1.48E+07	−5.79E+06
7.74E+06	−1.47E+07	−3.57E+06	3.62E+06	−3.12E+07	1.48E+07	2.67E+07	−9.51E+06
−8.65E+06	2.68E+05	1.15E+07	7.99E+06	8.80E+06	−5.79E+06	−9.51E+06	3.09E+07

$[K]_{12} =$

−4.28E+07	4.09E+07	7.48E+06	−1.60E+07
−1.92E+07	−2.04E+07	−4.49E+07	2.81E+07
−2.28E+06	−7.31E+07	−1.97E+07	2.87E+07
−4.00E+06	3.50E+07	3.81E+07	−3.66E+07
−8.57E+07	3.60E+07	8.93E+06	−1.53E+07
−2.74E+07	−2.92E+07	−6.41E+07	4.02E+07
3.46E+07	−4.08E+07	−3.54E+06	1.49E+07
1.10E+07	1.17E+07	2.57E+07	−1.61E+07

$[K]_{21} =$

−4.28E+07	−1.92E+07	−2.28E+06	−4.00E+06	−8.57E+07	−2.74E+07	3.46E+07	1.10E+07
4.09E+07	−2.04E+07	−7.31E+07	3.50E+07	3.60E+07	−2.92E+07	−4.08E+07	1.17E+07
7.48E+06	−4.49E+07	−1.97E+07	3.81E+07	8.93E+06	−6.41E+07	−3.54E+06	2.57E+07
−1.60E+07	2.81E+07	2.87E+07	−3.66E+07	−1.53E+07	4.02E+07	1.49E+07	−1.61E+07

$[K]_{22} =$

8.66E+08	0.00E+00	5.51E+07	0.00E+00
0.00E+00	2.36E+08	1.65E+08	−1.18E+08
5.51E+07	1.65E+08	3.52E+08	−1.24E+08
0.00E+00	−1.18E+08	−1.24E+08	3.05E+08

Considering $[K_c] = [[K_{11}] - [K_{12}][K_{22}]^{-1}[K_{21}]]$

7.68E+07	6.47E+06	−3.52E+07	−9.50E+06	−8.48E+07	−9.67E+06	1.83E+07	−8.77E+06
6.47E+06	3.12E+07	1.81E+07	−1.23E+07	−1.08E+07	−2.85E+07	−1.45E+07	4.02E+06
−3.52E+07	1.81E+07	3.77E+07	1.28E+06	3.24E+07	−1.68E+07	−1.92E+07	1.28E+07
−9.50E+06	−1.23E+07	1.28E+06	2.20E+07	6.23E+06	1.92E+07	8.38E+06	4.81E+06
−8.48E+07	−1.08E+07	3.24E+07	6.23E+06	9.79E+07	1.32E+07	−2.05E+07	8.90E+06
−9.67E+06	−2.85E+07	−1.68E+07	1.92E+07	1.32E+07	3.57E+07	1.50E+07	−4.30E+05
1.83E+07	−1.45E+07	−1.92E+07	8.38E+06	−2.05E+07	1.50E+07	1.60E+07	−9.62E+06
−8.77E+06	4.02E+06	1.28E+07	4.81E+06	8.90E+06	−4.30E+05	−9.62E+06	2.88E+07

Multiplying above by thickness t we finally have the stiffness matrix as

1.54E+07	1.29E+06	−7.04E+06	−1.90E+06	−1.70E+07	−1.93E+06	3.66E+06	−1.75E+06
1.29E+06	6.23E+06	3.61E+06	−2.46E+06	−2.16E+06	−5.70E+06	−2.90E+06	8.04E+05
−7.04E+06	3.61E+06	7.54E+06	2.57E+05	6.48E+06	−3.37E+06	−3.84E+06	2.55E+06
−1.90E+06	−2.46E+06	2.57E+05	4.41E+06	1.25E+06	3.84E+06	1.68E+06	9.61E+05
−1.70E+07	−2.16E+06	6.48E+06	1.25E+06	1.96E+07	2.65E+06	−4.09E+06	1.78E+06
−1.93E+06	−5.70E+06	−3.37E+06	3.84E+06	2.65E+06	7.13E+06	3.01E+06	−8.60E+04
3.66E+06	−2.90E+06	−3.84E+06	1.68E+06	−4.09E+06	3.01E+06	3.21E+06	−1.92E+06
−1.75E+06	8.04E+05	2.55E+06	9.61E+05	1.78E+06	−8.60E+04	−1.92E+06	5.75E+06

You can now check the values against stiffness matrix as derived in Example 2.12.1 and see that values of stiffness derived herein are lower in magnitude, meaning thereby that element is much more flexible compared to the original isoparametric formulation.

2.12.26 Higher order finite elements – The second generation members of the FEM family

Until now, we had derived element stiffness matrix for elements whose shape function varies linearly from one node to the other, where nodes are situated at the junction of two lines intersecting each other.

In this section, we discuss some higher order elements and the procedure to derive their shape functions vis-à-vis the element stiffness matrix.

2.12.26.1 Why Higher Order – What is its necessity?

A question many users possibly ask themselves who are new to the topic. What stops us remaining happy with what we have rather than unnecessarily complicating our life with more complex formulation? Is it research for research sake? Or was this really required?

For students who are still within the premise of the University (and care to go through this book) we can assure you that these elements were not developed to give you more tough time in the exam.

The specific reason for their development can be summarized as follows:

We had stated at the outset that FEA results converge as meshes are progressively refined.

The question which then naturally arises is – *"Mesh refinement to what extent?"* For instance for the beam as shown in Figure 2.12.30, how many elements would suffice 20, 30, 100 elements?

The answer to this query to be precise is dependent on the problem in hand and its boundary condition. However, to give you some qualitative idea results as reported by Abel and Popov (1968) are presented hereafter for your perusal.

For a cantilever beam, modeled with four node linear quadrilateral elements with a concentrated load P at the free end, tip deflections are as shown in Figure 2.12.30 and compared as hereunder.

Case	*No. of nodes*	*No. of elements*	*u*	*v*
1	9	4	1.417668	−1.207257
2	25	16	1.474063	−1.254745
3	81	64	1.492148	−1.269067
	Exact solution	–	1.500	−1.275

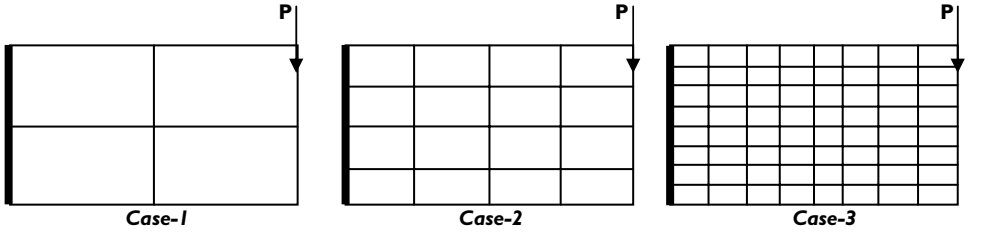


Figure 2.12.30 Cantilever beam with varying mesh.

It is apparent from the above data that mesh refinement (or the number of node to be considered) has to be quite high with linear elements to arrive at an accurate result. In the child hood of FEM when major software programs were developed in FORTRAN IV and VII and automatic mesh generation and renumbering of nodes to minimize the band width were not a part and parcel of the pre-processors, most of the input data were furnished in formatted forms (like I5, F10.4, E10.6 etc.). This called for significant effort from the user and was quite laborious in terms of data checking.

Even a small problem had quite a good amount of input data while with practical problems of even modest size the overall problem was getting sufficiently big thus creating serious memory space problem in many cases. For unlike the present generation of computers, the systems that were in use in late 60 to 80 did had limited memory space and speed.

It was perhaps at this juncture the eternal proverb "Necessity is the mother of invention" took over and people started looking into the possibility of higher order elements where *desired results could be arrived at by using cruder meshes thus reducing the modeling effort too.*

Though never documented clearly – this we believe is the major motivation behind the development of these second generation elements often termed as higher order elements. We start with the eight node rectangular element (of size $2a \times 2b$) and try to derive the $[N]$ matrix.

Since the objective is to use higher order polynomials based on compatibility law it is evident that number of nodes per element increase since number of coefficients must be equal to the number of nodal degrees of freedom.[58]

For eight nodded rectangular element we have 16 degrees of freedom (two per node, 2.12.31), when we have

$$u = \alpha_1 + \alpha_2 x + \alpha_3 y + \alpha_4 x^2 + \alpha_5 xy + \alpha_6 y^2 + \alpha_7 x^2 y + \alpha_8 xy^2 \tag{2.12.115}$$

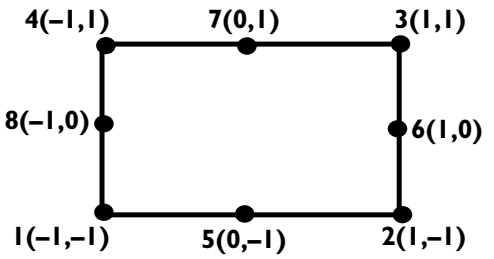


Figure 2.12.31 Eight-nodded rectangular element.

58 It should thus be noted that number of nodes may not decrease though number of elements used in a model may reduce with higher order elements.

The above in natural coordinate is expressed as

$$u = \alpha_1 + \alpha_2\xi + \alpha_3\eta + \alpha_4\xi^2 + \alpha_5\xi\eta + \alpha_6\eta^2 + \alpha_7\xi^2\eta + \alpha_8\xi\eta^2 \tag{2.12.116}$$

Thus substituting the co-ordinate values of nodes 1 to 8 as shown in the above Figure we have

$$\begin{aligned}
u_1 &= \alpha_1 - \alpha_2 - \alpha_3 + \alpha_4 + \alpha_5 + \alpha_6 - \alpha_7 - \alpha_8 \\
u_2 &= \alpha_1 + \alpha_2 - \alpha_3 + \alpha_4 - \alpha_5 + \alpha_6 - \alpha_7 + \alpha_8 \\
u_3 &= \alpha_1 + \alpha_2 + \alpha_3 + \alpha_4 + \alpha_5 + \alpha_6 + \alpha_7 + \alpha_8 \\
u_4 &= \alpha_1 - \alpha_2 + \alpha_3 + \alpha_4 - \alpha_5 + \alpha_6 + \alpha_7 - \alpha_8 \\
u_5 &= \alpha_1 - \alpha_3 + \alpha_6; \quad u_6 = \alpha_1 + \alpha_2 + \alpha_4 \\
u_7 &= \alpha_1 + \alpha_3 + \alpha_6; \quad u_8 = \alpha_1 - \alpha_2 + \alpha_4
\end{aligned} \tag{2.12.117}$$

The above when expressed in matrix notation can be represented as

$$\begin{Bmatrix} u_1 \\ u_2 \\ u_3 \\ u_4 \\ u_5 \\ u_6 \\ u_7 \\ u_8 \end{Bmatrix} = \begin{bmatrix} 1 & -1 & -1 & 1 & 1 & 1 & -1 & -1 \\ 1 & 1 & -1 & 1 & -1 & 1 & -1 & 1 \\ 1 & 1 & 1 & 1 & 1 & 1 & 1 & 1 \\ 1 & -1 & 1 & 1 & -1 & 1 & 1 & -1 \\ 1 & 0 & -1 & 0 & 0 & 1 & 0 & 0 \\ 1 & 1 & 0 & 1 & 0 & 0 & 0 & 0 \\ 1 & 0 & 1 & 0 & 0 & 1 & 0 & 0 \\ 1 & -1 & 0 & 1 & 0 & 0 & 0 & 0 \end{bmatrix} \begin{Bmatrix} \alpha_1 \\ \alpha_2 \\ \alpha_3 \\ \alpha_4 \\ \alpha_5 \\ \alpha_6 \\ \alpha_7 \\ \alpha_8 \end{Bmatrix} \tag{2.12.118}$$

Inversion of the matrix gives

$$\begin{Bmatrix} \alpha_1 \\ \alpha_2 \\ \alpha_3 \\ \alpha_4 \\ \alpha_5 \\ \alpha_6 \\ \alpha_7 \\ \alpha_8 \end{Bmatrix} = \frac{1}{4} \begin{bmatrix} -1 & -1 & -1 & -1 & 2 & 2 & 2 & 2 \\ 0 & 0 & 0 & 0 & 0 & 2 & 0 & -2 \\ 0 & 0 & 0 & 0 & -2 & 0 & 2 & 0 \\ 1 & 1 & 1 & 1 & -2 & 0 & -2 & 0 \\ 1 & -1 & 1 & -1 & 0 & 0 & 0 & 0 \\ 1 & 1 & 1 & 1 & 0 & -2 & 0 & -2 \\ -1 & -1 & 1 & 1 & 2 & 0 & -2 & 0 \\ -1 & 1 & 1 & -1 & 0 & -2 & 0 & 2 \end{bmatrix} \begin{Bmatrix} u_1 \\ u_2 \\ u_3 \\ u_4 \\ u_5 \\ u_6 \\ u_7 \\ u_8 \end{Bmatrix} \tag{2.12.119}$$

Similarly

$$\begin{Bmatrix} \alpha_9 \\ \alpha_{10} \\ \alpha_{11} \\ \alpha_{12} \\ \alpha_{13} \\ \alpha_{14} \\ \alpha_{15} \\ \alpha_{16} \end{Bmatrix} = \frac{1}{4} \begin{bmatrix} -1 & -1 & -1 & -1 & 2 & 2 & 2 & 2 \\ 0 & 0 & 0 & 0 & 0 & 2 & 0 & -2 \\ 0 & 0 & 0 & 0 & -2 & 0 & 2 & 0 \\ 1 & 1 & 1 & 1 & -2 & 0 & -2 & 0 \\ 1 & -1 & 1 & -1 & 0 & 0 & 0 & 0 \\ 1 & 1 & 1 & 1 & 0 & -2 & 0 & -2 \\ -1 & -1 & 1 & 1 & 2 & 0 & -2 & 0 \\ -1 & 1 & 1 & -1 & 0 & -2 & 0 & 2 \end{bmatrix} \begin{Bmatrix} \nu_1 \\ \nu_2 \\ \nu_3 \\ \nu_4 \\ \nu_5 \\ \nu_6 \\ \nu_7 \\ \nu_8 \end{Bmatrix} \tag{2.12.120}$$

Combining the above will give a 16×16 matrix which is expressed as

$$\{\alpha\} = [C]^{-1} \{\delta\} \tag{2.12.121}$$

and the $[M]$ Matrix is given by

$$[M] = \begin{bmatrix} 1 & \xi & \eta & \xi^2 & \xi\eta & \eta^2 & \xi^2\eta & \xi\eta^2 & 0 & 0 & 0 & 0 & 0 & 0 & 0 & 0 \\ 0 & 0 & 0 & 0 & 0 & 0 & 0 & 0 & 1 & \xi & \eta & \xi^2 & \xi\eta & \eta^2 & \xi^2\eta & \xi\eta^2 \end{bmatrix} \tag{2.12.122}$$

Multiplication of $[M]\,[C]^{-1}$ would give the desired shape function $[N]$.

But if you try to carry out this operation you will find it surprisingly laborious and chance of making a computational mistake is quite high. This made people realize *that conventional procedure used for linear elements to determine the shape function was not a very effective method in this case especially if we take elements of still higher order. The problem would become an absolute disaster for instance with higher order brick elements of say 20 nodes.*

Thus alternative method was devised to determine the shape functions which would not be labor intensive or unmanageable and at the same time would predict the expressions correctly and quickly.

We now present herein various techniques used to define shape function for these higher order elements other then the method as shown previously.

2.12.27 Lagrange's interpolation function – An extension to school co-ordinate geometry[59]

We start with an elementary problem of school co-ordinate geometry.

As shown in Figure 2.12.32 is a straight line which passes through two points A and B having co-ordinates (x_0, y_0) and (x_1, y_1) respectively, we would like to formulate its generic equation.

59 Professional Engineers whose mathematical base has eroded a bit due to lack of practice need not panic with the terminology (Lagrange's Interpolation) it is nothing but a little bit of high school coordinate geometry and its extension.

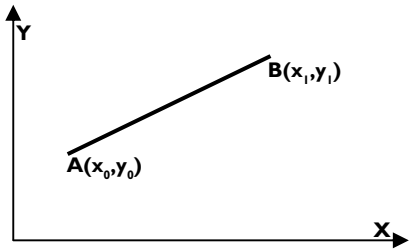


Figure 2.12.32 A straight line passing through two points *A* and *B*.

If the general equation of the line is, $y = mx + c$, we can argue that since the line passes through the points A and B the points (x_0, y_0) and (x_1, y_1) must satisfy the equation. Thus we have, $y_0 = mx_0 + c$ and, $y_1 = mx_1 + c$. Eliminating c from the above two equations we have $m = \frac{y_0 - y_1}{x_0 - x_1}$ which gives the gradient of the line. Substituting this value in the equation, $y_0 = mx_0 + c$, we have $c = \frac{x_0 y_1 - x_1 y_0}{x_0 - x_1}$. Thus the straight line equation can be expressed as

$$y = \frac{y_0 - y_1}{x_0 - x_1} x + \frac{x_0 y_1 - x_1 y_0}{x_0 - x_1}$$

The above on simplification and slight algebraic manipulation can be expressed as

$$y = \frac{x - x_1}{x_0 - x_1} y_0 + \frac{x - x_0}{x_1 - x_0} y_1$$

which is the desired expression for the straight line.

Now, the above can be further expressed as

$$y = L_0(x) y_0 + L_1(x) y_1$$

where, $L_0(x) = \frac{x - x_1}{x_0 - x_1}$ and $L_1(x) = \frac{x - x_0}{x_1 - x_0}$ are called *Lagrange's interpolation function.*

One should observe a feature of these coefficients is that

For $x = x_0$ $L_0(x) \to 1$ and $L_1(x) \to 0$ and for $x = x_1$ $L_0(x) \to 0$ and $L_1(x) \to 1$

The above can thus be generically represented as

$$\begin{aligned} L_i(x_j) &= 1 \quad \text{for } i = j \\ &= 0 \quad \text{for } i \neq j. \end{aligned}$$

Extending the above argument for a line passing through 3 points (x_0, y_0), (x_1, y_1) and (x_2, y_2) we have

$$y = \frac{(x - x_1)(x - x_2)}{(x_0 - x_1)(x_0 - x_2)} y_0 + \frac{(x - x_0)(x - x_2)}{(x_1 - x_0)(x_1 - x_2)} y_1$$

Observe here that while line passes through 3 points the relation is quadratic and can be expressed in terms of Lagrange's functions as

$$y = L_0(x)y_0 + L_1(x)\,y_1 + L_2(x)y_2$$

The Lagrange's coefficient thus passing through $(N+1)$-points can thus be expressed as

$$L_{N,k}(x) = \frac{(x-x_0)\cdot\cdots\cdot(x-x_{k-1})\,(x-x_{k+1})\cdot\cdots\cdot(x-x_N)}{(x_k-x_0)\cdot\cdots\cdot(x_k-x_{k-1})(x_k-x_{k+1})\cdot\cdots\cdot(x_k-x_N)} \tag{2.12.123}$$

The above in terms of natural co-ordinate can be can thus be expressed as

$$f_i(\xi) = \frac{(\xi-\xi_1)\cdot\cdots\cdot(\xi-\xi_{i-1})\,(\xi-\xi_{i+1})\cdot\cdots\cdot(\xi-\xi_N)}{(\xi_i-\xi_1)\cdot\cdots\cdot(\xi_i-\xi_{i-1})(\xi_i-\xi_{i+1})\cdot\cdots\cdot(\xi_i-\xi_N)} \tag{2.12.124}$$

It should be noted in the above expression that the node concerned *should be absent from the numerator and should only be present in the denominator.*

Thus, for a straight line as shown in Figure 2.12.33.

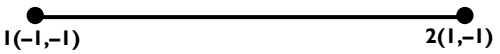


Figure 2.12.33 Lagrangian interpolation for a line element.

$$N_1 = f_1(\xi) = \frac{\xi-\xi_2}{\xi_1-\xi_2} = \frac{\xi-1}{-1-1} = \frac{1-\xi}{2} \quad \text{and}$$

$$N_2 = f_2(\xi) = \frac{\xi-\xi_1}{\xi_2-\xi_1} = \frac{\xi-(-1)}{1-(-1)} = \frac{\xi+1}{2}$$

We will now derive the shape function by Lagrange's interpolation formula of 4 node rectangular element shown in Figure 2.12.34, for which we had derived the shape function earlier.

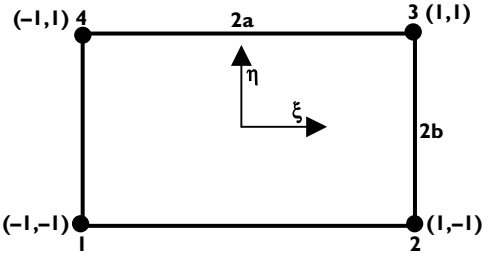


Figure 2.12.34 Lagrangian interpolation for a 4 nodded element.

$$N_1 = f_1(\xi)f_1(\eta) = \frac{\xi-\xi_2}{\xi_1-\xi_2}\frac{\eta-\eta_4}{\eta_1-\eta_4} = \frac{\xi-1}{-1-1}\frac{\eta-1}{-1-1} = \frac{1}{4}(1-\xi)(1-\eta)$$

$$N_2 = f_2(\xi)f_2(\eta) = \frac{\xi-\xi_1}{\xi_2-\xi_1}\frac{\eta-\eta_3}{\eta_2-\eta_3} = \frac{\xi+1}{2}\frac{\eta-1}{-1-1} = \frac{1}{4}(1+\xi)(1-\eta)$$

$$N_3 = f_3(\xi)f_3(\eta) = \frac{\xi-\xi_4}{\xi_3-\xi_4}\frac{\eta-\eta_2}{\eta_3-\eta_2} = \frac{1}{4}(1+\xi)(1+\eta)$$

$$N_4 = f_4(\xi)f_4(\eta) = \frac{\xi-\xi_3}{\xi_4-\xi_3}\frac{\eta-\eta_1}{\eta_4-\eta_1} = \frac{1}{4}(1-\xi)(1+\eta) \qquad (2.12.125)$$

This is same as what we had derived before but differently.

2.12.27.1 Nine node Rectangular Element

We present here the shape function for nine-nodded rectangular element (Figure 2.12.35) based on Lagrange's interpolation function having quadratic polynomial function. You should realize here that *eight node rectangular element is not possible directly*, for if we remove the internal node 9 the interpolation function between 8–6 and 5–7 becomes linear and does not remain quadratic – for we had shown earlier that a line must pass through minimum three nodes to develop quadratic polynomial.

The function being quadratic in this case we have

$$N_1 = \frac{(\xi-\xi_2)(\xi-\xi_5)}{(\xi_1-\xi_2)(\xi_1-\xi_5)}\frac{(\eta-\eta_4)(\eta-\eta_8)}{(\eta_1-\eta_4)(\eta_1-\eta_8)} = \frac{(\xi-1)(\xi-0)}{(-1-1)(-1-0)}\frac{(\eta-1)(\eta-0)}{(-1-1)(-1-0)}$$

$$= \frac{1}{4}[\xi\eta(\xi-1)(\eta-1)]$$

$$N_5 = \frac{(\xi-\xi_2)(\xi-\xi_1)}{(\xi_5-\xi_2)(\xi_5-\xi_1)}\frac{(\eta-\eta_9)(\eta-\eta_7)}{(\eta_5-\eta_9)(\eta_5-\eta_7)} = \frac{(\xi-1)(\xi+1)}{(0-1)(0+1)}\frac{(\eta-1)(\eta-0)}{(-1-0)(-1-1)}$$

$$= \frac{1}{2}\left[\eta(\eta-1)(1-\xi^2)\right]$$

$$N_2 = \frac{(\xi-\xi_5)(\xi-\xi_1)}{(\xi_2-\xi_5)(\xi_2-\xi_1)}\frac{(\eta-\eta_6)(\eta-\eta_3)}{(\eta_2-\eta_6)(\eta_2-\eta_3)} = \frac{1}{4}\xi\eta(\xi+1)(\eta-1)$$

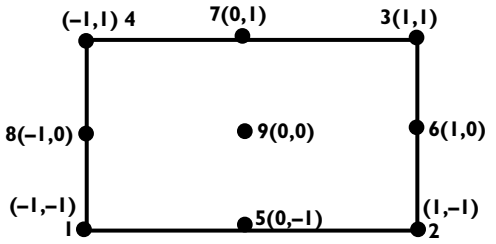


Figure 2.12.35 A nine nodded element.

$$N_6 = \frac{(\xi - \xi_9)(\xi - \xi_8)}{(\xi_6 - \xi_9)(\xi_6 - \xi_8)} \frac{(\eta - \eta_2)(\eta - \eta_3)}{(\eta_6 - \eta_2)(\eta_6 - \eta_3)} = \frac{1}{2}\xi(\xi + 1)(1 - \eta^2) \qquad (2.12.126)$$

Proceeding in identical manner we may have

$$N_3 = \frac{1}{4}[\xi\eta(\xi + 1)(\eta + 1)]; \quad N_4 = \frac{1}{4}[\xi\eta(\xi - 1)(\eta + 1)];$$
$$N_7 = \frac{1}{2}\eta(\eta + 1)(1 - \xi^2); \quad N_8 = \frac{1}{2}\xi(\xi - 1)(1 - \eta^2);$$
$$N_9 = (1 - \xi^2)(1 - \eta^2). \qquad (2.12.127)$$

The internal node 9 is an internal node as such after formulation of the element stiffness matrix (of order 18×18) needs to be condensed out. The condensed matrix which will finally have eight nodes will have a matrix of order 16×16.

2.12.28 Elements of Serendipidity family – named after Princes of Serendip

Though the word "Serendipdity" is not a commonly used English word, yet is a common terminology used by the members of FEM developers club. The word was coined originally by Horace Walpole (in literary sense) and adapted by Zienkiewicz. The reason for the same will be explained later.

First, let us see, what are the properties of these elements those belong to this group. While deriving the shape functions based on Lagrange's interpolation function, we had shown that for the polynomial functions having order more than one we have to take additional internal nodes. The internal node is finally condensed out to crunch the matrix considering only those nodes which are at the boundary of the element. As the degree of the polynomial increases cubic, quartic etc the number of internal nodes will also increase.

As an example we show in Figure 2.12.36, the number of node required for a rectangular element having cubic polynomial function.

In this case we see that after formulation of stiffness matrix we have to condense out the four nodes 13 to 16. Thus it is evident that for finite elements of higher order derived from Lagrange's interpolation formula the computational work that needs to be done at element level is more. For a finite element model of say 500 elements with this cubic 16 node element we have to thus perform condensation of 2000 nodes which would invariably kill a significant amount of computer time. To overcome this problem a different technique was devised where considering the internal nodes are not required.

Elements having polynomial functions developed by this method where internal nodes are not required for the formulating the desired polynomial functions are known as elements of Serendipidity family.

Eight-nodded quadrilaterals/rectangular elements belong to this group/family.

To understand the concept we start with four node rectangular elements shown in Figure 2.12.37 whose shape functions we had derived earlier.

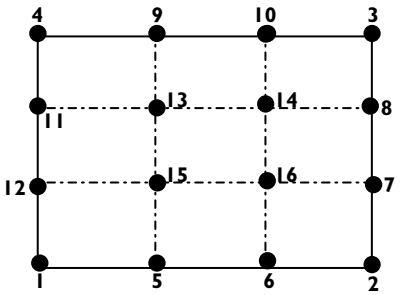


Figure 2.12.36 16-nodded rectangular element having cubic polynomial shape function.

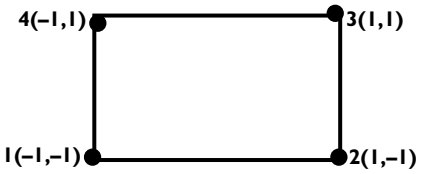


Figure 2.12.37 Four-nodded rectangular element.

We had shown earlier that for four node rectangular element

$$N_1 = \frac{1}{4}(1-\xi)(1-\eta); \quad N_2 = \frac{1}{4}(1+\xi)(1-\eta); \quad N_3 = \frac{1}{4}(1+\xi)(1+\eta);$$

$$N_4 = \frac{1}{4}(1-\xi)(1+\eta)$$

Looking at above it will observed that the above formula can be generalized as

$$N_i = \frac{1}{4}(1+\xi\xi_i)(1+\eta\,\eta_i) \tag{2.12.128}$$

where i is the node considered and (ξ_i, η_i) is the co-ordinate value corresponding to node i in natural coordinate.

For eight node rectangular elements (Figure 2.12.38) having quadratic shape function the generic formulation is given as

$$N_i = \frac{1}{4}(1+\xi\xi_i)\left(1+\eta\eta_i\right)\left(\xi\xi_i + \eta\eta_i - 1\right) \quad \text{for corner nodes}$$

$$N_i = \frac{1}{2}(1-\xi^2)(1+\eta\eta_i) \quad \text{for mid side nodes where } \xi_i = 0 \tag{2.12.129}$$

$$N_i = \frac{1}{2}(1-\eta^2)(1+\xi\xi_i) \quad \text{for mid side nodes where } \eta_i = 0$$

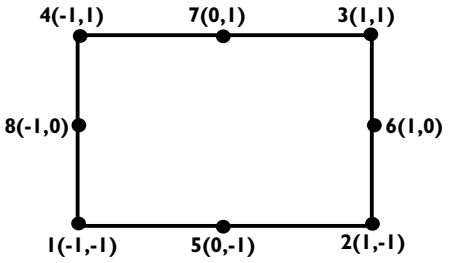


Figure 2.12.38 Eight-nodded rectangular element.

Thus for eight node rectangular element we have

$$N_1 = (1-\xi)(1-\eta)(1+\xi+\eta)/4; \quad N_2 = (1+\xi)(1-\eta)(\xi-\eta-1)/4;$$
$$N_3 = (1+\xi)(1+\eta)(1+\xi+\eta)/4; \quad N_4 = (1-\xi)(1+\eta)(\eta-\xi-1)/4;$$
$$N_5 = (1-\xi^2)(1-\eta)/2; \quad N_6 = (1+\xi)(1-\eta^2)/2;$$
$$N_7 = (1-\xi^2)(1+\eta)/2; \quad N_8 = (1-\xi)(1-\eta^2)/2 \tag{2.12.130}$$

For cubic function similarly the general equation for deriving the shape function is given by

$$N_i = \frac{1}{32}(1+\xi\xi_i)(1+\eta\eta_i)[-10+9(\xi^2+\eta^2)], \quad \text{for corner nodes}$$
$$N_i = \frac{9}{32}(1+\xi\xi_i)(1-\eta^2)[1+9\eta\eta_i]; \quad \text{for } \xi_i = \pm 1 \text{ and } \eta_i = \pm 1/3;$$
$$\text{and} \quad N_i = \frac{9}{32}(1+\eta\eta_i)(1-\xi^2)[1+9\xi\xi_i], \quad \text{for } \xi_i = \pm 1/3 \text{ and } \eta_i = \pm 1. \tag{2.12.131}$$

You will observe here that the formula for 4 node rectangle was furnished without any formal mathematical derivations and as such they were actually presented based on mere observation. While that for the higher order were actually derived based more on intuition-almost a chance discovery. *It was for this Zienkieiwicz named them as Serendip Elements after the princes of Serendip who were famous for their chance discoveries*[60].

Having established the basis of derivation of formulation for elements belonging to the Serendipidity family we present hereafter the element stiffness matrix derivation for an 8-node quadrilateral which is by far the most popular of all elements of Serendip group.

60 The place Serendip is actually the country known as Sri Lanka today. There lived three princes from Serendip who went on a journey to redeem their father's Kingdom from a dragon, and in their journey each one of them chanced upon treasures they neither sought or anticipated. We perceive the word Serendip is a actually an anglicized derivative of the Sanskrit word "Swarna Dweep" meaning Golden Island. For that was how Sir Lanka was known as in ancient times.

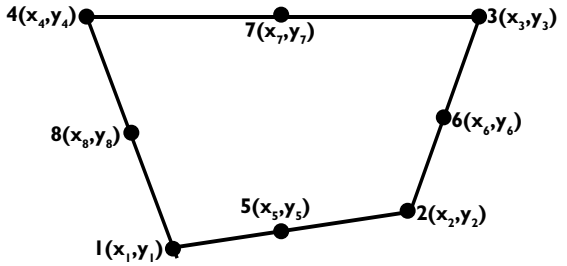


Figure 2.12.39 Eight-nodded quadrilateral element.

2.12.28.1 Eight-nodded quadrilateral of Serendipidity family

Shown in Figure 2.12.39, is a generic quadrilateral element having 8 nodes with their nodal coordinates.

To derive the [*B*] Matrix as a first step we tabulate the shape functions and their derivative as shown below

1	N_1	$(1-\xi)(1-\eta)(1+\xi+\eta)/4$	$\partial N_1/\partial\xi$	$(1-\eta)(2\xi+\eta)/4$	$\partial N_1/\partial\eta$	$(1-\xi)(2\eta+\xi)/4$
2	N_2	$(1+\xi)(1-\eta)(\xi-\eta-1)/4$	$\partial N_2/\partial\xi$	$(1-\eta)(2\xi-\eta)/4$	$\partial N_2/\partial\eta$	$(1+\xi)(2\eta-\xi)/4$
3	N_3	$(1+\xi)(1+\eta)(1+\xi+\eta)/4$	$\partial N_3/\partial\xi$	$(1+\eta)(2\xi+\eta)/4$	$\partial N_3/\partial\eta$	$(1+\xi)(2\eta+\xi)/4$
4	N_4	$(1-\xi)(1+\eta)(\eta-\xi-1)/4$	$\partial N_4/\partial\xi$	$(1+\eta)(2\xi-\eta)/4$	$\partial N_4/\partial\eta$	$(1-\xi)(2\eta-\xi)/4$
5	N_5	$(1-\xi^2)(1-\eta)/2$	$\partial N_5/\partial\xi$	$-(1-\eta)\xi$	$\partial N_5/\partial\eta$	$-(1-\xi^2)/2$
6	N_6	$(1+\xi)(1-\eta^2)/2$	$\partial N_6/\partial\xi$	$-(1-\eta^2)/2$	$\partial N_6/\partial\eta$	$-(1+\xi)\eta$
7	N_7	$(1-\xi^2)(1+\eta)/2$	$\partial N_7/\partial\xi$	$-(1+\eta)\xi$	$\partial N_7/\partial\eta$	$(1-\xi^2)/2$
8	N_8	$(1-\xi)(1-\eta^2)/2$	$\partial N_8/\partial\xi$	$-(1-\eta^2)\xi$	$\partial N_8/\partial\eta$	$-(1-\xi)\eta$

$$J_{11} = \frac{\partial}{\partial\xi}\sum_{i=1}^{8} N_i x_i = \frac{(1-\eta)(2\xi+\eta)}{4}x_1 + \frac{(1-\eta)(2\xi-\eta)}{4}x_2 + \frac{(1+\eta)(2\xi+\eta)}{4}x_3 + \frac{(1+\eta)(2\xi-\eta)}{4}x_4 - (1-\eta)\xi x_5 - \frac{(1-\eta^2)}{2}x_6 - (1+\eta)\xi x_7 - (1-\eta^2)\xi x_8$$

$$J_{12} = \frac{\partial}{\partial\xi}\sum_{i=1}^{8} N_i y_i = \frac{(1-\eta)(2\xi+\eta)}{4}y_1 + \frac{(1-\eta)(2\xi-\eta)}{4}y_2 + \frac{(1+\eta)(2\xi+\eta)}{4}y_3 + \frac{(1+\eta)(2\xi-\eta)}{4}y_4 - (1-\eta)\xi y_5 - \frac{(1-\eta^2)}{2}y_6 - (1+\eta)\xi y_7 - (1-\eta^2)\xi y_8 \tag{2.12.132}$$

$$J_{21} = \frac{\partial}{\partial \eta}\sum_{i=1}^{8} N_i x_i = \frac{(1-\xi)(2\eta+\xi)}{4}x_1 + \frac{(1+\xi)(2\eta-\xi)}{4}x_2$$
$$+ \frac{(1+\xi)(2\eta+\xi)}{4}x_3 + \frac{(1-\xi)(2\eta-\xi)}{4}x_4 - \frac{(1-\xi^2)}{2}x_5$$
$$- (1+\xi)\eta x_6 + \frac{(1-\xi^2)}{2}x_7 - (1-\xi)\eta x_8$$

$$J_{22} = \frac{\partial}{\partial \eta}\sum_{i=1}^{8} N_i y_i = \frac{(1-\xi)(2\eta+\xi)}{4}y_1 + \frac{(1+\xi)(2\eta-\xi)}{4}y_2$$
$$+ \frac{(1+\xi)(2\eta+\xi)}{4}y_3 + \frac{(1-\xi)(2\eta-\xi)}{4}y_4 - \frac{(1-\xi^2)}{2}y_5$$
$$- (1+\xi)\eta y_6 + \frac{(1-\xi^2)}{2}y_7 - (1-\xi)\eta y_8$$

Considering $|J| = J_{11} \times J_{22} - J_{12} \times J_{21}$ we have the strain matrix as

$$\begin{Bmatrix} \varepsilon_x \\ \varepsilon_y \\ \gamma_{xy} \end{Bmatrix} = \frac{1}{|J|}\begin{bmatrix} J_{22} & -J_{12} & 0 & 0 \\ 0 & 0 & -J_{21} & J_{11} \\ -J_{21} & J_{11} & J_{22} & -J_{12} \end{bmatrix}\left\langle \frac{\partial u}{\partial \xi}\ \frac{\partial u}{\partial \eta}\ \frac{\partial v}{\partial \xi}\ \frac{\partial v}{\partial \eta} \right\rangle^T$$

The above can be expanded to

$$\begin{Bmatrix} \varepsilon_x \\ \varepsilon_y \\ \gamma_{xy} \end{Bmatrix} = \frac{1}{|J|}\begin{bmatrix} J_{22} & -J_{12} & 0 & 0 \\ 0 & 0 & -J_{21} & J_{11} \\ -J_{21} & J_{11} & J_{22} & -J_{12} \end{bmatrix}$$
$$\times \begin{bmatrix} \frac{\partial N_1}{\partial \xi} & 0 & \frac{\partial N_2}{\partial \xi} & 0 & \frac{\partial N_3}{\partial \xi} & 0 & \frac{\partial N_4}{\partial \xi} & 0 & \frac{\partial N_5}{\partial \xi} & 0 & \frac{\partial N_6}{\partial \xi} & 0 & \frac{\partial N_7}{\partial \xi} & 0 & \frac{\partial N_8}{\partial \xi} & 0 \\ \frac{\partial N_1}{\partial \eta} & 0 & \frac{\partial N_2}{\partial \eta} & 0 & \frac{\partial N_3}{\partial \eta} & 0 & \frac{\partial N_4}{\partial \eta} & 0 & \frac{\partial N_5}{\partial \eta} & 0 & \frac{\partial N_6}{\partial \eta} & 0 & \frac{\partial N_7}{\partial \eta} & 0 & \frac{\partial N_8}{\partial \eta} & 0 \\ 0 & \frac{\partial N_1}{\partial \xi} & 0 & \frac{\partial N_2}{\partial \xi} & 0 & \frac{\partial N_3}{\partial \xi} & 0 & \frac{\partial N_4}{\partial \xi} & 0 & \frac{\partial N_5}{\partial \xi} & 0 & \frac{\partial N_6}{\partial \xi} & 0 & \frac{\partial N_7}{\partial \xi} & 0 & \frac{\partial N_8}{\partial \xi} \\ 0 & \frac{\partial N_1}{\partial \eta} & 0 & \frac{\partial N_2}{\partial \eta} & 0 & \frac{\partial N_3}{\partial \eta} & 0 & \frac{\partial N_4}{\partial \eta} & 0 & \frac{\partial N_5}{\partial \eta} & 0 & \frac{\partial N_6}{\partial \eta} & 0 & \frac{\partial N_7}{\partial \eta} & 0 & \frac{\partial N_8}{\partial \eta} \end{bmatrix}$$
$$\times \langle u_1\ \ v_1\ \ u_2\ \ v_2\ \ u_3\ \ v_3\ \ u_4\ \ v_4\ \ u_5\ \ v_5\ \ u_6\ \ v_6\ \ u_7\ \ v_7\ \ u_8\ \ v_8 \rangle^T$$

From which we get

$$[B] = \frac{1}{|J|}\begin{bmatrix} J_{22} & -J_{12} & 0 & 0 \\ 0 & 0 & -J_{21} & J_{11} \\ -J_{21} & J_{11} & J_{22} & -J_{12} \end{bmatrix}$$

$$\times \begin{bmatrix} \frac{\partial N_1}{\partial \xi} & 0 & \frac{\partial N_2}{\partial \xi} & 0 & \frac{\partial N_3}{\partial \xi} & 0 & \frac{\partial N_4}{\partial \xi} & 0 & \frac{\partial N_5}{\partial \xi} & 0 & \frac{\partial N_6}{\partial \xi} & 0 & \frac{\partial N_7}{\partial \xi} & 0 & \frac{\partial N_8}{\partial \xi} & 0 \\ \frac{\partial N_1}{\partial \eta} & 0 & \frac{\partial N_2}{\partial \eta} & 0 & \frac{\partial N_3}{\partial \eta} & 0 & \frac{\partial N_4}{\partial \eta} & 0 & \frac{\partial N_5}{\partial \eta} & 0 & \frac{\partial N_6}{\partial \eta} & 0 & \frac{\partial N_7}{\partial \eta} & 0 & \frac{\partial N_8}{\partial \eta} & 0 \\ 0 & \frac{\partial N_1}{\partial \xi} & 0 & \frac{\partial N_2}{\partial \xi} & 0 & \frac{\partial N_3}{\partial \xi} & 0 & \frac{\partial N_4}{\partial \xi} & 0 & \frac{\partial N_5}{\partial \xi} & 0 & \frac{\partial N_6}{\partial \xi} & 0 & \frac{\partial N_7}{\partial \xi} & 0 & \frac{\partial N_8}{\partial \xi} \\ 0 & \frac{\partial N_1}{\partial \eta} & 0 & \frac{\partial N_2}{\partial \eta} & 0 & \frac{\partial N_3}{\partial \eta} & 0 & \frac{\partial N_4}{\partial \eta} & 0 & \frac{\partial N_5}{\partial \eta} & 0 & \frac{\partial N_6}{\partial \eta} & 0 & \frac{\partial N_7}{\partial \eta} & 0 & \frac{\partial N_8}{\partial \eta} \end{bmatrix} \tag{2.12.133}$$

Here differential coefficients are as described in Table 2.11.1.

Thus the element stiffness matrix can now be obtained from the expression

$$[K]_e = t \int_{-1}^{1} \int_{-1}^{1} [B]^T [D] [B] |J| \, d\xi \, d\eta \tag{2.12.134}$$

Since the function is quadratic, two-point Gauss integration will give an accurate value for this element.

2.12.28.2 *Which to follow Lagrange or Serendip?*

Having gone through the two methods you might wonder which is superior and which formulation to follow in developing a higher order element?

Logically Lagrange would be a better choice (though not used very regularly) for the polynomial is complete and would thus be more accurate than elements of Serendip family. However the additional computation it incurs due to static condensation at element level does not make it an automatic choice. Serendip family elements are equally good and error accrued is not significant for practical engineering problems.

2.12.28.3 *Other Interpolation Formulas*

The Lagrange and Serendip family formulation are usually called C_0 type formulation, for in this case nodal displacements among adjacent elements are compatible while there derivatives are not. There are cases where not only the displacements need to be compatible at nodes there first and second derivatives also need to be compatible too. Plates/Slabs under bending is a classical example of this. In such case we use a different type of interpolation function called **Hermite Polynomials** (these are often referred to as C_1 and C_2 type for the continuity of their derivatives). Other then this Hierarchical and Heuristic type polynomial functions are also being used to develop Various types of elements – for more information on this one may refer Reference 22 (Advanced topics) given at the end of this chapter.

2.12.29 Other type of higher order elements

A number of other type of higher order elements are possible like *6-node triangular elements, 20 node brick element* etc.

Since, we are not writing this book on finite element only we have restricted our discussion only to those elements which or often used for practical engineering work. To know more about these elements reader may refer to the References cited at the end of the chapter.

2.12.30 Plate element – the problem child of FEM family

Though this book is not a comprehensive treatment on FEM, yet any discussion on FEM would possibly remain incomplete without some discussion on plates subjected to bending.

From the very outset, plate element has remained a problem to the finite element analysts, irrespective of whether he was a developer, assembler or a user.

Leaving aside the fact that basic equation of equilibrium of a plate element is bi-harmonic (∇^4) in nature, plate in bending creates far more complication than plane stress case. Plates have their own unique properties that require special manipulation. This has given the developers quite a rough time.

For assemblers, one of the major concerns was – since plates undergo bending normal to its plane the stress is discontinuous at edges (as are the slopes) and has created a lot of difficulty in terms of numerical computation as well as interpretations. For some cases (unlike 2D plane stress/strain case) formulation has proved to be quite difficult for neither the formulation were feasible based on hand computations (too laborious and tedious) nor were a logical algorithm emerging which was conducive to programming. Even if these were managed, many of them were failing important patch test or were giving poor result for certain geometrical orientations.

In-spite of all these initial frustrations the developers kept trying to come up with a complete and mathematically robust element – and the result is plethora of elements available in the market (not all of them are unconditionally stable though).

Users are in no better condition, for when it came to selecting the element available, numbers are confusingly high.

Clough and Felippa (1968), Veubeke (1967), Melosh (1963), Hughes and Taylor (1977), Toucher (1962), Pian and Tong (1969), Adini and Clough (1960), Bogner et al. (1965), LORA (Kardestuncer and Norrie 1987)... , the list is almost unending.

We perceive one can write a complete book presenting different plate elements available in the market for engineering application. It is thus impossible for an average engineer to know the strengths and weakness of every element he comes across before he puts it to use. The list still complicates when we further break it down to thin plate (Kirchoff type) and thick plate (Mindilin–Reissner type).

Since the literature is vast and it is not possible to cover all in such a short space we will restrict our discussions only to a few key elements that are mostly used in the industry and are generally considered reasonably stable.

To further concise the issue we will present in some cases only the final stiffness matrix describing (not deriving) the basic steps involved in formulating them.

If you put them to use by developing your own software we suggest you to test them before hand by running test samples for simple cases (like we did in our FDM example) and compare the results with exact solution. Or else you can run an eigen-value test to ensure the matrices are consistent and do not have any spurious modes.

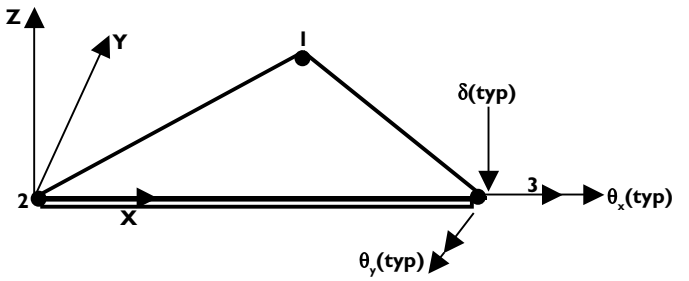


Figure 2.12.40 A triangular thin plate element in bending.

2.12.31 Triangular plate element in bending – the Catch-22 element

The element was found to be naturally non-conforming in bending mode. If you try to make complete polynomials as per Pascal triangle, the plate becomes *non-conforming*.

On the other hand if you try to make the element conforming, the polynomial *function becomes skewed or incomplete!*

To understand this problem further, let us consider the triangular element having three degrees of freedom per node (one translation and two rotations, Figure 2.12.40) having total nine degrees of freedom.

This means that when we formulate $\{f\} = [M]\{\alpha\}$ for triangular plate we must have $\{\alpha\} = \langle \alpha_1\ \alpha_2\ \alpha_3\ \ldots\ \alpha_9 \rangle^T$. Based on Pascal triangle we thus have

$$\delta = \alpha_1 + \alpha_2 x + \alpha_3 y + \alpha_4 x^2 + \alpha_5 xy + \alpha_6 y^2 + \alpha_7 x^3 + \alpha_8 x^2 y + \alpha_9 xy^2 \quad (2.12.135)$$

If you now check the Pascal triangle, you will see that the polynomial function is *incomplete*. This is because the term y^3 is missing (meaning thereby that the shape function is now skewed towards the x axis).

To make the polynomial complete the correct shape function should be

$$\delta = \alpha_1 + \alpha_2 x + \alpha_3 y + \alpha_4 x^2 + \alpha_5 xy + \alpha_6 y^2 + \alpha_7 x^3 + \alpha_8 x^2 y + \alpha_9 xy^2 + \alpha_{10} y^3 \quad (2.12.136)$$

The choice of polynomial is now correct but it violates the law "*number of coefficients must be equal to the number of degrees of freedom*", and has become *non-conforming*.

For argument sake, to cater to α_{10}, if we take another node then where do we take this node which is most appropriate? The situation is indeed confusing and left the developers somewhat confused for some time.

Toucher (1962) suggested considering the polynomial function as

$$\delta = \alpha_1 + \alpha_2 x + \alpha_3 y + \alpha_4 x^2 + \alpha_5 xy + \alpha_6 y^2 + \alpha_7 x^3 + \alpha_8 (x^2 y + xy^2) + \alpha_9 y^3 \quad (2.12.137)$$

This makes the function consistent and complete[61].

However, this did not mean the trouble was over. For it was found that for elements having two of its sides parallel to global X and Y axes, when we perform the operation $\{\alpha\} = [C]^{-1}\{\delta\}$, the determinant of the matrix $[C]$ becomes zero that is, *the matrix becomes singular*.

In-spite of this fallibility the element has been in past used for a number of practical engineering applications[62], though its overall performance with respect to stress is not deemed good unless sufficiently refined.

Irrespective of this short coming we will still proceed with this element to give a you a first hand idea of how we derive the element stiffness matrix for plate bending problem and the difficulties we face in the process, before we present more superior elements that are used now a days.

Here let

$$\delta = \alpha_1 + \alpha_2 x + \alpha_3 y + \alpha_4 x^2 + \alpha_5 xy + \alpha_6 y^2 + \alpha_7 x^3 + \alpha_8 (x^2 y + xy^2) + \alpha_9 y^3 \tag{2.12.138}$$

where $\{\delta\}^T = \langle w_1 \quad \theta_{x1} \quad \theta_{y1} \quad w_2 \quad \theta_{x2} \quad \theta_{y2} \quad w_3 \quad \theta_{x3} \quad \theta_{y3} \rangle$ and

$$\theta_x = -\frac{\partial w}{\partial y} \quad \text{and} \quad \theta_y = -\frac{\partial w}{\partial x}.$$

Thus

$$\langle w_1, \theta_{x1}, \theta_{y1}, w_2, \theta_{x2}, \theta_{y2}, w_3, \theta_{x3}, \theta_{y3} \rangle^T =$$

$$\begin{bmatrix}
1 & x_1 & y_1 & x_1^2 & x_1 y_1 & y_1^2 & x_1^3 & x_1^2 y_1 + x_1 y_1^2 & y_1^3 \\
0 & 0 & 1 & 0 & x_1 & 2y_1 & 0 & x_1^2 + 2x_1 y_1 & 3y_1^2 \\
0 & -1 & 0 & -2x_1 & -y_1 & 0 & -3x_1^2 & -2x_1 y_1 - y_1^2 & 0 \\
1 & x_2 & y_2 & x_2^2 & x_2 y_2 & y_2^2 & x_2^3 & x_2^2 y_2 + x_2 y_2^2 & y_2^3 \\
0 & 0 & 1 & 0 & x_2 & 2y_2 & 0 & x_2^2 + 2x_2 y_2 & 3y_2^2 \\
0 & -1 & 0 & -2x_2 & -y_2 & 0 & -3x_2^2 & -2x_2 y_2 - y_2^2 & 0 \\
1 & x_3 & y_3 & x_3^2 & x_3 y_3 & y_3^2 & x_3^3 & x_3^2 y_3 + x_3 y_3^2 & y_3^3 \\
0 & 0 & 1 & 0 & x_3 & 2y_3 & 0 & x_3^2 + 2x_3 y_3 & 3y_3^2 \\
0 & -1 & 0 & -2x_3 & -y_3 & 0 & -3x_3^2 & -2x_3 y_3 - y_3^2 & 0
\end{bmatrix}
\begin{Bmatrix}
\alpha_1 \\ \alpha_2 \\ \alpha_3 \\ \alpha_4 \\ \alpha_5 \\ \alpha_6 \\ \alpha_7 \\ \alpha_8 \\ \alpha_9
\end{Bmatrix}$$

i.e. $\{\delta\} = [C]\{\alpha\}$ this would give

$$\{\alpha\} = [C]^{-1}\{\delta\} \tag{2.12.139}$$

61 We feel this was done more out of intuition rather than any mathematical logic influencing the postulation. We could be wrong though. We have however not come across any formal proof on this issue and shall be grateful if somebody can furnish us with the same.

62 If you use this element just make sure that triangles chosen are not right angle triangles which circumvents the singularity error.

Observer here that it is not possible to find out the value of $[C]^{-1}$ explicitly based on algebraic expression and has to be evaluated numerically by a computer.

Here $[M]$ matrix is given by

$$[M] = \begin{bmatrix} 1 & x & y & x^2 & xy & y^2 & x^3 & x^2y + xy^2 & y^3 \\ 0 & 0 & 1 & 0 & x & 2y & 0 & x^2 + 2xy & 3y^2 \\ 0 & -1 & 0 & -2x & -y & 0 & -3x^2 & -2xy - y^2 & 0 \end{bmatrix}$$

This gives shape function as

$$[N] = [M]\ [C]^{-1}$$

The strain matrix is given by

$$\{\varepsilon\} = \begin{Bmatrix} -\dfrac{\partial^2 w}{\partial x^2} \\ -\dfrac{\partial^2 w}{\partial y^2} \\ -\dfrac{2\partial^2 w}{\partial x \partial y} \end{Bmatrix} = \begin{bmatrix} 0 & 0 & 0 & -2 & 0 & 0 & -6x & -2y & 0 \\ 0 & 0 & 0 & 0 & 0 & -2 & 0 & -2x & -6y \\ 0 & 0 & 0 & 0 & -2 & 0 & 0 & -4(x+y) & 0 \end{bmatrix} [C]^{-1} \begin{Bmatrix} w_1 \\ \theta_{x1} \\ \theta_{y1} \\ w_2 \\ \theta_{x2} \\ \theta_{y1} \\ w_3 \\ \theta_{x3} \\ \theta_{y3} \end{Bmatrix}$$

$$\rightarrow \{\varepsilon\} = [X]\,[C]^{-1}\,\{\delta\} \tag{2.12.140}$$

where $[X] = \begin{bmatrix} 0 & 0 & 0 & -2 & 0 & 0 & -6x & -2y & 0 \\ 0 & 0 & 0 & 0 & 0 & -2 & 0 & -2x & -6y \\ 0 & 0 & 0 & 0 & -2 & 0 & 0 & -4(x+y) & 0 \end{bmatrix}$

Again since $\{\varepsilon\} = [B]\,\{\delta\}$, we have $[B] = [X] \times [C]^{-1}$

Considering $[K] = \iiint [B]^T\,[D]\,[B]\ dv$

we have, $[K] = [C^{-1}]^T[C^{-1}] \iiint [X]^T[D]\,[X] dv$ (2.12.141)

The $[D]$ matrix is given by $[D] = \frac{Et^3}{12(1-\nu^2)} \begin{bmatrix} 1 & \nu & 0 \\ \nu & 1 & 0 \\ 0 & 0 & \frac{1-\nu}{2} \end{bmatrix}$, here t is the thickness of the plate putting this value in the stiffness expression we have

$$[K] = \frac{Et^3}{12(1-\nu^2)} [C^{-1}]^T[C^{-1}] \iint [X]^T \begin{bmatrix} 1 & \nu & 0 \\ \nu & 1 & 0 \\ 0 & 0 & \dfrac{1-\nu}{2} \end{bmatrix} [X]\, dx \cdot dy \tag{2.12.142}$$

$$= \frac{Et^3}{12(1-\nu^2)}[C^{-1}]^T[C^{-1}]$$

$$\times \iint \begin{bmatrix} 0\,0\,0 & 0 & 0 & 0 & 0 & 0 & 0 \\ 0\,0\,0 & 0 & 0 & 0 & 0 & 0 & 0 \\ 0\,0\,0 & 0 & 0 & 0 & 0 & 0 & 0 \\ 0\,0\,0 & 4 & 0 & 4\nu & 12x & 4(\nu x + y) & 12\nu y \\ 0\,0\,0 & 0 & 2(1-\nu) & 0 & 0 & 4(1-\nu)(x+y) & 0 \\ 0\,0\,0 & 4\nu & 0 & 4 & 12\nu x & 4(x+\nu y) & 12y \\ 0\,0\,0 & 12x & 0 & 12\nu x & 36x^2 & 12x(\nu x + y) & 36\nu xy \\ 0\,0\,0 & 4(\nu x+y) & 4(1-\nu)(x+y) & 4(x+\nu y) & 12x(\nu x+y) & (12-8\nu)(x+y)^2 - 8xy(1-\nu) & 12(x+\nu y)y \\ 0\,0\,0 & 12\nu y & 0 & 12y & 36\nu xy & 12(x+\nu y)y & 36y^2 \end{bmatrix}$$

$$\times\, dx \cdot dy$$

This gives the complete stiffness matrix for the triangular plate in bending mode. The integration parameters for the above matrix are as given hereafter:

Sl. No.	*Integral*	*Values*
1	$\iint dydx$	$\frac{1}{2}x_3y_2$
2	$\iint xdydx$	$\frac{1}{6}x_3^2y_2$
3	$\iint x^2dydx$	$\frac{1}{12}x_3^2y_2$
4	$\iint ydydx$	$\frac{1}{6}x_3y_2(y_2+y_3)$
5	$\iint y^2dydx$	$\frac{1}{12}x_3y_2\left(y_2^2+y_2y_3+y_3^2\right)$
6	$\iint xydydx$	$\frac{1}{24}x_3^2y_2(y_2+2y_3)$

It should be noted that to simplify the calculation here co-ordinate axes is made to coincide with edge 1–2 i.e. one has to convert $(x_1,\ y_1)$ to $(0, 0)$ and then make corresponding adjustments to $(x_2,\ y_2)$ and $(x_3,\ y_3)$ to carry out the integration of the stiffness matrix.

2.12.32 DKT Plate element

The finite element club does have its own language and jargons. Rummaging through literature on the topic, you will find a number of abbreviations as mentioned above like ACM element (named after Adini, Clough and Melosh), PLATE8 (means higher order plate element of serendipidity family with 8 nodes) etc.

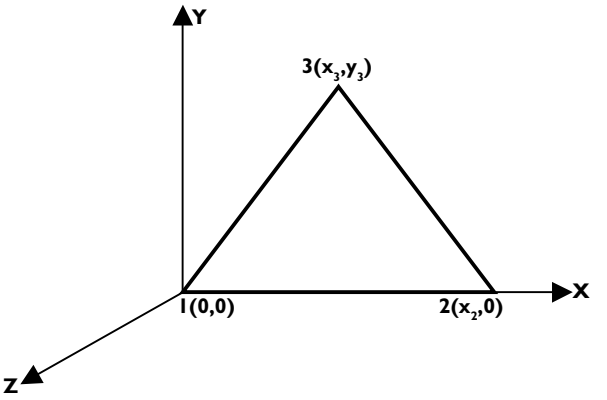


Figure 2.12.41 Triangular plate bending element-with nodal coordinates for DKT element.

Here the word DKT stands for **D**iscrete **K**irchoff **T**heory named after the famous German Mathematician Gustav R. Kirchoff, who was the first to formulate the theory of equilibrium for thin plate[63].

Developed by Batoz et. al. (1980) it is one of the best element available in the market and mathematically considered quite robust. DKT plate element is actually formulated based on thick plate theory of Mindilin and Reissner and converted into a thin plate by taking the transverse shear strain as zero at the specific points. Like the previous triangular element it has nine degrees of freedom and the stiffness matrix is derived in natural coordinate as shown in Figure 2.12.41.

In this case we will not derive the stiffness matrix as in the previous case but will give the final explicit expression as furnished by Batoz (1982).

Considering $[K] = \iiint [B]^T [D] [B] \, dv$, Batoz expressed this as

$$= \frac{1}{2A} [\Lambda]^T [\hat{D}] [\Lambda] \tag{2.12.143}$$

in which

$$[\hat{D}] = \frac{1}{24} \begin{bmatrix} DR & \nu DR & 0 \\ \nu DR & DR & 0 \\ 0 & 0 & 0 \end{bmatrix}, \quad [R] = \begin{bmatrix} 2 & 1 & 1 \\ 1 & 2 & 1 \\ 1 & 1 & 2 \end{bmatrix} \quad \text{and} \quad D = \frac{Et^3}{12(1-\nu^2)}$$

63 The Bi-harmonic equation of plate was actually first proposed by Sophie Germain (1776–1831) a lady mathematician who presented her papers under pseudonym La Blanc. In 1813 she correctly formulated the equation of vibration of plate albeit with some open ended issues and won a prize and citation on this. She can surely be given the credit of being the Mother of Plate Equation.

where $[\Lambda] =$

$$\begin{bmatrix}
y_3p_6 & 0 & -4y_3 & -y_3p_6 & 0 \\
-y_3p_6 & 0 & 2y_3 & y_3p_6 & 0 \\
y_3p_5 & -y_3q_5 & y_3(2-r_5) & y_3p_4 & y_3q_4 \\
-x_2t_5 & (x_2-x_3)+x_2r_5 & -x_2q_5 & 0 & x_3 \\
0 & x_2-x_3 & 0 & x_2t_4 & x_3+x_2r_4 \\
(x_2-x_3)t_5 & (x_2-x_3)(1-r_5) & (x_2-x_3)q_5 & -x_3t_4 & x_3(1-r_4) \\
[-x_3p_6 & & -4(x_2-x_3) & & \\
-x_2p_5] & x_2q_5+y_3 & +x_2r_5 & x_3p_6 & -y_3 \\
[(x_2-x_3)p_5+ & -(x_2-x_3)q_5+ & [(2-r_5)(x_2-x_3) & & [(r_4-1)y_3 \\
y_3t_5] & (1-r_5)y_3] & +y_3q_5] & -x_3p_4+y_3t_4 & -x_3q_4]
\end{bmatrix}$$

$$\begin{bmatrix}
-2y_3 & 0 & 0 & 0 \\
4y_3 & 0 & 0 & 0 \\
y_3(r_4-2) & -y_3(p_4+p_5) & y_3(q_4-q_5) & y_3(r_4-r_5) \\
0 & x_2t_5 & x_2(r_5-1) & -x_2q_5 \\
-x_2q_4 & -x_2t_4 & x_2(r_4-1) & -x_2q_4 \\
2x_3 & -x_2p_5 & x_2q_5 & (r_5-2)x_2 \\
-4x_3+x_2r_4 & -x_2p_4 & x_2q_4 & (r_4-2)x_2 \\
 & [-(x_2-x_3)p_5 & [-(x_2-x_3)q_5 & -(x_2-x_3)r_5 \\
[(2-r_4)x_3 & +x_3p_4- & -x_3q_4+ & -x_3r_4+4x_2 \\
-x_3q_4] & (t_4+t_5)y_3] & (r_4-r_5)y_3] & +(q_5-q_4)y_3
\end{bmatrix}$$

The parameters p, q, r and t etc. are as given hereafter

$$p_4 = \frac{-6(x_2-x_3)}{(x_2-x_3)^2+(y_2-y_3)^2}, \quad p_5 = \frac{-6x_3}{x_3^2+y_3^2}, \quad p_6 = \frac{6x_2}{x_2^2+y_2^2}$$

$$t_4 = \frac{-6(y_2-y_3)}{(x_2-x_3)^2+(y_2-y_3)^2}, \quad t_5 = \frac{-6y_3}{x_3^2+y_3^2}, \quad q_4 = \frac{3(x_2-x_3)(y_2-y_3)}{(x_2-x_3)^2+(y_2-y_3)^2},$$

$$q_5 = \frac{3x_3y_3}{x_3^2+y_3^2}, \quad r_4 = \frac{3(y_2-y_3)^2}{(x_2-x_3)^2+(y_2-y_3)^2}, \quad r_5 = \frac{3y_3^2}{x_3^2+y_3^2}. \tag{2.12.144}$$

2.12.33 Rectangular plate element in bending mode

Like triangular bending element rectangular element is also a naturally non-conforming element. Before we go to a generic 4 node quadrilateral under bending, we derive herein the stiffness matrix for a rectangular element which is quite similar to the stiffness matrix of triangular element derived previously.

As shown in Figure 2.12.42, is a rectangular plate element of length a and width b and thickness t having three degrees of freedom (one translation and two rotation). The total degrees of freedom for the plate is thus 12. So, as per law of polynomial as explained earlier the displacement function is expressed as

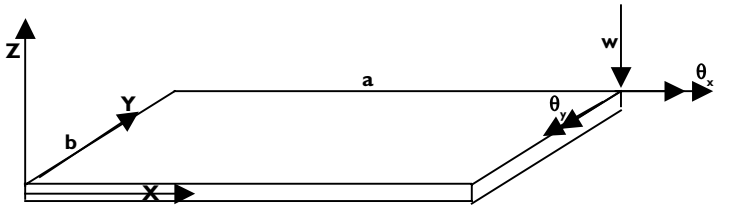


Figure 2.12.42 A rectangular plate element with three-degrees of freedom per node.

$$w(z) = \alpha_1 + \alpha_2 x + \alpha_3 y + \alpha_4 x^2 + \alpha_5 xy + \alpha_6 y^2 + \alpha_7 x^3 + \alpha_8 x^2 y + \alpha_9 xy^2 + \alpha_{10} y^3 + \alpha_{11} x^3 y + \alpha_{12} xy^3 \tag{2.12.145}$$

If you study the Pascal triangle, you will observe that the above is an incomplete fourth order polynomial in x and y where the terms x^4, x^2, y^2 and y^4 terms are missing.

In plate element, slopes normal to the surface are not compatible and as slope discontinuity occurs at adjacent edges this element is only C_0 compatible.

The stiffness matrix of the element we intend to derive herein was originally developed by Melosh, Zienkeiwicz and Chueng and is often termed as MCZ-element.

The explicit form of the stiffness matrix was derived by Adini, Clough and Melosh and is also sometimes addressed as ACM element.

Though the element is non-conforming, yet it has been found to produce reasonable good results in practice.

The reason for the same can be attributed to the following

- The presence of the terms, $1, x, y, x^2, xy, y^2$ ensure rigid body motion and constant curvature states of deformation.
- The fourth order term x^3y and xy^3 ensures that the governing differential equation of plate is satisfied at $\lim a \to 0$, and $\lim b \to 0$

Considering $\{\delta\} = [C]\{\alpha\}$, we have

$$\begin{bmatrix} w_1 \\ \theta_{x1} \\ \theta_{y1} \\ w_2 \\ \theta_{x2} \\ \theta_{y2} \\ w_3 \\ \theta_{x3} \\ \theta_{y3} \\ w_4 \\ \theta_{x4} \\ \theta_{y4} \end{bmatrix} = \begin{bmatrix} 1 & x_1 & y_1 & x_1^2 & x_1y_1 & y_1^2 & x_1^3 & x_1^2y_1 & x_1y_1^2 & y_1^3 & x_1^3y_1 & x_1y_1^3 \\ 0 & -1 & 0 & -2x_1 & -y_1 & 0 & -3x_1^2 & -2x_1y_1 & -y_1^2 & 0 & -3x_1^2y_1 & -y_1^3 \\ 0 & 0 & 1 & 0 & x_1 & 2y_1 & 0 & x_1^2 & 2x_1y_1 & 3y_1^2 & x_1^3 & 3x_1y_1^2 \\ 1 & x_2 & y_2 & x_2^2 & x_2y_2 & y_2^2 & x_2^3 & x_2^2y_2^2 & x_2y_2^2 & y_2^3 & x_2^3y_2 & x_2y_2^3 \\ 0 & -1 & 0 & -2x_2 & -y_2 & 0 & -3x_2^2 & -2x_2y_2 & -y_2^2 & 0 & -3x_2^2y_2 & -y_2^3 \\ 0 & 0 & 1 & 0 & x_2 & 2y_2 & 0 & x_2^2 & 2x_2y_2 & 3y_2^2 & x_2^3 & 3x_2y_2^2 \\ 1 & x_3 & y_3 & x_3^2 & x_3y_3 & y_3^2 & x_3^3 & x_3^2y_3^2 & x_3y_3^2 & y_3^3 & x_3^3y_3 & x_3y_3^3 \\ 0 & -1 & 0 & -2x_3 & -y_3 & 0 & -3x_3^2 & -2x_3y_3 & -y_3^2 & 0 & -3x_3^2y_3 & -y_3^3 \\ 0 & 0 & 1 & 0 & x_3 & 2y_3 & 0 & x_3^2 & 2x_3y_3 & 3y_3^2 & x_3^3 & 3x_3y_3^2 \\ 1 & x_4 & y_4 & x_4^2 & x_4y_4 & y_4^2 & x_4^3 & x_4^2y_4^2 & x_4y_4^2 & y_4^3 & x_4^3y_4 & x_4y_4^3 \\ 0 & -1 & 0 & -2x_4 & -y_4 & 0 & -3x_4^2 & -2x_4y_4 & -y_4^2 & 0 & -3x_4^2y_4 & -y_4^3 \\ 0 & 0 & 1 & 0 & x_4 & 2y_4 & 0 & x_4^2 & 2x_4y_4 & 3y_4^2 & x_4^3 & 3x_4y_4^2 \end{bmatrix} \begin{bmatrix} \alpha_1 \\ \alpha_2 \\ \alpha_3 \\ \alpha_4 \\ \alpha_5 \\ \alpha_6 \\ \alpha_7 \\ \alpha_8 \\ \alpha_9 \\ \alpha_{10} \\ \alpha_{11} \\ \alpha_{12} \end{bmatrix}$$

For, $\{\alpha\} = [C]^{-1}\{\delta\}$, it may again be noted that explicit expression for arriving at $[C]^{-1}$ is difficult, and is usually obtained numerically based on specific values of the coordinates by a computer.

Here $[M]$ matrix is given by

$$[M] = \begin{bmatrix} 1 & x & y & x^2 & xy & y^2 & x^3 & x^2y & xy^2 & y^3 & x^3y & xy^3 \\ 0 & -1 & 0 & -2x & -y & 0 & -3x^2 & -2xy & y^2 & 0 & 3x^2y & -y^3 \\ 0 & 0 & 1 & 0 & x & 2y & 0 & x^2 & 2xy & 3y^2 & x^3 & 3xy^2 \end{bmatrix}$$

This gives shape function as $[N] = [M][C]^{-1}$and the strain matrix is given by

$$\{\varepsilon\} = \left\langle -\frac{\partial^2 w}{\partial x^2}, -\frac{\partial^2 w}{\partial y^2}, -\frac{2\partial^2 w}{\partial x \partial y} \right\rangle^T = [X][C]^{-1}\{\delta\}$$

$$= \begin{bmatrix} 0 & 0 & 0 & -2 & 0 & 0 & -6x & -2y & 0 & 0 & -6xy & 0 \\ 0 & 0 & 0 & 0 & 0 & -2 & 0 & 0 & -2x & -6y & 0 & -6xy \\ 0 & 0 & 0 & 0 & -2 & 0 & 0 & -4xy & -4y & 0 & -6x^2 & -6y^2 \end{bmatrix} [C]^{-1}[\delta]$$

Considering $\{\varepsilon\} = [X][C]^{-1}\{\delta\} = [B]\{\delta\}$ we have

$$[X] = \begin{bmatrix} 0 & 0 & 0 & -2 & 0 & 0 & -6x & -2y & 0 & 0 & -6xy & 0 \\ 0 & 0 & 0 & 0 & 0 & -2 & 0 & 0 & -2x & -6y & 0 & -6xy \\ 0 & 0 & 0 & 0 & -2 & 0 & 0 & -4xy & -4y & 0 & -6x^2 & -6y^2 \end{bmatrix}$$

Thus knowing $[X]$ we have $[K] = \iiint [B]^T [D]\,[B]\,dv$ where $[B] = [X][C]^{-1}$, the stiffness reduces to

$$[K] = [C^{-1}]^T[C^{-1}] \iiint [X]^T[D][X]\,dv \tag{2.12.146}$$

The $[D]$ matrix is given by

$$[D] = \frac{Et^3}{12(1-\nu^2)} \begin{bmatrix} 1 & \nu & 0 \\ \nu & 1 & 0 \\ 0 & 0 & \dfrac{1-\nu}{2} \end{bmatrix},$$

where t is the thickness of the plate putting this value in the stiffness expression we have

$$[K] = \frac{Et^3}{12(1-\nu^2)}[C^{-1}]^T[C^{-1}] \iint [X]^T \begin{bmatrix} 1 & \nu & 0 \\ \nu & 1 & 0 \\ 0 & 0 & \dfrac{1-\nu}{2} \end{bmatrix} [X]\,dx \cdot dy \tag{2.12.147}$$

This expression has been explicitly derived by Adini and Clough (1960) as

$$[K] = \frac{Et^3}{180(1-\nu^2)} \times \begin{bmatrix} F & & & & & & & & & & & \\ G & R & & & \text{Symmetric} & & & & & & & \\ -H & -Z & V & & & & & & & & & \\ L & -M & N & F & & & & & & & & \\ -M & T & \psi & G & R & & & & & & & \\ -N & \psi & X & H & Z & V & & & & & & \\ O & P & Q & I & -J & K & F & & & & & \\ -P & U & \psi & J & S & \psi & -G & R & & & & \\ -Q & \psi & Y & K & \psi & W & H & -Z & V & & & \\ I & -J & -K & O & P & -Q & L & M & -N & F & & \\ J & S & \psi & -P & U & \psi & M & T & \psi & -G & R & \\ -K & \psi & W & Q & \psi & Y & N & \psi & X & -H & Z & V \end{bmatrix} \tag{2.12.148}$$

The values of matrix coefficients are as given as

Sl. No.	*Matrix coefficient*	*Expressions*
1	F	$\frac{\left(42-12\nu+60r^2+\frac{60}{r^2}\right)}{ab}$
2	G	$\frac{\left(30r+\frac{3}{r}+\frac{12\nu}{r}\right)}{b}$
3	H	$\frac{\left(\frac{30}{r}+3r+12\nu r\right)}{a}$
4	I	$\frac{\left(-42+12\nu-60r^2+\frac{30}{r^2}\right)}{ab}$
5	J	$\frac{30r+\frac{3(1-\nu)}{r}}{b}$
6	K	$\frac{\frac{15}{r}-3r-12\nu r}{a}$
7	L	$\frac{-42+12\nu-\frac{60}{r^2}+30r^2}{ab}$
8	M	$\frac{-15r+\frac{3}{r}+\frac{12\nu}{r}}{b}$
9	N	$\frac{\frac{30}{r}+3(1-\nu)r}{a}$
10	O	$\frac{42-12\nu-30r^2-\frac{30}{r^2}}{ab}$

(continued)

Sl. No.	Matrix coefficient	Expressions
11	P	$\frac{-15r + \frac{3(1-\nu)}{r}}{b}$
12	Q	$\frac{\frac{15}{r} - 3(1-\nu)r}{a}$
13	R	$20r + \frac{4(1-\nu)}{r}$
14	S	$10r - \frac{(1-\nu)}{r}$
15	T	$10r - \frac{4(1-\nu)}{r}$
16	U	$5r - \frac{(1-\nu)}{r}$
17	V	$\frac{20}{r} - 4(1-\nu)r$
18	W	$\frac{10}{r} - 4(1-\nu)r$
19	X	$\frac{10}{r} - (1-\nu)r$
20	Y	$\frac{5}{r} - (1-\nu)r$
21	Z	15ν
22	ψ	0
23	r	$\frac{a}{b}$ (Aspect ratio)

2.12.34 Four-nodded quadrilateral plate element in bending

Having presented the classical finite elements plates of regular geometric shape, we proceed hereafter to derive the stiffness matrix of a generalized quadrilateral element under bending.

Frankly speaking, this kept us confused for quite some time as to which one to pick and present, as we had a bewildering array of element to choose from. After much debate we decided to present the Hughes et al. (1977) element for the following reasons

- The formulation is relatively simple.
- It is quite robust in terms of mathematical formulation.
- Though have two spurious zero energy modes yet pass patch test successfully.
- Its record of accomplishment in industry is quite good and has been adapted by many commercial FEM software.
- The shape function is linear but still gives quite good result with reduced selective integration.
- Can cater to shear strain deformation, an important issue if the plate is thick.

- It can also cater to thin plate theory without shear locking.

Before getting involved in the direct derivation of the stiffness matrix, as a prelude, to those who are not so conversant with the thick plate theory we present briefly what makes it so special and different than thin plates[64].

2.12.34.1 Difference between thin and thick plate

Leaving aside the fact that thin plates are those whose thickness is negligible compared to its plan dimension ($t < L/10$) and thick plate have $t > L/10$, structurally speaking the difference is analogous to behavioral difference between a prismatic and a deep beam.

In a prismatic beam the flexural stiffness dominates. However, as the depth of the beam increases the effect of shear strain energy becomes more dominant and affects the element stiffness matrix.

For a plate element also, for thin plates while we can ignore shear effect, for thick plate we cannot do so. This effect needs to be taken into cognizance in its mathematical equation of equilibrium.

The explanation furnished herein is almost heuristic and is provided to give an insight into the problem only.

In this case the plate undergoes additional deformation ϕ_y over and above $\psi_x = -\frac{\partial w}{\partial y}$ which constitute the total angular deformation θ_x and hence

$$-\theta_x = \psi_x + \phi_y$$

$$\text{or} \quad -\theta_x = -\frac{\partial w}{\partial y} + \phi_y$$

similarly for other direction it can be proved that

$$\theta_y = -\frac{\partial w}{\partial x} + \phi_x,$$

$$\text{this gives,} \quad \phi_y = -\theta_x + \frac{\partial w}{\partial y} \quad \text{and} \quad \phi_x = \theta_y + \frac{\partial w}{\partial x} \tag{2.12.149}$$

The shear strain energy is given by

$$\Pi_s = \iint \frac{1}{2}\alpha GA\phi^2 dx \cdot dy, \quad \text{for the present case } = \iint \frac{1}{2}\alpha GA^2 \left[\phi_x^2 + \phi_y^2\right] dx \cdot dy \tag{2.12.150}$$

Here α is a correction factor usually considered normally as 5/6. For plates restrained fully against warping is considered as 1.0 and 2/3 for unrestrained against warping.

64 Those of you who are conversant with the plate theory can well skip this section.

This is the additional strain energy term that needs to be considered other then bending strain energy given by

$$\Pi_b = \frac{Et^3}{24(1-\nu^2)} \iint \left[\left(\frac{\partial \theta_x}{\partial x}\right)^2 + 2\nu \left(\frac{\partial \theta_x}{\partial x}\right)\left(\frac{\partial \theta_y}{\partial y}\right) + \left(\frac{\partial \theta_y}{\partial y}\right)^2 + \frac{1-\nu}{2}\left\{\frac{\partial \theta_x}{\partial y} + \frac{\partial \theta_y}{\partial x}\right\}^2 \right] dx \cdot dy \tag{2.12.151}$$

which is valid for thin plate.

Shown in Figure 2.12.44 is a generic thick plate quadrilateral element having node coordinates are as shown above. Considering the effect of shear deformation the strain matrix is given by

$$\{\varepsilon\}^T = \left\langle \frac{\partial \theta_y}{\partial x} - \frac{\partial \theta_x}{\partial y}\left(\frac{\partial \theta_y}{\partial y} - \frac{\partial \theta_x}{\partial x}\right)\theta_y + \frac{\partial w}{\partial x} - \theta_x + \frac{\partial w}{\partial y} \right\rangle, \tag{2.12.152}$$

Considering c_x, c_y, c_{xy} as the curvature of the plate in respective axes we have

$$\{\varepsilon\}^T = \langle c_x \quad c_y \quad c_{xy} \quad \phi_x \quad \phi_y \rangle. \tag{2.12.153}$$

The geometry of the element is given by

$$x = \sum_{i=1}^{4} N_i x_i \quad \text{and} \quad y = \sum_{i=1}^{4} N_i y_i, \tag{2.12.154}$$

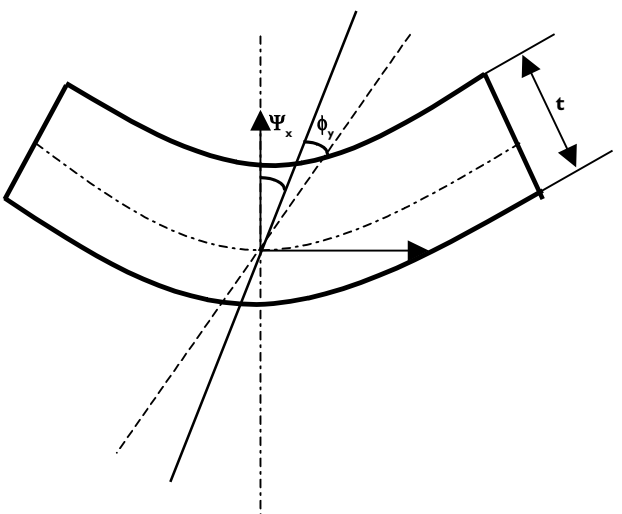


Figure 2.12.43 Thick plate under bending in exaggerated deformed shape.

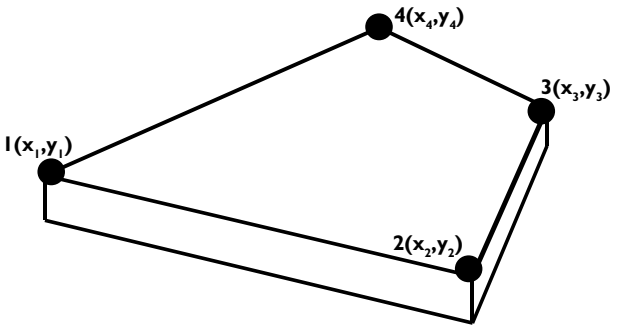


Figure 2.12.44 A quadrilateral thick plate element under bending.

thus for iso-parametric formulation

$$w = \sum_{i=1}^{4} N_i w_i, \quad \theta_x = \sum_{i=1}^{4} N_i \theta_{x_i} \quad \text{and} \quad \theta_y = \sum_{i=1}^{4} N_i \theta_{y_i} \tag{2.12.155}$$

where $N_i = \frac{1}{4}(1 + \xi\xi_i)\ (1 + \eta\eta_i)$

The Jacobian matrix is given by

$$[J] = \begin{bmatrix} \frac{\partial N_1}{\partial \xi} & \frac{\partial N_2}{\partial \xi} & \frac{\partial N_3}{\partial \xi} & \frac{\partial N_4}{\partial \xi} \\ \frac{\partial N_1}{\partial \eta} & \frac{\partial N_2}{\partial \eta} & \frac{\partial N_3}{\partial \eta} & \frac{\partial N_4}{\partial \eta} \end{bmatrix} \begin{bmatrix} x_1 & y_1 \\ x_2 & y_2 \\ x_3 & y_3 \\ x_4 & y_4 \end{bmatrix}$$

$$\text{Here} \quad J_{11} = \frac{\partial x}{\partial \xi} = \frac{\partial}{\partial \xi} \sum_{i=1}^{4} N_i x_i = \frac{\partial}{\partial \xi}\left[\frac{(1-\xi)(1-\eta)}{4} x_1 + \frac{(1+\xi)(1-\eta)}{4} x_2\right] + \frac{\partial}{\partial \xi}\left[\frac{(1+\xi)(1+\eta)}{4} x_3 + \frac{(1-\xi)(1+\eta)}{4} x_4\right]$$

or $J_{11} = \frac{1}{4}[(\eta - 1)x_1 + (1 - \eta)x_2 + (1 + \eta)x_3 - (1 + \eta)x_4]$

Similarly

$$J_{12} = \frac{1}{4}[(\eta - 1)y_1 + (1 - \eta)y_2 + (1 + \eta)y_3 - (1 + \eta)y_4]$$

$$J_{21} = \frac{1}{4}[(\xi - 1)x_1 - (1 + \xi)x_2 + (1 + \xi)x_3 + (1 - \xi)x_4]$$

$$J_{22} = \frac{1}{4}[(\xi - 1)y_1 - (1 + \xi)y_2 + (1 + \xi)y_3 + (1 - \xi)y_4]$$

Here $[J] = \begin{bmatrix} J_{11} & J_{12} \\ J_{21} & J_{22} \end{bmatrix}$ and $[J]^{-1} = \frac{1}{|J|}\begin{bmatrix} J_{22} & -J_{12} \\ -J_{21} & J_{11} \end{bmatrix}$.

This displacement relation in terms of Jacobian matrix can now be expressed as

$$\begin{bmatrix} \frac{\partial N_1}{\partial x} & \frac{\partial N_2}{\partial x} & \frac{\partial N_3}{\partial x} & \frac{\partial N_4}{\partial x} \\ \frac{\partial N_1}{\partial y} & \frac{\partial N_2}{\partial y} & \frac{\partial N_3}{\partial y} & \frac{\partial N_4}{\partial y} \end{bmatrix} = [J]^{-1} \begin{bmatrix} \frac{\partial N_1}{\partial \xi} & \frac{\partial N_2}{\partial \xi} & \frac{\partial N_3}{\partial \xi} & \frac{\partial N_4}{\partial \xi} \\ \frac{\partial N_1}{\partial \eta} & \frac{\partial N_2}{\partial \eta} & \frac{\partial N_3}{\partial \eta} & \frac{\partial N_4}{\partial \eta} \end{bmatrix}$$

The above can be further expressed as

$$\begin{bmatrix} \frac{\partial N_1}{\partial x} & \frac{\partial N_2}{\partial x} & \frac{\partial N_3}{\partial x} & \frac{\partial N_4}{\partial x} \\ \frac{\partial N_1}{\partial y} & \frac{\partial N_2}{\partial y} & \frac{\partial N_3}{\partial y} & \frac{\partial N_4}{\partial y} \end{bmatrix} = \frac{1}{|J|} \begin{bmatrix} J_{22} & -J_{12} \\ -J_{21} & J_{11} \end{bmatrix} \begin{bmatrix} \frac{\partial N_1}{\partial \xi} & \frac{\partial N_2}{\partial \xi} & \frac{\partial N_3}{\partial \xi} & \frac{\partial N_4}{\partial \xi} \\ \frac{\partial N_1}{\partial \eta} & \frac{\partial N_2}{\partial \eta} & \frac{\partial N_3}{\partial \eta} & \frac{\partial N_4}{\partial \eta} \end{bmatrix}$$

$$= \frac{1}{|J|} \times \begin{bmatrix} J_{22}\frac{\partial N_1}{\partial \xi} - J_{12}\frac{\partial N_1}{\partial \eta} & J_{22}\frac{\partial N_2}{\partial \xi} - J_{12}\frac{\partial N_2}{\partial \eta} & J_{22}\frac{\partial N_3}{\partial \xi} - J_{12}\frac{\partial N_3}{\partial \eta} & J_{22}\frac{\partial N_4}{\partial \xi} - J_{12}\frac{\partial N_4}{\partial \eta} \\ -J_{21}\frac{\partial N_1}{\partial \xi} + J_{11}\frac{\partial N_1}{\partial \eta} & -J_{21}\frac{\partial N_2}{\partial \xi} + J_{11}\frac{\partial N_2}{\partial \eta} & -J_{21}\frac{\partial N_3}{\partial \xi} + J_{11}\frac{\partial N_3}{\partial \eta} & -J_{21}\frac{\partial N_4}{\partial \xi} + J_{11}\frac{\partial N_4}{\partial \eta} \end{bmatrix}$$

Thus we have been equating term by term

$$\frac{\partial N_1}{\partial x} = \frac{1}{|J|}\left[J_{22}\frac{\partial N_1}{\partial \xi} - J_{12}\frac{\partial N_1}{\partial \eta}\right]$$

$$\frac{\partial N_2}{\partial x} = \frac{1}{|J|}\left[J_{22}\frac{\partial N_2}{\partial \xi} - J_{12}\frac{\partial N_2}{\partial \eta}\right]$$

.....

.....

$$\frac{\partial N_4}{\partial y} = \frac{1}{|J|}\left[-J_{21}\frac{\partial N_4}{\partial \xi} + J_{11}\frac{\partial N_4}{\partial \eta}\right]$$

The strain matrix $\{\varepsilon\}^T = \left\langle \left(\frac{\partial \theta_y}{\partial x}\right)\left(-\frac{\partial \theta_x}{\partial y}\right)\left(\frac{\partial \theta_y}{\partial y} - \frac{\partial \theta_x}{\partial x}\right)\left(\theta_y + \frac{\partial w}{\partial x}\right)\left(-\theta_x + \frac{\partial w}{\partial y}\right)\right\rangle$

And this can be expanded to

$$\{\varepsilon\} = \begin{bmatrix} 0 & 0 & \frac{\partial N_1}{\partial x} & 0 & 0 & \frac{\partial N_2}{\partial x} & 0 & 0 & \frac{\partial N_3}{\partial x} & 0 & 0 & \frac{\partial N_4}{\partial x} \\ 0 & -\frac{\partial N_1}{\partial y} & 0 & 0 & -\frac{\partial N_2}{\partial y} & 0 & 0 & -\frac{\partial N_3}{\partial y} & 0 & 0 & -\frac{\partial N_4}{\partial y} & 0 \\ 0 & -\frac{\partial N_1}{\partial x} & \frac{\partial N_1}{\partial y} & 0 & -\frac{\partial N_2}{\partial x} & \frac{\partial N_2}{\partial y} & 0 & -\frac{\partial N_3}{\partial x} & \frac{\partial N_3}{\partial y} & 0 & -\frac{\partial N_4}{\partial x} & \frac{\partial N_4}{\partial y} \\ \frac{\partial N_1}{\partial x} & 0 & N_1 & \frac{\partial N_2}{\partial x} & 0 & N_2 & \frac{\partial N_3}{\partial x} & 0 & N_3 & \frac{\partial N_4}{\partial x} & 0 & N_4 \\ \frac{\partial N_1}{\partial y} & -N_1 & 0 & \frac{\partial N_2}{\partial y} & -N_2 & 0 & \frac{\partial N_3}{\partial y} & -N_3 & 0 & \frac{\partial N_4}{\partial y} & -N_4 & 0 \end{bmatrix}$$

$$\times \langle w_1 \;\; \theta_{x1} \;\; \theta_{y1} \;\; w_2 \;\; \theta_{x2} \;\; \theta_{y2} \;\; w_3 \;\; \theta_{x3} \;\; \theta_{y3} \;\; w_4 \;\; \theta_{x4} \;\; \theta_{y4} \rangle^T$$

$$\rightarrow \{\varepsilon\} = [B]\{\delta\} \qquad (2.12.156)$$

$$\text{or} \quad [B] = \begin{bmatrix} 0 & 0 & \frac{\partial N_1}{\partial x} & 0 & 0 & \frac{\partial N_2}{\partial x} & 0 & 0 & \frac{\partial N_3}{\partial x} & 0 & 0 & \frac{\partial N_4}{\partial x} \\ 0 & -\frac{\partial N_1}{\partial y} & 0 & 0 & -\frac{\partial N_2}{\partial y} & 0 & 0 & -\frac{\partial N_3}{\partial y} & 0 & 0 & -\frac{\partial N_4}{\partial y} & 0 \\ 0 & -\frac{\partial N_1}{\partial x} & \frac{\partial N_1}{\partial y} & 0 & -\frac{\partial N_2}{\partial x} & \frac{\partial N_2}{\partial y} & 0 & -\frac{\partial N_3}{\partial x} & \frac{\partial N_3}{\partial y} & 0 & -\frac{\partial N_4}{\partial x} & \frac{\partial N_4}{\partial y} \\ \frac{\partial N_1}{\partial x} & 0 & N_1 & \frac{\partial N_2}{\partial x} & 0 & N_2 & \frac{\partial N_3}{\partial x} & 0 & N_3 & \frac{\partial N_4}{\partial x} & 0 & N_4 \\ \frac{\partial N_1}{\partial y} & -N_1 & 0 & \frac{\partial N_2}{\partial y} & -N_2 & 0 & \frac{\partial N_3}{\partial y} & -N_3 & 0 & \frac{\partial N_4}{\partial y} & -N_4 & 0 \end{bmatrix}$$

The stiffness matrix as usual is given by $[K] = \iiint [B]^T [D] [B] \, dv$, however in this case is broken up into two parts.

- The bending part which is valid for thin plate element
- The shear deformation part that needs to be added to above if the plate is considered thick.

$$\text{Thus} \quad [K] = t \iint [B]^T [D]_b [B] \left|J\right| d\xi d\eta + t \iint [B]^T [D]_s [B] \left|J\right| d\xi d\eta \quad (2.12.157)$$

$$\text{Here} \quad [D]_b = \frac{Et^3}{12\left(1-\nu^2\right)} \begin{bmatrix} 1 & \nu & 0 & 0 & 0 \\ \nu & 1 & 0 & 0 & 0 \\ 0 & 0 & \frac{1-\nu}{2} & 0 & 0 \\ 0 & 0 & 0 & 0 & 0 \\ 0 & 0 & 0 & 0 & 0 \end{bmatrix}$$

$$\text{and} \quad [D]_s = \frac{E}{2\left(1+\nu\right)} \begin{bmatrix} 0 & 0 & 0 & 0 & 0 \\ 0 & 0 & 0 & 0 & 0 \\ 0 & 0 & 0 & 0 & 0 \\ 0 & 0 & 0 & \alpha & 0 \\ 0 & 0 & 0 & 0 & \alpha \end{bmatrix}$$

Here $\alpha = 5/6$, $2/3$, 1 etc. the shear correction coefficient as discussed earlier. The developers suggest (Hughes et al.) that for numerical integration for the bending part, two point Gauss integration and for the shear deformation part one point Gauss integration at the centroid of the element suffice to give an accurate answer.

The beauty of the element is its simple approach and capability to handle both thick and thin element under one unified formula.

2.12.35 Three Dimensional Hexahedral Element – One last to bore you

We do not want to end this section in an incompatible mode as such we cajole you to go through this one last element and understand its derivation. The selection of this element is not without its reason and this will be unraveled subsequently.

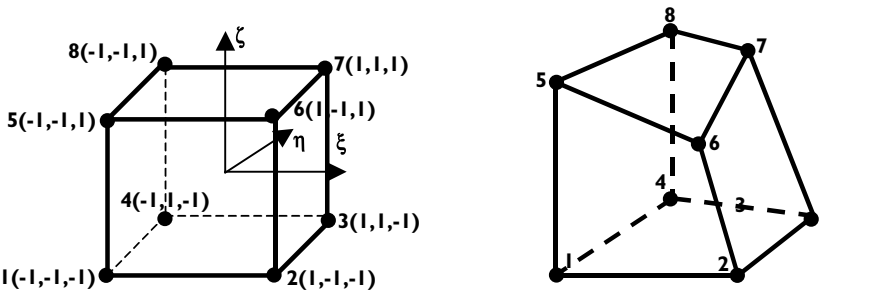


Figure 2.12.45 Iso-parametric representation of 3 dimensional eight node hexahedral element.

Shown Figure 2.12.45 is a eight nodded hexahedral element having three degrees of freedom at each node u, v and w. Thus in generalized co-ordinate the polynomial representation is given by

$$\begin{aligned} u &= \alpha_1 + \alpha_2 x + \alpha_3 y + \alpha_4 z + \alpha_5 xy + \alpha_6 yz + \alpha_7 xz + \alpha_8 xyz; \\ v &= \alpha_9 + \alpha_{10} x + \alpha_{11} y + \alpha_{12} z + \alpha_{13} xy + \alpha_{14} yz + \alpha_{15} xz + \alpha_{16} xyz \quad \text{and} \\ w &= \alpha_{17} + \alpha_{18} x + \alpha_{19} y + \alpha_{20} z + \alpha_{21} xy + \alpha_{22} yz + \alpha_{23} xz + \alpha_{24} xyz. \end{aligned} \tag{2.12.158}$$

In natural coordinate the shape function based on Serendip family is given as

$$N_i = \frac{1}{8}(1 + \xi\xi_i)(1 + \eta\eta_i)(1 + \zeta\zeta_i) \quad \text{where } i = 1, 2, 3 \ldots\ldots 8$$

The geometry of the element is given by $x = \sum_{i=1}^{8} N_i x_i$, $y = \sum_{i=1}^{8} N_i y_i$ and $z = \sum_{i=1}^{8} N_i z_i$, for iso-parametric formulation $u = \sum_{i=1}^{8} N_i u_i$, $v = \sum_{i=1}^{8} N_i v_i$ and $w = \sum_{i=1}^{8} N_i w_i$ where the relation between global and natural coordinate is given by

$$\begin{Bmatrix} \frac{\partial u}{\partial \xi} \\ \frac{\partial u}{\partial \eta} \\ \frac{\partial u}{\partial \zeta} \end{Bmatrix} = [J] \begin{Bmatrix} \frac{\partial u}{\partial x} \\ \frac{\partial u}{\partial y} \\ \frac{\partial u}{\partial z} \end{Bmatrix} \quad \text{which gives} \rightarrow \begin{Bmatrix} \frac{\partial u}{\partial x} \\ \frac{\partial u}{\partial y} \\ \frac{\partial u}{\partial z} \end{Bmatrix} = [J]^{-1} \begin{Bmatrix} \frac{\partial u}{\partial \xi} \\ \frac{\partial u}{\partial \eta} \\ \frac{\partial u}{\partial \zeta} \end{Bmatrix}$$

$$\text{Here} \quad [J] = \begin{bmatrix} J_{11} & J_{12} & J_{13} \\ J_{21} & J_{22} & J_{23} \\ J_{31} & J_{32} & J_{33} \end{bmatrix} = \begin{bmatrix} \frac{\partial x}{\partial \xi} & \frac{\partial y}{\partial \xi} & \frac{\partial z}{\partial \xi} \\ \frac{\partial x}{\partial \eta} & \frac{\partial y}{\partial \eta} & \frac{\partial z}{\partial \eta} \\ \frac{\partial x}{\partial \zeta} & \frac{\partial y}{\partial \zeta} & \frac{\partial z}{\partial \zeta} \end{bmatrix} \quad \text{where}$$

$$J_{11} = \frac{1}{8}\begin{bmatrix}(\eta-1)(1-\zeta)x_1 + (1-\eta)(1-\zeta)x_2 + (1+\eta)(1-\zeta)x_3 + (1+\eta)(\zeta-1)x_4\\ +(\eta-1)(1+\zeta)x_5 + (1-\eta)(1-\zeta)x_6 + (1+\eta)(1+\zeta)x_7 - (1+\eta)(1+\zeta)x_8\end{bmatrix}$$

$$J_{12} = \frac{1}{8}\begin{bmatrix}(\eta-1)(1-\zeta)y_1 + (1-\eta)(1-\zeta)y_2 + (1+\eta)(1-\zeta)y_3 + (1+\eta)(\zeta-1)y_4\\ +(\eta-1)(1+\zeta)y_5 + (1-\eta)(1-\zeta)y_6 + (1+\eta)(1+\zeta)y_7 - (1+\eta)(1+\zeta)y_8\end{bmatrix}$$

$$J_{13} = \frac{1}{8}\begin{bmatrix}(\eta-1)(1-\zeta)z_1 + (1-\eta)(1-\zeta)z_2 + (1+\eta)(1-\zeta)z_3 + (1+\eta)(\zeta-1)z_4\\ +(\eta-1)(1+\zeta)z_5 + (1-\eta)(1-\zeta)z_6 + (1+\eta)(1+\zeta)z_7 - (1+\eta)(1+\zeta)z_8\end{bmatrix}$$

$$J_{21} = \frac{1}{8}\begin{bmatrix}(\xi-1)(1-\zeta)x_1 + (1+\xi)(\zeta-1)x_2 + (1+\xi)(1-\zeta)x_3 + (1-\xi)(1-\zeta)x_4\\ +(\xi-1)(1+\zeta)x_5 + (1+\xi)(\zeta-1)x_6 + (1+\xi)(1+\zeta)x_7 + (1-\xi)(1+\zeta)x_8\end{bmatrix}$$

$$J_{22} = \frac{1}{8}\begin{bmatrix}(\xi-1)(1-\zeta)y_1 + (1+\xi)(\zeta-1)y_2 + (1+\xi)(1-\zeta)y_3 + (1-\xi)(1-\zeta)y_4\\ +(\xi-1)(1+\zeta)y_5 + (1+\xi)(\zeta-1)y_6 + (1+\xi)(1+\zeta)y_7 + (1-\xi)(1+\zeta)y_8\end{bmatrix}$$

$$J_{23} = \frac{1}{8}\begin{bmatrix}(\xi-1)(1-\zeta)z_1 + (1+\xi)(\zeta-1)z_2 + (1+\xi)(1-\zeta)z_3 + (1-\xi)(1-\zeta)z_4\\ +(\xi-1)(1+\zeta)z_5 + (1+\xi)(\zeta-1)z_6 + (1+\xi)(1+\zeta)z_7 + (1-\xi)(1+\zeta)z_8\end{bmatrix}$$

$$J_{31} = \frac{1}{8}\begin{bmatrix}(\xi-1)(1-\eta)x_1 + (1+\xi)(\eta-1)x_2 - (1+\xi)(1+\eta)x_3 + (\xi-1)(1+\eta)x_4\\ +(1-\xi)(1-\eta)x_5 + (1+\xi)(1-\eta)x_6 + (1+\xi)(1+\eta)x_7 + (1-\xi)(1+\eta)x_8\end{bmatrix}$$

$$J_{32} = \frac{1}{8}\begin{bmatrix}(\xi-1)(1-\eta)y_1 + (1+\xi)(\eta-1)y_2 - (1+\xi)(1+\eta)y_3 + (\xi-1)(1+\eta)y_4\\ +(1-\xi)(1-\eta)y_5 + (1+\xi)(1-\eta)y_6 + (1+\xi)(1+\eta)y_7 + (1-\xi)(1+\eta)y_8\end{bmatrix}$$

$$J_{33} = \frac{1}{8}\begin{bmatrix}(\xi-1)(1-\eta)z_1 + (1+\xi)(\eta-1)z_2 - (1+\xi)(1+\eta)z_3 + (\xi-1)(1+\eta)z_4\\ +(1-\xi)(1-\eta)z_5 + (1+\xi)(1-\eta)z_6 + (1+\xi)(1+\eta)z_7 + (1-\xi)(1+\eta)z_8\end{bmatrix}$$

Let the inverse of $[J]$ matrix be considered as

$$[J]^{-1} = \begin{bmatrix} j_{11} & j_{12} & j_{13}\\ j_{21} & j_{22} & j_{23}\\ j_{31} & j_{32} & j_{33}\end{bmatrix} \tag{2.12.159}$$

The strain matrix is given by

$$\begin{Bmatrix}\varepsilon_x\\ \varepsilon_y\\ \varepsilon_z\\ \gamma_{xy}\\ \gamma_{yz}\\ \gamma_{zx}\end{Bmatrix} = \begin{Bmatrix}\dfrac{\partial u}{\partial x}\\ \dfrac{\partial v}{\partial y}\\ \dfrac{\partial w}{\partial z}\\ \dfrac{\partial u}{\partial y} + \dfrac{\partial v}{\partial x}\\ \dfrac{\partial v}{\partial z} + \dfrac{\partial w}{\partial y}\\ \dfrac{\partial u}{\partial z} + \dfrac{\partial w}{\partial x}\end{Bmatrix}$$

Now considering $\{\varepsilon\} = [B]\{\delta\}$, the $[\varepsilon]$ matrix in terms of shape function can be expressed as

$$\{\varepsilon\} = \left[\begin{array}{ccc|ccc|ccc|ccc|c}
\frac{\partial N_1}{\partial x} & 0 & 0 & \frac{\partial N_2}{\partial x} & 0 & 0 & \frac{\partial N_3}{\partial x} & 0 & 0 & \frac{\partial N_4}{\partial x} & 0 & 0 \\
0 & \frac{\partial N_1}{\partial y} & 0 & 0 & \frac{\partial N_2}{\partial y} & 0 & 0 & \frac{\partial N_3}{\partial y} & 0 & 0 & \frac{\partial N_4}{\partial y} & 0 \\
0 & 0 & \frac{\partial N_1}{\partial z} & 0 & 0 & \frac{\partial N_2}{\partial z} & 0 & 0 & \frac{\partial N_3}{\partial z} & 0 & 0 & \frac{\partial N_4}{\partial z} \\
\frac{\partial N_1}{\partial y} & \frac{\partial N_1}{\partial x} & 0 & \frac{\partial N_2}{\partial y} & \frac{\partial N_2}{\partial x} & 0 & \frac{\partial N_3}{\partial y} & \frac{\partial N_3}{\partial x} & 0 & \frac{\partial N_4}{\partial y} & \frac{\partial N_4}{\partial x} & 0 \\
0 & \frac{\partial N_1}{\partial z} & \frac{\partial N_1}{\partial y} & 0 & \frac{\partial N_2}{\partial z} & \frac{\partial N_2}{\partial y} & 0 & \frac{\partial N_3}{\partial z} & \frac{\partial N_3}{\partial y} & 0 & \frac{\partial N_4}{\partial z} & \frac{\partial N_4}{\partial y} \\
\frac{\partial N_1}{\partial z} & 0 & \frac{\partial N_1}{\partial x} & \frac{\partial N_2}{\partial z} & 0 & \frac{\partial N_2}{\partial x} & \frac{\partial N_3}{\partial z} & 0 & \frac{\partial N_3}{\partial x} & \frac{\partial N_4}{\partial z} & 0 & \frac{\partial N_4}{\partial x}
\end{array}\right]
\left\{\begin{array}{c} u_1 \\ v_1 \\ w_1 \\ u_2 \\ v_2 \\ w_2 \\ u_3 \\ v_3 \\ w_3 \\ u_4 \\ v_4 \\ w_4 \end{array}\right\}$$

$$\left[\begin{array}{c|ccc|ccc|ccc|ccc}
\frac{\partial N_5}{\partial x} & 0 & 0 & \frac{\partial N_6}{\partial x} & 0 & 0 & \frac{\partial N_7}{\partial x} & 0 & 0 & \frac{\partial N_8}{\partial x} & 0 & 0 \\
0 & \frac{\partial N_5}{\partial y} & 0 & 0 & \frac{\partial N_6}{\partial y} & 0 & 0 & \frac{\partial N_7}{\partial y} & 0 & 0 & \frac{\partial N_8}{\partial y} & 0 \\
0 & 0 & \frac{\partial N_5}{\partial z} & 0 & 0 & \frac{\partial N_6}{\partial z} & 0 & 0 & \frac{\partial N_7}{\partial z} & 0 & 0 & \frac{\partial N_8}{\partial z} \\
\frac{\partial N_5}{\partial y} & \frac{\partial N_5}{\partial x} & 0 & \frac{\partial N_6}{\partial y} & \frac{\partial N_6}{\partial x} & 0 & \frac{\partial N_7}{\partial y} & \frac{\partial N_7}{\partial x} & 0 & \frac{\partial N_8}{\partial y} & \frac{\partial N_8}{\partial x} & 0 \\
0 & \frac{\partial N_5}{\partial z} & \frac{\partial N_5}{\partial y} & 0 & \frac{\partial N_6}{\partial z} & \frac{\partial N_6}{\partial y} & 0 & \frac{\partial N_7}{\partial z} & \frac{\partial N_7}{\partial y} & 0 & \frac{\partial N_8}{\partial z} & \frac{\partial N_8}{\partial y} \\
\frac{\partial N_5}{\partial z} & 0 & \frac{\partial N_5}{\partial x} & \frac{\partial N_6}{\partial z} & 0 & \frac{\partial N_6}{\partial x} & \frac{\partial N_7}{\partial z} & 0 & \frac{\partial N_7}{\partial x} & \frac{\partial N_8}{\partial z} & 0 & \frac{\partial N_8}{\partial x}
\end{array}\right]
\left\{\begin{array}{c} u_5 \\ v_5 \\ w_5 \\ u_6 \\ v_6 \\ w_6 \\ u_7 \\ v_7 \\ w_7 \\ u_8 \\ v_8 \\ w_8 \end{array}\right\} \tag{2.12.160}$$

From above it can be easily deduced that

$$[\mathbf{B}] = \left[\begin{array}{ccc|ccc|ccc|ccc|c}
\frac{\partial N_1}{\partial x} & 0 & 0 & \frac{\partial N_2}{\partial x} & 0 & 0 & \frac{\partial N_3}{\partial x} & 0 & 0 & \frac{\partial N_4}{\partial x} & 0 & 0 \\
0 & \frac{\partial N_1}{\partial y} & 0 & 0 & \frac{\partial N_2}{\partial y} & 0 & 0 & \frac{\partial N_3}{\partial y} & 0 & 0 & \frac{\partial N_4}{\partial y} & 0 \\
0 & 0 & \frac{\partial N_1}{\partial z} & 0 & 0 & \frac{\partial N_2}{\partial z} & 0 & 0 & \frac{\partial N_3}{\partial z} & 0 & 0 & \frac{\partial N_4}{\partial z} \\
\frac{\partial N_1}{\partial y} & \frac{\partial N_1}{\partial x} & 0 & \frac{\partial N_2}{\partial y} & \frac{\partial N_2}{\partial x} & 0 & \frac{\partial N_3}{\partial y} & \frac{\partial N_3}{\partial x} & 0 & \frac{\partial N_4}{\partial y} & \frac{\partial N_4}{\partial x} & 0 \\
0 & \frac{\partial N_1}{\partial z} & \frac{\partial N_1}{\partial y} & 0 & \frac{\partial N_2}{\partial z} & \frac{\partial N_2}{\partial y} & 0 & \frac{\partial N_3}{\partial z} & \frac{\partial N_3}{\partial y} & 0 & \frac{\partial N_4}{\partial z} & \frac{\partial N_4}{\partial y} \\
\frac{\partial N_1}{\partial z} & 0 & \frac{\partial N_1}{\partial x} & \frac{\partial N_2}{\partial z} & 0 & \frac{\partial N_2}{\partial x} & \frac{\partial N_3}{\partial z} & 0 & \frac{\partial N_3}{\partial x} & \frac{\partial N_4}{\partial z} & 0 & \frac{\partial N_4}{\partial x}
\end{array}\right]
\left\{\begin{array}{c} u_1 \\ v_1 \\ w_1 \\ u_2 \\ v_2 \\ w_2 \\ u_3 \\ v_3 \\ w_3 \\ u_4 \\ v_4 \\ w_4 \end{array}\right\}$$

$$\left[\begin{array}{c|ccc|ccc|ccc|ccc}
\frac{\partial N_5}{\partial x} & 0 & 0 & \frac{\partial N_6}{\partial x} & 0 & 0 & \frac{\partial N_7}{\partial x} & 0 & 0 & \frac{\partial N_8}{\partial x} & 0 & 0 \\
0 & \frac{\partial N_5}{\partial y} & 0 & 0 & \frac{\partial N_6}{\partial y} & 0 & 0 & \frac{\partial N_7}{\partial y} & 0 & 0 & \frac{\partial N_8}{\partial y} & 0 \\
0 & 0 & \frac{\partial N_5}{\partial z} & 0 & 0 & \frac{\partial N_6}{\partial z} & 0 & 0 & \frac{\partial N_7}{\partial z} & 0 & 0 & \frac{\partial N_8}{\partial z} \\
\frac{\partial N_5}{\partial y} & \frac{\partial N_5}{\partial x} & 0 & \frac{\partial N_6}{\partial y} & \frac{\partial N_6}{\partial x} & 0 & \frac{\partial N_7}{\partial y} & \frac{\partial N_7}{\partial x} & 0 & \frac{\partial N_8}{\partial y} & \frac{\partial N_8}{\partial x} & 0 \\
0 & \frac{\partial N_5}{\partial z} & \frac{\partial N_5}{\partial y} & 0 & \frac{\partial N_6}{\partial z} & \frac{\partial N_6}{\partial y} & 0 & \frac{\partial N_7}{\partial z} & \frac{\partial N_7}{\partial y} & 0 & \frac{\partial N_8}{\partial z} & \frac{\partial N_8}{\partial y} \\
\frac{\partial N_5}{\partial z} & 0 & \frac{\partial N_5}{\partial x} & \frac{\partial N_6}{\partial z} & 0 & \frac{\partial N_6}{\partial x} & \frac{\partial N_7}{\partial z} & 0 & \frac{\partial N_7}{\partial x} & \frac{\partial N_8}{\partial z} & 0 & \frac{\partial N_8}{\partial x}
\end{array}\right]
\left\{\begin{array}{c} u_5 \\ v_5 \\ w_5 \\ u_6 \\ v_6 \\ w_6 \\ u_7 \\ v_7 \\ w_7 \\ u_8 \\ v_8 \\ w_8 \end{array}\right\} \tag{2.12.161}$$

The relationship between the natural and local cordinate is expressed as

$$\begin{Bmatrix} \partial Ni/\partial x \\ \partial Ni/\partial y \\ \partial Ni/\partial z \end{Bmatrix} = [J]^{-1} \begin{bmatrix} \dfrac{\partial Ni}{\partial \xi} \\ \dfrac{\partial Ni}{\partial \eta} \\ \dfrac{\partial Ni}{\partial \zeta} \end{bmatrix} \tag{2.12.162}$$

The stiffness matrix is thus given by

$$[K]_e = \int_{-1}^{1}\int_{-1}^{1}\int_{-1}^{1} [B]^T [D] [B] \, d\xi \, d\eta \, d\zeta \tag{2.12.163}$$

The $[D]$ matrix is expressed as

$$[D] = \frac{E}{(1+\nu)(1-2\nu)} \begin{bmatrix} 1-\nu & \nu & \nu & 0 & 0 & 0 \\ \nu & 1-\nu & \nu & 0 & 0 & 0 \\ \nu & \nu & 1-\nu & 0 & 0 & 0 \\ 0 & 0 & 0 & \dfrac{1-2\nu}{2} & 0 & 0 \\ 0 & 0 & 0 & 0 & \dfrac{1-2\nu}{2} & 0 \\ 0 & 0 & 0 & 0 & 0 & \dfrac{1-2\nu}{2} \end{bmatrix}$$

This element has a lot of application in rock mechanics where stresses induced in rock due to external loads are often analyzed by modeling the rock mass in 3D as eight node brick elements.

Mechanical engineers often use this element to determine stresses in thick walled pressure vessels and heat exchangers subjected to internal pressure and thermal loading. We have seen Geotechnical engineers use this element for pile analysis in three dimensions, modeling the soil/elastic half space by this element.

We have also however observed gross misuse of this element in hands of rookies generating significant amount of garbage results.

In their over enthusiasm to produce something sophisticated we have seen people use this element at wrong places without understanding its limitations.

The classic example of this is thick rafts or jetty decks modeled by this element where the governing design force is flexural in nature.

For similar to 4 node quadrilateral element this element is quite stubborn under flexure and unless we take additional terms $(1-\xi^2)$, $(1-\eta^2)$ *and* $(1-\zeta^2)$ *thus make it a non conforming element and then apply Taylor's correction (like we did with 4-nodded iso-parametric element) the moments and shears obtained would be highly erroneous.*

Finally stress output for this element is usually furnished in terms of $\sigma_{xx}, \sigma_{yy}, \sigma_{zz}, \tau_{xy}, \tau_{yz}, \tau_{zx}$, while this is fine for stress in rocks or pressure vessel, for structural analysis in case of rafts or thick walls back calculating the Moments and shear is extremely tedious from such outputs unless the software has post processor to carry out this task.

It is possible to model such structural elements by 20 node higher order brick elements which would surely give better results. However if the software in hand does not have solid modeling post-processor and automatic band width minimization option playing around with 20 node brick element can be quite an arduous task.

2.12.36 Twenty-nodded hexahedral element

A twenty-nodded hexahedral element is as shown in Figure 2.12.46. This is a higher order quadratic element of Serendip family.

We will not derive the stiffness matrix for this but would present only the relevant shape function in natural coordinate, from which one can derive the stiffness matrix following the same steps as shown for the eight-nodded element.

Here,

$$\text{for nodes 1 to 8:} \quad N_i = (1+\xi\xi_i)(1+\eta\eta_i)(1+\zeta\zeta_i)(\xi\xi_i+\eta\eta_i+\zeta\zeta_i-2)/8,$$

$$\text{for nodes 10, 12, 14 and 16:} \quad N_i = (1-\xi^2)(1+\eta\eta_i)(1+\zeta\zeta_i)/4,$$

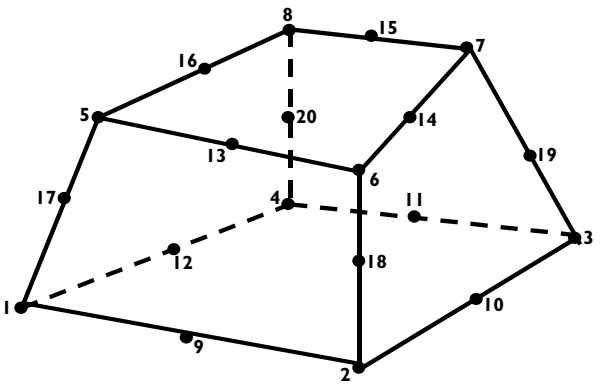


Figure 2.12.46 A 20-node generic hexahedral element.

for nodes 9, 11, 13 and 15: $N_i = (1 + \xi\xi_i)(1 - \eta^2)(1 + \zeta\zeta_i)/4$,

for nodes 17, 18, 19 and 20: $N_i = (1 + \xi\xi_i)(1 + \eta\eta_i)(1 - \zeta^2)/4$. (2.12.164)

2.12.37 The patch and eigenvalue test – The performance warranty certificates

When we buy an electronic or a mechanical gadget we are normally provided with a warranty certificate, which is nothing but a performance guarantee of the equipment.

In the finite element market though nobody furnishes a performance bond on the element in hand like the gadgets we buy, yet patch and eigenvalue test remain an important test to ensure that the element formulation is correct and the values indeed converge to the exact result as the mesh gets progressively refined.

In other words these tests are carried out to ensure that the element in hand indeed obeys the commandment of monotonic convergence.

Frankly speaking under the present scenario when a number of established commercially available FEM packages are available, the assemblers who develop these packages anyway carry out these tests on any new element rigorously to ensure their validity- before implementing them in the software. Thus, as an end user you would be rarely called upon to do this check, unless you become a developer yourself.

However, in case you get some unusual/doubtful results with any elements in hand these tests may be conveniently carried to ensure that there is no bug in the source code or a flaw in the formulation in the element in question.

2.12.37.1 Patch Test

Patch test was originally developed by Irons in an intuitive way by Irons & Razzaque (1972) and many researchers (Strang and Fix 1973), have tried to develop a mathematical proof of this. But then acknowledging the fact that mathematical intuition and capability of lesser mortals like us do not match with the geniuses of Strang and Irons we try to explain the patch test in a slightly different way.

We show in Figure 2.12.47, two identical samples of element one made of rubber and other of steel. Now if we apply a force of say P to each of them the stress induced in any section on the body is always same i.e. $\sigma = P/A$, where A is cross sectional area of the sample.

It is apparent that irrespective of what material it is made of, this is always true for any body that obeys Hooke's law.

Now we go back a bit to molecular or atomic physics. We know all elements are made up atoms whose basic characteristics are same (i.e. Proton + Neutron + Electron) and these atoms combine to make a molecule in a fixed pattern. The molecules in turn

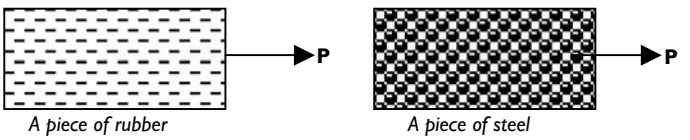


Figure 2.12.47 A patch of rubber and steel with load *P*.

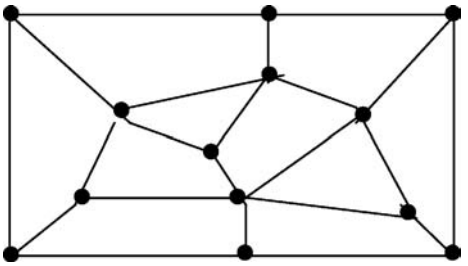


Figure 2.12.48 Arbitrary nodes within a body as a collection of molecules.

are bonded together in a particular structure that is unique for a particular element or a compound. As this molecular bond patterns are unique for every element, rubber is rubber and steel is steel.

Though the internal connectivity among the molecules within these two elements are different yet when an external load is applied to the bodies the molecules in some way[65] adjust themselves to carry the load in such a fashion that for the external load P, any arbitrary point within the body will always show same stress σ. If it does not, we conclude that the body is something different and does not obey Hooke's Law. In other words, if the body obeys Hooke's law, the stress strain relationship is invariant of the geometric bonding or patterns of the molecules.

Now look at the above pictures carefully (Fig. 2.12.47), and imagine that the patterns shown, represent the way the molecules are residing within the body (and are interconnected) then we can argue that irrespective of the geometric pattern of the molecules if the body obeys Hooke's law, stress is the same and would remain true irrespective of the size of the body whether big (say 2 m $\times$ 2 m) or a small patch (say 2 mm $\times$ 2 mm) of the same.

Now let us imagine that we collect all these small molecules (may be in thousands) and form a node, and then connect all these nodes constituting the body together as shown in Figure 2.12.48.

Now if the properties of molecules remain same as the original body we can argue that the stress will remain same at each node irrespective of how we have placed these nodes within the body since the stress distribution is independent of the location of the molecules and connectivity between them.

Thus if we apply a stress say σ on one of the edges of the body all these nodes will show a stress σ irrespective of whether the body is big, small or whatever pattern the nodes are located within the body. This is in essence is the basic philosophy of patch test though represented in slightly different way in terms of FEM.

The patch test is basically carried out to ensure that whether the body has rigid body modes and also has a constant strain deformation capability especially for the case when

65 We do not know how they manage this. Even classical physicists cannot explain this, possibly people with quantum mechanics background can explain as to – why and how this happen. But that is how it happen is indubitable.

- The element is non-conforming.
- Reduced or Selective Integration is carried out over elements deliberately to get a better stiffness value.

In this case consider a two dimensional element as shown in Figure 2.12.49, the displacement for a two dimensional body is represented by

$$u = \alpha_1 + \alpha_2 x + \alpha_3 y \quad \text{and} \quad v = \alpha_4 + \alpha_5 x + \alpha_6 y \tag{2.12.165}$$

and for this displacement induced at nodes, if the stresses developed matches the exact stress value obtained analytically, then it is concluded that the element has passed the patch test.

Now what does this really mean? To elucidate further let us consider the example as shown hereafter.

We show a patch of element (plane stress) having co-ordinates as shown in Figure 2.12.50. While selecting such a patch it should be ensured that the internal node 8 should be at an arbitrary location making each of the elements a generic quadrilateral. *The reason for this being some element with regular geometry may pass the patch test while the same element when made of quadrilaterals could fail.*

We need to test that for a displacement function considered does it simulate the constant strain relation or not.

To test this let us consider **an example**

$$u = 0.001 + 0.0035x + 0.005y \quad \text{and} \quad v = -0.001 - 0.0035x - 0.005y$$

Here $\varepsilon_x = \dfrac{\partial u}{\partial x} = 0.0035; \quad \varepsilon_y = \dfrac{\partial v}{\partial y} = -0.005; \quad$ and

$$\gamma_{xy} = \frac{\partial u}{\partial y} + \frac{\partial v}{\partial x} = 0.005 - 0.0035 = 0.0015$$

For plane stress case $\begin{bmatrix} \sigma_{xx} \\ \sigma_{yy} \\ \tau_{xy} \end{bmatrix} = \dfrac{E}{1-\nu^2} \begin{bmatrix} 1 & \nu & 0 \\ \nu & 1 & 0 \\ 0 & 0 & \dfrac{1-\nu}{2} \end{bmatrix} \begin{bmatrix} \varepsilon_{xx} \\ \varepsilon_{yy} \\ \gamma_{xy} \end{bmatrix}$

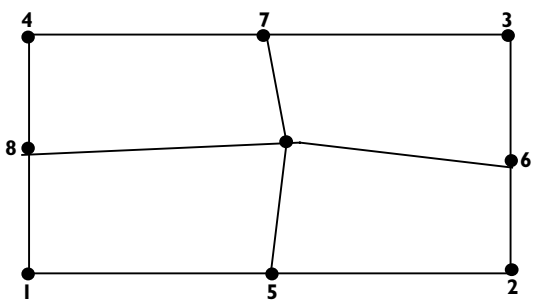


Figure 2.12.49 An arbitrary patch of two dimensional element.

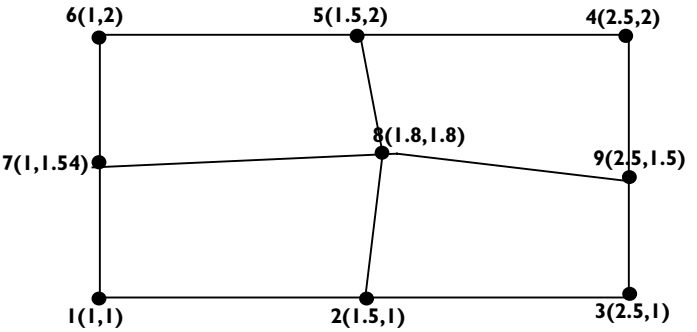


Figure 2.12.50 A two dimensional element with co-ordinates.

With $E = 2 \times 10^8$ kN/m^2 and $\nu = 0.25$ we have

$$\begin{bmatrix} \sigma_{xx} \\ \sigma_{yy} \\ \tau_{xy} \end{bmatrix} = \begin{bmatrix} 479.999999 \\ -879.999999 \\ 120 \end{bmatrix} \text{ N/mm}^2$$

Now based on the displacement function chosen the value of u and v at each node is given by

Node	*X*	*Y*	*u*	*v*
1	1	1	0.00950	−0.00950
2	1.5	1	0.01125	−0.01125
3	2.5	1	0.01475	−0.01475
4	2.5	2	0.01975	−0.01975
5	1.5	2	0.01625	−0.01625
6	1	2	0.01450	−0.01450
7	1	1.54	0.01220	−0.01220
8	**1.8**	**1.8**	**0.01630**	**−0.01630**
9	2.5	1.5	0.01725	−0.01725

To carry out the patch test we prescribe the displacements as obtained above for nodes 1 to 7 and 9 as given in the above table and carry out a simple static run in computer. *Note that we do not prescribe the displacement at the internal node 8*. Based on the computer output if we find that the nodal displacement at node 8 (value marked in bold above) and the stress in the nodes of the elements or the average stress at centroid of each of the element matches exactly to the values as calculated above analytically (to the last decimal place), we conclude that the patch has passed the test and the element formulation is correct. If not, something is wrong and we should preferably avoid such element.

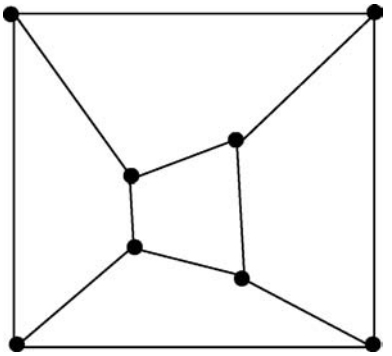


Figure 2.12.51 Alternate form of patch for which test may be carried out.

It is not necessary that the patch as shown in Figure 2.12.50 with one node inside can be the only geometry. The patch as shown in Figure 2.12.51 may also be used to carry out the test.

In this case again the displacement may be prescribed at external nodes only. The computer output should match the displacement at external and internal nodes as well as the stress at the nodes based on analytical solution.

2.12.37.2 Eigen value test

We had stated earlier that when Gauss Integration is carried out on an element exactly, the stiffness obtained is higher than actually what it should be. For this, sometimes it is beneficial to undertake reduced or selective integration to arrive at a more realistic result.

While deriving the Gauss integration scheme we mentioned that for the integration to be accurate one has take Gauss points $\cong 2n-1$, where n is the order of the shape function chosen for the element.

Thus for an twelve node iso-parametric element of Serendip family whose shape functions are cubic in nature we could carry out a three point Gauss integration for exact integration. Now suppose to get a more flexible stiffness (thus more realistic) we carry out a two point integration on this element, how correct will be the result? If two point integration give better results then why not one point integration ($\xi = \eta = 0$)?, this could perhaps converge to still better results. The quires as posed above we feel are natural and quite pertinent. We try to answer them hereafter.

One of the major problems with reduced or selective integration is that it makes the stiffness matrix rank deficient. Without getting into the details of what is a rank of matrix in mathematical term (Ayres 1962), for this particular case *the rank of the stiffness matrix is obtained as total degrees of freedom for the element minus the total number of rigid body modes.*

Thus for a two dimensional quadrilateral the number of rigid body modes are three (two translations and one rotation). Considering two degrees of freedom per node total degrees of freedom is 8, hence rank of the matrix is $8 - 3 = 5$.

The correct order of Gauss integration in this case is 2. However to make it more accurate if we try out one point integration it will be seen that the rank of the matrix becomes 3 that is two more zero modes develop beyond the normal rigid body modes. These are known *as mechanism, zero energy or hour glass modes*. The eigenvalue test helps us to detect these spurious zero energy modes or absence of rigid body modes in the element.

We had discussed at length on the mathematical and conceptual aspects of eigenvalue in Chapter 5 (Vol. 1), however, they are explained there in terms of dynamic analysis. For this particular test in context of FEM we explain the theory as follows.

We know that static equilibrium equation can be expressed as

$$[K]\{\delta\} = \{P\} \tag{2.12.166}$$

where $[K]$ is the stiffness matrix $\{\delta\}$ is the displacement and $\{P\}$ is the nodal load.

Now let us assume that the nodal load $\{P\}$ is proportional to the displacement as $\lambda[\delta]$. Then equating this we have

$$[K]\{\delta\} = \lambda[I]\{\delta\} \quad \text{or} \quad [[K] - \lambda[I]]\{\delta\} = 0 \tag{2.12.167}$$

The above is the eigen value problem of the equation $[K]\{\delta\} = \{P\}$ and the values λ_i are called the eigen values of $[K]$. The number of eigen values λ_i must be equal to the number of degrees of freedom $\{\delta\}$. For each value of λ_i there is a corresponding value $\{\delta_i\}$, these are called the eigen vectors of the problem. For the normalized eigen vectors it can be shown[66] that $\{\delta_i\}^T\{\delta_i\} = 1$ and $\{\delta_i\}^T[K]\{\delta_i\} = \lambda_i$.

From strain energy theorem for structural analysis it can be proved that strain energy of a body can be expressed as

$$U = \frac{1}{2}\{\delta\}^T[K]\{\delta\}, \tag{2.12.168}$$

Based on the normalized eigen vectors, we can express this as

$$2U_i = \{\delta_i\}^T[K]\{\delta_i\} = \lambda_i \tag{2.12.169}$$

It is apparent that when the eigenvalue is zero the strain energy of the body is also zero and this corresponds to the rigid body mode. From above we can also infer that mechanism can also induce for $\lambda = 0$.

Considering the fact that stiffness matrix of an element is obtained by

$$\int [B]^T[D][B]\,dv \tag{2.12.170}$$

at the Gauss points, the zero energy mode induces no strain at the Gauss points.

66 Refer Chapter 5 (Vol. 1) where we have proved this.

Thus in testing an element, we can compute the eigenvalues of $[K]$ when the stiffness matrix should have as many $\lambda i = 0$ as there are legitimate rigid body modes. If there are less, then it indicates that the element lacks the capability to undergo constant strain deformation, if they are more, it proves it has some mechanism or zero energy mode is prevalent in it.

It is not necessary that zero energy mode automatically qualify an element for rejection, for example the four-nodded plate element as developed by Hughes and Taylor has two zero energy mode, but this does not affect its performance when assembled in mesh, and pass the patch test quite well.

There are other ways and means by which the hour glass mode can be suppressed by incorporation of correction to the stiffness matrix but these are much more advanced topics and interested reader may refer to specialist literature (Hughes 2000) for further information.

2.12.38 A retrospection on what we presented so far

We have completed our reconnaissance of the Developers Club. By this survey, one should not have the impression that we have had a look at every nooks and corners of the institution but has only given you an exposure to the most often used elements that you would use in your day to day work in a design office or research work. We have skipped a few specialized elements like shell, axis symmetric, higher order triangular and tetrahedral elements for which one may refer to books totally dedicated to the topic.

On this study of what the developers does one should not carry an impression that considering the research carried out on this topic for last thirty odd years the show is over and no further development is envisaged. There are number of new areas which has emerged like finite volume, finite sphere and mesh less analysis which we hope in future would further enrich this powerful topic.

2.12.39 The assemblers – the tailors who stitches the pieces to give final shape

Having looked at what the developers do we would now enter the assemblers club to see what they do and how it benefits us.

While developers[67] develop the elements as discussed previously assemblers collect these building blocks to shape the over all problem.

In lighter vein, the picture in Figure 2.12.52 conceptually represents what the assemblers do. When we try to model a structure and its foundation by finite element it is rare when we will have same element considered over the whole system and neither the boundary conditions will remain identical. It will invariably be a combination of beams, plates, shells, boundary elements (springs), plane stress, plane strain elements etc with boundary conditions like free, fixed, hinged, partially restrained etc. This is otherwise, also called the overall problem where we assemble the elements to form the global stiffness matrix that represent the overall system.

67 Many of them are members of the assemblers club too.

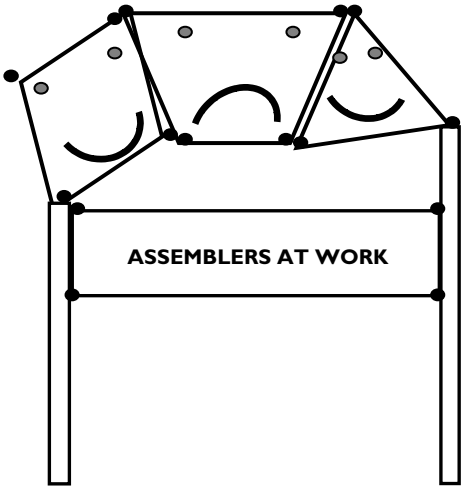


Figure 2.12.52 Gateway to assemblers' club.

We now present the mathematical background of such assembly and also explain a few techniques used in computer implementation of such assembly to optimize the computer storage.

2.12.40 Formulation of the global stiffness matrix

Like what we did with element stiffness matrix, here also we start with beam element to present the fundamental concepts of assembly before we graduate to the continuum. As discussed previously though beam is a discrete element and not a Finite Element, yet formulations applicable to beam are also applicable to continuum as will be seen subsequently.

Shown in Figure 2.12.53 is a beam of span 2L, supported on spring of stiffness *Ks* say at the center. The beam has two degrees of freedom at each node (on translation and one rotation). The mathematical model of the beam can thus be expressed as given in Figure 2.12.54. The above is actually an assembly of the following beam elements and the spring shown in Figure 2.12.55.

The stiffness matrix of individual beam elements are given as

$$[K]_1 = \begin{matrix} \\ \\ \\ \\ \end{matrix} \begin{matrix} 1 & 2 & 3 & 4 \end{matrix} \begin{bmatrix} \frac{12EI}{L^3} & \frac{6EI}{L^2} & \frac{-12EI}{L^3} & \frac{6EI}{L^2} \\ \frac{6EI}{L^2} & \frac{4EI}{L} & \frac{-6EI}{L^2} & \frac{2EI}{L} \\ \frac{-12EI}{L^3} & \frac{-6EI}{L^2} & \frac{12EI}{L^3} & \frac{-6EI}{L^2} \\ \frac{6EI}{L^2} & \frac{2EI}{L} & \frac{-6EI}{L^2} & \frac{4EI}{L} \end{bmatrix} \quad \text{and} \tag{2.12.171}$$

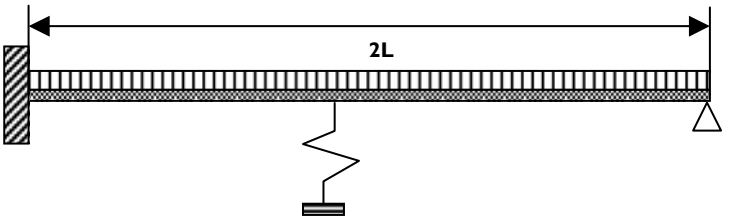


Figure 2.12.53 A propped cantilever beam supported on spring at mid span.

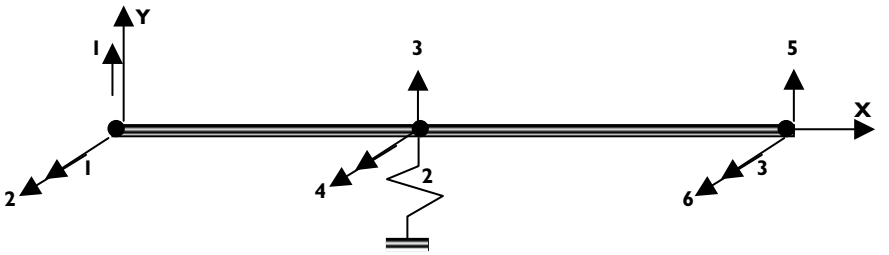


Figure 2.12.54 Mathematical model of the continuous beam.

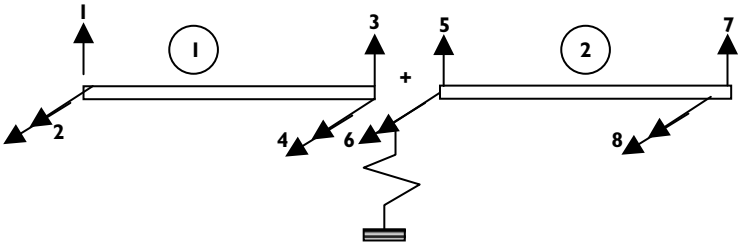


Figure 2.12.55 Mathematical model of beams and spring.

$$[K]_2 = \begin{matrix} \\ \frac{12EI}{L^3} \\ \frac{6EI}{L^2} \\ \frac{-12EI}{L^3} \\ \frac{6EI}{L^2} \end{matrix} \begin{matrix} \begin{matrix} 5 \end{matrix} \\ \begin{bmatrix} \frac{6EI}{L^2} \\ \frac{4EI}{L} \\ \frac{-6EI}{L^2} \\ \frac{2EI}{L} \end{bmatrix} \end{matrix} \begin{matrix} \begin{matrix} 6 \end{matrix} \\ \begin{bmatrix} \frac{-12EI}{L^3} \\ \frac{-6EI}{L^2} \\ \frac{12EI}{L^3} \\ \frac{-6EI}{L^2} \end{bmatrix} \end{matrix} \begin{matrix} \begin{matrix} 7 \end{matrix} \\ \begin{bmatrix} \frac{6EI}{L^2} \\ \frac{2EI}{L} \\ \frac{-6EI}{L^2} \\ \frac{4EI}{L} \end{bmatrix} \end{matrix} \begin{matrix} \begin{matrix} 8 \end{matrix} \\ \end{matrix} \tag{2.12.172}$$

While that of the spring is only $[K_s]$.

Now when we combine the stiffness matrix in this case we simply add the stiffness of individual stiffness of a particular node to their respective degrees of freedom as shown hereafter

$$[K]_G = \begin{matrix} \\ \\ \\ \\ \\ \\ \end{matrix} \begin{matrix} 1 & 2 & 3 & 4 & 5 & 6 \end{matrix} \begin{bmatrix} \frac{12EI}{L^3} & \frac{6EI}{L^2} & \frac{-12EI}{L^3} & \frac{6EI}{L^2} & 0 & 0 \\ \frac{6EI}{L^2} & \frac{4EI}{L} & \frac{-6EI}{L^2} & \frac{2EI}{L} & 0 & 0 \\ \frac{-12EI}{L^3} & \frac{-6EI}{L^2} & \frac{12EI}{L^3} + \frac{12EI}{L^3} + K_s & \frac{-6EI}{L^2} + \frac{6EI}{L^2} & \frac{-12EI}{L_3} & \frac{6EI}{L^2} \\ \frac{6EI}{L^2} & \frac{2EI}{L} & \frac{-6EI}{L^2} + \frac{6EI}{L_2} & \frac{4EI}{L} + \frac{4EI}{L} & \frac{-6EI}{L^2} & \frac{2EI}{L} \\ 0 & 0 & \frac{-12EI}{L^3} & \frac{-6EI}{L^2} & \frac{12EI}{L^3} & \frac{-6EI}{L^2} \\ 0 & 0 & \frac{6EI}{L^2} & \frac{2EI}{L} & \frac{-6EI}{L^2} & \frac{4EI}{L} \end{bmatrix} \tag{2.12.173}$$

or

$$[K]_G = \begin{matrix} \\ \\ \\ \\ \\ \\ \end{matrix} \begin{matrix} 1 & 2 & 3 & 4 & 5 & 6 \end{matrix} \begin{bmatrix} \frac{12EI}{L^3} & \frac{6EI}{L^2} & \frac{-12EI}{L^3} & \frac{6EI}{L^2} & 0 & 0 \\ \frac{6EI}{L^2} & \frac{4EI}{L} & \frac{-6EI}{L^2} & \frac{2EI}{L} & 0 & 0 \\ \frac{-12EI}{L^3} & \frac{-6EI}{L^2} & \frac{24EI}{L^3} + K_s & 0 & \frac{-12EI}{L_3} & \frac{6EI}{L^2} \\ \frac{6EI}{L^2} & \frac{2EI}{L} & 0 & \frac{8EI}{L} & \frac{-6EI}{L^2} & \frac{2EI}{L} \\ 0 & 0 & \frac{-12EI}{L^3} & \frac{-6EI}{L^2} & \frac{12EI}{L^3} & \frac{-6EI}{L^2} \\ 0 & 0 & \frac{6EI}{L^2} & \frac{2EI}{L} & \frac{-6EI}{L^2} & \frac{4EI}{L} \end{bmatrix} \tag{2.12.174}$$

The above matrix is singular as such cannot be inverted. So before the solution is to be carried out the boundary conditions for the structure has to be implemented.

For the given structure displacements 1, 2 and 5 (Figure 2.12.54) are zero thus the corresponding rows and columns from the above matrix are deleted when we are left with

$$[K]_G = \begin{bmatrix} \frac{24EI}{L^3} + K_s & 0 & \frac{6EI}{L^2} \\ 0 & \frac{8EI}{L} & \frac{2EI}{L} \\ \frac{6EI}{L^2} & \frac{2EI}{L} & \frac{4EI}{L} \end{bmatrix} \tag{2.12.175}$$

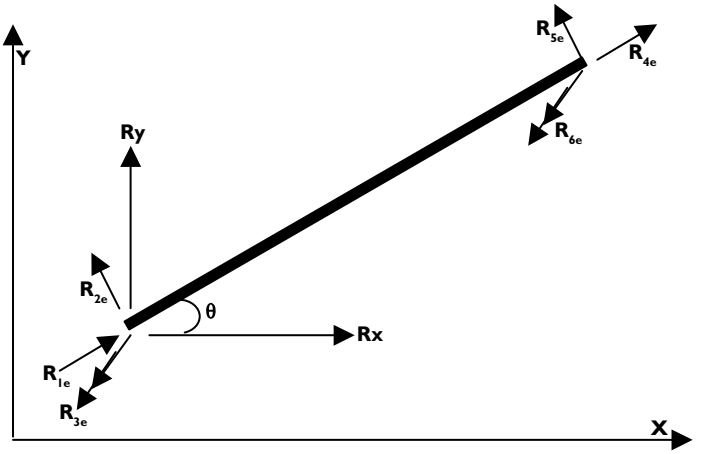


Figure 2.12.56 Beam Element inclined at an angle θ with the global axes.

In the above case the local and global co-ordinate of the structure matches. However, in our real world of engineering, nothing is ideal and there could always be cases when the beam could be at an angle say θ with global co-ordinate, we will now derive the effect of such inclination subsequently.

As shown in Figure 2.12.56 is a beam element inclined at an angle θ with global axes. The beam has three degrees of freedom per node as shown. In local co-ordinate axes let the reactions be expressed as R_{1e}, R_{2e}, R_{3e} be reactions at node 1 and R_{4e}, R_{5e}, R_{6e} be the reactions in node 2 in local axes and let this be R_x, R_y and R_θ in terms of global axes respectively. Here the subscript e represents the word element. Breaking up the forces in components it can be easily shown that

$$R_{1e} = R_x \cos\theta + R_y \sin\theta R_{2e} = -R_x \sin\theta + R_y \cos\theta \quad \text{and} \quad R_{3e} = R_{\theta x} \tag{2.12.176}$$

The above can be expressed in matrix form as

$$\begin{Bmatrix} R_{1e} \\ R_{2e} \\ R_{3e} \end{Bmatrix} = \begin{bmatrix} \cos\theta & \sin\theta & 0 \\ -\sin\theta & \cos\theta & 0 \\ 0 & 0 & 1 \end{bmatrix} \begin{Bmatrix} R_x \\ R_y \\ R_\theta \end{Bmatrix} \tag{2.12.177}$$

Thus for the two nodes we have the complete expression as

$$\begin{Bmatrix} R_{1e} \\ R_{2e} \\ R_{3e} \\ R_{4e} \\ R_{5e} \\ R_{6e} \end{Bmatrix} = \begin{bmatrix} \cos\theta & \sin\theta & 0 & 0 & 0 & 0 \\ -\sin\theta & \cos\theta & 0 & 0 & 0 & 0 \\ 0 & 0 & 1 & 0 & 0 & 0 \\ 0 & 0 & 0 & \cos\theta & \sin\theta & 0 \\ 0 & 0 & 0 & -\sin\theta & \cos\theta & 0 \\ 0 & 0 & 0 & 0 & 0 & 1 \end{bmatrix} \begin{Bmatrix} R_{1x} \\ R_{1y} \\ R_{1\theta} \\ R_{2x} \\ R_{2y} \\ R_{2\theta} \end{Bmatrix} \tag{2.12.178}$$

Here if (x_1, y_1) and (x_2, y_2) are the nodal coordinates of the node 1 and 2 then

$$\cos\theta = \frac{x_2 - x_1}{\sqrt{(x_2 - x_1)^2 + (y_2 - y_1)^2}} \quad \text{and} \quad \sin\theta = \frac{y_2 - y_1}{\sqrt{(x_2 - x_1)^2 + (y_2 - y_1)^2}} \tag{2.12.179}$$

Now let the above expression be expressed as

$$[R_e] = [T]\,[R_G] \tag{2.12.180}$$

where $[T]$ is called the *transformation matrix* and is expressed as

$$[T] = \begin{bmatrix} \cos\theta & \sin\theta & 0 & 0 & 0 & 0 \\ -\sin\theta & \cos\theta & 0 & 0 & 0 & 0 \\ 0 & 0 & 1 & 0 & 0 & 0 \\ 0 & 0 & 0 & \cos\theta & \sin\theta & 0 \\ 0 & 0 & 0 & -\sin\theta & \cos\theta & 0 \\ 0 & 0 & 0 & 0 & 0 & 1 \end{bmatrix} \tag{2.12.181}$$

and R_e is the element reaction and R_G is the global co-ordinate reaction.

One of the special property of the above matrix is $[T]^{-1} = [T]^T$. *That is inverse of the matrix is equal to its transpose.*

Proceeding in identical fashion it is elementary to show that displacements can also be expressed as

$$\{\delta_e\} = [T]\,\{\delta_G\} \tag{2.12.182}$$

The static equilibrium equation at element level can be expressed as

$$\{R_e\} = [K_e]\,\{\delta_e\} \tag{2.12.183}$$

Transferring them in global co-ordinate we have

$$\begin{aligned} &[T]\,\{R_G\} = [K_e]\,[T]\,\{\delta_G\} \\ &[T]\,[K_G]\,\{\delta_G\} = [K_e]\,[T]\,\{\delta_G\}; \quad \Longrightarrow [K_G] = [T]^{-1}\,[K_e]\,[T] \end{aligned} \tag{2.12.184}$$

Using the property as mentioned earlier that *inverse is equal to the transpose*, we have

$$[K_G] = [T]^T\,[K_e]\,[T] \quad \text{and} \quad [R_G] = [T]^T\,[\,R_e] \tag{2.12.185}$$

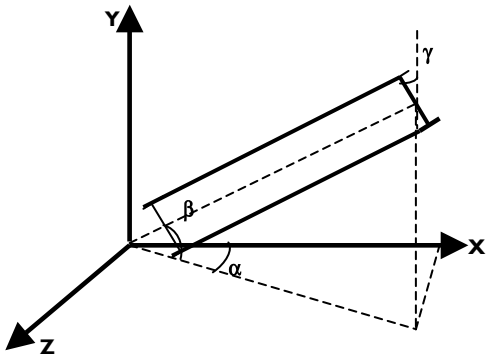


Figure 2.12.57 A beam element in space at angle α, β, γ with global *X*, *Y* and *Z* axis.

2.12.41 Transformation in space for 3D analysis

Having derived the transformation matrix in 2D we present now how transformation is carried out in 3D which is required for analysis of space frames.

Shown in Figure 2.12.57 is a beam element inclined at an angle α, β, and γ with global X, Y and Z axis. We do not derive the transformation matrix in detail but present the results only, which is anyway similar to what we have derived for the 2D case (Meek 1971).

Transferring the beam to the x-axis, the transformation matrix is given by

$$[T]_\alpha = \begin{bmatrix} \cos\alpha & 0 & \sin\alpha \\ 0 & 1 & 0 \\ -\sin\alpha & 0 & \cos\alpha \end{bmatrix} \tag{2.12.186}$$

similarly transferring to the y-axis, we have

$$[T]_\beta = \begin{bmatrix} \cos\beta & \sin\beta & 0 \\ -\sin\beta & \cos\beta & 0 \\ 0 & 0 & 1 \end{bmatrix} \tag{2.12.187}$$

and for the z-axis, we have

$$[T]_\gamma = \begin{bmatrix} 1 & 0 & 0 \\ 0 & \cos\gamma & \sin\gamma \\ 0 & -\sin\gamma & \cos\gamma \end{bmatrix}. \tag{2.12.188}$$

The transformation matrix is thus given by

$$\left[\bar{T}\right] = [T]_\gamma\,[T]_\beta\,[T]_\alpha$$

$$[\bar{T}] = \begin{bmatrix} L_x/L & L_y/L & L_z/L \\ (-L_xL_y\cos\gamma - LL_z\sin\gamma)/R\,L & \cos\gamma(R/L) & (-L_yL_z\cos\gamma + LL_x\sin\gamma)/R\,L \\ (L_yL_x\sin\gamma - LL_z\cos\gamma)/R\,L & -\sin\gamma(R/L) & (LyLz\sin\gamma + LLx\cos\gamma)/R\,L \end{bmatrix} \tag{2.12.189}$$

in which $R = \sqrt{L_x^2 + L_z^2}$; and for a beam of node i and j having nodal coordinates (x_i, y_i) and (x_j, y_j), we have

$$L_x = x_j - x_i, \quad L_y = y_j - y_i, \quad L_z = z_j - z_i \quad \text{and}$$
$$L = \sqrt{(x_j - x_i)^2 + (y_j - y_i)^2 + (z_j - z_i)^2}.$$

For a beam in space number of degrees of freedom per node is 6 which gives the element stiffness matrix of order 12×12.

Thus the total transformation matrix for the beam element is thus given by

$$[T] = \begin{bmatrix} [\bar{T}] & 0 & 0 & 0 \\ 0 & [\bar{T}] & 0 & 0 \\ 0 & 0 & [\bar{T}] & 0 \\ 0 & 0 & 0 & [\bar{T}] \end{bmatrix}_{12\times12} \tag{2.12.190}$$

You will notice that in the above transformation matrix, the angle γ is yet to be clarified. This is computed as given hereunder.

Here a node k having coordinate (x_k, y_k, z_k) is assumed on the x-y plane (Figure 2.12.58) it may be anywhere in the x-y plane but not on the x axis.

Thus with respect to node i

$$x_{ki} = x_k - x_i, \quad y_{ki} = y_k - y_i \quad \text{and} \quad z_{ki} = z_k - z_i \tag{2.12.191}$$

Making transformation through α and β we have

$$\langle x_k, y_k, z_k \rangle_{\alpha\beta}^T = [T]_\beta\,[T]_\alpha\,\langle x_{ki}, y_{ki}, z_{ki} \rangle^T \tag{2.12.192}$$

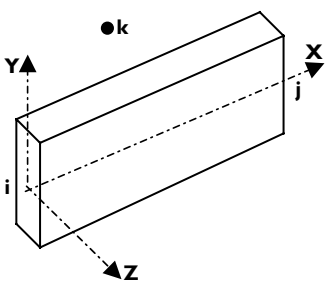


Figure 2.12.58 A beam element with k node on x-y plane.

i.e.

$$\begin{Bmatrix} x_k \\ y_k \\ z_k \end{Bmatrix}_{\alpha\beta} = \begin{bmatrix} R/L & L_y/L & 0 \\ -L_y/L & R/L & 0 \\ 0 & 0 & 1 \end{bmatrix} \begin{bmatrix} L_x/R & 0 & L_z/R \\ 0 & 1 & 0 \\ -L_z/R & 0 & L_x/R \end{bmatrix} \begin{Bmatrix} x_{ki} \\ y_{ki} \\ z_{ki} \end{Bmatrix} \tag{2.12.193}$$

in which $R = \sqrt{L_x^2 + L_z^2}$

The above on simplification gives

$$\begin{Bmatrix} x_k \\ y_k \\ z_k \end{Bmatrix}_{\alpha\beta} = \begin{Bmatrix} (L_x/L)x_{ki} + (L_y/L)y_{ki} + (L_z/L)z_{ki} \\ -(L_xL_y/R)x_{ki} + y_{ki}R - (L_yL_z/R)z_{ki} \\ -(L_z/R)x_{ki} + (L_x/R)z_{ki} \end{Bmatrix} \tag{2.12.194}$$

$$\text{Thus} \quad \sin\gamma = \frac{(z_k)_{\alpha\beta}}{\sqrt{(y_k^2)_{\alpha\beta} + (z_k^2)_{\alpha\beta}}} \quad \text{and} \quad \cos\gamma = \frac{(y_k)_{\alpha\beta}}{\sqrt{(y_k^2)_{\alpha\beta} + (z_k^2)_{\alpha\beta}}} \tag{2.12.195}$$

2.12.42 Members vertical in space – *a special case*

For members that are vertical that is its axes parallel to global y axes the transformation matrix $[\bar{T}]$ derived earlier converges to incorrect value.

In this case as L_x/L and L_z/L being zero the correct expression is

$$[\bar{T}] = \begin{bmatrix} 0 & L_y/L & 0 \\ -(L_y\cos\gamma)/L & 0 & \sin\gamma \\ (L_y\sin\gamma)/L & 0 & \cos\gamma \end{bmatrix} \tag{2.12.196}$$

where, using $Z = \sqrt{x_k^2 + z_k^2}$, $\sin\gamma = z_k/Z$, $\cos\gamma = x_k/Z$ for $0 \le \gamma \le \pi/2$ and $\sin\gamma = z_k/Z, \cos\gamma = -x_k/Z$ for $\pi/2 \le \gamma \le \pi$.

The element stiffness matrix and the element load can now be transferred to global axes by the expression

$$[K_G] = [T]^T [K_e] [T] \quad \text{and} \quad [R_G] = [T]^T [R_e] \tag{2.12.197}$$

The global assembly technique then remains same as in the case of 2D element as shown earlier.

Example 2.12.5

Shown in Figure 2.12.59 is a frame with loadings as shown. We solve this problem based on matrix method as described previously. The global axes are shown

in the figure. The nodal coordinates are as shown hereafter. Consider $E = 2 \times 10^7$ kN/m^2. Beam and column size 300 × 400.

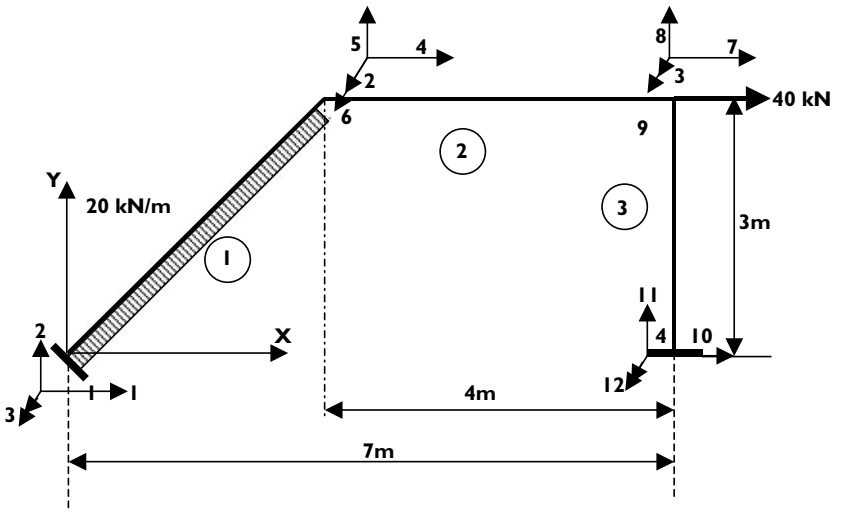


Figure 2.12.59 A 2D frame with udL and nodal load.

Node number	*X Coordinate (m)*	*Y Coordinate (m)*
1	0	0
2	3	3
3	7	3
4	7	0

The geometric properties are as given below

$$I = (0.3 \times 0.4^3)/12 = 0.0016 \text{ m}^4; \quad E = 2 \times 10^7 \text{ kN/m}^2$$

$$\rightarrow \quad EI = 32000 \text{ kN} \cdot \text{m}^2; \quad A = 0.12. \text{ m}^2; \quad AE = 2400000 \text{ kN}.$$

For Member-1 the fixed end moments are as given in Figure 2.11.60.

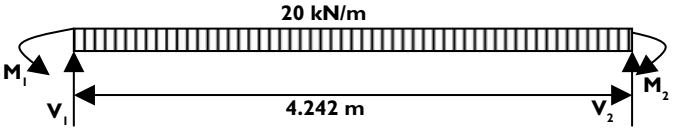


Figure 2.12.60 Free body diagram of member 1.

Here $M_1 = \dfrac{wL^2}{12} = \dfrac{20 \times 4.242^2}{12} = 29.99 \text{ kN} \cdot \text{m}$

$$M_2 = -\frac{wL^2}{12} = -\frac{20 \times 4.242^2}{12} = -29.99 \,\text{kN} \cdot \text{m};$$

$$V_1 = V_2 = \frac{wL}{2} = \frac{20 \times 4.242}{2} = 42.42 \,\text{kN}$$

$$[K]_{\text{beam}} = \begin{bmatrix} AE/L & 0 & 0 & -AE/L & 0 & 0 \\ 0 & 12EI/L^3 & 6EI/L^2 & 0 & -12EI/L^3 & 6EI/L^2 \\ 0 & 6EI/L^2 & 4EI/L & 0 & -6EI/L^2 & 2EI/L \\ -AE/L & 0 & 0 & AE/L & 0 & 0 \\ 0 & -12EI/L^3 & -6EI/L^2 & 0 & 12EI/L^3 & -6EI/L^2 \\ 0 & 6EI/L^2 & 2EI/L & 0 & -6EI/L^2 & 4EI/L \end{bmatrix}$$

For member 1, 2 and 3 element stiffness matrix is given by:

Member-1

614292	0	0	−614292	0	0
0	5460	11583	0	−5460	11583
0	11583	32762	0	−11583	16381
−614292	0	0	614292	0	0
0	−5460	−11583	0	5460	−11583
0	11583	16381	0	−11583	32762

Member-2

651555	0	0	−651555	0	0
0	6516	13031	0	−6516	13031
0	13031	34750	0	−13031	17375
−651555	0	0	651555	0	0
0	−6516	−13031	0	6516	−13031
0	13031	17375	0	−13031	34750

Member-3

868740	0	0	−868740	0	0
0	15444	23166	0	−15444	23166
0	23166	46333	0	−23166	23166
−868740	0	0	868740	0	0
0	−15444	−23166	0	15444	−23166
0	23166	23166	0	−23166	46333

For element 1 the transformation matrix [T] is given (for $\alpha = 45°$) by

0.707107	−0.707107	0	0	0	0
0.70711	0.707107	0	0	0	0
0	0	1	0	0	0
0	0	0	0.707107	−0.707107	0
0	0	0	0.70711	0.707107	0
0	0	0	0	0	1

Now performing the operation $[T]^T [K] [T]$ for element 1 we have the stiffness matrix in global co-ordinate as

309876.16	−304415.79	8190.56	−309876.16	304415.79	8190.56
−304415.79	309876.16	8190.56	304415.79	−309876.16	8190.56
8190.56	8190.56	32762.24	−8190.56	−8190.56	16381.12
−309876.16	304415.79	−8190.56	309876.16	−304415.79	−8190.56
304415.79	−309876.16	−8190.56	−304415.79	309876.16	−8190.56
8190.56	8190.56	16381.12	−8190.56	−8190.56	32762.24

Performing the operation $[T]^T [P]_e$ for element 1 the load matrix on global coordinate is given as

$$\begin{bmatrix} 0.707107 & 0.707107 & 0 & 0 & 0 & 0 \\ -0.707107 & 0.7070107 & 0 & 0 & 0 & 0 \\ 0 & 0 & 1 & 0 & 0 & 0 \\ 0 & 0 & 0 & 0.707107 & 0.707107 & 0 \\ 0 & 0 & 0 & -0.707107 & 0.707107 & 0 \\ 0 & 0 & 0 & 0 & 0 & 1 \end{bmatrix}$$

$$\times \begin{Bmatrix} 0 \\ -42.42 \\ -30 \\ 0 \\ -42.42 \\ 30 \end{Bmatrix} = \begin{Bmatrix} -30 \\ -30 \\ -30 \\ -30 \\ -30 \\ 30 \end{Bmatrix}$$

For element 2, as the axes is parallel to the global axes no transformation is required.

For element 3 which is vertical the transformation matrix (for $\alpha = 90°$) is given by

0	1	0	0	0	0
−1	0	0	0	0	0
0	0	1	0	0	0
0	0	0	0	1	0
0	0	0	−1	0	0
0	0	0	0	0	1

Thus the operation $[T]^T [K] [T]$ gives the stiffness matrix in global coordinate as

15444.27	0.00	−23166.40	−15444.27	0.00	−23166.40
0.00	868740.00	0.00	0.00	−868740.00	0.00
−23166.40	0.00	46332.80	23166.40	0.00	23166.40
−15444.27	0.00	23166.40	15444.27	0.00	23166.40
0.00	−868740.00	0.00	0.00	868740.00	0.00
−23166.40	0.00	23166.40	23166.40	0.00	46332.80

Thus we can now combine them to form the global stiffness matrix as given hereafter

COLUMNS 1	*2*	*3*	*4*	*5*	*6*
309876	−304416	8191	−309876	304416	8191
−304416	309876	8191	304416	−309876	8191
8191	8191	32762	−8191	−8191	16381
−309876	304416	−8191	961431	−304416	−8191
304416	−309876	−8191	−304416	316392	4841
8191	8191	16381	−8191	4841	67512
0	0	0	−651555	0	0
0	0	0	0	−6516	−13031
0	0	0	0	13031	17375
0	0	0	0	0	0
0	0	0	0	0	0
0	0	0	0	0	0

COLUMNS 7	*8*	*9*	*10*	*11*	*12*
0	0	0	0	0	0
0	0	0	0	0	0
0	0	0	0	0	0
−651555	0	0	0	0	0
0	−6516	13031	0	0	0
0	−13031	17375	0	0	0
666999	0	−23166	−15444	0	−23166
0	875256	−13031	0	−868740	0
−23166	−13031	81082	23166	0	23166
−15444	0	23166	15444	23166	23166
0	−868740	0	0	868740	0
−23166	0	23166	23166	0	46333

Since node 1 and 4 are fixed we can eliminate 1, 2, 3 and 10, 11, 12th degree of freedom. Thus deleting the corresponding rows and columns we have the stiffness matrix imposing the boundary conditions as

961431.16	−304415.79	−8190.56	−651555.00	0.00	0.00
−304415.79	316391.71	4840.54	0.00	−6515.55	13031.10
−8190.56	4840.54	67511.84	0.00	−13031.10	17374.80
−651555.00	0.00	0.00	666999.27	0.00	−23166.40
0.00	−6515.55	−13031.10	0.00	875255.55	−13031.10
0.00	13031.10	17374.80	−23166.40	−13031.10	81082.40

Inverting the above matrix we have

$[K]^{-1} =$

3.2586E-05	3.11821E-05	7.43431E-07	3.19708E-05	3.02933E-07	4.01248E-06
3.11821E-05	3.30215E-05	6.12932E-07	3.05764E-05	3.0477E-07	3.34671E-06
7.43431E-07	6.12932E-07	1.57354E-05	6.12826E-07	1.9023E-07	−3.26471E-06
3.19708E-05	3.05764E-05	6.12826E-07	3.28825E-05	3.02221E-07	4.3982E-06
3.02933E-07	3.0477E-07	1.9023E-07	3.02221E-07	1.15033E-06	1.81478E-07
4.01248E-06	3.34671E-06	−3.26471E-06	4.3982E-06	1.81478E-07	1.37806E-05

Performing the operation $\{\delta\} = [K]^{-1}\{P\}$ where

$\{P\} = \langle -30 \quad -30 \quad 30 \quad 40 \quad 0 \quad 0 \rangle^T$, we have

$\{\delta\} = \langle -0.00061 -0.00068 0.000456 -0.00054 - 4.3 \times 10^{-7} -0.00014 \rangle^T$.

Thus member 1 displacements in global coordinate is

$$\{\delta\}_1^G = \langle 0 \quad 0 \quad 0 \quad -0.0006116 \quad -0.0006843 \quad 0.0004558 \rangle^T$$

transferring it into local coordinate by operation $\{\delta\}_1^L = [T]\{\delta\}_1^G$ we have

$$\{\delta\}_1^L = \langle 0 \quad 0 \quad 0 \quad 5.1447 \times 10^{-5} \quad -0.0009164 \quad 0.00045589 \rangle^T$$

The element stress is obtained from the expression

$$\{\sigma\} = [K]_e \{\delta\}_e^L + \{P\}_f$$

where, $\{\sigma\}$ = stress vector which in this case is the shears and moments; $[K]_e$ = element stiffness matrix; $\{\delta\}_e^L$ = element defection matrix in local coordinate; $\{P\}_f$ = fixed end moments and shears.

Thus for element 1 we have

$$\begin{Bmatrix} P_1 \\ V_1 \\ M_1 \\ P_2 \\ V_2 \\ M_2 \end{Bmatrix} = \begin{bmatrix} 614292 & 0 & 0 & -614292 & 0 & 0 \\ 0 & 5460 & 11583 & 0 & -5460 & 11583 \\ 0 & 11583 & 32762 & 0 & -11583 & 16381 \\ -614292 & 0 & 0 & 614292 & 0 & 0 \\ 0 & -5460 & -11583 & 0 & -5460 & -11583 \\ 0 & 11583 & 16381 & 0 & -11583 & 32762 \end{bmatrix}$$

$$\times \begin{Bmatrix} 0 \\ 0 \\ 0 \\ 5.1447 \times 10^{-5} \\ -0.0009164 \\ 0.0004558 \end{Bmatrix} + \begin{Bmatrix} 0 \\ 42.42 \\ 30 \\ 0 \\ 42.42 \\ -30 \end{Bmatrix} = \begin{Bmatrix} -31.604 \\ 52.704 \\ 48.083 \\ 31.604 \\ 32.134 \\ -4.45 \end{Bmatrix}$$

For element 2 we have $[\sigma] = [K]_e \{\delta\}_e^L$ as there are no element force hence

$$\begin{Bmatrix} P_1 \\ V_1 \\ M_1 \\ P_2 \\ V_2 \\ M_2 \end{Bmatrix} = \begin{bmatrix} 651555 & 0 & 0 & -651555 & 0 & 0 \\ 0 & 6516 & 13031 & 0 & -6516 & 13031 \\ 0 & 13031 & 34750 & 0 & -13031 & 17375 \\ -651555 & 0 & 0 & 651555 & 0 & 0 \\ 0 & -6516 & -13031 & 0 & 6516 & -13031 \\ 0 & 13031 & 17375 & 0 & -13031 & 34750 \end{bmatrix}$$

$$\times \begin{Bmatrix} -0.0006116 \\ 0.000684 \\ 0.000456 \\ -0.000542 \\ -4.3256 \times 10^{-7} \\ -0.001427 \end{Bmatrix} = \begin{Bmatrix} -45.0705 \\ -0.3757 \\ 4.45 \\ 45.0705 \\ 0.3757 \\ -5.952 \end{Bmatrix}$$

For element 3 we have transferring the displacement from global to local coordinate by the operation $\{\delta\}_3^L = [T]\{\delta\}_3^G$

$$\{\delta\}_G = \langle -0.0005424 \quad -4.3256 \times 10^{-7} \quad -0.0001427 \quad 0 \quad 0 \quad 0 \rangle^T$$

in global axes and

$$\{\delta\}_L = \langle 4.3257 \times 10^{-7} \quad 0.0005424 \quad -0.00014275 \quad 0 \quad 0 \quad 0 \rangle^T$$

in local axes after transformation

$$\begin{Bmatrix} P_1 \\ V_1 \\ M_1 \\ P_2 \\ V_2 \\ M_2 \end{Bmatrix} = \begin{bmatrix} 868740 & 0 & 0 & -868740 & 0 & 0 \\ 0 & 15444 & 23166 & 0 & -15444 & 23166 \\ 0 & 23166 & 46333 & 0 & -23166 & 23166 \\ -868740 & 0 & 0 & 868740 & 0 & 0 \\ 0 & -15444 & -23166 & 0 & 15444 & -23166 \\ 0 & 23166 & 231665 & 0 & -23166 & 46333 \end{bmatrix}$$

$$\times \begin{Bmatrix} 4.3257 \times 10^{-7} \\ 0.0005424 \\ -0.00014275 \\ 0 \\ 0 \\ 0 \end{Bmatrix} = \begin{Bmatrix} -0.376 \\ 5.07 \\ 5.952 \\ 0.376 \\ -5.07 \\ 9.26 \end{Bmatrix}$$

Solution is given in Figure 2.12.61.

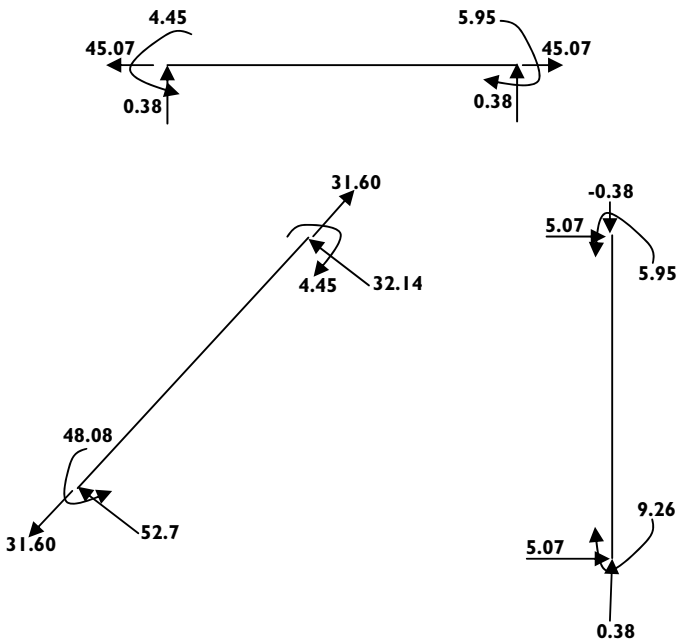


Figure 2.12.61 Nodal forces acting at the nodes of the frame.

2.12.43 Global stiffness matrix and transformation of finite element continuum

Some of you might feel apprehensive on going through the transformation technique for a beam element, on the complexity that could evolve for a continuum where element stiffness matrices are far more intricate. The typical reaction could be – If this is what happens with a simple beam in space! "God save us" – if I am handling a 20 node hexahedral in space.

Our suggestion is just relax, handling transformation for Finite elements are much simpler then a beam element in space. *On the contrary in majority of cases you need not carry out the transformation at all.*

Let us take the case of CST element, since the stiffness is independent of the x and y coordinate we need not undertake any transformation and just directly add the global stiffness values to the respective degrees of freedom.

The most beautiful of them all is the iso-parametric element. Just go back and have a re-look at the 4-nodded iso-parametric quadrilateral element.

What do you see? You will observe that though the stiffness matrix is derived based on natural coordinate is ultimately transferred to the global axes by the Jacobian matrix $[J]$.

Thus when we finally derive $[K]_e = t\iint [B]\,T\,[D]\,[B]\,|J|\,d\xi\,d\eta$ we have already transferred the matrix back into global coordinate and no further transformation is required. *As such your apprehension with 20 node hexahedral element is uncalled for as the job is already done at element stage.*

For DKT and ACM plate element also as the local axes is taken parallel to the global axes as such no axis transformation is required for these elements too.

The final global assemblage remains same as the beam element. For further clarification you can have a re-look now into the quadrilateral element derived earlier as an assemblage of 4 triangular elements to see the sanctity of the statement.

2.12.44 Implementing the boundary condition

For a structural or a soil foundation system as shown in Figs. 2.12.62 and 63 must have a specific boundary and a specified displacement (could be zero or have prescribed value). Without this being described it is not possible to have a solution as the global matrix become singular.

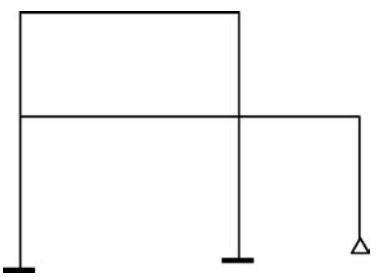


Figure 2.12.62 Plane frame structure.

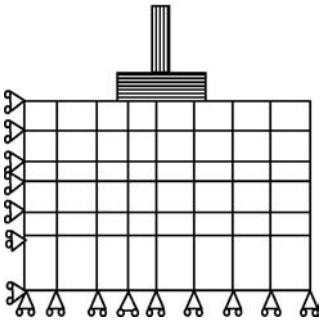


Figure 2.12.63 Footing and soil as finite elements.

If you look at the continuous beam problem we showed earlier (supported on spring at center) you will observe that since the left hand end was fixed the translation and rotation was zero as such we deleted the corresponding rows and columns 1 and 2 while at the right hand the displacement being zero we eliminated the row and column 5 thus the final matrix obtained is solvable and non-singular.

This of course is OK when the matrix is small or we are doing a hand computation. For solving a finite element problem when we are handling a matrix of order say >1000 it is not possible to eliminate the rows and columns as done earlier.

The reason for the same is

- Book keeping for the matrix becomes complicated
- Bandwidth of the matrix can get affected

One of the practical ways to deal with this is to multiply the diagonal element K_{ii} for the degree of freedom for which it is prescribed as zero by a value of 1×10^{10}. Thus for the beam we derived earlier Figure 2.12.53 boundary conditions are implemented as

$$[K]_G = \begin{bmatrix} \frac{12EI}{L^3} \times 10^{10} & \frac{6EI}{L^2} & \frac{-12EI}{L^3} & \frac{6EI}{L^2} & 0 & 0 \\ \frac{6EI}{L^2} & \frac{4EI}{L} \times 10^{10} & \frac{-6EI}{L^2} & \frac{2EI}{L} & 0 & 0 \\ \frac{-12EI}{L^3} & \frac{-6EI}{L^2} & \frac{12EI}{L^3} + \frac{12EI}{L^3} + K_s & \frac{-6EI}{L^2} + \frac{6EI}{L^2} & \frac{-12EI}{L_3} & \frac{6EI}{L^2} \\ \frac{6EI}{L^2} & \frac{2EI}{L} & \frac{-6EI}{L^2} + \frac{6EI}{L_2} & \frac{4EI}{L} + \frac{4EI}{L} & \frac{-6EI}{L^2} & \frac{2EI}{L} \\ 0 & 0 & \frac{-12EI}{L^3} & \frac{-6EI}{L^2} & \frac{12EI}{L^3} \times 10^{10} & \frac{-6EI}{L^2} \\ 0 & 0 & \frac{6EI}{L^2} & \frac{2EI}{L} & \frac{-6EI}{L^2} & \frac{4EI}{L} \end{bmatrix} \tag{2.12.198}$$

Now the question is how and why does it work? We can formulate the equation of equilibrium as

$$\begin{bmatrix} \frac{12EI}{L^3}\times 10^{10} & \frac{6EI}{L^2} & \frac{-12EI}{L^3} & \frac{6EI}{L^2} & 0 & 0 \\ \frac{6EI}{L^2} & \frac{4EI}{L}\times 10^{10} & \frac{-6EI}{L^2} & \frac{2EI}{L} & 0 & 0 \\ \frac{-12EI}{L^3} & \frac{-6EI}{L^2} & \frac{24EI}{L^3}+K_s & 0 & \frac{-12EI}{L^3} & \frac{6EI}{L^2} \\ \frac{6EI}{L^2} & \frac{2EI}{L} & 0 & \frac{8EI}{L} & \frac{-6EI}{L^2} & \frac{2EI}{L} \\ 0 & 0 & \frac{-12EI}{L^3} & \frac{-6EI}{L^2} & \frac{12EI}{L^3}1\times 10^{10} & \frac{-6EI}{L^2} \\ 0 & 0 & \frac{6EI}{L^2} & \frac{2EI}{L} & \frac{-6EI}{L^2} & \frac{4EI}{L} \end{bmatrix}$$

$$\times \begin{Bmatrix} \delta_1 \\ \theta_1 \\ \delta_2 \\ \theta_2 \\ \delta_3 \\ \theta_3 \end{Bmatrix} = \begin{Bmatrix} P_1 \\ M_1 \\ P_2 \\ M_2 \\ P_3 \\ M_3 \end{Bmatrix} \tag{2.12.199}$$

Now if we take first equation we have

$$\frac{12EI}{L^3}\times 10^{10}\delta_1 + \frac{6EI}{L^2}\theta_1 - \frac{12EI}{L^3}\delta_2 + \frac{6EI}{L^2}\theta_2 = P_1 \tag{2.12.200}$$

Dividing each term by the factor $\frac{12EI}{L^3}\times 10^{10}$ we have

$$\delta_1 + \frac{L}{2}\times 10^{-10}\theta_1 - 1\times 10^{-10}\delta_2 + \frac{L}{2}\times 10^{-10}\theta_2 = \frac{P_1L^3}{12EI}\times 10^{-10} \tag{2.12.201}$$

Observe here that except δ_1 each term has a common coefficient of 10^{-10} that makes it exceedingly small and for all practical purpose can be considered as zero.

Thus

$$\delta_1 + 0\times\theta_1 - 0\times\delta_2 + 0\times\theta_2 = 0 \quad \rightarrow \quad \delta_1 = 0 \tag{2.12.202}$$

You can now check with other equations and you will see that you can arrive at similar results.

2.12.45 Formulating specified support displacement

This often occurs when structures undergo settlement due to differential settlement of foundation.

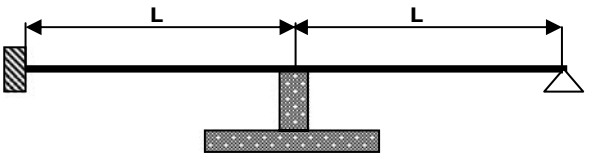


Figure 2.12.64 Beam on compliant foundation.

As shown in Figure 2.12.64, let the vertical displacement at the mid span be δ_F. Under no displacement condition the matrix is expressed as

$$\begin{bmatrix} \frac{12EI}{L^3}\times 10^{10} & \frac{6EI}{L^2} & \frac{-12EI}{L^3} & \frac{6EI}{L^2} & 0 & 0 \\ \frac{6EI}{L^2} & \frac{4EI}{L}\times 10^{10} & \frac{-6EI}{L^2} & \frac{2EI}{L} & 0 & 0 \\ \frac{-12EI}{L^3} & \frac{-6EI}{L^2} & \frac{24EI}{L^3} & 0 & \frac{-12EI}{L^3} & \frac{6EI}{L^2} \\ \frac{6EI}{L^2} & \frac{2EI}{L} & 0 & \frac{8EI}{L} & \frac{-6EI}{L^2} & \frac{2EI}{L} \\ 0 & 0 & \frac{-12EI}{L^3} & \frac{-6EI}{L^2} & \frac{12EI}{L^3}1\times 10^{10} & \frac{-6EI}{L^2} \\ 0 & 0 & \frac{6EI}{L^2} & \frac{2EI}{L} & \frac{-6EI}{L^2} & \frac{4EI}{L} \end{bmatrix} \times \begin{Bmatrix} \delta_1 \\ \theta_1 \\ \delta_2 \\ \theta_2 \\ \delta_3 \\ \theta_3 \end{Bmatrix} = \begin{Bmatrix} P_1 \\ M_1 \\ P_2 \\ M_2 \\ P_3 \\ M_3 \end{Bmatrix} \tag{2.12.203}$$

To simulate the displacement we modify the matrix as hereafter

$$\begin{bmatrix} \frac{12EI}{L^3}\times 10^{10} & \frac{6EI}{L^2} & \frac{-12EI}{L^3} & \frac{6EI}{L^2} & 0 & 0 \\ \frac{6EI}{L^2} & \frac{4EI}{L}\times 10^{10} & \frac{-6EI}{L^2} & \frac{2EI}{L} & 0 & 0 \\ \frac{-12EI}{L^3} & \frac{-6EI}{L^2} & \frac{24EI}{L^3}\times 10^{10} & 0 & \frac{-12EI}{L^3} & \frac{6EI}{L^2} \\ \frac{6EI}{L^2} & \frac{2EI}{L} & 0 & \frac{8EI}{L} & \frac{-6EI}{L^2} & \frac{2EI}{L} \\ 0 & 0 & \frac{-12EI}{L^3} & \frac{-6EI}{L^2} & \frac{12EI}{L^3}1\times 10^{10} & \frac{-6EI}{L^2} \\ 0 & 0 & \frac{6EI}{L^2} & \frac{2EI}{L} & \frac{-6EI}{L^2} & \frac{4EI}{L} \end{bmatrix}$$

$$\times \begin{Bmatrix} \delta_1 \\ \theta_1 \\ \delta_2 \\ \theta_2 \\ \delta_3 \\ \theta_3 \end{Bmatrix} = \begin{Bmatrix} P_1 \\ M_1 \\ \dfrac{24EI}{L^3} \times 10^{10}\delta_F \\ M_2 \\ P_3 \\ M_3 \end{Bmatrix} \tag{2.12.204}$$

Now expanding the third equation we have

$$-\frac{12EI}{L^3}\delta_1 - \frac{6EI}{L^2}\theta_1 + \frac{24EI}{L^3} \times 10^{10}\delta_2 + 0 \cdot \theta_2 + \frac{12EI}{L^3}\delta_3 + \frac{6EI}{L^2}\theta_3 = \frac{24EI}{L^3} \times 10^{10}\delta_F \tag{2.12.205}$$

Now Equation (2.12.205), we have

$$-\frac{\delta_1}{2} \times 10^{-10} - \frac{L}{4}\theta_1 \times 10^{-10} + \delta_2 + \frac{\delta_3}{2} \times 10^{-10} + \frac{L}{4}\theta_3 \times 10^{-10} = \delta_F \Rightarrow \delta_2 \cong \delta_F.$$

2.12.46 Calculation of element stress and displacements

Having imposed the boundary conditions we have now made the stiffness matrix of the system non singular (i.e. solvable) and are now ready to obtain the displacements and stress induced in the system.

Shown in Figure 2.12.65 is a structure assembled out of four triangular elements The structure is restrained at node 1 and 4.

Let $[K]_G$ be the assembled stiffness matrix after imposition of boundary conditions ($u_1 = v_1 = u_4 = v_4 = 0$) so that it is non-singular.

Then considering $[K]_G \{\delta\} = \{P\}$ we can solve to have the displacements as

$$\{\delta\} = [K]_G^{-1} \{P\} \tag{2.12.206}$$

where $\{\delta\}^T = \langle 0 \quad 0 \quad u_2 \quad v_2 \quad u_3 \quad v_3 \quad 0 \quad 0 \quad u_5 \quad v_5 \rangle$

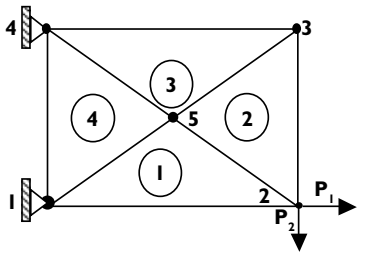


Figure 2.12.65 An assembly of finite element with nodal forces.

While deriving the stiffness matrix we have seen that the strain relationship may be expressed as

$$\{\varepsilon\}_e = [B]\{\delta\}_e \tag{2.12.207}$$

It is now possible to find out the strain in every element since while deriving the stiffness matrix we had derived the $[B]$ matrix for each individual element.

Thus for element 1 and 2 we have $\{\varepsilon\}_1 = [B]_1 \langle 0 \quad 0 \quad u_2 \quad v_2 \quad u_5 \quad v_5 \rangle^T$ and $\{\varepsilon\}_2 = [B]_2 \langle u_2 \quad v_2 \quad u_3 \quad v_3 \quad u_5 \quad v_5 \rangle^T$ etc.

The stress is thus expressed as $\{\sigma\}_e = [\boldsymbol{D}]\,[B]\{\delta\}_e$ (2.12.208)

Thus,

$$\{\sigma\}_1 = [D]\,[B]_1 \langle 0 \quad 0 \quad u_2 \quad v_2 \quad u_5 \quad v_5 \rangle^T \quad \text{and}$$

$$\{\sigma\}_2 = [D]\,[B]_2 \langle u_2 \quad v_2 \quad u_3 \quad v_3 \quad u_5 \quad v_5 \rangle^T \quad \text{and so on} \ldots$$

Example 2.12.6

Shown in Figure 2.12.66 is a wall 4 m × 3 m × 0.25 m subjected to load of 500 kN in *X* and *Y* direction. We determine the stress and deflection based on finite element analysis. The Elastic Modulus of the wall is $E = 2.8 \times 10^8$ kN/m^2 and consider $\nu = 0.25$

Also, shown in Figure 2.12.66 is the finite element assembly with global degrees of freedom as marked at each node (1 thru 10).

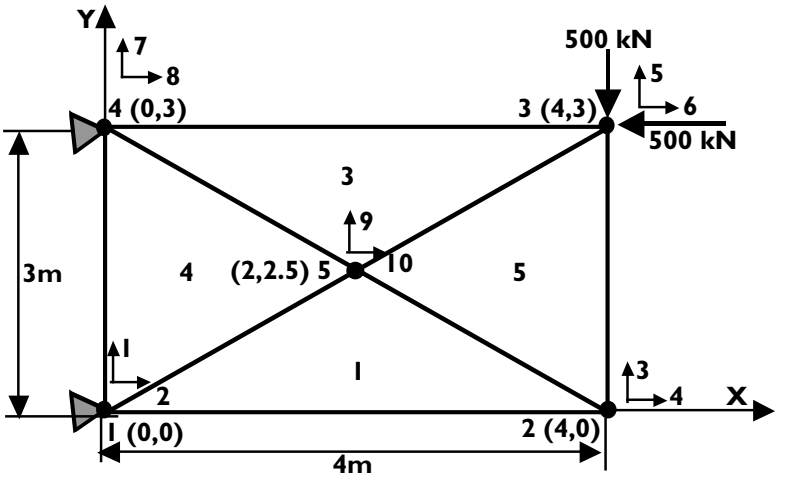


Figure 2.12.66 Finite element model of the wall.

The nodal coordinates of the assemblage is shown hereafter

Node No.	*X*	*Y*
1	0	0
2	4	0
3	4	3
4	0	3
5	2	2.5

Thus each element is defined by the nodal values as

Element No.	*Node-i*	*Node-j*	*Node-k*
1	1	2	5
2	2	3	5
3	3	4	5
4	1	4	5

We had already shown previously how to derive element stiffness matrix for individual triangular elements based on iso-parametric formulation. Based on this the [K] and [B] for each element are as shown hereafter.

For element 1:

[K] =

	1	2	3	4	9	10
1	$2.89 \times 10^{+07}$	$1.17 \times 10^{+07}$	$-1.77 \times 10^{+07}$	$-2.33 \times 10^{+06}$	$-1.12 \times 10^{+07}$	$-9.33 \times 10^{+06}$
2	$1.17 \times 10^{+07}$	$2.37 \times 10^{+07}$	$2.33 \times 10^{+06}$	$6.18 \times 10^{+06}$	$-1.40 \times 10^{+07}$	$-2.99 \times 10^{+07}$
3	$-1.77 \times 10^{+07}$	$2.33 \times 10^{+06}$	$2.89 \times 10^{+07}$	$-1.17 \times 10^{+07}$	$-1.12 \times 10^{+07}$	$9.33 \times 10^{+06}$
4	$-2.33 \times 10^{+06}$	$6.18 \times 10^{+06}$	$-1.17 \times 10^{+07}$	$2.37 \times 10^{+07}$	$1.40 \times 10^{+07}$	$-2.99 \times 10^{+07}$
9	$-1.12 \times 10^{+07}$	$-1.40 \times 10^{+07}$	$-1.12 \times 10^{+07}$	$1.40 \times 10^{+07}$	$2.24 \times 10^{+07}$	$0.00 \times 10^{+00}$
10	$-9.33 \times 10^{+06}$	$-2.99 \times 10^{+07}$	$9.33 \times 10^{+06}$	$-2.99 \times 10^{+07}$	$0.00 \times 10^{+00}$	$5.97 \times 10^{+07}$

In the above table the first row and column depicts the global degrees of freedom for each element.

The [*B*] matrix is given by

−0.25	0	0.25	0	0	0
0	−0.2	0	−0.2	0	0.4
−0.2	−0.25	−0.2	0.25	0.4	0

For element 2

$[K] =$

	3	4	5	6	9	10
3	$1.09 \times 10^{+07}$	$-3.89 \times 10^{+06}$	$-1.56 \times 10^{+06}$	$-1.01 \times 10^{+07}$	$-9.33 \times 10^{+06}$	$1.40 \times 10^{+07}$
4	$-3.89 \times 10^{+06}$	$2.55 \times 10^{+07}$	$-5.44 \times 10^{+06}$	$-2.20 \times 10^{+07}$	$9.33 \times 10^{+06}$	$-3.50 \times 10^{+06}$
5	$-1.56 \times 10^{+06}$	$-5.44 \times 10^{+06}$	$4.82 \times 10^{+07}$	$1.94 \times 10^{+07}$	$-4.67 \times 10^{+07}$	$-1.40 \times 10^{+07}$
6	$-1.01 \times 10^{+07}$	$-2.20 \times 10^{+07}$	$1.94 \times 10^{+07}$	$3.95 \times 10^{+07}$	$-9.33 \times 10^{+06}$	$-1.75 \times 10^{+07}$
9	$-9.33 \times 10^{+06}$	$9.33 \times 10^{+06}$	$-4.67 \times 10^{+07}$	$-9.33 \times 10^{+06}$	$5.60 \times 10^{+07}$	$0.00 \times 10^{+00}$
10	$1.40 \times 10^{+07}$	$-3.50 \times 10^{+06}$	$-1.40 \times 10^{+07}$	$-1.75 \times 10^{+07}$	$0.00 \times 10^{+00}$	$2.10 \times 10^{+07}$

The $[B]$ matrix is given by

0.0833333	0	0.4166667	0	−0.5	0
0	−0.333333333	0	0.333333	0	0
−0.333333	0.083333333	0.3333333	0.416667	0	−0.5

For element 3

$[K] =$

	5	6	7	8	9	10
5	$3.27 \times 10^{+07}$	$1.17 \times 10^{+07}$	$2.33 \times 10^{+07}$	$-2.33 \times 10^{+06}$	$-5.60 \times 10^{+07}$	$-9.33 \times 10^{+06}$
6	$1.17 \times 10^{+07}$	$7.64 \times 10^{+07}$	$2.33 \times 10^{+06}$	$7.29 \times 10^{+07}$	$-1.40 \times 10^{+07}$	$-1.49 \times 10^{+08}$
7	$2.33 \times 10^{+07}$	$2.33 \times 10^{+06}$	$3.27 \times 10^{+07}$	$-1.17 \times 10^{+07}$	$-5.60 \times 10^{+07}$	$9.33 \times 10^{+06}$
8	$-2.33 \times 10^{+06}$	$7.29 \times 10^{+07}$	$-1.17 \times 10^{+07}$	$7.64 \times 10^{+07}$	$1.40 \times 10^{+07}$	$-1.49 \times 10^{+08}$
9	$-5.60 \times 10^{+07}$	$-1.40 \times 10^{+07}$	$-5.60 \times 10^{+07}$	$1.40 \times 10^{+07}$	$1.12 \times 10^{+08}$	$0.00 \times 10^{+00}$
10	$-9.33 \times 10^{+06}$	$-1.49 \times 10^{+08}$	$9.33 \times 10^{+06}$	$-1.49 \times 10^{+08}$	$0.00 \times 10^{+00}$	$2.99 \times 10^{+08}$

$[B] =$

0.25	0	−0.25	0	0	0
0	1	0	1	0	−2
1	0.25	1	−0.25	−2	0

For element 4

$[K] =$

	1	2	7	8	9	10
1	$4.82 \times 10^{+07}$	$-1.94 \times 10^{+07}$	$-1.56 \times 10^{+06}$	$5.44 \times 10^{+06}$	$-4.67 \times 10^{+07}$	$1.40 \times 10^{+07}$
2	$-1.94 \times 10^{+07}$	$3.95 \times 10^{+07}$	$1.01 \times 10^{+07}$	$-2.20 \times 10^{+07}$	$9.33 \times 10^{+06}$	$-1.75 \times 10^{+07}$
7	$-1.56 \times 10^{+06}$	$1.01 \times 10^{+07}$	$1.09 \times 10^{+07}$	$3.89 \times 10^{+06}$	$-9.33 \times 10^{+06}$	$-1.40 \times 10^{+07}$
8	$5.44 \times 10^{+06}$	$-2.20 \times 10^{+07}$	$3.89 \times 10^{+06}$	$2.55 \times 10^{+07}$	$-9.33 \times 10^{+06}$	$-3.50 \times 10^{+06}$
9	$-4.67 \times 10^{+07}$	$9.33 \times 10^{+06}$	$-9.33 \times 10^{+06}$	$-9.33 \times 10^{+06}$	$5.60 \times 10^{+07}$	$0.00 \times 10^{+00}$
10	$1.40 \times 10^{+07}$	$-1.75 \times 10^{+07}$	$-1.40 \times 10^{+07}$	$-3.50 \times 10^{+06}$	$0.00 \times 10^{+00}$	$2.10 \times 10^{+07}$

$[B] =$

−0.416667	0	−0.083333	0	0.5	0
0	0.333333333	0	−0.333333	0	0
0.3333333	−0.416666667	−0.333333	−0.083333	0	0.5

On global assemblage the unconstrained matrix (i.e. without any boundary condition) is given by

$$[K]_G =$$

$$\left[\begin{array}{ccccc|ccccc}
\mathbf{7.72 \times 10^{+07}} & -7.78 \times 10^{+06} & -1.77 \times 10^{+07} & -2.33 \times 10^{+06} & 0.00 \times 10^{+00} \\
-7.78 \times 10^{+06} & \mathbf{6.32 \times 10^{+07}} & 2.33 \times 10^{+06} & 6.18 \times 10^{+06} & 0.00 \times 10^{+00} \\
-1.77 \times 10^{+07} & 2.33 \times 10^{+06} & \mathbf{3.98 \times 10^{+07}} & -1.56 \times 10^{+07} & -1.56 \times 10^{+06} \\
-2.33 \times 10^{+06} & 6.18 \times 10^{+06} & -1.56 \times 10^{+07} & \mathbf{4.92 \times 10^{+07}} & -5.44 \times 10^{+06} \\
0.00 \times 10^{+00} & 0.00 \times 10^{+00} & -1.56 \times 10^{+06} & -5.44 \times 10^{+06} & \mathbf{8.09 \times 10^{+07}} \\
0.00 \times 10^{+00} & 0.00 \times 10^{+00} & -1.01 \times 10^{+07} & -2.20 \times 10^{+07} & 3.11 \times 10^{+07} \\
-1.56 \times 10^{+06} & 1.01 \times 10^{+07} & 0.00 \times 10^{+00} & 0.00 \times 10^{+00} & 2.33 \times 10^{+07} \\
5.44 \times 10^{+06} & -2.20 \times 10^{+07} & 0.00 \times 10^{+00} & 0.00 \times 10^{+00} & -2.33 \times 10^{+06} \\
-5.79 \times 10^{+07} & -4.67 \times 10^{+06} & -2.05 \times 10^{+07} & 2.33 \times 10^{+07} & -1.03 \times 10^{+08} \\
4.67 \times 10^{+06} & -4.74 \times 10^{+07} & 2.33 \times 10^{+07} & -3.34 \times 10^{+07} & -2.33 \times 10^{+07}
\end{array}\right.$$

$$\left.\begin{array}{ccccc}
0.00 \times 10^{+00} & -1.56 \times 10^{+06} & 5.44 \times 10^{+06} & -5.79 \times 10^{+07} & 4.67 \times 10^{+06} \\
0.00 \times 10^{+00} & 1.01 \times 10^{+07} & -2.20 \times 10^{+07} & -4.67 \times 10^{+06} & -4.74 \times 10^{+07} \\
-1.01 \times 10^{+07} & 0.00 \times 10^{+00} & 0.00 \times 10^{+00} & -2.05 \times 10^{+07} & 2.33 \times 10^{+07} \\
-2.20 \times 10^{+07} & 0.00 \times 10^{+00} & 0.00 \times 10^{+00} & 2.33 \times 10^{+07} & -3.34 \times 10^{+07} \\
3.11 \times 10^{+07} & 2.33 \times 10^{+07} & -2.33 \times 10^{+06} & -1.03 \times 10^{+08} & -2.33 \times 10^{+07} \\
\mathbf{1.16 \times 10^{+08}} & 2.33 \times 10^{+06} & 7.29 \times 10^{+07} & -2.33 \times 10^{+07} & -1.67 \times 10^{+08} \\
2.33 \times 10^{+06} & \mathbf{4.36 \times 10^{+07}} & -7.78 \times 10^{+06} & -6.53 \times 10^{+07} & -4.67 \times 10^{+06} \\
7.29 \times 10^{+07} & -7.78 \times 10^{+06} & \mathbf{1.02 \times 10^{+08}} & 4.67 \times 10^{+06} & -1.53 \times 10^{+08} \\
-2.33 \times 10^{+07} & -6.53 \times 10^{+07} & 4.67 \times 10^{+06} & \mathbf{2.46 \times 10^{+08}} & 0.00 \times 10^{+00} \\
-1.67 \times 10^{+08} & -4.67 \times 10^{+06} & -1.53 \times 10^{+08} & 0.00 \times 10^{+00} & \mathbf{4.00 \times 10^{+08}}
\end{array}\right]$$

Since node 1 and 4 are fixed we impose this boundary condition by multiplying the k_{ii} element of the matrix of 1, 2, 7 and 8th degree of freedom by 10^{10} which gives

$$[K]_G =$$

$$\left[\begin{array}{ccccc|ccccc}
\mathbf{7.72 \times 10^{+17}} & -7.78 \times 10^{+06} & -1.77 \times 10^{+07} & -2.33 \times 10^{+06} & 0.00 \times 10^{+00} \\
-7.78 \times 10^{+06} & \mathbf{6.32 \times 10^{+17}} & 2.33 \times 10^{+06} & 6.18 \times 10^{+06} & 0.00 \times 10^{+00} \\
-1.77 \times 10^{+07} & 2.33 \times 10^{+06} & \mathbf{3.98 \times 10^{+07}} & -1.56 \times 10^{+07} & -1.56 \times 10^{+06} \\
-2.33 \times 10^{+06} & 6.18 \times 10^{+06} & -1.56 \times 10^{+07} & \mathbf{4.92 \times 10^{+07}} & -5.44 \times 10^{+06} \\
0.00 \times 10^{+00} & 0.00 \times 10^{+00} & -1.56 \times 10^{+06} & -5.44 \times 10^{+06} & \mathbf{8.09 \times 10^{+07}} \\
0.00 \times 10^{+00} & 0.00 \times 10^{+00} & -1.01 \times 10^{+07} & -2.20 \times 10^{+07} & 3.11 \times 10^{+07} \\
-1.56 \times 10^{+06} & 1.01 \times 10^{+07} & 0.00 \times 10^{+00} & 0.00 \times 10^{+00} & 2.33 \times 10^{+07} \\
5.44 \times 10^{+06} & -2.20 \times 10^{+07} & 0.00 \times 10^{+00} & 0.00 \times 10^{+00} & -2.33 \times 10^{+06} \\
-5.79 \times 10^{+07} & -4.67 \times 10^{+06} & -2.05 \times 10^{+07} & 2.33 \times 10^{+07} & -1.03 \times 10^{+08} \\
4.67 \times 10^{+06} & -4.74 \times 10^{+07} & 2.33 \times 10^{+07} & -3.34 \times 10^{+07} & -2.33 \times 10^{+07}
\end{array}\right.$$

$$\left.\begin{array}{ccccc}
0.00 \times 10^{+00} & -1.56 \times 10^{+06} & 5.44 \times 10^{+06} & -5.79 \times 10^{+07} & 4.67 \times 10^{+06} \\
0.00 \times 10^{+00} & 1.01 \times 10^{+07} & -2.20 \times 10^{+07} & -4.67 \times 10^{+06} & -4.74 \times 10^{+07} \\
-1.01 \times 10^{+07} & 0.00 \times 10^{+00} & 0.00 \times 10^{+00} & -2.05 \times 10^{+07} & 2.33 \times 10^{+07} \\
-2.20 \times 10^{+07} & 0.00 \times 10^{+00} & 0.00 \times 10^{+00} & 2.33 \times 10^{+07} & -3.34 \times 10^{+07} \\
3.11 \times 10^{+07} & 2.33 \times 10^{+07} & -2.33 \times 10^{+06} & -1.03 \times 10^{+08} & -2.33 \times 10^{+07} \\
\mathbf{1.16 \times 10^{+08}} & 2.33 \times 10^{+06} & 7.29 \times 10^{+07} & -2.33 \times 10^{+07} & -1.67 \times 10^{+08} \\
2.33 \times 10^{+06} & \mathbf{4.36 \times 10^{+17}} & -7.78 \times 10^{+06} & -6.53 \times 10^{+07} & -4.67 \times 10^{+06} \\
7.29 \times 10^{+07} & -7.78 \times 10^{+06} & \mathbf{1.02 \times 10^{+18}} & 4.67 \times 10^{+06} & -1.53 \times 10^{+08} \\
-2.33 \times 10^{+07} & -6.53 \times 10^{+07} & 4.67 \times 10^{+06} & \mathbf{2.46 \times 10^{+08}} & 0.00 \times 10^{+00} \\
-1.67 \times 10^{+08} & -4.67 \times 10^{+06} & -1.53 \times 10^{+08} & 0.00 \times 10^{+00} & \mathbf{4.00 \times 10^{+08}}
\end{array}\right]$$

The global force matrix is given by

$$\{P\}^T = \langle 0 \quad 0 \quad 0 \quad 0 \quad -500 \quad -500 \quad 0 \quad 0 \quad 0 \quad 0 \rangle$$

Now performing the operation $\{\delta\} = [K]_G^{-1}\{P\}$, we have

Node numbers	*Displacement (meters)*
U1	-5.11433×10^{-16}
V1	-8.08933×10^{-16}
U2	-1.12903×10^{-05}
V2	-2.57193×10^{-05}
U3	-5.07978×10^{-06}
V3	-3.01804×10^{-05}
U4	-2.41992×10^{-16}
V4	1.0684×10^{-17}
U5	-3.47989×10^{-06}
V5	-1.43565×10^{-05}

Observe here that at node 1 and 4 the displacements u_1, v_1, u_4 and v_4 are of the order 10^{-16} and 10^{-17} which means that the displacements are practically zero.

Thus for element 1 we have the displacements as

U1	-5.11433×10^{-16}
V1	-8.08933×10^{-16}
U2	-1.12903×10^{-05}
V2	-2.57193×10^{-05}
U5	-3.47989×10^{-06}
V5	-1.43565×10^{-05}

Now performing the operation $\{\sigma\} = [D]\,[B]\,\{\delta\}$, we have

Stress type	*Stress values (kN/m^2)*
σ_{yy}	-887.717876
σ_{xx}	-389.5798805
τ_{xy}	-623.1369766

Here the matrix $[D]$ is given by

$$[D] = \begin{bmatrix} 2.99 \times 10^8 & 7.47 \times 10^7 & 0 \\ 7.47 \times 10^7 & 2.99 \times 10^8 & 0 \\ 0 & 0 & 1.12 \times 10^8 \end{bmatrix}$$

Proceeding in identical fashion we find out the stresses in element 2, 3, 4 when we finally get

Stress type	*Element 1*	*Element 2*	*Element 3*	*Element 4*
σ_{yy}	−887.717876	−504.5225795	−619.4772176	−519.6633413
σ_{xx}	−389.5798805	−542.5015936	683.3827532	−129.9158354
τ_{xy}	−623.1369766	−612.6410133	−1205.162941	−803.9665098

All stresses have unit of kN/m^2.

Whatever we have explained till now in this section is what the assemblers do generically in developing a FEM package that usually consists of various types of elements in its library like truss, beam, 2D plane strain and stress, plates, shells, boundary elements (springs) 3D hexahedral elements etc. You may feel that compared to developers they have a relatively easy time, but is surely not the case.

For one of the major constraint within which the assemblers operate is the limitation in computer storage and speed. Thus the major challenge is to overcome the limitation of the system (computer) and come up with an optimal solution that is efficient and also present the output in a manner with enough diagnostic flags making the results easily interpretable by the user, especially when he would not have access to the source code. Trying to interpret an ill conceived output can become a nightmare job for the user who could get easily lost in maze of numbers and get totally confused with the outcome of the analysis. Recent developments in computer graphics with colored contours of stress and displacement plots have however made things relatively easier.

In a practical finite element analysis the size of the problem is normally not very modest. People do not blink in surprise in design office to hear a problem size having say 2,000 nodes. Thus a major focus of the assemblers has been how to form the global stiffness matrix in a most efficient manner and arrive at solution which uses the computer in-core storage most efficiently.

We should remember here that unlike today with Pentium chips incorporated in personal computers when speed and storage problem has reduced considerably, in the early 60 and 70s when engineers and scientists started the coding of FEM this was a serious bottleneck they had to circumvent. Considerable time and effort were given to devise techniques to overcome these limitations.

We describe here briefly some of the techniques used for efficient coding of FEM. You must have noticed by this time that stiffness matrix obtained for an element as well as the assembled global stiffness matrix is symmetrical. Thus storing the upper or the lower triangular matrix for the stiffness only would suffice.

Also observe that in the upper triangular matrix shown in Figure 2.12.67, not all the elements are non zero. These two properties are effectively used in storing the data in computer which greatly optimizes the data storage. The dotted line shown in the above matrix is called *a skyline*, which is a fictitious boundary chosen where all elements above this line are zero.

The computer only stores the upper matrix (including the zeros within the skyline) and all zeros above the skyline are ignored. There is a special implementation technique (Bathe and Wilson 1976) based on which this matrix is stored in a single array $A[K]$ where the address of each element are stored in another array called MAXA[J].

If you are interested to learn more about this technique, you may refer to Bathe (1984) that works out this implementation in quite detail.

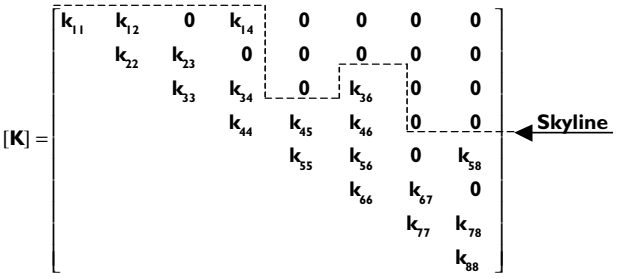


Figure 2.12.67 The upper triangle of a symmetric stiffness matrix.

Though skyline technique is a very effective technique for economic storage of global stiffness matrix it computes the overall stiffness matrix anyway. Thus for very large problems (say >80,000 equations) we have seen this can still sometimes produce problems in solution and data management.

Thus commercial FEM software which uses skyline method of assembly many of them give a limitation to the node for problem like say Maximum node to be used may be 50,000 with 6 degrees of freedom meaning the computer for the problem can handle maximum 300,000 simultaneous equations.

There is an alternate way of developing the matrix and solving for the same. This is known as *frontal wave solution*. Here rather then developing the full matrix for all the elements, the solution is sought sequentially at element level. Once the solution is obtained, its effect is carried over to the next element and the particular degree of freedom for which the solution has already been sought is eliminated. This sequence of steps is carried over for all the elements till all unknowns for all elements are solved.

One of the major advantages with this method is that the global assembly of the stiffness matrix is not required at any stage and goes on to save significant space and time. Originally developed by Melosh but later popularized by Irons and Ahmad (1980), the technique is also adapted by many General purpose Finite Element Software. With use of this technique, one can usually do away with the maximum nodal restriction and number of nodes and elements chosen can well be without any limits. We will have a brief look at the technique in the next section where we show how we solve large number of linear equations.

2.12.47 Solution of equilibrium equation

While solving the equation $[K]\{\delta\} = \{P\}$ you must have noticed that it is necessary to invert the matrix $[K]$ to find out the solution of $\{\delta\}$. Now a days where in many object oriented languages and special purpose software like MATLAB inversion of matrix is a built in function which has significantly eased the problem however, in the early days of coding with FORTRAN IV inversion of a matrix especially if the order was high was something that all programmers dreaded, for it ate away significant memory and time and was something to be avoided by all means if practicable.

So naturally techniques were devised to avoid such inversion yet arrive at a solution of $\{\delta\}$ that was accurate.

We discuss herein a few techniques that are in practice for solution of such linear simultaneous equations.

2.12.48 Gaussian elimination – The technique of back substitution

Let us consider the equation $[K]\{\delta\} = \{P\}$ which we intend to solve. For ease of our understanding let us assume that order of the matrices is 3. Then we have

$$\begin{bmatrix} k_{11} & k_{12} & k_{13} \\ k_{21} & k_{22} & k_{23} \\ k_{31} & k_{32} & k_{33} \end{bmatrix} \begin{Bmatrix} \delta_1 \\ \delta_2 \\ \delta_3 \end{Bmatrix} = \begin{Bmatrix} P_1 \\ P_2 \\ P_3 \end{Bmatrix} \tag{2.12.209}$$

Now by some mathematical operation if we can convert the above into a form

$$\begin{bmatrix} a_{11} & a_{12} & a_{13} \\ 0 & a_{22} & a_{23} \\ 0 & 0 & a_{33} \end{bmatrix} \begin{Bmatrix} \delta_1 \\ \delta_2 \\ \delta_3 \end{Bmatrix} = \begin{Bmatrix} Q_1 \\ Q_2 \\ Q_3 \end{Bmatrix} \tag{2.12.210}$$

The solution becomes easy for then we have

$$\delta_3 = \frac{Q_3}{a_{33}}, \quad \delta_2 = \frac{Q_2}{a_{22}} - \frac{a_{23}}{a_{22}}\frac{Q_3}{a_{33}}, \quad \delta_1 = \frac{Q_1}{a_{11}} - \frac{a_{12}}{a_{11}}\left[\frac{Q_2}{a_{22}} - \frac{a_{23}}{a_{22}}\frac{Q_3}{a_{33}}\right] - \frac{a_{13}}{a_{11}}\frac{Q_3}{a_{33}} \tag{2.12.211}$$

Example 2.12.7

Let us consider the matrix

$$\begin{bmatrix} \mathbf{10} & \mathbf{-5} & \mathbf{2} \\ \mathbf{-5} & \mathbf{12} & \mathbf{3} \\ \mathbf{2} & \mathbf{3} & \mathbf{18} \end{bmatrix} \begin{Bmatrix} \boldsymbol{u_1} \\ \boldsymbol{u_2} \\ \boldsymbol{u_3} \end{Bmatrix} = \begin{Bmatrix} \mathbf{10} \\ \mathbf{15} \\ \mathbf{0} \end{Bmatrix}$$

Multiplying row 2 by 2 and row 3 by 5 we have

$$\begin{bmatrix} 10 & -5 & 2 \\ -10 & 24 & 6 \\ 10 & 15 & 90 \end{bmatrix} \begin{Bmatrix} u_1 \\ u_2 \\ u_3 \end{Bmatrix} = \begin{Bmatrix} 10 \\ 30 \\ 0 \end{Bmatrix}$$

Adding row 1 to row 2 and subtracting row 1 from row 3 we have

$$\begin{bmatrix} 10 & -5 & 2 \\ 0 & 19 & 8 \\ 0 & 20 & 88 \end{bmatrix} \begin{Bmatrix} u_1 \\ u_2 \\ u_3 \end{Bmatrix} = \begin{Bmatrix} 10 \\ 40 \\ -10 \end{Bmatrix}$$

Multiplying row 2 by 20 and row 3 by 19 we have

$$\begin{bmatrix} 10 & -5 & 2 \\ 0 & 380 & 160 \\ 0 & 380 & 1672 \end{bmatrix} \begin{Bmatrix} u_1 \\ u_2 \\ u_3 \end{Bmatrix} = \begin{Bmatrix} 10 \\ 800 \\ -190 \end{Bmatrix}$$

Subtracting row 2 from row 3 we have

$$\begin{bmatrix} 10 & -5 & 2 \\ 0 & 380 & 160 \\ 0 & 0 & 1512 \end{bmatrix} \begin{Bmatrix} u_1 \\ u_2 \\ u_3 \end{Bmatrix} = \begin{Bmatrix} 10 \\ 800 \\ -990 \end{Bmatrix}$$

From above we can directly get $u_3 = \dfrac{-990}{1512} = -0.65476$

Now considering the equation

$$380u_2 + 160u_3 = 800$$

Substituting the value of $u_3 = -0.65476$ above, we have $u_2 = 2.380952$

On subsequent back substitution in equation

$$10u_1 - 5u_2 + 2u_3 = 10 \quad \rightarrow \quad u_1 = 2.321429$$

We will not go into the details of the computer logic or implementation of Gauss elimination technique for there are numbers of books in Numerical Analysis available (Krishnamurthy and Sen 1989), which has provided with the source code both in BASIC and FORTRAN and one can simply adapt them for solution.

Gauss elimination method is usually considered more efficient than solving equations by matrix inversion. Using looping functions (DO loop) and data stored in arrays it is a considered a superior technique than matrix inversion method. Moreover if one exploits the symmetric property of the Finite elements the program logic also gets quite simplified.

2.12.49 The LDL^T decomposition technique

For a Finite Element analysis where the number of equations is large, a special technique is used to solve the equations which is actually an extension of Choklesky's scheme and is as explained hereunder.

Let us consider the equation, $[K]\{\delta\} = \{P\}$. Now let us assume that the stiffness matrix $[K]$ is made up of a product of an upper triangular matrix and lower triangular matrix. Now since for finite element formulation the matrix $[K]$ is positive definite and symmetric we can say that the upper and lower triangular matrix should also have the same property.

Thus we can write

$$[K] = [L]\,[L]^T \tag{2.12.212}$$

where, $[L] =$ is the upper triangular matrix and $[L]^T =$ lower triangular matrix.

The equilibrium equation can now be expressed as

$$[L]\,[L]^T\{\delta\} = \{P\} \tag{2.12.213}$$

Considering $[L]\{\delta\} = \{f\}$ we can write the equation of equilibrium as

$$[L]^T\ \{f\} = \{P\} \tag{2.12.214}$$

Now since $[L]$ is a upper triangular matrix the above becomes a straight forward case of Gauss elimination where the values of $\{f\}$ can obtained from successive back substitution provided we know the coefficients of the matrix $[L]$. The value of matrix can obtained as shown below.

$$\begin{bmatrix} l_{11} & l_{12} & l_{13} & . & . & l_{1n} \\ & l_{22} & l_{23} & . & . & l_{2n} \\ & & l_{33} & . & . & l_{3n} \\ . & & & . & & . \\ . & & & & . & . \\ & & & & & l_{nn} \end{bmatrix} \begin{bmatrix} l_{11} & & & & \\ l_{21} & l_{22} & & & \\ l_{31} & l_{32} & l_{33} & & \\ . & & & & \\ . & & & & \\ l_{n1} & . & . & . & l_{nn} \end{bmatrix}$$
$$= \begin{bmatrix} k_{11} & k_{12} & . & & k_{1n} \\ k_{21} & k_{22} & . & . & k_{2n} \\ . & . & . & & . \\ . & & & & . \\ . & & & & \\ k_{n1} & . & . & . & k_{nn} \end{bmatrix} \tag{2.12.215}$$

Multiplying the LHS of the above equation and equating it to the $[K]$ matrix term by term it can be shown that

$$l_{ii} = \sqrt{k_{ii} - \sum_{p=1}^{p=i-1} l_{ip}^2} \quad \text{and} \quad l_{ij} = \frac{k_{ii} - \sum_{p=1}^{p=j-1} l_{ip} l_{jp}}{l_{jj}} \text{ for } i > j \tag{2.12.216}$$

Thus knowing the coefficients of the matrix $[L]$ we can now say that

$$\begin{bmatrix} l_{11} & & & & \\ l_{21} & l_{22} & & & \\ l_{31} & l_{32} & l_{33} & & \\ . & & & & \\ . & & & & \\ l_{n1} & . & . & . & l_{nn} \end{bmatrix} \begin{Bmatrix} f_1 \\ f_2 \\ f_3 \\ . \\ . \\ f_n \end{Bmatrix} = \begin{Bmatrix} P_1 \\ P_2 \\ P_3 \\ . \\ . \\ P_n \end{Bmatrix} \tag{2.12.217}$$

From above we have

$$f_1 = \frac{P_1}{l_{11}}; \quad f_2 = \frac{P_2 - f_1 l_{21}}{l_{22}}; \quad f_3 = \frac{P_3 - f_1 l_{31} - f_2 l_{32}}{l_{33}}; \ldots\ldots$$
$$f_n = \frac{P_n - f_1 l_{n1} - f_2 l_{n2} - \cdots\cdots f_{n-1} l_{nn-1}}{l_{nn}} \tag{2.12.218}$$

Thus knowing the values of $\{f\}$, we can write

$$\begin{bmatrix} l_{11} & l_{12} & l_{13} & . & . & l_{1n} \\ & l_{22} & l_{23} & . & . & l_{2n} \\ & & l_{33} & . & . & l_{3n} \\ . & & & . & & . \\ . & & & & . & . \\ & & & & & l_{nn} \end{bmatrix} \begin{Bmatrix} \delta_1 \\ \delta_2 \\ \delta_3 \\ . \\ . \\ \delta_n \end{Bmatrix} = \begin{Bmatrix} f_1 \\ f_2 \\ f_3 \\ . \\ . \\ f_n \end{Bmatrix} \tag{2.12.219}$$

This gives,

$$\delta_n = \frac{f_n}{l_{nn}}, \quad \delta_{n-1} = \frac{f_{n-1} l_{nn-1} \delta_n}{l_{n-1n-1}} \quad \text{and so on } \ldots . \tag{2.12.220}$$

The solution in this case is in reverse order.

The Global stiffness matrix coefficients of $[K]$ in a Finite Element Method at times have values whose order vary a lot especially for coupled analysis like soil structure or fluid structure interaction problems. This can at times result in numerical difficulty. To overcome this the $[K]$ matrix is pre- and post-multiplied by a diagonal matrix $[D]^{-\frac{1}{2}}$ where $D_{ii} = \frac{1}{K_{ii}}$ leading to all diagonal terms of the matrix to be unity and reduces the equilibrium equation to

$$[[D]^{\frac{-1}{2}} [K] [D]^{\frac{-1}{2}}] [D]^{\frac{1}{2}} [\delta] = [D]^{\frac{-1}{2}} [P] \tag{2.12.221}$$

This can be expressed as $[K_s] \{\Delta\} = \{P\}$ where

$$[K_s] = [[D]^{\frac{-1}{2}} [K] [D]^{\frac{-1}{2}}] \quad \rightarrow \quad \{\Delta\} = [D]^{\frac{1}{2}} \{\delta\} \quad \text{and } \{P_S\} = [D]^{-\frac{1}{2}} \{P\} \tag{2.12.222}$$

On solution of $\{\Delta\}$ it is pre-multiplied by the term $[D]^{-\frac{1}{2}}$ to obtain the values of the displacement $\{\delta\}$. Though the matrix $[D]^{-\frac{1}{2}}$ is a square matrix practically no extra storage is required as the terms can well be stored in a single array.

2.12.50 Frontal wave solution – Iron's technique reflecting present consumer market

The trend in today's consumer market is simply *"use and throw"*. In line with this trend we get a number of commodities that are simply disposable after use, like saucers, cups, glass, ball pens, cigarette lighters, the list is simply huge. The reason for this trend is simple, "save space".

Say, you have a party in your house that would be catering to 100 people. You would normally not store 100 plates and glasses in your house considering the fact that a party of such magnitude would be a once in a blue moon affair. So, either you hire 100 plates and glasses with a risk that a few of them could get damaged during handling and you would compensate the lender in such case else, you go to the market and buy one gross of disposable plates and glasses for the party. You serve your food to your guests in them and once the party is over you throw them off in the garbage can. No storage requirement, no maintenance, and no hassle. *Frontal wave technique is very much synonymous to this. The reason for its evolution is also – "save space"*.

We had stated earlier while explaining the global assemblage of stiffness matrix that in skyline technique irrespective of however economy we achieve in data storage we ultimately form the global stiffness matrix of the whole system. Thus, in some cases if the problem is very large can create computational difficulties. Increasing the MTOT array[68] may still run the problem but can reduce the speed of the computer considerably.

In such case the frontal methodology as proposed by Irons (1970) is of great advantage and is discussed herein to give you some idea on how it functions. The algorithm is simply marvelous, though the coding is not easy, since it requires significant management of array addresses which, if you are not an experienced programmer or a programmer with bad coding habits can put you in a lot of difficulties.

In skyline technique, the key issue on which the solution pivots is the nodal number or the bandwidth while in case of frontal solution it is the element number or the sequence of element that holds the key to the solution.

The biggest advantage as mentioned briefly earlier is that at no stage it is necessary to form the full stiffness matrix and solution is only sought at element level sequentially. To clarify it further, let us have a look at Figure 2.12.68.

We show above in a plane stress element assemblage where node and element numbers (marked inside the circles) are shown. Every node has 2 degrees of freedom (u, v) thus in solution for the displacements the first equation that needs to be considered would be that related to node 1, 2, 8 and 7 of element-1. To eliminate the nodal degrees of freedom of node 1 we need to only assemble the element stiffness matrix related to node-1. Now the question is *why do we want to eliminate the nodal degree of freedom of node 1?*

68 Total data storage allocation array.

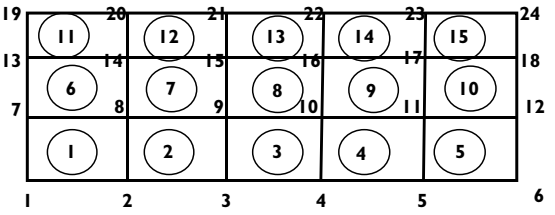


Figure 2.12.68 A finite element mesh with element and node number.

We should remember here that while solving the simultaneous equation to solve the displacement based on Gauss elimination we are eliminating the degrees of freedom sequentially from each equation until we arrive at an upper triangular matrix where from the last row we can directly derive the displacement. In this case after the element matrix is formed we simply perform a static condensation to eliminate the degree of freedom of the related node. Once this is done the original element stiffness matrix has no use and can be discarded and only the condensed matrix is retained. Next, the nodal degrees of freedom for node 2 must be eliminated. For this, element stiffness matrix for element 2 must be assembled and added to previously calculated condensed matrix (from which we have eliminated node 1) and then, we again condense it to eliminate the degrees of freedom of node 2. This is carried out successively over all the elements till we have the last equation from which we get the unknown displacement (in above case it is node 24). Once this is done rest of the displacements can by obtained by sequential back substitution.

It is obvious from above that due to this use and throw away logic adapted here at no stage the full matrix is assembled. The solution is simply carried out at element level which saves significant computer storage and does not impose any limit to the size of the problem.

However, as we have pointed out earlier the programming for the same is quite complex and requires significant skill in computer coding.

As the sequential elimination propagates through the element like a dispersive wave, the technique is termed as Frontal wave solution.

To further enhance your understanding we present herein a conceptual problem to give you at least an idea as to how it operates and what is the basic philosophy.

Example 2.12.8

Shown in Figure 2.12.69 is a three truss assembly having nodal force as shown. The individual stiffness matrix for the elements are shown hereafter. Find the displacements at node 2, 3 and 4 based on frontal solution and direct method.

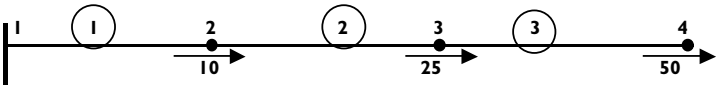


Figure 2.12.69 An assembly of truss elements.

Here $K_1 = \begin{bmatrix} 2 & -2 \\ -2 & 2 \end{bmatrix}$, $K_2 = \begin{bmatrix} 3 & -3 \\ -3 & 3 \end{bmatrix}$, $K_3 = \begin{bmatrix} 5 & -5 \\ -5 & 5 \end{bmatrix}$

While solving by direct method we assemble the global stiffness matrix as shown hereafter

$$K_G = \begin{bmatrix} 2 & -2 & 0 & 0 \\ -2 & 2+3 & -3 & 0 \\ 0 & -3 & 3+5 & -5 \\ 0 & 0 & -5 & 5 \end{bmatrix},$$

since node 1 is fixed we eliminate the first row and column to impose this boundary condition to get the equation of equilibrium as

$$\begin{bmatrix} 5 & -3 & 0 \\ -3 & 8 & -5 \\ 0 & -5 & 5 \end{bmatrix} \begin{Bmatrix} u_2 \\ u_3 \\ u_4 \end{Bmatrix} = \begin{Bmatrix} 10 \\ 25 \\ 50 \end{Bmatrix} \quad \rightarrow \quad [K]\ \{\delta\} = \{P\}$$

Solving the above by any of the previously mentioned method like Gauss elimination, Choklesky or even direct inversion one gets

$$\begin{Bmatrix} u_2 \\ u_3 \\ u_4 \end{Bmatrix} = \begin{Bmatrix} 42.5 \\ 67.5 \\ 77.5 \end{Bmatrix}$$

We now solve it by Frontal technique.

We consider the element stiffness matrix of element 1 and its equilibrium equation.

This gives

$$\begin{bmatrix} 2 & -2 \\ -2 & 2 \end{bmatrix} \begin{Bmatrix} u_1 \\ u_2 \end{Bmatrix} = \begin{Bmatrix} 0 \\ 10 \end{Bmatrix}$$

Since $u_1 = 0$ we eliminate the 1st row and column to have, $2u_2 = 10$.

We throw away the element stiffness matrix of element 1 and only retain the condensed form 2.

We add this to the element stiffness matrix of element 2 to get

$$\begin{bmatrix} 5 & -3 \\ -3 & 3 \end{bmatrix} \begin{Bmatrix} u_2 \\ u_3 \end{Bmatrix} = \begin{Bmatrix} 10 \\ 25 \end{Bmatrix}$$

We eliminate the u_2 degree of freedom by static condensation when the condensed stiffness and load matrix is expressed as

$$[K_c] = [K_{22} - K_{21}K_{11}^{-1}K_{12}] \quad \text{and} \quad \{P_c\} = \{P_3 - K_{21}K_{11}^{-1}P_2\}$$

here $K_{22} = 3, K_{21} = K_{12} = -3;\ K_{11} = 5,\ P_2 = 10$ and $P_3 = 25$

Substituting above we have

$$[K_c] = 3 - \frac{(-3)(-3)}{5} = 1.2 \quad \text{and} \quad \{P_c\} = 25 - \frac{(-3)(10)}{5} = 31$$

We now add this to the third element when we have

$$\begin{bmatrix} 6.2 & -5 \\ -5 & 5 \end{bmatrix} \begin{Bmatrix} u_3 \\ u_4 \end{Bmatrix} = \begin{Bmatrix} 31 \\ 50 \end{Bmatrix}$$

Again applying the expression

$$[K_c] = [K_{22} - K_{21}K_{11}^{-1}K_{12}] \quad \text{and} \quad \{P_c\} = \langle P_4 - K_{21}K_{11}^{-1}P_3 \rangle^T$$

we have, $[K_c] = 5 - \frac{(-5)(-5)}{6.2} = 0.967742$ and $\{P_c\} = 50 - \frac{(-5)(31)}{6.2} = 75$

This being last equation it gives $0.967742u_4 = 75 \Rightarrow u_4 = 77.5$

Now back substituting this in second equation of element 3 we have $-5u_3 + 5u_4 = 50$, this results in $u_3 = 67.5$

Back substituting this in first or second equation of element 2 (we have taken the first) we get

$$5u_2 - 3u_3 = 10 \Rightarrow u_2 = 42.5.$$

Comparing the results with direct method, we find that the values are exactly matching. You should however note here that we have never bothered to assemble the overall stiffness matrix, but have just assembled the stiffness matrix of the elements only and arrived at the exact solution.

2.12.51 The World of Boris Galerkin[69] – A look at finite element beyond stress analysis

Till now we have discussed FEM in terms of displacement and stress. In this section, we will have a generalized look at FEM (though briefly) to see how this can be extended to other areas of technology not related to stress. In this process of digression, we start with stress though as our fundamental vehicle, for as civil engineers this is what we understand best. We recall here the fourth order beam equation we posed while presenting the Weighted Residual Method.

69 Boris G Galerkin (1871–1945) was a Russian Engineer who published his first technical paper on the buckling of Bars while imprisoned in 1906 by the Tzar in pre-Bolshevik Russia. In CSI countries Galerkin's Finite Element Method is also known as the Bubonov-Galerkin Method. He published a paper using this idea in 1915. Thus, we feel Russians knew the mathematics of FEM earlier-though by a different name.

The equation was of the form

$$EI\frac{d^4u}{dx^4} + q = 0 \tag{2.12.223}$$

The solution of u may be obtained by solving this fourth order linear differential equation analytically by putting the appropriate boundary condition.

Now suppose we do not want to solve the differential equation analytically, we had shown earlier that we can use a suitable shape function (that satisfy the boundary condition of the equation) and come to a solution, but since the analysis is not exact, we will have an error residue.

In Galerkin's method this error is set to zero by multiplying the residue by the shape function itself and integrating the same over the full domain of the problem.

Thus considering an assumed shape function w, we have as per Galerkin's method

$$R = \int_{x_1}^{x_2} EI\left[\frac{d^2}{dx^2}\left\{\frac{d^2u}{dx^2}\right\} + q\right] w dx = 0 \tag{2.12.224}$$

where, R = residual error; EI = flexural stiffness of the beam; u = displacement of the beam @ $N_1u_1 + N_2u_2 + N_3u_3 + N_4u_4 = N_iu_i$, where $i = 1, 2, 3, 4$; q = load on the beam and w is the assumed shape function having same basis as u.

$$\text{or} \quad \int_{x_1}^{x_2} EI\left[w\frac{d^2}{dx^2}\left\{\frac{d^2u}{dx^2}\right\}\right] dx + \int_{x_1}^{x_2} wqdx = 0 \tag{2.12.225}$$

Integrating the above by parts, we have

$$EI\left[\left\{w\frac{d^3u}{dx^3}\right\}_{x_1}^{x_2} - \int_{x_1}^{x_2}\left\{\frac{dw}{dx}\frac{d}{dx}\left(\frac{d^2u}{dx^2}\right)\right\} dx\right] + \int_{x_1}^{x_2} wqdx = 0$$

$$\text{or} \quad EI\left[\left\{w\frac{d^3u}{dx^3}\right\}_{x_1}^{x_2} - \left\{\frac{dw}{dx}\frac{d^2u}{dx^2}\right\}_{x_1}^{x_2} + \int_{x_1}^{x_2}\frac{d^2w}{dx^2}\frac{d^2u}{dx^2}\right] + \int_{x_1}^{x_2} wqdx = 0 \tag{2.12.226}$$

$$\text{or} \quad EI\int_{x_1}^{x_2}\frac{d^2w}{dx^2}\frac{d^2u}{dx^2}dx = -wV + \frac{dw}{dx}M - q\int_{x_1}^{x_2} wdx \tag{2.12.227}$$

Here as w has the same basis as u we can write $w_j = \sum_{j=1}^{4} N_jw_j$ and $u_i = \sum_{i=1}^{4} N_iu_i$ thus the above expression can now be expressed as

$$EI\int_{x_1}^{x_2}\frac{d^2N_i}{dx^2}\frac{d^2N_j}{dx^2}dxu_i = -wV + \frac{dw}{dx}M - q\int_{x_1}^{x_2} wdx \tag{2.12.228}$$

The above can be further expressed as

$$[K]\{u\} = \{P\} \tag{2.12.229}$$

where $\left[K_{ij}\right] = EI\int_{x_1}^{x_2}\frac{d^2N_i}{dx^2}\frac{d^2N_j}{dx^2}dx$ is the stiffness matrix of the beam.

For the shape functions we had already derived them earlier while deriving the stiffness matrix of beam based on displacement method. Using,

$$N_1 = 1 - \frac{3x^2}{L^2} + \frac{2x^3}{L^3}, \quad N_2 = x - \frac{2x^2}{L} + \frac{x^3}{L^2}, \quad N_3 = \frac{3x^2}{L^2} - \frac{2x^3}{L^3},$$
$$N_4 = -\frac{x^2}{L} + \frac{x^3}{L^2},$$

the stiffness matrix can be obtained as

$$\left[K_{ij}\right] = EI\int_0^L \begin{bmatrix} \frac{d^2N_1}{dx^2}\frac{d^2N_1}{dx^2} & \frac{d^2N_1}{dx^2}\frac{d^2N_2}{dx^2} & \frac{d^2N_1}{dx^2}\frac{d^2N_3}{dx^2} & \frac{d^2N_1}{dx^2}\frac{d^2N_4}{dx^2} \\ \frac{d^2N_2}{dx^2}\frac{d^2N_1}{dx^2} & \frac{d^2N_2}{dx^2}\frac{d^2N_2}{dx^2} & \frac{d^2N_2}{dx^2}\frac{d^2N_3}{dx^2} & \frac{d^2N_2}{dx^2}\frac{d^2N_4}{dx^2} \\ \frac{d^2N_3}{dx^2}\frac{d^2N_1}{dx^2} & \frac{d^2N_3}{dx^2}\frac{d^2N_2}{dx^2} & \frac{d^2N_3}{dx^2}\frac{d^2N_3}{dx^2} & \frac{d^2N_3}{dx^2}\frac{d^2N_4}{dx^2} \\ \frac{d^2N_4}{dx^2}\frac{d^2N_1}{dx^2} & \frac{d^2N_4}{dx^2}\frac{d^2N_2}{dx^2} & \frac{d^2N_4}{dx^2}\frac{d^2N_3}{dx^2} & \frac{d^2N_4}{dx^2}\frac{d^2N_4}{dx^2} \end{bmatrix} dx \tag{2.12.230}$$

This gives

$$[K] = EI\begin{bmatrix} \frac{12}{L^3} & \frac{6}{L^2} & -\frac{12}{L^3} & \frac{6}{L^2} \\ \frac{6}{L^2} & \frac{4}{L} & -\frac{6}{L^2} & \frac{2}{L} \\ -\frac{12}{L^3} & -\frac{6}{L^2} & \frac{12}{L^3} & -\frac{6}{L^2} \\ \frac{6}{L^2} & \frac{2}{L} & -\frac{6}{L^2} & \frac{4}{L} \end{bmatrix}$$ the element stiffness matrix for the beam. (2.12.231)

2.12.52 Thermal analysis of composite wall in one dimension

Thermal analysis par-se is not the forte of a civil engineer. Mechanical and Chemical Engineers are usually far more adept in handling them. However there are certain situations where a civil /structural engineer is faced with the problem related to thermal analysis. A typical example shown in Figure 2.12.70 is chimney wall with brick lining

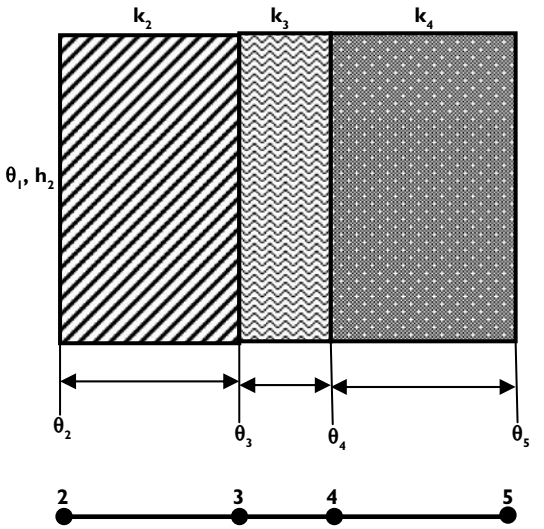


Figure 2.12.70 Composite wall and its Finite Element Model by line element.

where there exists a temperature gradient between inside and outside of chimney and unless one estimates this temperature gradient cannot assess the thermal stress. We try to explain this based on FEM principle.

Just to re-capitulate in case the physics of the problem has got rusted a bit, the thermal conductivity of a material is given by

$$Q = \frac{kA(\theta_i - \theta_f)t}{L} \tag{2.12.232}$$

where Q = Total quantity of heat flowing; k = thermal conductivity of the wall; A = area of the wall exposed to the heat; θ_i and θ_f = Initial and final temperature of the body; t = time in seconds and L = thickness of the body.

Under steady state condition,

$$Q = \frac{kA(\theta_i - \theta_f)}{L} \tag{2.12.233}$$

For the given wall

Let Q_1 be the heat energy inside the wall (where temperature is θ_1), then

$$Q_1 = h_2 A_2 (\theta_1 - \theta_2)$$

Here, in thermodynamic term, h is known as heat transfer coefficient for the wall surface, W/m^2 C.

$$Q_2 = \frac{k_2 A_2}{L_2}(\theta_2 - \theta_3); \quad Q_3 = \frac{k_3 A_3}{L_3}(\theta_3 - \theta_4);$$
$$Q_4 = \frac{k_4 A_4}{L_4}(\theta_4 - \theta_5) \quad \text{and} \quad Q_5 = q_5 A_5,$$

where q = Surface heat flux in W/m^2.

Under steady state condition we have, $Q_1 = Q_2$; $Q_2 = Q_3$; $Q_3 = Q_4$ and $Q_4 = Q_5$ and this gives

$$\begin{aligned}
\frac{k_2 A_2}{L_2}(\theta_2 - \theta_3) &= h_2 A_2 (\theta_1 - \theta_2) \\
\frac{k_2 A_2}{L_2}(\theta_2 - \theta_3) &= \frac{k_3 A_3}{L_3}(\theta_3 - \theta_4) \\
\frac{k_3 A_3}{L_3}(\theta_3 - \theta_4) &= \frac{k_4 A_4}{L_4}(\theta_4 - \theta_5) \\
\frac{k_4 A_4}{L_4}(\theta_4 - \theta_5) &= q_5 A_5
\end{aligned} \tag{2.12.234}$$

Expanding and writing the above equations in matrix form we have

$$\begin{bmatrix}
\frac{k_2 A_2}{L_2} + h_2 A_2 & -\frac{k_2 A_2}{L_2} & 0 & 0 \\
-\frac{k_2 A_2}{L_2} & \left[\frac{k_2 A_2}{L_2} + \frac{k_3 A_3}{L_3}\right] & -\frac{k_3 A_3}{L_3} & 0 \\
0 & -\frac{k_3 A_3}{L_3} & \left[\frac{k_3 A_3}{L_3} + \frac{k_4 A_4}{L_4}\right] & -\frac{k_4 A_4}{L_4} \\
0 & 0 & -\frac{k_4 A_4}{L_4} & \frac{k_4 A_4}{L_4}
\end{bmatrix}
\begin{Bmatrix} \theta_2 \\ \theta_3 \\ \theta_4 \\ \theta_5 \end{Bmatrix}$$

$$= \begin{Bmatrix} h_2 A_2 \theta_1 \\ 0 \\ 0 \\ q_5 A_5 \end{Bmatrix} \quad \rightarrow \quad [K]\{\theta\} = \{Q\} \tag{2.12.235}$$

One should observe a couple of things here.

1 The matrix is positive definite and symmetric, and
2 The nature of matrix is banded

We had not used Galerkin's technique above, but used an identical technique of assembling truss elements (refer example cited in the Frontal Solution example) in this case.

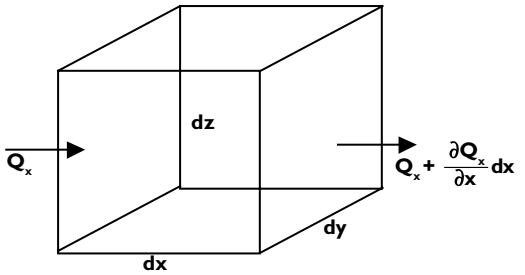


Figure 2.12.71 Propagation of heat through an elemental volume.

2.12.52.1 Thermal analysis of walls in three dimensions

The problem cited previously was of course elementary. Things do complicate a bit when we attempt a three or two dimensional analysis of this wall under temperature. For some very critical structures[70] this is sometimes mandatory.

We present such a case herein where we show how Galerkin's technique is adapted for FEM solution for the problem.

Since as civil engineers we are mainly focused on stress thus as a prelude to the FEM derivation we derive the equilibrium equation of heat flow in three dimension.

Let us consider an elemental volume of dimension dx, dy and dz shown Figure 2.12.71. Let k_x, k_y and k_z are the thermal conductivity of this element in x, y and z direction. If the increment in temperature is $d\theta$ then amount of heat absorbed (Q_x) in x direction

$$Q_x = k_x dy \cdot dz \left(\frac{\partial \theta}{\partial x}\right) \tag{2.12.236}$$

Now, looking at the above element it is evident that net heat absorbed by the body is given by

$$\Delta Q = Q_x + \frac{\partial Q_x}{\partial x} dx - Q_x = \frac{\partial Q_x}{\partial x} dx = \frac{\partial}{\partial x}\left[k_x \left(\frac{\partial \theta}{\partial x}\right)\right] dxdydz$$

This will raise the temperature of the body, given by the calorimetric principle as

$$\Delta Q = m \times s \times d\theta = \rho dxdydz \times s \times d\theta$$

where, ρ = mass density of the material; s = specific heat of the body.

70 For instance, the concrete wall that protects the core of the reactor in Reactor Building of a Nuclear Power Plant.

Thus combining all such heat balance equation in x, y and z direction we have

$$\frac{\partial}{\partial x}\left[k_x\frac{\partial\theta}{\partial x}\right]+\frac{\partial}{\partial y}\left[k_y\frac{\partial\theta}{\partial y}\right]+\frac{\partial}{\partial z}\left[k_z\frac{\partial\theta}{\partial z}\right]+H_v=\rho s\frac{\partial\theta}{\partial t} \tag{2.12.237}$$

in which, H_v = rate of heat generated per unit volume.

For isotropic body when $k_x = k_y = k_z$ i.e. the thermal conductivity is same in all direction we have

$$\frac{\partial^2\theta}{\partial x^2}+\frac{\partial^2\theta}{\partial y^2}+\frac{\partial^2\theta}{\partial z^2}+\frac{H_v}{k}=\frac{\rho s}{k}\frac{\partial\theta}{\partial t} \tag{2.12.238}$$

If the body is without any source or sink, the above equation reduces to

$$\frac{\partial^2\theta}{\partial x^2}+\frac{\partial^2\theta}{\partial y^2}+\frac{\partial^2\theta}{\partial z^2}=\frac{\rho s}{k}\frac{\partial\theta}{\partial t} \tag{2.12.239}$$

For steady state case the equation is expressed as

$$\frac{\partial^2\theta}{\partial x^2}+\frac{\partial^2\theta}{\partial y^2}+\frac{\partial^2\theta}{\partial z^2}+\frac{H_v}{k}=0 \tag{2.12.240}$$

The boundary condition for this problem is given as $\theta(x, y, t) = \theta_0$, for $t > 0$ on surface-A_1:

$$k_x\frac{\partial\theta}{\partial x}l+k_y\frac{\partial\theta}{\partial y}m+k_z\frac{\partial\theta}{\partial z}n+q=0 \quad \text{on surface } A_2 \text{ for } t>0$$
$$\text{and} \quad k_x\frac{\partial\theta}{\partial x}l+k_y\frac{\partial\theta}{\partial y}m+k_z\frac{\partial\theta}{\partial z}n+h\,(\theta-\theta_s)=0 \quad \text{on surface } A_3 \text{ for } t>0 \tag{2.12.241}$$

where, q = surface heat flux W/m^2; h = convection heat transfer coefficient W/m^2 K; θ_s = surrounding temperature in degree centigrade; l, m, n = direction cosine of outward normal to the surfaces A_1, A_2, A_3; A_1 = area on which temperature is specified; A_2 = area on which heat flux is defined; A_3 = area on which convective heat loss $h(\theta - \theta_s)$ is defined.

For finite element formulation let us assume

$$\theta=\sum_{i=1}^{p}N_i\theta i_i \tag{2.12.242}$$

Let the assumed shape function having the same basis as $\sum_{j=1}^{p}N_j$.

Applying Galerkin's technique under steady state condition we then have

$$\iiint_V N_j \left[\frac{\partial}{\partial x}\left(k_x \frac{\partial \theta}{\partial x}\right) + \frac{\partial}{\partial y}\left(k_y \frac{\partial \theta}{\partial y}\right) + \frac{\partial}{\partial z}\left(k_z \frac{\partial \theta}{\partial z}\right) + H_v \right] dxdydz = 0 \tag{2.12.243}$$

Considering the first term of the integral we have

$$\iiint_V N_j \left[\frac{\partial}{\partial x}\left(k_x \frac{\partial \theta}{\partial x}\right)\right] dxdydz = \iint N_j k_x \frac{\partial \theta}{\partial x} dydz - \iiint_V \left[\frac{\partial N_j}{\partial x} k_x \frac{\partial \theta}{\partial x}\right] dxdydz$$

$$= \iint_S N_j k_x \frac{\partial \theta}{\partial x}\, l \cdot ds - \iiint_V \left[k_x \frac{\partial N_j}{\partial x}\frac{\partial N_i}{\partial x}\right] \{\theta_i\}\, dxdydz$$

Adding all the terms we thus have

$$\iint_S N_j \left[k_x \frac{\partial \theta}{\partial x} l + k_y \frac{\partial \theta}{\partial y} m + k_z \frac{\partial \theta}{\partial z} n \right] ds$$

$$- \iiint_V \left[k_x \frac{\partial N_i}{\partial x}\frac{\partial N_j}{\partial x} + k_y \frac{\partial N_i}{\partial y}\frac{\partial N_j}{\partial y} + k_z \frac{\partial N_i}{\partial z}\frac{\partial N_j}{\partial z}\right] \{\theta\}$$

$$\times\, dxdydz + \iiint_V H_v dxdydz = 0 \tag{2.12.244}$$

Now since from the boundary condition is given by

$$k_x \frac{\partial \theta}{\partial x} l + k_y \frac{\partial \theta}{\partial y} m + k_z \frac{\partial \theta}{\partial z} n = q - h\,(\theta - \theta_s), \quad \text{we have}$$

$$\iiint_V \left[k_x \frac{\partial N_i}{\partial x}\frac{\partial N_j}{\partial x} + k_y \frac{\partial N_i}{\partial y}\frac{\partial N_j}{\partial y} + k_z \frac{\partial N_i}{\partial z}\frac{\partial N_j}{\partial z}\right] \{\theta\} dxdydz + \iint_S h N_i N_j \{\theta\} ds$$

$$= \iiint_V H_v dxdydz + \iint_S q N_j ds + \iint_S h\theta_s ds$$

or

$$\iiint_V \left[k_x \frac{\partial N_i}{\partial x}\frac{\partial N_j}{\partial x} + k_y \frac{\partial N_i}{\partial y}\frac{\partial N_j}{\partial y} + k_z \frac{\partial N_i}{\partial z}\frac{\partial N_j}{\partial z}\right] \{\theta\}\, dxdydz$$

$$= \iiint_V H_v dxdydz + \iint_S q N_j ds + \iint_S h\theta_s ds - \iint_S h N_i N_j ds. \tag{2.12.245}$$

The above can thus be expressed as

$$[K]\,\{\theta\} = \{Q\} \tag{2.12.246}$$

The stiffness matrix may be expressed as

$$[K] = \iiint_V [B]^T [D]\, [B]\, dv \tag{2.12.247}$$

where,

$$[B] = \begin{bmatrix} \frac{\partial N_i}{\partial x} & \frac{\partial N_j}{\partial x} & .. & .. & .. & \frac{\partial N_p}{\partial x} \\ \frac{\partial N_i}{\partial y} & \frac{\partial N_j}{\partial y} & .. & .. & .. & \frac{\partial N_p}{\partial x} \\ \frac{\partial N_i}{\partial z} & \frac{\partial N_j}{\partial z} & .. & .. & .. & \frac{\partial N_p}{\partial x} \end{bmatrix} \quad \text{and} \quad [D] = \begin{bmatrix} k_x & 0 & 0 \\ 0 & k_y & 0 \\ 0 & 0 & k_z \end{bmatrix}$$

2.12.52.2 Formulation of triangular element under heat flow

The formulation you will find is relatively easy, compared to stress analysis

Using triangular element shown in Figure 2.12.72 and based on iso-parametric formulation, we have derived earlier

$$[B] = \frac{1}{|J|} \begin{bmatrix} y_2 - y_3 & y_3 - y_1 & y_1 - y_2 \\ x_3 - x_2 & x_1 - x_3 & x_2 - x_1 \end{bmatrix}$$

Now considering, $[K] = \iiint_V [B]^T [D]\, [B]\, dv$, we had derived

$$[K_e] = \Delta t \begin{bmatrix} y_2 - y_3 & x_3 - x_2 \\ y_3 - y_1 & x_1 - x_3 \\ y_1 - y_2 & x_2 - x_1 \end{bmatrix} [D] \begin{bmatrix} y_2 - y_3 & y_3 - y_1 & y_1 - y_2 \\ x_3 - x_2 & x_1 - x_3 & x_2 - x_1 \end{bmatrix}$$

where, Δ = area of the triangle; t = thickness of the element.

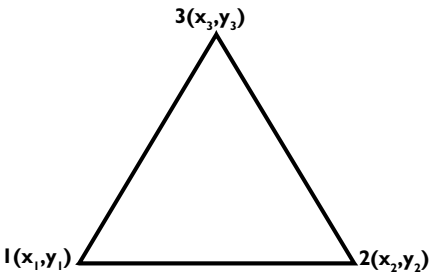


Figure 2.12.72 Triangular Element under heat flow.

For heat flow case, this reduces to

$$[K_e] = \Delta t \begin{bmatrix} y_2 - y_3 & x_3 - x_2 \\ y_3 - y_1 & x_1 - x_3 \\ y_1 - y_2 & x_2 - x_1 \end{bmatrix} \begin{bmatrix} k_x & 0 \\ 0 & k_y \end{bmatrix} \begin{bmatrix} y_2 - y_3 & y_3 - y_1 & y_1 - y_2 \\ x_3 - x_2 & x_1 - x_3 & x_2 - x_1 \end{bmatrix} \tag{2.12.248}$$

It should be noted that the steady state heat equation and seepage of water through soil are same, as such the same stiffness matrix may be used for seepage problems also where k_x and k_y stands for permeability of the two dimensional soil element.

2.12.53 The user domain-rookies, fakes, control freaks and clever Ivans[71]

Unlike the Developers and Assemblers club, where the association is elite (and membership restricted) the user domain is a spectacularly huge global market. In every country where engineering is practiced, we would invariably have users who would be using this technique today, one way or other.

While one should feel happy with its popularity is not without its danger. For it is a powerful tool and in an inexperienced hand can be as dangerous as a child being let out in Trafalgar square in peak hours with a Magnum 44 in his hand [72]!!

Improper interpretation and modeling carried out based on half digested theoretical knowledge the outcome can be as disastrous as an aftermath of a hurricane in Florida.

We seriously hope we would not see such spate of recurring accidents so that a day may come when companies using this tool would stop the usage and go back to traditional analysis based on hand computation. However (God forbid) if this ever be the case we feel, it is the companies and educational institutions who use this tool or offer it as a course work are to be completely blamed for this tragic decision.

For industry, simply buying a general purpose FEM package and letting the software company taking a weeks training session[73] with few young engineers for a few hours – if it is felt is sufficient, then we need not have any ESP to predict that the organization itself is the biggest perpetrator of its own trouble.

The most important thing we believe is to imbibe the right culture. To start with, train or educate first the discipline managers in this topic before any other guy, for this is where we have seen major communication gap exists.

Many of these so called bosses of today (especially in Indian Industry), had graduated in late 70's and early 80's when FEM was just a name in many Indian engineering colleges – just heard as a passing remark, and not surprisingly very few of them have a very clear idea as to what has gone into this.

71 In Russian Folklore you will find invariably in family of clever brothers – the youngest called Ivan who is considered not so smart by the other brothers but in reality – he is the cleverest and would invariably win the princess's heart at the end of the story.

72 It is heaviest handgun manufactured ever – see the movie Dirty Harry starring Clint Eastwood.

73 Where they mostly tell you how to run the software and would never get into any theoretical discussions on the FEM library in the software or tell you what the software CANNOT handle.

Out of sheer necessity (could be promotion or just not being perceived as old fashioned) a few of them have superficially gone through a book and has accumulated a half baked knowledge but poses they know it quite well (the fakers).

We assure you this is the most dangerous breed that can seriously damage a design office culture. They enforce their half witted knowledge on juniors to follow and when problem rears its head are completely out of their wits and conveniently leaves the engineer on whom he has imposed his so called wisdom to handle it or at worst take the blame – the net result, a serious erosion of talented manpower. People usually do not change jobs but change bosses especially one who are fakes, yet are big enforcers and not ready to learn or upgrade themselves.

While there are others who are at least honest enough to say they are not so conversant with it but would avoid it to their best of ability. For digressing into the twilight zone they feel the work would go out of their control (the control freaks). So, nip it in the bud. They would leave no stones unturned to discourage young engineers working under them (having some theoretical background) trying to solve a problem applying FEM – the reason is simple his own ignorance and fear of loosing control on the job standing in the way and stone walling the issue. The result is a big communication gap, after six months the frustrated young engineer seek jobs elsewhere the company looses a good talented engineer – but the biggest loser is the company itself for the design culture or the technology of the company does not improve and remains stagnant. Thus from application side we seriously believe first *educate the design heads* thoroughly before implementing this technology in-house.

For this is surely not an area where as a manager you can manage it without knowing it well[74], and neither pushing your subordinates and reminding him of his deliverable date for umpteen time[75] would do any good. If this is what you believe in and yet want to implement the FEM culture, its time you either take a voluntary retirement, or do something else than engineering design or go and seek a job in another industry trying to be as far as possible from this madding crowd.

Finite element as a coursework also needs to have a serious re-look. We firmly believe that derivation of the integral $\iiint_V [B]^T [D]\, [B]\, dv$ or merely deriving a few fundamental element stiffness matrix (and that too in a short cut way) on the blackboard is surely not the ultimate. Making students believe (on taking such coursework) that he knows what needs to know on FEM based on this sessions – this is not only unethical but we would go to the extent of attributing it as a criminal offence and unlike the Non conforming element formulation, cannot be pardoned for such wrongs. Students are innocent and should be clearly stated that it is only the tip of the iceberg and not the end. Same goes for computer coding. We believe, too much focus (in India) is being given on computer coding. While software development is a part and parcel of FEM education it is a means and not the end. The most important thing is the end results its interpretation and modeling the problem in hand which is an art – and this is where many educators themselves lack experience for they have never digressed beyond stiffness derivations on blackboard

74 Your soft skill will surely not tide you over this ...

75 Without bothering to know what difficulties he is facing – for the boss can't help him anyway.

or trying their hand out with a cantilever beam with maximum 10 elements to solve.

It is not so important whether a student can derive the stiffness matrix of iso-parametric 4-nodded finite element correctly in examination hall or not. He is worth an Ex^+ if he in a project assignment can properly model a problem in a commercially available FEM package. If the results obtained based on his model are not encouraging can write an effective report on why there is error in his results and what were the deficiencies in the model either in terms of boundary condition, mesh refinement or bad selection of an inappropriate element. The results correct to six place of decimal, is not important but the interpretation is. The correctness of solution will automatically come provided he is trained to develop the error diagnostic skills and the intuition of what works and what does not work based on his theoretical background being taught in his coursework.

Sadly, we lack in all these issues and need some serious retrospection. But on the other hand we do have a few clever Ivans, who are either lucky to get a knowledgeable teacher (who can look far beyond the blackboard) or a manger (who knows what is in hand) or at least a flexible boss who encourages him to take the dive and provide support. Years of honing his skill, makes him the real expert who knows the subject's strength and weaknesses clearly. It is these few individuals whose constant efforts push a company to the frontline of technology.

Enough sermonizing, and would like to change the subject for we do not want to face a hostile manager or an equally hostile academic counsel for giving it bluntly (without any sugar coating) as to where we believe we stand on this issue.

But seriously speaking educator and the industry, both has a collective responsibility in successful implementation of this otherwise an extremely powerful technology.

In this section, we show you some practical example of application of FEM pertaining to civil engineering applications.

But before we digress into this would like to share a story with you. Though we say it is a story it is not a conjured one but a real life fact[76].

In a particular industrial project of great economic importance the total quantity of concrete work involved was about 20,000 m^3. After about 30% of the project was implemented, the client felt since the project was important it was essential to check and ensure that quality of concrete work was being maintained. To audit this, they flew in a concrete expert as a consultant to the site for checking the concrete work. The man came in and took a look at the site of what work has been executed. Next day he walked into the Construction manager's office and after preliminary exchange of pleasantries asked the manager how much cubic meter of concrete work has been executed? To this the manager stated it was 6,500 m^3 to be precise. To this the expert asked and how many cubic meter of that has been broken and re-cast? The construction manager smiled proudly and said they have broken none, all concrete caste was adhering strictly to the technical specification. To this answer the expert quipped that if this be the case then he can simply conclude that *quality assurance for concrete work in this site is absolutely nil!*

76 We are indebted to Mr P.K. Som, Technical Specialist of Petrofac International for sharing this story with us.

The story might look irrelevant but is *NOT* and has a big moral, especially pertaining to Finite Element Analysis. For we have seen innumerable analysis outputs where the result is just a one pass affair. If you have an analysis output, that is an outcome of a one shot analysis, be rest assured all you are holding in your hand is a big bunch of garbage and nothing else. For by this time we hope you have realized it needs a few number of trials to arrive at the most optimized mesh and tinker around with a number of elements before coming to the right model.

We will not discuss the intricacies of modeling here, for we have talked on this issue on a number of places in the whole book in different chapters. But having applying this technology for last two decades to a number of problems we believe we do have developed some knowledge in this subject to give you some useful tips here which would stand you in good stead in your work or research.

- Never use an element whose stiffness matrix you cannot derive yourself or do not understand as to how it has been derived. Do not bother what your software dealer's sales engineer says regarding how good and robust this particular element is.
- If on reading the theoretical manual you find an element stiffness derivation or explanation vague you are completely within your rights to ask the dealer to provide you with the theoretical paper from which this element has been implemented – he is morally, as well as commercially bound to provide you with this support.
- When you have FEM software in your hand and that you intend to use, it is more important to know what it CANNOT DO rather then what it can do. So quiz the support company as much as possible on this to have a clear picture.
- Always run a prototype model of the actual problem before you take up the actual job with lesser elements or a typical problem that can be solved analytically or by other methods (like moment distribution say) to check that the results are consistent.
- Run a small problem with similar aspect ratio of the actual structure (especially if it is a continuum) to test what order of meshing gives consistent result. On progressive refinement of mesh when average stress and displacement gives almost same result with two successive runs you can conclude the results have more or less converged. Use the same meshing size proportionally for the actual problem.
- Do not try to over-sophisticate a model by using higher order elements when lower order elements suffice.
- The basic behavior of the system should be clear to you in terms of displacement and where maximum stress could be-as far as practicable from the outset.
- If analytical or any other method exists or possible for a particular problem do *NOT* jump into a FEM solution unless it is an absolute necessity.

2.12.54 Finite element model of table top centrifugal compressor with dynamic soil-structure interaction

We present a practical problem of a table top centrifugal compressor resting on a frame of height is 13.6 meter above ground level. The foundation which is a raft of

size 10 m × 8 × 1.25 meter is resting 2.25 meter below G.L. The plinth beams are of size 1 m × 1 m the deck beams are 1.25 m × 1m and Column sections are 1.25 m × 1.25 m. The total compressor weight is 155 kN having operating RPM of 12,300. The bearing capacity of soil is 195 kN/m^2 having dynamic shear wave modulus as 194 N/mm^2.

The frame is modeled by beam element while the slab is modeled as plate element supported on equivalent soil springs obtained based on Richart's formulation.

The FEM Model is as shown in Figure 2.12.73.

The total model has 742 nodes the frame is broken up into 3D beam elements and the raft as 3D thick plate elements. The model after node numbering is shown Figure 2.12.74.

The analysis consists of three parts

- Eigen solution of the system
- Response of the system under transient condition
- Psuedo Static analysis for shears and Bending Moments

We carried out the analysis in GTSTRUDL. Eigen solutions were carried out for first thirty modes – of which 15 of them are presented. Then checking the % of modal mass participation the mode for which transient load will induce excitation is calculated. Finally a combined static and dynamic load run is carried out to determine the Bending and shear force in the frame and the raft considering the elastic deformation soil modeled here as spring elements.

The eigen solution of the frame with the foundation and soil for first fifteen modes are as shown hereafter.

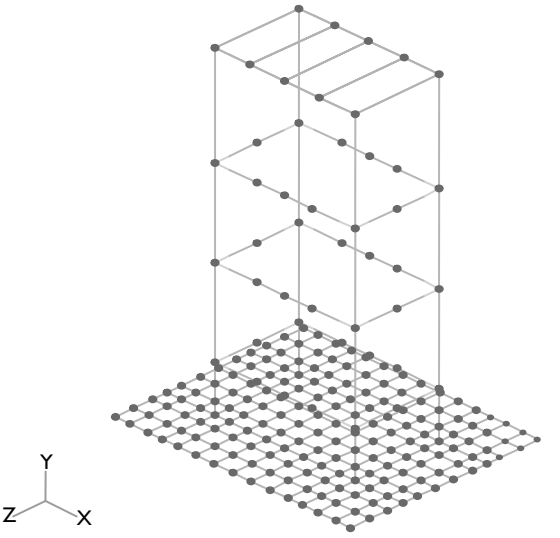


Figure 2.12.73 Computer model for framed type foundation for turbo expander/recompressor.

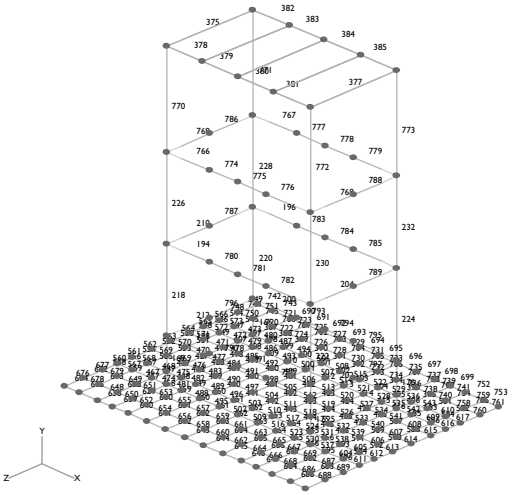


Figure 2.12.74 Member numbers for computer model of framed type foundation for turbo expander/recompressor.

Mode number	*Frequency (rad/sec)*
1	4.12
2	4.25
3	6.912
4	12.44
5	13.02
6	13.20
7	20.18
8	20.40
9	20.78
10	31.49
11	34.07
12	34.61
13	35.91
14	37.32
15	38.04

In Z direction maximum modal participation is 55.1% in 2nd mode having frequency of 4.25 rad/sec. The transient displacement under this condition is given as shown in Figure 2.12.75.

Similarly in the X direction, the transient displacement is given in Figs. 2.12.76 and 77.

The Bending Moment and shear force under the equipment load and combination of static and dynamic load are as given in Figs. 2.12.78 and 79.

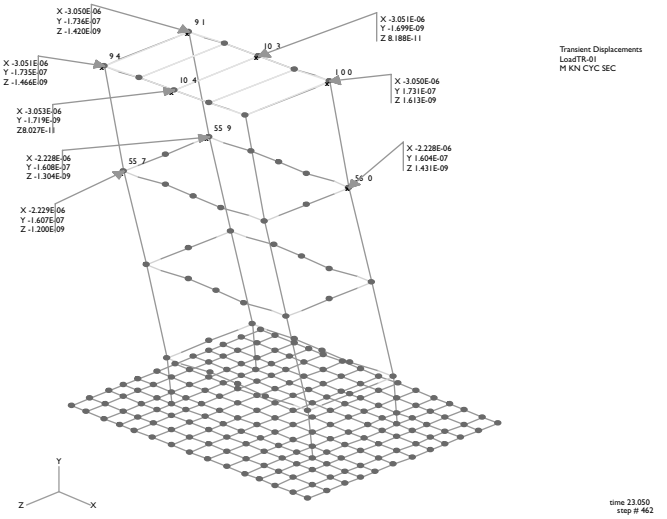


Figure 2.12.75a Maximum displacement of structure due to transient load at frequency 4.25 Hz.

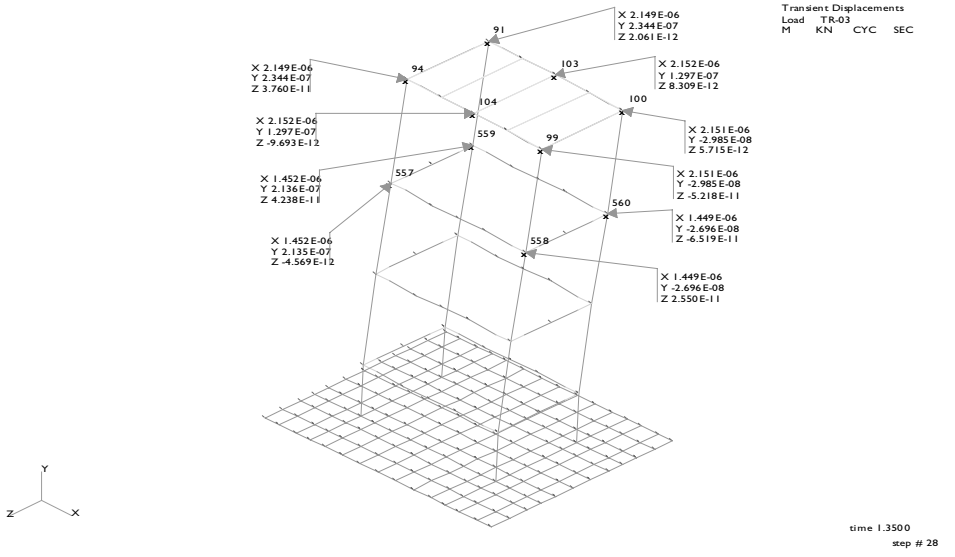


Figure 2.12.76a Maximum displacement of structure due to transient load at frequency 20.18 Hz.

We show below another problem of practical interest, "A Pedestrian tunnel below a city area".

As shown in the Figure 2.12.80 is the tunnel with loads coming on it from the surface. We would Like to know the bending moment, shear and displacement of the tunnel as well as the stress and strain induced in the soil.

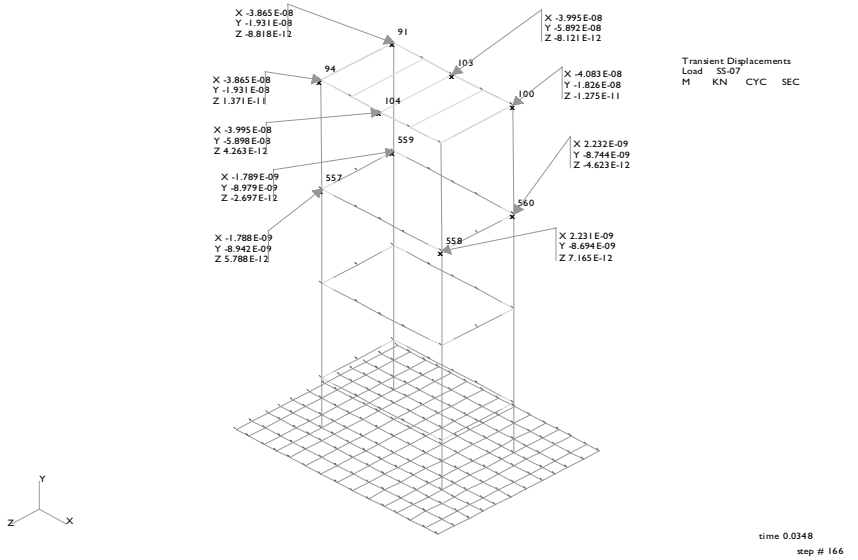


Figure 2.12.77 Maximum displacement of structure due to steady state load at frequency 236.78 Hz (operating speed of machine).

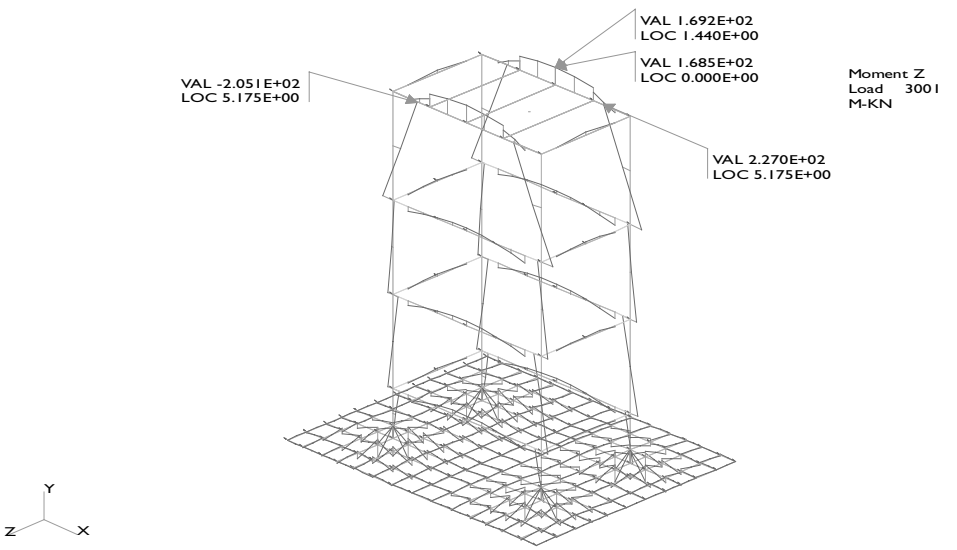


Figure 2.12.78 Bending moment diagram of structure.

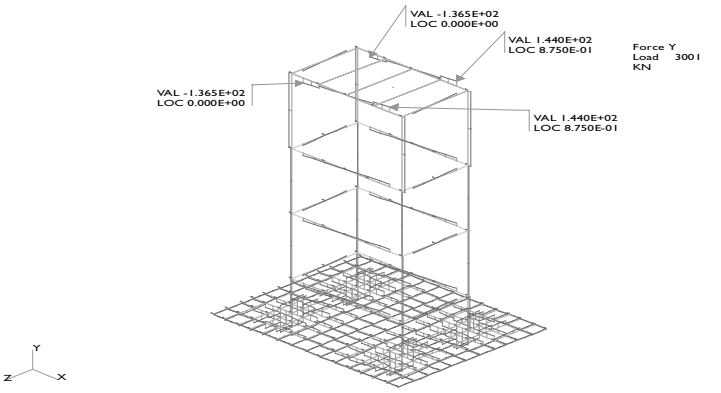


Figure 2.12.79 Shear force diagram of structure.

2.12.55 Static soil-structure interaction analysis of a pedestrian subway below ground

We solve this problem through an example as given below.

Example 2.12.9

The problem is as shown in Figure 2.12.80.

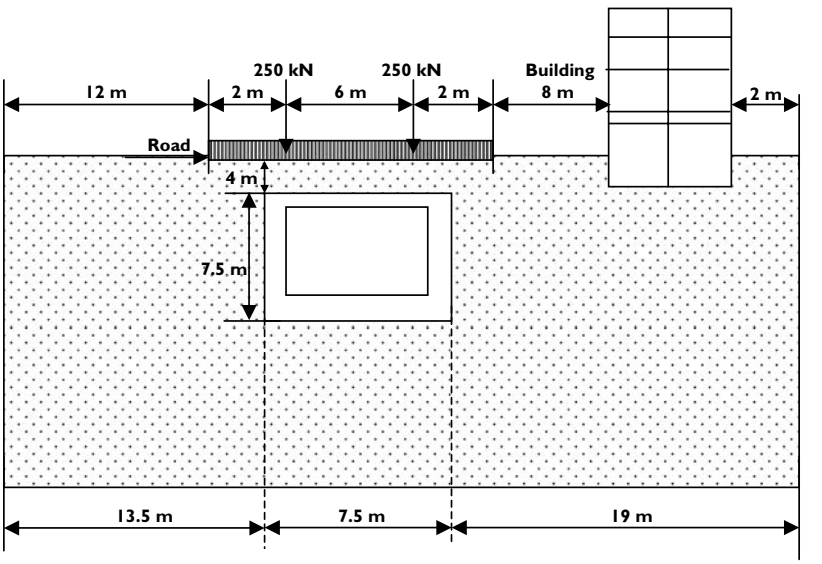


Figure 2.12.80 A box culvert below ground with road and building.

The RCC box culvert wall and base thickness is 750 mm
E_{soil}=11,0000 kN/m^2 ν = 0.35. Consider the soil as plane strain.
Density of soil-200 kN/m^3 – ignore ground water.
For the building consider a surface pressure @ 150 kn/m^2.
The maximum traffic load on surface is two wheel loads @ 250 kN.

Solution:

The finite element model of the problem is as shown in Figure 2.12.81.

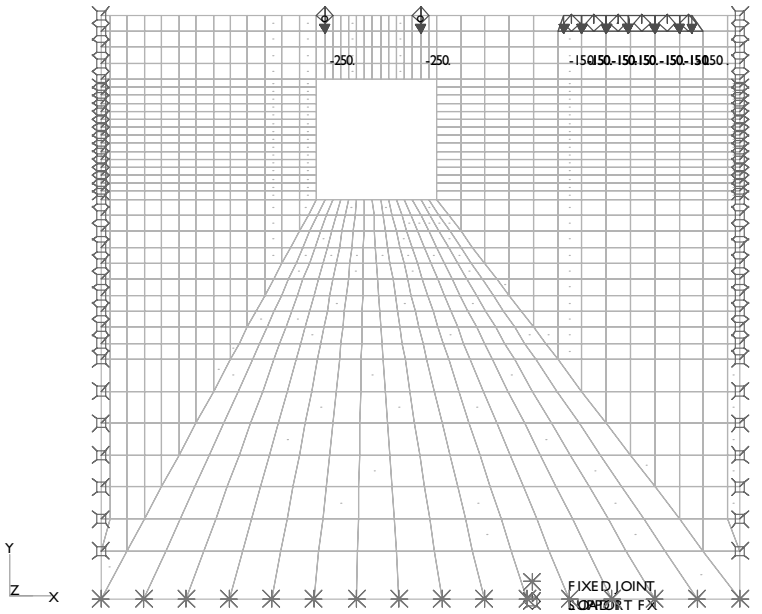


Figure 2.12.81 Geometry, element division and loading.

Here the model consists of three type of elements

1 Beam element of 1 meter width used to define the box culvert.
2 The soil modeled as iso-parametric quadrilaterals with meshes getting progressively cruder when taken away from the culvert to the boundary. The iso-parametric elements are non conforming in nature.
3 CST plane strain element are used at places to change the shape of the element or to match them. Observe here that CSTs are taken at places well away from the area where stress could be critical.

The boundary of the soil are taken as rollers at vertical edges and pinned at base. The loads induced due to wheel load and the building, are shown in the above figure. The self weight of soil is auto generated by the computer.

The problem was run on GTSTRUDL for static analysis and the displacement for the overall system is shown in Figure 2.12.82.

Observe here that the soil settles locally below the building inducing a rotation in the system.

This induces some pressure relief on the wall of the culvert as will be seen subsequently. The displacement scale is made big to make tangible for review.

The vertical and horizontal stress in the soil is as shown Figs. 2.12.83 and 84.

The Bending Moment and Shear force for the box culvert is as shown in Figure 2.12.85 and 86. We plot a colored stress contour which shows the distribution of vertical stress in the soil in Figure 2.12.87 which show the distribution of vertical stress in the soil. A Colored plot of displacement in the soil is shown in Figure 2.12.88.

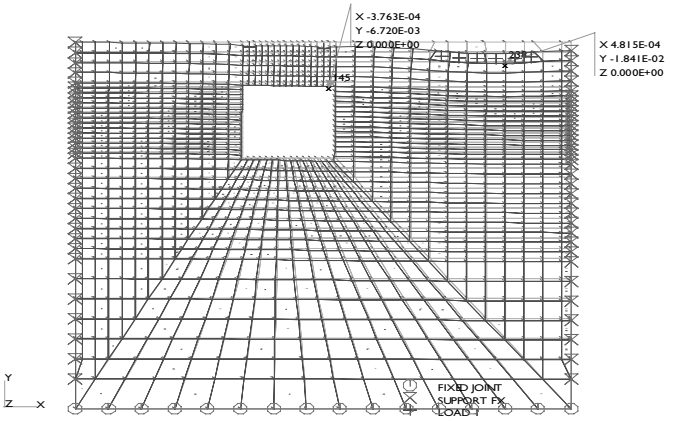


Figure 2.12.82 Displacement of the finite element model-under given load.

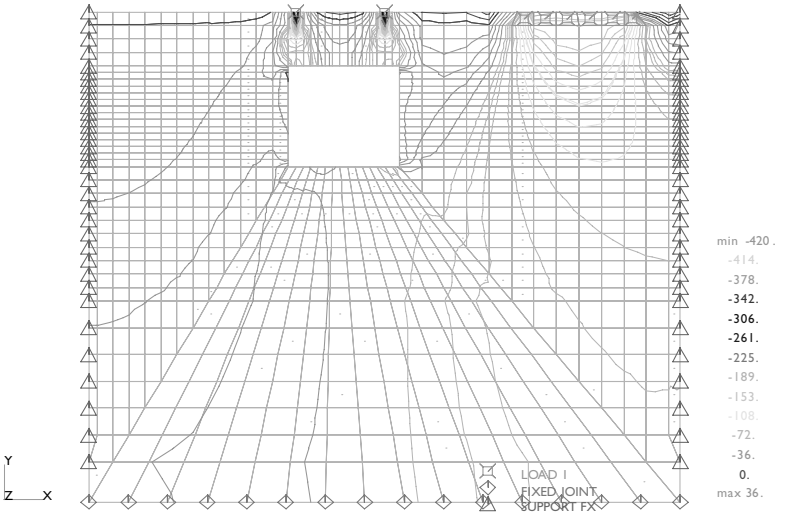


Figure 2.12.83 Contour for vertical stress.

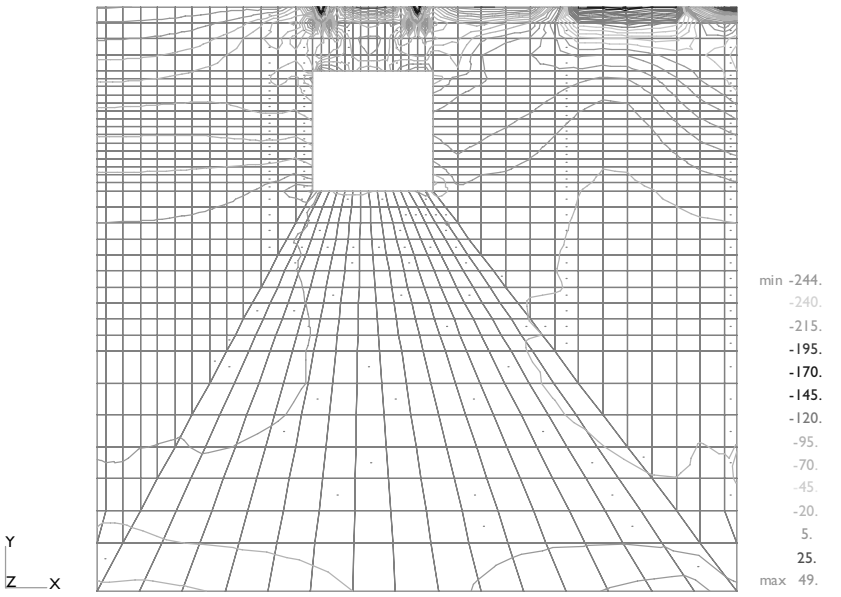


Figure 2.12.84 Contour of horizontal stress.

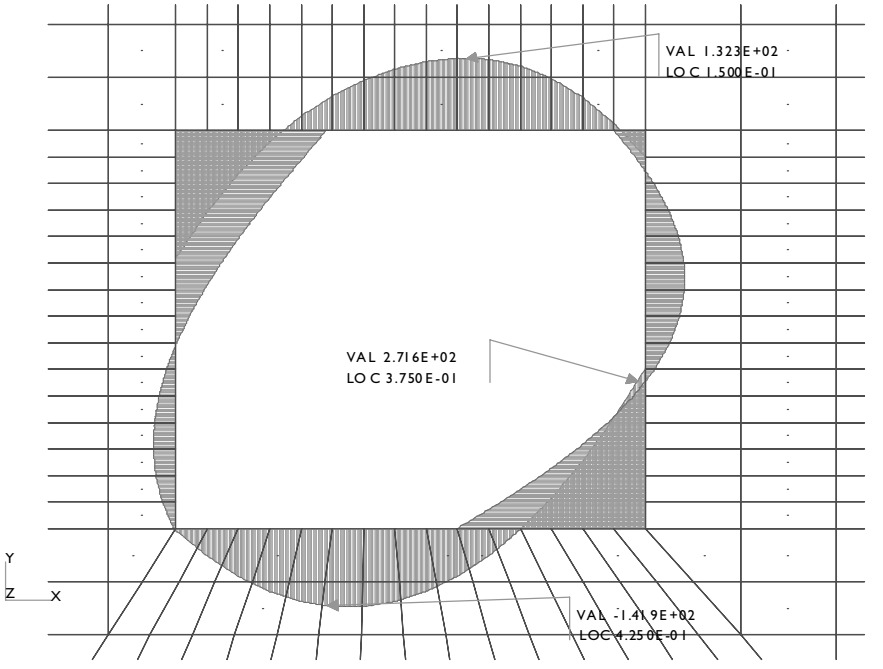


Figure 2.12.85 Bending moment diagram of the box culvert.

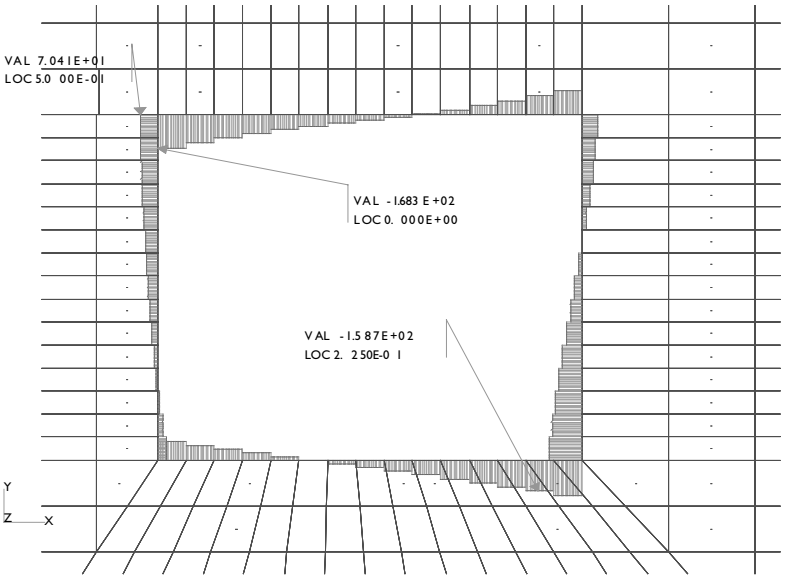


Figure 2.12.86 Shear force diagram of the box culvert.

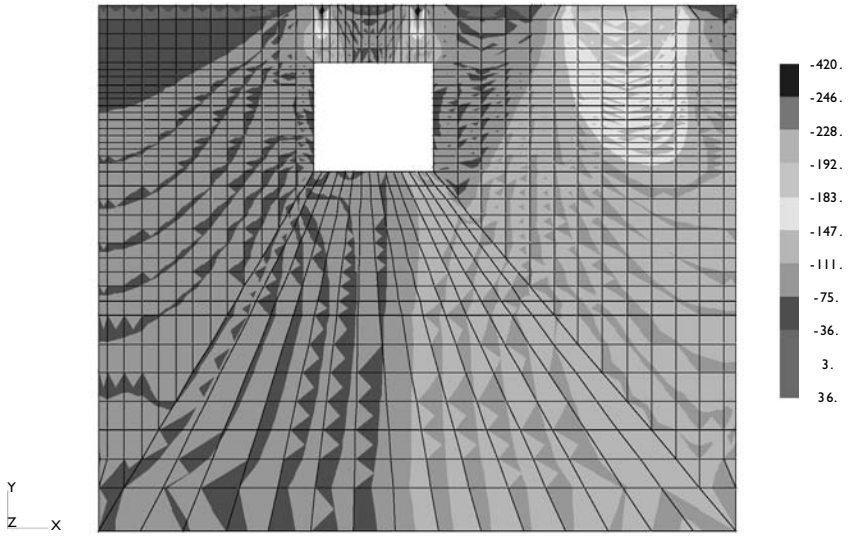


Figure 2.12.87 Vertical stress distribution in soil medium.

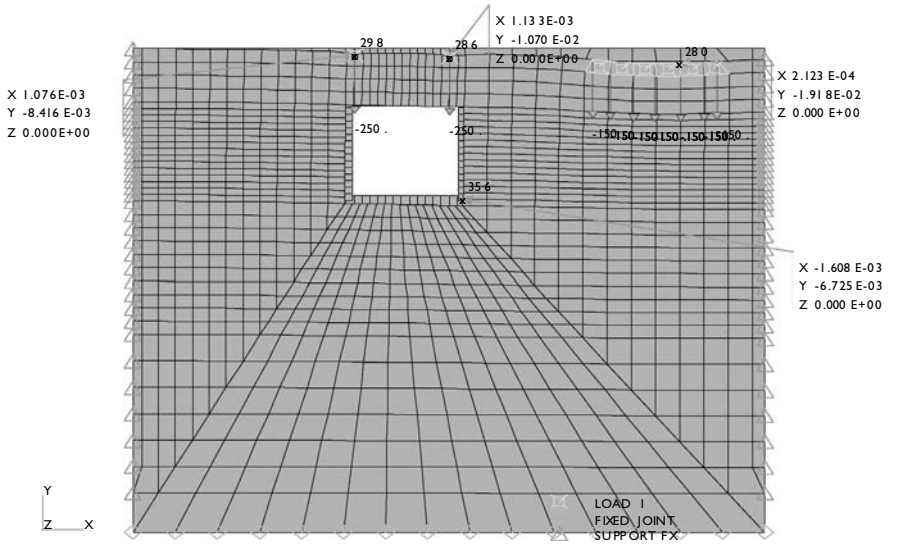


Figure 2.12.88 Colored plot of displacement.

The above analysis gives a comprehensive solution of the system under static load for the soil structure system.

SUGGESTED FURTHER READING

There are a number of excellent books and literatures available, totally dedicated to this topic. We acknowledge that we have not gone through all of them (not possible too) and many of them indeed could be an excellent reference. The reference of papers on topics that we have covered, are already mentioned in the footnotes in the chapter.

For further reading, we mention herein only books those that we have personally read and feel would benefit you. The reference are broken up in two categories 1) The Beginners 2) Advanced Theories

The Beginners

1 Akin, J.E. 1986, *Finite Element Analysis for Undergraduates,* London Academic, London.
2 Bickford, W.M. 1990, *A First Course in Finite Element Method*, Homewood IL R.D. Irwin.
3 Bowles, J.E. 1974, *Analytical and Computer Methods in Foundation Engineering*, McGraw-Hill Book Co., NY.
4 Cook, R.D., Malkus, D.S. & Plesha, M.E. 1989, *Concepts and Applications of Finite Element Analysis*, Third Edition, John Wiley and Sons, NY.

5 Chandruptala, T.R. & Belegundu, A.D. 1997, *Introduction to Finite Elements in Engineering* Prentice-Hall of India Pvt. Ltd., New Delhi.
6 Desai, C.S. 1979, *Elementary Finite Element Method* Prentice-Hall, NJ.
7 Desai, C.S. & Abel, J. 1972, *Introduction to Finite Element Method*, Van Nostrand Reinhold Company, NY.
8 Davies, A.J. 1980, *The Finite Element Method – first approach*, Oxford Clarendon.
9 Ghali, A & Neville, A.M. 1997, *Structural Analysis*, F & FN Spon, 4th Edition.
10 Irons, B.M. & Shrive, N. 1980, *Finite Element Primer*, John Wiley& Sons, NY.
11 Livesley, R.K. 1983, *Finite Element an introduction to Engineers*, Cambridge University Press, London.
12 Logan, D.L. 1986, *A First Course on Finite Element Method*, PWS Publishers, Boston, MA.
13 Martin, H.C. & Carey, G.F. 1973, *An introduction to Finite Element Analysis*, Theory and Application, McGraw-Hill, NY.
14 Mukhopadhyay, M. 1984, *Matrix, Finite Element, Computer and Structural Analysis*, Oxford & IBH Publishing Company, New Delhi.
15 Nath, B. 1974, *Fundamentals of Finite Elements for Engineers*, Athlone, London.
16 Sastry, S.S. 1986, *Numerical Methods for Engineers and Scientists,* Prentice-Hall of India Pvt. Ltd., New Delhi.
17 Salvadori, M.G. & Baron, M.L. 1966, *Numerical Methods in Engineering,* Prentice-Hall of India Pvt. Ltd, New Delhi.
18 Zienkiewics, O.C. & Morgan, K. 1982, *Finite Elements and Approximations,* Wiley Interscience, NY.

Advanced Topics

1 Bathe, K.J. 1984, *Finite Element Procedures in Engineering Analysis*, Prentice-Hall of India, New Delhi.
2 Bathe, K.J. & Wilson, E.L. 1976, *Numerical Methods in Finite Element Analysis,* Prentice-Hall of India, New Delhi.
3 Bowes, W.H. & Russel, L.T. 1975, *Stress Analysis by the Finite element method for Practicing Engineers*, Lexington Books.
4 Carey, G.F. & Oden, J.T. 1983, *Finite Element*, Vol. 1 and 2, Prentice-Hall Inc. NJ.
5 Cook, R.D., Malkus, D.S. & Plesha, M.E. 1989, *Concepts and Applications of Finite Element Analysis*, 3rd edn, John Wiley & Sons, NY.
6 Gallagher, R.H. 1975, *Finite Element Analysis Fundamentals,* Prentice-Hall Inc. NJ.
7 GTSTRUDL *Theoretical and Users Manual* Georgia University, Atlanta.
8 Hughes, T.J.R. 1987, *The Finite Element Method: Linear Static and Dynamic Finite Element Analysis*, Prentice-Hall, Englewood Cliffs, NJ.
9 Irons, B.M. & Ahmad, S. 1980, *Techniques of Finite Elements,* Ellis Horwood Chichester, UK.
10 Krishnamurthy, E.V. & Sen, S.K. 1989, *Numerical Algorithms: Computations in Science and Engineering*, Affiliated East West Press, Pvt. Ltd., New Delhi.
11 Norrie, D.H. & Vries De, G. 1973, *The Finite Element Method Fundamentals and Applications*, Academic Press, NY.
12 Oden, J.T. & Reddy, J.N. 1976, *An Introduction to Mathematical Theory of Finite Element,* John Wiley, NY.
13 Przemieniecki, J.S. 1968, *Theory of Matrix Structural Analysis*, McGraw-Hill Book Co., NY.

14 Rajasekaran, S. 1983, *Finite Element Analysis in Engineering Practice*, A.H. Wheeler Publication, New Delhi.
15 Rao, S.S. 1980, *The Finite Element method in Engineerin*, Pergamon Press, NY.
16 Reddy, J.N. 1993, *An introduction to finite element method*, McGraw-Hill, NY.
17 Segerlind, L.J. 1984, *Applied Finite Element Analysis*. John Wiley & Sons, NY.
18 Shames, I.H. & Dym, C.L. 1995, *Energy and Finite Element Method in Structural Mechanics,* New Age International Publishers Ltd., New Delhi.
19 Strang, G. & Fix, G. 1973, *An Analysis of Finite Element Method*, Prentice-Hall Inc. NJ.
20 SAP 2000 *Theoretical and Users Manual*, University of California, Berkeley.
21 Tong, P. & Rossetos, J.N. 1977, *Finite Element Method Basic Techniques and Implementation,* Cambridge MIT Press.
22 Zienkiewics, O.C & Taylor, R.L. 1991, *The Finite Element Method,* Vol. 1&2 McGraw-Hill Book Co., London.

Chapter 3

Basics of lumped parameter vibration

3.1 INTRODUCTION

The title of this chapter may intrigue you a bit!, however, to our perception the topic is of great importance for this is the first stepping stone towards the study of structural and soil dynamics.

Theory of vibration and mathematical modeling of bodies as discrete lumped mass and spring was studied by mechanical engineers much before dynamic forces became a major design consideration for civil engineers. As such, when civil engineers started to develop their own theories for design a structures subjected to dynamic loads[1] they drew heavily from many of these established theories that mechanical engineers were already using to suite their purpose. Thus theory of vibration also known as *theory of mechanical vibration* is the corner stone on which dynamics of structures and foundations are based upon, at least to start with.

In this chapter we present some of the conceptual and mathematical background that we would use later in Chapters 5 (Vol. 1) and 2 (Vol. 2) to develop the theories of structural and soil dynamics.

John and his son Daniel Bernouli did a pioneering study on the dynamics of a line of connected masses. It was shown that a system of n-masses has exactly n independent modes of vibration in one dimension. Daniel Bernoulli in 1753 enunciated that the general motion of a vibrating system can be written as a superposition of its normal modes. Normally a physical system that we think of is a continuous system (continuum). It is a fact that the discrete system and a continuous system represent mathematical models of identical physical systems. Whereas a discrete system has a finite number of degrees of freedom, a continuous system has an infinite number of degrees of freedom. However there is no such thing as a truly continuous medium. Again, discrete systems are governed by ordinary differential equations whereas continuous systems are by partial differential equations. However they represent similar dynamical behaviour. It may be noticed that concepts that we shall introduce in the following sections have their counterparts in the continuum model.

1 Popularly known as "Structural dynamics", which we are going to study in detail in Chapter 5 (Vol. 1).

3.2 SINGLE-DEGREE-OF FREEDOM

In many cases structural bodies like a beam, shaft etc can be effectively idealized as an equivalent spring and lumped mass. Analogous quantities of mechanical and electrical systems are shown in Table 3.2.1. We study hereafter how this model behaves under a time dependent load and its vibration characteristics.

3.2.1 Free vibration: Undamped case

Consider a spring-mass system shown in Figure 3.2.1.

From the free-body diagram shown in Figure 3.2.1, the force balance can be written as:

Table 3.2.1 Analogous quantities of mechanical and electrical systems.

Mechanical systems	*Electrical systems*
Displacement x	Charge q
Driving force F	Driving voltage V
Mass m	Inductance L
Viscous force constant c	Resistance R
Spring constant k	Reciprocal capacitance $1/C$
Resonant frequency $\sqrt{k/m}$	Resonant frequency $1/\sqrt{LC}$
Resonance width $\gamma = c/m$	Resonance width $\gamma = R/L$
Potential energy $1/2\ kx^2$	Energy of static charge $1/2q^2/C$
Kinetic energy $1/2\ m(dx/dt)^2 = 1/2\ mv^2$	Electromagnetic energy of moving charge $1/2L(dq/dt)^2 = 1/2Li^2$
Power absorbed at resonance $F_0^2/2c$	Power absorbed at resonance $V_0^2/2R$

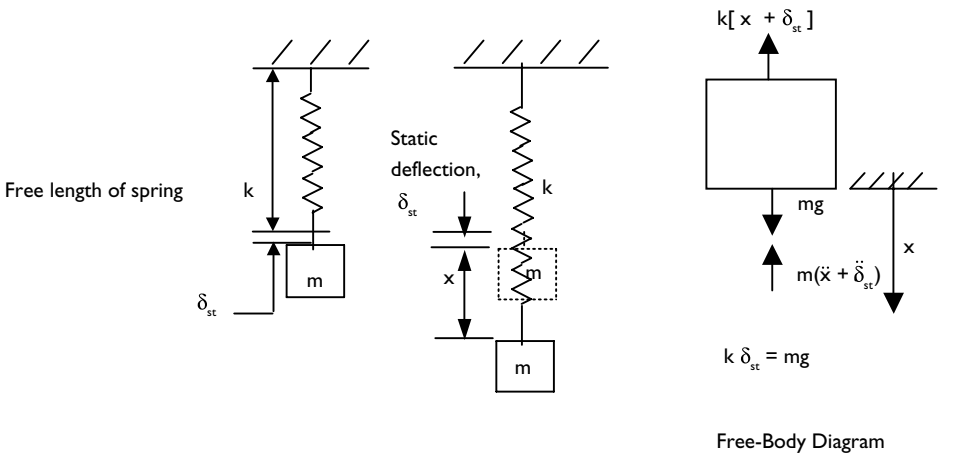


Figure 3.2.1 A single-degree-of-freedom system.

$$m\ddot{x} + kx = 0 \quad \rightarrow \quad \ddot{x} + \omega_n^2 x = 0 \tag{3.2.1}$$

where $\omega_n = \sqrt{\mathrm{k/m}} = \sqrt{\mathrm{gk/W}}$ rad/sec.

Defining, $f_n = \frac{1}{2\pi}\sqrt{\mathrm{gk/W}} = \frac{1}{2\pi}\sqrt{g/\delta_{st}}$ = natural frequency in cps or Hz, where $\delta_{\mathrm{stat}} = W/k$ = static deflection and we can conclude the following:

δ_{st}(mm):	0.0254	0.254	2.54	25.4
f_n (cps or Hz):	99	31.3	9.9	3.13

$\Rightarrow$ *stiffer the system, larger is the natural frequency.*

To solve Equation (3.2.1), the initial conditions to be imposed are at, $t = 0 : x = x_0; \dot{x} = \dot{x}_0$,

The solution is $$x = x_0 \cos \omega_n t + \frac{\dot{x}_0}{\omega_n} \sin \omega_n t \tag{3.2.2}$$

Solution in Equation (3.2.2) is the sum of the two responses shown in Figure 3.2.2.

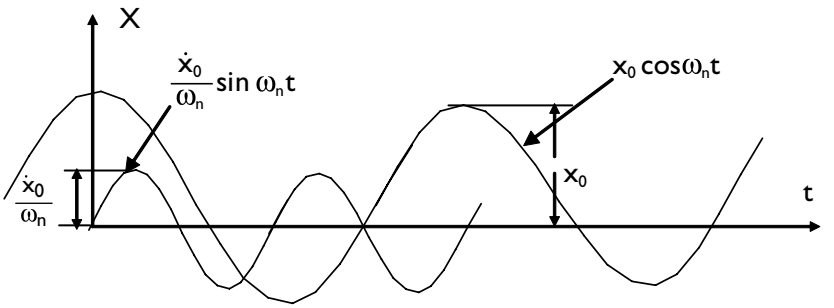


Figure 3.2.2 Response of a single-degree-of-freedom system.

3.2.1.1 Examples of single degree-of-freedom systems

Different cases of single-degree-of-freedom system are given in Figure 3.2.3.

Example 3.2.1

A RCC cantilever beam of span 3.0 m of size 500 × 800 supporting an electric motor of weight 25 kN at its unsupported end. Determine the natural frequency of the beam. Consider $E_{\mathrm{conc}} = 2.85 \times 10^7$ kN/m^2. Unit weight of concrete = 25 kN/m^3.

Solution:

Moment of inertia of the beam = $(1/12) \times 500 \times 800^3 = 2.133 \times 10^{10}$ mm^4 = 0.02133 m^4

Self weight of beam (w) $= 500 \times 800 \times 25 \times 10^{-6} = 10$ kN/m
Displacement due to beam self weight $\delta_1 = wL^4/8EI$
Here $L = 3.0$ m and $EI = 607905$ kN $\cdot$ m^2.

$$\text{Thus } \delta_1 = \frac{10 \times 3^4}{8 \times 607905} = 1.665 \times 10^{-4} \text{ m}$$

Displacement due to the motor (considered as a lumped mass) resting on beam $= \delta_2 = WL^3/3EI$

$$\delta_2 = \frac{25 \times 3^3}{3 \times 607905} = 3.701 \times 10^{-4} \text{ m}$$

Thus total static displacement is given by $\delta_{\text{stat}} = \delta_1 + \delta_2 = 5.366 \times 10^{-4}$ m.
Considering $f_n = \frac{1}{2\pi}\sqrt{g/\delta_{st}}$ we have

$$f_n = \frac{1}{2\pi}\sqrt{\frac{9.81}{5.366 \times 10^{-4}}} = 21.5 \text{ Hz}$$

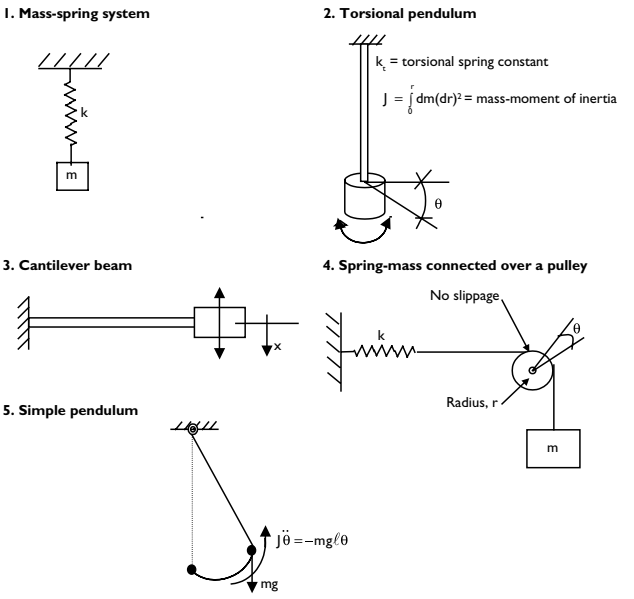


Figure 3.2.3 Different cases of single-degree-of-freedom system.

3.2.1.2 Energy methods

In any conservative system, sum of the kinetic and potential energy is constant. For free vibration of an undamped system, the energy is partly potential and partly kinetic. That is

$$T + U = \text{constant} \Rightarrow \frac{d}{dt}(T + U) = 0 \tag{3.2.3}$$

The kinetic energy $= T = \frac{1}{2}m\dot{x}^2$

The potential energy can be obtained for the mass-spring system (Figure 3.2.4) as: The change in potential energy of the system, for a displacement $x(t)$, is equal to the strain energy in the spring minus the potential energy change of the mass due to the difference in elevation. Hence, the potential energy is

$$U = \int_0^x (\text{total spring force})dx - \int_0^x mg\,dx = \int_0^x (mg + kx)dx - mgx = \frac{1}{2}kx^2$$

Thus $\frac{d}{dt}\left[\frac{1}{2}m\dot{x}^2 + \frac{1}{2}kx^2\right] = 0 \Rightarrow \dot{x}[m\ddot{x} + kx] = 0$, since $\dot{x} \neq 0 : m\ddot{x} + kx = 0$: same as Equation (3.2.1).

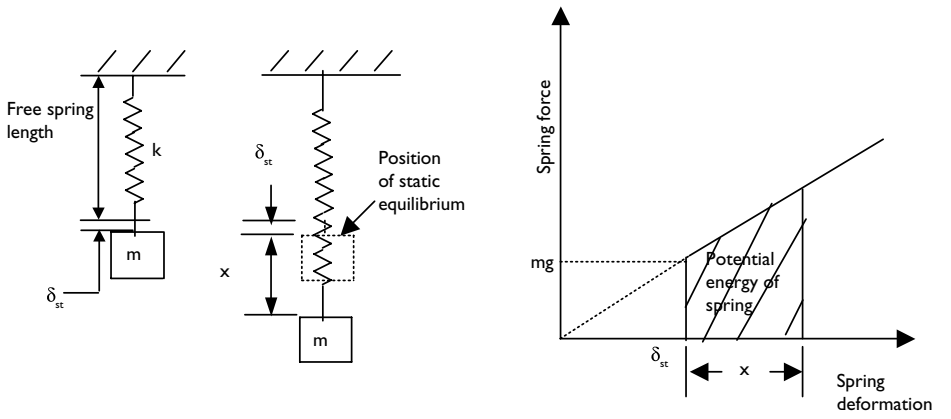


Figure 3.2.4 A single-degree-of-freedom (mass-spring) system.

This is a very useful technique for obtaining the natural frequency of a physical system. We would see a number of applications of this method latter while deriving response of various types of structures and foundations.

Example 3.2.2

Consider the vibration of a simple pendulum shown in Figure 3.2.5. Obtain the natural frequency of vibration of the system.

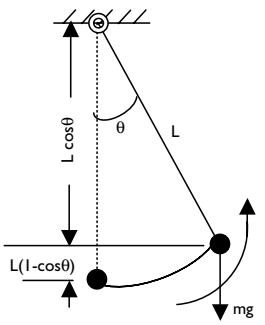


Figure 3.2.5 Vibration of a simple pendulum.

Solution:

Consider a pendulum shown in Figure 3.2.5.

$$\text{Total energy} = T + U = \frac{1}{2}mL^2(\dot{\theta})^2 + (1 - \cos\theta)Lmg$$

$$\text{Hence,} \quad \frac{d}{dt}(T+U) = \frac{1}{2}mL^2 \cdot 2\left(\frac{d\theta}{dt}\right) \cdot \frac{d^2\theta}{dt^2} + Lmg\sin\theta\frac{d\theta}{dt} = 0;$$

$$\because \frac{d\theta}{dt} \neq 0 \Rightarrow mL^2\frac{d^2\theta}{dt^2} + mgL\sin\theta = 0$$

$$\text{That is, } \ddot{\theta} + \frac{g}{L}\theta = 0 \quad \because \theta \text{ is small} \Rightarrow \theta = \sin\theta$$

$$\therefore \quad \omega_n = \sqrt{\frac{g}{L}} : f_n = \frac{1}{2\pi}\sqrt{\frac{g}{L}}.$$

Example 3.2.3

Shown in Figure 3.2.6, is a cylinder of mass *m* and radius *r* rolling without slipping on a curved surface of radium *R*. Obtain the equation of motion of the system and obtain the natural frequency of vibration of the system.

Translational velocity of the cylinder-centre $= (R_1 - R)\dot{\theta}$. Rotational velocity of the cylinder-center $= (\dot{\theta}_b - \dot{\theta})$. As the cylinder rolls without slippage, the *arc* $(a - b) = arc(a_1 - b)$, i.e. $R_1\theta = R\theta_b$.

Thus, the angular velocity can be written as $\left(\frac{R_1}{R} - 1\right)\dot{\theta}$ and total kinetic energy is

$$T = \frac{1}{2}m[(R_1 - R)\dot{\theta}]^2 + \frac{1}{2}m\frac{R^2}{2}\left[\left(\frac{R_1}{R} - 1\right)\dot{\theta}\right]^2$$

in which $m\frac{R^2}{2}$ is the mass moment of inertia of the cylinder about its longitudinal axis. Potential energy can be written as: $U = mg(R_1 - R)(1 - \cos\theta)$

$$\text{Using} \quad \frac{d(T+U)}{dt} = \left[\frac{3}{2}m(R_1 - R)^2\ddot{\theta} + mg(R_1 - R)\sin\theta\right]\dot{\theta} = 0$$

That is

$$\ddot{\theta} + \frac{2g}{3(R_1 - R)}\theta = 0 \text{ and this results in } \omega_n = \sqrt{\frac{2g}{3(R_1 - R)}}.$$

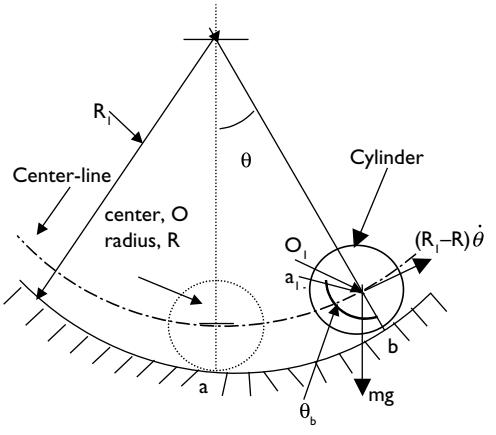


Figure 3.2.6 Oscillation of a cylinder on a curved surface.

Example 3.2.4

Using the energy method find out the natural period of oscillation of the fluid in a *U*-tube manometer shown in Figure 3.2.7.

Solution:

Although the motion is two-dimensional, it can be completely described in terms of the vertical displacement x of the fluid surface from equilibrium. If a = cross sectional area; ℓ = length of fluid column; g = acceleration due to gravity, the total mass of the fluid is $\rho\ a\ell$. Every part of the fluid can be assumed to move with the same speed, $\dot{x}$. The potential energy corresponds to taking a column of fluid of length x from the left-hand tube by raising it through the distance x and placing it on the top of the right-hand column.

$$\text{Thus,} \quad U = (\rho g a x)x \quad \text{and } T = \frac{1}{2}\rho\ a\ell\ \dot{x}^2$$

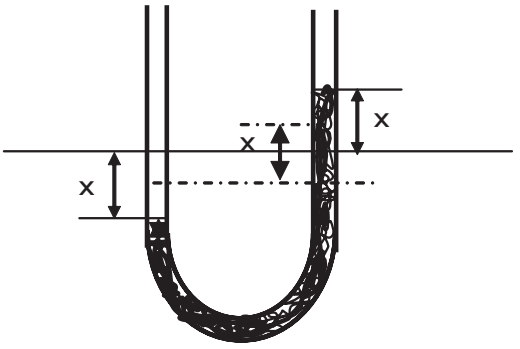


Figure 3.2.7 Oscillation in a U-tube.

$$\text{Now Total energy} = T + U, \quad \text{and } \frac{d(T+U)}{dt} = \frac{d}{dt}\left[\frac{1}{2}\rho\ a\ell\dot{x}^2 + a\rho\ gx^2\right] = 0$$

$$\rightarrow \quad \ddot{x} + \frac{2g}{\ell}x = 0 : \omega_n = \sqrt{\frac{2g}{\ell}}.$$

3.2.1.3 Effect of weight of the spring

Let ρ = mass density of the spring [mass per unit length]. Now, if the free-end of the spring as shown in Figure 3.2.8, has a displacement $Z(t)$ and it is assumed that an intermediate point of the spring at a distance x from the fixed end has a displacement equal to $(x/L) \cdot Z(t)$, then $Z(t)$ defines the configuration, and the system has but

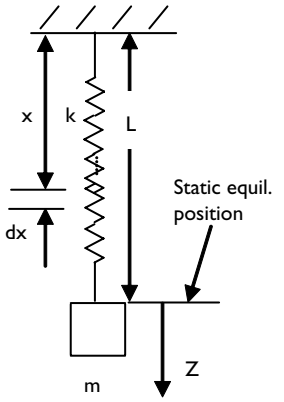


Figure 3.2.8 A single-degree-of-freedom system with spring having mass.

one-degree-of-freedom. This is possible because the mass per unit length of the spring is constant.

$$\text{For an element } dx : dT = \frac{1}{2}(\rho\ dx)\left[\frac{x}{L}\dot{Z(t)}\right]^2; \quad T_{\text{spring}} = \int_0^L \frac{1}{2}\rho\ dx\ \frac{x^2}{L^2}\dot{Z}^2 = \frac{1}{2}\rho\ \frac{L}{3}\dot{Z}^2$$

This may be the reason for having an 'added mass' to the footing-mass while computing its natural frequency and dynamic response. However, it must be noted that if we remove the mass m altogether, the natural frequency ω_n is not equal to $\sqrt{3k/\rho L}$. The derivation above assumes the static extension of a uniform spring, an extension proportional to the distance from the fixed end. But this holds only if the stretching force is the same at all points along the spring. This condition will not be applicable if there is a distributed mass along the spring. There must be a variation of the stretching force with distance along the spring. The derivation, however, will be valid if $\rho L << m$, in which case the force along the spring is roughly constant (whereas, for $m = 0$, the restoring force must fall to zero at the free-end, there being at this point an acceleration but no attached mass).

3.2.1.4 Equivalent spring constants

Consider the case of a cantilever beam shown in Figure 3.2.9, subjected to an end-load and the deflection of the beam-end be assumed to be only in the vertical direction.

$$x_{\text{static}} = \frac{WL^3}{3EI} = \frac{mgL^3}{3EI} \quad :: \quad k_{\text{eq}} = \frac{W}{x_{\text{static}}} = \frac{3EI}{L^3}$$

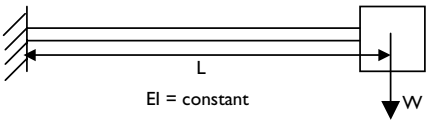


Figure 3.2.9 Cantilever beam with end loads.

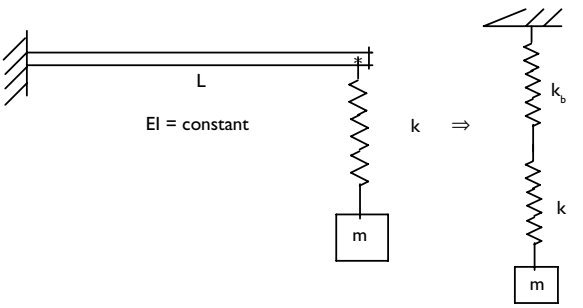


Figure 3.2.9a A single-degree-of-freedom system with equivalent springs.

Now, let a spring is suspended at the end of a cantilever, shown in Figure 3.2.9a:

$$x_{\text{static}} = \frac{mg}{k_b} + \frac{mg}{k_1} \quad \text{and} \quad k_{\text{eq}} = \frac{mg}{x_{\text{static}}} = \frac{mg}{\frac{mg}{k_b} + \frac{mg}{k_1}} \Rightarrow k_{eq} = \frac{1}{\frac{1}{k_b} + \frac{1}{k_1}} \tag{3.2.4}$$

Consider a solid pendulum shown in Fig. 3.2.10.

Mass moment of inertia, $J = \int_0^{2\pi} \int_0^R (r d\theta\, dr) r^2 = \frac{\pi R^4}{2}$; Angle of twist $= \frac{TL}{GJ}$;

$$T = \frac{\pi\, d^4}{32} \frac{G}{L} \theta = k_t\, \theta$$

where θ's are same in both the shafts.

$$\text{Hence,} \quad T = T_1 + T_2 = (k_{t_1} + k_{t_2})\theta : \omega_n = \sqrt{\frac{k_{eq}}{J}} = \sqrt{\frac{k_{t_1} + k_{t_2}}{J}}$$

$$= \sqrt{\frac{\pi}{32J}\left[\frac{d_1^4 G_1}{L_1} + \frac{d_2^4 G_2}{L_2}\right]} \tag{3.2.5}$$

Consider two springs connected as shown in Figure 3.2.11:
Equilibrium demands: $\Rightarrow P_1 + P_2 = W$
In this case x_{static} is same for the whole block: $W = k_1 + k_2 = x_{\text{static}}(k_1 + k_2)$

$$\text{Hence} \quad k_{eq} = k_1 + k_2. \tag{3.2.6}$$

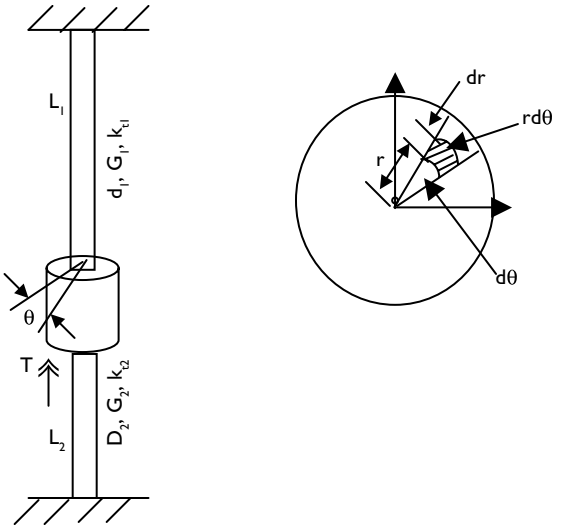


Figure 3.2.10 A single-degree-of-freedom system with equivalent spring.

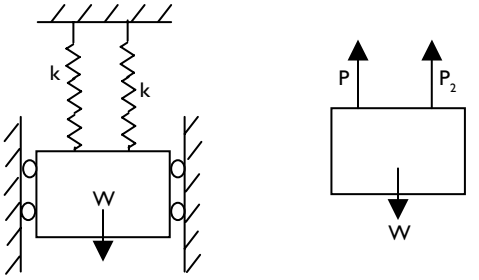


Figure 3.2.11 A single-degree-of-freedom system with equivalent springs.

3.2.1.5 Springs connected in series

If we have n-springs in series, equivalent spring constant may be computed from

$$k_{eq} = \frac{1}{\frac{1}{k_1} + \frac{1}{k_2} + \cdots + \frac{1}{k_n}}. \tag{3.2.7}$$

3.2.1.6 Springs connected parallely

If we have n-springs connected in parallel, equivalent spring constants may be obtained from

$$k_{eq} = k_1 + k_2 + \cdots + k_n. \tag{3.2.8}$$

Example 3.2.5

Find the natural frequency of a single-degree-of-freedom system shown in Figure 3.2.12. The sketch reflects the same system with different orientation. Assume that θ is small.

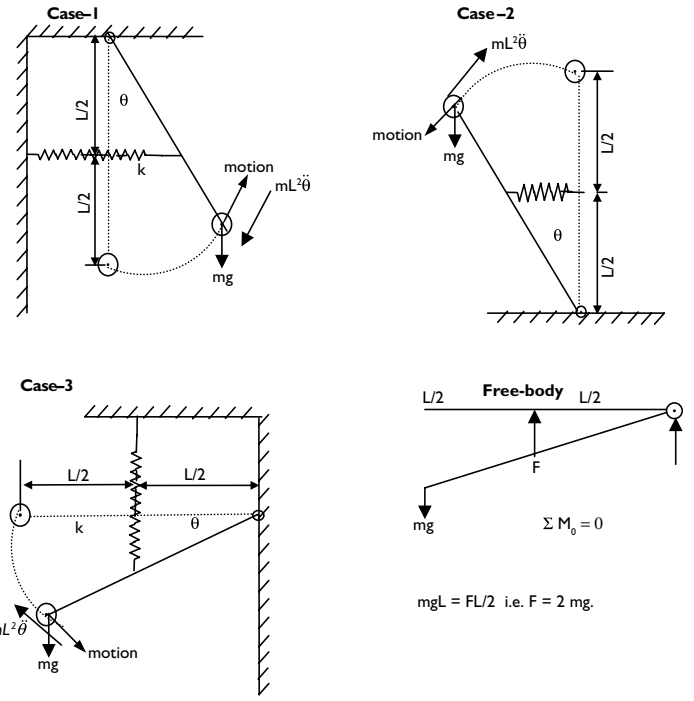


Figure 3.2.12 Spring-connected pendulum with different orientations.

Solution:

We have $mL^2\ddot{\theta} = \sum$ torques

Case-1: $\sum M_o = 0$: Assuming $\left(+\circlearrowright\right)$ +ve

$$mL^2\ddot{\theta} + mgL\sin\theta + k\frac{L\theta}{2}\frac{L}{2}\cos\theta = 0 \quad \Rightarrow \quad \ddot{\theta} + \left(\frac{g}{L} + \frac{k}{4m}\right)\theta = 0$$

Hence, natural frequency, $\omega_n = \sqrt{\dfrac{g}{L} + \dfrac{k}{4m}}$.

Case-2: $\sum M_o = 0$: Assuming $\left(+\circlearrowright\right)$ +ve

$$mL^2\ddot{\theta} - mgL\sin\theta + k\frac{L\theta}{2}\frac{L\cos\theta}{2} = 0 \quad \Rightarrow \quad \ddot{\theta} + \left(\frac{k}{4m} - \frac{g}{L}\right)\theta = 0$$

Hence, natural frequency, $\omega_n = \sqrt{\frac{k}{4m} - \frac{g}{L}}$.

Case-3: $\sum M_o = 0$: Assuming $\circlearrowleft$ +ve

$$mL^2\ddot{\theta} + k\frac{L\theta}{2}\frac{L\cos\theta}{2} + 2mg\frac{L\cos\theta}{2} - mgL\cos\theta = 0 \quad \Rightarrow \quad \ddot{\theta} + \frac{k}{4m}\theta = 0$$

Hence, natural frequency, $\omega_n = \sqrt{\frac{k}{4m}}$.

3.2.1.7 Damped free vibration (SDOF)

The displacement $x(t)$ of the mass m, shown in Figure 3.2.13, is measured from the static equilibrium position and is considered positive in the downward direction, and so are the velocity $\dot{x}(t)$ and the acceleration $\ddot{x}(t)$.

Considering the motion in x-direction and using d'Alembert's principle one can write

$$-m\ddot{x} + \sum \text{ forces in the } (+\text{V}e)\ x\text{-direction} = 0$$

Thus,

$$-m\frac{d^2}{dt^2}(x + \delta_{st}) - k(x + \delta_{st}) - c\frac{d}{dt}(x + \delta_{st}) + mg = 0 \tag{3.2.9}$$

As, $mg = k\delta_{st}$ i.e. $\delta_{st} = W/k$, Equation (3.2.13) reduces to

$$m\ddot{x} + c\dot{x} + kx = 0 \tag{3.2.10}$$

in which $c\dot{x}$ is the damping force and unit of c is (FTL^{-1}) in SI unit it is (N-s/m).

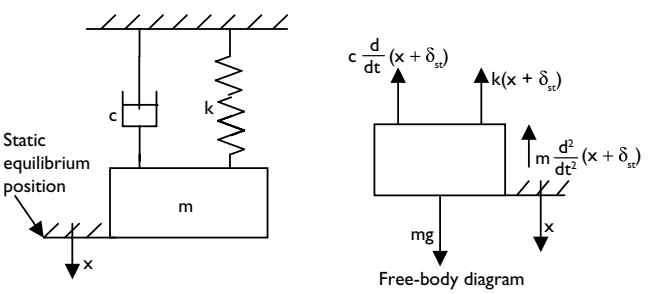


Figure 3.2.13 Damped free vibration (mass-spring-dashpot system).

The damping force considered here is linearly proportional to velocity. When a mass-spring system is set in motion with a little pull of the mass, the mass keeps on oscillating indefinitely. This is under an ideal situation. But in reality the movement of the mass attenuates with time due to air or other environmental resistance to the motion. Taking queue from the motion of a solid body in a viscous fluid and keeping in mind the Stoke's viscous drag concept, the resisting motion, treated as a damping force, is assumed to be linearly proportional to velocity of motion. This is treated as viscous damping. For solving Equation (3.2.10), assume $x = e^{\beta t}$, Auxiliary or characteristic equation of (3.2.14) can be written as

$$m\beta^2 + c\beta + k = 0 \quad \Rightarrow \quad \beta = \frac{-c \pm \sqrt{c^2 - 4mk}}{2m} \tag{3.2.11}$$

Case (a): When $c^2 > 4mk$; β is always $-$Ve.

Solution of Equation (3.2.11) is then, $x = C_1 e^{\beta_1 t} + C_2 e^{\beta_2 t}$, where β_1 and β_2 are the roots of Equation (3.2.11) and both are negative.

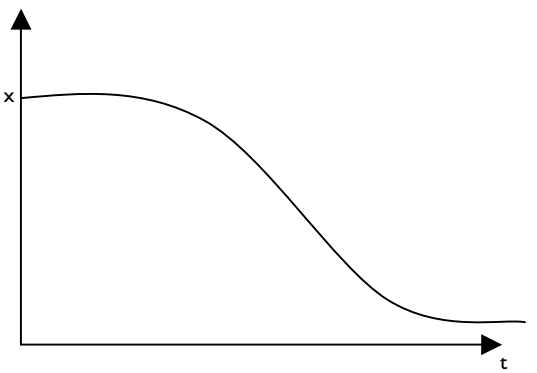


Figure 3.2.14 Over-damped case.

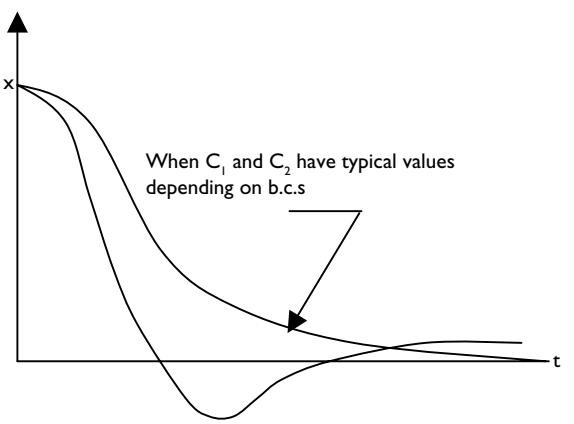


Figure 3.2.15 Case of critical damping.

The response, shown in Figure 3.2.14, is an exponentially decaying function and produces a non-harmonic solution. This is the case of over-damping.

Case (b): $c^2 = 4mk$, roots are $\beta_1, \beta_2 = -c/2m$: have equal roots.

Solution is, $x = (C_1 + C_2 t)e^{\beta t}$. $\rightarrow$ Again a non-periodic solution.

Undamped natural frequency

This is the case of critical damping. $c = C_c : C_c = 2\sqrt{km} = 2\sqrt{\omega_n^2 m^2} = 2m\,\omega_n$

Case (c): $c^2 < 4km$: A very practical situation, results in harmonic solution.

Roots are $\beta_{1,2} = \dfrac{1}{2m}\left[-c \pm i\sqrt{4km - c^2}\right]$.

Solution is $\quad x = C_1 e^{\beta_1 t} + C_2 e^{\beta_2 t}$. This is shown in Figure 3.2.16. (3.2.12)

To simplify above, consider

$$\frac{c}{2m} = \frac{c \cdot 2\omega_n}{2 \cdot C_c} = \frac{c}{C_c}\omega_n = D\omega_n : \; D = \frac{c}{C_c} = \text{Damping ratio.}$$

and, $\sqrt{\frac{4k}{4m} - \frac{c^2}{4m^2}} = \sqrt{\omega_n^2 - \frac{c^2 . 4\omega_n^2}{4 . C_c^2}} = \sqrt{\omega_n^2 - D^2\omega_n^2} = \omega_n\sqrt{1 - D^2} = \omega_{nd} =$ Damped natural frequency

Thus, the solution is

$$\begin{aligned} x &= C_1 e^{(-D\omega_n + i\omega_{nd})t} + C_2 e^{(-D\omega_n - i\omega_{nd})t} \\ \Rightarrow x &= e^{-D\omega_n t}\left[A\cos\,\omega_{nd}t + B\sin\,\omega_{nd}t\right] \end{aligned} \tag{3.2.13}$$

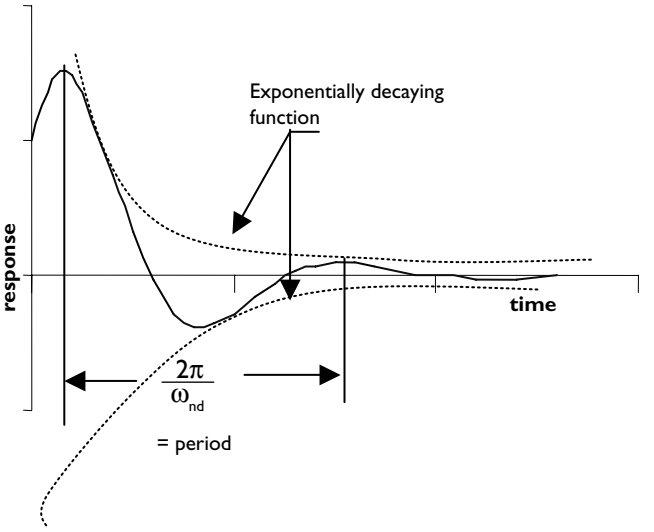


Figure 3.2.16 Damped free vibration.

When $D = 0.4, \omega_{nd} \approx 90\%$ of $\omega_n; D = 0.8, \omega_{nd} \approx 60\%$ of ω_n. It is for this reason that in many practical problems where D varies between 5–10%, we usually consider the natural frequency rather than damped natural frequency for it hardly makes any significant difference.

Consider $x = e^{-D\omega_n t}\,[A \cos\, \omega_{nd} t + B \sin\, \omega_{nd} t]$;

In Figure 3.2.17, $t_2 = t_1 + \dfrac{2\pi}{\omega_{nd}}$

$$x_1 = e^{-D\omega_n t_1}\,[A \cos \omega_{nd} t_1 + B \sin \omega_{nd} t_1]\,;$$

$$x_2 = e^{-D\omega_n t_2}\left[A \cos \omega_{nd}\left(t_1 + \frac{2\pi}{\omega_{nd}}\right) + B \sin \omega_{nd}\left(t_1 + \frac{2\pi}{\omega_{nd}}\right)\right]$$

Hence, $\dfrac{x_1}{x_2} = e^{D\omega_n(t_2 - t_1)} = e^{D\omega_n \frac{2\pi}{\omega_n\sqrt{1-D^2}}} = e^{\frac{2\pi D}{\sqrt{1-D^2}}}$

Also, $\log_e\left(\dfrac{x_1}{x_2}\right) = \dfrac{2\pi\, D}{\sqrt{1 - D^2}} = \delta =$ Logarithmic decrement. (3.2.14)

Hence $\delta = \frac{1}{n}\ell n \frac{x_1}{x_{n+1}}$ in which n is the number of peak value recorded.

To obtain D, find out x_1 and x_{n+1}, say, from an oscilloscope record of any two peak-amplitudes x_1 and x_{n+1}.

Equation (3.2.13) is solved using the initial condition: at $t = 0 \rightarrow x = x_0$ and $\dot{x} = \dot{x}_0$.

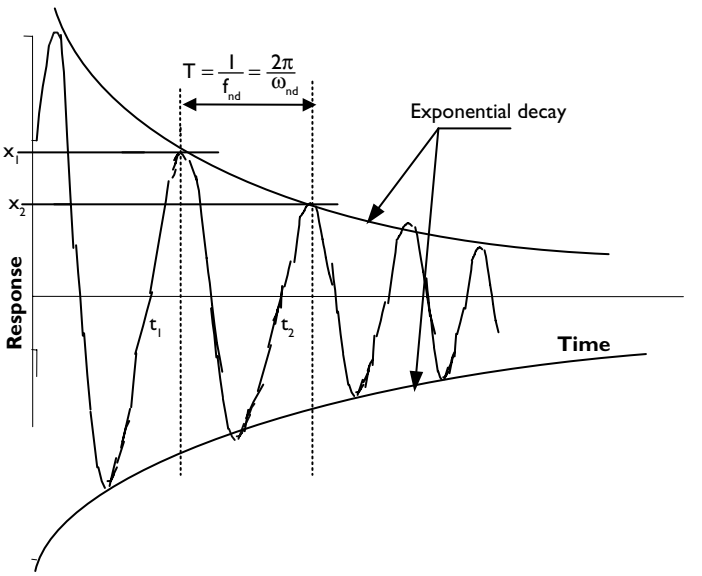


Figure 3.2.17 Damped free vibration, logarithmic decrement.

Hence the complete solution may be written as

$$x = e^{-D\omega_n t}\,[A\cos\,\omega_{nd}t + B\sin\omega_{nd}t] \quad \text{or}$$
$$x = e^{-D\omega_n t}\sqrt{[A^2 + B^2]}\sin(\omega_{nd}t + \phi) \tag{3.2.15}$$

in which $A = x_0$; $B = \dfrac{\dot{x}_0 + Dx_0\omega_n}{\omega_n\sqrt{1-D^2}}$; $\tan\,\phi = \dfrac{B}{A} = \dfrac{\dot{x}_0 + Dx_0\omega_n}{x_0\,\omega_n\sqrt{1-D^2}}$.

3.2.2 Forced vibration

The system is shown in Figure 3.2.18.

The governing equation for this case can be written as

$$m\ddot{x} + c\dot{x} + kx = F_0\sin\omega t \tag{3.2.16}$$

General solution of Equation (3.2.16) is

$$x(t) = x_c + x_p = \text{ Complementary solution (C.F.) + Particular integral (P.I.).} \tag{3.2.17}$$

$$\text{C.F.} = x_c = e^{-D\omega_n t}\,[A\cos\omega_{nd}t + B\sin\omega_{nd}t] \tag{3.2.18}$$

Since Equation (3.2.16) is a linear second order differential equation with constant coefficients, one may expect the particular integral to have a combination of harmonic functions. Again, the C.F. will die out after a few cycles, PI will be the only part of solution which will remain as the response of the vibrating system. As forcing function is sinusoidal, solution of the differential equation with constant coefficients will be of the form of a combination of $\sin\omega t$ and $\cos\omega t$.

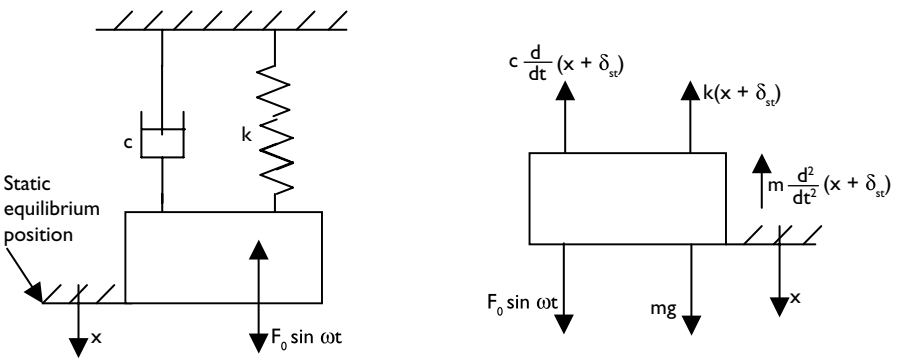


Figure 3.2.18 Single-degree-of-freedom, damped forced vibration.

For particular integral: $\text{P.I.} = x_p = A_1 \sin \omega t + A_2 \cos \omega t$ (3.2.19)

On differentiating Equation (3.2.19), we have

$$\dot{x} = \omega A_1 \cos \omega t - \omega A_2 \sin \omega t; \quad \ddot{x} = -\omega^2 A_1 \sin \omega t - \omega^2 A_2 \cos \omega t \tag{3.2.20}$$

Substituting in Equation (3.2.16) and separating sine and cosine terms, we have

$$-m\omega^2 A_1 - c\omega A_2 + kA_1 = F_0 \quad \text{and} - m\omega^2 A_2 + c\omega A_1 + kA_2 = 0 \tag{3.2.21}$$

Solving Equation (3.2.21) for A_1 and A_2 results in

$$A_2 = \frac{-F_0 c\omega}{(k - \omega^2 m)^2 + c^2\omega^2} \quad A_1 = \frac{-(m\omega^2 - k)F_0}{(k - \omega^2 m)^2 + c^2\omega^2} \tag{3.2.22}$$

$$\text{Thus} \quad x_p = \frac{F_0}{(k - \omega^2\, m)^2 + c^2\omega^2}[-(m\omega^2 - k)\sin \omega t - c\omega \cos \omega t] \tag{3.2.23}$$

$$= \frac{F_0}{\sqrt{(k - \omega^2 m)^2 + c^2\omega^2}} \sin(\omega t - \phi) \quad \text{and} \ \tan \phi = \frac{c\omega}{k - m\omega^2}$$

$$= \frac{-F_0}{\sqrt{(k - \omega^2 m)^2 + c^2\omega^2}} \cos(\omega t + \phi) \quad \text{and} \ \tan \phi = \frac{k - m\omega^2}{c\omega} \tag{3.2.24}$$

The solution of x_p and x_c are shown in Figure 3.2.19.

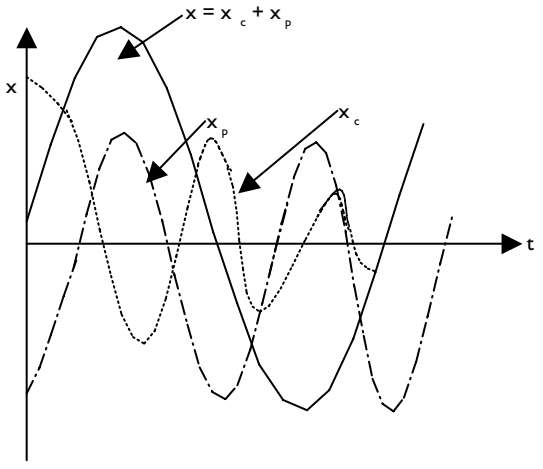


Figure 3.2.19 Response of SDOF damped system.

3.2.2.1 Non-dimensionalisation

Substituting Equation (3.2.20) in l.h.s. of Equation (3.2.16) and considering the value of A_1 an A_2 from Equations (3.2.21) and (3.2.22) we have

$$m^2\left[\left(\frac{k}{m}-\omega^2\right)^2+\frac{c^2}{m^2}\omega^2\right]=m^2\omega_n^4[(1-r^2)^2+(2Dr)^2] \quad \text{and } DC_c\omega=2D\omega_n\omega m \tag{3.2.25}$$

Equation (3.2.24) can thus be written as

$$\begin{aligned} x_p &= \frac{F_0/k}{\sqrt{(1-r^2)^2+(2Dr)^2}}\sin(\omega_n t-\phi) \quad \text{and } \tan\phi=\frac{2Dr}{1-r^2} \\ x_p &= \frac{-F_0/k}{\sqrt{(1-r^2)^2+(2Dr)^2}}\cos(\omega_n t+\phi) \quad \text{and } \tan\phi=\frac{1-r^2}{2Dr} \end{aligned} \tag{3.2.26}$$

Following observations can be made from Equation (3.2.26), the particular integral:

1 The motion is harmonic and is of same frequency as the exciting force. For a given harmonic excitation of constant amplitude and frequency, the amplitude of the response is constant. Hence the motion is steady state response or is called steady state vibration.
2 x_p does not contain any arbitrary constants, the response is independent of the initial conditions imposed on the system.
3 The amplitude of x_p is a function of magnitude and frequency of the exciting force, x_{static} defined by F_0/k is the response of the system to a static force defined by F_0 and the ratio $x_{\max}/x_{\text{static}}$ is the ratio of steady state response to the static response of the system. This is defined as magnification factor.
4 At $r = 1$, the resonant frequency of an undamped system, the magnification factor is limited by D.
5 Excitation and response do not attain their maximum values at the same time. The phase angle φ is a measure of the time difference between them. For a given D and r, the phase angle is a constant. Phase angle may vary from 0 to 180°, at $r = 1$, the phase angle is always 90°. For an undamped system, the phase angle is always either 0 or 180°.

Magnification factor $= M = \frac{x_{\max}}{x_{\text{static}}} = \frac{x_{\max}}{F_0/k}$ attains its maximum value $M_{\max}$ depending upon the value of r for a particular D value. This is shown in Figure 3.2.20.

At $r = 1$ = Undamped natural frequency, $M = 0.5/D$.

Thus, for $D = 0.2$, $M = 2.5$, and $D = 1/\sqrt{2}$, $M = 0.707 < 1 \rightarrow$ amplitude less than the statical value.

To obtain maximum M i.e. $M_{\max}$, we follow the following procedure

$$M=\frac{1}{\sqrt{((1-r^2)^2+(2Dr)^2)}} \tag{3.2.27}$$

To have a maximum M, denominator should be a minimum,

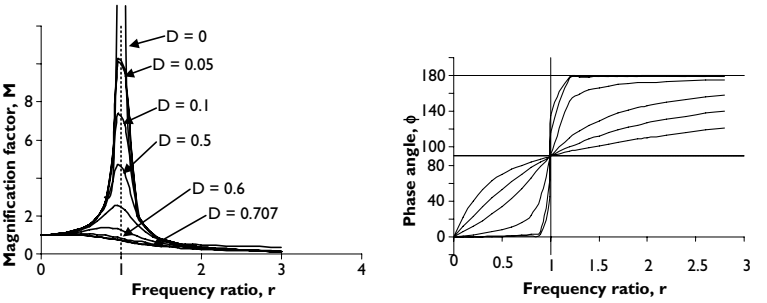


Figure 3.2.20 Magnification factor and phase angle variations with frequency ratios.

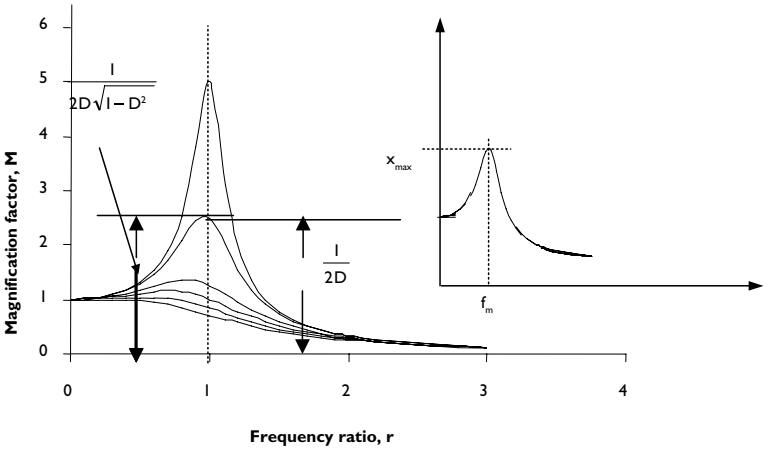


Figure 3.2.21 Maximum values.

i.e. $\dfrac{d}{dr}[(1-r^2)^2 + (2Dr)^2] = 0$

or $2(1-r^2)(-2dr) + 2(4D^2 r) = 0$; as $r = 0 \rightarrow$ gives only a trivial solution,

$$2(1-r^2) = 4D^2 \rightarrow r = \sqrt{1-2D^2}$$

Thus

$$\omega = \omega_n \sqrt{1-2D^2} : M_{\max} = \frac{1}{2D\sqrt{1-D^2}}; \quad x_{\max} = \frac{F_0/k}{2D\sqrt{1-D^2}}. \tag{3.2.28}$$

Resonant frequencies are: Response curve for a particular run looks like the one shown in Figure 3.2.21.

$$f_m = f_n\sqrt{1-2D^2} : \omega_m = \sqrt{\frac{k}{m}} \times \sqrt{1-2D^2} : f_m = \frac{1}{2\pi} \times \sqrt{\frac{k}{m}} \times \sqrt{1-2D^2} \tag{3.2.29}$$

One can have D and k provided m is known as F_0, $x_{\max}$ and f_m are known.

3.2.3 Steady-state analysis: Mechanical impedance method

If both the excitation and the steady-state response are harmonic and of the same frequency, they can be represented by rotating vectors with the same angular velocity. If the excitation force Fsin ωt be represented by $\boldsymbol{F} = Fe^{i\omega t}$ and if the response lags the excitation force by a phase angle, ψ, the displacement vector can be written as $\boldsymbol{X} = Xe^{i(\omega t-\psi)}$. The velocity and acceleration vectors can be written as

$$\text{Displacement } \boldsymbol{X} = Xe^{i(\omega t-\psi)} \tag{3.2.30}$$

$$\text{Velocity } \frac{d}{dt}(\boldsymbol{X}) = i\omega\boldsymbol{X} = i\omega Xe^{i(\omega t+\frac{\pi}{2}-\psi)} \tag{3.2.31}$$

$$\text{Acceleration } \frac{d^2}{dt^2}(\boldsymbol{X}) = (i\omega)^2\boldsymbol{X} = -\omega^2 Xe^{i(\omega t+\pi-\psi)} \tag{3.2.32}$$

These relative vectors are shown in Figure 3.2.22.

The harmonic force in the system obtained by multiplying the displacement, velocity and acceleration by appropriate constants as follows:

The spring force, $kx(t)$ resist the displacement $x(t)$, corresponding spring force vector is $-k\boldsymbol{X}$.

The damping force $c\dot{x}(t)$ resist the motion, corresponding damping force vector is $-$ic$\omega\boldsymbol{X}$.

The inertia force $m\ddot{x}(t)$ always resists the motion; corresponding force vector is m$\omega^2\boldsymbol{X}$.

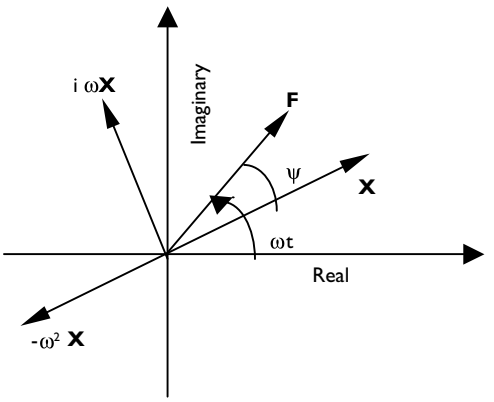


Figure 3.2.22 Force, displacement, velocity and acceleration presented by rotating vectors.

These force vectors are shown in Figure 3.2.22.

The impedance method can be deduced directly from the vector representation of harmonic forces.

The equation of motion of one-degree-of-freedom is given by

$$m\ddot{x} + c\dot{x} + kx = F\sin\omega t \tag{3.2.33}$$

Substitution of Eqns. (3.2.30)–(3.2.32) in Equation (3.2.33) results in

$$(-m\omega^2 + ic\omega + k)Xe^{i(\omega t-\psi)} = Fe^{i\omega t} \tag{3.2.34}$$

Factoring out $e^{i\omega t}$ and rearranging, it results in

$$X\,e^{-i\psi} = \frac{F}{(k - m\omega^2) + ic\omega} \tag{3.2.35}$$

Hence $\boldsymbol{X}$ is the magnitude of displacement vector and can be written as

$$X = \left|\frac{F}{(k - m\omega^2) + ic\omega}\right| = \frac{F}{\sqrt{(k - m\omega^2)^2 + (c\omega)^2}}; \quad \text{and}$$
$$\psi = \tan^{-1}\left[\frac{c\omega}{k - m\omega^2}\right] = \tan^{-1}\left[\frac{2Dr}{1 - r^2}\right] \tag{3.2.36}$$

Equation (3.2.33) can also be written as

$$\ddot{x} + (c/m)\dot{x} + (k/m)x = (F_0/m)\sin\omega t; \quad \text{or } \ddot{x} + \gamma\,\dot{x} + \omega_n^2 x = (F_0/m)\sin\omega t \tag{3.2.37}$$

3.2.4 Q-values and their interpretation

In vibration analysis it is customary to use Q-values, a pure number defined as (ω_n/γ). Q is known as quality factor (Main, 1995). When damping is light Q is very high; in a lightly damped case, $Q > 1/2$ and a very lightly damped case $Q >> 1$. Under normal vibratory system Q is around 10. Q is numerically equal to $(1/2D)$ and D is the damping coefficient defined in Equation (3.2.13).

Properties of lightly damped case are generally expressed in terms of Q. After Q cycles i.e. after a time $Q_t = 2\pi Q/\omega_f$ where $\omega_f = \omega_n$ sqrt $(1-[\gamma/2\omega_n])$ the amplitude is reduced by a factor, $\exp[-1/2(2\pi Q/\omega_f)] \approx \exp[-1/2\gamma(2\pi Q/\omega_n)] = e^{-\pi} = 0.043$. Thus a Q for a lightly damped vibration system is to note how many cycles it takes for the amplitude to fall to bout 4% of its initial value.

A vector diagram for Equation (3.2.37) is given Figure 3.2.23. In a steady state, if we assume the displacement of the forced vibrating system as $x = A\sin(\omega t + \phi)$, components of the diagram can be obtained as follows:

$\ddot{x}$ has amplitude $\omega^2\,A$ and is 90° behind $\dot{x}$. $\dot{x}$ has amplitude ωA and is 90° ahead of x. The values of A and ϕ are chosen so that a closed figure Figure 3.2.23 is formed

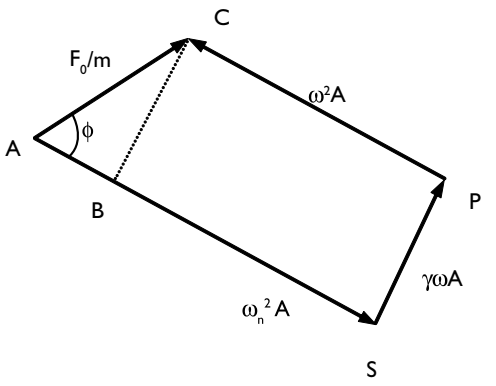


Figure 3.2.23 Vector diagram of Equation (3.2.37).

when we add the right hand side vector of Equation (3.2.37) As time progresses the figure will rotate without changing its shape and we can match up the four vectors at any time that we choose. Let us assume that the vector plot shown in Figure 3.2.23 defines the state at $t = 0$.

From Figure 3.2.23, it may be noticed that ϕ must lie between $-\pi < \phi \leq 0$. As we assume forcing function as the standard, x, the displacement is the phase advance of ϕ relative to the forcing function. Again, we have found that ϕ always negative (clockwise from the force), the displacement always lags the driving force. The magnitude of ϕ can be obtained from the vector diagram as

$$\tan\phi = \frac{\gamma\ \omega}{\omega_n^2 - -\omega^2} \tag{3.2.38}$$

The phase lag just discussed depends on the frequency and not on the forcing function. Considering triangle ABC of Figure 3.2.23, one can write

$$(\omega_n^2 - \omega^2)A^2 + \gamma^2\omega^2A^2 = (F_0/m)^2 \tag{3.2.39}$$

$$\text{i.e.} \quad A = \frac{F_0/m}{\sqrt{(\omega_n^2 - \omega^2)^2 + \gamma^2\omega^2}} \tag{3.2.40}$$

This can be expressed also in the form

$$A = (F_0/k)\ X\ \frac{1}{\sqrt{(1 - r^2)^2 + (r/Q)^2}} \tag{3.2.41}$$

in which $r = \omega/\omega_n$ and A becomes infinite at $\omega = \omega_n$ and $\gamma = 0$.

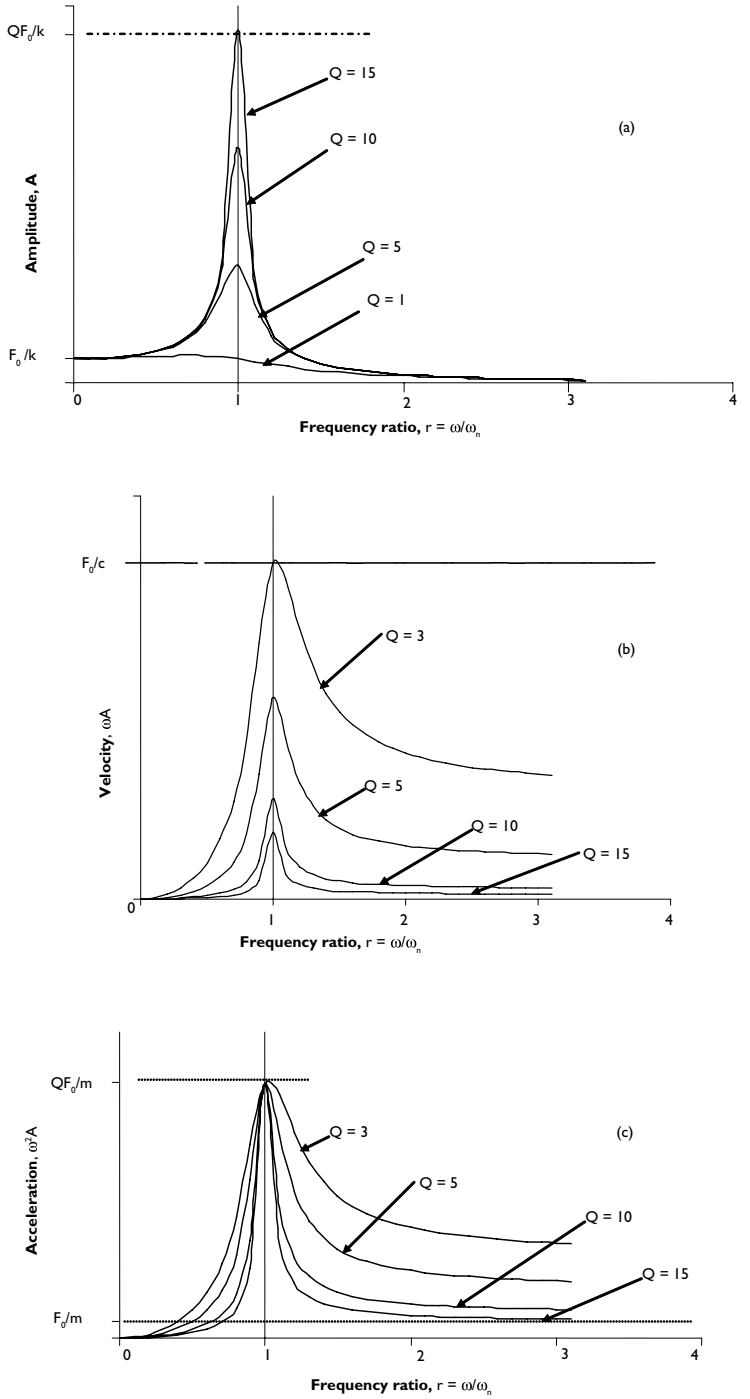


Figure 3.2.24 Resonant curves for various values of Q. [Note: Q = 5.0 = 1/2 D]

We define in the following a non-dimensional expression R, known as Response function, is given as follows

$$R(\omega) = \frac{\gamma^2\omega^2}{(\omega_n^2 - \omega^2)^2 + \gamma^2\omega^2} \tag{3.2.42}$$

In terms of Q, it can also be expressed as

$$R(r) = \frac{(r/Q)^2}{(1 - r^2)^2 + (r/Q)^2} \tag{3.2.43}$$

The response function lies between 0 and 1, the latter value is reached when $\omega = \omega_n$. One can write displacement, velocity and acceleration in terms of R as

$$\begin{aligned} \text{Displacement:} \quad & A = (F_0/c\omega)[R(\omega)]^{1/2}; \\ \text{Velocity:} \quad & \omega A = (F_0/c)[R(\omega)]^{1/2} \\ \text{Acceleration:} \quad & \omega^2 A = (F_0\omega/c)[R(\omega)]^{1/2} \end{aligned} \tag{3.2.44}$$

Three amplitudes are plotted against r, the frequency ratio, r for a system with $Q = 5$. These curves are called response curves. The variation of phase angle with r having $Q = 5$, are also shown in Figure 3.2.24. The damping used here is light. First three plots shows resonance near $r = 1$. The frequency corresponding to this phenomenon is called resonant frequency. Since the velocity amplitude ωA is proportional to the square root of $R(\omega)$, it has its maximum value exactly at $r = 1$. The displacement amplitude A has ω in the denominator, this pulls down the curve at high frequencies more than at low frequency and so A peaks at a frequency slightly below the resonance frequency. The acceleration amplitude contains ω in the numerator and therefore it peaks slightly above the resonant frequency. At resonant frequency, the phase angle is $-\pi/2$; then the displacement lags the forcing function by exactly $\pi/2$. For any harmonic function displacement lags the velocity by $\pi/2$. Thus *the velocity is in phase with the forcing function at resonance*.

At very low operating frequency where $\omega << \omega_n$, $\phi \approx 0$; $A \approx F_0/m\omega_n^2 = F_0/k \rightarrow x \approx (F_0/k)\sin\omega t$: this response is independent of m and γ, and a low frequency response is said to be stiffness controlled. The mass has very small acceleration which requires only a small part of the driving force, most of the energy goes to balance the spring force $= -kx$. Since the spring force is the restoring force, the driving force must be nearly in phase with x.

At high operating frequency, where $\omega >> \omega_n\phi \approx -\pi/2$; $A \approx F_0/m\omega_n^2 \rightarrow x \approx (F_0/m\omega^2)\sin\omega t$: this response is independent of k, and at high frequency response is mass controlled. The force is required to give the mass a large acceleration at these frequencies. The existence of spring is not felt. Since the driving force provides almost the entire return force, it is naturally almost anti-phase with the displacement.

At low frequencies, the acceleration is small but the displacement amplitude A is never smaller than F_0/k. At higher frequencies the acceleration amplitude is $\omega^2 A$ is

never smaller than F_0/m, but the displacement is small. This high frequency behaviour can be fruitfully utilised to provide vibration isolation. To protect a system from vibration of frequency ω taking place at the other end of a supporting mass, we should choose a spring whose stiffness makes $\omega_n << \omega$.

Resonance results in amplification in response. If vibrating the anchor point of the spring at the resonance frequency with amplitude, F_0/k causes the mass to vibrate, at the same frequency but with the larger amplitude $F_0/m\gamma\omega_n$. The quantity Q is the amplification factor ω_n/γ.

There is a similar amplifying effect on the acceleration, with the result that the force acting at the point where the mass is attached to the spring has amplitude QF_0 at resonance, not merely F_0: A potential source of danger in a careless engineered system liable to resonance.

In each of the cases shown in Figure 3.2.11, the amplification factor is Q exactly when $\omega = \omega_n$ exactly. Since the displacement and the acceleration have their maxima at slightly different frequencies, they are amplified by a slightly larger factor at these frequencies.

3.2.5 Power absorption

To maintain the steady state vibration the system requires a sustained supply of energy through the driving force and it has to replenish the dissipation of energy through the damping. When the mass of the system moves from x to $x + \Delta x$, the work done against the damping force is $-F_d\Delta x$. If the movement takes place in time Δt, the rate at which energy is dissipated is $-F_d[\Delta x/\Delta t]$. In the limit as $\Delta t \to 0$ this becomes the instantaneous power absorption, i.e.

$$\text{Power,} \quad P = -F_d\dot{x} = [c\dot{x}]\dot{x} = c\dot{x}^2 \tag{3.2.45}$$

Since the velocity varies harmonically and has an amplitude ωA, the average of P over many cycles can be obtained over a complete cycle as

$$\text{Average of} \quad \dot{x}^2 = 1/2[F_0/c]^2 R(\omega) \tag{3.2.46}$$

Thus the average power

$$\bar{P} = [F_0^2/2c]R(\omega) = \frac{F_0^2}{2m\gamma}\left[\frac{\gamma^2\omega^2}{(\omega_n^2 - \omega^2)^2 + \gamma^2\omega^2}\right] = \frac{F_0^2}{2c}\left[\frac{(r/Q)^2}{\left(1 - r^2\right)^2 + (r/Q)^2}\right] \tag{3.2.47}$$

This is the average power absorbed from the driving force when the system is driven with an angular velocity ω; it is now plotted against the frequency ratio r and for varying values of Q in Figure 3.2.25. The maximum value of the average power $F_0^2/2c$, is reached at the resonant frequency. It is inversely proportional to the resistance. The absorbed power produces heat in the system. It can be noticed that when damping is light, i.e. c is small the problem increases manyfold as average power increasingly

becomes unbounded. The shape of the absorption curve is essentially the shape of $R(\omega)$ with maximum value as 1. As ω decreases from the resonant value, $R(\omega)$ falls its maximum value of 1.

At some frequency, say ω_1, we have

$$R(\omega_1) = 1/2 \rightarrow \gamma^2\omega_1^2 = (\omega_n^2 - \omega_1^2)^2 \rightarrow \gamma\omega_1 = \omega_n^2 - \omega_1^2, \quad \text{for } \omega_1 < \omega_n. \quad (3.2.48)$$

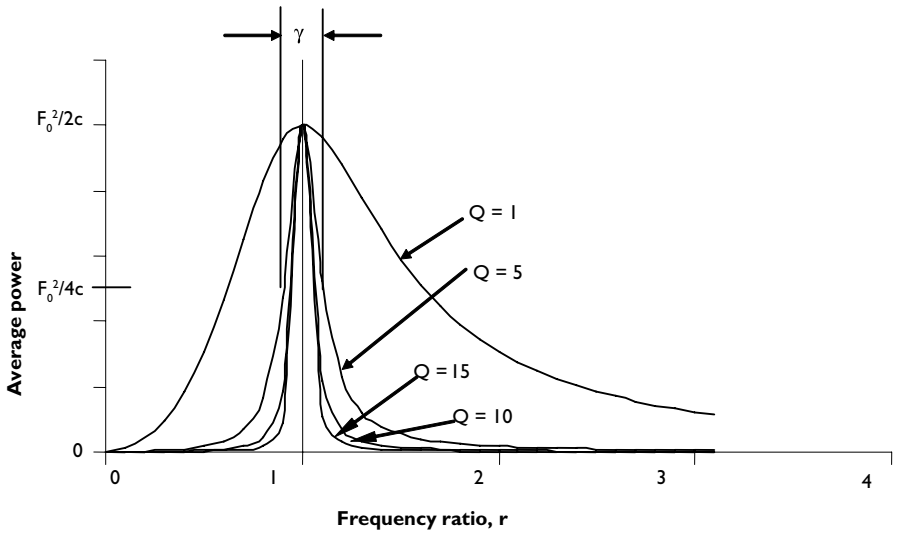


Figure 3.2.25 The average power absorption with varying Q values.

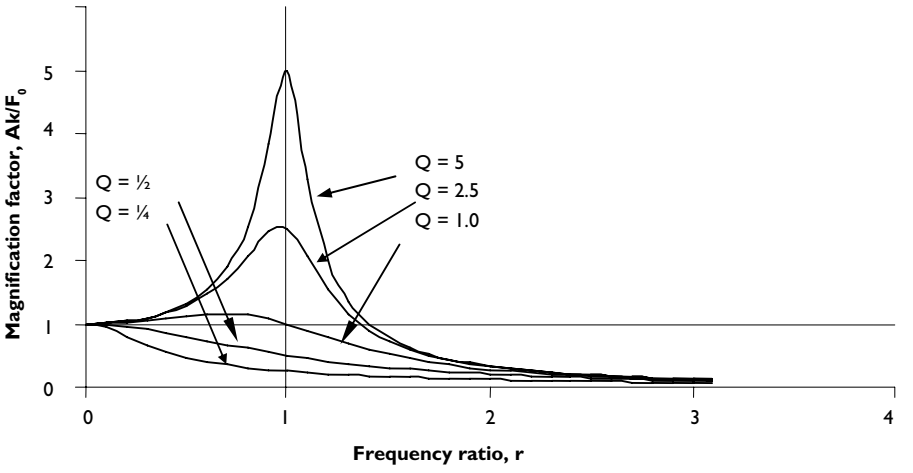


Figure 3.2.26 Magnification factors for varying, Q.

Similarly as ω increases from resonance, $R(\omega)$ decreases again and at, say ω_2, we have

$$R(\omega) = 1/2 \rightarrow \gamma\omega_2 = \omega_n^2 - \omega_2^2, \quad \text{for } \omega_2 > \omega_n. \tag{3.2.49}$$

From the above, we may write,

$$\gamma = (\omega_1 - \omega_2). \tag{3.2.50}$$

Thus γ is the size of the angular frequency range within which the average power is greater than half its maximum value. This is precisely the reason to call γ as 'width'.

With Q increasing (low damping), the figure sharpens around $r = 1$, that is the resonant frequency, free vibrations die out slowly and vice versa. Hence width of the power absorption curve is identical with the energy decay constant for free vibration of the same system. Thus measurement of the resonant curve can be used as a practical way of obtaining the decay constant.

3.2.6 Heavy damping

Free vibration cannot occur when the damping is heavy, i.e. $Q > 1/2$ and $\gamma > 2\omega_n$. The system in this case returns asymptotically to $x = 0$. However forced vibrations are possible. Figure 3.2.24(a) can be obtained for all degrees of damping. The corresponding plot is shown in Figure 3.2.26.

For heavy damping we can obtain an approximate expression for the response function $R(\omega)$ from which we obtain other responses like velocity and acceleration. For heavy damping we expect appreciable movement only at the lowest frequencies, hence we may put $\omega << \omega_n$ in the exact formula of $R(\omega)$, i.e.

$$R(\omega) \approx \frac{\gamma^2\omega^2/\omega_n^4}{1 + (\gamma^2\omega^2/\omega_n^4)} \tag{3.2.51}$$

Substituting the relaxation time, $\tau_r = \gamma/\omega_n^2 = c/k$: the time it takes for the displacement to be reduced by a factor $1/e$ and is a quantity independent of the mass, m. Hence we can write Equation (3.2.51) as

$$R(\omega) \approx \frac{\tau_r^2\omega^2}{1 + \tau_r^2\omega^2} \tag{3.2.52}$$

A plot of Eqn. (3.2.52) is shown in Figure 3.2.27.

The plot is very unlike the resonant curve we saw earlier. We are interested here in the frequency range.

$\omega\tau_r = 1$, and this implies, $\omega = 1/\tau_r = Q\omega_n << \omega_n$.

The absorbed power, directly proportional to $R(\omega)$, will increase from a very small value to its maximum possible value of $F_0^2/2c$ as the frequency increases past $1/2\pi\tau_r$, whereas we can 'heat' a lightly damped system efficiently by choosing an operating frequency in the region of the resonant frequency, with very heavy damping the criterion is to choose ω well above $1/\tau_r$. The concept is used in microwave cooking.

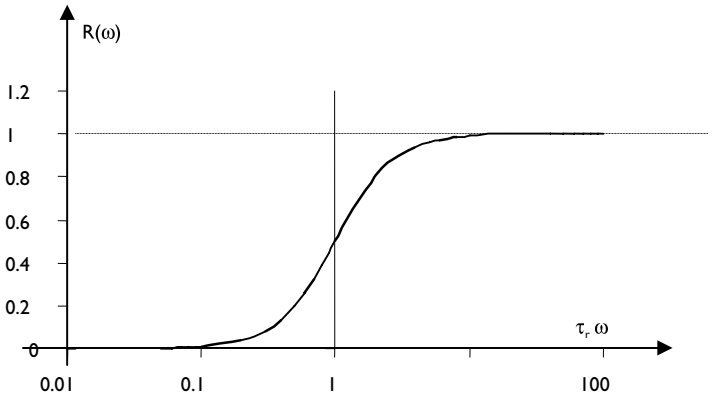


Figure 3.2.27 Response function for heavy damping.

3.2.7 Frequency dependent loading

A sinusoidal dynamic force is represented by $F(t) = F_0 \sin \omega t$. Here, F_0 is of constant magnitude. However dynamic forces emanating from unbalanced rotating mass is frequency dependent. Consider, for example an eccentric mass rotating with a constant circular frequency ω, around a fixed point O as in Figure 3.2.28.

The mass is rotating with an angular velocity, ω.

Hence, $\omega = \frac{d\theta}{dt}$; normal or centripetal acceleration $a_n = \rho\omega^2 = \rho\dot{\theta}^2$; and the tangential acceleration $a_t = d\frac{(\rho\omega)}{dt} = \rho\dot{\omega} + \dot{\rho}\omega = \rho\ddot{\theta} + \dot{\rho}\dot{\omega}$

As ρ is a constant $\rightarrow \dot{\rho} = 0$, a symmetric case, and $a_t = 0$ as $\omega =$ constant.

The idealized system is shown in Figure 3.2.28.

$F = m\rho\omega^2 \Rightarrow F_H = m\rho\omega^2 \cos\theta = m\rho\omega^2 \cos\omega t; \quad F_V = m\rho\omega^2 \sin\omega t.$

Hence forth the eccentricity ρ will be termed as e. So, we have a system subjected to the exciting force of the type shown in Figure 3.2.29(b). Figure 3.2.29(b) also indicates that the horizontal forces get cancelled; only the vertical component of oscillation remains and two such components get added up.

3.2.7.1 Mechanical oscillators

Two counter-rotating eccentric weights are used to produce forced oscillations. By varying the speed of rotation the magnitude of the resultant force can be varied. This is described in Figure 3.2.30.

Using, $F_V = 0 : F_H = 0$.

Net vertical force $= 4em\omega^2 \sin\omega t + 8em\omega^2 \sin\omega t$

$= m[2a_n \cos(\omega t + \alpha) - 2a_n \cos\omega t]$

When $\alpha = 0; F_V = 0 : \alpha = 180°; F_V$ is maximum.

A typical value of the vertical force:

$F = [1.875 \sin\frac{\alpha}{2} N^2]$ in lbs. in which $N = 2\pi f$ in rpm.

So, a S.D.O.F. system with frequency dependent amplitude, may be written as

$$m\ddot{x} + c\dot{x} + kx = me\omega^2 \sin\omega t = F_0 \sin\omega t \tag{3.2.53}$$

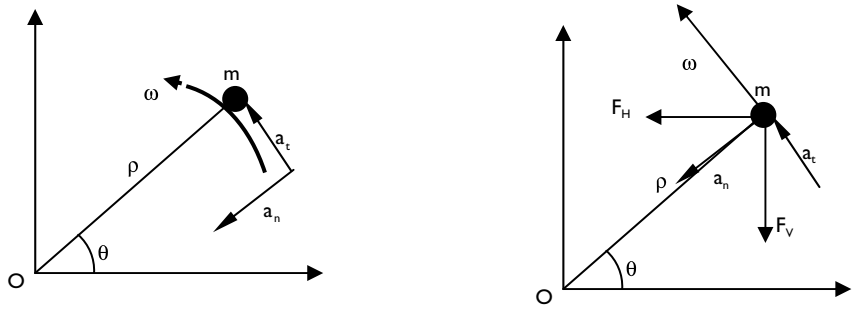


Figure 3.2.28 Eccentric rotating mass.

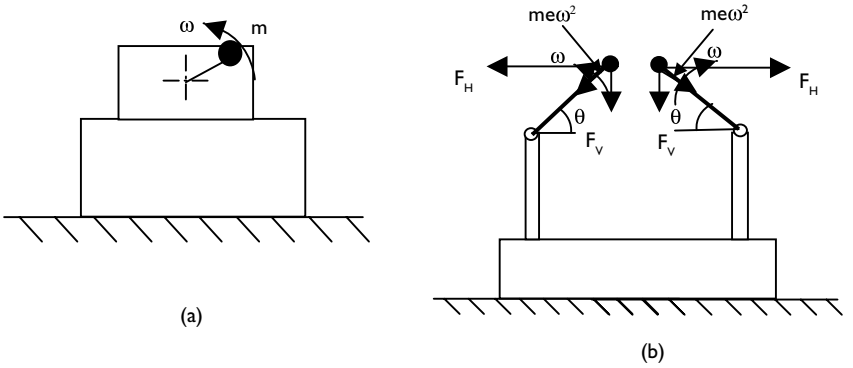


Figure 3.2.29 Generation of frequency dependent loading.

A typical foundation-soil system may be shown in Figure 3.2.31.
Thus from Equation (3.2.53),

$$x_{\max} = \frac{m_0 e\omega^2/k}{\sqrt{(1-r^2)^2+(2Dr)^2}} = \frac{m_0 e\omega^2/m\omega_n^2}{\sqrt{(1-r^2)^2+(2Dr)^2}} \quad \text{and} \tan\phi = \frac{2Dr}{1-r^2}. \tag{3.2.54}$$

$$\frac{x_{\max}}{\frac{m_0 e}{m}} = \frac{r^2}{\sqrt{(1-r^2)^2+(2Dr)^2}} = r^2 M = M' \tag{3.2.55}$$

$=$ Magnification factor for rotating mass type oscillator.

Response M' versus frequency ratio are shown in Figure 3.2.32 along with phase angle variation with frequency ratios. The phase angle of the steady state response is same as that shown in Figure 3.2.20.

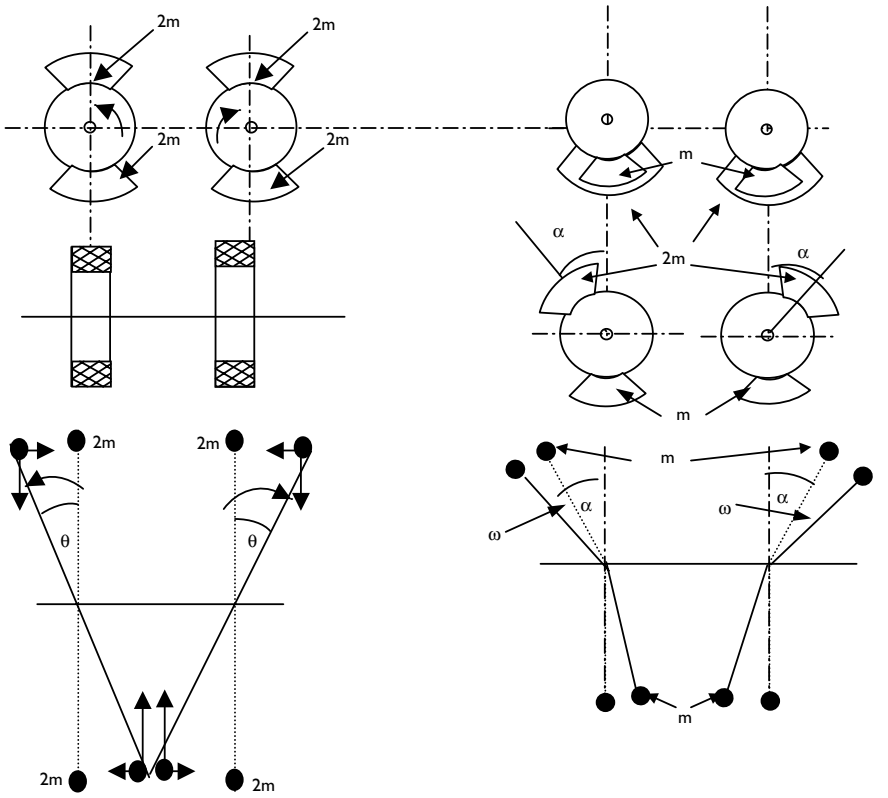


Figure 3.2.30 Principles of mechanical oscillator.

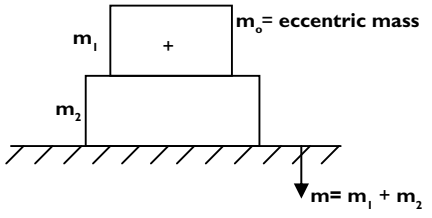


Figure 3.2.31 Footing-mass system.

3.2.7.2 *To obtain* M'_{max}

Equation (3.2.55) may be rewritten as

$$M' = \left(\frac{x_{\max}}{\frac{m_0 e}{m}}\right) = \frac{r^2}{\sqrt{(1-r^2)^2 + (2Dr)^2}} = \frac{1}{\sqrt{\left(\frac{1}{r^2} - 1\right)^2 + \left(\frac{2D}{r}\right)^2}} \tag{3.2.56}$$

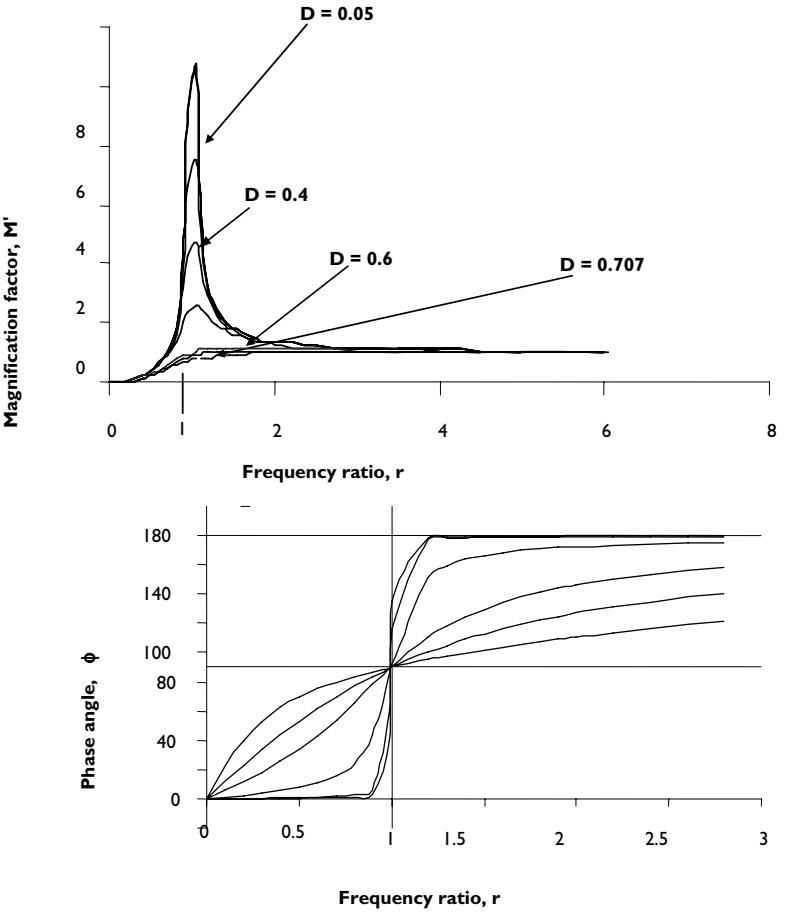


Figure 3.2.32 Response curves for different damping factors and phase angle.

Assume $\frac{1}{r} = r'$; this reduces Equation (3.2.55) to

$$M' = \frac{1}{\sqrt{(1 - r'^2)^2 + (2Dr')^2}} \tag{3.2.57}$$

and for M' to be maximum, $(1-r'^2)^2+(2Dr')^2$ is to be minimum. Now, from Equation (3.2.57) we can write that for a maximum value of $M', r' = \sqrt{1 - D^2}$.

Thus, for maximum M', r should be equal to $\dfrac{1}{\sqrt{1 - 2D^2}}$. (3.2.58)

Hence $\quad r_{\text{res}} = \dfrac{1}{\sqrt{1 - 2D^2}} \quad$ or $\quad \omega_{\text{res}} = \dfrac{\omega_n}{\sqrt{1 - 2D^2}}$. (3.2.59)

Thus ω_{res} is always less than ω_n.

$$M'_{\max} = \frac{1}{2D\sqrt{1-D^2}} \quad \text{so } M' = \frac{1}{2D}. \tag{3.2.60}$$

At low speed, the force $me\omega^2$ is small, and the amplitude is nearly zero. At resonance, when the frequency ratio, r is unity, the magnification factor M' is equal to $1/2Dr$. When frequency ratio is large the mass m has an amplitude (m_0e/m).

3.2.7.3 Physical significance of (m_0e/m)

We have, $\frac{m_0e\omega^2}{k}$: Now, if $\omega = \omega_n \rightarrow$ the mass is rotating at its natural frequency.

The force produced by the eccentric mass $= m_0e\omega_n^2$, and if $k =$ spring constant of the system,

$$\frac{m_0e\omega_n^2}{k} \Rightarrow \frac{m_0e}{m}. \tag{3.2.61}$$

1 When r is increased far beyond 1,

$$x_{\max} = \frac{m_0e}{m}. \tag{3.2.62}$$

This concludes that a rotating mass, if unrestrained, will tend to rotate about its centre of gravity. For this case, the vibration amplitude is e, since $m_0 = m$. For most systems m_0 is only a part of the total mass resulting in a limiting vibration amplitude of $(m_0/m)e$.

This phenomenon is the basis of adding more mass to a system when it is vibrating above resonant frequency in order to reduce its dynamic amplitude (Richart et al. 1970).

3.2.7.4 Summary of S.D.O.F vibrating systems

Free vibration $\rightarrow$ two natural frequencies, ω_n, ω_{nd}

Forced vibration $\rightarrow$ two resonant frequencies,

$$r_{\text{res}} = \sqrt{1-2D^2} = \frac{\omega_{\text{res}}}{\omega_n}[\text{constant amplitude}]; \tag{3.2.63}$$

$$r_{\text{res}} = \frac{1}{\sqrt{1-2D^2}} = \frac{\omega_{\text{res}}}{\omega_n}[\text{rotating mass}]. \tag{3.2.64}$$

As shown in Figure 3.2.34, up to $D = 0.2$ all natural and resonant frequencies are within 5% of the undamped natural frequency of the system. For higher D, difference is more. For $D \geq 1/\sqrt{2}$, no peak is produced for forced vibration. For $D \geq 1$, no oscillating motion is generated for damped free vibrations.

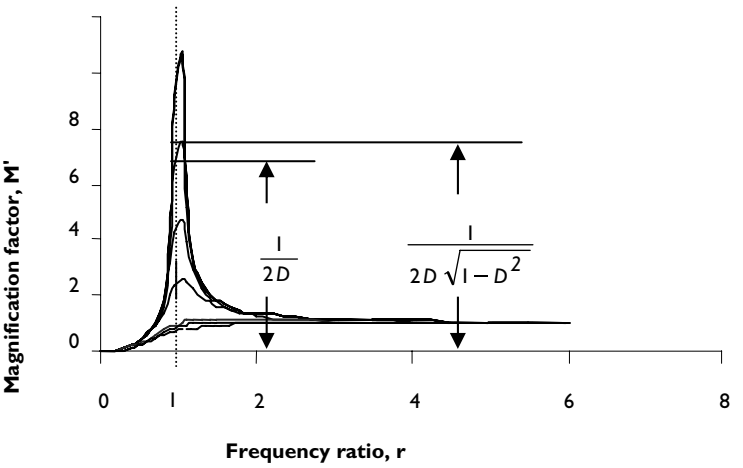


Figure 3.2.33 Maximum values of magnification factors.

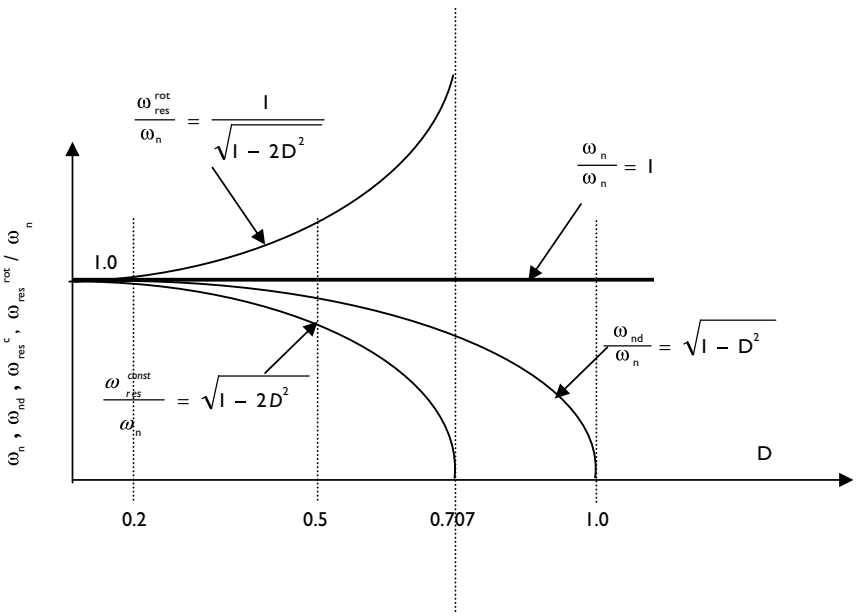


Figure 3.2.34 Natural and resonant frequencies of S.D.O.F. systems. [After Richart et al. (1970)]

3.2.7.5 Soil properties from response curves

If an experiment is conducted and response curves have been obtained for a signle-degree-of-freedom system, one can determine the following soil properties:

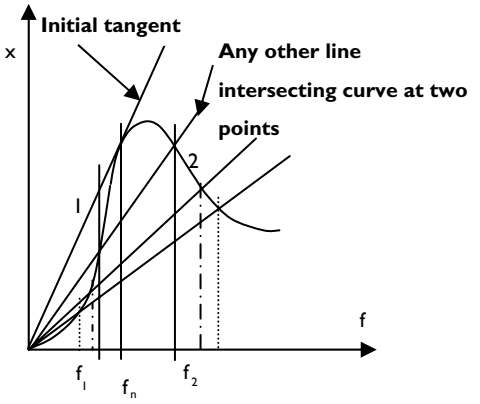


Figure 3.2.35 Single response of rotating mass type oscillator.

1 Rotating mass type oscillator (Figure 3.2.35): f_n, the undamped natural frequency, can be obtained from tangency of a line originating from origin to the curve.

However, the following relationship exists

$$f_n^2 = f_1 \cdot f_2 \tag{3.2.65}$$

Thus from a single curve can give several calculations can be made and an average is, normally used to obtain the undamped natural frequency of the system.

2 Constant amplitude force

A classical case for this type of behaviour (Figure 3.2.36) is the logarithmic decrement, as mentioned earlier.

$$\delta = \frac{\pi}{2} \frac{f_2^2 - f_1^2}{f_{\text{res}}^2} \sqrt{\frac{x_1^2}{x_{\max}^2 - x_1^2}} \left(\frac{\sqrt{1 - 2D^2}}{1 - D^2} \right) \tag{3.2.66}$$

for D, this equation has to be solved by trial and error, as D is involved on r.h.s. When D is small $\frac{\sqrt{1-2D^2}}{1-D^2} \approx 1$ and if x is chosen such that $x = 0.707\, x_{\max}$, then

$$\delta = \frac{\pi (f_2 - f_1)}{f_{\text{res}}}. \tag{3.2.67}$$

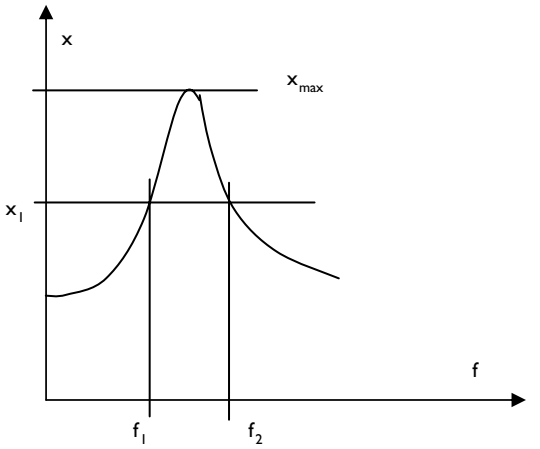


Figure 3.2.36 Single response of constant amplitude oscillator.

Example 3.2.6

Set up differential equations of motion for the systems shown in Figure 3.2.37. Determine expressions for: i) critical damping coefficient and, ii) the natural frequencies of the damped oscillation.

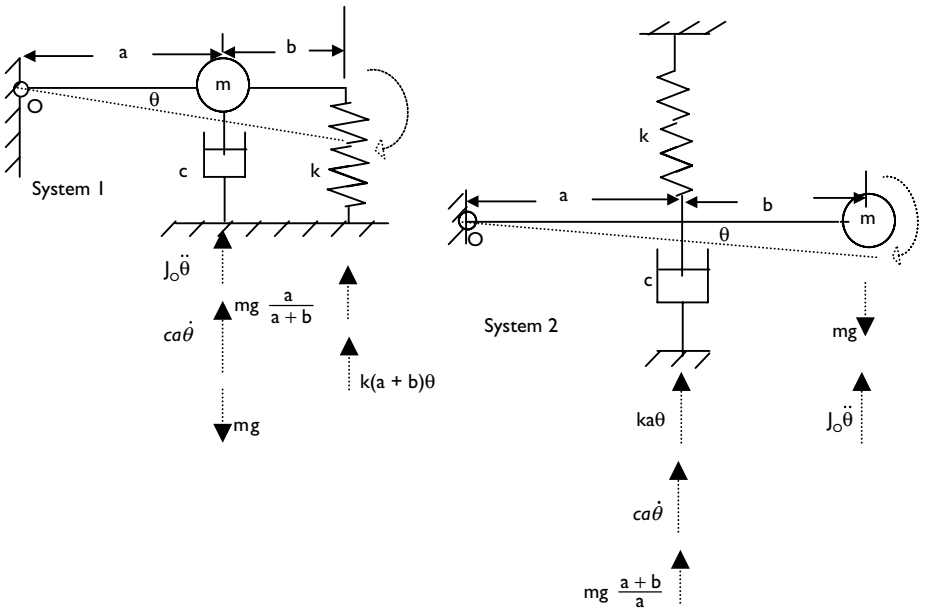


Figure 3.2.37 A system with mass-spring-dashpot.

Solution:

System 1: Taking moment about O: $J_0\ddot{\theta} + ca^2\dot{\theta} - mga + mg\frac{a(a+b)}{a+b} + k(a+b)^2\theta = 0$

Here J_0 = mass moment of inertia of the body = ma^2, and hence,

$$[ma^2]\ddot{\theta} + [ca^2]\dot{\theta} + [k(a+b)^2]\theta = 0; \text{ Comparing with } m\ddot{x} + c\dot{x} + kx = 0$$

$$C_c = \sqrt{4km} = \sqrt{4k(a+b)^2\, ma^2} = a(a+b)\sqrt{4km};$$

$$\omega_n = \sqrt{\frac{k}{m}} = \sqrt{\frac{k(a+b)^2}{ma^2}} = \frac{a+b}{a}\sqrt{\frac{k}{m}} \quad \text{and}$$

$$D = \frac{c}{C_c} = \frac{ca^2}{a(a+b)\sqrt{4km}} = \frac{ca}{(a+b)\sqrt{4km}}.$$

System 2: Similarly taking moment about O:

$m(a+b)^2 + ca^2\dot{\theta} + ka^2\theta - mg(a+b) + mg\frac{(a+b)}{a}a = 0$

$[m(a+b)^2]\ddot{\theta} + [ca^2]\dot{\theta} + [ka^2]\theta = 0$; Comparing with $m\ddot{x} + c\dot{x} + kx = 0$

$$C_c = \sqrt{4km} = \sqrt{4ka^2\, m(a+b)^2} = a(a+b)\sqrt{4km};$$

$$\omega_n = \sqrt{\frac{k}{m}} = \sqrt{\frac{ka^2}{m(a+b)^2}} = \frac{a}{a+b}\sqrt{\frac{k}{m}}.$$

$$D = \frac{c}{C_c} = \frac{ca^2}{a(a+b)\sqrt{4km}} = \frac{ca}{(a+b)\sqrt{4km}}.$$

The results are identical.

3.2.8 Dissipation of energy

Consider the general equation of motion, given by

$$m\ddot{x} + c\dot{x} + kx = F_0 \sin\omega t \tag{3.2.68}$$

Solution of Equation (3.2.68) is

$$x = \frac{F_0/k}{\sqrt{(1-r^2)^2 + (2Dr)^2}} \sin(\omega t - \phi) = A\, \sin(\omega t - \phi);$$

where, $\tan\phi = \dfrac{2Dr}{1-r^2}$.

Now, $x = A\sin(\omega t - \phi)$ and $\dot{x} = \omega A\cos(\omega t - \phi)$

3.2.8.1 Work done by the force F in one cycle

With reference to the forcing function shown in Figure 3.2.38 with time period τ

$$\Delta E_F = \int_0^\tau F dx = \int_0^\tau F_0 \sin \omega t \, \frac{dx}{dt} dt = F_0 \int_0^\tau \sin \omega t \, A\omega \cos(\omega t - \phi) dt \tag{3.2.69}$$

Equation (3.2.69) can be solved substituting $\omega t = \theta \rightarrow dt = \frac{d\theta}{\omega}$ and for $t = 0 \rightarrow \theta = 0$; $t = \tau \rightarrow \theta = 2\pi$. Eqn. (3.2.69), then, reduces to

$$\Delta E = F_0 \int_0^{2\pi} \sin\theta \cos(\theta - \phi) d\theta = \pi \, A \, F_0 \sin\phi \tag{3.2.70}$$

Thus, when the phase angle ϕ between the force and the displacement is zero, the work done per cycle is zero, since the spring and the mass are conservative elements. When $\phi = 90°$, the work done per cycle is a maximum. Hence the harmonic force F can be considered to be composed of two components, one in phase, or 180° out of phase, with the displacement, and the other in phase with the velocity. The net work is due to the force in phase with the velocity; the damping force is opposed to this force component.

3.2.8.2 Work done by the damping (viscous) force

$$\Delta E_d = \int_0^\tau c \frac{dx}{dt} \frac{dx}{dt} dt \; = \int_0^\tau c A^2 \omega^2 \cos^2(\omega t - \phi) dt \tag{3.2.71}$$

Equation (3.2.74) can be solved by substituting, $\omega t - \phi = z \rightarrow dt = dz/\omega$, and for $t = 0 \rightarrow z = -\phi$, $t = \tau = 2\pi/\omega \rightarrow z = 2\pi - \phi$.

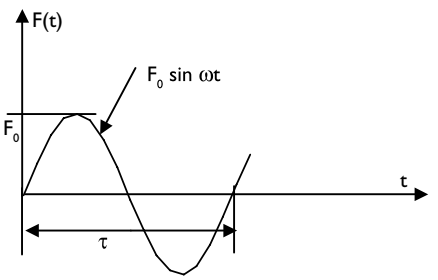


Figure 3.2.38 General sinusoidal motion.

Equation (3.2.71), then, reduces to

$$\Delta E_d = \frac{cA^2\omega}{2}\int_{\phi}^{2\pi-\phi}(1+\cos 2z)dz = \pi\, cA^2\omega \tag{3.2.72}$$

If the damping is non-viscous, an equivalent viscous damping coefficient c_{eq} can be assumed to describe the damping. However, a steady state motion with non-viscous damping need not be harmonic, a reasonable harmonic motion can be approximated if the damping is not large enough to change its wave form appreciably from its harmonic counterpart.

3.2.9 Velocity squared damping

When a mass vibrates in a fluid or a fluid is forced through an orifice, fluid friction is generally *assumed* to be proportional to the square of the velocity.

Let the damping force be $= a\dot{x}^2$ and if the motion is harmonic of the type: $x = x_0 \sin\omega t$,

Energy dissipation per cycle

$$\Delta E = 2\int_{-x}^{x} a\dot{x}^2 dx = 2x_0^2\int_{-\pi/2}^{\pi/2} a\omega^2\cos^3\omega t\, d(\omega t) = \frac{8}{3}a\omega^2 x_0^3 \tag{3.2.73}$$

If c_{eq} = equivalent viscous damping, we have

$$\rightarrow \quad c_{eq}\pi\omega x_0^2 = \frac{8}{3}a\omega^2 x_0^3 \quad \Rightarrow \quad c_{eq} = \frac{8a\omega x_0}{3\pi}. \tag{3.2.74}$$

Here we find that c_{eq} is not a constant, it depends on the excitation frequency and the amplitude of vibration. For a single-degree-of-freedom system, we can write

$$x_0 = \frac{F_0/k}{\sqrt{(1-r^2)^2 + (c_{eq}\frac{\omega}{k})^2}} \tag{3.2.75}$$

Squaring both sides, $\quad x_0^4 + \frac{9m^2\pi^2(1-r^2)^2}{64a^2r^4}x^2 - \frac{9m^2\pi^2}{64a^2r^4}\frac{F_0}{k^2} = 0. \tag{3.2.76}$

This gives real root as

$$x_0 = \left(\frac{3m\pi}{8ar^2}\right)\sqrt{-\frac{(1-r^2)^2}{4} + \sqrt{\frac{(1-r^2)^4}{4} + \left(\frac{8ar^2F_0}{3m\pi\ k}\right)^2}}. \tag{3.2.77}$$

3.2.10 Solid damping

Solid damping exists in a material if it is imperfectly elastic. When a spring of such material is subjected to cyclic load, the same strain has different values for increasing and decreasing stresses. The stress-strain diagram for a system with such materials forms a close loop, and the energy dissipation per cycle is proportional to the area enclosed by the loop. This is a very common phenomenon in geomaterials. However its magnitude is quite small. This damping is variously called hysteresis damping, material damping, structural damping and displacement damping.

Consider a damping force proportional to the displacement and independent of frequency: damping force $= ax = bkx$; where a and b are constants and a has the dimension of spring constant k and b are dimensionless constants.

As the damping force is opposite in phase to the velocity, to have this force proportional to the displacement, we write the equation of motion in exponential form and obtain a steady state amplitude X by impedance method

$$m\ddot{x} + k(1 + ib)x = F_0 e^{i\omega t} \tag{3.2.78}$$

$$\therefore X = \frac{F_0}{|k - m\omega^2 + ibk|} = \frac{F_0/k}{\sqrt{(1 - r^2)^2 + b^2}} \tag{3.2.79}$$

This implies $c_{eq}\omega/k = b \rightarrow c_{eq} = \frac{bk}{\omega} = a/\omega$.

Hence energy dissipation per cycle $= c_{eq}\omega\pi X^2 = a\pi X^2$.

So the energy dissipation in solid damping may be assumed to be independent of frequency but proportional to the square of displacement (strains) amplitude. This observation reduces the equation of motion to be linear. For mild steel, the energy dissipation is found to be proportional to $X^{2,3}$ and for other materials the amplitude exponent may range from 2 to 3.

3.2.11 Analysis of friction forces (Coulomb friction, dry friction)

Since the steady state motion with non-viscous damping may not be harmonic, the assumption of harmonic motion is reasonable only if damping is not large enough to change its wave appreciably. In many practical problems the damping in a system is small, and its effect may be neglected except near resonance. At resonance it is the damping that governs the amplitude of the motion. Hence, equivalent damping is often used to determine the resonant amplitude.

The coulomb damping force (Timoshenko & Young 1964) is generally assumed to be proportional to the normal force between the two sliding bodies. Hence, it is independent of the displacement and its derivatives, and, for a given sliding body, the frictional force is of constant magnitude.

It should be remembered that in a physical system the force required to start the motion is usually greater than that is required to maintain the motion. Frictional

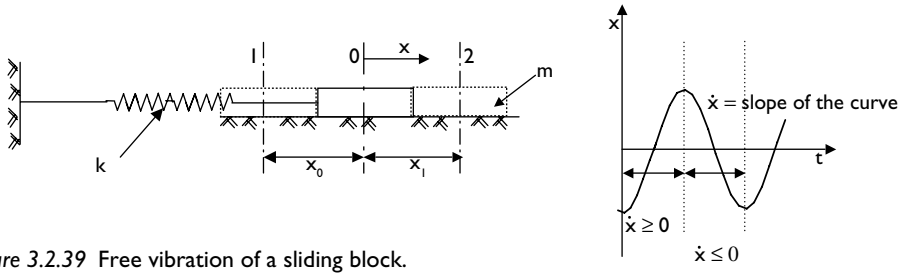


Figure 3.2.39 Free vibration of a sliding block.

coefficient is not necessarily constant, depending somewhat on the surface roughness of the sliding surface.

3.2.11.1 Free vibration considering the friction force

Let m is a mass sliding on a rough surface shown in Figure 3.2.39. Let the spring is at unstressed condition at position '0'. The direction of x is positive as shown in the Figure. The mass m is given an initial displacement $-x_0$ and is at position '1' at $t = 0$. Subsequently the mass is released and slides to position '2' through position '0'. While moving from '1' to '2', $\dot{x} \geq 0$; again the mass slides back from '2' to '1' and through '0', here $\dot{x} \leq 0$.

Cases

a Movement from left to right ($\dot{x} \geq 0$) (Figure 3.2.40)
Equation of motion can be written as

$$m\ddot{x} + kx = -f$$

b Movements from right to left ($\dot{x} \leq 0$) (Figure 3.2.41).
Equation of motion can be written as

$$m\ddot{x} + kx = f$$

General equation of motion of a mass sliding over a rough surface may be written as

$$m\ddot{x} + kx = \mp f \tag{3.2.80}$$

Solution: Substitute $x = z \pm \frac{f}{k}$ in Equation (3.2.80) to obtain $m\ddot{z} + k(z \pm \frac{f}{k}) = \pm f$ i.e

$$m\ddot{z} + kz = 0 \tag{3.2.81}$$

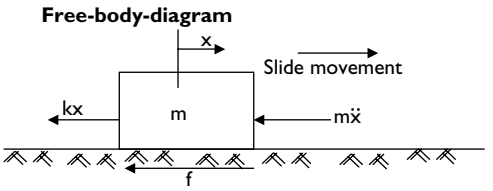


Figure 3.2.40 Block sliding left to right.

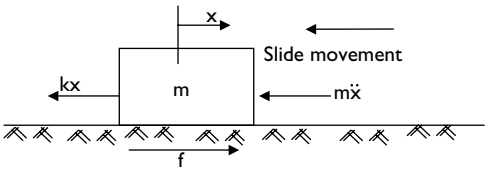


Figure 3.2.41 Block sliding right to left.

Solution of Equation (3.2.84) is

$$z = C_1 \cos \omega_n t + C_2 \sin \omega_n t; \quad \text{or, } x = C_1 \cos \omega_n t + C_2 \sin \omega_n t \mp \frac{f}{k} \tag{3.2.82}$$

in which negative sign is for block motion left to right and positive sign for the movement right to left; C_1 and C_2 are to be found out from the initial conditions.

Let it be given that, at $t = 0$; $x = x_0$ and $\dot{x} = 0$, substituting in Equation (3.2.82) $\rightarrow C_2 = 0$.

Movement from left to right

$$x = C_1' \cos \omega_n t - f/k; -x_0 = C_1' - f/k \quad \rightarrow \quad C_1' = -(x_0 - f/k)$$

$$\text{Solution is:} \quad x = -(x_0 - f/k) \cos \omega_n t - f/k; \quad \text{valid for } \dot{x} > 0. \tag{3.2.83}$$

Now at the end of $\omega_n t = \pi$, the movement from right to left starts (i.e. $\dot{x} < 0$). Hence displacement at the end of $\omega_n t = \pi$ for left to right is equal to the displacement at $t = 0$ for right to left (velocity is $\dot{x}_0 < 0$).

$$\text{Thus} \quad x_0^{r\,\text{to}\,\ell} = x_0 - \frac{f}{k} - \frac{f}{k} = x_0 - 2\frac{f}{k}.$$

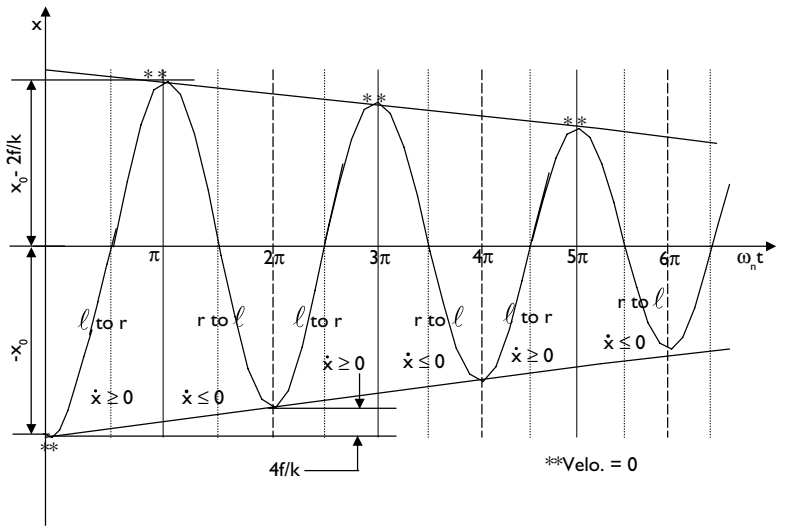


Figure 3.2.42 Response curve for a SDOF system with frictional damping.

Movement from right to left

$x = C_1'' \cos \omega_n t + f/k$, substituting initial condition,

$$x_0^{r \text{ to } \ell} = C_1'' + \frac{f}{k} \quad \Rightarrow \quad C_1'' = x_0 - 3\frac{f}{k},$$

$$\text{Solution is:} \quad x = \left(x_0 - 3\frac{f}{k}\right) \cos \omega_n t + \frac{f}{k}; \quad \text{valid for } \dot{x} < 0. \tag{3.2.84}$$

And $x_0^{\ell \text{ to } r} = -\left(x_0 - 3\frac{f}{k}\right) + \frac{f}{k}$, using $\omega_n t = \pi$. $\Rightarrow x_0^{\ell \text{ to } r} = -x_0 + 4\frac{f}{k}$ and so on.

Thus, the amplitude diminishes by $4f/k$ in each cycle, i.e. the sequence of amplitudes forms an arithmetic progression and the envelope of the curve ia a straight line and the tangent of the angle that the line makes with the t-axis is $4f/kT$. Calculations can be continued only until the the amplitude becomes less than say, a small value α, and the motion ceases completely since the elastic force kx_0 at beginning of movement, from right to left or from left to right will not be large enough to resist the friction force.

A graphical representation of Eqns. (3.2.83) and (3.2.84) is shown in Figure 3.2.42. It can be observed that attenuation of the response in this case is linear unlike an asymptotic attenuation in viscous damping shown earlier.

3.2.11.2 Forced vibration considering the friction force

System is shown in Figure 3.2.43.

Motions from left to right: $m\ddot{x} + kx = -f + F_0 \sin \omega t$

Motions from right to left: $m\ddot{x} + kx = f + F_0 \sin \omega t$

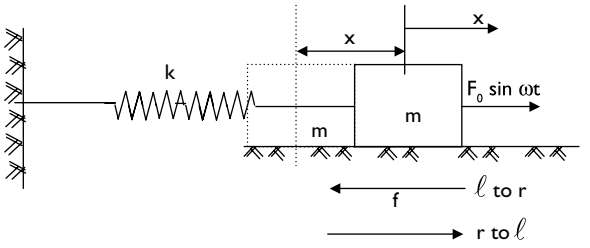


Figure 3.2.43 Forced vibration of a sliding block.

If an equivalent viscous damping to friction is used, we have from energy consideration:

Energy dissipation per cycle = $4fA$ (friction) [left to right $(2A)$ + right to left $(2A)$] = $C_{eq}\pi\omega A^2$ (viscous)

$$\text{Hence,} \quad C_{eq} = \frac{4f}{\pi\omega A}. \tag{3.2.85}$$

The difference in using C_{eq} is that we have an asymptotic dissipation in equivalent viscous damping whereas coulomb damping is linear. However, for small values of f, it gives a reasonable value for the response.

In forced vibration, we have,

$$m\ddot{z} + C_{eq}\dot{z} + kz = F_0 \sin\omega t; \quad \text{as the governing equation of motion.} \tag{3.2.86}$$

Steady state solution is given by

$$z = \frac{F_0/k}{\sqrt{(1-r^2)^2 + \left(C_{eq}\frac{\omega}{k}\right)^2}} \sin(\omega t - \phi) = A\sin(\omega t - \phi) \tag{3.2.87}$$

From Eqn. (3.2.87), we can obtain $A^2\left[(1-r^2)^2 + \left(\frac{4f}{\pi A k}\right)^2\right] = \left(\frac{F_0}{k}\right)^2$ and a value of A can be obtained as

$$A = \frac{\frac{F_0}{k}}{(1-r^2)}\sqrt{1 - \left(\frac{4f}{\pi F_0}\right)^2} \tag{3.2.88}$$

Equation (3.2.88) gives a real value of A only if $(4f/\Pi F_0) < 1$. It is clear that the amplitude at resonance is always theoretically infinite.

3.2.12 Response under impulsive loading

If the duration of loading is very small in comparison to the natural period of the system, the load is called an impulsive load or an impulse. The impulse $\hat{F}$ acting on a mass will result in a sudden change in its velocity equal to $\hat{F}/m$ without any appreciable change in its displacement. A mass m, which is initially at rest, will gain a velocity, say v_0, and can be written in the following form

$$\hat{F} = \int_0^{\Lambda t} F(t)dt = mv_0 \tag{3.2.89}$$

and with any change in displacement. This can be shown as given in Figure 3.2.44.

A free undamped vibration of a single-degree-of freedom system can be written as

$$x = (v_0/\omega_n)\sin\omega_n t = \hat{F}\,g(t) \tag{3.2.90}$$

where, $g(t) = \sin\omega_n t/\omega_n m =$ impulse response function.

The response is, thus, a sinusoidal vibration at the natural frequency with amplitude $(\hat{F}/m\omega_n)$. This is shown in Figure 3.2.45.

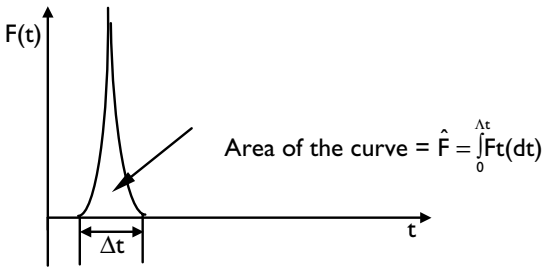


Figure 3.2.44 Definition of an impulse.

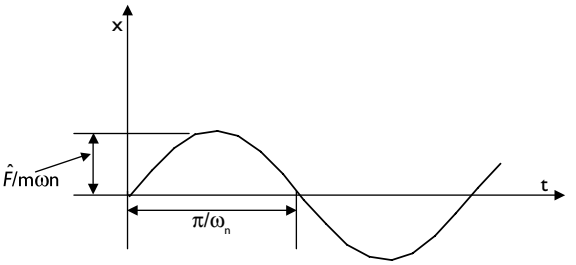


Figure 3.2.45 Sinusoidal response due to an impulse.

For a damped (viscous) single-degree-of freedom system Equation (3.2.90) can be written as

$$x = \frac{v_0}{\omega_n} e^{-D\omega_n t} \sin \omega_{nd} t \; = \; \hat{F} g(t) \tag{3.2.91}$$

in which $g(t) = \frac{e^{-D\omega_n t} \sin \omega_{nd} t}{m\omega_n}$; and $\omega_{nd} = \omega_n \sqrt{(1 - D^2)}$ = damped natural frequency of the system.

3.2.13 General solution for any arbitrary forcing system

Consider an undamped single-degree-of freedom system subjected to an arbitrary forcing function as shown in Figure 3.2.46. The force diagram can be considered to be consisting of a large number of thin slices each having area $F(\xi)d\xi$. Contribution of this force to the response of the system at any time t is dependent upon the elapsed time $(t - \xi)$. The response of each of these impulses can be obtained through Eqns. (3.2.90) and (3.2.91), as the case may be. To obtain the response of an arbitrary force $F(t)$, individual contribution of all these slices can be added up to obtain the complete response of the system. Thus, by combining all such contributions, the response to the arbitrary excitation $F(t)$ is represented by the integral over a total time t for a linear system can be written as

$$x(t) = \int_0^t F(t - \xi)\, g(\xi)\, d\xi = \int_0^t F(\xi)\, g(t - \xi)\, d\xi; \quad \text{for } t < t_p \tag{3.2.92}$$

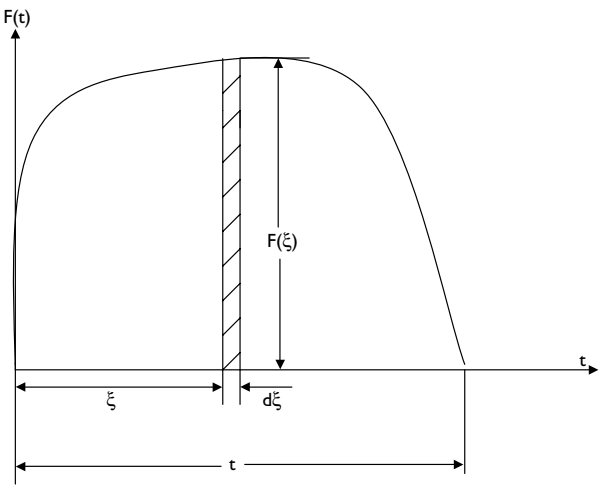


Figure 3.2.46 General loading.

When t is greater than the pulse time, say t_p, the upper limit of the general equation, remains at t_p; the integral then can be written as

$$x(t) = \int_0^{t_p} F(\xi)\, g(t-\xi)\, d\xi + \int_{t_p}^{t} F(\xi)\, g(t-\xi)\, d\xi$$
$$= \int_0^{t_p} F(\xi)\, g(t-\xi)\, d\xi \quad \text{as } F(\xi) = 0, \quad \text{for } \xi > t_p. \tag{3.2.93}$$

For an undamped and damped system can be written as

$$x = \frac{\hat{F}}{m\omega_n} \int_0^t F(\xi) \sin\, \omega_n\, (t-\xi) d\xi \quad \text{and} \tag{3.2.94}$$

$$x = \frac{\hat{F}}{m\omega_{nd}} \int_0^t F(\xi)\; e^{-D\omega_n t} \sin\, \omega_{nd}\, (t-\xi) d\xi \tag{3.2.95}$$

Equations (3.2.94) and (3.2.95) present a complete solution for transient as well as steady state problems. This is also known as convolution integral or Duhamel integral or superposition integral valid for linear problems. If $F(t)$ is given in a simple analytical form, Equation (3.2.94) can be obtained in closed form whereas for a complicated $F(t)$, one has to go in for a numerical technique. A general solution of the problem having initial conditions like, $x_0 = \dot{x}_0 = 0$ can be written as

3.2.13.1 For an undamped system

$$x = x_0 \cos \omega_n t + \frac{\dot{x}_0}{\omega_n} \sin \omega_n t + \frac{\hat{F}}{m\omega_n} \int_0^t F(\xi) \sin \omega_n (t-\xi) d\xi \tag{3.2.96}$$

3.2.13.2 For a damped system

$$x = e^{-\omega_n D t} \left[x_0 \cos \omega_{nd} t + \frac{\dot{x}_0}{\omega_{nd}} \sin \omega_{nd} t \right] + \frac{\hat{F}}{m\omega_{nd}} \int_0^t F(\xi) \sin \omega_{nd} (t-\xi) d\xi \tag{3.2.97}$$

Example 3.2.7

1 A single-degree-of freedom system subjected to step excitation (Figure 3.2.47):

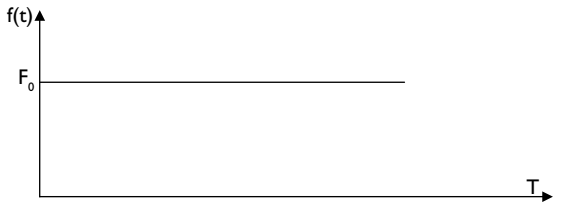


Figure 3.2.47 Unit step function.

Solution:

a Consider an undamped system

From Equation (3.2.93), $g(t) = \dfrac{1}{m\omega_n} \sin\, \omega_n t$

Solution is $x(t) = \dfrac{F_0}{m\omega_n} \displaystyle\int_0^t \sin\, \omega_n (t-\xi) d\xi = \frac{F_0}{k}(1 - \cos \omega_n t)$

Peak response to step excitation of magnitude F_0 is twice the statical value.

b Consider a damped system

From Equation (3.2.94), $g(t) = \dfrac{e^{-D\omega_n t}}{m\omega_n \sqrt{(1-D^2)}} \sin\, (\sqrt{1-D^2})\, \omega_n t$

Solution is $x(t) = \displaystyle\int_0^t \frac{F_0 e^{-D\omega_n\,(t-\xi)}}{m\omega_{nd}} \sin \omega_{nd}\,(t-\xi) d\xi;$

substitute $\omega_{nd}\,(t-\xi) = z\,; \rightarrow dz = -\omega_{nd}\, d\xi$

$$x(t) = \frac{F_0}{m\,\omega_{nd}^2} \int_0^t e^{-\frac{D\omega_n}{\omega_{nd}} z} \sin z dz = \frac{F_0}{k}[1 - \cos(\omega_{nd} t - \Psi) e^{-D\omega_n t}]$$

in which $\tan \Psi = \frac{D\omega_n}{\omega_n \sqrt{1-D^2}} = \frac{D}{\sqrt{1-D^2}}$.

A plot of xk/F_0 versus $\omega_n t$ with D as a parameter is shown in Figure 3.2.48 and it is evident that the peak response is less than $2F_0/k$ when damping is present.

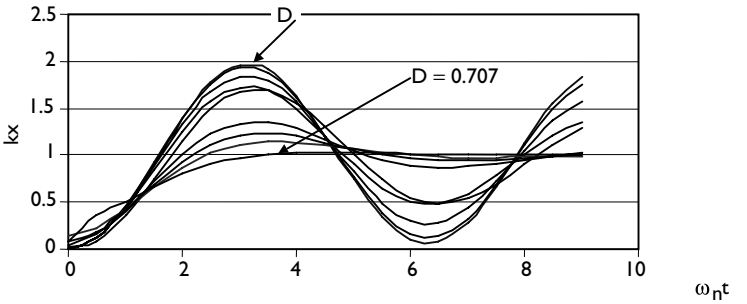


Figure 3.2.48 Peak response for unit step function.

Alternative solution

Alternatively, one can simply consider the differential equation as $\ddot{x} + 2D\omega_n \dot{x} + \omega_n^2 x = F_0/m$, whose solution is the sum of homogeneous equation plus that of the particular integral $(-F_0/m\omega_n^2)$. Thus the solution is:

$$x(t) = C_2\, e^{-D\omega_n t}\, \sin\left[\sqrt{1-D^2}\,\omega_n t - \psi\right] + \frac{F_0}{m\omega_n^2}$$

fitted to the initial conditions of $x(0) = 0 = \dot{x}(0)$ will result in

$$x = \frac{F_0}{k}\left[1 - \frac{e^{-D\omega_n t}}{\sqrt{1-D^2}}\cos\left(\sqrt{1-D^2}\,\omega_n t - \psi\right)\right]; \quad \text{with } \tan\psi = \frac{D}{\sqrt{1-D^2}}.$$

2 Consider an undamped mass-spring system where the motion of the base is specified by a velocity pulse of the form (Figure 3.2.49)

$\dot{y}(t) = v_0\, e^{-t/t_0}$, the time rate of change is $a = \dot{v}$.

Solution:

Velocity pulse at $t = 0$ has a sudden jump from zero to its rate of change (or acceleration) is infinite.

Acceleration of the base becomes [differentiating $\dot{y}(t)$], $\ddot{y}(t) = v_0\delta(t) - \frac{v_0}{t_0}e^{-\frac{t}{t_0}}$.

These functions can be brought under the head of "singularity Functions" defined hereunder:

Unit step function $u(t) = \langle t-\tau\rangle^0$,
Differentiation of $\langle t-\tau\rangle^0 = \langle t-\tau\rangle_*^{-1}$ = delta function = $\delta(t-\tau)$,

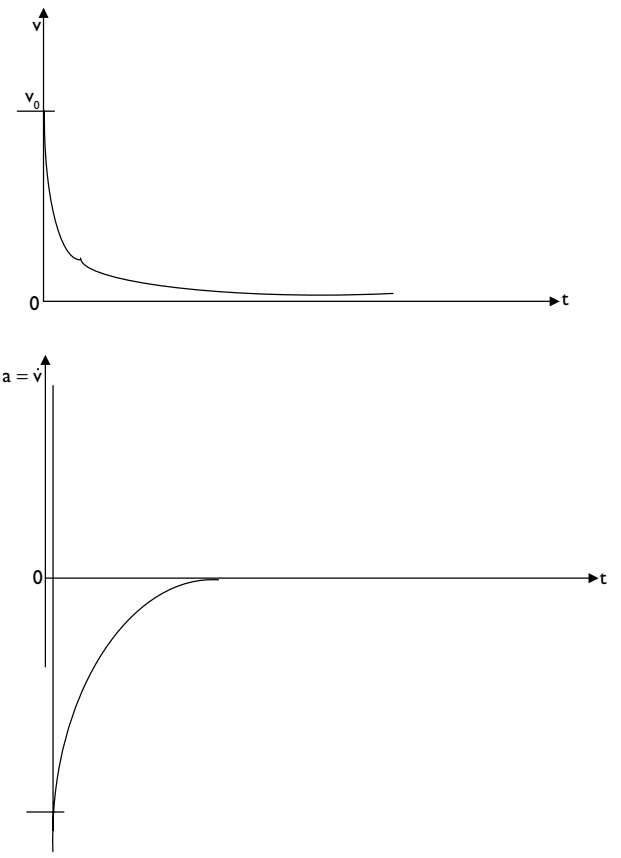


Figure 3.2.49 Velocity excitation.

Differentiation of $\langle t-\tau\rangle_*^{-1} = \langle t-\tau\rangle_*^{-2}$ = unit doublet function.

These functions have the magnitude unity only argument $(t-\tau)$ is zero or else the value is zero and they follow integration and differentiation as given above.

$$\text{Thus } z(t) = -\frac{1}{\omega_n}\int_0^t \ddot{y}(\xi)\,\sin\omega_n\,(t-\xi)d\xi$$

$$= \frac{v_0\,t_0}{1+(\omega_n\,t_0)^2}[e^{-t/t_0} - \omega_n\,t_0\,\sin\omega_n t - \cos\omega_n t].$$

3 An undamped system subjected to a rectangular pulse (Figure 3.2.50):

An undamped spring-mass system can be written as $g(t) = \dfrac{1}{m\omega_n} \sin \omega_n t$

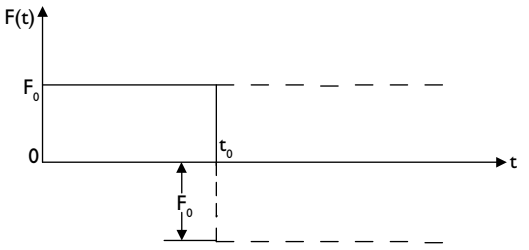


Figure 3.2.50 Rectangular impulse.

Solution is, $x(t) = \dfrac{F_0}{m\omega_n} \int_0^t \sin \omega_n (t - \xi)\, d\xi - \dfrac{F_0}{m\omega_n} \int_{t_0}^t \sin \omega_n (t - \xi) d\xi$

i.e. $x(t) = \dfrac{F_0}{k}(1 - \cos \omega_n t) - \dfrac{F_0}{k}[1 - \cos \omega_n (t - t_0)]$ for $t > t_0$.

3.2.14 Response spectra

A shock represents a sudden application of a force or other form of disruption which results in a transient response of a system. The maximum value of the response is a good measure of the severity of the shock and is, of course, dependent upon the dynamic characteristics of the system. In order to categorize all types of shock excitation, a single-degree-of freedom undamped oscillator is chosen as a standard system.

A response spectrum is a plot of the maximum peak response of the single-degree-of freedom oscillator and represented as a function of the natural frequency of the oscillator. Different types of shock excitation will then result in different response spectra.

Since the response spectrum is determined from a single point on the time response curve, which is in itself an incomplete bit of information, it does not uniquely define the shock input. It is possible for two different shock excitations to have very similar response spectra.

The response of a system to an arbitrary excitation can be expressed as given in Equation (3.2.97) and the peak response for an undamped single-degree-of freedom is given by

$$x(t)_{\max} = \left| \frac{1}{m\omega_n} \int_0^t f(\xi) \sin \omega_n (t - \xi) d\xi \right|_{\max} \tag{3.2.98}$$

In the case where the shock is due to a sudden motion of the support point, $f(t)$ in the above equation is replaced by $-\ddot{y}(t)$, the acceleration of the support point and the peak response is given by

$$x(t)_{\max} = \left| \frac{1}{m\omega_n} \int_0^t -\ddot{y}(\xi) \sin \omega_n (t-\xi) d\xi \right|_{\max} . \tag{3.2.99}$$

Associated with the shock excitation $f(t)$ or $-\ddot{y}(t)$ is some characteristic time t_1, such as the duration of the shock pulse. With T as the period of natural frequency of oscillator, the maximum value of $x(t)$ is plotted as a function of t_1/T. Following figures represent response spectra for three different excitations.

Example 3.2.8

Determine the undamped response spectrum for a step function (Figure 3.2.51) with a rise time t_1.

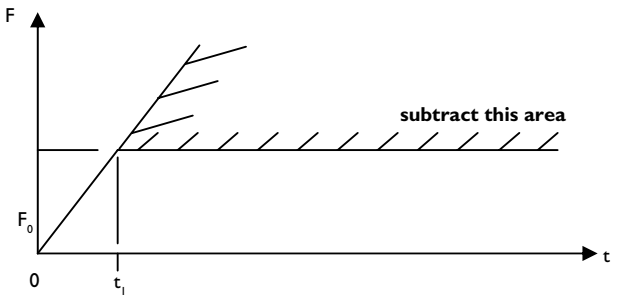


Figure 3.2.51 Ramp excitation.

Solution:

The input can be considered to be the sum of two ramp functions $F_0(t/t_1)$, the second of which is negative and delayed by the time t_1.

For the first ramp: $f(t) = F_0(t/t_1) = (F_0/t_1) < t >_*^1$; $g(t) = \sin \omega_n t/k$ and the response is

$$x(t) = \frac{\omega_n}{k} \int_0^t \frac{F_0 \xi}{t_1} \sin \omega_n (t-\xi) d\xi = \frac{F_0}{k} \left[\frac{t}{t_1} - \frac{\sin \omega_n t}{\omega_n t_1} \right] \quad \text{for } t < t_1.$$

For the second ramp, starting at t_1; $f(t) = -F_0 \left(\frac{t-t_1}{t_1} \right) = \frac{F_0}{t_1} < t - t_1 >_*^1$

$$x(t) = \frac{F_0}{k} \left[\frac{t}{t_1} - \frac{\sin \omega_n t}{\omega_n t_1} \right] \quad \text{at } t = t_1^{-0};$$

$$x(t) = -\frac{F_0}{k} \left[\frac{t-t_1}{t_1} - \frac{\sin \omega_n (t-t_1)}{\omega_n t_1} \right] \quad \text{at } t = t_1^{+0}$$

For $t > t_1 \quad x(t) = \dfrac{F_0}{k}\left[1 - \dfrac{\sin \omega_n t}{\omega_n t_1} + \dfrac{\sin \omega_n (t - t_1)}{\omega_n t_1}\right]$

Differentiating w.r.t. time, t and equating it to zero, the peak time t_p is obtained from

For $t < t_1$

$\dot{x}(t) = \frac{F_0}{k}\left[\frac{1}{t_1} - \frac{\cos \omega_n t}{t_1}\right] = 0$, i.e. $\cos \omega_n t_p = 1$, or $\omega_n t_p$ must be more than 2π as $t_p = 0$ is not possible.

Hence $\omega_n t_p$ must be more than π.

Again, for $t > t_1$

$$\dot{x}(t) = \frac{F_0}{k}\left[-\frac{\cos \omega_n t}{t_1} + \frac{\cos \omega_n (t - t_1)}{t_1}\right] = 0 : \rightarrow \tan \omega_n t = \frac{1 - \cos \omega_n t_1}{\sin \omega_n t_1}$$

$$\rightarrow \tan \omega_n t_p = \tan \frac{\omega_n t_1}{2} \rightarrow t_p = \frac{t_1}{2} = \pi$$

Since $\omega_n t_p$ must be greater than π

$$\sin \omega_n t_p = -\sqrt{\frac{1}{2}(1 - \cos \omega_n t_1)}; \qquad \cos \omega_n t_p = -\frac{\sin \omega_n t_1}{\sqrt{2(1 - \cos \omega_n t_1)}}.$$

Substituting these quantities into the expression for $x(t)$, peak amplitude is found as

$\left(\frac{xk}{F_0}\right)_{\max} = 1 + \frac{1}{\omega_n t_1}\sqrt{2(1 - \cos \omega_n t_1)}$, letting $T = 2\pi/\omega_n$ be the period of the oscillator the above equation is plotted as shown in Figure 3.2.52.

$\left[\frac{xk}{F_0}\right] \rightarrow a$ measure of the dynamic effect over the statically applied load.

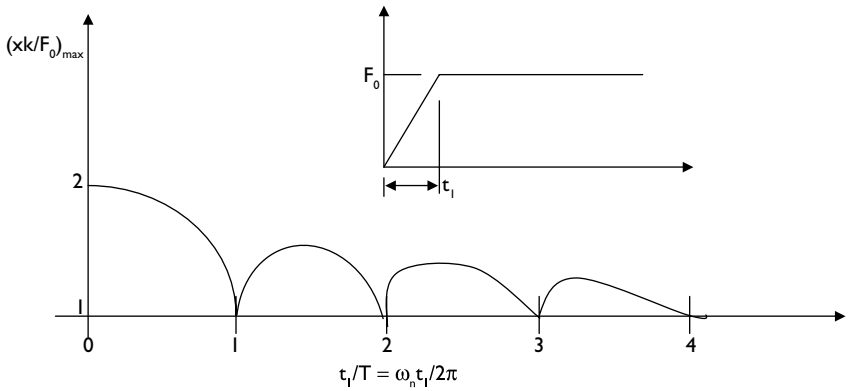


Figure 3.2.52 Response spectra for ramp excitation.

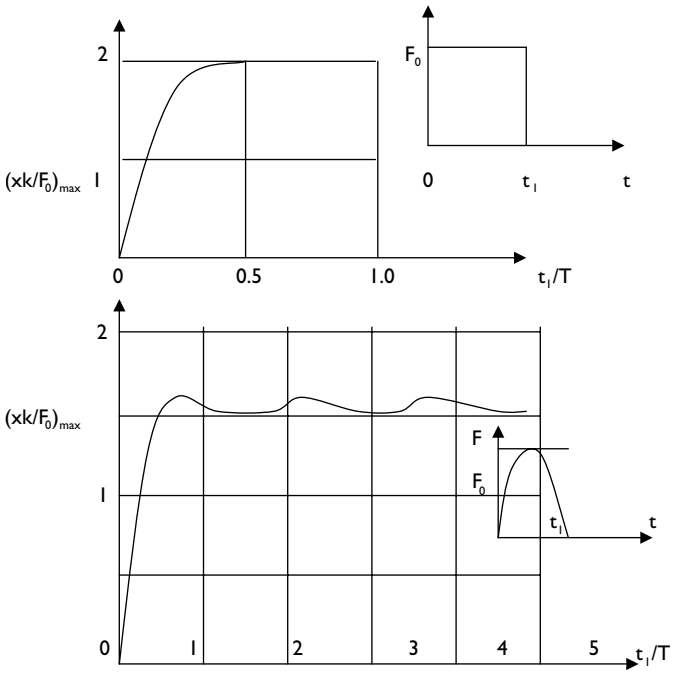


Figure 3.2.53 Response spectra for variety of loading.

Response spectra for a variety loading is shown in Figure 3.2.53.

Example 3.2.9

Determine the response spectrum for the base velocity input (Figure 3.2.54), $\dot{y}(t) = v_0\, e^{-t/t_0}$.

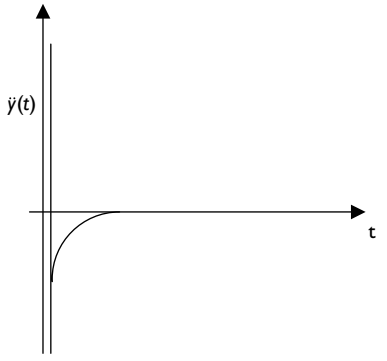


Figure 3.2.54 Base velocity input.

Solution:

The relative displacement $z(t)$ was found earlier,

$$z(t) = \frac{v_0\, t_0}{1 + (\omega_n t_0)^2}[e^{-t/t_0} - \omega_n t_0 \sin \omega_n t - \cos \omega_n t]$$

To determine the peak value z_p, the usual procedure is to differentiate the equation with respect to t, set it equal to zero, and substitute this time back into the equation for $z(t)$. This is a complicated procedure. Instead, one can follow a different approach.

For a very stiff system [$k/m = \omega_n^2$, stiff means k is large], which corresponds to large ω_n, the peak response will certainly occur at small t, and one would obtain for the time varying part of the equation, the peak value as $(1 - \omega_n t_0 - 1) = \omega_n t_0$.

For large ω_n, the peak value will be nearly equal to

$$|Z_p| \approx \frac{v_0 t_0}{1 + (\omega_n t_0)^2}(\omega_n t_0) \approx \frac{v_0 t_0}{\omega_n t_0}.$$

So that $z_p/v_0 t_0$ plots against $\omega_n t_0$ as a rectangular hyperbola.

For small ω_n, or a very soft system, the duration of the input would be small compared to the period of the system. Hence the input would appear as an impulsive doublet as shown below strength being $v_0 t_0 \delta'(t)$ [$v_0 t_0 < t >_*^{-2}$, singularity function].

The solution for $z(t)$ is then: $z(t) = v_0 t_0 cos \omega_n t$

[General, $z(t) = \frac{v_0 t_0}{1+(\omega_n t_0)^2}[e^{-t/t_0} - \omega_n t_0 \sin \omega_n t - \cos \omega_n t]$, when ω_n is small and t is small compared to the period of the system]

---

and its peak value is $|z| \approx v_0\, t_0$

With these extreme conditions evaluated, one can now fill in the response spectrum as shown in Figure 3.2.55.

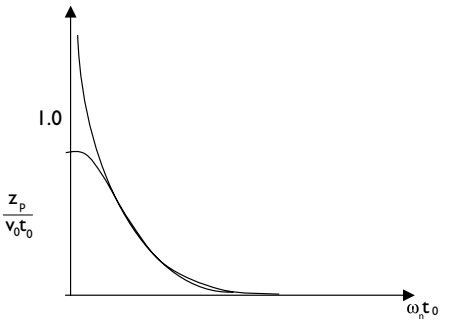


Figure 3.2.55 Response spectra for base velocity input.

3.2.15 Earthquake type of excitation

Response of a structure or a foundation to earthquake type excitation is a very important study for a civil engineer. For other than earthquake itself the phenomenon can also occur due to movement of rapid mass transit systems like underground metro rail, underground blasts in mining areas, driving of piles near sensitive structures etc.

However to understand the same in proper perspective we feel presenting the same in detail herein may be a bit pre-matured and would prefer that you first go through Chapter 5 (Vol. 1) first and then would be in a better position to appreciate its significance.

Thus this has been dealt in some detail in Chapter 3 (Vol. 2) where we study earthquake engineering as a topic itself.

3.3 STABILITY OF DYNAMIC SOLUTIONS

3.3.1 Phase planes and stability of solution

Other than the people, who specialize in the theory of vibration in the realms of applied physics and mathematics, study of phase plane and stability solution is usually

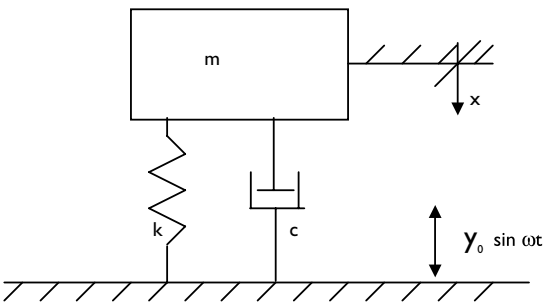


Figure 3.2.56 A single-degree-of freedom system subjected to ground motion $y(t)$.

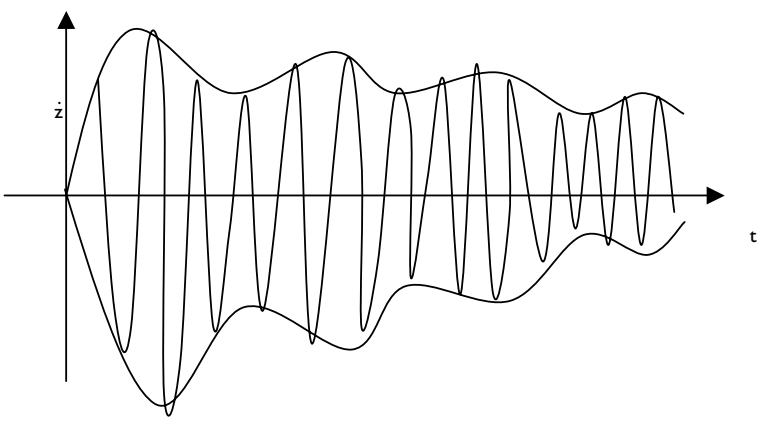


Figure 3.2.57 Modulated wave.

an ignored topic in the realms of engineering technology. As such, it is not surprising that there are many engineers who are aware of this topic, yet are not very clear as to its application and usefulness.

In the most simplistic term phase plane study can be termed as a geometric interpretation of the differential equation of motion and could be stated as a qualitative study of the behaviour of the body under motion.

This has a great application especially when the oscillation of a body is deemed non-linear.

Though non linear dynamic analysis of civil engineering structures and foundations is a recent trend yet many of the basic characteristics of non linear dynamic equation of motion has been long been studied in different branch of physics and science.

The study has revealed that systems undergoing non linear vibration and especially having large amplitudes develop completely different behaviour and pattern and that which cannot be predicted based on linear analysis.

Systems have also been found to suddenly become unstable showing no previous sign of such behaviour. It is in such cases, phase plane and phase portrait study is of great help to understand pictorially how the body would behave under such non linear condition.

3.3.2 Basics of differential equation

An *n*th order differential equation can be reduced to a system of *n* first-order differential equations. Thus, it permits the study and solution of single equations by methods for systems. An nth order differential equation

$$y^{(n)} = F(t, y, y', \ldots, y^{(n-1)}) \tag{3.3.1}$$

can be reduced to a system of n first-order differential equations by setting

$$y_1 = y, \quad y_2 = y', \ldots, y_n = y^{(n-1)}. \tag{3.3.2}$$

and the system of first-order equations can be written as

$$\begin{aligned} y_1' &= y_2 \\ y_2' &= y_3 \\ &\vdots \\ y_{n-1}' &= y_n \\ y_n' &= F(t, y_1, y_2, \ldots, y_n) \end{aligned} \tag{3.3.3}$$

The first order system in Equation (3.3.3) can be expressed in a more general way as

$$\begin{aligned} y_1' &= f_1(t, y_1, y_2, \ldots, y_n) \\ y_2' &= f_2(t, y_1, y_2, \ldots, y_n) \\ y_3' &= f_3(t, y_1, y_2, \ldots, y_n) \end{aligned} \tag{3.3.4}$$

$$\vdots$$

$$y_n' = f_n(t, y_1, y_2, \ldots, y_n)$$

A solution of Equation (3.3.4) in some interval $a < t < b$ is a set of n-differentiable functions, namely,

$$y_1 = q_1(t), y_2 = q_2(t), \ldots, y_n = q_n(t).$$

Thus the solution vector may be written as

$$\boldsymbol{y} = \boldsymbol{q}(t)$$

An initial value problem for Equation (3.3.4) consists of n given initial conditions

$$y_1(t_0) = k_1, y_2(t_0) = k_2, \ldots, y_n(t_0) = k_n, \tag{3.3.5}$$

In vector form:

$$\boldsymbol{y}(t_0) = \boldsymbol{k},$$

t_0 is a specified value of time t in the interval considered and the components $\boldsymbol{k} = <k_1, k_2, \ldots, k_n>$ are given values.

Example 3.3.1

Consider the mass-spring-dashpot system:

$$y'' + \frac{c}{m}y' + \frac{k}{m}y = 0$$

Using $y_1' = y_2$; $y_2' = -\frac{k}{m}y_1 - \frac{c}{m}y_2$, and writing $y^T = <y_1\ y_2>$, the matrix form of the equations is

$$\{\boldsymbol{y}\} = \begin{bmatrix} 0 & 1 \\ -\frac{k}{m} & -\frac{c}{m} \end{bmatrix} \begin{Bmatrix} y_1 \\ y_2 \end{Bmatrix}$$

the characteristic equation is

$$\det(\boldsymbol{A} - \lambda \boldsymbol{I}) \begin{vmatrix} -\lambda & 1 \\ -\frac{k}{m} & -\frac{c}{m} - \lambda \end{vmatrix} = \lambda^2 + \frac{c}{m}\lambda + \frac{k}{m} = 0.$$

Assuming $m = 1$, $c = 1$ and $k = 1$, solution is $\lambda_1 = -(1 + i\sqrt{3})/2$, and $\lambda_2 = -(1 - i\sqrt{3})/2$ are the eigenvalues, eigenvectors are obtained from:

$$[(1 + i\sqrt{3})/2]x_1 + x_2 = 0 \quad \rightarrow \quad x = <2/(1 + i\sqrt{3}) - 1>^T$$
$$[(1 - i\sqrt{3})/2]x_1 + x_2 = 0 \quad \rightarrow \quad x = <1 - (1 - i\sqrt{3})/2>^T$$

The solution is

$$\boldsymbol{y} = A_1 \begin{Bmatrix} 2/(1 + i\sqrt{3}) \\ -1 \end{Bmatrix} e^{-[(1+i\sqrt{3})/2]t} + A_2 \begin{Bmatrix} 1 \\ -(1 - i\sqrt{3})/2 \end{Bmatrix} e^{-[(1-i\sqrt{3})/2]t}$$

Thus $y_1 = A_1[2/(1 + i\sqrt{3})]e^{-[(1+i\sqrt{3})/2]t} + A_2 e^{-[(1-i\sqrt{3})/2]t}$

and $y_2 = -A_1 e^{-[(1+i\sqrt{3})/2]t} - A_2[-(1 - i\sqrt{3})/2]e^{-[(1-i\sqrt{3})/2]t} = y_1'$

3.3.3 Homogeneous Systems with Constant Coefficients, Phase Plane, Critical Points

Let us consider a homogeneous linear system of the type

$$\frac{dy_i}{dt} = \sum_{j=1}^{n} a_{ij} y_j \quad i = 1, 2, \ldots, n \tag{3.3.6}$$

Let us assume that a_{ij} are constants and do not depend on t. For a single equation $y' = ky$ has the solution $y = Ce^{kt}$, accordingly we may try

$$y_i = x_i e^{\lambda t}, \quad i = 1, 2, \ldots, n \tag{3.3.7}$$

as a solution to Equation (3.3.6). Substituting this as a solution to Equation (3.3.6) and writing in matrix $(n \times n)$ form, we have

$$\boldsymbol{y}' = \lambda \boldsymbol{X} e^{\lambda t} = \boldsymbol{A}\boldsymbol{X} e^{\lambda t}$$

Dividing by $e^{\lambda t}$, we are left with the eigenvalue problem

$$\boldsymbol{A}\boldsymbol{X} = \lambda \boldsymbol{X} \tag{3.3.8}$$

The non-trivial solution of Equation (3.3.6) are of the form Equation (3.3.7), where λ is an eigenvalue of $\boldsymbol{A}$ and $\boldsymbol{X}$ is a corresponding eigenvector.

Now, let us assume that $\boldsymbol{A}$ has a basis of n-eigenvectors $\boldsymbol{x}^1, \boldsymbol{x}^2, \ldots, \boldsymbol{x}^n$ corresponding to eigenvalues $\lambda_1, \lambda_2, \ldots, \lambda_n$ [which may be all different or some of which or all of which may be equal].

Basis. General solution, Wronskian

By a basis or a fundamental system of solution of the homogeneous system:

$$\boldsymbol{y}' = \boldsymbol{A}\boldsymbol{y} \tag{a}$$

on some interval J we mean a linearly independent set of n-equations $\boldsymbol{y}^1, \boldsymbol{y}^2, \ldots, \boldsymbol{y}^n$ of the equation on that interval. The following linear combination of solutions

$$\boldsymbol{y} = c_1\boldsymbol{y}^1 + c_2\boldsymbol{y}^2 + \cdots + c_n\boldsymbol{y}^n, \quad c_1, c_2, \ldots, c_n \text{ being arbitrary.} \tag{b}$$

is called a general solution of Equation (a) on J. It can be shown that if the $a_{ij}(t)$ in Equation (a) are continuous on J then Equation (3.3.4) has a basis of solution on J, hence a general solution, which include every solution of Equation (3.3.4) on J.

One can write n-solutions $\boldsymbol{y}^1, \boldsymbol{y}^2, \ldots, \boldsymbol{y}^n$ of Equation (3.3.4) on some interval J as columns of an $n \times n$ matrix

$$\boldsymbol{Y} = [\boldsymbol{y}^1\ \boldsymbol{y}^2 \ldots \boldsymbol{y}^n] \tag{c}$$

The determinant of $\boldsymbol{Y}$ is called the Wronskian of $\boldsymbol{y}^1, \boldsymbol{y}^2, \ldots, \boldsymbol{y}^n$ and is written as

$$W(\boldsymbol{y}^1, \boldsymbol{y}^2, \ldots, \boldsymbol{y}^n) = \begin{vmatrix} y_1^1 & y_1^2 & \cdots & y_1^n \\ y_2^1 & y_2^2 & \cdots & y_2^n \\ \cdots & \cdots & \cdots & \cdots \\ y_n^1 & y_n^2 & \cdots & y_n^n \end{vmatrix} \tag{d}$$

The columns are these solutions, each in terms of components. These solutions form a basis on J if W is not zero at any $t = t_1$ in this interval. W either is identically zero or is nowhere zero in J. If these solutions form a basis (a fundamental system), then Equation (d) is called the fundamental matrix.

Example 3.3.2

If y and z are solutions of a second order homogeneous linear differential equation, their Wronskian is

$$W = \begin{vmatrix} y & z \\ y' & z' \end{vmatrix}$$

If we write this equation as a system, we have to set $y = y_1, y' = y_1' = y_2$, and similarly for z. Thus $W(y, z)$ becomes Equation (d) with $n = 2$.

Then the corresponding solution of Equation (3.3.7) are

$$\boldsymbol{y}^1 = \boldsymbol{x}^1 e^{\lambda_{11} t}, \quad \boldsymbol{y}^2 = \boldsymbol{x}^2 e^{\lambda_2 t}, \ldots, \boldsymbol{y}^n = \boldsymbol{x}^n e^{\lambda_n t} \tag{3.3.9}$$

Their Wronskian is

$$W(\boldsymbol{y}^1, \boldsymbol{y}^2, \ldots, \boldsymbol{y}^n) = e^{(\lambda_1 + \lambda_2 + \cdots + \lambda_n)t} \begin{vmatrix} x_1^1 & x_1^2 & \ldots & x_1^n \\ x_2^1 & x_2^2 & \ldots & x_2^n \\ \ldots & \ldots & \ldots & \ldots \\ x_n^1 & x_n^2 & \ldots & x_n^n \end{vmatrix} \tag{3.3.10}$$

In Equation (3.3.10), the exponential terms are never zero, and the determinant is not zero either because its columns are the linearly independent eigenvectors that form a basis. Hence, we have the theory for a general solution as follows:

If the constant matrix $\boldsymbol{A}$ *in Equation (3.3.6) has a linearly independent set of n eigenvectors {holds if* $\boldsymbol{A}$ *is symmetric or if it has n distinct eigenvalues] then the corresponding solutions* $\boldsymbol{y}^1, \boldsymbol{y}^2, \ldots, \boldsymbol{y}^n$ *in Equation (3.3.10) form a basis of solutions of Equation (3.3.6), and the corresponding general solution is*

$$\boldsymbol{y} = c_1 \boldsymbol{x}^1 e^{\lambda_1 t} + c_2 \boldsymbol{x}^2 e^{\lambda_2 t} + \cdots + c_n \boldsymbol{x}^n e^{\lambda_n t} \tag{3.3.11}$$

3.3.3.1 Phase plane

With the advent and advances in of computer graphics, phase plane projections have become an integral part of solution procedures. Let the linear system in Equation (3.3.6) consists of two equations:

$$\boldsymbol{y}' = \boldsymbol{A}\boldsymbol{y} : \text{in long hand notation: } \boldsymbol{y}_1' = a_{11}\, y_1 + a_{12}\, y_2 : y_2' = a_{21}\, y_{11} + a_{22}\, y_2 \tag{3.3.12}$$

$$\text{We can plot solutions: } \boldsymbol{y}(t) = < y_1(t) \quad y_2(t) >^T \tag{3.3.13}$$

of Equation (3.3.12) as two curves against the t-axis, one for each component of $\boldsymbol{y}(\boldsymbol{t})$. We can also plot Equation (3.3.13) as a single curve in the $\boldsymbol{y}_1\ \boldsymbol{y}_2$-plane. This is a parametric representation with parameter t, known from calculus. Such a curve is called a trajectory (an orbit or path) of Equation (3.3.12) The $\boldsymbol{y}_1\ \boldsymbol{y}_2$-plane is called the phase plane of Equation (3.3.6). If we fill the phase plane with trajectories of Equation (3.3.12), we obtain the so-called phase portrait of Equation (3.3.12).

Example 3.3.3

Plot the phase-plane trajectories for the problem

$$\boldsymbol{y}' = \boldsymbol{A}\boldsymbol{y} : \text{given } \boldsymbol{A} = \begin{bmatrix} -3 & 1 \\ 1 & -3 \end{bmatrix}$$

Equations are: $y_1' = -3y_1 + y_2 : y_2' = y_1 - 3y_2$ (3.3.14)

Solution:

Using the solution as $\boldsymbol{y} = \boldsymbol{x}e^{\lambda t}$ and $\boldsymbol{y}' = \lambda \boldsymbol{x}e^{\lambda t}$ and dropping the exponential terms, we have $\boldsymbol{A}\boldsymbol{x} = \lambda \boldsymbol{x}$

The characteristic equation as

$$\det(\boldsymbol{A} - \lambda \boldsymbol{I}) = \begin{vmatrix} -3-\lambda & 1 \\ 1 & -3-\lambda \end{vmatrix} = \lambda^2 + 6\lambda + 8 = 0 : \text{eigenvalues are :}$$

$\lambda_1 = -2;\ \lambda_2 = -4.$

Eigenvectors are obtained from: $(-3 - \lambda)x_1 + x_2 = 0$

For $\lambda_1 = -2$, this is $-x_1 + x_2 = 0$; hence we can write $\boldsymbol{x}^1 = <1 \quad 1>^T$.

For $\lambda_2 = -4$, this is $x_1 + x_2 = 0$; hence we can write $\boldsymbol{x}^2 = <1 \quad -1>^T$.

This gives the general solution: $y = <y_1 \quad y_2>^T = c_1 y^1 + c_2 y^2 = c_1 <1 \quad 1>^T e^{-2t} + c_2 <1 \quad -1>^T e^{-4t}$.

Figure 3.3.1 shows a phase plane-portrait of some of the trajectories. Straight trajectories refer to $c_1 = 0$ and $c_2 = 0$.

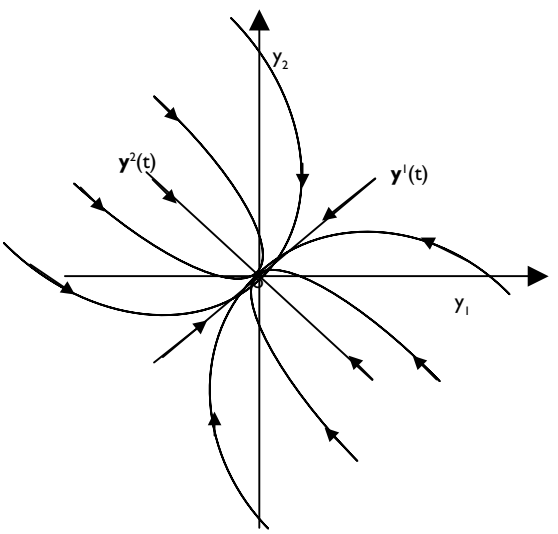


Figure 3.3.1 Trajectorie s of the system [Equation (3.2.14)] *[Improper node].*

3.3.3.2 *Critical points of the system*

In Figure 3.3.1, The point $y(0, 0)$ is a common tangent to all the trajectories, the reason for this remarkable observation can be obtained by using Equation (3.3.14), as follows

$$\frac{dy_2}{dt} \Big/ \frac{dy_1}{dt} = \frac{dy_2}{dy_1} = \frac{a_{21}y_1 + a_{22}y_2}{a_{11}y_1 + a_{12}y_2} \tag{3.3.15}$$

For every point, say $P(y_1, y_2)$ there is a unique tangent direction dy_2/dy_1 of the trajectory passing through P; except for the point $P = P_0(0, 0)$ [at P_0, we have $dy_2/dy_1 \equiv 0/0$ form] at which (dy_2/dy_1) becomes undetermined and the point is called a *critical point* of Equation (3.3.14).

There are five types of critical points depending upon the geometrical shape of the trajectories near them. These points are called *improper nodes, proper nodes, saddle points, centres and spiral points.*

Improper node

An improper node is a critical point P_0 at which all the trajectories, except two of them, have same limiting direction of the tangent. The two exceptional trajectories also have a limiting direction of the tangent at P_0 which, however, is different.

Equation (3.3.14) has an improper node at '0' as shown in Figure 3.3.1. The common limiting directions at 0 is that of the eigenvectors $\boldsymbol{x}^1 = <1\ 1>^T$ because e^{-4t} tends to zero faster than t increases. The exceptional limiting tangent direction is that of $\boldsymbol{x}^2 = <1\ -1>^T$.

Proper nodes

A proper node is critical point P_0 at which every trajectory has a definite limiting direction and for any given direction 'd' at P_0 there is a trajectory having 'd' as its limiting direction.

The system:

$$\boldsymbol{y}' = \begin{bmatrix} 1 & 0 \\ 0 & 1 \end{bmatrix} \boldsymbol{y} \quad \text{means} : y_1' = y_1 \text{ and } y_2' = y_2 \tag{3.3.16}$$

has a proper node at the origin as shown in Figure 3.3.2 as it has a general solution

$$y = c_1 <1\ \ 0>^T e^t + c_2 <0\ \ 1>^T e^t \quad \text{or } y_1 = c_1 e^t : y_2 = c_2 e^t$$

$$\rightarrow\ c_1 y_2 = c_2 y_1.$$

Saddle point

A saddle point is a critical point P_0 at which there are two incoming trajectories, two outgoing trajectories and all other trajectories in a neighbourhood of P_0 bypass P_0.

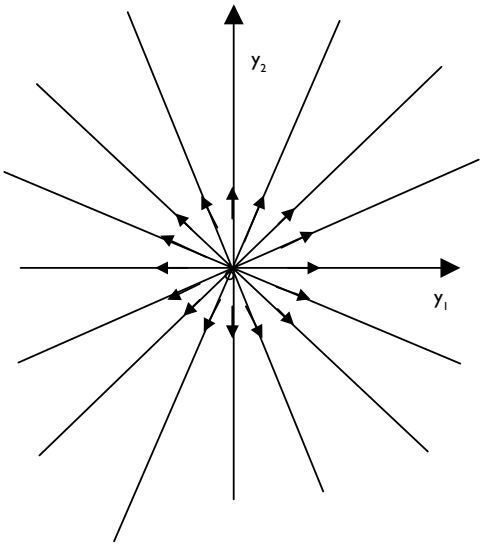


Figure 3.3.2 Trajectories of [Equation (3.2.16)] *[Proper node].*

The system:

$$\boldsymbol{y}' = \begin{bmatrix} 1 & 0 \\ 0 & -1 \end{bmatrix} \boldsymbol{y} \quad \text{means} : y_1' = y_1 \text{ and } y_2' = -y_2 \tag{3.3.17}$$

has a saddle point at the origin as shown in Figure 3.3.3 as it has a general solution.

This gives a system of hyperbolas shown in Figure 3.3.3.

$$y = c_1 <1 \;\; 0>^T e^t + c_2 <0 \;\; 1>^T e^{-t} \quad \text{or } y_1 = c_1 e^t : y_2 = c_2 e^{-t}$$

$$\rightarrow y_2 y_1 = \text{constant.}$$

Centre

A centre is a critical point that is enclosed by infinitely many closed trajectories.

The system:

$$\boldsymbol{y}' = \begin{bmatrix} 0 & 1 \\ -4 & 0 \end{bmatrix} \boldsymbol{y} \quad \text{means} : y_1' = y_2 \text{ and } y_2' = -4y_1 \tag{3.3.18}$$

has a centre at the origin. The characteristic equation is: $\lambda^2 + 4 = 0$. It has the eigen values $2i$ and $-2i$ and eigenvectors $<1 \;\; 2i>^T$ and $<1 \;\; -2i>^T$, respectively. The general solution is given by

$$\begin{aligned} &y = c_1 <1 \;\; 2i>^T e^{2it} + c_2 <0 \;\; -2i>^T e^{-2it} \quad \text{or} \\ &y_1 = c_1 e^{2it} + c_2 e^{-2it}; \quad y_2 = 2ic_1 e^{2it} - 2ic_2 e^{-2it} \end{aligned} \tag{3.3.18a}$$

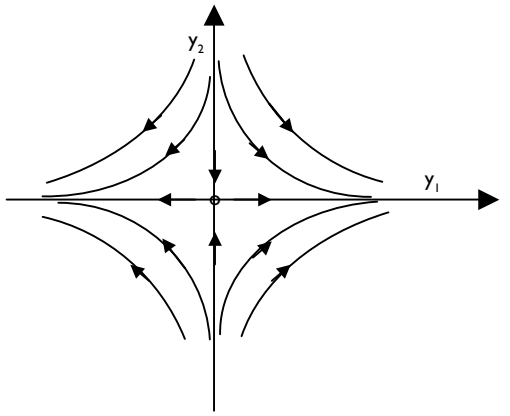


Figure 3.3.3 Trajectories of Equation (3.2.17) [Saddle point].

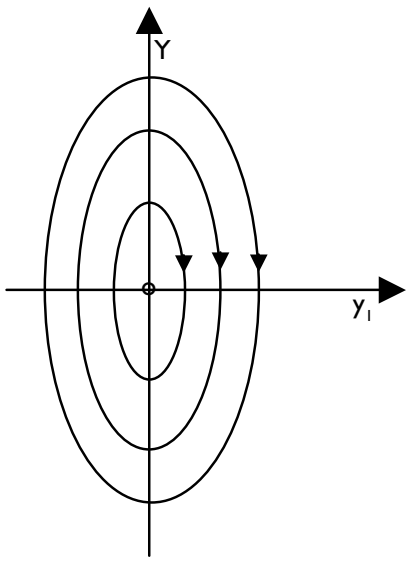


Figure 3.3.4 Trajectories of Equation (3.3.18) [Centre].

We can get a similar type of information as in the earlier cases by separating the solutions to real and imaginary parts.

Again, from Equation (3.3.18) we may write $4y_1y_1' = -y_2y_2'$ and by integration $2y_1^2 + 1/2\ y_2^2 =$ constant.

This gives a family of ellipses shown in Figure 3.3.4.

Spiral Points

A spiral point is a critical point P_0 about which the trajectories are spirals approaching P_0 as $t \to \propto$ (or tracing these spirals in the opposite sense away from P_0).

The system:

$$\boldsymbol{y}' = \begin{bmatrix} -1 & 1 \\ -1 & -1 \end{bmatrix} \boldsymbol{y} \text{ means : } y_1' = -y_1 + y_2 \quad \text{and} \quad y_2' = -y_1 - y_2 \tag{3.3.19}$$

has a spiral point at the origin. The characteristic equation is $\lambda^2 + 2\lambda + 2 = 0$ and has eigen values $-1+i$ and $-1-i$ with corresponding eigenvectors are obtained from $(-1-\lambda)x_1 + x_2 = 0$. This gives a complex solution

$$\boldsymbol{y} = c_1 <1 \;\; i>^T e^{(-1+i)t} + c_2 <1 \;\; -i>^T e^{(-1-i)t}.$$

This equation can be converted to real solution through transformations.

Again, multiply the first equation of (3.3.19) by y_1 and the second by y_2 and add to obtain

$$y_1 y_1' + y_2 y_2' = (y_1^2 + y_2^2)$$

Introducing polar coordinates (r, θ), using $r^2 = y_1^2 + y_2^2$, the equation reduces to $1/2(r^2)' = -r^2$: we can obtain $r = ce^{-\theta}$. For each real c this is a spiral as shown in Figure 3.3.5.

When no basis of eigenvectors available

So long as the matrix $\boldsymbol{A}$ is symmetric or skew-symmetric and also in many cases like eqns. (3.3.18) and (3.3.19), we have basis of eigenvectors. Let $\boldsymbol{A}$ be an n × n matrix having double eigenvalues p [i.e. the product representation of det $(\boldsymbol{A}-\lambda \boldsymbol{I})$ has a factor $(\lambda - p)^2$ with only one eigenvector (and its multiples) corresponding to it, instead of two linearly independent eigenvectors, so that we first get only one solution $\boldsymbol{y}^1 = \boldsymbol{x}e^{\boldsymbol{pt}}$. In this case we can obtain a second independent solution by substituting

$$\boldsymbol{y}^2 = \boldsymbol{x}te^{pt} + \boldsymbol{u}e^{pt} \tag{3.3.20}$$

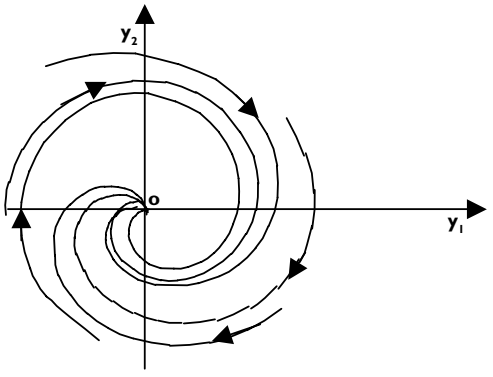


Figure 3.3.5 Trajectories of the system [Equation (3.2.19)] [Spiral point].

into Equation (3.3.6) [with having t-terms also], we have

$$\boldsymbol{y}^{2'} = \boldsymbol{x}e^{pt} + p\boldsymbol{x}te^{pt} + p\boldsymbol{u}e^{pt} = \boldsymbol{A}\boldsymbol{y}^2 = \boldsymbol{A}\boldsymbol{x}te^{pt} + \boldsymbol{A}\boldsymbol{u}e^{pt}$$

since $p\boldsymbol{x} = \boldsymbol{A}\boldsymbol{x}$, the terms $(p\boldsymbol{x}te^{pt})$ and $(\boldsymbol{A}\boldsymbol{x}e^{pt})$ would cancel and a division by e^{pt} would result in

$$\boldsymbol{x} + p\boldsymbol{u} = \boldsymbol{A}\boldsymbol{u} \quad \text{and hence } [\boldsymbol{A} - p\boldsymbol{I}]\boldsymbol{u} = \boldsymbol{x}. \tag{3.3.21}$$

Although $\det(\boldsymbol{A} - p\boldsymbol{I}) = 0$, this can always be solved for $\boldsymbol{u}$.

Degenerated node

The system:

$$\boldsymbol{y}' = \begin{bmatrix} 4 & 1 \\ -1 & 2 \end{bmatrix} \boldsymbol{y} = \boldsymbol{A}\boldsymbol{y}$$

The matrix $\boldsymbol{A}$ is not skew-symmetric, its characteristic equation is

$$\det(\boldsymbol{A} - \lambda\boldsymbol{I}) = \begin{vmatrix} 4-\lambda & 1 \\ -1 & 2-\lambda \end{vmatrix} = \lambda^2 - 6\lambda + 9 = 0 = (\lambda - 3)^2.$$

It has a double root $\lambda = 3$. Eigenvectors are obtained from $(4 - \lambda)x_1 + x_2 = 0$ ➔ $x_1 + x_2 = 0$, say $x^1 = <1\ -1>^T$ and multiples of this. This does not help.

Now, from Equation (3.3.21) we can have

$$(\boldsymbol{A} - 3\boldsymbol{I})\boldsymbol{u} = \begin{bmatrix} 1 & 1 \\ -1 & -1 \end{bmatrix} \boldsymbol{u} = \begin{Bmatrix} 1 \\ 1 \end{Bmatrix} \quad \rightarrow \quad u_1 + u_2 = 1 : -u_1 - u_2 = -1$$

and we can take simply $\boldsymbol{u} = <0\ \ 1>^T$. This solves the problem

$$\boldsymbol{y} = c_1\boldsymbol{y}^1 + c_2\boldsymbol{y}^2 = c_1<1\ -1e^{3t} + c_2> \quad (<1\ \ 1>^T t + <0\ \ 1>^T)e^{3t}.$$

This critical point at the origin is called a degenerate node or sometimes an improper node.

Shown in Figure 3.3.6, $c_1\boldsymbol{y}^1$ gives the heavy straight line with $c_1 > 0$ corresponding to the lower part in the fourth quadrant and $c_1 < 0$ corresponding to the upper part. $\boldsymbol{y}^2$ gives the right part of the heavy curve from 0 through the second, first and finally fourth quadrants. $-\boldsymbol{y}^2$ gives the other part of that curve.

Consider the system in Equation (3.3.6) consists of three or more equations and that $\boldsymbol{A}$ has triple eigenvalue p with only a single linearly independent eigenvector corresponding to it. Then we get a second solution (3.3.20) with a vector satisfying (3.3.21) and a third of the form

$$\boldsymbol{y}^3 = \frac{1}{2}\boldsymbol{x}t^2e^{pt} + \boldsymbol{u}te^{pt} + \boldsymbol{v}e^{pt} \tag{3.3.22}$$

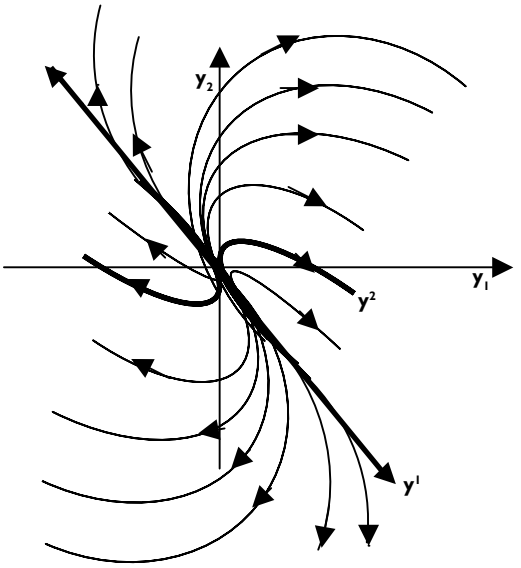


Figure 3.3.6 Degenerated node.

with $\boldsymbol{u}$ satisfying (3.3.21) and v determined from

$$(\boldsymbol{A} - p\boldsymbol{I})\boldsymbol{v} = \boldsymbol{u} \tag{3.3.23}$$

and this can be solved.

Finally we may mention that if A has a triple eigenvalue p and two linearly independent eigenvectors x^1, x^2 corresponding to it, then three linearly independent solutions are

$$\boldsymbol{y^1} = \boldsymbol{x}^1 e^{pt}, \quad \boldsymbol{y}^2 = x^2 e^{pt} \quad \text{and} \quad \boldsymbol{y}^3 = \boldsymbol{x}te^{pt} + \boldsymbol{u}e^{pt} \tag{3.3.24}$$

where $\boldsymbol{x}$ is a linear combination of $\boldsymbol{x}^1$ and $\boldsymbol{x}^2$ such that

$$(\mathbf{A} - p\boldsymbol{I})\boldsymbol{u} = \boldsymbol{x} \tag{3.3.25}$$

is solvable for u.

3.3.4 Phase plane method for SDOF system

When the response of a vibrating system is plotted graphically in terms of, say $\boldsymbol{Z}$ and $\dot{\boldsymbol{Z}}/\omega_n$, we obtain a curve referred to as the phase-plane trajectory. This curve is very useful for problems involving transient motion, since it allows the engineer to 'see' how the properties of the system affect its response to impact or transient loads. Consider

$$Z = A\sin\ \omega_n t + B\cos\omega_n t = C[(A/C)\sin\omega_n t + (B/C)\cos\omega_n t]$$
$$= C[\cos\ \phi\cos\omega_n t\ + \sin\ \phi\sin\omega_n t]$$

That is

$$Z = C\cos(\omega_n t - \phi);\ \text{phase angle}, \phi = \tan^{-1}(B/A)\quad \text{and } C = \sqrt{(A^2 + B^2)}. \tag{3.3.26}$$

Differentiating Equation (3.3.26) w.r.t. t

$$\rightarrow\quad \dot{Z}/\omega_n = -C\ \sin(\omega_n t - \phi) \tag{3.3.27}$$

From Eqns. (3.3.26) and (3.3.27), one can get

$$Z^2 + (\dot{Z}/\omega_n)^2 = C^2 \tag{3.3.28}$$

$\Rightarrow$ equation of a circle with centre at the origin, having a radius of C.

Plot of Equation (3.3.26) and Equation (3.3.27) on coordinates of Z and $\dot{Z}/\omega_n$, gives a point starting at Z_0 and $\dot{Z}_0/\omega_n$ traveling clockwise on the circular arc describing by Equation (3.3.28) and moving with an angular velocity ω_n. Plots of Z and $\dot{Z}/\omega_n$ are shown in Figure 3.3.7, start with Z_0 and $\dot{Z}_0/\omega_n$ traveling clockwise on the circular arc described by Equation (3.3.28) and moving with an angular velocity ω_n. At any time

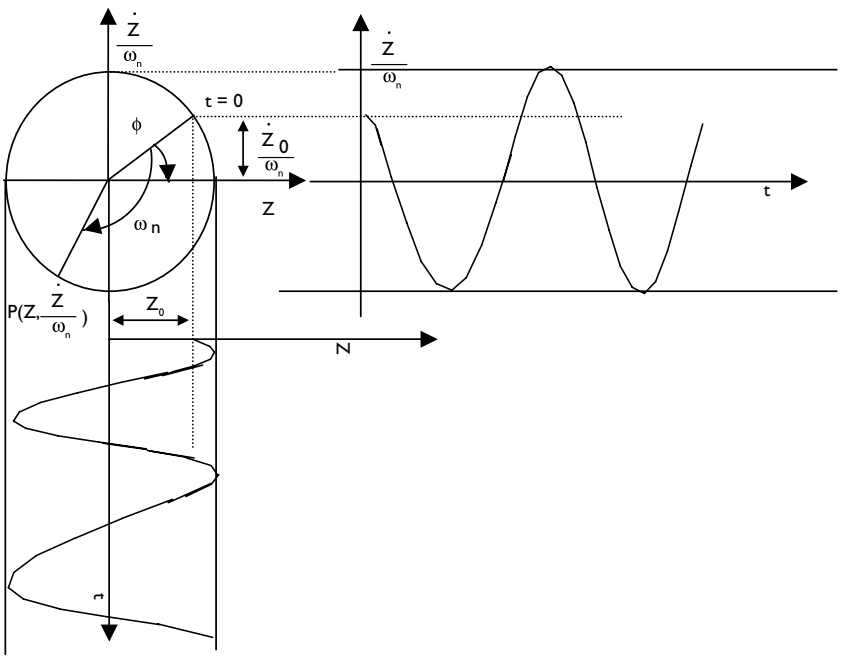


Figure 3.3.7 Phase plane solutions to SDOF system.

t, the angular distance traveled around the circle is $\omega_n t$. Quantities Z or $\dot{Z}/\omega_n$ can be obtained as a function of t and plotted by extending lines from the phase-plane shown in Figure 3.3.7.

3.3.5 Self-excited oscillations

When oscillation of a system depends on the motion itself the oscillation of the system is termed as a self-excited or self-induced vibration. Included under this category are the flutter of aeroplane wings and shimmy of automobiles. The van der Pole equation is a classic mathematical form of such oscillations. The oscillations may be linear or a nonlinear. Forcing function in this case may be some function of velocity or a combination of the velocity and the displacement. The system becomes unstable when the motion tends to increase the energy of the system. Consider the case of a mass-spring-dashpot system subjected to a forcing function dependent on velocity alone

$$m\ddot{x} + c\dot{x} + kx = F(\dot{x}) \tag{3.3.29}$$

Equation (3.3.29) may be written in the form

$$m\ddot{x} + [c\dot{x} - F(\dot{x})] + kx = m\ddot{x} + \alpha(\dot{x}) + kx = 0 \tag{3.3.30}$$

The damping, $\alpha(\dot{x})$ in Equation (3.3.30) may be negative if $F(\dot{x})$ becomes greater than $c\dot{x}$. This leads to a negative damping. When damping is negative amplitude of oscillation tends to increase while for a negative-positive cyclic damping oscillations tend to a limit cycle.

3.3.6 Autonomous system

Self-excited system is an autonomous system wherein time does not appear in the governing equation of motion quite explicitly and only the differential of time 'dt' may appear in the Equation. Thus the governing equation may take a shape like

$$\ddot{x} + f(x, \dot{x}) = 0 \tag{3.3.31}$$

in which $f(x, \dot{x})$ may be a linear or nonlinear function of x and $\dot{x}$.

3.3.7 State space method

In this method we express Equation (3.3.31) in terms of two first order differential equations as follows:

$$\dot{x} = y \quad \text{and } \dot{y} = -f(x, y) \tag{3.3.32}$$

If x and y are the Cartesian coordinates, the x-y plane is called the phase plane. The state of a system is defined by the coordinates $x \equiv x =$ displacement and $y \equiv \dot{x} =$ velocity in x-y plane. As the state of a system changes, the point $(x, \dot{x})$ traces a path known as trajectory.

3.3.8 State speed

The state speed V is defined as

$$V = \sqrt{\dot{x}^2 + \dot{y}^2} \tag{3.3.33}$$

An equilibrium state is reached when V is zero. It is obvious that in such a situation both velocity and acceleration i.e. $\dot{x}$ and $\dot{y}$ are zero. Dividing $\dot{y}$ by $\dot{x}$ in Equation (3.3.32), one can obtain

$$\frac{\dot{y}}{\dot{x}} = \frac{dy}{dx} = -\frac{f(x,y)}{y} = \phi(x,y) \tag{3.3.34}$$

Hence for every point x, y in the phase plane for which $\phi(x,\ y)$ is not indeterminate, there is a unique slope of the trajectory.

3.3.8.1 Various cases

When $y = 0$ and $f(x,y) \neq 0$, the slope of the trajectory is infinite. All trajectories corresponding to such points must cross the x-axis at right angles.

When $y = 0$ and $f(x,y) = 0$, the slope is indeterminate. These points are called singular points. A singular point corresponding to a state of equilibrium occurs when both the velocity and the force are zero $y = \dot{x} = \ddot{x} = \dot{y} = -f(x,y) = 0$. This is the necessary condition; the sufficient condition for stability of a system requires still further conditions.

A classical example may be sighted from an undamped S.D.O.F. system, as follows:

$$\ddot{x} + \omega_n^2 x = 0 \tag{3.3.35}$$

Here, with $y = \dot{x}$, we have $\dot{y} = -\omega_n^2 x$ and $\dot{x} = y$ and dividing

$$\frac{dy}{dx} = -\frac{\omega_n^2 x}{y}. \tag{3.3.36}$$

Integrating the above, we can write:

$$y^2 + \omega_n^2 x^2 = \text{a constant } C \tag{3.3.37}$$

and this represents a series of ellipses, the size of which is determined through C.

The equation given above is also the equation of conservation of energy given as follows:

$$\frac{1}{2}m\dot{x}^2 + \frac{1}{2}kx^2 = \text{const.} = A \tag{3.3.38}$$

At any given instant the state of a system can be expressed by the displacement x and velocity y; to this state corresponds a generic point of coordinates x and, y in the phase plane. The generic point will move with time on the phase plane describing phase trajectory. In the above case of harmonic vibration, we have:

$$x = x_0 \sin(\omega_n t + \phi) : y = x_0 \omega_n \cos(\omega_n t + \phi) \tag{3.3.39}$$

This set of equations may be regarded as a phase trajectory prescribed in parametric form, with t as parameter. To obtain the equation of phase trajectory in explicit form, it is necessary to eliminate the time t from Equation (3.3.11); we obtain

$$\frac{x^2}{x_0^2} + \frac{y^2}{x_0^2 \omega_n^2} = 1 \tag{3.3.40}$$

➔ equation of an ellipse.

To the initial condition $x = x_0$, $y_0 = \dot{x}_0$ corresponds to the initial generic point of the phase trajectory from which the motion is started. The periodicity of the system expresses itself in the fact that the generic point will run around one and the same elliptic orbit.

Singular point is at $x = y = 0$, the phase plane plot appears as shown in Figure 3.3.8(a). If y is replaced by (y/ω_n), ellipses will reduce to circles.

When the initial conditions are changed, the phase trajectory is found to be a different ellipse; the set of all possible states of the system is described by a family of ellipses embedded into one another as shown in Figure 3.3.8(b). The set of phase trajectories forms the phase diagram of the system. The parameters of the system determine the phase diagram and the initial conditions fix a particular trajectory.

In order to construct the phase diagram of a damped system, let us consider the following equations:

$$\begin{aligned} x &= Ae^{-D\omega_n t} \sin(\omega_{nd} t + \phi); \\ \dot{x} &= e^{-D\omega_n t} [\omega_{nd} \cos(\omega_{nd} t + \phi) - D\omega_n \sin(\omega_{nd} + \phi)] \end{aligned} \tag{3.3.41}$$

as the equation of the phase trajectory in parametric form.

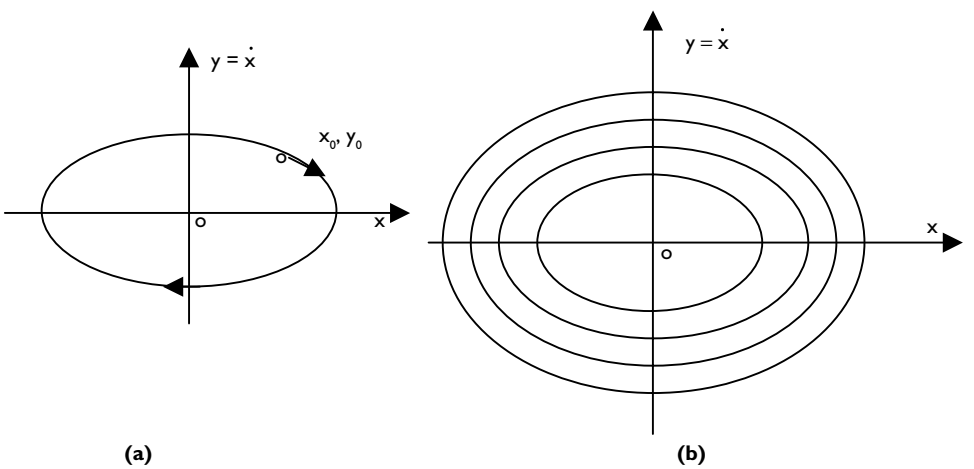


Figure 3.3.8 Phase-plane plot.

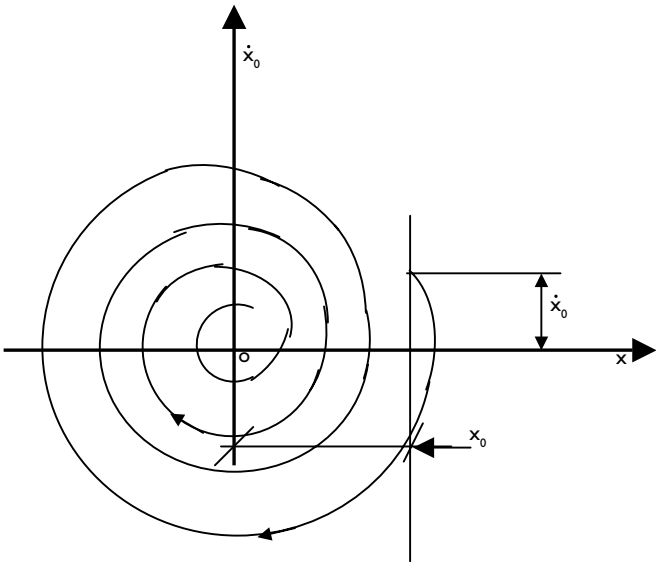


Figure 3.3.9 Phase plane plot for damped free vibration.

A typical phase trajectory is shown in Figure 3.3.9. It represents a spiral wound around the origin. The phase diagram is found by a system of such spirals surrounding the singular point 0; the later is called the stable focus in this case.

3.3.9 Stability of the solution

Let us consider the Cauchy's problem, similar to Equation (3.3.1), as follows

$$\frac{dy}{dt} = f(t, y), \text{subjected to initial condition } y(t_0) = y_0. \tag{3.3.42}$$

If the function $f(t,\ y)$ is continuous jointly with respect to the arguments and possesses a bounded derivative $\partial f/\partial y$ in a certain domain Ω of variation of t and y, which contains a point $(t_0,\ y_0)$, then the solution of Cauchy's problem Equation (3.3.42) exists and is unique. If we vary the values of t_0 and y_0, then the solution also varies. Then a question arises which is important in applications: how will the solution vary? This is a matter of principle. If some physical problem leads to Cauchy's problem, then the initial values are found from an experiment and we cannot guarantee the accuracy of measurement. And if, negligibly small changes in the initial data lead to a drastic change in the solution, then the mathematical model will be hardly suitable for describing a real process.

If f(t, y) of the differential equation Equation (3.3.42) is continuous jointly with respect to variables and possesses a bounded partial derivative $\partial f/\partial y$ in a certain domain Ω of variation of t and y, then the solution $y(t) = y(t,\ t_0, y_0)$, satisfying the initial condition $y(t)=y_0$, where $(t_0, y_0) \in \Omega$, continuously depends on the initial data.

If we assume that the solution $y(t)$, defined on the interval $\alpha \leq t \leq \beta, \in (\alpha, \beta)$, passes through the point (y_0, t_0). Then, for any $\varepsilon > 0$ there is $\delta > 0$ such that for $|\tilde{t}_0 - t_0| < \delta$, $|\tilde{x}_0 - x_0| < \delta$, the solution $\tilde{x}(t)$ of Equation (3.3.42), which passes through the point $(\tilde{t}_0, \tilde{x}_0)$, exists on the interval $[\alpha, \beta]$ and differs from $x(t)$ by less than $\varepsilon : |x(t) - \tilde{x}(t)| < \varepsilon \; \forall \; t \in [\alpha, \beta]$.

3.3.9.1 Existence and uniqueness theorem

A similar theorem is valid for the system of differential equations for Equation(3.3.4) can be stated as follows:

Let $f_1, f_2, f_3, \ldots, fn$ in Equation (3.3.4) be continuous having continuous partial derivatives $\partial f_1/\partial y_1, \partial f_{12}\partial y_2, \partial f_3/\partial y_3, \ldots, \partial f_n/\partial y_n$ in some domain Ω of t, $y_1, y_2, y_3, \ldots, y_n$ – space containing the point $(t_0, k_1, k_2, k_3, \ldots, k_n)$ then Equation (3.3.4) has a solution on some interval $t_0 - \alpha < t < t_0 + \alpha$ satisfying Equation (3.3.5) and this solution is unique. When the conditions just laid down are satisfied, the solution of Cauchy's problem exists, is unique, and continuously depends on the initial data. In that case we say that Cauchy's problem is correctly posed. The fact that the interval $[\alpha, \beta]$ of variation of t is finite is essential. In many problems, we are interested in the relationships between the solution and the initial data in the infinite interval, i.e. $t_0 \leq t \leq \infty$. The passage from a finite interval, in which we consider a continuous dependence of the solution on the initial data, to an infinite interval changes essentially the nature of the problem and the investigation methods. This problem is from the theory of stability created by Lyapunov.

3.3.9.2 Stability in the sense of Lyapunov

Consider Equation (3.3.42): $\dfrac{dy}{dt} = f(t, y)$ (3.3.42)

Where the function $f(t, y)$ is defined and continuous for $t \in (a, +\infty)$ and y from a certain domain Ω and possesses a bounded partial derivative $\partial f/\partial y$. Let us assume that the function $y = \varphi(t)$ is a solution of Equation (3.3.42), which satisfies the initial condition $y|_{t=t0} = \varphi(t_0), t_0 > a$. We assume, furthermore, that the function $y = y(t)$ is a solution of the same equation, which satisfies another initial condition $y|_{t=t0} = y(t_0)$. It is assumed that the solution $\varphi(t)$ and $y(t)$ are defined for all $t \geq t_0$, i.e. can be extended indefinitely to the right.

Definition I. The solution $y = \varphi(t)$ of Equation (3.3.42) is said be stable in the sense of Lypunov as $t \to +\infty$ (to the right) if, for any $\varepsilon > 0$, there is $\delta = \delta(\varepsilon) > 0$ such that for every solution $y = y(t)$ of that equation the inequality

$$|y(t_0) - \varphi(t_0)| < \delta \tag{3.3.43}$$

yields an inequality

$$|y(t_0) - \varphi(t_0)| < \varepsilon \tag{3.3.44}$$

for all $t \geq t_0$, we can always assume that $\delta \leq \varepsilon$.

This means that the solution that are close to the solution $y = \varphi(t)$ as concerns the initial values remain close for all $t \geq t_0$ as well. Geometrically the solution $y = \varphi(t)$ of Equation (3.3.42) is stable if, however narrow the ε-strip containing the curve $y = \varphi(t)$, all the integral curves $y = y(t)$ of the equation, which are sufficiently close to the strip at the initial moment $t = t_0$, lie entirely in the indicated ε-strip for all $t \geq t_0$. This is shown in Figure 3.3.10.

If for an arbitrarily small $\delta > 0$ inequality [Equation (3.3.44)] does not hold for at least one solution $y = y(t)$ of Equation (3.3.42), then the solution $y = \varphi(t)$ of that equation is said to be unstable. A solution which cannot be extended to the right as $t \to +\infty$ must be considered to be unstable.

Definition II. The solution $y = \varphi(t)$ of Equation (3.3.42) is said to be asymptotically stable if: a) the solution $y = \varphi(t)$ is stable: b) there is $\delta_1 > 0$ such that for any solution $y = y(t)$ of Equation (3.3.42), which satisfies the condition $|t(t_0) - \varphi(t)| < \delta_1$, we have

$$\lim_{t \to +\infty} |y(t) - \varphi(t)| = 0.$$

This means that all the solutions $y = y(t)$, which are close to the asymptotically stable solution $y = \varphi(t)$ as concerns the initial conditions, not only remain close to it for $t \geq \infty$.

Assume that a ball rests at the bottom of a hollow hemispheric body (stable equilibrium position). If the all is disturbed from the equilibrium position by a small

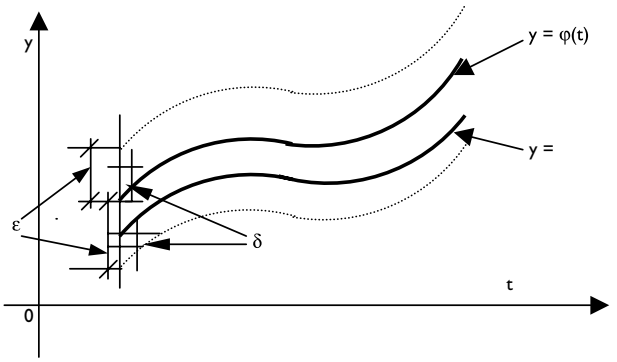


Figure 3.3.10 Stability in the sense of Lypunov.

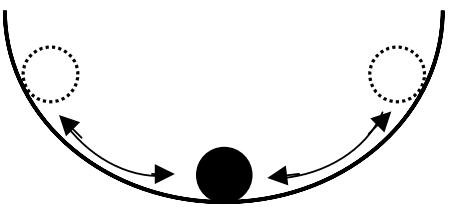


Figure 3.3.11 Stability.

perturbation then it will oscillate about it. If the body is frictionless, then the equilibrium position will be stable, and if there is some friction, the oscillations of the ball will decrease with time, that is the equilibrium position will be asymptotically stable [Figure 3.3.11].

Example 3.3.4

Investigate the solution of $y \equiv 0$ of the equation $\frac{dy}{dt} = 0$, for stability. (3.3.45)

Solution:

The solution satisfies the initial condition $y|_{t=t0} = 0$. Evidently the solution of Equation (3.3.45), which satisfies the initial condition $y|_{t=t0} = y_0$, has the form $y \equiv y_0$. One can observe in Figure 3.3.12 that whatever the strip about the integral curve $y = 0$, there is a $\delta > 0$, say $\delta = \varepsilon$, such that any integral curve $y = y_0$, for which $|y_0 - 0| < \delta$, lies entirely in the indicated ε-strip for all $t \geq t_0$. Consequently, as shown in Figure 3.3.12, the solution $y \equiv y_0$ does not tend to the straight line $y = 0$ as $t \to \infty$.

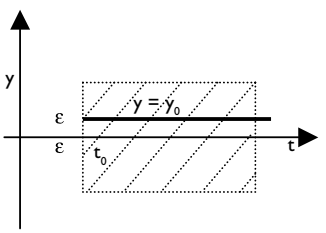


Figure 3.3.12

Example 3.3.5

Investigate the solution $y \equiv 0$ of the equation

$$\frac{dy}{dt} = -\lambda^2 y, \quad (\lambda = \text{constant}) \text{ for stability.} \tag{3.3.46}$$

Solution:

Solution of Equation (3.3.46) which satisfies the initial condition $y_{t=t_0} = y_0$ has the form

$$y = y_0\, e^{-\lambda^2 (t - t_0)} \tag{3.3.47}$$

Take any $\varepsilon > 0$ and consider the difference between the solutions $y(t)$ and $\varphi(t)$, i.e.

$$y(t) - \varphi(t) = y_0 e^{-\lambda^2(t-t_0)} - 0 = (y_0 - 0)e^{-\lambda^2(t-t_0)} \tag{3.3.48}$$

Since $e^{-\lambda^2(t-t_0)} \leq 1$ for all $t \geq t_0$, it follows from Equation (3.3.48) that there is $\delta > 0$, say, $\delta = \varepsilon$, such that for $|y_0 - 0| < \delta = \varepsilon$, we have

$$|y(t) - \varphi(t)| = |y_0 - 0|e^{-\lambda^2(t-t_0)} < \varepsilon \quad \forall t \geq t_0 \tag{3.3.49}$$

According to Definition I this means that the solution $\varphi(t) \equiv 0$ of Equation (3.3.46) is stable.

In addition we have

$\lim_{t\to+\infty} |y(t) - \varphi(t)| = \lim_{t\to+\infty} |y_0|e^{-\lambda^2(t-t_0)} = 0$ and, therefore the solution $\varphi(t) \equiv 0$ is asymptotically stable. This is shown in Figure 3.3.13.

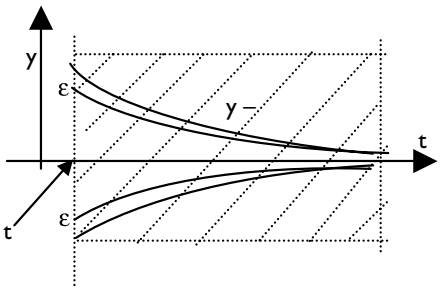


Figure 3.3.13

Example 3.3.6

Show that the solution $\varphi(t) \equiv 0$ of the equation $\dfrac{dy}{dt} = \lambda^2 y$ is unstable.

Solution:

For an arbitrarily small y_0 the solution $y(t) = y_0 e^{\lambda^2(t-t_0)}$ of this equation does not satisfy the condition $|y(t) - 0| = |y_0|e^{\lambda^2(t-t_0)} < \varepsilon$ for sufficiently large $t > t_0$. For any $y_0 \neq 0$, we have, $|y(t)|_{t\to+\infty} \to +\infty$. This is shown in Figure 3.3.14.

Let us consider now a system of equations

$$\frac{dy_i}{dt} = f_i(t, y_1, y_2, \ldots, y_n), \quad i = 1, 2, 3, \ldots, n \tag{3.3.50}$$

where the function f_i are defined for $a < t < +\infty$ and $y_1, y_2, \ldots, y_n$ belonging to a certain domain Ω of variation of $y_1, y_2, \ldots, y_n$ and satisfies the conditions of the unique existence theorem of the solution of Cauchy's problem. We may assume that all solutions of system in Equation (3.3.50), can be extended indefinitely to the right for $t \geq t_0 > a$.

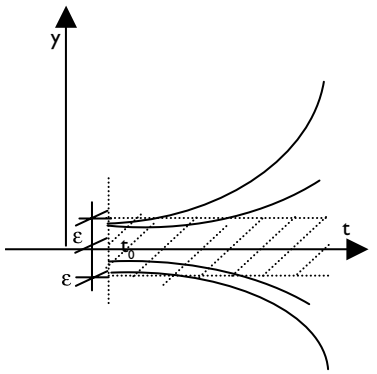


Figure 3.3.14

Definition III. The solution $\varphi_i(t), i = 1, 2, 3, \ldots, n$ of system Equation (3.3.50) is said to be stable in the sense of Lyapunov as $t \to +\infty$ if for any $\varepsilon > 0$ there is a $\delta = \delta(\varepsilon) > 0$ such that for every solution $y_i(t), i = 1, 2, 3, \ldots, n$ of that system, whose initial values satisfy the inequalities

$$|y_i(t_0) - \varphi_i(t_0)| < \delta, \quad i = 1, 2, 3, \ldots, n$$

the inequalities $\quad |y_i(t) - \varphi_i(t)| < \varepsilon, \quad i = 1, 2, 3, \ldots, n \qquad (3.3.51)$

are satisfied for all $t \geq t_0$, i.e. the solutions close as concerns the initial values remain close for all $t \geq t_0$.

If, for an arbitrarily small $\delta > 0$, inequalities Equation (3.3.51) do not hold even for one solution $y_i(t), i = 1, 2, 3, \ldots, n$, then the solution $\varphi_i(t)$ is unstable.

Definition IV. The solution $\varphi_i(t), i = 1, 2, 3, \ldots, n$ of system Equation (3.3.50) is asymptotically stable if

1 The solution is stable;
2 There is $\delta_1 > 0$ such that any solution $y_i(t), i = 1, 2, 3, \ldots, n$, of the system for which

$$|y_i(t_0) - \varphi_i(t_0)| < \delta_1 \quad i = 1, 2, 3, \ldots, n$$

satisfies the condition

$$\lim_{t\to\infty} |y_i(t) - \varphi_i(t)| < 0, \quad i = 1, 2, 3, \ldots, n \tag{3.3.52}$$

Example 3.3.7

From the definition of the Lyapunov stability, show that the solution of the system

$$\frac{dx}{dt} = y \quad \text{and} \quad \frac{dy}{dt} = -x \tag{3.3.53}$$

which satisfies the initial condition $x(0) = 0$, and $y(0) = 0$ is stable.

Solution:

The solution of Equation (3.3.53), which satisfies the initial conditions, is $x(t) \equiv 0, y(t) \equiv 0$. The solution of this system, which satisfies the conditions $x(0) = x_0$, $y(0) = y_0$, has the form

$$x(t) = x_0 \cos t + y_0 \sin t; \quad y(t) = -x_0 \sin t + y_0 \cos t$$

Let us take an arbitrary $\varepsilon > 0$ and show that there is a $\delta(\varepsilon) > 0$ such that for $|x_0 - 0| < 0$ and $|y_0 - 0| < \delta$ the inequalities $|x(t) - 0| = |x_0 \cos t + y_0 \sin t| < \varepsilon, |y(t) - 0| = |-x_0 \sin t + y_0 \cos t| < \varepsilon$ hold for all $t \geq 0$. This signifies that the zero solution $x(t) \equiv 0$, $y(t) \equiv 0$ of Equation (3.3.53) is stable in the sense of Lyapunov, we have, again

$$|x_0 \cos t + y_0 \sin t| \leq |x_0 \cos t| + |y_0 \sin t| \leq |x_0| + |y_0|$$
$$|-x_0 \sin t + y_0 \cos t| \leq |-x_0 \sin t| + |y_0 \cos t| \leq |-x_0| + |y_0|$$

If we take $\delta(\varepsilon) = \varepsilon/2$, then for $|x_0| < \delta$ and $|y_0| < \delta$, the inequalities $|x_0 \cos t + y_0 \sin t| < \varepsilon, |-x_0 \sin t + y_0 \cos t| < \varepsilon$ hold for all $t \geq 0$, i.e. the zero solution of the system is stable in the sense of Lyapunov but the stability is not asymptotic. The stability of a nontrivial solution of a differential equation does not imply that the solution is bounded. Let us consider an equation of the type $dy/dt = 1$. The solution of this equation, which satisfies the condition $y(0) = 0$, is a function $\varphi(t) = t$. The solution which satisfies the initial condition $y(0) = y_0$, has the form $y(t) = y_0 + t$. It is geometrically shown in Figure 3.3.15 and for any $\varepsilon > 0$, there is a $\delta > 0$, say ε, such that any solution $y(t)$ of the equation, for which the inequality $|y_0 - 0| < \delta$ holds, satisfies the condition $|y(t) - 0| < \varepsilon$ for every $t \geq 0$. This latter signifies that the solution $\varphi(t) = t$ is a stable in the sense of Lyapunov; this solution is bounded, however, as $t \to \infty$.

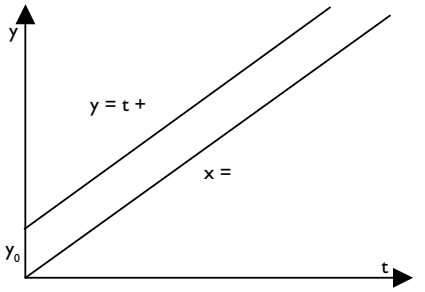


Figure 3.3.15

The boundedness of solutions of a differential equation does not imply that the solutions are stable. Let us consider an equation

$$\frac{dy}{dt} = \sin^2 y \tag{3.3.54}$$

It has solutions $y = k\pi, k = 0, \pm 1, \pm 2, \ldots$

Integrating Equation (3.3.54), we find that $\cot y =$ All these solutions are bounded on $(-\propto, +\propto)$.

However, the solution $\varphi(\mathrm{t}) \equiv 0$ is unstable for $t \to +\propto$ since for any $y_0 \in (0, \pi)$, shown in Figure 3.3.16, we have

$$\lim_{t \to +\propto} y(t) = \pi.$$

Thus the concepts of boundedness and stability of solutions are mutually independent.

The solution $\varphi_i(t) \equiv 0, i = 1, 2, 3, \ldots, n$ of system Equation (3.3.50), investigated for stability can always be reduced to a trivial solution $y_i \equiv 0$ of another system by substituting $y_i = x_i - \varphi_i(t), i = 1, 2, 3, \ldots, n$. Let we have a differential equation of the type

$$\frac{dx}{dt} = f(t, x) \tag{3.3.55}$$

and assume that we have to investigate a certain solution $\varphi(t)$ of that equation for stability.

We set $y(t) = x(t) - \varphi(t)$ [this is known as perturbation]. Then $x(t) = y(t) + \varphi(t)$ and its substitution into Equation (3.3.55) leads to

$$\frac{dy}{dt} + \frac{d\varphi}{dt} = f(t, y(t) + \varphi(t)) \tag{3.3.56}$$

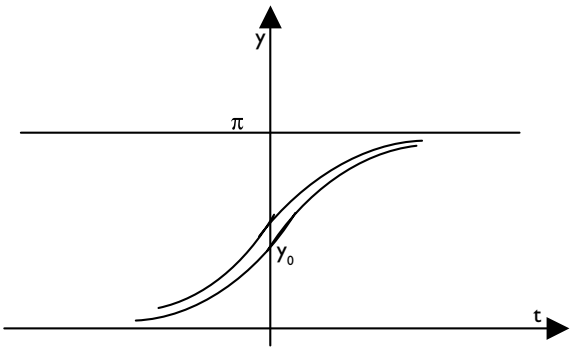


Figure 3.3.16

But $\varphi(t)$ is a solution of Equation (3.3.55), and hence, $d\varphi/dt \equiv f(t, \varphi(t))$ and we have from Equation(3.3.56)

$$\frac{dy}{dt} = f(t, y(t) + \varphi(t)) - f(t, \varphi(t)) = F(t, y) \tag{3.3.57}$$

Equation (3.3.57) has a solution $y \equiv 0$ since for $y \equiv 0$ its l.h.s. and r.h.s. are identically zero with respect to t, i.e.

$$F(t, 0) = f(t, \varphi(t)) - f(t, \varphi(t)) \equiv 0.$$

Thus the equation as to the stability of the solution $\varphi(t)$ of Equation (3.3.55) leads to the question concerning the stability of the trivial solution $y \equiv 0$ of Equation (3.3.57) to which Equation (3.3.55) can be reduced. Therefore, in what follows we shall assume, as a rule, that a trivial solution is investigated for stability.

3.3.9.3 The stability of autonomous systems: Simplest kind of rest points

A normal system of differential equations is called autonomous if its right hand side f_i does not depend explicitly on t, i.e. if it has the form

$$\frac{dy_i}{dt} = f_i(y_1, y_2, \ldots, y_n), \quad i = 1, 2, 3, \ldots, n \tag{3.3.58}$$

This means that the law of variation of the unknown functions, which is described by the autonomous system, does not vary with time as is the case for many physical systems.

Let us assume that $(a_1, a_2, a_3, \ldots, a_n)$ is a set of numbers such that

$$f_i(a_1, a_2, a_3, \ldots, a_n) = 0, \quad i = 1, 2, 3, \ldots, n.$$

Now, the system of functions $y_i(t) \equiv a_i, i = 1, 2, 3, \ldots, n$, is a solution of Equation (3.3.58). The point $(a_1, a_2, a_3, \ldots, a_n)$ of the phase space $(y_1, y_2, y_3, \ldots, y_n)$ is called a rest point (position of equilibrium) of the given system.

Let us consider Equation (3.3.58) for which $f_i(0, 0, 0, \ldots, 0) = 0, i = 1, 2, 3, \ldots, n$, so that the point $x_i = 0, i = 1, 2, 3, \ldots, n$, is a rest point of that system.

We denote by $S(R)$ a sphere: $\sum_{i=1}^{n} x_i^2 < R^2$: we assume that the condition of Theorem:

Given a normal system of differential equations (Cauchy's problem)

$$\frac{dx_i}{dt} = f_i(t, x_1, x_2, \ldots, x_n), \quad i = 1, 2, \ldots, n \tag{3.3.59}$$

Assume that the functions, $f_i(t, x_1, x_2, \ldots, x_n), i = 1, 2, \ldots, n$, are defined in a certain $(n + 1)$-dimensional domain Ω of variation of the variables $t, x_1, x_2, \ldots, x_n$. If there is a neighbourhood Ω' of the point $M_0\,(t_0, x_1^0, x_2^0, \ldots, x_n^0)$ at which the function f_i are continuous jointly with respect to the arguments and possess bounded partial derivatives with respect to the variables $x_1, x_2, x_3, \ldots, x_n$, then there is an interval $t_0 - h_0 < t_0 + h_0$ of variation of t on which there is a unique solution of the normal system satisfying the initial conditions are fulfilled for the system being considered in $S(R)$.

Definition V. We say that the rest point $x_i = 0, i = 1, 2, \ldots, n$, of Equation (3.3.58) is stable if for any $\varepsilon > 0 (0 < \varepsilon < R)$ there is $\delta = \delta(\varepsilon) > 0$ such that any trajectory of the system, which begins at the initial moment $t = t_0$ at the point $M_0 \in S(\delta)$, remains all the time in the sphere $S(\varepsilon)$.

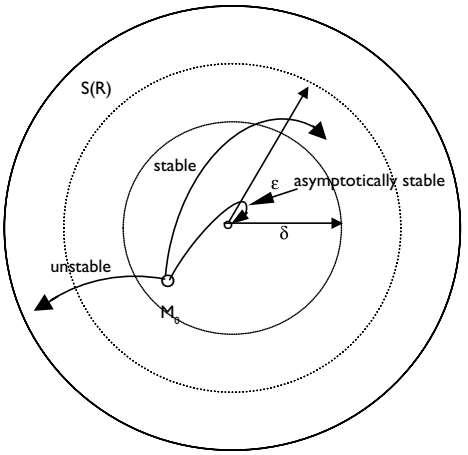


Figure 3.3.17

The rest point is asymptotically stable if

1 it is stable;
2 there is a $\delta_1 > 0$ such that every trajectory of the system, which begins at the point M_0 of the domain $S(\delta_1)$, approaches the origin when the time t increases indefinitely, as shown in Figure 3.3.17.

Example 3.3.8

Consider a system: $\dfrac{dx}{dt} = y : \dfrac{dy}{dt} = -x$

In this case the trajectories are concentric circles: $x^2 + y^2 = h^2$ with centre at the origin, which is the only rest point of the system. If we take $\delta = \varepsilon$, then any trajectory beginning in the circle $S(\delta)$ remains in the interior of $S(\delta)$ all the time, and, consequently, in the interior of $S(\varepsilon)$ as well, so that we have stability here. However, the trajectories do not approach the origin as $t \to \infty$ and the rest point is not asymptotically stable.

Example 3.3.9

Consider a system : $\dfrac{dx}{dt} = -x : \dfrac{dy}{dt} = -y$

Its solution are $x = C_1 e^{-t}; y = C_2 e^{-t}$. Hence we have $y/x = C_2/C_1 = k =$ constant, and therefore, the trajectories are rays which converge at the origin (Figure 3.3.18). We can choose $\delta = \varepsilon$. Any point of trajectory, which is in the interior of $S(\delta)$ at the initial moment, remains in the circle $S(\varepsilon)$ all the time, and, in addition, approaches indefinitely the origin as $t \to \infty$. Thus we have an asymptotic stability here.

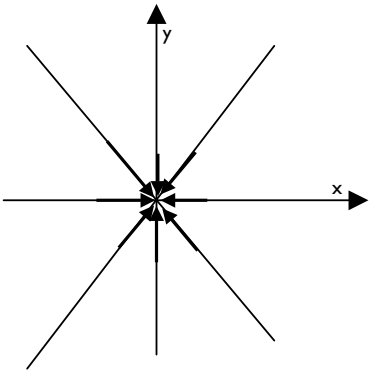


Figure 3.3.18

Example 3.3.10

Consider another system: $\dfrac{dx}{dt} = x : \dfrac{dy}{dt} = y$

Its solutions are $x = C_1e^t; y = C_2e^t$. Here we also have $y/x = C_2/C_1 = k =$ constant and the trajectories are rays beginning at the origin, but, as distinct from the last example, the direction of motion along the rays is away from the centre. The rest point is unstable.

Let us investigate the positions of the trajectories in the neighbourhood of the rest point $x = 0$, $y = 0$ of a system of two homogeneous linear equations with constant coefficients, i.e.

$$\frac{dx}{dt} = a_{11}x + a_{12}y : \frac{dy}{dt} = a_{21}x + a_{22}y \tag{3.3.60}$$

in which $\begin{vmatrix} a_{11} & a_{12} \\ a_{21} & a_{22} \end{vmatrix} \neq 0.$

We seek a solution in the form $x = Ae^{pt}$, $y = Be^{pt}$. To determine p we get a characteristic equation

$$\begin{vmatrix} a_{11} - p & a_{12} \\ a_{21} & a_{22} - p \end{vmatrix} = 0 \tag{3.3.61}$$

The quantities A and B can be found from the system
$(a_{11} - p)A + a_{12}B = 0$; $a_{21}A + (a_{22} - p)\ B = 0$, with an accuracy to a constant factor.

The following cases are possible:

1 The roots p_1 and p_2 of Equation (3.3.61) are *real* and *distinct*.
The general solution of Equation (3.3.60) is

$$x(t) = C_1\alpha_1e^{p_1t} + C_2\alpha_2e^{p_2t} : y(t) = C_1\beta_1e^{p_1t} + C_2\beta_2e^{p_2t} \tag{3.3.62}$$

a Assume that $p_1 < 0$ and $p_2 < 0$; the rest point (0, 0) is asymptotically stable in this case since due to the presence of the factors e^{p_1t} and e^{p_2t} all the points of any trajectory, which are in any δ-neighbourhood of the origin at the initial moment $t = t_0$, for a sufficiently large t pass into points lying in an arbitrarily small ε-neighbourhood of the region, and as $t \to \infty$, approach the origin.

Such a rest point is called a stable nodal point.

For $C_2 = 0$, we get from Equation (3.3.62) $x = C_1\alpha_1e^{p_1t} : y = C_1\beta_1e^{p_1t}$
when $y = (\beta_1/\alpha_1)x$ and the trajectories are two rays entering the origin with the slope $k_1 = (\beta_1/\alpha_1)$.

Similarly, for $C_1 = 0$ we obtain another two rays entering the origin with the slope $k_2 = \beta_2/\alpha_2$.

Assume now that $C_1 \neq 0$ and $C_2 \neq 0$, and let, for definiteness, $|p_1| > |p_2|$. Then by using Equation (3.3.62) $\frac{dy}{dx} = \frac{C_1\beta_1 p_1 e^{p_1 t} + C_2\beta_2 p_2 e^{p_2 t}}{C_1\alpha_1 p_1 e^{p_1 t} + C_2\alpha_2 p_2 e^{p_2 t}} \to \frac{\beta_2}{\alpha_2}$ for $t \to +\infty$, i.e. all the trajectories, except for the rays $y = (\beta_1/\alpha_1)x$, have the direction of the ray $y = (\beta_2/\alpha_2)x$ in the neighbourhood of the point O(0, 0).

This is shown in Figure 3.3.19.

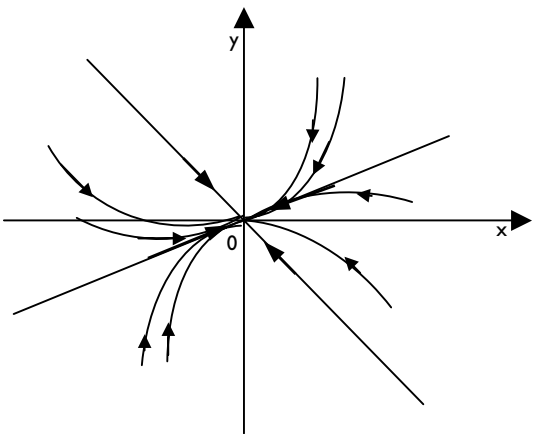


Figure 3.3.19

b If $p_1 < 0$ and $p_2 > 0$, then the position of the trajectories is the same as in the earlier case but the points move along the trajectories in the opposite direction. A rest point of this kind is shown in Figure 3.3.20 and is called an *unstable nodal point*.

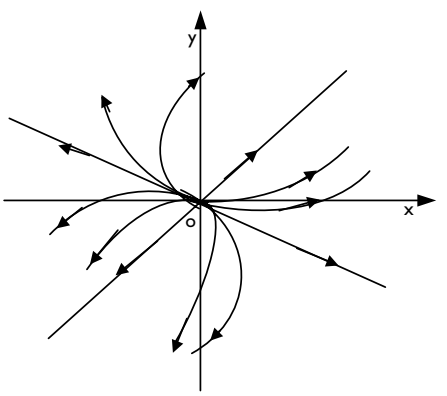


Figure 3.3.20

For example, consider a system : $\dfrac{dx}{dt} = x : \dfrac{dy}{dt} = 2y$

For this system the origin (0, 0) is a rest point. The characteristic equation is

$$\begin{vmatrix} 1-p & 0 \\ 0 & 2-p \end{vmatrix} = 0$$

and it has roots $p_1 = 1$ and $p_2 = 2$, so that we have an unstable nodal point. We pass from the given system to an equation $dy/dx = 2y/x$ or $xdx - 2ydy = 0$. It has solutions $y \equiv 0, x \equiv 0$, and $y = -Cx^2$, so that the trajectories of the system are rays which coincide with the coordinate semi-axis, and the family of parabolas which touch the x-axis at the origin (Figure 3.3.21).

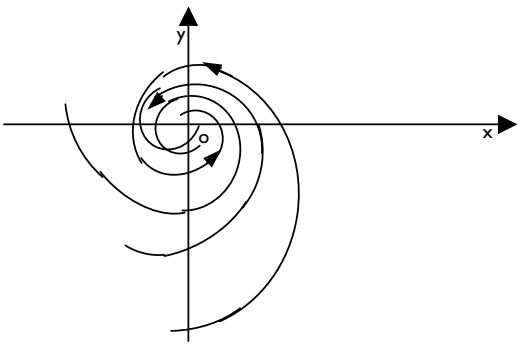


Figure 3.3.21

c Assume that $p_1 > 0$ and $p_2 > 0$, then the rest point is unstable e.g. For $C_2 = 0$, we get the motion: $x = C_1\alpha_1 e^{p_1 t} : y = C_1\beta_1 e^{p_1 t}$

In which with an increase in t the point moves along the ray $y = (\beta_1/\alpha_1)x$ in the direction from the origin ($p_1 > 0$), moving away from it indefinitely.

For $C_1 = 0, x = C_2\alpha_2 e^{p_2 t} : y = C_2\beta_{21} e^{p_2 t}$, it can be seen that with an increase in t the point moves along the ray $y = (\beta_2/\alpha_2)x$ in the direction towards the origin ($p_2 < 0$).

If $C_1 \neq 0$ and $C_2 \neq 0$, then both for $t \to +\infty$ and for $t \to -\infty$ the trajectory leaves the neighbourhood of the rest point. A stationary point of this kind is called a *saddle point* (Figure 3.3.20).

Let us investigate the character of the rest point O(0, 0) of the system:

$$\frac{dx}{dt} = -x : \frac{dy}{dt} = y \tag{3.3.63}$$

The characteristic equation of the system is $p^2 - 1 = 0$ and has roots: $p_1 = 1$ and $p_2 = -1$. Here we have one equation

$$\frac{dy}{dx} = -\frac{y}{x} \quad \text{or } xdx + ydy = 0 \tag{3.3.64}$$

whose integration yields $xy = C = a$ constant.

Equation (3.3.64) also has a solution $y \equiv 0$ and $x \equiv 0$. Thus the integrated curves of Equation (3.3.63) are equilateral hyperbolas and rays coinciding with the coordinate semi-axes.

2 The roots p_1 and p_2 of a characteristic equation are *complex:* $p_{1,2} = r \pm is$ and $s \neq 0$. The general solution of Equation (3.2.60) can be written as

$$x(t) = e^{rt}[C_1 \cos st + C_2 \sin st] : y(t) = e^{rt}[C_1^* \cos st + C_2^* \sin st] \tag{3.3.65}$$

where C_1 and C_2 are arbitrary constants, and C_1^* and C_2^* are some linear combinations of these constants.

a Assume that $p_{1,2} = r \pm i$ s, $r < 0$, $s \neq 0$. In this case the factor e^{rt}, $p < 0$, tends to zero as $t \to +\infty$, and the second factors in Equation (3.3.65) are bounded periodic functions. The trajectories are spirals, as shown in Figure 3.3.21, approaching asymptotically to the origin as $t \to +\infty$. The rest point $x = 0$, $y = 0$ is asymptotically stable. It is known as a *stable focal point*.

If $p_{1,2} = r \pm i$ s, $r > 0$, $s \neq 0$, then this case passes into the preceding one when t is replaced by $-t$. The trajectories do not differ from those in the preceding case, but with a increase in t the movement along them is in the opposite direction. The rest point is unstable. It is known as an *unstable focal point*.

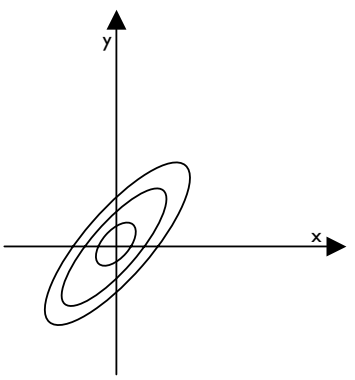


Figure 3.3.22

b If $p_{1,2} = \pm i\,s$, $s \neq 0$, then the solutions of Equation (3.3.60) are periodic functions. The trajectories are closed curves possessing in their interior a rest point which, in this case, is called a *vortex point* and is shown in Figure 3.3.22. The vortex point ias a stable rest point: however, there is no asymptotic stability since the solution

$$x(t) = C_1 \cos st + C_2 \sin st : y(t) = C_1^* \cos st + C_2^* \sin st \qquad (3.3.66)$$

does not tend to zero as $t \to \infty$.

Example 3.3.11

As an example consider a system of equations

$$\frac{dx}{dt} = ax - y : \frac{dy}{dt} = x + ay, \quad \textbf{a is a constant.} \qquad (3.3.67)$$

The characteristic equation of the system is: $(a - p)^2 + 1 = 0$ has complex roots $p_{1,2} = a \pm i$.

We pass from the system to one equation

$$\frac{dy}{dx} = \frac{x + ay}{ax - y} \qquad (3.3.68)$$

and introduce polar coordinates $x = \rho \cos\theta$ and $y = \rho \sin\theta$ and hence $\rho^2 = x^2 + y^2$, $\tan\theta = y/x$ and

$$\rho \frac{d\rho}{dx} = x + y\frac{dy}{dx} : \rho^2 \frac{d\theta}{dx} = x\frac{dy}{dx} - y \qquad (3.3.69)$$

and this is reduced to

$$\frac{d\rho}{d\theta} = \rho \frac{x + yy'}{xy' - y} \qquad (3.3.70)$$

From Equation (3.3.68), we obtain

$$\frac{d\rho}{d\theta} = a\rho, \text{ and the solution is } \rho = Ce^{a\theta}$$

The solution of this equation is logarithmic spiral. The curves winding on the origin reach the limit as $\theta \to \pm\infty$, depending upon $a < 0$ or $a > 0$. We have

here a rest point of the kind of a focal point. In a particular case, when $a = 0$, Equation (3.3.68) assumes the form:

$$\frac{dy}{dx} = -\frac{x}{y}.$$

The integral curves of this equation are circles with centre at the origin, which, for $a = 0$, ia a rest point of the system, Equation (3.3.67), of the kind of a vortex point.

The roots p_1 and p_2 of a characteristic equation are *Multiple*: i.e. $p_1 = p_2$.

This case is rather an exception rather than a rule. An arbitrarily small variation of the coefficients of the system disturbs it. If we use, say, the elimination method, we find that the general solution of Equation (3.3.60) has the form

$$x(t) = (C_1 + C_2 t)\, e^{p_1 t} : y(t) = (C_1^* + C_2^* t)\, e^{p_1 t}$$

where C_1^* and C_2^* are certain linear combinations of C_1 and C_2.

If $p_1 = p_2 < 0$, then, because of the presence of the factor, $e^{p_1 t}$, $p_1 < 0$, the solution $x(t)$ and $y(t)$ tend to zero as $t \to \infty$. The rest point $x = 0$, $y = 0$ is asymptotically stable. It is known as a stable degenerate nodal point and shown in Figure 3.3.23. It differs from the nodal point in case 1a since in that case one trajectory had a tangent different from all the others. A proper nodal point is also possible (Figure 3.3.17).

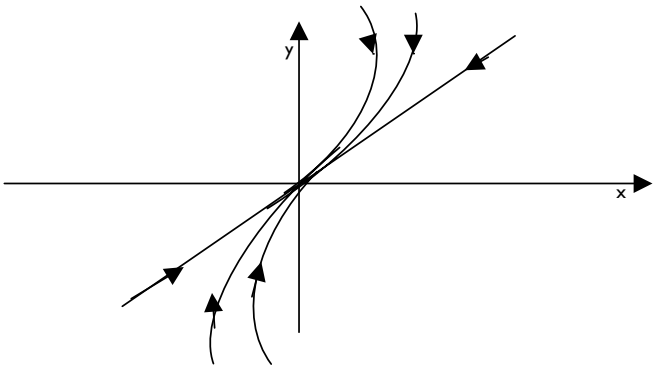


Figure 3.3.23

Example 3.3.12

Consider small oscillation of a pendulum, taking damping into account:

$$\frac{d^2x}{dt^2} = -x - c\frac{dx}{dt} \tag{3.3.71}$$

We can replace Equation (3.3.71) by an equivalent system

$$\frac{dx}{dt} = x_1 \quad \frac{dx_1}{dt} = -x - cx_1 \tag{3.3.72}$$

The characteristic equation of Equation (3.3.72) is

$$\begin{vmatrix} -p & 1 \\ -1 & -c-p \end{vmatrix} = 0 \quad \text{i.e. } p^2 + cp + 1 = 0 \tag{3.3.73}$$

and has roots $p_{1,2} = -\frac{c}{2} \pm \sqrt{\frac{c^2}{4} - 1}$. If $0 < c < 2$, then the roots are complex with a negative real part so that the lower position of equilibrium of the pendulum $x = x_1 = 0$ is a *stable focal point*. The solution of Equation (3.3.71) is a function

$$x(t) = Ae^{-ct/2} \sin(\omega t + \alpha),$$

where $\omega = \sqrt{1 - c^2/4}$ is the oscillation frequency, and the quantities A and α can be found from the initial conditions.

For $0 < c < 2$ the time-domain solution and phase plane solution are shown in Figs. 3.3.24 and 25. As $c \to 0$, i.e. for undamped condition, the *focal point* turns into a *vortex point*: the pendulum will make undamped periodic oscillation.

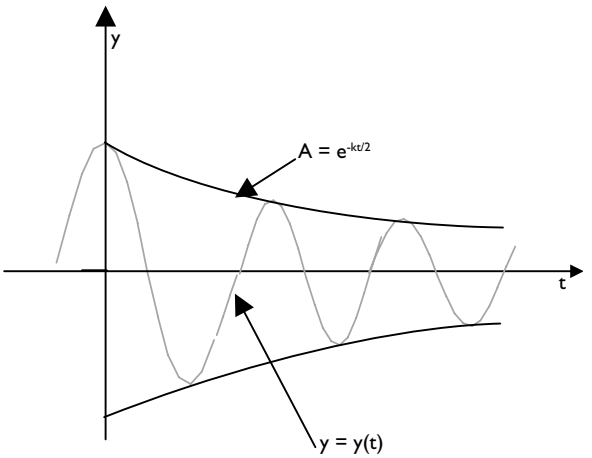


Figure 3.3.24

Now we will extend our attempts to the study of the stability of solutions of a system of n-homogeneous linear differential equations of the first order with constant coefficients, namely

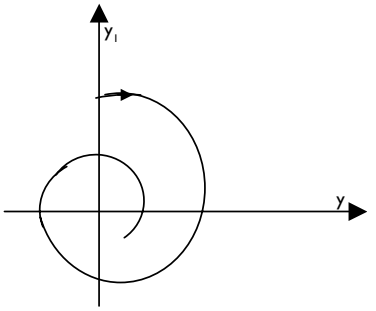


Figure 3.3.25

$$\frac{dx_i}{dt} = \sum_{j=1}^{n} a_{ij}x_j, \quad i = 1, 2, 3, \ldots, n, \quad a_{ij} = \text{constant}. \tag{3.3.74}$$

For system above we consider the characteristic equation as

$$\begin{vmatrix} a_{11} - p & a_{12} & \ldots & a_{1n} \\ a_{21} & a_{22} - p & \ldots & a_{2n} \\ \ldots & \ldots & \ldots & \ldots \\ a_{n1} & a_{n2} & \ldots & a_{nn} - p \end{vmatrix} = 0 \tag{3.3.75}$$

We have following propositions to make:

1 If all the roots of a characteristic equation have a negative real part, then all the solutions of Equation (3.3.75) are asymptotically stable. In this case all the terms of the general solution contain factors $e^{\text{Real}(p)} \cdot k^t$ which tends to zero as $t \to \infty$;
2 If at least one root p_k of Equation (3.3.75) has a positive real part, the all the solutions of the system are unstable;
3 If Equation (3.3.75) has simple roots with a zero real part (purely imaginary or zero roots) and the other roots, provided they exist, have a negative real part, then all the solutions are stable, but there is no asymptotic stability.

These results also refer to one linear differential equation with constant coefficients. A linear system all the solutions are simultaneously either stable or unstable.

Theorem 1. *The solution of a system of differential equations*

$$\frac{dx_i}{dt} = \sum_{j=1}^{n} a_{ij}(t)x_j + f_i(t), \quad i = 1, 2, 3, \ldots, n \tag{3.3.76}$$

are all simultaneously either stable or unstable.

Proof. Transform any particular solution $\varphi_i(t), i = 1, 2, 3, \ldots, n$ of system (Equation 3.3.60) into a trivial solution by means of a substitution $y_i = x_i(t) - \varphi_i(t)$. Then Equation(3.3.76) turns out into a homogeneous linear system with respect to $y_i(t)$:

$$\frac{dy_i}{dt} = \sum_{j=1}^{n} a_{ij}(t) y_j, \quad i = 1, 2, 3, \ldots, n \tag{3.3.77}$$

Now, all particular solutions of Equation (3.3.76) behave similarly i.e. as a trivial solution of homogeneous system (Equation 3.3.61).

In fact, let the trivial solution $y_i(t) \equiv 0$, $i = 1, 2, 3, \ldots, n$, of Equation (3.3.77) be stable. This means that for any $\varepsilon > 0$ there is $\delta = \delta(\varepsilon) > 0$ such that for every other solution $y_i(t)$, $i = 1, 2, 3, \ldots, n$ of the system it follows from the condition $|y_i(t_0)| < \delta$, $i = 1, 2, 3, \ldots, n$, that

$$|y_i(t)| < \varepsilon, \quad i = 1, 2, 3, \ldots, n, \quad \forall t \geq t_0$$

Noting that $y_i(t) = x_i(t) - \varphi_i(t)$, we find that the condition $|x_i(t_0) - \varphi_i(t_0)| < \delta$, $i = 1, 2, 3, \ldots, n$, implies that $|x_i(t) - \varphi_i(t)| < \varepsilon$, $i = 1, 2, 3, \ldots, n$, $\forall t \geq t_0$ for every solution $x_i(t)$, $i = 1, 2, 3, \ldots, n$, of the original system [Equation (3.3.76)]. According to the definition, this signifies the stability of the solution $\varphi_i(t)$, $i = 1, 2, 3, \ldots, n$ of that system.

This proposition does not hold for nonlinear systems, some of whose solutions may be stable while the others may be unstable.

Let us consider a nonlinear equation of the type $\frac{dx}{dt} = 1 - x^2$.

It has obvious solutions $x(t) = -1$ and $x(t) = 1$. The solution $x(t) = -1$ is unstable, and the solution $x(t) = 1$ is asymptotically stable. As $t \to +\infty$ all the solutions

$$x(t) = \frac{(1 + x_0)e^{2(t-t_0)} - (1 - x_0)}{(1 + x_0)e^{2(t-t_0)} + (1 - x_0)}, \quad x_0 \neq -1$$

tend to $+\infty$. According to the definition, this means that the solution $x(t) = 1$ is asymptotically stable.

For example in a case for $n = 2$, we can investigate the position of the trajectories in the neighbourhood of the rest point O(0, 0) of system in Equation (3.3.77). For $n = 3$ the so called nodal–focal points are shown in Figure 3.3.26 and saddle points shown in Figure 3.3.27 are the possibilities.

Theorem 2. Lyapunov's theorem of asymptotic stability
If, for the system of differential equations

$$\frac{dx_i}{dt} = f_i(x_1, x_2, x_3, \ldots, x_n), \quad i = 1, 2, 3, \ldots, n \tag{3.3.78}$$

there is a differentiable definite function $V(x_1, x_2, x_3, \ldots, x_n)$, whose total derivative with respect to time, formed out of the system, is also a definite function of the sign

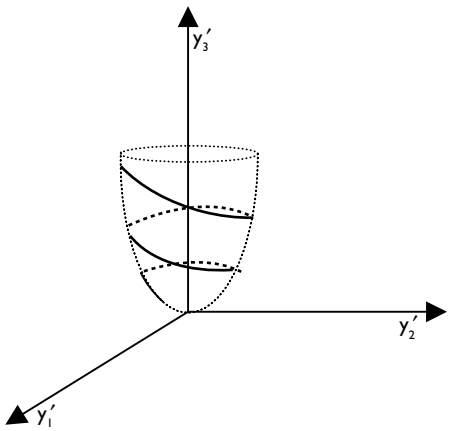


Figure 3.3.26

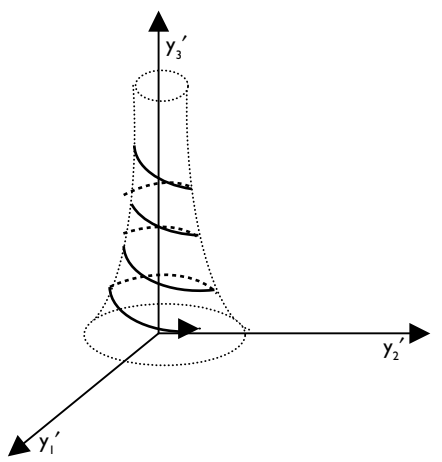


Figure 3.3.27

opposite to that of V, then the rest point $x_i = 0$, $i = 1, 2, 3, \ldots, n$, *of Equation (3.3.78) is asymptotically stable.*

Example 3.3.13

Test for stability of the system: $\dfrac{dx}{dt} = y; \dfrac{dy}{dt} = -x$. **rest point being O**$(0, 0)$ (3.3.79)

Consider a function $V(x, y) = x^2 + y^2$ as the function $V(x, y)$. This function is positive definite. From Equation (3.3.79) we obtain

$$\frac{dV}{dt} = \frac{\partial V}{\partial x}\frac{dx}{dt} + \frac{\partial V}{\partial y}\frac{dy}{dt} = 2xy - 2xy = 0$$

It follows from theorem 1 that the rest point O(0, 0) of Equation (3.3.79) is stable (vortex point). There is no asymptotic stability since the trajectories of Equation (3.3.79) are circles and they do not tend to the point O(0, 0) as $t \to \infty$.

Example 3.3.14

Test for stability of the system: $\frac{dx}{dt} = y - x^3; \frac{dy}{dt} = -x - y^3;$

rest point being O$(0, 0)$. (3.3.80)

Taking $V(x, y) = x^2 + y^2$, we find that

$$\frac{dV}{dt} = 2x(y - x^3) + 2y(-x - y^3) = -2(x^4 + y^4)$$

Thus dV/dt is a negative definite function. From theorem 2, the rest point O(0, 0) of Equation (3.3.80) is asymptotically stable.

Theorem 3. Lyapunov's theorem of instability

Assume that for the system of differential equations

$$\frac{dx_i}{dt} = f_i(x_1, x_2, x_3, \ldots, x_n), \quad (f_i(0, 0, 0, \ldots, 0) = 0) \quad i = 1, 2, 3, \ldots, n \quad (3.3.81)$$

there is a function $V(x_1, x_2, x_3, \ldots, x_n)$, differentiable in the neighbourhood of the origin, such that $V(0, 0, 0, \ldots, 0) = 0$. If its total derivative dV/dt formed out of Eqn. (3.3.81), is a positive definite function, and there are points, arbitrarily close to the origin, at which the function $V(x_1, x_2, x_3, \ldots, x_n)$ assumes positive values, then the rest point $x_i = 0, i = 1, 2, 3, \ldots, n$, of Equation (3.3.81) is unstable.

Example 3.3.15

Test for stability of the system: $\frac{dx}{dt} = x; \frac{dy}{dt} = -y,$ **having rest point O**$(0, 0)$. (3.3.82)

We take a function $V(x, y) = x^3 - y^2$ for which the function

$$\frac{dV}{dt} = \frac{\partial V}{\partial x}\frac{dx}{dt} + \frac{\partial V}{\partial y}\frac{dy}{dt} = 2(x^2 + y^2)$$

is positive definite. Since there are points at which $V > 0$, say $V = x^2 > 0$ along the straight line $y = 0$, arbitrarily close to the origin, All the conditions of theorem 3 are fulfilled and the rest point O(0, 0) is unstable, a saddle point.

3.3.9.4 *Stability in the first (linear) approximation*

Let the given equation be

$$\frac{dx_i}{dt} = f_i(x_1, x_2, x_3, \ldots, x_n), \quad i = 1, 2, 3, \ldots, n \tag{3.3.83}$$

It is given that $x_i = 0$, $i = 1, 2, 3, \ldots, n$, is a rest point of the system i.e.

$$F_i(0, 0, 0, \ldots, 0) = 0, \quad i = 1, 2, 3, \ldots, n, \tag{3.3.84}$$

We assume that the function f_i $(x_1, x_2, x_3, \ldots, x_n)$ are differentiable in the neighbourhood of the origin a sufficient number of times. We apply Taylor's formula to expand the function f_i in terms of x in the neighbourhood of the origin:

$$f_i(x_1, x_2, x_3, \ldots, x_n) = f_i(0, 0, 0, \ldots, 0) + \sum_{j=1}^{n} \frac{\partial f_i(0, 0, 0, \ldots, 0)}{\partial x_j} x_j + R_i(x_1, x_2, x_3, \ldots, x_n)$$

or using Equation (3.3.84), we can have

$$f_i(x_1, x_2, x_3, \ldots, x_n) = \sum_{j=1}^{n} a_{ij} x_j + R_i(x_1, x_2, x_3, \ldots, x_n)$$

in which $a_{ij} = \frac{\partial f_i(0,0,0,\ldots,0)}{dx_j}$ = constant, and R_i include terms not lower than the second order of smallness w.r.t $x_1, x_2, x_3, \ldots, x_n$. The system of differential equations (3.3.83) assumes the form:

$$\frac{dx_i}{dt} = \sum_{j=1}^{n} a_{ij} x_j + R_i(x_1, x_2, x_3, \ldots, x_n), \quad i = 1, 2, 3, \ldots, n; \quad a_{ij} \text{ is a constant.} \tag{3.3.85}$$

Since the concept of stability of a rest point O$(0, 0, 0, \ldots, 0)$ is connected with small neighbourhood of the origin in the phase space, it is natural; to expect that

the behaviour of solution (3.3.83) will be defined by the principal linear terms of the expansion of the functions f_i in terms of x. Therefore, alongside the system (3.3.85) we consider a system

$$\frac{dx_i}{dt} = \sum_{j=1}^{n} a_{ij}x_j : i = 1, 2, 3, \ldots, n \tag{3.3.86}$$

There is, strictly no connection between systems (3.3.85) and (3.3.86). Let us consider, for example, an equation

$$\frac{dx}{dt} = x^2 \tag{3.3.87}$$

Here $f(x) \equiv x^2$. The linearised equation for (3.3.87) has the form:

$$\frac{dx}{dt} = 0 \tag{3.3.88}$$

The solution $x(t) \equiv 0$ of Equation (3.3.88) is stable. But it is not stable when it is a solution of the original Equation (3.3.87). Indeed, every real solution of Equation (3.3.87), which satisfies the initial condition $x|_{t=t0} = x_0 > 0$, has the form $x = x_0/(1 - tx_0)$ and ceases to exist for $t = 1/x_0$, i.e. the solution cannot be extended to the right.

Theorem 1. *If all the roots of the characteristic equation*

$$\begin{vmatrix} a_{11} - p & a_{12} & \ldots & a_{1n} \\ a_{21} & a_{22} - p & \ldots & a_{2n} \\ \ldots & \ldots & \ldots & \ldots \\ a_{n1} & a_{n2} & \ldots & a_{nn} - p \end{vmatrix} = 0 \tag{3.3.89}$$

have negative real parts, then the rest point $x_i = 0$, $i = 1, 2, 3, \ldots, n$, of Eqns. (3.3.84) and (3.3.87) is asymptotically stable.

When the conditions of the theorem are satisfied, it is possible to test the rest point for stability in the first approximation.

Theorem 2. *If at least one root of the characteristic equation (3.3.89) has a positive real part, then the rest point $x_i = 0$ of the systems in Eqns. (3.3.85) and (3.2.86) is unstable.*

In this case it is also possible to test the rest point for stability in the first approximation.

Proof. Let us assume that the roots $p_1, p_2, p_3, \ldots, p_n$ of Equation (3.3.89) are real and distinct. We know that in this case there is a non-singular matrix $B = (b_{ij})_{i,j=1}^{n}$

with constant elements b_{ij} such that the matrix $B^{-1}AB$ is diagonal, i.e.

$$B^{-1}AB = \begin{bmatrix} p_1 & 0 & \dots & 0 \\ 0 & p_2 & \dots & 0 \\ \dots & \dots & \dots & \dots \\ 0 & 0 & \dots & p_n \end{bmatrix}$$

where $A = (a_{ij})_{i,j=1}^{n}$ is a coefficient matrix of Equation (3.3.86).

Now we set

$$X = B\,Y, \text{ in which } X = \begin{Bmatrix} x_1 \\ x_2 \\ \dots \\ x_n \end{Bmatrix} \quad \text{and} \quad Y = \begin{Bmatrix} y_1 \\ y_2 \\ \dots \\ y_n \end{Bmatrix}$$

Then $dX/dt = B\,dY/dt$, and Equation (3.3.86) is reduced to the form $B\,dY/dt = ABY$. Hence we obtain $dY/dt = B^{-1}ABY$, or, by the choice of the matrix B

$$\frac{dy_i}{dt} = p_i y_i,\ i = 1, 2, 3, \dots, n$$

Under the same transformation, Equation (3.3.51) reduces to

$$\frac{dy_i}{dt} = p_i y_i + \tilde{R}_i(y_1, y_2, \dots, y_n) \tag{3.3.90}$$

and $\tilde{R}_i$ include terms not lower than that of the second order of smallness w.r.t. y_i as $y_i \to 0$.

Possibilities:

1 All the roots p_k are negative. We set, $V = y_1^2 + y_2^2 + \dots + y_n^2$

The from Equation (3.3.90), the derivative dV/dt will have the form

$$\frac{dV}{dt} = 2(p_1 y_1^2 + p_2 y_2^2 + \dots + p_n y_n^2) + S(y_1, y_2, \dots, y_n).$$

where $S(y_1, y_2, \dots, y_n)$ for $\sum_{i=1}^{n} y_i^2 \to 0$, which is an infinitesimal of the order higher than that of the quadratic form $\sum_{i=1}^{n} p_i y_i^2$.

Thus, in a sufficiently small neighbourhood Ω of the point O$(0, 0, 0, \dots, 0)$ the function $V(y_1, y_2, \dots, y_n)$ is positive definite, and the derivative dV/dt is negative definite, and, hence the rest point O$(0, 0, 0, \dots, 0)$ is asymptotically stable.

2 Some of the roots p_k, say $p_1, p_2, \ldots, p_m$, $m \leq n$, are positive and others are negative. We set

$$V = y_1^2 + y_2^2 + \cdots + y_m^2 - y_{m+1}^2 - \cdots - y_n^2.$$

Then,

$$dV/dt = 2[p_1 y_1^2 + p_2 y_2^2 + \cdots + p_m y_m^2 - p_{m+1} y_{m+1}^2 - \cdots - p_n y_n^2] + S(y_1, y_2, \ldots, y_n).$$

It can be seen that, arbitrarily close to the origin, there are points (such points say, for which $y_{m+1} = \cdots = y_n = 0$), at which $V > 0$. As to the derivative dV/dt, it is a positive definite function since $p_{m+1}, \ldots, p_n$ are negative. From theorem 3, the rest point O $(0, 0, 0, \cdots, 0)$ is unstable.

In a critical case, when all the real parts of the roots of the characteristic equation are nonnegative, and the real part of at least one root is zero, the stability of the trivial solution of Equation (3.3.85) begins to be affected by the nonlinear terms of R_i and it becomes impossible to carry out a test for stability in the first approximation.

Example 3.3.16

Test for stability in the first approximation the rest point $x = 0$, $y = 0$, of the equation

$$\boldsymbol{dx/dt = -x + 2y - 5y^2; \quad dy/dt = 2x - y + x^3/2} \tag{3.3.91}$$

The system of the first approximation has the form

$$dx/dt = -x + 2y; \quad dy/dt = 2x - y \tag{3.3.92}$$

The nonlinear terms satisfy the necessary conditions: their order is not smaller than 2. We derive a characteristic equation for Equation (3.3.92) as

$$\begin{vmatrix} -1-p & 2 \\ 2 & -1-p \end{vmatrix} = 0, \quad \text{or } p^2 + 2p - 3 = 0.$$

The roots of the characteristic equations are $p_1 = 1$ and $p_2 = -3$. Since $p_1 > 0$, the zero solution $x \equiv 0$, $y \equiv 0$ of Equation (3.3.91) is unstable.

Example 3.3.17

Test for stability the rest point O(0, 0) of the system:

$$dx/dt = y - x^3; \quad dy/dt = -x - y^3. \tag{3.3.93}$$

The rest point $x = 0$, and $y = 0$, of Equation (3.3.93) is asymptotically stable since for this system Lyapunov's function $V = x^2 + y^2$ satisfies the conditions of Lyapunov's theorem of an asymptotic stability. In particular,

$$dV/dt = 2x(y - x^3) + 2y(-x - y^3) = -2(x^4 + y^4) \leq 0.$$

At the same time the rest point $x = 0$, $y = 0$, of the system

$$dx/dt = y + x^3, \quad dy/dt = -x + y^3 \text{ is unstable.} \tag{3.3.94}$$

From Equation (3.3.94) we have for the function $V(x, y) = x^2 + y^2$

$$\frac{dV}{dt} = \frac{\partial V}{\partial x}\frac{dx}{dt} + \frac{\partial V}{\partial y}\frac{dy}{dt} = 2x(y + x^2) + 2y(-x + y^3) = 2(x^4 + y^4)$$

i.e. dV/dt is a positive definite function. Arbitrarily close to the origin O(0, 0) there are points at which $V(x, y) > 0$.

By theorem 3, we infer that the rest point O(0, 0) of Equation (3.3.94) is unstable.

For system in Eqns. (3.3.93) and (3.3.94) the system of the first approximation is the same, i.e.

$$dx/dt = y; \; dy/dt = -x \tag{3.3.95}$$

For Equation (3.3.95), the characteristic equation is $p^2 + 1 = 0$ and has pure imaginary roots, which is a critical case [the real parts of the roots of the characteristic equation are zero]. For the system of the first approximation Equation (3.3.95), the origin is a stable rest point, a vortex point. Eqns. (3.2.93) and (3.2.94) results from a small perturbation of the right hand sides of Equation (3.2.95) in the neighbourhood of the origin. However, as a result of the small perturbations, the rest point O(0, 0) for Equation (3.3.93) becomes asymptotically stable, whereas for system Equation (3.3.94) it becomes unstable.

This shows that in a critical case the nonlinear terms can affect the stability of the rest point.

3.4 MULTIPLE-DEGREES-OF-FREEDOM SYSTEMS

3.4.1 Free vibration: Undamped system

In this section we give you just an introduction to what do we mean by a system having multi-degrees of freedom. In general, the number of degrees of freedom of a system is equal to the sum of the number of independent coordinates necessary to describe each mass into which the system has been discretised. Also when the exciting force is not acting at the c.g. of the system, it will develop a coupled motion (rocking and translation simultaneously) resulting in a two-degrees-of-freedom system. Shown in Figure 3.4.1 is a general machine foundation system resting on the ground. It is apparent that mathematical model of the system boils down to a multi-degrees-of-freedom system.

A general multi-storied Frame structure is shown in Figure 3.4.2. This is usually idealized as a multi-mass system. It is usual to assume the masses to be lumped at the floor levels and the lumped mass having a value corresponding to weight of the floor plus part of the supporting system above and below the floor level and also the effective live load. If the frame is set to vibrate horizontally in the vertical plane, the floor supporting systems provide the restoring forces (spring force). Each mass would provide one-degree-of freedom and the entire frame in Figure 3.4.2, has five-degrees-of freedom.

When the system is set into vibration and all the masses attain maximum amplitude simultaneously and all the masses pass through the equilibrium position simultaneously, then it is said to be vibrating in its *natural* or *normal* or *principal mode* of vibration.

For an undamped system, the response in such a mode of vibration would be sinusoidal and correspond to one of the frequencies of the system termed as natural or principal frequency. If all the masses vibrate in phase, i.e. all the masses have same sign of amplitude at any particular instant of time, the mode is called the first mode or the lowest or fundamental mode of vibration. The frequency corresponding to this mode will be the lowest in magnitude. If all adjacent masses vibrate out of phase with

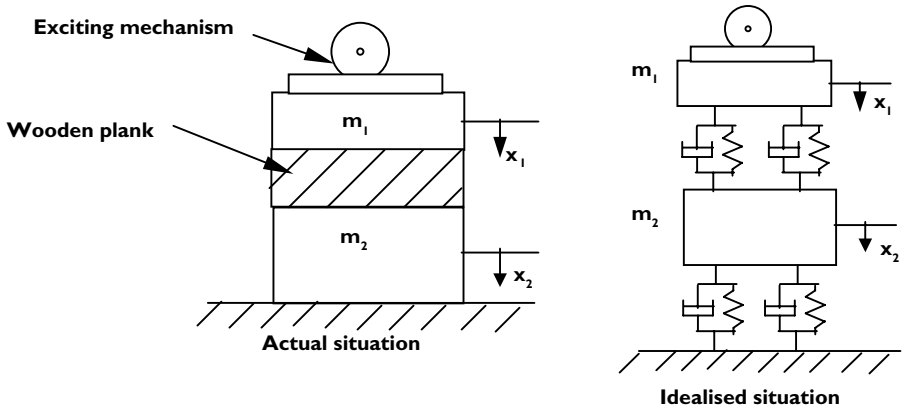


Figure 3.4.1 A two-degrees-of-freedom system.

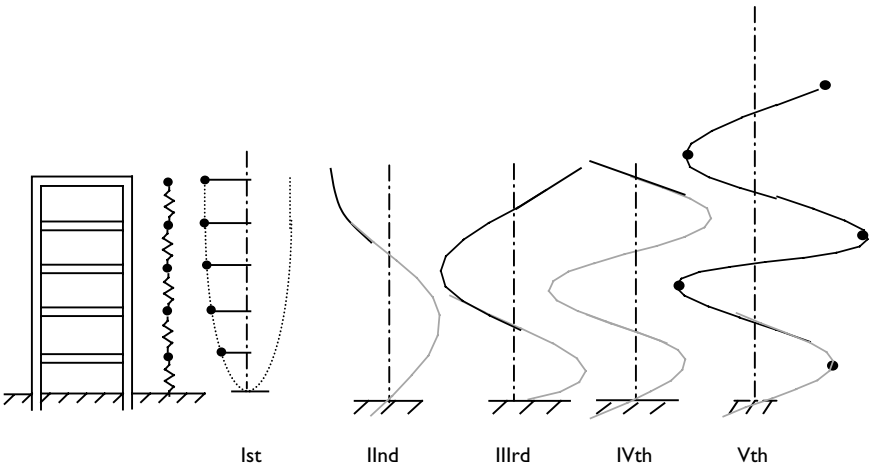


Figure 3.4.2 A multi-storied frame structure: idealisation and mode shapes.

one another, i.e. adjacent masses have opposite sign of amplitude at any particular instant of time, the mode is termed as the highest mode of vibration. The frequency corresponding to this mode would be the highest in magnitude.

We will not pursue the matter further here, and would come back to it latter in Chapter 5 (Vol. 1) where we have exhaustively developed the mathematical theories underlying this. We would however like to elaborate hereafter the mechanical impedance theory as applied to multi-degrees of freedom that is sometimes used also by structural and foundation engineers in analysis and design of some typical structures-especially subjected to harmonic loads.

3.4.2 Steady-state analysis: Mechanical impedance method

Mechanical impedance method described for a single-degree-of-freedom system can be extended to a multi-degree-of-freedom system (n-degree) and expressed as

$$\underset{n\times n\ \ n\times 1}{[m]\ \{\ddot{X}\}} + \underset{n\times n\ \ n\times 1}{[C]\ \{\dot{X}\}} + \underset{n\times n\ n\times 1}{[K]\ \{X\}} = \underset{n\times 1}{\{F\}} \tag{3.4.1}$$

For a harmonic of response of the type $e^{i\omega t}$ Equation (3.4.1) can be reduced to

$$[-\omega^2[M] + i\omega\,[C] + [K]\,]\{X\} = \{F\} \tag{3.4.2}$$

This can be rewritten as

$$[Z]\{\boldsymbol{X}\} = \{\boldsymbol{F}\},\ \text{that is}\ \{\boldsymbol{X}\} = [Z]^{-1}\{\boldsymbol{F}\} \tag{3.4.3}$$

where Z is known as mechanical impedance.

For a two-degrees-of-freedom system as an example (say),

$$\left[-\omega\begin{bmatrix}m_{11} & m_{12}\\ m_{21} & m_{22}\end{bmatrix}+i\,\omega\begin{bmatrix}c_{11} & c_{12}\\ c_{21} & c_{22}\end{bmatrix}+\begin{bmatrix}k_{11} & k_{12}\\ k_{21} & k_{22}\end{bmatrix}\right]\begin{Bmatrix}X_1\\ X_2\end{Bmatrix}=\begin{Bmatrix}F_{01}\\ F_{02}\end{Bmatrix} \tag{3.4.4}$$

the rest is similar to the one given in Equation (3.4.3) that is $[Z]\{X\}=\{F\}$ and results are shown below

$$X_1=\frac{Z_{22}F_{01}-Z_{12}F_{02}}{Z_{11}Z_{22}-Z_{12}Z_{21}};\quad X_1=\frac{-Z_{21}F_{01}+Z_{11}F_{02}}{Z_{11}Z_{22}-Z_{12}Z_{21}} \tag{3.4.5}$$

If we substitute $F_{01}e^{i\omega t}$ for $F_{01}\sin\omega t$, $\boldsymbol{X}_1e^{i\omega t}$ for $x_1(t)$ and $F_{02}e^{i\omega t}$ for $F_{02}\sin\omega t$, $\boldsymbol{X}_2e^{i\omega t}$ for $x_2(t)$ in Equation (3.4.5), $\boldsymbol{X}_1$ and $\boldsymbol{X}_2$ are the complex amplitude of $x_1(t)$ and $x_2(t)$, respectively. After some rearranging and factoring out $e^{i\omega t}$ we obtain

$$\begin{aligned}&[(k_1+k_2)-m_1\omega^2+i(c_1+c_2)]X_1-(k_2+ic\omega)X_2=F_{01}\\ &-(k_2+ic\omega)X_1+[(k_2+k_3)-m_2\omega^2+i(c_2+c_2)\omega\,]X_2=F_{02}\end{aligned} \tag{3.4.6}$$

$\boldsymbol{X}_1$ and $\boldsymbol{X}_2$ can be obtained from these equations by using Cramer's rule as follows

$$X_1=\frac{\begin{vmatrix}F_{01} & -(k_2+ic_2\omega)\\ F_{02} & k_2+k_3-m_2\omega^2+i(c_2+c_3)\omega\end{vmatrix}}{\Delta(\omega)}=X_1e^{-i\psi_1}$$

$$X_2=\frac{\begin{vmatrix}k_1+k_2-m_1\omega^2+i(c_1+c_2)\omega & F_{01}\\ -(k_2+ic_2\omega) & F_{02}\end{vmatrix}}{\Delta(\omega)}=X_2e^{-i\psi_2}$$

in which

$$\Delta(\omega)=\begin{vmatrix}k_1+k_2-m_1\omega^2+i(c_1+c_2)\omega & -(k_2+ic_2\omega)\\ -(k_2+ic_2\omega) & k_2+k_3-m_2\omega^2+i(c_2+c_3)\omega\end{vmatrix} \tag{3.4.7}$$

and ψ_1 and ψ_2 are the phase angles of the complex amplitudes $\boldsymbol{X}_1$ and $\boldsymbol{X}_2$, respectively.

Corresponding to the excitation forces $F_{01}\sin\omega t$ and $F_{02}\sin\omega t$, the steady state response of the masses are

$$x_1=\boldsymbol{X}_1\sin(\omega t-\psi_1)\quad\text{and}\quad x_2=\boldsymbol{X}_2\sin(\omega t-\psi_1) \tag{3.4.8}$$

3.4.3 Coupled translation and rotation

Consider a situation wherein a rigid body like say a foundation block is resting on an non-uniform spring support as shown in Figure 3.4.3.

Say $k_4 > k_1$: Line of reaction of the spring force will not pass through the c.g. of the rigid footing whereby there will be a rotation of the footing as shown in Figure 3.4.4 Let the c.g. be fixed while the footing rotates about the horizontal axis

Assumptions:

1 We have a centre of rotation, O.
2 Centre of pressure moves only in vertical direction.
3 Replacement of all sprins k_1 to k_4 by k_z.
4 Spring constant of rotation k_θ exists.

Translation Using force balance:

$$m\ddot{z} = -k_z(z + R\theta) \Rightarrow m\ddot{z} + k_z\,(z + R\theta) = 0 \tag{3.4.9}$$

Rotation Moment balance about O:

$$J\ddot{\theta} = -k_\theta\theta\, - k_z(z + R\theta\,)R \Rightarrow J\ddot{\theta} + k_\theta\,\theta + k_z(z + R\theta\,)R = 0 \tag{3.4.10}$$

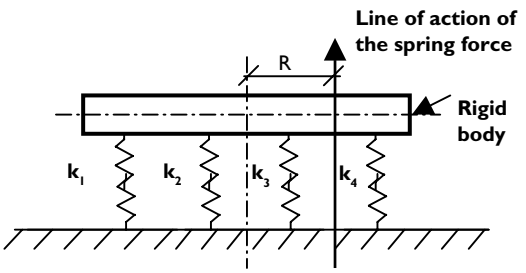


Figure 3.4.3

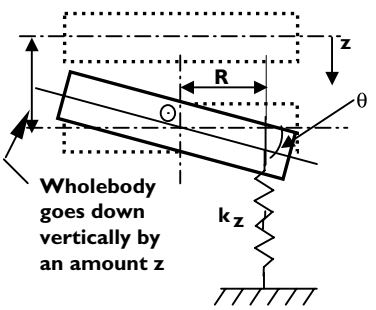


Figure 3.4.4 Coupled translation and rotation with no lateral movement.

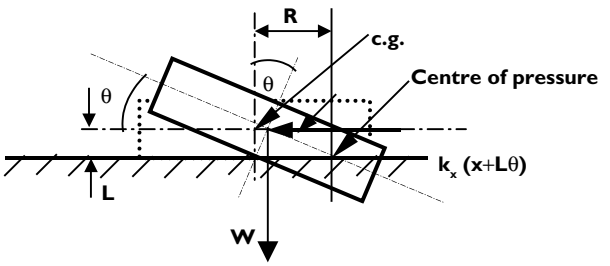


Figure 3.4.5 Combined lateral movement and rocking.

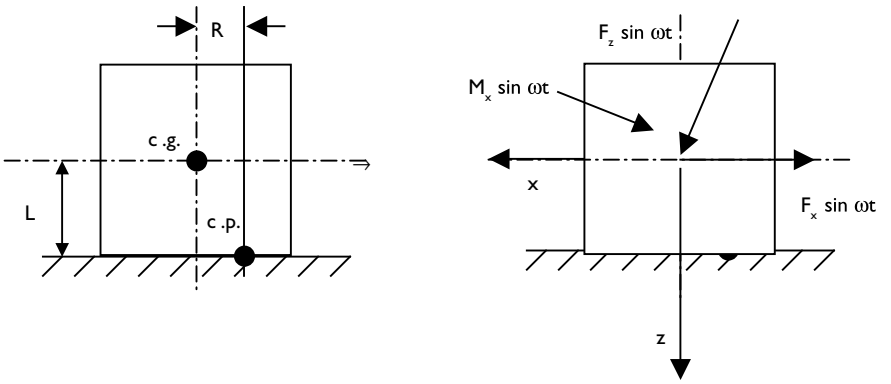


Figure 3.4.6 Coupled translation and rocking.

Equations (3.4.9) and (3.4.10) can be solved by assuming

$$z = A_z \sin \omega t \quad \text{and } \theta = A_\theta \sin \omega t \tag{3.4.11}$$

Centre of gravity has a free movement in lateral direction (Figure 3.4.5)
Governing equations of motion:

Vertical $$m\ddot{z} = -k_z z - (\theta\, R k_z) \Rightarrow m\ddot{z} + z k_z + R\theta\, k_z = 0 \tag{3.4.12}$$

Horizontal $$m\ddot{x} = -k_x x - k_x(L\theta\,) \Rightarrow m\ddot{x} + x k_x + L\theta\, k_x = 0 \tag{3.4.13}$$

Rotation about O'
$$J\ddot{\theta} = -\theta\, k_\theta - [k_z(z + R\theta\,)R] + WL\theta - [k_x(x + L\theta\,)L]$$
$$J\ddot{\theta} + \theta\, k_\theta + [k_z(z + R\theta\,)R] + [k_x(x + L\theta\,)L] - WL\theta = 0 \tag{3.4.14}$$

➔ Results in three-degrees-of-freedom.

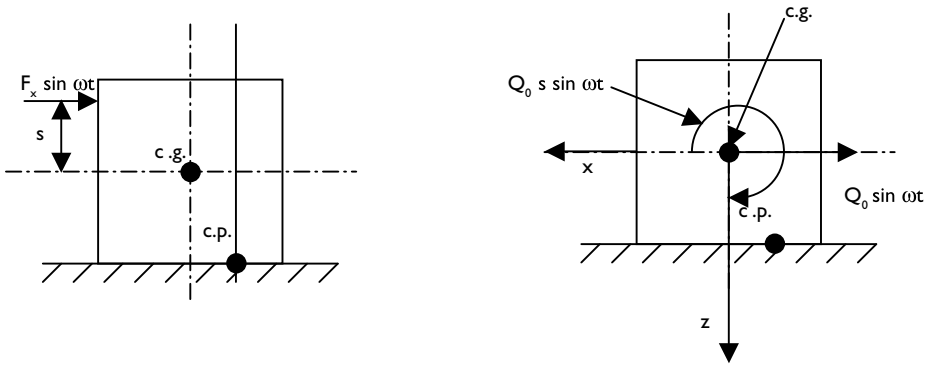


Figure 3.4.7 Coupled translation and rotation.

Cases:

1 If $R = 0 \rightarrow$ Two-degrees-of-freedom: Equations (3.4.12) and (3.4.13) are uncoupled while Equations (3.4.13) and (3.4.14) are always coupled.
2 If there is no horizontal movement: Equation (3.4.13) will not be there and corresponding terms in Equation (3.4.14) will be absent.

3.4.4 Forced vibration

Consider the situation shown in Figure 3.3.6
Governing equations are:

$$\begin{aligned} &m\ddot{z} + zk_z + R\theta\, k_z = F_z \sin\, \varpi\, t \\ &m\ddot{x} + xk_x + L\theta\, k_x = -F_x \sin\, \varpi\, t \\ &J\ddot{\theta} + \theta\, k_\theta - WL\theta + Rzk_z + R^2\theta\, k_z + xLk_x + k_xL^2\theta = M \sin\, \varpi t \end{aligned} \tag{3.4.15}$$

A practical situation may look like the one shown in Figure 3.4.7.

Example 3.4.1

1 **An elastically supported damper system, shown in Figure 3.4.8, can be used to successfully isolate the force transmitted to the foundation of the machine. Analyse the response.**

Solution:

We have two equations from the free-body diagram of the problem:

$$m\ddot{x}_1 + c(\dot{x}_1 - \dot{x}_2) + kx_1 = F \sin \omega t \quad \text{and } c(\dot{x}_1 - \dot{x}_2) = k_1x_2 \tag{3.4.16}$$

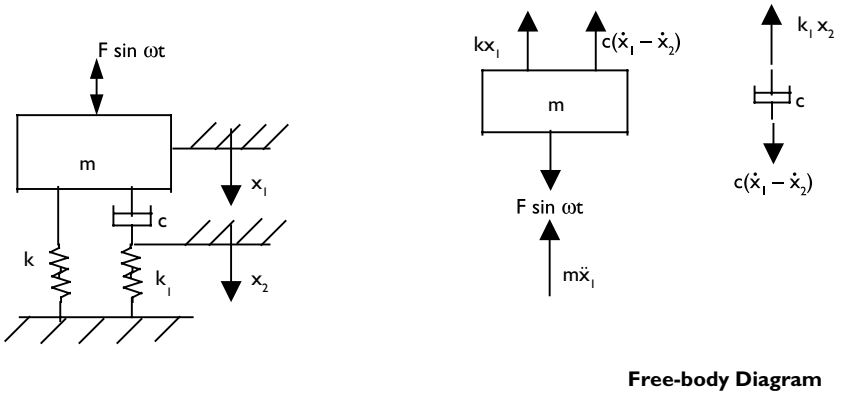


Figure 3.4.8 Elastically supported damper.

Replacing viscous term from the first equation using the second equation, we have

$$m\ddot{x}_1 + k_1 x_2 + kx_1 = F\sin\omega t \Rightarrow x_2 = [F\sin\omega t - m\ddot{x}_1 - kx_1]/k_1 \quad (3.4.17)$$

Substituting the value of x_2 in the first equation and a little rearrangement of terms, one can have

$$\dddot{x}_1 + \frac{k_1}{c}\ddot{x}_1 + \frac{k+k_1}{m}\dot{x}_1 + \frac{kk_1}{mc}x_1 = \frac{k_1}{mc}F\sin\omega t + \frac{\omega}{m}F\cos\omega t \quad (3.4.18)$$

This is a third order differential equation to be solved for obtaining the value of x_1.

The problem can be solved by using impedance method as follows:

Let the excitation be represented by $Fe^{i\omega t}$ and the displacements $x_1(t)$ and $x_2(t)$, respectively by $\boldsymbol{X}_1 e^{i\omega t}$ and $\boldsymbol{X}_2 e^{i\omega t}$, where $\boldsymbol{X}_1$ and $\boldsymbol{X}_2$ are complex amplitudes. Now, the free-body equations may be written as (by factoring out $e^{i\omega t}$)

$$[k - m\omega^2 + ic\omega]\,\boldsymbol{X}_1 - ic\omega\,\boldsymbol{X}_2 = \boldsymbol{F} : -ic\omega\,\boldsymbol{X}_1 + [k_1 + i\ c\ \omega]\boldsymbol{X}_2 = 0 \quad (3.4.19)$$

$\boldsymbol{X}_1$ and $\boldsymbol{X}_2$ can be solved by Cramer's rule as

$$\boldsymbol{X}_1 = \frac{F(k_1 + ic\omega)}{k_1(k - m\omega^2) + ic\omega\,(k + k_1 - m\omega^2)} :$$
$$\boldsymbol{X}_2 = \frac{ic\omega F}{k_1(k - m\omega^2) + ic\omega\,(k + k_1 - m\omega^2)} \quad (3.4.20)$$

Taking non-dimensional parameters like: $n = k_1/k$, $\omega_n = \sqrt{(k/m)}, c/m = 2D\omega_n = \omega/\omega_n$, $\boldsymbol{X}_1$ and $\boldsymbol{X}_2$ can be expressed as

$$\begin{aligned}\boldsymbol{X}_1 &= \frac{F}{k}\frac{\sqrt{1+(2Dr/n)^2}}{\sqrt{(1-r^2)^2+\left[2Dr\left(1+\frac{1}{n}-\frac{r^2}{n}\right)\right]^2}}e^{-i\phi} = \boldsymbol{X}_1 e_1^{-i\phi}\\ \boldsymbol{X}_2 &= \frac{F}{k}\frac{2Dr/n}{\sqrt{(1-r^2)^2+\left[2Dr\left(1+\frac{1}{n}-\frac{r^2}{n}\right)\right]^2}}e_2^{-i\phi} = \boldsymbol{X}_2 e_2^{-i\phi}\end{aligned} \tag{3.4.21}$$

In which

$$\begin{aligned}\phi_1 &= \tan^{-1}\left[\frac{2Dr\left[1+\frac{1}{n}-\frac{r^2}{n}\right]}{1-r^2}\right] - \tan^{-1}\left[\frac{2Dr}{n}\right];\\ \phi_2 &= \tan^{-1}\left[\frac{2Dr\left[1+\frac{1}{n}-\frac{r^2}{n}\right]}{1-r^2}\right] - \frac{\pi}{2}.\end{aligned} \tag{3.4.22}$$

The steady-state response can be written as

$$x_1 = \boldsymbol{X}_1 \sin(\omega t - \phi_1) \quad \text{and } x_2 = \boldsymbol{X}_2 \sin(\omega t - \phi_2). \tag{3.4.23}$$

Example 3.4.2

Effect of earthquake on a rigid building is simulated as shown in Figure 3.4.9 The building base is idealized through two springs k_H and k_θ for ground's translational and rotational stiffnesses respectively. The ground is now given a harmonic motion $x_G = x_g \sin \omega t$. Set up the equations of motion in terms of coordinates shown in the Figure

Solution:

Vibration due to the translation x_0 of the foundation, Eqns. (3.4.13) and (3.4.14) may be written as

$$m\ddot{x} + k_x(x + \theta\ell_0) = -m\ddot{x} \quad \text{and } J_0\ddot{\theta} + \theta\, k_\theta + k_x(x + \theta\, \ell_0) = 0 \tag{3.4.24}$$

where x is the displacement of the mass-c.g. along the X-axis, less the displacement of the foundation; θ is the angular rotation of the mass-c.g. or the mass point; ℓ_0 is the eccentricity of the mass centre relative to the stiffness centre; k_x

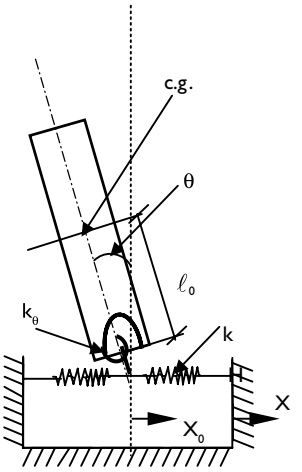


Figure 3.4.9 An earthquake type of disturbance to a rigid building frame.

and k_θ are the stiffness factors of the system in linear and angular deflection, respectively; and J_0 is the mass moment of inertia about the mass centre.

Physically, the first equation of Equation (3.4.24) is the equation of the dynamic equilibrium of the force projection on the ***X***-axis, whereas the second describes the equilibrium of the moments about the mass c.g. Setting $x_G = x_g \sin \omega t$, Equation (3.4.24) reduces to

$$m\ddot{x} + k_x(x + \theta\ell_0) = m\omega^2 \sin \omega t \quad \text{and } J_0\ddot{\theta} + \theta k_\theta + k_x(x + \theta\ell_0) = 0 \tag{3.4.25}$$

➔ Consider a case where

$\omega_x^2 = k_x/m; \omega_\theta^2 = k_\theta/J_0 = k_\theta/[m\rho_c^2]$; and $[\rho_c/\ell_0]^2 = 1/3$; and $(\omega_r/\omega_x)^2 = 4$ and $J_0 = m\ell_c^2$, where ℓ_c *is the radius of gyration.*

Now, we can have the equations for free vibration as

$$m\ddot{x} + k_x(x + \theta\ell_0) = 0 \quad \text{and } J_0\ddot{\theta} + \theta k_\theta + k_x(x + \theta\ell_0) = 0 \tag{3.4.26}$$

The solution of Equation (3.4.26), from which the natural frequencies and mode of the translational and rotational vibrations could be obtained, are written in the form $x = A_x \sin \omega t$ and $\theta = A_\theta \sin \omega t$. Substituting them, Equation (3.4.26), we have

$$\begin{bmatrix} k_x - m\omega^2 & \ell_0 k_x \\ \ell_0 k_x & k_\theta + k_x\ell_0^2 - j_0\omega^2 \end{bmatrix} \begin{Bmatrix} A_1 \\ A_2 \end{Bmatrix} = \begin{Bmatrix} 0 \\ 0 \end{Bmatrix} \tag{3.4.27}$$

Thus, the characteristic equation reduces to

$$(-m\omega^2 + k_x)(k_\theta - J_0\omega^2 + k_x\ell_0^2) + \ell_0^2 k_x^2 = 0 \tag{3.4.28}$$

Finally, it reduces to $\omega^4 - \dfrac{\omega^2}{mJ_0}[k_\theta m + k_x(J_0 + m\ell_0^2)] + \dfrac{k_x k_\theta}{mJ_0} = 0$ (3.4.29)

Two roots of Equation (3.4.29) may be written as

$$\omega_{1,2}^2 = \phi \pm \left[\phi^2 - \frac{k_x k_\theta}{mJ_0}\right]^{1/2} \tag{3.4.30}$$

where $\phi = \frac{1}{2mJ_0}[k_x(J_0 + m\ell_0^2) + mk_\theta]$.

Substituting the values outlined for the present case, we have, $\phi = 4\omega_x^2$ and $\omega_{1,2}^2$ may be written as

$$\omega_{1,2}^2 = 4\omega_x^2 \pm \sqrt{16\omega_x^2 - \frac{\omega_\theta^2}{\omega_x^2}\omega_x^4} = \omega_x^2[4 \pm 3.464]$$

$\bar{\omega}_1 = (\omega_1/\omega_x) = 0.732$ and $\bar{\omega}_2 = (\omega_2/\omega_x) = 2.732$.

From Equation (3.4.27), the mode shapes can be expressed as

$$\frac{A_{1i}}{A_{2i}} = -\frac{\ell_0 k_x}{k_x - m\omega_i^2} = -\frac{k_\theta + k_x\ell_0^2 - J_0\omega_i^2}{k_x\ell_0}, \quad \text{at } i = 1, 2. \tag{3.4.31}$$

Here we assume A_{11}, A_{12}, A_{21} and A_{22} are values of A_1 and A_2 for ω_1 and ω_2, with the parameters given for this problem, Equation (3.4.31) reduces to

$$\frac{A_{1i}}{\ell_0 A_{2i}} = -\frac{1}{1 - \bar{\omega}_i^2} = -\frac{7 - \bar{\omega}_i^2}{3} = -2.154, -0.154,$$

for $i = 1$ and 2, respectively.

x-displacement of the mass can be written as $x + \ell_0\theta$, hence $\frac{X_1}{\ell_0\theta} = 1 - 2.154 = -1.154$; and $\frac{X_2}{\ell_0\theta} = 0.854$ and $\frac{X_2}{X_1} = -0.732$.

3.4.5 Semi-definite systems

When one of the natural frequencies of a system is zero, i.e. one of the roots of the frequency equation vanishes; the system reduces to a degenerated system. Physically,

the system may move as a rigid body without any exciting force. This class of system represents a large group of engineering problems and is called a semi-definite system.

Example 3.4.3

Examples are shown in Figure 3.4.10.

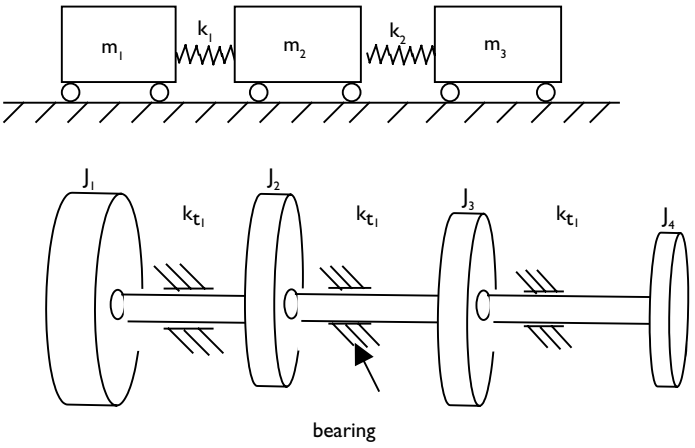


Figure 3.4.10 Semi-definite systems.

3.4.5.1 Rectilinear system

The system consists of a number of masses connected through springs. This system may used to study the vibration of a locomotive or a similar vehicle.

3.4.5.2 The rotational system

It may consist of a number of discs coupled together by torsional shafts.

As for example we may select two-mass and two-disk systems shown in Figure 3.4.11.

3.4.5.3 Rotational system

Summing up torques about the longitudinal axis of the shaft (Figure 3.4.11), equations of motion may be written as

$$J_1\ddot{\theta}_1 = -k_{t_1}(\theta_1 - \theta_2) : J_2\ddot{\theta}_2 = -k_{t_1}(\theta_2 - \theta_1) \tag{3.4.32}$$

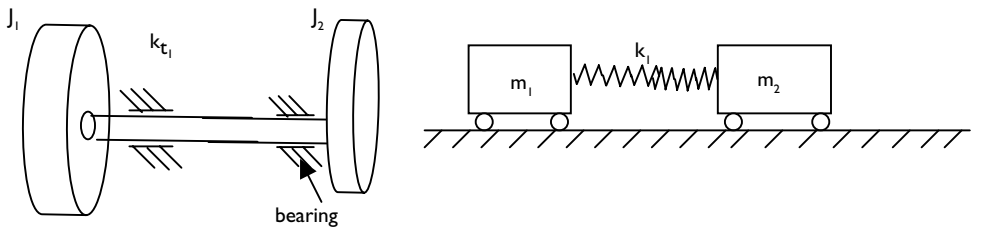


Figure 3.4.11 Two-disc and two-mass semi-definite systems.

Equation (3.4.32) may my rearranged in the form of

$$J_1\ddot{\theta}_1 + k_{t_1}\theta_1 - k_{t_1}\theta_2 = 0 : J_2\ddot{\theta}_2 + k_{t_1}\theta_2 - k_{t_1}\theta_1 = 0 \tag{3.4.33}$$

With solution of the type $\theta_1(t) = A_{\theta 1}\sin(\omega t + \psi) : \theta_2(t) = A_{\theta 2}\sin(\omega t + s\psi)$, frequency equation may be written as

$$\Delta(\omega) = \begin{vmatrix} k_{t_1} - J_1\omega^2 & -k_{t_1} \\ -k_{t_1} & k_{t_1} - J_2\omega^2 \end{vmatrix} = 0 \tag{3.4.34}$$

Equation (3.4.34) reduces to

$$\left[\omega^2 - \left(\frac{k_{t_1}}{J_1} + \frac{k_{t_1}}{J_2}\right)\right]\omega^2 = 0 \tag{3.4.35}$$

Two roots of ω^2 are zero and $\left(\frac{k_{t_1}}{J_1} + \frac{k_{t_1}}{J_2}\right)$ respectively.
The amplitude ratios of the principal modes are

$$\begin{aligned} &\frac{A_{\theta 1}}{A_{\theta 2}} = \frac{k_{t_1}}{k_{t_1} - J_1\omega^2} = \frac{k_{t_1} - J_2\omega^2}{k_{t_1}} = 1 \quad \text{for } \omega^2 = 0 \\ &= -\frac{J_2}{J_1} \text{ for } \omega^2 = \left(\frac{k_{t_1}}{J_1} + \frac{k_{t_1}}{J_2}\right). \end{aligned} \tag{3.4.36}$$

These amplitude ratios indicate that the discs may rotate either together as a rigid body or oscillate in opposite directions with a frequency $\omega^2 = \left(\frac{k_{t_1}}{J_1} + \frac{k_{t_1}}{J_2}\right)$.

3.4.5.4 Rectilinear system

Summing up torques about the longitudinal axis of the shaft (Figure 3.4.11), equations of motion may be written as

$$m_1\ddot{x}_1 = -k_1(x_1 - x_2) : m_2\ddot{x}_2 = -k_1(x_2 - x_1) \tag{3.4.37}$$

Equation (3.4.37) may be rearranged in the form of

$$m_1\ddot{x}_1 + k_1 x_1 - k_1 x_2 = 0 : m_2\ddot{x}_2 + k_1 x_2 - k_1 x_1 = 0 \tag{3.4.38}$$

With solution of the type $x_1(t) = A_1 \sin(\omega t + \psi) : x_2(t) = A_2 \sin(\omega t + \psi)$, frequency equation may be written as

$$\Delta(\omega) = \begin{vmatrix} k_1 - m_1\omega^2 & -k_1 \\ -k_1 & k_1 - m_2\omega^2 \end{vmatrix} = 0 \tag{3.4.39}$$

Equation (3.4.39) reduces to

$$\left[\omega^2 - \left(\frac{k_{t_1}}{J_1} + \frac{k_{t_1}}{J_2}\right)\right]\omega^2 = 0 \tag{3.4.40}$$

Two roots of ω^2 are zero and $\left(\frac{k_1}{m_1} + \frac{k_1}{m_2}\right)$ respectively.
The amplitude ratios of the principal modes are

$$\begin{aligned} \frac{A_1}{A_2} = \frac{k_1}{k_1 - m_1\omega^2} &= \frac{k_1 - m_2\omega^2}{k_1} = 1 \quad \text{for } \omega^2 = 0 \\ &= -\frac{m_2}{m_1} \quad \text{for } \omega^2 = \left(\frac{k_1}{m_1} + \frac{k_1}{m_2}\right). \end{aligned} \tag{3.4.41}$$

These amplitude ratios indicate that the discs may rotate either together as a rigid body or oscillate in opposite directions with a frequency $\omega^2 = \left(\frac{k_1}{m_1} + \frac{k_1}{m_2}\right)$.

Example 3.4.4

A dynamic absorber is shown in Figure 3.4.12(a) in which a damper c is installed in parallel with the spring k_2. Discuss the effect of the damper c on the motion of the mass m_1.

Solution:

Equivalent system is shown in Figure 3.4.12(b). Summing up the forces in the vertical direction we have

$$\begin{aligned} m_1\ddot{x}_1 + c\dot{x}_1 + (k_1 + k_2)x_1 - c\dot{x}_2 - k_2 x_2 &= F_{01}\sin\omega t \\ m_2\ddot{x}_2 + c\dot{x}_2 + k_2 x_2 - c\dot{x}_1 - k_2 x_1 &= 0 \end{aligned} \tag{3.4.42}$$

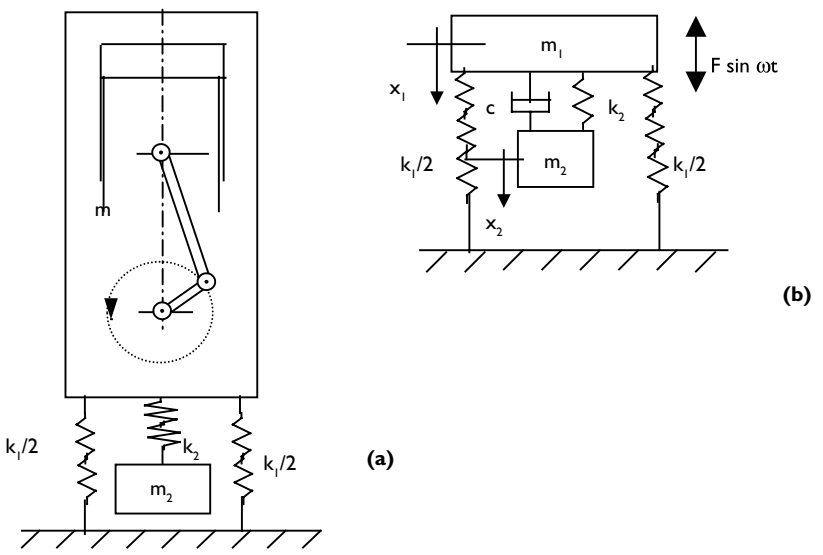


Figure 3.4.12 Dynamic Absorber.

From Equation (3.4.42), we have complex amplitudes

$$X_1 = \frac{\begin{vmatrix} F_{01} & -(k_2 + ic\omega) \\ 0 & k_2 - m_2\,\omega^2 + ic\,\omega \end{vmatrix}}{\Delta(\omega)} = X_1\, e^{-i\psi_1} :$$
$$X_2 = \frac{\begin{vmatrix} k_1 + k_2 - m_1\,\omega^2 + ic\omega & F_{01} \\ -(k_2 + ic\omega) & 0 \end{vmatrix}}{\Delta(\omega)} = X_2\, e^{-i\psi_2} \tag{3.4.43}$$

$$\text{and } \Delta(\omega) = \begin{vmatrix} k_1 + k_2 - m_1\,\omega^2 + ic\omega & -(k_2 + ic\omega) \\ -(k_2 + ic\omega) & k_2 - m_2\,\omega^2 + ic\,\omega \end{vmatrix} \tag{3.4.44}$$

The steady state responses of two masses are $x_1 = X_1 \sin(\omega t - \psi_1)$; $x_2 = X_2 \sin(\omega t - \psi_2)$.

If $c = 0$, the system is that of an undamped dynamic absorber. Hence,

$$X_1 = \frac{\begin{vmatrix} F_{01} & -k_2) \\ 0 & k_2 - m_2\,\omega^2 \end{vmatrix}}{\Delta(\omega)} = X_1\, e^{-i\psi_1} :$$
$$X_2 = \frac{\begin{vmatrix} k_1 + k_2 - m_1\,\omega^2 & F_{01} \\ -k_2 & 0 \end{vmatrix}}{\Delta(\omega)} = X_2\, e^{-i\psi_2} \tag{3.4.45}$$

$$\Delta(\omega) = \begin{vmatrix} k_1 + k_2 - m_1\omega^2 & -k_2 \\ -k_2 & k_2 - m_2\omega^2 \end{vmatrix} = \omega^4 - \left[\frac{k_1 + k_2}{m_1} + \frac{k_2 + k_3}{m_2}\right]\omega^2 + \left[\frac{k_1k_2 + k_2k_3 + k_3k_1}{m_1m_2}\right] = 0 \quad (3.4.46)$$

ψ_1 and ψ_2 are either zero or 180°.

These expressions indicate that when $k_2 - m_2\,\omega^2 = 0, X_1 = 0$ and $X_2 = -F_{01}/k_2$, i.e. $x_1(t)$ is zero and the force is transmitted to the foundation is zero. The force transmitted through spring k_2 to the base of the machine is $k_2x_2 = -F_{01}\sin\omega t$. This means that the motion of m_2 is 180° out of phase with the exciting force and the force due to the deformation of the spring k_2 is equal and opposite to the exciting force.

The dynamic absorber minimizes the vibration of the original system when operating frequency is nearly equal to $\sqrt{k_1/m_1}$. It can be shown that when the exciting frequency ω is equal to $\sqrt{k_2/m_2}$, the amplitude of $x_1(t)$ is zero. Hence an undamped dynamic absorber is normally tuned so that $k_1/m_1 = k_2/m_2$. Frequency equation of the system is then, $\frac{m_1m_2}{k_1k_2}\omega^4 - \left[\left(1 + \frac{k_1}{k_2}\right)\frac{m_2}{k_2} + \frac{m_1}{k_1}\right]\omega^2 + 1 = 0$, if the dynamic absorber is tuned i.e. $k_1/m_1 = k_2/m_2$, using $\omega/\sqrt{k_1/m_1} = \omega/\sqrt{k_2/m_2} = r$ and equating $k_1/k_2 = m_1/m_2$, the equation reduces to $r^4 - \left[2 + \frac{m_2}{m_1}\right]r^2 + 1 = 0$. The resonant frequency of the tuned system can be determined from the root of this equation with mass ratio as a parameter.

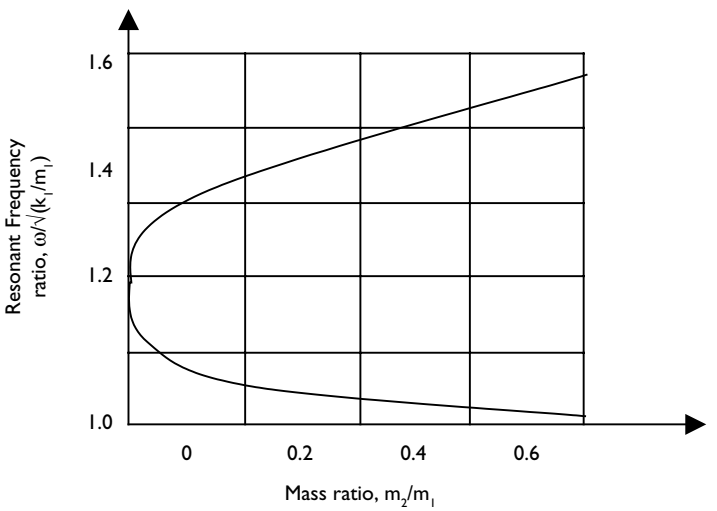


Figure 3.4.13 Variation on Resonant frequency with mass ratio.

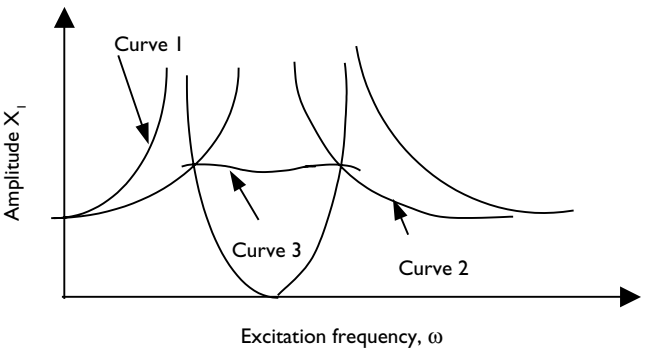


Figure 3.4.14 Response curves.

There are two resonant frequencies. Figure 3.4.13 shows that the effect of the size of the absorber mass m_2 is to change the range of resonant frequencies. When m_2/m_1 is very small, the absorber mass has very little effect, and the resonant frequencies are close to those of the original system. When m_2/m_1 is appreciable, the resonant frequencies are separated. For example, when $m_2/m_1 = 0.4$, the resonant frequency ratio are, 0.73 and 1.37; that is, resonance occurs at frequencies 0.732 and 1.36 times those of the original system. If $c = \infty$, which means that the mass m_2 is securely attached to the mass m_1, the response of the system is that of a single-degree-of-freedom system. The vibrating mass is equal to $(m_1 + m_2)$ and the spring constant is k_1. The response is now sinusoidal. Hence, for $0 < c < \infty$, the steady state response of mass m_1 must be intermediate between these two extreme conditions. The steady state response curves of m_1 for $0 < c < \infty$ are shown in Figure 3.4.14.

Curve 1 in Figure 3.4.14, shows an undamped system and Curve 2 corresponds to $c = \infty$. Where these two curves intersect, the damping can range from zero to infinity. Curve 3 is that of a properly tuned dynamic absorber with appropriate damping.

3.5 NONLINEAR SYSTEMS

3.5.1 Free vibrations

In the Preceding sections it was assumed that the force in a spring is linearly proportional to the deformation; damping force is a linear function of velocity of motion. The resulting governing equation of motion always resulted in a linear differential equation with constant coefficients. There are practical problems in which this linearity proposition is violated and in such situations, one has to deal with systems having nonlinear characteristics. For most of geomaterials, the modulus of elasticity (if one still takes recourse to elastic behaviour) decreases with deformation. Therefore some decrease in the frequency with increase in amplitude of vibration must be expected.

If due to resonance, the amplitude of vibration begins to increase, the frequency of vibration changes, i.e. the resonant condition disappears.

A Summary of the properties of linear and nonlinear systems is given in Table 3.5.1.

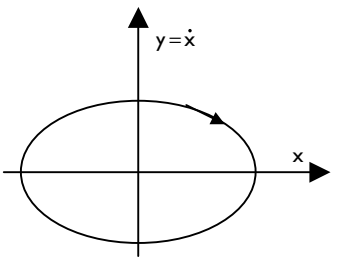
Let us consider Van der Pol equation (in the form of a nonlinear differential equation)

$$\ddot{x} + \varepsilon\,[x^2 - 1]\dot{x} + x = 0;\ \text{where } \varepsilon \text{ is a constant.} \tag{3.4.1}$$

If one assumes $0 \leq x \leq 1$, Equation (3.5.1) resembles to the free vibration of a damped single-degree-of-freedom system with nonlinear damping. If $x < 1$, the damping term is negative and the amplitude x will increase with time. If $x > 1$, the damping term is positive and amplitude x will decrease with time. Thus, if the system is given a small initial displacement or velocity, the motion will build up and will eventually become periodic with constant amplitude. Conversely, if a large initial

Table 3.5.1 Summary of the properties of linear and nonlinear systems.

	Linear system	*Nonlinear systems*
1.	Only one static equilibrium position exists around which the system vibrates.	More than one stable equilibrium positions may exists and the system can vibrate around any, or all of these.
2.	With time independent system parameters, constant forces do not play any role except changing the static equilibrium position.	The presence of a constant force may significantly change the nature of the response.
3.	Free undamped vibration is harmonic with a characteristic (natural frequency ω_n which is a system property, independent of the amplitude).	Free undamped vibration is not harmonic and the time period of oscillation is amplitude dependent, not a system property.
4.	The principle of superposition holds good which implies that the response is proportional to the level of excitation.	The principle of super position is not valid.
5.	For a harmonic excitation, the steady state response (for a damped system) has the same frequency as that of the excitation.	Besides the excitation frequency, super and subharmonics of different orders may be contained in the response.
6.	The amplitude of harmonic response is unique for a given excitation frequency.	At a given frequency of excitation, the amplitude of response can have multiple values. Which one, among the possible a stable amplitude, is reached depends on the initial conditions (and the method of experimentation). For a multi-frequency excitation, only simple responses can occur when the natural frequency coincides with one of the excitation frequencies.
7.	Besides simple (primary), subharmonic and super harmonic resonances, combination of resonances can occur when certain combinations of forcing frequencies bear specific relationships with the natural frequency.	For a damped, forced system, the steady state response is not governed by the initial disturbances. Even in the presence of damping, the response of a forced system after a long time interval may be highly sensitive to the initial disturbances and the motion may not show any periodicity.



(a) ε = 0

Figure 3.5.1 Phase plane trajectories of Van der Pol equation.

displacement or velocity is imposed on the system, its motion will diminish until the same periodic motion with constant amplitude is attained.

If $\varepsilon = 0$, the equation is same as linear mass-spring system and the phase trajectories for this case is an ellipse shown in Figure 3.5.1.

If $\varepsilon > 0$, the motion tends to build up for small oscillations and tends to decrease for large oscillations. Hence after the initial transient, the motion becomes periodic, represented by a closed trajectory. This phase trajectory is called a limit cycle. Shown in Figure 3.5.2, are the phase trajectories of Van der Pol equation for various values of ε. In each of these figures, the limit cycle is indicated by heavy lines. For a given ε, the same limit cycle is obtained whether the system is set into motion with initial conditions inside or outside the limit cycle.

3.5.1.1 Non-linear springs

In the Preceding sections it was assumed that the force in a spring is linearly proportional to the deformation; damping force is a linear function of velocity of motion. The resulting governing equation of motion always resulted in a linear differential equation with constant coefficients. There are practical problems in which this linearity proposition is violated and in such situations, one has to deal with systems having nonlinear characteristics. For geomaterials, where modulus of elasticity (if one sill takes recourse to elastic behaviour) decreases with deformation, some decrease in the frequency with increase in amplitude of vibration must be expected. If due to resonance, the amplitude of vibration begins to increase, the frequency of vibration changes, i.e. the resonant condition disappears.

Consider the general equation of motion in the form of

$$m\ddot{x} + f(x) = 0 \quad \rightarrow \quad \ddot{x} + \omega_n^2 f(x) = 0 \tag{3.4.2}$$

where $\omega_n^2 f(x)$ is the restoring force per unit mass as function of the displacement x.

$$\text{Now} \quad \ddot{x} = \frac{d\dot{x}}{dt} = \frac{d\dot{x}}{dx}\frac{dx}{dt} = \frac{d\dot{x}}{dx}\dot{x} = \frac{1}{2}\frac{d(\dot{x})^2}{dx} \tag{3.4.3}$$

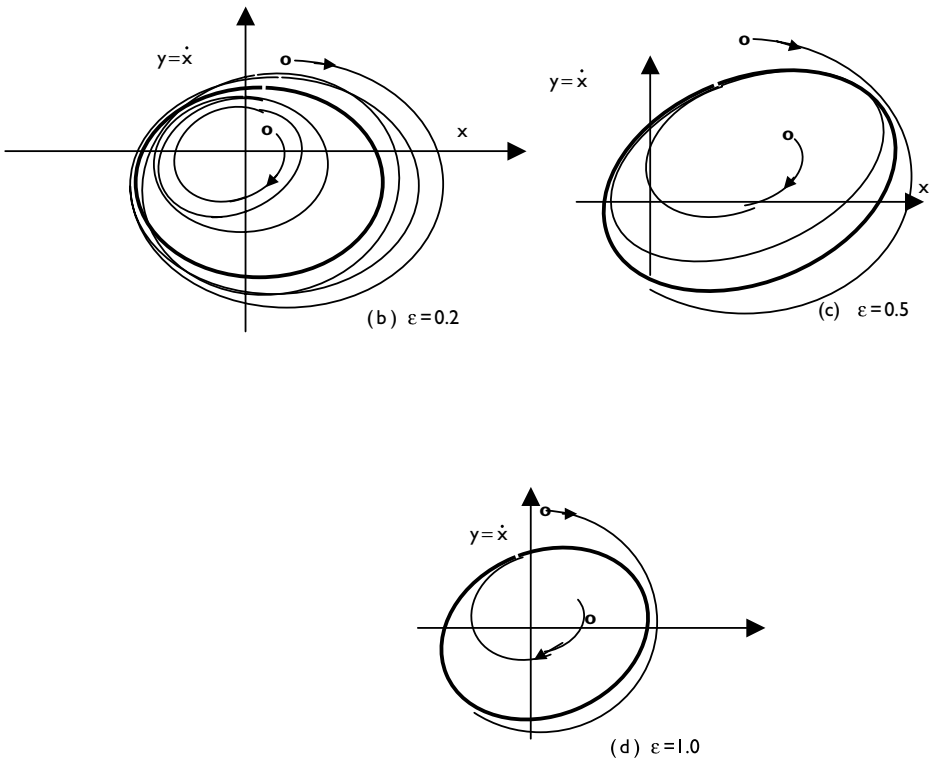


Figure 3.5.2 Phase plane trajectories of Van der Pol equation.

Equation (3.5.2) then reduces to

$$\frac{1}{2}\frac{d(\dot{x})^2}{dx} + \omega_n^2 f(x) = 0 \tag{3.4.4}$$

Assume that the restoring force is given by the curve OA in Figure 3.5.3 and at $t = 0, x = x_0, \dot{x} = 0$

Integrating Equation (3.5.4)

$$\frac{1}{2}\dot{x}^2 = -\omega_n^2 \int_{x_0}^{x} f(x)dx = \omega_n^2 \int_{x}^{x_0} f(x)dx = \text{Area of the shaded part.}$$

Means that for any position of the vibrating mass, m, its kinetic energy is equal to the difference of the potential energy stored in the spring initially due to the deflection x_0 and the potential energy at the moment under consideration.

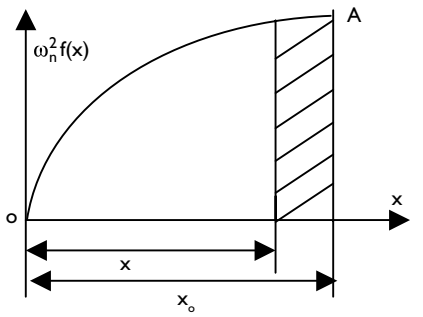


Figure 3.5.3 Restoring force-deformation behaviour.

3.5.1.2 Non-harmonic motions

Vibration is harmonic only if the return force controlling it is directly proportional to the corresponding displacement. A system where return force depends upon x in some other way is called a non-linear system. Vibrations of non-linear systems are non-harmonic. Again, many springs take a slightly different magnitude of force to produce a given extension than to produce an equal compression. The simplest asymmetry of this kind is represented by a term in restoring force proportional to x^2. Or it may be that the spring is symmetrical with respect to positive and negative displacements, but that there is not strict proportionality of the restoring force to x. The simplest symmetrical effect of this kind is described by a term in the restoring force proportional to x^3. The equation of motion of these cases may be written as

$$\begin{aligned} &m\ddot{x} + kx + \alpha\, x^2 = 0: \text{ In nonlinear, asymmetric situation.} \\ &m\ddot{x} + kx + \beta\, x^3 = 0: \text{ In nonlinear, symmetric situation.} \end{aligned} \tag{3.4.5}$$

Nonlinear systems are described by nonlinear differential equations [Equation (3.5.5)] and these are usually impossible to solve exactly. If we try a solution of the form $x = A\cos\omega_n t$ in either of the Equation (3.5.5), we find that it does not work. The motion is no longer describable as a harmonic vibration at some unique frequency ω_n. Some times it is possible to use a linear equation as an approximation and assume that any small vibration is approximately harmonic. To start with let us consider systems where there is only slight non-linearity and let us consider the case of free vibration.

a Symmetric return force

Let a mass is attached to a spring which exerts a return force with a cubic function of the displacement i.e.

$$F_{\text{spring force}} = -F_s = (1 + \alpha x^2)kx \tag{3.4.6}$$

where α and k are constants.

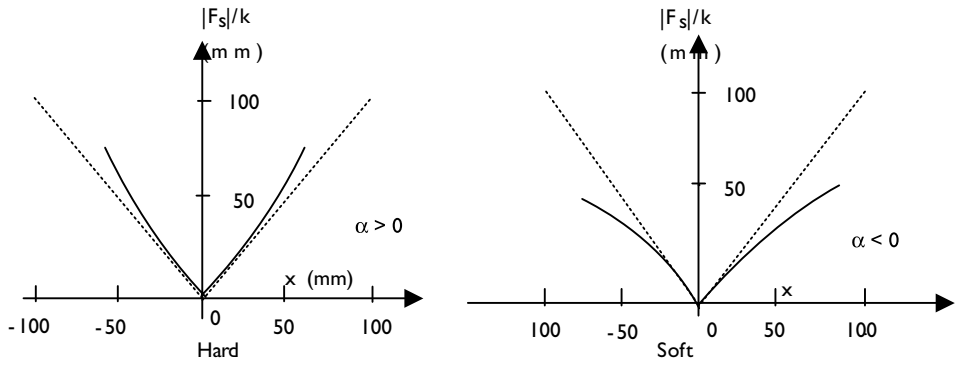


Figure 3.5.4 Non linear symmetric return forces.

This force $|F_s|$ is symmetric against displacement both positive and negative and shown in Figure 3.5.4.

Slight nonlinearity is implied by assuming $|\alpha x^2| << 1$. However, we can ensure αx^2 to be small by limiting the maximum value that $|x|$ reaches during vibration.

If damping is ignored, the equation of motion assumes the form

$$\ddot{x} + (1 + \alpha\, x^2)\omega_n^2 x = 0 \tag{3.4.7}$$

1 We now assume that the motion must be periodic, as there is no damping. If T is the period then

$$x(t) = x(t + T) \tag{3.4.8}$$

2 'Inward' part of any cycle (|x| decreasing) will be exactly same as the 'outward' part (|x| increasing) run backwards i.e.

$$|x(t_0 - t)| = |x(t_0 + t)|, \tag{3.4.9}$$

where t_0 is any value of t for which $x(t_0) = 0$.

3 Since $|F_s|$ is symmetric about $x = 0$, the motion during a movement to the left, $x < 0$, will be a mirror image of the motion during a movement to the right, $x > 0$. Both these movements take exactly the same time, half a period to be precise and hence

$$x(t + 1/2\, T) = -x(t). \tag{3.4.10}$$

For a solution of Equation (3.5.7), we think of harmonic functions, and consider x, in general, to be the sum of the terms $\cos(\omega t+\phi)$, $\cos(2\omega t+\phi)$, $\cos(3\omega t+\phi)$, ..., where $\omega = 2\pi/T$. With symmetric restoring force, one can exclude all the terms involving

even multiples of ωt and again, without any loss of generality using $\dot{x}(0) = 0$, we may write

$$x = A[\cos \omega t + \varepsilon \cos 3\omega t + \cdots] \tag{3.4.11}$$

The first term is fundamental and the other terms are called harmonics and ε is a small multiplier. Thus a vibration controlled by a symmetric returning force will not contain any even harmonics. From Equation (3.5.11) we have

$x^3 = A^3[\cos^3 \omega t + 3\varepsilon \cos^2 \omega t \cos 3\omega t + \cdots]$ omitting higher order terms of ε;

$\ddot{x} = -A\omega^2[\cos \omega t + 9\varepsilon \cos 3\omega t + \cdots]$ omitting higher order terms of ε.

Using $\cos^3 \omega t = 1/4 \cos 3\omega t + 3/4 \cos \omega t$, we have now

1 Coefficient of $\cos \omega t$: $[-\omega^2 A + \omega_n^2 A + {}^3\!/_4\, \alpha \omega_n^2 A^3] = 0$

$$\omega^2 = \omega_n^2(1 + 3/4\ \alpha A^2) \ \rightarrow\ \omega = \omega_n(1 + 3/4\ \alpha A^2)^{1/2} \ \rightarrow\ \omega \approx \omega_n(1 + 3/8\ \alpha A^2). \tag{3.4.12}$$

This implies that the nonlinear term in Equation (3.5.6) can either increase or decrease the fundamental frequency from its value with $\alpha = 0$, depending upon the sign of α and frequency shift becomes larger as the maxima of $|x|$ become larger. *Mass and the spring do not fix the period of vibration alone as in the case of a linear system.*

2 Collecting the coefficients of $\cos 3\omega t$: $-9\varepsilon\omega^2 A + \varepsilon\omega_n^2 A + 1/4\alpha A^3 = 0$

$$\text{Selecting } \omega \text{ from Equation (3.5.8), we have } \ \rightarrow\ \varepsilon \approx \alpha A^2/32. \tag{3.4.13}$$

When the quantities ω and ε given by Equations (3.5.12) and (3.5.13) are substituted in Equation (3.5.11) it gives the solution of Equation (3.5.7). The adequacy of the solution should be judged from its utility for we have discarded the terms of order of magnitude one order smaller than $\alpha\ A^2$. Any value of ω and ε that we calculate using these formulas will have an error of the order of $(\alpha A^2)^2$. Thus, if we have a vibration with $\alpha A^2 = 0.1$, then $(\alpha A^2)^2$ is 0.01 and the error will be of the order of 1%.

For a more precise solution, we have to go in for retaining second order terms in ε. For zeroth order approximation, nonlinear terms are ignored entirely and it will yield errors of 1%.

Example 3.5.1

Let us consider the case of pendulum, we have motion

$$\ddot{\theta} + \frac{g}{\ell} \sin\theta = 0 \tag{3.4.14}$$

For small amplitudes, sin $\theta \approx \theta$ and the system vibrate in simple harmonic motion. The simple pendulum is a 'soft' nonlinear system. The amplitude of the return torque is plotted as shown in Figure 3.5.5. The plot indicates that the exact curve i.e. θ versus $|sin\theta| = T/mg\ell$ and also shown are the linear approximation (dotted line) as well as cubic approximation $|(1-\theta)^2/6\theta|$

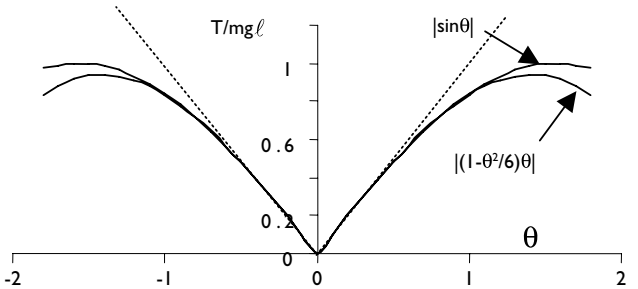


Figure 3.5.5 Restoring torque of a simple pendulum.

If small oscillation is not assumed, Equation (3.5.14) is a nonlinear differential equation, elliptical integral has to be used to solve the equation von Karman and Biot (1940) gave solution to this problem as

$$t = \int_{\theta_0}^{\theta} \frac{d\theta}{\sqrt{\dot{\theta}_0^2 + \frac{2mg\ell}{J_0}(\cos\theta - \cos\theta_0)}} \tag{3.4.15}$$

where θ_0 and $\dot{\theta}_0$ are the initial conditions at $t = 0$. If the pendulum is given a sufficiently large initial velocity to set it into motion, the pendulum will continue to rotate about the hinge point. Thus $\theta(t)$ will increase with time, and motion is not periodic. Small oscillation assumption simplifies the solution procedure and a periodic will result.

If the amplitudes are not small sin θ may be expanded in power series and we have, say,

$$\ddot{\theta} + \frac{g}{\ell}\left[\theta - \frac{\theta^3}{6} + \cdots\right] = 0 \tag{3.4.16}$$

Here we see that the nonlinear term has opposite sign and is a case of soft system. Normally it is sufficient to consider only the first two terms, i.e.

$$\text{Restoring force} = -mg\ell\left[\theta - \frac{\theta^3}{6} + \cdots\right] = kx + \alpha k x^3 \tag{3.4.17}$$

$\rightarrow \alpha = -1/6$ and $|\alpha A^2| \ll 1$ 'A' should be small compared to $\sqrt{6}$ radian $= 140°$.

Thus,

$$\rightarrow \quad \omega \approx \omega_n(1 - \alpha A^2/16) \quad \text{and } \varepsilon \approx A^2/192. \tag{3.4.18}$$

Hence, for an amplitude 10°, $\alpha A^2 = -0.005$ and error will be of the order of 0.001%.

b Unsymmetric returning force

Here we consider an unsymmetric returning force in quadratic form as follows:

$$F_S = -(1 + \beta x)kx \tag{3.4.19}$$

β and k are constants and $|\beta x| \ll 1$ and if β is positive as shown in Figure 3.5.6(a), the spring is stiffer for $x > 0$ but becomes softer when $x < 0$. If β is negative just an opposite case develops as shown in Figure 3.5.6(b).

In an undamped situation the equation of motion can be written as

$$\ddot{x} + (1 + \beta x)\omega_n^2 x = 0 \tag{3.4.20}$$

Setting $\dot{x}(0) = 0$ as initial the condition and seek a solution of Equation (3.5.20) in the form of a series of harmonics we cannot ignore the even-harmonics as we do not

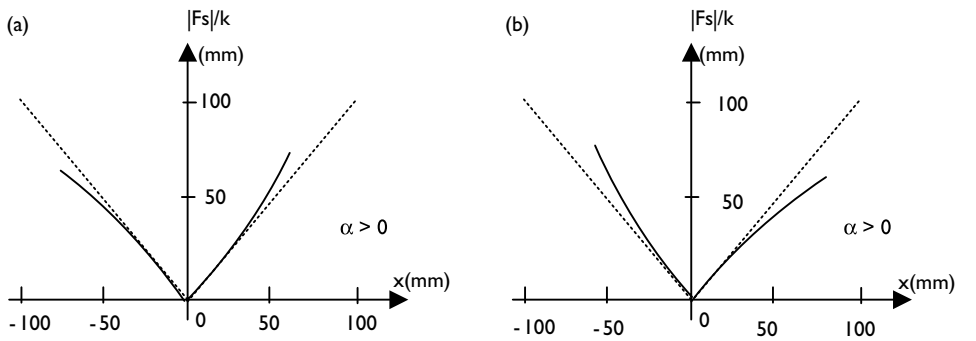


Figure 3.5.6 Unsymmetric returning force.

have a symmetric force. Most important harmonic will be now the second term and one may write the solution as

$$x = A_0 + A[\cos \omega t + \eta \cos 2\omega t + \cdots] \tag{3.4.21}$$

The term A_0 can be taken as the zeroth harmonic. Figure 3.5.7 describes the individual and combined effect of harmonics. It may be noticed that on the positive displacement side loop is sharpened in comparison to the negative side showing how the 'hard' force turns the mass round more rapidly than the 'soft' force.

From Equation (3.5.21) we have

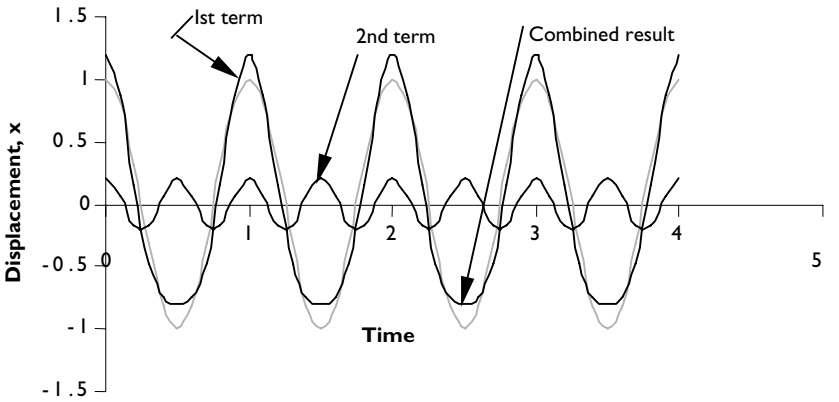
$$x^2 = A_0^2 + 2A_0A[\cos \omega t + \eta \cos 2\omega t] + A^2[\cos^2 \omega t + 2\eta \cos \omega t \cos 2\omega t + \cdots]$$
$$\times \ \ddot{x} = -\omega^2 A[\cos \omega t + 4\eta \cos 2\omega t + \cdots] \tag{3.4.22}$$

Substituting these values in Equation (3.5.19) and using the identity $\cos^2 \omega t = 1/2[1 + \cos 2\omega t]$ and ignoring η^2, $(\beta A)^2$ and $\eta\beta A$ and higher order terms of η and (βA), we obtain

$$-\omega^2 A[\cos \omega t + 4\eta cos2\omega t + \cdots] + \omega_n^2[A_0 + A(\cos \omega t + \eta \cos 2\omega t + \cdots)]$$
$$+ \beta^2\omega_n^2[A_0^2 + 2AA_0 \cos \omega t + A^2(1/2 + 1/2 \ \cos 2\omega t + \cdots)] = 0 \tag{3.4.23}$$

Now collecting coefficients of cos ωt and equating them to zero leads to

$$-\omega^2 A + \omega_n^2 A + 2\beta\omega_n^2 \, AA_0 = 0 \quad \rightarrow \quad \omega^2 = \omega_n^2(1 + 2\beta A_0) \tag{3.4.24}$$



(The individual harmonics are plotted in the first period)

Figure 3.5.7 Superposition of harmonics.

Table 3.5.2 Free Vibrations under cubic (symmetric) and quadratic (axisymmetric) restoring forces.

Cubic restoring force	Quadratic restoring force
$X = A(\cos\omega t + \varepsilon\cos 3\omega t + \cdots)$	$x = A_0 + A(\cos\omega t + \eta\cos 2\omega t + \cdots)$
$\omega \approx \omega_0(1 + 3/8\alpha A^2)$	$\omega \approx \omega_n$
$\varepsilon \approx 1/32\alpha A^2$	$\eta \approx 1/6\beta A$
$\bar{x} = 0$	$\bar{x} = A_0 \approx -\frac{1}{2}\beta A^2$

Collecting coefficients of $\cos 2\omega t$ and equating them to zero leads to

$$-4\eta\omega^2 A + \eta\omega_n^2 A + 1/2\ \beta\omega_n^2 A^2 = 0 \quad \rightarrow \quad -\eta(1 + 2\beta A_0) + \eta + 1/2\ \beta A = 0$$
$$\rightarrow \quad \eta \approx 1/6\ \beta A \tag{3.4.25}$$

neglecting a term in (βA) (βA_0).

We also have constant terms and they will also add up to zero

$$\omega_n^2 A_0 + \beta\omega_n^2 A_0^2 + 1/2\ \beta\omega_n^2 A^2 = 0 \tag{3.4.26}$$

Neglecting $(\beta A)^2$ term, we have

$$A_0 \approx -1/2\ \beta A^2 \tag{3.4.27}$$

Equation (3.5.27) indicates that A_0 is much smaller than A, the amplitude of the fundamental mode.

Approximate value of ω^2 may be given as

$$\omega^2 \approx \omega_0^2(1 - \beta A^2) \approx \omega_0^2 \tag{3.4.28}$$

Thus we have the following conclusions to make for an asymmetric return force

1 Within the approximation made, there is no frequency shift.
2 There is a presence of small constant term A_0 and the average position of the mass during the vibration is given by

$$\bar{x} = A_0 \approx -\frac{1}{2}\beta\ A^2 \tag{3.4.29}$$

Since the average of each cosine term in Equation (3.5.21) is zero, Equation (3.5.27) indicates that A_0 has the opposite sign to β, and so, as we might expect the mass spends more time on the 'soft' side of $x = 0$, than on the 'hard' side.

A summary of the results is shown in Table 3.5.2.

3.5.2 Forced vibrations

Since there is no exact solution for a general nonlinear vibration problem we must resort to an approximate solution.

Method of superposition is not valid which was always applicable to problems solved earlier. Thus even if the free vibration of a system as well as its forced vibration can be found, the sum of these two motions does not give the resultant vibration. Also if there are several harmonics in the disturbing force, the resultant forced vibrations cannot be obtained by summing up vibrations due to each harmonics alone as was done in the earlier sections.

To start with a solution procedure, let us consider a lightly damped vibrator subjected to harmonic driving force of moderate amplitude and nonlinearity is slight. We also assume that driving force is of much less frequency that the resonance. Thus $\omega \ll \omega_n$ and at this range motion of the system depends mostly on the stiffness and mass or the damping hardly have any influence. The effects of nonlinearity in the spring may be expected to be the most pronounced under these conditions.

Hence the response of the system x may be expressed as

$$x \approx a\,F + b\,F^3 + c\,F^3 + \cdots \tag{3.4.30}$$

in which a, b, c, etc are constants and F is the driving force which, for stiffness controlled motion, is at all times nearly equal and opposite to the spring force.

Assuming the force to be harmonic and of the type $F = F_0 \cos \omega t$ and using the identity $\cos^2 \omega t = 1/2[1 + \cos 2\omega t]$ and $\cos^3 \omega t = 1/4 \cos^3 \omega t + 3/3 \cos \omega t$, and substituting it in Equation (3.5.30), we have

$$x = \frac{bF_0^2}{2} + \left(aF_0 + \frac{3cF_0^3}{4}\right)\cos \omega t + \frac{bF_0^2}{2}\cos 2\omega t + \frac{cF_0^3}{4}\cos 3\omega t + \cdots \tag{3.4.31}$$

Equation (3.5.31) reveals that the solution has also second, third and higher harmonics as well as a constant term present. These new contributions to x will become increasingly important as the force amplitude is increased.

3.5.2.1 Sub-harmonic resonance

If the driving frequency is at resonance, ω_n, and we gradually decrease it, ω will successively pass through the values $\omega_n/2$, $\omega_n/3, \ldots$, at which the harmonics in the driven motion are close to the resonance frequency. At one of these frequencies, we should expect the relevant component to go through a resonance so that the dominant motion will be at the resonant frequency. Subsidiary resonance peaks will appear at each of these driving frequencies, which are sub-harmonics of the resonance frequency.

3.5.2.2 Driving force with a combination of two frequencies

A new situation arises when we consider the driving force is consisting of two coherent driving forces with different frequencies, say $\omega_1 < \omega_n$. As an example, let the force be

written as

$$F = F_1 \cos \omega_1 t + F_2 \cos \omega_2 t \tag{3.4.32}$$

Substituting Equation (3.5.32) in Equation (3.2.29), we have

$$\begin{aligned} x = {} & a[F_1 \cos \omega_1 t + F_2 \cos \omega_2 t] + b[F_1 \cos \omega_1 t + F_2 \cos \omega_2 t]^2 \\ & + c[F_1 \cos \omega_1 t + F_2 \cos \omega_2 t]^3 \end{aligned} \tag{3.4.33}$$

The first expression on the right is the linear case and it will give rise to beats for $\omega_1 \approx \omega_2$. The second and third terms will result in

$$\begin{aligned} [F_1 \cos \omega_1 t + F_2 \cos \omega_2 t]^2 &= F_1^2 \cos \omega_1^2 t + F_2^2 \cos \omega_2^2 t + 2F_1 F_2 \cos \omega_1 t \cos \omega_2 t \\ [F_1 \cos \omega_1 t + F_2 \cos \omega_2 t]^3 &= F_1^3 \cos \omega_1^3 t + F_2^3 \cos \omega_2^3 t \\ &\quad + 3F_1 F_2 \cos \omega_1 t \cos \omega_2 t [F_1 \cos \omega_1 t + F_2 \cos \omega_2 t] \end{aligned} \tag{3.4.34}$$

Higher power terms in $\cos \omega t$ will result in second and third harmonics of both driving frequencies and a constant term. The product terms are

$$\begin{aligned} & 2F_1 F_2 \cos \omega_1 t \cos \omega_2 t = F_1 F_2 [cos(\omega_1 + \omega_2)t + \cos(\omega_2 - \omega_1)t] \\ & 3F_1 F_2 \cos \omega_1 t \cos \omega_2 t [F_1 \cos \omega_1 t + F_2 \cos \omega_2 t] \\ & \quad = 3/2\, F_1 F_2 [F_1 \cos \omega_1 t \{\cos(\omega_1 + \omega_2)t + \cos(\omega_2 - \omega_1)t\} \\ & \qquad + F_2 \cos \omega_2 t \{\cos(\omega_1 + \omega_2)t + \ cos(\omega_2 - \omega_1)t\}] \\ & x = 1/2[F_1^2 + F_2^2]b + a[F_1 \cos \omega_1 t + F_2 \cos \omega_2 t] + (1/2\, bF_1^2) \cos 2\omega_1 t \\ & \qquad + (1/2\, bF_2^2) \cos 2\omega_2 t + (cF_1^3/4) \cos\ 3\omega_1 t + (3cF_1^3/4) \cos \omega_1 t \\ & \qquad + (cF_2^3/4) \cos\ 3\omega_2 t + (3cF_2^3/4) \cos \omega_2 t + 3/4\ F_1 F_2 [F_1 \{\cos(2\omega_1 + \omega_2)t \\ & \qquad + 2 \cos \omega_2 t + \cos(\omega_2 - 2\omega_1)t\} + F_2 \{\cos(\omega_1 + 2\omega_2)t + 2 \cos \omega_1 t \\ & \qquad + \cos(2\omega_2 - \omega_1)t\}] \end{aligned} \tag{3.4.35}$$

We have now four completely new terms: sums of frequencies: $(2\omega_1 \pm \omega_2)/2\pi$, and, $(2\omega_2 \pm \omega_1)/2\pi$.

These combinations of frequencies will become important with increasing the driving force amplitudes. Thus we can expect a subsidiary resonance whenever the driving forces have a combination frequency equal to the resonance frequency.

An important characteristic of nonlinearity in forced vibration is that the system vibration will be having components, namely harmonics, combination frequencies or a constant term which are not present in the driving force. This is always undesirable in practice.

Table 3.5.3 Fourth order Runge-Kutta method with Gill's variation.

```
      program pendulum
      dimension y(3), dy(3)
c
      hi = 0.001
      t0 = 0.
      x0 = 0.0
      v0 = 0.0
      n = 2
      a1 = 1.0
      tmgl = 1.35
      y(1) = t0
      y(2) = x0
      y(3) = v0
      h = hi
      yfin = .0
10    continue
      call rkg(y, dy, yfin, h, n, tmgl, a1)
      f1 = tmgl* cos(2.*y(1)/3.) − sin(y(2)) − 0.5*a1*y(3)
      f = dy(3) − f1
      yfin = yfin + 0.001
      if(y(1).gt.1.001)yfin = yfin + .1
      if(y(1).gt.10.001)yfin = yfin + 1.
      if(y(1).gt.100.001)yfin = yfin + 10.
      if(y(1).gt.1000.001)yfin = yfin + 100.
      write(4,* )y(1), y(2), y(3), f
      if(yfin.lt.400.001) goto 10
      stop
      end
      subroutine func(y, dy, tmgl, a1)
      dimension y(3), dy(3)
      dy(1) = 1.
      dy(2) = y(3)
      dy(3) = tmgl ∗ cos(2.*y(1)/3.) − sin(y(2)) − 0.5*a1*y(3)
      return
      end
      subroutine rkg(y, dy, yfin, h, n, tmgl, a1)
      dimension a(4), b(4), c(4), q(4), y(3), dy(3)
      a(1) = 0.5
      a(2) = 1. − sqrt(0.5)
      a(3) = 1. + sqrt(0.5)
      a(4) = 1./6.
      b(1) = 2.0
      b(2) = 1.0
      b(3) = 1.0
      b(4) = 2.0
      c(1) = a(1)
      c(2) = a(2)
      c(3) = a(3)
      c(4) = 0.5
      i = n + 1
```

(*Continued*)

Table 3.5.3 (*Continued*)

```
      do 5j = 1, i 5      q(j) = 0.0
50    do 10j = 1, i
      do 15k = 1, 4
      call func(y, dy, tmgl, a1)
      temp = a(k)*(dy(j) − b(k)*q(j))
      y(j) = y(j) + h*temp
      q(j) = q(j) + 3.*temp − c(k)*dy(j)
15    continue
10    continue
      if(y(1).lt.yfin)goto 50
      return
      end
```

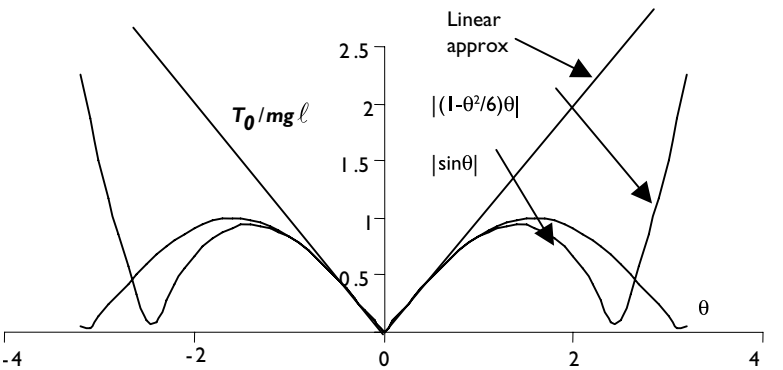


Figure 3.5.8 Restoring torque versus angular rotation.

3.5.3 Large amplitudes in response: Order and chaos

Response of a nonlinear system, particularly at high amplitudes cannot be extrapolated from small amplitude vibration results. Let us consider the behaviour of simple pendulum [Equation (3.5.14)] for high amplitude vibration. At large amplitudes the return torque of the pendulum begins to decrease beyond $\theta = 1/2\,\pi$ and may become negative for $\theta > \pi$, when the mass swings over the top [Figure 3.5.8].

Following Equation (3.5.36), the forced vibration equation for pendulum may be written as

$$\ddot{\theta} + \frac{c}{m\ell^2}\,\dot{\theta} + \frac{g}{\ell}\sin\theta = \frac{T_0}{m\ell^2}\cos\omega t \tag{3.4.36}$$

Equation (3.5.36) cannot be solved analytically and a numerical method has to be used for solving it.

Runge-Kutta integration given in Table 3.5.1 is given for a set of first order differential equation and as such Equation (3.5.36) is to be converted into a set of two

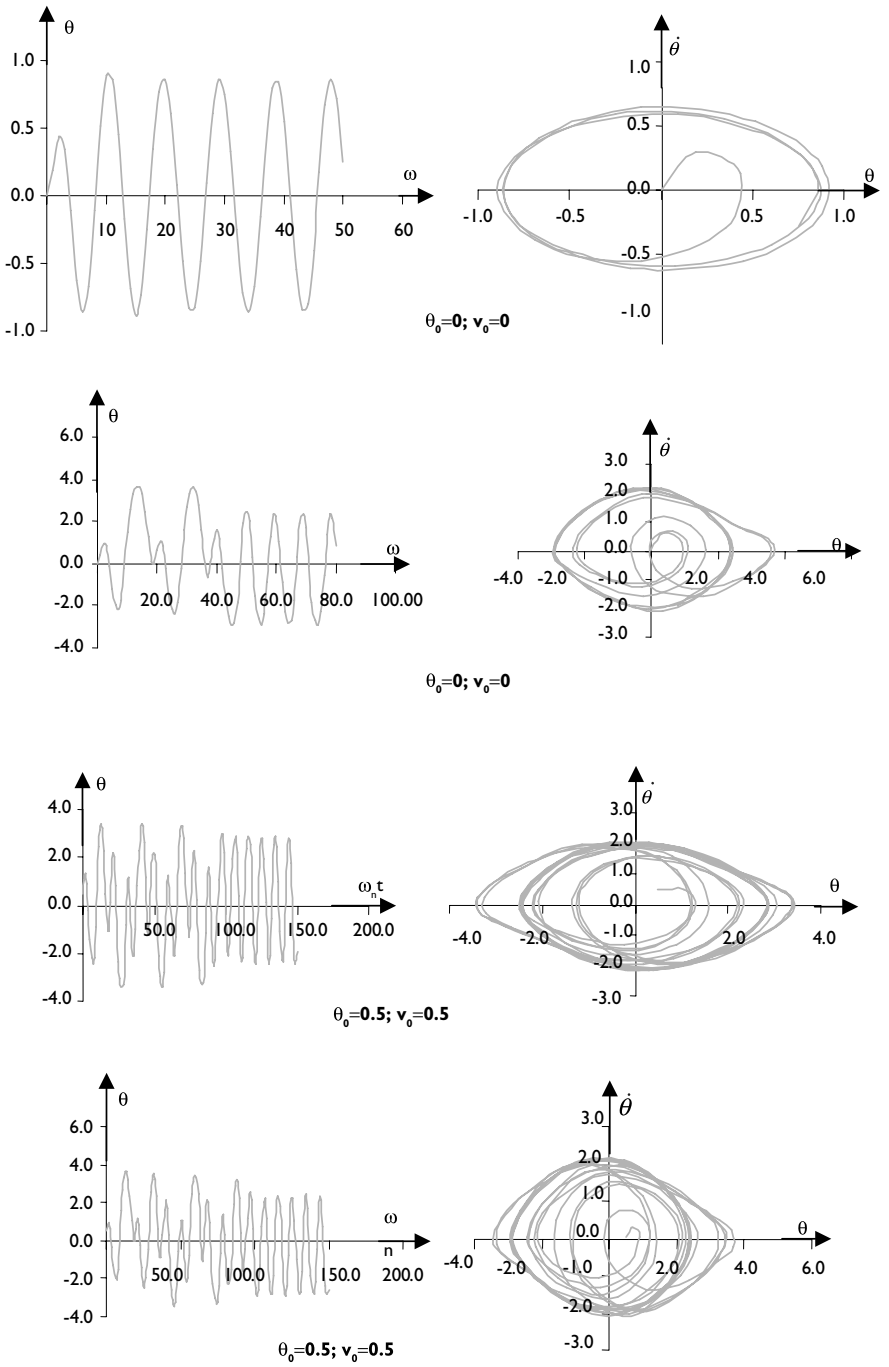


Figure 3.5.9 Oscillation of pendulum: $T_0/mgl = 1.025$.

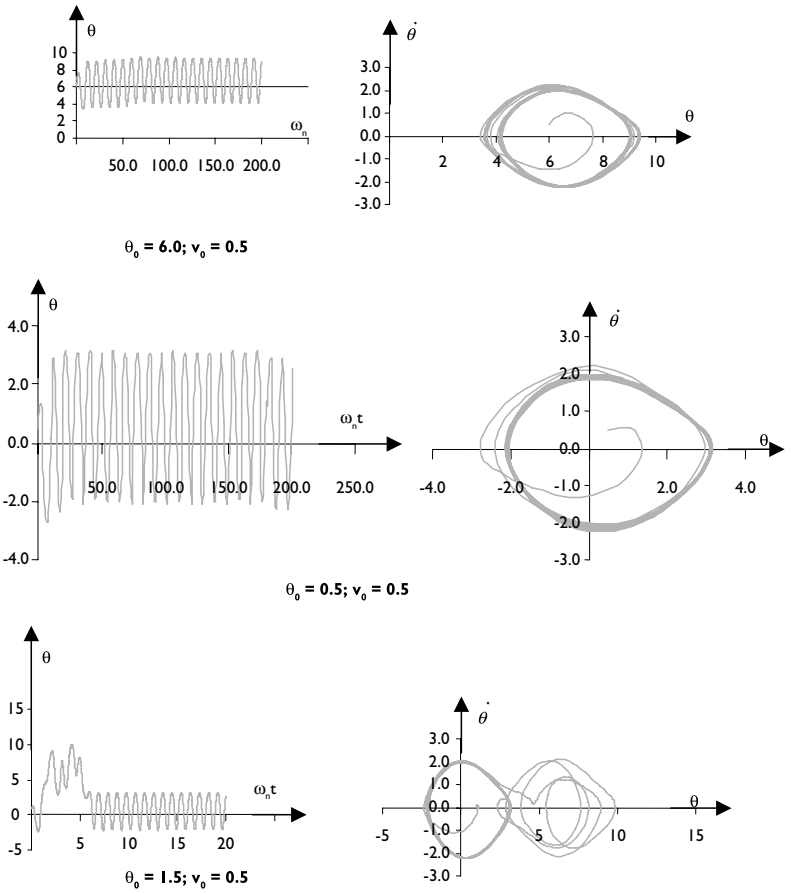


Figure 3.5.10 Oscillation of pendulum: $T_0/mgl = 5$.

simultaneous first order differential equations using

$$y = \dot{\theta} = \frac{d\theta}{dt} \quad \text{and} \quad \frac{dy}{dt} = \ddot{\theta} \tag{3.4.37}$$

Equation (3.5.36) may be written as

$$\frac{d\theta}{dt} = y$$

$$\frac{dy}{dt} = \frac{T_0}{m\ell^2}\cos\omega t - \frac{c}{m\ell^2}y - \frac{g}{\ell}\sin\theta$$

with $\theta(t=0) = \theta_0$ and $y(t=0) = \dot{\theta}\,(t=0) = \dot{\theta}_0$

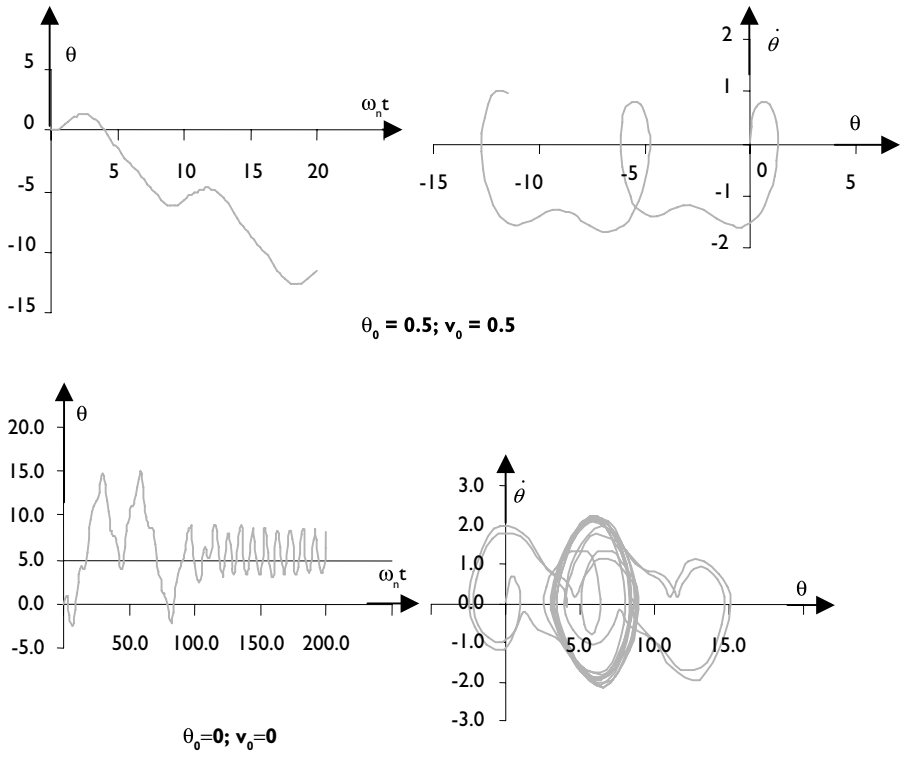


Figure 3.5.11 Oscillation of pendulum: $T_0/mgl = 1.35$.

Eqns. (3.5.38) are to be non-dimensionalised before using them in numerical solution technique and these may be realised by assuming

$$T = \omega_n t \rightarrow dT = \omega_n dt \quad \text{and} \quad \frac{d\theta}{dt} = \frac{d\theta}{dT} \cdot \frac{dT}{dt} = y$$
$$\rightarrow y = \omega_n \frac{d\theta}{dT}; \rightarrow \frac{dy}{dt} = \frac{d}{dt}\left(\frac{d\theta}{dt}\right) = \frac{d}{dT}\left(\frac{d\theta}{dT}\right)\omega_n^2 = \omega_n^2 \frac{dy}{dT}$$

Hence using $\omega_n^2 = g/\ell, Q = \omega_n/\gamma$ and $\gamma = \frac{c}{m\ell^2}$, Eqn. (3.5.38) may be written as

$$\begin{aligned} \frac{d\theta}{dT} &= \frac{y}{\omega_n} \\ \frac{dy}{dT} &= \left(\frac{T_0}{mg\ell}\right)\cos\left(\frac{\omega}{\omega_n}T\right) - \left(\frac{1}{Q}\right)\left(\frac{y}{\omega_n}\right) - \sin\theta \end{aligned} \tag{3.4.38}$$

with the boundary conditions given in Equation (3.5.38).

A computer experiment with R-K-G method on the numerical result of Equation (3.5.39) for $Q = 2; \omega = (2/3)\omega_n$ and $\gamma = (1/2)\omega_n$; and $(T_0/mgl) = 0.5; 1.025\ 1.07$

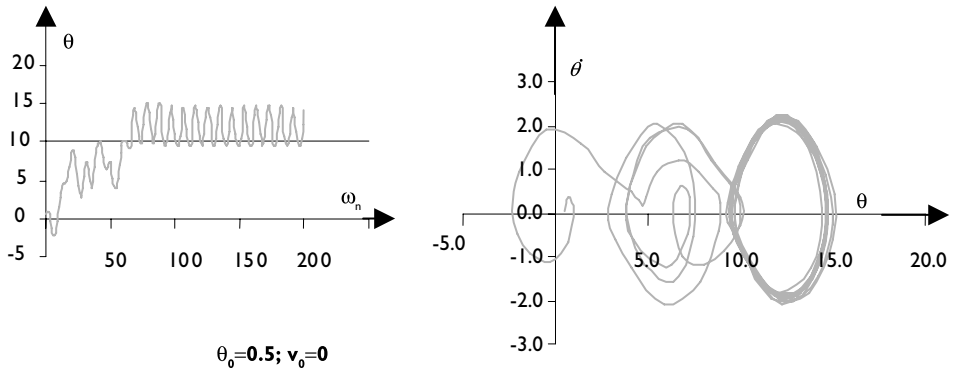


Figure 3.5.12 Oscillation of pendulum: $T_0/mgl = 10$.

and 1.35 , with $\theta_0 = 0, 0.5$ and $\dot{\theta}_0 = 0, 0.5$ are shown in Figs. 3.5.7 to 3.5.12. The RKG subroutine is appended in the Table 3.5.3. Runge-Kutta method with Gill's variation (RKG) or an adaptive Runge Kutta method may be used for solving this type of initial value problem easily.

Chapter 4

An introduction to soil-structure systems under statical condition

4.1 INTRODUCTION

This chapter deals with coupled analysis of soil and structure under static load.

Though we focus on the dynamic analysis of structures and foundations in this book yet understanding the static phenomenon is important for without having this concept clear the engineers often make mistakes especially in the mathematical modelling. Moreover, having insufficient concepts in coupled analysis of a system under static load surely makes behaviour under dynamic load difficult to perceive and as such we give a brief overview of this topic hereunder.

4.1.1 What we did twenty years ago...

Even some twenty years ago coupled analysis was not usually the practice followed in a normal design office.

- A structural engineer would do his frame analysis considering the frame as fixed base. On completion of his analysis, he will possibly furnish the fixed end moment shear and reaction at the base of the structure to a foundation engineer for the design of foundation.
- Soil mechanics specialist will perform a soil investigation at the site; study the various engineering parameters of the soil based on various laboratory and field investigations conducted and will suggest an *allowable bearing capacity* of the soil, which becomes the input to the foundation engineer.
- The foundation engineer would carefully review the soil report, find out the allowable bearing capacity of the soil, study the recommendations of geotechnical report to arrive at the nature of foundation and design the foundation.

Each of the above activities were done in isolation except some interface data and each specialist would execute his task in isolation with no interface amongst each other.

While a structural/foundation engineer would hardly ever bother to know about the voluminous detail given in the soil report except the bearing capacity value of the soil which he is only interested in, a soil mechanics specialist will hardly try to look

beyond the soil (and its properties) to see what is being built, how well the scheme fits in to his recommendation in terms of money time and safety.

4.1.2 The Present Scenario...

But things started changing, with advent of digital computer, Finite element method, development of complex industrial structures (like reactor building in nuclear power plant, HRSG raft in combined cycle plant, High speed compressor foundation in oil and gas industry, tall chimneys in fossil fuel plant to name only a few) it was slowly realized that doing things in isolation do have its limitations (and at times can be dangerous too) and often results in a design which is either far too conservative (thus cost is more) or unsafe.

This gave rise to a new field of study which synthesized the individual behavior of all these special branches of technology and brought them under one roof to develop a new branch of analysis termed Coupled Analysis and some salient features of the same is studied herein.

Our discussion pertaining to Civil/Structural engineering is restricted to the following class of soil-structure interaction problems:

- Static Soil-Structure interaction (for e.g. a flexible beam/plate on elastic foundation, Secondary moments in frames due to differential settlements...)
- Dynamic Soil-Structure interaction[1].

4.2 SOIL-STRUCTURE INTERACTION

Before we go in to the details it may be worthwhile to examine the following questions:

- What is soil structure interaction?
- What do we really mean by it?

4.3 STATIC SOIL-STRUCTURE INTERACTION

Shown in Figure 4.3.1 are frame structures, which could have raft or isolated footings as their foundation and which in turn are resting on soil. For analysis of this frame to obtain the design moments, shears under various loads and its combination, we would usually consider the bottom of the column as fixed and proceed with the structural or frame analysis.

The moments and shears induced at the base of the column based on the fixed base analysis are considered separately for design of foundation.

But does this analysis give a correct picture?

The basic lacuna in this method is possibly the assumption that the columns are fixed at the base. For if we ponder at this point a bit it is obvious that the foundation (be a raft or an isolated pad) acts together with the superstructure and the underlying

1 This we are going to take up in Chapter 1 (Vol. 2) subsequently.

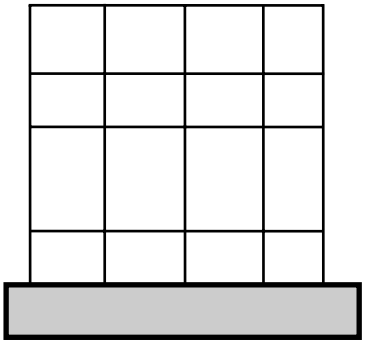


Figure 4.3.1a Frame on Raft.

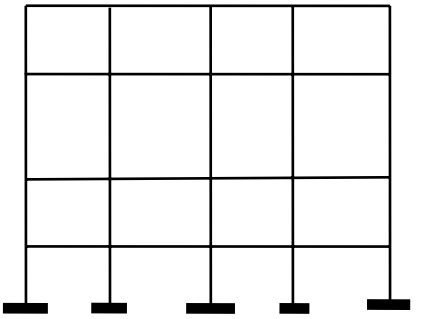


Figure 4.3.1b Frame on isolated footing.

soil if considered as a de-formable material will undergo some deformation which in turn will affect the moments and shears in the superstructure frame.

Thus, we see that deformation in soil affects the stress parameters in the superstructure and vice-versa and are inter-related with each other and constitutes the case of *soil structure interaction for the frame/foundation system.*

So long as this settlement is uniform over all the foundation, the structure does not undergo any additional stresses. But when their exists differential settlement or the contact pressure at various points of the foundation varies analysis of the superstructure assuming the column base fixed may not yield a realistic picture. *The above can possibly be further explained through a simple example.*

Example 4.3.1

Shown in Figure 4.3.2 is a bridge girder across a river and resting at points *A* and *B* on rock abutments at the ends, and resting on a pier at the center of the girder (point *C*) which is resting on the soil bed of the river and is subjected to load of 200 kN/m. The flexural stiffness of the girder is $EI = 10{,}000$ kN-m^2. Calculate the moments at *A*, *B* and *C* considering no deformation at *C* and with deformation at *C*.

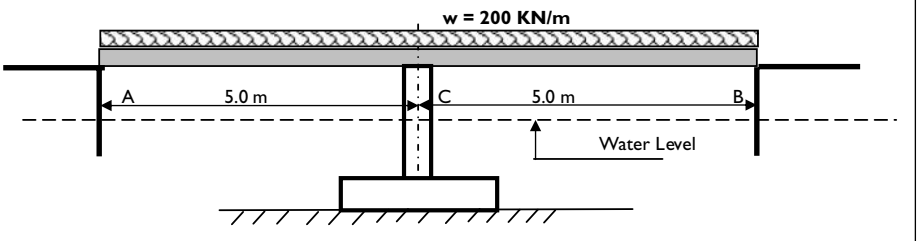


Figure 4.3.2 Bridge girder – with a supporting pier.

Solution:

We can assume the girder as a beam element supported at the points A, B and C (Figure 4.3.3a). Since the point A and B are lying on rock it can well be argued that deformation at point A & B will be negligible and it would not be unrealistic to assume that point A & B are unyielding support. Presuming the pier at point C is unyielding the analytical model may be depicted as shown in Figure 4.3.3a.

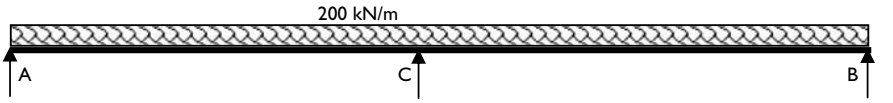


Figure 4.3.3a Idealisation ignoring soil effect.

Then based on our knowledge of structural mechanics it is quite elementary to find out that

$$M_A = 0 = 0;$$

$$M_c = \frac{wl^2}{8} = 625\,\text{kN}\cdot\text{m};$$

$$M_B = 0;$$

$$M_{AC} = M_{CB} = \frac{wl^2}{16} = 312.5\,\text{kN}\cdot\text{m}$$

Now considering the soil deformation below the pier the obvious choice to model the soil and pier is as a linear spring and let this value be $K = 8000\,\text{kN/m}$ for simplicity of calculation.[2]

Thus based on the above the mathematical model for the girder may be depicted as shown in Figure 4.3.3b.

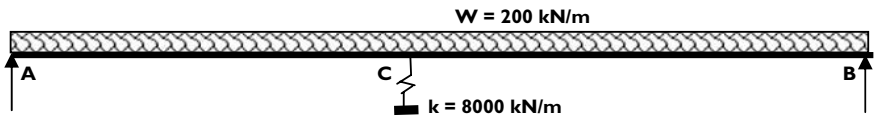


Figure 4.3.3b Idealisation, considering soil effect.

To determine the moments the first thing that we have to do is to find out the value of the reaction at point C which is an unknown.

2 It may be noted that there are different approaches available for evaluating this spring value and will be discussed subsequently.

For this let us presume initially there is no support at point C, thus the girder behave as simply supported beam between points A and B then

$$\delta_{CD} = \frac{5wl^4}{384EI}, \quad \text{acting downward} \tag{4.3.1}$$

where $l = 10$ m, the whole length of the girder.

Presuming R_C as the unknown reaction at spring support acting upward we have

$$\delta_{CU} = \frac{R_C l^3}{48EI}, \quad \text{acting upward} \tag{4.3.2}$$

Thus under the combined action of the load and the spring net deflection (δ_n) is given by

$$\delta_n = \delta_{CD} - \delta_{CU}; \quad \Rightarrow \delta_n = \frac{5wl^4}{384EI} - \frac{R_C l^3}{48EI}; \quad \Rightarrow R_c = k\delta_n;$$

$$\delta_n = \frac{5wl^4}{384EI} - \frac{k\delta_n l^3}{48EI}$$

On simplification we have $\delta_n = \dfrac{5wl^4}{8(48EI + kl^3)}$ (4.3.3)

Back-substituting the above value of δ_n above R_C can be obtained as

$$R_C = \frac{5}{8} wl \left[1 \Big/ \left(1 + \frac{48EI}{kl^3} \right) \right] \text{kN} \tag{4.3.4}$$

Now substituting the numerical values we have

$$R_C = 1179 \text{ kN}; \quad \text{Again } R_A + R_B + R_C = 2000 \text{ kN}$$

Or, $R_A + R_B = 820.75$ kN

Considering, AC (Figure 4.3.4):

Taking moment about point B we have, $R_A \times 10 + R_C \times 5 = 2000 \times 5$

Substituting $R_C = 1179$ kN, we have $R_A = 410.55 \text{ kN} = R_B$.

Once R_A, R_B, R_C is known moments at support and span are obtained by drawing the free body diagram of the span AC and applying the equilibrium equation about the joint C.

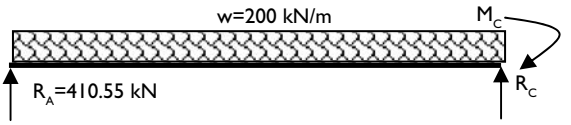


Figure 4.3.4 Free body diagram of Span *AC*.

$$M_A = 0 = M_B; \quad M_C = 447.553\ \text{kN} \cdot \text{m}; \quad M_{AC} = 401.25\,\text{kN} \cdot \text{m} = M_{BC}$$

Thus comparing the values we have obtained above, we find the values as shown in Table 4.3.1.

Table 4.3.1

Sl. No.	*Support/Span*	*Moment with no interaction*	*Moments with soil structure interaction*	*Variation in %*
1	A	0	0	0
2	B	0	0	0
3	C	625	448	−28%
4	AC	313	401	+28%
5	BC	313	401	+28%

Based on the above calculations it is observed that due to deformation of the pier, the support moments *reduce by 28% while the span moment is increased by* 28%.

Thus we see that if we do not take into cognizance the effect of the soil deformation we would be under-designing the span moment and the girder could eventually exhibit cracks at bottom face of the span due to inadequate reinforcement.

4.4 NON UNIFORM CONTACT PRESSURE

A similar situation can occur with frames resting on combined foundation supporting multiple columns.

Based on the contact pressure distribution the moments in the frame can vary as shown in Figure 4.4.1. If the combined footing supporting the frame settles uniformly it is obvious that there is no effect on the frame but if there is variation in the contact pressure depending on the relative stiffness of the soil and the foundation the foundation might deform as a saucer (as shown by the dotted line) it will surely have an effect on the final moments and shear of the frame

The above phenomenon gave rise to the topic of soil structure interaction where research is still in continuation to understand the phenomenon properly.

There also exists another class of problem which has intrigued many a design engineers in the Industry. The above phenomenon can best be elucidated by a real life problem as mentioned hereafter.

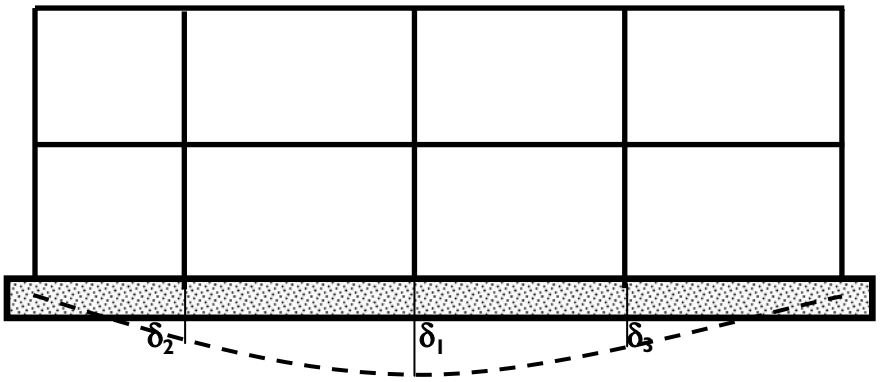


Figure 4.4.1 Deflection of foundation under non-uniform contact pressure.

Example 4.4.1

A combined cycle power plant of 240 MW-unit is to be built at two sites *A* and *B*. It was decided to go to a single vendor to buy the two identical cooling tower plants for the two sites. The plan area of the cooling water basin for the towers are 30 m × 60 m in plan, 800 mm thick, with maximum center to center distance between the columns is 10.3 m. The soil report states that for site-*A*, bearing capacity of soil is 80 kN/m^2 and that for site *B* is 450 kN/m^2. Will there be a unified approach for design of these rafts? If not, what needs to be done?

Solution:

Under various combination of loads and moments the basin the may be designed based on the soil pressure generated due to the superstructure load given by

$$q = Q/A \pm (Qe_y/I_x)y \pm (Qe_x/I_y)x \tag{4.4.1}$$

where, q = stress in soil; Q = vertical load on raft including self weight; e_x, e_y, I_x, I_y = eccentricities and moments of inertia about the principal axes through the centroid of the section; x, y = co-ordinates of any given point on the raft with respect to x and y axes passing through the centroid of the area of the raft.

When we apply the above equation, we start with an implicit assumption that- *"the raft is rigid. By which we imply that it is stiff enough to distribute the load coming on it to all the points in contact with the soil uniformly". But is this assumption valid for all cases?*

Certainly not, for it has been observed that depending on the overall stiffness of the raft, sub-grade modulus of the soil and center to center distance between the column the raft may either behave as *rigid or may behave as flexible* (i.e. stress distribution will be localized) and there is indeed a substantial variation in

the design moments and shears based on these two methods. It has been observed that if L the c/c distance between columns resting on a raft. Then for

- $\lambda L \leq \pi/4$ the raft will behave as *rigid raft*;
- For $\lambda L \geq \pi$ the raft will behave as *flexible raft*;
- For all values between $\pi/4 \leq \lambda L \leq \pi$ the slab behave *in between rigid/flexible* in which,

$$\lambda = \sqrt[4]{kB/4E_C I} \tag{4.4.2}$$

where, if, k = modulus of sub-grade reaction in kN/m^3, B = width of raft in m, E_c = modulus of elasticity of concrete in kN/m^2, and, I = moment of inertia of the raft in m^4.

The basic difference between the two methods are that in conventional rigid analysis the effect of soil deformation is negligible on the raft while in flexible analysis the deformation of soil plays a significant role in affecting the deformation in the raft ('the soil stiffness interacts with the raft stiffness') and modifies the moment and shear profile. Usually for soft soils like normally consolidated clay, peat, organic silts etc., the assumption involved in conventional rigid method are commonly justified. Now let us see what conclusion we arrive at on solving the problem.

The sub-grade modulus of the soil is given by the expression[3] $k_s = 100 \times q_{\text{all}}$, where q_{all} = allowable bearing capacity of soil.

Thus for site A, $k_{sA} = 100 \times 80 = 8{,}000$ kN/m^3 and for site B, $k_{sB} = 100 \times 450 = 45{,}000$ kN/m^3.

Now, $\lambda = \sqrt[4]{\frac{k_s B}{4E_c I}}$ where, $I = \frac{Bh^3}{12}$ in which, h = thickness of the raft, we have on substitution on the above equation, $\lambda = \sqrt[4]{\frac{3k_s}{E_c h^3}}$.

Using $E_c = 28500000$ kN/m^2, for site A $\lambda_A = \sqrt[4]{\frac{3 \times 8{,}000}{28500000 \times (0.8)^3}} = 0.2013$

Therefore $\lambda L = 0.2013 \times 10.3 = 2.073$ m $\geq \pi/4$ but $< \pi$ thus *the raft will be intermediate between rigid and flexible.*

For site B $\lambda_B = \sqrt[4]{\frac{3 \times 45{,}000}{28500000 \times (0.8)^3}} = 0.310$

$\therefore \lambda L = 0.310 \times 10.3 = 3.193 \geq \pi$, thus the *raft behaves as a flexible raft.*

Designing the cooling tower basin based on rigid method (Teng 1962) for site A is justified while designing the raft as flexible, considering the interaction effect of soil for site B, is more prudent.

Flexible analysis can be done by two methods

- Based on closed form solution as given in IS 2950 (part1)
- By numerical methods like finite element or finite grid method (Selvadurai 1979).

3 The basis of this is explained later.

The method to be adapted in analyzing a raft based on FEM or FDM has already been discussed in detail in Chapter 2 (Vol. 1) while discussing numerical methods in engineering.

4.5 VARIOUS SOIL MODELS–THE TOOLS IN THE TOOLKIT...

The two most common models which are in vogue for static soil-structure interaction problems are

- *Winkler springs where soil is modeled as linear springs.*
- *Finite element models usually when the problem is a 2D plane strain one.*

4.5.1 Winkler springs

In this method soil medium is assumed to constitute of a series of closely spaced springs on which the foundation slab lies. The springs are linear in nature and can be expressed as:

$$P = k\delta \tag{4.5.1}$$

in which, P = force on the node at which the spring is connected; k = the spring constant having units of force per unit displacement; δ = displacement at the node.

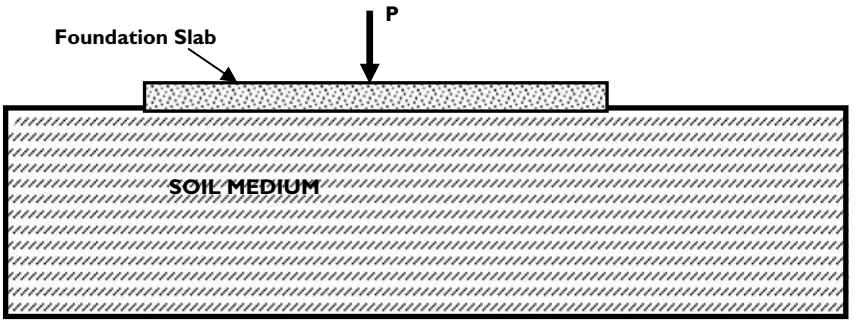


Figure 4.5.1 Foundation resting on soil medium.

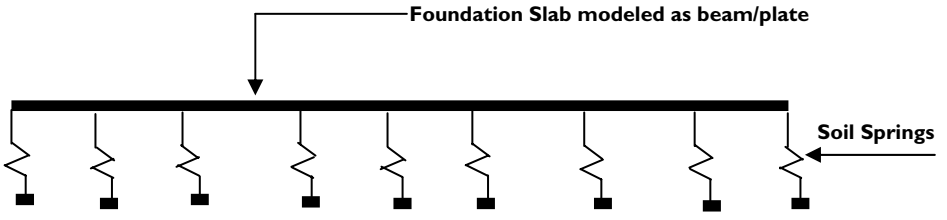


Figure 4.5.2 Equivalent foundation resting on Winkler spring bed.

This can be figuratively shown as mentioned in Figure 4.5.1 and mathematically represented as shown in Figure 4.5.2.

For springs, the soil parameter on which it is chiefly dependent is the *sub-grade modulus* of soil and there exists a major problem in estimating its numerical value.

Terzaghi and Peck (1967) suggested that this may be obtained from plate load test where the load versus deflection for a plate loaded gradually is plotted and based on the curve obtained, the sub-grade modulus is estimated.

4.5.2 Estimation of sub-grade modulus

For footings on sand

$$k_s = k_1 \left(\frac{B + 0.3}{2B} \right)^2 \tag{4.5.2}$$

while that in clay is given by,

$$k_s = k_1 \cdot B \tag{4.5.3}$$

where, k_s = sub-grade modulus of the soil for footing of width B in kN/m^3; k_1 = sub-grade modulus of the soil obtained from plate load test for a plate of area 300 mm × 300 mm in kN/m^3.

4.5.2.1 Sub-grade modulus from allowable bearing capacity of soil...

In the absence of this data, the sub-grade modulus can also be estimated from allowable bearing capacity of the soil based on the following equation (Bowles 1988). This has been found to be in excellent agreement with observed field data

$$k_s = 40(S.F.)q_a \text{ kN/m}^3 \tag{4.5.4}$$

in which, $S.F.$ = factor of safety to bearing capacity of soil; q_a = allowable bearing capacity of soil, and $q_{\text{ult.}}$ = ultimate bearing capacity of soil.

This equation is based on $q_a = q_{\text{ult.}}/S.F.$ and the ultimate soil pressure is at an elastic settlement of $\Delta H = 25$ mm. For $\Delta H = 10$ mm, the factor 40 gets modified to 100, while for $\Delta H = 50$ mm the value 40 gets modified to 20 (*meaning thereby that this is linearly proportional to the ratio of the displacement*).

Once the sub-grade modulus is estimated the equivalent spring connected to a particular node of a foundation is given by

$$k_i = k_s x A_f \tag{4.5.5}$$

where, k_i = spring data at node i of the foundation; k_s = sub-grade modulus of the soil for a specified displacement δ; A_f = influence area of the foundation pertaining to node I.

How to evaluate the influence area A_f we will see it shortly.

4.5.2.2 *Effect of consolidation on the sub-grade modulus*

Based on the above discussion it is quite evident that discussions where restricted to the elastic deformation of the soil. So long as the soil is cohesionless/granular in nature the above is quite right. But for soil constituting of medium to soft clay, the elastic part of the settlement is secondary and the major deformation in this type of soil is attributed to consolidation settlement. So what do we do about it?

It must be remembered that consolidation settlement is non-linear in nature and time dependent while we are restricting our analysis to linear and time independent frame work.

One of the techniques that is often used to account for the consolidation is to modify the value of k_s as mentioned hereafter.

On clayey type of soil for net pressure Δp, total displacement may be defined as

$$\Delta H_t = \Delta H_e + \Delta H_c \tag{4.5.6}$$

where, ΔH_t = total deformation of the foundation; ΔH_e = elastic deformation of the foundation; ΔH_c = consolidation settlement of the foundation.

Let k_s' be the modified sub-grade modulus of the soil considering the consolidation effect under pressure Δp. Then,

$$k_s' = \frac{\Delta p}{\Delta H_e + \Delta H_c}; \tag{4.5.7}$$

Again as, $\Delta p = k_s \cdot \Delta H_e$ we have,

$$k_s' = \frac{k_s \cdot \Delta H_e}{\Delta H_e + \Delta H_c} \tag{4.5.8}$$

This value of modified sub-grade modulus (k_s') is to be considered for evaluating the spring taking into consideration the consolidation effect of the soil.

The above is best explained by the following example.

Example 4.5.1

A certain site has been observed to have a ultimate bearing capacity of 150 kN/m^2. For a 14 m × 6 m raft on the same site is observed to have consolidation settlement of 50 mm. Evaluate the subgrade modulus for computer analysis of the raft with springs.

Solution:

Based on Bowles's equation: $k_s = 40 \cdot q_u;\ \Rightarrow k_s = 6000\ \text{kN/m}^3$

As stated earlier for application above equation $\Delta H_e = 25$ mm

Therefore, $k_s' = 6000\ x\ \left(\frac{25}{25+50}\right); k_s' = 2000\ \text{kN/m}^3$.

Thus we see that the sub-grade modulus value gets reduced when consolidation of the soil is taken into cognizance[4].

4.6 EVALUATION OF NODAL SPRINGS

Next comes the evaluation of the nodal springs which we have shown earlier is dependent on the influence area. How do we evaluate the influence area?

Example 4.6.1

Shown in Figure 4.6.1 is a raft discretised into finite element meshes supported on soil what is the influence area for the spring calculation for nodes 1, 2 and 3? Consider meshes to be equally spaced. K_s value considered for the site is 2000 kN/m^3.

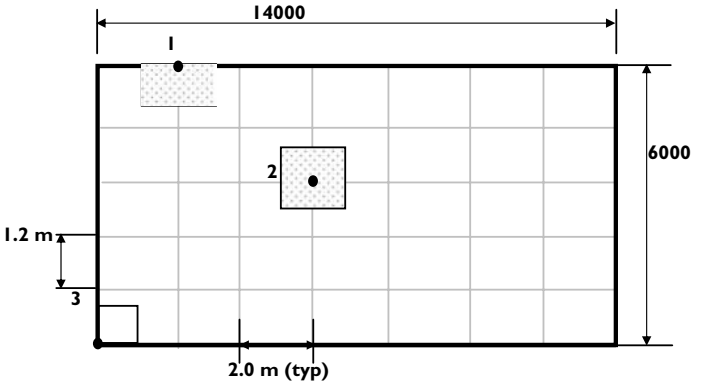


Figure 4.6.1 Raft with finite element meshing of slab supported on Winkler springs.

4 Consolidation is basically time dependent and most of the soil report deals with settlement data at 90–95% consolidation. But as settlement function is time dependent it is obvious that at different stage of consolidation the sub-grade modulus value will be different and so will be the spring constant. With spring stiffness changing with time, the moments and shears in the foundation and the frame will also vary with time. It is for this, analysis is usually carried out for 40%, 60%, 80%, 95% consolidation stage and the most critical case amongst the same is selected.

Solution:

Considering equally spaced meshes dimension of each mesh is 2 m × 1.2 m.
Hence for
node 1 $k_1 = 2000 \times 1/4 \times 2 \times 1.2 \times 2(\text{nos}) = 2400$ kN/m
node 2 $k_2 = 2000 \times 1/4 \times 2 \times 1.2 \times 4(\text{nos}) = 4800$ kN/m
node 3 $k_3 = 2000 \times 1/4 \times 2 \times 1.2 \times 1(\text{nos}) = 1200$ kN/m

4.6.1 So the ground rule is. . .

- For each rectangular/quadrilateral mesh 1/4 of the contact area of each mesh connecting a node constitutes the influence area[5].
- For triangular meshes 1/3 of the total area influence a particular node.

Table 4.6.1 gives some range of values for sub-grade modulus of soil and may be used as a guide for comparison when using the above equations.

Table 4.6.1 (After Bowles 1988).

Sl. No.	*Soil type*	*Sub-grade Modulus* (kN/m^3)
1	Loose sand	4800–16000
2	Medium dense sand	9600–80000
3	Dense sand	64000–128000
4	Clayey medium dense sand	32000–80000
5	Silty medium dense sand	24000–48000
6	Clayey soil	
6a	$q_a \leq 250$ kPa	12000–24000
6b	$200 \leq q_a \leq 400$ kPa	24000–48000
6c	$q_a > 800$ kPa	>48000

q_a = Allowable bearing capacity of Foundation in kN/m^2.

4.7 LIMITATIONS/ADVANTAGES OF WINKLER SPRING MODEL

One of the major approximations attributed to Winkler's model is that the springs assumed to idealize the soil is discrete in nature.

For a nodal load acting on the spring, affects that particular spring only. While in reality, soil is a continuous medium and the interaction between them (soil to soil) do exists.

It is for this many engineers prefers to use finite element modeling specially when the problem constitute of plane strain case like

5 For computer input of spring data the values at node 1 and 3 needs to be doubled. See Section 4.10 for further explanations.

- Analysis of box culverts below ground
- Study of influence of one foundation over the other
- Analysis of retaining walls, sheet piles
- Analysis of vertical cuts in soil etc.

But for contact pressure problem of beams and plates and super-structure/foundation interaction Winkler spring model still *remains the most popular mathematical model in use*.

Though mathematical formulation exists based on plates on elastic half space they are far too complex for handling of day to day engineering work. Moreover most of the software available in the market cannot handle the special conditions invoked in it.

Some of the major advantages that lie with Winkler model can be stated as follows:

- The idealization is simple yet realistic.
- In spite of its limitations, if used judiciously, has been found to yield results in excellent agreement with field observed data.
- Most of the commercially available finite element package like SAP, GTSTRUDL, ANSYS, PAFEC, STAAD, SACS etc. are capable of handling spring elements and it is easy to furnish the data correctly (the accuracy is of course dependent on to the extent of the realistic estimation of the sub-grade modulus of the soil).
- Finally a number of structures analyzed and designed based on Winkler spring model *has stood the test of time*.

Though finite element model is becoming increasingly popular with classes of problems as mentioned above, for contact problems of soils with beams or plates and for foundation/super-structure interaction analysis Winkler spring models will continue to dominate the scenario of industrial design till further enhancements like boundary element theory or sub-structuring technique becomes popular or a part and parcel of standard FEM analysis packages.

4.8 FINITE ELEMENT MODELS

Finite element modelling is increasingly becoming popular for its sheer versatility of satisfying varied boundary conditions like:

- Irregular boundary conditions.
- Non-homogenous medium (layered soil, different materials in structure like RCC and steel).
- Complex loading conditions etc.

We have discussed earlier above that for problems classified as contact problems, Winkler spring model is by far the most popular.

It is quite possible to model a similar structure by finite element in 3D, with soils modelled as brick elements as shown Figure 4.8.1.

This is a conceptual model only and it should not be thought that the numbers of element as shown suffices and for real life problem number of brick elements could be in thousands.

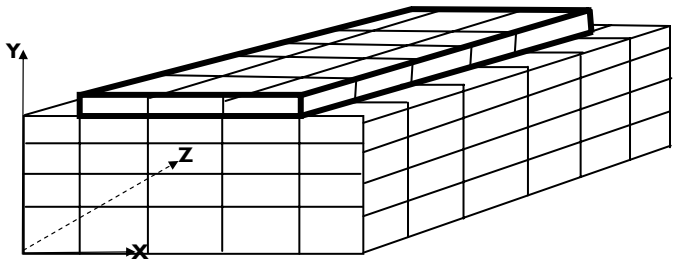


Figure 4.8.1 Finite element model of raft resting on soil modelled as 8-noded brick element.

Though this is the most comprehensive model one can conceive, yet, it is quit obvious that analysis of such model in terms preparation of the model, generation of input data interpretation of output results will be extremely intensive (and expensive too) and is really not called for (Even this small conceptual model as shown above constitute of 210 nodes 120 brick elements and 15 plate elements). Moreover the problem cannot be converted to 2D problem for the mat have a finite dimension in Z direction and strain is not invariant in this direction.

Finally what are we looking for? We are not interested to find out the stress within the soil but the stress induced at the plate/soil interface.

Intuitively it can be seen that modelling the soil as Winkler model do have its distinct advantages. Like we said earlier that "accuracy of the structural foundation system with Winkler springs are valid to the extent of realistic estimation of the sub-grade modulus", similarly for the FEM the accuracy is valid to the extent of realistic estimate of the Elastic modulus of the soil (E_s) and Poisson's Ratio (ν).

How to evaluate the value of E_s and ν we will see subsequently.

Though we advocate to model the soil as Winkler spring for contact stress class of problem it is evident that the foundation (which could be isolated footing, raft, combined footing etc.) is a continuum and can be modeled as finite element which in turn is connected to the springs.

We give here some details of modeling by FEM of raft foundation resting on soil.

The first step is what element we choose for the raft?

As discussed earlier two options are usually used

- Plate Element
- Equivalent beam element

4.8.1 Plate element

We had already discussed in Chapter 2 (Vol. 1) the advantages and disadvantages of plate element and have shown that if we use lower order 4-noded plate elements substantial refinement needs to be done to cater for the discontinuity of slope at edges. This in turn increases the computational effort substantially.

Provided the software in use supports it, it is advised (Bathe 1990) that 9 nodded plates based on iso-parametric formulation be used for all plate bending problems.

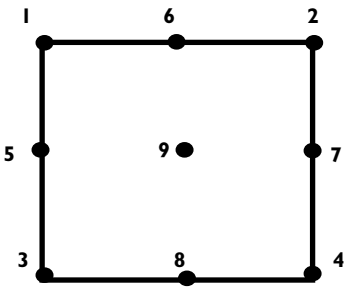


Figure 4.8.2 Nine node plate element.

The advantages with this element are

- The edge discontinuities are reduced due to imposition of internal nodes (5, 6, 7, 8).
- Elements being of higher order than 4 nodded plates coarser meshes while modeling will not effect the accuracy to the extent with 4 nodded elements.
- The transition from refined to coarser meshes becomes very simple.
- With nodes at center of plate displacement/stress can be directly obtained (else this needs to be interpolated from the edge nodes) [Figure 4.8.2].

The above is described by a simple example as follows:

Example 4.8.1

Solution:

Shown in Figure 4.8.3 are two identical models with two different types of elements it is obvious that in first model with 4 nodded elements the transitioning takes place with triangular or quadrilateral element if this elements are too skewed in their geometric shape can create numerical ILL-conditioning and the stress thus obtained will not be a realistic one.

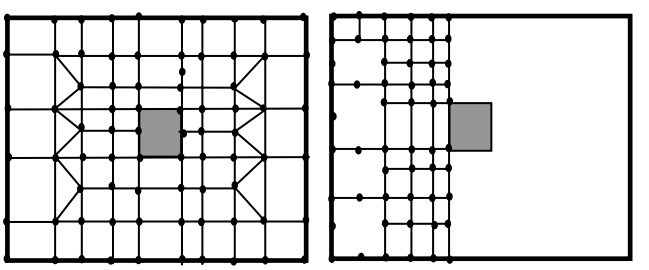


Figure 4.8.3 Finite element model of a portion of raft near column with 4-noded and 8-noded plate elements.

Moreover, the elements at edge of the raft (connected to tri-angular elements) have large edges where slope will be discontinuous and results obtained therein will again not be too realistic.

For the second model with 8/9 nodded plate elements it is obvious that the transition from refined to coarser mesh is smoother with no elements having geometric shape which is irregular.

Edge elements having additional nodes at the middle of the side edge the slope discontinuity is reduced to half. This goes on to give much better results in comparison to 4 nodded plates.

Other than this, plate elements based on Hybrid formulation (Kardestuncer and Norrie 1987) due to their lower bound stiffness property are found to give much improved results even with coarse meshes and may also be used provided the software in hand have this type of element in its finite element library.

4.9 FINITE ELEMENT ANALYSIS OF PLATE WITH SOIL STIFFNESS BASED ON ISOTROPIC ELASTIC HALF SPACE THEORY

One of the major complains against the Winkler model as we had stated earlier was that the springs being localized the displacement of the raft is restricted within the foundation boundary only.

In reality the soil being a continuous medium the displacements also affects zones outside the foundation area as shown in Figure 4.9.1.

4.9.1 Displacement profile of soil under a foundation based on half space theory

In this method based on direct solution of differential equation the displacement of the elastic half space under vertical loading is obtained. Since this solution is close form the disadvantage of discrete modelling like in spring does not exists. The displacements are obtained based on unit load to generate the flexibility matrix of the soil and this on inversion is added to the element stiffness of the plate to generate the combined matrix of the soil and the plate (Zienkiewicz and Cheung 1964).

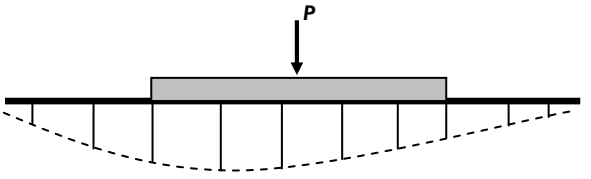


Figure 4.9.1 Displacement profile of soil under a foundation.

The basic steps of the method are discussed herein. Let us consider one plate element of size $a_0 \times b_0$. For a load Q on the plate the uniform contact stress induced in the plate is

$$q = Q/(a_0 \times b_0) \tag{4.9.1}$$

The response function for the elastic half space model in closed form takes the integral form

$$w(x, y) = \frac{(1 - \nu_s^2)}{\pi E_s} \iint_A \frac{q\,(\xi, \zeta)\, d\xi\, d\zeta}{[(x - \xi)^2 + (y - \zeta)^2]^{1/2}} \tag{4.9.2}$$

where ν_s = Poisson's ratio of the soil; E_s = modulus of elasticity of the soil; x, y = Co-ordinates in x and y direction; $w(x, y)$ = vertical displacement which is a function of x and y; A = contact area of the finite element ($a_0 \times b_0$).

In case of a nodal point i the deflection at center of the loaded area $a_0 \times b_0$, namely, w_{ii} (by w_{ii} we mean deflection at point i due to a load at i) can be obtained from integrating the above equation between appropriate limits, when we have

$$w_{ii} = \frac{Qi(1 - \nu_s^2)}{a_0 \pi E_s} f_{ii} \tag{4.9.3}$$

$$\text{where} \quad f_{ii} = \frac{4}{b_0} \int_{\xi=0}^{a_0/2} \int_{\zeta=0}^{b_0/2} \frac{d\xi\, d\zeta}{[\xi^2 + \zeta^2]^{1/2}}$$

The coefficients f_{ii} depends on the aspect ratio b_0/a_0 of the loaded area and numerical values are tabulated in Table 4.9.1.

The surface deflection w_{ni} (here w_{ni} means displacement at node n due to a load at node i) at any arbitrary nodal point n which lies outside the loaded area can be similarly expressed as:

$$w_{ni} = \frac{Qi(1 - \nu_s^2)}{a_0 \pi E_s} f_{ni} \tag{4.9.4}$$

where

$$f_{ni} = \left| \left[\left\{ \frac{x_n - x_i}{a_0} \right\}^2 + \left\{ \frac{y_n - y_i}{b_0} \right\}^2 \right]^{-1/2} \right|$$

Based on the above it is possible to find out the soil displacement at the four nodes of the plate element represent by 1, 2, 3, 4 (Figure 4.9.1). And this is represented by the displacement matrix as follows:

Table 4.9.1

b_0/a_0	2/3	1	2	3	4	5
f_{ii}	4.265	3.525	2.406	1.867	1.543	1.322

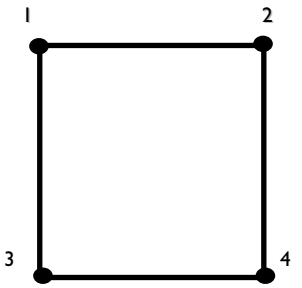


Figure 4.9.2 A four node rectangular plate element.

If $\{w\}$ = the displacement vector of the soil at the four nodes 1, 2, 3, 4, then the total soil displacement for node can be described as

$$\{w\} = \frac{(1 - \nu_s^2)}{a_0 \pi E_s} [f_s]\{Q\} \tag{4.9.5}$$

where $[f_s]$ = Flexibility matrix of the soil (the diagonal elements are obtained from the term f_{ii} and off-diagonals from the term f_{ni}); $\{Q\}$ = vector for nodal reactive force.

On inversion of the flexibility matrix, we have

$$\{Q\} = \frac{a_0 \pi E_s}{(1 - \nu_s)^2} [K_s] \{w\} \tag{4.9.6}$$

where $[K_s]$ = stiffness matrix of the soil = $[f_s]^{-1}$.

For external load vector $\{P\}$ acting at the plate nodes with a net reaction $\{Q\}$, the stiffness can be defined (Cheung and Nag 1968) as

$$\{P\} - \{Q\} = \frac{D}{15 a_0 b_0} [K_p]\{w\} \tag{4.9.7}$$

in which $[K_p]$ = the stiffness matrix of the plate element, and

$$D = E_p h^3 / 12(I - \nu_b^2) \tag{4.9.8}$$

where E_p = elastic modulus of the plate element; h = thickness of the plate; ν_b = Poisson's ratio of the plate material.

Substituting the value of $\{Q\}$ above we have

$$\{P\} = \frac{D}{15a_0b_0}[[K_p] + \gamma * [K_s]]\{w\} \tag{4.9.9}$$

Considering $\{P\} = [K_{sp}]\ \{w\}$ we have

$$[K_{sp}] = [[K_p] + \gamma * [K_s]] \tag{4.9.10}$$

where $[K_{sp}]$ = combined stiffness matrix of the plate element and the soil.

$$\gamma* = \frac{180\pi a_0^2 b_0}{h^3} \frac{\left(1-\nu_b^2\right)}{\left(1-\nu_s^2\right)} \frac{E_p}{E_s} \tag{4.9.11}$$

Thus once the stiffness matrix of the combined plate and soil is obtained it can be assembled in the usual way based on matrix analysis of structure and for the external load imposed on it can be solved for the displacement and stress (Weaver and Gere 1986).

4.10 FINITE GRID METHOD/EQUIVALENT BEAM ELEMENT, THE UNSUNG WORK HORSE

For engineers inclined mathematically this method may not look appealing for it does not appear so mathematically elegant. For followers of classical finite element analysis, the method may also look somewhat crude. But from the point of view of practical application and simplicity as well as fit for purpose engineering this method has possibly been most successful.

We had already discussed in previously some of the merits and practical advantages in using beams to model the raft (Figure 4.10.1) which in turn is connected to Winkler springs.

In this method the raft instead of plate is broken up into equivalent beam elements and each of the beam elements have degrees of freedom as shown in Figure 4.10.2.



Figure 4.10.1 Equivalent beam element connected to soil springs.

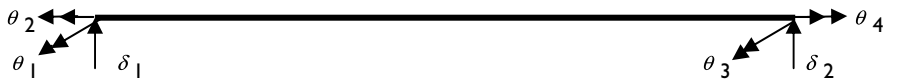


Figure 4.10.2 Mathematical model of the equivalent beam element.

Based on matrix analysis of structure the element stiffness for this element is given by

$$[K_{\text{beam}}] = \frac{EIz}{L^3}\begin{bmatrix} 12 & 6L & 0 & -12 & 6L & 0 \\ 6L & 4L^2 & 0 & -6L & 2L^2 & 0 \\ 0 & 0 & \dfrac{IxL^2}{2Iz(1+\nu)} & 0 & 0 & \dfrac{-IxL^2}{2Iz(1+\nu)} \\ -12 & 6L & 0 & 12 & 6L & 0 \\ 6L & 2L^2 & 0 & 6L & 4L^2 & 0 \\ 0 & 0 & \dfrac{-IxL^2}{2Iz(1+\nu)} & 0 & 0 & \dfrac{IxL^2}{2Iz(1+\nu)} \end{bmatrix} \tag{4.10.1}$$

The displacement vector is given by

$$\{\delta\} = \langle \delta_1\ \theta_1\ \theta_2\ \delta_2\ \theta_3\ \theta_4 \rangle^T \tag{4.10.2}$$

When the soil spring are added to the nodes the overall stiffness becomes

$$[K'_{\text{beam}}] = \frac{EIz}{L^3}\begin{bmatrix} \left(12 + \dfrac{L^3K_{ii}}{EIz}\right) & 6L & 0 & -12 & 6L & 0 \\ 6L & 4L^2 & 0 & -6L & 2L^2 & 0 \\ 0 & 0 & \dfrac{IxL^2}{2Iz(1+\upsilon)} & 0 & 0 & \dfrac{-IxL^2}{2Iz(1+\upsilon)} \\ -12 & 6L & 0 & \left(12 + \dfrac{L^3K_{jj}}{EIz}\right) & 6L & 0 \\ 6L & 2L^2 & 0 & 6L & 4L^2 & 0 \\ 0 & 0 & \dfrac{-IxL^2}{2Iz(1+\upsilon)} & 0 & 0 & \dfrac{IxL^2}{2Iz(1+\upsilon)} \end{bmatrix} \tag{4.10.3}$$

where $[K'_{\text{beam}}]$ = combined stiffness matrix for the beam and the spring; $K_{ii} = K_{jj}$ = spring values of soil at node I and node j of the beam respectively.

Once the combined stiffness of beam and spring element is obtained at element level the overall stiffness matrix of the raft can be assembled globally and solved for the displacement and stresses for the imposed loads.

The main objections rose for the equivalent beam method by many engineers is that

- It is less accurate than FEM based on plate elements, for the slab looses it continuum character.
- The discrete nature of the of the Soil springs.

Actually there is hardly any evidence that FEM based on plate elements are more accurate than equivalent beam method.

It has been found by some authors that results are very nearly matching when compared for the same problem by the two methods.

"*To cater to the coupling effect of the soil it has been suggested by Bowles (1988) to* ***double the value*** *of the edge springs during computations of the soil springs to give better correlation with the field observations.*"

Over and above, less handling of the input and output data getting results which are easily interpretable and can be directly used for design, *This method still remains the most popular mathematical model in application in the design offices in the industry.*

4.11 FEM APPLICATION FOR PROBLEMS OF CLASS 2D

There are certain classes of problems in 2D where the solution, based on FEM, is possibly unmatched and possibly furnishes the most realistic value.

Consider the following type of problems:

Example 4.11.1

Effect of Building Structure on the Box Culvert below Ground shown in Figure 4.11.1.

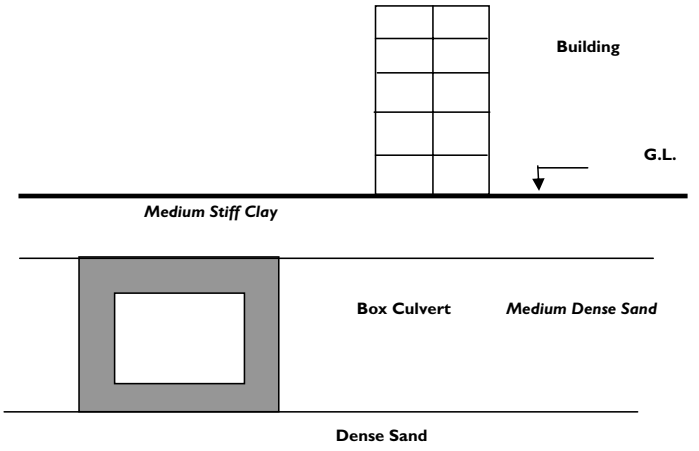


Figure 4.11.1 Effect of building structure on the box culvert below ground.

Example 4.11.2

Vertical cuts in soil with horizontal struts to support the excavation shown in Figure 4.11.2.

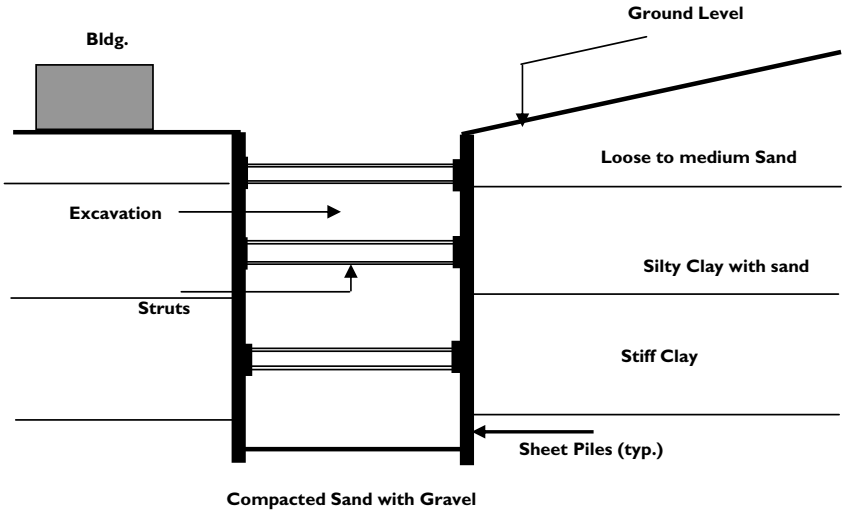


Figure 4.11.2 Vertical cuts soil with horizontal struts to support the excavation.

Solution:

On observing the two problems as mentioned above, it does not take super intelligence to realize that because of the layered nature of the soil solution based on conventional method will not be possible.

The reason are as follows

- Due to layered nature of the soil conventional pressure diagram is not valid.
- The building at the site induces overburden pressure. But the stress induced due to it in the soil cannot be evaluated based on Westergaard's analysis for the evaluation of stress in elastic medium is valid only for homogenous isotropic material only.
- It is not possible to evaluate the effect it will have on the surrounding when sheet piles are driven in the ground and soil is excavated with progressive strutting of the walls are taking place.

Based on the conventional analysis the pressure on the sheet pile walls due to earth is given by the following expressions (Terzaghi and Peck 1967, Tschebotarioff 1973) [Figure 4.11.3].

Here,

γ = Density of soil in kN/m^3;

$p_a = \gamma\, HK_A$; for $\delta = 0$ to $20° < \phi$

$p_a = 0.8\gamma\, HK_A$; $K_A = \tan^2(45 - \phi/2)$

(Here ϕ = internal angle of friction of the soil).

For cohesive soils the pressure diagram is as shown in Figure 4.11.4.

Based on the above formulation it is obvious that none of the formulation can be applied directly because of the heterogeneous property of the soil.

Since we cannot apply formulations based on conventional closed form expressions the obvious choice would to seek an approximate solution based on FEM.

Here we will discuss Example 4.11.2 in detail since a similar problem like Example 4.11.1 has already been solved in Chapter 2 (Vol. 1) dealing with FEM.

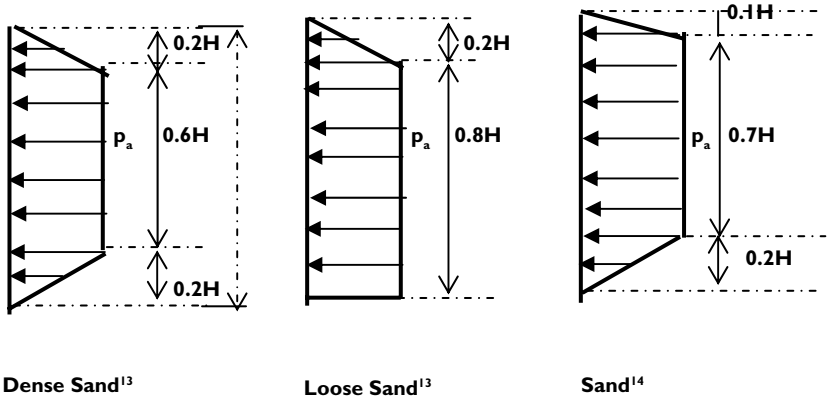


Figure 4.11.3 Pressure diagram on sheet piles for cohesionless soil.

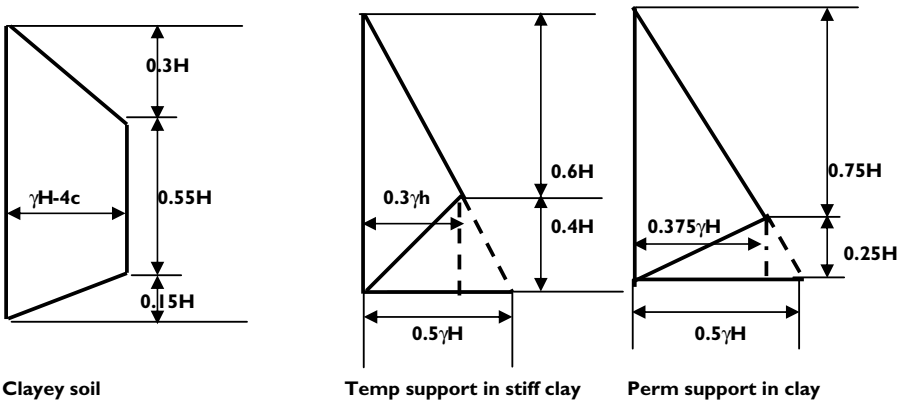


Figure 4.11.4 Pressure diagram on sheet piles for cohesive soil.

Before we go into the detail of selection of the various elements it would possibly be worth to recapitulate the state of equilibrium of an elastic medium in 2D.

4.12 PLANE STRESS AND PLANE STRAIN CONDITION

The equilibrium of a body under the application of external loads has been categorized based on theory of elasticity (Timoshenko and Goodier1970), into two states;

- *Plane stress condition*
- *Plane strain condition*

4.12.1 Plane stress condition

As shown in Figure 4.12.1 is a thin plate loaded by an UDL in the XY plain only. As the plate is very thin the variation of stress in Z-direction (i.e. perpendicular to the plane of the paper) is ignored. Based on the above we have, $\sigma_z = 0$; $\tau_{xz} = 0$; $\tau_{yz} = 0$; the stress in the body is completely defined by σ_x, σ_y, τ_{xy}. The relation between the stress and strain is defined by the following matrix

$$\{\sigma\} = [D]\{\varepsilon\} \tag{4.12.1}$$

where, $\{\sigma\}$ = the stress vector; $[D]$ = the material or elasticity matrix; $\{\varepsilon\}$ = strain vector.

In matrix form the constitutive relation for plane stress case becomes

$$\begin{Bmatrix} \sigma_x \\ \sigma_y \\ \tau_{xy} \end{Bmatrix} = \frac{E}{1-\upsilon^2} \begin{bmatrix} 1 & \upsilon & 0 \\ \upsilon & 1 & 0 \\ 0 & 0 & \frac{1-\upsilon}{2} \end{bmatrix} \begin{Bmatrix} \varepsilon_x \\ \varepsilon_y \\ \gamma_{xy} \end{Bmatrix} \tag{4.12.2}$$

Here, E = Young's modulus of the material; υ = Poisson's ratio of the material.

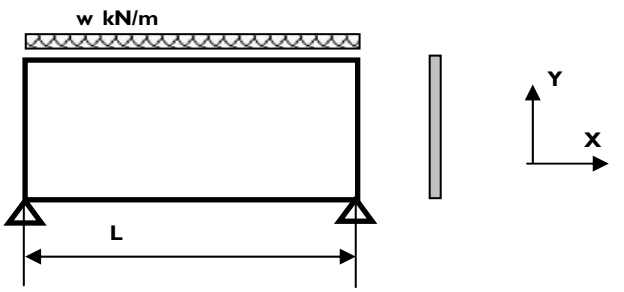


Figure 4.12.1 A thin plate subjected to load in x-y plane.

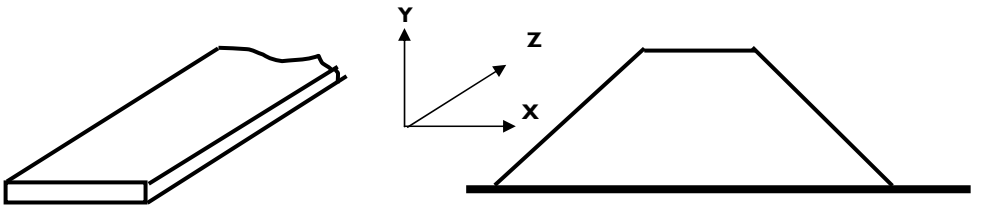


Figure 4.12.2 Plane strain situations.

4.12.2 Plane strain condition

In contrast to plane stress problem there are case in the other extreme where the length of the system is large in the Z direction like a continuous strip footing, embankments dams etc. as shown in Figure 4.12.2.

In this case as the Z-direction is large it is assumed that the displacement component of the body in Z direction is zero at every cross section and the strain component ε_{zz}, γ_{yz} and γ_{zx} will vanish and the remaining non zero components will be given by:

$$\varepsilon_x = \frac{\partial u}{\partial x}; \quad \varepsilon_y = \frac{\partial v}{\partial y}; \quad \gamma_{xy} = \frac{\partial u}{\partial y} + \frac{\partial v}{\partial x} \tag{4.12.3}$$

The constitutive law for plane strain element is as given hereafter:

$$\begin{Bmatrix} \sigma_x \\ \sigma_y \\ \tau_{xy} \end{Bmatrix} = \begin{bmatrix} 1-\nu & \nu & 0 \\ \nu & 1-\nu & 0 \\ 0 & 0 & \frac{1-2\nu}{2} \end{bmatrix} \begin{Bmatrix} \varepsilon_x \\ \varepsilon_y \\ \gamma_{xy} \end{Bmatrix} \tag{4.12.4}$$

The thickness considered in the Z-direction in this case is always the unit length.

4.13 FEM MODEL FOR THE VERTICAL CUT PROBLEM

Based on the above logic it is evident that the in sheet pile problem the soil can be modeled as a 2D plain strain problem for the cut soil tends to large distance in Z direction. The element to be chosen from the FEM library of the software in use should have a bilinear polynomial function[6] or an incompatible element subjected to Taylor's correction.

The total model including the point to which its boundary should extend is shown hereafter.

As shown in Figure 4.13.1, the different elements of the whole system is broken up into various structural elements like

6 Refer Chapter 2 (Vol. 1) to find why bilinear polynomial function should be used for this elements.

- Truss element (for the struts)
- Beam elements (one meter width in Z direction) for the sheet pile
- The soil as plain strain element.

One of the major advantage here is that due to layering of the soil no approximation is required and all one has to do is define three material card sets and define the plain strain element accordingly while furnishing the input to the software.

It is evident that the extent to which the boundary shall extend in both X and Y direction should be significant enough as not to have any distortion effect on the problem in hand. The depth beyond the cut to which one should usually go is 1.5 to $2B$ in direction, where B is the width of the cut.

This is surely one disadvantage with FEM in infinite domain problems especially under time dependent force.

In order to cater for the infinite boundary condition on has to go substantial distance from the point of interest to ensure no spurious deflections effect the system.

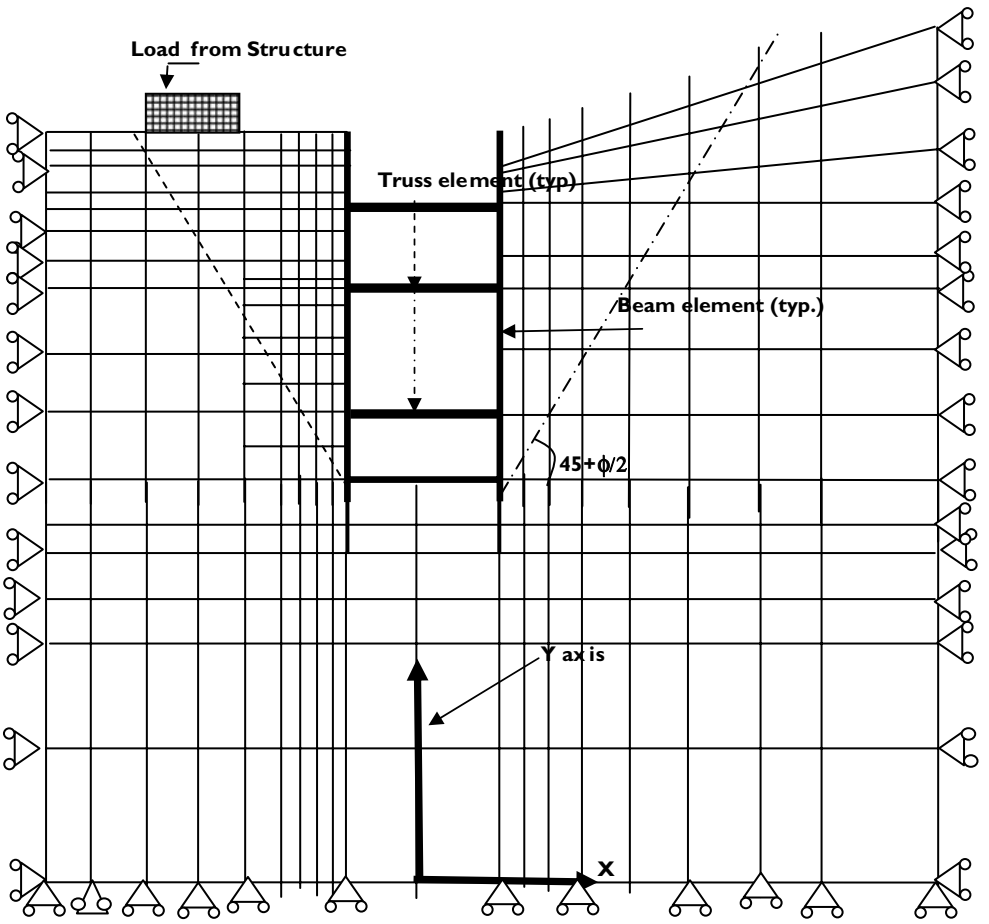


Figure 4.13.1 Finite element model of sheet pile with vertical cut.

This obviously makes the problem big, time consuming and at times expensive in terms of man-hours spent in preparation of data input, debugging the input, review of the model and output interpretation.

At the boundary of the model at every node we provide supports on roller. This helps the soil medium to deform on its own without any distortion and simulate the correct field condition.

4.14 INFINITE FINITE ELEMENT A LOGICAL PARADOX...

On reading the definition itself the reader might say "OOPS". For, surely the terminology looks like a riddle. But in the Swansean world of finite element analysts, the element appears perfectly sane and at times worshipped as the Virgin Mary itself.

Any FEM package supporting this element saves a lot of time energy of the user and makes his life much simpler.

Based on such raving review given above, the reader might by this time be a bit curios to know as to

- What constitutes this paradox?
- How does it make life easy for us?

We had discussed above that one of the major disadvantage in FEM of solving infinite domain problem is that to ensure proper field condition, we usually take the boundary at a large distance from the point of interest and in the process makes the problem in hand big, thus laborious and at times expensive.

Let us for instance take the case of Boussinesq's equation of point load Q on an elastic medium where the vertical stress is given by:

$$\sigma_z = \left[\frac{3Q}{2\pi z^2}\right] \frac{1}{\left(1+\left(\frac{r}{z}\right)^2\right)^{5/2}} \tag{4.14.1}$$

It is quite evident that as $z \to \infty$ $\sigma_z \to 0$.

Thus if we are doing a FEM analysis of this problem by intuition we can say that limit of σ_z will approach the value zero when the distance will be *very large*[7].

To cater to this we have seen earlier how the problem tends to become voluminous in terms of input data.

Suppose now we find an element which can be attached to the finite element at a *finite_depth* and whose mathematical formulation can define the condition that ε_z and σ_z tends to zero as z tends to infinity. We surely can drastically reduce the magnitude of the problem.

7 Of course the question remains as to what is the definition of this very large distance?

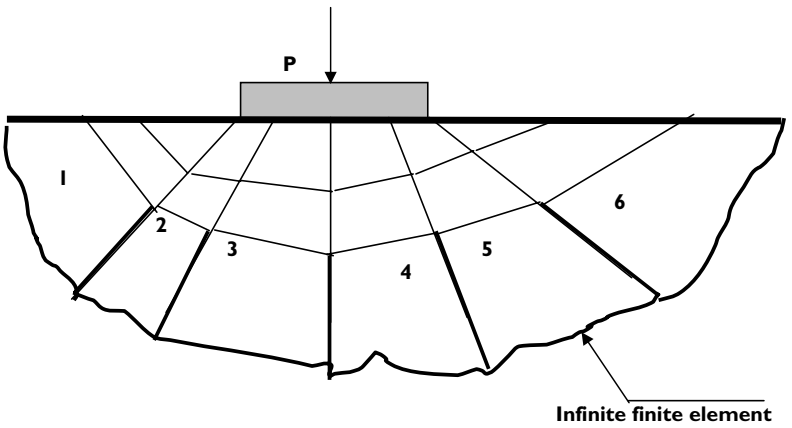


Figure 4.14.1 Soil foundation modeled with infinite finite element.

The above is explained by an example as shown in Figure 4.14.1. We try to model a foundation subjected to a point load P. Now for the first two rows, we apply standard finite elements and for the third row we provide an element whose mathematical formulation defines condition of stress and displacement approaches the value zero at infinity we get a model as shown above. By providing these special elements we have surely bypassed the problem of extending the boundary to a large distance.

This is no more required for the intrinsic mathematical property of the infinite finite element satisfies the boundary condition implicitly.

Elements 1 to 6 as shown above are element of this kind and are called infinite finite element (Bettes 1977, Beer and Meek 1981).

4.15 BASIS OF FORMULATION OF THE INFINITE ELEMENT

The mathematical logic behind the element stiffness generation is simple and intuitive. We know that the basis of generation of stiffness matrix based on virtual work for any element is based on selecting a suitable polynomial function for the displacement function which is complete and continuous.

We now describe an element whose *nodal* displacement term, u is defined by a polynomial

$$u = \frac{\alpha_1}{x} + \frac{\alpha_2}{x^2} + \frac{\alpha_3}{x^3} + \frac{\alpha_4}{x^4} + \cdots\cdots\cdots\cdots \tag{4.15.1}$$

where, $u =$ displacement at a particular node; $\alpha_1, \alpha_2, \alpha_3, \alpha_4 \ldots\ldots =$ constants; $x =$ polynomial of nth degree, defining the displacement u.

4.15.1 What does it really mean?

This means that the polynomial function is decaying exponentially and approaches zero when x tends to infinity.

We will see here how the above concept is adapted in generating the element stiffness. The concept though above looks simple but while implementation of the same based on polynomial function as mentioned above generates two basic problems:

- At what order of x we truncate the polynomial?
- What would be the error induced due to this truncation?

It is quite obvious that theoretically, $x \to \infty$, but while defining the polynomial, we have to cut off at some finite value which could be quite high say $1/x^{100}$.

But x^{100} though could be a high value it is surely *not infinity* and would surely induce some truncation error.

Secondly using a polynomial of such high order would increase the computational effort significantly.

To by-pass the above difficulties polynomial function is generated based on mapping system as shown below.

The mapping is first generated in term of one co-ordinate and is then extended to two-dimension.

Let us consider a line (Figure 4.15.1), with points C, P, Q and R where R *is an imaginary point at infinity.*

In Cartesian co-ordinate system the co-ordinates of each of the point are as mentioned hereafter:

$$C = (x_c, 0); \quad P = (x_p, 0)$$

where, $x_p = (x_q + x_c)/2$; $Q = (x_q, 0)$ and $R = (\infty, 0)$.

Suppose we impose an arbitrary co-ordinate system $\xi - \eta$ such that the co-ordinate of point P, Q and R becomes

$$P = (-1, 0); \quad Q = (0, 0); \quad R = (1, 0)$$

Then any point x on the line C, P, Q, R can be expressed as in term of ξ as

$$x = -\frac{\xi}{1-\xi} x_c + \left(1 + \frac{\xi}{1-\xi}\right) x_q \tag{4.15.2}$$

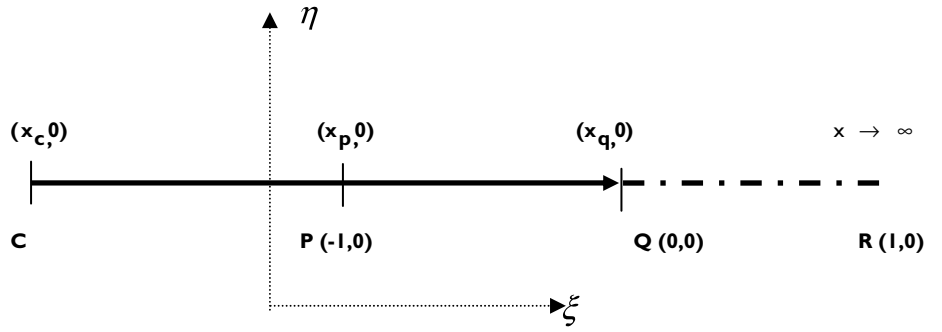


Figure 4.15.1 Mapping co-ordinate in one dimension.

Thus we find that for $\xi = 0$ we have, $x = x_q$
For $\xi = -1$ we have, $x = (x_q + x_c)/2$
For $\xi = 1$ we have $x = \infty$.

The point C is here very *significant for it is the origin of disturbance or the point from which the stress propagates.*

Now suppose we designate r as the radius vector from point C then

$$r = x - x_c \tag{4.15.3}$$

Now based on the expression of x in terms ξ as mentioned above, on solving for ξ we have

$$\xi = 1 - \frac{x_q - x_c}{x - xc} \Rightarrow \xi = 1 - \frac{x_q - x_c}{r} \tag{4.15.4}$$

Now suppose we define the displacement function in terms ξ as:

$$u = \alpha_0 + \alpha_1 \xi + \alpha_2 \xi^2 + \alpha_3 \xi^3 + \cdots\cdots\cdots\cdots \tag{4.15.5}$$

on replacing ξ in term of x_q, x_c and r we find that the shape function takes the form of exponential decay with $u \to 0$ as $r \to \infty$.

Based on the expressions deduced above one basic question still remains unanswered?

4.15.2 Why did we transform the co-ordinate and what did we gain out of it?

The answer to this is that based on the virtual work principle the stiffness matrix of any finite element is given by[8]

$$[K] = \int_A [B]^T [D] [B] \, dA \tag{4.15.6}$$

where $[B] = f(u)$

Now for the above line element it is obvious that integral becomes *indefinite* for the limits in X-Y co-ordinate are

$$[K] = \int_{x=xc}^{x=\infty} [B]^T [D] [B] \, dA \tag{4.15.7}$$

Now as the integration has to be done numerically it is not possible to integrate between ∞ and x_c. When the reference co-ordinate is changed the above expression gets converted to

8 Refer Chapter 2 (Vol. 1) for derivation of the expression.

$$[K] = \int_{\xi=-1}^{\xi=1} [B]^T [D] [B] \, dA \tag{4.15.8}$$

This is a definite integral between the boundary -1 and 1 and numerical integration of the function between the specified boundary is possible.

For two dimensional element we can introduce another function η where

$$\eta = 1 - \frac{yq - yc}{y - yc} \quad \text{with its boundary values lying between 1 and } -1. \tag{4.15.9}$$

Now based on the problem in hand we can select the functions

$$\begin{aligned} u &= \alpha_0 + \alpha_1 \xi + \alpha_2 \eta \\ v &= \alpha_4 + \alpha_5 \xi + \alpha_6 \eta \end{aligned} \tag{4.15.10}$$

and derive the stiffness matrix based on the expression

$$[K] = \int_{\xi=-1}^{\xi=1} \int_{\eta=-1}^{\eta=1} [B]^T [D] [B] \, d\xi \, d\eta \tag{4.15.11}$$

This element (if available in the finite element library of the software in hand) is one of the most powerful tool in reducing the problem size of an infinite domain problem. Since element satisfies the boundary condition at infinity it is called the infinite finite element.

4.16 MATERIAL PROPERTY AFFECTING THE MODEL

As we had seen earlier that Winkler springs values are dependant on the sub-grade modulus property of the soil, similarly for Finite element the material property which on which it is dependent are:

E = Modulus of Elasticity of the material; ν = Poisson's Ratio.
For concrete this value is usually taken as (IS-456), $E_{\text{conc}} = 5700\sqrt{fck}$ N/mm^2; $\nu = 0.3$.

Because concrete is generally man made and manufactured under controlled condition there is not much variation in the quality, and in majority of the cases the value of E_{conc} will be near around the value as mentioned above.

Moreover laboratory techniques for evaluation of Modulus of elasticity of concrete are sufficiently advanced to evaluate its value (Neville 1981), accurately.

When it comes to soil the problem becomes complicated because:

- For cohesion less soil collecting undisturbed sample form the field is very difficult (if not impossible)

Table 4.16.1 Equation of E_s by several test methods. [after Bowles (1988)]

Sl. No.	*Soil*	*SPT*	*CPT*
1	Sand (Normally Consolidated)	$E_s = 500(N + 15)$ $E_s = (15000 \text{ to } 22000) \log_e N$	$E_s = 2$ to 4 qc
2	Sand (Saturated)	$E_s = 250(N + 15)$	
3	Sand (over-consolidated)	$E_s = 18000 + 750N$	$E_s = 6$ to 30 qc
4	Gravelly sand and gravel	$E_s = 1200(N + 6)$	
4.1		$E_s = 600(N + 6)$ for $N \leq 15$	
4.2		$E_s = 600(N + 6) + 2000$ for $N \geq 15$	
5	Clayey sand	$E_s = 320(N + 15)$	$E_s = 3$ to 6 qc
6	Silty sand	$E_s = 300(N + 6)$	$E_s = 1$ to 2 qc
7	Soft clay		$E_s = 3$ to 8 qc

Here value of E_s is in kPa, N = No. of blows in a SPT test.

- For cohesive soil though samples can be collected in sampler, due to the thixotropic changes during collection of samples the sample undergoes re-distribution in its shear strength and as such laboratory results of modulus of soil may vary greatly with the actual field condition.

It is for this it is preferable that Elasticity modulus of soil (E_s) be measured in-situ.

Menard pressure meter test (Murthy 1991) is one such test where it is possible to measure the in-situ modulus of soil in the field. One of the disadvantages of this test is that the probing rod placed inside a vertical hole gives the modulus in lateral direction. If the soil is not isotropic in nature the value in the vertical direction will not be the same as in the lateral direction.

Because of the difficulty in obtaining the value of E_s in laboratory and also due to the limitation in application of pressure meter test, Modulus of elasticity is usually obtained from co-relation to various field tests carried out in the field like Standard Penetration Test (SPT) for sand and Cone penetration Test (CPT). The relation between E_s and various test methods for various kinds of soils are given in Table 4.16.1.

4.17 RELATION BETWEEN SUB-GRADE MODULUS AND MODULUS OF ELASTICITY

It is also possible to obtain the modulus of elasticity from the sub-grade modulus value. The relationship is given by (Vesic 1961)

$$k's = 0.65 \sqrt[12]{\frac{E_s B^4}{E_f I f}} \frac{E_s}{1 - \upsilon^2} \tag{4.17.1}$$

where $k_s = k_s'/B, E_s, E_f$ = modulus of soil and footing in consistent units; B, I_f = footing width and moment of inertia based on cross section in consistent units.

Since the twelfth root of any value multiplied by 0.65 is very near to 1, for all practical purposes, the equation can be modified to

$$ks = \frac{Es}{B(1 - \nu^2)} \tag{4.17.2}$$

4.18 SELECTION OF POISSON'S RATIO

The Poisson's ratio for soil usually varies between 0.3 and 0.5.

Considering $\nu = 0.4$ *shall serve the purpose for most of the practical problems.*

4.19 LIMITATION AND ADVANTAGES OF FINITE ELEMENT METHOD IN STATIC SOIL STRUCTURE INTERACTION PROBLEM

Biggest advantage of the finite element method is its versatility to cater to varying boundary condition.

- Soil is a heterogeneous medium any closed form solution is at best an approximation. We had shown in our example of vertical cut as to how FEM can overcome this problem.
- Though out of scope in this treatise it is possible to solve non-structural problems like consolidation, seepage heat mass transfer etc., based on variational formulation of the differential equation and seek a solution based on appropriate boundary condition.
- Material non-linearity, plastic flow and crack propagation problems are now routinely solved by FEM.

But this is not without its pitfall. For the major danger lies in the present trend of using a FEM software as a *black box* with many a times the end result tantamounting to "*Garbage in and Garbage Out*".

FEM is surely a powerful tool for analysis but when gets into the hand of an inexperienced user or a user with inadequate theoretical knowledge it is as good as performing a *Hara-Kiri*[9].

Leaving aside the philosophical aspect of the disadvantage FEM, one of the major debate which is still on as far as Geo-technical Engineering is concerned, is that one of the major constituent of the FEM analysis is the **material matrix** (Made up of E_s and ν).

As there exists a major problem in correct estimation of these values...

9 If the reader is unaware of the terminology "Hara-Kiri" he is advised to see Bruce Lee's movie 'Enter the Dragon'.

- What is the sanctity of using such a sophisticated analysis?
- How accurate will be results where basic parameter could quite be suggestive?

Based on this we still find many engineers[10] quite skeptical about the usage of FEM specially to problems related to Foundation Engineering.

It is not without any semblance of truth. It is for this at times it is worth running a problem for a certain range of data pertaining to a certain kind of soil and use our judgement to arrive at the best design figure. Finally the importance of field observations *like load testing should not be undermined.*

The analyst is sitting in the design office far away from the site and selecting his parameters based on his judgment and from the soil report on his desk (*which could also be erroneous due to wrong field reading or faulty instrumentation too*).

Based on the load testing of a similar foundation at site if the results vary then what his theoretical predictions say, he should re-modify his parameters to suite the field reading and re-analyze. He may be spending some more hours in his engineering design[11] but at the end may end up with saving a lot of money in terms of *damage management and repair of faulty foundation and structures.*

For just to remind the readers we end with Terzaghi's[12] famous quotation.

> "*Foundation can appropriately be described as a necessary evil. If a building is to be constructed on an outcrop of sound rock, no foundation is required. Hence in contrast to the building itself which satisfies specific needs, appeals to the aesthetic sense, and fills its matters with pride, the foundation merely serve as a remedy for the deficiencies of whatever nature has provided for the support of the structure at the site which has been selected.*
>
> *On account of the fact that there is no glory attached to the foundations and that the sources of success or failures are hidden deep in the ground, building foundations have always been treated as step children and their acts of revenge for the lack of attention can be very embarrassing*".

10 Specially the Geo-technical specialists of orthodox school, who think FEM is a rude intrusion by the structural engineers in their domain of semi-empirical approach.

11 And might get a bit of kick in his butt from his boss for over-running the man-hours.

12 The Influence of Modern Soil Studies on Design and Construction of Foundations – Dr. Karl Terzaghi International Conference of Soil Mechanics & Foundation Engineering ,Opening Lecture 1951.

Chapter 5

Concepts in structural and soil dynamics

5.1 INTRODUCTION

This section focuses on different theories of Structural Dynamics. Here we have emphasized on the *modal response technique* and *step-by-step integration* that forms the backbone of analysis of most of the structures.

Advance techniques like random vibration, non-linear dynamics and probabilistic analysis have not been dealt here. For study of this more advanced topic you may go through the reference list furnished at the end of the chapter. While introducing this chapter we have tried to focus on the fundamental concepts and designed the numerical problems accordingly. We have deliberately restricted to matrices of the second and third order in most of the cases, so that one may follow the essence using a simple calculator.

5.2 A BRIEF HISTORY OF DYNAMIC ANALYSIS OF STRUCTURE AND FOUNDATION IN CIVIL ENGINEERING

Though civil engineering as a profession itself has been in existence from the early dawn of civilization, yet even fifty years ago civil engineers did not use dynamic analysis as an essential tool as a part of their daily work.

Most of the analyses were done based on equivalent static methods. Any dynamic effect due to movements of cranes or operation of machines were catered to in the static analysis by considering an impact factor, or an arbitrary magnification factor. Unlike aircraft or shipping industry where engineers were extensively using various analytical tools for dynamic response of structure in flight or in motion on sea, the civil engineers were quite content with there approach of designing there buildings and structures based on their method (which can be stated in today's terminology) *of a crude form of pseudo-static analysis.*

Then *four* things happened almost simultaneously after the Second World War ...

- *A big boom in high rise building in USA.*
- *A big demand in energy sector specially power plants in war ravaged Europe and USA, (both thermal and nuclear) generating requirements of supporting heavy and high speed machines.*

- *Tehachapi Earthquake in California USA in 1952.*
- *IBM coming up with business machines capable of doing automatic calculations.*

The damages occurred during the 1952 earthquake brought civil engineers out of their slumber and it was realized that the traditional tools used for designing the structure that were the order of the day were inadequate.

Tehachapi earthquake clearly demonstrated the seismic vulnerability of a number of traditional structures.

The potential of a severe earthquake hitting a major populated area and the catastrophe it can create looming large over their head, the civil engineers had no other option but to take stock of the analytical tools they had in their hand and went back to the hallowed domain of academics to understand and harness *the most complex and the fearful force that the nature has ever created.*

An intensive research work started in a number of American Universities namely, the University of California at Berkley, California Institute of Technology, and Massachusetts Institute of Technology under the leadership of the likes of R S Bisplinghoff, Ray W Clough, Edward L Wilson and S H Crandall and a number of interesting results came out from their research.

Dynamic analysis was then restricted to finding out the frequencies and mode shapes of the first few modes based on manual calculations. Engineers in design offices still abhorred dynamic analysis for the laborious and intense calculation it demanded.

It was in the late fifties that an engineer by the name of Gabriel Kron who was working with the IBM developed a logic based on his indigenous method of diakoptics[1] and showed how matrix operations can be manipulated through computers[2]. Engineers working in area of dynamic analysis quickly realized the potential and the development of software for analysis of structures with a large number of degrees of freedom soon became a reality.

In the meantime engineers working in the energy sector were going through a tough time. With more and more demand for power, manufacturers were churning out more and more heavy machines with progressively increasing operating speed. It was observed that in many cases the rule of thumb in vogue to provide a support or foundation having weight 2 to 2.5 times weight of the machine were not working all the time. In many cases the machines malfunctioned due to excessive vibration, the foundations cracked and there were repeated breakdowns resulting in poor output and productivity.

During this time Gregory P Tschebotarioff migrated to USA from erstwhile USSR. He published some papers prepared by one of his Russian colleague, Dominic D Barkan where it was shown in a systematic way that the problem of foundations supporting the rotating machines could be solved. Tschebotarioff on his own initiative translated all the works in English from Russian and got it published in the form of a book (Barkan 1962). **Soil dynamics saw its first light on birth.**

1 It means the method of cutting.
2 It was an era when a 17 by 17 matrix inversion roughly took about 17 hours.

In the meantime civil engineers were building the high-rise building considering their foundations as rigid with the earthquakes inducing a base motion to it. The tall buildings, which are identified as potential earthquake hazard, were slender, flexible and were mostly resting on firm ground. The fixed based assumptions the engineers made for these tall buildings were valid for most of the cases.

The analytical techniques for the calculating the dynamic response of such tall structures was quite developed by that time. They were mostly programmed into the computers based on matrix analysis of structure and were found to be quite efficient in predicting the static and dynamic response of tall buildings.

The civil engineers leaned back in their chairs with a satisfied grin on their faces. *'He has come a long way from his days of paper, pencil, eraser and a slide rule'*. **Dynamic analysis thus reached it teens.**

But history has a peculiar way of changing the course and destiny of human civilization. It forced upon human beings two issues, which catapulted the whole technology into a new era.

The issues were...

- *The advent of Nuclear power plants*
- *Two earthquakes one in Mexico and the other in Turkey*

With the fast depletion of conventional energy sources like coal and the environmental hazard it created, many developed countries like USA, France, Germany and others resorted to Nuclear Power Plants as an alternate source of energy.

The dynamic analysis techniques that were developed as mentioned above when applied to the structures related to Nuclear Power Plant (N.P.P.) were found to be insufficient.

For from functional and other safety requirements, most of the structures pertaining to N.P.P. were massive and rigid in nature. It was realized that considering them as lightweight and flexible structures were not valid. Moreover from the point of view of economy and technical feasibility of the project many of them were to be built on soft soil. It became clearly apparent that the response of such massive and stiff structures resting on soft soil would induce significant dynamic deformation of the foundation system. This in turn will alter the dynamic response of the structure.

The two earthquakes (in Mexico and Turkey) as mentioned above, resulted in extensive damage to the buildings though most of them were designed for earthquake considering them as fixed base flexible structures.

Study revealed that the underlying soil condition played a major hand in their damage resulting in amplification of the earthquake response.

Realization of these facts has brought a new era in the dynamic analysis of structures pertaining to Civil Engineering termed **Dynamic Soil-Structure Interaction,** *where conventional techniques applied in structure and soil dynamics are coupled together to understand the overall response of the system (by the word system we mean here to constitute both the structure and the supporting soil medium). Dynamic soil structure interaction is by far the most complex analysis in the annals of civil engineering and research is still on to understand the phenomenon properly and minimize the uncertainties, which dogs it.*

5.2.1 Basic concepts

In Chapter 3 (Vol. 1) while introducing you to the theory of mechanical vibration we stated that vibration/dynamics as a topic got inducted in civil engineering quite late (sometimes around 1950). In the pre-computer era when engineers were restricted to hand computations or mechanical computers (at best), the objective was- trying to find out the first few modes or at least the fundamental mode of vibration of a system.

For this, many structures were mathematically modeled as a system with single degree of freedom to determine their dynamical characteristics. In this process engineers initially depended heavily on the spring lumped mass model as cited earlier in Chapter 3 (Vol. 1). To give you some further idea let us consider the portal frame as shown in Figure 5.2.1(a) and we are interested in determining the fundamental time period in the horizontal and vertical directions. For a quick calculation, considering single degree of freedom, we first need to establish the mass (m) and equivalent spring (k) for the system[3].

In the vertical direction for each column the spring stiffness can be stated to be EA/L. Here E = Young's modulus of the column material, A = cross sectional area and L its length[4]. Considering two columns of the frame and these being in parallel the net spring stiffness is $2EA/L$. Considering self weight of column and beam and whatever is the superimposed load, we can arrive at the effective lumped mass, m. Thus in effect, the real structure as shown in Figure 5.2.1(a) has now been idealized as an equivalent spring and mass as shown in Figure 5.2.1(b).

Similarly for lateral direction it can be shown that equivalent spring for the system is $24EI/L^3$. Here I = Moment of inertia of the column and again the system can be idealized as a spring mass system as shown in Figure 5.2.1(b).

Though apparently this may look to be a crude procedure, yet is a very effective and realistic tool even today as the first step to asses the dynamic behavior of a body under vibrating force and thus it becomes an important topic of study.

5.2.1.1 Vibration of systems having single degree of freedom

A structure having single degree of freedom under vibration can be mathematically modeled as a lumped mass connected to a spring where the spring data is obtained from the elastic property of the system is as shown in Figure 5.2.1(b). The mathematical derivation being same as that developed in Chapter 3 (Vol. 1) we will not derive them in detail herein but for quick recapitulation would only present the basic essence[5].

3 Since time period is given by the expression $T = 2\pi\sqrt{m/k}$.

4 Refer Table 5.1.1 where equivalent spring stiffness for beams with various boundary conditions are furnished.

5 For those who have skipped Chapter 3 (Vol. 1), would find it beneficial to go through the analysis of single degree of freedom as elaborated there.

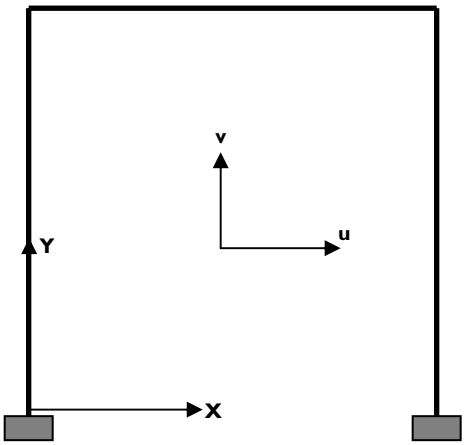


Figure 5.2.1a Single storey portal frame with two translational degrees of freedom per node.

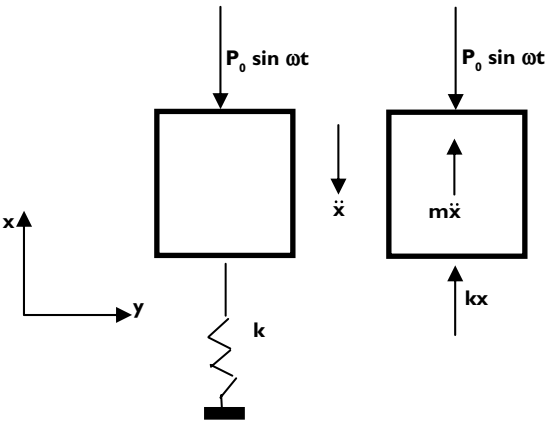


Figure 5.2.1b Mathematical model and the free body diagram.

5.2.1.2 Calculation of natural frequency

For the applied load the free body diagram is as shown and applying D'Alembert's principle we have the equation of equilibrium as

$$m\ddot{x} + kx = P_0 \sin \omega_m t \tag{5.2.1}$$

Considering $\omega_n^2 = k/m$ for the homogenous equation, we have

$$\ddot{x} + \omega_n^2 x = 0; \quad \rightarrow x = A \sin \omega_n t + B \cos \omega_n t \tag{5.2.2}$$

Where, $\omega_n =$ the natural frequency of the structure.

Differentiating Equation (5.2.2) twice with respect to time, we have

$$\ddot{x} = -A\omega_n^2 \sin \omega_n t - B\omega_n^2 \cos \omega_n t$$

For $t = 0$, $x = 0$ which implies $B = 0$; again for $t = 0$ $\ddot{x} = 0$ which implies $\sin \omega_n T = 0$ and

$$T = 2\pi/\omega_n \quad \text{and} \quad T = 2\pi\sqrt{m/k} \tag{5.2.3}$$

where T is the time period of the body defined as the time taken for the body to complete one cycle of vibration.

5.2.1.3 Calculation of amplitude

Let $x = \bar{x} \sin(\omega_m t + \alpha)$ be the assumed displacement function where α is the phase difference with the exciting force $P_0 \sin \omega_m t$. Then $\ddot{x} = -\bar{x}\omega_m^2 \sin(\omega_m t + \alpha)$ and substituting the value in Equation (5.2.1), we have

$$\bar{x} \sin(\omega_m t + \alpha) = P_0 \sin(\omega_m t)/(k - m\omega_m^2)$$

For maximum value of x, taking $\sin(\omega_m t + \alpha) = 1$ and $\sin(\omega_m t) = 1$, and we have

$$\bar{x} = P_0/(k - m\omega_m^2) \tag{5.2.4}$$

Now since $\omega_n^2 = k/m$, and using, $r = \omega_m/\omega_n$, we have

$$\bar{x} = \frac{P_0/k}{(1 - r^2)}, \tag{5.2.5}$$

It may be noted that when $\omega_m = \omega_n$, $r = 1$ *which gives the value of* $\bar{x}$ *infinity.*

This means that when the natural frequency of the system has the same frequency of the exciting force, for an un-damped system the displacement is infinite.

This is known as the *resonant condition* of the system and is a very important factor for further study.

The system shown above is known as an *un-damped system*. By this, what happens is that a system once starts vibrating will continue to be in motion, *indefinitely*[6].

For instance a simple pendulum once starts moving to and fro from its mean position will continue to do so and will never stop.

But things do not happen so in nature, "like all good things comes to an end", a motion once starts also stops after a certain period of time.

6 This is called perpetual motion.

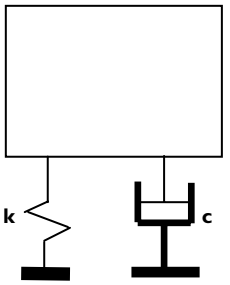


Figure 5.2.2 Mathematical model of single degree damped system.

5.2.1.4 Why does it happen so?

This happens because nature has built in our system a retarding property, which implicitly acts against motion from the very advent of the motion and brings it to a stop. *This is known as the damping of a system.*

Damping is indeed a difficult concept. While the physicist are still in quest to understand the mechanics behind the concept as to how exactly it works and quantify its value, the Mathematicians and Numerical Analysts despise it for it makes a mess of a lot of their elegant looking equations and complicates the issue[7].

There are different kinds of damping like material damping, radiation damping, hysteretic damping etc.

We will see this in more detail later and for the time being let us assume that it is mathematically represented by a dash-pot where the force induced is expressed as $F_c = c\dot{x}$.

The system is mathematically shown in Figure 5.2.2.

The differential equation of motion is given by

$$m\ddot{x} + c\dot{x} + kx = P_0 \sin(\omega_m t) \tag{5.2.6}$$

For the homogeneous equation, the solution is usually taken as $x = e^{st}$ and substituting this value in Equation (5.2.6), we have $(ms^2 + cs + k)e^{st} = 0$, which is satisfied for all values of, t, when

$$s^2 + cs/m + k/m = 0$$

On solution of the above quadratic equation, we have,

$$s_{1,2} = -c/2m \pm \sqrt{[(c/2m)^2 - k/m]}.$$

7 But that is how mother nature is built . . . . And one has to learn to live and solve the riddles she possesses.

Hence the general solution is given by

$$x = Ae^{s_1 t} + b\,e^{s_2 t} \tag{5.2.7}$$

where A and B are constants to be evaluated from the initial conditions $x(0)$ and $\dot{x}(0)$.

On substitution of the value of s_1 and s_2 we have

$$x = e^{-(c/2m)t}[Ae^{\sqrt{\{(c/2m)^2 - k/m\}}t} + Be^{-\sqrt{\{(c/2m)^2 - k/m\}}t}] \tag{5.2.8}$$

The first term $e^{-(c/2m)t}$ is simply an *exponentially decaying function of time*. The behavior within the parenthesis however will depend upon numerical value within the radical i.e. if it is negative, zero or positive.

Case-1 $\sqrt{[(c/2m)^2 - k/m]} \geq 0 : (\mathrm{c/2m})^2 > k/m$, the exponent in the above equation is a real number and no oscillation is possible. *This case is termed as over damped system.*

Case-2 $\sqrt{[(c/2m)^2 - k/m]} = 0 : (\mathrm{c/2m})^2 = k/m$, this is known as *critically damped case*.

In this case the damping is represented by $c = c_c$ as such $(c_c/2m)^2 = k/m = \omega_n^2$ which, on simplification gives $c_c = 2\sqrt{km} = 2m\omega_n$. It is convenient to express the value of any damping in terms of the critical damping as a ratio $D = c/c_c$ and is known as the *critical damping ratio*.

Case-3 when $\sqrt{[(c/2m)^2 - k/m]} \leq 0 : (\mathrm{c/2m})^2 < k/m$ the case is known as *under damped case*. The factor $c/2m$ in terms of D can be written as, $c/2m = D\omega_n$.

Then the general solution becomes

$$x = e^{-D\omega_n t}(Ae^{i\omega dt} + Be^{-i\omega dt}) \tag{5.2.9}$$

where $\omega_d = \omega_n\sqrt{1 - D^2}$ is known as *the damped natural frequency*.

Now using the identity $e^{i\theta} = \cos\theta + i\sin\theta$, $e^{-i\theta} = \cos\theta - i\sin\theta$ and applying these expressions in Equation (5.2.9), we have

$$x = e^{-D\omega_n t}[(A + B)\cos\omega_d t + i(A - B)\sin\omega_d t]$$

$$\rightarrow \quad x = e^{-D\omega_n t}[C_1\cos\omega_d t + C_2\sin\omega_d t] \tag{5.2.10}$$

where C_1 and C_2 are arbitrary constants and the expression above is the solution to the homogenous equation.

5.2.1.5 Solution to the Particular Integral

Let the solution be, $x = \bar{x}\sin(\omega_m t - \varphi)$, then we have

$$\dot{x} = \bar{x}\omega_m \cos(\omega_m t - \phi) \quad \text{and} \quad \ddot{x} = -\bar{x}\omega_m^2 \sin(\omega_m t - \varphi).$$

Substituting the above in Equation (5.2.6), we have,

$$\bar{x}[(k - m\omega_m^2)\sin(\omega_m t - \phi) + c\omega_m \cos(\omega_m t - \varphi)] = P_0 \sin\omega_m t$$

Using $\theta = \omega_m t - \varphi$ and $A = (k - m\omega_m^2)$ and $B = c\omega_m$, the above equation reduces to

$$\bar{x}(A\sin\theta + B\cos\theta) = P_0 \sin\omega_m t$$

$$\rightarrow \quad \bar{x} = \frac{P_0 \sin\omega_m t}{A\sin\theta + B\cos\theta}$$

Again, $\bar{x} = \bar{x}_{\max}$ and $\frac{d\bar{x}}{d\theta} = 0$ give, $\bar{x}_{\max} = [P_0 \sin\omega_m t]/\sqrt{[(k - m\omega_m^2)^2 + c^2\omega_m^2]}$ which on simplification becomes

$$\bar{x}_{\max} = \frac{(P_0/k)\sin\omega_m t}{\sqrt{[(1 - r^2)^2 + (2Dr)^2]}} \tag{5.2.11}$$

where $r = \omega_m/\omega_n$ and $D = c/c_c$; c_c = critical damping of the system and is $2\sqrt{mk}$.

Thus the complete solution is

$$x = e^{-D\omega_n t}(Ae^{i\omega_d t} + Be^{-i\omega_d t}) + \frac{(P_0/k)\sin\omega_m t}{\sqrt{[(1 - r^2)^2 + (2Dr)^2]}}$$

$$\text{where,} \quad \omega_d = \omega_n\sqrt{[1 - D^2]}. \tag{5.2.12}$$

In the above equation the first part is known as the *transient response* and the second part is known as the *steady state response*.

The transient response dies down after initial first few cycles while the steady state response continues and becomes the main factor.

Above is a very important expression and it will be seen that time and again we would be utilizing this expression for both structures and foundations of both single and multi-degree of freedom.

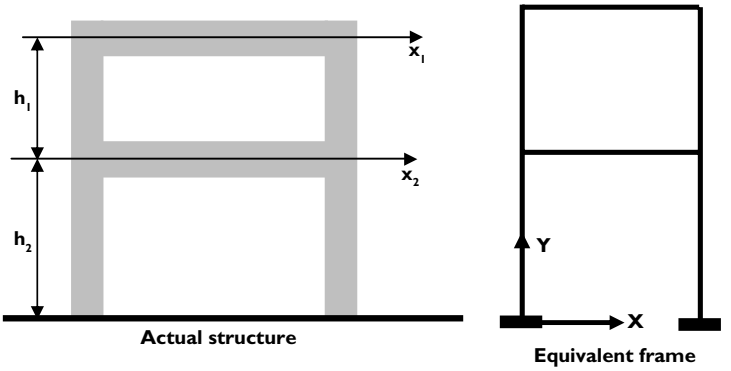


Figure 5.2.3 A two-storied building resting on ground.

5.2.1.6 Vibrations of systems with two/multi-degree of freedom

This is also known as *modal response method* and is one of the most popular methods in design offices for dynamic analysis of structure and foundation.

Two understand the principle of vibration of a structure with n degrees of freedom we start as a pre-requisite to understand the concepts of a structure with two degrees of freedom in matrix form.

As a 2×2 matrix is amenable to hand calculation the underlying concepts are easy to understand. Based on these concepts we will extend the techniques to dynamic analysis of structures and foundations having a large number of degrees of freedom and its computer implementation.

Shown in Figure 5.2.3 is a two storied building with two degrees of freedom in x directions. The slabs connected to transverse beams are assumed to act as deep diaphragm and induces infinite stiffness to beams by virtue of which the flexural mode of the beam is ignored and the frame is assumed to act as a shear frame[8].

The equivalent two storied frame is converted into a stick model as shown in Figure 5.2.4. In the model, the weight in each floor is converted to equivalent mass and is lumped as shown. While the stiffness constitute of summation of the individual stiffness of columns on each floor, we neglect the damping effect for the time being and presume the system to be subjected to an un-damped free vibration.

The free body diagram is as shown in Figure 5.2.5, is based on D'Alembart's equation.

Then taking $\sum F_x = 0$ we have for mass m_2

$$m_2\ddot{x}_2 + k_2(x_2 - x_1) = 0 \tag{5.2.13a}$$

8 In fact this is the basic assumption for dynamic analysis of all multistoried buildings where for calculation of eigen-values shear type of frames are found to be quite sufficient.

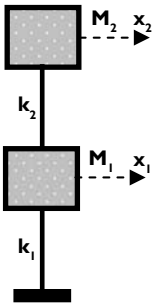


Figure 5.2.4 Stick model.

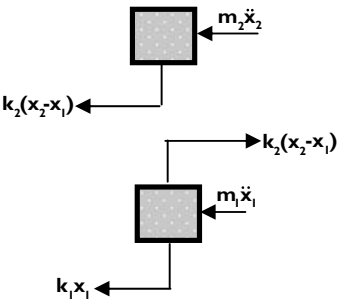


Figure 5.2.5 Free body diagram.

and from the free body diagram of mass m_1 we have

$$m_1\ddot{x}_1 + k_1x_1 - k_2(x_2 - x_1) = 0, \tag{5.2.13b}$$

re-arranging the above two equations in matrix form we have

$$\begin{bmatrix} m_1 & 0 \\ 0 & m_2 \end{bmatrix} \begin{Bmatrix} \ddot{x}_1 \\ \ddot{x}_2 \end{Bmatrix} + \begin{bmatrix} k_1 + k_2 & -k_2 \\ -k_2 & k_2 \end{bmatrix} \begin{Bmatrix} x_1 \\ x_2 \end{Bmatrix} = 0 \tag{5.2.14}$$

The above constitute the equation of free vibration for a two storied building as shown above. In *matrix form* the above is usually represented as

$$[M]\{\ddot{X}\} + [K]\{X\} = 0 \tag{5.2.15}$$

where, $[M]$ = a square matrix of the order 2; $[K]$ = a square matrix of size (2×2) and X = a column matrix of size (2×1).

It should be noted here that

- *The mass matrix is a diagonal matrix having all off diagonal elements as zero.*
- *The stiffness matrix is a 2 × 2 matrix and is symmetric i.e.* $[K]^T = [K]$.

5.2.1.6.1 Determination of the natural frequency

For calculation of natural frequency let us assume

$$\{X\} = x_i \sin(\omega_n t - \alpha) \tag{5.2.16}$$

where i indicates the total degrees of freedom (here 2).

Now $\{\ddot{X}\} = -\{X\}\omega^2 \sin(\omega t - \alpha)$ and on substitution of the same in the equation of free vibration we have

$$-[M]\ \omega^2 \sin(\omega t - \alpha)\{X\} + [K]\{X\}\sin(\omega t - \alpha) = 0 \tag{5.2.17}$$

which on simplification gives

$$[K] - [M]\,\omega^2 = 0 \tag{5.2.18}$$

The above is mathematically known as the *eigen value problem* of a matrix of order $n \times n$ where on simplification it yields a polynomial of order n. The n roots of the equation are known as the *eigen values* of the system and the corresponding vectors spanning the n space is known as the *eigen vectors*. We will devote more on eigen values and different computer techniques adopted for solving the same while discussing the solution of dynamic problems with large degree of freedom.

For the time being let us see how the eigen values effect the overall dynamic analysis procedure based on a 2×2 matrix which is amenable to hand calculation.

Based on the above explanation the second order differential equation for the two storied building becomes

$$\begin{bmatrix} k_1 + k_2 - m_1\lambda & -k_2 \\ -k_2 & k_2 - m_2\lambda \end{bmatrix} = 0 \quad \text{where } \lambda = \omega^2 \tag{5.2.19}$$

Now considering, $k_1 + k_2 = A$ and $k_2 = B$ we have

$$\begin{bmatrix} A - m_1\lambda & -B \\ -B & B - m_2\lambda \end{bmatrix} = 0 \tag{5.2.20}$$

on expansion of the above we have

$$(A - m_1\lambda)(B - m_2\lambda) - B^2 = 0, \tag{5.2.21}$$

on simplification it becomes $m_1 m_2 \lambda^2 - (m_1 B + m_2 A)\lambda + (AB - B^2) = 0$, resulting in

$$\lambda_{1,2} = \frac{(m_1 B + m_2 A) \pm \sqrt{[(m_1 B + m_2 A)^2 - 4m_1 m_2 (AB - B^2)]}}{2m_1 m_2} \tag{5.2.22}$$

in which, $\omega_1 = \sqrt{\lambda_1}$ and $\omega_2 = \sqrt{\lambda_2}$, where ω_1 and ω_2 are the *natural frequency of the structure*.

We know that, $T = 2\pi/\omega$, so for converting the values of ω_1 and ω_2, one can find the *fundamental time periods T_1 and T_2 of the two storied building*. Once the value of λ_1 and λ_2 are obtained we substitute the values in the matrix equations to have

$$\begin{bmatrix} A - m_1\lambda_1 & -B \\ -B & B - m_2\lambda_1 \end{bmatrix} \begin{Bmatrix} x_1 \\ x_2 \end{Bmatrix} = 0 \quad \text{for the first mode, and}$$

$$\begin{bmatrix} A - m_1\lambda_2 & -B \\ -B & B - m_2\lambda_2 \end{bmatrix} \begin{Bmatrix} x_1 \\ x_2 \end{Bmatrix} = 0 \quad \text{for the second mode.} \tag{5.2.23}$$

For *the first mode*, on expanding, we have

$$-Bx_2 + (A - m_1\lambda_1)x_1 = 0 \quad \text{and}$$

$$-Bx_1 + (B - m_2\lambda_1)x_2 = 0, \tag{5.2.24}$$

the above being a homogenous equation having zero in the right hand side of both the equations a unique solution is not possible; as such presuming one value as unity or any arbitrary value the other term may be obtained.

For the first mode considering, $x_1 = 1$, $x_2 = (A - m_1\lambda_1)/B$, and for the second mode with, $x_1 = 1$, $x_2 = (A - m_1\lambda_2)/B$.

It will be observed that the other equations in the first and second mode are automatically satisfied.

We will now explain the above theory based on a suitable numerical example.

Example 5.2.1

The plan view of a two storied R.C.C. building is as shown in Figure 5.2.6. The building has following data

1. **Thickness of roof slab = 150 mm**
2. **Thickness of floor slab = 200 mm**
3. **Size of roof beams = 600 × 750**
4. **Size of floor beams = 600 × 900**
5. **Size of columns = 600 × 600**
6. **Wall thickness at first floor = 250 mm**
7. **Live load on roof slab = 1 kN/m^2**
8. **Live load on floor = 1.5 kN/m^2**
9. **Equipment load on floor = 500 kN**
10. **Unit weight of brick = 20 kN/m^3**
11. **Dynamic modulus of concrete = 3×10^8 kN/m^2**
12. **Unit weight of concrete = 25 kN/m^3**

Calculate the natural frequency, time period and the modal shapes for each mode.

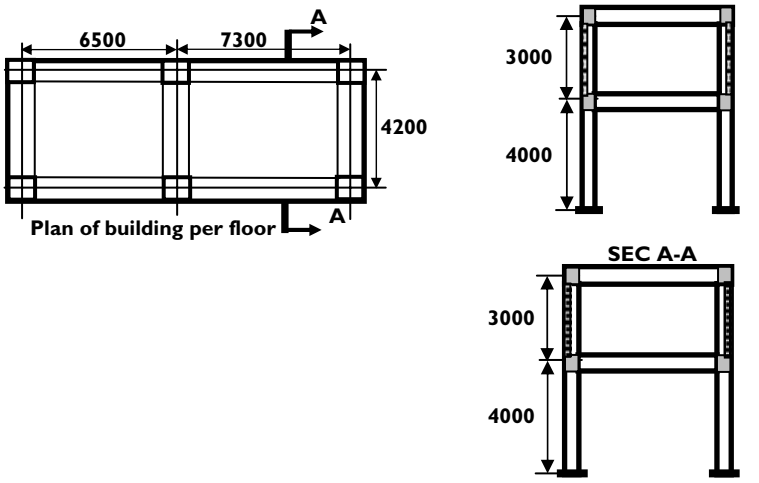


Figure 5.2.6 Two storied R.C.C. building.

Solution:

Mass calculation per floor:

Sl. No.	*Roof/system*	*Calculation*	*Load/9.81*	*CF2*	*CF1*	M_2	M_1
1	Slab	$14.4 \times 4.8 \times 0.15 \times 25 = 259.2$	26.422	1	0	26.42	0
1.1	Beam	$36 \times 0.6 \times (0.75-0.15) \times 25 = 324$	33.03	1	0	33.03	0
1.2	Column	$0.6 \times 0.6 \times 3 \times 25 \times 6 = 162$	16.51	1/3	2/3	5.50	11
1.3	Live load	$14.4 \times 4.8 \times 1.0 = 69$	7.03	1	0	7.03	0
2	Floor/System						
2.1	Slab	$(259.2/0.15) \times 0.2 = 345.6$	35.229	0	1	0	35.23
2.2	Beam	$36 \times 0.6 \times (0.9-0.2) \times 25 = 378$	38.53	0	1	0	38.53
2.3	Equipment load	500	50.97	0	1	0	50.97
2.4	Live load	$(69/1.0) \times 1.5 = 103.5$	10.55	0	1	0	10.55
2.5	Brick-wall	$36 \times 0.25 \times (3-0.375-0.45) \times 20 = 391$	39.908	1/3	2/3	13.3	26.6
2.6	Column	$0.6 \times 0.6 \times 4 \times 6 \times 25 = 216$	22.02	0	1/3	0	7.34
						85.31	180.22

Note: Here CF1 and CF2 are contributing factors of mass to the floor level and roof level.

Calculation of stiffness

For floor level

$$k_1 = \sum_{1}^{6} \frac{12EI}{L_1^3} \quad \text{where } I = \frac{(0.6)^4}{12} = 0.0108\,\text{m}^4$$

$$\therefore k_1 = 6 \times (12 \times 3 \times 10^8 \times 0.0108)/(4)^3 = 3645000\,\text{kN/m};$$

$$k_2 = 6 \times (12 \times 3 \times 10^8 \times 0.0108)/(3)^3 = 8640000\,\text{kN/m}$$

The stiffness matrix is given by

$$[K] = \begin{bmatrix} 3645000 + 8640000 & -8640000 \\ -8640000 & 8640000 \end{bmatrix}, \quad \text{while mass matrix is}$$

$$[M] = \begin{bmatrix} 180 & 0 \\ 0 & 85 \end{bmatrix}$$

Thus, the characteristic equation of the system as mentioned above is given by the determinant of

$$\begin{bmatrix} 122850000 - 180\lambda & -8640000 \\ -8640000 & 8640000 - 85\lambda \end{bmatrix} = 0$$

The solution to the same is given by the equation

$$\lambda_{1,2} = \frac{(m_1 B + m_2 A) \pm \sqrt{[(m_1 B + m_2 A)^2 - 4m_1 m_2 (AB - B^2)]}}{2m_1 m_2}$$

where, $m_1 = 180$; $m_2 = 85$; $B = 8640000$ and $A = 122850000$.

Substituting the above mentioned data, we have

$\lambda_1 = 93365.32$ and $\lambda_2 = 690781.7$ ➔ $\omega_1 = 306$ rad./sec and $\omega_2 = 831$ rad/sec.

Knowing $T = 2\pi/\omega$, we have $T_1 = 0.02$ sec and $T_2 = 0.0075$ sec.

Mode shapes

For the first mode,

$$\begin{bmatrix} 122850000 - 180 \times 93365 & -8640000 \\ -8640000 & 8640000 - 85 \times 93365 \end{bmatrix} \begin{Bmatrix} x_1 \\ x_2 \end{Bmatrix} = 0$$

On expansion, we have,

$$106044300x_1 - 8640000x_2 = 0$$

$$-8640000x_1 + 703975x_2 = 0$$

Thus, assuming $x_1 = 1.0$ we have, $x_2 = \frac{106044300}{8640000} = 12.2736$

Thus the mode shape for **the first mode** is

$$\begin{Bmatrix} x_1 \\ x_2 \end{Bmatrix} = \begin{Bmatrix} 1.0 \\ 12.2736 \end{Bmatrix}$$

Similarly for **the second mode**

$$\begin{bmatrix} 122850000 - 180 \times 690781.7 & -8640000 \\ -8640000 & -8640000 - 85 \times 680781.7 \end{bmatrix} \begin{Bmatrix} x_1 \\ x_2 \end{Bmatrix} = 0$$

On expansion, the above equations give

$$-14907060x_1 - 8640000x_2 = 0; \quad -8640000x_1 - 66506444x_2 = 0$$

Substituting, $x_1 = 1.0$, we have $x_2 = -14907060/8640000 = -0.1725362$. Thus, the mode shapes for the second mode is

$$\begin{Bmatrix} x_1 \\ x_2 \end{Bmatrix} = \begin{Bmatrix} 1.0 \\ -0.1725632 \end{Bmatrix}$$

The mode shapes are shown in Figure 5.2.7.

Thus, under any arbitrary loading, the displacements x_1 and x_2 will be a multiple of the modal values.

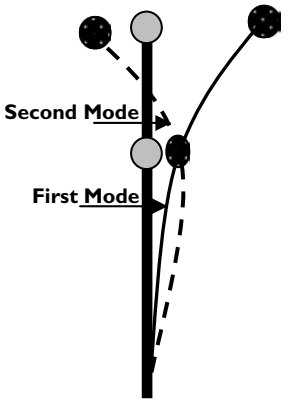


Figure 5.2.7 Eigen vectors or modeshapes of the building.

Based on the above problem we have come to realize that the evaluation of eigen values and eigenvectors are in essence evaluation of the natural frequency and mode shapes of a system. As such, before we proceed further, it would be worth to understand the physical as well as mathematical concepts underlying it.

5.2.1.7 Concepts of eigen value analysis

The *eigen value problem* in terms of matrix algebra (Ayres 1962) is defined as follows:

If there exists a matrix $[A]$ and $\{X\}$ such that

- $[A]\ \{X\} = [\lambda]\ \{X\}$, then problem is said to be an *eigen value problem*; where λ is the eigen value.
- The matrix expression as mentioned above on expansion gives *a polynomial equation*, and the order of the polynomial is *same as the size of the matrix [A] and {X}* (i.e. if the size of the matrix is 2×2 the polynomial equation will be a quadratic equation, if the size is 3×3 it will be a cubic equation and so on...). *The characteristic roots of the polynomial give the eigen value solution* (λ) *of the problem.*
- For each definite value of λ we get a set of homogeneous equation in terms of X and the same can be expressed in terms of the other and are known as the eigenvectors.
- For any particular mode j, the term $\sum_{k=1}^{3} a_k[[M]^{-1}[K]]^k =$ is known as the eigen pair for the jth mode. This is elaborated later in Equation (5.2.30).

The definition mentioned above looks fine but reads more like a lecture in the graduate course in mathematics. But engineers though use mathematics as a day to day tool in their regular work prefers to first comprehend the physical concept behind the problem rather than the obscure abstractions which mathematicians prefer at times.

So the question boils down to...

5.2.1.8 What is the physics of the eigen value?

To understand the physical concept behind it for the time being we digress from our present topic and go back to some fundamentals of elasticity and strength of materials.

Shown in Figure 5.2.8 is an element cut out from a 2D body subjected to bi-axial stress. We know that the stress tensor in plane subtending an angle ϕ with vertical is represented by

$$\begin{bmatrix} \sigma_x & \tau_{xy} \\ \tau_{xy} & \sigma_y \end{bmatrix} \begin{Bmatrix} l \\ m \end{Bmatrix} = \begin{Bmatrix} X \\ Y \end{Bmatrix} \tag{5.2.25}$$

where ℓ and m are direction cosines X and Y are the external forces.

We also know (Timoshenko and Goodier 1970) if s is the principal stress then the same is represented by the expression

$$s_{1,2} = (\sigma_x + \sigma_y)/2 \pm \sqrt{([\sigma_x - \sigma_y]/2)^2 + (\tau_{xy})^2} \tag{5.2.26}$$

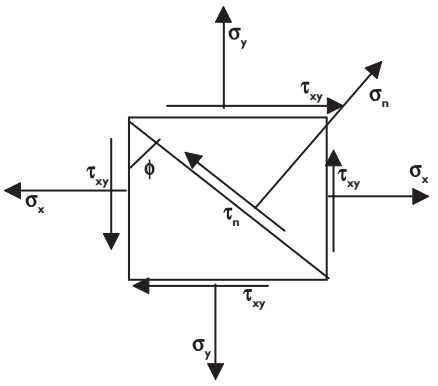


Figure 5.2.8 Plane stress at a point.

Here the principal stress is defined as a set of unique stresses in a plane where the shear stress, τ vanishes and the total stress tensor is represented by two complimentary forces one with positive and the other with negative sign and is given by

$$s_1 = (\sigma_x + \sigma_y)/2 + \sqrt{([\sigma_x - \sigma_y]/2)^2 + (\tau_{xy})^2};$$

$$s_2 = (\sigma_x + \sigma_y)/2 - \sqrt{([\sigma_x - \sigma_y]/2)^2 + (\tau_{xy})^2}$$

The forces represented by σ_x, σ_y and τ_{xy} are transformed into a different co-ordinate system (X′Y′) which we can attribute as a change of basis and represent them in terms of the two stress parameters s_1 and s_2.

Substituting $X = S \cdot \ell$ and $Y = S \cdot m$, we can write equation (5.2.25) as

$$\begin{bmatrix} \sigma_x - S & \tau_{xy} \\ \tau_{xy} & \sigma_y - S \end{bmatrix} \begin{Bmatrix} \ell \\ m \end{Bmatrix} = 0, \quad \text{since } \ell \text{ and } m \text{ is not equal to zero}$$

hence

$$\begin{bmatrix} \sigma_x - S & \tau_{xy} \\ \tau_{xy} & \sigma_y - S \end{bmatrix} = 0, \quad \text{and on expansion we may get}$$

$$S^2 - (\sigma_x + \sigma_y)S + (\sigma_x\sigma_y - \tau_{xy}^2) = 0$$

$$\rightarrow \quad S_{1,2} = (\sigma_x + \sigma_y)/2 \pm \sqrt{([\sigma_x - \sigma_y]/2)^2 + (\tau_{xy})^2} \tag{5.2.27}$$

We see that principal stresses are actually the ***eigen values of the stress matrix*** *and can be represented as* $[\sigma_{x,y}]\{\phi\} = [S]\{\phi\}$.

Thus we can conclude that ...

A system of forces spanning a space of n dimension and represented by a matrix of order n × n can be subjected to transformation of basis and converted into n number of unique values.

These unique values on the change of the basis from its original form gets de-coupled and are known as the ***eigen values*** *of the system and the space it spans are termed as the* ***eigen vectors****.*

5.2.1.9 Eigen value problem in dynamics

First let us see how the second order linear differential equation of motion can be converted to a standard eigen value problem. We know that

$$[M]\{\ddot{X}\} + [K]\{X\} = 0 \tag{5.2.28}$$

Considering $\{X\} = \{\varphi\}\sin(\omega t - \alpha)$, we may write $\{\ddot{X}\} = -\{\varphi\}\omega^2 \sin(\omega t - \alpha)$

Substituting the value of $\{\ddot{X}\}$ in the equation of motion we have

$$-[M]\omega^2\{\varphi\}\sin(\omega t - \phi) + [K]\{\varphi\}\sin(\omega t - \alpha) = 0$$

$$\rightarrow [K]\{\varphi\} = \omega^2[M]\{\varphi\} \quad \rightarrow \quad [K][M]^{-1}\{\varphi\} = \omega^2\{\varphi\}$$

$$\rightarrow \quad [A]\{\varphi\} = \lambda\{\varphi\} \tag{5.2.29}$$

which is the standard eigen value format.

5.2.1.9.1 What does eigen value signify in dynamics?

Based on the previous discussion it would perhaps be not too difficult to conceive now the physical concept underlying eigen value problem in dynamics.

A structure or a foundation as we have seen earlier is an assemblage of individual elements. In terms of dynamic analysis, it is actually an assemblage of a complex system of idealized springs and lumped masses and we assemble them to form global matrix and perform the analysis.

Shown in Figure 5.2.9, is a system of space truss assembled as a mathematical model of springs and lumped masses.

While performing the eigen value analysis we transform it into a different co-ordinate system and define the parameters in terms of a set of distinct value λ.

$$[\lambda] = [K]\,[M]^{-1} = \frac{[K]}{[M]} \tag{5.2.30}$$

Here we are actually breaking up the complex system into *individual sets of spring and lumped mass of 'single degree of freedom' and try to analyse the behaviour* in the transformed axes.

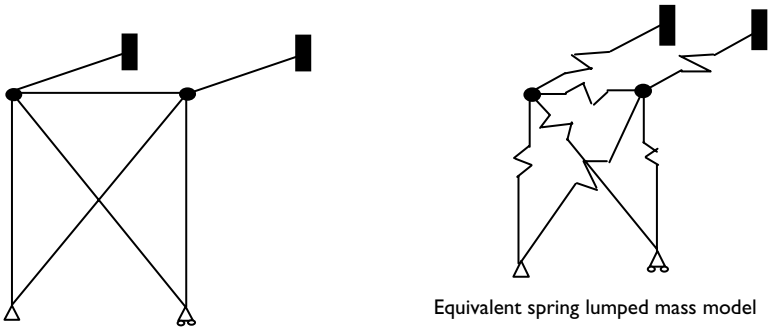


Figure 5.2.9 Space truss.

The term 'λ' actually measures stiffness per unit mass i.e. it gives us a measure of how stiff or how flexible is the structure/foundation and the eigen vectors give us a physical idea of how it will deform on application of a time dependent load.

5.2.2 Orthogonal transformation or the transformation basis

We had mentioned while explaining the eigen value that the transformation of co-ordinate de-couples the matrix into an independent distinct set of data.

This transformation is known as the orthogonal transformation and we discuss here some of the fundamental concepts regarding the same.

5.2.2.1 What is orthogonal transformation?

By orthogonal transformation we mean that the scalar product of two vectors is zero.

Suppose

$$\hat{A} = A_x i + A_y j + A_z k \quad \text{and} \quad \hat{B} = B_x i + B_y j + B_z k$$

are two vectors then the scalar product of the two vectors are given as, $[A]\,[B]^T$, in which using $i^2 = j^2 = k^2 = 1$, and $ij = jk = ki = 0$, the scalar product the vectors $[A]$ and $[B]$ is given by

$$[A] \cdot [B]^T = A_x B_x + A_y B_y + A_z B_z, \tag{5.2.31}$$

and this is said to be orthogonal, when $A_x B_x + A_y B_y + A_z B_z = 0$.

For a matrix of order $n \times n$ having n numbers of eigen pairs $\sum_{i=1}^{n} (\lambda_i, \phi_i)$, the eigen vectors are orthogonal to each other.

We prove this by a suitable numerical example.

Example 5.2.2

Let $[A]\{\phi\} = [\lambda]\{\phi\}$ **where** $[A] = \begin{bmatrix} 30 & 10 \\ 10 & 30 \end{bmatrix}$

Then for **eigen value analysis** we have

$$\begin{bmatrix} 30-\lambda & 10 \\ 10 & 30-\lambda \end{bmatrix} \begin{Bmatrix} \phi_1 \\ \phi_2 \end{Bmatrix} = 0, \quad \text{since} \{\varphi\} \neq 0 \text{ we have } (30-\lambda)^2 - (10)^2 = 0$$

or, $\lambda_1 = 40$ and $\lambda_2 = 20$.

Then for first mode we have; $-10\phi_1 + 10\phi_2 = 0$ and $10\phi_1 - 10\phi_2 = 0$ which gives, for $\phi_1 = 1 \rightarrow \phi_2 = 1$.

Similarly for second mode substituting the value of $\lambda = 20$ in the above matrix we have $\phi_1 = 1$ and $\phi_2 = -1$ which gives us the two eigen vectors for the two modes.

Thus the two eigen vectors are represented by

$$\{\varphi\}_1 = \begin{Bmatrix} 1 \\ -1 \end{Bmatrix} \text{ and } \{\varphi\}_2 = \begin{Bmatrix} 1 \\ -1 \end{Bmatrix} \text{ when we have}$$

$$[\varphi]_1^T [\varphi]_2 = \begin{bmatrix} 1 & 1 \end{bmatrix} \begin{bmatrix} 1 \\ -1 \end{bmatrix} = (1 \times 1 + 1 \times (-1)) = 0$$

Thus, we see that the eigen vectors are orthogonal to each other[9].

Based on the above orthogonal property let us see how we transform the basis of the equation of motion and what happens after the transformation.

We have seen earlier that the equation of motion under undamped free vibration is

$$[M]\{\ddot{X}\} + [K]\{X\} = 0 \tag{5.2.32}$$

Where the relationship between the global co-ordinate of the structure and the transformed co-ordinate is given by

$$\{X\} = \{\varphi\}\{\xi\} \tag{5.2.33}$$

We had also seen earlier that the above equation of motion can be written as

$$[K][\varphi] = \omega^2 [M][\varphi] \tag{5.2.34}$$

9 Here for clarity of calculation we have selected a simple matrix but the reader may check the orthogonality with the Example 5.2.1 and will still see that the scalar product of the eigenvectors become zero.

Now substituting the value of $\{X\}$ in the equation of motion based on the transformed co-ordinate we have

$$[M][\varphi]\{\ddot{\xi}\} + [K][\varphi]\{\xi\} = 0, \tag{5.2.35}$$

pre-multiplying $[\varphi]^T$ on both sides, yields

$$[\varphi]^T[M][\varphi]\{\ddot{\xi}\} + [\varphi]^T[K][\varphi]\{\xi\} = 0$$

Since $[K][\varphi] = \omega^2[M][\varphi]$ on substitution, it results in

$$[\varphi]^T[M][\varphi]\{\ddot{\xi}\} + [\omega^2][\varphi]^T[M][\varphi]\{\xi\} = 0.$$

Taking $[\varphi]^T[M][\varphi]$ as common from the both term we have

$$[\varphi]^T[M][\varphi]\left\langle\{\ddot{\xi}\} + [\omega^2]\{\xi\}\right\rangle = 0 \tag{5.2.36}$$

As [M] is a diagonal matrix, using the orthogonality relationship, we have

$$[\varphi]^T[M][\varphi] = \langle\phi_1\ \phi_2 \ldots \phi_n\rangle \begin{bmatrix} m_1 & & & & & \\ & m_2 & & & & \\ & & m_3 & & & \\ & & & \cdot & & \\ & & & & \cdot & \\ & & & & & m_n \end{bmatrix} \begin{Bmatrix} \phi_1 \\ \phi_2 \\ \cdot \\ \cdot \\ \cdot \\ \phi_n \end{Bmatrix}$$

$$= \langle\phi_1 m_1 \quad \phi_2 m_2 \ldots \phi_n m_n\rangle\langle\phi_1\ \phi_2 \ldots \phi_n\rangle^T$$

$$= \phi_1 m_1^2 + \phi_2 m_2^2 + \phi_3 m_3^2 + \ldots \phi_n m_n^2 = m_r \tag{5.2.37}$$

As the off-diagonal elements of $[\varphi]^T[M][\varphi]$ are zeroes, because of the orthogonal relationship, the equation $[\varphi]^T[M][\varphi]\langle\{\ddot{\xi}\} + [\omega^2]\{\xi\}\rangle = 0$ therefore gets uncoupled into n number of independent equations where the rth equation can be written as

$$m_r\langle\{\ddot{\xi}_r\} + [\omega_r^2]\{\xi_r\}\rangle = 0,$$

$$\rightarrow \quad \langle\{\ddot{\xi}_r\} + [\omega_r^2]\{\xi_r\}\rangle = 0, \tag{5.2.38}$$

the solution for the above equation is

$$\xi_r = A_r \sin\omega_r t + B_r \cos\omega_r t$$

Thus, an n-degree freedom system is represented by

$$[M]\{\ddot{X}\} + [K]\{X\} = 0 \tag{5.2.39}$$

is reduced to n single degree freedom system of equations represented by

$$\langle\{\ddot{\xi}_r\} + [\omega_r^2]\{\xi_r\}\rangle = 0, \tag{5.2.40}$$

using the transformed co-ordinates.

As the transformation uses the orthogonal properties of the eigen vectors this method of transforming the matrix into n-uncoupled equations are known as *orthogonal transformation.*

The advantage now is that we know the closed form solution of an un-damped system of motion for single degree of freedom and can be solved easily.

Once the values of displacement are obtained they are again back transferred to the global co-ordinate of the structure.

The theory as explained above is now explained with reference to the extension of Example 5.2.1.

Example 5.2.3

For the two storied building frame as shown in Example 5.2.1 and Figure 5.2.10, a compressor having an unbalanced force of 500 sin 600 t kN is under operation at the first floor level.

- **Determine amplitude of vibration**
- **Shear forces at each floor.**
- **How would the amplitude and shear force change if we put this compressor on roof?**

Solution:

Case-1

We had seen earlier that the equation of motion for the two storied building is given by

$$\begin{bmatrix} 180 & 0 \\ 0 & 85 \end{bmatrix} \begin{Bmatrix} \ddot{x}_1 \\ \ddot{x}_2 \end{Bmatrix} + \begin{bmatrix} 122850000 & -8640000 \\ -8640000 & 8640000 \end{bmatrix} \begin{Bmatrix} x_1 \\ x_2 \end{Bmatrix} = 0$$

Under the forced vibration the equation of motion becomes

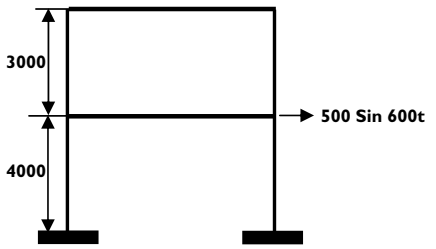


Figure 5.2.10

$$\begin{bmatrix} 180 & 0 \\ 0 & 85 \end{bmatrix} \begin{Bmatrix} \ddot{x}_1 \\ \ddot{x}_2 \end{Bmatrix} + \begin{bmatrix} 122850000 & -8640000 \\ -8640000 & 8640000 \end{bmatrix} \begin{Bmatrix} x_1 \\ x_2 \end{Bmatrix}$$

$$= \begin{Bmatrix} 500 \sin 600\, t \\ 0 \end{Bmatrix}$$

We had seen earlier that for free vibration based on eigen value analysis

$$\lambda_1 = 93365 \rightarrow \omega_1 = 305 \,\text{rad/sec}; \quad \lambda_2 = 690781 \rightarrow \omega_2 = 831 \,\text{rad/sec}.$$

The eigen vectors are

$$\{\phi_1\} = \begin{Bmatrix} 1.0 \\ 12.273639 \end{Bmatrix} \quad \text{and} \quad \{\phi_2\} = \begin{Bmatrix} 1.0 \\ -0.172536 \end{Bmatrix}$$

For the first mode

$$\{\phi_1\}^T [M] \{\phi_1\} = \langle 1.0 \quad 12.273639 \rangle \begin{bmatrix} 180 & 0 \\ 0 & 85 \end{bmatrix} \begin{Bmatrix} 1.0 \\ 12.273639 \end{Bmatrix}$$

$$= 12984.5882$$

Therefore the scaling factor $(SF) = \sqrt{12984.5882} = 113.9499373$.

The normalized eigen vector for the first mode is given by

$$[\phi_{n1}] = \begin{Bmatrix} \dfrac{\phi_{11}}{SF} \\ \dfrac{\phi_{12}}{SF} \end{Bmatrix} = \begin{Bmatrix} 0.008775783 \\ 0.1077108 \end{Bmatrix}.$$

For the second mode

$$\{\phi_2\}^T[M]\{\phi_2\} = \langle 1.0 \quad -0.172536\rangle \begin{bmatrix} 180 & 0 \\ 0 & 85 \end{bmatrix} \begin{Bmatrix} 1.0 \\ -0.172536 \end{Bmatrix}$$

$$= 182.5701922$$

Therefore **scaling factor** $(SF) = \sqrt{182.5701922} = 13.51185377$.
The normalized eigen vector for first mode is given by

$$[\phi_{n2}] = \begin{Bmatrix} \frac{\phi_{21}}{SF} \\ \frac{\phi_{22}}{SF} \end{Bmatrix} = \begin{Bmatrix} 0.074009089 \\ -0.012769232 \end{Bmatrix}.$$

The normalized eigen vector matrix is given by,

$$[\phi] = \begin{bmatrix} 0.008775783 & 0.074009089 \\ 0.1077108 & -0.012769293 \end{bmatrix}.$$

The equation of motion for the frame is given by

$$[M]\{\ddot{X}\} + [K]\{X\} = \{P_0\}\sin\omega_m t$$

In the transformed co-ordinate, $\{X\} = [\varphi]\{\xi\}$, we have, $[M][\varphi]\{\ddot{\xi}\} + [K][\varphi]\{\xi\} = \{P_0\}\sin\omega_m t$
Multiplying the above equation by $[\varphi]^T$
$[\varphi]^T[M][\varphi]\{\ddot{\xi}\} + [\varphi]^T[K][\varphi]\{\xi\} = [\varphi]^T\{P_0\}\sin\omega_m t$ and this gets de-coupled into two equations

$$\{\ddot{\xi}_1\} + [\lambda_1]\{\xi_1\} = \{p_1\}\sin\omega_m t; \quad \{\ddot{\xi}_2\} + [\lambda_2]\{\xi_2\} = \{p_2\}\sin\omega_m t$$

Multiplying $\{P_0\}\sin\omega_m t$ by $[\varphi]^T$

$$[\varphi]^T\{P_0\}\sin\omega_m t = \begin{bmatrix} 0.008775783 & 0.1077108 \\ 0.074009089 & -0.012769293 \end{bmatrix}$$

$$\times \begin{Bmatrix} 500 \\ 0 \end{Bmatrix} \sin 600\,t$$

$$= \begin{Bmatrix} 4.385 \\ 37 \end{Bmatrix} \sin 600\,t$$

Thus the two de-coupled equation of motion becomes

$$\{\ddot{\xi}_1\} + 93365\{\xi_1\} = 4.385 \sin 600\,t; \quad \{\ddot{\xi}_2\} + 690781\{\xi_2\} = 37 \sin 600\,t$$

Therefore,

$$\xi_1 = \frac{p_1/k_1}{(1-r^2)} \sin 600\,t = \frac{4.385/93365}{1-(600/305)^2} \sin 600\,t$$

$$= -1.63757 \times 10^{-5} \sin 600\,t$$

$$\xi_2 = \frac{p_2/k_2}{(1-r^2)} \sin 600\,t = \frac{37/690781}{1-(600/831)^2} \sin 600\,t$$

$$= 1.11909 \times 10^{-4} \sin 600\,t$$

As $\{X\} = [\varphi]\{\xi\}$, we have for **the first mode**

$$\begin{Bmatrix} x_1 \\ x_2 \end{Bmatrix} = \begin{Bmatrix} 0.00877 \\ 0.10771 \end{Bmatrix} (-1.6445 \times 10^{-5} \sin 600\,t); \quad \text{or}$$

$$\begin{Bmatrix} x_1 \\ x_2 \end{Bmatrix} = \begin{Bmatrix} -1.4371 \\ -17.6384 \end{Bmatrix} \times 10^{-7} \sin 600\,t\ \text{m}.$$

Shear forces/per floor in first mode is given by

$$\{V_i\}_1 = \begin{bmatrix} 12285 & -864 \\ -864 & 864 \end{bmatrix} \times \begin{Bmatrix} -1.4371 \\ -17.6384 \end{Bmatrix} \times 10^{-3} \sin 600\,t$$

$$\rightarrow \quad \{V_i\}_1 = \begin{Bmatrix} -2.415 \\ -13.997 \end{Bmatrix} \sin 600\,t$$

The second mode

$$\begin{Bmatrix} x_1 \\ x_2 \end{Bmatrix} = \begin{Bmatrix} 0.074 \\ -0.0127 \end{Bmatrix} \times (1.11909 \times 10^{-4} \sin 600\,t)$$

$$\rightarrow \quad \begin{Bmatrix} x_1 \\ x_2 \end{Bmatrix} = \begin{Bmatrix} 8.2823 \\ -1.428 \end{Bmatrix} \times 10^{-6} \sin 600\,t\ \text{m}.$$

Therefore, shear force/per floor in the second mode is given by

$$\{V_i\}_2 = \begin{bmatrix} 12285 & -864 \\ -864 & 864 \end{bmatrix} \times \begin{Bmatrix} 8.30 \\ -1.428 \end{Bmatrix} \times 10^{-2} \sin 600\, t$$

$$= \begin{Bmatrix} 1029.82 \\ -83.9 \end{Bmatrix} \sin 600\, t$$

Case-2

Compressor located on roof

When the compressor is located on the roof the force vector gets modified to

$$\{P\} = \begin{Bmatrix} 0 \\ 500 \end{Bmatrix} \sin 600\, t.$$

Multiplying the above by $[\varphi]^T$, we have

$$[\varphi]^T\{P_0\} \sin \omega_m t = \begin{bmatrix} 0.008775783 & 0.1077108 \\ 0.074009089 & -0.01276929 \end{bmatrix}$$

$$\times \begin{Bmatrix} 0 \\ 500 \end{Bmatrix} \sin 600\, t$$

$$= \begin{Bmatrix} 53.855 \\ -6.385 \end{Bmatrix} \sin 600\, t$$

The two equations of motion are

$$\{\ddot{\xi}_1\} + 93365\{\xi_1\} = 53.855 \sin 600\, t;$$
$$\{\ddot{\xi}_2\} + 690781\{\xi_2\} = -6.385 \sin 600\, t$$

Therefore

$$\xi_1 = \frac{p_1/k_1}{(1 - r^2)} \sin 600\, t = \frac{53.855/93365}{1 - (600/305)^2} \sin 600\, t$$

$$= -2.01 \times 10^{-4} \sin 600\, t$$

$$\xi_2 = \frac{p_2/k_2}{(1 - r^2)} \sin 600\, t = \frac{-6.385/690781}{1 - (600/831)^2} \sin 600\, t$$

$$= -1.931 \times 10^{-5} \sin 600\, t$$

For the first mode,

$$\begin{Bmatrix} x_1 \\ x_2 \end{Bmatrix} = \begin{Bmatrix} 0.00877 \\ 0.10771 \end{Bmatrix} (-2.01 \times 10^{-4} \sin 600\, t)$$

$$\rightarrow \quad \begin{Bmatrix} x_1 \\ x_2 \end{Bmatrix} = \begin{Bmatrix} -1.76 \\ -21.6 \end{Bmatrix} \times 10^{-6} \sin 600\, t \text{ m}.$$

Therefore **shear force/per floor in first mode** is given by

$$\{V_i\}_1 = \begin{bmatrix} 12285 & -864 \\ -864 & 864 \end{bmatrix} \times \begin{Bmatrix} -1.76 \\ -21.6 \end{Bmatrix} \times 10^{-2} \sin 600\, t$$

$$= \begin{Bmatrix} -29.64 \\ -171.8 \end{Bmatrix} \sin 600\, t.$$

For the second mode

$$\begin{Bmatrix} x_1 \\ x_2 \end{Bmatrix} = \begin{Bmatrix} 0.074 \\ -0.0127 \end{Bmatrix} (-1.931 \times 10^{-5})$$

$$\rightarrow \quad \begin{Bmatrix} x_1 \\ x_2 \end{Bmatrix} = \begin{Bmatrix} -1.429 \\ 0.2465 \end{Bmatrix} \times 10^{-6} \sin 600\, t \text{ m}.$$

Therefore **shear force/per floor in the second mode** is given by

$$\{V_i\}_2 = \begin{bmatrix} 12285 & -864 \\ -864 & 864 \end{bmatrix} \times \begin{Bmatrix} -1.429 \\ 0.2465 \end{Bmatrix} \times 10^{-2} \sin 600\, t$$

$$= \begin{Bmatrix} -177.7 \\ 14.476 \end{Bmatrix} \sin 600\, t$$

It is to be observed that based on application of the force, the amplitude and shear force become completely different for the two cases.

5.2.2.2 *Vibration of damped multi-degree freedom system*

Its time we introduce the damping . . .

As we had stated earlier that damping is an inherent property of the system by which there is a progressive decay in the amplitude and the system ultimately stops.

The mechanics of damping of how it works is still a matter of research and to dynamic analyst a source of headache and discomfort . . .

The reasons that can be attributed to the same are

- *It makes a mess of his elegant looking equations.*
- *After all the eigen value and matrix algebra, he is forced to guess certain values which is judgmental.*

- *The correctness of these assumptions cannot be validated beforehand.*
- *For coupled analysis like soil-structure or fluid-structure interaction either he has to deal with the problem completely differently based on direct integration method or else has to live with his guess-estimated values.*

This is surely not a happy state of affair.

We will study this subject subsequently and see what dogs the phenomenon quite in detail.

For the time being let us see what happens when we introduce the damping in our equation of motion of a system of multi-degree of freedom.

The equation of motion of a damped free vibration may be written as

$$[M]\{\ddot{X}\} + [C]\{\dot{X}\} + [K]\{X\} = 0 \tag{5.2.41}$$

where, $[M]$ = the mass matrix having masses lumped along the diagonal of the matrix; $[C]$ = the damping matrix of the system; $[K]$ = the stiffness matrix, symmetric in nature; $\{\ddot{X}\}$, $\{\dot{X}\}, \{X\}$ are the acceleration, velocity and displacement vectors respectively.

We had shown earlier that on orthogonal transformation the mass matrix becomes *an identity* and the stiffness matrix gets diagonalised into the *square of the natural frequency*. Based on a numerical example cited earlier we had also shown the advantage we get in such orthogonal transformation when a multi-degree freedom system (of order $n \times n$) gets decoupled into n number of independent equations of single degree of freedom making our calculations spectacularly simple. So while trying to fit in the damping people obviously wondered.

What happens when we do the operation $[\varphi]^T[C][\varphi]$?

For a single degree of freedom we have the equation of motion as

$$m\ddot{x} + c\dot{x} + kx = 0 \tag{5.2.42}$$

On dividing each term by m we have

$$\ddot{x} + \frac{c}{m}\dot{x} + \omega^2 x = 0 \tag{5.2.43}$$

Now the damping ratio D is defined as $D = c/c_c$ where c_c is the critical damping $(2\sqrt{mk})$, and $c = Dc_c$ which results in $c = 2D\sqrt{mk}$ and $c/m = 2D\sqrt{k}/\sqrt{m} = 2D\omega$.

Thus based on the orthogonal transformation if the mass matrix get transformed to an identity matrix and the stiffness matrix get transformed to a diagonal matrix whose diagonal terms are the eigen value *then by mathematical symmetry we can argue that the operation* $[\varphi]^T[C][\varphi]$ *will transform it into a matrix whose diagonal term will be* $2D\omega$.

Thus on orthogonal transformation of a matrix of size $n \times n$ will yield n numbers of uncoupled equations

$$\{\ddot{\xi}_1\} + 2D_1\omega_1\{\dot{\xi}_1\} + [\omega_1^2]\{\xi_1\} = 0; \quad \{\ddot{\xi}_2\} + 2D_2\omega_2\{\dot{\xi}_2\} + [\omega_2^2]\{\xi_{21}\} = 0;$$

$$\{\ddot{\xi}_3\} + 2D_3\omega_3\{\dot{\xi}_3\} + [\omega_3^2]\{\xi_{31}\} = 0; \ \ldots\ldots, \quad \{\ddot{\xi}_n\} + 2D_n\omega_n\{\dot{\xi}_n\} + [\omega_n^2]\{\xi_n\} = 0. \tag{5.2.44}$$

Thus, for any time dependent forcing function we can now solve these equations as single degree freedom and solve for the amplitude.

Apparently, though the transformation of the equation of motion with damping included looks quite fine, but there is a serious catch in it.

The catch is that the equation will uncouple only on orthogonal transformation provided that the damping matrix is proportional to the mass and stiffness matrices.

Unfortunately in many cases it has been found that the matrix is non-proportional.

Some of the classic examples of non-proportional damping are when soil and structure vibrates together (e.g. machine foundation, analysis of building with soil deformations), vibration of structures submerged in fluid (e.g. off-shore structures, vibration of jetty piles under earthquake) etc.

Moreover even if the damping matrix is proportional to the stiffness and mass matrices, ***we have to guess the damping ratio*** D ***for the modes under consideration.***

The damping ratio can only be guessed from experience and there exists no rational basis for prior evaluation of the same.

Even if the matrix is proportional to the mass and stiffness matrix, we are only considering what is known as the *material damping* of the system.

There exists other kinds of damping too like radiation damping, geometric damping etc. and we are yet to have a realistic model for the same.

5.2.2.3 Proportional or Rayleigh damping

This is by far the most popular form of representing the damping where the damping matrix is represented by a form

$$[C] = \alpha[M] + \beta[K] \tag{5.2.45}$$

where α and β are two arbitrary coefficients to be determined from two unequal frequencies of vibration.

Now let us see what happens when we perform the orthogonal transformation of the matrix [C].

$$[\varphi]^T[C][\varphi] = \alpha[\varphi]^T[M][\varphi] + \beta[\varphi]^T[K][\varphi]$$

$$\rightarrow \quad 2[D_i]\,[\omega_i] = \alpha + \beta[\omega_i^2] \tag{5.2.46}$$

Thus, for two different modes we have

$$2[D_1][\omega_1] = \alpha + \beta[\omega_1^2]; \quad 2[D_2][\omega_2] = \alpha + \beta[\omega_2^2] \tag{5.2.47}$$

Solving these two equations we can get the value of α and β.

Once α and β are known, we form the damping matrix from the expression $[C] = \alpha[M\} + \beta[K]$.

In Equation (5.2.47), we see that ω_1 and ω_2 can be obtained from free undamped equation but *to obtain α and β we have to guess the values of the damping ratio.*

We will now explain this with a numerical problem.

Example 5.2.4

For the two storied building analyzed in Example 5.2.1.

- **Form the damping matrix for damping ratio of 10% and 15% for the first two modes.**
- **Show that the matrix does not de-couple for any other symmetric matrix?**

Solution:

For the present problem, $D_1 = 0.10$ and $D_2 = 0.15$.

We had deduced in Example 4.1 that the natural frequency and the eigen values (ω^2) are given as

$$\omega_1 = 305, \Rightarrow \omega_1^2 = 93365 \quad \text{and} \quad \omega_2 = 831, \Rightarrow \omega_2^2 = 690781$$

and the mass matrix $[M] = \begin{bmatrix} 180 & 0 \\ 0 & 85 \end{bmatrix}$ while the stiffness matrix is

$$[K] = \begin{bmatrix} 12285 & -864 \\ -864 & 864 \end{bmatrix} \times 10^4$$

Based on the Rayleigh damping factors the equations are

$$2D_1\omega_1 = \alpha + \beta\omega_1^2; \quad 2D_2\omega_2 = \alpha + \beta\omega_2^2$$

Substituting the value the frequencies and damping ratio @ 0.10 and 0.15 we have

$$\alpha + 93365\beta = 61; \quad \alpha + 690781\beta = 249.3$$

The solution of the above two equations gives

$$\alpha = 31.572 \quad \text{and} \quad \beta = 3.152 \times 10^{-4}$$

Considering $[C] = \alpha[M] + \beta[K]$ we have

$$[C] = 31.572\begin{bmatrix}180 & 0\\ 0 & 85\end{bmatrix} + 3.152 \times 10^{-4}\begin{bmatrix}12285 & -864\\ -864 & 864\end{bmatrix} \times 10^4$$

$$= \begin{bmatrix}5682.96 + 38722 & -2723\\ -2723 & 2683 + 2723\end{bmatrix}$$

$$[C] = \begin{bmatrix}44405 & -2723\\ -2723 & 5406\end{bmatrix}; \quad \text{which is the required damping matrix.}$$

Thus we see that provided we can guess the damping ratios correctly it is possible to form a damping matrix which is orthogonal.

Now let us see what happens if we try to deal with an arbitrary damping matrix which has been pre-selected based on material property[10].

$$\text{Let} \quad [C] = \begin{bmatrix}10000 & -5000\\ -5000 & 40000\end{bmatrix} \text{ say.}$$

Then based on the definition of Rayleigh damping we have

$$\alpha\begin{bmatrix}180 & 0\\ 0 & 85\end{bmatrix} + \beta\begin{bmatrix}12285 & -864\\ -864 & 864\end{bmatrix} \times 10^4 = \begin{bmatrix}10000 & -5000\\ -5000 & 40000\end{bmatrix}$$

$$\text{i.e.} \quad \begin{bmatrix}0.018\alpha + 12285\beta & -864\beta\\ -864\beta & 0.0085\alpha + 864\beta\end{bmatrix} = \begin{bmatrix}1 & -0.5\\ -0.5 & 40\end{bmatrix}.$$

On expansion, we find three equations

$$0.018\alpha + 12285\beta = 1$$

$$0.00885\alpha + 864\beta = 40$$

$$-864\beta = -0.5$$

Now solving the first two equations, we have $\beta = 8 \times 10^{-3}$; $\alpha = 5515.56$.

But when we substitute this value in the third equation we find that the value of β does not satisfy this equation.

➔ *This proves that the orthogonal relationship is NOT satisfied.*

Thus in the above example it was shown that to de-couple the equations with damping effect we have to

- *Guess a value of the damping ratio.*

10 A common thing when we induce dynamic soil springs and damping in a structural system.

- *Evaluate the Rayleigh coefficients α and β to de-couple the damping matrix.*
- *The de-coupling does not take place for any other damping matrix even if it is symmetric.*

For a two-degrees of freedom system evaluation of α and β is simple. For, on expansion of matrices, we get two unknown equations with α and β and solving the two equations, we get two values of the Rayleigh coefficients.

But when the degree of freedom of structure is more than 2, the question arises as to which two equations to use?

An effective way to arrive at a meaningful value for the Rayleigh coefficient is described hereafter.

5.2.2.4 Selection of α and β for systems with large degrees of freedom

In almost all general-purpose FEM software like SAP, GTSTRUDL, ANSYS etc. provisions are there to give direct input for the Rayleigh coefficient α and β.

We have shown previously that when the structure has two degree of freedom it is simple to obtain the value of α and β from the equations

$$2[D_1][\omega_1] = \alpha + \beta[\omega_1^2]; \quad 2[D_2][\omega_2] = \alpha + \beta[\omega_2^2] \tag{5.2.48}$$

We simply solve the two simultaneous equations to obtain the values of α and β.

However when we are solving a system having a large degrees of freedom having say 400 or 1000 equations the obvious question which comes to mind is which two equations to use to obtain α and β which will be valid for all significant modes?

Surely there is no straight forward solution to arrive at these values and an iterative solution is only possible which would arrive at a possibly best fit value of α and β for a particular system.

We describe below this method (Chowdhury and Dasgupta 2004) which we hope would eradicate a lot of confusion in selection of this particular data in solving practical problems.

We have seen previously that orthogonal transformation of the damping matrix is done by

$$[\varphi]^T[C][\varphi] = \alpha[\varphi]^T[M][\varphi] + \beta[\varphi]^T[K][\varphi] \quad \rightarrow \quad 2[D_i][\omega_i] = \alpha + \beta[\omega_i^2],$$

this on simplification reduces to

$$[D_i] = \frac{\alpha}{2\omega_i} + \frac{\beta\omega_i}{2}, \tag{5.2.49}$$

meaning thereby that the damping ratio is in someway proportional to the natural frequency. We now show two typical plots of the equation $\frac{\alpha}{2\omega_i} + \frac{\beta\omega_i}{2}$ for frequency having ranges

- 2 to 13.5 rad/sec and 10 to 23.5 rad/sec.

The two curves in Figures 5.2.11 and 12, show some very interesting result.

For the first case (frequency range 2–13.5 rad/sec) the curve shows *marked non-linearity* at the start and after frequency of 6.35 rad/sec (step 92) is almost linearly varying.

While for the second case (having frequency range of 10 to 21.35 rad/sec) the equation is *practically linearly varying with x*.

From this we can conclude that *when x is small, the first term a/x dominates at the initial stage and as x increases the value a/x diminishes and approaches zero and the term b/x starts dominating the equation.*

In other words if a structure is very flexible and have a very low fundamental frequency will show non linear damping properties at the start with respect to frequency and would converge to a linear proportionality with frequency as the eigen value increases with each subsequent mode.

Flexible antennas, very long piles, or tall chimney (height >275 m) would possibly show this type of behavior at the outset.

However most of the civil engineering structures are usually designed to have a reasonable rigidity and would have a much higher value of the frequency when the $\beta x/2$ will usually pre-dominate.

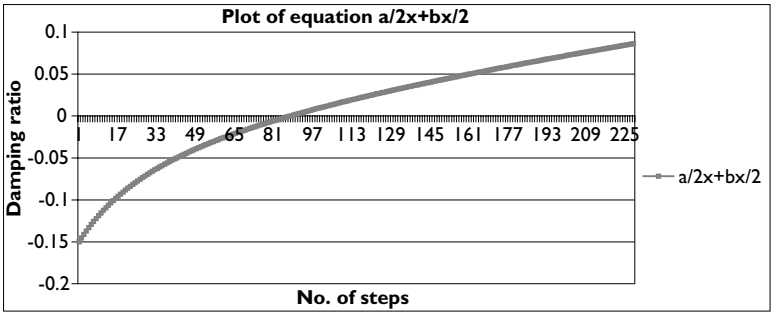


Figure 5.2.11 Plot of curve $a/2x + bx/2$ for frequency range 2 to 13.5 rad/sec.

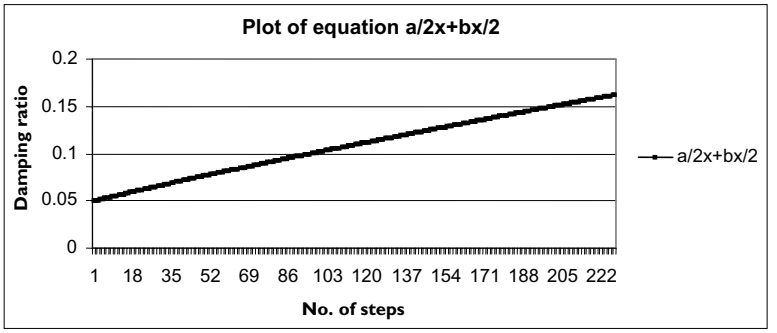


Figure 5.2.12 Plot for curve $ax/2 + bx/2$ for frequency range 10 to 21.35 rad/sec.

Moreover, considering the fact that the nonlinear range is very small for normal structures it will not induce much error to assume that *the damping ratio for each mode is linearly proportional to the frequency of the system.*

Thus if we have a set of value $\omega_1, \omega_2, \omega_3 \ldots\ldots\ldots\ldots \omega_n$ and $D_1, D_2, D_3 \ldots\ldots\ldots\ldots D_n$ as the corresponding damping ratio then for *i*th mode the damping ratio is given by

$$D_i = \frac{D_n - D_1}{\omega_n - \omega_1}(\omega_i - \omega_1) + D_1 \tag{5.2.50}$$

It is a well established that even for structures having large degrees of freedom it is only the first few modes, which contribute to the significant dynamic forces[11].

Let us presume that for a particular structure having n degrees of freedom (where, $n \gg 6$) the first six modes are significant, and having damping ratio varying between say 0.05 for 1st mode and 0.1 for the 6th mode.

As a first step we perform the eigen value considering *modes at least 2.5 times the first significant modes i.e. 15 modes for this case.*

We set the value damping ratio @ 0.05 to mode #1 and 0.1 to mode #6 and interpolate the values of damping ratio for mode 2 to 5 from equation (5.2.50) as mentioned above. We also extrapolate the values for mode 7 to 15.

Now we select two ranges of values

- One between modes 1 to 6, the last significant mode.
- The other between 1 to 15 the complete range of the eigen values.

Based on the above we find two sets of α and β from the equation

$$\beta = \frac{2D_i\omega_i - 2D_f\omega_f}{\omega_i^2 - \omega_f^2} \tag{5.2.51}$$

and back substitute, the value of β in Equation (5.2.49), we obtain α.

Based on the above two sets of value of α and β calculate *a third set by averaging the two values as obtained above.*

Next, we plot the three sets of data and see which data fits best the curve of the damping ratio *based on linear interpolation* and select the corresponding value α and β. This is the desired Rayleigh coefficient to be given as an input, which would give damping ratio reasonably correct for the first six (or whatever the modes considered) significant modes.

In some cases it might so happen that values will show significant variation in higher modes but this is irrelevant so long as the values are closely matching for the first few significant modes since the contribution of higher modes are insignificant for the system.

We now explain the above technique by a suitable numerical problem.

11 The modal mass participation factor is a very good indicator of to what mode does the vibration is significant. We will discuss more about it in the Chapter 3 (Vol. 2) on Earthquake engineering.

Example 5.2.5

A structure having 100 degrees of freedom has first six values of natural frequency as 3.0, 4.0, 7.0, 8.0, 12.0 and 20.0 rad/sec respectively. It is presumed that the significant dynamic response of the system will die down within first six modes with damping ratios varying between 5% and 15% within the first six modes.

Select a suitable value of α and β based for the above.

Solution:

We show below the eigen values for the first 15 mode as hereafter and taking first modal damping ratio as 5% and sixth modal damping ratio as 15% we linearly interpolate and extrapolate the data for the full range of the eigen values are as shown hereafter.

Sl. No.	*Natural frequency (rad/sec)*	*Damping ratio*
1	3	0.05
2	4	0.055882353
3	7	0.073529412
4	8	0.079411765
5	12	0.102941176
6	20	0.15
7	25	0.179411765
8	32	0.220588235
9	38	0.255882353
10	47	0.308823529
11	62	0.397058824
12	75	0.473529412
13	110	0.679411765
14	135	0.826470588
15	140	0.855882353

For the first six modes the range values are

$\omega_2 = 20$ rad/sec and $D_2 = 0.15$; and $\omega_1 = 3$ rad/sec and $D_2 = 0.05$.

Based on the above values $\beta = \frac{2\times0.15\times20-2\times0.05\times3}{400-9} = 0.01457801$ and $\alpha = 2 \times 0.15 \times 20 - 0.01457801 \times 400 = 0.16879795$.

For the full range of 15 modes we have

$\omega_2 = 140$ rad/sec and $D_2 = 0.855882353$; and $\omega_1 = 3$ rad/sec and $D_2 = 0.05$.

Based on the above values $\beta = \frac{2\times0.8588\times140-2\times0.05\times3}{19600-9} = 0.01221719$ and $\alpha = 2 \times 0.8588 \times 1400 - 0.01221719 \times 19600 = 0.05549134$.

Thus, based on the above values the average values α and β are: $\alpha = 0.1121446$ and $\beta = 0.0133976$.

Thus based on the above values the damping ratios are found to vary as follows:

No. of modes	*Frequency*	*Linear damping*	*damping upto 6th mode approximation*	*Damping upto full range approximation*	*Damping with average data*
1	3	0.05	0.05	0.027574349	0.038787
2	4	0.055882353	0.050255754	0.031370807	0.040813
3	7	0.073529412	0.063080015	0.046723848	0.054902
4	8	0.079411765	0.068861893	0.052336987	0.060599
5	12	0.102941176	0.094501279	0.075615307	0.085058
6	20	0.15	0.15	0.123559229	0.13678
7	25	0.179411765	0.185601023	0.153824759	0.169713
8	32	0.220588235	0.23588555	0.196342165	0.216114
9	38	0.255882353	0.279203123	0.232856846	0.25603
10	47	0.308823529	0.344378843	0.287694406	0.316037
11	62	0.397058824	0.453279432	0.379180543	0.41623
12	75	0.473529412	0.547800512	0.458514739	0.503158
13	110	0.679411765	0.802557545	0.672197935	0.737378
14	135	0.826470588	0.984640523	0.824866157	0.904753
15	140	0.855882353	1.021063208	0.855401803	0.938233

On plotting the data we find the variations as given in Figure 5.2.13.

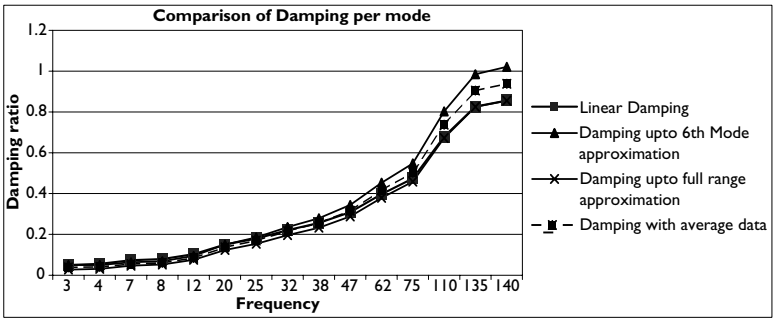


Figure 5.2.13

It will be observed that at lower modes the six mode value and average value matches the best. Though these shows variation in data beyond 13th mode this may be ignored for modes beyond 6th mode is considered to have no effect.

Thus the design Rayleigh coefficient are $\alpha = 0.1121446$ and $\beta = 0.0133976$.

5.2.2.5 Other methods of evaluating damping matrix

We have shown previously how damping matrix can be established with two damping ratios for a structure having multi-degree of freedom. When more then two values of damping ratios are to be used, the damping matrix can be represented by series known as *Caughey Damping (Caughey 1960)*.

Here the damping matrix is represented as

$$[C] = [M]\sum_{k=0}^{p-1} a_k[[M]^{-1}[K]]^k \tag{5.2.52}$$

where the coefficients a_k, $k = 1, 2, 3 \ldots . p$ are calculated from p simultaneous equations.

Now multiplying both side with the orthogonal eigen vectors we have

$$[\varphi_n]^T[C][\varphi] = [\varphi_n]^T[M]\sum_{k=0}^{p-1} a_k[[M]^{-1}[K]]^k[\varphi]$$

$$\text{or,} \quad 2\{D_n\}[\omega_n] = [\varphi_n]^T[M]\sum_{k=0}^{p-1} a_k[[M]^{-1}[K]]^k[\varphi_n]$$

Now since $[K] = [M]\omega^2$, we have

$$2\{D_n\}[\omega_n] = [\varphi_n]^T[M]\sum_{k=0}^{p-1} a_k[[M]^{-1}[M][\omega_n]^2]^k[\varphi_n]$$

$$\text{i.e.} \quad 2\{D_n\}[\omega_n] = [\varphi_n]^T[M][\varphi]\sum_{k=0}^{p-1} a_k[[M]^{-1}[M][\omega_n]^2]^k$$

Since $[\phi_n]^T[M][\phi] = [I]$ and $[M]^{-1}[M] = [I]$, we may write

$$2\{D_n\}[\omega_n] = [I]\sum_{k=0}^{p-1} a_k[[I][\omega_n]^2]^k \quad \text{where } [I] = \text{Identity matrix}$$

$$\rightarrow \quad \{D_n\} = \frac{1}{2[\omega_n]}\sum_{k=0}^{p-1} a_k[[\omega_n]^2]^k \tag{5.2.53}$$

Thus for a matrix of order $n \times n$ the above equation can be expressed as

$$\begin{Bmatrix} D_1 \\ D_2 \\ . \\ . \\ D_n \end{Bmatrix} = \frac{1}{2}\begin{bmatrix} \omega_1 & \omega_1^3 & . & . & \omega_1^{2n-1} \\ \omega_2 & \omega_2^3 & . & . & \omega_2^{2n-1} \\ . & . & . & . & . \\ . & . & . & . & . \\ \omega_n & \omega_n^3 & . & . & \omega_n^{2n-1} \end{bmatrix}\begin{Bmatrix} a_1 \\ a_2 \\ a_3 \\ a_4 \\ a_5 \end{Bmatrix} \tag{5.2.54}$$

Thus based on assumed values of damping ratio and calculated natural frequency we put it in the above equation and find the values of $a_1, a_2, \ldots\ldots a_n$.

Once these values are obtained we back substitute them in the equation $[C] = [M]\sum_{k=0}^{p-1} a_k[[M]^{-1}[K]]^k$ and obtain the damping matrix of the system.

We will now explain the above with a numerical example

Example 5.2.6

A three-storied structure having stiffness and mass matrix as below is assumed to have damping ratio of 5% in the first mode and 15% in the third mode.

The three natural frequencies of the structure are $\omega_1 = 2.197$ rad/sec, $\omega_2 = 6$ rad/sec, $\omega_3 = 8.33$ rad/sec form the Caughey damping for the structure. Here

$$[K] = \begin{bmatrix} 2000 & -2000 & 0 \\ -2000 & 4000 & -2000 \\ 0 & -2000 & 5000 \end{bmatrix} \quad \text{and} \quad [M] = \begin{bmatrix} 100 & 0 & 0 \\ 0 & 100 & 0 \\ 0 & 0 & 100 \end{bmatrix}$$

Solution:

For $\omega_1 = 2.197$ rad/sec, $\xi_1 = 0.05$; For $\omega_3 = 8.33$ rad/sec $\xi_3 = 0.15$

Thus based on linear interpolation we have for $\omega_2 = 6.00$ rad/sec

$$\xi_2 = 0.05 + \left[\frac{0.15 - 0.05}{8.33 - 2.197}\right] \times (6 - 2.197) = 0.112$$

Based on the previous deduction we have

$$\begin{Bmatrix} D_1 \\ D_2 \\ D_3 \end{Bmatrix} = \frac{1}{2}\begin{bmatrix} \omega_1 & \omega_1^3 & \omega_1^5 \\ \omega_2 & \omega_2^3 & \omega_2^5 \\ \omega_3 & \omega_3^3 & \omega_3^5 \end{bmatrix}\begin{Bmatrix} a_1 \\ a_2 \\ a_3 \end{Bmatrix} \quad \text{or}$$

$$\begin{Bmatrix} 0.05 \\ 0.112 \\ 0.150 \end{Bmatrix} = \frac{1}{2}\begin{bmatrix} 2.197 & 10.6 & 51.2 \\ 6 & 216 & 7776 \\ 8.33 & 57.8 & 40107 \end{bmatrix}\begin{Bmatrix} a_1 \\ a_2 \\ a_3 \end{Bmatrix}$$

On expansion we have the following three equations

$$1.1a_1 + 5.3a_2 + 25.6a_3 = 0.05$$

$$3a_1 + 108a_2 + 3888a_3 = 0.112$$

$$4.17a_1 + 289a_2 + 20054a_3 = 0.15$$

Solution of the above three equations gives

$$a_1 = 0.04314; \quad a_2 = -4.49 \times 10^{-4}; \quad a_3 = 4.0857 \times 10^{-6}$$

The mass matrix is given by

$$[M] = \begin{bmatrix} 100 & 0 & 0 \\ 0 & 100 & 0 \\ 0 & 0 & 100 \end{bmatrix},$$

and the inverse is given by

$$[M]^{-1} = \begin{bmatrix} 10^{-2} & 0 & 0 \\ 0 & 10^{-2} & 0 \\ 0 & 0 & 10^{-2} \end{bmatrix}$$

$$\therefore [M]^{-1}[K] = \begin{bmatrix} 10^{-2} & 0 & 0 \\ 0 & 10^{-2} & 0 \\ 0 & 0 & 10^{-2} \end{bmatrix} \times \begin{bmatrix} 2000 & -2000 & 0 \\ -2000 & 4000 & -2000 \\ 0 & -2000 & 5000 \end{bmatrix}$$

$$= \begin{bmatrix} 20 & -20 & 0 \\ -20 & 40 & -20 \\ 0 & -20 & 50 \end{bmatrix}$$

The damping matrix is given by $[C] = [M] \sum_{k=1'}^{3} a_k [[M]^{-1}[K]]^k$ for which we have

$$\sum_{k=1'}^{3} a_k [[M]^{-1}[K]]^k = 0.04314 \begin{bmatrix} 20 & -20 & 0 \\ -20 & 40 & -20 \\ -20 & -20 & 50 \end{bmatrix}$$

$$- 4.49 \times 10^{-4} \begin{bmatrix} 20 & -20 & 0 \\ -20 & 40 & -20 \\ 0 & -20 & 50 \end{bmatrix}^2$$

$$+ 4.086 \times 10^{-6} \begin{bmatrix} 20 & -20 & 0 \\ -20 & 40 & -20 \\ 0 & -20 & 50 \end{bmatrix}^3$$

The above on simplification gives

$$\sum_{k=1'}^{3} a_k [[M]^{-1}[K]]^k = \begin{bmatrix} 66.66 & -60.58 & 0.63 \\ -60.58 & 128.46 & -61.76 \\ 0.63 & -61.76 & 163.5 \end{bmatrix} \times 10^{-2} \quad \text{and}$$

$$[C] = [M] \sum_{k=1'}^{3} a_k [[M]^{-1}[K]]^k = \begin{bmatrix} 66.66 & -60.58 & 0.63 \\ -60.58 & 128.46 & -61.76 \\ 0.63 & -61.76 & 163.5 \end{bmatrix}$$

One disadvantage of this method is that for the damping matrix to be defined, we have to take into consideration all the n number of eigen values (where n is the total degrees of freedom) to obtain the [C] matrix of size $n \times n$. While this is OK with small structures, for large structures this surely becomes computationally expensive.

While in Rayleigh damping case we can only take into consideration the first few significant modes and on calculating the values of α and β can still produce the [C] matrix of size $n \times n$.

For most of the practical analysis a reasonable value of Rayleigh damping is usually assumed based on observed material damping of various materials or from observed data of real structures and similar level of damping is used similar/identical structure.

One disadvantage of Rayleigh damping is that it gives higher damping values at the higher modes. However if the modal mass participation is restricted to first few modes (which is usually true for most of the cases), Rayleigh damping gives quite reasonable values in predicting the damped behavior of a structure.

The table hereafter gives some suggestive damping ratio for different type of materials which may be used for dynamic analysis for structure and soil foundation system.

Suggestive damping ratio for different materials

Sl. No.	*Material in use*	*Damping ratio*
1	Concrete	5–10%
2	Steel	2–5%
3	Soil	10–30%
4	Timber	2–5%

In the above discussion we have shown how damping characteristic of structure can be made proportional to the stiffness and mass matrix and can be used for modal analysis based on orthogonal transformation.

In many analyses, the assumption of proportional damping is valid. But as stated earlier in cases like foundation structure interaction, fluid structure interaction gives rise to non-proportional damping where on orthogonal transformation the equations do not uncouple we use completely different techniques for analyzing such systems.

Before we discuss these techniques, we see how the equation of motion can also be formed based on other techniques namely the *energy equations*.

5.2.2.6 The Lagrangian formulation

French mathematician Lagrange developed equations based on differential equations of motion expressed in terms of generalized co-ordinates of the kinetic and potential energy of a system.

This is one of the most versatile tools in formulating the equations of motion of a dynamical system, specially when the system motion is complicated.

While formulating the equation based on D'Alembert's principle we have to clearly write down the equations taking into consideration the vector directions of the motions. There could be systems for which writing down such equations become quite complicated (specially for structures and foundations where horizontal and rocking degree of freedom becomes coupled) and under such situation the Lagrange's equation prove to be a powerful tool for formulation of the equations of motions[12]. Let us now understand the principle underlying the concept.

For any conservative system in this universe we know that the sum of Kinetic and Potential energy is a constant.

Thus, if T = kinetic energy of a system (KE) and U = potential energy of a system (PE), we have by the law of physics:

The total energy = $T + U$ = constant; which gives

$$d(T + U) = 0, \tag{5.2.55}$$

where d is the first derivative or differential of the total energy.

Now suppose q_i and $\dot{q}_i$ are the displacement and velocity vector in the generalized co-ordinate, we know that

$$\begin{aligned} &T = f(q_1, q_2, q_3 \ldots\ldots q_n; \quad \dot{q}_1, \dot{q}_2, \dot{q}_3, \ldots\ldots\ldots, \dot{q}_n) \quad \text{and} \\ &U = f(q_1, q_2, q_3, \ldots\ldots\ldots q_n) \end{aligned} \tag{5.2.56}$$

Then the differential of T is given by[13].

$$dT = \sum_{i=1}^{n} \frac{\partial T}{\partial q_i} dq_i + \sum_{i=1}^{n} \frac{\partial T}{\partial \dot{q}_i} d\dot{q}_i \tag{5.2.57}$$

The kinetic energy of a system can be expressed as

$$T = \frac{1}{2} \sum_{i=1}^{n} \sum_{j=1}^{n} m_{ij} \dot{q}_i \dot{q}_j.$$

Differentiating the above with $\dot{q}_i$ and multiplying by $\dot{q}_i$, we have

$$\sum_{i=1}^{n} \frac{\partial T}{\partial \dot{q}_i} \dot{q}_i = \sum_{i=1}^{n} \sum_{j=1}^{n} m_{ij} \dot{q}_i \dot{q}_j = 2T \quad \text{i.e. } 2T = \sum_{i=1}^{n} \frac{\partial T}{\partial \dot{q}_i} \dot{q}_i.$$

12 We will see the advantages in of this form of equation when we tackle different form of coupled analysis.

13 If $u = f(x, y)$ then $du = \frac{\partial u}{\partial x} dx + \frac{\partial u}{\partial y} dy$.

Now considering $u = \sum_{i=1}^{n} \frac{\partial T}{\partial \dot{q}_i}$ and $v = \dot{q}_i$, we have $2T = u \cdot v$ and differentiating the above, one may write

$$2dT = u \cdot dv + v \cdot du \quad \rightarrow \quad \text{or } 2dT = \sum_{i=1}^{n} d\left(\frac{\partial T}{\partial \dot{q}_i}\right)\dot{q}_i + \sum_{i=1}^{n}\left(\frac{\partial T}{\partial \dot{q}_i}\right)d\dot{q}_i$$

Subtracting from above the expression of dT as shown above by a black border, we have

$$dT = \sum_{i=1}^{n}\left[\frac{d}{dt}\left(\frac{\partial T}{\partial \dot{q}_i}\right) - \frac{\partial T}{\partial q_i}\right]dq_i$$

Taking differential of U we may write

$$dU = \sum_{i=1}^{n}\frac{\partial U}{\partial q_i}dq_i$$

Thus, considering $d(T + U) = 0$, we can write

$$d(T+U) = \sum_{i=1}^{n}\left[\frac{d}{dt}\left(\frac{\partial T}{\partial \dot{q}_i}\right) - \frac{\partial T}{\partial q_i} + \frac{\partial U}{\partial q_i}\right]dq_i = 0 \tag{5.2.58}$$

This is Lagrange's energy equation for derivation of equation of motion in generalized co-ordinate.

Based on the above let us see how we can form the equation of motion for a structure having two degrees of freedom [Figure 5.2.14].

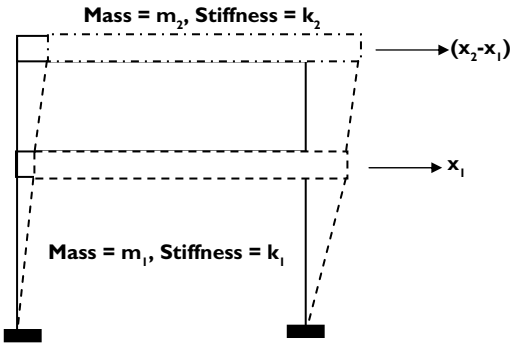


Figure 5.2.14 A two storied frame under free vibration.

Here, $KE = T = \frac{1}{2}m_1\dot{x}_1^2 + \frac{1}{2}m_2\dot{x}_2^2$, and $PE = U = \frac{1}{2}k_1x_1^2 + \frac{1}{2}k_2(x_2 - x_1)^2$

Based on Lagrange's equation we have

$$\frac{\partial T}{\partial x_1} = m_1\dot{x}_1; \quad \frac{d}{dt}\left(\frac{\partial T}{\partial x_1}\right) = m_1\ddot{x}_1. \tag{5.2.59}$$

Similarly

$$\frac{\partial U}{\partial x_1} = k_1x_1 - k_2(x_2 - x_1) \tag{5.2.60}$$

Thus combining the differential of the kinetic and potential energy in terms of x_1 we have

$$m_1\ddot{x}_1 + k_1x_1 - k_2(x_2 - x_1) = 0$$

Similarly we have for x_2

$$\frac{d}{dt}\left(\frac{\partial T}{\partial x_2}\right) = m_2\ddot{x}_2; \quad \text{and} \quad \frac{\partial U}{\partial x_2} = k_2(x_2 - x_1)$$

Thus combining the two terms we have

$$m_2\ddot{x}_2 + k_2(x_2 - x_1) = 0$$

Now writing the equations in matrix notation we have

$$\begin{bmatrix} m_1 & 0 \\ 0 & m_2 \end{bmatrix} \begin{Bmatrix} \ddot{x}_1 \\ \ddot{x}_2 \end{Bmatrix} + \begin{bmatrix} k_1 + k_2 & -k_2 \\ -k_2 & k_2 \end{bmatrix} \begin{Bmatrix} x_1 \\ x_2 \end{Bmatrix} = 0 \tag{5.2.61}$$

This is the same expression we had derived based on D'Alembert's equation.

5.2.3 Direct integration technique, the alternate approach

This technique is also otherwise known as *step-by-step integration* and is basically a numerical method based on the *principles of finite difference*.

Before we get into the detail of the topic it would be worthwhile to understand the advantage of this method.

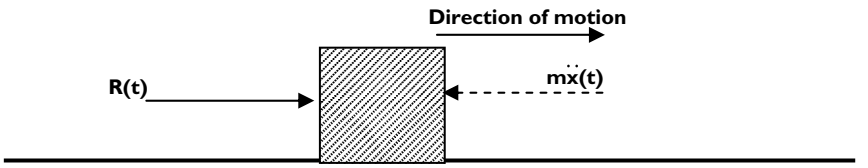


Figure 5.2.15 Free body diagram of a body in motion.

We had already stated while explaining the modal response technique that there are situations when due to the non-proportional damping the matrix does not de-couple and the analyst find it difficult to predict the damping ratio specially when the material are widely varying.

- He at best guesses a value of the damping ratio for different and lives with it or... Does the operation $[\varphi]^T[C][\varphi]$ and considers only the diagonal terms neglecting the off-diagonal terms as *secondary effects*[14]. When his assumption of the neglecting the off-diagonal terms as secondary effect *may or may not be correct or accurate*.

It is in this type of cases that step-by-step integration is advantageous and much superior to modal response technique in predicting the response of the dynamic system because here no transformation of the equation is required as the integrals are directly operable on the acceleration velocity and the displacement vectors.

To understand the concept we go back a bit to our basic course of engineering mechanics (or high school level physics...) in undergraduate class.

We pose the question...

Why does a body move in space?

The answer is that it moves because it has an unbalanced force within the system and tends to move in the same direction in which the unbalanced force works.

Now if we want to formulate the equation of motion as per D'Alembert's principle we apply a *fictitious force* in the direction opposite to the motion (i.e. the unbalanced force) and state the body to be in a condition *of dynamic equilibrium* at an instant of time t when the *laws of static do apply* (Figure 5.2.15).

The equation of motion is then depicted by

$$m\ddot{x} = R(t) \quad \text{where } \ddot{x} = \frac{d^2x}{dt^2} \text{ and the above can then be depicted as}$$

$$F_m(t) = R(t) \quad \text{where } F_m(t) \text{ is the inertial force of the system.}$$

14 There are techniques by which non-proportional damping can be to certain extent modified to de-couple. We will study this technique in our chapter of Analysis and design of Machine foundation.

For a body in motion having n degrees of freedom the equation of motion is given by

$$[M][\ddot{X}] + [C][\dot{X}] + [K][X] = R(t) \tag{5.2.62}$$

Then at any instantaneous time Δt (we can write the above equation as)

$$F(m)_{\Delta t} + F(c)_{\Delta t} + F(k)_{\Delta t} = R(t)_{\Delta t} \tag{5.2.63}$$

where $F(m)_{\Delta t}$ = inertial force; $F(c)_{\Delta t}$ = damping force and $F(k)_{\Delta t}$ = stiffness force.
Thus,

$$\sum [\text{Inertial force} + \text{Damping force} + \text{Stiffness force}]$$

$$= \text{External force at any instant of time} \Delta t.$$

From the above expression it is quite obvious that the dynamic equation of motion is under static equilibrium at the time instant Δt.

Now suppose by some mathematical manipulation we can express each of the force terms in terms of displacement term say Δx, then we can represent the above equation of motion as follows:

$$f(m)\Delta x + f(c)\Delta x + f(k)\Delta x = R(t)_{\Delta t} \tag{5.2.64}$$

where, $f(m)\Delta x$ = function of $F(m)_{\Delta t}$ in terms of Δx; $f(c)\Delta x$ = function of $F(c)_{\Delta t}$ in terms of Δx, and $f(k)\Delta x$ = function of $F(k)_{\Delta t}$ in terms of Δx.

From which we can develop an expression

$$f(m, c, k)\Delta x = R(t)$$

when

$$\Delta x = \frac{R(t)}{f(m, c, k)} \tag{5.2.65}$$

The value of $\Delta x = \frac{R(t)}{f(m,c,k)}$, thus obtained, becomes the initial input for finding out the displacement of the next step at an interval $2\Delta t$ and so on...

This is known as *step-by-step integration* and is usually carried out based on *finite difference equation.*

5.2.3.1 The central difference technique

The equation of motion for a dynamic system having n degrees of freedom at any instant of time t is given by

$$[M]\{\ddot{X}(t)\} + [C]\{\dot{X}(t)\} + [K]\{X(t)\} = \{R(t)\} \tag{5.2.66}$$

Now applying *central difference formula*[15] to $\{\ddot{X}\}$ and *average central difference* formula to $\{\dot{X}\}$ for *time step increment of* Δt, we have

$$\ddot{X}(t) = \frac{1}{\Delta t^2}[X(t+\Delta t) - 2X(t) + X(t-\Delta t)] \quad \text{and}$$
$$\dot{X}(t) = \frac{1}{2\Delta t}[X(t+\Delta t) - X(t-\Delta t)]$$

For easier manipulation while writing the equations let us represent the expressions as

$$\ddot{X}_t = \frac{1}{\Delta t^2}[X_{t+\Delta t} - 2X_t + X_{t-\Delta t}] \quad \text{and} \quad \dot{X}_t = \frac{1}{2\Delta t}[X_{t+\Delta t} - X_{t-\Delta t}]$$

Thus substituting the values of $\{\ddot{X}\}$ and $\{\dot{X}\}$ in the equation of motion we have

$$[M]\frac{1}{\Delta t^2}\{X_{t+\Delta t} - 2X_t + X_{t-\Delta t}\} + [C]\frac{1}{2\Delta t}\{X_{t+\Delta t} - X_{t-\Delta t}\} + [K]\{X(t)\} = \{R(t)\} \tag{5.2.67}$$

Now separating the terms of $X_{t+\Delta t}, X_t$ and $X_{t-\Delta t}$ we have

$$\left[\frac{M}{\Delta t^2} + \frac{C}{2\Delta t}\right] X_{t+\Delta t} = R_t - \left(K - \frac{2M}{\Delta t^2}\right) X_t - \left(\frac{M}{\Delta t^2} - \frac{C}{2\Delta t}\right) X_{t-\Delta t}$$

Now considering $\hat{M} = \left[\frac{M}{\Delta t^2} + \frac{C}{2\Delta t}\right]; \hat{K} = \left(K - \frac{2M}{\Delta t^2}\right)$ and $\hat{M}_0 = \left(\frac{M}{\Delta t^2} - \frac{C}{2\Delta t}\right)$, we can write the above equations as

$$\hat{M} \cdot X_{t+\Delta t} = R_t - \hat{K} \cdot X_t - \hat{M}_0 \cdot X_{t-\Delta t}. \tag{5.2.68}$$

It is obvious that in order to find out the value of $X_{t+\Delta t}$ it is necessary to find out the displacements at X_t and $X_{t-\Delta t}$.

15 Refer Chapter 2 (Vol. 1) where we have developed the theory of finite difference for second order differential equations.

Thus to calculate for the solution at time Δt a special condition has to be invoked.

Usually the displacement and velocity vector at time $t = 0$ is known as *the initial boundary condition*.

For instance if $X_{t=0} = 0$ and $\dot{X}_{t=0} = 0$ then we have

$$[M][\ddot{X}_0] + [C][0] + [K][0] = R_{t=0} \quad \rightarrow \quad [\ddot{X}_0] = [M]^{-1} R_{t=0}. \tag{5.2.69}$$

To find out the value of $[X]_{-\Delta t}$ we proceed as follows ...

We have seen earlier that based on *Taylor's series expansion* that

$$f(x-h) = f(x) - h\dot{f}(x) + \frac{h^2 f(x)}{2} + \cdots\cdots$$

Thus $X_{t-\Delta t}$ can be expressed as

$$X_{t-\Delta t} = X_t - \Delta t \dot{X}_t + \frac{\Delta t^2}{2}\ddot{X}_t + \cdots\cdots$$

Thus ignoring the higher order terms, $X_{-\Delta t}$ may be represented by

$$X_{-\Delta t} = X_0 - \Delta t \dot{X}_0 - \frac{\Delta t^2}{2} X_0$$

Thus once $X_{-\Delta t}$ is established we substitute the same in our equation of motion to obtain

$$\hat{M} \cdot X_{\Delta t} = R_0 - \hat{K} \cdot X_0 - \hat{M}_0 \cdot X_{-\Delta t} \tag{5.2.70}$$

and step by step proceed to find out the displacements at steps $X_{2\Delta t}, X_{3\Delta t} \ldots X_t$.

The above expression can be structured as follows

- Assemble the mass matrix M, Damping matrix C and stiffness matrix K
- Initialize $X_0, \dot{X}_0$
- Obtain $\{\ddot{X}_0\} = [M]^{-1}\{\{R_0\} - [C]\{\dot{X}_0\} - [K]\{X_0\}\}$
- Select time step Δt and calculate the integration constants
  - $\alpha_0 = \frac{1}{\Delta t^2}$, $\alpha_1 = \frac{1}{2\Delta t}$, $\alpha_2 = 2\alpha_0$, and $\alpha_3 = \frac{1}{\alpha_2}$
  - Calculate $X_{-\Delta t} = X_0 - \Delta t \dot{X}_0 + \alpha_3 \ddot{X}_0$
  - Form effective Mass matrix $\hat{M} = \alpha_0[M] + \alpha_1[C]$

- For each time step calculate.....
  - Calculate effective load at time t

$$\{\hat{R}_t\} = \{R_t\} - [[K] - \alpha_2[M]]\{X_t\} - [\alpha_0[M] - \alpha_1[C]]\{X_{t-\Delta t}\}$$

  - Solve for displacement at time $t + \Delta t$ by

$$[\hat{M}]\{X_{t+\Delta t}\} = \{\hat{R}_t\} \tag{5.2.71}$$

We show here a numerical problem of finding out the amplitude of a dynamic system based on Central Difference Technique with the following data:

Example 5.2.7

$$[M] = \begin{bmatrix} 50 & 0 \\ 0 & 100 \end{bmatrix} \quad [C] = \begin{bmatrix} 700 & -2800 \\ -2800 & 12300 \end{bmatrix} \quad [K] = \begin{bmatrix} 3000 & -1200 \\ -1200 & 51000 \end{bmatrix}$$

The load vector is given by $\{P\} = \begin{Bmatrix} 500 \sin 12.5t \\ 200 \sin 12.5t \end{Bmatrix}$

For a time step of 0.04 seconds determine the amplitudes by Central difference technique.

Solution:

We start with the following assumptions

- Let displacement vector be $\{X\} = \begin{Bmatrix} X_1 \\ X_2 \end{Bmatrix}$
- As the function is a sine curve hence at t = 0, $\{P\} = 0$ as such $\{X\}_{t=0} = 0$ and $\{\dot{X}\}_{t=0} = 0$

Thus

$$\begin{bmatrix} 50 & 0 \\ 0 & 100 \end{bmatrix} \begin{Bmatrix} \ddot{X}_1 \\ \ddot{X}_2 \end{Bmatrix} + \begin{bmatrix} 700 & -2800 \\ -2800 & 12300 \end{bmatrix} \begin{Bmatrix} \dot{X}_1 \\ \dot{X}_2 \end{Bmatrix}$$

$$+ \begin{bmatrix} 3000 & -1200 \\ -1200 & 51000 \end{bmatrix} \begin{Bmatrix} X_1 \\ X_2 \end{Bmatrix} = \begin{bmatrix} 500 \sin 12.5t \\ 200 \sin 12.5t \end{bmatrix}$$

$\therefore$ For $\{X\}_{t=0} = 0$ and $\{\dot{X}\}_{t=0} = 0$ we have

$$\begin{bmatrix}50 & 0\\ 0 & 100\end{bmatrix}\begin{Bmatrix}\ddot{X}_1\\ \ddot{X}_2\end{Bmatrix}+\begin{bmatrix}700 & -2800\\ -2800 & 12300\end{bmatrix}\begin{Bmatrix}0\\ 0\end{Bmatrix}$$

$$+\begin{bmatrix}3000 & -1200\\ -1200 & 51000\end{bmatrix}\begin{Bmatrix}0\\ 0\end{Bmatrix}=\begin{Bmatrix}500\sin 12.5t\\ 200\sin 12.5t\end{Bmatrix}$$

$$\rightarrow \quad \begin{Bmatrix}\ddot{X}_1\\ \ddot{X}_2\end{Bmatrix}_{t=0}=\begin{Bmatrix}0\\ 0\end{Bmatrix}$$

The integration constant are, $\alpha_0=\frac{1}{\Delta t^2}=\frac{1}{(0.04)^2}=625$; $\alpha_1=\frac{1}{2\Delta t}=\frac{1}{0.08}=12.5$

$$\alpha_2=2\alpha_0=2\times 625=1250; \quad \alpha_3=1/\alpha_2=1/1250=0.0008$$

Calculation of effective mass matrix

$$\alpha_0[M]=\begin{bmatrix}31250 & 0\\ 0 & 62500\end{bmatrix} \quad \text{and} \quad \alpha_1[C]=\begin{bmatrix}8750 & -35000\\ -35000 & 153750\end{bmatrix}$$

$$\rightarrow \quad [\hat{M}]=\alpha_0[M]+\alpha_1[C]=\begin{bmatrix}40000 & -35000\\ -35000 & 216250\end{bmatrix}$$

Inversion of the effective mass matrix

$$|\hat{M}|=40000\times 216250-35000\times 35000=7425000000$$

$$\text{Cofactor matrix of } [\hat{M}]=\begin{bmatrix}216250 & 35000\\ 35000 & 40000\end{bmatrix}=\text{adjoint Matrix of } [\hat{M}]$$

$$[\hat{M}]^{-1}=\frac{\text{Adj.}[\hat{M}]}{|M|}=\begin{bmatrix}29.12 & 4.71\\ 4.71 & 5.39\end{bmatrix}\times 10^{-6}$$

Calculation of effective stiffness matrix

$$[\hat{K}]=[K]-\alpha_2[M]=\begin{bmatrix}3000 & -1200\\ -1200 & 51000\end{bmatrix}-1250\times\begin{bmatrix}50 & 0\\ 0 & 100\end{bmatrix}$$

$$=\begin{bmatrix}-59500 & -1200\\ -1200 & -74000\end{bmatrix}$$

Calculation of effective inertial cum damping matrix

$$[\hat{M}_0] = \alpha_0[M] - \alpha_1[C] = 625 \times \begin{bmatrix} 50 & 0 \\ 0 & 100 \end{bmatrix} - 12.5 \times \begin{bmatrix} 700 & -2800 \\ -2800 & 12300 \end{bmatrix}$$

$$= \begin{bmatrix} 22500 & 35000 \\ 35000 & -91250 \end{bmatrix}$$

Setting up of initial condition

Now, $\{X\}_{-0.04} = \{X\}_0 - 0.04 \times \{\dot{X}\}_0 - \frac{(0.04)^2}{2}\{\ddot{X}\}_0 = \begin{Bmatrix} 0 \\ 0 \end{Bmatrix}$

Start of step by step integration

1 At $\Delta t = 0.04$

$$\{\hat{R}\}_{0.04} = \{R\}_{0.04} - [\hat{K}]\{X\}_0 - [\hat{M}_0]\{X\}_{-0.04} \quad \text{or,}$$

$$\{\hat{R}\}_{0.04} = \begin{Bmatrix} 500 \sin 12.5t \\ 200 \sin 12.5t \end{Bmatrix} - \begin{bmatrix} -59500 & -1200 \\ -1200 & -74000 \end{bmatrix} \begin{Bmatrix} 0 \\ 0 \end{Bmatrix}$$

$$- \begin{bmatrix} 22500 & 35000 \\ 35000 & -91250 \end{bmatrix} \begin{Bmatrix} 0 \\ 0 \end{Bmatrix} \quad \text{with } t = 0.04$$

$$\rightarrow \quad \{\hat{R}\}_{0.04} = \begin{Bmatrix} 239.713 \\ 95.885 \end{Bmatrix}$$

$$\therefore \begin{Bmatrix} X_1 \\ X_2 \end{Bmatrix}_{t=0.04} = \begin{bmatrix} 29.12 & 4.71 \\ 4.71 & 5.39 \end{bmatrix} \times 10^{-6} \left\{\hat{R}\right\}_0 = \begin{bmatrix} 29.12 & 4.71 \\ 4.71 & 5.39 \end{bmatrix}$$

$$\times \begin{Bmatrix} 239.713 \\ 95.885 \end{Bmatrix} 10^{-6} = \begin{Bmatrix} 239.713 \\ 95.885 \end{Bmatrix} \times 10^{-3}$$

2 At $\Delta t = 0.08$

$$\{\hat{R}\}_{0.08} = \{R\}_{0.08} - [\hat{K}]\{X\}_{0.04} - [\hat{M}_0]\{X\}_0$$

$$= \begin{Bmatrix} 500 \sin 12.5t \\ 200 \sin 12.5t \end{Bmatrix} - \begin{bmatrix} -59500 & -1200 \\ -1200 & -74000 \end{bmatrix} \begin{Bmatrix} 7.4316 \\ 1.6458 \end{Bmatrix} \times 10^{-3}$$

$$- \begin{bmatrix} 22500 & 35000 \\ 35000 & -91250 \end{bmatrix} \begin{Bmatrix} 0 \\ 0 \end{Bmatrix} \quad \text{with } \Delta t = 0.08$$

$$\rightarrow \quad \{\hat{R}\}_{0.08} = \begin{Bmatrix} 420.73 \\ 168.29 \end{Bmatrix} + \begin{Bmatrix} 444.15 \\ 130.77 \end{Bmatrix} - \begin{Bmatrix} 0 \\ 0 \end{Bmatrix} = \begin{Bmatrix} 864.88 \\ 299.06 \end{Bmatrix}$$

$$\therefore \begin{Bmatrix} X_1 \\ X_2 \end{Bmatrix}_{t=0.08} = \begin{bmatrix} 29.12 & 4.71 \\ 4.71 & 5.39 \end{bmatrix} \times 10^{-6} \left\{\hat{R}\right\}_{0.08}$$

$$= \begin{bmatrix} 29.12 & 4.71 \\ 4.71 & 5.39 \end{bmatrix} \begin{Bmatrix} 864.88 \\ 299.06 \end{Bmatrix} \times 10^{-6} = \begin{Bmatrix} 0.0265 \\ 0.00568 \end{Bmatrix}$$

3 At $\Delta t = 0.12$

$$\{\hat{R}\}_{0.12} = \{R\}_{0.12} - [\hat{K}]\{X\}_{0.08} - [\hat{M}_0]\{X\}_{0.04}$$

$$= \begin{Bmatrix} 500 \sin 12.5t \\ 200 \sin 12.5t \end{Bmatrix} - \begin{bmatrix} -59500 & -1200 \\ -1200 & -74000 \end{bmatrix} \begin{Bmatrix} 0.0265 \\ 0.00568 \end{Bmatrix}$$

$$- \begin{bmatrix} 22500 & 35000 \\ 35000 & -91250 \end{bmatrix} \begin{Bmatrix} 7.4316 \times 10^{-3} \\ 1.6458 \times 10^{-3} \end{Bmatrix} \text{ with } \Delta t = 0.12$$

$$\rightarrow \quad \{\hat{R}\}_{0.12} = \begin{Bmatrix} 498.747 \\ 199.499 \end{Bmatrix} + \begin{Bmatrix} 1583.566 \\ 452.120 \end{Bmatrix} - \begin{Bmatrix} 224.814 \\ 109.926 \end{Bmatrix} = \begin{Bmatrix} 1857.499 \\ 541.693 \end{Bmatrix}$$

$$\begin{Bmatrix} X_1 \\ X_2 \end{Bmatrix}_{t=0.12} = \begin{bmatrix} 29.12 & 4.71 \\ 4.71 & 5.39 \end{bmatrix} \times 10^{-6} \{\hat{R}\}_{0.12}$$

$$= \begin{bmatrix} 29.12 & 4.71 \\ 4.71 & 5.39 \end{bmatrix} \begin{Bmatrix} 1857.499 \\ 541.6593 \end{Bmatrix} \times 10^{-6} = \begin{Bmatrix} 0.0566 \\ 0.0116 \end{Bmatrix}$$

In this way we can proceed to find out step by step the displacement for each time step at an increment of time @ 0.04 sec.

The table below gives the value of displacement and force for 30 time steps based CDT and plotted in Figure 5.2.16.

Sl. No.	*Time step*	R_1	R_2	X_1	X_2
1	0.04	239.7128	95.88511	0.00743	0.00165
2	0.08	865.0056	299.0563	0.02660	0.00569
3	0.12	1863.547	542.4456	0.05683	0.01171
4	0.16	3052.544	704.3392	0.09222	0.01818
5	0.2	4119.941	655.0561	0.12308	0.02295
6	0.24	4709.854	305.5834	0.13861	0.02385
7	0.28	4528.179	−352.7345	0.13022	0.01944
8	0.32	3439.481	−1231.554	0.09437	0.00958
9	0.36	1527.15	−2156.784	0.03431	−0.00442
10	0.4	−901.792	−2906.572	−0.03997	−0.01991
11	0.44	−3371.882	−3266.585	−0.11360	−0.03349
12	0.48	−5343.218	−3088.552	−0.17018	−0.04183
13	0.52	−6339.924	−2336.345	−0.19566	−0.04247
14	0.56	−6071.389	−1106.647	−0.18204	−0.03458
15	0.6	−4515.196	382.7451	−0.12970	−0.01922
16	0.64	−1939.169	1835.805	−0.04782	0.00075
17	0.68	1145.615	2943.208	0.04724	0.02126

(*continued*)

Sl. No.	Time step	R_1	R_2	X_1	X_2
18	0.72	4092.124	3454.226	0.13546	0.03790
19	0.76	6261.167	3238.21	0.19762	0.04696
20	0.8	7168.248	2320.254	0.21971	0.04629
21	0.84	6598.443	881.4853	0.19633	0.03585
22	0.88	4661.193	−777.2352	0.13209	0.01778
23	0.92	1770.754	−2300.583	0.04073	−0.00405
24	0.96	−1444.358	−3358.237	−0.05790	−0.02490
25	1	−4282.619	−3720.077	−0.14227	−0.04023
26	1.04	−6128.804	−3309.321	−0.19410	−0.04672
27	1.08	−6594.064	−2220.837	−0.20252	−0.04305
28	1.12	−5603.828	−699.9693	−0.16651	−0.03019
29	1.16	−3412.734	913.4549	−0.09509	−0.01117
30	1.2	−543.0643	2262.977	−0.00515	0.00963

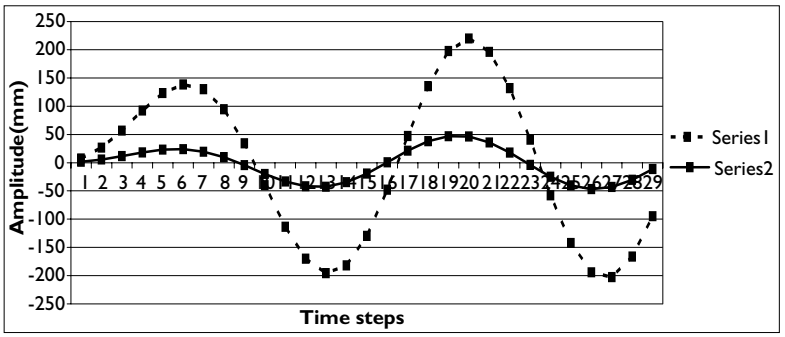


Figure 5.2.16 Time history response for first 30 steps ased on CDT.

5.2.4 Wilson-Theta method

The method was developed by Wilson et al. (1973) wherein a linear variation of acceleration with time between t and $t + \Delta t$ has been assumed.

Referring to Figure 5.2.17, which shows linear variation of acceleration with time t to $t + \theta\Delta t$, θ is assumed to be ≥ 1.4. Let τ denote the increase in time such that, $0 \leq \tau \leq \theta\Delta t$.

Then by similar triangle

$$\frac{\ddot{X}_{t+\theta\Delta t} - \ddot{X}_t}{t + \theta\Delta t - t} = \frac{\ddot{X}_{t+\tau} - \ddot{X}_t}{t + \tau - t} \tag{5.2.72}$$

$$\text{or}, \quad \frac{\ddot{X}_{t+\tau} - \ddot{X}_t}{\tau} = \frac{\ddot{X}_{t+\theta\Delta t} - \ddot{X}_t}{\theta\Delta t} \quad \rightarrow \quad \{\ddot{X}_{t+\tau}\} = \{\ddot{X}_t\} + \frac{\tau}{\theta\Delta t}\{\ddot{X}_{t+\theta\Delta t} - \ddot{X}_t\} \tag{5.2.73}$$

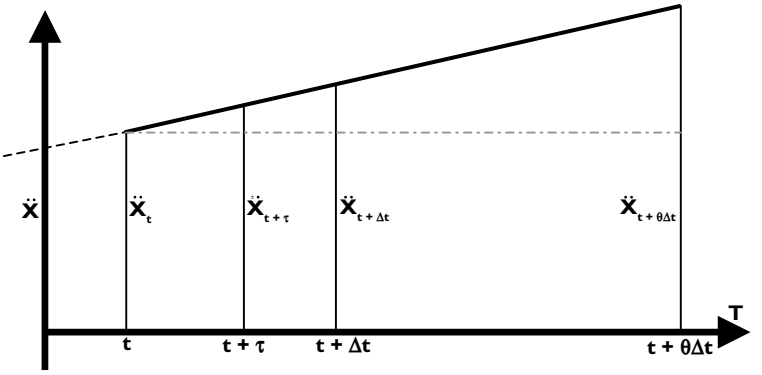


Figure 5.2.17 Linear variation of time period with respect to time.

To find the velocity vector at time interval $t+\tau$, we integrate the L.H.S. between $t+\tau$ to t and right hand side between τ to 0, to have

$$\int_{t}^{t+\tau} \{\ddot{X}_{t+\tau}\}dt = \int_{0}^{\tau} \{\ddot{X}_t\}dt + \int_{0}^{\tau} \frac{\tau}{\theta\Delta t}\{\ddot{X}_{t+\theta\Delta t} - \ddot{X}_t\}dt$$

$$\rightarrow \quad \{\dot{X}_{t+\tau}\} = \{\dot{X}_t\} + \tau\{\ddot{X}_t\} + \frac{\tau^2}{2\theta\Delta t}\{\ddot{X}_{t+\theta\Delta t} - \ddot{X}_t\} \tag{5.2.74}$$

To find out the displacement vector at $t+\tau$ we have on further integration of the velocity vector

$$\int_{t}^{t+\tau} \{\dot{X}_{t+\tau}\}dt = \int_{0}^{\tau} \{\dot{X}_t\}dt + \int_{0}^{\tau} \tau\{\ddot{X}_t\}dt + \int_{0}^{\tau} \frac{\tau^2}{2\theta\Delta t}\{\ddot{X}_{t+\theta\Delta t} - \ddot{X}_t\}\cdot dt$$

$$\rightarrow \quad \{X_{t+\tau}\} = \{X_t\} + \tau\{\dot{X}_t\} + \frac{\tau^2}{2}\{\ddot{X}_t\} + \frac{\tau^3}{6\theta\Delta t}\{\ddot{X}_{t+\theta\Delta t} - \ddot{X}_t\} \tag{5.2.75}$$

For $\tau = \theta\Delta t$, we have

$$\{\dot{X}_{t+\theta\Delta t}\} = \{\dot{X}_t\} + \theta\Delta t\{\ddot{X}_t\} + \frac{\theta^2\Delta t^2}{2\theta\Delta t}\{\ddot{X}_{t+\theta\Delta t} - \ddot{X}_t\}$$

Thus,

$$\{\dot{X}_{t+\theta\Delta t}\} = \{\dot{X}_t\} + \frac{\theta\Delta t}{2}\{\ddot{X}_{t+\theta\Delta t} + \ddot{X}_t\} \quad \text{and}$$

$$\{X_{t+\theta\Delta t}\} = \{X_t\} + \theta\Delta t\{\dot{X}_t\} + \frac{\theta^2\Delta t^2}{6}\{\ddot{X}_{t+\theta\Delta t} + 2\ddot{X}_t\}$$

The above two equations can be solved to obtain $\{\ddot{X}_{t+\theta\Delta t}\}$ and $\{\dot{X}_{t+\theta\Delta t}\}$ in terms of $\{X_{t+\theta\Delta t}\}$ and this gives:

$$\{\ddot{X}_{t+\theta\Delta t}\} = \frac{6}{\theta^2\Delta t^2}\{X_{t+\theta\Delta t} - X_t\} - \frac{6}{\theta\Delta t}\{\dot{X}_t\} - 2\{\ddot{X}_t\}$$
$$\{\dot{X}_{t+\theta\Delta t}\} = \frac{3}{\theta\Delta t}\{X_{t+\theta\Delta t} - X_t\} - 2\{\dot{X}_t\} - \frac{\theta\Delta t}{2}\{\ddot{X}_t\} \tag{5.2.76}$$

To start the solution for the dynamic equation we start with the expression

$$[M]\{\ddot{X}_{t+\theta\Delta t}\} + [C]\{\dot{X}_{t+\theta\Delta t}\} + [K]\{X_{t+\theta\Delta t}\} = \{R_{t+\theta\Delta t}\} \tag{5.2.77}$$

Now as acceleration is varying linearly hence the applied force within this small time step can also be assumed to vary linearly. Thus we can draw a similar force diagram as shown in Figure 5.2.18.

By similar triangle we have

$$\frac{R_{t+\theta\Delta t} - R_t}{t + \theta\Delta t - t} = \frac{R_{t+\Delta t} - R_t}{t + \Delta t - t}$$

or $$R_{t+\theta\Delta t} = R_t + \theta\,(R_{t+\Delta t} - R_t) \tag{5.2.78}$$

Now substituting the value of $\{\ddot{X}_{t+\theta\Delta t}\}$ and $\{\dot{X}_{t+\theta\Delta t}\}$ in the equilibrium equation we have

$$[M]\frac{6}{\theta^2\Delta t^2}\{X_{t+\theta\Delta t} - X_t\} - [M]\frac{6}{\theta\Delta t}\{\dot{X}_t\} - 2[M]\{X_t\} + [C]\frac{3}{\theta\Delta t}\{X_{t+\theta\Delta t} - X_t\}$$
$$- 2[C]\{\dot{X}_t\} - \frac{\theta\Delta t}{2}[C]\{\ddot{X}_t\} + [K]\{X_{t+\theta\Delta t}\} = \{R_t\} + \theta\{R_{t+\Delta t} - R_t\}$$

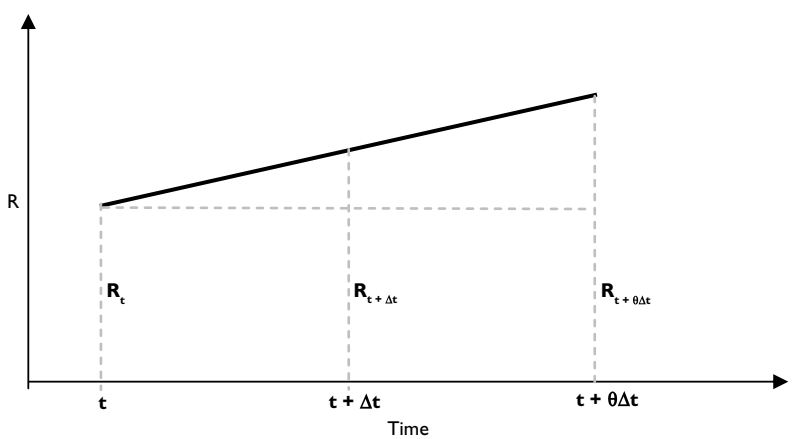


Figure 5.2.18 Linear variation of *R* with time.

The above equation can be further simplified to

$$\left[\frac{6[M]}{\theta^2\Delta t^2}+\frac{3[C]}{\theta\Delta t}+[K]\right]\{X_{t+\theta\Delta t}\}-\left[\frac{6[M]}{\theta^2\Delta t^2}+\frac{3[C]}{\theta\Delta t}\right]\{X_t\}$$

$$-\left[\frac{6[M]}{\theta^2\Delta t^2}+2[C]\right]\{\dot{X}_t\}-\left[2[M]-\frac{\theta\Delta t}{2}[C]\right]\{\ddot{X}_t\}=\{R_{t+\theta\Delta t}\}$$

The above expression can now be further simplified and written in more compact form as

$$[\hat{K}]\cdot\{X_{t+\theta\Delta t}\}=\{\hat{R}_{t+\theta\Delta t}\}+[\hat{M}_0]\{X_t\}+[\hat{M}_1]\{\dot{X}_t\}+[\hat{M}_2]\{\ddot{X}_t\} \tag{5.2.79}$$

where, $[\hat{K}]=\left[\frac{6[M]}{\theta^2\Delta t^2}+\frac{3[C]}{\theta\Delta t}+[K]\right]$; $[\hat{M}_0]=\left[\frac{6[M]}{\theta^2\Delta t^2}+\frac{3[C]}{\theta\Delta t}\right]$;

$[\hat{M}_1]=\left[\frac{6[M]}{\theta^2\Delta t^2}+2[C]\right]\{\dot{X}_t\}$; $[\hat{M}_2]=\left[2[M]-\frac{\theta\Delta t}{2}[C]\right]$.

We have,

$$\{\hat{R}_{t+\theta\Delta t}\}=\{R_t\}+\theta\{R_{t+\Delta t}-R_t\} \tag{5.2.80}$$

from which we can find out the value of $\{X_{t+\theta\Delta t}\}$.

Once $X_{t+\theta\Delta t}$ is obtained we can now back-substitute its values in the equations

$$\{\ddot{X}_{t+\theta\Delta t}\}=\frac{6}{\theta^2\Delta t^2}\{X_{t+\theta\Delta t}-X_t\}-\frac{6}{\theta\Delta t}\{\dot{X}_t\}-2\{\ddot{X}_t\} \quad \text{and}$$

$$\{\dot{X}_{t+\theta\Delta t}\}=\frac{3}{\theta\Delta t}\{X_{t+\theta\Delta t}-X_t\}-2\{\dot{X}_t\}-\frac{\theta\Delta t}{2}\{\ddot{X}_t\} \tag{5.2.81}$$

Thus all data at the time intervals $t+\theta\Delta t$ is evaluated.

The above method can thus be structured as follows:

- Assemble the mass matrix $[M]$ the damping matrix $[C]$ and stiffness matrix $[K]$
- Initialize $\{X_0\}$ and $\{\dot{X}_0\}$
- Evaluate $\{\ddot{X}_0\}$ (Refer Central difference method to see how this is evaluated)
- Select the time step Δt and calculate the integration constant θ (this usually taken as 1.4)
- Select the values

$$\alpha_0=\frac{6}{\theta^2\Delta t^2},\quad \alpha_1=\frac{3}{\theta\Delta t},\quad \alpha_2=2\alpha_1,\quad \alpha_3=\frac{\theta\Delta t}{2},\quad \alpha_4=\frac{\alpha_0}{\theta},$$

$$\alpha_5=\frac{-\alpha_2}{\theta},\quad \alpha_6=1-\frac{3}{\theta},\quad \alpha_7=\frac{\Delta t}{2},\quad \alpha_8=\frac{\Delta t^2}{6}.$$

- Form modified stiffness matrix $[\hat{K}]$

$$[\hat{K}] = [K] + \alpha_0[M] + \alpha_1[C]$$

- Calculate the external load $\{\hat{R}_{t+\theta\Delta t}\}$

$$\{\hat{R}_{t+\theta\Delta t}\} = \{R_t\} + \theta\{R_{t+\Delta t} - R_t\} + [M]\{\alpha_0\{X_t\} + \alpha_2\{\dot{X}_t\} + 2\{\ddot{X}_t\}\}$$
$$+ [C]\{\alpha_1\{X_t\} + 2\{\dot{X}_t\} + \alpha_3\{\ddot{X}_t\}\}$$

- Solve for displacement at time $t + \theta\Delta t$

$$[\hat{K}]\ \{X_{t+\theta\Delta t}\} = \{\hat{R}_{t+\theta\Delta t}\}$$

- Calculate the acceleration, velocity and at time displacement $t + \Delta t$
  - $\{\ddot{X}_{t+\Delta t}\} = \alpha_4\{X_{t+\theta\Delta t} - X_t\} + \alpha_5\{\dot{X}_t\} + \alpha_6\{\ddot{X}_t\}$
  - $\{\dot{X}_{t+\Delta t}\} = \{\dot{X}_t\} + \alpha_7\{\ddot{X}_{t+\Delta t} + \ddot{X}_t\}$
  - $\{X_{t+\Delta t}\} = \{X_t\} + \{\dot{X}_t\}\Delta t + \alpha_8\{\ddot{X}_{t+\Delta t} + 2\ddot{X}_t\}$

We repeat the numerical problem in Example 5.2.7, for finding out the amplitude of a dynamic system based on Wilson-θ method with the following data:

Example 5.2.8

$$[M] = \begin{bmatrix} 50 & 0 \\ 0 & 100 \end{bmatrix} \quad [C] = \begin{bmatrix} 700 & -2800 \\ -2800 & 12300 \end{bmatrix} \quad [K] = \begin{bmatrix} 3000 & -1200 \\ -1200 & 51000 \end{bmatrix}$$

The load vector is given by $\{P\} = \begin{Bmatrix} 500\sin 12.5t \\ 200\sin 12.5t \end{Bmatrix}$

For a time step of 0.04 seconds determine the amplitudes by Wison-θ method. Consider $\theta = 1.4$.

Solution:

We start with the following assumptions

- Let displacement vector be $\{X\} = \begin{Bmatrix} X_1 \\ X_2 \end{Bmatrix}$
- As the function is a sine curve hence at $t = 0\{P\} = 0$ as such $\{X\}_t = 0 = 0$ and $\{\dot{X}\}_{t=0} = 0$

Thus

$$\begin{bmatrix}50 & 0\\ 0 & 100\end{bmatrix}\begin{Bmatrix}\ddot{X}_1\\ \ddot{X}_2\end{Bmatrix}+\begin{bmatrix}700 & -2800\\ -2800 & 12300\end{bmatrix}\begin{Bmatrix}\dot{X}_1\\ X_2\end{Bmatrix}+\begin{bmatrix}3000 & -1200\\ -1200 & 51000\end{bmatrix}\begin{Bmatrix}X_1\\ X_2\end{Bmatrix}$$

$$=\begin{Bmatrix}500\sin 12.5t\\ 200\sin 12.5t\end{Bmatrix}$$

$\therefore$ For $\{X\}_{t=0}=0$ and $\{\dot{X}\}_{t=0}=0$ we have,

$$\begin{bmatrix}50 & 0\\ 0 & 100\end{bmatrix}\begin{Bmatrix}\ddot{X}_1\\ \ddot{X}_2\end{Bmatrix}+\begin{bmatrix}700 & -2800\\ -2800 & 12300\end{bmatrix}\begin{Bmatrix}0\\ 0\end{Bmatrix}$$

$$+\begin{bmatrix}3000 & -1200\\ -1200 & 51000\end{bmatrix}\begin{Bmatrix}0\\ 0\end{Bmatrix}=\begin{Bmatrix}500\sin 12.5t\\ 200\sin 12.5t\end{Bmatrix}$$

or, $$\begin{Bmatrix}\ddot{X}_1\\ \ddot{X}_2\end{Bmatrix}_{t=0}=\begin{Bmatrix}0\\ 0\end{Bmatrix}$$

The integration constant are

$$\alpha_0=\frac{6}{(\theta\Delta t)^2}=1913,\quad \alpha_1=\frac{3}{\theta\Delta t}=53.57,\quad \alpha_2=2\alpha_1=107.14,$$

$$\alpha_3=\frac{\theta\Delta t}{2}=0.028,\quad \alpha_4=\frac{\alpha_0}{\theta}=1366,\quad \alpha_5=\frac{-\alpha_2}{\theta}=-76.53,$$

$$\alpha_6=1-\frac{3}{\theta}=-1.14,\quad \alpha_7=\frac{\Delta t}{2}=0.02,\quad \alpha_8=\frac{\Delta t^2}{6}=0.000266$$

$$[\hat{K}]=[K]+\alpha_0[M]+\alpha_1[C]$$

$$[\hat{K}]=\begin{bmatrix}3000 & -1200\\ -1200 & 51000\end{bmatrix}+1913\begin{bmatrix}50 & 0\\ 0 & 100\end{bmatrix}+53.57\begin{bmatrix}700 & -2800\\ -2800 & 12300\end{bmatrix}$$

$$=\begin{bmatrix}136150 & -151160\\ -151160 & 901211\end{bmatrix}$$

$$[\hat{K}]=136150\times 901211-(151160)^2=9.985\times 10^{10}$$

$$\text{Adj.}[\hat{K}]=\begin{bmatrix}901211 & 151160\\ 151160 & 136150\end{bmatrix};\quad [\hat{K}]^{-1}=\begin{bmatrix}9.03 & 1.514\\ 1.514 & 1.363\end{bmatrix}\times 10^{-6}$$

Now, $\{\hat{R}_{t+\theta\Delta t}\} = \{R_t\} + \theta\{R_{t+\Delta t} - R_t\} + [M]\{\alpha_0 X_t + \alpha_2 \dot{X}_t + 2\ddot{X}_t\}$

$$+ [C]\{\alpha_1 X_t + 2\dot{X}_t + \alpha_3 \ddot{X}_t\}$$

At $t = 0.04$ sec

$$\{\hat{R}\}_{0.04} = \begin{Bmatrix} 500 \sin 12.5 \times 0.4 \\ 200 \sin 12.5 \times 0.4 \end{Bmatrix} + 1.4 \left\{ \begin{Bmatrix} 500 \sin 12.5 \times 0.04 \\ 200 \sin 12.5 \times 0.04 \end{Bmatrix} - \begin{Bmatrix} 0 \\ 0 \end{Bmatrix} \right\}$$

$$+ \begin{bmatrix} 50 & 0 \\ 0 & 100 \end{bmatrix} \left\{ 1913 \begin{Bmatrix} 0 \\ 0 \end{Bmatrix} + 107 \begin{Bmatrix} 0 \\ 0 \end{Bmatrix} + 2 \begin{Bmatrix} 0 \\ 0 \end{Bmatrix} \right\}$$

$$+ \begin{bmatrix} 700 & -2800 \\ -2800 & 12300 \end{bmatrix} \left\{ 53.57 \begin{Bmatrix} 0 \\ 0 \end{Bmatrix} + 2 \begin{Bmatrix} 0 \\ 0 \end{Bmatrix} + 0.028 \begin{Bmatrix} 0 \\ 0 \end{Bmatrix} \right\}$$

$$= \begin{Bmatrix} 575.28 \\ 230.20 \end{Bmatrix}$$

As $[\hat{K}]\{X_{t+\theta\Delta t}\} = \{\hat{R}_{t+\theta\Delta t}\}$

$$\{\hat{X}\}_{0.04} = \begin{bmatrix} 9.03 & 1.514 \\ 1.514 & 1.363 \end{bmatrix} \begin{Bmatrix} 575.28 \\ 230.20 \end{Bmatrix} \times 10^{-6} = \begin{Bmatrix} 5.543 \\ 1.185 \end{Bmatrix} \times 10^{-3}$$

$$\{\ddot{X}_{t+\Delta t}\} = \alpha_4\{X_{t+\theta\Delta t} - X_t\} + \alpha_5\{\dot{X}_t\} + \alpha_6\{\ddot{X}_t\}$$

$$= 1366.42 \left\{ \begin{Bmatrix} 5.543 \times 10^{-3} \\ 1.185 \times 10^{-3} \end{Bmatrix} - \begin{Bmatrix} 0 \\ 0 \end{Bmatrix} \right\} - 76.53 \begin{Bmatrix} 0 \\ 0 \end{Bmatrix} - 1.14 \begin{Bmatrix} 0 \\ 0 \end{Bmatrix}$$

$$= \begin{Bmatrix} 7.5714 \\ 1.619 \end{Bmatrix}$$

$$\{\dot{X}_{t+\Delta t}\} = \{\dot{X}_t\} + \alpha_7\{\ddot{X}_{t+\Delta t} + \ddot{X}_t\} = \begin{Bmatrix} 0 \\ 0 \end{Bmatrix} + 0.02 \left\{ \begin{Bmatrix} 7.574 \\ 1.619 \end{Bmatrix} + \begin{Bmatrix} 0 \\ 0 \end{Bmatrix} \right\}$$

$$= \begin{Bmatrix} 0.15148 \\ 0.0324 \end{Bmatrix}$$

$$\{X_{t+\Delta t}\} = \{X_t\} + \{\dot{X}_t\}\Delta t + \alpha_8\{\ddot{X}_{t+\Delta t} + 2\ddot{X}_t\}$$

$$= \begin{Bmatrix} 0 \\ 0 \end{Bmatrix} + 0.04 \begin{Bmatrix} 0 \\ 0 \end{Bmatrix} + 0.000266 \left\{ \begin{Bmatrix} 7.5714 \\ 1.619 \end{Bmatrix} + \begin{Bmatrix} 0 \\ 0 \end{Bmatrix} \right\}$$

$$= \begin{Bmatrix} 2.014 \times 10^{-3} \\ 4.306 \times 10^{-4} \end{Bmatrix}$$

At $t = 0.08$ again

$$\{\hat{R}_{t+\theta\Delta t}\} = \{R_t\} + \theta\{R_{t+\Delta t} - R_t\} + [M]\{\alpha_0 X_t + \alpha_2 \dot{X}_t + 2\ddot{X}_t\}$$

$$+ [C]\{\alpha_1 X_t + 2\dot{X}_t + \alpha_3 \ddot{X}_t\}$$

$$\{\hat{R}\}_{0.08} = \begin{Bmatrix} 500 \sin 12.5 \times 0.08 \\ 200 \sin 12.5 \times 0.08 \end{Bmatrix} + 1.4 \left\{ \begin{Bmatrix} 420.735 \\ 168.294 \end{Bmatrix} - \begin{Bmatrix} 239.713 \\ 95.885 \end{Bmatrix} \right\}$$

$$+ \begin{bmatrix} 50 & 0 \\ 0 & 100 \end{bmatrix} \left\{ 1913 \begin{Bmatrix} 2.014 \times 10^{-3} \\ 4.306 \times 10^{-4} \end{Bmatrix} + 107 \begin{Bmatrix} 0.15148 \\ 0.0324 \end{Bmatrix} \right.$$

$$\left. + 2 \begin{Bmatrix} 7.574 \\ 1.619 \end{Bmatrix} \right\} + \begin{bmatrix} 700 & -2800 \\ -2800 & 12300 \end{bmatrix} \left\{ 53.57 \begin{Bmatrix} 2.014 \times 10^{-3} \\ 4.306 \times 10^{-4} \end{Bmatrix} \right.$$

$$\left. + 2 \begin{Bmatrix} 0.15148 \\ 0.0324 \end{Bmatrix} + 0.028 \begin{Bmatrix} 7.574 \\ 1.619 \end{Bmatrix} \right\} = \begin{Bmatrix} 2498.32 \\ 914.00 \end{Bmatrix}$$

$$\{\hat{X}\}_{0.08} = \begin{bmatrix} 9.03 & 1.514 \\ 1.514 & 1.363 \end{bmatrix} \begin{Bmatrix} 2498.32 \\ 914 \end{Bmatrix} \times 10^{-6} = \begin{Bmatrix} 0.02394 \\ 0.00502 \end{Bmatrix}$$

$\{\ddot{X}_{t+\Delta t}\} = \alpha_4\{X_{t+\theta\Delta t} - X_t\} + \alpha_5\{\dot{X}_t\} + \alpha_6\{\ddot{X}_t\}$ at $t = 0.08$ is

$$= 1366.42 \left\{ \begin{Bmatrix} 0.02394 \\ 0.00502 \end{Bmatrix} - \begin{Bmatrix} 2.014 \times 10^{-3} \\ 4.306 \times 10^{-4} \end{Bmatrix} \right\}$$

$$- 76.53 \begin{Bmatrix} 0.01548 \\ 0.0324 \end{Bmatrix} - 1.14 \begin{Bmatrix} 7.574 \\ 1.619 \end{Bmatrix} = \begin{Bmatrix} 9.726 \\ 1.946 \end{Bmatrix}$$

$\{\dot{X}_{t+\Delta t}\} = \{\dot{X}_t\} + \alpha_7\{\ddot{X}_{t+\Delta t} + \ddot{X}_t\}$ at $_{t=0.08}$

$$= \begin{Bmatrix} 0.15148 \\ 0.0324 \end{Bmatrix} + 0.02 \left\{ \begin{Bmatrix} 9.726 \\ 1.946 \end{Bmatrix} + \begin{Bmatrix} 7.5740 \\ 1.619 \end{Bmatrix} \right\} = \begin{Bmatrix} 0.49748 \\ 0.1037 \end{Bmatrix}$$

or, $\{X_{t+\Delta t}\} = \{X_t\} + \{\dot{X}_t\}\Delta t + \alpha_8\{\ddot{X}_{t+\Delta t} + 2\ddot{X}_t\}$ at $t = 0.08$ is

$$= \begin{Bmatrix} 2.014 \times 10^{-3} \\ 4.306 \times 10^{-4} \end{Bmatrix} + 0.04 \begin{Bmatrix} 0.15148 \\ 0.0324 \end{Bmatrix}$$

$$+ 0.000266 \left\{ \begin{Bmatrix} 9.726 \\ 1.946 \end{Bmatrix} + 2 \begin{Bmatrix} 7.5740 \\ 1.619 \end{Bmatrix} \right\}$$

$$= \begin{Bmatrix} 1.47 \times 10^{-2} \\ 3.1055 \times 10^{-4} \end{Bmatrix}$$

Thus, we proceed step by step to find out the displacement, velocity and acceleration at each time step.

The displacement time history for 30 time steps are shown hereafter.

The table below gives the force and amplitudes for 30 time steps based on Wilson-Theta Method and a plot is given in Figure 5.2.19.

Sl. No.	*Time step*	R_1 *(t)*	R_2 *(t)*	X_1 *(m)*	X_2 *(m)*
1	0.04	239.7128	95.88511	2.02×10^{-03}	4.32×10^{-04}
2	0.08	420.7355	168.2942	1.47×10^{-02}	3.11×10^{-03}
3	0.12	498.7475	199.499	4.17×10^{-02}	8.65×10^{-03}
4	0.16	454.6487	181.8595	7.93×10^{-02}	1.59×10^{-02}
5	0.20	299.2361	119.6944	1.18×10^{-01}	2.27×10^{-02}
6	0.24	70.56	28.224	1.46×10^{-01}	2.64×10^{-02}
7	0.28	−175.3916	−70.15665	1.51×10^{-01}	2.48×10^{-02}
8	0.32	−378.4012	−151.3605	1.26×10^{-01}	1.69×10^{-02}
9	0.36	−488.7651	−195.506	7.18×10^{-02}	3.41×10^{-03}
10	0.40	−479.4621	−191.7849	-4.80×10^{-03}	-1.35×10^{-02}
11	0.44	−352.7702	−141.1081	-8.92×10^{-02}	-3.02×10^{-02}
12	0.48	−139.7077	−55.8831	-1.64×10^{-01}	-4.29×10^{-02}
13	0.52	107.56	43.024	-2.10×10^{-01}	-4.83×10^{-02}
14	0.56	328.4933	131.3973	-2.17×10^{-01}	-4.44×10^{-02}
15	0.60	469.00	187.6	-1.80×10^{-01}	-3.13×10^{-02}
16	0.64	494.6791	197.8716	-1.04×10^{-01}	-1.13×10^{-02}
17	0.68	399.2436	159.6974	-3.57×10^{-03}	1.18×10^{-02}
18	0.72	206.0592	82.4237	1.00×10^{-01}	3.31×10^{-02}
19	0.76	−37.57556	−15.03022	1.86×10^{-01}	4.80×10^{-02}
20	0.80	−272.0106	−108.8042	2.34×10^{-01}	5.32×10^{-02}
21	0.84	−439.8479	−175.9392	2.35×10^{-01}	4.74×10^{-02}
22	0.88	−499.9951	−199.998	1.87×10^{-01}	3.17×10^{-02}
23	0.92	−437.7261	−175.0904	1.02×10^{-01}	9.56×10^{-03}
24	0.96	−268.2865	−107.3146	-2.91×10^{-03}	-1.43×10^{-02}
25	1.00	−33.16095	−13.26438	-1.04×10^{-01}	-3.48×10^{-02}
26	1.04	210.0835	84.03341	-1.80×10^{-01}	-4.74×10^{-02}
27	1.08	401.8922	160.7569	-2.15×10^{-01}	-4.96×10^{-02}
28	1.12	495.3037	198.1215	-2.02×10^{-01}	-4.11×10^{-02}
29	1.16	467.4475	186.979	-1.45×10^{-01}	-2.41×10^{-02}
30	1.20	325.1439	130.0576	-5.93×10^{-02}	-2.61×10^{-03}

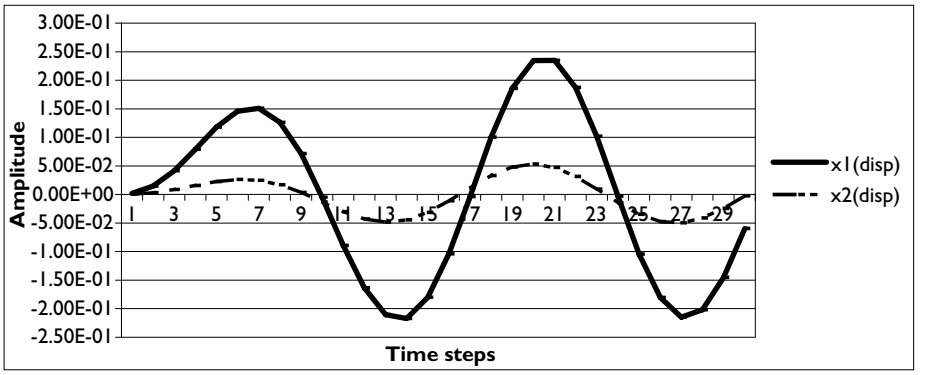


Figure 5.2.19 Time history response using Wilson-Theta method for first 30 steps.

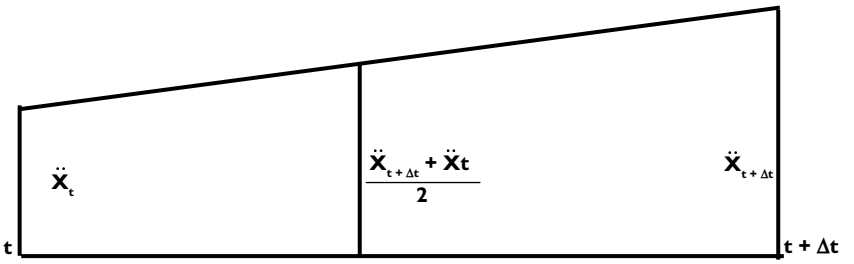


Figure 5.2.20 Description of Newmark's method.

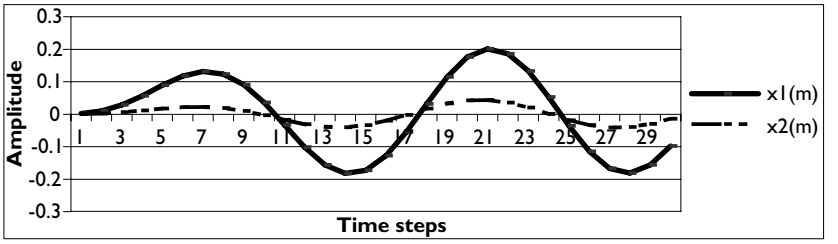


Figure 5.2.21 Time history response using Newmark-β method for first 30 steps.

5.2.4.1 Newmark-Beta method

Newmark (1959) developed an integration scheme based on constant average acceleration method as described in Figure 5.2.20. Considering $\ddot{X}_t$ and $\ddot{X}_{t+\Delta t}$ as acceleration at time t and $t + \Delta t$ he assumed that average acceleration of a body within the time interval t and $t + \Delta t$ is

$$\ddot{X}_{av} = \frac{\ddot{X}_{t+\Delta t} + X_t}{2}$$

Let $\frac{dv}{dt} = \ddot{X}_{av}$, we may write

$$\int_t^{t+\Delta t} dv = \int_t^{t+\Delta t} \ddot{X}_{av} dt \quad \rightarrow \quad \dot{X}_{t+\Delta t} - \dot{X}_t = \ddot{X}_{av}\,(t + \Delta t - t) \tag{5.2.82}$$

i.e. $\dot{X}_{t+\Delta t} = \dot{X}_t + \ddot{X}_{av}\Delta t$ implying $\dot{X}_{t+\Delta t} = \dot{X}_t + \frac{\ddot{X}_{t+\Delta t} + \dot{X}_t}{2}\Delta t$

Hence, $\dot{X}_{t+\Delta t} = \dot{X}_t + \{(1-\delta)\ddot{X}_t + \delta\ddot{X}_{t+\Delta t}\}\Delta t$, where $\delta = 1/2$.

To obtain the displacement vector, we integrate the above between the limits t and $t + \Delta t$

$$\int_t^{t+\Delta t} \dot{X}_{t+\Delta t} = \int_t^{t+\Delta t} \dot{X}_t + \int_t^{t+\Delta t} \{(1-\delta)\ddot{X}_t + \delta\ddot{X}_{t+\Delta t}\}\Delta t$$

or, $$X_{t+\Delta t} - X_t = \dot{X}_t \cdot \Delta t + \{(1-\delta)\ddot{X}_t + \delta X_{t+\Delta t}\}\frac{\Delta t^2}{2}$$

i.e. $$X_{t+\Delta t} = X_t + \dot{X}_t \cdot \Delta t + \left\{\left(\frac{1}{2} - \beta\right)\ddot{X}_t + \beta X_{t+\Delta t}\right\}\Delta t^2 \quad \text{where, } \beta = \frac{1}{4}.$$

Here you should note the similarity in the above procedure with Wilson-Theta Method.

In Wilson-Theta method we had expression of displacement as $\{X_{t+\Delta t}\} = \{X_t\} + \{\dot{X}_t\}\Delta t + \alpha_8\{X_{t+\Delta t} + 2\ddot{X}_t\}$ where, $\alpha_8 = \frac{\Delta t^2}{6}$ and on substitution we get $\{X_{t+\Delta t}\} = \{X_t\} + \{\dot{X}_t\}\Delta t + \frac{\Delta t^2}{6}\{X_{t+\Delta t} + 2\ddot{X}_t\}$

Considering $\beta = 1/6$ in Newmark's equation, we have

$$X_{t+\Delta t} = X_t + \dot{X}_t \cdot \Delta t + \left[\left(\frac{1}{2} - \frac{1}{6}\right)\ddot{X}_t + \frac{1}{6}X_{t+\Delta t}\right]\Delta t^2$$

$$\rightarrow \quad \{X_{t+\Delta t}\} = \{X_t\} + \{\dot{X}_t\}\Delta t + \frac{\Delta t^2}{6}\{X_{t+\Delta t} + 2\ddot{X}_t\} \tag{5.2.83}$$

Thus we see that for $\beta = 1/6$ we arrive at the same expression as arrived in the Wilson-Theta Method.

Thus we start here with the basic equation of motion as

$$[M]\{\ddot{X}_{t+\Delta t}\} + [C]\{\dot{X}_{t+\Delta t}\} + [K]\{X_{t+\Delta t}\} = \{R_{t+\Delta t}\} \tag{5.2.84}$$

and proceeding in the similar manner as shown in the Wilson-Theta method, we find out the value of $X_{t+\Delta t}$ which can be systematically structured as follows

- Assemble the mass matrix [M] the damping matrix [C] and stiffness matrix [K]
- Initialize $\{X_0\}$ and $\{\dot{X}_0\}$
- Evaluate $\{\ddot{X}_0\}$ (Refer Central difference method to see how this is evaluated)
- Select time step size Δt and parameters δ and β where $\delta \geq 0.50$ and $\beta = 0.25\,(0.5+\delta)^2$
- Calculate integration constant . . .

$$\alpha_0 = \frac{1}{\beta \Delta t^2}, \quad \alpha_1 = \frac{\delta}{\beta \Delta t}, \quad \alpha_2 = \frac{1}{\beta \Delta t},$$

$$\alpha_3 = \frac{1}{2\beta} - 1, \quad \alpha_4 = \frac{\delta}{\beta} - 1, \quad \alpha_5 = \frac{\Delta t}{2}\left(\frac{\delta}{\beta} - 2\right),$$

$$\alpha_6 = \Delta t\,(1-\delta), \quad \alpha_7 = \Delta t \delta$$

- Form the modified stiffness matrix as

$$[\hat{K}] = [K] + \alpha_0[M] + \alpha_1[C]$$

- Calculate modified load at time $t + \Delta t$

$$\{\hat{R}_{t+\Delta t}\} = \{R_{t+\Delta t}\} + [M]\{\alpha_0 X_t + \alpha_2 \dot{X}_t + \alpha_3 \ddot{X}_t\} + [C]\{\alpha_1 X_t + \alpha_4 \dot{X}_t + \alpha_5 \ddot{X}_t\}$$

- Solve for displacement vector

$$[\hat{K}]\,\{X_{t+\Delta t}\} = \{\hat{R}_{t+\Delta_t}\}$$

- Calculate the acceleration and velocity at time $t + \Delta t$

$$\{\ddot{X}_{t+\Delta t}\} = \alpha_0\{X_{t+\Delta t} - X_t\} - \alpha_2\{\dot{X}_t\} - \alpha_3\{\ddot{X}_t\}$$

$$\{\dot{X}_{t+\Delta t}\} = \{\dot{X}_t\} + \alpha_6\{\ddot{X}_t\} + \alpha_7\{\ddot{X}_{t+\Delta t}\}$$

We repeat the numerical problem in Example 5.2.7 for finding out the amplitude of a dynamic system based on Newmark-β method with the following data.

Example 5.2.9

$$[M] = \begin{bmatrix} 50 & 0 \\ 0 & 100 \end{bmatrix} \quad [C] = \begin{bmatrix} 700 & -2800 \\ -2800 & 12300 \end{bmatrix}$$

$$[K] = \begin{bmatrix} 3000 & -1200 \\ -1200 & 51000 \end{bmatrix}$$

The load vector is given by $\{P\} = \begin{Bmatrix} 500 \sin 12.5t \\ 200 \sin 12.5t \end{Bmatrix}$

For a time step of 0.04 seconds determine the amplitudes by Newmark-β method. Consider $\delta = 0.5$ and $\beta = 0.25$

Solution:

We start with the following assumptions

- Let displacement vector be $\{X\} = \begin{Bmatrix} X_1 \\ X_2 \end{Bmatrix}$
- As the function is a sine curve hence at $t = 0$ $\{P\} = 0$ as such $\{X\}_{t=0} = 0$ and $\{\dot{X}\}_{t=0} = 0$

Thus

$$\begin{bmatrix} 50 & 0 \\ 0 & 100 \end{bmatrix} \begin{Bmatrix} \ddot{X}_1 \\ \ddot{X}_2 \end{Bmatrix} + \begin{bmatrix} 700 & -2800 \\ -2800 & 12300 \end{bmatrix} \begin{Bmatrix} \dot{X}_1 \\ X_2 \end{Bmatrix} + \begin{bmatrix} 3000 & -1200 \\ -1200 & 51000 \end{bmatrix} \begin{Bmatrix} X_1 \\ X_2 \end{Bmatrix} = \begin{Bmatrix} 500 \sin 12.5t \\ 200 \sin 12.5t \end{Bmatrix}$$

$\therefore$ For $\{X\}_{t=0} = 0$ and $\{\dot{X}\}_{t=0} = 0$ we have

$$\begin{bmatrix} 50 & 0 \\ 0 & 100 \end{bmatrix} \begin{Bmatrix} \ddot{X}_1 \\ \ddot{X}_2 \end{Bmatrix} + \begin{bmatrix} 700 & -2800 \\ -2800 & 12300 \end{bmatrix} \begin{Bmatrix} 0 \\ 0 \end{Bmatrix} + \begin{bmatrix} 3000 & -1200 \\ -1200 & 51000 \end{bmatrix} \begin{Bmatrix} 0 \\ 0 \end{Bmatrix} = \begin{Bmatrix} 500 \sin 12.5t \\ 200 \sin 12.5t \end{Bmatrix}$$

or, $\begin{Bmatrix} \ddot{X}_1 \\ \ddot{X}_2 \end{Bmatrix}_{t=0} = \begin{Bmatrix} 0 \\ 0 \end{Bmatrix}$

The integration constant are

$$\alpha_0 = \frac{1}{\beta \Delta t^2} = 2500, \quad \alpha_1 = \frac{\delta}{\beta \Delta t} = 50,$$

$$\alpha_2 = \frac{1}{\beta \Delta t} = 100, \quad \alpha_3 = \frac{1}{2\beta} - 1 = 1.0,$$

$$\alpha_4 = \frac{\delta 1}{\beta} - 1 = 1.0, \quad \alpha_5 = \frac{\Delta t}{2}\left(\frac{\delta}{\beta} - 2\right) = 0.0,$$

$$\alpha_6 = \Delta t\,(1 - \delta) = 0.02.$$

$$[\hat{K}] = [K] + \alpha_0[M] + \alpha_1[C] = \begin{bmatrix} 3000 & -1200 \\ -1200 & 51000 \end{bmatrix}$$

$$+ 2550 \begin{bmatrix} 50 & 0 \\ 0 & 100 \end{bmatrix} + 50 \begin{bmatrix} 700 & -2800 \\ -2800 & 12300 \end{bmatrix}$$

$$= \begin{bmatrix} 16300 & -141200 \\ -141200 & 916000 \end{bmatrix}$$

$$\det.|\hat{K}| = 16300 \times 916000 - (141200)^2 = 1.29E + 11;$$

$$\text{Adj.}[\hat{K}] = \begin{bmatrix} 916000 & 141200 \\ 141200 & 163000 \end{bmatrix}$$

$$[\hat{K}]^{-1} = \begin{bmatrix} 7.08 & 1.09 \\ 1.09 & 1.259 \end{bmatrix} \times 10^{-6}$$

Now $\{\hat{R}_{t+\Delta t}\} = \{R_{t+\Delta t}\} + [M]\{\alpha_0\{X_t\} + \alpha_2\{\dot{X}_t\} + \alpha_3\{\ddot{X}_t\}\}$
$+[C]\{\alpha_1\{X_t\} + \alpha_4\{\dot{X}_t\} + \alpha_5\{\ddot{X}_t\}\}$

For $t = 0.04$ sec

$$\{\hat{R}\}_{0.04} = \begin{bmatrix} 500 \sin 12.5 \times 0.04 \\ 200 \sin 12.5 \times 0.04 \end{bmatrix} + \begin{bmatrix} 50 & 0 \\ 0 & 100 \end{bmatrix}$$

$$\times \left\{ 2500 \begin{Bmatrix} 0 \\ 0 \end{Bmatrix} + 100 \begin{Bmatrix} 0 \\ 0 \end{Bmatrix} + 1 \begin{Bmatrix} 0 \\ 0 \end{Bmatrix} \right\} + \begin{bmatrix} 700 & -2800 \\ -2800 & 12300 \end{bmatrix}$$

$$\times \left\{ 50 \begin{Bmatrix} 0 \\ 0 \end{Bmatrix} + 1.0 \begin{Bmatrix} 0 \\ 0 \end{Bmatrix} + 0.0 \begin{Bmatrix} 0 \\ 0 \end{Bmatrix} \right\} = \begin{Bmatrix} 239.7 \\ 95.885 \end{Bmatrix}$$

$$\{\hat{X}\}_{t+\Delta t} = [\hat{K}]^{-1}\{\hat{R}\}_{t+\Delta t}$$

$$\{X\}_{0.04} = \begin{bmatrix} 7.08 & 1.09 \\ 1.09 & 1.259 \end{bmatrix} \begin{Bmatrix} 239.7 \\ 95.885 \end{Bmatrix} \times 10^{-6} = \begin{Bmatrix} 1.801 \\ 0.381 \end{Bmatrix} \times 10^{-3}$$

$$\{\ddot{X}_{t+\Delta t}\} = \alpha_0\{X_{t+\Delta t} - X_t\} - \alpha_2\{\dot{X}_t\} - \alpha_3\{\ddot{X}_t\}$$

$$\{\ddot{X}\}_{0.04} = 2500 \left\{ \begin{Bmatrix} 1.801 \times 10^{-3} \\ 0.381 \times 10^{-3} \end{Bmatrix} - \begin{Bmatrix} 0 \\ 0 \end{Bmatrix} \right\}$$

$$- 100 \begin{Bmatrix} 0 \\ 0 \end{Bmatrix} - 1.0 \begin{Bmatrix} 0 \\ 0 \end{Bmatrix} = \begin{Bmatrix} 4.5025 \\ 0.9525 \end{Bmatrix}$$

$$\{\dot{X}_{t+\Delta t}\} = \{\dot{X}_t\} + \alpha_6\{\ddot{X}_t\} + \alpha_7\{\ddot{X}_{t+\Delta t}\}$$

$$\{\dot{X}\}_{0.04} = \begin{Bmatrix} 0 \\ 0 \end{Bmatrix} + 0.02 \begin{Bmatrix} 0 \\ 0 \end{Bmatrix} + 0.02 \begin{Bmatrix} 4.5025 \\ 0.9525 \end{Bmatrix} = \begin{Bmatrix} 0.090 \\ 0.019 \end{Bmatrix}$$

For $t = 0.08$ sec

$$\{\hat{R}_{t+\Delta t}\} = \{R_{t+\Delta t}\} + [M]\{\alpha_0 X_t\} + \alpha_2\{\dot{X}_t\} + \alpha_3\{\ddot{X}_t\}$$
$$+ [C]\{\alpha_1\{X_t\} + \alpha_4\{\dot{X}_t\} + \alpha_5\{\ddot{X}_t\}\}$$

$$\{\hat{R}\}_{0.08} = \begin{Bmatrix} 500 \sin 12.5 \times 0.08 \\ 200 \sin 12.5 \times 0.08 \end{Bmatrix} + \begin{bmatrix} 50 & 0 \\ 0 & 100 \end{bmatrix}$$
$$\times \left\{ 2500 \begin{Bmatrix} 1.801 \times 10^{-3} \\ 0.381 \times 10^{-3} \end{Bmatrix} + 100 \begin{Bmatrix} 0.090 \\ 0.019 \end{Bmatrix} + 1.0 \begin{Bmatrix} 4.5025 \\ 0.9525 \end{Bmatrix} \right\}$$
$$+ \begin{bmatrix} 700 & -2800 \\ -2800 & 12300 \end{bmatrix} \{50 \begin{Bmatrix} 1.801 \times 10^{-3} \\ 0.381 \times 10^{-3} \end{Bmatrix}$$
$$+ 1.0 \begin{Bmatrix} 0.090 \\ 0.019 \end{Bmatrix} + 0\} = \begin{Bmatrix} 1340.335 \\ 512.294 \end{Bmatrix}$$

For $\{X\}_{t+\Delta t} = [\hat{K}]^{-1}\{\hat{R}\}_{t+\Delta t}$, we have

$$\{X\}_{0.08} = \begin{bmatrix} 7.08 & 1.09 \\ 1.09 & 1.259 \end{bmatrix} \begin{Bmatrix} 1340.335 \\ 512.294 \end{Bmatrix} \times 10^{-6} = \begin{Bmatrix} 1.004 \times 10^{-2} \\ 2.106 \times 10^{-3} \end{Bmatrix}$$

$$\{\ddot{X}_{t+\Delta t}\} = \alpha_0\{X_{t+\Delta \mathrm{t}} - X_t\} - \alpha_2\{\dot{X}_t\} - \alpha_3\{\ddot{X}_t\}$$

$$\{\ddot{X}\}_{0.08} = 2500 \left\{ \begin{Bmatrix} 1.004 \times 10^{-2} \\ 2.106 \times 10^{-3} \end{Bmatrix} - \begin{Bmatrix} 1.801 \times 10^{-3} \\ 0.381 \times 10^{-3} \end{Bmatrix} \right\}$$
$$- 100 \begin{Bmatrix} 0.090 \\ 0.019 \end{Bmatrix} - 1.0 \begin{Bmatrix} 4.5025 \\ 0.9525 \end{Bmatrix} = \begin{Bmatrix} 7.0945 \\ 1.460 \end{Bmatrix}$$

Again $\{\dot{X}_{t+\Delta \mathrm{t}}\} = \{\dot{X}_t\} + \alpha_6\{\ddot{X}_t\} + \alpha_7\{\ddot{X}_{t+\Delta \mathrm{t}}\}$

or $\{\dot{X}\}_{0.08} = \begin{Bmatrix} 0.090 \\ 0.019 \end{Bmatrix} + 0.02 \begin{Bmatrix} 4.5025 \\ 0.9525 \end{Bmatrix}$
$$+ 0.02 \begin{Bmatrix} 7.0945 \\ 1.460 \end{Bmatrix} = \begin{Bmatrix} 0.3218 \\ 0.068 \end{Bmatrix}$$

This way we proceed step-by-step to find out the displacement velocity and acceleration at a time step of 0.04, 0.08, 0.12 ...

The table below gives the force and amplitudes for 30 time steps based on Newmark-Beta method and plots are given in Figure 5.2.21.

Finally we compare the values obtained by the three methods to see how they match in terms of each other.

Sl. No.	*Time steps*	$R_1(t)$	$R_2(t)$	$X_1(t)$	$X_2(t)$
1	0.04	239.71	95.89	1.80×10^{-03}	3.82×10^{-04}
2	0.08	420.74	168.29	1.01×10^{-02}	2.11×10^{-03}
3	0.12	498.75	199.50	2.85×10^{-02}	5.89×10^{-03}
4	0.16	454.65	181.86	5.66×10^{-02}	1.14×10^{-02}
5	0.20	299.24	119.69	8.90×10^{-02}	1.73×10^{-02}
6	0.24	70.56	28.22	1.17×10^{-01}	2.16×10^{-02}
7	0.28	−175.39	−70.16	1.31×10^{-01}	2.25×10^{-02}
8	0.32	−378.40	−151.36	1.24×10^{-01}	1.85×10^{-02}
9	0.36	−488.77	−195.51	9.09×10^{-02}	9.57×10^{-03}
10	0.40	−479.46	−191.78	3.58×10^{-02}	-3.27×10^{-03}
11	0.44	−352.77	−141.11	-3.29×10^{-02}	-1.77×10^{-02}
12	0.48	−139.71	−55.88	-1.02×10^{-01}	-3.06×10^{-02}
13	0.52	107.56	43.02	-1.56×10^{-01}	-3.89×10^{-02}
14	0.56	328.49	131.40	-1.82×10^{-01}	-4.02×10^{-02}
15	0.60	469.00	187.60	-1.73×10^{-01}	-3.38×10^{-02}
16	0.64	494.68	197.87	-1.28×10^{-01}	-2.03×10^{-02}
17	0.68	399.24	159.70	-5.49×10^{-02}	-2.19×10^{-03}
18	0.72	206.06	82.42	3.20×10^{-02}	1.69×10^{-02}
19	0.76	−37.58	−15.03	1.15×10^{-01}	3.30×10^{-02}
20	0.80	−272.01	−108.80	1.75×10^{-01}	4.26×10^{-02}
21	0.84	−439.85	−175.94	2.01×10^{-01}	4.34×10^{-02}
22	0.88	−500.00	−200.00	1.86×10^{-01}	3.53×10^{-02}
23	0.92	−437.73	−175.09	1.33×10^{-01}	1.99×10^{-02}
24	0.96	−268.29	−107.31	5.30×10^{-02}	4.01×10^{-04}
25	1.00	−33.16	−13.26	-3.59×10^{-02}	-1.89×10^{-02}
26	1.04	210.08	84.03	-1.15×10^{-01}	-3.39×10^{-02}
27	1.08	401.89	160.76	-1.67×10^{-01}	-4.15×10^{-02}
28	1.12	495.30	198.12	-1.81×10^{-01}	-4.00×10^{-02}
29	1.16	467.45	186.98	-1.56×10^{-01}	-3.00×10^{-02}
30	1.20	325.14	130.06	-9.79×10^{-02}	-1.40×10^{-02}

Sl. No.	*Time steps*	x_1 (*Central difference*)	x_1 (*Wilson-*θ)	x_1 (*Newmark-*β)
1	0.04	7.43×10^{-03}	2.02×10^{-03}	1.80×10^{-03}
2	0.08	2.66×10^{-02}	1.47×10^{-02}	1.01×10^{-02}
3	0.12	5.68×10^{-02}	4.17×10^{-02}	2.85×10^{-02}
4	0.16	9.22×10^{-02}	7.93×10^{-02}	5.66×10^{-02}
5	0.2	1.23×10^{-01}	1.18×10^{-01}	8.90×10^{-02}
6	0.24	1.39×10^{-01}	1.46×10^{-01}	1.17×10^{-01}
7	0.28	1.30×10^{-01}	1.51×10^{-01}	1.31×10^{-01}
8	0.32	9.44×10^{-02}	1.26×10^{-01}	1.24×10^{-01}
9	0.36	3.43×10^{-02}	7.18×10^{-02}	9.09×10^{-02}
10	0.4	-4.00×10^{-02}	-4.80×10^{-03}	3.58×10^{-02}

(continued)

Sl. No.	*Time steps*	x_1 (*Central difference*)	x_1 (*Wilson-θ*)	x_1 (*Newmark-β*)
11	0.44	-1.14×10^{-01}	-8.92×10^{-02}	-3.29×10^{-02}
12	0.48	-1.70×10^{-01}	-1.64×10^{-01}	-1.02×10^{-01}
13	0.52	-1.96×10^{-01}	-2.10×10^{-01}	-1.56×10^{-01}
14	0.56	-1.82×10^{-01}	-2.17×10^{-01}	-1.82×10^{-01}
15	0.6	-1.30×10^{-01}	-1.80×10^{-01}	-1.73×10^{-01}
16	0.64	-4.78×10^{-02}	-1.04×10^{-01}	-1.28×10^{-01}
17	0.68	4.72×10^{-02}	-3.57×10^{-03}	-5.49×10^{-02}
18	0.72	1.35×10^{-01}	1.00×10^{-01}	3.20×10^{-02}
19	0.76	1.98×10^{-01}	1.86×10^{-01}	1.15×10^{-01}
20	0.8	2.20×10^{-01}	2.34×10^{-01}	1.75×10^{-01}
21	0.84	1.96×10^{-01}	2.35×10^{-01}	2.01×10^{-01}
22	0.88	1.32×10^{-01}	1.87×10^{-01}	1.86×10^{-01}
23	0.92	4.07×10^{-02}	1.02×10^{-01}	1.33×10^{-01}
24	0.96	-5.79×10^{-02}	-2.91×10^{-03}	5.30×10^{-02}
25	1	-1.42×10^{-01}	-1.04×10^{-01}	-3.59×10^{-02}
26	1.04	-1.94×10^{-01}	-1.80×10^{-01}	-1.15×10^{-01}
27	1.08	-2.03×10^{-01}	-2.15×10^{-01}	-1.67×10^{-01}
28	1.12	-1.67×10^{-01}	-2.02×10^{-01}	-1.81×10^{-01}
29	1.16	-9.51×10^{-02}	-1.45×10^{-01}	-1.56×10^{-01}
30	1.2	-5.15×10^{-03}	-5.93×10^{-02}	-9.79×10^{-02}

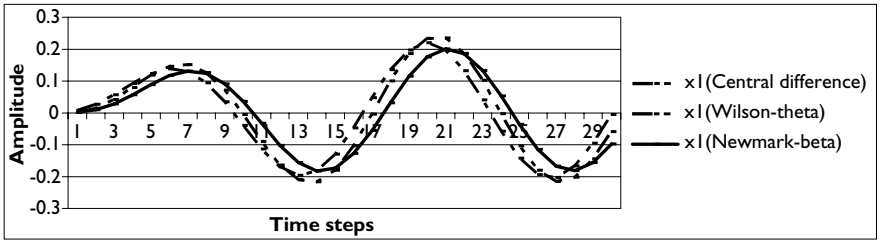


Figure 5.2.22 Comparison of response for displacement x_1 by three methods.

It may be observed from Figure 5.2.22 that the results are quite closely matching.

5.2.4.2 *Discussions on selection of time step for step by step integration*

In central difference method, the value of displacement $\{X_{t+\Delta t}\}$ is sought based on equilibrium equation of $[M]\{\ddot{X}_t\} + [C]\{\dot{X}_t\} + [K]\{X_t\} = \{R_t\}$ while in Wilson-Theta method and Newmark-beta method the equation is solved for $\{X_{t+\Delta t}\}$ based on the equilibrium of the equation of motion at

$$[M]\{\ddot{X}_{t+\Delta t}\} + [C]\{\dot{X}_{t+\Delta t}\} + [K]\{X_{t+\Delta t}\} = \{R_{t+\Delta t}\} \tag{5.2.85}$$

The central difference method is known as *explicit integration scheme* while Wilson-Theta method and Newmark–Beta are known as *implicit integration schemes*.

Most of the explicit integration schemes like central difference method are *conditionally stable*, while implicit integration schemes like, Wilson-Theta, and Newmark-Beta method are *unconditionally stable*.

By conditional stability we mean that there exists a certain condition beyond which the scheme does not produce meaningful results.

For central difference method there exists a particular limiting value of the time step Δt_{lim}, which if exceeded, the scheme becomes unstable and displacement, velocity and acceleration vectors grow without limit.

If the damping is high the solution may not undergo core overflow but may contain errors that may not be easily recognizable.

Thus selection of an appropriate time period for meaningful evaluation of response based on direct integration method is of utmost importance.

The time step should neither be too small to make the analysis too expensive and nor too big to render results which have values which are far too crude/rough for any practical use.

This is the essence of our further discussion.

It has been observed that for central difference technique when, $\Delta t \leq \Delta t_{\text{lim}} \leq T_n/\pi$, *the solution is stable.* Here, T_n is the highest un-damped time period of the dynamic system having n degrees of freedom.

Let us now see what does the term, $\Delta t \leq \Delta t_{\text{lim}} \leq T_n/\pi$ signify.

For a structure or a foundation system having limited degrees of freedom finding T_n is surely not a problem.

For instance a block foundation supporting a centrifugal/reciprocating compressor subjected to coupled horizontal and rocking mode and we have to deal with two degrees of freedom system.

Similarly for dynamic analysis of tall R.C.C. chimney where we usually apply a stick model and have a maximum of 20 to 30 nodes with about 40 to 60 degrees of freedom and the value of T_n can easily be obtained by an *inverse iteration technique*[16].

But when we undertake a large finite element analysis with more than 1000 or 1500 nodes, finding out T_n, based on standard eigen value solution, could be time consuming and expensive too. Moreover, the value of T_n for such problems could be quite small, making $\Delta t \leq T_n/\pi$ very small.

As the cost of analysis increases directly with the decrement of the time step, for a value $\Delta t \to 0$, the analysis could be prohibitively expensive.

We discuss below a few of the cases when due to the typical characteristics of a problem, the time step becomes prohibitively small.

- There could be cases where due to opening or re-entrant corners it becomes necessary for mesh refinements this goes on to add additional degrees of freedom and makes the value of T_n small.

16 In most of the iterative techniques for evaluation eigenvalue the iteration converges first to the lowest eigen value. In inverse iteration technique it converges to the highest eigen value.

- The use shell elements in structure where in plane membrane mode is far stiffer than the bending or flexural mode.
- A large structure with mass matrix considered as lumped mass having one or two nodes having very small mass will make the value of T_n very small.

Systems which are flexible *having long time period gives very good result based on explicit integration scheme*. One of the best examples is response of fluid in a container in a fluid structure interaction problem.

For implicit integration schemes there exists a condition if satisfied the scheme becomes *unconditionally stable*. However the choice of magnitude of an appropriate time step also depends upon the accuracy of the scheme as well as on *the co-relation between modal response method and direct integration method*.

As such we first try to understand the co-relation between modal response and direct integration.

In modal analysis we have seen that the orthogonal transformation de-couples an equation of n degrees of freedom into the form

$$\{\ddot{\xi}_1\} + 2D_1\omega_1\{\dot{\xi}_1\} + [\omega_1^2]\{\xi_1\} = 0; \quad \{\ddot{\xi}_2\} + 2D_2\omega_2\{\dot{\xi}_2\} + [\omega_2^2]\{\xi_2\} = 0;$$

$$\{\ddot{\xi}_3\} + 2D_3\omega_3\{\dot{\xi}_3\} + [\omega_3^2]\{\xi_3\} = 0; \quad \cdots \quad \{\ddot{\xi}_n\} + 2D_n\omega_n\{\dot{\xi}_n\} + [\omega_n^2]\{\xi_n\} = 0. \tag{5.2.86}$$

where D_i = damping ratio per mode; ω_i = natural frequency per mode, and ξ_i = displacement value in transformed orthogonal plane.

Now for each mode we have time periods $T_1, T_2, T_3 \ \ldots \ T_n$

Suppose we want to do a time history analysis in the transformed co-ordinates for each uncoupled degree of freedom, we can find $\sum_{i=1}^{n} \Delta t_i = \frac{T_1}{\pi}, \frac{T_2}{\pi}, \frac{T_3}{\pi}, \ \ldots \ . \ \frac{T_n}{\pi}$ and can find a solution based on step by step integration.

However if we can solve the equations for all modes based on common time step modal analysis in essence becomes direct integration method.

Thus how to arrive at a common time step to solve the equation of motion becomes of the topic of our subsequent discussion. For most of the practical structure the significant contributions are restricted to a first few mode beyond which the inertial contribution for higher modes become insignificant. Now for a structural system having n degrees of freedom if first *m-modes* are significant then for $\Delta t \leq T_m/\pi$ *or say* $\Delta t \leq T_m/10$ *would suffice*.

This also has the advantage that the time step Δt becomes larger to Δt_{lim} by the ratio T_m/T_n and makes the cost of analysis much cheaper.

However, it should also be remembered that during direct integration method the effects of the higher modes also get directly integrated into the system.

Thus the question boils down what response does the structure give for large $\Delta t/T$ and what is the contribution of the higher modes which are deemed insignificant.

This is basically the crux of the stability concept for by stability of integration we mean that for large value of $\Delta t/T$, the results do not get artificially amplified rendering the lower mode responses useless.

We will not discuss the mathematics underlying the stability of integration for excellent treatment is available elsewhere but will only discuss the end results[17].

- For Central difference method we have already discussed that the condition of stability to be $\Delta t \leq \Delta t_{\text{lim}} \leq T_n/\pi$.
- For Wilson-Theta method, unconditional stability is obtained for $\theta \geq 1.37$ (usually taken as 1.4).
- For Newmark-Beta method, the unconditional stability is satisfied when $\delta \geq 0.5$ and $\beta \geq 0.25(\delta + 0.5)^2$.

For accuracy analysis specially for central difference method we don't have much choice except to abide by the conditional stability rule of putting, $\Delta t \leq \Delta t_{\text{lim}} \leq T_n/\pi$. However for implicit integration scheme it has been shown that for Wilson-Theta method for $\theta \geq 1.37$ and for Newmark-Beta method for $\delta \geq 0.5$ and $\beta \geq 0.25(\delta+0.5)^2$ gives the best solution.

Even with higher value of $\Delta t/T$ it has been observed that due to amplitude decay inherent in the numerical procedure the effect of higher modes effectively gets damped out.

Thus for a modeling a finite element problem falling under the purview of structural dynamics problem for selection of Δt we have to proceed as follows[18]:

- Select the frequency to which there is a significant contribution from load
    - For instance for Turbine foundation say the operating frequency is 3000 rpm. then the forcing function will be given by $P(t) = P \sin 314\, t$ where $\omega_m = 314$ rad/sec Then consider the cut off frequency as $\omega_{co} = 4\omega_m = 1256$ rad /sec
    - Similarly for earthquake analysis it is possible to undertake a Fourier analysis to find out the significant frequency to which the load has contribution and establish the cut off frequency based on the relation $\omega_{co} = 4\omega_m$. Alternatively one can check the modal mass participation factor and find out to which mode does 95% of mass contribute and *consider the cut off frequency as four times the corresponding frequency of that mode.*
- Once the cut off frequency is established it should be ensured that the finite element has enough nodes to accurately predict the modal response to the cutoff frequency level.
- Find out the cut off time period from the expression $T_{co} = 2\pi/\omega_{co}$.
- Select $\Delta t = T_{co}/20$.

You might wonder at this point as to what is the basis of the selection of $\omega_{co} = 4\omega_{m.}$

17 For detailed discussion on study of stability and accuracy of Numerical integration technique applied to dynamic problems in Finite element method, read section 9.4 of the book "Finite Element Procedures – Bathe Klaus Jurgen Prentice Hall Publication. It possibly gives the best insight into the topic we feel.

18 For soil dynamics and wave propagation problems the considerations are a bit different. We will discuss this problem in detail in when we take up the subject of Soil Dynamics.

The logic is simple for we know that $\bar{x} = \frac{P_0/k}{(1-r^2)}$ where, $r = \frac{\omega_m}{\omega_n}$. For $\frac{\omega_m}{\omega_n} \leq 0.25$ the value of $\bar{x} \to \frac{P_0}{k}$, which means that the value approaches *static deflection.*

As the response for higher modes are insignificant for static deflection case a cut off frequency four times the significant mode is found to be quite logical.

We have already stated earlier that dynamic analysis is nothing but equivalent to static analysis at an instant of time Δt. Thus all logic pertaining to modeling of FEM for static problems holds good including the use of higher order elements which gives a better result.

As we had stated earlier that refined meshes at times render exceedingly low value of T_n it would possibly be worth to go for higher order elements with cruder meshes to have an economic and optimal analysis model.

We solve a bench mark problem here which covers the complete gamut of modal analysis as discussed in this chapter.

Example 5.2.9

As shown in Figure 5.2.23 is a three storied steel frame subjected to dynamic forces as shown. The damping ratio for steel is found to vary between 2 to 5%. Determine

- **The natural frequencies of the structure.**
- **The eigen-vectors**
- **The mode shapes**
- **Normalised eigen-vectors**
- **Form the Rayleigh Damping Matrix**
- **Determine the damped amplitude of vibrations.**
- **Nodal shear forces.**

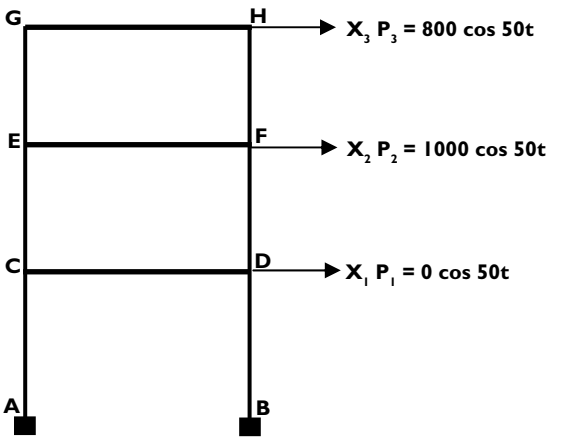


Figure 5.2.23 A three storied frame under harmonic load.

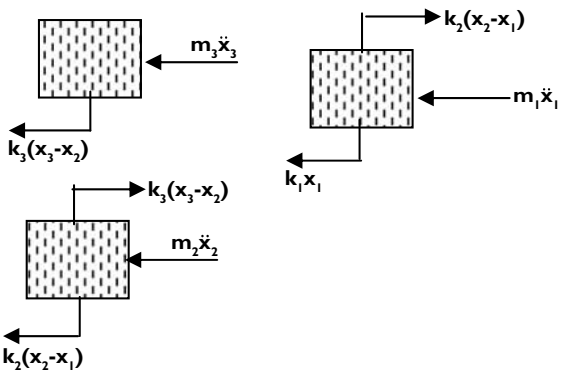


Figure 5.2.24

Here

1 $K_{AC} = K_{DB} = \mathbf{1.5 \times 10^3}$ kN/m $M_{GH} = 200$ kN sec^2/m
2 $K_{CE} = K_{DF} = \mathbf{1.0 \times 10^3}$ kN/m $M_{EF} = \mathbf{400}$ kN sec^2/m
3 $K_{EG} = K_{FH} = \mathbf{0.75 \times 10^3}$ kN/m $M_{CD} = \mathbf{400}$ kN sec^2/m

Solution:

The free body diagram of the structure is as shown in Figure. 5.2.24.
Based on the F.B.D we have:

$$m_3\,\ddot{x}_3 + k_3(x_3 - x_2) = P_3 \cos \omega_m t$$
$$m_2\,\ddot{x}_2 + k_2(x_2 - x_1) - k_3(x_3 - x_2) = P_2 \cos \omega_m t$$
$$m_1\,\ddot{x}_1 + k_1 x_1 - k_2(x_2 - x_1) = P_1 \cos \omega_m t$$

The above on simplification while writing in the matrix form gives

$$\begin{bmatrix} m_1 & 0 & 0 \\ 0 & m_2 & 0 \\ 0 & 0 & m_3 \end{bmatrix} \begin{Bmatrix} \ddot{x}_1 \\ \ddot{x}_2 \\ \ddot{x}_3 \end{Bmatrix} + \begin{bmatrix} k_1 + k_2 & -k_2 & 0 \\ -k_2 & k_2 + k_3 & -k_3 \\ 0 & -k_3 & k_3 \end{bmatrix} \begin{Bmatrix} x_1 \\ x_2 \\ x_3 \end{Bmatrix} = \begin{Bmatrix} P_1 \cos \omega_m t \\ P_2 \cos \omega_m t \\ P_3 \cos \omega_m t \end{Bmatrix}$$

The above, on substituting the values, gives the following matrices:

$$[K] = \begin{bmatrix} 5000 & -2000 & 0 \\ -2000 & 3500 & -1500 \\ 0 & -1500 & 1500 \end{bmatrix} \quad \text{and} \quad [M] = \begin{bmatrix} 400 & 0 & 0 \\ 0 & 400 & 0 \\ 0 & 0 & 200 \end{bmatrix}$$

- **To find out the natural frequencies** we have,

$$\begin{bmatrix} 5000 - 400\lambda & -2000 & 0 \\ -2000 & 3500 - 400\lambda & -1500 \\ 0 & -1500 & 1500 - 200\lambda \end{bmatrix} = 0$$

On expansion we have

$$(5000 - 400\lambda)\begin{vmatrix} 3500 - 400\lambda & -1500 \\ -1500 & 1500 - 200\lambda \end{vmatrix} + 2000\begin{vmatrix} -2000 & -1500 \\ 0 & 1500 - 200\lambda \end{vmatrix} = 0$$

The above on expansion and further simplification gives a cubical equation as follows

$$\lambda^3 - 28.75\lambda^2 + 215.625\lambda - 281.25 = 0$$

We find the first root by Newton Raphson method
Let $f(\lambda) = \lambda^3 - 28.75\lambda^2 + 215.625\lambda - 281.25$ and $f'(\lambda) = 3\lambda^2 - 57.5\lambda + 215.625$

$$\lambda_{i+1} = \lambda_i - \frac{f(\lambda)}{f'(\lambda)}$$

Let $\lambda = 50$, say an arbitrary value we start with, then $\lambda_1 = 50 - \frac{63625}{4840.6} = 36.586$

$$\lambda_2 = 36.586 - \frac{18676}{2171.499} = 28.255 \ldots \quad \lambda_6 = 17.753 - \frac{83.66}{140.33} = 17.156;$$

$$\lambda_7 = 17.156 - \frac{5.569}{112.14} = 17.106; \quad \lambda_8 = 17.106 - \frac{0.1944}{109.87} = 17.104.$$

Thus the first root of the above equation is 17.104.
Now as 17.104 is one of the roots of the equation hence it must satisfy the expression

$$\lambda^3 - 28.75\lambda^2 + 215.625\lambda - 281.25 = 0$$

i.e. $(\lambda - 17.104)\lambda^2 - (\lambda - 17.104)11.646\lambda + (\lambda - 17.104)16.431816 = 0$

or, $(\lambda - 17.104)(\lambda^2 - 11.646\lambda + 16.431816) = 0;$

$\rightarrow$ $(\lambda^2 - 11.646\lambda + 16.431816) = 0$

Hence,

$$\lambda = \frac{11.646 \pm \sqrt{(11.646)^2 - 4 \times 16.431816}}{2}$$

$$= \frac{11.646 \pm 8.360}{2} = 1.6426, \quad 10.00$$

Thus

$\omega_1 = \sqrt{1.6426} = 1.281$ rad/sec; $\omega_2 = \sqrt{10.00} = 3.162$ rad/sec;

$\omega_3 = \sqrt{17.104} = 4.135$ rad/sec.

- To calculate **the mode shapes** or **the eigenvectors**

For first mode we have ($\lambda = 1.6426$)

$$\begin{bmatrix} 5000 - 400 \times 1.6426 & -2000 & 0 \\ -2000 & 3500 - 400 \times 1.6426 & -1500 \\ 0 & -1500 & 1500 - 200 \times 1.6426 \end{bmatrix} \times \begin{Bmatrix} \phi_1 \\ \phi_2 \\ \phi_3 \end{Bmatrix} = 0$$

where $[\phi_i]_{i=1}^{3}$ are the modal vectors

$$\text{or,} \quad \begin{bmatrix} 4343 & -2000 & 0 \\ -2000 & 2843 & -1500 \\ 0 & -1500 & 1171.48 \end{bmatrix} \begin{Bmatrix} \phi_1 \\ \phi_2 \\ \phi_3 \end{Bmatrix} = 0$$

$$\text{or} \quad 4343\phi_1 - 2000\phi_2 = 0$$

$$-2000\phi_1 + 2843\phi_2 - 1500\phi_3 = 0$$

$$-1500\phi_2 + 1171\phi_3 = 0$$

For $\phi_1 = 1.00$, $\phi_2 = 2.1715$ and $\phi_3 = \frac{1500 \times 2.1715}{1171} = 2.7816$

$$\therefore \quad \phi_1 : \phi_2 : \phi_3 = 1.00 : 2.1715 : 2.7816$$

For second mode ($\lambda = 10.00$)

$$\begin{bmatrix} 5000 - 400 \times 10 & -2000 & 0 \\ -2000 & 3500 - 400 \times 10 & -1500 \\ 0 & -1500 & 1500 - 200 \times 10 \end{bmatrix} \begin{Bmatrix} \phi_1 \\ \phi_2 \\ \phi_3 \end{Bmatrix} = 0$$

The above on simplification gives

$$\phi_1 = 1.00, \quad \phi_2 = 0.500 \quad \text{and} \quad \phi_3 = \frac{1500 \times 0.5}{500} = -1.50$$

$$\phi_1 : \phi_2 : \phi_3 = 1.00 : 0.50 : -1.50$$

For third mode we have ($\lambda = 17.104$)

$$\begin{bmatrix} 5000 - 400 \times 17.104 & -2000 & 0 \\ -2000 & 3500 - 400 \times 17.104 & -1500 \\ 0 & -1500 & 1500 - 200 \times 17.104 \end{bmatrix} \times \begin{Bmatrix} \phi_1 \\ \phi_2 \\ \phi_3 \end{Bmatrix} = 0$$

The above on simplification gives

$$\phi_1 = 1.00, \quad \phi_2 = -0.9208 \quad \text{and} \quad \phi_3 = \frac{1500 \times -0.9208}{1920.8} = 0.719$$

$$\phi_1 : \phi_2 : \phi_3 = 1.00 : -0.9208 : 0.719$$

Thus for three modes eigen-vectors are given by

$$[\phi] = \begin{bmatrix} 1.00 & 1.0 & 1.0 \\ 2.1715 & 0.5 & -0.9208 \\ 2.7816 & -1.50 & 0.719 \end{bmatrix}$$

Normalised eigen vectors
For first mode

$$\{\varphi\}^T[M]\{\varphi\} = \langle 1.00 \quad 2.1715 \quad 2.7816 \rangle \begin{bmatrix} 400 & 0 & 0 \\ 0 & 400 & 0 \\ 0 & 0 & 200 \end{bmatrix} \begin{Bmatrix} 1.00 \\ 2.1715 \\ 2.7816 \end{Bmatrix}$$

$$= 3833.56$$

$$M_r = \sqrt{3833.56} = 6.191 \quad \rightarrow \quad \{\phi_i\} = \begin{Bmatrix} \frac{1.00}{6.191} \\ \frac{2.1715}{6.191} \\ \frac{2.7816}{6.191} \end{Bmatrix} = \begin{Bmatrix} 0.01615 \\ 0.0350718 \\ 0.0449255 \end{Bmatrix}$$

For second mode

$$\{\varphi\}^T[M]\{\varphi\} = \langle 1.00 \quad 0.5 \quad -1.50 \rangle \begin{bmatrix} 400 & 0 & 0 \\ 0 & 400 & 0 \\ 0 & 0 & 200 \end{bmatrix} \begin{Bmatrix} 1.00 \\ 0.5 \\ -1.50 \end{Bmatrix}$$

$$= 950; \quad M_r = \sqrt{950} = 30.822$$

$$\{\phi_i\} = \begin{Bmatrix} 0.03244 \\ 0.016322 \\ -0.02433 \end{Bmatrix}$$

For third mode

$$\{\varphi\}^T[M]\{\varphi\} = \langle 1.00 \quad -0.9208 \quad 0.719 \rangle \begin{bmatrix} 400 & 0 & 0 \\ 0 & 400 & 0 \\ 0 & 0 & 200 \end{bmatrix}$$

$$\times \begin{Bmatrix} 1.00 \\ -0.9208 \\ 0.719 \end{Bmatrix} = 842.54$$

$$M_r = \sqrt{842.54} = 29.0265 \quad \rightarrow \quad \{\phi_i\} = \begin{Bmatrix} 0.03445 \\ -0.031723 \\ 0.02477 \end{Bmatrix}$$

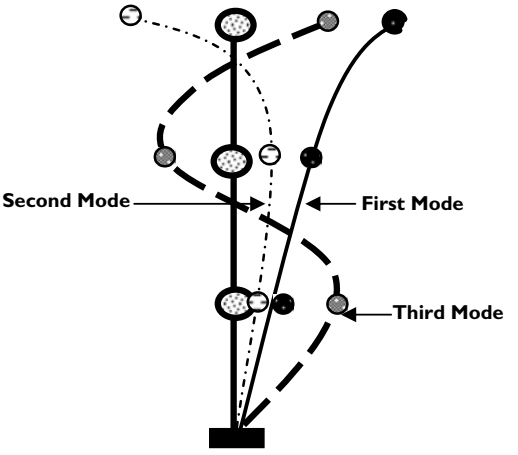


Figure 5.2.25 Mode shape of the frame.

Thus **the normalised eigen-vector** is

$$[\varphi_i] = \begin{bmatrix} 0.01615 & 0.03244 & 0.0344512 \\ 0.0350718 & 0.01622 & -0.03172 \\ 0.04493 & -0.02433 & 0.02477 \end{bmatrix}$$

Mode shapes are shown in Figure. 5.2.25.

- **Determination of Rayleigh Damping**

For $\omega_1 = 1.281$ rad/sec. $D_1 = 0.02$
For $\omega_3 = 4.135$ rad/sec. $D_3 = 0.05$ then by linear interpolation
For $\omega_2 = 3.162$ rad/sec. $D_2 = 0.0397$

Thus based on successive averaging technique

Sl. No.	*Damping ratio*	*Average damping*	*Frequency*	*Average frequency*
1	0.02	0.02985	1.281	2.2215
2	0.0397	0.0448	3.162	3.6485
3	0.05		4.135	

As $\alpha + \beta\omega_i^2 = 2D_i\omega_i$

For the above two conditions we have

$$\alpha + 2.2215^2\beta = 2 \times 0.02985 \times 2.215 \quad \text{or,} \alpha + 4.906\beta = 0.1326 \quad \text{and}$$

$$\alpha + 3.6458^2\beta = 2 \times 0.0448 \times 3.6485 \quad \text{or,} \alpha + 13.311\beta = 0.326$$

Solving the above two equations we have $\alpha = 0.0198; \quad \beta = 0.023$

Considering $[C] = \alpha\,[M] + \beta[K]$ we have

$$[C] = 0.0198\begin{bmatrix}400 & & \\ & 400 & \\ & & 200\end{bmatrix} + 0.023\begin{bmatrix}5000 & -2000 & 0\\ -2000 & 3500 & -1500\\ 0 & -1500 & 1500\end{bmatrix}$$

$$= \begin{bmatrix}122.92 & -46 & 0\\ -46 & 88.42 & -34.5\\ 0 & -34.5 & 38.46\end{bmatrix}$$

- Determination of damped amplitude of vibration.

The force vector is given by

$$P(t) = \begin{Bmatrix}0\\ 1000\cos 50t\\ 800\cos 50t\end{Bmatrix}$$

On the transformed co-ordinate the force vector is

$$[\varphi]^T P(t) = \begin{bmatrix}0.01615 & 0.03507 & 0.04492\\ 0.03244 & 0.01622 & -0.02433\\ 0.03445 & -0.01372 & 0.02477\end{bmatrix}\begin{Bmatrix}0\\ 1000\ \cos\ 50t\\ 800\ \cos\ 50t\end{Bmatrix}$$

$$= \begin{Bmatrix}75\ \cos\ 50t\\ -3.244\ \cos\ 50t\\ -11.904\ \cos\ 50t\end{Bmatrix}$$

The equation of motion on transformed co-ordinate is given by

$$\{\ddot{\xi}_i\} + 2D_i\omega_i\{\dot{\xi}_i\} + [\omega_i^2]\{\xi_i\} = \{p(t)\}$$

i.e. $\ddot{\xi}_1 + 2 \times 0.02 \times 1.281\ \dot{\xi}_1 + 1.642\ \xi_1 = 75\cos 50\ t$

$$\ddot{\xi}_2 + 2 \times 0.039 \times 3.162\ \dot{\xi}_2 + 10\ \xi_2 = -3.244\cos 50\ t$$

$$\ddot{\xi}_3 + 2 \times 0.05 \times 4.135\ \dot{\xi}_3 + 17.1\ \xi_3 = -11.904\cos 50\ t$$

The above on simplification gives the following equations

$$\ddot{\xi}_1 + 0.0512\ \dot{\xi}_1 + 1.642\ \xi_1 = 75\cos 50\ t$$

$$\ddot{\xi}_2 + 2.466\ \dot{\xi}_2 + 10\ \xi_2 = -3.244\cos 50\ t$$

$$\ddot{\xi}_3 + 0.4135\ \dot{\xi}_3 + 17.1\ \xi_3 = -11.904\cos 50\ t$$

Knowing that amplitude for harmonic force is given by

$$\xi_{\max} = \frac{\frac{P_0}{K}\cos\omega_m t}{\sqrt{[(1-r^2)^2 + (2\zeta r)^2]}}$$

$$\begin{Bmatrix}\xi_1\\ \xi_2\\ \xi_3\end{Bmatrix} = \begin{Bmatrix}0.03\cos 50t\\ -1.3012\times 10^{-3}\cos 50t\\ -4.794\times 10^{-3}\cos 50t\end{Bmatrix}$$

For first mode :

$$\Delta_1 = \langle 0.0615, 0.0350, 0.0492\rangle^T \times 0.03\cos\ 50\ t\,\text{m}$$

or $\Delta_1 = \langle 1.845, 1.052, 1.498\rangle^T \times 10^{-3}\cos 50\ t\,\text{m}$

Nodal shear force is given by

$$\text{V1} = \text{K}\text{X}\Delta_1$$

$$= \begin{bmatrix}5000 & -2000 & 0\\ -2000 & 3500 & -1500\\ 0 & -1500 & 1500\end{bmatrix} \times \begin{bmatrix}1.845\\ 1.052\\ 1.498\end{bmatrix} \times 10^{-3}\cos 50\,t$$

$$= \begin{Bmatrix}7.21\\ -2.25\\ 0.668\end{Bmatrix}\cos 50\,t\ \text{kN}$$

Proceeding in identical manner for second mode

$$\Delta_2 = \langle -4.22, -2.11, 3.166\rangle^T \times 10^{-5}\cos\ 50\,t\,\text{m}$$

$$V_2 = \langle -0.169, -0.337, 0.079\rangle^T \cos 50\,t\ \text{kN}$$

For third mode

$$\Delta_3 = \langle 1.652, -1.521, 1.187\rangle^T \times 10^{-4}\cos\ 50t\ \text{m}$$

$$V_3 = \langle 1.13, -1.041, 0.406\rangle^T \cos\ 50t\ \text{kN}.$$

5.3 EIGEN VALUE ANALYSIS

5.3.1 Some techniques for eigen value analysis

In this section we deal with some of the techniques that are used for eigen value analysis for small and large structures and also their computer implementation. In various domains of science and engineering, eigen value solution plays a very important role. Mathematicians, physicists and engineers are grappling with this problem for perhaps more then a century and have put forward various techniques for solution to this problem.

Some concept of eigen value was already explained to you previously where we defined briefly the mathematical definition of eigen value and also explained it's physical significance in terms of principal stress in an elastic body. We also explained what it means in terms of Dynamic Analysis of a physical system.

In this chapter we first discuss different techniques that may be used for calculation of eigen values of small systems like buildings (two or three storied), simple framed

structures, chimneys, retaining walls etc to name a few and finally digress into techniques used for eigen value solution of large systems based on Finite element method and its computer implementation.

The *eigen value problem* in terms of matrix algebra is defined as follows (Ayres 1962):

If there exists a matrix $[A]$ and $\{X\}$ such that

- $[A]\{X\} = [\lambda]\{X\}$ then problem is said to be an *eigen value*[19] *problem*. Where $\lambda$is the eigen value.
- The matrix expression as mentioned above on expansion gives *a polynomial equation*, and the order of the polynomial is *same as the order of the matrix* $[A]$ *and* $\{X\}$ (i.e. if the size of the matrix is 2×2 the polynomial equation will be a quadratic equation, if the size is 3×3 it will be a cubic equation and so on...). *The characteristic roots of the polynomial gives the eigen value solution* (λ) *of the problem*.
- For each definite value of λ we get a set of homogeneous equation in terms of X and the same can be expressed in terms of the other and are known as the eigenvectors.
- For any particular mode j the term (λ_j, x_j) is known as the eigen pair for the jth mode.

In terms of structural dynamics considering the free vibration equation

$$[M]\{\ddot{X}\} + [K]\{X\} = 0 \tag{5.3.1}$$

Using $\{X\} = \{\varphi\}\sin(\omega t - \alpha)$, we have $\{\ddot{X}\} = -\{\varphi\}\omega^2 \sin(\omega t - \alpha)$and substituting the value of $\{\ddot{X}\}$ in Equation. (5.2.94) one can have

$$-[M]\omega^2\{\varphi\}\sin(\omega t - \phi) + [K]\{\varphi\}\sin(\omega t - \alpha) = 0$$

$$\rightarrow \quad [A]\{\varphi\} = \lambda\{\varphi\}, \quad \text{where } [A] = [K][M]^{-1} \tag{5.3.2}$$

which is the standard eigen value format in terms of structural dynamics.

Based on the above statements it will be observed that eigen value solution boils down to finding the roots of polynomial of n degrees where n is the order of the matrix.

Thus for a system having three degrees of freedom we have the free vibration equation of motion as

$$\begin{bmatrix} m_1 & 0 & 0 \\ 0 & m_2 & 0 \\ 0 & 0 & m_3 \end{bmatrix} \begin{Bmatrix} \ddot{x}_1 \\ \ddot{x}_2 \\ \ddot{x}_3 \end{Bmatrix} + \begin{bmatrix} k_1 + k_2 & -k_2 & 0 \\ -k_2 & k_2 + k_3 & -k_3 \\ 0 & -k_3 & k_3 \end{bmatrix} \begin{Bmatrix} x_1 \\ x_2 \\ x_3 \end{Bmatrix} = \begin{Bmatrix} 0 \\ 0 \\ 0 \end{Bmatrix}$$

19 The word "eigen" is a German term whose equivalent English word means "proper".

The above can be expressed as

$$\begin{bmatrix} k_1 + k_2 - m_1\lambda & -k_2 & 0 \\ -k_2 & k_2 + k_3 - m_2\lambda & -k_3 \\ 0 & -k_3 & k_3 - m_3\lambda \end{bmatrix} \begin{Bmatrix} x_1 \\ x_2 \\ x_3 \end{Bmatrix} = \{0\} \tag{5.3.3}$$

Expansion of the above would give a cubical polynomial whose roots would give the three eigen values λ_1, $\lambda_2 s$, λ_3.

In other words eigen value is obtained by determination of roots of the polynomial of order n where $n = 1, 2, 3\ldots$

We discuss hereafter some techniques that may be used for determination of roots of such n degree polynomial.

5.3.1.1 Visual inspection

With the advent of desktop and laptop computer, technology application has undergone a profound change in last two decades.

What was perceived as a Herculean effort even twenty years ago can now be very well done quite easily – thanks to the computer and different software now available commercially.

Thus method of visual inspection though one of the most simplified method, can very well be used to identify the roots very easily.

For instance in Example 5.2.10, we have shown that stiffness and mass matrix of a structural system as

$$[K] = \begin{bmatrix} 5000 & -2000 & 0 \\ -2000 & 3500 & -1500 \\ 0 & -1500 & 1500 \end{bmatrix} \quad \text{and} \quad [M] = \begin{bmatrix} 400 & & \\ & 400 & \\ & & 200 \end{bmatrix}, \quad \text{the eigen}$$

value equation is given by $\begin{bmatrix} 5000 - 400\lambda & -2000 & 0 \\ -2000 & 3500 - 400\lambda & -1500 \\ 0 & -1500 & 1500 - 200\lambda \end{bmatrix} = 0$, the above on expansion gives a cubical polynomial equation as

$$\lambda^3 - 28.75\lambda^2 + 215.625\lambda - 281.25 = 0$$

One of the simplest thing would be to plot this equation in utility tools like Excel, Mathcad or Matlab and visually find out the points where values tend to zero.

The value for which the equation tends to zero would give the eigenvalues of the equation.

For example if we plot the above polynomial equation in excel we have a graph as shown in Figure. 5.3.1.

Based on the above plot, we see that the values approach zero at three points and is given by

$$\lambda_1 = 1.7, \quad \lambda_2 = 10.2 \quad \text{and} \quad \lambda_3 = 17.1$$

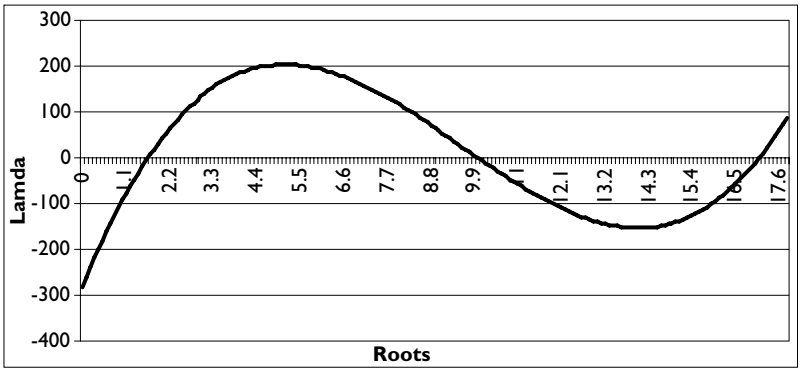


Figure 5.3.1 Plot of equation $\lambda^3 - 28.75\lambda^2 + 215.625\lambda - 281.25 = 0$.

The above represent three eigen values of the cubical polynomial[20].

5.3.1.2 Newton Raphson method

This is one of the most powerful iterative methods which can be very effectively used for determination of roots of an equation. Without mathematically making it too abstract the theory underlying the method can be explained as follows. Let

$$f(x) = Ax^3 + Bx^2 + Cx + D \tag{5.3.4}$$

where x_0 be an approximate value perceived as a root of the equation when the correct root is actually x_1, such that $f(x_1) = 0$.

Also let, $x_1 = x_0 \pm h$, (which would of course be problem dependent.)

Since $f(x_1) = 0$, we have $f(x_0 \pm h) = 0$ and now expanding it by Taylor series about x_0,

$$f(x_0) + hf'(x_0) + \frac{h^2}{2!}f''(x_0) + \frac{h^3}{3!}f'''(x_0) + \cdots\cdots = 0$$

Neglecting the higher terms, we have

$$f(x_0) + hf'(x_0) = 0; \quad h = -\frac{f(x_0)}{f'(x_0)}$$

An improved approximation is then given by,

$$x_1 = x_0 - \frac{f(x_0)}{f'(x_0)} \tag{5.3.5}$$

20 Reader to note that in Example 5.2.10 we found the three eigen values as 1.643,10.00,17.104 by Newton Raphson method which we have explained in the next section.

Successive approximation is given by $x_1, x_2, x_3 \ldots\ldots x_n$, where,

$$x_{n+1} = x_n - \frac{f(x_n)}{f'(x_n)} \quad \text{till the value of } x_{n+1} - x_n \cong 0. \tag{5.3.6}$$

The value thus obtained is one of the roots of the equation and let it be depicted by α. If α is one of the root of the equation then $(x - \alpha) = 0$ and the equation $Ax^3 + Bx^2 + Cx + D = 0$, can be represented by, $(x - \alpha)(A'x^2 + B'x + C') = 0$

The expression $(A'x^2 + B'x + C') = 0$ is next considered and we repeat the process to find out the next root β. We reduce the degree of the polynomial for each successive root, till all the roots are found.

We shall explain the above by a suitable numerical example.

Example 5.3.1

Find out the roots of the equation $\lambda^3 - 28.75\lambda^2 + 215.625\lambda - 281.25 = 0$ based on Newton-Raphson method.

Solution:

Let $f(\lambda) = \lambda^3 - 28.75\lambda^2 + 215.625\lambda - 281.25$, then, $f'(\lambda) = 3\lambda^2 - 28.75\lambda$.

Let $g\lambda = 1.2$, then we have $f(\lambda) = -62.172$ and $f'(\lambda) = 150.945$

Thus $\lambda_1 = 1.2 - \frac{-62.172}{150.945} = 1.611885$; $\lambda_2 = 1.61185 - \frac{-4.1968}{130.736} = 1.6439$

$$\lambda_3 = 1.6439 - \frac{-0.035}{129.208} = 1.6444$$

The values being nearly constant we conclude that $\lambda = 1.644$ is one of the roots of the equation.

Thus equation $\lambda^3 - 28.75\lambda^2 + 215.625\lambda - 281.25 = 0$ can be simplified to

$$(\lambda - 1.644)\lambda^2 - (\lambda - 1.644)27.106\lambda + 171.106(\lambda - 1.644) = 0$$

or, $(\lambda - 1.644)(\lambda^2 - 27.106\lambda + 171.106) = 0$

Thus the reduced equation is $(\lambda^2 - 27.106\lambda + 171.106) = 0$

With this we start our next cycle of iteration[21], as shown hereafter

Let $f(\lambda) = \lambda^2 - 27.106\lambda + 171.106$

Then $f'(\lambda) = 2\lambda - 27.106$

As a first trial let $\lambda = 9$ then we have

$$\lambda_1 = 9 - \frac{8.152}{-9.106} = 9.895; \quad \lambda_2 = 9.895 - \frac{0.757}{-7.316} = 9.998;$$

and $\lambda_3 = 9.998 - \frac{0.06021}{-7.11} = 10.00.$

21 Note the equation being a quadratic one, we can directly solve it by the expression $\lambda_{j,k} = \frac{-b \pm \sqrt{b^2 - 4ac}}{2a}$, however for clarity we proceed with as depicted above.

Thus values being nearly constant we conclude that $\lambda = 10.00$ is another root of the equation.

Thus on further reduction of the equation $\lambda^2 - 27.106\lambda + 171.106 = 0$ we have

$$(\lambda - 10)(\lambda - 17.106) = 0$$

Thus, the third root is $\lambda = 17.106$.

Three roots are

$$\{\lambda\}_{i=1}^{3} = \begin{Bmatrix} 1.644 \\ 10.00 \\ 17.106 \end{Bmatrix}$$

It is to be noted that the initial assumption is very important in terms of iterations. For instance in Example 5.2.10 we started with $\lambda = 50$ and took *eight (8) iterations* to arrive at the first root. On the contrary in this case starting with $\lambda = 1$ it took us only *three (3) iterations* to arrive at the first root.

This means closer the first approximation to a root, lesser is the number of iterations it will take to converge.

To make the process quicker one can directly plot the values in excel and find out the point where the value changes sign, you can select a value close to this point as the first iteration vector which would considerably accelerate the process.

The above technique can be very easily adapted in a spreadsheet to arrive at the roots as shown hereafter

$A = 1, B = -28.75, C = 215.625, D = -281.25$

Iteration	λ	$f(\lambda)$	$f'(\lambda)$	$\lambda\, f(\lambda)/f'(\lambda)$
1	1.2	−62.172	150.945	1.611885
2	1.611885124	−4.19681	130.7361	1.643986
3	1.643986467	−0.02461	129.2039	1.644177
4	1.644176945	−8.6E-07	129.1948	1.644177
5	1.644176952	0	129.1948	1.644177

It will be observed that at 5th iteration the values has converged to $\lambda = 1.644177$.

5.3.1.3 Ramanujan's method[22]

Ramanujan's method can be stated as follows

22 Srinivasa Ramanujan born in Chennai in 1887 a mathematical genius who died tragically of tuberculosis at the young age of only 33 in England. With practically minimal formal education he managed to solve some of the most complex mathematical riddles, which has intrigued many a mathematician.

Let there be an equation represented by,

$$f(\lambda) = A\lambda^3 + B\lambda^2 + C\lambda + D = 0$$

The above equation can then be written as

$$f(\lambda) = D - A\lambda^3 - B\lambda^2 - C\lambda \tag{5.3.7}$$

or, $f(\lambda) = [1 - (A\lambda^3 + B\lambda^2 + C\lambda)/D] = 0$ as D$\neq 0$

Considering, $x = (A\lambda^3 + B\lambda^2 + C\lambda)/D$, we can represent Equation (5.3.7) as the first two terms of the equation

$$f(\lambda) = [1 - x]^{-1} = 0$$

Thus[23],

$$\begin{aligned} f(\lambda) &= [1 + (a_1\lambda + a_2\lambda^2 + a_3\lambda^3) + (a_1\lambda + a_2\lambda^2 + a_3\lambda^3)^2 + \cdots\cdots\cdots] \\ &= b_1 + b_2\lambda + b_3\lambda^2 \end{aligned} \tag{5.3.8}$$

where $a_1 = C/D$, $a_2 = B/D$ and $a_3 = A/D$

Comparing the like powers of λ we have

$$\begin{aligned} &b_1 = 1 \\ &b_2 = a_1 = a_1 b_1 \\ &b_3 = a_1^2 + a_2 = a_1 b_2 + a_2 b_1 \\ &\cdots\cdots\cdots\cdots\cdots\cdots\cdots\cdots\cdots\cdots\cdots\cdots \\ &b_n = a_1 b_{n-1} + a_2 b_{n-2} + \cdots\cdots\cdots + a_{n-1} b_1, \quad \text{for } n = 2, 3.\ldots\ldots\ldots \end{aligned} \tag{5.3.9}$$

Ramanujan showed that successive value of $\frac{b_n}{b_{n+1}}$ approaches the lowest root of the equation, $f(\lambda) = 0$.

Example 5.3.2

Find out the lowest root of the equation $\lambda^3 - 28.75\lambda^2 + 215.625\,\lambda - 281.25 = 0$ based on Ramanujan's Method.

Solution:

Here $\lambda^3 - 28.75\lambda^2 + 215.625\lambda - 281.25 = 0$

23 From Binomial theorem .. $(1+x)^p = 1 + {}^pC_1 x + {}^pC_2 x^2 + {}^pC_3 x^3 + \cdots\ldots\cdots\cdots$ where p could be negative, zero or positive integer

Transferring the above in the Ramanujan's form, we have $\left[1 - \frac{215.625\lambda - 28.75\lambda^2 + \lambda^3}{281.25}\right] = 0$

Thus by the problem

$$a_1 = \frac{215.625}{281.25} = 0.766667, \quad a_2 = \frac{-28.75}{281.25} = -0.10222,$$
$$a_3 = \frac{1}{281.25} = 0.003556; \quad a_4 = a_5 = 0$$

$b_1 = 1$
$b_2 = a_1 = 0.766667$ $\quad b_1/b_2 = 1.304348$
$b_3 = a_1 b_2 + a_2 b_1 = 0.485556$ $\quad b_2/b_3 = 1.578947$
$b_4 = a_1 b_3 + a_2 b_2 + a_3 b_1 = 0.297444$ $\quad b_3/b_4 = 1.632424$
$b_5 = a_1 b_4 + a_2 b_3 + a_3 b_2 + a_4 b_1 = 0.178406$ $\quad b_4/b_5 = 1.667232$
$b_6 = a_1 b_5 + a_2 b_4 + a_3 b_3 + a_4 b_2 + a_5 b_1 = 0.108099$ $\quad b_5/b_6 = 1.650395$
.....
$b_9 = 0.024298$
$b_{10} = 0.014778$ $\quad b_9/b_{10} = 1.644184$

Based on above calculation it is observed that successive ratio has converged to the value of 1.6441.

5.3.1.4 Matrix deflation method

This method is often used for large system when we are interested to find out the fundamental time period (or the lowest frequency) or the highest frequency /time period.

We had shown earlier that in terms of structural dynamics the eigen-values can be expressed as

$$[K]\{\phi\} = \omega^2[M]\{\phi\} \quad \text{or } [B]\{\phi\} = \frac{1}{\omega^2}\{\phi\} \tag{5.3.10}$$

where $[B] = [K]^{-1}[M]$ when the value converges to the *lowest eigen value*, or can be expressed as $[A]\{\phi\} = \omega^2\{\phi\}$, where $[A] = [K][M]^{-1}$ when the value converges to the *highest eigen value*.

The iteration starts with a trial value of the column vector which is pre-multiplied by $[B]$ or $[A]$ depending on what is the value we are seeking. The resulting column matrix is then normalized by reducing one of its value to unity.

The resulting normalized vector is then again pre-multiplied by the matrix $[B]$ or $[A]$. The process is repeated till we arrive at a normalized column matrix which becomes stationary with respect to the preceding step. The constant thus obtained gives the highest/lowest eigen value.

We explain the above method now with a suitable example.

Example 5.3.3

For structure having stiffness and mass matrix as mentioned below determine the highest eigen-value by matrix deflation method

$$[K] = \begin{bmatrix} 5000 & -2000 & 0 \\ -2000 & 3500 & -1500 \\ 0 & -1500 & 1500 \end{bmatrix} \quad \textbf{and} \quad [M] = \begin{bmatrix} 400 & & \\ & 400 & \\ & & 200 \end{bmatrix}.$$

Solution:

For the above matrices

$$[M]^{-1} = \begin{bmatrix} 0.0025 & 0 & 0 \\ 0 & 0.0025 & 0 \\ 0 & 0 & 0.005 \end{bmatrix}$$

Considering $[A] = [K][M]^{-1}$ we have

$$[A] = \begin{bmatrix} 5000 & -2000 & 0 \\ -2000 & 3500 & -1500 \\ 0 & -1500 & 1500 \end{bmatrix} \times \begin{bmatrix} 0.0025 & 0 & 0 \\ 0 & 0.0025 & 0 \\ 0 & 0 & 0.005 \end{bmatrix}$$

$$= \begin{bmatrix} 12.5 & -5 & 0 \\ -5 & 8.75 & -7.5 \\ 0 & -3.75 & 7.5 \end{bmatrix}$$

Considering $\{\varphi\} = \begin{Bmatrix} 1.0 \\ 1.0 \\ 1.0 \end{Bmatrix}$ as trial vector, we have

$$[A]\{\varphi\} = \begin{bmatrix} 12.5 & -5 & 0 \\ -5 & 8.75 & -7.5 \\ 0 & -3.75 & 7.5 \end{bmatrix} \begin{Bmatrix} 1.0 \\ 1.0 \\ 1.0 \end{Bmatrix} = \omega^2\{\varphi\} = 7.5 \begin{Bmatrix} 1.0 \\ -0.5 \\ 0.5 \end{Bmatrix}$$

For **second cycle**

$$[A]\{\varphi\} = \begin{bmatrix} 12.5 & -5 & 0 \\ -5 & 8.75 & -7.5 \\ 0 & -3.75 & 7.5 \end{bmatrix} \begin{Bmatrix} 1.0 \\ -0.5 \\ 0.5 \end{Bmatrix} = \omega^2\{\varphi\} = 15 \begin{Bmatrix} 1.0 \\ -0.875 \\ 0.375 \end{Bmatrix}$$

For **third cycle**

$$[A]\{\varphi\} = \begin{bmatrix} 12.5 & -5 & 0 \\ -5 & 8.75 & -7.5 \\ 0 & -3.75 & 7.5 \end{bmatrix} \begin{Bmatrix} 1.0 \\ -0.875 \\ 0.375 \end{Bmatrix}$$

$$= \omega^2\{\varphi\} = 16.875 \begin{Bmatrix} 1.0 \\ -0.91667 \\ 0.361111 \end{Bmatrix}$$

4th Cycle

$$[A]\{\varphi\} = \begin{bmatrix} 12.5 & -5 & 0 \\ -5 & 8.75 & -7.5 \\ 0 & -3.75 & 7.5 \end{bmatrix} \begin{Bmatrix} 1.0 \\ -0.91667 \\ 0.361111 \end{Bmatrix}$$

$$= \omega^2\{\varphi\} = 17.08333 \begin{Bmatrix} 1.0 \\ -0.92073 \\ 0.359756 \end{Bmatrix}$$

5th Cycle

$$[A]\{\varphi\} = \begin{bmatrix} 12.5 & -5 & 0 \\ -5 & 8.75 & -7.5 \\ 0 & -3.75 & 7.5 \end{bmatrix} \begin{Bmatrix} 1.0 \\ -0.92073 \\ 0.359756 \end{Bmatrix}$$

$$= \omega^2\{\varphi\} = 17.10366 \begin{Bmatrix} 1.0 \\ -0.92112 \\ 0.359626 \end{Bmatrix}$$

6th Cycle

$$[A]\{\varphi\} = \begin{bmatrix} 12.5 & -5 & 0 \\ -5 & 8.75 & -7.5 \\ 0 & -3.75 & 7.5 \end{bmatrix} \begin{Bmatrix} 1.0 \\ -0.92112 \\ 0.359626 \end{Bmatrix} = \omega^2\{\varphi\}$$

$$= 17.10561 \begin{Bmatrix} 1.0 \\ -0.92116 \\ 0.359613 \end{Bmatrix}$$

7th Cycle

$$[A]\{\varphi\} = \begin{bmatrix} 12.5 & -5 & 0 \\ -5 & 8.75 & -7.5 \\ 0 & -3.75 & 7.5 \end{bmatrix} \begin{Bmatrix} 1.0 \\ -0.92116 \\ 0.359613 \end{Bmatrix} = \omega^2\{\varphi\}$$

$$= 17.1058 \begin{Bmatrix} 1.0 \\ -0.92116 \\ 0.359612 \end{Bmatrix}$$

As the column matrix has now become stationary we conclude that the highest eigen value of the system is given by $\lambda = 17.1058$.

It is to be noted that as per example 5.2.11 we arrived at this value based on Newton Raphson method as $\lambda = 17.106$.

This is also sometimes called as inverse iteration technique for the value having converged to the highest eigen value.

Now that we have explained the above method based on a numerical example it would perhaps be relevant to contemplate as to how and why does it converge to the desired eigen value.

5.3.1.5 Mathematical proof of convergence to lowest eigen value

For a matrix $[A]$ of order nxn, we know that we can obtain n number of eigen values and n eigen vectors $\{\varphi\}$ which span n space and linearly independent of each other[24] i.e.

$$\{\varphi_1\} = C_1\{\phi_1\} + C_2\{\phi_2\} + C_3\{\phi_3\} + \cdots\cdots\cdots\cdots + C_n\{\phi_n\} \tag{5.3.11}$$

where, $\{\varphi_1\}$ = the first trial vector, $C_1, C_2, C_3, \cdots\cdots C_n$ = constants; $\{\phi_1\}, \{\phi_2\}, \{\phi_3\} \ldots \{\phi_n\} = n$ number of eigenvectors.

Now pre-multiplying the above equation with $[A]$, we have

$$[A]\{\varphi_1\} = C_1[A]\{\varphi_1\} + C_2[A]\{\phi_2\} + C_3[A]\{\phi_3\} + \cdots\cdots\cdots\cdots C_n[A]\{\phi_n\} \tag{5.3.12}$$

Since $[A][\varphi] = \frac{1}{\omega^2}[\varphi]$, we can interpret this expression as the $[A]$ matrix representing a linear transformation that transforms any eigenvector $\{\varphi_1\}$ into itself within a constant scalar multiplier $(1/\omega_r^2)$.

Thus, the above equation can be represented as

$$[A]\{\varphi_1\} = \{\varphi_2\} = \frac{C_1}{\omega_1^2}\{\phi_1\} + \frac{C_2}{\omega_2^2}\{\phi_2\} + \frac{C_3}{\omega_3^2}\{\phi_3\} + \cdots\cdots\cdots\cdots \frac{C_n}{\omega_n^2}\{\phi_n\} \tag{5.3.13}$$

Here $\{\varphi_2\}$ is the second trial vector.

The second iteration would give

$$[A]\{\varphi_2\} = \{\varphi_3\} = \frac{C_1}{\omega_1^4}\{\phi_1\} + \frac{C_2}{\omega_2^4}\{\phi_2\} + \frac{C_3}{\omega_3^4}\{\phi_3\} + \cdots\cdots\cdots\cdots \frac{C_n}{\omega_n^4}\{\phi_n\} \tag{5.3.14}$$

24 We will discuss more about this property of eigen vectors when we talk about eigen value determination of large systems.

Thus r numbers of iteration would give

$$[A]\{\varphi_r\} = \{\varphi_{r+1}\} = \frac{C_1}{\omega_1^{2r}}\{\phi_1\} + \frac{C_2}{\omega_2^{2r}}\{\phi_2\} + \frac{C_3}{\omega_3^{2r}}\{\phi_3\} + \cdots\cdots\cdots\cdots \frac{C_n}{\omega_n^{2r}}\{\phi_n\} \tag{5.3.15}$$

As $\omega_1 < \omega_2 < \omega_3 < \cdots\cdots\cdots\cdots < \omega_n$ it is evident that for the value r (number of iterations) being sufficiently large,

$$\frac{1}{\omega_1^{2r}} >> \frac{1}{\omega_2^{2r}} >> \frac{1}{\omega_3^{2r}} >> \cdots\cdots\cdots\cdots \frac{1}{\omega_n^{2r}} \tag{5.3.16}$$

Equation (5.3.15) reduces to

$$[A]\{\varphi_r\} = \{\varphi_{r+1}\} = \frac{C_1}{\omega_1^{2r}}\{\phi_1\} + \frac{C_2}{\omega_2^{2r}}\{\phi_2\} + \frac{C_3}{\omega_3^{2r}}\{\phi_3\} + \cdots\cdots\cdots\cdots \frac{C_n}{\omega_n^{r}}\{\phi_n\} \tag{5.3.17}$$

thus the first term in Equation (5.3.17) only become significant with other terms having higher order becoming exceedingly small and can be neglected.

Hence, for r number of iterations required to achieve the accuracy, the resulting equation is

$$\{\varphi_{r+1}\} = \frac{C_1}{\omega_1^{2r}}\{\phi_1\} \tag{5.3.18}$$

Thus we see that the $(r+1)$th trial vector becomes identical to the first natural mode shape to within a multiplicative constant and converges to the lowest eigenvalue.

5.3.1.6 Calculation of higher modes

For calculation of higher eigen values the matrix $[A]$ has to be modified to eliminate the effect of the first eigen value.

This is done by the following mathematical operations

$$[A_2] = [A] - \frac{1}{\omega_1^2}\{\varphi_1\}_n\{\varphi_1\}_n^T[M] \tag{5.3.19}$$

where $\{\varphi_1\}_n =$ Is the normalized eigen vector, based on orthogonal property[25] we have $\{\varphi_1\}_n[M]\{\varphi_1\}_n^T = 1$.

25 Recall our discussion earlier.

Thus the above sweeps out the effect of the first eigen value and if we repeat our process with a second trial vector we will converge to the next higher eigen value.

The above will now be explained with a suitable numerical example.

Example 5.3.4

For structure having stiffness and mass matrix as mentioned below determine the lowest eigen value by matrix deflation method and also find out the other values based on sweeping technique.

$$[K] = \begin{bmatrix} 5000 & -2000 & 0 \\ -2000 & 3500 & -1500 \\ 0 & -1500 & 1500 \end{bmatrix} \quad \textbf{and} \quad [M] = \begin{bmatrix} 400 & & \\ & 400 & \\ & & 200 \end{bmatrix}$$

Solution:

For the above matrices

$$[K]^{-1} = \begin{bmatrix} 0.0003333 & 0.000333 & 0.000333 \\ 0.0003333 & 0.000833 & 0.000833 \\ 0.0003333 & 0.000833 & 0.0015 \end{bmatrix}$$

Considering $[A] = [K]^{-1}[M]$ we have

$$[A] = \begin{bmatrix} 0.0003333 & 0.000333 & 0.000333 \\ 0.0003333 & 0.000833 & 0.000833 \\ 0.0003333 & 0.000833 & 0.0015 \end{bmatrix} \times \begin{bmatrix} 400 & 0 & 0 \\ 0 & 400 & 0 \\ 0 & 0 & 2000 \end{bmatrix}$$

$$= \begin{bmatrix} 0.133333 & 0.133333 & 0.066667 \\ 0.133333 & 0.333333 & 0.166667 \\ 0.133333 & 0.333333 & 0.3 \end{bmatrix}$$

Considering $\{\varphi\} = \begin{Bmatrix} 1.0 \\ 1.0 \\ 1.0 \end{Bmatrix}$ as the first trial vector we have

$$[A]\{\varphi\} = \begin{bmatrix} 0.133333 & 0.133333 & 0.066667 \\ 0.133333 & 0.333333 & 0.166667 \\ 0.133333 & 0.333333 & 0.3 \end{bmatrix} \begin{Bmatrix} 1.0 \\ 1.0 \\ 1.0 \end{Bmatrix}$$

$$= \frac{1}{\omega^2}\{\varphi\} = 0.766667 \begin{Bmatrix} 0.434783 \\ 0.826087 \\ 1.0 \end{Bmatrix}$$

For second cycle we have

$$[A]\{\varphi\} = \begin{bmatrix} 0.133333 & 0.133333 & 0.066667 \\ 0.133333 & 0.333333 & 0.166667 \\ 0.133333 & 0.333333 & 0.3 \end{bmatrix} \begin{Bmatrix} 0.434783 \\ 0.826087 \\ 1.0 \end{Bmatrix}$$

$$= \frac{1}{\omega^2}\{\varphi\} = 0.63333 \begin{Bmatrix} 0.3707 \\ 0.7894 \\ 1.0 \end{Bmatrix}$$

For third cycle we have

$$[A]\{\phi\} = \begin{bmatrix} 0.133333 & 0.133333 & 0.066667 \\ 0.133333 & 0.333333 & 0.166667 \\ 0.133333 & 0.333333 & 0.3 \end{bmatrix} \begin{Bmatrix} 0.370709 \\ 0.789474 \\ 1.0 \end{Bmatrix}$$

$$= \frac{1}{\omega^2}\{\phi\} = 0.612856 \begin{Bmatrix} 0.36135 \\ 0.782343 \\ 1.0 \end{Bmatrix}$$

.....

Proceeding in this way after 9 cycles we arrive at a value
9th Cycle

$$[A]\{\varphi\} = \begin{bmatrix} 0.133333 & 0.133333 & 0.066667 \\ 0.133333 & 0.333333 & 0.166667 \\ 0.133333 & 0.333333 & 0.3 \end{bmatrix} \begin{Bmatrix} 0.359612 \\ 0.780776 \\ 1.0 \end{Bmatrix}$$

$$= \frac{1}{\omega^2}\{\varphi\} = 0.608207 \begin{Bmatrix} 0.359612 \\ 0.780776 \\ 1.0 \end{Bmatrix}$$

where the value becomes stationary

Thus as per the problem $\omega^2 = 1/0.608207 = 1.64416$ which has converged to the lowest eigenvalue[26].

Calculation of next lowest eigen value

The scaling factor is given by

$$\{\varphi\}^T[M]\{\varphi\} = \langle 0.359612 \quad 0.780776 \quad 1.0 \rangle \times \begin{bmatrix} 400 & 0 & 0 \\ 0 & 400 & 0 \\ 0 & 0 & 200 \end{bmatrix} \begin{Bmatrix} 0.359612 \\ 0.780776 \\ 1.0 \end{Bmatrix} = 495.572$$

$$\text{S.F.} = \sqrt{495.572 = 22.26}$$

26 We arrived at a value of 1.644 based on Newton Raphson Method in Example 5.2.11.

Thus normalized eigen vector is given by

$$\{\varphi\}_n = \begin{Bmatrix} 0.01654018 \\ 0.035072995 \\ 0.044920688 \end{Bmatrix}$$

Considering the expression $[A_2] = [A] - \frac{1}{\omega_1^2}\{\phi_1\}_n \{\phi_1\}_n^T [M]$ we have

$$[A_2] = \begin{bmatrix} 0.133333 & 0.133333 & 0.066667 \\ 0.133333 & 0.333333 & 0.166667 \\ 0.133333 & 0.333333 & 0.3 \end{bmatrix} - \begin{Bmatrix} 0.016154 \\ 0.035072 \\ 0.04492 \end{Bmatrix} \begin{Bmatrix} 0.01654 \\ 0.035072 \\ 0.04492 \end{Bmatrix}^T \begin{bmatrix} 400 & & \\ & 400 & \\ & & 200 \end{bmatrix}$$

$$[A_2] = \begin{bmatrix} 0.0698 & -0.0045 & -0.0216 \\ -0.0045 & 0.0341 & -0.025 \\ -0.0432 & -0.05 & 0.0545 \end{bmatrix}$$ which is the revised matrix with

which we start **our new cycle** of iteration

Considering $\{\varphi\} = \begin{Bmatrix} 1.0 \\ -1.0 \\ 1.0 \end{Bmatrix}$ as trial vector we have

$$[A]\{\varphi\} = \begin{bmatrix} 0.0698 & -0.0045 & -0.0216 \\ -0.0045 & 0.0341 & -0.025 \\ -0.0432 & -0.05 & 0.0545 \end{bmatrix} \begin{Bmatrix} 1.0 \\ -1.0 \\ 1.0 \end{Bmatrix}$$

$$= \frac{1}{\omega^2}\{\varphi\} = 0.0613 \begin{Bmatrix} 0.859706 \\ -1.03752 \\ 1.0 \end{Bmatrix}$$

For **second cycle** we have

$$[A]\{\varphi\} = \begin{bmatrix} 0.0698 & -0.0045 & -0.0216 \\ -0.0045 & 0.0341 & -0.025 \\ -0.0432 & -0.05 & 0.0545 \end{bmatrix} \begin{Bmatrix} 0.859706 \\ -1.03752 \\ 1.0 \end{Bmatrix}$$

$$= \frac{1}{\omega^2}\{\varphi\} = 0.069237 \begin{Bmatrix} 0.622161 \\ -0.97295 \\ 1.0 \end{Bmatrix}$$

. . . . . .

Proceeding in this way after 13 cycles we arrive at a value

13th Cycle

$$[A]\{\varphi\} = \begin{bmatrix} 0.0698 & -0.0045 & -0.0216 \\ -0.0045 & 0.0341 & -0.025 \\ -0.0432 & -0.05 & 0.0545 \end{bmatrix} \begin{Bmatrix} -0.65011 \\ -0.34136 \\ 1.0 \end{Bmatrix} = \frac{1}{\omega^2}\{\varphi\}$$

$$= 0.099653 \begin{Bmatrix} -0.6567 \\ -0.33832 \\ 1.0 \end{Bmatrix}$$

where the value becomes stationary

Thus as per the problem $\omega^2 = \frac{1}{0.0996503} = 10.035$ which has converged to the next lowest eigen value[27].

It is to be noted in the above problem that it took 9 cycles of iteration to converge to the lowest eigen-value and subsequently took 13 cycles of iteration to converge to the next eigen value.

How many iterations it would take to converge to a reasonable accuracy varies from case to case. However it is generally seen that higher modes take larger iteration to converge.

For systems with large degrees of freedom or cases where significant modes needs to be considered the technique may turn out to be less efficient compared to other techniques used for systems with large degrees of freedom.

5.3.1.7 Stodola's Method

Stodola's Method is actually a refined version of matrix deflation method which is very effective in finding out the values of first few modes of a large structural system[28].

The steps involved in calculation of the first lowest eigen value remains exactly same as that like matrix deflation method, it is only for the higher modes where for matrix deflation method order of matrix remains unchanged, in this method gets reduced by the degree one for each successive higher modes.

Suffice it to say this successive reduction of matrix considerably reduces the computational effort and can surely be considered as an improvement on the matrix deflation method.

The steps involved in this method can thus be structured as hereunder:

- Form the matrix $[A]$ as

$$[A] = [K]^{-1}[M] \tag{5.3.20}$$

27 The same problem gave a value of 10.0 in Example 5.31 by Newton Raphson method.

28 We should remember that in most of the cases it is the first few modes which contribute to maximum dynamic response of a system.

- Choose a trial vector $\{\phi\}$ and proceed with the iteration as shown in the matrix deflation method till it converges to the desired value. The constant will give the lowest eigen value and the corresponding values in the column matrix gives the first mode eigen vectors.
- For obtaining higher modes modify the basis based on orthogonality relationship[29]

$$m_1\phi_1^1\phi_1^2 + m_2\phi_2^1\phi_2^2 + \cdots\cdots\cdots + m_n\phi_n^1\phi_n^2 = 0 \tag{5.3.21}$$

- Knowing the eigen vectors for first mode find out the expression.

$$\phi_1^2 = -\frac{m_2\phi_2^1}{\phi_1^1}\phi_2^2 - \frac{m_3\phi_3^1}{\phi_{1_1}}\phi_3^2 - \cdots\cdots\cdots - \frac{m_n\phi_n^1}{\phi_1^1}\phi_n^2 \tag{5.3.22}$$

- Now expanding the term

$$[A]\{\varphi\} = \frac{1}{\omega^2}\{\varphi\} \tag{5.3.23}$$

  and substituting the eigen vector as obtained above we eliminate the effect of the first eigen value and eigen vector and are left with a matrix of order $(n-1)$
- We start new iteration with this matrix (of order $n-1$) to find out the next higher eigen value.

The method will now be explained by a suitable numerical example.

Example 5.3.5

Repeat Example 5.3.4 to solve by Stodola's method to find out the eigen values and eigen vectors given:

$$[K] = \begin{bmatrix} 5000 & -2000 & 0 \\ -2000 & 3500 & -1500 \\ 0 & -1500 & 1500 \end{bmatrix} \quad \textbf{and} \quad [M] = \begin{bmatrix} 400 & & \\ & 400 & \\ & & 200 \end{bmatrix}$$

Solution:

Based on example 10.4 we have seen that $[A] = [K]^{-1}[M]$ gives the value

$$[A] = \begin{bmatrix} 0.133333 & 0.133333 & 0.066667 \\ 0.133333 & 0.333333 & 0.166667 \\ 0.133333 & 0.333333 & 0.3 \end{bmatrix}$$ and starting with a trial vector

29 Here superscript denotes order of mode (1st, 2nd etc.) and not power.

$\{\varphi\} = \begin{Bmatrix} 1.0 \\ 1.0 \\ 1.0 \end{Bmatrix}$ after 9 cycles of iteration we arrive at a value of

$\frac{1}{\omega^2}\{\varphi\} = 0.608207\langle 0.359612 \quad 0.780776 \quad 1.0\rangle^T$ where $\lambda = 0.608207$ and the corresponding eigen vectors for first mode is given by $\{\varphi\} = \langle 0.359612 \quad 0.780776 \quad 1.0\rangle^T$.

For calculation of higher modes considering the orthogonality relation, we have

$$m_1\phi_1^1\phi_1^2 + m_2\phi_2^1\phi_2^2 + m_3\phi_3^1\phi_3^2 = 0$$

or, $400 \times 0.359162\phi_1^2 + 400 \times 0.780776\phi_2^2 + 200 \times 1\phi_3^2 = 0$

$$\rightarrow \quad \phi_1^2 = -2.173883\phi_2^2 - 1.39213\phi_3^2.$$

Now expanding the term $[A]\{\varphi\} = \lambda\{\varphi\}$we have (neglecting the superscript for ease of presentation)

$$0.13333\phi_1 + 0.13333\phi_2 + 0.06667\phi_3 = 0.21872$$
$$0.13333\phi_1 + 0.33333\phi_2 + 0.16667\phi_3 = 0.47487$$
$$0.13333\phi_1 + 0.33333\phi_2 + 0.3\phi_3 = 0.608207.$$

Substituting the value $\phi_1 = -2.173883\phi_2 - 1.39213\phi_3$ in the last two equations we have

$$0.04348\phi_2 - 0.018939\phi_3 = 0.47487$$
and $\quad 0.04348\phi_2 + 0.114391\phi_3 = 0.60807$

Thus the modified $[A]$ matrix becomes

$[A] = \begin{bmatrix} 0.04348 & -0.018939 \\ 0.04348 & 0.114391 \end{bmatrix}$, we start with new eigen vector $\{\phi\} = \begin{Bmatrix} 1 \\ 1 \end{Bmatrix}$ when we have

$$[A]\{\phi\} = \begin{bmatrix} 0.04348 & -0.018939 \\ 0.04348 & 0.114391 \end{bmatrix} \begin{Bmatrix} 1 \\ 1 \end{Bmatrix}$$
$$= \lambda\{\phi\} = 0.157871 \begin{Bmatrix} 0.15545 \\ 1 \end{Bmatrix}$$

For 2nd cycle

$$[A]\{\phi\} = \begin{bmatrix} 0.04348 & -0.018939 \\ 0.04348 & 0.114391 \end{bmatrix} \begin{Bmatrix} 0.15545 \\ 1 \end{Bmatrix}$$

$$= \lambda\{\phi\} = 0.12115 \begin{Bmatrix} -0.10054 \\ 1 \end{Bmatrix}$$

For 3rd cycle

$$[A]\{\phi\} = \begin{bmatrix} 0.04348 & -0.018939 \\ 0.04348 & 0.114391 \end{bmatrix} \begin{Bmatrix} 0.15545 \\ 1 \end{Bmatrix}$$

$$= \lambda\{\phi\} = 0.106025 \begin{Bmatrix} -0.25753 \\ 1 \end{Bmatrix}$$

.....

After **10th cycle,** we have

$$[A]\{\phi\} = \begin{bmatrix} 0.04348 & -0.018939 \\ 0.04348 & 0.114391 \end{bmatrix} \begin{Bmatrix} -0.3316 \\ 1 \end{Bmatrix}$$

$$= \lambda\{\phi\} = 0.099973 \begin{Bmatrix} -0.33366 \\ 1 \end{Bmatrix}$$

when the value becomes stationary.

Thus the desired eigen value[30] is = 0.099973

The corresponding eigen vector is given by $\{\phi\} = \begin{Bmatrix} -0.66676 \\ -0.33366 \\ 1.0 \end{Bmatrix}$

Now proceeding in the identical manner we can find out the next eigenvalue[31].

5.3.1.8 Rayleigh Ritz method

In many cases, for different class of structures it is sufficient to find out the fundamental time period or response of a first few modes.

In such cases Rayleigh Ritz method is one of the most powerful methods for calculation of time period and can be applied to wide class of problems in engineering[32].

The beauty of the method is that it is equally versatile in its application based on *closed form and numerical solution.*

The underlying principle of this method can be explained as follows:

30 In example 5.3.4 we had obtained this value as 0.0996.

31 This we leave as an exercise for the reader.

32 For further application of this method refer to the topic of retaining wall and tall chimneys in Chapter 3 (Vol. 2) for earthquake analysis.

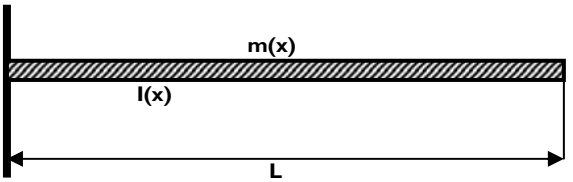


Figure 5.3.2 Cantilever beam under flexure.

For a flexural member shown in Figure 5.3.2, the kinetic energy of the system is given by

$$T = \frac{1}{2}\int_0^L m(x)\left[\frac{\partial y(x,t)}{\partial t}\right]^2 dx \tag{5.3.24}$$

Considering $y(x,t) = \phi(x)\cdot q(t)$ we have

$T = \frac{1}{2}\int_0^L m(x)\left[\sum_{i=1}^{n}\phi_i(x)\dot{q}_i(t)\right]\left[\sum_{j=1}^{n}\phi_j(x)\dot{q}_j(t)\right]dx$, which can be expressed as

$$T = \frac{1}{2}\sum_{i=1}^{n}\sum_{j=1}^{n}\dot{q}_i(t)\dot{q}_j(t)\left[\int_0^L m(x)\phi_{i(}x)\phi_j(x)dx\right] \tag{5.3.25}$$

from which it can be concluded that the mass coefficient has the form

$$m_{i_j} = \int_0^L m(x)\phi_i(x)\phi_j(x)dx \quad \text{for } i,j = 1,2,3\ldots\ldots\ldots n \tag{5.3.26}$$

On the other hand the potential energy of the system is given by

$$U(t) = \frac{1}{2}\int_0^L EI_x\left[\frac{\partial^2 y(x,t)}{\partial x^2}\right]^2 dx$$

$$= \frac{1}{2}\int_0^L EI_x\left[\sum_{i=1}^{n}\frac{d^2\phi_i(x)}{dx^2}q_i(t)\right]\left[\sum_{j=1}^{n}\frac{d2\phi_j(x)}{dx^2}q_j(t)\right]dx$$

$$\rightarrow \quad U(t) = \frac{1}{2}\sum_{i=1}^{n}\sum_{j=1}^{n}q_i(t)q_j(t)\left[\int_0^L EI_x\frac{d^2\phi_{i(}x)}{dx^2}\frac{d^2\phi_j(x)}{dx^2}dx\right] \tag{5.3.27}$$

from which we conclude that stiffness coefficient may be written as

$$k_{i_j} = \int_0^L EI(x)\phi_i''(x)\phi_j''(x)dx \tag{5.3.28}$$

The natural frequency is given by the expression

$$\lambda_{i_j} = \omega_{ij}^2 = \frac{k}{m} = \frac{\int_0^L EI(x)\varphi''_i(x)\varphi''_j(\mathrm{x})\mathrm{dx}}{\int_0^L m(x)\varphi_i(x)\varphi_j(x)dx} \tag{5.3.29}$$

Based on the above expression it is evident that the correctness of the result will depend on how correctly we have guessed the eigen vectors $\phi_i(x)$, $\phi_j(x)$.

The closer the value of the eigen vectors to the reality more accurate will be the value of the frequency or the time period.

There are certain classes of structures like chimneys, vertical vessels, distillation columns, retaining walls etc whose time periods can be very effectively obtained by this method.

We now show the application of this theory by a practical problem hereafter.

Example 5.3.6

A vertical vessel of height 40 m as shown in Figure 5.3.2a, has outside diameter 2.0 meter and shell thickness 20 mm. Operating weight of the vessel is 750 kN and empty weight of vessel is 380 kN. Determine the fundamental time period under operation and when the vessel is empty. Consider the structure to be fixed at the foundation level.

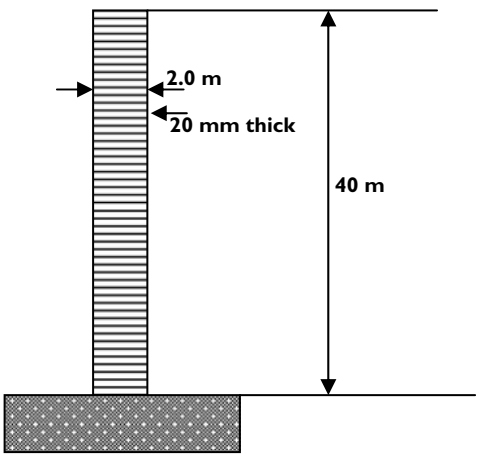


Figure 5.3.2a Vertical vessel resting on foundation.

Solution:

For applying Rayleigh-Ritz method we had stated earlier that the first step is to select an appropriate displacement function. For choosing the displacement consider the Figure 5.3.3.

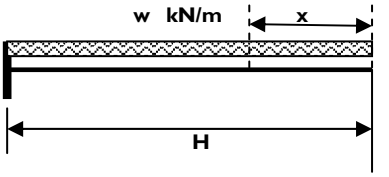


Figure 5.3.3

From our basic knowledge of mechanics of material we know that $EI\frac{d^2y}{dx^2} = -M_x$, and for the above cantilever beam we have

$$EI\frac{d^2y}{dx^2} = \frac{wx^2}{2}; \quad \text{or } EI\int\frac{d^2y}{dx^2} = \int\frac{wx^2}{2}dx \quad \rightarrow \quad \text{or } EI\frac{dy}{dx} = \frac{wx^3}{6} + C_1$$

Now at $x = H$ as $dy/dx = 0$ we have $C_1 = -wH^3/6$ from which we have, $EI\frac{dy}{dx} = \frac{wx^3}{6} - \frac{wH^3}{6}$

On subsequent integration, we have $EIy = \frac{wx^4}{24} - \frac{wH^3x}{6} + C_2$.

At $x = H$ as $y = 0$ we have $C_2 = wH^4/8$, from which we have, $EIy = \frac{wx^4}{24} - \frac{wH^3x}{6} + \frac{wH^4}{8}$

It is evident from above, that the beam will follow generically a curve of nature $\phi = \frac{H^4}{8} - \frac{H^3x}{6} + \frac{x^4}{24}$ for any value of w and EI.

From which we conclude that possible mode shape of the system for first mode as

$$\phi = \frac{H^4}{8} - \frac{H^3x}{6} + \frac{x^4}{24}.$$

Differentiating the above expression twice, we have, $\phi'' = \frac{x^2}{2}$.

Thus based Rayleigh's method $k_{ij} = \int_0^H EI\phi_i''\phi_j''dx$ from which we have for the first mode

$$k_{11} = \int_0^H EI\frac{x^4}{4}\,dx = \frac{EIH^5}{20}.$$

The mass coefficient is given by $m_{ij} = \int_0^H m(x)\phi_i\phi_j dx$ from which we have for the first mode

$$m_{11} = \int_0^H m\left[\frac{H^4}{8} - \frac{H^3x}{6} + \frac{x^4}{24}\right]^2 dx$$

$$= \int_0^H m\left[\frac{H^8}{64} + \frac{H^6x^2}{36} + \frac{x^8}{576} - \frac{H^7x}{24} - \frac{H^3x^5}{72} + \frac{H^4x^4}{96}\right]dx$$

The above on intergration gives

$$m_{11} = \frac{mH^9}{249.23}.$$

Considering, $\omega^2 = \frac{k}{m} = \frac{EIH^5}{20} \times \frac{249.23}{mH^9} = 12.4615\frac{EI}{mH^4}$, which gives, $\omega = 3.53\sqrt{\frac{EI}{mH^4}}$ rad/sec.

Considering $T = -2\pi/\omega$ we have (Dowrick 1987)[33], $T = 1.779\sqrt{\frac{mH^4}{EI}}$secs.
For the present problem

$$I = \frac{\pi(2.0^4 - 1.96^4)}{64} = 0.06097\,\text{m}^4; \quad E = 2x10^8\,\text{kN/m}^2$$

Thus, $EI = 12194381\ \text{kN/m}^2$.

Under operating condition; m = $\frac{750}{40\times9.81} = 1.9113\,\textbf{kN} \cdot \textbf{sec}^2\textbf{/m}.$

➔ $T = 1.779\sqrt{\frac{1.9113 \times 40^4}{12194381}} = 1.126\text{secs}$

When the vessel is empty $m = \frac{380}{40\times9.81} = 0.9684\ \text{kN} \cdot \text{sec}^2/\text{m}$; $T = 1.779\sqrt{\frac{0.9684\times40^4}{12194381}} = 0.802$ secs.

In the above example we solved for the fundamental time period of a vertical vessel based on closed form solution. However for complicated geometry we usually resort to numerical solution for calculation of such time period[34].

5.3.1.9 Calculation of eigen value for free–free structure

Though, a common phenomenon in aircraft structure analysis or ship floating in sea is not so common in civil engineering[35].

There are cases where a structure or a system does not have a physical boundary.

33 It suggests a formula for self supporting steel chimney and vessels as $T = 1.79\text{H}^2[\text{w/EIg}]^{0.5} \cdot$ w = weight per unit height.

34 This we have dealt in detail in Chapter 3 (Vol. 2) under Earthquake Engineering.

35 Except special cases of soil/fluid structure interaction depending on how the coupling of soil/fluid is considered.

One of the classic cases for the same is an aircraft in flight or a ship floating on sea. Finding eigen value for such cases becomes tricky for the $[K]$ matrix becomes singular[36].

As the matrix inversion becomes inadmissible trying to solve for the eigen value by normal methods are not possible.

One of the major property of such matrices is that there are eigen values equal to the number of degrees of freedom which are zero, i.e. under such circumstance the body undergoes rigid body modes and induces no stress within the body initially before the body itself starts bending deformation when stress starts getting induced with the body[37].

Since as stress engineers we are more interested to know the stress deformation within the body we get rid of the rigid body mode by a technique which is *called shifting technique*.

We had shown previously that eigen value equation of a physical system is expressed as

$$[K]\{\varphi\} = \omega^2[M]\{\varphi\} \tag{5.3.30}$$

Now since $[K]$ is singular for unconstrained system the strategy is to make $[K]$ non-singular but at the same time retain the intrinsic property of the system undisturbed.

The following is done in such cases.

Adding the term $\psi[M]\{\varphi\}$ on both sides we have

$$\begin{aligned}[K]\{\varphi\} + \psi[M]\{\varphi\} &= \omega^2[M]\{\varphi\} + \psi[M]\{\varphi\} \quad \rightarrow \quad \{[K] + \psi[M]\}\{\varphi\} \\ &= (\omega^2 + \psi)[M]\{\varphi\}\end{aligned}$$

The above can now be expressed as

$$[K]'\{\varphi\} = \omega'^2\{\varphi\} \tag{5.3.31}$$

where $[K]' = [K] + \psi[M]$ and $\omega^2 = \omega'^2\psi$.

The modified matrix $[K]'$ will be non singular and shall produce eigen values which are non zero from which the relevant eigen values can be obtained based on $\omega^2 = \omega'^2\psi$.

It should be noted that ψ^2 should be of the same order of ω^2 for the results to give meaningful results.

The theory is further elaborated by an example hereafter.

36 By singular we mean determinant of the matrix $[K]$ becomes zero.As inverse of $[K]$ is given by Adj$[K]$/Det$[K]$, thus the inversion of the matrix becomes inadmissible.

37 A classic case of this is a plate resting on elastic medium. When the first few modes the body undergoes a rigid body mode (though non-zero) and finally at higher modes undergoes its own bodily deformations.

Example 5.3.7

For a structure having [K] and [M] as shown below determine the eigen values based shifting technique

$$[K] = \begin{bmatrix} 100 & -200 \\ -20 & 40 \end{bmatrix} \quad \textbf{and} \quad [M] = \begin{bmatrix} 10 & 0 \\ 0 & 20 \end{bmatrix}$$

Solution:
Solving the above by polynomial method we have

$$\begin{bmatrix} 100 - 10\lambda & -200 \\ -20 & 40 - 20\lambda \end{bmatrix} = 0$$

The above on expansion gives $\lambda\,(200\lambda - 2400) = 0$ and $\lambda = 0$ and 12.

However if we try to solve the same by Matrix deflation method to arrive at he lowest eigen-value, we have to perform the operation

$$[A] = [K]^{-1}[M]$$

But the stiffness matrix [K] being singular inversion of [K] is inadmissible and arriving at matrix [A] is not possible[38].

Hence we have to perform a mathematical operation based on which the singularity of the matrix [K] is disturbed.

Considering the expression $[K]' = [K] + \psi[M]$ and taking $\psi = 5.0$, we have

$$[K]' = \begin{bmatrix} 100 & -200 \\ 20 & 40 \end{bmatrix} + 5\begin{bmatrix} 10 & 0 \\ 0 & 20 \end{bmatrix}$$

$$= \begin{bmatrix} 100 + 50 & -200 \\ 20 & 40 + 100 \end{bmatrix} = \begin{bmatrix} 150 & -200 \\ 20 & 140 \end{bmatrix}$$

The modified matrix being non-singular the operation $[A] = [K]^{-1}[M]$ is now admissible and solution by vector iteration method is now possible.

Expanding the above by polynomial method

$\begin{bmatrix} 150 - 10\lambda & -200 \\ -20 & 140 - 20\lambda \end{bmatrix} = 0$ which gives the characteristic equation as

$200\lambda^2 - 4400\lambda - 17000 = 0$ and this results in $\lambda = 5$ and 17
from which we can predict that the corrected actual eigen values as $\lambda = 0$ and 12.

38 We should remember that polynomial method is only used for small system. For systems with large degrees of freedom eigen values are generally obtained based on vector iteration method (as explained above) or by transformation techniques that will be explained subsequently.

5.3.1.10 Calculation of eigen-values based on vector transformation

We had shown previously how eigen values are obtained based on vector iteration method based on matrix deflation and Stodola's sweeping technique. We now show here after techniques which are commonly used for eigen value determination of systems based on co-ordinate transformation.

The underlying concepts are not difficult to understand.

Let us consider the free vibration equation

$$[K]\{\varphi\} = \omega^2[M]\{\varphi\} \tag{5.3.32}$$

We have shown earlier that if $\{\varphi\}$ is the eigen vector matrix of the system then

$$\{\varphi\}^T[K]\{\varphi\} = [\lambda] \quad \text{and} \quad \{\varphi\}^T[M]\{\varphi\} = [I] \tag{5.3.33}$$

Here $[\lambda]$ is the diagonal matrix consisting of eigen values of the system and $[I]$ is an identity matrix

For the eigen vector $\{\varphi\}$ as this diagonalisation is unique, in transformation method we try to construct based on iteration -a vector, which reduce $[K]$ and $[M]$ into a diagonal matrix by successively pre and post multiplying by the transformation matrices $[T_r]^T$ and $[T_r]$ where, $r =$ number of iterations $1, 2, 3\ldots$

Thus,

$$\begin{aligned}
&[K_2] = [T_1]^T[K_1][T_1]\\
&[K_3] = [T_2]^T[K_2][T_2]\\
&\ldots\ldots\\
&[K_{r+1}] = [T_r]^T[K_r][T_r]
\end{aligned} \tag{5.3.34}$$

and similarly for mass matrix we have

$$\begin{aligned}
&[M_2] = [T_1]^T[M_1][T_1]\\
&[M_2] = [T_1]^T[M_1][T_1]\\
&\ldots\\
&[M_{r+1}] = [T_r]^T[M_r][T_r]
\end{aligned} \tag{5.3.35}$$

and, the transformation matrix $[T]$ is chosen in such a manner that

$$[K_{r+1}] \rightarrow [\lambda] \text{ and } \quad [M_{r+1}] \rightarrow [I] \quad \text{as} \quad r \rightarrow [\infty]. \tag{5.3.36}$$

In practice, it is not necessary for the matrix $[K_{r+1}]$ converge to $[\lambda]$ or $[M_{r+1}]$ tend to $[I]$. All that is necessary is that they converge to a diagonal form

$$[K_{r+1}] \rightarrow \text{Diag}[K_{ii}^r] \quad \text{and} \quad [M_{r+1}] \rightarrow \text{Diag}[M_{ii}^r] \tag{5.3.37}$$

when the eigen values are given by

$$[\lambda] = \text{Diag}\left[\frac{K_{ii}^r}{M_{ii}^r}\right]. \tag{5.3.38}$$

It is to be noted that here the eigen values may not be obtained in sequential ascending or descending order.

The eigen vectors of the system is then given by

$$\{\phi\} = [T_1]\,[T_2]\ldots\ldots\ldots[T_r]\,\text{Diag}\left[\frac{1}{\sqrt{M_{nn}^{r+1}}}\right] \tag{5.3.39}$$

where n = order of the matrix.

Based on the above principle we now explain two techniques which have a wide ranging application in dynamics and Finite element analysis, and are usually adapted for systems with large degrees of freedom.

5.3.2 Standard Jacobi's technique

This is a longstanding technique (Jacobi 1846), which has been found to be very reliable and has wide ranging application in different branch of physics and engineering (Goldstein et al. 1959).

The method is very powerful for symmetric matrices and is capable of evaluating negative, zero and positive eigen values.

Jacobi's method can be very effectively used for both standard and general eigen value problem.

We first discuss the solution of standard eigen value problem.

Considering the free vibration equation

$$[K]\{\varphi\} = \omega^2[M]\{\varphi\} \tag{5.3.40}$$

the above can be expressed as

$$[A]\{\varphi\} = \omega^2\{\varphi\} \quad \text{where } [A] = [K]\,[M]^{-1}. \tag{5.3.41}$$

The above format is known as the standard eigen value problem such that on transformation

$$[A_{r+1}] = [T_r]^T[A_r]\,[T_r] \tag{5.3.42}$$

where $[T_r]$ is an orthogonal matrix gives

$$[T_r]^T[T_r] = I \tag{5.3.43}$$

As per Jacobi, the rotation matrix $[T_r]$ is so chosen that the off diagonal element of $[A_r]$ is zeroed. If element (j, k) is to be reduced to zero the corresponding transformation matrix is chosen as

$$[T_r] = \begin{bmatrix} & & & j \text{ col} & k \text{ col} \\ 1 & 0 & 0 & 0 & 0 \\ . & . & . & . & . \\ 0 & 0 & 1 & 0 & 0 \\ & & & \cos\theta & -\sin\theta \\ & & & \sin\theta & \cos\theta \end{bmatrix} \tag{5.3.44}$$

where $\tan 2\theta = \frac{2A^r_{jk}}{A^r_{jj} - A^r_{kk}}$, in which $A^r_{jj} \neq A^r_{kk}$ and $\theta = \frac{\pi}{4}$ for $A^r_{jj} = A^r_{kk}$.

In this case the matrix being symmetric transformation need to be only applied to either the lower or upper triangle matrix including the diagonal term. For optimal solution and computer implementation a special form of the solution known as *Threshold Jacobi Technique*[39] is usually applied. In this case off diagonal elements are tested column by column or row by row and transformation is only applied if the value is greater than a pre-defined threshold value for that sweep.

Since in this technique we ultimately want to reduce the matrix into a diagonal form the strategy is to diminish the coupling effect between the j and k degrees of freedom. An estimate of this coupling effect is given by $(A^2_{jk}/A_{jj}A_{kk})^{0.5}$. This factor can be effectively used to decide if a rotation has to be applied or not. The convergence is measured based on the threshold tolerance for a finite number of iterations[40].

Thus for a particular number of finite iterations q it is assumed to have converged to a tolerance t if

$$\frac{|A^{(q+1)}_{jj} - A^{(q)}_{jj}|}{A^{(q+1)}_{jj}} \leq 10^{-t} \quad \text{and} \quad \sqrt{\frac{(A^{(q+1)}_{jk})^2}{A_{jj_{(q+1)}} A^{(q+1)}_{kk}}} \leq 10^{-t}; \quad \text{for all} \quad i < j \text{ and}$$

$$i = 1, 2, 3 \ldots\ldots\ldots n. \tag{5.3.45}$$

Having defined the method it would be worthwhile to understand why and how the matrix get reduced to a diagonal form.

Consider the matrix

$$[A] = \begin{bmatrix} A_{jj} & A_{jk} \\ A_{jk} & A_{kk} \end{bmatrix} \tag{5.3.46}$$

—a symmetric 2×2 matrix.

39 For further insight to this refer "Finite Element Analysis for Engineering Procedure" – by K.J. Bathe which has some superb discussion on this issue.

40 This is logical for q number of iterations as theoretically $Aq + 1 \rightarrow \lambda$ as $q \rightarrow \propto$.

Considering the transformation matrix as

$$[T] = \begin{bmatrix} \cos\theta & -\sin\theta \\ \sin\theta & \cos\theta \end{bmatrix}, \tag{5.3.47}$$

we have

$$[T]^T[A][T] = \begin{bmatrix} \cos\theta & \sin\theta \\ -\sin\theta & \cos\theta \end{bmatrix} \begin{bmatrix} A_{jj} & A_{jk} \\ A_{jk} & A_{kk} \end{bmatrix} \begin{bmatrix} \cos\theta & -\sin\theta \\ \sin\theta & \cos\theta \end{bmatrix} \tag{5.3.48}$$

which gives

$$[T]^T[A][T] = \begin{bmatrix} A_{jj}\cos^2\theta + A_{jk}\sin 2\theta + A_{kk}\sin^2\theta & (A_{kk} - A_{jj})\sin\theta\cos\theta + A_{jk}\cos 2\theta \\ (A_{kk} - A_{jj})\sin\theta\cos\theta + A_{jk}\cos 2\theta & A_{jj}\sin^2\theta - A_{jk}\sin 2\theta + A_{kk}\cos^2\theta \end{bmatrix} \tag{5.3.49}$$

Considering the fact that the off diagonal terms are to be reduced to zero we have

$$\frac{1}{2}(A_{kk} - A_{jj})\sin 2\theta + A_{jk}\cos 2\theta = 0$$

$$\rightarrow \quad \tan 2\theta = \frac{2A_{jk}}{\mathbf{A}_{jj} - A_{kk}} \quad \text{when } A_{jj} \neq A_{kk}, \quad \text{for } A_{jj} = A_{kk} \tag{5.3.50}$$

$$\theta = \frac{\pi}{4} \quad \text{when } A_{jk} > 0 \quad \text{and } \theta = -\frac{\pi}{4} \quad \text{when } A_{jk} < 0.$$

Thus based on above transformation considering i and j degrees of freedom the matrix is systematically transformed into a diagonal form. It has been proved that once the off diagonal element are small the convergence is quadratic in nature and minimal cost is required to calculate eigen pairs to high accuracy once an approximate solution is obtained (Wilkinson 1968).

The symmetric eigen value analysis also has an important application in finite element analysis.

It is a very effective tool to check the stability and conformity of finite elements and is often used by FEM researchers to test the numerical sanctity of a new finite element.

Example 5.3.8

For symmetric matrix [*A*] as shown below determine the eigen values based on Jacobi's method.

$$[A] = \begin{bmatrix} 5000 & -2000 & 0 \\ -2000 & 3500 & -1500 \\ 0 & -1500 & 1500 \end{bmatrix}$$

Solution:

For 1st row (j) and 2nd column (k)

As $\tan 2\theta = \frac{2A_{jk}}{A_{jj}-A_{kk}} = \frac{2\times(-)2000}{5000-3500} = -2.6667$, we have $\sin\theta = -0.569594$ and $\cos\theta = 0.821925$.

Thus the transformation matrix is given by

$$T_1 = \begin{bmatrix} 0.821926 & 0.569594 & 0 \\ -0.569594 & 0.821926 & 0 \\ 0 & 0 & 1 \end{bmatrix} \rightarrow$$

$$T_1^T = \begin{bmatrix} 0.821926 & -0.569594 & 0 \\ 0.569594 & 0.821926 & 0 \\ 0 & 0 & 1 \end{bmatrix}$$

and $$T_1^T A T_1 = \begin{bmatrix} 6386.000936 & -3.41061\times10^{-13} & 854.3922566 \\ 0 & 2113.999064 & -1232.888426 \\ 854.3922566 & -1232.888426 & 1500 \end{bmatrix}$$

For $j = 1$ and $k = 3$ we have, $\tan 2\theta = \frac{2A_{jk}}{A_{jj}-A_{kk}} = \frac{2\times854.3922566}{6386.000935-1500} = 0.349730697$ which gives $\sin\theta = 0.167425$ and $\cos\theta = 0.98588$ and the transformation matrix is given by

$$T_2 = \begin{bmatrix} 0.98588 & 0 & -0.167425 \\ 0 & 1 & 0 \\ 0.167425 & 0 & 0.98588 \end{bmatrix}$$ which results in

$$T_2^T T_1^T A T_1 T_2 = \begin{bmatrix} 6386.000936 & -3.41061\times10^{-13} & 854.3922566 \\ 0 & 2113.999064 & -1232.888426 \\ 854.3922566 & -1232.888426 & 1500 \end{bmatrix}$$

For $j = 2$ and $k = 3$, we have $\tan 2\theta = \frac{2A_{jk}}{A_{jj}-A_{kk}} = \frac{2\times-1232.888426}{2113.999064-1500} = -4.0159$ which gives $\sin\theta = -0.61578$ and $\cos\theta = 0.787918$ and the transformation matrix is

$$T_3 = \begin{bmatrix} 1 & 0 & 0 \\ 0 & 0.787918 & 0.61578 \\ 0 & -0.61578 & 0.787918 \end{bmatrix}$$ which results in

$$T_3^T T_2^T T_1^T A T_1 T_2 T_3 = \begin{bmatrix} 6386.000936 & -526.1177 & 673.19112 \\ -526.1177 & 3077.535869 & -1.13687\times10^{-13} \\ 673.1911 & 2.27374\times10^{-13} & 536.4632 \end{bmatrix}$$

$$\text{and} \quad T_1T_2T_3 = \begin{bmatrix} 0.81032 & 0.5335 & 0.2423 \\ -0.56155 & 0.5888 & 0.5812648 \\ 0.16742 & -0.607088 & 0.77679 \end{bmatrix}$$

This completes the **first cycle** of sweep.

We start the 2nd Cycle with modified value of $[A]$ as

$$[A] = \begin{bmatrix} 6386.000936 & -526.1177 & 673.19112 \\ -526.1177 & 3077.535869 & -1.13687 \times 10^{-13} \\ 673.1911 & 2.27374 \times 10^{-13} & 536.4632 \end{bmatrix}$$

For 1st row(i) and 2nd column (k)

As $\tan 2\theta = \frac{2A_{jk}}{A_{jj}-A_{kk}} = \frac{2\times(-)526.1177}{6386.00936-3077.535869} = -0.31804$ from which we have $\sin\theta = -0.15335$ and $\cos\theta = 0.98817101$

Thus, the transformation matrix is given by

$$T_1 = \begin{bmatrix} 0.988171 & 0.15335 & 0 \\ -0.15335 & 0.988171 & 0 \\ 0 & 0 & 1 \end{bmatrix} \quad \text{and}$$

$$T_1^T A T_1 = \begin{bmatrix} 6467.650055 & -1.70531 \times 10^{-13} & 665.227 \\ 0 & 2995.88675 & 103.2378 \\ 665.227 & -103.2378 & 536.463 \end{bmatrix}.$$

Now proceeding in identical manner with $j = 1$ and $k = 3$ and then subsequently $j = 2$, $k = 3$ we finally arrive at a value of

$$T_3^T T_2^T T_1^T A T_1 T_2 T_3 = \begin{bmatrix} 6541.344802 & 11.35799 & -0.45933 \\ 11.35799 & 3000.0364 & -2.131 \times 10^{-14} \\ -0.45933 & 1.98952 \times 10^{-13} & 458.6187 \end{bmatrix}$$

$$\text{and} \quad T_1T_2T_3 = \begin{bmatrix} 0.98216 & 0.14883 & -0.11491 \\ -0.152435 & 0.9804 & 0.02306 \\ 0.110107 & -0.04016 & 0.993107 \end{bmatrix}$$

For **3rd Cycle,** considering the modified matrix as

$$[A] = \begin{bmatrix} 6541.344802 & 11.35799 & -0.45933 \\ 11.35799 & 3000.0364 & -2.131 \times 10^{-14} \\ -0.45933 & 1.98952 \times 10^{-13} & 458.6187 \end{bmatrix}$$ and proceeding in identical manner, we have

$$T_3^T T_2^T T_1^T A T_1 T_2 T_3 = \begin{bmatrix} 6541.381265 & 1.11245 \times 10^{-7} & 6.45 \times 10^{-14} \\ 1.11245 \times 10^{-7} & 3000 & 4.878 \times 10^{-19} \\ 3.85507 \times 10^{-13} & 1.76595 \times 10^{-13} & 458.6187 \end{bmatrix}$$

$$\text{and} \quad T_1T_2T_3 = \begin{bmatrix} 0.999999 & -0.003207 & -7.55131 \times 10^{-5} \\ 0.003207 & 0.99999 & 3.37487 \times 10^{-7} \\ -7.55131 \times 10^{-5} & 5.79678 \times 10^{-7} & 0.999999 \end{bmatrix}$$

Since the matrix has almost diagonalised with off diagonal terms reducing to negligible terms we conclude that

$$[\lambda] = \begin{bmatrix} 6541.38 \\ 3000 \\ 458.6187 \end{bmatrix} \quad \text{and}$$

$$[\varphi] = \begin{bmatrix} 0.999999 & -0.003207 & -7.55131 \times 10^{-5} \\ 0.003207 & 0.99999 & 3.37487 \times 10^{-7} \\ -7.55131 \times 10^{-5} & 5.79678 \times 10^{-7} & 0.999999 \end{bmatrix}.$$

In most of the practical structural dynamics problem mass matrix $[M]$ is considered as a lumped mass matrix[41] thus obtaining the matrix $[A] = [K][M]^{-1}$ is simple and does not take much computational effort and can be converted into a standard eigen value form very easily. Once the same is done we can apply the above procedure to find out the eigen pairs of the system. However for cases where the mass matrix is distributed or dynamic coupling exists generalized Jacobi technique operable on both $[K]$ and $[M]$ are usually used.

Before we move into this technique let us see what happens to the problem we had solved earlier by Newton-Raphson method based on standard Jacobi technique.

Example 5.3.9

For structure having stiffness and mass matrix as mentioned below determine the eigen-values by standard Jacobi's technique.

$$[K] = \begin{bmatrix} 5000 & -2000 & 0 \\ -2000 & 3500 & -1500 \\ 0 & -1500 & 1500 \end{bmatrix} \quad \text{and} \quad [M] = \begin{bmatrix} 400 & & \\ & 400 & \\ & & 200 \end{bmatrix}$$

Solution:

For the above matrices

$$[M]^{-1} = \begin{bmatrix} 0.0025 & 0 & 0 \\ 0 & 0.0025 & 0 \\ 0 & 0 & 0.005 \end{bmatrix}$$

41 Meaning thereby that it is diagonal matrix.

Considering $[A] = [K][M]^{-1}$ we have

$$[A] = \begin{bmatrix} 5000 & -2000 & 0 \\ -2000 & 3500 & -1500 \\ 0 & -1500 & 1500 \end{bmatrix} \times \begin{bmatrix} 0.0025 & 0 & 0 \\ 0 & 0.0025 & 0 \\ 0 & 0 & 0.005 \end{bmatrix}$$

$$= \begin{bmatrix} 12.5 & -5 & 0 \\ -5 & 8.75 & -7.5 \\ 0 & -3.75 & 7.5 \end{bmatrix}$$

For 1st row(i) and 2nd column (k)

As $\tan 2\theta = \frac{2A_{jk}}{A_{jj}-A_{kk}} = \frac{2\times(-)5}{12.5-8.75} = -2.6667$ which gives $\sin\theta = -0.569594$ and $\cos\theta = 0.821925$.

Thus the transformation matrix is given by

$$T_1 = \begin{bmatrix} 0.821926 & 0.569594 & 0 \\ -0.569594 & 0.821926 & 0 \\ 0 & 0 & 1 \end{bmatrix} \quad \text{thus}$$

$$T_1^T = \begin{bmatrix} 0.821926 & -0.569594 & 0 \\ 0.569594 & 0.821926 & 0 \\ 0 & 0 & 1 \end{bmatrix}$$

$$\text{Thus} \quad T_1^T A T_1 = \begin{bmatrix} 15.965 & -4.44 \times 10^{-16} & 4.2719 \\ 0 & 5.284 & -6.164 \\ 2.1359 & -3.0822 & 7.5 \end{bmatrix}$$

For $j = 1$ and $k = 3$, we have $\tan 2\theta = \frac{2A_{jk}}{A_{jj}-A_{kk}} = \frac{2\times 4.2719}{15.965-7.5} = 1.00932$ which gives $\sin\theta = 0.384826$ and $\cos\theta = 0.82192$ which gives the transformation matrix as

$$T_2 = \begin{bmatrix} 0.82192 & 0 & -0.384826 \\ 0 & 1 & 0 \\ 0.384826 & 0 & 0.982192 \end{bmatrix} \quad \text{which gives}$$

$$T_2^T T_1^T A T_1 T_2 = \begin{bmatrix} 15.965 & 4.44 \times 10^{-16} & 4.2719 \\ 0 & 5.2849 & -6.1644 \\ 2.13598 & -3.0822 & 7.5 \end{bmatrix}.$$

Now proceeding in identical manner as shown in the previous problem of example 11.8 after three cycles we arrive at[42]

$$T_3^T T_2^T T_1^T A T_1 T_2 T_3 = \begin{bmatrix} 17.112 & 0.039 & 9.92 \times 10^{-5} \\ -2.746 & 1.637 & 5.444 \times 10^{-7} \\ -0.6059 & 2.4365 & 9.9999 \end{bmatrix} \quad \text{and}$$

42 The intermediate steps are left as an exercise to the reader.

$$T_1T_2T_3 = \begin{bmatrix} 0.99896 & -0.04344 & -0.013889 \\ 0.04343 & 0.99905 & -0.00107 \\ 0.01392 & 0.0004 & 0.99903 \end{bmatrix}$$

From which we have

$$\{\lambda\} = \begin{Bmatrix} 17.112 \\ 1.637 \\ 9.99999 \end{Bmatrix} \quad \text{and} \quad [\varphi] = \begin{bmatrix} 0.99896 & -0.04344 & \mathbf{-0.013889} \\ 0.04343 & 0.99905 & \mathbf{-0.00107} \\ 0.01392 & 0.0004 & \mathbf{0.99903} \end{bmatrix}$$

It will be observed that results are closely matching with the results solved previously by other techniques though the off diagonal term convergence to tolerance value is poor, for on transformation of $[K][M]^{-1}$ to matrix $[A]$ the matrix has lost its symmetric property.

A significant fact is to be noticed here. Unlike Matrix Deflation or Stodola's method where number of iterations increased significantly beyond the fundamental mode in Jacobi's method the number of iterations are spectacularly less.

Suffice it to say that computational effort being much less the technique becomes a very attractive choice for computer implementation for eigen value solutions of large systems.

5.3.3 Generalized Jacobi technique

As discussed earlier we now explain herein how Jacobi Technique is applied to generalized equation $[K]\{\varphi\} = \omega^2[M]\{\varphi\}$ where we do not convert it into a standard eigen value problem.

The transformation matrix used in this case is given by (for i row and j column)

$$[T_r] = \begin{bmatrix} 1 & 0 & 0 & . & . \\ . & 1 & 0 & a & . \\ . & . & 1 & . & . \\ . & b & . & 1 & . \\ . & . & . & . & 1 \end{bmatrix} \tag{5.3.51}$$

The values of the coefficients a and b are chosen in such a way that on application it simultaneously reduces elements of i row and j column of matrix $[K_r]$ and $[M_r]$ to zero.

It is not difficult to infer from the above statement that the coefficients a and b (for rth iteration) is a dependent function of $k^r_{ii}, k^r_{jj}, k^r_{ij}, m^r_{ii}, m^r_{jj}, m^r_{ij}$.

Performing the matrix operation $[T_r]^T[K_r][T_r]$ and $[T_r]^T[M_r][T_r]$ and satisfying the condition that k^{r+1}_{ij}, m^{r+1}_{ij} will tend to zero results in the following boundary equations

$$ak^r_{ii} + (1+ab)k^r_{ij} + bk^r_{jj} = 0 \quad \text{and} \quad am^r_{ii} + (1+ab)m^r_{ij} + bm^r_{jj} = 0 \tag{5.3.52}$$

For solving for a and b we express

$$\begin{aligned} k_{ii}^r &= k_{ii}^r m_{ij}^r - m_{ii}^r k_{ij}^r \\ k_{jj}^r &= k_{jj}^r m_{ij}^r - m_{jj}^r k_{ij}^r \quad \text{and} \\ \hat{k}^r &= k_{ii}^r m_{jj}^r - m_{ii}^r k_{jj}^r \end{aligned} \tag{5.3.53}$$

where, $b = -\frac{k_{ii}^r}{x}$ and $a = \frac{k_{jj}^r}{x}$ in which x is defined as

$$x = \frac{\hat{k}^r}{2} + \text{sign}(\hat{k}^r)\sqrt{\left(\frac{\hat{k}^r}{2}\right) + k_{ii}^r k_{jj}^r} \tag{5.3.54}$$

Here the function $sign(\hat{k}^r)$means if the value of $\hat{k}^r > 0$ then we consider it as $(+)1$ and when $\hat{k}^r < 0$ we consider this as $(-)1$.

Based on above the steps to find out the eigen values based on generalized Jacobi Technique can be structured as follows

- For the matrix $[K]$ and $[M]$ determine for each row i and j (where $i, j = 1, 2, 3\ldots$)
  - $k_{ii}^r = k_{ii}^r m_{ij}^r - m_{ii}^r k_{ij}^r$
  - $k_{jj}^r = k_{jj}^r m_{ij}^r - m_{jj}^r k_{ij}^r$
  - $\hat{k}^r = k_{ii}^r m_{jj}^r - m_{ii}^r k_{jj}^r$
- If $\hat{k}^r > 0$ then $x = \frac{\hat{k}^r}{2} + \sqrt{\left(\frac{\hat{k}^r}{2}\right) + k_{ii}^r k_{jj}^r}$ else
- $x = \frac{\hat{k}^r}{2} - \sqrt{\left(\frac{\hat{k}^r}{2}\right) + k_{ii}^r k_{jj}^r}$
- find $b = -\frac{k_{ii}^r}{x}$ and $a = \frac{k_{jj}^r}{x}$
- Form the matrix T as $[T_r] = \begin{bmatrix} 1 & 0 & 0 & . & . \\ . & 1 & 0 & a & . \\ . & . & 1 & . & . \\ . & b & . & 1 & . \\ . & . & . & . & 1 \end{bmatrix}$
- Form $[K]^{r+1} = [T^r]^T [K][T^r]$ and $[M]^{r+1} = [T^r]^T [M][T^r]$
- Repeat this cycle till the matrix gets diagonalised i.e. off diagonal elements get reduced below the tolerance value of 10^{-t}
- Find the eigen values based on the expression $[\lambda] = \text{Diag}\left[\frac{K_{ii}^r}{M_{ii}^r}\right]$
- Find the eigen vectors based on the expression

$$\{\varphi\} = [T_1][T_2]\ldots\ldots\ldots\ldots[T_r]\,\text{Diag}\left[\frac{1}{\sqrt{M_{nn}^{r+1}}}\right]$$

The above steps now will be expressed further by a numerical problem.

Example 5.3.10

For the stiffness and mass matrix as shown below determine the eigen-pair based on generalized Jacobi Technique.

$$[K] = \begin{bmatrix} 5000 & -2000 & 0 \\ -2000 & 3500 & -1500 \\ 0 & -1500 & 1500 \end{bmatrix} \quad \text{and} \quad [M] = \begin{bmatrix} 400 & & \\ & 400 & \\ & & 200 \end{bmatrix}$$

Solution:

For $i = 1$ and $j = 2$ we have $k_{11}^1 = k_{11}^1 m_{12}^1 - m_{11}^1 k_{12}^1$

or $k_{11} = 5000 \times 0 - 400 \times -2000 = 800000$

Again $k_{22}^1 = k_{22}^1 m_{12}^1 - m_{22}^1 k_{12}^1$

or, $k_{22} = 3500 \times 0 - 400 \times -2000 = 800000$

$$\hat{k} = k_{11} m_{22} - m_{11} k_{22} = 5000 \times 400 - 400 \times 3500 = 600000.$$

As $\hat{k} > 0$ hence $x = \frac{\hat{k}}{2} + \sqrt{\left(\frac{\hat{k}}{2}\right) + k_{11} k_{22}}$

$$x = \frac{600000}{2} + \sqrt{\left(\frac{600000}{2}\right) + (800000)^2} \quad \rightarrow \quad x = 1154400.375$$

Then

$$b = -\frac{k_{11}}{x} = -\frac{800000}{1154400.375} = -0.693000468 \quad \text{and}$$

$$a = \frac{k_{22}}{x} = \frac{800000}{1154400.375} = 0.693000468.$$

Thus the transformation matrix is given by

$$[T_1] = \begin{bmatrix} 1 & 0.693000468 & 0 \\ -0.693000468 & 1 & 0 \\ 0 & 0 & 1 \end{bmatrix}$$

Based on this we have

$$[K]^{(2)} = [T^{(1)}]^T [K][T^{(1)}] = \begin{bmatrix} 9452.875664 & 0 & 1039.500702 \\ 9.09495 \times 10^{-13} & 3129.246372 & -1500 \\ 1039.500702 & -1500 & 1500 \end{bmatrix}$$

and $[M]^{(2)} = [T^{(1)}]^T[M][T^{(1)}] = \begin{bmatrix} 592.0998596 & 0 & 0 \\ 0 & 592.0998586 & 0 \\ 0 & 0 & 200 \end{bmatrix}$

For $i = 1$ and $j = 3$ we have

$$k_{11}^1 = k_{11}^1 m_{13}^1 - m_{11}^1 k_{13}^1$$
$$= 9452.875664 \times 0 - 592.0998596 \times 1039.500702$$
$$= -615488.2198.$$

Again, $k_{33}^1 = k_{33}^1 m_{13}^1 - m_{33}^1 k_{13}^1 = 1500 \times 0 - 200 \times 10039.500702 = -207900.1404$.

$$\hat{k} = k_{11}m_{33} - m_{11}k_{33} = 9452.875664 \times 200 - 592.0998596 \times 1500$$
$$= 1002425.339.$$

As $\hat{k} > 0$, hence $x = \frac{\hat{k}}{2} + \sqrt{\left(\frac{\hat{k}}{2}\right) + k_{11}k_{33}}$

Substituting the value k_{11}, k_{33}, etc ... we have, $x = 1116983.916$.
Then

$$b = -\frac{k_{11}}{x} = -\frac{-615488.2198}{1002425.339} = 0.551026932 \quad \text{and}$$
$$a = \frac{k_{33}}{x} = \frac{-207900.1404}{1002425.339} = -0.186126351.$$

Thus the transformation matrix is given by

$$[T_2] = \begin{bmatrix} 1 & 0 & -0.186126351 \\ 0 & 1 & 0 \\ 0.551026932 & 0 & 1 \end{bmatrix} \quad \text{then}$$

$$[K]^{(3)} = [\mathbf{T}^{(2)}]^T[K][T^{(2)}]$$
$$= \begin{bmatrix} 11053.90743 & -826.5403974 & -2.27374 \times 10^{-13} \\ -826.5403974 & 3129.246372 & -1500 \\ -4.54747 \times 10^{-13} & -1500 & 1440.519201 \end{bmatrix}$$

and $[M]^{(3)} = [T^{(2)}]^T[M][T^{(2)}]$

$$= \begin{bmatrix} 652.825994 & 0 & -2.84217 \times 10^{-14} \\ 0 & 592.0998586 & 0 \\ -2.84217 \times 10^{-14} & 0 & 220.5121264 \end{bmatrix}$$

For $i = 2$ and $j = 3$ we have proceeding in identical manner

$$k_{22}^1 = k_{22}^1 m_{23}^1 - m_{22}^1 k_{23}^1 = 888149.7893$$

Again $\quad k_{33}^1 = k_{33}^1 m_{23}^1 - m_{33}^1 k_{23}^1 = 330768.1896.$

$$\hat{k} = k_{22} m_{33} - m_{22} k_{33} = -162894.4451$$

As $\hat{k} < 0$, hence $x = \frac{\hat{k}}{2} - \sqrt{\left(\frac{\hat{k}}{2}\right) + k_{11} k_{33}}$.
Substituting the value k_{22}, k_{33}, etc ... we have, $x = -629539.6856$.
Then $b = -\frac{k_{22}}{x} = 1.410792377$ and $a = \frac{k_{33}}{x} = -0.525413$.
Thus the transformation matrix is given by

$$[T_3] = \begin{bmatrix} 1 & 0 & 0 \\ 0 & 1 & -0.525413 \\ 0 & 1.410792377 & 1 \end{bmatrix} \quad \text{then}$$

$$[K]^{(4)} = [T^{(3)}]^T [K][T^{(3)}]$$

$$= \begin{bmatrix} 11053.90743 & -826.5403974 & 434.2748792 \\ -826.5403974 & 1763.985213 & -9.09495 \times 10^{-13} \\ 434.2748792 & -2.27374 \times 10^{-13} & 3880.612814 \end{bmatrix}$$

and

$$[M]^{(4)} = [T^{(2)}]^T [M][T^{(2)}]$$

$$= \begin{bmatrix} 652.825994 & -4.009 \times 10^{-14} & -2.84217 \times 10^{-14} \\ -4.009 \times 10^{-14} & 1030.992891 & 0 \\ -2.84217 \times 10^{-14} & 0 & 383.9663718 \end{bmatrix}$$

and

$$[T_1][T_2][T_3] = \begin{bmatrix} 1 & 0.430414831 & -0.550237646 \\ -0.693000468 & 1.18197197 & -0.396427121 \\ 0.551026932 & 1.410792377 & 1 \end{bmatrix}$$

This completes the first cycle. We start the second cycle with new stiffness and mass matrix as

$$[K] = \begin{bmatrix} 11053.90743 & -826.5403974 & 434.2748792 \\ -826.5403974 & 1763.985213 & -9.09495 \times 10^{-13} \\ 434.2748792 & -2.27374 \times 10^{-13} & 3880.612814 \end{bmatrix} \quad \text{and}$$

$$[M] = \begin{bmatrix} 652.825994 & -4.009 \times 10^{-14} & -2.84217 \times 10^{-14} \\ -4.009 \times 10^{-14} & 1030.992891 & 0 \\ -2.84217 \times 10^{-14} & 0 & 383.9663718 \end{bmatrix} \text{ and}$$

proceeding in identical fashion as mentioned above we arrive at the figures

$$[K]^{(4)} = [T^{(3)}]^T [K][T^{(3)}] = \begin{bmatrix} 11387.13 & 5.811795352 & 0.024159556 \\ 5.811795352 & 1702.578035 & 0 \\ 0.02416 & 6.74127 \times 10^{-13} & 3898.55867 \end{bmatrix}$$

and

$$[M]^{(4)} = [T^{(2)}]^T [M][T^{(2)}]$$

$$= \begin{bmatrix} 665.6875 & -3.559 \times 10^{-14} & -2.857 \times 10^{-14} \\ -3.56 \times 10^{-14} & 1035.518 & 8.88178 \times 10^{-16} \\ -2.86 \times 10^{-14} & 8.88178 \times 10^{-16} & 389.855 \end{bmatrix} \text{ and}$$

$$[T_1][T_2][T_3] = \begin{bmatrix} 1 & 0.08386 & -0.09428 \\ -0.05244 & 0.99999 & 0.009119 \\ 0.161594 & -0.01104 & 1 \end{bmatrix}$$

This completes the **second cycle**.

For **third cycle** proceeding in identical manner, we have

$$[K]^{(4)} = [T^{(3)}]^T$$

$$[K][T^{(3)}] = \begin{bmatrix} 11387.13 & 1.18 \times 10^{-10} & 6.75 \times 10^{-18} \\ 1.18 \times 10^{-10} & 1702.575103 & 0 \\ 5.66 \times 10^{-13} & 6.744 \times 10^{-13} & 3898.55867 \end{bmatrix} \text{ and}$$

$$[M]^{(4)} = [\boldsymbol{T}^{(2)}]^T$$

$$[M][T^{(2)}] = \begin{bmatrix} 665.6875 & -3.559 \times 10^{-14} & -2.857 \times 10^{-14} \\ -3.56 \times 10^{-14} & 1035.518 & 9.044 \times 10^{-16} \\ -2.86 \times 10^{-14} & 9.044 \times 10^{-16} & 389.855 \end{bmatrix} \text{ and}$$

$$[T_1][T_2][T_3] = \begin{bmatrix} 1 & -0.00056 & 5.107 \times 10^{-6} \\ 0.000363 & 1 & -3.4305 \times 10^{-9} \\ 8.72 \times 10^{-6} & 4.187 \times 10^{-9} & 1 \end{bmatrix}$$

Considering $\{\lambda\} = \text{Diag}\left[\frac{K_{ii}^r}{M_{ii}^r}\right]$, we have $\{\lambda\} = \begin{Bmatrix} 17.10582 \\ 1.644177 \\ 10 \end{Bmatrix}$ as the eigen values[43] and considering $\{\varphi\} = [T_1][T_2] \ldots\ldots\ldots [T_r]$ Diag $\left[\frac{1}{\sqrt{M_{nn}^{r+1}}}\right]$ we can get

43 Compare the results with previous examples … …

$$\{\varphi\} = \begin{bmatrix} 1 & -0.00056 & 5.107 \times 10^{-6} \\ 0.000363 & 1 & -3.4305 \times 10-^{9} \\ 8.72 \times 10^{-6} & 4.187 \times 10^{-9} & 1 \end{bmatrix} \times \begin{bmatrix} 0.03876 & & \\ & 0.031076 & \\ & & 0.050646 \end{bmatrix}$$

$$\{\varphi\} = \begin{bmatrix} 0.038758 & -1.7547 \times 10^{-5} & -2.586 \times 10^{-7} \\ 1.407 \times 10^{-5} & 0.03107 & -1.7374 \times 10^{-10} \\ 3.3801 \times 10^{-7} & 1.3013 \times 10^{-10} & 0.05064 \end{bmatrix}$$

as the eigenvectors.

5.3.4 Dynamic analysis based on finite element method

In our previous discussions we had mostly dealt with frames to explain to you the basic principles that are used for dynamic analysis of structural systems. It is but evident that this can be extended to Finite Element Method (FEM) where the theory can be extended to perform analysis for any general physical system also.

For readers who have gone through Chapter 2 (Vol. 1) can intuitively deduce that like for a static analysis in this case we assemble the $[K]$ and $[M]$ matrix and perform the eigen value analysis based on the equation $[K] - [M]\,\omega^2 = 0$.

To give you further conceptual insight into the problem we first give you some preparatory background.

5.3.4.1 Flexibility and stiffness matrices

Influence coefficients: An influence coefficient a_{ij} is defined as the static deflection of the system at point i due to a unit force at j. Let us consider a simply supported beam of Figure 5.3.4 in which two vertical forces f_1 and f_2 are applied at points 1 and 2. Influence coefficients are then, a_{11}, a_{12}, a_{21}, a_{22}. For example, the deflection at 1 due to force f_2 at 2 is $f_2\ a_{12}$. Let us assume that a force f_1 is first applied at 1 and then f_2 is applied at 2.

When f_1 alone is applied, the potential energy in the beam, for its deformation, is equal to $(1/2)f_1^2 a_{11}$. Again, when the force f_2 is applied, the additional deflection at the point 1 due to the force f_2 is $f_2\ a_{12}$. The work done by f_1 corresponding to this

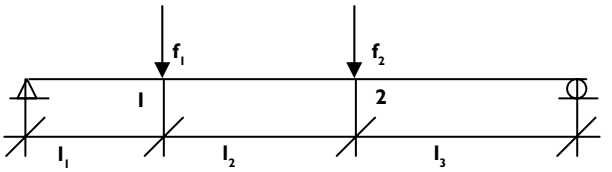


Figure 5.3.4 Simply supported beam with two concentrated loads.

deflection is $f_1(f_2\ a_{12})$. Hence the total potential energy in the system is

$$U = \frac{1}{2}f_1^2 a_{11} + f_1[f_2 a_{12}] + \frac{1}{2}f_2^2 a_{22} \tag{5.3.55}$$

Again when the force f_2 is applied at 2 and then the force f_1 is applied at 1. The total potential energy of the system is

$$U = \frac{1}{2}f_2^2 a_{22} + f_2[f_1 a_{21}] + \frac{1}{2}f_1^2 a_{11} \tag{5.3.56}$$

Since the final two stages are identical, by the law of conservation of energy, the potential energy computed by the two methods should be same. This implies $a_{12} = a_{21}$. This can be generalised for several loads and is known as Maxwell's reciprocal theorem.

Example 5.3.11

A simply supported uniform beam of length L, shown in Figure 5.3.5, is loaded with weights at positions $0.25L$ and $0.6L$. Determine the flexibility matrix for the beam.

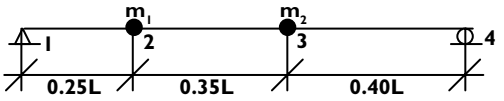


Figure 5.3.5 Simply supported beam with two concentrated loads.

Solution:

Influence coefficients may be determined by placing unit loads at 2 and 3.

In Figure. 5.3.5a,
For span AD:

Vertical deflection, $v = \frac{Pbx}{6EIL}(x^2 + b^2 - L^2)$

Slope at $A\ \theta = \frac{Pb}{6EIL}(L^2 - b^2)$

For span DB:

Vertical deflection, $v = \frac{Pb}{6EIL}\left[-\frac{L}{b}(x-a)^3 - (L^2 - b^2)x + x^3\right]$

Slope at $B\ \theta = \frac{Pab}{6EIL}(2L - b)$.

Thus, consider the simply supported beam shown in the Figure 5.3.5 in which two vertical unit loads are applied at points 2 and 3, respectively. First assume that the unit force is applied first at station 2 and then another unit load is applied at station 3.

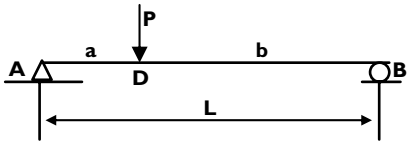


Figure 5.3.5a

When the unit load is applied at 2 and the at 3, we have

$$a_{11} = \frac{0.75L \times 0.25L}{6EIL}(0.25^2 + 0.75^2 - 1)L^2 = \frac{0.0117L^3}{EI};$$
$$a_{22} = \frac{0.4L \times 0.6L}{6EIL}(0.6^2 + 0.4^2 - 1)L^2 = \frac{0.0192L^3}{EI}$$

similarly,

$$a_{12} = a_{21} = \frac{0.75L}{6EIL}\left(0.6^2 - 0.6(1 - 0.75^2) - \frac{(0.6 - 0.25)^3}{0.75}\right)L^3$$

$$= \frac{0.01296L^3}{EI} \quad (\textit{All values are negative}).$$

Hence the flexibility matrix can be written as

$$[A] = \begin{bmatrix} .0117 & .01296 \\ .01926 & .0192 \end{bmatrix} \frac{L^3}{EI}.$$

Example 5.3.12

The natural frequencies of a system, shown in Figure 5.3.6, are to be obtained. Assume a constant flexural rigidity *EI* of the shaft with no inertial effect. Radius of the shaft is *L*/4 and the system is in its static equilibrium.
Solution:

From the figure: $a_{11} = \frac{L^3}{3EI}$; $a_{22} = \frac{L}{EI}$; $a_{12} = a_{21} = \frac{L^2}{2EI}$.

y-delection of the mass: $y(t) = -m\ddot{y}\,a_{11} - J\ddot{\theta}\,a_{12} = -(2\,L\,m\ddot{y} + 3\,J\ddot{\theta})(L^2/6EI)$

Rotation of the mass: $\theta(t) = -m\ddot{y}a_{21} - J\ddot{\theta}a_{22} = -(Lm\ddot{y} + 2J\ddot{\theta})(L/2EI)$

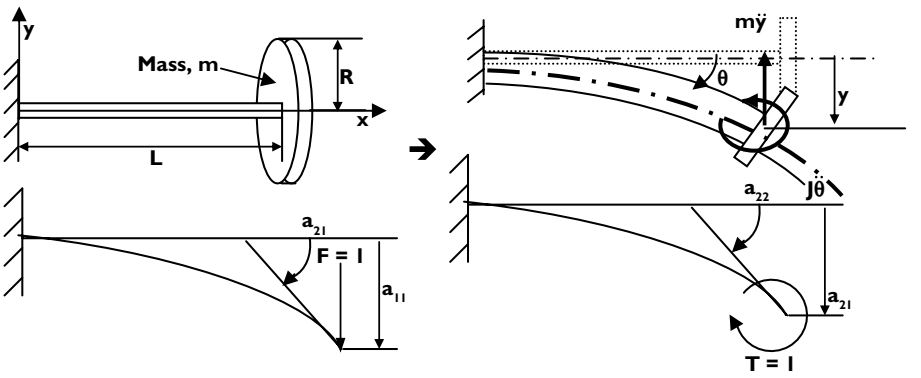


Figure 5.3.6 Determination of influence coefficients.

Assuming: $y = A1 \sin \omega t$ and $\theta = A2 \sin \omega t$, and substituting them for y(t) and $\theta(t)$, we have,

$$\frac{6EI}{L^2} y + 2Lm\ddot{y} + 3J\ddot{\theta} = 0; \quad \frac{2EI}{L}\theta + Lm\ddot{y} + 2J\ddot{\theta} = 0$$

Above equation further reduce to

$$A1[6EI - 2mL^3\omega^2] - 3JL^2\omega^2 A2 = 0$$

$$-L^2 m\omega^2 A1 + [2EI - 2JL\omega^2]A2 = 0$$

Characteristic equation may thus be written as

$$\Delta(\omega) = \begin{vmatrix} 6EI - 2mL^3\omega^2 & -3JL^2\omega^2 \\ -L^2 m\omega^2 & 2EI - 2JL\omega^2 \end{vmatrix} = 0$$

Now using $J = mR^2/4$ and $R = L/4$, and expanding the above determinant we have

$$\omega^4 - 268\left(\frac{EI}{mL^3}\right)\omega^2 + 768\left(\frac{EI}{mL^3}\right)^2 = 0$$

Solution is $\omega_1 = 1.962\sqrt{EI/mL^3} : \omega_2 = 16.37\sqrt{EI/mL^3}$

5.3.4.2 Generalisation

With forces $f_1, f_2, f_3, \ldots, f_n$ acting at points $1, 2, 3, \ldots, n$ displacements, thus produced can be written as

$$x_1 = a_{11}f_1 + a_{12}f_2 + a_{13}f_3 + \cdots + a_{1n}f_n$$

$$x_2 = a_{21}f_1 + a_{22}f_2 + a_{23}f_3 + \cdots + a_{2n}f_n$$

$$
\begin{aligned}
x_3 &= a_{31}f_1 + a_{32}f_2 + a_{33}f_3 + \cdots + a_{3n}f_n \\
&\cdot \\
&\cdot \\
&\cdot \\
x_n &= a_{n1}f_1 + a_{n2}f_2 + a_{n3}f_3 + \cdots + a_{nn}f_n.
\end{aligned} \tag{5.3.57}
$$

These equations can be written in matrix for as

$$
\begin{Bmatrix} x_1 \\ x_2 \\ x_3 \\ . \\ . \\ . \\ x_n \end{Bmatrix} = \begin{bmatrix} a_{11} & a_{12} & a_{13} & . & . & . & a_{1n} \\ a_{21} & a_{22} & a_{23} & . & . & . & a_{2n} \\ a_{31} & a_{32} & a_{33} & . & . & . & a_{3n} \\ . & . & . & . & . & . & . \\ . & . & . & . & . & . & . \\ . & . & . & . & . & . & . \\ a_{n1} & a_{n2} & a_{n3} & . & . & . & a_{nn} \end{bmatrix} \begin{Bmatrix} f_1 \\ f_2 \\ f_3 \\ . \\ . \\ . \\ f_n \end{Bmatrix} \tag{5.3.58}
$$

This can be written as $\{x\} = [A]\{f\}$, in which $[A]$ is called flexibility matrix. If $[A]$ is non-singular, $[A]^{-1}$ exists and $\{f\}$ can be expressed as

$$
\{f\} = [A]^{-1}\{x\} = [K]\{x\} \tag{5.3.59}
$$

where $[K]$ is called the stiffness matrix.

In terms of stiffness, Equation (5.1.11) can be rewritten as

$$
\begin{bmatrix} k_{11} & k_{12} & k_{13} & . & . & . & k_{1n} \\ k_{21} & k_{22} & k_{23} & . & . & . & k_{2n} \\ k_{31} & k_{32} & k_{33} & . & . & . & k_{3n} \\ . & . & . & . & . & . & . \\ . & . & . & . & . & . & . \\ . & . & . & . & . & . & . \\ k_{n1} & k_{n2} & k_{n3} & . & . & . & k_{nn} \end{bmatrix} \begin{Bmatrix} x_1 \\ x_2 \\ x_3 \\ . \\ . \\ . \\ x_n \end{Bmatrix} = \begin{Bmatrix} f_1 \\ f_2 \\ f_3 \\ . \\ . \\ . \\ f_n \end{Bmatrix}. \tag{5.3.60}
$$

Elements of the stiffness matrix in Equation (5.3.60) can be interpreted as follows:

If $x_1 = 1$ and all other x's are zero, the forces at $1, 2, 3, \ldots, n$ are that which are required to maintain this displacement are $k_{11}, k_{21}, k_{31}, \ldots, k_{n1}$ in the first column.

Example 5.3.13

Consider a system with *n*-springs in series as presented in Figure 5.3.7. Compute the stiffness matrix of the over-all system.

Solution:

Let $x_1 = 1$, and other x's are zero. The forces required at $1, 2, 3, \ldots, n$, considering positive direction forces as the forces to the right, we have, say,

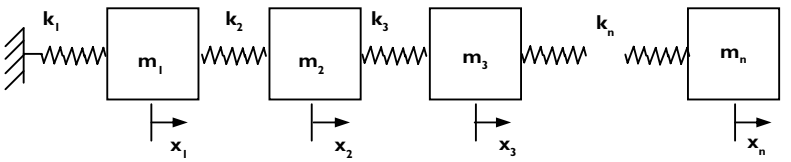


Figure 5.3.7 Vibration of a system with n-springs arranged in series.

Reference to Figure 5.3.8.



Figure 5.3.8

$$f_1 = (k_1 + k_2)x_1 : f_2 = -k_2 x_1 : f_3 = f_4 = \ldots = f_n = 0$$

$$\rightarrow \quad k_{11} = k_1 + k_2 : k_{21} = -k_2 : k_{31} = k_{41} = \ldots = k_{n1} = 0.$$

Similarly setting $x_2 = 1$, and all other x's zero;
Reference to Figure 5.3.9.

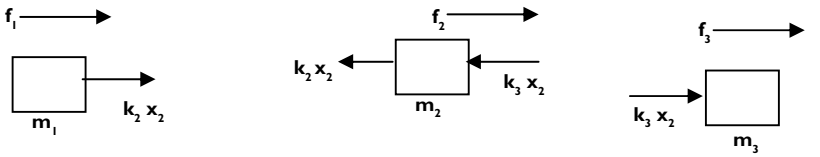


Figure 5.3.9

$$f_1 = -k_2 x_2 : f_2 = (k_2 + k_3)x_2 : f_3 = -k_3 x_2 : f_4 = f_5 = \ldots = f_n = 0.$$

$$\rightarrow \quad k_{12} = -k_2 : k_{22} = (k_2 + k_3) : k_{32} = -k_3 : k_{42} = k_{52} = \ldots = k_{n2} = 0.$$

Continuing with setting unit values to $x_{n-1} = 1$ and all other x's zero;
Reference to Figure 5.3.10.

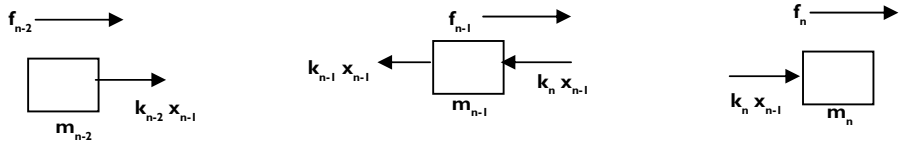


Figure 5.3.10

$$f_{n-2} = -k_{n-2}x_{n-1} : f_{n-1} = (k_{n-1} + k_n)x_{n-1} :$$
$$f_n = -k_{n\times n-1} : f_1 = f_2 = f_3 = \ldots = f_{n-3} = 0.$$
$$\rightarrow \quad k_{n-2,n-1} = -k_{n-1} : k_{n-1,n-1} = (k_{n-1} + k_n) :$$
$$k_{n,n-1} = -k_n : k_{1,n-1} = k_{2,n-1} = \ldots = k_{n-3,n-1} = 0.$$

Reference to Figure 5.3.11.



Figure 5.3.11

Hence, $f_{n-1} = -k_n x_n : f_n = k_n x_n : f_1 = f_2 = f_3 = \ldots = f_{n-3} = f_{n-2} = 0.$

$$\rightarrow \quad k_{n-1,n} = -k_n : k_{n,n} = k_n : k_{1,n} = k_{2,n} = \ldots = k_{n-3,n} = k_{n-2,n} = 0.$$

$$\begin{bmatrix} k_1+k_2 & -k_2 & 0 & 0 & . & 0 & 0 \\ -k_2 & k_2+k_3 & . & . & . & 0 & 0 \\ 0 & -k_3 & . & . & . & . & . \\ 0 & . & . & . & . & . & . \\ . & . & . & . & . & . & . \\ 0 & 0 & . & . & -k_{n-1} & k_{n-1}+k_n & -k_n \\ 0 & 0 & . & . & . & -k_n & k_n \end{bmatrix} \begin{Bmatrix} x_1 \\ x_2 \\ . \\ . \\ . \\ x_{n-1} \\ x_n \end{Bmatrix} = \begin{Bmatrix} f_1 \\ f_2 \\ \\ \\ \\ f_{n-1} \\ f_n \end{Bmatrix}$$

The governing equation shown above indicates a banded form of stiffness matrix with a band along the diagonal.

The influence coefficients have been defined for static elastic property of a system and the inertial effects neglected. When this method is applied to a dynamical system, the inertial forces are to be substituted for the assumed static forces. The total deflection at a point of a system is the sum of the product of the inertial forces and the appropriate influence coefficients.

The above numerical example makes a very important deduction. For a system having multi-degree of freedom the overall stiffness of the system is nothing but an assemblage of the individual stiffness of the elements constituting the structure. Thus principles of assemblage of global stiffness matrix as explained in Chapter 2 (Vol. 1) for finite element is valid. However for assemblage of mass matrix an additional step has to be carried out.

5.3.4.3 Distributed or consistent mass matrix

In the previous sections in most of the cases we have considered masses lumped at the node which makes the mass matrix diagonal and makes it very convenient for further

computation. However the lumped mass approximation do induce some error (not very profound though) in the eigenvalues thus obtained especially for members having pre-dominant flexural modes.

Thus when considering continuum, especially plates and shells where flexural mode governs, it is preferable to consider distributed mass for more accurate results.

The development of consistent mass matrix is as explained by Archer (1963) is given below.

For a body of volume V the kinetic energy of the system can be expressed as $K.E. = 1/2\,\mathrm{mv}^2$. Here m is the mass of the body and v its velocity.

For an elemental volume dV this can thus be expressed in terms of FEM as

$$K.E. = \frac{1}{2}\int_V \dot{u}T\dot{u}\rho dV \tag{5.3.61}$$

Here ρ = mass density of the body and $\dot{u}$ = the velocity of the body.

The displacement vector u is thus expressed in terms of shape function and time as

$$[u] = [N][q(t)] \tag{5.3.62}$$

Thus the velocity vector $\dot{u}$ can be expressed as $$[\dot{u}] = [N][\dot{q}(t)] \tag{5.3.63}$$

Substituting Equation (5.3.63) in (5.3.61) we finally we have

$$K.E. = \frac{1}{2}\dot{q}(t)[\int_V \rho N^T N dV]\dot{q}(t) \tag{5.3.64}$$

Comparing this with Equation (5.3.61) it is obvious that the element mass matrix is given by

$$[M_e] = \int_V \rho N^T N dV \tag{5.3.65}$$

5.3.4.4 Distributed and lumped mass matrix of beam element

We had shown in Chapter 2 (Vol. 1) that shape function of a beam having two degrees of freedom per node (one translation and one rotation) is given by

$$[N] = \left\langle \left(1 - \frac{3x^2}{L^2} + \frac{2x^3}{L^3}\right) \left(x - \frac{2x^2}{L} + \frac{x^3}{L^2}\right) \left(\frac{3x^2}{L^2} - \frac{2x^3}{L^3}\right) \left(\frac{-x^2}{L^2} + \frac{x^3}{L^3}\right) \right\rangle \tag{5.3.66}$$

Substituting this in Equation (5.3.65) we have

$$[M_e] = \frac{\rho AL}{420}\begin{bmatrix} 156 & 22L & 54 & 13L \\ 22L & 4L^2 & 13L & -3L^2 \\ 54 & 13L & 156 & -22L \\ 13L & -3L^2 & -22L & 4L^2 \end{bmatrix} \tag{5.3.67}$$

The lumped mass matrix for beam element where the masses are assumed to be lumped at the node is expressed as

$$[M_e] = \frac{\rho AL}{2}\begin{bmatrix} 1 & 0 & 0 & 0 \\ 0 & 0 & 0 & 0 \\ 0 & 0 & 1 & 0 \\ 0 & 0 & 0 & 0 \end{bmatrix} \tag{5.3.68}$$

It is evident from Equation (5.3.67) that lumped mass approach cannot simulate the rotational inertia as such induces some error in eigen-value solution especially for systems with pre-dominant flexural mode. But irrespective of this short coming its popularity with professional engineers is immense for its ease of computation.

5.3.4.5 Distributed and lumped mass matrix of triangular elements (CST)

For plain stress and plain strain triangular elements the shape function as cited in Chapter 2 (Vol. 1) is given by

$$[N] = \frac{1}{2\Delta} \times \begin{bmatrix} d_{11} & 0 & d_{22} & 0 & d_{33} & 0 \\ 0 & d_{11} & 0 & d_{22} & 0 & d_{33} \end{bmatrix} \tag{5.3.69}$$

in which, $d_{11} = a_i + b_i x + c_i y$; $d_{22} = a_j + b_j x + c_j y$; $d_{33} = a_m + b_m x + c_m y$; and $\Delta =$ Area of the triangle.

Substituting this in Equation (5.3.65) we have

$$[M_e] = \frac{\rho At}{12}\begin{bmatrix} 2 & & & & & \\ 0 & 2 & & \text{Symmetric} & & \\ 1 & 0 & 2 & & & \\ 0 & 1 & 0 & 2 & & \\ 1 & 0 & 1 & 0 & 2 & \\ 0 & 1 & 0 & 1 & 0 & 2 \end{bmatrix} \tag{5.3.70}$$

Here t is the thickness of the element.

Similar to stiffness matrix the element mass matrix has to undergo the transformation $[M_G] = [T]^T[M_e][T]$ before one carries out the global assemblage.

Example 5.3.14

A Portal frame as shown in Figure 5.3.12 having three degrees of freedom per node (two translation and one rotation) supports a pulsating pipe of weight 200 kN when the frequency of the pulsating fluid is 6 Hz and 12 Hz in the first and second harmonics. Determine the natural frequencies of frame based on FEM to check if there is any resonance in the system or not. Also determine the fundamental frequency of the system as a body with single degree of freedom. The material and geometric property of columns and beams are mentioned hereafter. $E = 2 \times 10^7\ \text{kN/m}^2$, $I_{\text{col}} = 1.2 \times 10^{-4}\ \text{m}^4$, $A_{\text{col}} = 0.03\ \text{m}^2$, $I_{\text{beam}} = 1.5 \times 10^{-4}\ \text{m}^4$ **and** $A_{\text{beam}} = 0.035\ \text{m}^2$. **Density of material** $= 25\ \text{kN/m}^3$.

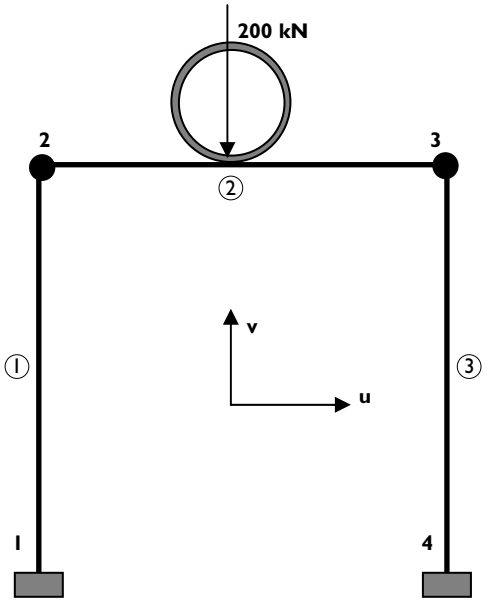


Figure 5.3.12 A portal frame supporting a pulsating pipe.

Solution:

Calculation of global stiffness matrix:

The element stiffness matrix of the beam element in this case is expressed as

$$[K]_{\text{beam}} = \begin{bmatrix} AE/L & 0 & 0 & -AE/L & 0 & 0 \\ 0 & 12EI/L^3 & 6EI/L^2 & 0 & -12EI/L^3 & 6EI/L^2 \\ 0 & 6EI/L^2 & 4EI/L & 0 & -6EI/L^2 & 2EI/L \\ -AE/L & 0 & 0 & AE/L & 0 & 0 \\ 0 & -12EI/L^3 & -6EI/L^2 & 0 & 12EI/L^3 & -6EI/L^2 \\ 0 & 6EI/L^2 & 2EI/L & 0 & -6EI/L^2 & 4EI/L \end{bmatrix}$$

For member 1 and 3 (the vertical members), the element stiffness matrix is given by

$$[K_e] = \begin{bmatrix} 150000 & 0 & 0 & -150000 & 0 & 0 \\ 0 & 450 & 900 & 0 & -450 & 900 \\ 0 & 900 & 2400 & 0 & -900 & 1200 \\ -150000 & 0 & 0 & 150000 & 0 & 0 \\ 0 & -450 & -900 & 0 & 450 & -900 \\ 0 & 900 & 1200 & 0 & -900 & 2400 \end{bmatrix}$$

The transformation matrix for the vertical members are given as

$$[T] = \begin{bmatrix} 0 & 1 & 0 & 0 & 0 & 0 \\ -1 & 0 & 0 & 0 & 0 & 0 \\ 0 & 0 & 1 & 0 & 0 & 0 \\ 0 & 0 & 0 & 0 & 1 & 0 \\ 0 & 0 & 0 & -1 & 0 & 0 \\ 0 & 0 & 0 & 0 & 0 & 1 \end{bmatrix}$$

Performing the operation $[K_g] = [T]^T[K_e]T$ we have

$$[K_e] = \begin{bmatrix} 450 & 0 & -900 & -450 & 0 & -900 \\ 0 & 150000 & 0 & 0 & -150000 & 0 \\ -900 & 0 & 2400 & 900 & 0 & 1200 \\ -450 & 0 & 900 & 450 & 0 & 900 \\ 0 & -150000 & 0 & 0 & 150000 & 0 \\ -900 & 0 & 1200 & 900 & 0 & 2400 \end{bmatrix}$$

For member 2 whose axis matches with the global direction the stiffness matrix is given by

$$[K_e] = \begin{bmatrix} 200000 & 0 & 0 & -200000 & 0 & 0 \\ 0 & 840 & 1469 & 0 & -840 & 1469 \\ 0 & 1469 & 3429 & 0 & -1469 & 1714 \\ -200000 & 0 & 0 & 200000 & 0 & 0 \\ 0 & -840 & -1469 & 0 & 840 & -1469 \\ 0 & 1469 & 1714 & 0 & -1469 & 3429 \end{bmatrix}$$

Performing the global assemblage and eliminating the degrees of freedom for the fixed base of the column we finally have the global stiffness matrix as

$$[K_g] = \begin{array}{|cccccc|}\hline 200450 & 0 & 900 & -200000 & 0 & 0 \\ 0 & 150840 & 1469 & 0 & -840 & 1469 \\ 900 & 1469 & 5829 & 0 & -1469 & 1714 \\ -200000 & 0 & 0 & 200450 & 0 & -900 \\ 0 & -840 & -1469 & 0 & 150840 & -1469 \\ 0 & 1469 & 1714 & -900 & -1469 & 5829 \\ \hline \end{array}$$

Calculation of mass matrix:

Load from pipe on each node = 100 kN
Load from column (assumed 1/3rd mass affects the node 2 and 3) = 1.00 kN
Load from beam (50% on each node) = 1.54 kN
Thus mass per node = 102.54/9.81 = 10 kN.
The mass matrix which is a diagonal matrix is thus given by[44]

$$[M] = \begin{array}{|cccccc|}\hline 10 & 0 & 0 & 0 & 0 & 0 \\ 0 & 10 & 0 & 0 & 0 & 0 \\ 0 & 0 & 0 & 0 & 0 & 0 \\ 0 & 0 & 0 & 10 & 0 & 0 \\ 0 & 0 & 0 & 0 & 10 & 0 \\ 0 & 0 & 0 & 0 & 0 & 0 \\ \hline \end{array}$$

Solving by Jacobi method for eigenvalue analysis as shown earlier we have $[\lambda] = \langle 25.316 \quad 1.5 \times 10^4 \quad 1.505 \times 10^4 \quad 4.003 \times 10^4 \rangle_{\text{diag}}$ which gives $[\omega] = \langle 5.031 \quad 122.474 \quad 122.693 \quad 200.086 \rangle_{\text{diag}}$ rad/sec

$$\Rightarrow [f] = \langle 0.801 \quad 19.492 \quad 19.527 \quad 31.845 \rangle_{\text{diag}} \text{ Hz}$$

It may be noticed that while the total degrees of freedom for the system is 6 we have only shown 4 frequencies. *This is because as the rotational inertia is ignored considering lumped mass* (zero diagonal element in the mass matrix) the eigen values are theoretically infinite for these degrees of freedoms are of no physical significance and are ignored.

The corresponding eigenvectors are given by

$$[\varphi] = \begin{bmatrix} 0.691 & 0.702 & 9.246 \times 10^{-4} & 0 \\ 0 & -9.853 \times 10^{-4} & 0.659 & 0.707 \\ -0.151 & -0.083 & -0.257 & 1.862 \times 10^{-14} \\ 0.691 & -0.702 & -9.246 \times 10^{-4} & 0 \\ 0 & 9.853 \times 10^{-4} & -0.659 & 0.707 \\ 0.151 & -0.083 & -0.257 & -2.024 \times 10^{-14} \end{bmatrix}$$

Frequency based on single degree of freedom:

In lateral direction
$K_{col} = 24EI/L^3 = 900$ kN/m, total mass $(M) = 20.89$ kN-sec^2/m
Thus $\omega = \sqrt{K_{col}/M}$ or $\omega = 6.563$ rad/sec i.e. $f = 1.044$ Hz.
In vertical direction
$K_{col} = 2EA/L = 3 \times 10^5$ kN/m, total mass $(M) = 20.89$ kN-sec^2/m
Thus $\omega = \sqrt{K_{col}/M}$ or $\omega = 119.817$ rad/sec i.e. $= 19.07$ Hz.

It may be observed that even such simplistic model gives quite a reasonable result for practical application.

Having established the basis of dynamic analysis of a system by FEM based on a framed structure we now extend the above for continuum.

Example 5.3.15

Shown in Figure 5.3.13 is a wall 4 m × 3 m × 0.25 m subjected to load of 1500 kN vertical direction. We need to determine the time periods based on finite element analysis. The Elastic Modulus of the wall is E = 2.8 x 10^8 kN/m^2 and consider ν=0.25. Material density of the wall is 25 kN/m^3.

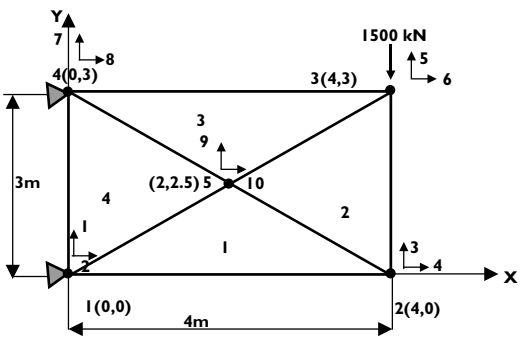


Figure 5.3.13

Also, shown in Figure 5.3.13 is the finite element assembly with global degrees of freedom as marked at each node (1 thru 10).

Solution:

In this case to avoid repetition we will not derive the assembled global stiffness matrix with the enforced boundary condition. This has already been worked out in detail in Example 2.12.6 in Chapter 2 (Vol. 1).

The global stiffness matrix for the assembly considering plain stress triangular element is given by $[K_g] =$

44 Observe here that we have ignored the rotational inertia of the system.

7.72 $\times 10^{+17}$	$-7.78 \times 10^{+06}$	$-1.77 \times 10^{+07}$	$-2.33 \times 10^{+06}$	$0.00 \times 10^{+00}$	$0.00 \times 10^{+00}$	$-1.56 \times 10^{+06}$	$5.44 \times 10^{+06}$	$-5.79 \times 10^{+07}$	$4.67 \times 10^{+06}$
$-7.78 \times 10^{+06}$	**6.32 $\times 10^{+17}$**	$2.33 \times 10^{+06}$	$6.18 \times 10^{+06}$	$0.00 \times 10^{+00}$	$0.00 \times 10^{+00}$	$1.01 \times 10^{+07}$	$-2.20 \times 10^{+07}$	$-4.67 \times 10^{+06}$	$-4.74 \times 10^{+07}$
$-1.77 \times 10^{+07}$	$2.33 \times 10^{+06}$	**3.98 $\times 10^{+07}$**	$-1.56 \times 10^{+07}$	$-1.56 \times 10^{+06}$	$-1.01 \times 10^{+07}$	$0.00 \times 10^{+00}$	$0.00 \times 10^{+00}$	$-2.05 \times 10^{+07}$	$2.33 \times 10^{+07}$
$-2.33 \times 10^{+06}$	$6.18 \times 10^{+06}$	$-1.56 \times 10^{+07}$	**4.92 $\times 10^{+07}$**	$-5.44 \times 10^{+06}$	$-2.20 \times 10^{+07}$	$0.00 \times 10^{+00}$	$0.00 \times 10^{+00}$	$2.33 \times 10^{+07}$	$-3.34 \times 10^{+07}$
$0.00 \times 10^{+00}$	$0.00 \times 10^{+00}$	$-1.56 \times 10^{+06}$	$-5.44 \times 10^{+06}$	**8.09 $\times 10^{+07}$**	$3.11 \times 10^{+07}$	$2.33 \times 10^{+07}$	$-2.33 \times 10^{+06}$	$-1.03 \times 10^{+08}$	$-2.33 \times 10^{+07}$
$0.00 \times 10^{+00}$	$0.00 \times 10^{+00}$	$-1.01 \times 10^{+07}$	$-2.20 \times 10^{+07}$	$3.11 \times 10^{+07}$	**1.16 $\times 10^{+08}$**	$2.33 \times 10^{+06}$	$7.29 \times 10^{+07}$	$-2.33 \times 10^{+07}$	$-1.67 \times 10^{+08}$
$-1.56 \times 10^{+06}$	$1.01 \times 10^{+07}$	$0.00 \times 10^{+00}$	$0.00 \times 10^{+00}$	$2.33 \times 10^{+07}$	$2.33 \times 10^{+06}$	**4.36 $\times 10^{+17}$**	$-7.78 \times 10^{+06}$	$-6.53 \times 10^{+07}$	$-4.67 \times 10^{+06}$
$5.44 \times 10^{+06}$	$-2.20 \times 10^{+07}$	$0.00 \times 10^{+00}$	$0.00 \times 10^{+00}$	$-2.33 \times 10^{+06}$	$7.29 \times 10^{+07}$	$-7.78 \times 10^{+06}$	**1.02 $\times 10^{+18}$**	$4.67 \times 10^{+06}$	$-1.53 \times 10^{+08}$
$-5.79 \times 10^{+07}$	$-4.67 \times 10^{+06}$	$-2.05 \times 10^{+07}$	$2.33 \times 10^{+07}$	$-1.03 \times 10^{+08}$	$-2.33 \times 10^{+07}$	$-6.53 \times 10^{+07}$	$4.67 \times 10^{+06}$	**2.46 $\times 10^{+08}$**	$0.00 \times 10^{+00}$
$4.67 \times 10^{+06}$	$-4.74 \times 10^{+07}$	$2.33 \times 10^{+07}$	$-3.34 \times 10^{+07}$	$-2.33 \times 10^{+07}$	$-1.67 \times 10^{+08}$	$-4.67 \times 10^{+06}$	$-1.53 \times 10^{+08}$	$0.00 \times 10^{+00}$	**4.00 $\times 10^{+08}$**

Calculation of mass matrix:

Area of element #1 = 5.0 m2. Thickness = 0.25 m. Thus considering material wt density = 25 kN/m^3
we have

$$[m_1] = \begin{bmatrix} 1.062 & & & & & & \\ & 1.062 & & & & & \\ & & 1.062 & & & & \\ & & & 1.062 & & & \\ & & & & 1.062 & & \\ & & & & & 1.062 & \end{bmatrix} \text{ and}$$

$$[m_2] = [m_4] = \begin{bmatrix} 0.637 & & & & & & \\ & 0.637 & & & & & \\ & & 0.637 & & & & \\ & & & 0.637 & & & \\ & & & & 0.637 & & \\ & & & & & 0.637 & \end{bmatrix}$$

$$[m_3] = \begin{bmatrix} 0.212 & & & & & & \\ & 0.212 & & & & & \\ & & 0.212 & & & & \\ & & & 0.212 & & & \\ & & & & 0.212 & & \\ & & & & & 0.212 & \end{bmatrix}$$

The global mass matrix(10×10) including the effect of nodal load (1500 kN) is thus given by[45]

$$[m_g] = \begin{bmatrix} 1.698 & & & & & & & & & \\ & 1.698 & & & & & & & & \\ & & 1.698 & & & & & & & \\ & & & 1.698 & & & & & & \\ & & & & 154 & & & & & \\ & & & & & 154 & & & & \\ & & & & & & 0.85 & & & \\ & & & & & & & 0.85 & & \\ & & & & & & & & 2.55 & \\ & & & & & & & & & 2.55 \end{bmatrix}$$

Solving the eigen value equation $[K]\{\phi\} = \lambda[M]\{\phi\}$ by the Jacobi method as explained earlier we have

$$[\lambda] = \langle 1.2 \times 10^{18} \quad 4.54 \times 10^{17} \quad 3.72 \times 10^{17} \quad 5.13 \times 10^{17} \quad 1.61 \times 10^{8} \quad 9.99 \times 10^{7} \quad 2.96 \times 10^{5} \quad 1.67 \times 10^{7} \quad 2.51 \times 10^{5} \quad 6.35 \times 10^{4} \rangle$$

Considering $\omega = \sqrt{\lambda}$ and $T = 2\pi/\omega$ we have the time periods[46] for all the active degrees of freedom as

$$[T] = \langle 0.025 \quad 0.013 \quad 0.00153 \quad 0.00115 \quad 0.0006 \quad 0.0004 \text{ sec.}$$

5.3.4.6 *Static and dynamic condensation – the eigen value economizer*

Based on above examples it is evident that for dynamic analysis based on FEM the major effort is directed towards the computation of the eigen-values and eigen vectors and this is *computationally expensive* when the structure in hand is large.

More refined are the meshes, larger is the stiffness and mass matrix and more expensive is the cost of computation. However for most of the structures from practical engineering point of view it is only necessary to compute the first few modes when all the eigenvalues (as computed in the above examples) is not required. For instance a 3D building frame of say 500 nodes having six degrees of freedom will have total 3000 degrees of freedom. Ignoring the rotational inertia and considering lumped mass the size of the stiffness and mass matrix would actually be of the order 1500×1500. However for practical engineering design the first 3 to 4 eigen values and corresponding eigenvectors suffice. Naturally the question arose as to – is there a way by which we can compute the first few significant eigen values of a matrix of order n without solving all the n equations? The biggest advantage then would obviously be that it would bring a lot of economy in computational time and effort.

45 The mass matrices are diagonal matrix having all non diagonal terms as zero.

46 This is just to show you the procedure and may not be the correct model in terms of mesh refinement when the value has converged to a correct result.

This issue has been a topic of significant research in the last decade and huge amount of literature are available on the issue. A detailed discussion would rightfully be a complete chapter as such we give briefly here the conceptual aspects only.

One of the most popular method is static and dynamic condensation which are used in many commercially available software to compute the desired number of eigen values and vectors as prescribed by the user.

We had already explained the principle of static condensation in Chapter 2 (Vol. 1) while deriving stiffness matrix of quadrilateral elements from triangular elements however in such case the nodal degree of freedom that needs to be eliminated (the internal node) was known priori. For a complex structure on the other hand how do we know which degrees of freedom can be ignored?

For instance for the portal frame problem worked out above it is evident that since we are considering lumped mass the rotational degree of freedoms are ignored as such on can condense out the rotational degrees of freedom at element level and then assemble the global matrix which would reduce its size. Thus for small or simple structures one can possibly identify these mass less degree of freedom based on inspection and can eliminate them.

However when the order of the stiffness and mass matrix is say 1000, condensation of only rotational or mass less degrees of freedom may not be sufficient enough to give any significant computational advantage for an eigen value solution.

Thus techniques had to be developed where even translational mass which does not affect the first few modes, can be eliminated-however keeping the fact in mind that condensation do incur error in the final eigen values and vectors thus obtained[47].

The technique that is used for such case is as follows.

For any structure or foundation when we assemble the global stiffness and mass matrix, it is observed that the values are invariably dominated by the major diagonal element (i.e. K_{ii} and M_{ii}). Since our objective is to obtain the first few lowest eigen value, the target is to eliminate the higher eigen-values whose values are not important/relevant to us.

To this end an array constituting the term K_{ii}/M_{ii} is computed and the computer is asked to search for the highest value in this array[48]. Once this is identified the particular degree of freedom is eliminated to crunch the matrix by one degree based on static condensation. The step is repeated again and the next highest value of K_{ii}/M_{ii} is identified and is subsequently crunched. In this process if we get two values in the array that have the same highest value, then the first value encountered is eliminated first. It has been observed that the procedure do induce some error in the eigen values thus obtained but is not significant provided the order of the matrix is restricted to at least 3 times the number of modes we are seeking.

The technique though looks simple requires significant book keeping while programming to track the correct addresses of the degree of freedom that are to be eliminated and in many cases the stiffness and mass matrix looses its inherent banded property and becomes a full matrix.

47 It is obvious that this error should be within an acceptable limit and not significant.

48 In terms of Fortran programming this is address as LAMBDA = MAX($K(I, J)/M(I, J)$) when $I = J$

5.4 INTRODUCTION TO SOIL AND ELASTO-DYNAMICS

In this section we will study some basic concepts of soil dynamics and its theoretical developments within the domain of civil engineering. Before we start this chapter we would expect you to have some background on

- Theory of elasticity
- Solution of linear and partial differential equation
- Some basics of wave motion (not mandatory though)

This would greatly help in understanding the mechanics of the subject.

5.4.1 Development of soil dynamics to the present state of art

Most of the developments in natural science go through certain phases of metamorphosis. The experimental observations, followed by empirical and semi-empirical formulation, are used to match observed phenomena. This is usually followed by a spurt of theoretical hypothesis that forms the basis of rigorous mathematical developments.

The development of soil dynamics has however defied the above trend. Though researchers have been aware of its importance for quite some time yet its development has been at best sporadic.

The root of its developments lies within the annals of continuum mechanics where considering a linear stress-strain relationship under small strain range, many of the solutions were obtained by applying laws of elasticity coupled with Newtonian equation of motion where characteristic property of the soil hardly played any role except for Young's modulus and Poisson's ratio.

Development of dynamics related to foundations subjected to vibrations under rotating equipment is one of the areas where above mentioned hypothesis fitted quite well.

The pioneering work in this area was the work of Lamb (1904) and that of Rayleigh (1885) and Love (1942) based upon which most of the developments took place in future.

Russians unknown to the Western World[49] made a significant contribution in this area that perhaps formed the first scientific study of this emerging science.

Theory of mechanical vibration based on lumped mass, spring and dashpot was a significantly developed science by then. When analogues of elastic half space theory based on continuum were developed, observations matched the field results quite well.

Reissner, Sung, Quinlan, Hsieh, and Shekter developed the elastic half space theories pertaining to continuous medium which were brought into the day to day application of design office practice by developing equivalent spring analogs by Lysmer, Richart, Whitman and Novak only to name the pioneering few. However soil when subjected to severe shock and subjected to large strain started showing peculiar characteristics of its own especially liquefaction, that defied many of the above hypothecation.

49 Till D.D. Barkan published his book – Dynamics of Bases and Foundations in English.

Further development almost came to a standstill for a significant period of time, till 1964 when Nigaata Earthquake in Japan and Alaskan earthquake created massive damage due to soil liquefaction.

This started a second spurt of research activities where significant development took place in this area under the pioneering leadership of Seed, Idriss and Newmark including some areas of seismology; a new area of technology called *geotechnical earthquake engineering* was developed. Geotechnical earthquake engineering mainly deals with liquefaction potential of soil, dynamic pressures induced due to propagation of waves through the soil medium, behavior of earth structures like dams and retaining walls under earthquake and dynamic bearing capacity of soil.

Though theoretical developments have been significant, many of these theories are yet to be put to rigorous test awaiting a major earthquake to occur. In spite of such developments, structures and foundations still fail with monotonic regularity in different parts of the world under earthquake[50] clearly proving that there do exist a significant gap or limitation in our knowledge in the behavior of soil under propagation of waves due to earthquake. The continuing research in this field would hopefully clear the picture further in time to come which to our perception is still a growing technology.

5.4.1.1 How do soil dynamics differ from structural dynamics?

Soil dynamics is relatively a new addition in the annals of civil engineering, though geo-physicists and seismologists have been using these techniques in their own study for a significant period of time.

Engineers working in the design office, many though are conversant with the basic mechanics involving the dynamic behavior of structure has been observed hardly to have any or very limited background on this particular topic or its significance in the design of structures and its foundation.

So for people new to this topic the basic question which comes to mind is – *what is the difference between the two?*

In structural dynamics as has been shown in the earlier section, we basically analyze behavior of a structure considering the body as an assemblage of discrete elements like beams, plates, shells, springs, trusses etc. and then apply the equation of motion to arrive at the displacement *vis a vis* dynamic stresses induced within the body.

While in case of soil dynamics we study the same thing within a soil body[51] and find out displacement, stresses within the body itself and also its effect on structures overlying it[52].

However in case of soil dynamics the soil body considered to be a *continuum* the approach for analysis is quite different than what we do in structural dynamics. It would be enlightening to point out at this juncture as to why this topic has remained almost a mystique science understood and applied by a handful few in the industry.

50 For instance Bhuj Earthquake in India, 26th January 2001.
51 Often idealized as an isotropic homogenous elastic medium.
52 Often termed as Dynamic soil structure interaction.

One of the major reasons is perhaps that root of its development lies in domain of applied mathematics and physics where mathematician/physicist explains a number of these elastodynamic phenomena in their own abstract mathematical way that an average engineer finds difficult to comprehend. It is for this perhaps many engineers feel uncomfortable with the subject to deal with in their day to day work.

Finally unlike structural dynamics where solution of equation of motion is a second order linear differential equation whose solution is mostly sought resorting to Matrix notation and algebra[53], solutions of equation of motion for elastodynamic problem mostly gives rise to fear evoking partial differential equations, integral transforms with complex functions, and other complicated functions like Bessel and Hankel functions, Bateman–Pekeris integral etc. with which most engineers are not too familiar with. Moreover most of the interpretations being more mathematical than physical and intuitive (where structural dynamics has a great advantage), engineers find it indeed difficult to tackle the subject.

We surely agree at the very outset that it is not an easy topic to deal with[54]. But with little bit of patience and dogged wrestling with a few mathematical theorems and retrospection it is not an impossible topic to cope with.

Before we proceed further *we would request puritans in structural engineering not to neglect this chapter.*

For in the analysis of many important structures like reactor buildings in nuclear power plant, high rise commercial complexes on soft soil, frame top compressors and turbines it is now almost mandatory to consider the effect of soil within the structural frame work and arrive at a solution which is far more realistic than the traditional *fixed base analysis*.

To understand the basic behavior of a continuum (could be soil, fluid or any elastic medium), let us examine a case, many of us have often observed in our childhood.

If we drop a pebble in a pool of water – what do we see?

We will see concentric circles of waves generated from the source of disturbance (i.e. the point where the pebble is dropped in the fluid) which dissipates away (in intensity) from the source and dampens away as it moves away from the source of the disturbance as shown in Figure 5.4.1.

Now if we look at the waves carefully it will be observed that the wave patterns dissipate with distance in the fashion as shown in Figure 5.4.2. Thus, we can conclude that when a continuum is subjected to a disturbance which varies with time,

- it generates waves within the body.
- the intensity of the wave amplitude attenuates with distance.[55]
- the travel of these waves through the body would obviously induce deformation within the body which in turn would induce stresses within the body.

53 With which most of the engineers are familiar with .....

54 We are quite sympathetic to those engineers in the industry whose routine commitment of releasing drawings in design office often severely blunts their mathematical edge with course of time.

55 Often defined as Radiation damping of the system.

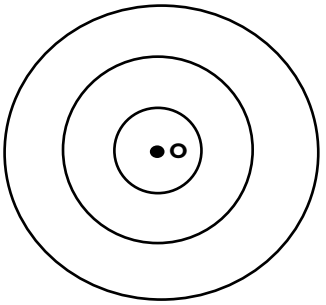


Figure 5.4.1 Concentric wave patterns and its dissipation from the disturbing source.

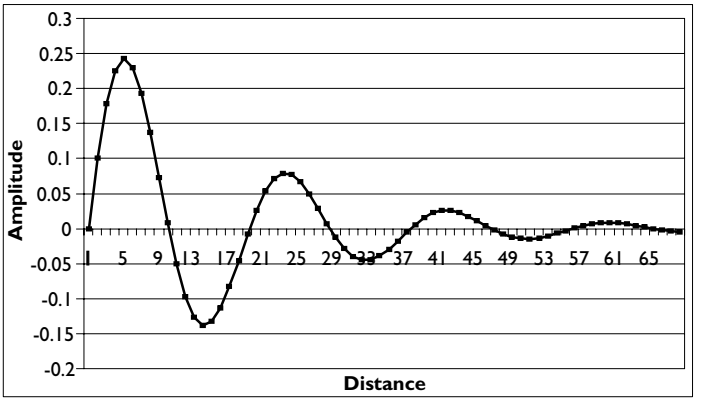


Figure 5.4.2 Dissipation of waves from the disturbing source.

- if the body through which the waves are propagating is considered a homogeneous isotropic elastic medium, laws of elasticity may be applied and consequently it may be possible to arrive at the stiffness of this body based on stress strain relationship.
- this stiffness if added to the stiffness of overlying structure, it is possible to arrive at stiffness of the overall assemblage from which it is possible to assess the global behaviour of the continuum plus discrete system.

The above has been the basic philosophy of a number of studies in soil-structure, fluid-structure interactions and also in coupled thermo-mechanical behavior of spacecrafts flight in the space.

Thus as a first step it is essential to understand the behavior of waves propagating through elastic medium which constitutes the foundation of soil dynamics.

5.4.2 One-dimensional propagation of wave through an elastic medium

In our real world everything we see and feel is three dimensional (3D), however there are many cases where simplifying a 3D problem to a two or one dimensional problem

adequately serves the purpose[56]. Thus as a first step we study herein the solution of propagation of waves through an elastic media in one dimension.

Before we delve into the mathematical aspect of such analysis it would be preferable to understand the various types of waves, which propagate through an elastic medium.

The waves propagating through an elastic medium constitute mainly of four types of waves which are of interest to civil engineers.

1 *P*-waves (body waves)
2 *S*-waves (body waves)
3 *R*-waves: Rayleigh Waves (surface waves)
4 *L*-waves: Love waves (surface waves)

The primary or *P*-waves are the fastest traveling of all the waves and generally produces longitudinal compression and extension within a soil media. These waves can travel both through soil and water and are the first one to arrive at a site during an earthquake. However soil being relatively more resistant to compression and dilation effects, *its impact on ground distortion is minimal*.

The *S*-waves, also otherwise known as secondary or shear waves usually causes shear deformation in the medium through which it propagates. The *S*-waves can usually propagate through soil only. It travels at a much slower speed through the ground than the primary waves, the soil being weak in resisting shear deformation, *these waves are found to cause maximum damage (along with Rayleigh waves) to the ground surface during an earthquake*.

The Rayleigh waves are surface waves which are found to produce ripples on the surface of the ground. These waves produce both horizontal and vertical movement of the earth surface. As the waves travel away from the source it dissipates maximum amount of energy while traveling through a medium, and is an important aspect in study of response of *foundations supporting vibrating equipment foundations and earthquake force transmitting through the ground*.

Love waves are similar to *S*-waves and produce transverse shear deformation to the ground and have a very important bearing for cases *where an elastic half space is overlain by a finite elastic layer*.

We will study the properties of the above waves here in reasonable details to understand how it affects various aspects of foundation and structural design.

The expression of wave propagation in a semi-infinite elastic medium in one dimension is given by the equation

$$\frac{\partial^2 u}{\partial z^2} = \frac{1}{v^2}\frac{\partial^2 u}{\partial t^2} \tag{5.4.1}$$

where u = displacement of the medium and is a function of time and space coordinate z; v = velocity of the medium and may be v_p for primary wave, v_s for shear wave, v_R for Rayleigh wave and v_L for Love wave etc.

56 For instance consolidation of soil is basically three dimensional in nature. However for many practical engineering problems treating it as a one dimensional plane strain body adequately serves the analysis.

Considering, $u(z,t) = \varphi(z)\psi(t)$ this on substitution in Equation (5.4.1) gives

$$\phi(z)\ddot{\psi}(t)\frac{1}{v^2} = \ddot{\phi}(z)\psi(t) \tag{5.4.2}$$

i.e. $\frac{\ddot{\psi}(t)}{\psi(t)} = v^2\,\frac{\ddot{\phi}(z)}{\phi(z)} = -\omega_n^2$, and ω_n is the natural frequency of the system.

The above can now be broken up into two linear differential equations

$$\frac{d^2\psi(t)}{dt^2} + \omega_n^2\psi(t) = 0 \quad \text{and} \quad \frac{d^2\phi(z)}{dz^2} + \frac{\omega_n^2}{v^2}\,\phi(z) = 0 \tag{5.4.3}$$

The solutions of Equation (5.4.3), are given by

$$\phi(z) = A\cos\frac{\omega_n}{v}z + B\sin\frac{\omega_n}{v}z \quad \text{and} \quad \psi(t) = C\cos\omega_n t + D\sin\omega_n t. \tag{5.4.4}$$

The complete solution to the above equation may be written as

$$u(z,t) = \phi(z)\,\psi(t) = \left[A\cos\frac{\omega_n}{v}z + B\sin\frac{\omega_n}{v}z\right][C\cos\omega_n t + D\sin\omega_n t] \tag{5.4.5}$$

in which, the integration constants A, B, C, D and ω_n are obtained from the boundary conditions.

Having gone through Equation (5.4.5), one might wonder, fair enough, – *where do we apply this equation in our day-to-day design engineering?*

At least three applications of this equation have been presented in this book in different chapters, namely,

1 determination of dynamic shear modulus of soil (G) of a site under high strain earthquake in Section-1.5.1 (Vol. 2).-Geo-technical consideration for DSSI.
2 determination of fundamental time period of a site and how we can avoid resonance at the planning stage of a structure in Chapter-1 (Vol. 2)-Fundamentals of DSSI.
3 finally, we have used this equation extensively to arrive at the dynamic pressure on an unyielding wall for a building basement under earthquake in Chapter-3 (Vol. 2)-Analysis and design of structures and foundations under Earthquake.

Going through the above mentioned applications, we hope you'd realize how powerful is the above equation in solving certain types of problems related to earthquake engineering.

5.4.3 Three-dimensional propagation of waves in an infinite elastic medium

Having derived the basic expression for propagation of waves in one dimension, we now examine the behavior of a soil element under wave propagation in three dimensions.

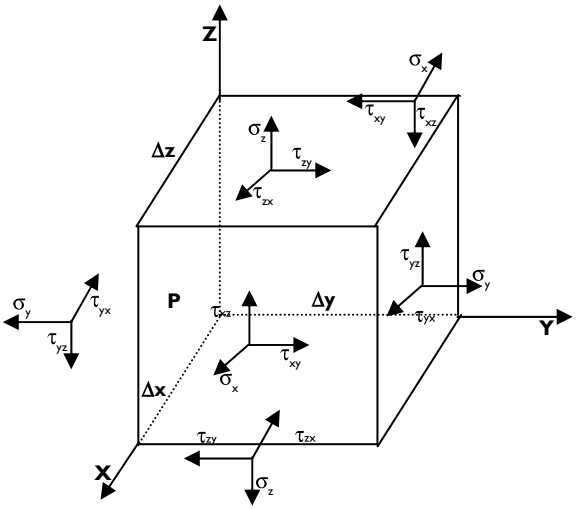


Figure 5.4.3 Stresses on an elemental body in three dimensions.

However, before we go into the details of the derivation it would be worthwhile to re-capitulate some of the fundamental properties of elasticity, which has important bearing on the derivation.

For an elemental body of length Δx, Δy and Δz (Figure 5.4.3), the stress matrix[57] or stress tensor, at a point within the body is represented as

$$[\sigma] = \begin{bmatrix} \sigma_{xx} & \tau_{xy} & \tau_{xz} \\ \tau_{yx} & \sigma_{yy} & \tau_{yz} \\ \tau_{zx} & \tau_{zy} & \sigma_{zz} \end{bmatrix},$$

and strain relationship is given by

$$\varepsilon_{xx} = \frac{du}{dx}, \quad \varepsilon_{yy} = \frac{dv}{dy}, \quad \varepsilon_{zz} = \frac{dw}{dz}, \quad \gamma_{xy} = \frac{dv}{dx} + \frac{du}{dy}, \quad \gamma_{yz} = \frac{dw}{dy} + \frac{dv}{dz},$$
$$\gamma_{zx} = \frac{du}{dz} + \frac{dw}{dx},$$

and the rigid body rotation is given by

$$\Omega_x = \frac{1}{2}\left(\frac{dw}{dy} - \frac{dv}{dz}\right); \quad \Omega_y = \frac{1}{2}\left(\frac{du}{dz} - \frac{dw}{dx}\right), \quad \Omega_z = \frac{1}{2}\left(\frac{dv}{dx} - \frac{du}{dy}\right) \qquad (5.4.6)$$

57 The matrix is symmetric about its diagonal.

The stress strain relationship is now given by the relation

$$\begin{Bmatrix} \sigma_{xx} \\ \sigma_{yy} \\ \sigma_{zz} \\ \tau_{xy} \\ \tau_{yz} \\ \tau_{zx} \end{Bmatrix} = \begin{bmatrix} \lambda+2G & \lambda & \lambda & 0 & 0 & 0 \\ \lambda & \lambda+2G & \lambda & 0 & 0 & 0 \\ \lambda & \lambda & \lambda+2G & 0 & 0 & 0 \\ 0 & 0 & 0 & G & 0 & 0 \\ 0 & 0 & 0 & 0 & G & 0 \\ 0 & 0 & 0 & 0 & 0 & G \end{bmatrix} \begin{Bmatrix} \varepsilon_{xx} \\ \varepsilon_{yy} \\ \varepsilon_{zz} \\ \gamma_{xy} \\ \gamma_{yz} \\ \gamma_{zx} \end{Bmatrix} \tag{5.4.7}$$

where λ and G are the Lame's constants and are expressed as

$$\lambda = \frac{\nu E}{(1+\nu)(1-2\nu)}; \quad G = \frac{E}{2(1+\nu)} \tag{5.4.8}$$

Based on the above relationship one can easily derive that

$$\sigma_{xx} = \lambda e_v + 2G\varepsilon_{xx}, \quad \sigma_{yy} = \lambda e_v + 2G\varepsilon_{yy}, \quad \sigma_{zz} = \lambda e_v + 2G\varepsilon_{zz} \tag{5.4.9}$$

$\tau_{xy} = G\gamma_{xy}, \tau_{yz} = G\gamma_{yz}, \tau_{zx} = G\gamma_{zx}; e_v = \varepsilon_{xx} + \varepsilon_{yy} + \varepsilon_{zz}$ is defined as the volumetric strain.

The equation of motion in the x direction can be expressed as

$$\begin{aligned} \rho\Delta x \cdot \Delta y \cdot \Delta z \cdot \frac{\partial^2 u}{\partial t^2} &= \left(\sigma_{xx} + \frac{\partial \sigma_{xx}}{\partial x}\Delta x\right)\Delta y\Delta z - \sigma_{xx}\Delta y\Delta z \\ &\quad + \left(\tau_{xy} + \frac{\partial \tau_{xy}}{\partial y}\Delta y\right)\Delta x\Delta z - \tau_{xz}\Delta x\Delta y \end{aligned} \tag{5.4.10}$$

in which, ρ = mass density of the elemental body; $\frac{\partial^2 u}{\partial t^2}$ is the acceleration in x-direction.

Equation (5.4.10) can be further simplified to

$$\rho\frac{\partial^2 u}{\partial t^2} = \frac{\partial \sigma_{xx}}{\partial x} + \frac{\partial \tau_{xy}}{\partial y} + \frac{\partial \tau_{xz}}{\partial z} \tag{5.4.11}$$

Proceeding in identical fashion for the other directions (y and z), we have

$$\rho\frac{\partial^2 v}{\partial t^2} = \frac{\partial \tau_{yx}}{\partial x} + \frac{\partial \sigma_{yy}}{\partial y} + \frac{\partial \tau_{yz}}{\partial z} \quad \text{and} \quad \rho\frac{\partial^2 w}{\partial t^2} = \frac{\partial \tau_{zx}}{\partial x} + \frac{\partial \tau_{zy}}{\partial y} + \frac{\partial \sigma_{zz}}{\partial z} \tag{5.4.12}$$

The above three expressions represent the equations of motion of an elastic body in three dimensions.

It may be observed that since these equations were derived based on the condition of equilibrium only and is valid for all materials.

Subsequent solution of the above equations will reveal that the wave propagation breaks up into two major body waves namely P and S waves whose property we are going to study subsequently.

5.4.3.1 Derivation of P waves

Substituting the values of stress-strain relationship of Equation (5.4.9), we have

$$\rho\frac{\partial^2 u}{\partial t^2} = \frac{\partial}{\partial x}(\lambda e_v + 2G\varepsilon_{xx}) + \frac{\partial}{\partial y}G\gamma_{xy} + \frac{\partial}{\partial z}G\gamma_{xz} \tag{5.4.13}$$

Again substituting the strain displacement relations $\varepsilon_{xx} = \frac{\partial u}{\partial x}; \gamma_{xy} = \frac{\partial v}{\partial x} + \frac{\partial u}{\partial y}, \gamma_{xz} = \frac{\partial w}{\partial x} + \frac{\partial u}{\partial z}$ in the x-direction.

We can further express the equation of motion as

$$\rho\frac{\partial^2 u}{\partial t^2} = \frac{\partial e_v}{\partial x}(\lambda + G) + G\nabla^2 u \tag{5.4.14}$$

where, the Laplacian operator ∇^2 is expressed as $\nabla^2 = \frac{\partial^2}{\partial x^2} + \frac{\partial^2}{\partial y^2} + \frac{\partial^2}{\partial z^2}$.

Similarly, the equation of motion in the y and z-directions may be given by

$$\rho\frac{\partial^2 v}{\partial t^2} = \frac{\partial e_v}{\partial y}(\lambda + G) + G\nabla^2 v; \quad \rho\frac{\partial^2 w}{\partial t^2} = \frac{\partial e_v}{\partial z}(\lambda + G) + G\nabla^2 w \tag{5.4.15}$$

Differentiating the equation of motion in the x-direction with respect to x, we have

$$\rho\frac{\partial^2}{\partial t^2}\left(\frac{\partial u}{\partial x}\right) = \frac{\partial^2 e_v}{\partial x^2}(\lambda + G) + G\nabla^2\left(\frac{\partial u}{\partial x}\right) \;\rightarrow\; \rho\frac{\partial^2 \varepsilon_{xx}}{\partial t^2} = \frac{\partial^2 e_v}{\partial x^2}(\lambda + G) + G\nabla^2\varepsilon_{xx},$$

and in the y and z-directions,

$$\rho\frac{\partial^2 \varepsilon_{yy}}{\partial t^2} = \frac{\partial^2 e_v}{\partial x^2}(\lambda + G) + G\nabla^2\varepsilon_{yy} \quad \text{and} \quad \rho\frac{\partial^2 \varepsilon_{zz}}{\partial t^2} = \frac{\partial^2 e_v}{\partial x^2}(\lambda + G) + G\nabla^2\varepsilon_{zz}.$$

Now, adding all three equations, we have

$$\rho\left(\frac{\partial^2 \varepsilon_{xx}}{\partial t^2} + \frac{\partial^2 \varepsilon_{yy}}{\partial t^2} + \frac{\partial^2 \varepsilon_{zz}}{\partial t^2}\right) = (\lambda + G)\left(\frac{\partial^2 e_v}{\partial x^2} + \frac{\partial^2 e_v}{\partial y^2} + \frac{\partial^2 e_v}{\partial z^2}\right) + G\left(\frac{\partial^2 \varepsilon_{xx}}{\partial x^2} + \frac{\partial^2 \varepsilon_{yy}}{\partial y^2} + \frac{\partial^2 \varepsilon_{zz}}{\partial z^2}\right)$$

Using $e_v = \varepsilon_{xx} + \varepsilon_{yy} + \varepsilon_{zz}$ = the volumetric strain, we can simplify the equation as

$$\frac{\partial^2 e_v}{\partial t^2} = \frac{\lambda + 2G}{\rho}\nabla^2 e_v \tag{5.4.16}$$

Since the volumetric strain e_v in the above equation does not involve any deformation which is shearing or rotational in nature, it shows that the dilatational waves will propagate through the body with a velocity,

$$v_p = \sqrt{(\lambda + 2G)/\rho} \tag{5.4.17}$$

— *which is the velocity of P or primary wave.*

The above can be written in terms of Shear Modulus (G) and Poisson's ratio (ν) as

$$v_p = \sqrt{\frac{2G\,(1-\nu)}{\rho\,(1-2\nu)}} \tag{5.4.18}$$

5.4.3.2 Derivation for S waves

Another type of wave which generates in the infinite elastic body may be obtained by differentiating the equation of motion in y-direction with respect to z and the equation of motion in z-direction with respect to y and subtracting them from one another gives

$$\rho \frac{\partial^2}{\partial t^2}\left(\frac{\partial w}{\partial y} - \frac{\partial v}{\partial z}\right) = G\nabla^2\left(\frac{\partial w}{\partial y} - \frac{\partial v}{\partial z}\right) \tag{5.4.19}$$

Recalling the previously defined expression for rotation, Equation (5.4.19) can be simplified to

$$\rho \frac{\partial^2 \Omega_x}{\partial t^2} = G\nabla^2 \Omega_x \quad \text{or} \quad \frac{\partial^2 \Omega_x}{\partial t^2} = \left(\frac{G}{\rho}\right)\nabla^2 \Omega_x \tag{5.4.20}$$

Above expression describes a distortional wave of rotation about the x-axis[58], while the waves are observed to travel with a velocity of

$$V_s = \sqrt{G/\rho} \tag{5.4.21}$$

This wave is commonly known as S or shear waves which due to its distortional nature causes ground damage during an earthquake. S-waves during their motion are often broken up into two components SH and SV-waves.

SH waves are those waves whose particle motion is restricted to the horizontal plane only. While SV waves are waves when the particle motion lies only in the vertical plane. A given S-waves with an arbitrary particle motion can be expressed as vector sum of SH and SV components.

From the above expressions of v_p and v_s, the relation ship between the two can now be expressed as

$$\frac{V_p}{V_s} = \sqrt{\frac{2(1-\nu)}{1-2\nu}}, \tag{5.4.22}$$

for typical value of $\nu = 0.25$, the ratio of $V_p/V_s = \sqrt{3}$ which shows that in an infinite elastic medium the primary waves travel at a much faster velocity than the shear waves and are the first to arrive at a site during an earthquake, followed by a minor tremor which develops due to the shear waves which comes at a slower speed[59].

58 Similar expression can be derived for the y and z axes also.

59 The major tremor occurs to due to Rayleigh waves whose properties we are going to study subsequently.

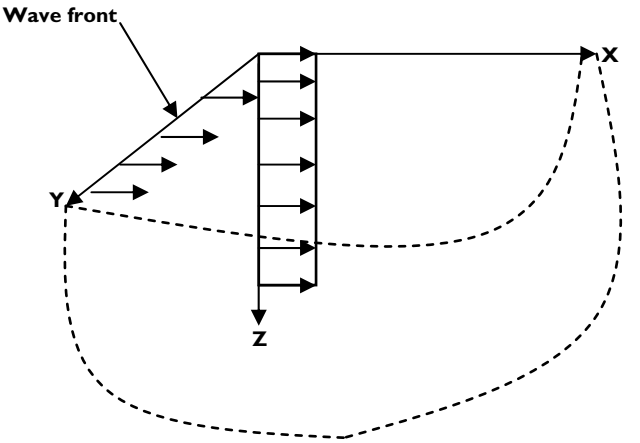


Figure 5.4.4 Propagating wave in an elastic half space.

5.4.3.3 Derivation of Rayleigh waves

In the earlier section we had derived propagation of waves through an infinite elastic media. However in our real world situation an infinite domain is only an idealization and the earth we live in though big is still a finite sphere where neglecting its spherical curvature can be considered as a semi-infinite elastic half space.

Waves propagating through such elastic half space develop special waves near the surface called Rayleigh Waves[60] whose effect both for earthquake induced vibration and machine foundation is of primary importance.

We will study its property in some detail herein.

Shown in Figure 5.4.4 are the waves propagating through an elastic half space expressed by the x-y plane. Let u and w be the displacements in the direction of x and z axes, independent of y.

Let u and w be a function of stream potentials ϕ and ψ such that

$$u = \frac{\partial \phi}{\partial x} + \frac{\partial \psi}{\partial z} \quad \text{and} \quad w = \frac{\partial \phi}{\partial z} - \frac{\partial \psi}{\partial x}$$

Considering e_v = volumetric strain where,

$$e_v = \varepsilon_x + \varepsilon_y + \varepsilon_z = \frac{\partial u}{\partial x} + \frac{\partial v}{\partial y} + \frac{\partial w}{\partial z} \tag{5.4.23}$$

Substituting the values of u and w in terms of potential functions we have

$$e_v = \frac{\partial}{\partial x}\left(\frac{\partial \phi}{\partial x} + \frac{\partial \psi}{\partial z}\right) + \frac{\partial}{\partial y}0 + \frac{\partial}{\partial z}\left(\frac{\partial \phi}{\partial z} - \frac{\partial \psi}{\partial x}\right) \tag{5.4.24}$$

60 Originally studied by Lord Rayleigh and named after him.

$$\text{or,} \quad e_v = \frac{\partial^2 \phi}{\partial x^2} + \frac{\partial^2 \phi}{\partial z^2} = \nabla^2 \phi \tag{5.4.25}$$

Again considering, $\Omega_y = \frac{1}{2}\left(\frac{du}{dz} - \frac{dw}{dx}\right)$, and substituting the values of u and w in terms of their potential function we have

$$\Omega_y = \frac{1}{2}\left(\frac{\partial}{\partial z}\left(\frac{\partial \phi}{\partial x} + \frac{\partial \psi}{\partial z}\right) - \frac{\partial}{\partial x}\left(\frac{\partial \phi}{\partial z} - \frac{\partial \psi}{\partial x}\right)\right) = \frac{\partial^2 \psi}{\partial x^2} + \frac{\partial^2 \psi}{\partial z^2} = \nabla^2 \psi \tag{5.4.26}$$

Substituting the above into the equation of motion in x direction, we have

$$\rho \frac{\partial^2 u}{\partial t^2} = \frac{\partial e_v}{\partial x}(\lambda + G) + G\nabla^2 u \tag{5.4.27}$$

$$\text{or} \quad \rho \frac{\partial^2}{\partial t^2}\left(\frac{\partial \phi}{\partial x} + \frac{\partial \psi}{\partial z}\right) = (\lambda + G)\frac{\partial}{\partial x}\nabla^2 \phi + G\nabla^2\left(\frac{\partial \phi}{\partial x} + \frac{\partial \psi}{\partial z}\right) \tag{5.4.28}$$

If we look carefully at the above equation we will see that it is a combination of two wave equations namely,

$$\frac{\partial^2 \phi}{\partial t^2} = \frac{\lambda + 2G}{\rho}\nabla^2 \phi \quad \rightarrow \quad \frac{\partial^2 \phi}{\partial t^2} = V_p^2 \nabla^2 \phi \tag{5.4.29}$$

$$\frac{\partial^2 \psi}{\partial t^2} = \frac{G}{\rho}\nabla^2 \psi \quad \rightarrow \quad \frac{\partial^2 \psi}{\partial t^2} = V_s^2 \nabla^2 \psi \tag{5.4.30}$$

In similar manner for rotational case we have

$$\rho \frac{\partial}{\partial z}\left(\frac{\partial^2 \phi}{\partial t^2}\right) - \rho \frac{\partial}{\partial x}\left(\frac{\partial^2 \psi}{\partial t^2}\right) = (\lambda + 2G)\frac{\partial}{\partial z}\nabla^2 \phi - G\frac{\partial}{\partial x}(\nabla^2 \psi) \tag{5.4.31}$$

Above again on close scrutiny will be seen to constitute of two type of wave equations as expressed by Equations (5.4.29) and (5.4.30).

For a sinusoidal wave traveling in x direction let the potential functions be represented by

$$\phi = F(z)e^{[i\omega t - nx]}; \quad \psi = G(z)e^{[i\omega t - nz]}, \tag{5.4.32}$$

where $F(z)$ and $G(z)$ are functions of depth and $n = 2\pi/L_w$, where L_w = wave length

Substituting the above in Equations (5.4.29) and (5.4.30), we have

$$\frac{\partial^2}{\partial t^2}F(z)e^{[i\omega t-nx]} = V_p^2\nabla^2 F(z)e^{[i\omega t-nx]}; \quad \rightarrow -\omega^2 F(z) = V_p^2[F''(z) - n^2F(z)] \tag{5.4.33}$$

$$\frac{\partial^2}{\partial t^2}G(z)e^{[i\omega t-nz]} = V_s^2\nabla^2 G(z)e^{[i\omega t-nz]}; \quad \rightarrow -\omega^2 G(z) = V_s^2[G''(z) - n^2G(z)] \tag{5.4.34}$$

Equation (5.4.34) can be re-arranged and expressed as

$$F''(z) - q^2F(z) = 0 \quad \text{and} \quad G''(z) - s^2G(z) = 0 \tag{5.4.35}$$

where $q^2 = n^2 - \omega^2/V_p^2$ and $s^2 = n^2 - \omega^2/V_s^2$.

Solution of Equation (5.4.35) is given by

$$F(z) = A_1e^{-qz} + A_2e^{qz} \quad \text{and} \quad G(z) = B_1e^{-sz} + B_2e^{sz} \tag{5.4.36}$$

where A_1, A_2, B_1, B_2 are integration constants whose values will depend upon the boundary condition.

In Equation (5.4.36), it will be seen that the values $F(z)$ and $G(z)$ will tend to infinity as z tends to infinity, and this is inadmissible. Thus for a realistic solution A_2 and B_2 must be equal to zero. This gives the solution as

$$F(z) = A_1e^{-qz} \quad \text{and} \quad G(z) = B_1e^{-sz}. \tag{5.4.37}$$

Thus the potential functions can now be expressed as

$$\phi = A_1e^{-qz}e^{[i\omega t-nx]}; \quad \psi = B_1e^{-sz}e^{[i\omega t-nz]} \tag{5.4.38}$$

The boundary condition of Equation (5.4.37) can be expressed as

$$\sigma_{zz} = 0, \quad \tau_{zx} = \tau_{zy} = 0$$

$$\sigma_{zz}(z=0) = \lambda e_v + 2G\varepsilon_z = \lambda e_v + 2G\left(\frac{\partial w}{\partial z}\right) = 0 \tag{5.4.39}$$

$$\tau_{zx}(z=0) = G\gamma_{zx} = G\left(\frac{\partial w}{\partial x} + \frac{\partial u}{\partial z}\right) = 0 \tag{5.4.40}$$

Using the definition of u and w and solution of ϕ and ψ as given in Equation (5.4.38), Equations (5.4.39) and (5.4.40) can be written as

$$A_1[(\lambda + 2G)\,q^2 - \lambda n^2] - 2iGnsA_2 = 0 \quad \text{and}$$

$$2iA_1nq + A_2(s^2 + n^2) = 0 \tag{5.4.41}$$

Rearranging Equation (5.4.41), we have

$$\frac{A_1}{A_2}\frac{(\lambda+2G)\,q^2-\lambda n^2}{2insG}-1=0 \quad \text{and} \quad \frac{A_1}{A_2}\frac{2qin}{(s^2+n^2)}+1=0 \tag{5.4.42}$$

Eliminating the factor A_1 and A_2 from Equation (5.4.42), we have

$$\frac{(\lambda+2G)\,q^2-\lambda n^2}{2insG}=-\frac{2qin}{s^2+n^2} \tag{5.4.43}$$

This can be further simplified to

$$4qsn^2G=(s^2-n^2)[(\lambda+2G)\,q^2-\lambda n^2] \tag{5.4.44}$$

Squaring Equation (5.4.44) and substituting the value of s and n from Equation (5.4.35), we have

$$16G^2n^4\left(n^2-\frac{\omega^2}{V_p^2}\right)\left(n^2-\frac{\omega^2}{V_s^2}\right)$$
$$=\left[(\lambda+2G)\left(n^2-\frac{\omega^2}{V_p^2}\right)-\lambda n^2\right]^2\left[n^2+\left(n^2-\frac{\omega^2}{V_s^2}\right)\right]^2 \tag{5.4.45}$$

Equation (5.4.45) can be further reduced to

$$16\left(1-\frac{\omega^2}{n^2V_p^2}\right)\left(1-\frac{\omega^2}{n^2V_s^2}\right)=\left[2-\left(\frac{\lambda+2G}{G}\right)\left(\frac{\omega^2}{n^2V_p^2}\right)-\lambda n^2\right]^2\left(2-\frac{\omega^2}{n^2V_s^2}\right)^2 \tag{5.4.46}$$

Before we proceed further it is essential to define certain mathematical parameters which are derived hereafter[61].

Let L_R = wave length of Rayleigh wave expressed as $L_R = 2\pi/n$; and V_R be the Rayleigh wave velocity of the propagating waves; $n = \omega/V_R$; $R = V_R/V_s$ and $\alpha R = V_R/V_P$; and $V_R^2/V_P^2 = \alpha^2 = (1-2\nu)/[2(1-\nu)]$; $\nu = \lambda/[2(\lambda+G)]$.

Substituting these values in Equation (5.4.46), we have

$$16(1-\alpha^2R^2)(1-R^2)=(2-R^2)^4 \tag{5.4.47}$$

On expansion and re-arrangement, Equation (5.4.47) can be expressed as

$$R^6-8R^4+(24-16\alpha^2)R^2+16(\alpha^2-1)=0 \tag{5.4.48}$$

61 We are working this out in detail for else the solution might look a bit too abrupt.

Above is actually a cubic equation in terms of R^2 which when solved for various values of ν (Poisson's ratio) we get the values of Rayleigh wave velocity (V_R) in terms of compression wave velocity (V_p) and shear wave velocity (V_s).

For $\nu = 0.5$, incompressible solid Equation (5.4.48) reduces to

$$R^6 - 8R^4 + 24R^2 - 16 = 0 \tag{5.4.49}$$

The real root of the above equation (other two roots are complex) is given by

$$V_R^2 = 0.91275V_s^2 \quad \text{or } V_R = 0.95538V_s \tag{5.4.50}$$

Similarly for $\nu = 0.25$, it can be shown that three roots for the Equation (5.4.48) are $R^2 = 4, 2 + 2/\sqrt{3}$ and $2 - 2/\sqrt{3}$ of which only the last root satisfies the condition of the surface waves being real.

Thus for $R^2 = 2 - 2/\sqrt{3}$, we have

$$V_R = 0.9194V_s \tag{5.4.51}$$

It has been shown by Richart et al. (1970) that for practical engineering problems where Poisson's ratio of soil usually varies between 0.3 and 0.4 *the V_R and V_s can be considered same for all practical purpose.*

5.4.3.4 Displacement due to Rayleigh waves

The basis of our above explained derivation was based on assuming potential functions φ and ψ for the displacements u and w; where $u = \frac{\partial \phi}{\partial x} + \frac{\partial \psi}{\partial z}$ and $w = \frac{\partial \phi}{\partial z} - \frac{\partial \psi}{\partial x}$, and we had also derived earlier [vide Equation (5.4.38)] that

$$\phi = A_1 e^{-qz} e^{[i\omega t - nx]} \quad \text{and} \quad \psi = B_1 e^{-sz} e^{[i\omega t - nz]}$$

Substituting the above for u and w, we have

$$u = -iA_1\, ne^{[-qz + i(\omega t - nx)]} + A_2 s e^{[-sz + i(\omega t - nx)]} \tag{5.4.52}$$

Considering the value of $A_2 = -\frac{2iqnA_1}{s^2 + n^2}$ as from Equation (5.4.41), we have

$$u = -A_1 \left[-ine^{-qz} + \frac{2iqsn}{s^2 + n^2} e^{-sz} \right] e^{i(\omega t - nx)}$$

$$= A_1 in \left[-e^{\frac{q}{n}(zn)} + \frac{(2qs)/n^2}{1 + (s^2/n^2)} e^{-sz} \right] e^{i(\omega t - nx)} \quad \text{and}$$

$$w = A_1 n \left[\frac{(2q/n)}{(s^2/n^2) + 1} e^{[-\frac{s}{n}(zn)]} - \frac{q}{n} e^{[-\frac{q}{n}(zn)]} \right] e^{i(\omega t - nx)} \tag{5.4.53}$$

Having derived the above expressions for u and w the variation with respect to depth can be expressed as

$$u(z) = -e^{-qz} + \frac{(2qs)/n^2}{1 + (s^2/n^2)} e^{-sz} \quad \text{and} \quad w(z) = \frac{(2q/n)}{(s^2/n^2) + 1} e^{-sz} - \frac{q}{n} e^{-qz} \tag{5.4.54}$$

Based on definitions given in Equation (5.4.35), we can re-write q and s as

$$\frac{q^2}{n^2} = 1 - \frac{\omega^2}{n^2 V_p^2} = 1 - \alpha^2 R^2 \quad \text{and} \quad \frac{s^2}{n^2} = 1 - \frac{\omega^2}{n^2 V_s^2} = 1 - R^2 \tag{5.4.55}$$

Thus $u(z)$ and $w(z)$ can now be represented by the Poisson's ratio and any wave number n.

For instance for $\nu = 0.25$, $u(z)$ and $w(z)$ can be represented by

$$u(z) = -e^{[-0.8475(zn)]} + 0.5773e^{-0.3993(zn)} \quad \text{and}$$

$$w(z) = 0.8475e^{-0.8475(zn)} - 1.469e^{-0.3933(zn)} \tag{5.4.56}$$

Rayleigh surface wave is shown in Figure 5.4.5. From the figure it may be observed that the Rayleigh waves propagate in x-z plane and any displacement in y direction vanishes. It can be shown from theoretical consideration that the wave perpendicular to the plane of the motion is not possible in a homogenous half space. However such waves- popularly known as SH waves are observed prominently on earth surface with other surface waves.

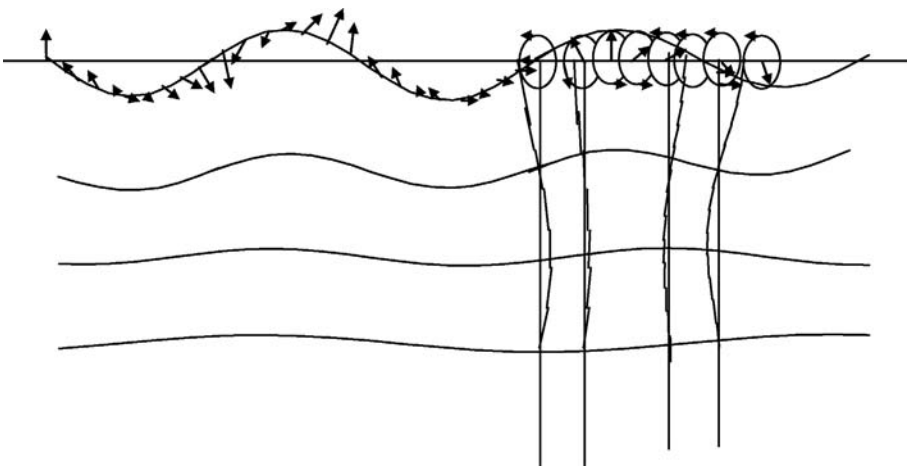


Figure 5.4.5 View of Rayleigh surface waves.

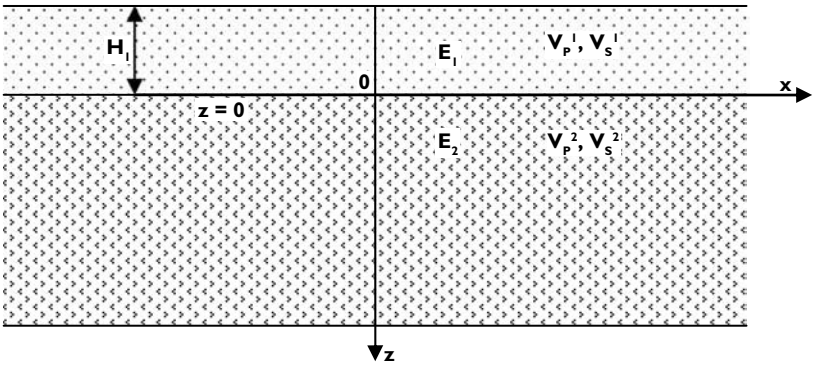


Figure 5.4.6 A layered half space.

Love (1944) showed that a theory sufficient to include SH surface waves can be constructed by having homogenous layer of medium E_1 of uniform thickness H_1 overlying a homogenous half space of another medium E_2 as shown Figure 5.4.6.[62]

5.4.3.5 Derivation of Love wave

In Figure 5.4.6, we see an elastic half space overlain by another layer of elastic medium having height H_1. As stated earlier, Love wave (SH waves) propagating in positive x direction would render a ground motion in y direction which can be expressed as

$$v(x, z, t) = V(z)e^{i(n_L x - \omega t)} \tag{5.4.57}$$

where v is the displacement of ground in y direction, $V(z)$ depicts the variation of displacement with depth z and n_L is the Love wave number.

The propagation of wave must satisfy the two-dimensional wave equation for both the overburden elastic medium and the elastic half space thus the expression

$$\frac{\partial^2 v}{\partial t^2} = \frac{G}{\rho_1}\left(\frac{\partial^2 v}{\partial x^2} + \frac{\partial^2 v}{\partial z^2}\right) \quad \text{is valid for } 0 < z < H$$

$$\text{and} \quad \frac{\partial^2 v}{\partial t^2} = \frac{G}{\rho_2}\left(\frac{\partial^2 v}{\partial x^2} + \frac{\partial^2 v}{\partial z^2}\right) \quad \text{valid for } Z \geq H \tag{5.4.58}$$

The amplitude of vibration will vary with depth according to the expression (Aki & Richards 1980)

$$\begin{aligned} v(z) &= S_1 e^{-V_1 z} + T_1 e^{V_1 z} \quad \text{for } 0 < z < H \\ \text{and} \quad v(z) &= S_2 e^{-V_2 z} + T_2 e^{V_2 z} \quad \text{for } z > H \end{aligned} \tag{5.4.59}$$

62 Love waves can be visualized similar to a snake wriggling on the ground.

Here the terms S and T are amplitude of waves propagating down and up respectively.

$$\text{Here} \quad V_1 = \sqrt{\frac{n_L^2 - \omega^2}{G_1/\rho_1}} \quad \text{and} \quad V_2 = \sqrt{\frac{n_L^2 - \omega^2}{G_2/\rho_2}} \tag{5.4.60}$$

As the layered half-space extends to infinity T_2 must be equal to zero as no waves can reflect back from infinity and considering all stresses (and consequently strain) vanishes at the surface is satisfied if now, $\frac{\partial v}{\partial z} = 0$, which on differentiation gives $(S_1 - T_1)V_1(e^{-V_1 z} + e^{V_1 z}) = 0$; since V_1 is not equal to zero it gives $S_1 = T_1$.

The amplitude function can thus be expressed as

$$v(z) = S_1(e^{-V_1 z} + e^{V_1 z}), \quad \text{for } 0 < z < H; \quad \text{and}$$

$$v(z) = S_2 e^{-V_2 z}, \quad \text{for } z\ H \tag{5.4.61}$$

At $z = H$, the stress compatibility yields the equation

$$2iG_1 V_1 S_1 \sin(iV_1 H) = G_2 V_2 S_2 e^{-V_2 H} \tag{5.4.62}$$

Similarly displacement compatibility yields

$$2S_1 \cos(iV_1 H) = S_2 e^{-V_2 H} \tag{5.4.63}$$

Combining the above two equations gives

$$v(x, z, t) = 2S_1 \cos\left[\omega\left(\sqrt{(1/V_1^2) - (1/V_L^2)}\right) z\right] e^{i(n_L x - \omega t)}; \quad \text{for } 0 < z < H \tag{5.4.64}$$

and

$$v(x, z, t) = 2S_1 \cos\left[\omega\left(\sqrt{(1/V_1^2) - (1/V_L^2)}\right) H\right]$$

$$\times\, e^{[-\omega(\sqrt{(1/V_L^2) - (1/V_2^2)})(z-H)]} e^{i(n_L x - \omega t)} \quad \text{for } Z > H \tag{5.4.65}$$

Here V_1 and V_2 are shear wave velocities of the layers 1 and 2 while V_L is the love wave velocity. Equations (5.4.64) and (5.4.65) show that the amplitude of Love wave velocity varies as a sinusoidal function for top layer of depth H, while at a depth greater than H, it decays exponentially. It is for this they are often described as SH waves that remain trapped in surface layers.

The Love wave velocity is obtained by the solution of the equation

$$\tan \omega H \sqrt{(1/V_1^2) - (1/V_L^2)} = \frac{G_2}{G_1} \frac{\sqrt{(1/V_L^2) - (1/V_2^2)}}{\sqrt{(1/V_1^2) - (1/V_L^2)}} \tag{5.4.66}$$

This wave is basically dispersive in nature.

5.4.4 Propagation of waves in polar co-ordinates

This is a very important derivation and has many applications in seismology, blast analysis, and vibration of footing and we derive the general solution herein.

With reference to Figure 5.4.7, consider $r = \sqrt{x^2 + y^2}$ and vertical axis as Z, the displacement function in cylindrical co-ordinates (r, z and t), can be expressed as

$$u(r, z, t) = \phi(r)\psi(z)\xi(t). \tag{5.4.67}$$

The equation of wave propagation in polar co-ordinate can be expressed as

$$\frac{\partial^2 u}{\partial t^2} = V_s^2 \left[\frac{\partial^2 u}{\partial r^2} + \frac{1}{r}\frac{\partial u}{\partial r} + \frac{\partial u}{\partial z^2} \right] \tag{5.4.68}$$

Here the angular function θ is ignored for the case being axis symmetric substituting Equations (5.4.67) in (5.4.68), we have

$$\phi(r)\psi(z)\ddot{\xi}(t) = V_s^2 \left[\ddot{\phi}(r)\psi(z)\xi(t) + \frac{1}{r}\dot{\phi}(r)\psi(z)\xi(t) + \phi(r)\ddot{\psi}(z)\xi(t) \right] \tag{5.4.69}$$

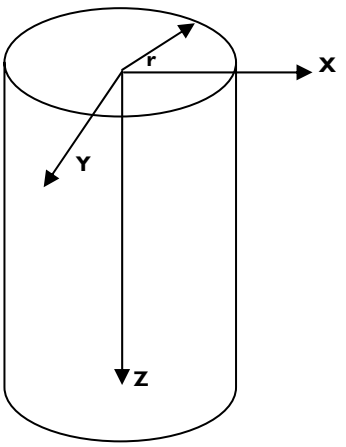


Figure 5.4.7 Propagation of elastic waves in cylindrical co-ordinate.

Dividing each term of Equation (5.4.69) by the term $\phi(r)\ \psi(z)$ we have

$$\ddot{\xi}(t) = V_s^2 \left[\frac{\ddot{\phi}(r)}{\phi(r)} \xi(t) + \frac{1}{r} \frac{\dot{\phi}(r)}{\phi(r)} \xi(t) + \frac{\ddot{\psi}(z)}{\psi(z)} \xi(t) \right]$$

$$\rightarrow \quad \frac{\ddot{\xi}(t)}{V_s^2 \xi(t)} = \left[\frac{\ddot{\phi}(r)}{\phi(r)} + \frac{1}{r} \frac{\dot{\phi}(r)}{\phi(r)} + \frac{\ddot{\psi}(z)}{\psi(z)} \right] = -k^2 (\text{say}) \tag{5.4.70}$$

Equation (5.4.70) can be separated into

$$\ddot{\xi}(t) + k^2 V_s^2 \xi(t) = 0 \quad \ddot{\xi}(t) + \lambda^2 \xi(t) = 0 \quad \text{where } \lambda^2 = k^2 V_s^2 \tag{5.4.71}$$

Again, let us consider

$$\frac{\ddot{\psi}(z)}{\psi(z)} = m^2 \quad \text{which gives } \ddot{\psi}(z) - m^2 \psi(z) = 0 \tag{5.4.72}$$

And finally, considering $\left[\frac{\ddot{\phi}(r)}{\phi(r)} + \frac{1}{r} \frac{\dot{\phi}(r)}{\phi(r)} + m^2 \right] = -k^2$, we have

$$\left[\frac{\ddot{\phi}(r)}{\phi(r)} + \frac{1}{r} \frac{\dot{\phi}(r)}{\phi(r)} \right] = -k^2 - m^2 \text{ or } \left[\frac{\ddot{\phi}(r)}{\phi(r)} + \frac{1}{r} \frac{\dot{\phi}(r)}{\phi(r)} \right] = -h^2 \quad \text{where } h^2 = k^2 + m^2$$

which finally results in

$$\ddot{\phi}(r) + \frac{1}{r} \dot{\phi}(r) + h^2 \phi(r) = 0 \tag{5.4.73}$$

Thus the partial differential equation based on the method of separation of variables has been broken up into three linear differential equations

$$\frac{d^2 \phi}{ds^2} + \frac{1}{s} \frac{d\phi}{ds} + \phi = 0 \quad \text{here } s = hr \tag{5.4.74}$$

$$\frac{d^2 \psi}{dz^2} - m^2 \psi = 0 \quad \text{and} \quad \frac{d^2 \xi}{dt^2} + \lambda^2 \xi = 0 \tag{5.4.75}$$

The solutions are respectively

$$\phi(r) = C_1 J_0(hr) + C_2 K_0(hr) \tag{5.4.76}$$

$$\psi(z) = C_3 e^{mz} + C_4 e^{-mz}; \quad \xi(t) = C_5 \cos \lambda t + C_6 \sin \lambda t \tag{5.4.77}$$

where $J_0(hr)$, $K_0(hr)$ = Bessel's function of first and second kind of order zero.

Thus the complete solution is given by

$$u(r,z,t) = [C_1 J_0(hr) + C_2 K_0(hr)][C_3 e^{mz} + C_4 e^{-mz}][C_5 \cos \lambda t + C_6 \sin \lambda t]$$

For $r \to \infty$, $K_0(hr) = 0$

For $z \to \infty$ as waves cannot reflect back and nor can its intensity increase, hence we have $e^{mz} = 0$.

For harmonic motion as at, $t = 0$ $u = 0$, we have $C_5 = 0$ which finally gives

$$u(r,z,t) = C' J_0(hr) e^{-mz} \sin \lambda t \tag{5.4.78}$$

5.4.5 Reflection/Refraction

The problem we will be studying is the propagation of plane harmonic waves in an unbounded medium consisting of two joined elastic halfspaces of different material properties. The wave that emanates from the infinite depth in one of the media and strikes at the interface is called the incident wave. The problem now is what combination of additional waves is required in order that the stresses and the displacements are continuous at the interface. These waves are called reflected and refracted waves.

The medium that does not transmit elastic waves, the system waves consists of incident and reflected waves only. It is known that the nature of the waves is in general changed when it is reflected or refracted at the interface separating the two media. If a purely transverse or purely longitudinal wave is incident on a surface of separation, the result is a mixed wave containing both transverse and longitudinal parts. The nature of the wave remains unchanged only when it is incident normally on the interface, or a transverse wave whose oscillations are parallel to the interface, may be at any angle.

Although all the waves are steady state traveling waves extending throughout the two joined half spaces, the incident wave is taken to be the cause of the interface-disturbance and the reflected and refracted waves are effects. This leads to the causality requirement that the reflected and refracted waves must propagate away from the interface. This is shown in Figure 5.4.8.

We consider here that the plane waves representing disturbances are uniform in planes of constant phase, i.e. in planes normal to the propagation vector. However, for bodies with a surface of material discontinuity there are plane waves, which are not uniform in planes of constant phase. These waves propagate parallel to the surface of discontinuity, and are called surface waves. They have the property that the disturbance decays rapidly as the distance from the surface increases. For free surface they are known as Rayleigh waves, as described earlier. Surface waves at an interface of two media are called Stonely waves.

Let us consider the consistency of the frequency and of the tangential components of the wave vector. We may now obtain the directions of the reflected and refracted waves. Let α_1 and α_2 be the angles of the incidence and reflection (or refraction) and

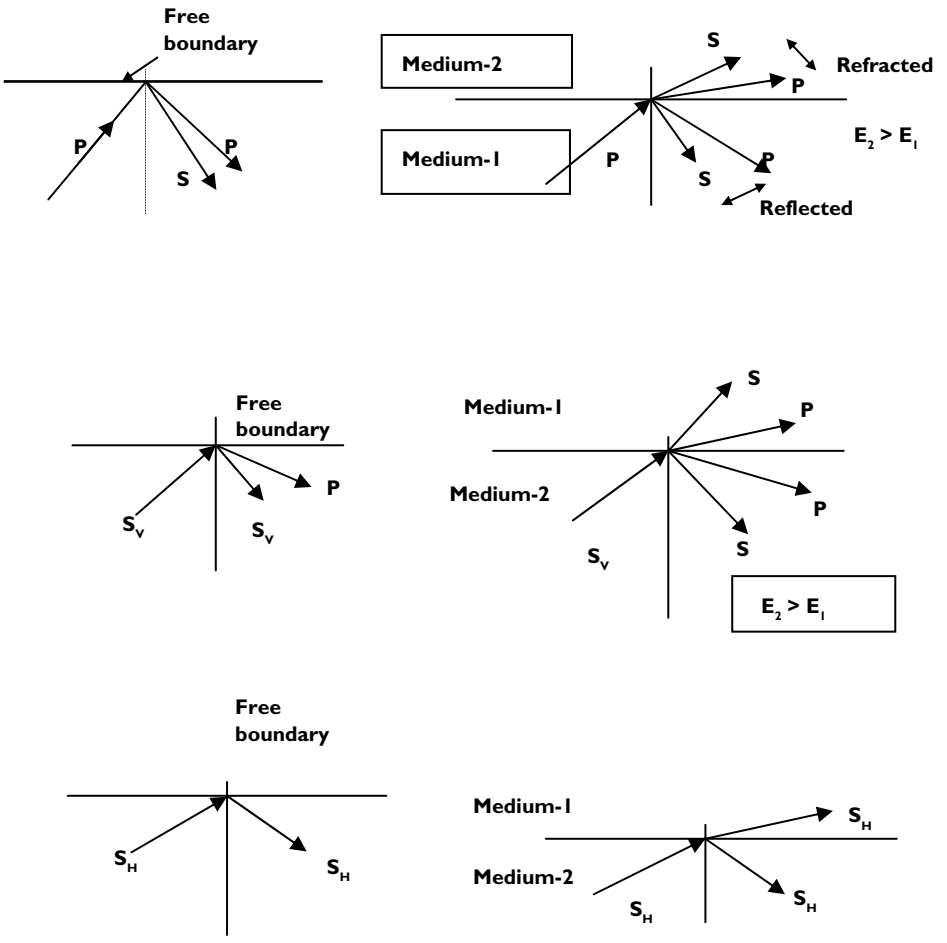


Figure 5.4.8 Reflection and Refraction under a variety of conditions.

V_1 and V_2 the velocities of the two waves.

$$\text{Then} \quad \frac{\sin\alpha_1}{\sin\alpha_2} = \frac{V_1}{V_2} \tag{5.4.79}$$

Let the incident wave be longitudinal: then $V_1 = V_{P1}$ is the velocity of longitudinal wave in the medium '1'. For longitudinal reflected wave $V_2 = V_{P1}$ also, so that Equation (5.4.79) gives $\alpha_1 = \alpha_2$, that is angle of incidence equal to angle of reflection. For the transverse reflected wave, $V_2 = V_{S1}$ and hence

$$\frac{\sin\alpha_1}{\sin\alpha_2} = \frac{V_{P1}}{V_{S1}} \tag{5.4.80}$$

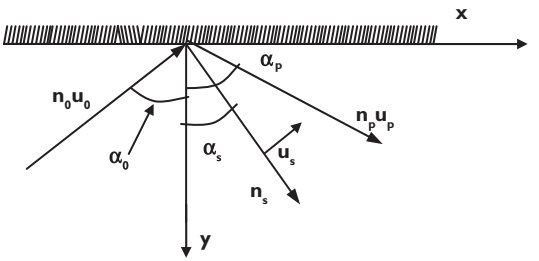


Figure 5.4.9 Reflection of elastic waves on the surface of a body.

For the longitudinal part of the refracted wave, $V_2 = V_{P2}$ and for longitudinal incident wave

$$\frac{\sin\alpha_1}{\sin\alpha_2} = \frac{V_{P1}}{V_{P2}} \tag{5.4.81}$$

Similarly the transverse part of the refracted wave, $V_2 = V_{S2}$

$$\frac{\sin\alpha_1}{\sin\alpha_2} = \frac{V_{P1}}{V_{S2}} \tag{5.4.82}$$

The reflection coefficient for a longitudinal monochromatic wave incident at any angle on the surface of a body is shown in Figure 5.4.9.

Reflected elastic waves have, in general both longitudinal and transverse waves. From Figure 5.4.9 and symmetry that the displacement vector in the transverse reflected wave lies in the plane of incidence. n_0, n_P and n_S are the unit vectors in the direction of propagation of the incident, longitudinal reflected and transverse reflected waves, and u_0, u_P and u_S, the corresponding displacement vectors. The total displacement in the body is given (Landau & Lifshitz 1989) by

$$u = A_0\, n_0\, e^{i(k_0\cdot r-\omega t)} + A_P\, n_P\, e^{i(_P\cdot \mathbf{r}-\omega t)} + A_S\, a \times n_S\, e^{i(\mathbf{k}_S\cdot\mathbf{r}-\omega t)} \tag{5.4.83}$$

in which a is a unit vector perpendicular to the plane of incidence.

Magnitude of wave vectors are $k_0 = k_P = \omega/V_P$; $k_S = \omega/V_S$ and the angle of incidence α_0 and of reflection α_P, α_S are related by $\alpha_P = \alpha_0$, $\sin\alpha_S = (V_S/V_P)\sin\alpha_0$.

With boundary conditions $\sigma_x = \tau_{yx} = 0 :: \sigma_{ik}n_k = 0$, we have

$$A_P = A_0\frac{V_S^2\sin 2\alpha_S\,\sin 2\alpha_0 - V_P^2\cos^2 2\alpha_S}{V_S^2\sin 2\alpha_S\,\sin 2\alpha_0 + V_P^2\cos^2 2\alpha_S} \tag{5.4.84}$$

$$A_S = -A_0\frac{2V_PV_S\sin 2\alpha_0\cos 2\alpha_S}{V_S^2\sin 2\alpha_S\sin 2\alpha_0 + V_P^2\cos^2 2\alpha_S} \tag{5.4.85}$$

For $\alpha_0 = 0$, $A_P = -A_0$ and $A_S = 0$, i.e. the wave is reflected as a purely longitudinal wave. The ratio of energy flux density components normal to the surface in the reflected

and incident longitudinal wave is $R_P = |A_P/A_0|^2$. The corresponding ratio for the reflected transverse wave is

$$R_S = \frac{V_S \cos\alpha_S}{V_P \cos\alpha_0} \left|\frac{A_S}{A_0}\right|^2; \quad \text{sum of } R_P \text{ and } R_S \text{ is 1.} \tag{5.4.86}$$

The same problem, but for transverse incident wave (with the vibration in the plane of incidence).

The wave is reflected as a transverse and a longitudinal wave, with $\alpha_S = \alpha_0$, $V_S \sin\alpha_P = V_P \sin\alpha_0$. The total displacement vector is

$$u = a \times n_0 A_0 \, e^{i(k_0 \cdot r - \omega t)} + n_P A_P \, e^{i(k_P \cdot r - \omega t)} + a \times n_S A_S \, e^{i(k_S \cdot r - \omega t)} \tag{5.4.87}$$

The expressions for the amplitudes of the reflected waves are

$$\frac{A_S}{A_0} = \frac{V_S^2 \sin 2\alpha_P \sin 2\alpha_0 - V_P^2 \cos^2 2\alpha_0}{V_S^2 \sin 2\alpha_P \sin 2\alpha_0 + V_P^2 \cos^2 2\alpha_0};$$

$$\frac{A_P}{A_0} = \frac{2 V_P V_S \sin 2\alpha_0 \cos 2\alpha_0}{V_S^2 \sin 2\alpha_P \sin 2\alpha_0 + V_P^2 \cos^2 2\alpha_0}. \tag{5.4.88}$$

If the displacement vector (u, v, w, t) is represented by a scalar potential $\Phi(x, y, z, t)$ and vector potential $\Psi(x, y, z, t)$ so that (in indicial notation with e_{ijk} as permutation vector)

$$u_i = \frac{\partial \varphi}{\partial x_i} + e_{ijk} \frac{\partial \psi_k}{\partial x_j} \quad \text{with } \psi_{i,i} = 0 \tag{5.4.89}$$

they satisfy the wave equation

$$\frac{\partial^2 \varphi}{\partial x^2} + \frac{\partial^2 \varphi}{\partial y^2} + \frac{\partial^2 \varphi}{\partial z^2} = \frac{1}{V_P^2} \frac{\partial^2 \varphi}{\partial t^2} \tag{5.4.90}$$

$$\frac{\partial^2 \psi_k}{\partial x^2} + \frac{\partial^2 \psi_k}{\partial y^2} + \frac{\partial^2 \psi_k}{\partial z^2} = \frac{1}{V_S^2} \frac{\partial^2 \psi_k}{\partial t^2} \tag{5.4.91}$$

The functions Φ and Ψ define dilatational (P) and distortional (S) waves. S-waves are polarized. If an S-wave train propagates along the x-axis in the x-z plane (x-horizontal, z-vertical), and the material particles move in the z-direction (vertical), we name these waves as SV-waves. If the S-waves propagate along x in the x-z plane but particles move in the y-direction (horizontal), we then speak of SH waves.

The Plane P-waves when hit the boundary $z = 0$, are reflected into plane P-waves and plane S-waves. Similarly, incident SV waves are reflected as both P and SV waves. If two elastic media are in contact and have welded interface, the P-waves will be

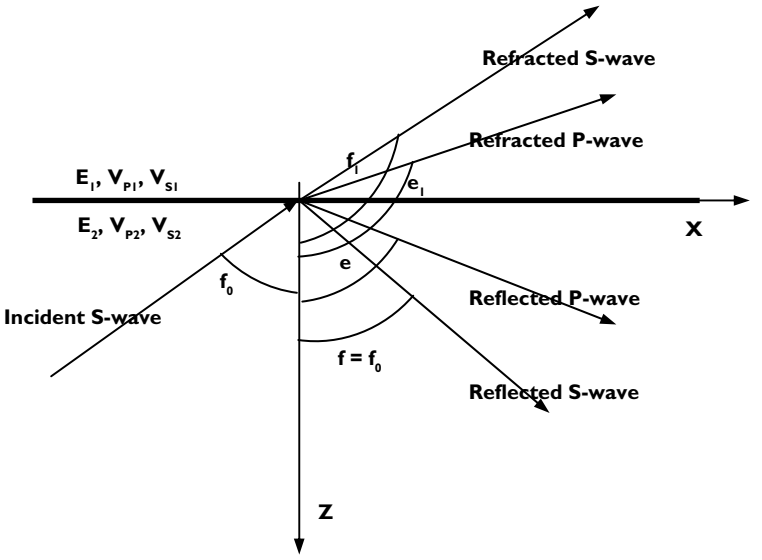


Figure 5.4.10 Reflection of *P*-ray incident in a plane boundary.

reflected in the incident medium into *P* and SV waves, whereas they will be refracted in the second medium as *P* and SV waves. Similar statement holds for SV waves as well.

The SH waves behave in a simple manner; they will be reflected and refracted into SH waves only. Reflection and refraction of elastic waves follow the same Snell's law of Optics.

From Figure 5.4.10 and from Snell's law, we have for incident SV-wave

$$\frac{V_S^2}{\sin f_0} = \frac{V_S^2}{\sin f} = \frac{V_P^2}{\sin e} = \frac{V_S^1}{\sin f_1} = \frac{V_P^1}{\sin e_1} \qquad (5.4.92)$$

$$(f = f_0)$$

For incident *P*-wave $$\frac{V_P^2}{\sin e_0} = \frac{V_P^2}{\sin e} = \frac{V_S^2}{\sin f} = \frac{V_P^1}{\sin e_1} = \frac{V_S^1}{\sin f_1} \qquad (5.4.93)$$

$$(e = e_0)$$

For incident SH-wave $$\frac{V_S^2}{\sin f_0} = \frac{V_S^2}{\sin f} = \frac{V_S^1}{\sin f_1}. \qquad (5.4.94)$$

5.4.5.1 SV-waves

For emerging SV waves from a free boundary, the wave front has a normal in the direction of a unit vector with direction cosines $(\sin f_0, 0, \cos f_0)$ whereas the normal to the incident SV-wave front has a direction cosines $(\sin f_0, 0, -\cos f_0)$. This change in direction cosine excites a reflected *P*-wave.

Thus

$$\varphi = \Phi(x \sin e + z \cos e - V_P t), \quad \psi_1 = \psi_2 = 0, \quad \text{and}$$

$$\psi_3 = \Psi_0(x \sin f_0 - z \cos f_0 - V_S t) + \Psi(x \sin f + z \cos f - V_S t) \tag{5.4.95}$$

The displacements are

$$u = \frac{\partial \varphi}{\partial x} - \frac{\partial \psi}{\partial z}; \quad w = \frac{\partial \varphi}{\partial z} + \frac{\partial \psi}{\partial x} \tag{5.4.96}$$

The stresses are given by

$$\sigma_z = \lambda \left[\frac{\partial^2 \varphi}{\partial x^2} + \frac{\partial^2 \varphi}{\partial z^2} \right] + 2G \left[\frac{\partial^2 \varphi}{\partial z^2} + \frac{\partial^2 \psi}{\partial x \partial z} \right]; \quad \tau_{zx} = G \left[2 \frac{\partial^2 \varphi}{\partial x \partial z} + \frac{\partial^2 \psi}{\partial x^2} - \frac{\partial^2 \psi}{\partial z^2} \right] \tag{5.4.97}$$

The boundary conditions are: at $z = 0$, $\sigma_z = \tau_{zx} = 0$ (5.4.98)

From Equations (5.4.96), (5.7.97) and (5.7.98),

$$\begin{aligned} &(\lambda + 2G \sin^2 e)\, \varphi''(x \sin e - V_P t) + 2G V_S \sin f\, [\psi''(x \sin f_0 - V_S t) \\ &\quad - \psi''(x \sin f - V_S t)] = 0 \\ &- 2\alpha \cos e\, \varphi''(c \sin e - V_P t) + (\sin^2 f_0 - \cos^2 f_0) \psi''(x \sin f_0 - V_S t) \\ &\quad + (\sin^2 f - \cos^2 f) \psi''(x \sin f - V_S t) = 0 \end{aligned} \tag{5.4.99}$$

These equations can be satisfied for all values of x and t provided the arguments of the various φ and ψ functions are in a constant ratio.

Hence $$\frac{V_P}{\sin e} = \frac{V_S}{\sin f_0} = \frac{V_S}{\sin f}. \tag{5.4.100}$$

5.4.5.2 Plane waves

5.4.5.2.1 Reflections

Plane waves in the halfspace $y \geq 0$. Let us assume that the wave normal n lies in the x-y plane, call it vertical plane. For a primary wave the particle motion will be in the direction of the wave normal and will lie completely in the vertical plane as shown in Figure 5.4.11 (Graff 1975).

The normal displacement component is u_n and the transverse components are u_v and u_z which are in the vertical and horizontal planes. Since every point along the plane the plane of the wave is executing the same motion, we have that the motion is invariant with respect to z if the wave normal is in the vertical plane.

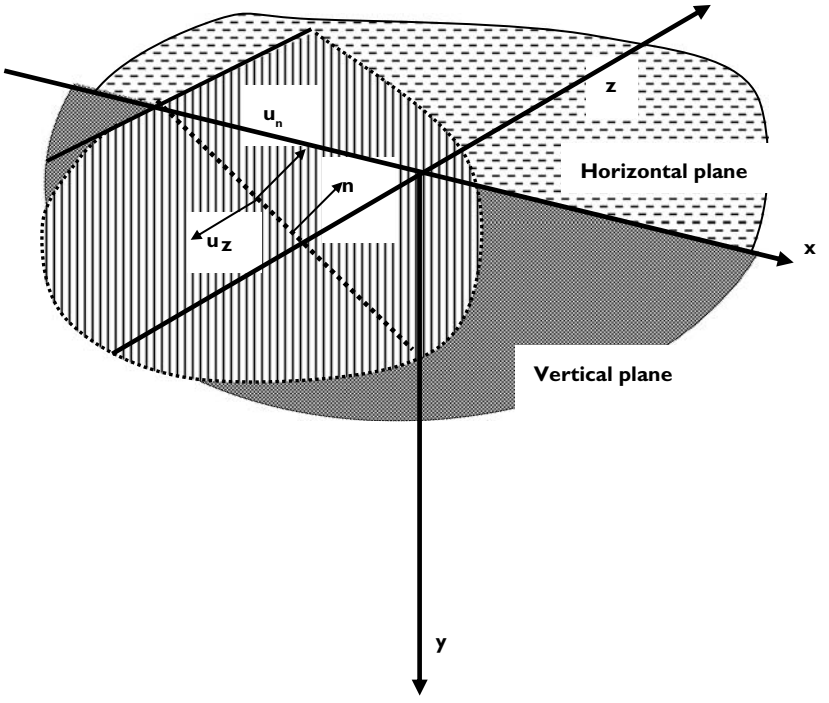


Figure 5.4.11 Plane wave, with wave normal in the *x*-*y* plane (vertical) advancing towards a free surface.

Following earlier notation for the wave equation, we have

$$u_x = \frac{\partial \phi}{\partial x} + \frac{\partial \psi_z}{\partial y}; \quad u_y = \frac{\partial \phi}{\partial y} - \frac{\partial \psi_z}{\partial x}; \quad u_z = -\frac{\partial \psi_x}{\partial y} + \frac{\partial \psi_y}{\partial x}; \quad \frac{\partial \psi_x}{\partial x} + \frac{\partial \psi_y}{\partial y} = 0 \tag{5.4.101}$$

and this leads to the wave equation

$$\nabla^2 \phi = \frac{1}{V_P^2} \frac{\partial^2 \phi}{\partial t^2}; \quad \nabla^2 \psi_i = \frac{1}{V_s^2} \frac{\partial^2 \psi_i}{\partial t^2} \tag{5.4.102}$$

$i = x, y, z.$

Stress-displacement relations are:

$$\sigma_x = (\lambda + 2G)\left(\frac{\partial u_x}{\partial x} + \frac{\partial u_y}{\partial y}\right) - 2G\frac{\partial u_y}{\partial y}; \quad \sigma_y = (\lambda + 2G)\left(\frac{\partial u_x}{\partial x} + \frac{\partial u_y}{\partial y}\right) - 2G\frac{\partial u_x}{\partial x}$$

$$\sigma_z = \frac{\lambda}{2(\lambda + G)}\left(\sigma_x + \sigma_y\right); \quad \tau_{xy} = G\left(\frac{\partial u_x}{\partial y} + \frac{\partial u_y}{\partial x}\right); \quad \tau_{yx} = \frac{\partial u_z}{\partial y}; \quad \tau_{xz} = 0 \tag{5.4.103}$$

In terms of potentials

$$\sigma_x = (\lambda + 2G)\left(\frac{\partial^2\phi}{\partial x^2} + \frac{\partial^2\phi}{\partial y^2}\right) - 2G\left(\frac{\partial^2\phi}{\partial y^2} - \frac{\partial^2\psi_z}{\partial y \partial x}\right);$$

$$\sigma_y = (\lambda + 2G)\left(\frac{\partial^2\phi}{\partial x^2} + \frac{\partial^2\phi}{\partial y^2}\right) - 2G\left(\frac{\partial^2\phi}{\partial x^2} + \frac{\partial^2\psi_z}{\partial x \partial y}\right)$$

$$\tau_{xy} = G\left(2\frac{\partial^2\phi}{\partial x \partial y} + \frac{\partial^2\psi_z}{\partial y^2} - \frac{\partial^2\psi_z}{\partial x^2}\right); \quad \tau_{yz} = G\left(-\frac{\partial^2\psi_z}{\partial y^2} + \frac{\partial^2\psi_y}{\partial y \partial x}\right); \quad \tau_{xz} = 0. \tag{5.4.104}$$

We have the boundary conditions:

$$\text{At} \quad y = 0, \quad \sigma_y = \tau_{yx} = \tau_{yz} = 0. \tag{5.4.105}$$

It is to be noted that u_x, u_y, σ_x, σ_y and τ_{xy} depend only on φ and ψ_z and for solution we must be dealing with two uncoupled equations in Equation (5.4.102). Again the displacement component u_z is necessary to obtain τ_{yz} which in turn depends on ψ_x, ψ_y. This makes it possible to resolve the motion into two parts, the one is **plane strain** and the other is **SH** wave motion.

5.4.5.2.2 Plane strain wave motion

$$\text{Constraints:} \quad u_z = \partial u_z / \partial z = 0. \tag{5.4.106}$$

$$\text{Governing equations:} \quad \text{with } u_x = \frac{\partial\phi}{\partial x} + \frac{\partial\psi_z}{\partial y}; \quad u_y = \frac{\partial\phi}{\partial y} - \frac{\partial\psi_z}{\partial x} \tag{5.4.107}$$

$$\sigma_x = (\lambda + 2G)\left(\frac{\partial^2\phi}{\partial x^2} + \frac{\partial^2\phi}{\partial y^2}\right) - 2G\left(\frac{\partial^2\phi}{\partial y^2} - \frac{\partial^2\psi_z}{\partial y \partial x}\right); \tag{5.4.108}$$

$$\sigma_y = (\lambda + 2G)\left(\frac{\partial^2\phi}{\partial x^2} + \frac{\partial^2\phi}{\partial y^2}\right) - 2G\left(\frac{\partial^2\phi}{\partial x^2} + \frac{\partial^2\psi_z}{\partial x \partial y}\right) \tag{5.4.109}$$

$$\tau_{xy} = G\left(2\frac{\partial^2\phi}{\partial x \partial y} + \frac{\partial^2\psi_z}{\partial y^2} - \frac{\partial^2\psi_z}{\partial x^2}\right); \quad \sigma_z = \frac{\lambda}{2(\lambda + G)}(\sigma_x + \sigma_y) \tag{5.4.110}$$

$$\rightarrow \quad \nabla^2\phi = \frac{1}{V_P^2}\frac{\partial^2\phi}{\partial t^2}; \quad \nabla^2\psi_z = \frac{1}{V_s^2}\frac{\partial^2\psi_z}{\partial t^2} \tag{5.4.111}$$

Boundary conditions:

$$\text{At} \quad y = 0; \quad \sigma_y = \tau_{xy} = 0. \tag{5.4.112}$$

$$\text{Assume the solution of the type:} \quad \phi = f(y)e^{i(px - \omega t)}; \quad \psi_z = h_z(y)e^{i(qx - \omega t)} \tag{5.4.113}$$

Substituting these expressions in the governing equation, Equation (5.4.111), we have

$$\frac{d^2f}{dy^2} + \alpha^2 f = 0 \quad \text{and} \quad \frac{d^2h_z}{dy^2} + \beta^2 h_z = 0 \tag{5.4.114}$$

in which $\alpha^2 = \omega^2/V_P^2 - p^2 : \beta^2 = \omega^2/V_s^2 - q^2$.

The plane wave solution for Φ and Ψ_z are given by

$$\varphi = A_1 e^{i(px-\alpha y-\omega t)} + A_2 e^{i(qx+\alpha y-\omega t)}; \quad \psi_z = B_1 e^{i(qx-\beta y-\omega t)} + B_2 e^{i(qx+\beta y-\omega t)} \tag{5.4.115}$$

If θ_1 and θ_2 are the angles between the y-axis and the wave normal of the P and S waves, we can write

$$p = k_1 \sin\theta_1, \quad q = k_2 \sin\theta_2, \quad \alpha = k_1 \cos\theta_1 \quad \text{and} \quad \beta = k_2 \cos\theta_2. \tag{5.4.116}$$

where, k_1 and k_2 are the wave numbers along the respective waves. Φ and Ψ_z may also be written as

$$\varphi = A_1 e^{ik_1(\sin\theta_1 x - \cos\theta_1 y - c_1 t)} + A_2 e^{ik_1(\sin\theta_1 x + \cos\theta_1 y - c_1 t)}$$

$$\psi_z = B_1 e^{ik_2(\sin\theta_2 x - \cos\theta_2 y - c_2 t)} + B_2 e^{ik_2(\sin\theta_2 x + \cos\theta_2 y - c_2 t)} \tag{5.4.117}$$

The results are shown in Figure 5.4.12 for the Φ-wave. $2\pi/k_1$ is the wavelength along the direction of propagation and k_1 is the wave number. p and α are horizontal and vertical wave numbers resulting in $2\pi/p$ and $2\pi/\alpha$ horizontal and vertical wavelengths.

Substituting Equation (5.4.117) into the plane strain boundary conditions, we have $\sigma_y = 0$:

$$k_1^2(2\sin^2\theta_1 - k^2)(A_1 + A_2)e^{i(k_1 \sin\theta_1 x - k_1 V_P t)}$$

$$- k_2^2 \sin 2\theta_2 (B_1 - B_2) e^{i(k_2 \sin\theta_2 x - k_2 V_s t)} = 0$$

$$k_1^2 \sin 2\theta_1 (A_1 - A_2) e^{i(k_1 \sin\theta_1 x - k_1 V_P t)} - k_2^2 \cos 2\theta_2 (B_1 + B_2) e^{i(k_2 \sin\theta_2 x - k_2 V_s t)} = 0 \tag{5.4.118}$$

in which $k = \frac{V_P}{V_s} = \sqrt{\frac{\lambda+2G}{G}}$.

Since $\omega = k_1 V_P = k_2\ V_s$ and $k_2/k_1 = V_p/V_s = \mathrm{k}$, we may write

$$(2\sin^2\theta_1 - k^2)(A_1 + A_2)e^{ik_1 \sin\theta_1 x} - k^2 \sin 2\theta_2 (B_1 - B_2) e^{ik_2 \sin\theta_2 x} = 0 \tag{5.4.119}$$

$$\sin 2\theta_1 (A_1 - A_2) e^{ik_1 \sin\theta_1 x} - k^2 \cos 2\theta_2 (B_1 + B_2) e^{ik_2 \sin\theta_2 x} = 0 \tag{5.4.120}$$

—done by factoring out $e^{i\omega t}$ from the Equation (5.4.118).

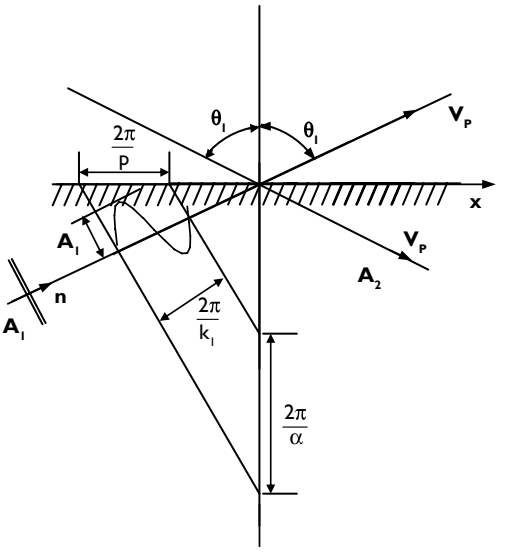


Figure 5.4.12 Incident and reflected wave system for $\Phi(x, y, t)$.

If Equations (5.4.119) and (5.4.120) are to hold good, for any arbitrary x, we must have

$$\rightarrow \quad k_1 \sin\theta_1 = k_2 \sin\theta_2 \tag{5.4.121}$$

This is *Snell's law* for elastic waves.

As a consequence, we have the following from Equations (5.4.119) and (5.4.120)

$$\frac{(A_1 + A_2)}{(B_1 - B_2)} = \frac{k^2 \sin 2\theta_2}{(2\sin^2\theta_1 - k^2)} : \frac{(A_1 - A_2)}{(B_1 + B_2)} = \frac{k^2 \cos 2\theta_2}{\sin 2\theta_1} \tag{5.4.122}$$

These equations govern the reflection of plane waves in a half space.

5.4.5.2.3 *Case (a) P-waves at oblique incidence*

Here we have $B_1 = 0$, and Equation (5.4.112) reduces to

$$\frac{A_2}{A_1} = \frac{\sin 2\theta_1 \sin 2\theta_2 - k^2 \cos^2 2\theta_2}{\sin 2\theta_1 \sin 2\theta_2 + k^2 \cos^2 2\theta_2}; \quad \frac{B_2}{A_1} = \frac{2 \sin 2\theta_1 \cos 2\theta_2}{\sin 2\theta_1 \sin 2\theta_2 + k^2 \cos^2 2\theta_2} \tag{5.4.123}$$

The reflection angle and wave number are given by Equation (5.4.120), also θ_2 is always less than θ_1.

Important outcome of this exercise is that for a single *P*-incident, two waves, *P* and SV, are reflected. Normally two waves namely *P* and *S* waves propagate independently,

they are uncoupled. But when a free boundary is encountered coupling of the two waves occurs through the boundary conditions. This phenomenon is called mode conversion.

5.4.5.2.4 Case (b) SV-waves at oblique incidence

In this case we have $A_1 = 0$ and the boundary conditions Equation (5.4.122) result in

$$\frac{B_2}{B_1} = \frac{\sin 2\theta_1 \sin 2\theta_2 - k^2 \cos^2 2\theta_2}{\sin 2\theta_1 \sin 2\theta_2 + k^2 \cos^2 2\theta_2}; \quad \frac{A_2}{B_1} = \frac{-k^2 2 \sin 2\theta_2 \cos 2\theta_2}{\sin 2\theta_1 \sin 2\theta_2 + k^2 \cos^2 2\theta_2} \tag{5.4.124}$$

As in the case of *P*-waves, mode conversion occurs again for incident SV-waves. For normal incidence, given by $\theta_2 = 0$, we have,

$$A_2/A_1 = 0, \quad \text{and} \quad B_2/B_1 = -1. \tag{5.4.125}$$

In case when $\theta_2 = 45°$,

$$A_2/B_1 = 0, \quad B_2/B_1 = 1, \tag{5.4.125a}$$

It has application in plate theory. It is also possible to have an incident SV-wave with only a reflected *P*-wave ($B_2 = 0$). This occurs for

$$(\sin 2\theta_1 \sin 2\theta_2) = k^2 \cos^2 2\theta_2. \tag{5.4.126}$$

Again, there is a value of θ_2 beyond this critical angle for which the reflected *P* wave will be tangential to the surface. This result in

$$\rightarrow \quad \sin\theta_1 = k \sin\theta_2 = 1, \quad \text{and } k \text{ is always greater than 1.} \tag{5.4.127}$$

5.4.5.2.5 SH wave motion

$$\text{Constraints :} \quad u_x = u_z = \partial/\partial z = 0 \tag{5.4.128}$$

$$\text{Governing equations:} \quad \text{with } u_z = -\frac{\partial \psi_x}{\partial y} + \frac{\partial \psi_y}{\partial x}; \quad \frac{\partial \psi_x}{\partial x} + \frac{\partial \psi_y}{\partial y} = 0$$

$$\tau_{yz} = G\left(-\frac{\partial^2 \psi_z}{\partial y^2} + \frac{\partial^2 \psi_y}{\partial y \partial x}\right) \tag{5.4.129}$$

$$\rightarrow \quad \nabla^2 \psi_x = \frac{1}{V_s^2} \frac{\partial^2 \psi_x}{\partial t^2}; \quad \nabla^2 \psi_y = \frac{1}{V_s^2} \frac{\partial^2 \psi_y}{\partial t^2} \tag{5.4.130}$$

Boundary conditions:

$$\text{At,} \quad y = 0; \quad \tau_{yz} = 0.$$

In the case of SH wave propagation; we may use the displacement equations directly,

$$\nabla^2 u_z = \frac{1}{V_s^2} \frac{\partial^2 u_z}{\partial t^2} \tag{5.4.131}$$

Assume the solution of the type:

$$\psi_x = h_x(y) e^{i(px-\omega t)}; \quad \psi_y = h_y(y) e^{i(qx-\omega t)} \tag{5.4.132}$$

Substituting these expressions in the governing equation, Equation (5.4.130), we have

$$\frac{d^2 h_x}{dy^2} + \eta^2 f = 0 \quad \text{and} \quad \frac{d^2 h_y}{dy^2} + \eta^2 h_y = 0 \tag{5.4.133}$$

where, $\eta^2 = (\omega^2/V_s^2) - p^2$.

The plane wave solution for Ψ_x and Ψ_y are given by

$$\psi_x = C_1 e^{i(px-\eta y-\omega t)} + C_2 e^{i(px+\eta y-\omega t)} : \psi_y = D_1 e^{i(px-\eta y-\omega t)} + D_2 e^{i(px+\eta y-\omega t)} \tag{5.4.134}$$

It may be noticed that u_x and u_y depend only on φ and ψ_z and u_z depends on ψ_x and ψ_y. Applying the divergence condition $\nabla \cdot \psi = 0$, factoring out $e^{i(px-\omega t)}$, we may write

$$ip(C_1 e^{-i\eta y} + C_2 e^{i\eta y}) + i\eta(-D_1 e^{-i\eta y} + D_2 e^{i\eta y}) = 0 \tag{5.4.135}$$

This further leads to

$$(pC_1 - \eta D_1) e^{-i\eta y} + (pC_2 + \eta D_2) e^{i\eta y} = 0 \tag{5.4.136}$$

In order for the above to hold good for all values of y, we must have

$$pC_1 = \eta D_1, \quad pC_2 = -\eta D_2. \tag{5.4.137}$$

Arbitrarily eliminating D_1 and D_2, We may write the solution as

$$\psi_x = C_1 e^{i(px-\eta y-\omega t)} + C_2 e^{i(px+\eta y-\omega t)}; \quad \psi_y = \frac{p}{\eta} C_1 e^{i(px-\eta y-\omega t)} - \frac{p}{\eta} C_2 e^{i(px+\eta y-\omega t)} \tag{5.4.138}$$

Substituting ψ_x and ψ_y into the boundary condition we may obtain

$$\eta^2(C_1 + C_2) + p^2(C_1 + C_2) = 0 \tag{5.4.139}$$

Equation (5.4.139) implies that $C_2 = -C_1$.

Thus the reflection angle is equal to the incidence angle and there is no mode conversion. This is analogous to acoustic wave reflection. If a shear wave of arbitrary polarization strikes on a free surface, the SV portion of the wave will lose a portion of its energy to *p*-waves, whereas the SH portion of the amplitude and energy will reflect with only change of phase.

5.4.6 Where does this all lead to?

OK, so we have solved a few exotic/nasty[63] looking differential equations one might wonder where does it all lead to?

We will show some application of it subsequently, however for the present we would only like to point out that study of Rayleigh and Love wave has great application in seismology, geophysical prospecting and locating oil deposits below earth.

Study of these two waves are of great importance to estimate the arrival time of seismic waves at a particular site from which it is possible to estimate the focus and epicenter of an earthquake.

Analysis in polar co-ordinate and expression similar to of the form as expressed in the preceding has a lot of application especially in solution of Lamb's problem which was the first stepping stone for study of waves in elastic media.

Before we delve further into the topic we explain herein some integral transforms and other mathematical theorems that form the background of subsequent development. We do not apologize for not putting them in an appendix and would prefer you to get through the same first for these are the stepping stones on which further developments are shown subsequently.

We are apprehensive, that without having this background it could be difficult for you to comprehend the further derivations and one might draw a wrong conclusion that the subject is a utopian exercise only, having little applications.

The mathematical derivations given hereafter are surely not rigorous[64] but are presented in a heuristic form to give you a reasonable background to appreciate the elastodynamic problems.

5.4.7 Some background on integral transforms and other mathematical theorems

We start with Fourier series and integrals which most of us are familiar with.

63 Depends on whether you love or despise it .....

64 For which reference are furnished at appropriate place.

5.4.7.1 Trigonometric Fourier series

A wave form expressed by a function $f(t)$ can be represented by a trigonometric series as

$$f(t) = a_0 + a_1 \cos \omega t + a_2 \cos 2\omega t + a_3 \cos 3\omega t + \cdots\cdots\cdots + a_n \cos n\omega t$$
$$+ b_1 \sin \omega t + b_2 \sin 2\omega t + b_3 \sin 3\omega t + \cdots\cdots\cdot b_n \sin n\omega t \tag{5.4.140}$$

The above can be further expressed in compact form as $f(t) = a_0 + \sum_{n=1}^{\infty} (a_n \cos \omega_n t + b_n \sin \omega_n t)$, where $\omega_n = n\omega$ and $n = 1, 2, 3.\ldots\ldots$

Considering $\omega_n = 2\pi n/T$ where T is the time period of the wave front we have

$$f(t) = a_0 + \sum_{n=1}^{\infty} \left(a_n \cos \frac{2\pi nt}{T} + b_n \sin \frac{2\pi nt}{T} \right) \tag{5.4.141}$$

Now the question here is how do we evaluate a_0, a_n, b_n etc.

To this end we first define some standard integral values that we will use for subsequent derivations.

$$\int_0^{2\pi} (\cos n\theta) d\theta = -\frac{1}{n} [\sin n\theta]_0^{2\pi} = 0 \tag{5.4.142}$$

$$\int_0^{2\pi} (\sin n\theta) d\theta = -\frac{1}{n} [\cos n\theta]_0^{2\pi} = 0 \tag{5.4.143}$$

$$\int_0^{2\pi} (\sin^2 n\theta) d\theta = \frac{1}{2} \int_0^{2\pi} (1 - \cos 2n\theta) d\theta = \frac{1}{2} \left[\theta - \frac{1}{2n} \sin 2n\theta \right]_0^{2\pi} = \pi \tag{5.4.144}$$

$$\int_0^{2\pi} (\cos^2 n\theta) d\theta = \frac{1}{2} \int_0^{2\pi} (1 + \cos 2n\theta) d\theta = \frac{1}{2} \left[\theta + \frac{1}{2n} \sin 2n\theta \right]_0^{2\pi} = \pi \tag{5.4.145}$$

$$\int_0^{2\pi} (\sin m\theta \cos n\theta) d\theta = \frac{1}{2} \int_0^{2\pi} \{\sin(m+n)\theta + \sin(m-n)\theta\} d\theta$$
$$= \frac{1}{2} \left[-\frac{1}{m+n} \cos(m+n)\theta + \frac{1}{m-n} \cos(m-n)\theta \right]_0^{2\pi} = 0 \tag{5.4.146}$$

for $n \neq m$. Similarly it can be proved that

$$\int_0^{2\pi} (\cos m\theta \cos n\theta) d\theta = 0 \quad \text{for } n \neq m \quad \text{and}$$

$$\int_0^{2\pi} (\sin m\theta \sin n\theta) d\theta = 0 \quad \text{for } n \neq m \tag{5.4.147}$$

Considering $\omega t = \theta$ we can now write the trigonometric series as

$$f(\theta) = a_0 + a_1 \cos\theta + a_2 \cos 2\theta + a_3 \cos 3\theta + \cdots\cdots\cdots + a_n \cos n\theta + b_1 \sin\theta + b_2 \sin 2\theta + b_3 \sin 3\theta + \cdots\cdots\cdots b_n \sin n\theta$$

Now integrating both sides between limits 2π to 0 we have

$$\int_0^{2\pi} f(\theta) d\theta = \int_0^{2\pi} (a_0 + a_1 \cos\theta + a_2 \cos 2\theta + a_3 \cos 3\theta + \cdots\cdots\cdots + a_n \cos n\theta + b_1 \sin\theta + b_2 \sin 2\theta + b_3 \sin 3\theta + \cdots\cdots\cdots b_n \sin n\theta) d\theta$$

$$\int_0^{2\pi} f(\theta) = a_0 [\theta]_0^{2\pi} = 2\pi a_0 \text{ (Other coefficient values becomes zero on integration)}$$

$$\rightarrow \quad a_0 = \frac{1}{2\pi} \int_0^{2\pi} f(\theta) d\theta \tag{5.4.148}$$

Thus over one complete cycle of period T, $a_0 = \frac{1}{T} \int_0^T f(t) dt$ which also can be expressed, as

$$a_0 = \frac{1}{T} \int_{-\frac{T}{2}}^{\frac{T}{2}} f(t) dt = a_0 = \frac{1}{T} \int_{0\tau}^{T+\tau} f(t) dt \tag{5.4.149}$$

where τ is any arbitrary value.

To determine a_n we multiply both sides by cos nθ and integrating between 2π to 0 we have

$$\int_0^{2\pi} (f(\theta) \cos n\theta) d\theta = \int_0^{2\pi} (a_0 \cos n\theta + a_1 \cos\theta \cos n\theta + a_2 \cos 2\theta \cos n\theta + \cdots\cdots + a_n \cos^2 n\theta + b_1 \sin\theta \sin n\theta + b_2 \sin 2\theta \sin n\theta + \cdots\cdots\cdots b_n \sin^2 n\theta) d\theta$$

$$\rightarrow \int_0^{2\pi} (f(\theta)\cos n\theta)d\theta = a_0 \cdot 0 + a_1 \cdot 0 + a_2 \cdot 0 + \cdots\cdots + a_n \cdot \pi$$

$$+ b_1 \cdot 0 + b_2 \cdot 0 + \cdots\cdots\cdot b_n 0$$

$$\rightarrow a_n = \frac{1}{\pi}\int_0^{2\pi} (f(\theta)\cos n\theta)d\theta \quad \text{or, } a_n = \frac{2}{2\pi}\int_0^{2\pi} (f(\theta)\cos n\theta)d\theta$$

Thus for one complete cycle of period T we have

$$a_n = \frac{2}{T}\int_0^{T} f(t)\cos\frac{2\pi nt}{T}dt \quad \text{or } a_n = \frac{2}{T}\int_{-\frac{T}{2}}^{\frac{T}{2}} f(t)\cos\frac{2\pi nt}{T}dt \tag{5.4.150}$$

To determine b_n we multiply both sides by $\sin n\theta$ and integrating between 2π to 0 proceeding in similar manner as shown above we have

$$\int_0^{2\pi} (f(\theta)\sin n\theta)d\theta = a_0 \cdot 0 + a_1 \cdot 0 + a_2 \cdot 0 + \cdots\cdots + a_n 0\pi$$

$$+ b_1 \cdot 0 + b_2 \cdot 0 + \cdots\cdots\cdots b_n\pi$$

$$\rightarrow \quad b_n = \frac{1}{\pi}\int_0^{2\pi} (f(\theta)\sin n\theta)d\theta$$

Thus for one complete cycle of period T we have

$$b_n = \frac{2}{T}\int_0^{T} f(t)\sin\frac{2\pi nt}{T}dt \quad \rightarrow \quad b_n = \frac{2}{T}\int_{-T/2}^{T/2} f(t)\sin\frac{2\pi nt}{T}dt \tag{5.4.151}$$

Thus, from above we see that any wave form which is a periodic function can be subjected to Fourier analysis to evaluate the coefficient and express it as a continuous function.

5.4.7.2 Fourier series in complex form

We have shown earlier that a wave form can be represented (Pipes & Harvill 1970) as

$$f(t) = a_0 + \sum_{n=1}^{\infty} (a_n \cos\omega_n t + b_n \sin\omega_n t) \tag{5.4.152}$$

Now as $e^{i\theta} = \cos\theta + i\sin\theta$ and $e^{-i\theta} = \cos\theta - i\sin\theta$, we can express cosine and sine function as

$$\cos\theta = \frac{e^{i\theta} + e^{-i\theta}}{2} \quad \text{and} \quad \sin\theta = \frac{e^{i\theta} - e^{-i\theta}}{2i}$$

Substituting above formula in Equation (5.4.152), we have

$$f(t) = a_0 + \sum_{n=1}^{\infty}\left(a_n\frac{e^{i\omega t} + e^{-i\omega t}}{2} + b_n\frac{e^{i\omega t} - e^{-i\omega t}}{2i}\right)$$

$$= a_0 + \sum_{n=1}^{\infty}\left(\frac{1}{2}(a_n - ib_n)e^{i\omega t} + \frac{1}{2}(a_n + ib_n)e^{-i\omega t}\right)$$

$$= a_0 + \sum_{n=1}^{\infty}\left(\frac{1}{2}\hat{a}_n e^{i\omega t} + \frac{1}{2}\hat{b}_n e^{-i\omega t}\right)$$

where $\hat{a}_n = \frac{1}{2}(a_n - ib_n)$ and $\hat{b}_n = \frac{1}{2}(a_n + ib_n)$ (5.4.153)

Substituting the value of a_n and b_n obtained from Equations (5.4.150) and (5.4.151) in Equation (5.4.153), we have

$$\hat{a}_n = \frac{1}{T}\left[\int_0^T f(t)\cos\omega t dt - i\int_0^T \sin\omega t dt\right] \quad \text{or } \hat{a}_n = \frac{1}{T}\left[\int_0^T f(t)e^{-i\omega t}dt\right] \tag{5.4.154}$$

Proceeding in similar fashion we can arrive at the solution

$$\hat{b}_n = \frac{1}{T}\left[\int_0^T f(t)e^{i\omega t}dt\right] \tag{5.4.155}$$

Now looking at $\hat{a}_n$ and $\hat{b}_n$, it can be seen that $\hat{b}_n$ is nothing but complex conjugate of $\hat{a}_n$.

Thus $\hat{b}_n = \hat{a}_{-n}$ when the function $f(t)$ can be expresses (Kreyszig 2001) as

$$f(t) = a_0 + \hat{a}_1 e^{i\omega t} + \hat{a}_2 e^{2i\omega t} + \cdots + \hat{a}_n e^{ni\omega t} + \hat{a}_{-1}e^{-i\omega t} + \hat{a}_{-2}e^{-2i\omega t} + \hat{a}_{-n}e^{-ni\omega t}$$

$$\rightarrow \quad f(t) = \sum_{-\infty}^{\infty}\hat{a}_n e^{i\omega t}$$

where $\hat{a}_n$ is as given in Equation (5.4.154).

Above is usually termed as complex representation of Fourier series.

5.4.7.3 Fourier Integral-Trigonometric form

We had seen that any periodic function can be expressed by Fourier series expressed (Riley et al. 2002) by the form

$$f(t) = a_0 + \sum_{n=1}^{\infty} (a_n \cos \omega_n t + b_n \sin_n t), \quad \text{where} \quad a_0 = \frac{1}{T} \int_{-\frac{T}{2}}^{\frac{T}{2}} f(t)dt;$$

$$a_n = \frac{2}{T} \int_{-\frac{T}{2}}^{\frac{T}{2}} f(t) \cos \frac{2\pi nt}{T} dt \quad \text{and} \quad b_n = \frac{2}{T} \int_{-\frac{T}{2}}^{\frac{T}{2}} f(t) \sin \frac{2\pi nt}{T} dt$$

Thus for any function $f(x)$ we represent it in Fourier series as

$$f(x) = a_0 + \sum_{n=1}^{\infty} \left(a_n \cos \frac{2\pi nx}{T} + b_n \sin \frac{2\pi nx}{T} \right)$$

Substituting the value of a_0, a_n and b_n we have

$$f(x) = \frac{1}{T} \int_{-T/2}^{T/2} f(t)dt + \sum_{n=1}^{\infty} \left(\frac{2}{T} \int_{-T/2}^{T/2} f(t) \cos \frac{2\pi nt}{T} \cos \frac{2\pi nx}{T} dt \right.$$

$$\left. + \frac{2}{T} \int_{-T/2}^{T/2} f(t) \sin \frac{2n\pi t}{T} \sin \frac{2\pi nx}{T} dt \right)$$

$$\text{or} \quad f(x) = \frac{1}{T} \int_{-T/2}^{T/2} f(t)dt + \frac{2}{T} \sum_{n=1}^{\infty} \left(\int_{-T/2}^{T/2} f(t) \left\{ \cos \frac{2\pi n}{T} (x-t) dt \right\} \right).$$

Now we are interested to find out what happens to the function $f(x)$ when $T \to \infty$?

For $T \to \infty (T/2, -T/2) \to (+\infty, -\infty)$. Taking limit of $T \to \infty$ for the first term in $f(x)$ tends to 0, when we have

$$f(x) = \frac{2}{T} \sum_{n=1}^{\infty} \left(\int_{-T/2}^{T/2} f(t) \left\{ \cos \frac{2\pi n}{T} (x-t) dt \right\} \right)$$

Now considering $\omega_n = \frac{2\pi n}{T}$ and $\omega_{n+1} = \frac{2\pi (n+1)}{T}$, we have

$$\Delta\omega = \omega_{n+1} - \omega_n = \frac{2\pi}{T} \quad \to \quad T = \frac{\Delta\omega}{2\pi}$$

Thus the function can be represented as $f(x) = \sum_{n=1}^{\infty} \frac{\Delta\omega}{2\pi} \left(\int_{-\infty}^{\infty} f(t) \{ \cos \frac{2\pi n}{T} (x-t) \right) dt$ which can be further expressed as

$$f(x) = \frac{1}{2\pi} \int_0^{\infty} d\omega \int_{-\infty}^{\infty} f(t) \cos \omega (x-t) dt \tag{5.4.156}$$

Above is known as the trigonometric form of Fourier integral.

5.4.7.4 Fourier integral complex form

We had shown above that, based on trigonometric form $f(x) = \frac{1}{2\pi}\int_0^\infty d\omega \int_{-\infty}^{\infty} f(t)\cos\omega(x-t)dt$, which can be again expressed between $(\pm)\infty$ as $f(x) = \frac{1}{2\pi}\int_{-\infty}^{\infty} d\omega \int_{-\infty}^{\infty} f(t)\cos\omega(x-t)dt$ while it can be shown (Arfken & Weber 2001) that the integral

$$\frac{1}{2\pi}\int_{-\infty}^{\infty} d\omega \int_{-\infty}^{\infty} f(t)\sin\omega(x-t)dt = 0$$

Thus the function $f(x)$ can be expressed as

$$f(x) = \frac{1}{2\pi}\int_{-\infty}^{\infty} d\omega \int_{-\infty}^{\infty} f(t)\cos\omega(x-t)dt - \frac{1}{2\pi}\int_{-\infty}^{\infty} d\omega \int_{-\infty}^{\infty} f(t)i\sin\omega(x-t)dt$$

or, $$f(x) = \frac{1}{2\pi}\int_{-\infty}^{\infty} d\omega \int_{-\infty}^{\infty} f(t)\left[\cos\omega(x-t) - i\sin\omega(x-t)\right]dt \quad \text{i.e.}$$

$$f(x) = \frac{1}{2\pi}\int_{-\infty}^{\infty} d\omega \int_{-\infty}^{\infty} f(t)e^{-i\omega(x-t)}dt$$

$$\rightarrow \quad f(x) = \frac{1}{2\pi}\int_{-\infty}^{\infty} e^{-i\omega x}d\omega \int_{-\infty}^{\infty} f(t)e^{i\omega t}dt \tag{5.4.157}$$

Above is known as complex form of Fourier integral.

5.4.7.5 Fourier transform

We had shown above that in complex form the Fourier integral is expressed as

$$f(x) = \frac{1}{2\pi}\int_{-\infty}^{\infty} e^{-i\omega x}d\omega \int_{-\infty}^{\infty} f(t)e^{i\omega t}dt$$

Considering $\Im(\omega) = \frac{1}{\sqrt{2\pi}}\int_{-\infty}^{\infty} f(t)e^{i\omega t}dt$, we can write

$$f(t) = \frac{1}{\sqrt{2\pi}}\Im(\omega)\int_{-\infty}^{\infty} e^{-i\omega x}d\omega$$

where $\Im(\omega)$ = Fourier transform

Inverse of Fourier transform $\Im(\omega)$ is given by

$$f(t) = \frac{1}{\sqrt{2\pi}} \int_{-\infty}^{\infty} \Im(\omega) e^{-i\omega t} d\omega. \tag{5.4.158}$$

Two other Fourier transforms which are very useful, are as mentioned hereafter

$$\Im(\omega) = \sqrt{\frac{2}{\pi}} \int_{-\infty}^{\infty} f(t) \cos \omega t dt, \quad \text{and inverse is given as } f(t) = \sqrt{\frac{2}{\pi}} \int_{-\infty}^{\infty} \Im(\omega) \cos \omega t d\omega \tag{5.4.159}$$

this is known as **cosine Fourier transform.**

Similarly $\Im(\omega) = \sqrt{\frac{2}{\pi}} \int_{-\infty}^{\infty} f(t) \sin \omega t dt$ whose inverse is given as

$$f(t) = \sqrt{\frac{2}{\pi}} \int_{-\infty}^{\infty} \Im(\omega) \sin \omega t d\omega \tag{5.4.160}$$

this is known as **sine Fourier transform.**

5.4.7.6 Fourier transform in three dimensions

Fourier transformation in three-dimension can be expressed as

$$\Im(k_x, k_y, k_z) = \frac{1}{(2\pi)^{\frac{3}{2}}} \iiint f(x, y, z) e^{ikx} e^{iky} e^{ikz} dx \cdot dy \cdot dz$$

where, the inverse of the same is given by

$$f(x, y, z) = \frac{1}{(2\pi)^{\frac{3}{2}}} \iiint \Im(k_x, k_y, k_z) e^{-ikx} e^{-iky} e^{-ikz} dk_x \cdot dk_y \cdot dk_z \tag{5.4.161}$$

5.4.7.7 Laplace transform

Basics

If $f(t)$ is a function which is piecewise and continuous, then $f(t)$ is said to be of exponential order α, if there exists a real and finite positive number N such that

$$\lim_{t \to \infty} |f(t)| e^{-\alpha t} \leq N \quad \Rightarrow \quad |f(t)| = 0(e^{\alpha t})$$

If $f(t)$ be a continuous single valued function of the real variable t defined for all t, when $0 < t < \infty$ and is also of exponential order. Then the Laplace Transform $f(t)$ is defined as

$$L\{f(t)\} = \bar{f}(s) = \int_0^\infty e^{-st} f(t)dt \tag{5.4.162}$$

The above is valid subject to the condition that the integral on the right hand side exists. Here s is a parameter that could be real or imaginary (complex number) and $\bar{f}(s)$ is a function of s.

Table 5.4.1. gives the Laplace Transform and its inverse for a number of functions.

There are many cases where the results cannot be obtained directly from the table. In such case the first principle method of inverting a transformed solution can be applied irrespective of the availability of the tabulated values. To develop the needed inversion process it is essential to extend the theory of Laplace Transform by letting s represent a complex variable and then on extension of Cauchy Integral formula provides the desired result.

For complex variable Cauchy's integral formula states that if $f(z)$ is an analytic function inside a closed curve C and if z_0 is a point within C then

Table 5.4.1 Typical Laplace transform and its inverse.

No.	$f(t)$	$\bar{f}(s) = L\{f(t)\}$	$\bar{f}(t) = L^{-1}\{f(t)\}$
1	0	0	0
2	1	$1/s$	1
3	t	$1/s^2$	t
4	t^n	$\Gamma(n)/s^{n+1}$	t^n
5	e^{at}	$1/(s-a)$	e^{at}
6	$\sin at$	$a/(s^2+a^2)$	$\sin at$
7	$\cos at$	$s/(s^2+a^2)$	$\cos at$
8	$\sinh at$	$a/(s^2-a^2)$	$\sinh at$
9	$\cosh at$	$s/(s^2-a^2)$	$\cosh at$
10	$t \sin at$	$2as/(s^2+a^2)^2$	$t \sin at$
11	$t \cos at$	$(s^2-a^2)/(s^2+a^2)^2$	$t \cos at$
12	$H(t-a)$	$e^{-as}/s, s > 0$	$H(t-a)$
13	$f(t-a)H(t-a)$	$e^{-as}f(s)$	$f(t-a)H(t-a)$
14	$\delta(t-a)$	$e^{-as}, a > 0$	$\delta(t-a)$
15	$J_0(t)$	$1/\sqrt{1+s^2}$	$J_0(t)$
16	$tJ_0(t)$	$s/(1+s^2)^{3/2}$	$tJ_0(t)$
17	$e^{at}f(t)$	$f(s+a)$	$e^{at}f(t)$
18	$t^n f(t)$	$(-1)n\frac{d^n}{ds^n}f(s)$	$t^n f(t)$
19	$e^{at}f(t)$	$\frac{1}{s}e^{\frac{s^2}{4}}erfc\left(\frac{s}{2}\right)$	$e^{at}f(t)$
20	$\int_0^t f(t-u)g(u)du$	$f(s)g(s)$	$\int_0^t f(t-u)g(u)du$
21	$\frac{f(t)}{t}$	$\int_s^\infty f(s)ds$	$\frac{f(t)}{t}$

$$f(z_0) = \frac{1}{2\pi i}\int_C \frac{f(z)dz}{z - z_0} \tag{5.4.163}$$

If $f(z)$ be analytic for all real values of $z \geq \gamma$ where γ is a real constant greater than 0 than for all real $z > \gamma$

$$f(z_0) = \frac{1}{2\pi i_{Lt\beta\to\infty}} \int_{\gamma - i\beta}^{\gamma + i\beta} \frac{f(z)dz}{z - z_0} \tag{5.4.164}$$

This can be proved by choosing a closed rectangular contour $C = C1+C2+C3+C4$ enclosing the point z_0 and having sides parallel to the real and imaginary axes as shown in Figure 5.4.13.

Based on above figure we have

$$f(z_0) = \frac{1}{2\pi i}\left[\int_{C1} + \int_{C2} + \int_{C3} + \int_{C4}\right] \frac{f(z)}{z - z_0} dz \tag{5.4.165}$$

By some limiting arguments and inequalities it can be shown that the contribution from the paths C1, C2 and C3 vanishes on letting $\beta \to \infty$ and the expression becomes

$$f(s) = \frac{1}{2\pi i_{Lt\beta\to\infty}} \int_{\gamma - i\beta}^{\gamma + i\beta} \frac{f(z)}{s - z} dz,$$

where z has been replaced by $s = x + iy$ and $f(s)$ is assumed to be analytic in the half-plane, $Re(s) > \gamma$.

Applying inverse of Laplace transform on both sides of this equation we get,

$$f(t) = L^{-1}\{f(s)\} = \frac{1}{2\pi i} L^{-1}\left\{ Lt\beta\to\infty \int_{\gamma - i\beta}^{\gamma + i\beta} \frac{f(z)}{s - z} dz \right\}$$

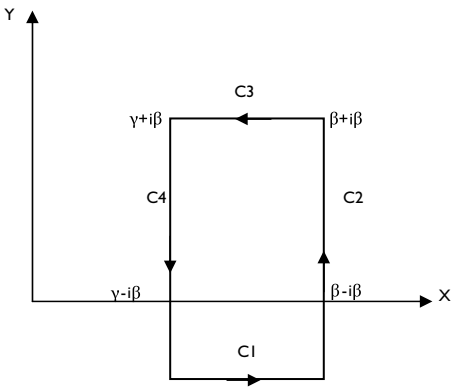


Figure 5.4.13 Path of integration.

$$= \frac{1}{2\pi i_{Lt\beta\to\infty}} \int_{\gamma-i\beta}^{\gamma+i\beta} f(z) L^{-1}\left(\frac{1}{s-z}dz\right)$$

$$= \frac{1}{2\pi i_{Lt\beta\to\infty}} \int_{\gamma-i\beta}^{\gamma+i\beta} e^{st} f(s)ds \qquad \left[\because L^{-1}\left(\frac{1}{s-z}\right) = e^{st}\right]$$

Thus in general Laplace transform is given by

$$f(t) = \frac{1}{2\pi i} \int_{\gamma-i\infty}^{\gamma+i\infty} e^{st}\bar{f}(s)ds \tag{5.4.166}$$

for t >0 and γ being a positive constant.

The path of integration in this inversion integral of Laplace Transform, is often called "**Bromwich contour**" since Bromwich first devised this method of handling certain integrals that arose in operational mathematics.

Example 5.4.1

Obtain a *LT* of function $f(t) = c$ for $t > 0$.

$$L[f(t)] = \int_0^\infty e^{-st} f(t)dt = \int_0^\infty e^{-st} cdt = \frac{c}{s} \quad \textbf{exists for Real (s)} > 0.$$

If c = unity, we have unit step function, $u(t)$.

Thus $u(t) = 0$, for $t < 0$

$= 1$, for $t > 0 \rightarrow L[u(t)] = \dfrac{1}{s}$

Example 5.4.2

Obtain *LT* for $f(t) = t$, for $t > 0$.

$$L[f(t)] = \int_0^\infty t\, e^{-st}dt = \left|\frac{-te^{-st}}{s}\right|_0^\infty + \frac{1}{s}\int_0^\infty e^{-st}dt = \frac{1}{s^2}, \quad \text{for Real } (s) > 0.$$

5.4.7.8 Laplace transform for derivatives

If $L[f(t)] = \bar{f}(s)$ exists, where $f(t)$ is continuous, then $f(t)$ tends to $f(0)$ as t $\to$ 0 and the LT of its derivative $f'(t) = \frac{df(t)}{dt}$ *is* $L\,[f'(t)] = s\bar{f}(s) - f(0)$.

$$[f'(t)] = \int_0^\infty e^{-st} f'(t)dt = \left|e^{-st} f(t)\right|_0^\infty + s\int_0^\infty e^{-st} f(t)dt = -f(0) + s\bar{f}(s) \quad (5.4.167)$$

Similarly

$L[f''(t)]$ can be written as $L[f''(t)] = s^2\bar{f}(s) - sf(0) - f'(0)$. (5.4.168)

5.4.7.9 Shifting theorem

$$L[e^{at} f(t)] = \int_0^\infty e^{-st}[e^{at} f(t)]dt = \int_0^\infty e^{-(s-a)t} f(t)dt = \bar{f}(s-a) \quad (5.4.169)$$

➔ multiplication of $f(t)$ by e^{at} shifts the transform by a, where a may be any number, real or complex.

5.4.7.10 Ordinary differential equation (ODE)

Consider: $m\ddot{x} + c\dot{x} + kx = f(t)$ (5.4.170)

LT of l.h.s. and r.h.s. can be written as

$$m[s^2\bar{x}(s) - sx(0) - \dot{x}(0)] + c[s\bar{x}(s) - x(0)] + k\bar{x}(s) = \bar{f}(s)$$

This can be rearranged to

$$\bar{x}(s) = \frac{\bar{f}(s)}{ms^2 + cs + k} + \frac{(ms + c)x(0) + m\dot{x}(0)}{ms^2 + cs + k} \quad (5.4.171)$$

force response due to initial condition.

This is called subsidiary equation of the ODE. $x(t)$ is found by the inverse transformation i.e. $L^{-1}[\bar{f}(s)]$.

The subsidiary equation, in general, can be written as,

$$\bar{x}(s) = \frac{A(s)}{B(s)} \tag{5.4.172}$$

Let $B(s)$ has n-roots $a_k, k = 1, 2, \ldots, n$, which are distinct [*known as simple poles in* $\bar{x}(s)$]

$$\rightarrow \quad B(s) = (s - a_1)(s - a_2)\ldots(s - a_n).$$

$\bar{x}(s)$ can be written as

$$\bar{x}(s) = \frac{A(s)}{B(s)} = \frac{c_1}{(s - a_1)} + \frac{c_2}{(s - a_2)} + \cdots + \frac{c_n}{(s - a_n)} \tag{5.4.173}$$

To determine c_k, multiply both the sides by $(s - a_k)$. Every term on the right hand side of the above will then be zero except c_k. Thus in the limit

$$C_k = \lim_{s \to a_k} (s - a_k) \frac{A(s)}{B(s)} \tag{5.4.174}$$

Since $L^{-1}\left[\frac{c_k}{s - a_k}\right] = c_k e^{a_k t}$, inverse of $\bar{x}(s)$ will be

$$x(t) = \sum_{k=1}^{n} \lim\ s \to a_k\ \ (s - a_k) \frac{A(s)}{B(s)} e^{a_k t}. \tag{5.4.175}$$

Again, say, $B(s) = (s - a_k)B_1(s)$; hence $B'(s) = (s - a_k)B_1'(s) + B_1(s) : \lim_{s \to a_k} B'(s) = B_1(a_k)$

$$\text{Since,} \quad (s - a_k)\frac{A(s)}{B(s)} = \frac{A(s)}{B_1(s)} \quad \Rightarrow \quad x(t) = \sum_{k=1}^{n} \frac{A(a_k)}{B'(a_k)} e^{a_k t}. \tag{5.4.176}$$

5.4.7.11 Poles of higher order

Consider $\bar{x}(s) = \frac{A(s)}{B(s)}$ and $\bar{x}(s)$ has an mth order pole.

Assuming that there is an mth order pole at a_1, $B(s)$ will have the form: $B(s) = (s - a_1)^m\ (s - a_2)(s - a_3)\ \ldots$

The partial fraction expansion of $\bar{x}(s)$ then becomes

$$\bar{x}(s) = \frac{C_{11}}{(s - a_1)^m} + \frac{C_{12}}{(s - a_1)^{m-1}} + \cdots + \frac{C_{1m}}{(x - a_1)} + \frac{C_2}{(x - a_2)} + \cdots \tag{5.4.177}$$

The coefficients C_{11} is determined by multiplying both the sides of the equation by $(x - a_1)^m$ and letting $s = a_1$

$$(s-a_1)^m\bar{x}(s) = C_{11}+(s-a_1)C_{12}+\cdots+(s-a_1)^{m-1}C_{1m}+\frac{(s-a_1)^m}{(s-a_2)}C_2+\frac{(s-a_1)^m}{(s-a_3)}C_3+\cdots$$

$$\therefore C_{11} = [(s-a_1)^m\bar{x}(s)]_{s=a_1}$$

The coefficient C_{12}, by differentiating $(s-a_1)^m\bar{x}(s)$, w.r.t. s and setting $s = a_1$,

$$C_{12} = \left[\frac{d(s-a_1)^m}{ds}\bar{x}(s)\right]_{s=a_1}$$

$$\rightarrow \quad C_{1n} = \frac{1}{(n-1)!}\left[\frac{d^{n-1}(s-a_1)^m}{ds^{n-1}}\bar{x}(s)\right]_{s=a_1} \tag{5.4.178}$$

The remaining C_2, C_3, etc. are evaluated as in the previous section for simple poles.

Since by the shifting theorem $\quad L^{-1}\left[\frac{1}{(s-a_1)^n}\right] = \frac{t^{n-1}}{(n-1)!}a_1t$

Inverse of $\bar{x}(s)$ becomes

$$x(t) = \left[C_{11}\frac{t^{m-1}}{(m-1)!} + C_{12}\frac{t^{m-2}}{(m-2)!}+\cdots\right]e^{a_1t} + C_2e^{a_2t} + C_3e^{a_3t}+\cdots \tag{5.4.179}$$

5.4.7.12 *Viscously damped spring-mass system with x(0) and ẋ(0)*

Consider, $\quad m\ddot{x} + c\dot{x} + kx = f(t)$ (5.4.180)

Taking LT of both the sides, we have,

$$m[s^2\bar{x}(s) - sx(0) - \dot{x}(0)] + c[s\bar{x}(s) - x(0)] + k\bar{x}(s) = \bar{f}(s)$$

Subsidiary equation:

Forced Vibration ↓ Transient solution due to end ↓

$$\bar{x}(s) = \frac{\bar{f}(s)}{ms^2+cs+k} + \frac{(ms+c)x(0)+m\dot{x}(0)}{ms^2+cs+k} \tag{5.4.181}$$

$$x(t) = L^{-1}[\bar{x}(s)] \tag{5.4.182}$$

Subsidiary equation is: $x(s) = \frac{A(s)}{B(s)}$, where $A(s)$ and $B(s)$ are polynomials in s and $B(s)$ is of higher order than $A(s)$.

5.4.7.13 Forced vibration

$$\frac{\bar{f}(s)}{\bar{x}(s)} = z(s) = ms^2 + cs + k = \text{Impedance transform.} \tag{5.4.183}$$

$$\text{Its reciprocal is admittance Transform given by} \quad H(s) = \frac{1}{z(s)}. \tag{5.4.184}$$

$$\text{Usually this is shown by} \quad \overset{\text{Input } \bar{f}(s)}{\longrightarrow} \boxed{\text{H(s)}} \quad \overset{\text{Output } \bar{x}(s)}{\longrightarrow} \tag{5.4.185}$$

With initial conditions zero; $H(s)$ can be called *system transfer function*.

Example 5.4.3

Spring-mass system subjected to a step function excitation = $F_0 u(t)$

$$m\ddot{x} + c\dot{x} + kx = F_0 u(t)$$

Taking LT of both sides $(ms^2 + cs + k)\bar{x}(s) = F_0/s$
If initial conditions are zero then

$$x(s) = \frac{F_0}{m}\frac{1}{s(s^2 + 2D\omega_n s + \omega_n^2)} = \frac{F_0}{m}\left[\frac{A_1}{s} + \frac{A_2 s + A_3}{s^2 + 2D\omega_n s + \omega_n^2}\right]$$

in which $A_1 = \frac{1}{\omega_n^2}; A_2 = -\frac{1}{\omega_n^2}; A_3 = -\frac{2D\omega_n}{\omega_n^2}$.

$$\rightarrow \quad x(t) = \frac{F_0}{k}\left[1 - e^{-D\omega_n t}\left(\cos\omega_{nd}t + \frac{D}{\sqrt{1-D^2}}\sin\omega_{nd}t\right)\right].$$

Important outcomes:

$$\int_0^\infty f(t)\delta(t-a)dt = f(a): \quad \text{if } f(t) = e^{-st}, \text{ we have}$$

$$\int_0^\infty e^{-st}\delta(t-a)dt = e^{-as}.$$

5.4.7.14 Hankel transform

Hankel transform is basically an analog to Fourier transform which often arises in problems involving Bessel's function. This is also otherwise known as *Fourier Bessel's* transform.

To elaborate it further we start with two dimensional Fourier transform.

$$f(x,y) = \frac{1}{2\pi}\int_{-\infty}^{\infty}\int_{-\infty}^{\infty} \Im(\xi,\eta)e^{i(\xi x+\eta y)}d\xi d\eta \quad \text{where}$$

$$\Im(\xi,\eta) = \frac{1}{2\pi}\int_{-\infty}^{\infty}\int_{-\infty}^{\infty} f(x,y)e^{-i(\xi x+\eta y)}dxdy \tag{5.4.186}$$

Changing the above Cartesian co-ordinate system to polar co-ordinate we have $f(x,y) = F(r)$ where $x = r\cos\theta, y = r\sin\theta, \xi = \kappa\cos\phi, \eta = \kappa\sin\phi$

$$\therefore \xi x + \eta y = r\kappa(\cos\theta\cos\phi + \sin\theta\sin\phi) = r\kappa\cos(\theta-\phi) \tag{5.4.187}$$

Since in polar co-ordinate differential area dA can be expressed as

$$dA = rdr\cdot d\theta \quad \text{we have } \Im(\xi,\eta) = \frac{1}{2\pi}\int_{-\infty}^{\infty}\int_{0}^{2\pi} F(r)e^{-ir\kappa\cos(\theta-\phi)}(rdr\cdot d\theta)$$

Let $\beta = \theta - \phi$ thus as $\theta \to 2\pi, \beta \to 2\pi - \phi$ and

As $\theta \to 0, \beta \to -\phi$ and $d\beta \to d\theta$

Thus[65]

$$\Im(\xi,\eta) = \frac{1}{2\pi}\int_{-\infty}^{\infty}\int_{-\phi}^{2\pi-\phi} F(r)e^{-ir\kappa\cos(\theta-\phi)}(rdr\cdot d\theta) = \frac{1}{2\pi}\int_{-\infty}^{\infty} rF(r)dr\int_{0}^{2\pi} e^{-ir\kappa\cos\beta}\cdot d\beta$$

Without going into detailed derivation, it can be shown that

$$\int_{0}^{2\pi} e^{ir\kappa\cos\beta}d\beta = 2\pi J_0(\kappa r) \quad \text{which gives } \Im(\xi,\eta) = \frac{1}{2\pi}\int_{-\infty}^{\infty} rF(r)J_0(\kappa r)\cdot dr$$

Since the last integral is clearly a function of the single variable κ, this shows that $\Im(\xi,\eta)$ is actually a function of ξ and η only through the combination, $\kappa = \sqrt{\xi^2+\eta^2}$. Thus considering $H(\kappa) = \Im(\xi,\eta)$ and we can write

$$H(\kappa) = \int_{-\infty}^{\infty} rF(r)J_0(\kappa r)\cdot dr. \tag{5.4.188}$$

65 Since the last integral in periodic it does not matter where it begins so long as it completes one full period.

Here $H(\kappa)$ is known as the Hankel Transform pair for Bessel function of order $\nu = 0$

$$\text{Thus,} \quad f(x,y) = F(r) = \frac{1}{2\pi}\int_{-\infty}^{\infty}\int_{0}^{2\pi} \Im(\xi,\eta)e^{ir\kappa\cos(\theta-\phi)}\kappa\, d\kappa\, d\phi = \int_{0}^{\infty}\kappa H(\kappa)J_0(\kappa r)d\kappa \tag{5.4.189}$$

More generally it can be shown that if $F(r)$ is a piecewise continuous function and provided $\int_0^\infty F(r)\cdot dr$ exists then

$$F(r) = \int_{0}^{\infty}\kappa H(\kappa)J_\nu(\kappa r)d\kappa \quad \text{and} \quad H(\kappa) = \int_{0}^{\infty} rF(r)J_\nu(\kappa r)dr. \tag{5.4.190}$$

5.5 HALFSPACE ELASTODYNAMIC SOLUTION

5.5.1 Lamb's solution for two-dimensional problem

Having cleared the basic mathematical background required for study of the subject of soil dynamics we are now ready to study the pioneering work of Lamb (1904) on response of an infinite and semi infinite media under action of dynamic load[66].

This though basically is of only historical importance now forms the basis on which Reissner and others developed the solution of response of machine foundations under dynamic load while seismologists realized why a major earthquake shock is preceded by a minor shock or tremor.

5.5.1.1 Action of dynamic vertical load in an infinite 2-D medium

Consider an infinite two-dimensional medium shown in Figure 5.5.1. While deriving the propagation of Rayleigh's wave we have shown that

$$\frac{\partial^2\phi}{\partial t^2} = \frac{\lambda+2G}{\rho}\nabla^2\phi \quad \text{and} \quad \frac{\partial^2\psi}{\partial t^2} = \frac{G}{\rho}\nabla^2\psi \tag{5.5.1}$$

where $\nabla^2 = \frac{\partial^2}{\partial x^2} + \frac{\partial^2}{\partial z^2}$, the Laplacian operator in two-dimension.

Considering the load to be of the nature, $P_0e^{i\omega t}$, it would be logical to assume that displacement nature shall also be of the form $\Phi = \phi e^{i\omega t}$ and $\Psi = \psi e^{i\omega t}$.

Now expressing the above equation of motion in the form

$$\frac{\partial^2\Phi}{\partial t^2} = V_p^2\nabla^2\Phi \quad \text{and } (V_p \text{ is the compression wave velocity})$$

$$\frac{\partial^2\Psi}{\partial t^2} = V_s^2\frac{G}{\rho}\nabla^2\Psi \quad (V_s \text{ is the shear wave velocity})$$

66 This is also otherwise known as dynamic Boussinesq's Problem.

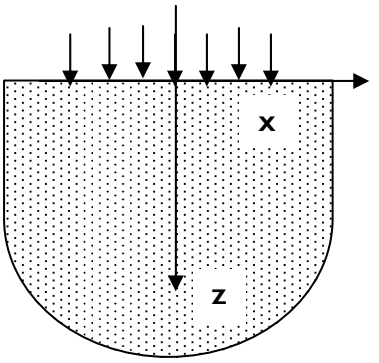


Figure 5.5.1 Vertical dynamic load acting on a two-dimensional semi-infinite elastic medium.

Considering $\Phi = \phi e^{i\omega t}$ and substituting in equation of motion, we have $-\omega^2 e^{i\omega t}\phi = V_p^2 \nabla^2 \phi e^{i\omega t}$ or $-\frac{\omega^2}{V_p^2}\phi = \nabla^2\phi$, using $h^2 = \frac{\omega^2}{V_p^2}$ we have[67]

$$\nabla^2\phi + h^2\phi = 0$$

Similarly considering $\Psi = \psi e^{i\omega t}$ we have

$$\nabla^2\psi + k^2\psi = 0 \quad \text{where } k^2 = \omega^2/V_s^2.$$

Now considering the differential equation

$$\nabla^2\phi + h^2\phi = 0$$

we can express this as $\dfrac{\partial^2\phi}{\partial x^2} + \dfrac{\partial^2\phi}{\partial y^2} + h^2\phi = 0$

Let $\phi = X(x)Z(z) \cong X \cdot Z$ which, on substitution gives

$$\ddot{X}Z + \ddot{Z}X + h^2XZ = 0$$

Dividing each of the above term by XZ (where $XZ \neq 0$), we have

$$\frac{\ddot{X}}{X} + \frac{\ddot{Z}}{Z} + h^2 = 0 \quad \rightarrow \quad \frac{\ddot{X}}{X} = -\left(\frac{\ddot{Z}}{Z} + h^2\right) = -\alpha^2 \text{ (say)} \tag{5.5.2}$$

67 Here h is actually the inverse of compression wave length.

This gives two linear differential equations

$$\frac{d^2X}{dx^2} + \alpha^2 X = 0 \quad \text{and} \quad \frac{d^2Z}{dz^2} - \xi^2 Z = 0 \tag{5.5.3}$$

where $\xi^2 = (\alpha^2 - h^2)$

The solutions is, $X = C_1 e^{i\alpha x} + C_2 e^{-i\alpha x}$ and $Z = C_3 e^{\xi z} + C_4 e^{-\xi z}$

The complete solution is given by

$$\phi = X \cdot Z = (C_1 e^{i\alpha x} + C_2 e^{-i\alpha x})(C_3 e^{\xi z} + C_4 e^{-\xi z}) \tag{5.5.4}$$

Proceeding in an identical fashion as done earlier, it can be shown that

$$\psi = (C_5 e^{i\alpha x} + C_6 e^{-i\alpha x})(C_7 e^{\eta z} + C_8 e^{-\eta z}) \quad \text{where } \eta^2 = \alpha^2 - k^2 \tag{5.5.4a}$$

Thus for $Z > 0$ as wave intensity cannot build up at infinity we have

$$\Phi = A e^{i\alpha x} e^{-\xi z} e^{i\omega t} \quad \text{and} \quad \psi = B e^{i\alpha x} e^{-\eta z} e^{i\omega t}$$

where A and B are integration constants.

To determine the integration constants A and B, we go back to the following stress strain relation derived earlier.

$$\sigma_{xx} = \lambda e_v + 2G\varepsilon_{xx}, \quad \tau_{zx} = G\gamma_{zx} \quad \text{and} \quad \sigma_{zz} = \lambda e_v + 2G\varepsilon_{zz}$$

where, $e_v = \varepsilon_{xx} + \varepsilon_{zz}$ in two-dimension,

in which $\varepsilon_{xx} = \dfrac{du}{dx}$, $\varepsilon_{zz} = \dfrac{dw}{dz}$ and $\gamma_{zx} = \dfrac{du}{dz} + \dfrac{dw}{dx}$.

While deriving propagation of Rayleigh waves we have shown that u and w can expressed in terms of potential as

$$u = \frac{\partial \phi}{\partial x} + \frac{\partial \psi}{\partial z} \quad \text{and} \quad w = \frac{\partial \phi}{\partial z} - \frac{\partial \psi}{\partial x}$$

$$\text{Thus,} \quad \varepsilon_{xx} = \frac{du}{dx} = \frac{\partial^2 \phi}{\partial x^2} + \frac{\partial^2 \psi}{\partial x \partial z}; \quad \varepsilon_{zz} = \frac{dw}{dz} = \frac{\partial^2 \phi}{\partial z^2} - \frac{\partial^2 \psi}{\partial x \partial z} \quad \text{and} \tag{5.5.5}$$

$$\gamma_{zx} = \frac{du}{dz} + \frac{dw}{dx} = \frac{\partial^2 \phi}{\partial z \partial x} + \frac{\partial^2 \psi}{\partial z^2} + \frac{\partial^2 \phi}{\partial x \partial z} - \frac{\partial^2 \psi}{\partial x^2} \tag{5.5.6}$$

$$\text{Thus,} \quad \gamma_{zx} = \frac{\partial^2 \psi}{\partial z^2} + 2\frac{\partial^2 \phi}{\partial x \partial z} - \frac{\partial^2 \psi}{\partial x^2} = \nabla^2 \psi + 2\frac{\partial^2 \phi}{\partial x \partial z} - 2\frac{\partial^2 \psi}{\partial x^2} \tag{5.5.7}$$

$$e_v = \varepsilon_{xx} + \varepsilon_{zz} = \nabla^2 \phi \tag{5.5.8}$$

Substituting the above in stress equation, we have

$$\frac{\sigma_{xx}}{G} = \frac{\lambda}{G}\nabla^2\phi + 2\frac{\partial^2\phi}{\partial z^2} + 2\frac{\partial^2\psi}{\partial x \partial z} \tag{5.5.9}$$

$$\frac{\sigma_{zz}}{G} = \frac{\lambda}{G}\nabla^2\phi + 2\frac{\partial^2\phi}{\partial z^2} - 2\frac{\partial^2\psi}{\partial x \partial z} \tag{5.5.10}$$

$$\frac{\tau_{xz}}{G} = \nabla^2\psi + 2\frac{\partial^2\phi}{\partial x \partial z} - 2\frac{\partial^2\psi}{\partial x^2} \tag{5.5.11}$$

5.5.1.2 *Lamb's simplification by considering $\nu = 0.25$ for which $\lambda = G$*

Considering the above assumption, the stress equation simplifies (Kausel 2005) to

$$\frac{\sigma_{xx}}{G} = \nabla^2\phi + 2\frac{\partial^2\phi}{\partial z^2} + 2\frac{\partial^2\psi}{\partial x \partial z} \tag{5.5.12}$$

$$\frac{\sigma_{zz}}{G} = \nabla^2\phi + 2\frac{\partial^2\phi}{\partial z^2} - 2\frac{\partial^2\psi}{\partial x \partial z} \tag{5.5.13}$$

$$\frac{\tau_{xz}}{G} = \nabla^2\psi + 2\frac{\partial^2\phi}{\partial x \partial z} - 2\frac{\partial^2\psi}{\partial x^2} \tag{5.5.14}$$

Since, $\nabla^2\phi + h^2\phi = 0$ and $\nabla^2\psi + k^2\psi = 0$ we can further write the stress equations as

$$\frac{\sigma_{xx}}{G} = -h^2\phi + 2\frac{\partial^2\phi}{\partial z^2} + 2\frac{\partial^2\psi}{\partial x \partial z} \tag{5.5.15}$$

$$\frac{\sigma_{zz}}{G} = -h^2\phi + 2\frac{\partial^2\phi}{\partial z^2} - 2\frac{\partial^2\psi}{\partial x \partial z} \tag{5.5.16}$$

$$\frac{\tau_{xz}}{G} = -k^2\psi + 2\frac{\partial^2\phi}{\partial x \partial z} - 2\frac{\partial^2\psi}{\partial x^2} \tag{5.5.17}$$

Next we determine the displacement and stress at z = 0.

Considering the time function the displacements in x and z direction can be expressed as

$$u = \frac{\partial\Phi}{\partial x} + \frac{\partial\Psi}{\partial z} \quad \text{and} \quad w = \frac{\partial\Phi}{\partial z} - \frac{\partial\Psi}{\partial x}.$$

$$\text{Thus,} \quad u = \frac{\partial}{\partial x}Ae^{i\alpha x}e^{-\xi z}e^{i\omega t} + \frac{\partial}{\partial z}Be^{i\alpha x}e^{-\eta z}e^{i\omega t}$$

$$\rightarrow \quad u = Ai\alpha e^{i\alpha x}e^{-\xi z}e^{i\omega t} - \eta Be^{i\alpha x}e^{-\eta z}e^{i\omega t} \tag{5.5.18}$$

For $z = 0$ we thus have

$$(u)_{z=0} = (Ai\alpha - \eta B)e^{i\alpha x}e^{i\omega t}$$

Considering,

$$w = \frac{\partial \Phi}{\partial z} - \frac{\partial \Psi}{\partial x} \quad \rightarrow \quad w = \frac{\partial}{\partial z}Ae^{i\alpha x}e^{-\xi z}e^{i\omega t} - \frac{\partial}{\partial x}Be^{i\alpha x}e^{-\eta z}e^{i\omega t}$$

$$\rightarrow \quad w = -A\xi e^{i\alpha x}e^{-\xi z}e^{i\omega t} - iB\alpha e^{i\alpha x}e^{-\eta z}e^{i\omega t} \tag{5.5.19}$$

For $z = 0$ thus we have

$$(w)_{z=0} = -(A\xi - iB\alpha)e^{i\alpha x}e^{i\omega t}$$

Again, considering the stress in vertical direction, we have

$$\frac{\sigma_{zz}}{G} = -h^2\phi + 2\frac{\partial^2 \phi}{\partial z^2} - 2\frac{\partial^2 \psi}{\partial x \partial z}$$

On substitution of the values of function Φ and ψ we have

$$\sigma_{zz} = G\left[-h^2 Ae^{i\alpha x}e^{-\xi z}e^{i\omega t} + 2A\xi^2 e^{i\alpha x}e^{-\xi z}e^{i\omega t} + 2Bi\alpha\eta e^{i\alpha x}e^{-\eta z}e^{i\omega}t\right]$$

At $z = 0$ the above value simplifies to

$$(\sigma_{zz})_{z=0} = G\left[(2\xi^2 - h^2)A + 2Bi\alpha\eta\right]e^{i\alpha x}e^{i\omega t}$$

Proceeding in identical fashion it can be shown that

$$(\tau_{xz})_{z=0} = G\left[(2\alpha^2 - k^2)B - 2Ai\alpha\xi\right]e^{i\alpha x}e^{i\omega t}$$

For $Z < 0$ the function Φ and ψ an be expressed by replacing A and B by A' and B'. Now for a force $P_0 e^{i\alpha x}e^{i\omega t}$ acting per unit area in vertical Z direction on the plane $Z = 0$, the normal stress will thus have a jumped discontinuity and can be expressed as

$$(\sigma_{zz})_{z=0+} - (\sigma_{zz})_{z=0-} = -P_0 e^{i\alpha x}e^{i\omega t}$$

Thus substituting the value of σ_{zz}, we have

$$(2\xi^2 - h^2)(A - A') + 2i\alpha\eta(B - B') = -P_0/G, \quad \text{this plane is continuous.} \tag{5.5.20}$$

For $z = 0$ as $\tau_{xz} = 0$ we have for $Z < 0$ and $Z > 0$

$$-2i\alpha\xi(A + A') + (2\alpha^2 - k^2)(B + B') = 0 \tag{5.5.21}$$

For displacement compatibility we have

$$(u)_{z=0+} - (u)_{z=0-} = 0 \quad \text{and} \tag{5.5.22}$$

$$(w)_{z=0+} - (w)_{z=0-} = 0 \quad \text{this gives} \tag{5.5.23}$$

$$i\alpha(A - A') - \eta(B - B') = 0 \quad \text{and} \quad \xi(A - A') + i\alpha(B - B') = 0 \tag{5.5.24}$$

Now knowing $\xi^2 = (\alpha^2 - h^2)$ and for $\nu = 0.25$ $3h^2 = k^2$, we have on substitution in Equation (5.4.187), four equation with four unknowns (A, A', B, B') to solve.

$$(2\alpha^2 - k^2)(A - A') + 2i\alpha\eta(B - B') = -P_0/G \tag{5.5.25}$$

$$-2i\alpha\xi(A + A') + (2\alpha^2 - k^2)(B + B') = 0 \tag{5.5.26}$$

$$i\alpha(A - A') - \eta(B - B') = 0 \tag{5.5.27}$$

$$\xi(A - A') + i\alpha(B - B') = 0 \tag{5.5.28}$$

Solutions of these four equations give

$$A = -A' = \frac{P_0}{2k^2G} \quad \text{and} \quad B = B' = \frac{iP_0\alpha}{2k^2G\eta} \tag{5.5.29}$$

Hence for $Z > 0$ the potential functions are expressed as

$$\Phi = \frac{P_0}{2k^2G} e^{i\alpha x} e^{-\xi z} e^{i\omega t} \quad \text{and} \quad \Psi = \frac{iP_0\alpha}{2k^2G\eta} e^{i\alpha x} e^{-\xi z} e^{i\omega t} \tag{5.5.30}$$

The above values will now be used for subsequent derivation for various load cases.

5.5.1.3 Action of concentrated dynamic vertical load in an infinite 2D medium

Consider an infinite 2D medium under dynamic vertical load shown in Figure 5.5.2. While explaining the Fourier integral we have shown that any general function in complex form can be expressed as

$$f(x) = \frac{1}{2\pi} \int_{-\infty}^{\infty} e^{-i\omega x} d\omega \int_{-\infty}^{\infty} f(t) e^{i\omega t} dt$$

With respect to our derivation for general vertical load as shown above we modify $f(x)$ to write

$$f(x) = \frac{1}{2\pi} \int_{-\infty}^{\infty} e^{-i\alpha x} d\alpha \int_{-\infty}^{\infty} f(t) e^{i\omega t} dt$$

Assuming $\int_{-\infty}^{\infty} f(t)dt = Q_0$ we have, $f(x) = \frac{1}{2\pi} \int_{-\infty}^{\infty} Q_0 e^{i\omega t} e^{i\alpha x} d\alpha$

Now considering $P_0 = \frac{Q_0 d\alpha}{2\pi}$, we have

$$\Phi = \frac{Q_0 e^{i\omega t}}{4\pi k^2 G} \int_{-\infty}^{\infty} e^{i\alpha x} e^{-\xi z} d\alpha \quad \text{and} \quad \Psi = \frac{iQ_0 e^{i\omega t}}{4\pi \eta k^2 G} \int_{-\infty}^{\infty} \alpha e^{i\alpha x} e^{-\eta z} d\alpha \tag{5.5.31}$$

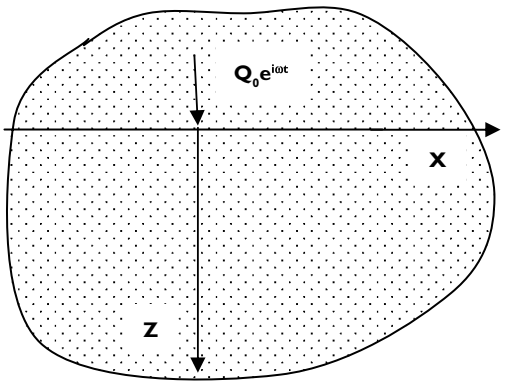


Figure 5.5.2 Vertical concentrated load acting in two-dimensional infinite elastic medium.

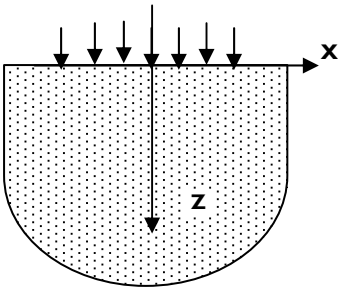


Figure 5.5.3 Vertical dynamic load acting on a two-dimensional semi-infinite elastic media.

5.5.1.4 Line load on a semi-infinite elastic media[68]

In this case as shown in Figure 5.5.3, we consider a force $P_0 e^{i\alpha x} e^{i\omega t}$ is a periodic force acting at $z = 0$ per unit area. The boundary conditions are at $z = 0$, $(\tau_{xz})_{z=0} = 0$ and $(\sigma_{zz})_{z=0} = 0$.

Based on our derivation earlier for infinite elastic media we had shown that

$$(\sigma_{zz})_{z=0} = G[(2\xi^2 - h^2)A + 2Bi\alpha\eta]e^{i\alpha x}e^{i\omega t} \quad \text{and}$$

$$(\tau_{xz})_{z=0} = G[(2\alpha^2 - k^2)B - 2Ai\alpha\xi]e^{i\alpha x}e^{i\omega t}$$

Imposing the boundary conditions as mentioned above, we have

$$[(2\xi^2 - h^2)A + 2Bi\alpha\eta] = 0 \quad \text{and} \quad [(2\alpha^2 - k^2)B - 2Ai\alpha\xi] = 0$$

Solution of these two equations gives

$$A = \frac{2\alpha^2 - k^2}{(2\alpha^2 - k^2)^2 - 4\alpha^2\xi\eta}\frac{P_0}{G} \quad \text{and} \quad B = \frac{2i\alpha\xi}{(2\alpha^2 - k^2)^2 - 4\alpha^2\xi\eta}\frac{P_0}{G}$$

Thus the surface displacements can now be expressed as

$$(u)_{z=0} = \frac{i\alpha(2\alpha^2 - k^2 - 2\xi\eta)}{(2\alpha^2 - k^2)^2 - 4\alpha^2\xi\eta}\frac{P_0}{G}e^{i\alpha x}e^{i\omega t} \quad \text{and} \tag{5.5.32}$$

$$(w)_{z=0} = \frac{ik^2\xi}{(2\alpha^2 - k^2)^2 - 4\alpha^2\xi\eta}\frac{P_0}{G}e^{i\alpha x}e^{i\omega t} \tag{5.5.33}$$

5.5.1.5 Concentrated load on a semi-infinite elastic media

In this case we assume a concentrated load acting at $x = z = 0$ as shown in Figure 5.5.4.

68 A semi-infinite medium is also known as elastic half space which could be 2D or 3D.

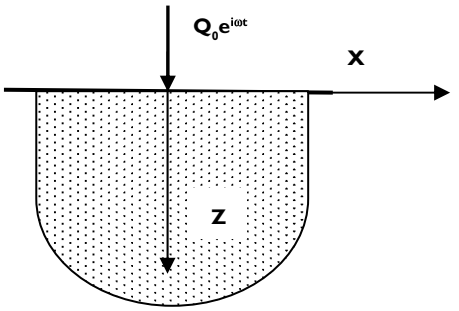


Figure 5.5.4 Concentrated load acting on a two-dimensional semi-infinite elastic media.

Similar to as shown in elastic full space, consider $P_0 = \frac{Q_0 d\alpha}{2\pi}$ and we have

$$(u)_{z=0} = \frac{Q_0 e^{i\omega t}}{2\pi G} \int_{-\infty}^{\infty} \frac{\alpha(2\alpha^2 - k^2 - 2\xi\eta)}{(2\alpha^2 - k^2)^2 - 4\alpha^2\xi\eta} e^{i\alpha x} d\alpha \quad \text{and} \tag{5.5.34}$$

$$(w)_{z=0} = \frac{Q_0 e^{i\omega t}}{2\pi G} \int_{-\infty}^{\infty} \frac{k^2\xi}{(2\alpha^2 - k^2)^2 - 4\alpha^2\xi\eta} e^{i\alpha x} d\alpha \tag{5.5.35}$$

5.5.1.6 Tangential Load on a semi-infinite elastic media

For this case, shown in Figure 5.5.5, we have the boundary condition as at $z = 0$, $(\tau_{xz})_{z=0} = P_x e^{i\alpha x} e^{i\omega t}$ and $(\sigma_{zz})_{z=0} = 0$.

Imposing the above boundary conditions to determine A and B the integration constants and proceeding in identical fashion as in previous case we have

$$(u)_{z=0} = \frac{P_x e^{i\omega t}}{2\pi G} \int_{-\infty}^{\infty} \frac{k^2\eta}{(2\alpha^2 - k^2)^2 - 4\alpha^2\xi\eta} e^{i\alpha x} d\alpha \tag{5.5.36}$$

$$(w)_{z=0} = \frac{iP_x e^{i\omega t}}{2\pi G} \int_{-\infty}^{\infty} \frac{\alpha(2\alpha^2 - k^2 - 2\xi\eta)}{(2\alpha^2 - k^2)^2 - 4\alpha^2\xi\eta} e^{i\alpha x} d\alpha \tag{5.5.37}$$

A very interesting phenomenon may be observed now if we put $P_x = Q_0$, it can be observed that the horizontal displacement due to the vertical force is equal to the vertical displacement due to the tangential load. *This is known as dynamic reciprocity property*.

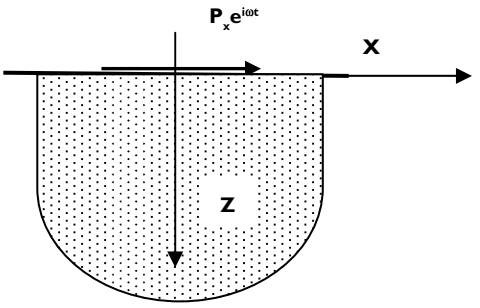


Figure 5.5.5 Tangential load acting on a two-dimensional semi-infinite elastic media.

The above were the solution proposed by Lamb for 2 dimensional problems. It will be observed that the solutions are theoretical for the integrals involved in the displacement functions are indeterminate.

5.5.1.7 Lamb's solution for 3-dimensional problems

We had shown earlier vide Equations (5.4.14) and (5.4.15) that equation of motion in 3D in an elastic body is given by the expression

$$\rho\frac{\partial^2 u}{\partial t^2} = \frac{\partial e_v}{\partial x}(\lambda + G) + G\nabla^2 u; \quad \rho\frac{\partial^2 v}{\partial t^2} = \frac{\partial e_v}{\partial y}(\lambda + G) + G\nabla^2 v \quad \text{and}$$

$$\rho\frac{\partial^2 w}{\partial t^2} = \frac{\partial e_v}{\partial z}(\lambda + G) + G\nabla^2 w$$

Here u, v, w are displacement vectors in x, y and z co-ordinate, λ and G = Lame's constant

$$e_v = \varepsilon_{xx} + \varepsilon_{yy} + \varepsilon_{zz} = \frac{\partial u}{\partial x} + \frac{\partial v}{\partial y} + \frac{\partial w}{\partial z} \quad \text{and}$$

$$\nabla^2 = \frac{\partial^2}{\partial x^2} + \frac{\partial^2}{\partial y^2} + \frac{\partial^2}{\partial z^2} \quad \text{the Laplacian operator.}$$

Now considering the displacement vector is of the nature $e^{i\omega t}$ we have

$$(\lambda + G)\frac{\partial e_v}{\partial x} + G\nabla^2 u = -\rho u\omega^2 \tag{5.5.38}$$

$$(\lambda + G)\frac{\partial e_v}{\partial y} + G\nabla^2 v = -\rho v\omega^2 \tag{5.5.39}$$

$$(\lambda + G)\frac{\partial e_v}{\partial z} + G\nabla^2 w = -\rho w\omega^2 \tag{5.5.40}$$

The above equations of motion are satisfied if we put

$$u = \frac{\partial \phi}{\partial x} + u'; \quad v = \frac{\partial \phi}{\partial y} + v'; \quad w = \frac{\partial \phi}{\partial z} + w';$$

This gives

$$\varepsilon_{xx} = \frac{\partial^2 \phi}{\partial x^2} + \frac{\partial u'}{\partial x}; \quad \varepsilon_{yy} = \frac{\partial^2 \phi}{\partial y^2} + \frac{\partial v'}{\partial y} \quad \text{and} \quad \varepsilon_{zz} = \frac{\partial^2 \phi}{\partial z^2} + \frac{\partial w'}{\partial z}$$

from which we have

$$e_v = \varepsilon_{xx} + \varepsilon_{yy} + \varepsilon_{zz} = \nabla^2 \phi + \frac{\partial u'}{\partial x} + \frac{\partial v'}{\partial y} + \frac{\partial w'}{\partial z} = \nabla^2 \phi + e_1$$

Substituting the above in the first equation of motion we have

$$(\lambda + G)\frac{\partial}{\partial x}\nabla^2 \phi + (\lambda + G)\frac{\partial e_1}{\partial x} + G\nabla^2 \frac{\partial \phi}{\partial x} + G\nabla^2 u' + \rho\omega^2 \frac{\partial \phi}{\partial x} + \rho\omega^2 u' = 0$$

The above can be re-structured and expressed as

$$(\lambda + 2G)\left[\frac{\partial}{\partial x}\nabla^2 \phi + \frac{\rho\omega^2}{\lambda + 2G}\frac{\partial \phi}{\partial x}\right] + G\left[\nabla^2 u' + \frac{\rho\omega^2}{G}u'\right] + (\lambda + G)\frac{\partial e_1}{\partial x} = 0$$

Now considering $h^2 = \frac{\rho\omega^2}{\lambda + 2G}, k^2 = \frac{\rho\omega^2}{G}$, we have

$$(\lambda + 2G)\frac{\partial}{\partial x}[\nabla^2 \phi + h^2 \phi] + G[\nabla^2 u' + k^2 u'] + (\lambda + G)\frac{\partial e_1}{\partial x} = 0 \tag{5.5.41}$$

Similarly for y and z direction we have

$$(\lambda + 2G)\frac{\partial}{\partial y}[\nabla^2 \phi + h^2 \phi] + G[\nabla^2 v' + k^2 v'] + (\lambda + G)\frac{\partial e_1}{\partial y} = 0 \quad \text{and} \tag{5.5.42}$$

$$(\lambda + 2G)\frac{\partial}{\partial z}[\nabla^2 \phi + h^2 \phi] + G[\nabla^2 w' + k^2 w'] + (\lambda + G)\frac{\partial e_1}{\partial z} = 0 \tag{5.5.43}$$

Since $(\lambda + 2G), G \neq 0$ the above equations can only be satisfied, if

$$[\nabla^2 + h^2]\phi = 0 \tag{5.5.44}$$

$$[\nabla^2 + k^2]u' = 0 \tag{5.5.45}$$

$$[\nabla^2 + k^2]v' = 0 \tag{5.5.46}$$

$$[\nabla^2 + k^2]w' = 0 \tag{5.5.47}$$

$$\text{and} \quad e_1 = \frac{\partial u'}{\partial x} + \frac{\partial v'}{\partial y} + \frac{\partial w'}{\partial z} = 0 \tag{5.5.48}$$

The last equation $e_1 = 0$ shows that u', v', w' are equi-voluminal rotational components of displacement thus a functional value has to be so chosen that it satisfies the other equations

$$[\nabla^2 + k^2](u', v', w') = 0.$$

Let us consider[69]

$$u' = \frac{\partial^2 \psi}{\partial x \partial z}, \quad v' = \frac{\partial^2 \psi}{\partial y \partial z} \quad \text{and} \quad w' = \frac{\partial^2 \psi}{\partial z^2} + k^2 \psi \quad \text{thus we have}$$

$$e_1 = \frac{\partial^3 \psi}{\partial x^2 \partial z} + \frac{\partial^3 \psi}{\partial y^2 \partial z} + \frac{\partial^3 \psi}{\partial z^3} + k^2 \frac{\partial \psi}{\partial z} = 0; \quad \text{or}$$

$$e_1 = \frac{\partial}{\partial z}\left(\frac{\partial^2 \psi}{\partial x^2} + \frac{\partial^2 \psi}{\partial y^2} + \frac{\partial^2 \psi}{\partial z^2} + k^2 \psi\right) = 0$$

$$\rightarrow \quad e_1 = \frac{\partial}{\partial z}(\nabla^2 + k^2)\psi = 0 \tag{5.5.49}$$

which shows the function satisfies the required boundary condition.

$$\text{Thus} \quad u = \frac{\partial \phi}{\partial x} + u'; \quad v = \frac{\partial \phi}{\partial y} + v'; \quad w = \frac{\partial \phi}{\partial z} + w'; \quad \text{gets modified to}$$

$$u = \frac{\partial \phi}{\partial x} + \frac{\partial^2 \psi}{\partial x \partial z}; \quad v = \frac{\partial \phi}{\partial x} + \frac{\partial^2 \psi}{\partial x \partial z} \quad \text{and} \quad w = \frac{\partial \phi}{\partial z} + \frac{\partial^2 \psi}{\partial z^2} + k^2 w$$

Having derived the above, we have now developed enough background to derive Lamb's solution in three-dimension, which was actually derived in polar co-ordinates.

69 This is where the mathematicians show that unusual Extra Sensory Perceptions (ESP) which makes complex problems solvable.....

The advantage with polar co-ordinate as would be seen, is that it reduces the problem from three variable to two and is easier to handle than in x, y and z co-ordinate.

In cylindrical or polar co-ordinate, $r = \sqrt{x^2 + y^2}$, such that $x, y, z = f(r, \theta, z)$, where f is a function of r, θ and z. Moreover for axis-symmetric case it becomes independent of θ.

The Laplacian operator ∇^2 in polar co-ordinate becomes

$$\nabla^2 = \frac{\partial^2}{\partial r^2} + \frac{1}{r}\frac{\partial}{\partial r} + \frac{\partial^2}{\partial z^2} \tag{5.5.50}$$

Let displacement function be $q(r, z)$ and $w(r, z)$, then with analogy to u, v, w as derived earlier we can say that

$$q(r, z) = \frac{\partial \phi}{\partial r} + \frac{\partial^2 \psi}{\partial r \partial z} \tag{5.5.51}$$

$$w(r, z) = \frac{\partial \phi}{\partial r} + \frac{\partial^2 \psi}{\partial z^2} + k^2 \psi = 0 \tag{5.5.52}$$

We had shown earlier that one of the conditions that satisfies the differential equation of motion is

$$[\nabla^2 + h^2]\phi = 0,$$

substituting the value of Laplacian operator in polar co-ordinate, we have

$$\left[\frac{\partial^2}{\partial r^2} + \frac{1}{r}\frac{\partial}{\partial r} + \frac{\partial^2}{\partial z^2} + h^2\right]\phi = 0 \tag{5.5.53}$$

Let $\phi = R(r)Z(z) \cong R \cdot Z$ which gives

$$\ddot{R}Z + \frac{1}{r}\dot{R}Z + R\ddot{Z} + h^2 RZ = 0$$

Since R and Z are not equal to zero dividing each of the above term by RZ we have

$$\frac{\ddot{R}}{R} + \frac{1}{r}\frac{\dot{R}}{R} + \frac{\ddot{Z}}{Z} + h^2 = 0 \quad \rightarrow \quad \frac{\ddot{R}}{R} + \frac{1}{r}\dot{R} = -h^2 - \frac{\ddot{Z}}{Z} = -\alpha^2 \text{ (say)}$$

The above gives two linear differential equations $\ddot{Z} - \xi^2 Z = 0$, where $\xi^2 = \alpha^2 - h^2$ and $\ddot{R} + \frac{1}{r}\dot{R} + \alpha^2 R = 0$

The solution to these equations are given by

$$Z = C_1 e^{\xi z} + C_2 e^{-\xi z} \tag{5.5.54}$$

The second equation is Bessel's equation whose solution is given by

$$R = C_3 J_0(\alpha r) + C_4 K_0(\alpha r) \tag{5.5.55}$$

Here $J_0(\alpha r)$ = Bessel's function of first kind of order zero and $K_0(\alpha r)$ = Bessel's function of second kind of order zero.

For $Z > 0$ as waves cannot increase in intensity and nor can it reflect back, thus to satisfy this condition we have $C_1 = 0$.

For $r \to \infty$, $K_0(\alpha r) = 0$ when we have

$$\phi = A e^{-\xi z} J_0(\alpha r) e^{i\omega t} \tag{5.5.56}$$

Proceeding in similar manner one can prove that

$$\psi = B e^{-\eta z} J_0(\alpha r) e^{i\omega t}, \quad \text{here } \eta^2 = \alpha^2 - k^2 \tag{5.5.57}$$

Considering $q(r,z) = \frac{\partial \phi}{\partial r} + \frac{\partial^2 \psi}{\partial r \partial z}$ we have

$$q(r,z) = \alpha \lfloor -A e^{-\xi z} + \eta B e^{-\eta z} \rfloor J_1(\alpha r) e^{i\omega t} \quad (\text{here } \frac{\partial}{\partial r} J_0(\alpha r) = J_1(\alpha r)) \tag{5.5.58}$$

$$w(r,z) = \lfloor -\xi A e^{-\xi z} + \alpha^2 B e^{-\eta z} \rfloor J_0(\alpha r) e^{i\omega t} \tag{5.5.59}$$

Also the stress at $Z = 0$ is given by $(\tau_{rz})_{z=0} = G\left[\frac{\partial q}{\partial z} + \frac{\partial w}{\partial r}\right]_{z=0}$ or $(\tau_{rz})_{z=0} = G \lfloor 2\alpha\xi A - (2\alpha^2 - k^2)\alpha B \rfloor J_1(\alpha r) e^{i\omega t}$ and $(\sigma_{zz})_{z=0} = \lambda e + 2G\frac{\partial w}{\partial z}$ or, $(\sigma_{zz})_{z=0} = G \lfloor (2\alpha^2 - k^2)A - 2\alpha^2 \eta B \rfloor J_0(\alpha r) e^{i\omega t}$, it should be noted here again $\nu = 0.25$ for which $\lambda = G$.

For region $Z < 0$ the functions can be expressed as

$$\phi = A' e^{-\xi z} J_0(\alpha r) e^{i\omega t} \quad \text{and} \quad \psi = B' e^{-\eta z} J_0(\alpha r) e^{i\omega t}.$$

Now applying a force of $P_0 J_0(\alpha r) e^{i\omega t}$ per unit area along z direction a $tz = 0$ and considering the stress jump

$$(\sigma_{zz})_{z=0+} - (\sigma_{zz})_{z=0-} = -P_0 J_0(\alpha r) e^{i\omega t}$$

We have, $(2\alpha^2 - k^2)(A - A') - 2\alpha^2 \eta (B + B') = \frac{P_0}{G}$.

For the tangential stress to be continuous in this plane we have

$$2\xi(A + A') - (2\alpha^2 - k^2)(B - B') = 0$$

The displacement continuity along r and z direction gives

$$(A - A') - \eta(B + B') = 0 \quad \text{and} \quad \xi(A + A') - \alpha^2(B - B') = 0$$

Solution of these four equations give $A = -A' = \frac{P_0}{2k^2G}$ and $B = B' = \frac{P_0}{2k^2G\eta}$.
Hence for region $Z > 0$ we have

$$\phi = \frac{P_0}{2k^2G} e^{-\xi z} J_0(\alpha r) \quad \text{and} \quad \psi = \frac{P_0}{2k^2G\eta} e^{-\eta z} J_0(\alpha r) \tag{5.5.60}$$

5.5.1.8 Application of point load in infinite elastic space

Shown in Figure 5.5.6 is an elastic full space with point load $Q_0\, e^{i\omega t}$. We make use here a special function called Fourier-Bessel Integral based on which

$$f(r) = \int_0^\infty J_0(\alpha r)\alpha d\alpha \int_0^\infty f(\lambda) J_0(\alpha\lambda)\lambda d\lambda \tag{5.5.61}$$

For $\lim \lambda \to 0$, considering $\int_0^\infty f(\lambda) 2\pi\lambda d\lambda = Qe^{i\omega t}$

Considering $P_0 = \frac{Q\alpha d\alpha}{2\pi}$, we have

$$\phi = \frac{Q_0\, e^{i\omega t}}{4\pi\omega^2\rho} \int_0^\infty e^{-\xi z} J_0(\alpha r)\alpha d\alpha \quad \text{and} \quad \psi = \frac{Q_0\, e^{i\omega t}}{4\pi\omega^2\rho} \int_0^\infty \frac{e^{-\eta z}}{\eta} J_0(\alpha r)\alpha d\alpha \tag{5.5.62}$$

where ρ = mass density of the elastic medium.

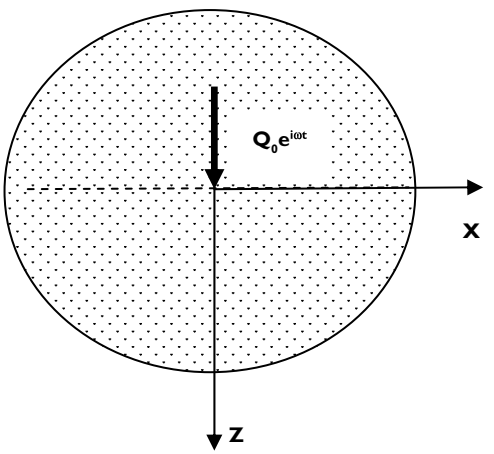


Figure 5.5.6 Elastic full space with concentrated load at $Z = 0$.

5.5.1.9 Application of point load in elastic half space

Shown in Figure 5.5.7, is an elastic half space subjected to a point load. Let us consider the point load applied at $Z = 0$ as $P_0 J_0(\alpha r) e^{i\omega t}$.

Then at the surface

$$(\sigma_{zz})_{z=0} = P_0 J_0(\alpha r) e^{i\omega t} \quad \text{and} \quad (\tau_{rz})_{z=0} = 0$$

Based on the above boundary condition and referring to previous case of elastic full space we get

$$(2\alpha^2 - k^2)A - 2\alpha^2 \eta B = \frac{P_0}{G} \quad \text{and} \quad 2\xi A - (2\alpha^2 - k^2)B = \frac{P_0}{G}$$

Solutions of these two equations give

$$A = \frac{2\alpha^2 - k^2}{(2\alpha^2 - k^2)^2 - 4\alpha^2 \xi \eta} \frac{P_0}{G} \quad \text{and} \quad B = \frac{2\xi}{(2\alpha^2 - k^2)^2 - 4\alpha^2 \xi \eta} \frac{P_0}{G}$$

The surface displacement can thus be computed for $Z > 0$ as

$$q(r, z) = \frac{-\alpha(2\alpha^2 - k^2 - 2\xi\eta)}{(2\alpha^2 - k^2)^2 - 4\alpha^2 \xi \eta} J_1(\alpha r) \frac{P_0}{G} e^{i\omega t}$$

$$w(r, z) = \frac{k^2 \xi}{(2\alpha^2 - k^2)^2 - 4\alpha^2 \xi \eta} J_0(\alpha r) \frac{P_0}{G} e^{i\omega t}$$

For a concentrated load $Qe^{i\omega t}$ considering $P_0 = -Q\alpha d\alpha / 2\pi$ and integrating it between ∞ to 0 we have

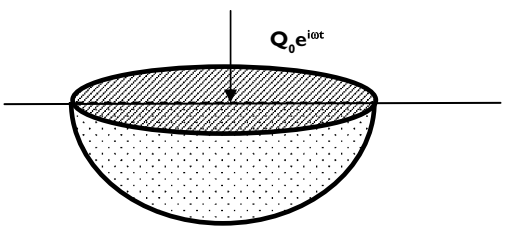


Figure 5.5.7 Point load on elastic half space.

$$(q)_{z=0} = \frac{Q_0 e^{i\omega t}}{2\pi G} \int_0^\infty \frac{\alpha^2(2\alpha^2 - k^2 - 2\xi\eta)}{(2\alpha^2 - k^2)^2 - 4\alpha^2\xi\eta} J_1(\alpha r) d\alpha \quad \text{and}$$

$$(w)_{z=0} = \frac{Q_0 e^{i\omega t}}{2\pi G} \int_0^\infty \frac{k^2\alpha\xi}{(2\alpha^2 - k^2)^2 - 4\alpha^2\xi\eta} J_0(\alpha r) d\alpha \tag{5.5.63}$$

These are the Lamb's solution in three-dimension.

So what we have achieved?

All right, so we have managed to propose the solution as furnished by Lamb for the propagation of waves in an elastic medium in two and three dimension.

And in the process we believe we have managed to sufficiently infuriate the professional engineers, for after all those ghastly and boring Del, Zi, Phi, Fourier transform etc. we arrive at a solution

- Which is an indefinite integral
- Whose solution is not known and difficult to solve analytically
- Whose boundary limits are either $(\pm)\,\infty$ or $0 \rightarrow \infty$!

The first reaction would be OK after all this complex mathematical manipulation can we compute or find out the surface displacement for the applied load directly from those results? The answer would surely be an embarrassing −NO.

So where do we go from here?

Being a mathematician Lamb's job was to find a solution that could be finite in terms of our technical perception. He solved the problem in generic term and it was left to others like Reissner and Pekeris to solve those maddening indefinite integrals and interpret the problem in a form understandable to others.

5.5.2 Pekeris' solution for surface pulse

As discussed in the previous section Lamb gave the basic solution for impulsive force acting on or within an elastic full space. It was left to Pekeris (1955) and others to further enhance it and give solutions, which are readily usable.

As shown in Figure 5.5.8, at source (a buried point shown by a shaded box) a pulse load which is varying with time as a Heaveside function $H(t)$ is applied. The solution for surface pulse is obtained by letting the depth of the surface approach zero.

Choosing a cylindrical co-ordinate system with origin at depth H below surface, zone below the source is depicted as zone-1 and that above the source as zone-2.

The surface integral of the applied vertical stress is expressed as

$$2\pi \int_0^\infty [(\sigma_{zz})_1 - (\sigma_{zz})_2] r \cdot dr = Z \tag{5.5.64}$$

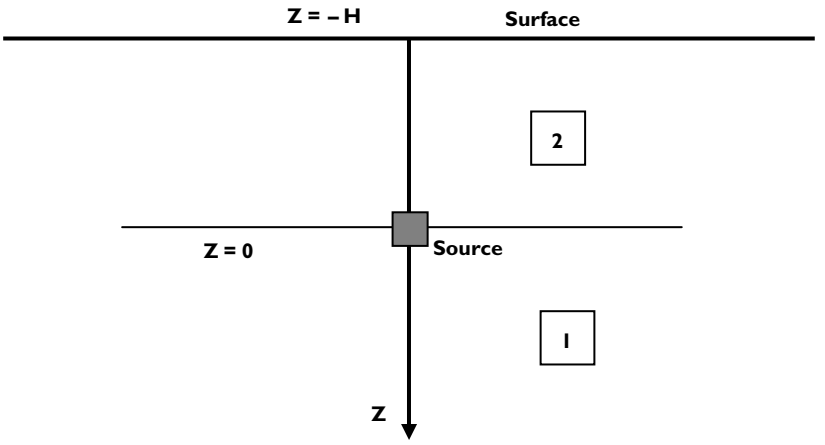


Figure 5.5.8 Conceptual model for Pekeris' solution for surface pulse.

While solving Lamb's problem in 3D we have shown that if $q(r,z)$ and $w(r,z)$ are the displacements in horizontal and vertical direction then

$$q(r,z) = \frac{\partial \phi}{\partial r} + \frac{\partial^2 \psi}{\partial r \partial z} \quad \text{and} \quad w(r,z) = \frac{\partial \phi}{\partial r} + \frac{\partial^2 \psi}{\partial z^2} + k^2 \psi \tag{5.5.65}$$

where ϕ and ψ are dilatational and equi-voluminal motion respectively.

Here Pekeris used slightly different notation[70] than what we used earlier. As per his derivation

$$q(r,z) = \frac{\partial \phi}{\partial r} + \frac{\partial^2 \psi}{\partial r \partial z} \quad \text{and} \quad w(r,z) = \frac{\partial \phi}{\partial r} + \frac{\partial^2 \psi}{\partial z^2} - k^2 \psi \tag{5.5.66}$$

$$\rightarrow \quad \nabla^2 \phi - h^2 \phi = 0; \quad \nabla^2 \psi - h^2 \psi = 0 \tag{5.5.67}$$

$$\text{where,} \quad h^2 = \frac{\omega^2}{V_p^2}; \quad k^2 = \frac{\omega^2}{V_s^2}; \quad V_s^2 = \frac{G}{\rho}; \quad V_p^2 = \frac{\lambda + 2G}{\rho} = 3V_s^2, \quad \text{for } \nu = 0.25. \tag{5.5.68}$$

The normal and shear stress in polar co-ordinate based on elasticity equation is given by

$$\sigma_{zz} = \lambda h^2 \phi + 2G\left[\frac{\partial^2 \phi}{\partial z^2} + \frac{\partial^3 \psi}{\partial z^3} - k^2 \frac{\partial \psi}{\partial z}\right] \quad \text{and} \quad \tau_{rz} = G\frac{\partial}{\partial r}\left[2\frac{\partial \phi}{\partial z} + 2\frac{\partial^2 \psi}{\partial z^2} - k^2 \psi\right] \tag{5.5.69}$$

70 This depends on how one considers the vector function. Here considered as e^{-iwt} by Pekeris.

Thus in time domain applying the general Fourier transform we have

$$w(r,z,t) = \frac{1}{2\pi i}\int_{\alpha-i\infty}^{\alpha+i\infty}\left[\frac{e^{\omega t}}{\omega}\right]w(r,z,\omega)d\omega \tag{5.5.70}$$

Solution to ϕ and ψ in zone 1 and 2 are given by

$$\phi_1 = Ae^{-k\alpha z}J_0(\xi r), \quad \psi_1 = Be^{-k\beta z}J_0(\xi r) \tag{5.5.71}$$

$$\phi_2 = [Ce^{-k\alpha z}J_0(\xi r) + De^{k\alpha z}]J_0(\xi r); \quad \psi_2 = [Ee^{-k\beta z}J_0(\xi r) + Fe^{k\beta z}J_0(\xi r)] \tag{5.5.72}$$

$$\text{where} \quad k\alpha = \sqrt{\xi^2 + h^2} \quad \text{and} \quad k\beta = \sqrt{\xi^2 + k^2} \tag{5.5.73}$$

It is to be noted here that Pekeris' notation are slightly different than what we solved for Lamb's problem earlier. We are trying to derive this with same notation of Pekeris while trying to keep the form similar to what we derived earlier as far as possible.

At $z = 0$ considering the displacement and stress compatibility, we have

$$|q_1|_{z=0} = |q_2|_{z=0} \quad \text{and} \quad |w_1|_{z=0} = |w_2|_{z=0} \tag{5.5.74}$$

$$|\tau_{rz1}|_{z=0} = |\tau_{rz2}|_{z=0} \tag{5.5.75}$$

This gives

$$\left[\frac{\partial\phi}{\partial r} + \frac{\partial^2\psi}{\partial r\partial z}\right]_1 = \left[\frac{\partial\phi}{\partial r} + \frac{\partial^2\psi}{\partial r\partial z}\right]_2 \tag{5.5.76}$$

$$\left[\frac{\partial\phi}{\partial r} + \frac{\partial^2\psi}{\partial z^2} - k^2\psi\right]_1 = \left[\frac{\partial\phi}{\partial r} + \frac{\partial^2\psi}{\partial z^2} - k^2\psi\right]_2 \tag{5.5.77}$$

$$\frac{\partial}{\partial r}\left[2\frac{\partial\phi}{\partial z} + 2\frac{\partial^2\psi}{\partial z^2} - k^2\psi\right]_1 = \frac{\partial}{\partial r}\left[2\frac{\partial\phi}{\partial z} + 2\frac{\partial^2\psi}{\partial z^2} - k^2\psi\right]_2 \tag{5.5.78}$$

Considering $|\sigma_{zz}|_{z=0+} - |\sigma_{zz}|_{z=0-} = \left(\frac{Z}{2\pi}\right)J_0(\xi r)d\xi$ and integrating with respect to from $0 \to \infty$. Again considering at $Z = -H$ $\sigma_{zz} = 0$ and $\tau_{rz} = 0$ we can solve for six(6) boundary conditions to get A, B, C, D, E and F when

$$F = \frac{Z\xi}{12\pi G k\beta h^2}, \quad D = -k\beta F, \quad B = E + F, \quad A = C - D \tag{5.5.79}$$

$$e^{k\alpha H}C = \frac{k\beta F}{M}[\{(2\xi^2 + k^2)^2 + 4k^2\xi^2\alpha\beta\}e^{-k\alpha H} - 4\xi^2(2\xi^2 + k^2)e^{-k\beta H}] \tag{5.5.80}$$

$$e^{k\beta H}E = \frac{F}{M}[4k^2(2\xi^2 + k^2)\alpha\beta e^{-k\alpha H} - \{(2\xi^2 + k^2)^2 + 4k^2\xi^2\alpha\beta\}e^{-k\beta H}] \tag{5.5.81}$$

where $M = [(2\xi^2 + k^2)^2 - 4k^2\xi^2\alpha\beta]$ (5.5.82)

Substituting these values for ϕ and ψ in Equation (5.5.61) and for $q(r, z)$ and $w(r, z)$ we have

$$w(r,z) = \frac{Zk}{2\pi G}\int_0^\infty J_0(\xi r)\xi[-(2\xi^2 + k^2)e^{-k\alpha H} + 2\xi^2 e^{-k\beta H}]\left(\frac{\alpha}{M}\right)d\xi \tag{5.5.83}$$

$$q(r,z) = -\frac{Z}{2\pi G}\int_0^\infty J_1(\xi r)\xi^2[(2\xi^2 + k^2)e^{-k\alpha H} - 2k^2\alpha\beta e^{-k\beta H}]\left(\frac{d\xi}{M}\right) \tag{5.5.84}$$

5.5.2.1 Vertical displacement at surface

Thus vertical displacement at surface is given by considering the depth $H = 0$, when we have

$$w(r) = \frac{Zk}{2\pi G}\int_0^\infty J_0(\xi r)\xi[-(2\xi^2 + k^2) + 2\xi^2]\left(\frac{\alpha}{M}\right)d\xi$$

$$w(r) = -\frac{Zk^3}{2\pi G}\int_0^\infty J_0(\xi r)\frac{\xi\alpha}{[(2\xi^2 + k^2)^2 - 4k^2\xi^2\alpha\beta]}d\xi \tag{5.5.85}$$

Considering $\xi = kx$ the above expression can be simplified to

$$w(r) = -\frac{Zk}{2\pi G}N(kr) \tag{5.5.86}$$

where $N(kr) = \int_0^\infty J_0(krx)xm(x)dx$, $m(x) = \frac{\alpha}{[(2x^2+1)^2-4x^2\alpha\beta]}$,

$$\alpha = \sqrt{\frac{1}{3} + x^2}, \quad \beta = \sqrt{1 + x^2} \quad \text{and} \quad k = \frac{\omega}{V_s} \tag{5.5.87}$$

Having derived the above it is now left to determine the indefinite integral $N(kr)$.

Solution of $N(kr)$ requires a special theorem called Bateman-Pekeris (1945) theorem involving analytical functions in complex domain when $N(kr)$ gets converted into

$$N(kr) = \int_0^{\infty} J_0(krx)xm(x)dx = -\left(\frac{2}{\pi}\right) IP \int_{\frac{1}{\sqrt{3}}}^{\infty} K_0(krv)vm(iv)dv \tag{5.5.88}$$

Here, I denotes the imaginary part of the function and P is the principal value.

We will not go into the detail of mathematical derivation of this integral but will present the subsequent results as mentioned hereafter.

Considering $\tau = \frac{v_s t}{r}$ where V_s = shear wave velocity of the soil, t = time, and r = radial distance from the surface pulse source, we have

$$w(\tau) = 0 \quad \text{for } \tau < \frac{1}{\sqrt{3}} \tag{5.5.89}$$

$$w(\tau) = \left(\frac{3Z}{\pi^2 Gr}\right) G_1(\tau) \quad \text{for } \frac{1}{\sqrt{3}} < \tau < 1 \quad \text{and} \tag{5.5.90}$$

$$w(\tau) = \left(\frac{3Z}{\pi^2 Gr}\right) [G_1(\tau) + G_2(\tau)] \quad \text{for } \tau > 1 \quad \text{where} \tag{5.5.91}$$

$$G_1(\tau) = P \int_{\frac{1}{\sqrt{3}}}^{\tau} \frac{v(1-2v^2)\sqrt{v^2 - \frac{1}{3}}}{\left(3 - 24v^2 + 56v^4 - 32v^6\right)\sqrt{\tau^2 - v^2}} dv \tag{5.5.92}$$

$$G_2(\tau) = P \int_{1}^{\tau} \frac{v^3\left(4v^2 - \frac{4}{3}\right)\sqrt{v^2 - 1}}{(3 - 24v^2 + 56v^4 - 32v^6)\sqrt{\tau^2 - v^2}} dv \tag{5.5.93}$$

Taking $v^2 = \frac{1}{3} + \chi^2 \sin^2\theta$ and $\chi^2 = \tau^2 - \frac{1}{3}$ we have

$$G_1(\tau) = \frac{P}{96} \int_0^{\frac{\pi}{2}} \left[-12 + \frac{1}{\frac{1}{12} + \chi^2 \sin^2\theta} - \frac{B}{-b + \chi^2 \sin^2\theta} - \frac{C}{c + \chi^2 \sin^2\theta}\right] d\theta \tag{5.5.94}$$

Here $B = 3 + \frac{5}{\sqrt{3}}$, $C = 3 - \frac{5}{\sqrt{3}}$, $b = \frac{5}{12} + \frac{\sqrt{3}}{4}$ and $c = \frac{\sqrt{3}}{4} - \frac{5}{12}$.

Now considering,

$$\int_0^{\frac{\pi}{2}} \frac{d\theta}{\alpha^2 + \chi^2 \sin^2\theta} = \frac{\pi}{2\alpha} \frac{1}{\sqrt{\alpha^2 + \chi^2}} \quad \text{and,}$$

$$P\int_0^{\frac{\pi}{2}} \frac{d\theta}{-\beta^2+\chi^2\sin^2\theta} = 0 \quad \text{for } \beta < \chi$$

$$= -\frac{\pi}{2\beta}\frac{1}{\sqrt{\beta^2-\chi^2}} \quad \text{for } \beta > \chi \text{ we obtain}$$

$$G_1(\tau) = \frac{\pi}{96}\left[-6+\frac{\sqrt{3}}{\sqrt{\tau^2-\frac{1}{4}}}+\frac{\sqrt{3\sqrt{3}+5}}{\sqrt{\frac{1}{4}(3+\sqrt{3})-\tau^2}}-\frac{\sqrt{3\sqrt{3}-5}}{\tau^2-\frac{1}{4}(3-\sqrt{3})}\right] \quad \text{for } \tau < \gamma \tag{5.5.95}$$

$$\text{and} \quad G_1(\tau) = \frac{\pi}{96}\left[-6+\frac{\sqrt{3}}{\sqrt{\tau^2-\frac{1}{4}}}-\frac{\sqrt{3\sqrt{3}-5}}{\tau^2-\frac{1}{4}(3-\sqrt{3})}\right] \quad \text{for } \tau > \gamma \tag{5.5.96}$$

Here $\gamma = \frac{1}{2}\sqrt{3+\sqrt{3}}$.

Similarly considering, $\nu^2 = \frac{1}{3} + \bar{\chi}^2\sin^2\theta$ where $\bar{\chi}^2 = \tau^2 - 1$, we have

$$G_2(\tau) = \frac{1}{24}\int_0^{\frac{\pi}{2}}\left[-3-\frac{3}{(3+4\bar{\chi}^2\sin^2\theta)}-\frac{(1+\sqrt{3})}{1-\sqrt{3}+4\bar{\chi}^2\sin^2\theta}\right]d\theta \tag{5.5.97}$$

Integrating above we have

$$G_2(\tau) = \frac{\pi}{96}\left[-6-\frac{\sqrt{3}}{\sqrt{\tau^2-\frac{1}{4}}}+\frac{\sqrt{3\sqrt{3}+5}}{\sqrt{\frac{1}{4}(3+\sqrt{3})-\tau^2}}+\frac{\sqrt{3\sqrt{3}-5}}{\tau^2-\frac{1}{4}(3-\sqrt{3})}\right] \quad \text{for } \tau < \gamma \tag{5.5.98}$$

$$\text{and} \quad G_2(\tau) = \frac{\pi}{96}\left[-6-\frac{\sqrt{3}}{\sqrt{\tau^2-\frac{1}{4}}}+\frac{\sqrt{3\sqrt{3}-5}}{\tau^2-\frac{1}{4}\left(3-\sqrt{3}\right)}\right] \quad \text{for } \tau > \gamma \tag{5.5.99}$$

Substituting these values for $w(r)$ finally gives

$$w(r) = 0 \quad \text{for } \tau < \frac{1}{\sqrt{3}} \tag{5.5.100}$$

$$w(r) = \left(\frac{3Z}{\pi^2 Gr}\right)\left[-6-\frac{\sqrt{3}}{\sqrt{\tau^2-\frac{1}{4}}}-\frac{\sqrt{3\sqrt{3}+5}}{\sqrt{\frac{3}{4}+\frac{\sqrt{3}}{4}-\tau^2}}+\frac{\sqrt{3\sqrt{3}-5}}{\sqrt{\tau^2+\frac{\sqrt{3}}{4}-\frac{3}{4}}}\right]$$

for $\dfrac{1}{\sqrt{3}} < \tau < 1$

$$w(r) = -\left(\frac{Z}{16\pi Gr}\right)\left[6 - \frac{3\sqrt{3+5}}{\sqrt{\frac{3}{4}+\frac{\sqrt{3}}{4}-\tau^2}}\right] \quad \text{for } 1 < \tau < \gamma = \frac{1}{2}\sqrt{3+\sqrt{3}} \tag{5.5.101}$$

$$w(r) = -\left(\frac{3Z}{8\pi Gr}\right) \quad \text{for } \tau > \gamma \tag{5.5.102}$$

If we observe the values of $w(r)$ now we see that all the values are definite and finite. It is possible to find out the value of $w(r)$ for a surface pulse at $H = 0$ for any instant of time t or τ at any radial distance r from the source.

5.5.2.2 Horizontal displacement at surface

We had shown earlier that

$$q(r,z) = -\frac{Z}{2\pi G}\int_0^\infty J_1(\xi r)\xi^2[(2\xi^2+k^2)e^{-k\beta H} - 2k^2\alpha\beta e^{-k\beta H}]\left(\frac{d\xi}{M}\right) \tag{5.5.103}$$

At the surface for $H = 0$ we have

$$q(r) = -\frac{Z}{2\pi G}\int_0^\infty J_1(\xi r)\xi^2[(2\xi^2+k^2) - 2k^2\alpha\beta]\left(\frac{d\xi}{M}\right) \tag{5.5.104}$$

where M is as defined earlier.

Considering $\xi = kx$ we can simplify $q(r)$ as

$$q(r) = \frac{Z}{2\pi G}\frac{\partial}{\partial r}\int_0^\infty J_0(krx)n(x)xdx \tag{5.5.105}$$

$$\text{Here} \quad n(x) = \frac{(2x^2+1) - 2\sqrt{1+x^2}\sqrt{\frac{1}{3}+x^2}}{(2x^2+1)^2 - 4x^2\sqrt{1+x^2}\sqrt{\frac{1}{3}+x^2}} \tag{5.5.106}$$

Again based on Bateman-Pekeris theorem it can be shown that

$$\int_0^\infty J_0(krx)n(x)xdx = -\frac{2}{\pi}I\int_0^\infty K_0(krv)n(iv)vdv - \frac{1}{4}K_0(kr) \tag{5.5.107}$$

Skipping the details of derivation of the above integral in complex domain based on analytical function it can be finally shown that

$$q(\tau) = 0 \quad \text{for } \tau < \frac{1}{\sqrt{3}} \tag{5.5.108}$$

$$q(\tau) = -\left(\frac{Z}{2\pi^2 Gr}\right)\tau R_1(\tau) \quad \text{for } \frac{1}{\sqrt{3}} < \tau < 1 \tag{5.5.109}$$

$$q(\tau) = -\left(\frac{Z}{2\pi^2 Gr}\right)\tau R_2(\tau) \quad \text{for } 1 < \tau < \gamma \tag{5.5.110}$$

$$q(\tau) = -\left(\frac{Z}{2\pi^2 Gr}\right)\tau R_2(\tau) + \frac{Z}{8\pi Gr}\frac{1}{\sqrt{\tau^2 - \gamma^2}} \quad \text{for } \tau > \gamma \tag{5.5.111}$$

where

$$R_1(\tau) = \int_{\frac{1}{\sqrt{3}}}^{\tau} \frac{v\sqrt{v^2 - \frac{1}{3}}\sqrt{1 - v^2}\left(12 - 24v^2\right)}{\sqrt{\tau^2 - v^2}\left(3 - 24v^2 + 56v^4 - 32v^6\right)} dv \quad \text{and} \tag{5.5.112}$$

$$R_2(\tau) = \int_{\frac{1}{\sqrt{3}}}^{1} \frac{v\sqrt{v^2 - \frac{1}{3}}\sqrt{1 - v^2}\left(12 - 24v^2\right)}{\sqrt{\tau^2 - v^2}\left(3 - 24v^2 + 56v^4 - 32v^6\right)} dv \tag{5.5.113}$$

By decomposing the above integrals in partial fraction and again assuming $v^2 = \frac{1}{3} + \bar{\chi}^2 \sin^2\theta$ where $\bar{\chi}^2 = \tau^2 - 1$ we have

$$R_1(\tau) = -\frac{1}{8}\sqrt{\frac{3}{2}} \int_0^{\frac{\pi}{2}} \frac{d\theta}{\sqrt{1 - k^2 \sin^2\theta}}$$

$$\times \left\{6 - \frac{18}{1 + 8k^2 \sin^2\theta} + \frac{(6 - 4\sqrt{3})}{[1 - (12\sqrt{3} - 20)k^2 \sin^2\theta]}\right.$$

$$\left. + \frac{(6 + 4\sqrt{3})}{[1 + (12\sqrt{3} + 20)k^2 \sin^2\theta]}\right\}$$

$$R_1(\tau) = -\frac{1}{8}\sqrt{\frac{3}{2}} \int_0^{\frac{\pi}{2}} \{6K(k) - 18\Pi(8k^2, k) + (6 - 4\sqrt{3})\Pi[-(12\sqrt{3} - 20)k^2, k]$$

$$+ (6 + 4\sqrt{3})\Pi[(12\sqrt{3} + 20)k^2, k]\}$$

$$\text{where} \quad k^2 = \frac{1}{2}(3\tau^2 - 1), \tag{5.5.114}$$

$$K(k) = \int_0^{\frac{\pi}{2}} \frac{d\theta}{\sqrt{1 - k^2 \sin^2\theta}}; \quad \Pi(n,k) = \int_0^{\frac{\pi}{2}} \frac{d\theta}{(1 + n\sin^2\theta)\sqrt{1 - k^2\sin^2\theta}} \tag{5.5.115}$$

Here $K(k)$ and $\Pi(n,k)$ are complete elliptical integral of first and third kind respectively.

Similarly substituting $v^2 = \frac{1+2\sin^2\theta}{3}$, we have

$$R_2(\tau) = -\frac{1}{4\chi}\int_0^{\frac{\pi}{2}} \frac{d\theta}{\sqrt{1-\kappa^2\sin^2\theta}}\left\{3 - \frac{9}{1+8\sin^2\theta} + \frac{(3+\sqrt{3})}{[8\sin^2\theta - 5 - 3\sqrt{3}]} + \frac{(3-\sqrt{3})}{[8\sin^2\theta - 5 + 3\sqrt{3}]}\right\}$$

$$R_2(\tau) = -\frac{1}{4\chi}\left\{3K(\kappa) - 9\Pi(8,\kappa) - (2\sqrt{3}-3)\Pi[-(12\sqrt{3}-20),\kappa] + (2\sqrt{3}+3)\Pi(12\sqrt{3}+20,\kappa)\right\}$$

$$\text{where} \quad \kappa^2 = \frac{2}{3\tau^2 - 1}. \tag{5.5.116}$$

Now substituting the values of $R_1(\tau)$ and $R_2(\tau)$ in displacement equation we have

$$q(r) = 0 \quad \text{for } \tau < \frac{1}{\sqrt{3}} \tag{5.5.117}$$

$$q(r) = -\left(\frac{Z\tau\sqrt{\frac{3}{2}}}{16\pi^2 Gr}\right)\{6K(k) - 18\Pi(8k^2,k) + (6-4\sqrt{3})\Pi[-(12\sqrt{3}-20)k^2,k] + (6+4\sqrt{3})\Pi(12\sqrt{3}+20)k^2,k)\} \quad \text{for } \frac{1}{\sqrt{3}} < \tau < 1 \tag{5.5.118}$$

$$q(r) = -\left(\frac{Z\tau\sqrt{\frac{3}{2}}}{16\pi^2 Gr}\right)\{6K(\kappa) - 18\Pi(8,\kappa) + (6-4\sqrt{3})\Pi[-(12\sqrt{3}-20),\kappa] + (6+4\sqrt{3})\Pi(12\sqrt{3}+20),\kappa)\} \quad \text{for } 1 < \tau < \gamma \tag{5.5.119}$$

$$q(r) = -\left(\frac{Z\tau\sqrt{\frac{3}{2}}}{16\pi^2 Gr}\right)\{6K(\kappa) - 18\Pi(8,\kappa) + (6-4\sqrt{3})\Pi[-(12\sqrt{3}-20),\kappa] + (6+4\sqrt{3})\Pi(12\sqrt{3}+20),\kappa)\} + \frac{Z\tau}{8\pi Gr\sqrt{\tau^2-\gamma^2}}$$

$$\text{for } \tau > \gamma \tag{5.5.120}$$

Looking at the value of $q(r)$ above it will be observed that all values in right hand side of the equation are finite and definite as such it is possible to find out values of $q(r)$ for any finite value of τ or t at any distance r provided we are in a position to find out the values of those complete elliptical integrals of first and third kind.

Well, mathematicians have not been so heartless. To ease our work, tables giving values of these elliptic integrals are available which may be effectively used (Abramowitz & Stegan 1964) or else, they can be solved numerically based on Simpson's 1/3rd rule or other standard algorithm.

5.5.3 Pekeris' solution for buried pulse

Pekeris (1955) also gave solution for buried pulse. We present here however a modified version of the same which is more amenable to numerical analysis (Pekeris & Lifson 1957).

While solving for the surface pulse we had shown that

$$2\pi\int_0^\infty [(\sigma_{zz})_1 - (\sigma_{zz})_2]r\cdot dr = Z \tag{5.5.121}$$

We had also shown that vertical and horizontal displacement in polar co-ordinate is given by

$$w(r,z) = \frac{Zk}{2\pi G}\int_0^\infty J_0(\xi r)\xi[-(2\xi^2+k^2)e^{-k\alpha H} + 2\xi^2 e^{-k\beta H}]\left(\frac{\alpha}{M}\right)d\xi \quad \text{and} \tag{5.5.122}$$

$$q(r,z) = -\frac{Z}{2\pi G}\int_0^\infty J_1(\xi r)\xi^2[(2\xi^2+k^2)e^{-k\alpha H} - 2k^2\alpha\beta e^{-k\beta H}]\left(\frac{d\xi}{M}\right) \tag{5.5.123}$$

where $M = [(2\xi^2+k^2)^2 - 4k^2\xi^2\alpha\beta]$.

Considering $\xi = kx$ and substituting the same for ξ, after some simplification we can write

$$w(r,z) = \frac{Zk}{2\pi G}\int_0^\infty J_0(krx)x[-f_1(x)e^{-k\alpha H} + f_2(x)e^{-k\beta H}]dx \tag{5.5.124}$$

where,

$$f_1(x) = \frac{\alpha(2x^2+1)}{(2x^2+1)^2 - 4x^2\alpha\beta} \quad \text{and} \quad f_2(x) = \frac{2\alpha x^2}{(2x^2+1)^2 - 4x^2\alpha\beta}$$

$$\text{for } \nu = 0.25 \; V_p = V_s\sqrt{3} \tag{5.5.125}$$

To determine the displacement due to buried pulse it is necessary to solve the integral equation

$$\omega \int_0^\infty e^{-\omega t}\, w(t,r,H) = \frac{Zk}{2\pi G} \int_0^\infty J_0(krx)x[-f_1(x)e^{-k\alpha H} + f_2(x)e^{-k\beta H}] \tag{5.5.126}$$

We do not intend to solve the above integral, but present the results directly which is amenable to numerical solution.

$$w(t,r,H) = \frac{3ZW}{\pi^2 GR}, \quad \text{where } R = \sqrt{r^2+H^2} \quad \text{and} \quad W = (-W_p + W_s) \tag{5.5.127}$$

Here W_p represents the compressional component of the wave and W_s represents the shear component of the wave.

$$3W_p = 0 \quad \text{for } \tau < 1/\sqrt{3} \tag{5.5.128}$$

$$3W_p = Re \int_0^{\frac{\pi}{2}} (h\tau + i\nu_0 \sin\phi) f_1(x) d\phi \quad \text{for } \tau > 1/\sqrt{3} \tag{5.5.129}$$

where

$$h = H/R; \quad \nu_0 = (1-h^2)(\tau^2 - 1/3); \quad \alpha = h\tau + i\nu_0 \sin\phi;$$
$$x = \sqrt{\alpha^2 - 1/3} \quad \text{and} \quad \beta = \sqrt{\alpha^2 + 2/3} \tag{5.5.130}$$

Here the word *Re* means that while performing the numerical integration only the real part of the final value need to be considered only.

Before we proceed further it would worthwhile to study the characteristics of waves as obtained from the expressions above.

Since $\nu_p = \nu_s\sqrt{3}$ meaning $\nu_p > \nu_s$, it is evident that compression waves (represented by the function W_p) first reaches the surface and varies monotonically throughout its course. The shear wave traveling with velocity $< V_p$ reaches latter and its variation is much more complicated due to diffraction. We study the characteristics for some of the cases below.

Case-1 Buried Pulse at $r < H/\sqrt{2}$

As shown in Figure 5.5.9 a shear wave S incident on the surface which is traveling in vertical direction (often depicted as SV waves) when $r < H/\sqrt{2}$. The wave gets partially reflected as an S' wave which is shearing in nature and a compressive wave P' where P' travels with velocity V_p.

Case-2 Buried pulse at $r = H/\sqrt{2}$

As shown in Figure 5.5.10, at $r = H/\sqrt{2}$ the P wave grazes the free surface and owes its existence entirely due to diffraction.

Case-3 Buried pulse at $r > H/\sqrt{2}$

When $r > H/\sqrt{2}$ like point B shown in Figure 5.5.11, in addition to direct shear wave S which travels along OB another wave with velocity v_s travels along OA and the horizontal distance AB with velocity V_p. This diffracted wave is often termed as SP wave. It can be shown that SP wave reaches point B earlier than S wave (traveling along OB) though it travels a longer distance OAB.

Thus for $r < H/\sqrt{2}$ the order of arrival of waves are P and S and for $r > H/\sqrt{2}$ the order of arrival is P, SP and S.

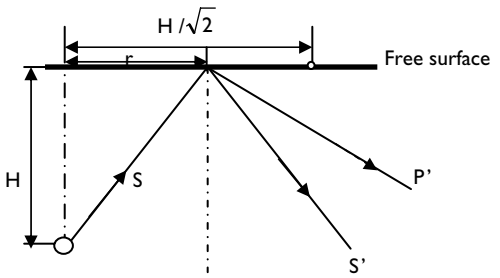


Figure 5.5.9 Reflection of waves from buried source at distance $r < H/\sqrt{2}$.

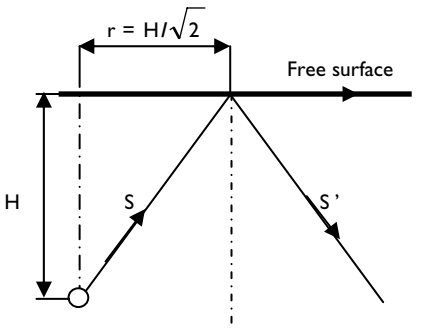


Figure 5.5.10 Reflection of waves from buried source at distance $r = H/\sqrt{2}$.

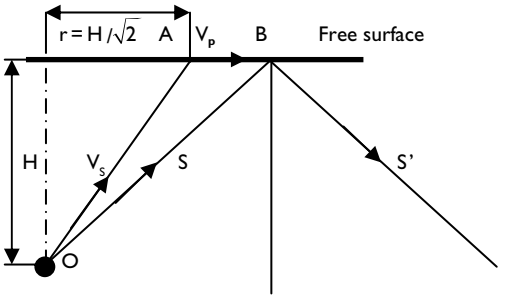


Figure 5.5.11 Reflection of waves from buried source at distance $r > H/\sqrt{2}$.

It is obvious based on above discussion that when r<$H/\sqrt{2}$ or $r > H/\sqrt{2}$ the characteristics of W_s would vary significantly.

For Vertical direction

For $r < H/\sqrt{2}$

$$3W_s = 0 \quad \text{for } \tau < 1 \tag{5.5.131}$$

$$3W_s = Re\int_0^{\infty} \left(h\tau + i\mu_0 \sin\phi\right) f_2(x)d\phi \quad \text{for } \tau > 1 \tag{5.5.132}$$

$$\text{Here} \quad \mu_0 = \sqrt{(1-h^2)(\tau^2-1)}, \quad h = \frac{H}{R}, \quad R = \sqrt{H^2+r^2} \tag{5.5.133}$$

$$\beta = h\tau + i\mu_0 \sin\phi, \quad x = \sqrt{(\beta^2-1)}, \alpha = \sqrt{\beta^2 - 2/3} \quad \text{and} \tag{5.5.134}$$

$$f_2(x) = \frac{2\alpha x^2}{(2x^2+1)^2 - 4x^2\alpha\beta} \tag{5.5.135}$$

For $r > H/\sqrt{2}$ as explained earlier SP waves arrive first at surface and starts at time function $\tau = \tau^*$ where

$$\tau^* = \left[h\sqrt{2/3} + \sqrt{(1-h^2)/3}\right] \tag{5.5.136}$$

$$3W_s = 0 \quad \text{for } \tau < \tau^* \tag{5.5.137}$$

$$3W_s = -I\int_0^{\frac{\pi}{2}} \beta f_2(x) \left[\frac{\cos\phi}{\sqrt{\kappa^2 + \sin^2\phi}}\right] d\phi \quad \text{for } \tau < \tau^* < 1 \tag{5.5.138}$$

Here I denotes that only the imaginary/complex part of the integration needs to be considered.

After arrival of the *S* waves (following the SP waves) W_s is given by

$$3W_s = Re\int_0^{\frac{\pi}{2}} (h\tau + i\mu_0 \sin\phi) f_2(x) d\phi - \delta \times \left[I \int_0^{\frac{\pi}{2}} (h\tau + \delta \sin\psi) f_2(x) \frac{\cos\psi}{\sqrt{\mu_0^2 + \delta^2 \sin^2\psi}} d\psi \right]$$

$$\text{for} \quad 1 < \tau < \frac{\sqrt{2/3}}{h} \tag{5.5.139}$$

$$\text{Here} \quad \delta = (\sqrt{2/3} - h\tau), \quad m = \sqrt{\delta^2 - \kappa^2 m^2}, \quad \kappa m = \sqrt{(1-h^2)(1-\tau^2)} \tag{5.5.140}$$

$$\beta = \left[h\tau + m\sqrt{\kappa^2 + \sin^2\phi} \right], \quad x = i\sqrt{1-\beta^2}, \quad \alpha = i\sqrt{2/3 \quad -\beta^2} \tag{5.5.141}$$

$$3W_s = Re\int_0^{\frac{\pi}{2}} (h\tau + i\mu_0 \sin\phi) f_2(x) d\phi \quad \text{for } \tau > \frac{\sqrt{2/3}}{h} \tag{5.5.142}$$

In the first integral of Equation (5.5.136) and in Equation (5.5.139), we substitute equation (5.5.132), while in second integral of Equation (5.5.137), we put

$$\beta = [h\tau + \delta \sin\psi], \quad x = i\sqrt{1-\beta^2}, \quad \text{and} \quad \alpha = i\sqrt{2/3 - \beta^2} \tag{5.5.143}$$

For Horizontal direction

Similar to the vertical displacement, the horizontal displacement at the surface is given by

$$q(\omega) = \frac{Zk}{2\pi G} \int_0^{\infty} J_1(krx) x^2 [g_1(x) e^{-k\alpha H} - g_2(x) e^{-k\beta H}] dx \tag{5.5.144}$$

$$\text{where} \quad g_1(x) = \frac{2\alpha\beta}{(2x^2+1)^2 - 4x^2\alpha\beta} \quad \text{and} \quad g_2(x) = \frac{2x^2+1}{(2x^2+1)^2 - 4x^2\alpha\beta} \tag{5.5.145}$$

Also, we can write

$$q(t, r, H) = -\frac{3Z}{\pi^2 Gr} Q \tag{5.5.146}$$

where, $Q = -Q_p + Q_s$ the compressional and shear component of the waves.

Again without going into the details of the solution of the integral equation, we proceed to give directly the solution of Q_p and Q_s.

$$3Q_p = 0 \quad \text{for } \tau < \frac{1}{\sqrt{3}} \tag{5.5.147}$$

$$3Q_p = -Re \int_0^{\frac{\pi}{2}} (h\tau + iv_0 \sin\phi)[\tau - h(h\tau + iv_0 \sin\phi)]g_1(x)d\phi \tag{5.5.148}$$

$$\text{for } \tau > \frac{1}{\sqrt{3}}$$

$$\text{where} \quad \tau = \frac{V_s t}{R}, \quad h = \frac{h}{R}, \quad \alpha = h\tau + iv_0 \sin\phi, \quad \beta = \sqrt{\alpha^2 + \frac{2}{3}}, \tag{5.5.149}$$

$$v_0 = \left\{(1-h^2)\sqrt{\tau^2 - \frac{1}{3}}\right\}, \quad x = \sqrt{\alpha^2 - \frac{1}{3}} \tag{5.5.150}$$

For $r < \frac{H}{\sqrt{2}}$ Q_s is given by

$$3Q_s = 0 \quad \text{for } \tau < 1 \tag{5.5.151}$$

$$3Q_s = -Re \int_0^{\frac{\pi}{2}} (h\tau + i\mu_0 \sin\phi)[\tau - h(h\tau + i\mu_0 \sin\phi)]\, g_2(x)d\phi \quad \text{for } \tau > 1 \tag{5.5.152}$$

$$\text{where} \quad g_2(x) = \frac{2x^2 + 1}{(2x^2+1)^2 - 4x^2\alpha\beta} \tag{5.5.153}$$

$$x = \sqrt{\alpha^2 - \frac{1}{3}}, \quad \alpha = h\tau + i\mu_0 \sin\phi, \quad \beta = \sqrt{\alpha^2 + \frac{2}{3}} \tag{5.5.154}$$

For $r < \frac{H}{\sqrt{2}}$, Q_s is given by

$$3Q_s = 0 \quad \text{for } \tau < \tau^* \tag{5.5.155}$$

$$3Q_s = I \int_0^{\frac{\pi}{2}} \beta(\tau - h\beta)g_2(x) \left[\frac{\cos\phi}{\sqrt{\kappa^2 + \sin^2\phi}}\right] d\phi \quad \text{for } \tau^* < \tau < 1 \tag{5.5.156}$$

$$3Q_s = -Re \int_0^{\frac{\pi}{2}} (h\tau + i\mu_0 \sin\phi)[\tau - h(h\tau + i\mu_0 \sin\phi)]g_2(x)d\phi$$

$$+\delta I \int_0^{\frac{\pi}{2}} \beta(\tau - h\beta) g_2(x) \left[\frac{\cos\psi}{\sqrt{\mu_0^2 + \delta^2 \sin^2\psi}} \right] d\psi \quad \text{for } 1 < \tau < \frac{\sqrt{2/3}}{h} \tag{5.5.157}$$

$$3Q_s = -Re \int_0^{\frac{\pi}{2}} (h\tau + i\mu_0 \sin\phi)[\tau - h(h\tau + i\mu_0 \sin\phi)] g_2(x) d\phi \quad \text{for } \tau > \frac{\sqrt{2/3}}{h} \tag{5.5.158}$$

In Equations (5.5.153) and (5.5.155), we substitute expressions of (5.5.146) while for the second integral in Equation (5.5.154), expression (5.5.141) is to be substituted.

5.5.4 Interpretation of Pekeris' solution

You may solve the above equations and plot them to find out the nature of wave propagation for different values of τ and r/H.

We give below the basic essence of Pekeris' findings at a far off distance from the source.

As shown in Figure 5.5.12, when the waves arrive at a site, the first to arrive are the compression (P) waves followed by the shear (S) waves which produce a *minor tremor* and finally with the arrival of the Rayleigh surface wave a *major tremor* is produced. This has been indeed observed when a far field earthquake occurs at a site.

When the focus of the source point is shallow, Pekeris' solution for the surface pulse can be used to estimate the amplitudes and stress induced in the medium.

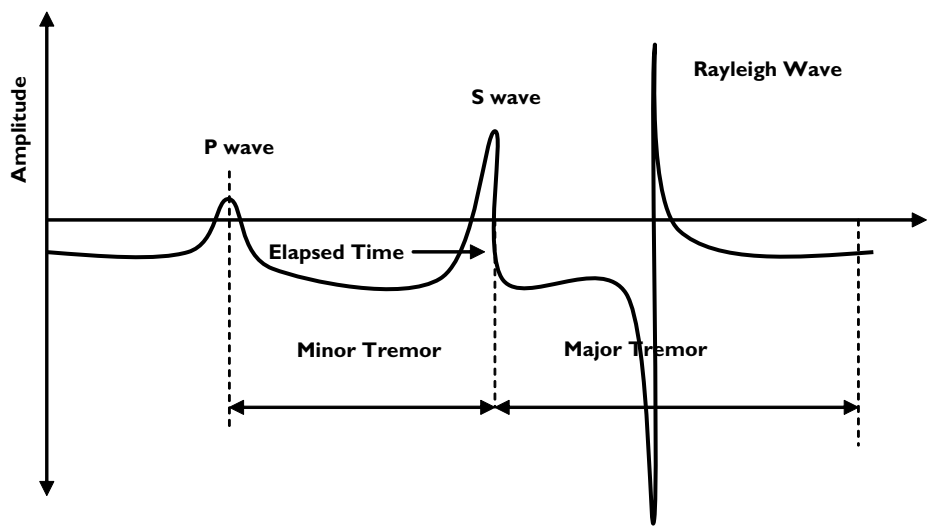


Figure 5.5.12 Propagation of wave from a far field source.

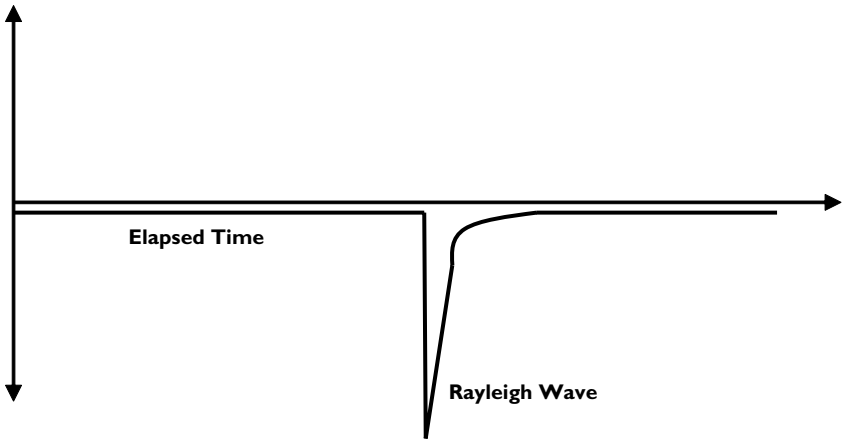


Figure 5.5.13 Propagation of wave for source at $r/h = 1000$.

Other than this, underground explosion in mines and its effect on surface structures, underground nuclear explosion[71] and its effect on surface can well be estimated by Pekeris' solution.

At a distance of r/H greater or equal to 1000, the characteristics of wave propagation is as shown Figure 5.5.13. Based on above it is clear that it is Rayleigh wave propagating on the surface is the major disturbing source and creates havoc during a major earthquake.

5.5.5 Chang's Solution to dynamic response for horizontal surface loading

While Pekeris gave solution to pulse load buried or on the surface of an elastic half space, Chang (1960) gave solution to dynamic response of a half-space subjected to tangential force acting on the surface of the half space. This surface loading cannot be simplified to axial symmetry. Chang obtained a closed form solution for the surface displacements and displacements (u, v, w in the x, y and z-directions, respectively) directly below the applied force varying with time as the Heaviside unit function. In order to simplify the calculations, Lame's constants λ is assumed to be equal to G i.e. Poisson's ratio, $\nu = 1/4$.

The boundary conditions on the elastic half-space $z \geq 0$ with traction-free surface $z = 0$, when a concentrated force, F, parallel to the x-axis is applied inside the medium and varies with time as a Heaviside unit function.

Case 1 $z = 0$, i.e. the surface displacements corresponding to a tangential force F, acting at a point on the surface:

Parameters used are: $r^2 = x^2 + y^2$; $\tau = v_s t/r$; and $v_s^2 = G/\rho$

71 A common occurrence in 1960–70 however banned presently under CTBT convention.

Here G and ρ are the shear modulus and mass density of the elastic half-space; v_s is the shear wave velocity. The solutions are mentioned hereafter.

$$u_1 = 0 \quad \tau < 1/\sqrt{3}$$

$$u_1 = \frac{F}{\pi G r}\left[\frac{9\tau^2}{8\sqrt{3\tau^2 - \frac{3}{4}}} - \frac{\tau^2\sqrt{6\sqrt{3}+10}}{16\sqrt{\tau^2-\beta^2}} - \frac{\tau^2\sqrt{6\sqrt{3}-10}}{16\sqrt{\gamma^2-\tau^2}}\right] \quad \text{for } 1/\sqrt{3} < \tau < 1$$

$$u_1 = \frac{F}{\pi G r}\left[\frac{1}{2} - \frac{\tau^2\sqrt{6\sqrt{3}-10}}{8\sqrt{\gamma^2-\tau^2}}\right] \quad \text{for } 1 < \tau < \gamma \tag{5.5.159}$$

$$u_1 = \frac{F}{2\pi G r} \quad \text{for } \gamma < \tau$$

$$u_2 = 0 \quad \text{for } \tau < 1/\sqrt{3}$$

$$u_2 = \frac{F}{\pi G r}\left[-\frac{3}{16} + \frac{3}{8}\sqrt{3\left(\tau^2 - \frac{1}{4}\right)} - \frac{1}{16}\sqrt{(10+6\sqrt{3})(\tau^2-\beta^2)}\right.$$

$$\left. + \frac{1}{16}\sqrt{(10-6\sqrt{3})(\gamma^2-\tau^2)}\right] \quad \text{for } 1/\sqrt{3} < \tau < 1$$

$$u_2 = \frac{F}{\pi G r}\left[-\frac{3}{8} + \sqrt{(6\sqrt{3}-10)(\gamma^2-\tau^2)}\right] \quad \text{for } 1 < \tau < \gamma \tag{5.5.160}$$

$$u_2 = -\frac{3F}{8\pi G r} \quad \text{for } \gamma < \tau$$

$$u_3 = 0 \quad \text{for } \tau < 1/\sqrt{3}$$

$$u_3 = \frac{F\tau\sqrt{6}}{32\pi^2 G r}[6K(m) - 18\Pi(8m^2, m) - (4\sqrt{3}-6)\Pi\{-(12\sqrt{3}-20)m^2, m\}]$$

$$+ (4\sqrt{3}+6)\Pi\{(12\sqrt{3}+20)m^2, m\} \quad \text{for } 1/\sqrt{3} < \tau < 1$$

$$u_3 = \frac{F\tau\sqrt{6n}}{32\pi^2 G r}[6K(n) - 18\Pi(8, n) - (4\sqrt{3}-6)\Pi\{-(12\sqrt{3}-20), n\}]$$

$$+ (4\sqrt{3}+6)\Pi\{(12\sqrt{3}+20), n\} \quad \text{for } 1 < \tau < \gamma$$

$$u_3 = \frac{F\tau\sqrt{6n}}{32\pi^2 G r}[6K(n) - 18\Pi(8, n) - (4\sqrt{3}-6)\Pi\{-(12\sqrt{3}-20), n\}]$$

$$+ (4\sqrt{3}+6)\Pi\{(12\sqrt{3}+20), n\} + \frac{F\tau}{8\pi G r\sqrt{\tau^2-\gamma^2}} \quad \text{for } \gamma < \tau \tag{5.5.161}$$

in which $m = \frac{3\tau^2-1}{2}$; $n = \frac{1}{m}$ and, $K(k) = \int_0^{\pi/2} \frac{d\theta}{\sqrt{1-k^2\sin^2\theta}}$, $\Pi(n,k) = \int_0^{\pi/2} \frac{d\theta}{(1+n\sin^2\theta)\sqrt{1-k^2\sin^2\theta}}$ are complete elliptical integral of the first and third kinds.

Case 2 $r = 0$, the displacements are along the z-axis directly below an applied tangential force which acts at a point (the origin) on the surface:

$$u_3 = 0$$

$$u_1 = -u_2 = 0 \quad \tau_1 < 1/\sqrt{3}$$

$$u_1 = -u_2 = -\frac{F}{2\pi Gz}\left[\frac{\tau_1\left(\tau_1^2-\frac{1}{3}\right)\sqrt{\tau_1^2+\frac{2}{3}}}{\left(2\tau_1^2+\frac{1}{3}\right)^2-4\tau_1\left(\tau_1^2-\frac{1}{3}\right)\sqrt{\tau_1^2+\frac{2}{3}}}\right]$$

for $1/\sqrt{3} < \tau_1 < 1$

$$u_1 = -u_2 = \frac{F\left(\tau_1^2+1\right)}{4\pi Gz} - \frac{F}{4\pi Gz}\left[\frac{2\tau_1\left(\tau_1^2-\frac{1}{3}\right)\sqrt{\tau_1^2+\frac{2}{3}}}{\left(2\tau_1^2+\frac{1}{2}\right)^2-4\tau_1\left(\tau_1^2-\frac{1}{3}\right)\sqrt{\tau_1^2+\frac{2}{3}}}\right]$$

$$+\frac{F}{4\pi Gz}\left[\frac{2\tau_1^2\left(\tau_1^2-1\right)\left[2\tau_1\sqrt{\tau_1^2-\frac{2}{3}}-\left(2\tau_1^2-1\right)\right]}{\left(2\tau_1^2-1\right)^2-4\tau_1\left(\tau_1^2-1\right)\sqrt{\tau_1^2-\frac{2}{3}}}\right] \quad \text{for } 1 < \tau_1,$$

$$\text{where} \quad \tau_1 = \frac{v_s t}{z}. \tag{5.5.162}$$

u_r, u_θ and u_z in (r, θ, z) coordinate system may be written as:

$$u_r = u_1\cos\theta; \quad u_\theta = u_2\sin\theta \quad \text{and} \quad u_z = u_3\cos\theta. \tag{5.5.163}$$

The non-zero displacement directly below the applied force is $u_x = u_r\cos\theta - u_\theta\sin\theta$. The solution shows that there exist three distinct wave fronts, traveling with velocities $v_p = \sqrt{(\lambda+2G)/\rho}$, $v_s = \sqrt{G/\rho}$ and v_s/γ respectively. For Poison's ratio, $\nu = 1/4$, $\gamma^2 = (3+\sqrt{3})/4$ (γ is the root of Rayleigh equation). These waves are identified as the pressure wave (P), the shear wave(S) and the Rayleigh surface wave (R), respectively.

Before the arrival of the P-wave, the medium was in complete rest. At the arrival of the P-wave the velocities experience a sudden jump. The arrival of the S-wave is marked by a finite jump in v; however, for displacements u_r and u_θ[in (r, θ, z) coordinate system] , it is marked only by discontinuities in the corresponding velocity components. The arrival of the R-wave is marked by infinite discontinuity in u_r and u_θ while for u_θ, only a discontinuity in velocity occurs.

In the neighbourhood of R-wave front, the major portion of the displacement is u_r and u_θ is proportional to

$$\frac{1}{r^2[\tau^2 - \gamma^2]^{1/2}} = \frac{1}{[\gamma(\tau + \gamma)]^{1/2}} \frac{1}{\sqrt{r\, r_R}} \tag{5.5.164}$$

where $|r_R| = |r - v_s t/\gamma|$ is the distance from the R-wave front and the displacement vary as $(1/rr_R)^{1/2}$ in the neighbourhood of the wave front of the surface wave. At large distances from the applied force, only small u_θ displacement occurs, while the other components still assume very large values when the surface wave arrives.

In steady-state solution, it can be observed that on the surface of the elastic half-space, the quantity $[u_\theta/F\cos\theta]$, corresponding to a tangential force on the surface, is equal to the quantity $[u_r/F]$, corresponding to a vertical force on the surface. Such a reciprocal relation is seen to be preserved for all time for the dynamic case by comparing the quantity $[u_\theta/F\cos\theta]$ of this derivation to the corresponding quantity $[u_r/F]$ of Pekeris (1957).

5.6 GEOTECHNICAL EARTHQUAKE ANALYSIS

5.6.1 Soil dynamics and earthquake

Even thirty years ago mechanics of propagation of wave due to earthquake was a subject that remained an exclusive haven of geologists and seismologists with civil engineers hardly having any idea as to the propagation mechanics. However times have changed. Civil engineers of today have to make a much more detailed assessment of seismic hazard a project would face if build in a seismic prone zone. He has to make a reasonable assessment of the risk involved and give feedback to the investors who are investing significant amount of money in such projects. In today's global scenario, oil and power companies are investing billions of dollars to develop oil and gas facilities and power plants across the world, where surely they would like to know the risk involved in case such happenstance occurred.

It is for this we have seen civil engineers in last three decades increasingly sitting with seismologists, geologists, geophysicists and trying to understand the mechanics and try to rationalize and seek the design parameters which affect his design procedure.

In this context how soil dynamics comes into play in understanding such mechanics is our topic of discussion in this section.

5.6.1.1 The seismological mechanics of earthquake

We have given some background on this in Chapter 3 (Vol. 2) while discussing earthquake resistant design of structures and foundations. In this chapter we only restrict the same by saying that strains build up in rock due to geologic upheaval finally comes to a point at which the rock no longer can sustain the strain and generates a crack in it[72], the strain energy built up within the body thus gets released as kinetic energy

72 These are called Fault lines in Geological science.

generating stress waves within the rock which propagates all around and causes the earthquake.

Let us consider further a scenario...

A power plant is being built at a place where it is known that there exists a fault say 150 kilometer away from the site? The fault has a history of generating a few minor tremors ($M < 5.0$ say) in the past what is the risk involved for an earthquake of $M \geq= 6.5$ to occur? One does not need to be a mathematical genius to guess that the problem is probabilistic.

However, a few questions immediately emerge out of the problem which could be summarized as follows:

- What chance is there that a major earthquake would emerge from the fault?
- What could be its intensity (usually measured in Richter scale)?
- What would be duration of shaking?
- What would be the peak ground acceleration at the site which is 150 KM away?
- The waves normally attenuate with distance thus the shock that would be felt at the site – would it decrease?
- Or the local geological condition of the site is such that it may amplify the response?

Before we answer these questions, we need to know a few seismological terms based on which we would try to quantify and answer the above-mentioned queries.

1 ***Focus*:** This is the point O or source on the fault line from where the earthquake generates. This is the point from where the rupture first generates.
2 ***Focal distance*:** The distance OA as shown in Figure 5.6.1 is called the focal distance. Based on this distance an earthquake may be deep focused (when OA

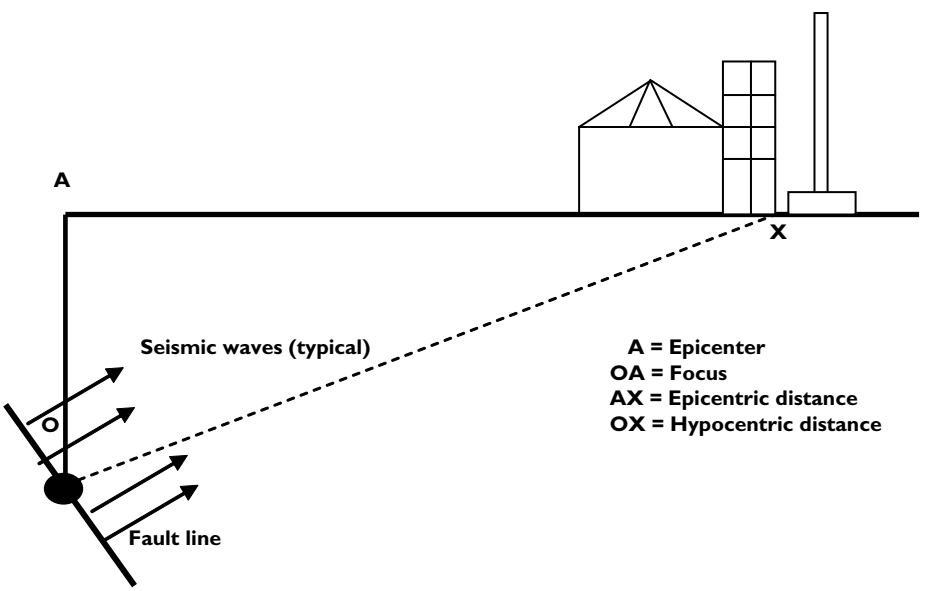


Figure 5.6.1 Common seismological terms used for evaluation of an earthquake for a given site.

>300 to700 km), intermediate focused (when OA >60 to 300 km) and short focused when (OA is ≤60 Km).

3 ***Epicenter*:** The point A that is vertically above the focus or point of rupture is called the epicenter.

4 ***Epicentric Distance*:** The horizontal distance AX from the epicenter to the given site (X) is called the epicentric distance. This distance is usually depicted by D.

5 ***Hypo-centric distance*:** The distance OX from the focus to the site is called the hypo-centric distance. For shallow focused earthquake and far field response hypo-centric distance becomes almost equal to epicentric distance. Hypocentric distance is usually depicted by *R*.

6 ***Earthquake Intensity*:** How strong is an earthquake when it shakes the ground? Richter (1958) was the first to propose a scale named after him as Richter scale which qualitatively measures the earthquake intensity. You may refer to IS-1893 the Indian standard for code of earthquake resistant design or similar international code, which gives the description of the scales. This is usually depicted by *M*, earthquake of intensity greater than 6 is usually known as strong motion earthquake which affects our civil engineering structures and foundation.

5.6.1.2 Energy released due to earthquake

Energy released due to an earthquake is given by the expression as per Richter as

$$\log_{10} E = 11.4 + 1.5M \tag{5.6.1}$$

Here E is the energy in ergs and M is the intensity of earthquake in Richter scale. Bath (1966) corrected the above formula as

$$\log_{10} E = 12.24 + 1.44M \tag{5.6.2}$$

5.6.1.3 Relation between length of fault rupture and earthquake intensity

Tocher (1958) based on observation of a number of earthquakes in California gave the relation as

$$\log L = 1.02M - 5.77 \tag{5.6.3}$$

Here L is the length of fault rupture in km.

Variation of length of rupture with Earthquake magnitude is shown in Figure 5.6.2.

5.6.1.4 Duration of earthquake

Duration of strong motion earthquake normally increase with the earthquake intensity and distance from the source and could also increase from rock to soil sites. However estimates are mostly probabilistic and based on observed data, which are the fitted based on regression analysis. Duration of earthquake with magnitude is given in Figure 5.6.3.

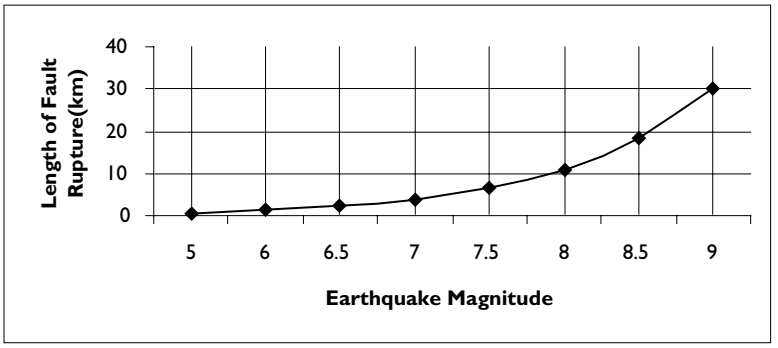


Figure 5.6.2 Length of rupture at earthquake source.

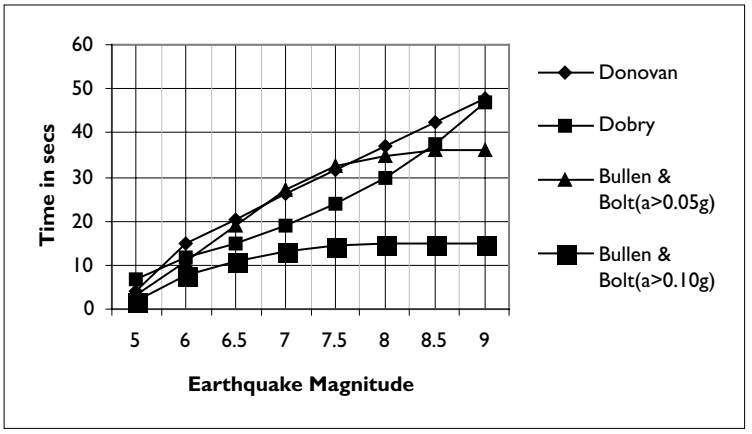


Figure 5.6.3 Duration of earthquake with magnitude.

Donovan (1974) based on data as observed for US and Japanese earthquake proposed a relationship

$$D = 4 + 11(M - 5) \quad \text{for } M > 5 \tag{5.6.4}$$

Dobry and other researchers based on observation of earthquake in US has given a relationship

$$\log D = 0.432M - 1.83 \tag{5.6.5}$$

Bullen & Bolt(1985) has proposed an expression based on the observed ground acceleration at site given by

$$D = 17.5 \tan h(M - 6.5) + 19 \tag{5.6.6}$$

for $a > 0.05$ g where a = ground acceleration,

$$D = 7.5 \tan h(M - 6) + 7.5 \quad \text{for } a > 0.10 \text{ g} \tag{5.6.7}$$

Here the epicentric distance is considered to be less or equal to 25 km.

5.6.1.5 Predominant period of rock motion

Gutenberg & Richter(1956) based on study of a number of Californian earthquake presented the following data vide Table 5.6.1 for the predominant periods of accelerations developed at different epicentral distances by earthquakes with magnitude ranging from 5.5 to 6.5.

Table 5.6.1

Epicentral distance in kM	0–50	51–100	101–150	151–200	201–250
Predominant period in seconds	0.25	0.3	0.4	0.4	0.6

5.6.1.6 Peak ground acceleration and velocity

The peak ground acceleration a and velocity v is related the to earthquake magnitude and hypo-centric distance as

$$a = \frac{5600e^{0.8M}}{(R+40)^2} \quad \text{and} \quad v = \frac{32e^{M}}{(R+25)^{1.7}} \tag{5.6.8}$$

The above is valid for a case when the focal distance is less than 15 km.

Esteva & Rosenblueth (1973) has given a modified version of the peak ground accelelration as

$$a = \frac{110e^{0.8M}}{(R)^{1.6}} \tag{5.6.9}$$

A very popular formulation that is in used in design office is one proposed by Mcguire (1974) and is expressed as

$$\log a = 2.649 + 0.278M - 1.301 \log(R + 25) \tag{5.6.10}$$

where, a is expressed in cm/sec^2.

It is to be noted that all these formulas are for acceleration in bedrock or through soil having stiffness as strong as rock (i.e. $V_s > 600$m/sec).

The Peak ground acceleration variations are shown in Figures 5.6.4 and 5.

5.6.1.7 Attenuation factor

Earthquakes have been observed to attenuate with distance. For predicting the design earthquake at particular site it is essential to know as to how it attenuates with distance.

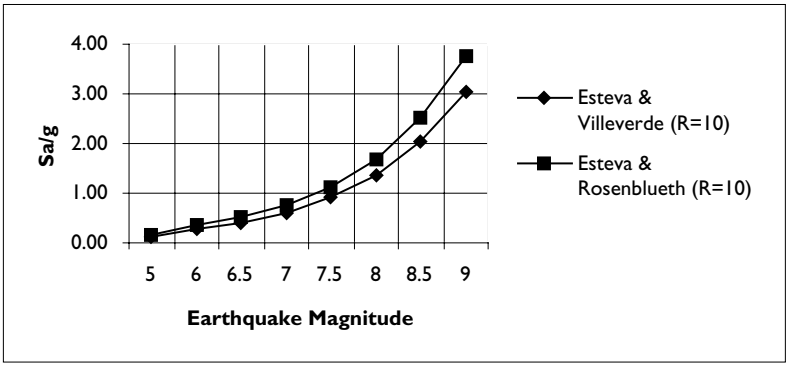


Figure 5.6.4 Peak ground acceleration at epicentric distance at $R = 10$ km.

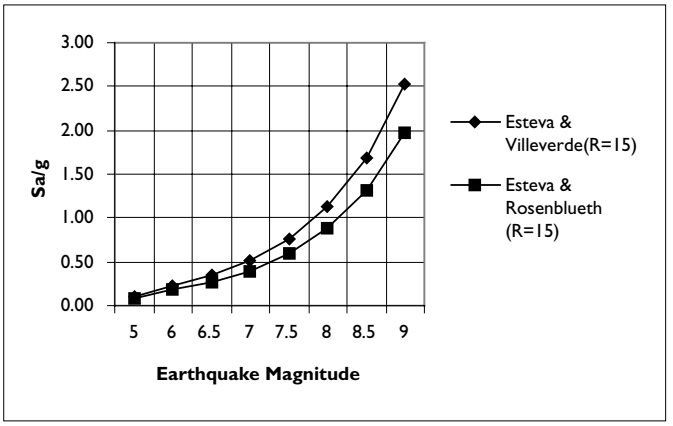


Figure 5.6.5 Peak ground acceleration at epicentric distance at $R = 15$ km.

Blume (1965) has given an attenuation factor as

$$F_d = \frac{1}{1 + (D/h)^2} \tag{5.6.11}$$

in which, h = depth of the earthquake source at focus, and D epicentral distance.

Gutenberg & Richter (1956) has given an expression for acceleration at the epicenter as

$$\log a_0 = -2.1 + 0.81M - 0.027M^2 \tag{5.6.12}$$

$$a_D = F_d \, a_0 \tag{5.6.13}$$

where $F_d = \left[\frac{1.25}{1+D/y_0}\right]^n$ in which $n = 1 + \frac{1}{2.5T_p}$

where Tp = predominant time period which varies with distance as given earlier $y_0 = 48$ miles; D = site distance which should be greater or equal to 12 miles.

5.6.1.8 One dimensional ground motion under earthquake

Engineers working in a design office are normally not called upon to tackle response of ground under earthquake. Their working interface starts from the simplified response curve as shown in Figure 5.6.6.

As per IS code peak force expected in a site with a probability of severe shock is given by

$$A_h = \frac{ZI}{2R}\left(\frac{S_a}{g}\right) \tag{5.6.14}$$

for severe case taking $Z = 0.24$ $I/R = 1.0$, maximum peak ground acceleration (S_a/g) expected is 0.3 g.

There are however cases due to local geological condition the acceleration at ground level can be much higher especially when bedrock is overlain by soft soil. This is usually known as *local ground amplification.*

Ground motion study is thus an estimate of what peak acceleration a particular site can generate. In special cases[73] it is also used to generate site specific response spectra for design of structures constructed on it.

Unless the site has peculiar configuration like being a valley or confined, one dimensional analysis of wave propagation is good enough to give an estimate of ground motion at a particular site.

We present herein two common techniques which are being used for finding out the response at surface of a soil underlain by rock.

1 Developed by Schnabel et al. (1972) based on frequency domain analysis.[74] Which usually considers the soil as linear and elastic.
2 Developed by Idriss and Seed (1968) based on time domain analysis[75] which also takes into cognizance the non linearity of the soil.

5.6.1.9 Schnabel's method of estimation of response of horizontal soil over over rigid rock

This technique was developed by Schanbel (1972) and is implemented in the software SHAKE.

We develop the method step by step starting with the simplest case and progressing to the complex one.

73 Like Nuclear Power plants.
74 The technique is often used across the world based on the software SHAKE developed at Dept of Civil Engineering University of California Berkeley.
75 The technique is implemented in the software called MASH developed by Martin and Seed at University of California Berkeley.

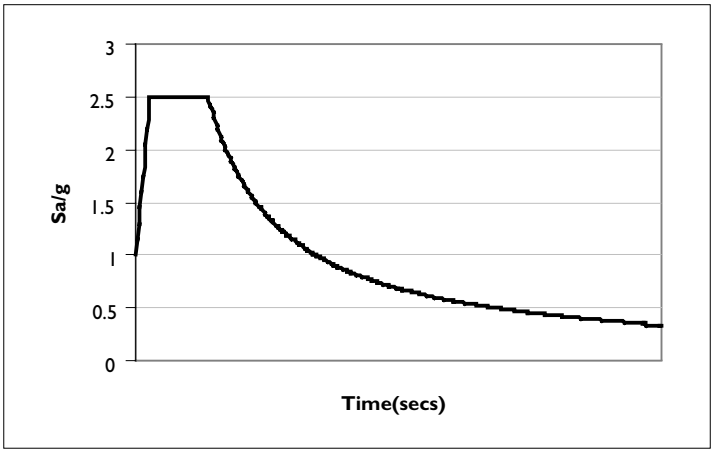


Figure 5.6.6 Typical response curve for medium soil as per IS 1893 (2002).

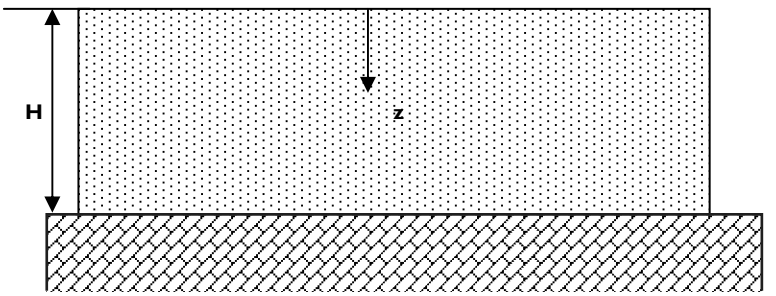


Figure 5.6.7 Horizontal soil layer of depth *H* underlain by rigid rock.

Case-1

Uniform undamped soil over rigid rock as shown in Figure 5.6.7.

We consider a soil column through which due to harmonic load the waves are propagating vertically. The soil layer has depth H and is considered undamped. The differential equation of motion in this case is thus

$$\rho \frac{\partial^2 u}{\partial t^2} = G \frac{\partial^2 u}{\partial z^2} \tag{5.6.15}$$

The solution to above equation in complex form is expressed as

$$u(z,t) = X_1 e^{i(\omega t + kz)} + X_2 e^{-i(\omega t - kz)} \tag{5.6.16}$$

where ω = Circular frequency of ground motion; k = wave number @ ω/v_s; v_s = shear wave velocity of the soil.

At free surface as the shear stress must be equal to zero we have

$$\tau(0,t) = G\frac{\partial u}{\partial z} = 0 \text{ which gives, } Gik(X_1 e^{ik_0} - X_2 e^{-ik_0})e^{i\omega t} = 0$$

It is evident that above can only be zero provided $X_1 - X_2 = 0$ or $X_1 = X_2$.
Thus, $u(z,t) = 2X_1 \frac{e^{ikz}+e^{-ikz}}{2} e^{i\omega t}$, considering $X_1 = X$, we have

$$u(z,t) = 2X \cos kz e^{i\omega t} \tag{5.6.17}$$

The above equation can be used to define a transfer function that can describe ratio of displacement amplitudes at any two points in the soil layer. Choosing these two points at top and bottom of the soil layer we have the transfer function as

$$H(\omega) = \frac{u(0,t)}{u(H,t)} = \frac{1}{\cos kH} \tag{5.6.18}$$

Since the denominator cannot be more than 1 it shows that surface motion at worst can be equal to the amplitude of the bedrock and for other values more than 1.
Resonance will obviously occur when the denominator is zero i.e.

$$\cos\frac{\omega_n H}{v_s} = 0 \quad \Rightarrow \frac{\omega_n H}{v_s} = \frac{(2n-1)\pi}{2} \quad \text{or}$$
$$\Rightarrow \omega_n = \frac{(2n-1)\pi v_s}{2H} \tag{5.6.19}$$

which is the free field natural frequency of the soil layer.
The variation of amplification factor with kH is as shown in Figure 5.6.8.

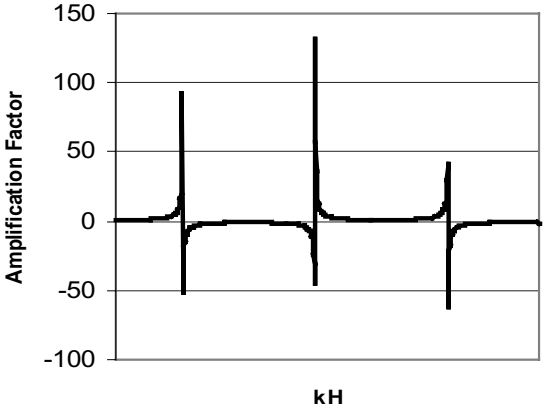


Figure 5.6.8 Amplifications of undamped soil overlaying rigid rock.

Case-2

Horizontal soil layer with damping underlain by rigid rock

In this case the differential equation of motion is given by

$$\rho \frac{\partial^2 u}{\partial t^2} = G \frac{\partial^2 u}{\partial z^2} + \eta \frac{\partial^3 u}{\partial z^2 \partial t} \tag{5.6.20}$$

Considering $u = \phi e^{i\omega t}$, when substituted in the above equation we have

$$-\rho\omega^2\phi = (G + i\omega\eta)\frac{d^2\phi}{dt^2} \quad \text{or} -\rho\omega^2\phi = G^*\frac{d^2\phi}{dt^2} \tag{5.6.21}$$

Here G^* is known as the complex Shear Modulus of the soil[76].

Solution to the above equation can thus be expressed as

$$u(z,t) = X_1 e^{i(\omega t + k^* z)} + X_2 e^{-i(\omega t - k^* z)} \tag{5.6.22}$$

Here k^* is the complex wave number expressed as, $k^* = \omega/v_s^*$, where $v_s^* = \sqrt{G^*/\rho}$ the complex shear wave velocity of the soil.

It can be shown that considering the soil constitutive model as a Kelvin-Vogt Model the viscosity factor $\eta = \frac{2GD}{\omega}$ where D is the material damping ratio of the soil. Substituting this value of D, we have $G^* = G(1 + 2iD)$. Now considering the expression

$v_s^* = \sqrt{G^*/\rho}$ we can approximate the complex shear wave velocity as

$$v_s^* = v_s\,(1 + iD). \tag{5.6.23}$$

At free surface as the shear stress must be equal to zero we have

$$\tau(0,t) = G^*\frac{\partial u}{\partial z} = 0 \quad \text{which gives, } G^* ik^* (X_1 e^{ik0} - X_2 e^{-ik0}) e^{i\omega t} = 0$$

This results in $X_1 - X_2 = 0$ or $X_1 = X_2 = X$.

Thus, $u(z,t) = 2X \cos k^* z e^{i\omega t}$

76 One need not get confused or puzzled with the concept of complex shear modulus – just treat it as a mathematical symbol you will finally see that it all boils down to real numbers in the end.

The transfer function in this case is thus expressed as

$$H(\omega) = \frac{u(0,t)}{u(H,t)} = \frac{1}{\cos k^* H} \quad \text{or } H(\omega) = 1/[\cos(\omega H/v_s^*)]$$

where $k^* = \dfrac{\omega}{v_s^*} = \dfrac{\omega}{v_s(1+iD)}$

$$\text{i.e.} \quad k^* = \frac{\omega}{v_s}(1+iD)^{-1} \approx \frac{\omega}{v_s}(1-iD) = k(1-iD) \tag{5.6.24}$$

Thus the transfer function can now be expressed as

$$H(\omega) = \frac{1}{\cos k(1-iD)H} = \frac{1}{\cos(kH - iDkH)}$$

Considering $kH = a$ and $-DkH = b$, we have $|\cos(a+ib)| = |\cos^2 a + \sin h^2 b|$

$$\text{which gives,} \quad |H(\omega)| = \frac{1}{\sqrt{\cos^2 kH + \sin h^2 kH}} \tag{5.6.25}$$

The variation of amplification factor for various damping ratio and kH are as shown in Figure 5.6.9.

Observing the above figure it will be seen that when bedrock is overlain by soil there can be significant amplification of acceleration at ground level which can be many times more than the bedrock motion. At resonance due to the presence of damping the value is magnified yet remains finite. A number of researches conducted (Zeevart 1983) with previous earthquakes show that is indeed the case and has been

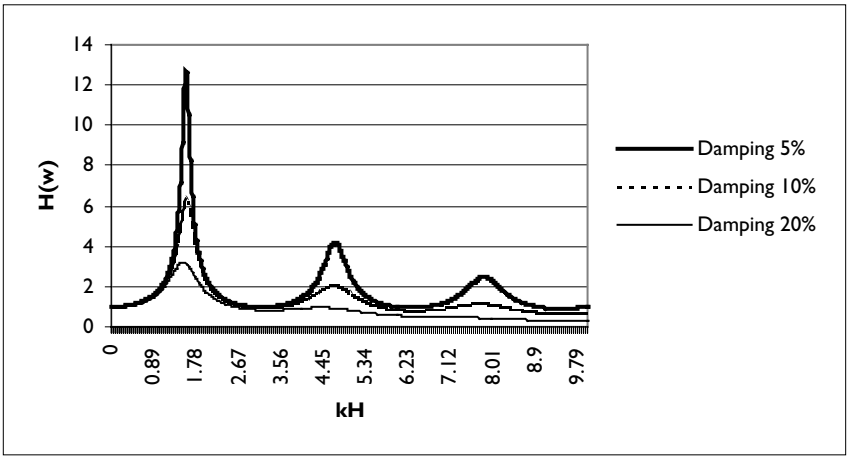


Figure 5.6.9 Soil amplification factor for damped soil overlying rigid rock.

the cause of significant destruction of a number of structures and facilities built on such ground.

Other than above, Schnabel's technique also takes into cognizance, layered soil strata overlying rock. Based on recursive technique one can compute the transfer functions at any point within the soil at any particular layer. Details of the same are available in Kramer (2004) or in the User manual of SHAKE, which gives the derivation in quite detail.

One of the major objections by many researchers in use of frequency domain analysis in geo-technical earthquake engineering is that the transfer function theory is valid only when the system is linear and elastic while soil (especially soft soil) is notorious for its non-linearity, specifically when the strain rate is high.

All strong ground motion induces enough strain in ground to make it behave in non linear fashion and compounded by the fact that soil undergoes stiffness degradation with progressive increment of strain and increases in damping ratio, many researchers perceive that frequency domain analysis remains only a qualitative assessment of the behavior of soil under such earthquake force.

Nevertheless the theory and the software still remains quite popular in design office for assessment of ground amplification due to local site condition that can affect the surface motion.

5.6.1.10 Idriss and Seed (1968)'s method of determination of ground motion

This is a time domain analysis where the differential equation of motion is considered as

$$\rho(z)\frac{\partial^2 u}{\partial t^2} + c(z)\frac{\partial u}{\partial t} - G(z)\frac{\partial^2 u}{\partial z^2} = -\rho(z)\frac{\partial^2 u_g}{\partial t^2} \tag{5.6.26}$$

in which, $\rho(z)$ = mass density of soil in z direction; $c(z)$ = damping of soil in z direction; $G(z)$ = dynamic shear modulus varying with depth $\cong Gz^{\alpha}$; gu = relative displacement of ground with respect to bedrock; u_g = displacement at bed rock level.

Considering $u(z,t) = \sum_{n=1}^{\infty} \phi_n(z)\psi_n(t)$ and applying the law of separation of variable the above partial differential equation can be broken up into two liner differential equations whose solutions are given by

$$\phi_n(z) = \left(\frac{1}{2}\beta_n\right)^b \Gamma(1-b)\left(\frac{z}{H}\right)^{b/\theta} J_{-b}\left[\beta_n\left(\frac{z}{H}\right)^{1/\theta}\right] \tag{5.6.27}$$

and $$\ddot{\psi}_n(t) + 2D\omega_n\dot{\psi}_n(t) + \omega_n^2\psi_n(t) = -P_n\ddot{u}_g \tag{5.6.28}$$

Here J_{-b} is the Bessel's function of first kind of order $-b$, β_n represents the roots of the equation $J_{-b}(\beta_n) = 0$ for $n = 0, 1, 2, 3.....$ (Abramowitz and Stegan1964)[77].

77 The roots are standard values available in many Mathematical Handbooks.

Γ is the gamma function

$$\omega_n = \frac{\beta_n\sqrt{G/\rho}}{(\theta H)^{1/\theta}} \quad \text{and} \quad D = \frac{c/2}{\rho\omega_n} \quad \text{and} \quad P_n = \left[(\beta_n/2)^{1+b}\,\Gamma(1-b)J_{1-b}\,(\beta_n)\right]^{-1}$$

$$\theta = \frac{2}{2-\alpha} \quad \text{and} \quad b = \frac{\alpha-1}{\alpha-2} \tag{5.6.29}$$

For calculating displacements the steps followed are as follows

1 Find out α, G, H, c etc.
2 Determine ϕ_n for various modes[78]
3 Perform time history response analysis for a given bedrock earthquake data to find out $\psi_n(t)$. This can be very easily done by Wilson–θ or Newmark-β method as shown earlier
4 Obtain $u(z, t_p = \phi_v \cdot D)\psi_v(\tau)$
5 Determine $\dot{u}(z,t)$ and $\ddot{u}(z,t)$ by differentiating above
6 The absolute total acceleration, velocity and displacement can be obtained as

$$u_{tot}(z,t) = u(z,t) + u_g(z,t); \quad \dot{u}_{\text{tot}}(z,t) = \dot{u}(z,t) + \dot{u}_g(z,t);$$

$$\ddot{u}_{tot}(z,t) = \ddot{u}(z,t) + \ddot{u}_g(z,t) \tag{5.6.30}$$

For cohesion less soil considering $\alpha = 1/3$ Idriss and Seed has given following expression for sandy soil

$$\phi_n(z) = \left(\frac{1}{2}\beta_n\right)^{0.4}\Gamma(0.6)\left(\frac{z}{H}\right)^{1/3}J_{-0.4}\left[\beta_n\left(\frac{z}{H}\right)^{5/6}\right] \tag{5.6.31}$$

$$\ddot{\psi}_n(t) + 2D\omega_n\dot{\psi}_n(t) + \omega_n^2\psi_n(t) = -\ddot{u}_g\left[(\beta_n/2)^{1.4}\,\Gamma(0.6)J_{0.6}\,(\beta_n)\right]^{-1} \tag{5.6.32}$$

$\omega_n = \frac{\beta_n\sqrt{G/\rho}}{1.2H^{5/6}}$ and $\beta_1 = 1.751$, $\beta_2 = 4.8785$, $\beta_3 = 11.157$ for the first three mode.

For purely cohesive soil i.e. $\alpha = 0$ the expression gets modified to

$$\phi_n(z) = \cos\left[\frac{1}{2}(2n-1)\left(\frac{y}{H}\right)\right] \quad \text{and}$$

$$\ddot{\psi}_n(t) + 2D\omega_n\dot{\psi}_n(t) + \omega_n^2\psi_n(t) = (-1)^n\ddot{u}_g\left[\frac{4}{(2n-1)\,\pi}\right]\omega_n = \frac{(2n-1)\pi\sqrt{G/\rho}}{2H}. \tag{5.6.33}$$

78 In most of the practical case fundamental mode should suffice.

For fundamental mode the time period is thus given by

$$T = 4H/Vs \quad \text{where } G = \rho Vs^2 \tag{5.6.33a}$$

One of the advantages with time domain method is that incorporating non-linearity of soil is quite straight forward.

At every step of integration based on incremental displacement average strain in the soil can be estimated and based on the reference strain at which G was obtained the new G can be obtained as $G_{i+1} = G_{\max}/[1 + \psi_i/\psi_{\max}]$ and $D_{i+1} = D_i/(1 - G_i/G_{\max})$ where 'i' is the number of the step of the iteration[79].

5.6.1.11 A practical method for linear and non-linear dynamic analysis of ground due to earthquake

We show in Figure 5.6.7, a practical method (Chowdhury & Dasgupta 2007) for evaluation of ground response due to earthquake which gives a qualitative assessment of the behavior of soil under earthquake.

The strain energy of body in three dimensions is given by

$$V = \frac{\lambda e^2}{2} + G(\varepsilon_x^2 + \varepsilon_y^2 + \varepsilon_z^2) + \frac{G}{2}(\gamma_{xy}^2 + \gamma_{yz}^2 + \gamma_{xz}^2) \tag{5.6.34}$$

where V = strain energy density of the soil body; $\lambda = 2G\nu/(1 - 2\nu)$; G = dynamic shear modulus of the soil medium and νg its Poisson's ratio; $e = \varepsilon_x + \varepsilon_y + \varepsilon_z$; $\varepsilon_{x,y,z}$ = strain in the x, y and z direction and $\gamma_{xy,yz,zx}$ = shear strains in the xy, yz and zx planes respectively.

Assuming the condition of plane strain the strain energy equation can be rewritten as

$$V = \frac{G\nu}{1 - 2\nu}(\varepsilon_x + \varepsilon_z)^2 + G(\varepsilon_x^2 + \varepsilon_z^2) + \frac{G}{2}(\gamma_{xz}^2)$$

For impulsive seismic response, $\varepsilon_z = 0$ which reduces the above equation further to

$$V = \frac{G(1 - \nu)}{1 - 2\nu}\varepsilon_x^2 + \frac{G}{2}\gamma_{xy}^2 \tag{5.6.35}$$

Considering $u(x, z) = \phi(x, z)q(t)$, one can have

$$\frac{\partial V}{\partial q_r} = \frac{2G(1 - \nu)}{1 - 2\nu}\frac{\partial u}{\partial x}\frac{\partial}{\partial q_r}\left(\frac{\partial u}{\partial x}\right) + G\frac{\partial u}{\partial z}\frac{\partial}{\partial q_r}\left(\frac{\partial u}{\partial z}\right)$$

79 We will elucidate this further later, in the chapter titled Geotechnical Consideration for DSSI.

That is

$$\frac{\partial V}{\partial q_r} = \frac{2G(1-\nu)}{1-2\nu}\frac{\partial \phi_i}{\partial x}\frac{\partial \phi_r}{\partial x}q_i q_r + G\frac{\partial \phi_i}{\partial z}\frac{\partial \phi_r}{\partial z}q_i q_r \tag{5.6.36}$$

where $\phi(x, z)$ = generalized shape function with respect to x and z co-ordinate; $q(t)$ = displacement function with respect to time in generalized co-ordinate.

From which the stiffness and mass matrix can be written as

$$K_{ir} = \int_0^H \int_0^a \left[\frac{2G\,(1-\nu)}{1-2\nu}\frac{\partial \phi_i}{\partial x}\frac{\partial \phi_r}{\partial x} + G\frac{\partial \phi_i}{\partial z}\frac{\partial \phi_r}{\partial z}\right] dx\,dz, \quad \text{and}$$

$$M_{ir} = \frac{\gamma_s}{g}\int_0^H \int_0^a \phi_i \phi_r dx \cdot dz \tag{5.6.37}$$

where K = stiffness matrix of the soil medium; M = mass matrix of the soil medium; i and r are different modes 1, 2, 3. . .. . .K and M for the fundamental mode are given by

$$K_{11} = \int_0^H \int_0^a \left[\frac{2G\,(1-\nu)}{1-2\nu}\left(\frac{\partial \phi}{\partial x}\right)^2 + G\left(\frac{\partial \phi}{\partial z}\right)^2\right] dx \cdot dz \quad \text{and}$$

$$M_{11} = \frac{\gamma_s}{g}\int_0^H \int_0^a (\phi)^2\, dx \cdot dz.$$

For one dimensional analysis when $\lim a \to \infty$, the first term can be dropped and the stiffness and mass expression can be reduced to

$$K_{11} = \int_0^H \left[G\left(\frac{\partial \phi}{\partial z}\right)^2\right] \cdot dz; \quad M_{11} = \frac{\gamma_s}{g}\int_0^H (\phi)^2\, dz \tag{5.6.38}$$

Considering the shape function as given, $\phi(z) = \cos\frac{(2n-1)\pi z}{2H}$ and substituting it in the above Equations for a constant G value and by integrating we have

$$K_{11} = \frac{\pi^2 G}{8H} \quad \text{and} \quad M_{11} = \frac{\gamma_s H}{2g} \tag{5.6.39}$$

Considering $T = 2\pi\sqrt{M/K}$ one can arrive at the same expression as $T = 4H/V_s$ derived earlier vide Equation (5.6.33a).

This shows that the stiffness and mass matrix formulation as represented here is correct.

Considering a suitable damping ratio of soil as D the damping of the soil C may be arrived at from the expression

$$C = 2D\sqrt{KM} \tag{5.6.40}$$

Having formed the mass (M), damping (C) and stiffness matrix (K) one can now easily form the equation

$$M\ddot{u} + C\dot{u} + Ku = -M\ddot{u}_g \tag{5.6.41}$$

where u = displacement of the soil body at ground level; $\dot{u}$ = velocity of the soil body at ground level; $\ddot{u}$ = acceleration of the soil at ground level; $\ddot{u}_g$ = bedrock acceleration usually available as a time history data.

The above equation of motion can very easily be solved by one of the time history analysis methods to obtain the acceleration response at the ground level.

5.6.1.12 Linear and Non linear analysis

For linear behavior the analysis is now quite straightforward for G(dyn) and damping remaining invariable with time.

We show below some results of a soil layer of height 40 meter overlying bedrock having shear wave velocity of 120 m/sec subjected to the time history response of San Fernanado earthquake.

The density of soil is 20 kN/m^3. The shear wave velocity *vis-a-vis* dynamic shear modulus and damping @ 10% was obtained at a reference strain of 0.001.

For non linear analysis the strain was calculated at each time step and Dynamic Modulus of soil was upgraded as per Seed and Idriss expression while damping was upgraded based on Ishibashi and Zang's expression[80].

The comparative results are shown in Figures 5.6.10 to 13 for first 5 second of shaking.

Looking at the results we see that in this case peak bed rock acceleration is 0.31 g and this gets amplified to 0.71 g at ground level during elastic analysis however when non linear behavior of soil is considered the amplification is only marginal @ 0.34 g.

The variations of shear stress characteristics are markedly different for linear and non linear case.

Thus from above following conclusions can be made.

- Soil overlying rock, response gets amplified during an earthquake.
- The amplification is more pre-dominant if the soil remains with elastic range (i.e. stress strain relationship remains linear.)
- The behavior may attenuate under non linear behavior the variation of stress strain with time is quite different for linear and non-linear response.

80 Refer Chapter 1 (Vol. 2) the section on Geotechnical aspects of dynamic soil structure interaction for these expressions.

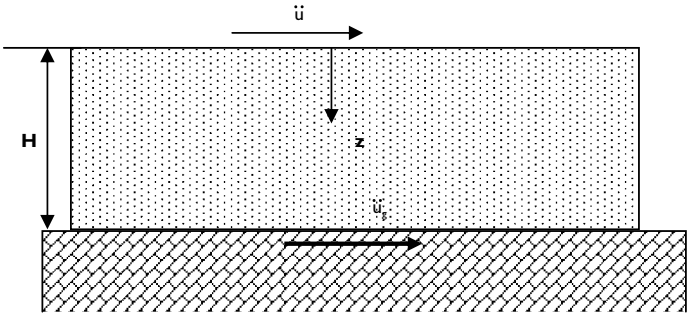


Figure 5.6.10 Horizontal soil layer of depth *H* underlain by rigid rock.

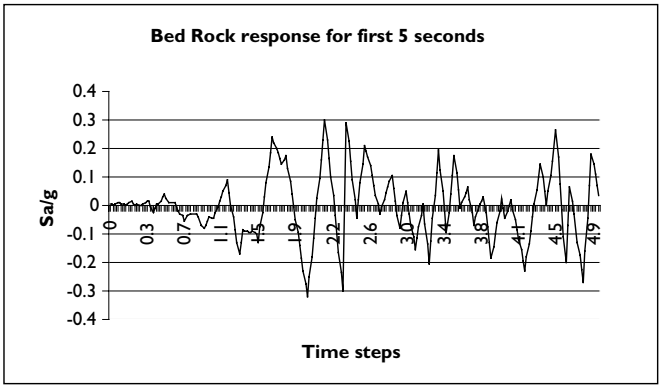


Figure 5.6.11 Bed rock response.

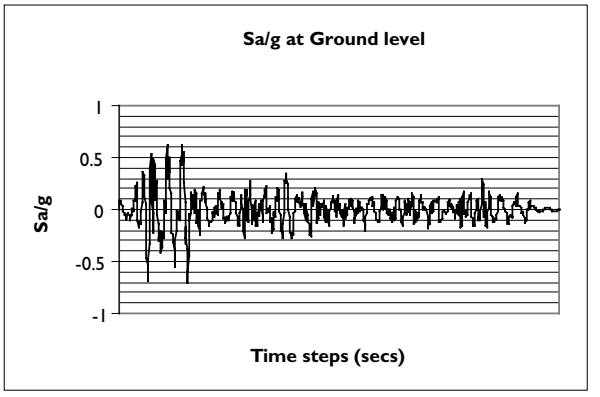


Figure 5.6.12 Amplified *Sa/g* at ground level.

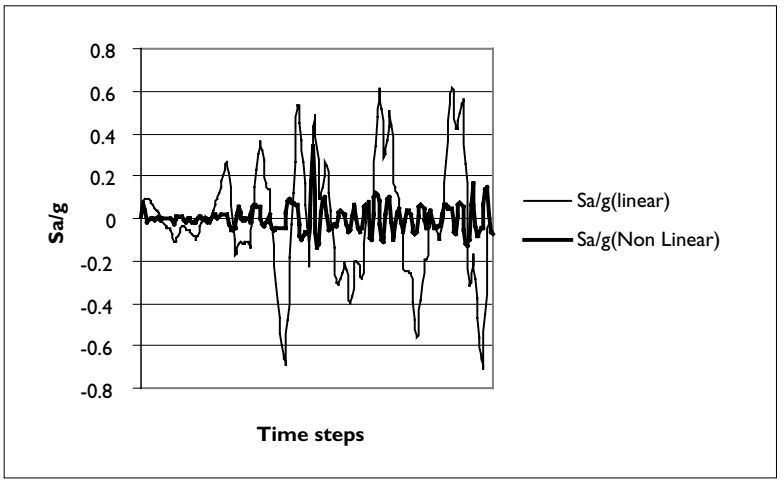


Figure 5.6.13 Comparison *Sa/g* for linear and non linear analysis at ground level.

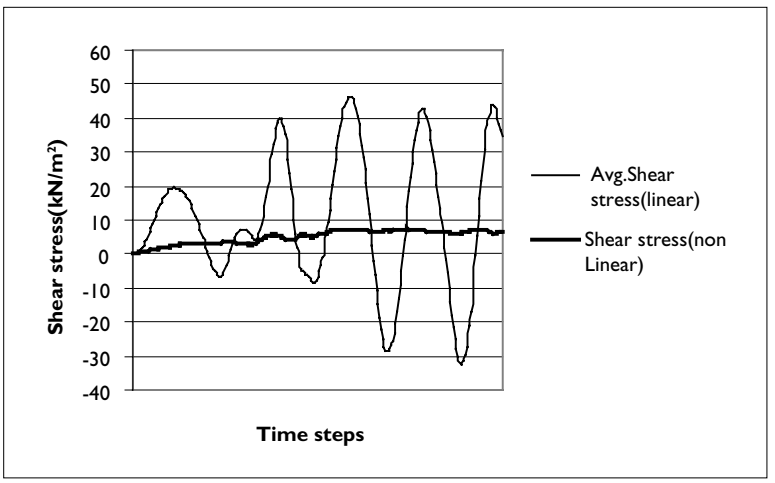


Figure 5.6.14 Variation of average shear stress for linear and nonlinear soil.

Other than the soil dynamics, many theories are extensively used to generate dynamic earth pressures on retaining structures, linear and non linear behavior of earth dam etc. These we have dealt separately later in Chapter 3 (Vol. 2) of earthquake resistant design and may be referred to further.

5.6.2 Waves induced by underground blast

Soil displacements at points located some distance away from the surface due to an underground disturbance is an interesting study. The waves emanating from the centre of the dynamic source, produced by an explosion, may be either longitudinal

or transverse waves propagating in an infinite media. Such a phenomenon refers to a military term 'Camouflet' and indicates an underground blast, the effect of which do not produce any visible displacement on the soil surface.

Barkan (1962) analysed the problem by treating the initial zone of excitement of the soil as spherical. The radial components of displacements are large in comparison with the tangential components. Thus for camouflet explosion the boundary condition of wave propagation, when $r = r_0$ may be taken as

$$u = \frac{x}{r} f(t); \quad v = \frac{y}{r} f(t); \quad w = \frac{z}{r} f(t) \tag{5.6.42}$$

where $f(t)$ is an assigned function of t.

Since the displacement is occurring only in the radial direction, only longitudinal waves will propagate from the explosion centre.

The displacement may be written as

$$u_r = -\frac{r_0^2 a\alpha}{r^2(\beta r_0 - a)} \left[\frac{r}{a} \left\{ 1 - \left(t - \frac{r}{a} + \frac{r_0}{\beta r_0 - a} \right) \beta \right\} + t - \frac{r}{a} + \frac{r_0}{\beta r_0 - a} \right] \times e^{[-\beta(t - \frac{r}{a})]} \quad \text{for } r > at. \tag{5.6.43}$$

where α and β depend on the properties of the explosion charge to be obtained experimentally.

The displacement of the camouflet surface created by the explosion is given by $f(t) = \alpha t e^{-\beta t}$, a is the velocity of compressional wave.

Equation (5.6.43) may be used to obtain the effect of an explosion at any distance from the charge. At small distance from the explosion centre the displacement dies out fast and the decrease is approximately proportional to the square of the distance. At large distance the decrease of the amplitude is inversely proportional to the distance.

5.7 GEOTECHNICAL ANALYSIS OF MACHINE FOUNDATIONS

5.7.1 Soil dynamics and machine foundation

Vibration of foundations under the influence of rotating machine is one of the most important developments in soil dynamics. We have dedicated one complete chapter in this book titled "Analysis and design of machine foundation", wherein we have shown various design techniques used for analysis and design of such foundations.

In this section we show some of the major theoretical development that took place in this area and how it got transformed from abstract and complex mathematical expression to what we see today in design offices around the world.

5.7.2 Reissner's method

We had shown earlier derivation of wave propagation in three dimensions as proposed by Lamb (1904). Based on Lamb's solution Reissner (1936) first developed the vertical response of a rigid footing resting on an elastic half space.

Shekter, as reported by Barkan (1962), corrected a mistake in Reissner's work and she presented a solution for the dynamic response of a uniformly loaded circular footing. The vertical displacement of the centre of a uniformly loaded [$Q_0 e^{i\omega t} = \pi r_0^2 q_0 e^{i\omega t}$] circular disc resting on the surface of an elastic halfspace obtained by Reissner is given by

$$w(0, 0, t) = \frac{Q_0 e^{i\omega t}}{G r_0}[f_1 + i f_2] \tag{5.7.1}$$

in which, $w(0, 0, t)$ = the vertical displacement at the centre of the cicular disc of radius r_0; Q_0 = force amplitude of the dynamic load; ω = circular frequency of the dynamic load; G = shear modulus of the elastic solid; and f_1, f_2 = compliance functions.

w and Q are in the same direction, downward (say z).

Reissner also defined non-dimensional parameters:

Dimensionless frequency $= a_0 = \omega r_0 \sqrt{\rho / G} = \omega r_0 / V_S$; V_S being the velocity of propagation of the shear wave in the elastic medium; ρ is its mass density, and mass ratio, $b_1 = m / \rho r_0^3$; m is the total mass of the vibrating footing and exciting mechanism on the elastic halfspace.

Reissner's solution for the amplitude of oscillator motion is given by

$$a_z = \frac{Q_0}{G r_0} \sqrt{\frac{f_1^2 + f_2^2}{(1 - b_1 a_0^2 f_1)^2 + (b_1 a_0^2 f_2)^2}} \tag{5.7.2}$$

The phase angle ϕ between the exciting force $Q = Q_0 e^{i\omega t}$ and the dynamic response z_0 is given by

$$\tan \varphi = \frac{f_2}{-f_1 + b_1 a_0^2 (f_1^2 + f_2^2)} \tag{5.7.3}$$

The power input required is given by

$$PR = \frac{Q_0^2}{r_0^2} \frac{a_0 f_1}{(1 - b_1 a_0^2 f_1)^2 + (b_1 a_0^2 f_2)^2} \tag{5.7.4}$$

For rotating mass type of oscillator (DEGEBO type), $Q_0 = m_e e \omega^2$, as described earlier.

Though Reissner's analysis and hence solution shown in Figs. 5.7.1 to 4, is an important landmark and has been the basis of subsequent development in this area it did not receive immediate credibility for application.

For when subjected to field test the theortical results varied significantly from observed data, and possibly the assumption of uniform contact pressure and application of the theory to only foundations of circular shape made its use very limited.

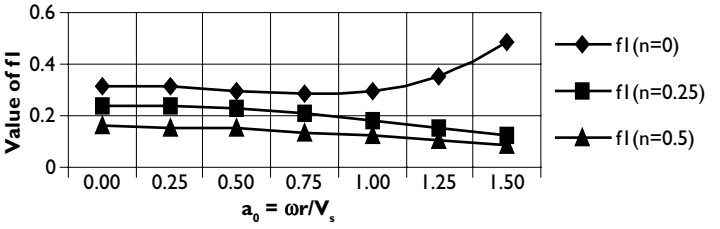


Figure 5.7.1 Coefficient f_1 for flexible foundation (Reissner 1936).

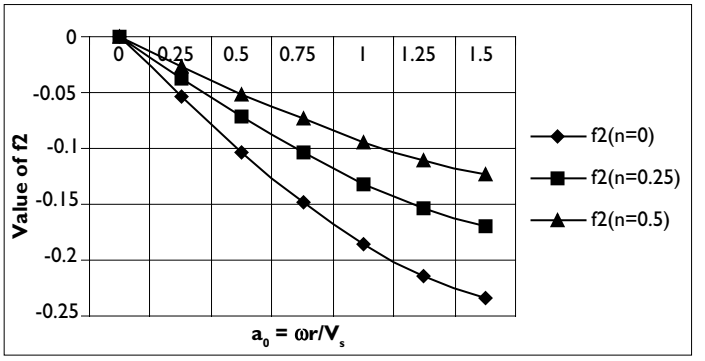


Figure 5.7.2 Coefficient f_2 for flexible foundation (Reissner 1936).

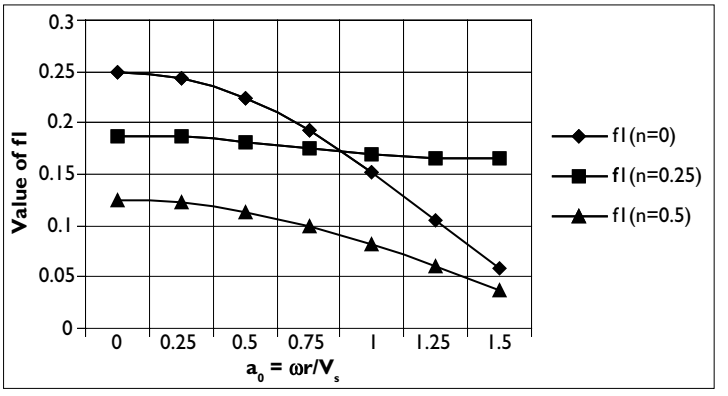


Figure 5.7.3 Coefficient f_1 for rigid foundation (Reissner 1936).

There was hardly any development for next 17 years[81] as the focus turned elsewhere possibly due to outbreak of Second World War.

81 At least there is no documentary evidence of this recorded.

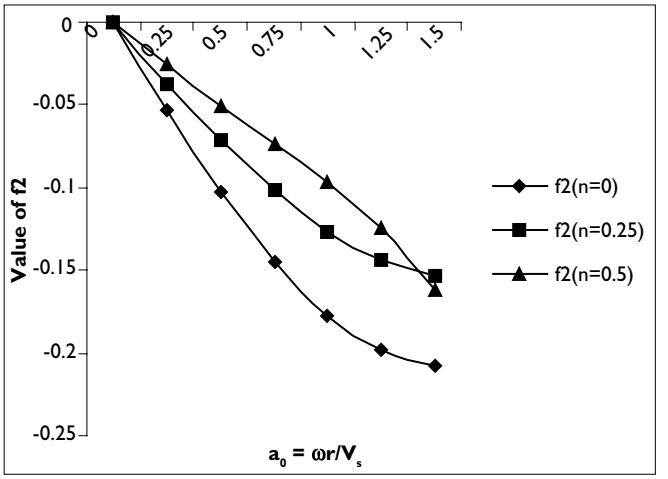


Figure 5.7.4 Coefficient f_2 for rigid foundation (Reissner 1936).
Note: Here *n* stands for Poisson's ratio in Figure 5.7.1 to 5.7.4.

5.7.3 Sung and Quinlan's method

Sung (1953) and Quinlan (1953) independently presented solutions for the dynamic response of a circular footing on an elastic halfspace shown in Figure 5.7.5. They considered three probable contact pressures at the footing-soil interface (Figure 5.7.6). These pressures are the dynamic equivalent to their static counterparts, namely, uniform, parabolic and the one corresponding to rigid base condition. They were able to evaluate the resonant frequency, amplitude, power input necessary to maintain the vibration and the displacement at the centre of the footing. A constant as well as frequency dependent loading was also considered in the analysis.

Sung extended Reissner's solution and developed equations for all the three cases of contact pressure distributions on a circular loaded area and reported the solution in series form with varying Poisson ratios. Sung considered an axially symmetric distributed total force $Q(r,t)$ with frequency ω, the footing-soil contact stress (stress boundary condition for elastic halfspace) can be expressed as given in the following.

Quinlan, although established equations for all three contact pressures, presented only the results for rigid base approximation. He also proposed the solution for a long rectangular vibrator assuming various contact pressure distributions using a different approach.

For numerical computation the functions f_1 and f_2 as proposed by Sung are as given Table 5.7.1 and shown in Figure 5.7.7.

The displacement at center of contact area of a circular foundation resting on half space is expressed as

$$w(0,0,t) = \frac{Q_0 e^{i\omega t}}{G r_0}\left[f_1 + i f_2\right] \tag{5.7.5}$$

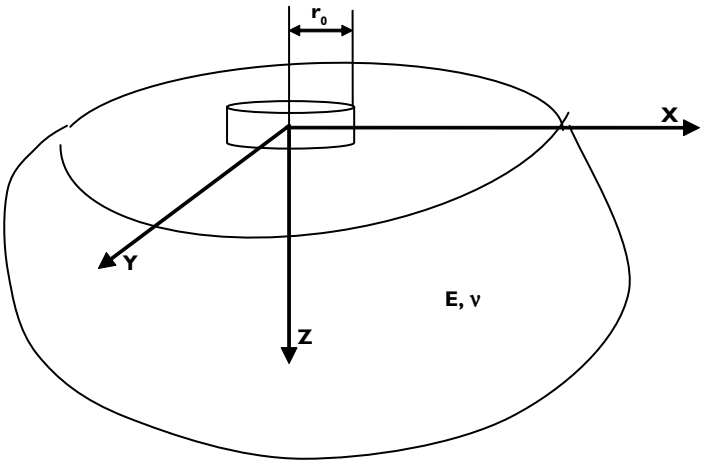


Figure 5.7.5 Geometrical description of a circular disc resting on elastic halfspace.

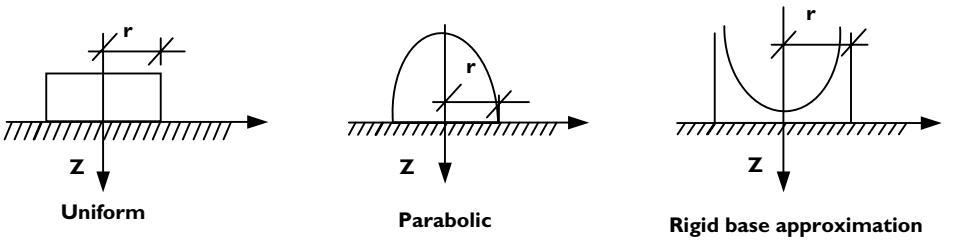


Figure 5.7.6 Contact pressure distributions.

where, $w(0, 0, t)$ = the vertical displacement at the centre of the cicular disc of radius r_0; Q_0 = force amplitude of the dynamic load; ω = circular frequency of the dynamic load; G = shear modulus of the elastic solid; and f_1, f_2 = compliance functions.

5.7.4 Bycroft's solution for dynamic response of foundation

Arnlod et al. (1955) computed the dynamic response of a rigid circular foundation on an elastic halfspace in the vertical mode of vibration as well as other modes namely, rocking and sliding. Contact pressures used by Quinlan and Sung are the equivalent dynamic pressure of their static counterparts. In rigid base a uniform dynamic displacement beneath the footing is not always true. It varies with frequency. With this in view, a weighted average of displacement under the footing and an average magnitude of displacement functions were evaluated. The weighted average solution corresponds to applying the total dynamic force, [say $Q = \int p dA$, where p and A are the contact pressure and area, respectively] to a rigid block whose area is such that the work done by the dynamic applied force is just equal to the work done by the contact pressures.

Table 5.7.1 Compliance functions f_1 and f_2.

Rigid Base	$\nu = 0$	$-f_1 = 0.2500 - 0.100375\ a_0^2 + 0.010205\ a_0^4$
	$\nu = 1/4$	$-f_1 = 0.187500 - 0.0703131\ a_0^2 + 0.006131\ a_0^4$
	$\nu = 1/3$	$-f_1 = 0.166667 - 0.060761\ a_0^2 + 0.005085\ a_0^4$
	$\nu = 1/2$	$-f_1 = 0.125000 - 0.046875\ a_0^2 + 0.003581\ a_0^4$
Uniform	$\nu = 0$	$-f_1 = 0.318310 - 0.092841\ a_0^2 + 0.007405\ a_0^4$
Loading	$\nu = 1/4$	$-f_1 = 0.238733 - 0.059683\ a_0^2 + 0.004163\ a_0^4$
	$\nu = 1/3$	$-f_1 = 0.212207 - 0.051578\ a_0^2 + 0.003453\ a_0^4$
	$\nu = 1/2$	$-f_1 = 0.159155 - 0.039789\ a_0^2 + 0.002432\ a_0^4$
Parabolic	$\nu = 0$	$-f_1 = 0.424414 - 0.074272\ a_0^2 + 0.004232\ a_0^4$
Loading	$\nu = 1/4$	$-f_1 = 0.318310 - 0.047747\ a_0^2 + 0.002379\ a_0^4$
	$\nu = 1/3$	$-f_1 = 0.282942 - 0.041262\ a_0^2 + 0.001973\ a_0^4$
	$\nu = 1/2$	$-f_1 = 0.212207 - 0.031831\ a_0^2 + 0.001389\ a_0^4$
Rigid Base	$\nu = 0$	$f_2 = 0.214714\ a_0 - 0.039116\ a_0^3 + 0.002414\ a_0^5$
	$\nu = 1/4$	$f_2 = 0.148594\ a_0 - 0.023677\ a_0^3 + 0.001291\ a_0^5$
	$\nu = 1/3$	$f_2 = 0.130630\ a_0 - 0.020048\ a_0^3 + 0.001052\ a_0^5$
	$\nu = 1/2$	$f_2 = 0.104547\ a_0 - 0.014717\ a_0^3 + 0.000717\ a_0^5$
Uniform	$\nu = 0$	$f_2 = 0.214474\ a_0 - 0.019708\ a_0^3 + 0.001528\ a_0^5$
Loading	$\nu = 1/4$	$f_2 = 0.148591\ a_0 - 0.017557\ a_0^3 + 0.000808\ a_0^5$
	$\nu = 1/3$	$f_2 = 0.130630\ a_0 - 0.015037\ a_0^3 + 0.000658\ a_0^5$
	$\nu = 1/2$	$f_2 = 0.101547\ a_0 - 0.011038\ a_0^3 + 0.000441\ a_0^5$
Parabolic	$\nu = 0$	$f_2 = 0.214474\ a_0 - 0.019708\ a_0^3 + 0.000761\ a_0^5$
Loading	$\nu = 1/4$	$f_2 = 0.148591\ a_0 - 0.011837\ a_0^3 + 0.000405\ a_0^5$
	$\nu = 1/3$	$f_2 = 0.130630\ a_0 - 0.010024\ a_0^3 + 0.000328\ a_0^5$
	$\nu = 1/2$	$f_2 = 0.104574\ a_0 - 0.007358\ a_0^3 + 0.000222\ a_0^5$

Bycroft computed the weighted average of the displacements beneath the footing to obtain the vaules of the compliance functions f_1 band f_2. All these solutions are valid for small frequency ratios ($a_0 < 1.5$), and it was shown by Richart (1962) that this range includes the operational frequencies of most of the practical problems. The compliance functions mentioned in Equation (5.7.1) are shown in Figure 5.7.8.

Bycroft (1977) extended his studies to the forced vibrations of a rigid circular plate attached to the surface of an elastic halfspace for large values of the frequency. Response under a non-sinusoidal forced motions of a system may be evaluated from the steady state solutions using a Fourier synthesis of the steady state solutions and a Fast Fourier Transform procedure to evaluate the resulting infinite integrals with their oscillatory integrands. The integrals are formally taken over an infinite range in the frequency domain, and this means that one needs the steady state solutions over finite fruency range depending upon the system and the frequency content of the input function. Again, while solving soil-structure interaction

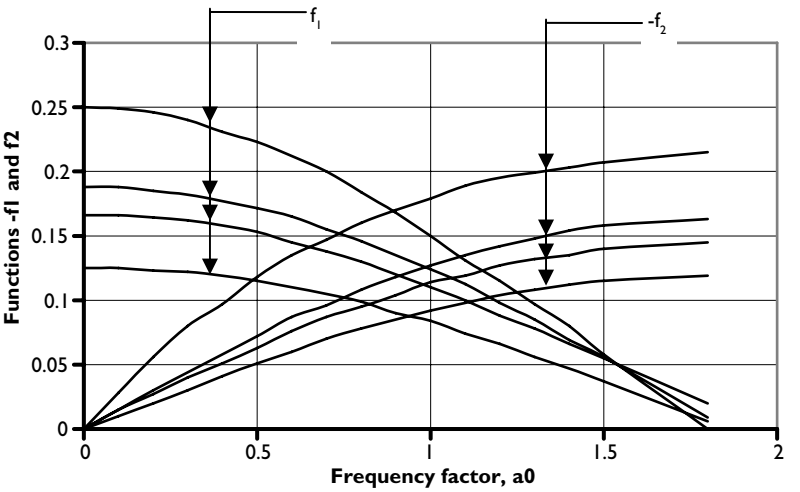


Figure 5.7.7 Compliance functions f_1 and f_2 for rigid circular plates (Sung 1953).

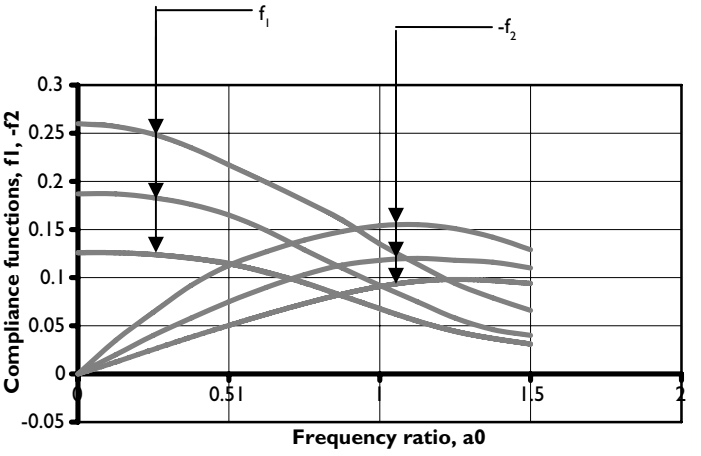


Figure 5.7.8 Displacement functions for rigid circular footing vibrating vertically on the surface of an elastic half-space (Bycroft 1956).

problems, such situation arises when high-frequency components of earthquakes are associated with a relatively rigid foundation of large base area and located on a soft terrain.

The displacements U, V and W of the plate is given by the real part of

$$U, V, W = (-Pe^{i\omega t}/Gr_0)(f_1 + if_2) \tag{5.7.6}$$

and the rotation is given by

$$\Phi = (-Me^{i\omega t}/Gr_0^3)(f_1 + if_2) \tag{5.7.7}$$

where the compliance functions f_1 and f_2 are functions of a_0 and τ, and are different for each of the four modes, $\tau = \sqrt{(1-2\nu)/2(1-\nu)}$ and ν is the Poisson's ratio.

5.7.4.1 Vertical translation

5.7.4.1.1 For compressible medium

The average displacement of the plate w is given by

$$w = \frac{Pe^{i\omega t}}{2\pi Gr_0}\left[\int_0^\infty \frac{\sqrt{\theta^2-\tau^2}J_1^2(a_0\theta_1)}{a_0\theta_1 f'(\theta_1)}d\theta - \frac{i\pi\sqrt{\theta_1^2-\tau^2}J_1^2(a_0\theta_1)}{a_0\theta_1 f'(\theta_1)}\right] \tag{5.7.8}$$

where θ_1 is the root of the equation: $f(\theta) = (\theta^2 - 1/2)^2 - \theta^2\sqrt{(\theta^2-\tau^2)}\sqrt{(\theta^2-1)}$.

Here the principal value of the infinite integral is to be taken and for large a_0 i.e for high frequency f_1 and f_2 may be evaluated as

$$f_1 = K_V/a_0^2; \quad f_2 = \tau/\pi a_0 \tag{5.7.9}$$

in which K_V may be obtained from Table 5.7.2.

5.7.4.1.2 Incompressible medium

The average vertical displacement is given by

$$w = \frac{Pe^{i\omega t}}{2\pi Gr_0}\left[\int_0^\infty \frac{\left[\frac{\sin a_0\theta}{a_0\theta} - \cos a_0\theta\right]^2 d\theta}{a_0^3\theta^2 f(\theta)} - \frac{i\pi\left[\frac{\sin a_0\theta_1}{a_0\theta_1} - \cos a_0\theta_1\right]}{a_0^3\theta_1^2 f'(\theta_1)}\right] \tag{5.7.10}$$

where θ_1 is as defined above.

Following the similar arguments as in the previous case,

$$f_1 = 3/4a_0^2; \quad f_2 = 1.93/a_0^2 \tag{5.7.11}$$

The surface wave contributes to the function f_2.

Table 5.7.2 Coefficients K_V.

τ^2	ν	K_V
0.250	0.333	−0.0596
0.333	0.25	−0.0820
0.500	0	−0.928

5.7.4.2 Rotation about a vertical axis

Only the shear wave exists in this case. For high frequencies the shear stress distribution is proportional to the radius from the axis of rotation. The average angle of rotation of the plate can be expressed as

$$\phi = -\frac{8M}{\pi G r_0^3} \int_0^\infty \frac{J_2^2(a_0\theta)d\theta}{a_0\theta\sqrt{\theta^2-1}}$$

from which it follows that

$$f_1 = \frac{-8}{\pi} \int_1^\infty \frac{J_2^2(a_0\theta)d\theta}{a_0\theta\sqrt{(\theta^2-1)}} \tag{5.7.12}$$

Finally,

$$f_1 = \frac{-8}{\pi^2 a_0^2}\left(1+\frac{2.34}{a_0^2}\right); \quad f_2 = \frac{2}{\pi a_0} \tag{5.7.13}$$

5.7.4.3 Rotation about a horizontal axis

5.7.4.3.1 Compressible medium

Wave lengths are taken to be small in comparison with the dimensions of the plate. The criterion for the shear waves to have a relatively short wave length is that the frequency factor a_0 is large and for the compressional waves that $a_0\tau$ be large. As long as τ is finite, which means that the medium is compressible, than these criteria are satisfied by large values of a_0. The shear stresses on the surface are set equal to zero. The average angle of rotation of the plate is given by

$$\phi = \frac{4Me^{ipt}}{G\pi r_0^3}\left[\int_0^\infty \frac{\left(\sqrt{\theta^2-\tau^2}\right)J_2^2(a_0\theta)d\theta}{a_0\theta f(\theta)} - \frac{i\pi\left(\sqrt{\theta_1^2-\tau^2}\right)J_2^2(a_0\theta_1)}{a_0\theta_1 f'(\theta_1)}\right] \tag{5.7.14}$$

where $f(\theta)$ has been written earlier and the principal part of the integral is to be taken.

Compliance functions f_1 and f_2 reduce to

$$f_1 = \frac{4}{\pi}\left[\int_\tau^1 \frac{(\sqrt{\theta^2-\tau^2})(\theta^2-1/2)^2 J_2^2(a_0\theta)d\theta}{a_0\theta[(\theta^2-1/2)^4-\theta^4(\theta^2-\tau^2)(\theta^2-1)]} + \int_1^\infty \frac{(\sqrt{\theta^2-\tau^2})J_2^2(a_0\theta)d\theta}{a_0\theta f(\theta)}\right] \tag{5.7.15}$$

Table 5.7.3

τ^2	ν	K_R
0.250	0.333	−0.476
0.333	0.25	−0.654
0.500	0	−0.741

$$f_2 = \frac{4}{\pi a_0}\int_0^{a_0\tau} \frac{\sqrt{[\tau^2 - (\xi^2/a_0^2)]}\, J_2^2(\xi)d\xi}{\xi\{[(\xi^2/a_0^2) - 1/2]^2 - (\xi^2/a_0^2)[\sqrt{(\xi^2/a_0^2) - 1}][\sqrt{(\xi^2/a_0^2) - \tau^2}]\}}$$

$$= \frac{16\tau}{\pi a_0}\int_0^{\infty} \frac{J_2^2(\phi)d\phi}{\phi} \tag{5.7.16}$$

When $a_0\tau$ is large asymptotic values of f_1 and f_2 reduce to

$$f_1 = \frac{K_R}{a_0^2} \quad \text{and} \quad f_2 = \frac{4\tau}{\pi a_0} \tag{5.7.17}$$

The values of K_R is shown in Table 5.7.3.

The function f_2 represents the energy propagated. The free wave term or Rayleigh wave term shown in Equation (5.7.14) is of the order of $1/a_0^2$. Thus for high frequencies the energy tend to propagate vertically.

5.7.4.3.2 Incompressible medium

$$\phi = \frac{450Me^{ipt}}{32\pi\mu r_0^3}\left[\int_0^{\infty} \frac{\left\{\sin a_0\theta\left[\frac{3}{(a_0\theta)^2} - 1\right] - \left[\frac{3\cos a_0\theta}{a_0\theta}\right]\right\}^2}{a_0^3\theta^2 f(\theta)}d\theta\right.$$

$$\left. - \frac{i\pi\left\{\sin a_0\theta_1\left[\frac{3}{(a_0\theta_1)^2} - 1\right] - \left[\frac{3\cos a_0\theta_1}{a_0\theta_1}\right]\right\}^2}{a_0^3\theta_1^2 f'(\theta_1)}\right] \tag{5.7.18}$$

Compliance functions f_1 and f_2 may be written as

$$f_1 = \frac{45}{8a_0^2}; \quad f_2 = \frac{24.7}{a_0^3} \tag{5.7.19}$$

This case is in contrast to the compressible case where f_2 decreases as a_0^{-1}.

5.7.4.4 Horizontal translation

If a horizontal force is applied to the centre of the plate, both horizontal translation and rotation about a horizontal axis will occur. To simplify the matter a constraint will be imposed to prevent rotation. In this case shear predominates, and the stress distribution under the plate may be shown to be constant for both the compressible and incompressible cases.

The horizontal displacement is then given by

$$U = \frac{-P}{\pi \mu r_0} \int_0^\infty \frac{J_1^2(a_0\theta)}{a_0\theta} \left[\frac{\theta^2}{\sqrt{\theta^2 - \tau^2}} - \sqrt{\theta^2 - 1} + \frac{1}{\sqrt{\theta^2 - 1}} \right] d\theta \tag{5.7.20}$$

5.7.4.4.1 Compressible media

$$f_1 = \frac{-1}{\pi^2 a_0^2}[2 - \log \tau]; \quad f_2 = 1/\pi a_0 \tag{5.7.21}$$

The expression for f_1 diverges as $\nu \to 0.5$ and $\tau \to 0$ and a different asymptotic value must be determined.

5.7.4.4.2 Incompressible media

In this case the expression for f_2 is the same as before, but f_1 has a different form

$$f_1 = \frac{-1}{\pi a_0} \int_0^1 J_1^2(\pi a_0) d\theta - \frac{1}{\pi} \int_1^\infty \frac{J_1^2(\pi a_0)}{\pi a_0} \left(\theta - \sqrt{\theta^2 - 1} + \frac{1}{\sqrt{\theta^2 - 1}} \right) d\theta \tag{5.7.22}$$

The first integral does not have an asymptotic value and must be evaluated numerically.

The second term may be evaluated and may be written as

$$f_1 = \frac{-1}{\pi^2 a_0^2}[2 - \log 2] - \frac{1}{\pi a_0} \int_0^1 J_1^2(\pi a_0) d\theta \tag{5.7.23}$$

5.7.5 Reissner and Sagoci's method of torsional oscillation

Reissner & Sagoci (1944) gave the solution for the torsional mode of vibration of a rigid circular footing resting on the surface of the elastic half-space. The oscillation is

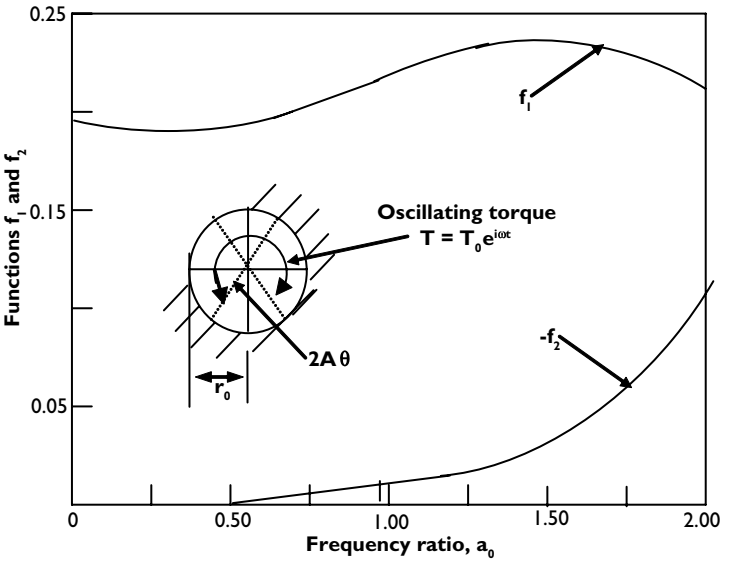


Figure 5.7.9 Compliance functions for torsional mode of rigid circular foundations (Reissner & Sagoci 1944).

about a vertical axis through the center of the contact area. Compliance functions for torsional mode of rigid circular Foundations are shown in Figure 5.7.9.

A linear variation of the displacement from the center of the rigid foundation to the periphery was assumed. The angle of rotation is given by

$$\varphi = \frac{T_0 e^{i\omega t}}{G r_0^3}[f_1 + i f_2] \tag{5.7.24}$$

in which ϕ = angle of rotation; T_0 = amplitude of torsional moment; G = shear modulus of the soil; ω angular frequency of vibration; f_1 and f_2 = compliance functions.

It has been observed that compliance functions are invariant to the variation of Poisson's ratio.

Again by using the dimensionless frequency ratio $a_0 = \omega r_0 / V_S$ and the mass ratio $b_\theta = I_\theta / \rho r_0^5$, where I_θ is the mass moment of inertia of the footing about the axis of rotation, the dynamicmic response has been computed.

5.7.6 Hseih's method for dynamic response of foundation

We will not work out in detail the derivation here as this has already been discussed in detail in Chapter 2 (Vol. 2) Analysis and Design of Machine Foundation.

Suffice it to say that Hseih (1962) first showed the possibility of an elastic half space that may be converted to a mechanical analog of spring and dashpot.

He first considered a weightless circular disc of radius r_0 resting on a elastic half space, subjected to a vertical oscillating force $Q = Q_0 e^{i\omega t}$.

The vertical displacement is given by

$$z = \frac{Q_0 e^{i\omega t}}{Gr_0}(f_1 + if_2) \tag{5.7.25}$$

Differentiating Equation (5.7.25) with respect to time one gets

$$\frac{dz}{dt} = \frac{\omega Q_0 e^{i\omega t}}{Gr_0}(if_1 - f_2)$$

which leads to $$f_1 \omega z - f_2 \frac{dz}{dt} = \frac{Q_0 \omega e^{i\omega t}}{Gr_0}(f_1^2 + f_2^2) \tag{5.7.26}$$

and gives $$Q_0 e^{i\omega t} = -\frac{Gr_0}{\omega}\frac{f_2}{f_1^2 + f_2^2}\frac{dz}{dt} + Gr_0 \frac{f_1}{f_1^2 + f_2^2} z. \tag{5.7.27}$$

The above can be represented in terms of mechanical analog now as

$$Q = \frac{Gr_0}{\omega}\frac{-f_2}{f_1^2 + f_2^2}\frac{dz}{dt} + Gr_0 \frac{f_1}{f_1^2 + f_2^2} z = c\frac{dz}{dt} + kz \tag{5.7.28}$$

where $c = \frac{Gr_0}{\omega}\frac{-f_2}{f_1^2+f_2^2} = \frac{r_0^2}{a_0}\sqrt{\rho G}\frac{-f_2}{f_1^2+f_2^2}$ and $k = Gr_0\frac{f_1}{f_1^2+f_2^2}$.

It is seen that both c and k are dependent on the Poisson's ratio(ν) and dimensionless frequency number a_0.

Hsieh also considered a rigid circular footing of weigh W resting on an elastic half space for which he derived the equation

$$\frac{W}{g}\frac{d^2 z}{dt^2} + c\frac{dz}{dt} + kz = P_0 e^{i\omega t} \tag{5.7.29}$$

where c and k are as derived above.

5.7.7 Lysmer and Richart's model for dynamic response of foundation

By 1960 the mathematics behind mechanics of a spring and dashpot connected to a lumped mass and its behavior under dynamic load was sufficiently developed. Civil engineers working in the area of structural dynamics were regularly using this model for analyzing the behavior of structures having single and multi-degrees of freedom. This model had great advantage, for in this case the equivalent springs developed to describe

the structural stiffness were frequency independent. This made the mathematical calculations much simplified and their physics relatively easy to interpret.

On the contrary applying the elastic half space theory with frequency dependent springs and dashpot not only made the foundation analysis tedious but also called for significant amount of trial and error which made its application very limited. Thus obviously a search was on to find an equivalent mechanical analog for the elastic half space theory which would be simple to apply yet give a result close to the rigorous solution based on the classical theory.

Lysmer and Richart (1966) considered a class of elastic systems a typical is shown in Figure 5.7.10. It consists of a linear elastic system S that is excited by a periodic vertical force $P(t)$, of frequency ω and amplitude P_0. The system may or may not contain viscous damping (Figure 5.7.11) and it may have finite or infinite dimensions.

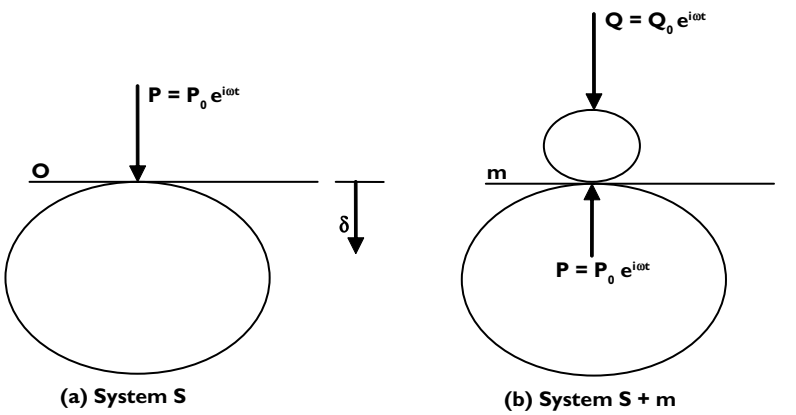


Figure 5.7.10 Typical linear system in elastic half space.

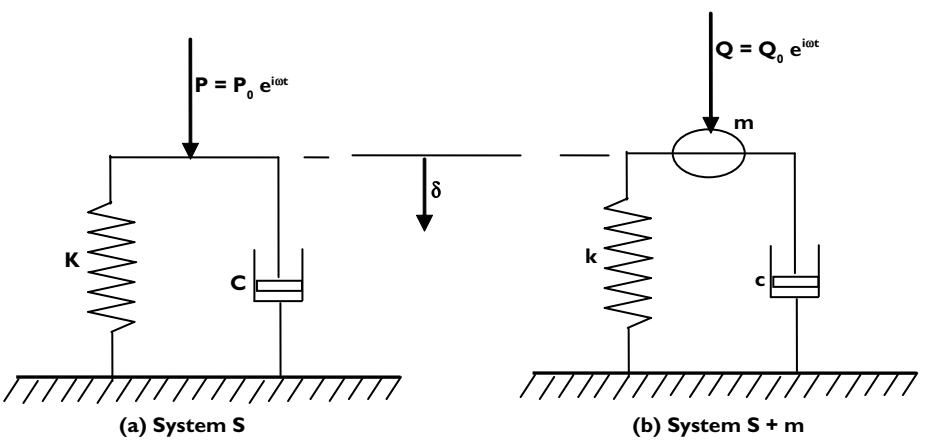


Figure 5.7.11 Simpled mechanical analog.

The force is given by $P = P_0 \exp(i\omega t)$ is assumed to act at a point O, which is such that the displacement a_z of point O is vertical at all times.

Following Bycroft, Lysmer started with compliant functions

$$f = f_1 + if_2$$

He however noticed that when the above function is multiplied by a factor $\frac{4}{1-\nu}$ the functions became independent of Poisson's ratio. Thus he defined a new compliance function

$$F = \frac{4}{1-\nu} f = F_1 + iF_2. \tag{5.7.30}$$

Based on above, the Bycroft's-curves (presented earlier) merge to almost a unique curve as shown in Figure 5.7.12.

When $a_z = \frac{P}{k} F$ as per analog figure as shown above

Lysmer also introduced a modified dimensionless mass ratio

$$B_z = \frac{1-\nu}{4} \frac{m}{\rho r_0^3} \tag{5.7.31}$$

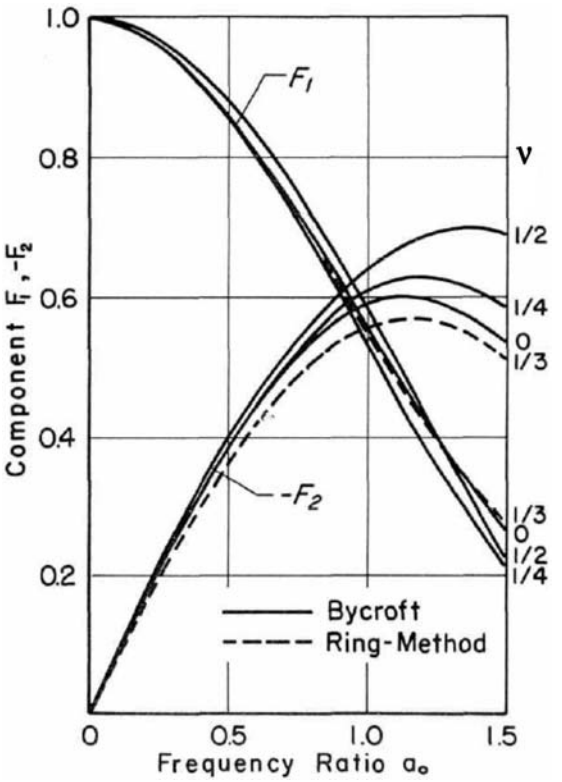


Figure 5.7.12 Compliance functions *F* (Lysmer & Richart 1966).

Substituting the above parameters in Reissner's solution for displacement

$$a_z = \frac{Q_0}{Gr_0}\sqrt{\frac{f_1^2 + f_2^2}{(1 - b_1 a_0^2 f_1)^2 + (b_1 a_0^2 f_2)^2}}, \tag{5.7.32}$$

Lysmer finally obtained an epxression

$$a_z = \frac{1 - \nu}{4Gr_0} P_0 M \tag{5.7.33}$$

where M is the magnification factor by which the equivalent static displacement produced by P_0 is mutiplied to give the dynamic dispalcement amplitude.

For a mechanical analog with spring and dashpot subjected to a dynamic force P_0 the amplitude is given by[82]

$$a_z = \frac{P_0}{k\sqrt{(1 - r^2) + 2D\,r^2}} \tag{5.7.34}$$

where r is the frequency ratio D is damping ratio, k is static spring stiffness and the magnification factor M is given by

$$M = \frac{1}{\sqrt{(1 - r^2) + 2Dr^2}} \tag{5.7.35}$$

thus above equation can now be expressed as $a_z = \frac{P_0}{k} M$; equating this with half space equation we have $a_z = \frac{P_0}{k} M = \frac{1-\nu}{4Gr_0} P_0 M$, which gives

$$k = \frac{4Gr_0}{1 - \nu} \tag{5.7.36}$$

which is a frequency independent static spring value for the soil[83].

Based on above Lysmer made a comparison of amplitudes for various mass ratio and the values are as shown in Figure 5.7.13.

Here the firm lines represent the response based on elastic half space theory, while the dotted lines show the corresponding response due to mechanical analog as proposed by Lysmer – the results are surely very encouraging.

The above, to our perception is a landmark contribution in analysis of machine foundation. It not only made the analysis much simplified but also brought the physics

82 For derivation of this expression refer Chapter 3 (Vol. 1).

83 It is interesting to note that though many engineers use these spring value in their day to day to work almost routinely for design of machine foundation or perform analysis of other structures considering dynamic soil-structure interaction, very few have the background on how this is arrived at. Many even believe that this value is empirical!

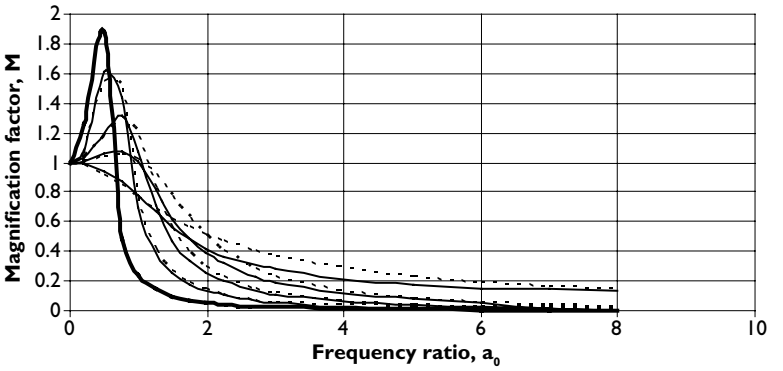


Figure 5.7.13 Steady state spectra for footing-soil system.

of the phenomenon well within the grasp of an average engineer undertaking analysis and design of such foundations.

Lysmer also compared the values of damping and found that the best fit value for the damping in the range of $0 < a_0 < 1.0$ is given by

$$c_z = \frac{3.4r_0^2}{1-\nu}\sqrt{\rho G} \tag{5.7.37}$$

based on which the equation of motion for a foundation under dynamic loading can now be expressed as

$$m\frac{dz^2}{dt^2} + \frac{3.4r_0^2}{1-\nu}\sqrt{\rho G}\frac{dz}{dt} + \frac{4Gr_0}{1-\nu}z = P(t) \tag{5.7.38}$$

5.7.8 Hall's analog for sliding and rocking vibration

Following Lysmer's success in developing an equivalent mechanical analog for elastic half space theory in vertical mode, Hall (1967) followed a similar procedure to develop equivalent static springs for sliding and rocking mode.

Starting with the solution to the motion of a rigid circular plate on the surface of an elastic half space given by Bycroft (1956), Hall developed coupled rocking and sliding motion for all Poisson's ratios. Shown in Figure 5.7.14 is a weightless disc on the surface of an elastic half space with shear modulus G, Poisson's ratio ν and mass density ρ.

Let the horizontal displacement of the disc be

$$x = x_0 e^{i\omega t}, \tag{5.7.39}$$

where, x_0 = the amplitude of the displacement; ω = the circular frequency and t = time.

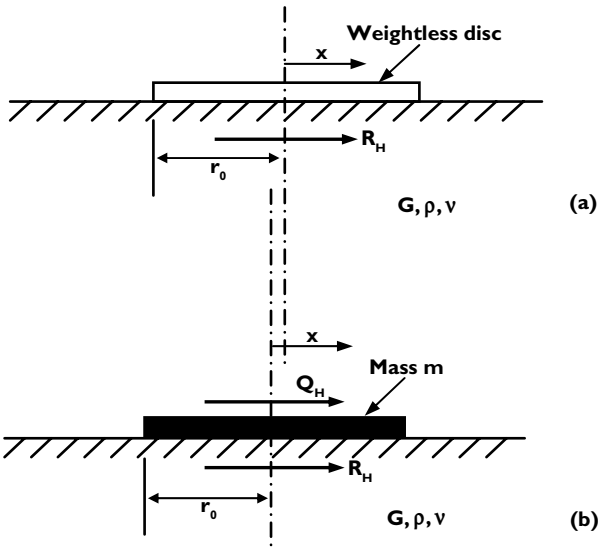


Figure 5.7.14 Sliding motion.

The reaction developed on the base of the disc may be written as

$$R_H = R_{H0} e^{i\omega t} \tag{5.7.40}$$

The displacement and reaction relation may be expressed as

$$x = \frac{R_{H_0}}{Gr_0} \left(f_1 + if_2\right) e^{i\omega t} \tag{5.7.41}$$

where the displacement functions f_1 and f_2 are the functions of ν and dimensionless frequency given by

$$a_0 = \omega r_0 \sqrt{\rho / G} \tag{5.7.42}$$

Following Hsieh's (1962) analysis Hall took the soil reaction as

$$R_{H0} = -\frac{Gr_0}{\omega} \frac{f_2}{f_1^2 + f_2^2} \frac{dx}{dt} + Gr_0 \frac{f_1}{f_1^2 + f_2^2} x \tag{5.7.43}$$

The velocity term arises from the fact that the energy is transmitted into the half space without being returned back to the footing and provides an apparent damping in the system known as *radiation damping*.

Equation (5.7.17) is further simplified by introducing the notation

$$F_1 = \frac{-f_1}{f_1^2 + f_2^2} \quad \text{and} \quad F_2 = \frac{f_2}{a_0\left(f_1^2 + f_2^2\right)} \tag{5.7.44}$$

From Bycroft's (1956) solution and using the best least-square approximation using seven points in the interval 0 to 1.5 for $\nu = 0$, and $0 \leq a_0 \leq 1.5$, Hall obtained F_1 and F_2 as follows

$$F_1 = 4.573 - 0.02004a_0 - 0.2122a_0^2; \quad F_2 = 2.610 - 0.01257a_0 + 0.1025a_0^2 \tag{5.7.45}$$

When the footing has a mass as shown in above figure a force $Q_H = Q_{H0}e^{i\omega t}$ acts on the mass, the equation of motion can be written as

$$m\frac{d^2x}{dt^2} + r_0^2\sqrt{G\rho}\,F_2\frac{dx}{dt} + Gr_0F_1x = Q_{H0}e^{i\omega t} \tag{5.7.46}$$

A similar equation used for a single degree-of-freedom system with viscous damping, only difference is that the damping and spring constants are frequency dependent.

Thus comparing the equations derived from elastic half space with the mechanical analog we have $k_x = Gr_0F_1$ and $c_x = r_0^2\sqrt{\rho G}F_2$.

For static case when $a_0 = 0$, $F_1 = 4.573$ for $\nu = 0$ thus the spring stiffness can now be expressed as $k_x = 4.573Gr_0$ this can thus be further expressed as $k_x = (32Gr_0)/7$. For $\nu \neq 0$ the value is further expressed as

$$k_x = \frac{32\,(1-\nu)}{7-8\nu}Gr_0 \tag{5.7.47}$$

For damping we had shown above that $c_x = r_0^2\sqrt{\rho G}F_2$.

This can be further expressed $c_x = r_0^2F_1\frac{\sqrt{\rho G}F_2}{F_1}$ for static case this becomes

$$c_x = r_0^2F_1\frac{\sqrt{\rho G}2.61}{4.573} = 0.5707413r_0^2F_1\sqrt{\rho G}$$

For $\nu \neq 0$ this can be further approximated to

$$c_x = \frac{18.4(1-\nu)}{7-8\nu}r_0^2\sqrt{\rho G} \tag{5.7.48}$$

5.7.8.1 Rocking motion

Figure 5.7.15 below shows a disc on an elastic half space with mass polar moment of inertia I_0 about a horizontal axis through the center of the base.

If *c.g.* is assumed to lie in the plane of the base, the equation of motion will be

$$I_0 \frac{d^2\theta}{dt^2} + r_0^4 \sqrt{\rho G}\, F_2' \frac{d\theta}{dt} + G r_0^3 F_1' \theta = T_0 e^{i\omega t} \tag{5.7.49}$$

Values of F_1' and F_2' were obtained from Bycroft's solution. However, Bycroft's solution was confined to $\nu = 0$ and the results were given in the range $0 \leq a_0 \leq 1.5$ and they are

$$\begin{aligned} F_1' &= 2.67 - 0.253a_0 - 0.493a_0^2 + 0.196a_0^3 \\ F_2' &= -.000353 + 0.1288a_0 + 0.557a_0^2 - 0.244a_0^3 \end{aligned} \tag{5.7.50}$$

At zero frequency, the static condition exists $F_1' = 2.67$, when static spring constant can be defined by

$$k_\theta = 2.67 G r_0 \Rightarrow k_\theta = \frac{8}{3} G r_0^3 \quad \text{when Poisson's ratio, } \nu = 0. \tag{5.7.51}$$

When $\nu \neq 0$ this value is expressed as

$$k_\theta = \frac{8}{3\,(1-\nu)} G r_0^3 \tag{5.7.52}$$

Comparing the elastic half space equation with the mechanical analog model we have

$$c_\theta = r_0^4 \sqrt{\rho G} F_2' \tag{5.7.53}$$

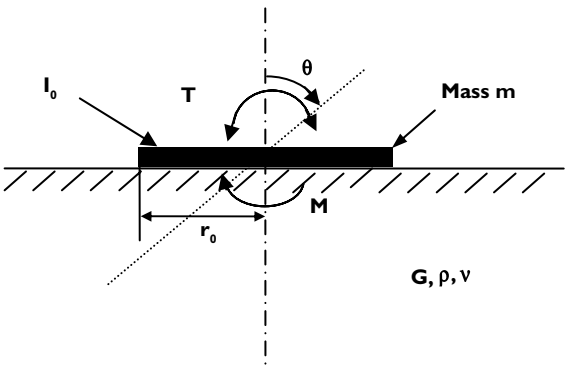


Figure 5.7.15 Rocking motion.

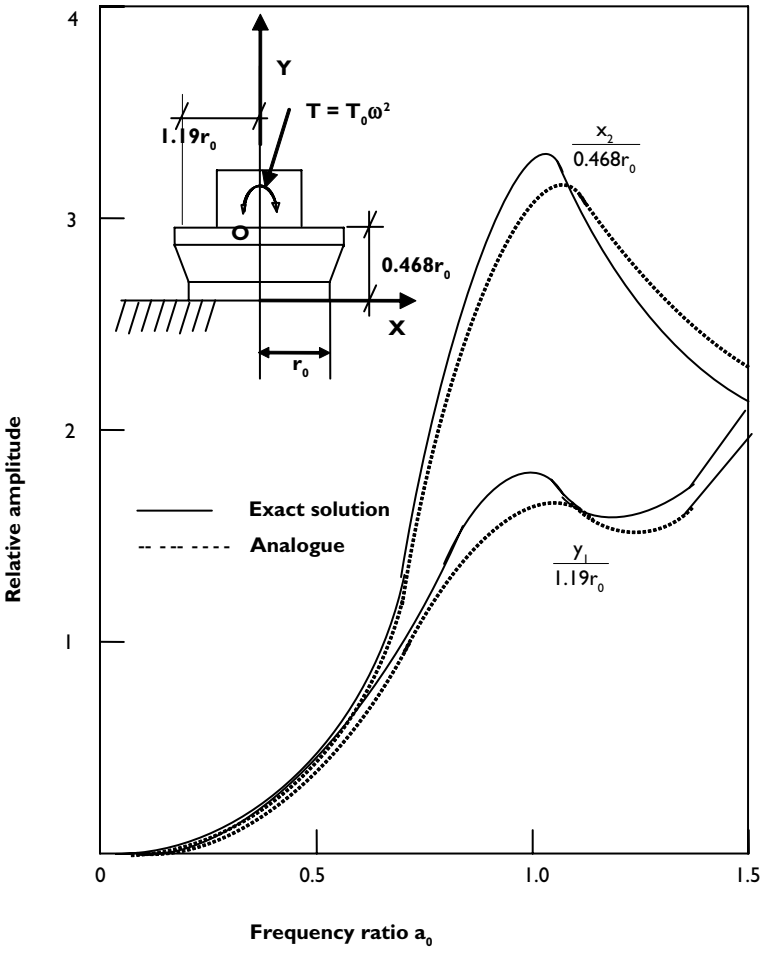


Figure 5.7.16 Comparison of Exact and Analogue solutions for coupled rocking and sliding (Hall 1967).

Hall, like Lysmer, found a dimensionless mass ratio

$$B_\psi = \frac{3(1-\nu)}{8}\frac{I_\psi}{\rho r_0^5} \tag{5.7.54}$$

based on which he modified the above equation of damping to derive

$$c_\theta = \frac{0.80 r_0^4 \sqrt{\rho G}}{(1-\nu)\,(1+B_\psi)}. \tag{5.7.55}$$

5.7.8.2 *Coupled analysis under rocking and sliding*

Foundations undergoing sliding and rocking motion usually have their response coupled. This equation of motion in Matrix form[84] can be expressed as

$$\begin{bmatrix} m & 0 \\ 0 & J_{x\phi} \end{bmatrix} \begin{Bmatrix} \ddot{x} \\ \ddot{\phi} \end{Bmatrix} + \begin{bmatrix} C_x & -C_x Z_c \\ -C_x Z_c & C_{\phi x} + C_x Z_c^2 \end{bmatrix} \begin{Bmatrix} \dot{x} \\ \dot{\phi} \end{Bmatrix} + \begin{bmatrix} K_x & -K_x Z_c \\ -K_x Z_c & K_{\phi x} + K_x Z_c^2 \end{bmatrix}$$

$$\begin{Bmatrix} x \\ \phi \end{Bmatrix} = \begin{Bmatrix} P_0 \\ M_0 \end{Bmatrix} \sin \omega_m t \tag{5.7.56}$$

Based on the stiffness and damping derived by Hall for mechanical analog he compared the dynamic response of foundation based on elastic half-space and the mechanical analog for coupled motion. The results derived by him are shown in Figure 5.7.16.

It will again be seen that the results obtained are quite encouraging and can well be used for practical design without any significant error.

5.7.9 Vibration of rectangular footings resting on elastic half-space

The following solution for calculating the displacements inside and outside a uniformly loaded rectangular footing resting on an elastic half space was proposed by *Holzlöner* (1969). The solution is approximate and can be obtained for any accuracy. The rectangular area is of side lengths $2a$ and $2b$. Half-space is provided with a rectangular system of coordinates (x, y, z), whose z-axis points vertically inwards.

With the modulus of elasticity E, the shear modulus G and Poisson's ratio ν for the half space, the vertical surface displacement at the surface ($z = 0$), w_0 was found as

$$w_0 = \frac{Q}{Ga} \cdot \frac{1}{16\pi^2 b_0} \left[2 \int_0^{\bar{b}} \frac{\sqrt{\bar{b}^2 - \bar{\xi}^2}}{(2\bar{\xi}^2 - 1)} + 4\bar{\xi}^2 \cdot \sqrt{\bar{b}^2 - \bar{\xi}^2} \cdot \sqrt{1 - \bar{\xi}^2} \phi(a_0 \bar{\xi}) d\bar{\xi} \right.$$

$$\left. + 8 \int_{\bar{b}}^{1} \frac{(\bar{\xi}^2 - \bar{b}^2) \cdot \sqrt{1 - \bar{\xi}^2} \cdot \bar{\xi}^2}{(2\bar{\xi}^2 - 1)^4 + 16(\bar{\xi}^2 - \bar{b}^2)(1 - \bar{\xi}^2)\bar{\xi}^4} \phi(a_0 \bar{\xi}) d\bar{\xi} \right] e^{i\omega t}$$

$$+ \frac{Q}{Ga} \cdot \frac{1}{16\pi^2 b_0} \left[\frac{c_2 \pi (2\chi^2 - 1)^2 \sqrt{\bar{\chi}^2 - \bar{b}^2}}{8\bar{\chi}\{1 - (6 - 4\bar{b}^2)\bar{\chi}^2 + 6(1 - \bar{b}^2)\bar{\chi}^4\}} \phi(a_0 \bar{\chi}) \right] e^{i\omega t} \tag{5.7.57}$$

84 Refer Chapter 2 (Vol. 2) on Design and Analysis of Machine foundation wherein this equation has been derived in detail.

in which

$$\phi\left(\mathrm{a}_0,\overline{\xi}\right)=\sum_{j=1}^{4}(-1)^{j+1}\int_{\theta_{j,2}}^{\theta_{j,1}}\frac{e^{-ia_0\overline{\xi}\left(a_j\cos\theta+c_j\sin\theta\right)}}{ia_0\overline{\xi}\cos\theta\sin\theta}d\theta$$

$$\text{and}\quad [a_j\cos\theta+c_j\sin\theta]>0;\quad \tan\theta_{j,1,2}=-\frac{a_j}{c_j} \tag{5.7.58}$$

The non-dimensional quantities used here are as follows:

$$ak=a_o,\quad \frac{b}{a}=b_0,\quad A_jk=xk\pm ak=ak\left(\frac{x}{a}\pm 1\right)=a_0a_j$$

$$B_jk=yk\pm bk=bk\left(\frac{y}{b}\pm 1\right)=ak\frac{b}{a}\left(\frac{y}{b}\pm 1\right)=a_0b_0b_j=a_0c_j$$

$$h^2=\omega^2\rho/\lambda+2G;\quad k^2=\omega^2\rho/G;\quad \overline{\alpha}=\sqrt{\overline{\zeta}^2-\overline{h}^2}=\frac{\alpha}{k};\quad \bar{\beta}=\frac{\beta}{\mathrm{k}}=\sqrt{\overline{\zeta}^2-1};$$

$$\lambda=\nu E/[(1+\nu)(1-2\nu)];\quad a_0=ak=a\omega\sqrt{\rho/G};\quad \overline{h}=\sqrt{\frac{(1-2\nu)}{2\,(1-\nu)}};$$

$$F\left(\xi\right)=\left(2\xi^2-k^2\right)^2-4\alpha\beta\xi^2$$

$$\text{where}\quad \alpha=\sqrt{\xi^2-h^2},\ \beta=\sqrt{\xi^2-k^2} \tag{5.7.59}$$

The relation $F(\xi)=0$ is the Rayleigh's equation and χ is a zero position of $F(\xi)$.

5.7.9.1 Static displacement

The integration with respect to θ is done by term-by-term integration of the Taylor series of the exponential function.

We have: $a_0=ak=a\omega\sqrt{\rho/G}$; in the static limiting case $\omega=0$, i.e. $a_0=0$.

The integral over the first term of the integrand in Equation (5.7.57) is given by

$$\int_{\theta_{j,2}}^{\theta_{j,1}}\frac{d\theta}{ia_0\overline{\xi}\cos\theta\sin\theta}=\lim_{a_0\to 0}\int_{\theta_{j,2}}^{\theta_{j,1}}\frac{d\theta}{ia_0\xi\cos\theta\sin\theta}=0 \tag{5.7.60}$$

The second term is independent of a_0 and $\overline{\xi}$ and can be expressed as

$$\int_{\theta_{j,2}}^{\theta_{j,1}}\frac{-ia_0\overline{\xi}\left(a_j\cos\theta+c_j\sin\theta\right)}{ia_0\overline{\xi}\cos\theta\sin\theta}d\theta=-a_j\int_{\theta_{j,2}}^{\theta_{j,1}}\frac{d\theta}{\sin\theta}-c_j\int_{\theta_{j,2}}^{\theta_{j,1}}\frac{d\theta}{\cos\theta}$$

$$=-a_j\ell n\frac{\sqrt{a_j^2+c_j^2}+c_j}{a_j}-c_j\ell n\frac{\sqrt{a_j^2+c_j^2}+a_j}{c_j} \tag{5.7.61}$$

Table 5.7.4 Dependence of different quantities on the Poisson's ratio ν.

ν	0	1/4	1/3	1/2
$\overline{h}$	0.707107	0.577350	0.5	0
$\overline{\chi}$	1.1444	1.0875	1.072	1.047
C_2	2.00	2.00	2.00	2.00

The following terms are all equal to zero for $a_0 = 0$. Hence, for $a_0 = 0$, we have:

$$\phi(0) = -\sum_{j=1}^{4} (-1)^{j+1} 2 \left[a_j l_n \frac{\sqrt{a_j^2 + c_j^2} + c_j}{a_j} + c_j l_n \frac{\sqrt{a_j^2 + c_j^2} + a_j}{c_j} \right]$$

$$a_j = \left(\frac{x}{a} \pm 1\right); \quad c_j = \frac{b}{a}.\left(\frac{y}{b} \pm 1\right) \tag{5.7.62}$$

C_2 is found to be independent of Poisson's ratio ν. Table 5.7.4 gives numerical values for other quantities.

5.7.9.2 *The displacement in the general dynamic case* ($a_0 \neq 0$)

The Taylor series of the integrated of Equation (5.7.57) is

$$\frac{e^{-ia_0\overline{\xi}(a_j \cos\theta + c_j \sin\theta)}}{ia_0\overline{\xi} \cos\theta \sin\theta} = -\sum_{N=0}^{\infty} \frac{\left(a_j \cos\theta + c_j \sin\theta\right)^N}{\cos\theta \sin\theta \; N!} \left(-ia_0\overline{\xi}\right)^{N-1} \tag{5.7.63}$$

When the expression $(a_j \cos\theta + c_j \sin\theta)^N$ is multiplied out the integrals of the individual summands can then be determined easily. Using abbreviation for the term

$$(m; d; \kappa) = m(m + d)(m + 2d) \ldots (m + \{\kappa - 1\}d); \kappa = 1, 2, \ldots \tag{5.7.64}$$

We have for even N,

$$R_{N,j} = \int_{\alpha}^{\alpha+\pi} \frac{\left(a_j \cos\theta + c_j \sin\theta\right)^N}{\cos\theta \sin\theta \cdot N!} d\theta$$

$$= \frac{\pi}{2^{N-2}\left(\frac{N-2}{2}\right)!} \sum_{n=0}^{N-2} \frac{\left(a_j^{n+1} c_j^{N-(n+1)}\right)}{(n+1)\,(N - [n+1])\,\left(\frac{n}{2}\right)!\left(\frac{N-[n+2]}{2}\right)!} \tag{5.7.65}$$

($N, n \geq 0$ and even and arbitrary).

For $N = 0$, the sum in (5.7.64) is zero, hence $R_{0,j} = 0$.

For odd N ($N \geq 1$),

$$R_{N,j} = \int_{\theta_{j,2}}^{\theta_{j,1}} \frac{(a_j \cos\theta + c_j \sin\theta)^N}{\cos\theta \sin\theta \cdot N!} d\theta = 2\frac{a_j c_j}{|a_j c_j|} \left\{ |c_j|^N \left(l_n \frac{1+\sin\theta_j}{\cos\theta_j} - \sum_{\vartheta=1,2,3\ldots}^{(N-1)/2} \frac{\sin^{2\vartheta-1}\theta_j}{2\vartheta-1} \right) \frac{1}{N!} \right.$$
$$+ |a_j|^N \left(l_n \frac{1+\cos\theta_j}{\sin\theta_j} - \sum_{\vartheta=1}^{(N-1)/2} \frac{\cos^{2\vartheta-1}\theta_j}{2\vartheta-1} \right) \frac{1}{N!}$$
$$+ \left[\sum_{n=0}^{(N-3)/2} \frac{n!}{(2n+2)!\,(N-[2n+2])!} \left(\frac{|a_j c_j|}{\sqrt{a_j^2 + c_j^2}} \right)^{N-(2n+2)} \right]$$
$$+ \left[|a_j|^{2n+2} \sum_{\vartheta=0}^{n} \frac{2^\vartheta \cos^{2n-2\vartheta}\theta_j}{(n-\vartheta)!\,(N-2;-2;\vartheta+1)} \right.$$
$$\left. \left. + |c_j|^{2n+2} \sum_{\vartheta=0}^{n} \frac{2^\vartheta \sin^{2n-2\vartheta}\theta_j}{(n-\vartheta)!\,(N-2;-2;\vartheta+1)} \right] \right\} \tag{5.7.66}$$

with, $\theta_j = \tan^{-1}[|a_j/c_j|], \quad 0 < \theta_j < \pi/2$ (5.7.67)

Note that for $N = 1$, some sums become zero. For $a_j = 0$ or/and $c_j = 0$, with even and odd N, and we get $R_{N,j} = 0$.

With the results in Equations (5.7.63) to (5.7.66), we can write Equation (5.7.58) as

$$\phi\left(a_0, \bar{\xi}\right) = -\sum_{j=1}^{4} (-1)^{j+1} \sum_{N=1}^{M} \left(-i a_0 \bar{\xi}\right)^{N-1} R_{N,j} \tag{5.7.68}$$

The number M is to be selected such that the terms following $(-ia_0\bar{\xi})^{M-1}R_{M,j}$ no longer have any influence on $\phi\left(a_0\bar{\xi}\right)$ within the desired accuracy of calculation. Naturally, M depends on the argument $\left(a_0\bar{\xi}\right)$. The integration with respect to $\bar{\xi}$ in (5.7.446) can be carried out numerically, e.g. with the help of Simpson's rule.

5.7.9.3 Numerical values

We first determine the vertical displacement at the midpoint of a square surface over which a dynamic load is uniformly distributed. This displacement is compared, among others, with that of the midpoint of a circle of equal area. There, the displacement is given (without time factor) in the form:

$$w_0 = \frac{Q}{Gr_0}(f_1 + if_2) \tag{5.7.69}$$

Here, r_0 is the radius of the loaded area, and f_1 and f_2 are the components of displacement in different phase positions. If we reduce Equation (5.7.57) to the form:

$$\omega_0 = \frac{Q\sqrt{\pi}}{2Ga\sqrt{b_0}}(f_1 + if_2) \tag{5.7.70}$$

Then the expression $(2a\sqrt{b_0}/\sqrt{\pi})$ is the radius of a circle whose surface is equal to the rectangular surface $(4ab)$. Normally, the vertical displacement of the midpoint of a square load area is compared with the solution of Thomson & Kobori (1963) and with the displacement of the midpoint of a circular load area of equal area. The functions plotted (f_1 and f_2) are defined by Equations (5.7.69) and (5.7.70). Here $a = b$, i.e. $b_0 = 1$. Since the tensile stress at the surface of the half space acts against the positive direction of displacement, the function values f_1 are negative for $a_0 = 0$.

However, while comparing the present results with the results of the circular are, in Equation (5.7.32) for a_0, the quantity a is to be replaced by r_0 which is equal to the distance of the edge from the midpoint of the loaded area. However, for the square, it is referred to the length a which is the minimum distance of the edge from the midpoint of the loaded area would have to be extended, i.e. the values calculated here would approach those of the circular loaded area.

It may also be mentioned that with the help of Equation (5.7.57), for any ratio of sites b_0 of the rectangular loaded area, we can determine the vertical displacement of any point of the half-space.

5.7.9.4 Particular possibilities of applications

Calculations of this type have been applied since the time of Reissner (1936) to the vibration of foundations on the building sites. For this, we should have the solutions of a boundary value problem in which a given displacement is impressed at the surface of half-space. Stress boundary value problems are however easier to solve. Lysmer (1965) approximately satisfied the displacement boundary condition for the base of a foundation which is itself rigid (equal displacement of all the base surface points), from the solution of the boundary value problems in the rotation symmetric case, by concentric superimposition of circular loaded areas. In the case of n loaded areas we get, for the displacement of n points, two systems of equations each with n solutions, for which stress boundary value problem solved here, we can correspondingly deal with foundations whose surface can be made up of rectangles. If the foundation plane of the foundation is not to be considered as a rigid, the stress components can be selected such that the displacement at the surface agrees with bending surface of the foundation plate. The problem solved here, we can also deal with tilting vibration of a foundation.

5.7.10 Rigid strip footing

A mathematical difficulty arises unless the stress distribution in the elastic medium immediately beneath the rigid body is known or assumed. Reissner (1936) and Miller and Pursey (1954) amongst others assumed, when considering a rigid circular body, a constant stress distribution in the elastic medium for vertical oscillation and a stress proportional to radial distance for rotation about an axis normal to the surface. Other authors, namely Arnold et al. (1955), Biot (1943), Hsieh (1962) only to name a few, assumed a stress distribution proportional to that obtained from considerations of static loading case. An assumed stress distribution will not yield a constant linear or angular displacement of the medium immediately under the rigid body as demanded

from physical consideration and it is then necessary to find a mean value for the displacement.

Awojobi & Grootenhuis (1965), Robertson (1966) solved this mixed boundary-value problem for rigid circular punch pressed into elastic half-space by a dual integral Equation Using a standard method the dual integral equations were reduced to a set of Fredholm integral equation, a series solution of which was obtained for low frequencies giving a perturbation of the static solution.

Karasudhi et al. (1968) studied the vertical, horizontal and rocking vibrations of a body on the surface of an unloaded half plane. An oscillation displacement was prescribed in the loaded region. The problem, thus, reduced to a mixed problem with respect to the prescribed displacement and the stress at the footing-soil interface. Each of these cases leads to a mixed boundary value problem represented by dual integral equations, which are reduced to a single Fredholm integral Equation.

5.7.10.1 Governing equations

The coordinate system and significant direction for the vibration of a rectangular plate of infinite length resting on an elastic half space is shown in Figure 5.7.17. The infinite plate is along the z-axis and the elastic half space occupies the region $y = 0$. Also, $w = 0$ and all derivatives with respect to z vanish.

Using harmonic time variation of the loading $\exp(i\omega t)$ and writing the response in the form $(u, v, 0)e^{i\omega t}$, the vector equation of motion may be written as

$$\nabla^2 e + \omega_1^2 e = 0; \quad \nabla^2 \phi_z + \omega_2^2 \phi_z = 0 \tag{5.7.71}$$

in which

$\nabla^2 = \dfrac{\partial^2}{\partial x^2} + \dfrac{\partial^2}{\partial y^2}$; e and φ_z are the dilatation and the z-component of rotation given by

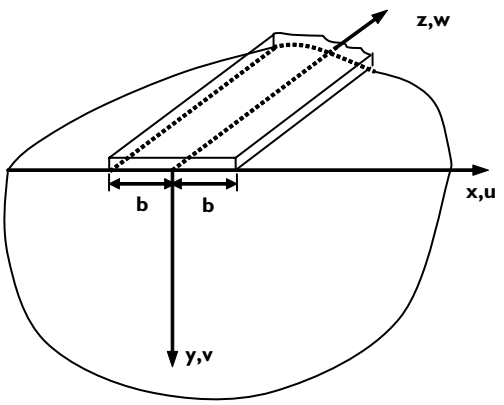


Figure 5.7.17 Coordinate axes and significant dimensions.

$$e = \frac{\partial u}{\partial x} + \frac{\partial v}{\partial y} \quad \text{and} \quad \phi_z = \frac{\partial u}{\partial y} - \frac{\partial v}{\partial x} \tag{5.7.72}$$

and $\omega_1 = \omega/V_P; \omega_2 = \omega/V_S$; V_P = dilatational wave velocity = $[(\lambda + 2G)/\rho]^{1/2}$; V_S = shear wave velocity = $[G/\rho]^{1/2}$, where λ and G are Lame's parameters and ρ the mass density of the medium. The solution of Equation (5.7.71) may be obtained in the form of Fourier Transform of e and ϕ_z and these may be written as

$$e(x,y) = \frac{1}{2\pi}\int_{-\infty}^{\infty} \bar{e}(p,y)e^{-ipx}dp; \quad \phi_z(x,y) = \frac{1}{2\pi}\int_{-\infty}^{\infty} \bar{\phi}_z(p,y)e^{-ipx}dp \tag{5.7.73}$$

where $\bar{e} = Ae^{-a_1 y}$; $\bar{\phi}_z = Be^{-k_2 y}$; $k_1^2 = p^2 - \omega_1^2$; $k_2^2 = p^2 - \omega_2^2$; A and B are arbitrary constants of p, to be determined from the boundary conditions.

Using Equation (5.7.73), the normal stress σ_y, the shearing stress τ_{xy} and the displacements u and v may be written as

$$\sigma_y(x,y) = -\frac{G}{2\pi\omega_2^2}\int_{-\infty}^{\infty}\left[\left(\frac{k_1^2}{\eta^2} - \frac{\lambda}{G}p^2\right)\frac{A}{\eta^2}e^{-k_1 y} + 4ik_2 pBe^{-k_2 y}\right]e^{-ipx}dp;$$

$$\tau_{xy}(x,y) = \frac{G}{\pi\omega_2^2}\int_{-\infty}^{\infty}\left[-\frac{ik_1 p}{\eta^2}Ae^{-k_1 y} + (k_2^2 + p^2)Be^{-k_2 y}\right]e^{-ipx}dp;$$

$$u(x,y) = \frac{1}{2\pi}\int_{-\infty}^{\infty}\left(\frac{1}{\omega_1^2}k_1 Ae^{-k_1 y} - \frac{2}{\omega_2^2}k_2 Be^{-k_2 y}\right)e^{-ipx}dp;$$

$$v(x,y) = \frac{1}{2\pi}\int_{-\infty}^{\infty}\left(\frac{1}{\omega_1^2}k_1 Ae^{-k_1 y} + \frac{2}{\omega_2^2}ipBe^{-k_2 y}\right)e^{-ipx}dp, \tag{5.7.74}$$

in which, $\eta = V_S/V_P = \sqrt{(1-2\nu)/2(1-\nu)}$ and ν is the Poisson's ratio.

5.7.10.2 Vertical vibration

With reference to Figure 5.7.17, the boundary conditions are

$$\begin{aligned}
&\tau_{xy}(x,0) = 0 : 0 = |x| < 8;\\
&\sigma_y(x,0) = 0 : b < |x| < 8;\\
&v(x,0) = v_0 : 0 = |x| = b.
\end{aligned} \tag{5.7.75}$$

where v_0 is the specified constant amplitude of the vertical displacement.

$$\text{Taking,} \quad \bar{\sigma}(p) = -\frac{G}{\omega_2^2}\left[\left(\frac{k_1^2}{\eta^2} - \frac{\lambda}{G}p^2\right)\frac{A}{\eta^2} + 4ik_2 pB\right], \tag{5.7.76}$$

σ_y in Equation (5.7.74) reduces to

$$\sigma_y(x,0) = \frac{1}{2\pi}\int_{-\infty}^{\infty} \bar{\sigma}(p)e^{-ipx}dp \tag{5.7.77}$$

From τ_{xy} in Equation (5.7.74) and using $\bar{\sigma}(p)$, we can evaluate the constants A and B, function of p, as follows:

$$A = -\frac{\omega_2^2\eta^2(k_2^2+p^2)}{GF(p)}\bar{\sigma}(p)\,; \quad B = -\frac{i\omega_2^2 p k_1}{GF(p)}\bar{\sigma}(p) \tag{5.7.78}$$

where $$F(p) = \left(2p^2-\omega_2^2\right)^2 - 4p^2\sqrt{\left(p^2-\omega_1^2\right)\left(p^2-\omega_2^2\right)} \tag{5.7.79}$$

Using expression for v in Equation (5.7.74) and substituting for the constants A and B, the boundary conditions for σ_y and v in Equation (5.7.75) and use of *symmetry*, lead to the dual integral equation as follows

$$\frac{\omega_2^2}{2\pi G}\int_{-\infty}^{\infty}\frac{k_1(p)\bar{\sigma}(p)\,e^{-ipx}}{F(p)}dp = v_0 : |x| < b \tag{5.7.80}$$

$$\int_{-\infty}^{\infty}\bar{\sigma}(p)\,e^{-ipx}dp = 0 : |x| > b \tag{5.7.81}$$

and $$\sigma_y(x,0) = \frac{1}{\pi}\int_0^{\infty}\bar{\sigma}(p)\cos(px)\,dp$$

Using notations, $r = x/b$; $n = bp$, $f(n) = f(bp) = \bar{\sigma}(p)$; $a_0 = b\omega_2 = a_0^*/\eta$, these equations reduce to the dual integral equation of the form

$$a_0^2\int_0^{\infty}\frac{k_1(n)}{F(n)}f(n)\cos(nr)dn = \pi G v_0; \quad 0 \le r \le 1 \tag{5.7.82}$$

$$\int_0^{\infty} f(n)\cos(nr)dn = 0; \quad r > 1. \tag{5.7.83}$$

where

$$F(n) = (2n^2-a_0^2)^2 - 4n^2k_1(n)k_2(n); \quad k_1(n) = \sqrt{(n^2-a_0^{*2})}; \quad k_2(n) = \sqrt{(n^2-a_0^2)}, \tag{5.7.84}$$

$F(n)$ is known as the Rayleigh's function and a_0 is referred to as the frequency factor.

To ensure that only outgoing waves are present, it is necessary to subtract one half of the residue at the Rayleigh pole from the left hand side of Equation (5.7.80). The residue can be shown to be equal to $2\pi i a_0^2 k_1(n_s)\cos(n_s r)/F'(n_s)$, where n_s is the root of $F(n)$ and $F'(n)$ is (dF/dn).

Thus, Equations (5.7.82) and (5.7.83) reduce to

$$a_0^2 \int_0^\infty \frac{k_1(\xi)}{\phi(\xi)} f(\xi)\cos(\xi\, r)d\xi - \frac{\pi i a_0^2 k_1(n_s) f(n_s)\cos(n_s r)}{F'(n_s)} = \pi G v_0; \quad 0 \le r \le 1 \tag{5.7.85}$$

$$\int_0^\infty f(\xi)\cos(\xi\, r)d\xi = 0; \quad r > 1 \tag{5.7.86}$$

The dual integral equations above is reduced to Fredholm integral equation by assuming a solution of the form

$$f(n) = C_0 J_0(n) + \int_0^1 t^{1/2}\,\theta(t) J_0(nt)dt \tag{5.7.87}$$

where J_0 is the 0th order Bessel function of the first kind and C_0 depends on a_0 and ν and it can be seen that Equation (5.7.86) is satisfied, with C_0 and $\theta(t)$ to be determined from Equation (5.7.85).

Differentiating and with some rearrangement Equation (5.7.84) may be written as

$$\int_0^\infty [C_1 + H(\xi)] f(\xi)\sin(\xi r)d\xi - \frac{\pi i a_0^2 n_s k_1(n_s) f(n_s)\sin(n_s r)}{F'(n_s)} = 0; \quad 0 \le r \le 1 \tag{5.7.88}$$

in which $C_1 = -[2(1-\eta^2)]^{-1}$ and $H(n) = a_0^2 n k_1(n)/F(n) - C_1$. (5.7.89)

Substituting Equation (5.7.87) into Equation (5.7.88) leads to

$$-C_1\theta(s) = \int_0^1 \sqrt{ts}\, k(t,s)\theta(t)dt + C_0\sqrt{s}\, K(s) \tag{5.7.90}$$

in which

$$k(t,s) = \int_0^\infty nH(n)J_0(nt)J_0(ns)dn - \pi i a_0^2 n_s^2 \frac{k_1(n_s)}{F'(n_s)} J_0(n_s t)J_0(n_s s); \quad \text{and} \tag{5.7.91}$$

$$K(s) = k(1,s) \tag{5.7.92}$$

Applying contour integration shown in Figure 5.7.18, with integrand $[\zeta H(\zeta)H_0^{(1)}(\zeta t)J_0(\zeta s)]$ for $t \geq s$ where $\zeta = \eta + i\mu$, $k(t,s)$ is evaluated in the form

$$\begin{aligned} k(t,s) &= k_1(t,s) \quad t \geq s \\ &= k_1(s,t) \quad t \leq s \end{aligned} \tag{5.7.93}$$

where

$$\begin{aligned} &k_1(t,s) \\ &= ia_0^2 \int_0^{\beta} \frac{\xi^2\sqrt{\eta^2-\xi^2}\,H_0^{(2)}(a_0\xi t)J_0(a_0\xi s)}{(2\xi^2-1)^2+4\xi^2\sqrt{\eta^2-\xi^2}\,\sqrt{1-\xi^2}}d\xi \\ &\quad + 4in_2^2 \int_{\beta}^{1} \frac{\xi^4(\eta^2-\xi^2)\sqrt{1-\xi^2}\,H_0^{(2)}(a_0\xi t)J_0(a_0\xi s)}{(2\xi^2-1)^4+16\xi^4(\eta^2-\xi^2)(1-\xi^2)}d\xi \\ &\quad - \frac{\pi i a_0^2\xi_s(\xi_s^2-\eta^2)\,(\sqrt{\xi_s^2-1})H_0^{(2)}(a_0\xi_s t)J_0(a_0\xi_s s)}{4[2(2\xi_s^2-1)(\sqrt{\xi_s^2-\eta^2})(\sqrt{\xi_s^2-1})-2(\xi_s^2-\eta^2)(\xi_s^2-1)-\xi_s^2(2\xi_s^2-\eta^2-1)]} \end{aligned} \tag{5.7.94}$$

in which $\xi = n/a_0$ and $\xi_s = n_s/a_0$; $H_m^{(1)}(\zeta)$ and $H_m^{(2)}(\zeta)$ are Hankel functions of order m.

An exhaustive solution of Equation (5.7.90) is given in Karasudhi et al. (1968) and an out line of its numerical implementation is given below:

1 Divide the unit interval into n-equal parts;
2 Let s_i be the ordinate of the mid-point of each interval, i.e. $s_i = (2i-1)/2n$, $i = 1, 2, \ldots, n$.
3 Introduce $k_{ij} = (s_i s_j)1/2xk(s_i, s_j)$, where $k(s_i, s_j)$ is evaluated numerically.

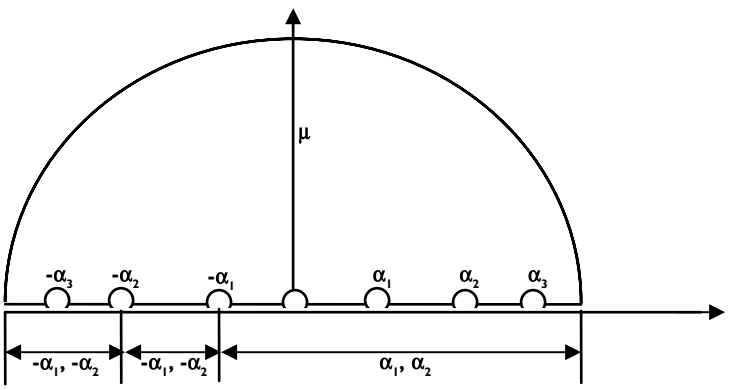


Figure 5.7.18 Contour for infinite integration.

Equation (5.7.90) is then approximated by a set of n-complex simultaneous equations by applying trapezoidal rule to the finite integrals and may be written as

$$\sum_{j=1}^{n}(k_{ij} + nC_1\delta_{ij})\theta(s_j) = -nC_0\sqrt{s_i}K(s_i), \quad (i = 1, 2, \ldots, n) \tag{5.7.95}$$

in which $\delta_{ij} = 0$ for $i \neq j$ and $= 1$, otherwise.

When a_0, ν and n are specified, Equation (5.7.95) can be solved numerically for $\theta(sj)$.

After several trials, $n = 10$ is found to be sufficient to obtain a solution within 0.5%. Normally, a closed form representation of $[s^{1/2}\theta(s)]$ is obtained from the least square approximation and for $a_0 \leq 1$, result is within 0.5% and for $1 \leq a_0 \leq 1.5$, the result is within 1.0%. Hence, we can write

$$s^{1/2}\theta(s) = C_0(A_1 s + A_2 s^2) \tag{5.7.96}$$

where A_1 and A_2 are complex coefficients determined by the curve fitting process and depend on the values of a_0 and ν.

Substituting Equation (5.7.96) into Equation (5.7.87), we may obtain

$$f(n) = C_0[J_0(n) + A_1' J_1(n)/n + A_2' J_2(n)/n^2] \tag{5.7.97}$$

where $A_1' = A_1 + A_2$ and $A_2' = -2A_2$.

Equation (5.7.97) satisfies only the stress boundary condition, Equation (5.7.83) and the slope of the displacement, Equation (5.7.88).

To satisfy the displacement boundary condition of Equation (5.7.80), Equation (5.7.97) is substituted into it leading to the evaluation of integrals of the form

$$a_0^2 \int_0^{\infty} \frac{\alpha_1(\xi)}{F(\xi)} \frac{J_m(\xi)}{\xi^m} \cos(\xi r) d\xi; \quad m = 0, 1, 2. \tag{5.7.98}$$

Integrals are to be evaluated by using contour integration with the integrand $a_0^2\alpha_1(\zeta)H_m^{(1)}(\zeta)\cos(\zeta r)/|F(\zeta)\zeta^m|$. Procedure is similar to the one used in determining $k(t, s)$.

Values for the real and imaginary parts of C_0 are determined for different values of r in the interval $0 = r = 1$. The variation of C_0 is found to be less than 0.5% for $a_0 = 1.0$ and less than 1% for $1.0 = a_0 = 1.5$.

The vertical stress and the vertical contact force P_r per unit length is given by

$$\sigma_y(x, 0) = (C_0/\pi)[(b^2 - x^2)^{-1/2} + A_1'(b^2 - x^2)^{1/2}/b^2 + A_2'(b^2 - x^2)^{3/2}/3b^4]; \quad 0 \leq x < b \tag{5.7.99}$$

$$P_r = C_0[1 + A_1'/2 + A_2'/8] = \pi G v_0(f_1 + if_2) \tag{5.7.100}$$

where f_1 and f_2 are the equivalent stiffness and are given in Figure 5.7.19a.

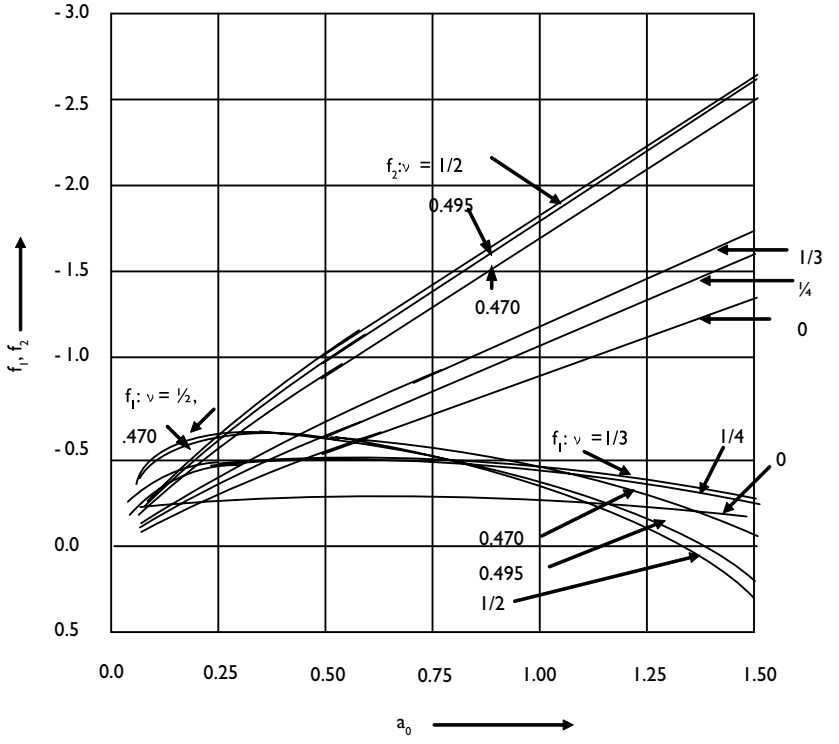


Figure 5.7.19a Equivalent stiffness versus frequency factor, vertical vibration.

Considering the system as having a single degree of freedom leads to the equation of equilibrium as

$$P_r e^{i(\omega t+\phi)} + Pe^{i\omega t} = [d^2/dt^2]mv_0 e^{i\omega t} \tag{5.7.101}$$

Assuming m = mass of the rigid body per unit length, and $b_1 = m/(\rho b^2)$ = mass ratio, the non-dimensional amplitude is given by

$$V = |\pi G v_0/P| = [(f_1 + a_0^2 b_0/\pi)^2 + f_2^2]^{-1/2}, \tag{5.7.102}$$

where P is the amplitude of the applied vertical force per unit length and, phase angle

$$\theta = \tan^{-1}[f_2/(f_1 + a_0^2 b_0/\pi)] \tag{5.7.103}$$

Let the frequency factors at $\theta = \pi/2$ and at the maximum amplitude be a_0^* and $\bar{a}_0^*$ and the corresponding amplitudes be$V_{\max}$ and $\bar{V}_{\max}$. These quantities are shown in Figures 19b,c.

The static values are obtained corresponding to $a_0 = 0$.

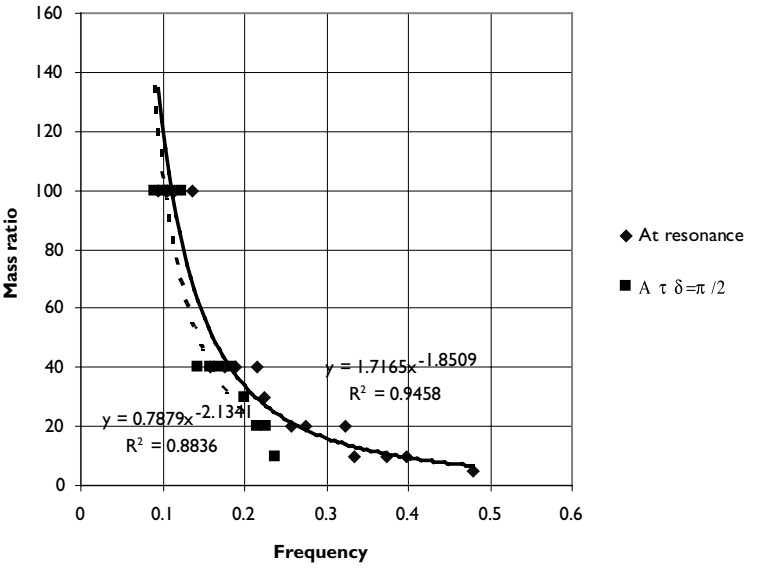


Figure 5.7.19b Mass ratio at resonance, a_0^* and at $\bar{a}_0^*$ (at $\delta = \pi/2$): for all Poisson ratios.

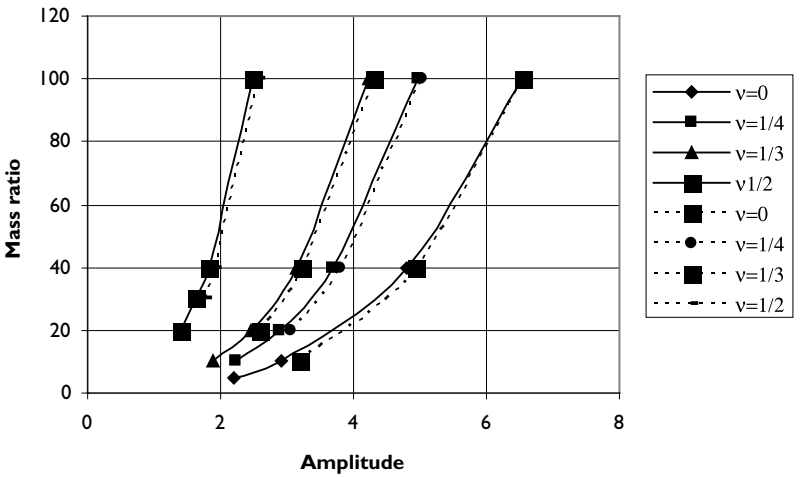


Figure 5.7.19c Mass ratio versus resonant amplitudes at a_0^* and at $\bar{a}_0^*$ (at $\delta = \pi/2$).

For this case $f(n) = C_0 J_0(n)$, using L'Hospital rule, Equation (5.7.85) reduces to

$$\int_0^\infty \frac{f(n)}{n} \cos(nr) dn = 2\pi G(\eta^2 - 1) v_0 : 0 \le r \le 1. \tag{5.7.104}$$

Equation (5.7.98) indicates that left hand side of the equation is singular. Differentiating Equation (5.7.104) with respect to r gives the correct value for the slope and the

problem can be specified only within an arbitrary displacement. C_0 can be expressed in terms of the static applied force P. By integration, $C_0 = P$ and the static vertical stress, $\sigma_y(x,0) = P/\pi(b^2 - x^2)^{1/2}$.

5.7.10.3 Horizontal vibration

Boundary conditions are:

$$\sigma_y(x,0) = 0 \quad 0 \le |x| < \infty \tag{5.7.105}$$

$$\tau_{xy}(x,0) = 0 \quad 0 < |x| < \infty \tag{5.7.106}$$

$$u_0(x,0) = u_0 \quad 0 \le |x| \le b \tag{5.7.107}$$

where u_0 is the specified amplitude of the horizontal vibration.

The non-dimensional governing dual integral equation are given by

$$a_0^2 \int_0^\infty \frac{k_2(\xi)}{F(\xi)} f(\xi)\cos(\xi r)d\xi - \pi i a_0^2 \frac{k_2(n_s)}{F'(n_s)} f(n_s)\cos(n_s r) = \pi G u_0 \tag{5.7.108}$$

$$\int_0^\infty f(\xi)\cos(\xi r)d\xi = 0 \tag{5.7.109}$$

where $f(\eta)$ is given by

$$\tau_{xy}(x,0) = \frac{1}{\pi}\int_0^\infty f(bp)\cos(px)dp \tag{5.7.110}$$

Equations (5.7.108) and (5.7.109) are modified by using

$$H(\xi) = a_0^2 \eta \frac{k_2(\xi)}{F(\xi)} - C_1 \tag{5.7.111}$$

where C_1 is given by Equation (5.7.89).

Assuming $f(n)$ similar to the one given in Equation (5.7.87), the non-homogeneous Fredholm equation of the second kind may be represented by Equation (5.7.90), in which

$$k(t,s) = \int_0^\infty \xi H(\xi) J_0(\xi t) J_0(\xi s) d\xi - \pi i a_0^2 n_s^2 \frac{k_2(n_s)}{F'(n_s)} J_0(n_s t) J_0(n_s s) \tag{5.7.112}$$

and $$K(s) = k(1,s) \tag{5.7.113}$$

Using Equation (5.7.93) for $k(t,s)$, it can be shown by using contour in Figure 5.7.6, that

$$\begin{aligned} k_1(t,s) &= i a_0^2 \int_0^\eta \frac{\xi^2 \sqrt{1-\xi^2}\, H_0^{(2)}(a_0 \xi t) J_0(a_0 \xi s)}{(2\xi^2-1)^2 + 4\xi^2 \sqrt{\eta^2-\xi^2}\,\sqrt{1-\xi^2}} d\xi \\ &\quad + i a_0^2 \int_\eta^1 \frac{\xi^2 (2\xi^2-1) \sqrt{1-\xi^2}\, H_0^{(2)}(a_0 \xi\, t) J_0(a_0 \xi_s)}{(2\xi^2-1)^2 + 4\xi^2 \sqrt{\eta^2-\xi^2}\,\sqrt{1-\xi^2}} d\xi \\ &\quad - \frac{\pi i a_0^2 \xi_s (\xi_s^2-\eta^2)\,(\sqrt{\xi_s^2-1}) H_0^{(2)}(a_0 \xi_s t) J_0(a_0 \xi_s s)}{4[2(2\xi_s^2-1)(\sqrt{\xi_s^2-\eta^2})(\sqrt{\xi_s^2-1}) - 2(\xi_s^2-\eta^2)(\xi_s^2-1) - \xi_s^2(2\xi_s^2-\eta^2-1)]} \end{aligned} \tag{5.7.114}$$

Rewriting the Fredholm equation similar to Equation (5.7.95), $\theta(s)$ can be approximated by Equation (5.7.96) and with sufficient accuracy. Hence $f(n)$ is given by Equation (5.7.97), which upon substitution into Equation (5.7.109), leads to an equation for determining C_0 and containing an infinite integral of the form

$$a_0^2 \int_0^\infty \frac{k_2(n)}{F(n)} \frac{J_m(n)}{n^m} \cos(nx) dn, \quad \text{where } m = 0, 1, 2. \tag{5.7.115}$$

The latter is evaluated by using the contour integration shown in Figure 5.7.18, the integrand being $\{a_0^2 k_2(n) H_m^{(2)}(\zeta) \cos(\zeta r)/[F(\zeta)\zeta^m]\}$.

Values for the real and imaginary parts of C_0 are determined for different values of r in the interval $0 = r = 1$. The variation of C_0 is found to be less than 0.5% for $n_2 = 1.0$ and less than 1% for $1.0 = n_2 = 1.5$.

The horizontal stress and the contact shear force Q per unit length along the z-axis is given by

$$\tau_{xy}(x,0) = (C_0/\pi)[(b^2-x^2)^{-1/2} + A_1'(b^2-x^2)^{1/2}/b^2 + A_2'(b^2-x^2)^{3/2}/3b^4]; \quad 0 \le x < b \tag{5.7.116}$$

$$Q = C_0[1 + A_1'/2 + A_2'/8] = \pi G u_0 (f_1 + i f_2) \tag{5.7.117}$$

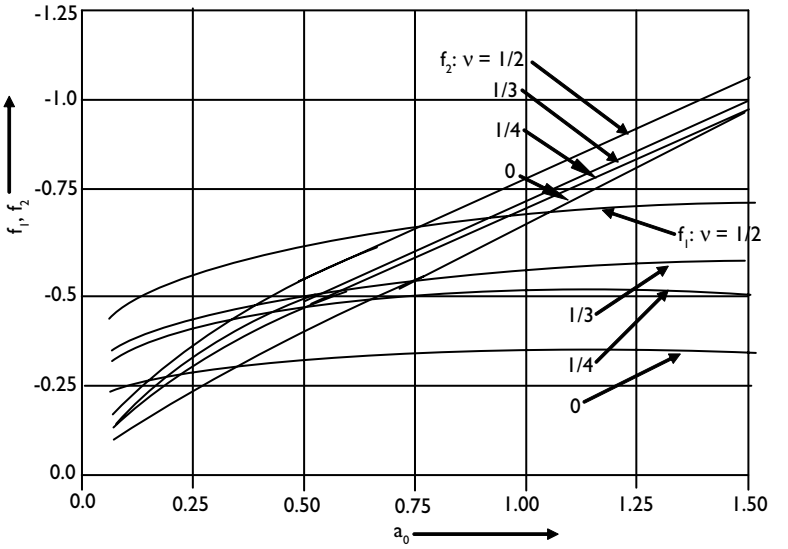


Figure 5.7.20a Equivalent stiffness versus frequency factor, uncoupled horizontal vibration.

where f_1 and f_2 are equivalent stiff nesses and are shown in Figure 5.7.20a, plotted against a_0. Assuming m = mass of the rigid body per unit length, and $b_0 = m/(\rho b^2)$ = mass ratio, the non-dimensional amplitude is given by

$$U = |\pi G u_0/Q_r| = [(f_1 + n_2^2 b_0/\pi)^2 + f_2^2]^{-1/2},$$

$$\text{Phase angle} \quad \theta = \tan^{-1}[f_2/(f_1 + n_2^2 b_0/\pi)] \tag{5.7.118}$$

Let the frequency factors at $\theta = \pi/2$ and at the maximum amplitude be a_0^* and $\bar{a}_0^*$ and the corresponding amplitudes be $V_{\max}$ and $\bar{V}_{\max}$. The result is shown in Figures 20b,c.

In terms of the static applied force Q, $C_0 = Q$, and the static shear stress distribution is

$$\tau_{xy}(x, 0) = Q/\pi(b^2 - x^2)^{1/2}. \tag{5.7.119}$$

5.7.10.4 Rocking vibration

Boundary conditions for vertical cases are already given as:

$$\tau_{xy}(x, 0) = 0 : 0 = |x| < 8;$$
$$\sigma_y(x, 0) = 0 : b < |x| < 8;$$
$$v(x, 0) = v_0 : 0 = |x| = b. \tag{5.7.120}$$

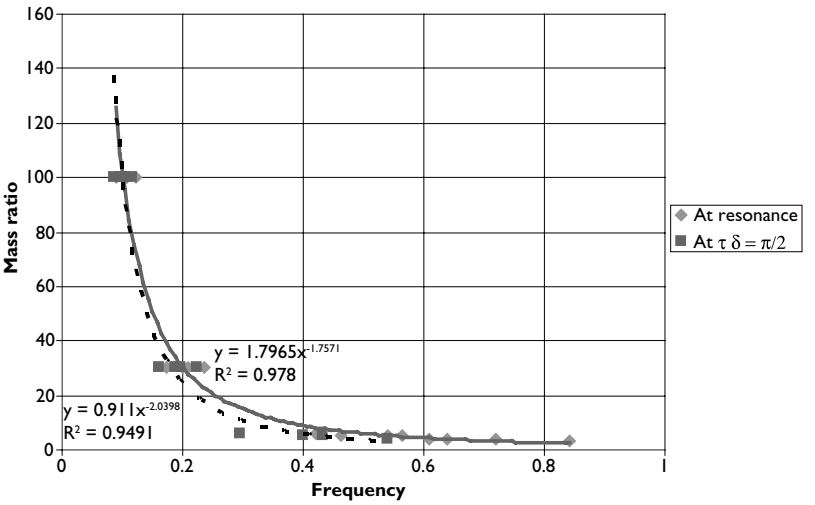


Figure 5.7.20b Mass ratio at resonance, a_0^* and at $\bar{a}_0^*$ (at $\delta = \pi/2$): for all Poisson ratios.

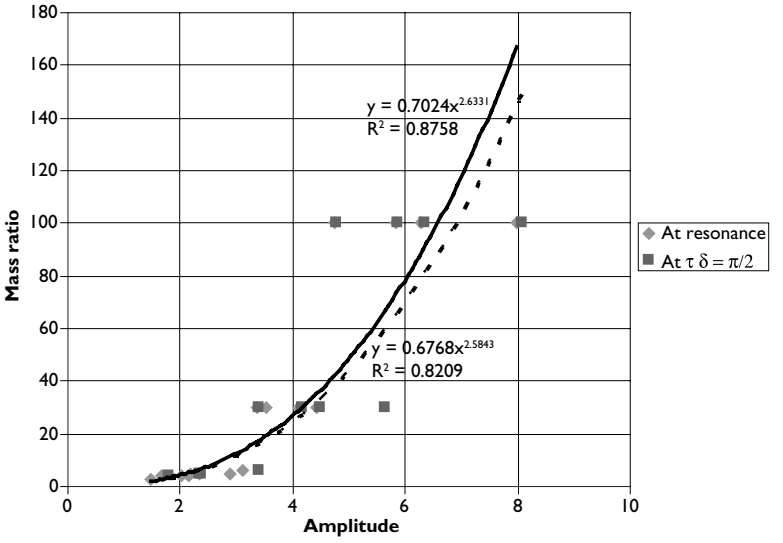


Figure 5.7.20c Amplitudes at resonance, a_0^* and at $\bar{a}_0^*$ (at $\delta = \pi/2$): for all Poisson ratios.

for rocking case v_0 is replaced by ψx, where ψ is the amplitude of the angle of rocking. The governing dual integral equations are

$$a_0^2 \int_0^\infty \frac{k_2(\xi)}{F(\xi)} f(\xi)\cos(\xi r)d\xi - \pi i a_0^2 \frac{\alpha_2(n_s)}{F'(n_s)} f(n_s)\cos(n_s r) = \pi G u_0 \quad 0 = r = 1 \tag{5.7.121}$$

$$\int_0^\infty f(\xi)\cos(\xi r)d\xi = 0; \quad r > 1 \tag{5.7.122}$$

where $f(\xi)$ is given by

$$\sigma_y(x,0) = \frac{1}{\pi}\int_0^\infty f(bp)\sin(px)dp \tag{5.7.123}$$

Assuming $f(n)$ to be of the form

$$f(n) = C_0 J_1(n) + \int_0^1 \sqrt{t}\,\theta(t)J_1(nt)dt \tag{5.7.124}$$

and using Equation (5.7.99), Equation (5.7.96) can be transformed into an non-homogeneous Fredholm equation of the second degree and can be represented by Equation (5.7.134), where $k(t,s)$ is given by Equation (5.7.112) with J_0 is replaced by J_1 and $K(s) = k(1,s)$. Using Equations (5.7.93) for $k(t,s)$, it can be shown that $k_1(t,s)$ given by Equation (5.7.94) with J_0 being replaced by J_1 and $H_0^{(2)}$ by $H_0^{(2)}$.

Rewriting the Fredholm equation in the form of Equation (5.7.95) $\theta(s)$ can be approximated with good accuracy as

$$s^{1/2}\theta(s) = C_0(A_1 s^2 + A_2 s^4) \tag{5.7.125}$$

Substituting Equation (5.7.125) into Equation (5.7.124), we may obtain

$$f(n) = C_0[J_1(n) + A_1' J_2(n)/n + A_2' J_3(n)/n^2] \tag{5.7.126}$$

where $A_1' = A_1 + A_2$ and $A_2' = -2A_2$.

To determine C_0, Equation (5.7.125) is substituted into Equation (5.7.121) leading to the evaluation of integrals of the form

$$a_0^2 \int_0^\infty \frac{k_1(\xi)}{F(\xi)}\frac{J_m(\xi)}{\xi^{m-1}}\sin(\xi r)d\xi; \quad m = 1,2,3. \tag{5.7.127}$$

Integrals are to be evaluated by using contour integration with the integrand $a_0^2 k_1(\zeta)H_m^{(1)}(\zeta)\sin(\zeta r)/|F(\zeta)\zeta^{m-1}|$. Procedure is similar to the one used earlier.

Values for the real and imaginary parts of C_0 are determined for different values of r in the interval $0 = r = 1$. The variation of C_0 is found to be less than 0.5% for $a_0 = 1.0$ and less than 1% for $1.0 = a_0 = 1.5$.

The contact stress and the torque per unit length along the z-axis is given by

$$\sigma_y(x,0) = C_0[x(b^2-x^2)^{-1/2} + A_1' x(b^2-x^2)^{1/2}/b^2 + A_2' x(b^2-x^2)^{3/2}/3b^4]/(\pi b); \quad 0 \le x < b \tag{5.7.128}$$

$$T = bC_0[1/2 + A_1'/8 + A_2'/48] = \pi G b^2 \psi_{a22} = \pi G b^2 \psi(f_1 + if_2) \tag{5.7.129}$$

where f_1 and f_2 are equivalent stiffness, shown in Figure 5.7.21a.

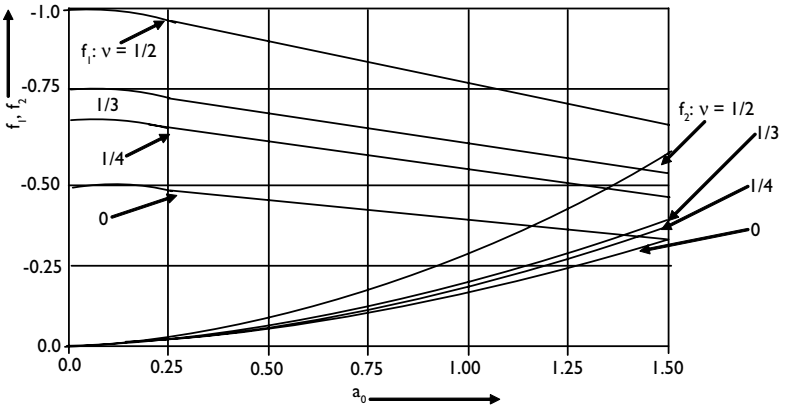


Figure 5.7.21a Equivalent stiffness versus frequency factor, rocking vibration.

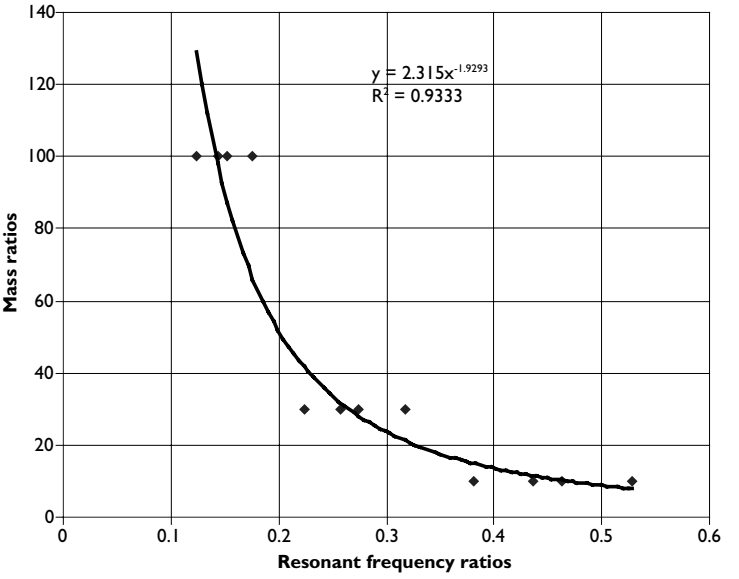


Figure 5.7.21b Mass ratio at resonance, a_0^*: for all Poisson ratios.

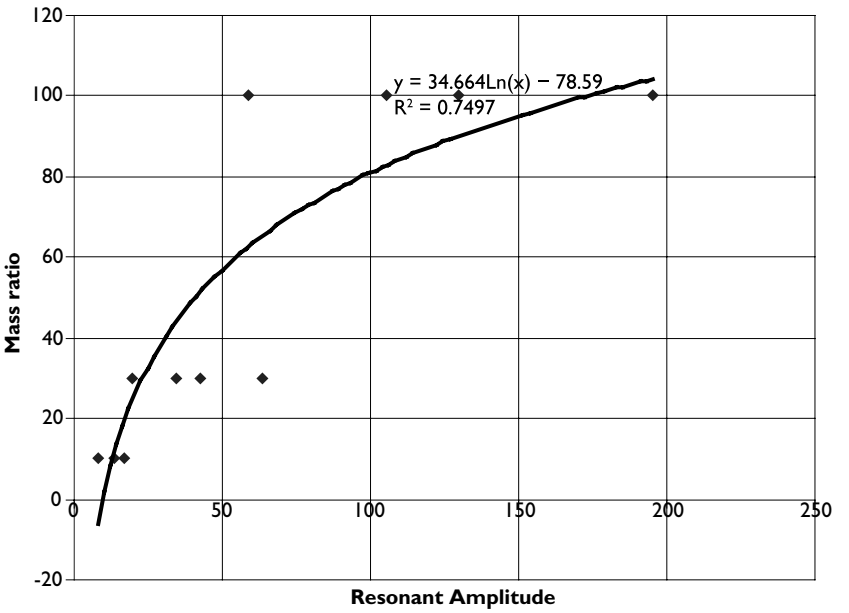


Figure 5.7.21c Mass ratio versus amplitude at resonance, a_0^*: for all Poisson ratios.

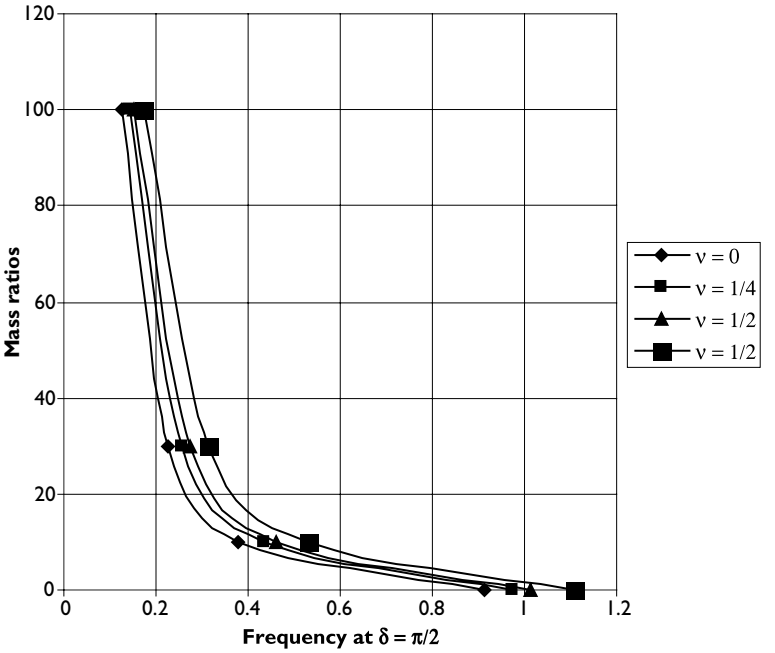


Figure 5.7.21d Amplitudes at resonance, at $\bar{a}_0^*$ (at $\delta = \pi/2$).

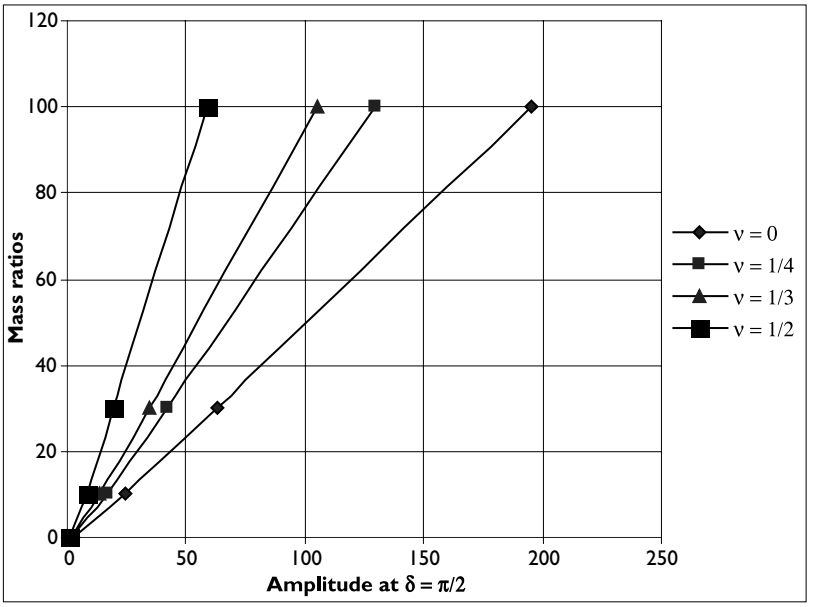


Figure 5.7.21e Mass ratio versus amplitudes at resonance, at $\bar{a}_0^*$ (at $\delta = \pi/2$).

The non-dimensional amplitude ψ is given by

$$\psi = |\pi G b^2 \psi / T| = [(f_1 + n_2^2 \tilde{J}/\pi)^2 + f_2^2]^{-1/2}, \tag{5.7.130}$$

where T is the amplitude of the applied torque per unit length along the z-axis and $\tilde{J}$ the inertia ratio equal to $(J/\rho b^4)$, where J denotes the mass polar inertia per unit length of the rigid body about the axis of rocking and the phase angle is given by

$$\delta = \tan^{-1}[f_2/(f_1 + a_0^2 \tilde{J}/\pi)] \tag{5.7.131}$$

It can be shown that for $a_0 = 0$, $\theta(s) = 0$, yielding $f(n) = C_0 J_1(n)$. Results are shown in Figures 21b,c,d,e.

5.7.11 Luco and Westmann solution for rigid strip footing

Luco and Westmann (1972) obtained a solution for the forced vibration of a rigid rectangular footing of infinite length and width 2b perfectly bonded to the free surface of an elastic half space is considered. The footing is subjected to vertical, shear and moment forces with harmonic time-dependence. The motion of the mass less footing is produced by line forces and moments with harmonic time dependence $e^{i\omega t}$ acting on the strip. Using the theory of singular integral equations the problem reduced to

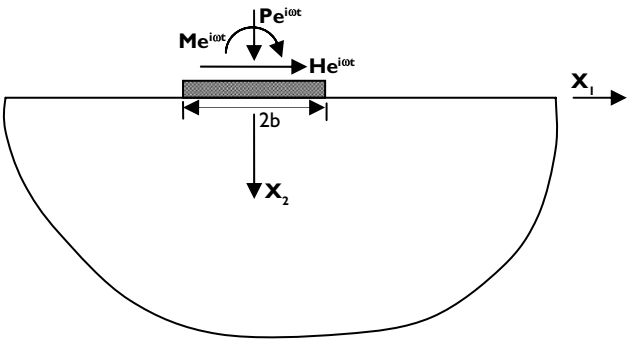


Figure 5.7.22 Footing and the coordinates.

the evaluation of the numerical solution of two Fredholm integral Equations. The statement problem is shown in Figure 5.7.22.

For this derivation Cartesian tensor notation has been used all through. If $u_i e^{i\omega t}$ are the Cartesian components of the displacement vector, due to the nature of applied forces, $u_3 = 0$ and all derivatives with respect to x_3 vanish. The x_3-axis coincides with the infinite direction of the strip. The space, $x_2 \geq 0$ is assumed to be homogeneous, isotropic elastic half space. Under these conditions the problem is two-dimensional and the equations of motion in the half space are given by

$$G u_{i,jj} + (\lambda + G) u_{j,ji} + \omega^2 \rho u_i = 0, \quad x_2 \geq 0; \quad i, j = 1, 2 \tag{5.7.132}$$

where λ and G are Lame's constants and ρ is the density of the medium.

The displacement boundary conditions are

$$u_1 = \Delta_1 \quad |x_1| < b, \; x_2 = 0 \tag{5.7.133}$$

$$u_2 = \Delta_2 + \varphi x_1 \quad |x_1| < b, x_2 = 0 \tag{5.7.134}$$

in which Δ_1 corresponds to the amplitude of the horizontal displacement of the strip, Δ_2 to the vertical displacement at the center of the strip, and φ is the amplitude of the footing rotation.

The components of surface traction T_i must satisfy the conditions

$$T_i(x_1) = -t_{2i}(x_1, 0) = 0, \quad |x_1| > b, i = 1, 2. \tag{5.7.135}$$

in which τ_{ij} represents the component of stress tensor referred to x_i coordinate system.

Also, the weightless footing requires that

$$b \int_{-1}^{1} T_1(b\xi) d\xi = H; \quad b \int_{-1}^{1} T_2(b\xi) d\xi = P; \quad b^2 \int_{-1}^{1} \xi T_2(b\xi) d\xi = M \tag{5.7.136}$$

where H, P, M are, respectively, the amplitude per unit length of the horizontal force, vertical force, and the moment applied to the strip.

Luco and Westmann (1972) used Green's function g_{ij} for the half space and now the problem of determining the unknown surface traction under the footing is reduced to

$$\int_{-b}^{b} g_{1i}(x_1 - \xi;\omega)T_i(\xi)d\xi = \Delta_1$$

$$\int_{-b}^{b} g_{2i}(x_1 - \xi;\omega)T_i(\xi)d\xi = (\Delta_2 + \phi x_1), \quad |x_1| < b, \ (i = 1,2) \tag{5.7.137}$$

The above integral equations were solved for the values of T_1 and T_2 and subsequently the stress field and displacements were obtained by solving the boundary value problem of class 1.

Differentiation of Equation (5.7.137) w. r. t. x_1 and use of the variable $x = x_1/b$, leads to

$$\frac{1}{\pi}\int_{-1}^{1}\frac{T_i(b\xi)}{\xi - x}d\xi - \eta^2\varepsilon_{ij}T_j(bx) = 2(1-\eta^2)\left[G\phi\delta_{2i} + \frac{a_0}{\pi}\int_{-1}^{1}T_j(b\xi)L_{ij}(x-\xi)d\xi\right]$$
$$|x| < 1, \ (i,j = 1,2) \tag{5.7.138}$$

where, e_{ij} is zero for $i = j$ and ± 1 if (i,j) is even or odd permutation of (1 and 2); other parameters used are: $a_0 = \omega b\sqrt{\rho/G} = bk$; $\eta = \sqrt{[(1-2\nu)/2(1-\nu)]}$ = ratio of shear and dilatation waves, ν = Poisson's ratio.

The integrals on the left hand side of Equation (5.7.137) are to be interpreted in the sense of a Cauchy principal value. The remaining terms are defined by

$$L_{ij}(x-\xi) = (-1)^{i+j}\int_0^{\infty} H_{ij}(k,\eta)\cos\left[a_0 k(x-\xi) + \delta_{ij}\frac{\pi}{2}\right]dk \tag{5.7.139}$$

The left hand side of Equation (5.7.137) is uncoupled by recombining may be written as

$$\frac{1}{\pi}\int_{-1}^{1}\frac{\rho_{i(\xi)}}{\xi - x}d\xi + i(-1)^i\eta^2\rho_j(x) = 2\left(1-\eta^2\right)\left[G\phi - \frac{i}{2\pi}\int_{-1}^{1}\rho_{j(\xi)K_{ij}(x-\xi)d\xi}\right]$$
$$|x| < 1, \ (i,j = 1,2)$$

in which $\rho_i(x) = T_2(bx) - i\,(-1)^i T_1(bx), (i = 1, 2); i = \sqrt{-1}$, and it finally leads to the following system of Fredholm integral equations

$$r_i(x) + \frac{1}{\pi}\int_{-1}^{1} \phi_{ij}(x,\xi) r_j(\xi) d\xi = -(-1)^i \frac{2Gi}{\kappa}\,(C_i + \phi x)\,; \quad |x| < 1,\ (i,j = 1,2) \tag{5.7.140}$$

where $\quad r_i(x) = \rho_i(x)/X_i(x);$ (5.7.141)

$$X_1(x) = -i\frac{\sqrt{\kappa}}{\sqrt{1-x^2}} \exp\left(i\theta \ln\left(\frac{1+x}{1-x}\right)\right);$$

$$X_2(x) = X_1(x); \quad \kappa = 3 - 4\nu; \quad \theta = \ln(\kappa)/(2\pi) \quad \text{and}$$

$$\phi_{ij}(x,\xi) = \kappa^{i-2} X_j(\xi) \left[\int_{-1}^{1} \frac{K_{ij}(t-\xi) - Kij(x-\xi)}{X_i(t)(t-x)} dt\right]; \quad i,j = 1,2 \text{ (no sum)}$$

$$\text{Also,} \quad K_{11}(x) = 2a_0 \int_0^\infty H_{12}(k,\eta)\cos(a_0 kx)dk - ia_0 \int_0^\infty [H_{11}(k,\eta) + H_{22}(k,\eta)\sin(a_0 kx)]dk$$

$$K_{21}(x) = 2a_0 \int_0^\infty H_{21}(k,\eta)\cos(a_0 kx)dk - ia_0 \int_0^\infty [H_{11}(k,\eta) + H_{22}(k,\eta)\sin(a_0 kx)]dk$$

$$K_{12}(x) = ia_0 \int_0^\infty [H_{11}(k,\eta) - H_{22}(k,\eta)\sin(a_0 kx)]dk = K_{21}(k,\eta)$$

where

$$H_{11}(k,\eta) = \frac{1}{2(1-\eta^2)} + \frac{n'k}{\Delta_0(k,\eta)}; \quad H_{22}(k,\eta) = \frac{1}{2(1-\eta^2)} + \frac{nk}{\Delta_0(k,\eta)}$$

$$H_{12}(k,\eta) = \frac{\eta^2}{1-\eta^2} + \frac{2(k^2-1)k^2 - 2k^2 nn'}{\Delta_0(k,\eta)} = -H_{21}(k,\eta)$$

in which $n = \sqrt{k^2 - \eta^2}$; $n' = \sqrt{k^2 - 1}$; $\mathrm{Re}[n], n' \geq 0$; and $\Delta_0(k,\eta) = (2k^2 -)^2 - 4k^2 nn'$.

φ, C_1 and C_2 are constants to be determined from Equation (5.7.136) and may be written as

$$b\int_{-1}^{1} X_1(x)r_1(x)dx = P + iH; \qquad b\int_{-1}^{1} X_2(x)r_2(x)dx = P - iH;$$

$$b^2\int_{-1}^{1} [X_1(x)r_1(x) + X_2(x)r_2(x)]xdx = 2M \tag{5.7.142}$$

The coupled integral equation, Equation (5.7.140), permits the expression of r_1 and r_2 in terms of φ_1, C_1 and C_2. It is then possible to find out Δ_1 and Δ_2 from Equation (5.7.137).

For an incompressible solid, the singularity at the edges of the strip footing reduces to a square root type singularity. Under this condition the Cauchy singular integral equations (Equation (5.7.138)) can be transformed into Fredholm integral equations with simplified kernels.

5.7.11.1 Vertical vibration

Surface tractions used are

$$T_1(b\xi) = -2G\xi\left[A_1(1-\xi^2)^{-1} + \int_{|\xi|}^{1} \nu^{-1/2}\theta_1(\nu)(\nu^2-\xi^2)^{-1/2}d\nu\right]$$

$$T_2(b\xi) = 2G\left[A_2(1-\xi^2)^{-1/2} + \int_{|\xi|}^{1} \nu^{1/2}\theta_2(\nu)(\nu^2-\xi^2)^{-1/2}d\nu\right], \quad |\xi| < 1. \tag{5.7.143}$$

in which, A_1 A_2 are unknown constants and $\theta_1(\nu)$ and $\theta_2(\nu)$ are functions to be determined. It is assumed that $\nu^{-1/2}\theta_1(\nu)$ and $\nu^{1/2}\theta_2(\nu)$ are $O(\nu)$ as $\nu \to 0$.

In Equation (5.7.138) if we set $\varphi = 0$, and $\nu = 1/2$ one may obtain the following set of Fredholm integral equations

$$\theta_i(u) - \int_0^1 M_{ij}(u,v)\theta_j(v) = A_j M_{ij}(u,1), \quad 0 \le u \le 1, \ (i,j=1,2) \tag{5.7.144}$$

where

$$M_{11}(u,v) = 2a_0^2\sqrt{uv}\int_0^\infty kH_{11}(k,0)J_1(a_0ku)J_1(a_0kv)dk;$$

$$M_{22}(u,v) = 2a_0^2\sqrt{uv}\int_0^\infty kH_{22}(k,0)J_0(a_0ku)J_0(a_0kv)dk;$$

$$M_{12}(u,v) = 2a_0^2\sqrt{uv}\int_0^\infty kH_{12}(k,0)J_1(a_0ku)J_0(a_0kv)dk;$$

$$M_{21}(u,v) = 2a_0^2\sqrt{uv}\int_0^\infty kH_{12}(k,0)J_0(a_0ku)J_1(a_0kv)dk.$$

The integral equations given above in Equation (5.7.144) would give the values of $\theta_1(u)$ and $\theta_2(u)$ in terms of the unknowns A_1 and A_2. These constants are determined in turn by Equation (5.7.137) with $\Delta_1 = \varphi = 0$. Both the sides of Equation (5.7.137) are differentiated with respect to x_1 and the results evaluated at $x_1 = 0$. An average of the vertical displacement with weight $b\pi^{-1}(b-x_1^2)^{-1/2}$ has been used to obtain Δ_2 and hence we have

$$0 = -2\left[A_jN_{1j}(1) + \int_0^1 N_{1j}(v)\theta_j(v)v^{1/2}dv\right];$$

$$\Delta_2 = -2b\left[A_jN_{2j}(1) + \int_0^1 N_{2j}(v)\theta_j(v)v^{1/2}dv\right] \quad (j=1,2) \tag{5.7.145}$$

where

$$N_{11}(v) = a_0\int_0^\infty H_{11}(k,0)J_1(a_0kv)dk - 1/2v;$$

$$N_{12}(v) = a_0\int_0^\infty H_{12}(k,0)J_0(a_0kv)dk;$$

$$N_{21}(v) = \int_0^\infty \frac{(2k^2-1)k - 2knn'}{\Delta_0(k,0)}J_0(a_0k)J_1(a_0kv)dk;$$

$$N_{22}(v) = \int_0^\infty \frac{n}{\Delta_0(k,0)}J_0(a_0k)J_1(a_0kv)dk$$

Equation (5.7.145) may be used to obtain A_1 and A_2 in terms of Δ_2.

Now, the amplitude of the applied vertical force is given by

$$P = 2\pi pb\left[A_2 + \int_0^1 v^{1/2}\theta_2(v)dv\right] \tag{5.7.146}$$

The dynamic compliance and corresponding stiffness may be obtained from

$$C_{vv}(a_0) = \pi\mu\Delta_2/P; \quad k_{vv}(a_0) = 1/C_{vv}(a_0) \tag{5.7.147}$$

For low frequencies

$$T_1(bx) = 0; \quad T_2(bx) = \frac{P}{\pi b\sqrt{1-x^2}} \quad |x| < 1. \tag{5.7.148}$$

Using Equations (5.7.139), (5.7.147) leads to

$$C_{vv}(a_0) = -\frac{1}{2}\left[\ln\left(\frac{a_0}{2}\right) + \bar{\gamma} + i\frac{\pi}{2}\right] \quad \text{as } a_0 \to 0; \bar{\gamma} = 0.577125 = \text{Euler's constant.} \tag{5.7.149}$$

5.7.11.2 Coupled horizontal and rocking vibration

The surface traction components are

$$T_1(b\xi) = 2G\left[A_1(1-\xi^2)^{-1/2} + \int_{|\xi|}^1 v^{1/2}\theta_1(v)(v^2-\xi^2)^{-1/2}dv\right]$$

$$T_2(b\xi) = 2G\left[A_2(1-\xi^2)^{-1/2} + \int_{|\xi|}^1 v^{-1/2}\theta_2(v)(v^2-\xi^2)^{-1/2}dv\right] \quad |\xi| < 1 \tag{5.7.150}$$

Using these expressions in Equation (5.7.138) and setting $\Delta_2 = 0$ and $\nu = 1/2$ leads to a system of Fredholm integral equations also as given in Equation (5.7.142), in which the kernels $M_{ij}(u, v)$ are the same as in Equation (5.7.142) except for the replacement of the Bessel function of order one by the corresponding Bessel function of order zero and vice-versa.

Substitution from Equation (5.7.150) into Equation (5.7.137) leads to

$$\Delta_1 = -2b\left[A_j N_{1j}(1) + \int_0^1 N_{1j}(v)\theta_j(v)v^{1/2}dv\right]$$
$$\phi = -2\left[A_j N_{2j}(1) + \int_0^1 N_{2j}(v)\theta_j(v)v^{1/2}dv\right] \quad (j = 1, 2) \tag{5.7.151}$$

in which

$$N_{11}(v) = \int_0^\infty \frac{n'}{\Delta_0(k,0)} J_0(a_0 k)J_0(a_0 kv)dk$$
$$N_{12}(v) = \int_0^\infty \frac{(2k^2-1)k - 2knn'}{\Delta_0(k,0)} J_0(a_0 k)J_1(a_0 kv)dk$$
$$N_{21}(v) = a_0\int_0^\infty H_{12}(k,0)J_1(a_0 kv)dk; \tag{5.7.152}$$
$$N_{22}(v) = a_0\int_0^\infty H_{22}(k,0)J_1(a_0 kv)dk - 1/2v$$

and an average with weight $b\pi^{-1}(b^2 - x_1^2)^{-1/2}$ has been used to obtain Equation (5.7.151).

Both the sides of Equation (5.7.137) has been differentiated w.r.t. x to obtain Equation (5.7.151) and the result is evaluated at the center of the strip.

The force displacement relationship is then reduced to

$$H = 2\pi Gb\left[A_1 + \int_0^1 v^{1/2}\theta_1(v)dv\right]; \quad M = 2Gb^2\left[A_2 + \int_0^1 v^{1/2}\theta_2(v)dv\right] \tag{5.7.153}$$

Once the integral equations have been solved in term as of A_1 and A_2, these constants can be determined in terms of Δ_1 and φ using Equation (5.7.151). These lead to

$$\begin{Bmatrix}\Delta_1 \\ b\phi\end{Bmatrix} = \frac{1}{\pi b}\begin{bmatrix}C_{HH}(a_0) & C_{HM}(a_0) \\ C_{MH}(a_0) & C_{MM}(a_0)\end{bmatrix}\begin{Bmatrix}H \\ M/b\end{Bmatrix} \tag{5.7.154}$$

where $C_{HM} = C_{MH}$.

$C_{HH}(a_0)$ has the same asymptotic behaviour as $C_{vv}(a_0)$ when a_0 tends to zero. To obtain the corresponding integral equations and compliances for the vertical, rocking and horizontal vibrations under relaxed conditions, it is necessary to set A_1 and θ_1 to zero for the first two cases, and set A_2 and θ_2 to zero for the last case.

It should be noted that only the equations representing constraints on the vertical displacement are considered for vertical and rocking vibrations, while only the equations constraining the horizontal displacement are considered for the horizontal vibrations. For solving integral equations the integrals are replaced by summations obtained by using standard numerical techniques, like the Simpson's rule. Once the integral equations have been solved, numerical integration is used to evaluate the applied forces and corresponding displacements. The kernels M_{ij}, N_{ij} are evaluated by numerical integrations after transforming them by the use of contour integration.

5.7.11.3 Approximate evaluation of compliances

A first approximation to the force-displacement relationship for Poisson's ratio other than one half has been obtained by solving the dominant part of Equation (5.7.140). This is given by the nonhomogeneous terms in Equation (5.7.140). Combining this solution with Equations (5.7.140), (5.7.141) and (5.7.142) leads to the surface traction for vertical vibration:

$$T_1(\xi b) = -\frac{1}{4\pi}\left(\frac{1+\kappa}{\kappa}\right)\frac{P}{b}\left[X_1(\xi) + X_2(\xi)\right]$$
$$T_2(\xi b) = -\frac{i}{4\pi}\left(\frac{1+\kappa}{\kappa}\right)\frac{P}{b}\left[X_1(\xi) - X_2(\xi)\right] \quad |\xi| < 1 \tag{5.7.155}$$

in the case of coupled horizontal-rocking vibration it is

$$T_1(\xi b) = \frac{G}{\kappa}[C_1^0\{X_1(\xi) - X_2(\xi)\} + \phi^0\xi\{X_1(\xi) + X_2(\xi)\}]$$

$$T_2(\xi b) = \frac{G\,i}{\kappa}[C_1^0\{X_1(\xi) + X_2(\xi)\} + \phi^0\xi\{X_1(\xi) - X_2(\xi)\}] \tag{5.7.156}$$

$$\text{in which} \quad C_1^0 = -i[2\theta\phi^0 - \frac{1+\kappa}{\kappa}\frac{H}{b}]; \quad \phi^0 = \frac{1}{2\pi}\left[\frac{1+\kappa}{1+\theta^2}\right]\left[\frac{M+2\theta bH}{\mu b^2}\right] \tag{5.7.157}$$

Substitution from Equation (5.7.152) in Equation (5.7.137) shows that the corresponding displacement u_2 under the strip for the vertical vibration is given by

$$u_2(bx) = -\frac{P}{2\pi G}\left[\int_0^\infty \frac{n}{\Delta_0(k,\eta)}\cos(a_0kx)M_+\left(\frac{1}{2}+i\theta,1,2ia_0k\right)dk\right.$$

$$\left.+\int_0^\infty \frac{(2k^2-1)k-2knn'}{\Delta_0(k,\eta)}\cos(a_0kx)M_-\left(\frac{1}{2}+i\theta,1,2ia_0k\right)dk\right];\quad |x|<1 \tag{5.7.158}$$

in which $M\pm(a,b,z) = [M(a,b,z)\pm M(\bar{a},b,z)]e^{-z/2}$ where $M(a,b,z)$ represents Kummer's confluent hypergeometric function.

Defining the average displacement under the strip footing as

$$\Delta_2 = \frac{2}{\pi}\int_0^1 \frac{u_2(bx)}{\sqrt{1-x^2}}dx \tag{5.7.159}$$

leads to the following estimate of the vertical compliance

$$C_{vv}(a_0) = -\frac{1}{2}\left[\int_0^\infty \frac{n}{\Delta_0(k,\eta)}J_0(a_0k)M_+\left(\frac{1}{2}+i\theta,1,2ia_0k\right)dk\right.$$

$$\left.+\int_0^\infty \frac{(2k^2-1)k-2knn'}{\Delta_0(k,\eta)}J_0(a_0k)M_-\left(\frac{1}{2}+i\theta,1,2ia_0k\right)dk\right] \tag{5.7.160}$$

Using a similar procedure compliance functions for horizontal and rocking compliances may be obtained as

$$C_{HH}(a_0)$$

$$= -\frac{1}{2}\left\{\int_0^\infty \frac{n'}{\Delta_0(k,\eta)}J_0(a_0k)\left[M_+\left(\frac{1}{2}+i\theta,1,2ia_0k\right)+2\theta a_0kM_-\left(\frac{3}{2}+i\theta,3,2ia_0k\right)\right]dk\right.$$

$$\left.+\int_0^\infty \frac{(2k^2-1)k-2knn'}{\Delta_0(k,\eta)}J_0(a_0k)\left[M_-\left(\frac{1}{2}+i\theta,1,2ia_0k\right)+2\theta a_0kM_+\left(\frac{3}{2}+i\theta,3,2ia_0k\right)\right]dk\right\} \tag{5.7.161}$$

$$C_{HM}(a_0) = -\frac{a_0}{2}\left\{\int_0^\infty \frac{n'k}{\Delta_0(k,\eta)}J_0(a_0k)\left[M_-\left(\frac{3}{2}+i\theta,3,2ia_0k\right)\right]dk\right.$$

$$\left.+\int_0^\infty \frac{(2k^2-1)k-2knn'}{\Delta_0(k,\eta)}J_0(a_0k)\left[M_+\left(\frac{3}{2}+i\theta,3,2ia_0k\right)\right]dk\right\} \tag{5.7.162}$$

$$C_{MH}(a_0)$$

$$= -\left\{\int_0^\infty \frac{n}{\Delta_0(k,\eta)} J_1(a_0k)\left[M_-\left(\frac{1}{2}+i\theta,1,2ia_0k\right)+2\theta a_0kM_+\left(\frac{3}{2}+i\theta,3,2ia_0k\right)\right]dk\right.$$

$$+\int_0^\infty \frac{(2k^2-1)k-2kn'n}{\Delta_0(k,\eta)} J_1(a_0k)$$

$$\left.\times\left[M_+\left(\frac{1}{2}+i\theta,1,2ia_0k\right)+2\theta a_0kM_-\left(\frac{3}{2}+i\theta,3,2ia_0k\right)\right]dk\right\} \tag{5.7.163}$$

$$C_{MM}(a_0) = -a_0\left\{\int_0^\infty \frac{n}{\Delta_0(k,\eta)} J_1(a_0k)M_+\left(\frac{3}{2}+i\theta,3,2ia_0k\right)dk\right.$$

$$\left.+\int_0^\infty \frac{(2k^2-1)k-2kn'n}{\Delta_0(k,\eta)} J_1(a_0k)M_-\left(\frac{3}{2}+i\theta,3,2ia_0k\right)dk\right\} \tag{5.7.164}$$

The corresponding approximation for the relaxed boundary conditions can be obtained by setting $\theta = 0$, in Equations (5.7.160) through (5.7.164).

5.7.12 Dynamic response of circular footings

The dynamic compliances for a larger frequency range is necessary for solving soil-structure interaction problems, particularly under earthquake loading condition. Further the knowledge of surface displacements is needed since these quantities are being experimentally measured.

Luco and Westmann (1971) computed the various dynamic compliances of the circular footing for a wide range of dimensionless frequency. Also presented are the surface tractions and far-field displacements as a function of frequency.

The footing is modeled as a rigid circular disc with radius r_0 resting on a homogeneous elastic half space. A cylindrical coordinate system r, θ, z is employed: the $r-\theta$ plane coincides with the half space surface with the z-axis directed into the half space. The origin of the coordinate system is located at the centre of the circular disc. The steady state displacement vector $(u_r, u_\theta, u_z)e^{i\omega t}$, corresponding to a harmonic loading frequency ω, satisfies the elastic equations of motion. Hence in the solution the factor $e^{i\omega t}$ is omitted. The basic criterion used is that since the loads are applied on a finite region of the surface of the half space, the displacements must satisfy the appropriate condition as (r^2+z^2) tends to infinity.

Solutions of the equations of motion in cylindrical coordinates, satisfying the radiation condition, for the displacements and components of stress τ_{rz}, $\tau_{\theta z}$, σ_z at $z = 0$, are specified in terms of the dimensionless variables $r' = r/r_0$, $z' = z/r_0$ are given by

$$u_r(r_0r', \theta, r_0z') = -r_0 \int_0^\infty kF_{11}(k, z')J_1(kr')dk;$$

$$u_\theta(r_0r', \theta, r_0z') = r_0 \int_0^\infty \frac{C_1(k)}{n_2} e^{-n_2z'} J_1(kr')dk;$$

$$u_z(r_0r', \theta, r_0z') = r_0 \int_0^\infty F_{21}(k, z')J_0(kr')dk; \tag{5.7.165}$$

$$\tau_{rz}(ar', \theta, 0) = -G \int_0^\infty kF_{31}(k)J_1(kr')dk;$$

$$\tau_{\theta z}(ar', \theta, 0) = -G \int_0^\infty C_1(k)J_1(kr')dk$$

$$\sigma_z(ar', \theta, 0) = G \int_0^\infty F_{41}(k)J_1(kr')dk \quad \text{and} \tag{5.7.166}$$

$$u_r(r_0r', \theta, r_0z') = r_0 \int_0^\infty \left[F_{12}(kz') \frac{\partial J_1(kr')}{\partial r'} - C_2(k) \frac{J_1(kr')}{r'} e^{-n_2z'} \right] dk \cos\theta$$

$$u_\theta(r_0r', \theta, r_0z') = -r_0 \int_0^\infty \left[F_{12}(kz') \frac{J_1(kr')}{r'} - C_2(k) \frac{\partial J_1(kr')}{\partial r'} e^{-n_2z'} \right] dk \sin\theta$$

$$u_z(r_0r', \theta, r_0z') = r_0 \int_0^\infty F_{22}(k, z')J_1(kr')dk \cos\theta \tag{5.7.167}$$

$$\tau_{rz}(r_0r', \theta, 0) = G \int_0^\infty \left[F_{32}(k) \frac{\partial J_1(kr')}{\partial r'} + n_2C_2(k) \frac{J_1(kr')}{r'} \right] dk \cos\theta$$

$$\tau_{\theta z}(r_0r', \theta, 0) = -G \int_0^\infty \left[F_{32}(k) \frac{J_1(kr')}{r'} + n_2C_2(k) \frac{\partial J_1(kr')}{\partial r'} \right] dk \sin\theta$$

$$\sigma_z(r_0r', \theta, 0) = G \int_0^\infty F_{42}(k)J_1(kr')dk \cos\theta \tag{5.7.168}$$

in which

$$
\begin{aligned}
F_{1i}(k,z') &= -A_i(k)e^{-n_1 z'} + n_2 B_i(k)e^{-n_2 z'} \quad i = 1,2 \\
F_{2i}(k,z') &= n_1 A_i(k)e^{-n_1 z'} - k^2 B_i(k)e^{-n_2 z'} \quad i = 1,2 \\
F_{3i}(k) &= 2n_1 A_i(k) + (a_0^2 - 2k^2)B_i(k) \quad i = 1,2 \\
F_{4i}(k) &= (a_0^2 - 2k^2)A_i(k) + 2n_2 k^2 B_i(k) \quad i = 1,2
\end{aligned}
\tag{5.7.169}
$$

where $n_1 = \sqrt{k^2 - \gamma^2 a_0^2}; n_2 = \sqrt{k^2 - a_0^2}$; $Re\ n_1, n_2 \geq 0$; $a_0^2 = \omega r_0(\rho/G); \gamma^2 = (1-2\nu)/[2(1-\nu)]$ and ρ, G and ν represent density, shear modulus and Poisson's ratio, respectively.

Equations (5.7.165) and (5.7.166) have been used to solve the torsional and vertical vibration response, while Equations (5.7.165) and (5.7.166) are used for the rocking and horizontal vibrations.

5.7.12.1 Boundary conditions

1 In all four cases it has been assumed that the surface traction outside the disc is zero.
2 For vertical and rocking vibrations, the vertical displacement under the disc is prescribed while the disc-foundation interface is taken to be frictionless.
3 For horizontal vibrations, the horizontal displacements are prescribed under the disc while it is assumed that the contact is such that the normal component of the surface traction is zero everywhere.

The boundary conditions described above lead to sets of dual integral equations in terms of the unknown functions $A_i(k)$, $B_i(k)$, $C_i(k)$. By appropriate substitutions, the dual integral equations reduce to Fredholm integral equations of the second kind, which are to be solved numerically.

5.7.12.2 Tortional vibration

For torsional vibration of the rigid disc of amplitude α_T, the displacement u_θ and the stress $\tau_{\theta z}$ under the disc, and the total applied torque T are given by

$$u_\theta(r_0 r', \theta, 0) = \alpha_T r_0 r' \quad (r' \leq 1) \tag{5.7.170}$$

$$
\begin{aligned}
&\tau_{\theta z}(r_0 r', \theta, 0) \\
&\quad = -\frac{4G\alpha_T}{\pi}\left[\frac{r'}{(1-r'^2)^{1/2}}\phi(1) - \int_{r'}^{1} \frac{r'}{(t^2 - r'^2)^{1/2}} \frac{d}{dt}[t^{-1/2}\phi(t)]dt\right] \quad (r' \leq 1)
\end{aligned}
\tag{5.7.171}
$$

$$T = 16G\alpha_T r_0^3 \int_0^1 t\phi(t)dt \tag{5.7.172}$$

in which $\phi(t)$ satisfies the Fredholm integral equation

$$\phi(t) + \int_0^1 K(t,t')\phi(t')dt' = t \quad (0 \le t \le 1) \tag{5.7.173}$$

The kernel $K(t,t')$ for Equation (5.7.173) and other kernels to be appeared later are listed in the Appendix. The expressions given therein have been obtained using Equations (5.7.165) and (5.7.166) with $A_1 = B_1 = 0$ and

$$C_1(k) = \frac{4k\alpha_T}{\pi} \int_0^1 \phi(t)\sin(kt)dt \tag{5.7.174}$$

5.7.12.3 Vertical vibration

For vertical vibrations of amplitude Δ_V

$$u_z(r_0 r', \theta, 0) = \Delta_V \quad (r' < 1) \tag{5.7.175}$$

$$\sigma_z(r_0 r', \theta, 0) = -\frac{2G\Delta_V}{\pi r_0(1-\nu)}\left[\frac{\phi(1)}{(1-r'^2)^{1/2}} - \int_{r'}^1 \frac{\frac{d}{dt}\phi(t)dt}{(t^2-r'^2)^{1/2}}\right] \quad (r' < 1) \tag{5.7.176}$$

$$V = \frac{4G\Delta_V r_0}{(1-\nu)} \int_0^1 \phi(t)dt \tag{5.7.177}$$

where V is the amplitude of the vertical force. The function $\phi(t)$ must satisfy the Fredholm integral equation

$$\phi(t) + \int_0^1 K(t,t')\phi(t')dt' = 1 \quad (0 \le t \le 1) \tag{5.7.178}$$

The expressions given in the Appendix have been obtained using Equations (5.7.165) and (5.7.166) with $C_1 = 0$ and

$$\begin{aligned} A_1(k) &= \frac{1}{1-\nu}\left[\frac{(a_0^2 - 2k^2)}{4n_1 n_2 k^2 - (2k^2 - a_0^2)^2}\right]\psi(k); \\ B_1(k) &= -\frac{1}{1-\nu}\left[\frac{2n_1}{4n_1 n_2 k^2 - (2k^2 - a_0^2)^2}\right]\psi(k) \end{aligned} \tag{5.7.179}$$

where

$$\psi(k) = \frac{2\Delta_V k}{\pi r_0} \int_0^1 \phi(k) \cos(kt) dt \tag{5.7.180}$$

The far-field displacements ($r \gg r_0$) on the surface of the half space, using Equations (5.7.165), (5.7.179) and (5.7.180) are given by

$$u_z(r,\theta,0) = -i\frac{\omega L_0 V}{2\beta^3\rho} R_V(a_0) H_0^{(2)}\left(\frac{\omega r}{C_R}\right) \quad (r \gg r_0)$$
$$u_r(r,\theta,0) = i\frac{\omega M_0 V}{2\beta^3\rho} R_V(a_0) H_1^{(2)}\left(\frac{\omega r}{C_R}\right) \quad (r \gg r_0) \tag{5.7.181}$$

where $H_0^{(2)}$ and $H_1^{(2)}$ are Hankel functions and

$$L_0 = \frac{s\sqrt{s^2-\gamma^2}}{F'(s)}; \quad M_0 = -\frac{s^2[2\sqrt{s^2-\gamma^2}\sqrt{s^2-1} - (2s^2-1)]}{F'(s)} \tag{5.7.182}$$

$$R_V(a_0) = \int_0^1 \phi(t)\cos(a_0 st)dt \Big/ \int_0^1 \phi(t)dt \tag{5.7.183}$$

in which

$$F(s) = 4s^2\sqrt{s^2-\gamma^2}\sqrt{s^2-1} - (2s^2-1)^2 = 0;$$

$F'(s)$ is the derivative of $F(x)$ at $x = s$, $\beta = (G/\rho)^{1/2}$ and $C_R = \beta/s$ is the velocity of the Rayleigh wave.

5.7.12.4 Rocking vibration

For rocking vibrations of amplitude α_M

$$u_z(r_0 r', \theta, 0) = \alpha_M r_0 r' \cos\theta \quad (r' < 1) \tag{5.7.184}$$

$$\sigma_z(r_0 r', \theta, 0)$$
$$= -\frac{4G\alpha_M}{\pi(1-\nu)}\left[\frac{r'\phi(1)}{(1-r'^2)^{1/2}} - \int_{r'}^1 \frac{r'\frac{d}{dt}[t^{-1}\phi(t)]dt}{(t^2-r'^2)^{1/2}}\right]\cos\theta \quad (r' < 1) \tag{5.7.185}$$

$$M = \frac{8G\alpha_M r_0^3}{1-\nu}\int_0^1 t\phi(t)dt \tag{5.7.186}$$

where M is the amplitude of rocking moment. The function $\theta(t)$ satisfies a Fredholm integral equation identical, except for the kernel, to Equation (5.7.172).

The above results are based on Equation (5.7.167) and (5.7.168) with $C_2 = 0$ and A_2, B_2 given, respectively, by the right hand side of Equation (5.7.179) in which

$$\psi(k) = \frac{4k\alpha_M}{\pi} \int_0^1 \phi(t) \sin(kt) dt \tag{5.7.187}$$

The part of the far-field displacement on the surface of the half space corresponding to Rayleigh wave is given by

$$\begin{aligned}
u_z(r,\theta,0) &= -\frac{i\omega^2 s L_0 M}{2\beta^4 \rho} R_M(a_0) H_1^{(2)}\left(\frac{\omega r}{C_R}\right)\cos\theta \\
u_r(r,\theta,0) &= \frac{i\omega^2 s L_0 M_0 M}{4\beta^4 \rho} R_M(a_0)\left[H_2^{(2)}\left(\frac{\omega r}{C_R}\right) - H_0^{(2)}\left(\frac{\omega r}{C_R}\right)\right]\cos\theta \\
u_\varphi(r,\theta,0) &= \frac{i\omega^2 s L_0 M_0 M}{4\beta^4 \rho} R_M(a_0)\left[H_2^{(2)}\left(\frac{\omega r}{C_R}\right) + H_0^{(2)}\left(\frac{\omega r}{C_R}\right)\right]\sin\theta \quad (r \gg r_0)
\end{aligned} \tag{5.7.188}$$

where L_0, M_0 are far-field displacement factors and

$$R_M(a_0) = \left\{\int_0^1 \phi(t)\sin(a_0 s t) dt\right\} \Big/ \left\{a_0 s \int_0^1 [t\phi(t) dt]\right\} \tag{5.7.189}$$

5.7.12.5 Horizontal vibrations

For horizontal vibration of amplitude Δ_H

$$u_r(r_0 r', \theta, 0) = \Delta_H \cos\theta \quad u_\theta(r_0 r', \theta, 0) = -\Delta_H \sin\theta \quad (r' < 1) \tag{5.7.190}$$

$$\tau_{rz}(r_0 r', \theta, 0) = \tau_{rz}^*(r')\cos\theta \quad \tau_{\theta z}(r_0 r', \theta, 0) = \tau_{\theta z}^*(r')\sin\theta \quad (r' < 1) \tag{5.7.191}$$

where

$$\begin{aligned}
\tau_{rz}^* - \tau_{\varphi z}^* &= -\frac{4G\Delta_H}{\pi r_0(2-\nu)}\left[\frac{2\phi_1(1) - \nu\phi_2(1)}{(1-r'^2)^{1/2}} - \int_{r'}^1 \left\{\frac{2\frac{d}{dt}\phi_1(t) - \nu t^{-1}\frac{d}{dt}\left(t\phi_2(t)\right)\frac{dt\phi_2(t)}{dt}}{(t^2 - r'^2)^{1/2}}\right\} dt\right] \\
\tau_{rz}^* + \tau_{\varphi z}^* &= \frac{4G\Delta_H}{\pi r_0}\left[\frac{r^2\phi_2(1)}{(1-r'^2)^{1/2}} - r'^2 \int_{r'}^1 \left\{\frac{\frac{d}{dt}\left(t^{-2}\phi_2(t)\right)}{(t^2 - r'^2)^{1/2}}\right\} dt\right]
\end{aligned} \tag{5.7.192}$$

The amplitude of the horizontal force H applied to the disc is given by

$$H = \frac{8Gr_0\Delta_H}{2-\nu}\int_0^1 \phi_1(t)dt \tag{5.7.193}$$

The functions ϕ_1 and ϕ_2 satisfy the pair of Fredholm integral equations given by

$$\phi_1(t) + \int_0^1 [K_{11}(t,t')\phi_1(t') + K_{12}(t,t')\phi_2(t')] = 1$$

$$(1-\nu)\phi_2(t) + \int_0^1 [K_{21}(t,t')\phi_1(t') + K_{22}(t,t')\phi_2(t')]dt' = 0 \quad (0 \le t \le 1) \tag{5.7.194}$$

The above expressions are obtained from Equations (5.7.167) and (5.7.168) by using

$$A_2(k) = -\frac{4n_2k}{4n_1n_2k^2 - (2k^2 - a_0^2)^2}\psi_1(k); \quad B_2(k) = \frac{2(a_0^2 - 2k^2)}{4n_1n_2k^2 - (2k^2 - a_0^2)^2}\psi_1(k);$$

$$C_2(k) = [2\psi_2(k)]/[kn_2] \tag{5.7.195}$$

where

$$\psi_1(k) = \frac{2\Delta_H k}{\pi r_0(2-\nu)}\int_0^1 \phi[(\phi_1(t) - \phi_2(t))\cos(kt) + [\phi_2(t)\sin(kt)]/kt]dt \tag{5.7.196}$$

$$\psi_2(k) = \frac{2\Delta_H k}{\pi r_0(2-\nu)}\int_0^1 [-(\phi_1(t) + (1-\nu)\phi_2(t))\cos(kt) + [(1-\nu)\phi_2(t)\sin(kt)]/kt]dt \tag{5.7.197}$$

The part of the far-field displacement on the surface of the half space corresponding to the Rayleigh wave is given by

$$u_z(r,\theta,0) = -i\frac{\omega M_0 H}{2\beta^3\rho}R_H(a_0)H_1^{(2)}\left(\frac{\omega r}{C_R}\right)\cos\theta$$

$$u_r(r,\theta,0) = \frac{i\omega N_0 H}{4\beta^3\rho}R_H(a_0)\left[H_2^{(2)}\left(\frac{\omega r}{C_R}\right) - H_0^{(2)}\left(\frac{\omega r}{C_R}\right)\right]\cos\theta$$

$$u_\varphi(r,\theta,0) = \frac{i\omega N_0 H}{4\beta^3\rho}R_H(a_0)\left[H_2^{(2)}\left(\frac{\omega r}{C_R}\right) + H_0^{(2)}\left(\frac{\omega r}{C_R}\right)\right]\sin\theta \quad (r \gg r_0) \tag{5.7.198}$$

in which

$$N_0 = \frac{s(s^2-1)^{1/2}}{F'(s)};$$

$$R_H(a_0) = \left[\int_0^1 [\phi_1(t) - \phi_2(t)]\cos(a_0 st)dt + \int_0^1 \phi_2(t)[\sin(a_0 st)/a_0 st]dt\right] \Big/ \left[\int_0^1 \phi_1(t)dt\right] \tag{5.7.199}$$

5.7.12.6 Coupling motions

Let a harmonic horizontal force of amplitude H is applied to a perfectly bonded elastic half space, a harmonic rocking motion α_H is produced, in addition to the horizontal displacement Δ_H. Again when a rocking moment M is applied, a horizontal motion Δ_M is produced in addition to the rocking motion α_M. These coupling motion α_H and Δ_M are related by the reciprocity condition. Since the solutions given in (c) and (d) are based on relaxed boundary conditions, only estimates of these coupled displacements can be obtained.

Bycroft (1956) used generalized weighted averages as

$$\bar{\alpha}_H = \frac{3}{2\pi r_0^3}\int_0^{2\pi}\int_0^{r_0} \frac{r^2}{(r_0^2-r^2)^{1/2}} u_z \cos\theta d\theta; \quad \bar{\Delta}_M = \frac{3}{2\pi r_0}\int_0^{2\pi}\int_0^{r_0}\left[\frac{u_r\cos\theta - u_\theta \sin\theta}{(r_0^2-r^2)^{1/2}}\right] r dr d\theta; \tag{5.7.200}$$

where, u_z is the vertical displacement produced by the horizontal force while u_r and u_θ are the horizontal components of the displacement produced by the rocking moment.

Again, from Equation (5.7.199), we have

$$H\Delta_M = M\alpha_H \tag{5.7.201}$$

Thus, using Equations (5.7.167), (5.7.168), (5.7.193), (5.7.194) and (5.7.197), one can have

$$\begin{aligned}\bar{\alpha}_H = \frac{3(1-\nu)}{8\pi}\frac{H}{Gr_0^2}\Bigg\{&\gamma^2 + I_{H1}(a_0) + \gamma^2\int_0^1 \frac{1+t^2}{2t^2}\Theta(t)\\ &\times\left[\gamma^2\int_0^1 \frac{1+t^2}{2t^2}\Theta(t)\left(\ln\left(\frac{1-t}{1+t}\right) + \frac{2t}{1+t^2}\right)dt - \int_0^1 t^{-1/2}\Theta(t) I_{H2}(a_0,t)dt\right]\\ &\times\left(\int_0^1 \phi_1(t)dt\right)^{-1}\Bigg\}\end{aligned} \tag{5.7.202}$$

$$\text{where} \quad \Theta(t) = t\phi_1(t) - \int_0^t \phi_1(t')dt' - t\phi_2(t) \tag{5.7.203}$$

$\phi_1(t)$, $\phi_2(t)$ are solutions of Equations (5.7.194) and $I_{H1}(a_0)$ and $I_{H2}(a_0, t)$ are given in the Appendix.

Similarly using Equations (5.7.167), (5.7.169), (5.7.185) and (5.7.187), we can have

$$\bar{\Delta}_M = \frac{1-\nu}{8\pi}\frac{M}{Gr_0^2}\left[\gamma^2 \int_0^1 \phi(t)\ln\left(\frac{1+t}{1-t}\right)dt + \int_0^1 \phi(t) I_M(a_0, t)dt\right]\left[\int_0^1 t\phi(t)dt\right]^{-1} \tag{5.7.204}$$

in which $I_M(a_0, t)$ is also given in the Appendix and $\theta(t)$ is the solution of Equation (5.7.173) for the rocking case.

5.7.12.7 Numerical solutions

The Fredholm integral equation for each case was solved numerically for a_0 in the range 0 to 10 for varying Poisson's ratio. The Fredholm integral equations were reduced to a system of algebraic equations using finite differences. Integrals were evaluated using Simpson's rule with ten to twenty intervals. The kernels were evaluated by Filon's method of numerical integration.

As regarding error in the numerical evaluation, by doubling the number of intervals the difference found was less than one percent for frequencies less than two, the error increases for higher frequencies.

The dynamic compliances are defined by the matrix equation as follows

$$\begin{Bmatrix} \alpha_T \\ \Delta_V \\ \alpha_M \\ \Delta_H \end{Bmatrix} \begin{bmatrix} C_T(a_0) & 0 & 0 & 0 \\ 0 & C_V(a_0) & 0 & 0 \\ 0 & 0 & C_M(a_0) & C_{MH}(a_0) \\ 0 & 0 & C_{HM}(a_0) & C_H(a_0) \end{bmatrix} \begin{Bmatrix} T \\ V \\ M \\ H \end{Bmatrix} \tag{5.7.205}$$

and were evaluated using Equations (5.7.172), (5.7.177), (5.7.186), (5.7.173), (5.7.200) and (5.7.204).

The static values obtained from above are:

$$C_T(0) = \frac{3}{16}\frac{1}{\pi r_0^3}; \quad C_V(0) = \frac{1}{4}\frac{1-\nu}{\pi r_0}; \quad C_M(0) = \frac{3}{8}\frac{1-\nu}{\pi r_0^3};$$

$$C_H(0) = \frac{1}{8}\frac{2-\nu}{\pi r_0}; \quad C_{HM}(0) = C_{MH}(0) = \frac{3}{16\pi}\frac{1-2\nu}{Gr_0^2} \tag{5.7.206}$$

In the neighbourhood of the edge of the disc, the stresses are as given below

$$\tau_{\theta z}(r_0 r', 0, 0) = -\frac{3}{4\pi r_0^3} T S_T \frac{r'}{(1-r'^2)^{1/2}}; \quad S_T = \frac{\phi(1)}{3\int_0^1 t\phi(t)dt} \text{(torsion) as } r' \to 1-$$

$$\sigma_z(r_0 r', 0, 0) = -\frac{V}{2\pi r_0^2} S_V \frac{1}{(1-r'^2)^{1/2}}; \quad S_V = \frac{\phi(1)}{\int_0^1 \phi(t)dt} \text{(vertical) as } r' \to 1-$$

$$\sigma_z(r_0 r', 0, 0) = -\frac{3M}{2\pi r_0^3} S_M \frac{r'}{(1-r'^2)^{1/2}}; \quad S_M = \frac{\phi(1)}{3\int_0^1 t\phi(t)dt} \text{(rocking) as } r' \to 1-$$

$$\tau^*_{rz}(r') - \tau^*_{\theta z}(r') = -\frac{H}{\pi r_0^2} S_{H1} \frac{1}{(1-r'^2)^{1/2}};$$

$$S_{H1} = \frac{2\phi_1(1) - \nu\phi_2(1)}{2\int_0^1 \phi_1(t)dt} \text{(horizontal) as r}' \to 1-$$

$$\tau^*_{rz}(r') + \tau^*_{\theta z}(r') = -\frac{H}{\pi r_0^2} S_{H2} \frac{r'^2}{(1-r'^2)^{1/2}};$$

$$S_{H2} = \frac{(2-\nu)\phi_2(1)}{2\int_0^1 \phi_1(t)dt} \text{(horizontal) as } r' \to 1- \tag{5.7.207}$$

The coefficients L_0, M_0, N_0 appearing in the expressions for the far-field are given in Table 5.7.5. It can be seen that only for extremely low values of the dimensionless frequency $a_0 = r_0\omega/\beta$, the far-field displacement is approximated by the corresponding displacement for a point load.

In Equation (5.7.205), when the force inputs are real, consider the following example involving the torsion problem. If the resultant torque acting on the footing is $T\cos\omega t$, then the response is given by

$$\alpha_T = T\{Re[C_T]\cos\omega t - Im[C_T]\sin\omega t\} = T|C_T|\cos(\omega t + \delta) \tag{5.7.208}$$

$$\text{where,} \quad |C_T| = \{(Re[C_T])^2 + (Im[C_T])^2\}^{1/2}; \quad \delta = \tan^{-1}\left[\frac{Im[C_T]}{Re[C_T]}\right] \tag{5.7.209}$$

Table 5.7.5

ν	γ^2	s	L_0	M_0	N_0
1/2	0	1.0468	0.1139	0.0620	0.0337
1/3	1/4	1.0724	0.1752	0.1066	0.0681
1/4	1/3	1.0877	0.1996	0.1360	0.0926
0	1/2	1.1441	0.3254	0.2558	0.2011

APPENDIX

(a) Torsional case

The kernel is given by

$$K(t,t') = L(t+t') - L(|t-t'|) \tag{a1}$$

where

$$L(t) = 0.5a_0[J_1(a_0t) - iH_1(a_0t)] \tag{a2}$$

in which J_1 and H_1 stand for Bessel and Struve functions of order one.

The asymptotic expansions of the compliance for low and high frequencies are

$$C_T(a_0) = \frac{3}{16Gr_0^3}\left\{\left[1 + a_0^2 - \frac{34}{525}a_0^4 + \cdots\right] - \frac{i}{\pi}\left[\frac{4}{9}a_0^3 - \frac{16}{225}a_0^5 + \cdots\right]\right\} \quad \text{as } a_0 \to 0 \tag{a3}$$

$$C_T(a_0) = \frac{3}{16Gr_0^3}\left\{\left[\frac{125}{3}\frac{1}{(\pi a_0)^2} + \cdots\right] - \frac{i}{4}\left[\frac{32}{3}\frac{1}{a_0} + \frac{64}{3}\frac{\sin(2a_0 - \pi/4)}{\sqrt{\pi}a_0^{5/2}} + \cdots\right]\right\}$$

$$\text{as } a_0 \to \infty \tag{a4}$$

(b) Vertical case

The kernel is given by

$$K(t,t') = L(t+t') + L(|t-t'|) \tag{b1}$$

in which

$$L(t) = \frac{-ia_0}{4\pi(1-\nu)}\left[\frac{4\pi s(s^2-\gamma^2)^{1/2}e^{-ia_0st}}{F'(s)} + \int_0^{\gamma}\frac{\xi(\gamma^2-\xi^2)^{1/2}e^{-ia_0\xi t}}{\Delta_1(\xi,\gamma)}d\xi\right]$$
$$+ \frac{-ia_0}{4\pi(1-\nu)}\left[\int_{\gamma}^{1}\frac{\xi^2(\xi^2-\gamma^2)(1-\xi^2)^{1/2}e^{-ia_0\xi t}}{\Delta_2(\xi,\gamma)}d\xi\right] \tag{b2}$$

where

$$\Delta_1(\xi,\gamma) = (\gamma^2-\xi^2)^{1/2}(1-\xi^2)^{1/2}\xi^2 + (\xi^2 - 1/2)^2$$

$$\Delta_2(\xi,\gamma) = (\gamma^2-\xi^2)(1-\xi^2)\xi^4 + (\xi^2 - 1/2)^4$$

The asymptotic expansion of the compliance for low frequencies

$$C_V(a_0) = \left(\frac{1-\nu}{4Gr_0}\right)\left\{\left[1+\left(\frac{2\pi I_2 - 6I_1^2}{3\pi^2}\right)a_0^2 + \left(\frac{19I_2^2 + 84I_1I_3 - 120\pi I_4}{180\pi^2}\right)a_0^4 + \cdots\right]\right\}$$
$$-\frac{i}{\pi}\left(\frac{1-\nu}{4Gr_0}\right)\left[I_1 a_0 + \left(\frac{\pi I_3 - 4I_1I_3}{3\pi}\right)a_0^3 + \cdots\right] \quad as\ a_0 \to 0 \tag{b3}$$

where I_1, I_2, I_3 and I_4 are as given below (Robertson, 1966) for $n = 1, 2, 3, 4$.

$$I_n = (1-\gamma^2)\left[\frac{-\pi(s^2-\gamma^2)^{1/2}s^n}{F'(s)}\right] + (1-\gamma^2)\left[\int_0^{\gamma} \frac{\xi^n(\gamma^2-\xi^2)^{1/2}d\xi}{(\xi^2-1/2)^2 + (\gamma^2-\xi^2)^{1/2}(1-\xi^2)^{1/2}\xi^2}\right]$$
$$+ (\gamma^2-\xi^2)^{1/2}\left[\int_{\gamma}^{1} \frac{\xi^{n+2}(\gamma^2-\xi^2)(1-\xi^2)^{1/2}d\xi}{(\xi^2-1/2)^4 + (\xi^2-\gamma^2)(1-\xi^2)\xi^4}\right] \tag{b4}$$

I_n-values have been computed numerically over the range $0 \le \gamma^2 \le 0.5$ using Simpson's rule and are shown in Table 5.7.6.

Table 5.7.6

γ^2	n	I_n	γ^2	n	I_n	γ^2	n	I_n
0.00	1	2.62118	0.10	1	2.51526	0.25	1	2.45791
	2	2.35291		2	2.29358		2	2.28989
	3	2.21709		3	2.20102		3	2.26230
	4	2.15658		4	2.17479		4	2.29960
	5	2.14177		5	2.18908		5	2.37603
	6	2.15660		6	2.23066		6	2.48038
	7	2.19196		7	2.29213		7	2.60706
	8	2.24252		8	2.36915		8	2.75320
0.33	1	2.48050		1	2.53203		1	2.59471
	2	2.35514		2	2.45891		2	2.57800
	3	2.37570		3	2.53543		3	2.71486
	4	2.46463		4	2.68599		4	2.93351
	5	2.59652		5	2.88676		5	3.21258
	6	2.76109		6	3.12898		6	3.54560
	7	2.95385		7	3.40978		7	3.93203
	8	3.17304		8	3.72909		8	4.37433
0.48	1	2.64472	0.49	1	2.66372	0.50	1	2.68862
	2	2.67176		2	2.70740		2	2.74876
	3	2.85636		3	2.91042		3	2.97068
	4	3.13010		4	3.20571		4	3.28871
	5	3.47400		5	3.57528		5	3.68589
	6	3.88380		6	4.01582		6	4.15998
	7	4.36133		7	4.53024		7	4.71504
	8	4.91170		8	5.12484		8	5.35874

(c) Rocking case

The kernel is

$$K(t,t') = -[L(t+t') - L(|t-t'|)] \tag{c1}$$

where $L(t)$ is given by Equation (b2).

The asymptotic expansion of the compliance for low frequencies is given by

$$C_M(a_0) = \frac{3(1-\nu)}{8Gr_0^3}\left[1 + \left(\frac{2}{5}\frac{I_2}{\pi}\right)a_0^2 - \left(\frac{90\pi I_4 + I_2^2}{525\pi^2}\right)a_0^4 + \cdots\right]$$
$$- \frac{i}{\pi}\left(\frac{3(1-\nu)}{8Gr_0^3}\right)\left[\left(\frac{I_3}{3}\right)a_0 - \left(\frac{I_5}{15}\right)a_0^3 + \cdots\right] \quad as\ a_0 \to 0 \tag{c2}$$

(d) Horizontal case

The kernel for $t \geq t'$ is given by

$$K_{11}(t,t') = -\frac{ia_0^2(tt')^{1/2}}{4(2-\nu)}\int_0^1 [G_1(\xi) + G_2(\xi)]H_{-1/2}^{(2)}(a_0t\xi)J_{-1/2}(a_0t'\xi)d\xi$$

$$K_{12}(t,t') = -\frac{ia_0^2(tt')^{1/2}}{4(2-\nu)}\int_0^1 [G_1(\xi) - (1-\nu)G_2(\xi)]H_{-1/2}^{(2)}(a_0t\xi)J_{3/2}(a_0t'\xi)d\xi$$

$$K_{21}(t,t') = -\frac{ia_0^2(tt')^{1/2}}{4(2-\nu)}\int_0^1 [G_1(\xi) - (1-\nu)G_2(\xi)]H_{3/2}^{(2)}(a_0t\xi)J_{-1/2}(a_0t'\xi)d\xi$$

$$K_{22}(t,t') = -\frac{ia_0^2(tt')^{1/2}}{4(2-\nu)}\int_0^1 [G_1(\xi) + (1-\nu)^2G_2(\xi)]H_{3/2}^{(2)}(a_0t\xi)J_{3/2}(a_0t'\xi)d\xi \tag{d1}$$

where

$$G_1(\xi) = \frac{4\pi(s^2-1)^{1/2}s^2}{F'(s)}\delta(\xi - s) + \frac{(1-\xi^2)^{1/2}\xi^2}{\Delta_1(\xi,\gamma)}H(\gamma - \xi)$$
$$+ \frac{(1-\xi^2)^{1/2}(\xi^2 - 1/2)^2\xi^2}{\Delta_2(\xi,\gamma)}H(\xi - \gamma)$$
$$G_2 = \frac{4\xi^2}{\sqrt{1-\xi^2}} \tag{d2}$$

where, $\delta(\xi)$ is Dirac's delta function and $H(\xi)$ is the Heaviside step function.

For $t' > t$, the kernels can be evaluated by use of the relationships

$$K_{11}(t,t') = K_{11}(t',t); \quad K_{12}(t,t') = K_{21}(t',t); \quad K_{22}(t,t') = K_{22}(t',t). \tag{d3}$$

The asymptotic expansion of C_H is given by

$$\begin{aligned} &C_H(a_0) \\ &\quad = \frac{2-\nu}{8Gr_0}[\{1-(C_2+C_1^2)a_0^2+\cdots\} - i\{a_0C_1+(C_3-2C_1C_2-C_1^3)a_0^3+\cdots\}] \\ &\quad \text{as } a_0 \to 0 \end{aligned} \tag{d4}$$

where the constants $C1$, $C2$, $C3$ are given in Luco (1971).

(e) Coupling case

The functions related to this case are as follows

$$\begin{aligned} I_{H1}(a_0) = -\frac{i\sqrt{2\pi}}{4(1-\nu)} \Bigg\{ &-4\pi s \left(\frac{2\sqrt{s^2-\gamma^2}\sqrt{s^2-1} - (2s^2-1)}{F'(s)} \right) H_{1/2}^{(2)}(a_0 s) J_{3/2}(a_0 s) \\ &+ \int_\gamma^1 \frac{k\sqrt{k^2-\gamma^2}\sqrt{1-k^2}\,(k^2-1/2)}{\Delta_2(k,\gamma)} H_{1/2}^{(2)}(a_0 k) J_{3/2}(a_0 k)\,dk \\ &- \frac{4i}{\pi} \int_0^\infty \left[\frac{\sqrt{k^2+\gamma^2}\sqrt{1+k^2} - (k^2+1/2)}{\Delta_3(k,\gamma)} k + \frac{\gamma^2}{k(1-\gamma^2)} \right] K_{1/2}(a_0 k) J_{3/2}(a_0 k)\,dk \Bigg\} \end{aligned} \tag{e1}$$

$$\begin{aligned} I_{H2}(a_0,t) = -\frac{ia_0\sqrt{2\pi}}{4(1-\nu)} \Bigg\{ &-4\pi \left(\frac{2\sqrt{s^2-\gamma^2}\sqrt{s^2-1} - (2s^2-1)}{F'(s)} \right) s^2 H_{3/2}^{(2)}(a_0 s) J_{3/2}(a_0 st) \\ &+ \int_\gamma^1 \frac{k^2\sqrt{k^2-\gamma^2}\sqrt{1-k^2}\,(k^2-1/2)}{\Delta_2(k,\gamma)} H_{3/2}^{(2)}(a_0 k) J_{3/2}(a_0 kt)\,dk \\ &- \frac{4i}{\pi} \int_0^\infty \left[\frac{\sqrt{k^2+\gamma^2}\sqrt{1+k^2} - (k^2+1/2)}{\Delta_3(k,\gamma)} k^2 + \frac{\gamma^2}{(1-\gamma^2)} \right] K_{3/2}(a_0 k) I_{3/2}(a_0 kt)\,dk \Bigg\} \end{aligned} \tag{e2}$$

$$I_{H1}(a_0) = -\frac{1}{2(1-\nu)} \left\{ 4\pi \left(\frac{2\sqrt{s^2-\gamma^2}\sqrt{s^2-1} - (2s^2-1)}{F'(s)} \right) s e^{ia_0 s} \sin(a_0 st) \right.$$

$$-\int_{\gamma}^{1} \frac{k\sqrt{k^2-\gamma^2}\sqrt{1-k^2}\,(k^2-1/2)}{\Delta_2(k,\gamma)} e^{-ia_0k} \sin(a_0kt)dk$$

$$+2\int_{0}^{\infty} \left[\left(\frac{k\sqrt{k^2+\gamma^2}\sqrt{1+k^2}-(k^2+1/2)}{\Delta_3(k,\gamma)}\right)k+\frac{\gamma^2}{k(1-\gamma^2)}\right] e^{-ia_0k} \sin\, h(a_0kt)dk\Bigg\} \tag{e3}$$

in which, $\Delta_3(k,\gamma) = \sqrt{k^2+1}\sqrt{k^2+\gamma^2}k^2 - (2k^2+1)^2$ and $K_{1/2}$, $I_{3/2}$ are modified Bessel functions of the second and first kind.

5.7.13 Vibration of an elastic half space under rectangular loading

The motion of a footing block can be described by six co-ordinates corresponding to two orthogonal horizontal translations, a vertical translation, rocking about two mutually perpendicular horizontal axes. The vertical translation mode and torsional rotational mode occurs as uncoupled motions when a complete symmetry exists. Present study is confined to the vertical, horizontal and rocking modes of vibration of a rectangular foundation (Dasgupta & Kallam 2006).

5.7.13.1 Rectangular Footing Vibrations

For homogenous isotropic elastic body, the displacement vector satisfies the following equation

$$(\lambda+G)\left\{\frac{\partial\Delta}{\partial x},\frac{\partial\Delta}{\partial y},\frac{\partial\Delta}{\partial z}\right\}+G\nabla^2\{u,v,w\}=\rho\frac{\partial^2}{\partial t^2}\{u,v,w\} \tag{5.7.210}$$

where,

$$\Delta = \frac{\partial u}{\partial x}+\frac{\partial u}{\partial y}+\frac{\partial w}{\partial z} = \text{ dilatation;}$$

$$\nabla^2 = \frac{\partial^2}{\partial x^2}+\frac{\partial^2}{\partial y^2}+\frac{\partial^2}{\partial z^2} = \text{ Laplacian operator.}$$

By eliminating the displacement components u, v and w, the wave equation for the dilatation is obtained as

$$\left(\nabla^2-\frac{1}{V_s^2}\frac{\partial^2}{\partial t^2}\right)\Delta=0 \tag{5.7.211}$$

where $V_s = \sqrt{\frac{\lambda+2G}{\rho}}$ = dilatational wave velocity.

To solve Equation (5.7.211) a triple Fourier Transform (F) of Δ on x, y and t has been introduced where

$$F^3(\Delta) = \left(\frac{1}{2\pi}\right)^{\frac{3}{2}} \int_{-\infty}^{\infty}\int_{-\infty}^{\infty}\int_{-\infty}^{\infty} \Delta(x,y,z,t)\ e^{-i(\beta x+\gamma y+\omega t)} dxdydt = \overline{\Delta} \tag{5.7.212}$$

Its inverse is then defined by the equation $F^{-3}(\overline{\Delta}) = \Delta$.
It can be shown that

$$\left(\frac{1}{2\pi}\right)^{\frac{3}{2}} \int_{-\infty}^{\infty}\int_{-\infty}^{\infty}\int_{-\infty}^{\infty} \left(\frac{\partial^2\Delta}{\partial x^2}, \frac{\partial^2\Delta}{\partial y^2}, \frac{\partial^2\Delta}{\partial t^2}\right) e^{-i(\beta x+\gamma y+\omega t)} dxdydt$$
$$= -\left(\beta^2, \gamma^2, \omega^2\right)\overline{\Delta}(\beta,\gamma,z,\omega) \tag{5.7.213}$$

So the tripple Fourier transform of Equation (5.7.211) becomes

$$\left[\frac{d^2}{dz^2} - \{(\beta^2+\gamma^2) - h^2\}\right]\overline{\Delta} = 0 \tag{5.7.214}$$

With the solution

$$\overline{\Delta} = Ae^{-\alpha_1 z} + A'e^{+\alpha_1 z} \quad \text{where } \alpha_1^2 = \beta^2+\gamma^2-h^2;\ h^2 = \frac{\omega^2}{V_s^2}. \tag{5.7.215}$$

In Equation (5.7.215), we must take $A' = 0$ in order to eliminate the physically inconsistent solution for an exponentially increasing $\overline{\Delta}$ with z. Thus, the solution to Equation (5.7.231) is reduced to

$$\overline{\Delta} = Ae^{-\alpha_1 z} \tag{5.7.216}$$

Inverting Equation (5.7.216)

$$\Delta(x,y,z,t) = F^{-3}\left(Ae^{-\alpha_1 z}\right)$$
$$= \left(\frac{1}{2\pi}\right)^{\frac{3}{2}} \int_{-\infty}^{\infty}\int_{-\infty}^{\infty}\int_{-\infty}^{\infty} A(\beta,\gamma,\omega)\ e^{-\alpha_1 z+i(\beta x+\gamma y+\omega t)} d\beta d\gamma d\omega \tag{5.7.217}$$

We introduce now the multiple Fourier transform of the displacement components u, v and w in Equation (5.7.226).

Making use of the solution for Equation (5.7.217), Equation (5.7.210) then becomes

$$\left(\frac{d^2}{dz^2} - (\beta^2 + \gamma^2 - k^2)\right)(\overline{u}, \overline{v}, \overline{w}) = \left(\frac{k^2}{h^2} - 1\right) A e^{-\alpha_1 z}\,(i\beta, i\gamma, \alpha_1) \tag{5.7.218}$$

where $\alpha_2^2 = \beta^2 + \gamma^2 - k^2; \frac{k^2}{h^2} - 1 = \frac{V_p^2}{V_s^2} - 1 = \frac{\lambda+G}{G}; k^2 = \frac{\omega^2}{V_s^2} : V_s = \sqrt{\frac{G}{\rho}}$ = shear wave velocity. The independent solutions of $\overline{u}, \overline{v}$ and $\overline{w}$ in Equation (5.7.218) are then,

$$(\overline{u}, \overline{v}, \overline{w}) = (i\beta, i\gamma, \alpha_1)\,\frac{A}{h^2} e^{-\alpha_1 z} + (B, C, D)\, e^{-\alpha_2 z} \tag{5.7.219}$$

And its inverse can be written as

$$(u,\, v,\, w) = F^{-3}\left\{(i\beta, i\gamma, \alpha_1)\,\frac{A}{h^2} e^{-\alpha_1 z} + (B, C, D)\, e^{-\alpha_2 z}\right\} \tag{5.7.220}$$

The general solutions for the displacements are expressed by the following

$$(u, v, w) = F^{-3}\left\{(i\beta, i\gamma, \alpha_1)\,\frac{A}{h^2} e^{-\alpha_1 z} + \left(B, C, -\frac{i}{\alpha_2}(\beta B + \gamma C)\right) e^{-\alpha_2 z}\right\} \tag{5.7.221}$$

where A, B and C are to be determined from the boundary conditions.

Assume that the boundary conditions are to be specified in terms of stresses which can be determined from the displacements of Equation (5.7.221).

These are

$$\begin{aligned}
\tau_{xz}]_{z=0} &= -GF^{-3}\left\{\frac{2i\alpha_1\beta}{h^2} A e^{-\alpha_1 z} + \left(\frac{1}{\alpha_2}(\beta^2 + \alpha_2^2)B + \frac{\beta\gamma}{\alpha_2} C\right) e^{-\alpha_2 z}\right\} \\
\tau_{yz}]_{z=0} &= -GF^{-3}\left\{\frac{2i\alpha_1\gamma}{h^2} A e^{-\alpha_1 z} + \left(\frac{\beta\gamma}{\alpha_2} B + \frac{1}{\alpha_2}(\gamma^2 + \alpha_2^2)C\right) e^{-\alpha_2 z}\right\} \\
\sigma_z]_{z=0} &= -GF^{-3}\left\{(2\alpha_2 + k^2)\frac{A}{h^2} e^{-\alpha_1 z} - 2i\,(\beta B + \gamma C)\, e^{-\alpha_2 z}\right\}
\end{aligned} \tag{5.7.222}$$

5.7.13.2 Ground compliance of a rectangular foundation

In estimating the dynamical behavior of an above-ground structure, the motion of the foundation is defined in terms of the ground compliance which is a function of the elastic properties of the ground, the shape of the foundation and the frequency of oscillation. In this section we consider a rectangular foundation of dimensions of the half-space boundary.

In the dynamical problem the stress distribution under the foundation is not known since it depends on the displacement which is yet unknown. Thus we will adopt the

procedure used by others, of assuming a stress distribution under the foundation and solving for corresponding displacement.

We designate the stress distribution under the foundation to be $q_j(x, y, t)$ where then subscript j defines the type loading. Its Fourier transform is given by

$$F^3 q_j(x, y, t) = \overline{q}_j(x, y, t) = \left(\frac{1}{2\pi}\right)^{\frac{3}{2}} \int_{-\infty}^{\infty}\int_{-\infty}^{\infty}\int_{-\infty}^{\infty} q(\xi, \eta, \zeta) e^{-i(\beta\xi+\gamma\eta+\omega\xi)} d\xi\, d\eta d\zeta \tag{5.7.223}$$

Furthermore, by assuming the function of the stress distribution to be separable, i.e.

$$q_j(x, y, t) = q_j(x, y)\, Q(t) \tag{5.7.224}$$

We have, $FQ(t) = \left(\frac{1}{2\pi}\right)^{\frac{1}{2}} \int Q(\zeta) e^{-i\omega\zeta} d\zeta = \overline{Q}(\omega)$

Then the Fourier transform of

$$q_j(x, y, t) = \frac{\overline{Q}(\omega)}{2\pi} \int_{-\infty}^{\infty}\int_{-\infty}^{\infty} q_j(\xi, \eta) e^{-i(\beta\xi+\gamma\eta)} d\xi\, d\eta \tag{5.7.225}$$

This way solving dynamic problems of rectangular footings is adopted by Thomson and Kobori to obtain dynamic compliance at centre of rectangular footings in vertical mode of vibrations. Our present attempt is to obtain dynamic compliance at any point of the rectangular footings for all modes of vibrations adopting the same procedure as Thomson and Kobori. In this investigation we will consider the following types of loading

1 vertical loading
2 horizontal loading
3 loading produced by the rocking of the foundation about its centerline.

5.7.13.3 Vertical loading

The boundary stress are defined as

$$\tau_{xz} = 0; \quad \tau_{yz} = 0; \quad \sigma_z = q_v(x, y)\, Q(t) \tag{5.7.226}$$

Taking the triple Fourier transform of the stresses as given by Equation (5.7.238) and substituting in Equations (5.7.225) and (5.7.226) we obtain three Equations for

the arbitrary functions A, B and C.

$$\frac{2i\alpha_1\beta}{h^2}Ae^{-\alpha_1 z}+\left(\frac{1}{\alpha_2}(\beta^2+\alpha_2^2)B+\frac{\beta\gamma}{\alpha_2}C\right)e^{-\alpha_2 z}=0 \tag{5.7.227}$$

$$\frac{2i\alpha_1\gamma}{h^2}Ae^{-\alpha_1 z}+\left(\frac{\beta\gamma}{\alpha_2}B+\frac{1}{\alpha_2}(\gamma^2+\alpha_2^2)C\right)e^{-\alpha_2 z}=0 \tag{5.7.228}$$

$$(2\alpha_2+k^2)\frac{A}{h^2}e^{-\alpha_1 z}-2i\,(\beta B+\gamma C)\,e^{-\alpha_2 z}$$
$$=-\frac{\overline{Q}\,(\omega)}{2\pi G}\int_{-\infty}^{\infty}\int_{-\infty}^{\infty}q_V\,(\xi,\eta)e^{-i(\beta\xi+\gamma\eta)}d\xi\,d\eta \tag{5.7.229}$$

Assuming $q_v\,(\xi,\eta)$ to be a uniform stress $-q_0=$ constant, in which case the right side of the Equation (5.7.229) becomes

$$\frac{q_0\overline{Q}\,(\omega)}{2\pi G}\int_{-b}^{b}e^{-i\beta\xi}d\xi\int_{-c}^{c}e^{-i\gamma\eta}d\eta=\frac{4q_0}{2\pi G}\frac{\sin\beta b\ \sin\gamma c}{\beta\gamma}\overline{Q}\,(\omega) \tag{5.7.230}$$

Then Equation (5.7.229) can be written as

$$(2\alpha_2+k^2)\frac{A}{h^2}e^{-\alpha_1 z}-2i\,(\beta B+\gamma C)\,e^{-\alpha_2 z}=\frac{4q_0}{2\pi G}\frac{\sin\beta b\ \sin\gamma c}{\beta\gamma}\overline{Q}\,(\omega) \tag{5.7.231}$$

Solving Equations (5.7.227), (5.7.228) and (5.7.231), A, B and C are obtained as

$$A=\frac{4q_0}{2\pi G}\left(\frac{\sin\beta b\ \sin\gamma c}{\beta\gamma}\right)\frac{h^2\left[2\left(\beta^2+\gamma^2\right)-k^2\right]}{F\,(\beta,\gamma)}\overline{Q}\,(\omega)$$

$$B=-i\frac{4q_0}{2\pi G}\left(\frac{\sin\beta b\ \sin\gamma c}{\beta\gamma}\right)\frac{2\alpha_1\alpha_2\beta}{F\,(\beta,\gamma)}\overline{Q}\,(\omega) \tag{5.7.232}$$

$$C=-i\frac{4q_0}{2\pi G}\left(\frac{\sin\beta b\ \sin\gamma c}{\beta\gamma}\right)\frac{2\alpha_1\alpha_2\gamma}{F\,(\beta,\gamma)}\overline{Q}\,(\omega)$$

where $F\,(\beta,\gamma)=[2(\beta^2+\gamma^2)-k^2]-4\alpha_1\alpha_2(\beta^2+\gamma^2)$

Now the compliance in the vertical direction at the center of the rectangular foundation can be determined from Equation (5.7.221)

$$w=F^{-3}\left[\frac{\alpha_1 e^{-\alpha_1 z}}{h^2}-\frac{i\,(\beta B+\gamma C)}{\alpha_2}e^{-\alpha_2 z}\right] \tag{5.7.233}$$

For $z = 0$

$$w = F^{-3}\left[\frac{\alpha_1 A}{h^2} - \frac{i(\beta B + \gamma C)}{\alpha_2}\right] \tag{5.7.234}$$

$$w = \frac{1}{(2\pi)^{\frac{3}{2}}}\int_{-\infty}^{\infty}\int_{-\infty}^{\infty}\int_{-\infty}^{\infty}\overline{w}e^{i(\beta x+\gamma y+\omega t)}d\gamma\, d\beta\, d\omega \tag{5.7.235}$$

Now

$$\begin{aligned}\beta B + \gamma C &= \beta\left[-i\frac{4q_0}{2\pi G}\left(\frac{\sin\beta b\ \sin\gamma c}{\beta\gamma}\right)\frac{2\alpha_1\alpha_2\beta}{F(\beta,\gamma)}\overline{Q}(\omega)\right] \\ &\quad + \gamma\left[-i\frac{4q_0}{2\pi G}\left(\frac{\sin\beta b\ \sin\gamma c}{\beta\gamma}\right)\frac{2\alpha_1\alpha_2\gamma}{F(\beta,\gamma)}\overline{Q}(\omega)\right] \\ &= -i\frac{4q_0}{2\pi G}\left(\frac{\sin\beta b\ \sin\gamma c}{\beta\gamma}\right)\frac{2\alpha_1\alpha_2\gamma}{F(\beta,\gamma)}[\beta^2+\gamma^2]\overline{Q}(\omega)\end{aligned} \tag{5.7.236}$$

$$\overline{w}(\beta,\gamma,\omega) = -\frac{4q_0\alpha_1 k^2}{2\pi G}\left(\frac{\sin\beta b\sin\gamma c}{\beta\gamma}\right)\frac{\overline{Q}(\omega)}{F(\beta,\gamma)} \tag{5.7.237}$$

$$w = \frac{1}{(2\pi)^{\frac{3}{2}}}\int_{-\infty}^{\infty}\int_{-\infty}^{\infty}\int_{-\infty}^{\infty} -\frac{4q_0}{2\pi G}\left(\frac{\sin\beta b\sin\gamma c}{\beta\gamma}\right)\frac{\alpha_1 k^2}{F(\beta,\gamma)}\overline{Q}(\omega)e^{i(\beta x+\gamma y+\omega t)}d\gamma\, d\beta\, d\omega \tag{5.7.238}$$

Omitting $e^{i\omega t}$

$$\frac{\mathrm{w}]_{z=0}}{p_v Q(t)} = \frac{-1}{\pi^2 bcG}\int_0^{\infty}\int_0^{\infty}\frac{\alpha_1 k^2}{F(\beta,\gamma)}\frac{\sin\beta b\ \sin\gamma \mathrm{c}}{\beta\gamma}\cos\beta x\cos\gamma y d\beta d\gamma \tag{5.7.239}$$

The ground compliance for vertical dynamic load obtained was in terms of double infinite integrals for numerical evaluation of this integral certain simplification is necessary, this can be done by transformation of coordinates to reduce one of infinite integral to finite one and render the integrals in a form more suitable for computation.

Omitting the time factor $Q(t)$ Equation (5.7.239) can be written in the following form

$$\frac{wcG}{p_v} = \frac{1}{\pi^2 b}\int_0^{\infty}\int_0^{\infty}\frac{\alpha_1 k^2}{F(\beta,\gamma)}\frac{\sin\beta b\ \sin\gamma \mathrm{c}}{\beta\gamma}\cos\beta x\cos\gamma y d\beta d\gamma \tag{5.7.240}$$

Making the following substitution

$$\beta = r'\cos\theta;\quad \gamma = r'\sin\theta \Rightarrow \beta^2+\gamma^2 = r'^2;\quad d\beta d\gamma = r' dr' d\theta$$

And substituting

$$h = \frac{\omega}{c_1} = \frac{c_2}{c_1}\frac{\omega}{c_2} = nk; \quad \text{where } n = \sqrt{(1-2\nu)/[2\,(1-\nu)]};\ \nu = \text{Poisson's ratio.}$$

The finite integral form of the Equation (5.7.240) is

$$\frac{wcG}{p_v} = \frac{1}{\pi^2 b}\int_0^{\infty}\int_0^{\frac{\pi}{2}}\left[\frac{k^2\sqrt{r'^2 - n^2k^2}}{F\left(r', k\right)}\right]\left[\frac{\sin\left(r'b\cos\theta\right)\ \sin\left(r'c\sin\theta\right)}{r'^2\sin\theta\cos\theta}\right]$$

$$\times\left[\cos\left(r'x\cos\theta\right)\cos\left(r'y\sin\theta\right)\right]r'd\theta dr' \tag{5.7.241}$$

substituting $r' = rk$ and $\frac{\omega \mathrm{b}}{V_s} = bk = a_0$, Equation (5.7.241) becomes

$$\frac{wcG}{p_v} = \frac{1}{\pi^2 b}\int_0^{\infty}\int_0^{\frac{\pi}{2}}\left[\frac{\sqrt{r^2 - n^2}}{F\left(r\right)}\right]\left[\frac{\sin\left(ra_0\cos\theta\right)\ \sin\left(r\frac{c}{b}a_0\sin\theta\right)}{r\sin\theta\cos\theta}\right]$$

$$\times\left[\cos\left(r\frac{x}{b}a_0\cos\theta\right)\cos\left(r\frac{y}{c}\frac{c}{b}a_0\sin\theta\right)\right]drd\theta \tag{5.7.242}$$

where, $F(r) = (2r^2 - 1)^2 - 4r^2\sqrt{r^2 - n^2}\sqrt{r^2 - 1}$.

While numerical evaluation of the above integral some singularities due to the nature of the Rayleigh function $F(r)$ will occur. In order to avoid this error it is necessary to subtract half the residual value at Rayleigh pole.

Thus Equation (5.7.242) must be added with the quantity

$$\frac{-i}{\pi a_0}\int_0^{\frac{\pi}{2}}\frac{\sqrt{z_0^2 - n^2}}{F'\left(z_0\right)}\frac{\sin\left(z_0a_0\cos\theta\right)\ \sin\left(z_0\frac{c}{b}a_0\sin\theta\right)}{z_0\sin\theta\cos\theta}d\theta \tag{5.7.243}$$

5.7.13.4 Horizontal loading

In this case a horizontal shear load P_H is applied to the foundation in the direction of X, leading to the boundary conditions

$$\sigma_z = 0; \quad \tau_{yz} = 0; \quad \tau_{xz} = q_H\left(x, y, t\right) = -q_0Q\left(t\right)$$

Assuming again that the distribution of shear stress under the foundation is to be uniform and is equal to $-q_0$ proceeding as in vertical case the quantities A,

B and C are

$$A = i\frac{4q_0}{2\pi G}\left(\frac{\sin\beta b\ \sin\gamma c}{\beta\gamma}\right)\frac{2\beta\alpha_2 h^2}{F(\beta,\gamma)}\overline{Q}(\omega)$$
$$B = \frac{4q_0}{2\pi G}\left(\frac{\sin\beta b\ \sin\gamma c}{\beta\gamma}\right)\frac{(2\alpha_2^2+k^2)(\gamma^2+\alpha_2^2)-4\alpha_1\alpha_2\gamma^2}{\alpha_2 F(\beta,\gamma)}\overline{Q}(\omega)$$
$$C = -\frac{4q_0}{2\pi G}\left(\frac{\sin\beta b\ \sin\gamma c}{\beta\gamma}\right)\frac{(2\alpha_2^2+k^2-4\alpha_1\alpha_2)}{\alpha_2 F(\beta,\gamma)}\overline{Q}(\omega)$$

Then the compliance in horizontal direction can be found out by substituting these A, B and C values in Equation (5.7.221) and solving the equation same as vertical case. The final expression for ground compliance in horizontal case then becomes.

$$\frac{\mathrm{u}]_{z=0}}{p_H\overline{Q}(t)} = \frac{1}{\pi^2 bcG}\int_0^\infty\int_0^\infty\left[\frac{F(\beta,\gamma)-\beta^2[k^2-4\alpha_2(\alpha_1-\alpha_2)]}{\alpha_2 F(\beta,\gamma)}\right]$$
$$\times\left[\frac{\sin\beta b\ \sin\gamma c}{\beta\gamma}\cos\beta x\cos\gamma y\right]d\beta d\gamma \qquad (5.7.244)$$

Making the substitutions same as in vertical case to make the infinite integral to finite the simplified expression for ground compliance for horizontal case then becomes.

$$\frac{ucG}{p_H} = \frac{1}{\pi^2 a_0}\int_0^\infty\int_0^{\frac{\pi}{2}}\left[\frac{F(r)\sin^2\theta-(r^2-1)\cos^2\theta}{\sqrt{r^2-1}F(r)}\right]\left[\frac{\sin(ra_0\cos\theta)\ \sin(r\frac{c}{b}a_0\sin\theta)}{r\sin\theta\cos\theta}\right]$$
$$\times\left[\cos\left(r\frac{x}{b}a_0\cos\theta\right)\cos\left(r\frac{y}{c}\frac{c}{b}a_0\sin\theta\right)\right]drd\theta \qquad (5.7.245)$$

While evaluating the numerical values, singularities will occur due to nature of the Rayleigh function one at the Rayleigh pole and other at $r = 1$ in order to avoid errors due to these singularities the above Equation should be added with the following quantity

$$-\frac{i}{\pi a_0}\int_0^{\frac{\pi}{2}}\left[\frac{(1-i)\sin^2\theta}{\sqrt{2}}-\frac{\sqrt{z_0^2-1}}{f'(z_0)}\cos^2\theta\right]$$
$$\times\left[\frac{\sin(z_0a_0\cos\theta)\ \sin\left(z_0\frac{c}{b}a_0\sin\theta\right)}{z_0\sin\theta\cos\theta}cos\left(z_0\frac{x}{b}a_0\cos\theta\right)\cos\left(z_0\frac{y}{c}\frac{c}{b}a_0\sin\theta\right)\right]d\theta \qquad (5.7.246)$$

5.7.13.5 Rocking loading

In this case foundation is assumed to undergo rotation about the x axis. The shear stress under the foundation is assumed to be zero as in the case (a) and the normal stress is assumed to increase linearly with y, the boundary conditions for the shear is same as vertical loading and additional boundary condition is given by

$$\sigma_z]_{z=0} = -q_0 \frac{y}{c} Q(t)$$

And the total moment M_R is $M_R = \frac{4}{3} q_0 b c^2$

Substituting these boundary conditions in Equation (5.7.222) and solving those Equations values of A, B and C can be found out. Substituting the values of A, B and C in Equation (5.7.223) and proceeding as in the case of vertical motion, the final expression for vertical compliance at any point can be obtained as

$$w = -\frac{q_0 Q(t)\, i}{\pi^2 G c} \int_{-\infty}^{\infty} \int_{-\infty}^{\infty} \frac{\alpha_1 k^2}{F(\beta,\gamma)} \frac{\sin \beta b}{\beta} \left(\frac{\sin \gamma c}{\gamma^2} - \frac{c \cos \gamma c}{\gamma} \right) e^{i(\beta x + \gamma y)} d\beta d\gamma \tag{5.7.247}$$

On simplification above equation becomes

$$w = \frac{3 M_R Q(t)}{\pi^2 G b c^3} \int_0^{\infty} \int_0^{\infty} \frac{\alpha_1 k^2}{F(\beta,\gamma)} \frac{\sin \beta b \sin \gamma y}{\beta \gamma} \left[\frac{\sin \gamma c}{\gamma} - c \cos \gamma c \right] \cos \beta x d\beta d\gamma \tag{5.7.248}$$

Making the substitutions same as in vertical case to make the infinite integral to finite the simplified expression for vertical ground compliance at any point in rocking mode of vibrations becomes

$$\frac{w G c^2}{M_R} = \frac{3}{\pi^2 a_0} \int_0^{\infty} \int_0^{\frac{\pi}{2}} \frac{\sqrt{r^2 - n^2}}{F(r)} \left[\frac{\sin\left(\frac{c}{b} a_0 r \sin\theta\right)}{\frac{c}{b} a_0 r \sin\theta} - \cos\left(\frac{c}{b} a_0 r \sin\theta\right) \right]$$

$$\times \left[\frac{\sin(a_0 r \cos\theta) \sin\left(\frac{c}{b}\frac{y}{c} a_0 r \sin\theta\right) \cos\left(\frac{x}{b} a_0 r \cos\theta\right)}{r \sin\theta \cos\theta} \right] dr d\theta \tag{5.7.249}$$

Rotation ϕ is then obtained as $\phi = \frac{w]_{z=0,y=c,x=0}}{c}$

$$\frac{\phi G c^3}{M_R} = \frac{3}{\pi^2 a_0} \int_0^{\infty} \int_0^{\frac{\pi}{2}} \frac{\sqrt{r^2 - n^2}}{F(r)} \left[\frac{\sin\left(\frac{c}{b} a_0 r \sin\theta\right)}{\frac{c}{b} a_0 r \sin\theta} - \cos\left(\frac{c}{b} a_0 r \sin\theta\right) \right]$$

$$\times \left[\frac{\sin(a_0 r \cos\theta) \sin\left(\frac{c}{b} a_0 r \sin\theta\right)}{r \sin\theta \cos\theta} \right] dr d\theta \tag{5.7.250}$$

While evaluating the numerical values singularities will occur due to nature of the Rayleigh function at the Rayleigh pole in order to avoid errors due to these singularities the above Equation should be added with the following quantity

$$\frac{\phi G c^3}{M_R} = -\frac{3i}{\pi a_0}\int_0^{\frac{\pi}{2}} \frac{\sqrt{z_0^2 - n^2}}{F(z_0)}\left[\frac{\sin\left(\frac{c}{b}a_0 z_0 \sin\theta\right)}{\frac{c}{b}a_0 z_0 \sin\theta} - \cos\left(\frac{c}{b}a_0 z_0 \sin\theta\right)\right] \times \left[\frac{\sin\left(a_0 z_0 \cos\theta\right)\sin\left(\frac{c}{b}a_0 z_0 \sin\theta\right)}{z_0 \sin\theta\cos\theta}\right] d\theta \tag{5.7.251}$$

5.7.13.6 Zero frequency (static) displacement

The above derived equations are not suitable for zero frequency case $a_0 = 0$, this limiting case $\omega = 0$ is solved in this section and a closed form solution is presented here.

5.7.13.7 Vertical loading

In Equation (5.7.241) for $k \to 0$; $\lim_{k\to 0}\left[\frac{k^2\sqrt{r'^2 - n^2k^2}}{F(r',k)}\right] = \frac{1}{2r'(n^2-1)}$, and Equation (5.7.241) will become

$$\left.\frac{wcG}{p_v}\right]_{\omega=0} = \frac{1}{\pi^2 b}\int_0^{\infty}\int_0^{\frac{\pi}{2}}\left[\frac{1}{2(n^2-1)}\right] \times \left[\frac{\sin\left(r'b\cos\theta\right)\ \sin\left(r'c\sin\theta\right)}{r'^2\sin\theta\cos\theta}\right] \times [\cos(r'x\cos\theta)\cos(r'y\sin\theta)]d\theta dr' \tag{5.7.252}$$

Simplifying the above equation it can be expressed as

$$\left.\frac{wcG}{p_v}\right]_{\omega=0} = \frac{1}{16\pi(n^2-1)}[I_1 + I_2 + I_3 + I_4]$$

where

$$I_{1,4} = \frac{c}{b}\left(1 \pm \frac{y}{c}\right)\int_0^{\theta}\frac{d\theta}{\cos\theta} + \left(1 \pm \frac{x}{b}\right)\int_0^{\frac{\pi}{2}-\theta}\frac{d\theta}{\cos\theta}; \quad \theta = \tan^{-1}\left(\frac{1 \pm \frac{x}{b}}{1 \pm \frac{y}{c}}\right)$$

$$I_{2,3} = \frac{c}{b}\left(1 \pm \frac{y}{c}\right)\int_0^{\theta} \frac{d\theta}{\cos\theta} + \left(1 \pm \frac{x}{b}\right)\int_0^{\frac{\pi}{2}-\theta} \frac{d\theta}{\cos\theta}; \quad \theta = \tan^{-1}\left(\frac{1 \pm \frac{x}{b}}{1 \pm \frac{y}{c}}\right)$$

5.7.13.8 Horizontal loading

The limiting value for static case will become

$$\lim_{k\to 0}\left[\frac{F(r',k) - r'^2\cos^2\theta[4r'^2 - 3k^2 - 4\sqrt{r'^2 - k^2}\sqrt{r'^2 - n^2k}]}{F(r',k)\sqrt{r'^2 - k^2}}\right]$$

$$= \frac{1}{r'}\left[1 - \frac{\cos^2\theta(2n^2 - 1)}{2(n^2 - 1)}\right]$$

The expression for zero frequency displacement then become

$$\frac{ucG}{P_H}\Big]_{\omega=0} = \frac{1}{\pi^2 b}\int_0^{\infty}\int_0^{\frac{\pi}{2}}\left[1 - \frac{\cos^2\theta(2n^2 - 1)}{2(n^2 - 1)}\right]$$

$$\times\left[\frac{\sin(r'b\cos\theta)\sin(r'c\sin\theta)}{r'^2\sin\theta\cos\theta}\right]$$

$$\times[\cos(r'x\cos\theta)\cos(r'y\sin\theta)]dr'd\theta$$

On simplification as in vertical case the above equation can be written as

$$\frac{wcG}{p_H}\Big]_{\omega=0} = \frac{I_1 + I_2}{4\pi} - \left(\frac{2n^2 - 1}{8\pi\left(n^2 - 1\right)}\right)I_3 - \left(\frac{2n^2 - 1}{8\pi\left(n^2 - 1\right)}\right)I_2 \tag{5.7.253}$$

$$I_1 = \frac{c}{b}\left(1 \pm \frac{y}{c}\right)\int_0^{\theta}\frac{d\theta}{\cos\theta} \quad \theta = \tan^{-1}\left(\frac{1 \pm \frac{x}{b}}{1 \pm \frac{y}{c}}\right)$$

$$I_2 = \left(1 \pm \frac{x}{b}\right)\int_0^{\frac{\pi}{2}-\theta}\frac{d\theta}{\cos\theta} \quad \theta = \tan^{-1}\left(\frac{1 \pm \frac{x}{b}}{1 \pm \frac{y}{c}}\right)$$

$$I_3 = \frac{c}{b}\left(1 \pm \frac{y}{c}\right)\sin\theta + \left(1 \pm \frac{x}{b}\right)\cos\theta \quad \theta = \tan^{-1}\left(\frac{1 \pm \frac{x}{b}}{1 \pm \frac{y}{c}}\right)$$

5.7.13.9 Rocking loading

Form Equation (5.7.251) by applying limits the final equation for rocking will become

$$\frac{\phi G c^3}{M_R} = \frac{3}{2\pi^2 \frac{c}{b}(n^2-1)} \int_0^{\infty} \int_0^{\frac{\pi}{2}} \left[\frac{\sin\left(\frac{c}{b} r \sin\theta\right) \sin(r\cos\theta) \sin\left(\frac{c}{b} r \sin\theta\right)}{r^3 \sin^2\theta \cos\theta} - \frac{\cos\left(\frac{c}{b} r \sin\theta\right) \sin(r\cos\theta) \sin\left(\frac{c}{b} r \sin\theta\right)}{r^2 \sin\theta \cos\theta} \right] dr d\theta \tag{5.7.254}$$

5.7.13.10 Programming algorithm

The equations we have to evaluate are complex functions and require special consideration. In evaluation of the integration it is necessary to use 96 points Gaussian quadrature because of the complicity of the sine and cosine functions. A closer interval should be needed to account these variations of sine and cosine functions. More over the entire interval should be divided in to parts to account for nature of function $f(r)$. The function $f(r)$ has the following characteristics (0 to 0.5) $\rightarrow$ real, (0.5 to Pn) $\rightarrow$ real, (Pn to 1) $\rightarrow$ complex, [1 to z_0 root of equation $f(r)$] $\rightarrow$ positive real and (z_0 to 8) $\rightarrow$ negative real.

5.7.13.11 Algorithm for dynamic case

1 Suitable values of Poisson's ratio, frequency ratio and also x/b, y/c, c/b values are selected.
2 Numerical value of the function $f(r)$ its derivative and $f'(r)$ were computed.
3 The compliance functions were evaluated by Gaussian double integration method.
4 96 Gauss points method was used for evaluation of the integral.
5 While evaluation of the integral the interval should be divided into parts to account for the complicities in evaluation of function $f(r)$.
6 The intervals are (0 to 0.5), (0.5 to pn), (pn to 1), [1 to z_0 (root of equation $f(r)$] and (z_0 to 8).
7 The interval z_0 to 8 can be evaluated by substituting $\frac{1}{r}$ instead of r in the integral.
8 The value suggested in the literature should be subtracted to account for singularities occur due to nature of the Rayleigh function $f(r)$.

5.7.13.12 Algorithm for static case

1 equation and derived and are presented in the literature, for vertical and horizontal case these are simplified to single integral form where numerical values found by integrating the terms and applying the limits.
2 To find numerical values in rotational case Gaussian double integration method
3 was used with a substitution $r = \frac{2\alpha}{(1+x_i)} - \alpha$, where $\alpha = 1$.

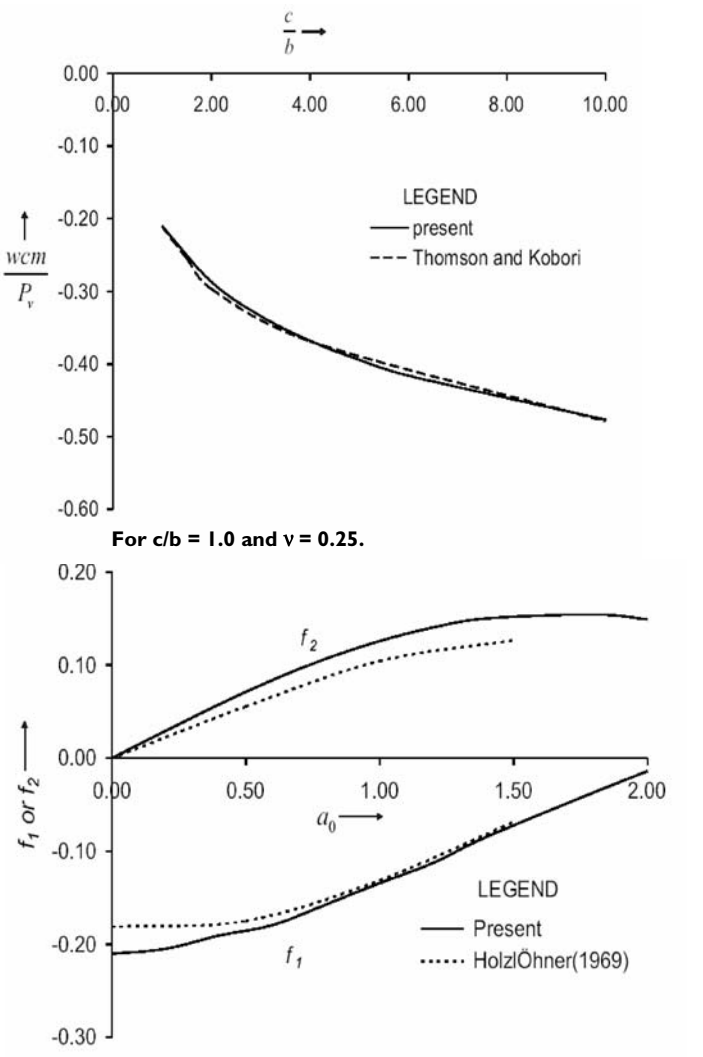
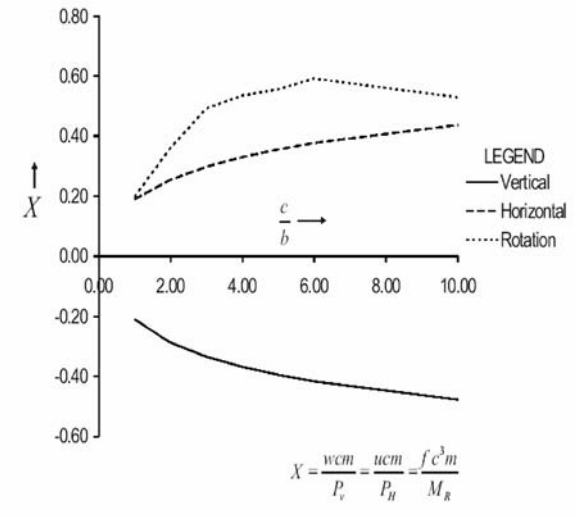
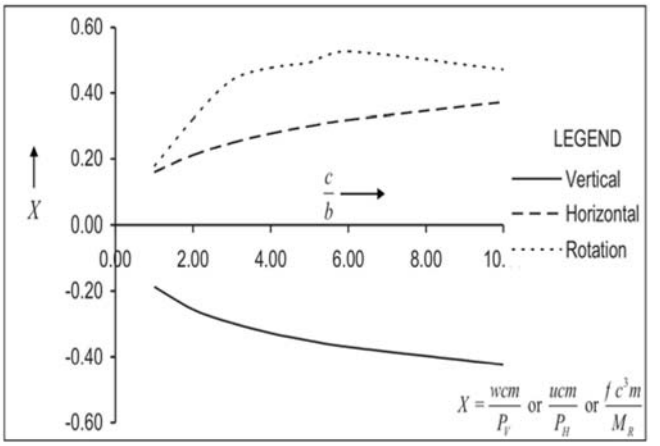


Figure 5.7.23 Comparison of non dimensional static vertical displacement *vrs. c/b* value for $v = 0.25$.

A numerical solution is presented for all three modes of vibrations of a rectangular footing resting on semi-infinite, homogeneous, isotropic, elastic medium. Fourier triple integration technique followed by Thomson and Kobori's was followed to solve the above problem. Solutions obtained for vertical, horizontal, rotation modes of vibrations The derived expressions are use full to find compliance functions for three modes of vibrations at any point of the footing. The expressions for zero frequency displacements i.e. static non-dimensional displacements are also obtained by applying limits to the above derived equations (Figs. 5.7.23 to 25).



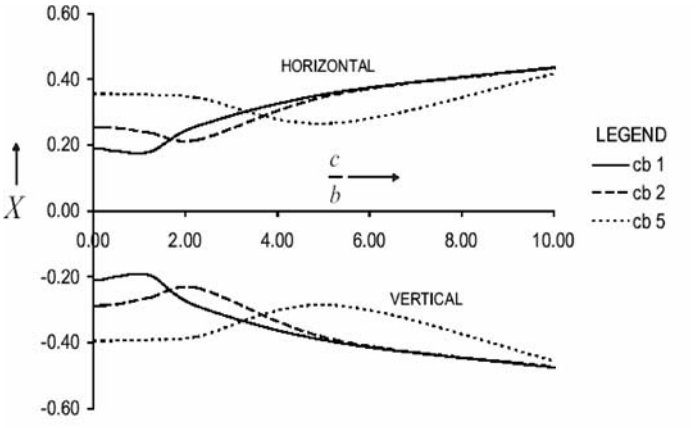
(a) For ν = 0.25



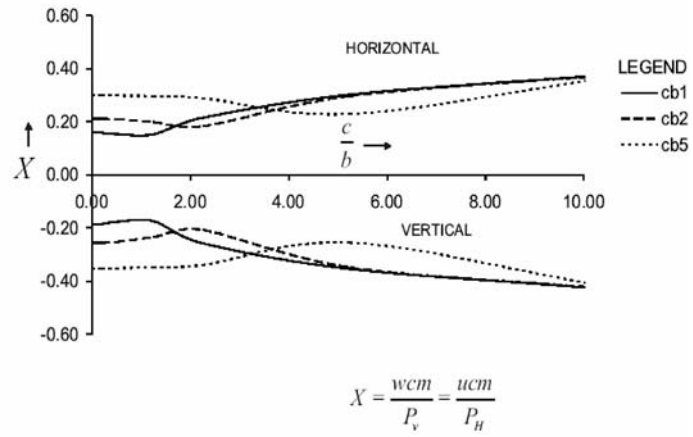
(b) For ν = 0.33

Figure 5.7.24 Non dimensional static displacement *vrs. c/b* values.

Compliance functions at any point of the rectangular footing are obtained for all three modes of vibrations by solving the integral expressions by using Gaussian double integration method. Compliance functions f_1 and f_2 at centre of the footing were drawn against frequency ratio for all three modes of vibrations. Plots are also made for compliance functions against the distance away from center of the footing. Non dimensional static displacement factors are also been obtained and are presented against c/b ratio.



(a) For ν = 0.25



(b) For ν = 0.33

Figure 5.7.25 Non dimensional static displacement away from center of the footing.

Magnification factor (M) has been calculated against different frequency ratios for the different mass ratio of 0, 5 and 10 and for various lengths to with ratio of the footing. Plots are also made between mass ratio against frequency ratio and mass ratio against magnification factor at resonant frequency. Comparisons are also made with the previous studies. These comparisons shows that the results obtained are in good agreement with the previous studies.

5.8 VIBRATION OF EMBEDDED FOOTINGS

5.8.1 Embedment effect on foundation

In previous section we had shown some theoretical developments of machine foundation resting on elastic half space and its mechanical analog. One of the major idealization in the above model is it is assumed that the foundation is resting on ground. In reality foundations are embedded in ground and experimental investigations have proved that the embedment effect do have considerable effect on the dynamic response of the foundation. Frankly speaking a rigorous analytical solution for the problem is still eluding us. A number of researchers in India and abroad have worked on this problem and we provide herein the pioneering few.

5.8.1.1 Novak and Berdugo's solution

Following Baranov's (1967) formulation, Novak and his colleagues (Novak and Beredugo, 1972; Novak et al. 1978) proposed a simplified model to compute the dynamic response of partially or fully embedded circular foundation. The soil at the side of foundation is considered to be decoupled from the soil at the base of the foundation and is treated as a Winkler model. Its stiffness parameters are formulated from vibrations of a horizontal, mass less, rigid, circular body of the foundation, contained in a horizontal layer of unit thickness in plane strain condition (no variation of displacement along the thickness of the layer). In this treatment, the soil medium at the side of the foundation is viewed as a stack of mutually uncoupled horizontal layers. Figure 5.8.1 shows the model of the embedded footing-soil system, and the forces acting on the foundation. The basic governing equation is given by

$$m\ddot{w}(t) = P(t) - R_z(t) - N_z(t) \tag{5.8.1}$$

in which, m, $w(t)$, $P(t)$, $R_z(t)$, $N_z(t)$ are respectively the mass, vertical displacement, time dependent vertical excitation force, dynamic vertical reaction at the base and the dynamic vertical reaction along the side of the footing.

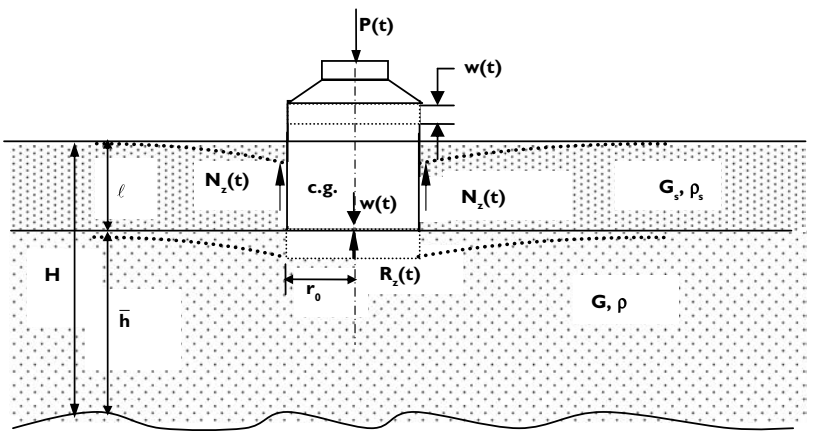


Figure 5.8.1 Vertically oscillating embedded footing.

5.8.1.2 Vibration in vertical direction

It has been assumed that the footing is a rigid cylindrical body with radius, r_0; the dynamic reaction at the base is independent of the depth of the footing; there is a perfect bond between the sides of the footing and the soil; the excitation force is harmonic and acts along the vertical direction and the soil is elastic.

The footing base displacement and elastic halfspace reaction is given by

$$R_z(t) = Gr_0(C_1 + C_2)z(t) \tag{5.8.2}$$

$$\text{in which} \quad C_1 = \frac{-f_1}{f_1^2 + f_2^2}; \quad C_2 = \frac{f_2}{f_1^2 + f_2^2} \tag{5.8.3}$$

where $f_{1,2}$ are compliance functions of the elastic half space as obtained from Bycroft's solution and depending on the dimensionless frequency $a_0 = \omega r_0\sqrt{\rho/G}$, Poisson's ratio and the stress distribution at the footing base, G = shear modulus of halfspace and r_0 = radius of the footing.

The dynamic soil reaction, $N_z(t)$, acting on the vertical sides of the footing is given by

$$N_z(t) = \int_0^{\ell} s(z,t)dz \tag{5.8.4}$$

in which $s = s(z,t)$ is the Baranov's solution for unit reaction (independent of z) and is given by

$$s(t) = G_s(S_1 + iS_2)w(t) \tag{5.8.5}$$

$$\text{and} \quad N_z(t) = \int_0^{\ell} s(z,t)dz = G_s\ell(S_1 + iS_2)w(t) \tag{5.8.6}$$

S_1 and S_2 are shown in Figure 5.8.2 and also given by

$$S_1 = 2\pi a_0 \frac{J_1(a_0)J_0(a_0) + Y_1(a_0)Y_0(a_0)}{J_0^2(a_0) + Y_0^2(a_0)}; \quad S_2 = \frac{4}{J_0^2(a_0) + Y_0^2(a_0)} \tag{5.8.7}$$

in which $J_0\, J_1$, Y_0, Y_1 are respectively Bessel functions of the first kind and of order zero and one and Bessel functions of the second kind and order zero and one; all of them have argument a_0.

Substituting R_z and N_z in Equation (5.8.1) one can obtain

$$m\ddot{w}(t) + Gr_0\left[C_1 + iC_2 + \frac{G_s}{G}\frac{\ell}{r_0}(S_1 + iS_2)\right]w(t) = P(t) \tag{5.8.8}$$

With excitation $P(t) = P_0 \exp(i\omega t)$, the steady state response is $w(t) = w \exp(i\omega t)$

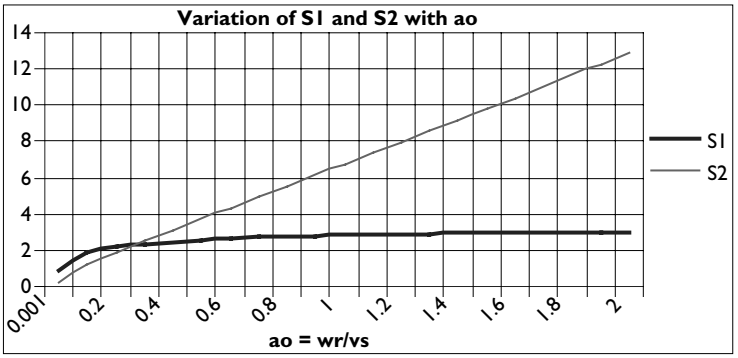


Figure 5.8.2 Variation of S_1 and S_2.

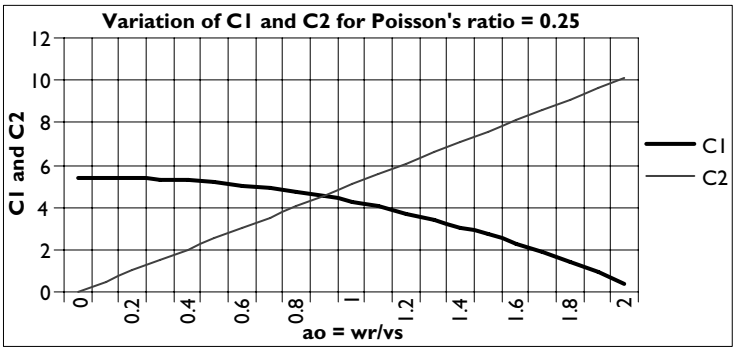


Figure 5.8.3 Variation of C_1 and C_2.

The frequency dependent stiffness and damping may be computed as

$$k = Gr_0\left[C_1 + \frac{G_s}{G}\frac{\ell}{r_0}S_1\right]; \quad c = Gr_0\left[C_2 + \frac{G_s}{G}\frac{\ell}{r_0}S_2\right] \tag{5.8.9}$$

Variation of C_1 and C_2 are shown in Figure 5.8.3.
The real part of the vibration is

$$w(t) = w_0\cos(\omega t + \phi) \tag{5.8.10}$$

in which the amplitude is given by

$$w_0 = \frac{P_0}{\sqrt{(k - m\omega^2)^2 + (c\omega)^2}} = \frac{P_0/k}{\sqrt{\left[1 - (\omega/\omega_n)^2\right]^2 + 4D^2\,(\omega/\omega_n)^2}} \tag{5.8.11}$$

Phase shift, $\phi = \tan^{-1}\left(\frac{c\omega}{k-m\omega^2}\right)$ and the damping ratio, $D = \frac{c}{2m\omega_n}$ and the natural undamped frequency of an embedded foundation is given by

$$\omega_0 = \sqrt{\frac{k}{m}} = \sqrt{\frac{Gr_0}{m}\left(C_1 + \frac{G_s}{G}\frac{\ell}{r_0}S_1\right)} \tag{5.8.12}$$

for a rotating mass (m_e) type of vibrator $P_0 = m_e e\omega^2$, where e = eccentricity of the rotating mass. Some times we introduce the dimensionless amplitude $A = w_0 m/(m_e e)$.

The response of footings embedded in a stratum can be analysed using the proper functions f_1 and f_2 to compute the stiffness and damping parameters $C_{1,2}$. The side reactions remain the same.

Stiffness and damping parameters are given in Table 5.8.1 and Table 5.8.2.

5.8.1.3 Simplified design parameters

Amplitudes and resonant frequencies can be considerably simplified if stiffness parameters C_1 and S_1 are assumed as frequency independent and parameters C_2 and S_2 as proportional to dimensionless frequency, a_0.

These assumptions are justified for the embedment parameters S_1 and S_2 if $a_0 \geq 0.1$, as they do for a halfspace; C_2 for a stratum is less linear but very small, thus adding little to the total damping. However, constancy of C_1 may be questioned, it seems acceptable in the shown frequency range [Table 5.8.1 and Table 5.8.2]. Thus, $C_1 = \bar{C}_1$ and $S_1 = \bar{S}_1$ and $C_2 = \bar{C}_2 a_0$ and $S_2 = \bar{S}_2 a_0$.

The constant stiffness parameters $\bar{C}_1$ and $\bar{S}_1$ may be substituted in Equation (5.8.9) to obtain the frequency independent stiffness constant and the natural undamped frequency ω_n may be computed directly from them.

Table 5.8.1 Stiffness and damping parameters for halfspace and side layers.

ν	*Halfspace values*	*Constant parameters*	*Validity range*
0.0	$C_1 = 4.00 - 0.08356\ a_0 + 0.6346\ a_0^2$ $-2.600\ a_0^3 + 1.801\ a_0^4 - 0.3646\ a_0^5$	$\bar{C}_1 = 3.90$	$0 \leq a_0 \leq 1.5$
	$C_2 = 3.438\ a_0 + 0.5742\ a_0^2 - 1.154\ a_0^3 + 0.7433\ a_0^2$	$\bar{C}_2 = 3.50$	
0.25	$C_1 = 5.37 + 0.346\ a_0 - 1.41\ a_0^2$	$\bar{C}_1 = 5.20$	$0 \leq a_0 \leq 1.5$
	$C_2 = 5.06\ a_0$	$\bar{C}_2 = 5.00$	
0.5	$C_1 = 8.00 + 2.180\ a_0 - 12.63\ a_0^2$ $+20.73\ a_0^3 - 16.47\ a_0^4 + 4.458\ a_0^5$	$\bar{C}_1 = 7.50$	$0 \leq a_0 \leq 1.5$
	$C_2 = 7.414\ a_0 - 2.986\ a_0^2 + 4.324\ a_0^3 - 1.782\ a_0^4$	$\bar{C}_2 = 6.80$	
	Side layer		
Any value	$S_1 = 0.2153\ a_0 + 2.760\ a_0/(a_0 + 0.06084)$	$\bar{S}_1 = 2.70$	$0 \leq a_0 \leq 2.0$
	$S_2 = 6.059 + 0.7022\ a_0/(a_0 + 0.01616)$	$\bar{S}_2 = 6.70$	

Table 5.8.2 Stiffness and damping parameters for stratum below foundation.

$\bar{h}/r_0$	*Stratum* $\nu = 0.25$	*Constant parameters*	*Validity range*
1.0	$C_1 = 12.23 - 1.178a_0 - 0.3056a_0^2 - 1.177\ a_0^3 + 0.4160a_0^4$	$\bar{C}_1 = 10.0$	$0 \le a_0 \le 1.5$
	$C_2 = 0.2395a_0^2 + 0.5646a_0^3 + 0.0227a_0^4 - 0.3403a_0^5 + 0.203\ a_0^6$	$\bar{C}_2 = 0.30$	
2.0	$C_1 = 8.13 + 0.8516a_0 - 3.664a_0^2 - 8.289a_0^3 + 11.18a_0^4 - 3.978a_0^5$	$\bar{C}_1 = 7.00$	$0 \le a_0 \le 1.25$
	$C_2 = 0.004044a_0 - 0.7386a_0^2 + 13.27a_0^3 - 39.61a_0^4 + 49.8a_0^5 - 26.95a_0^6 + 5.069a_0^7$	$\bar{C}_2 = 0.45$	
3.0	$C_1 = 7.04 + 0.4659a_0 - 6.989a_0^2$	$\bar{C}_1 = 5.5$	$0 \le a_0 \le 0.81$
	$C_2 = 0.7361a_0^2 - 1.462a_0^3 + 3.573a_0^4$	$\bar{C}_2 = 0.65$	
4.0	$C_1 = 6.579 - 0.2422a_0 - 0.3889a_0^2 - 29.69a_0^3 + 7.711a_0^4 + 76.44a_0^5 - 77.42a_0^6$	$\bar{C}_1 = 4.30$	$0 \le a_0 \le 0.62$
	$C_2 = 0.02804\ a_0 + 3.02\ a_0^2 + 7.458\ a_0^3 - 184.2\ a_0^4 + 655.7a_0^5 - 804.9a_0^6 + 314.2a_0^7$	$\bar{C}_2 = 1.00$	

The frequency independent damping constant for embedded footing can be computed from

$$c = r_0^2\sqrt{\rho G}\left[\bar{C}_2 + \bar{S}_2\frac{\ell}{r_0}\sqrt{\frac{\rho_s G_s}{\rho G}}\right] \quad \text{and}$$

$$D = \frac{1}{2\sqrt{b_1}}\left[\bar{C}_2 + \bar{S}_2\frac{\ell}{r_0}\sqrt{\frac{\rho_s G_s}{\rho G}}\right]\Bigg/\left[\bar{C}_1 + \frac{G_s}{G}\frac{\ell}{r_0}\bar{S}_1\right] \tag{5.8.13}$$

in which the mass ratio $b_1 = m/\rho r_0^3$.

The amplitude at natural frequency ω_n (slightly smaller than the maximum amplitude) is

$$w_0(\omega_n) = \frac{P_0}{k}\frac{1}{2D} = \frac{m_e e}{m}\frac{1}{2D} \quad \text{(for frequency dependent force amplitude).} \tag{5.8.14}$$

For horizontal direction, considering a cylindrical block of radius r_0 and height H and embedded to a depth h subject to a force $P_x(t) = P_x e^{iwt}$ the equation of motion is expressed as

$$m\ddot{x}(t) = P(t) - R_x(t) - N_x(t) \tag{5.8.15}$$

where $R_x(t) = Gr_0(C_{x1} + C_{x2})x(t)$ and $Nx(t) = G_s h(S_{x1} + iS_{x2})x(t)$ where S_{x1} and S_{x2} are parameters which are function of dimensionless frequency number $a = \omega r_0/v_s$.

Thus we have

$$m\ddot{x}(t) + Gr_0(C_{x1} + iC_{x2})x(t) + G_s h(S_{x1} + iS_{x2})x(t) = P_x(t)$$

$$\text{or,} \quad m\ddot{x}(t) + Gr_0\left[\left(C_{x1} + \frac{G_s}{G}\frac{h}{r_0}S_{x1}\right) + i\left(C_{x2} + \frac{G_s}{G}\frac{h}{r_0}S_{x2}\right)\right]x(t) = P_x e^{i\omega t} \quad (5.8.16)$$

Seperating the real imaginary part we have

$$k_x = Gr_0\left[\left(C_{x1} + \frac{G_s}{G}\frac{h}{r_0}S_{x1}\right)\right] \quad \text{and} \quad c_x = \frac{Gr_0}{\omega}\left[\left(C_{x2} + \frac{G_s}{G}\frac{h}{r_0}S_{x2}\right)\right] \quad (5.8.17)$$

Here both k_x, c_x are frequency dependent.

Beredugo and Novak proved that the values k_x, c_x may be approximated by frequency independent values for all practical purposes by substitution:

$$C_{x1} = \bar{C}_{x1}, \quad C_{x2} = \bar{C}_{x2}, \quad S_{x1} = \bar{S}_{x1}, \quad S_{x2} = \bar{S}_{x2}$$

The values of $C_{x1}, \bar{C}_{x1}, C_{x2}, \bar{C}_{x2}, S_{x1}, \bar{S}_{x1}, S_{x2}, \bar{S}_{x2}$ are as shown in Table 5.8.3.

Based on the above, frequency independent stiffness and damping value is given by

$$k_x = Gr_0\left[\left(\bar{C}_{x1} + \frac{G_s}{G}\frac{h}{r_0}\bar{S}_{x1}\right)\right] \quad \text{and} \quad c_x = \sqrt{\rho G}r_0^2\left[\left(\bar{C}_{x2} + \frac{h}{r_0}\sqrt{\frac{\rho_s G_s}{\rho G}}\bar{S}_{x2}\right)\right] \quad (5.8.18)$$

Table 5.8.3 Values of $C_{x1}, \bar{C}_{x1}, C_{x2}, \bar{C}_{x2}, S_{x1}, \bar{S}_{x1}, S_{x2}, \bar{S}_{x2}$.

Poisson's ratio	*Half space functions*	*Validity range*	*Constant parameters*
0.0	$C_{x1} = 4.571 - 4.653a_0 + \frac{89.09a_0}{a_0+19.14}$	$0 \le a_0 \le 2.0$	$\bar{C}_{x1} = 4.30$
0.0	$C_{x2} = 2.536a_0 - \frac{0.1345a_0}{a_0-1.923}$	$0 \le a_0 \le 2.0$	$C_{x2} = 2.70$
0.5	$C_{x1} = 5.333 - 1.584a_0 + \frac{10.39a_0}{a_0+6.522}$	$0 \le a_0 \le 2.0$	$\bar{C}_{x1} = 5.10$
0.5	$C_{x2} = 2.923a_0 - \frac{0.1741a_0}{a_0-1.927}$	$0 \le a_0 \le 2.0$	$\bar{C}_{x2} = 3.15$
0.0	$S_{x1} = 0.2328a_0 + \frac{3.609a_0}{a_0+0.06159}$	$0.2 \le a_0 \le 1.5$	$\bar{S}_{x1} = 3.60$
0.0	$S_{x1} = 150.3a_0 - 3630a_0^2 + 3948a_0^3 - 1934a_0^4 + 3488a_0^5$	$0.0 \le a_0 \le 0.2$	$\bar{S}_{x1} = 3.60$
0.0	$S_{x2} = 7.334a_0 + \frac{0.8652a_0}{a_0+0.00874}$	$0 \le a_0 \le 1.5$	$\bar{S}_{x2} = 8.20$
0.25	$S_{x1} = 2.474 + 4.119a_0 - 4.320a_0^2 + 2.057a_0^3 - 0.362a_0^4$	$0.2 \le a_0 \le 2.0$	$\bar{S}_{x1} = 4.00$
0.25	$S_{x1} = 1.468\sqrt{a_0} + 5.662\sqrt[4]{a_0}$	$0.0 \le a_0 \le 0.2$	$\bar{S}_{x1} = 4.00$
0.25	$S_{x2} = 0.83a_0 + \frac{41.59a_0}{3.90+a_0}$	$0 \le a_0 \le 1.5$	$\bar{S}_{x2} = 9.10$
0.4	$S_{x1} = 2.824 + 4.776a_0 - 5.539a_0^2 + 2.445a_0^3 - 0.394a_0^4$	$0.2 \le a_0 \le 2.0$	$\bar{S}_{x1} = 4.10$
0.4	$S_{x1} = -1.796\sqrt{a_0} + 6.539\sqrt[4]{a_0}$	$0.0 \le a_0 \le 0.2$	$\bar{S}_{x1} = 4.10$
0.4	$S_{x2} = 0.96a_0 + \frac{56.55a_0}{4.68+a_0}$	$0 \le a_0 \le 1.5$	$\bar{S}_{x2} = 10.60$

$$\omega_x = \sqrt{\frac{k_x}{m}}, \quad c_{cr} = 2\sqrt{k_x m} \quad \text{and} \quad D = c_x/c_{cr} \tag{5.8.19}$$

$$x(t) = \frac{P_x e^{i\omega t}}{k_x\sqrt{(1-r^2)^2 + (2Dr)^2}}, \quad \text{where } r = \frac{\omega}{\omega_n}. \tag{5.8.20}$$

5.8.1.4 Rocking motion

Cylinder embedded in soil to a depth h under rocking is shown in Figure 5.8.4 and the equation of motion in this case is given by

$$J_\phi \ddot{\phi}(t) + Gr_0^3(C_{\phi 1} + iC_{\phi 2})\phi(t) + G_s\left[r_0^2 h(S_{\phi 1} + iS_{\phi 2}) + \frac{h^3}{3}(S_{x1} + iS_{x2})\right]$$

$$\phi(t) = M_y(t) \tag{5.8.21}$$

which gives

$$J_\phi \ddot{\phi}(t) + Gr_0^3\left[(C_{\phi 1+} iC_{\phi 2}) + \frac{G_s}{G}\left\{\frac{h}{r_0}(S_{\phi 1} + iS_{\phi 2}) + \frac{1}{3}\left(\frac{h}{r_0}\right)^2 (S_{x1} + iS_{x2})\right\}\right]$$

$$\phi(t) = M_y e^{i\omega t} \tag{5.8.22}$$

Separating the real and imaginary part we have

$$k_\phi = Gr_0^3\left[C_{\phi 1} + \frac{G_s}{G}\frac{h}{r_0}\left(S_{\phi 1} + \frac{h^2}{3r_0^2}S_{x1}\right)\right],$$

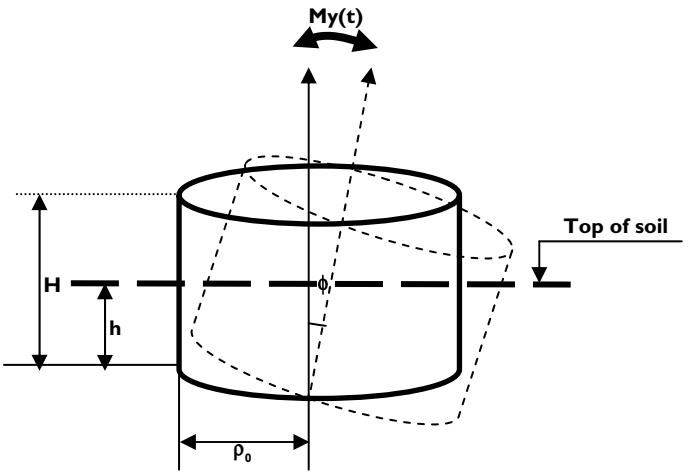


Figure 5.8.4 Cyclinder embedded in soil to a depth h under rocking.

Table 5.8.4

Poisson's ratio	*Half space functions*	*Valdity range*	*Constant parameters*
0.0	$C_{\phi 1} = 2.654 + 0.1962a_0 - 1.729a_0^2 + 1.485a_0^3 - 0.4881\ a_0^4 + 0.03498a_0^5$	$0 < a_0 < 1.0$	$\bar{C}_{\phi 1} = 2.5$
0.0	$C_{\phi 2} = 0.008025a_0 + 0.01583a_0^2 + 0.2035a_0^3 + 1.202a_0^4 - 1.448a_0^5 + 0.4491a_0^6$	$0 < a_0 < 1.0$	$\bar{C}_{\phi 2} = 0.43$
Any value	$S_{\phi 1} = 3.142 - 0.421a_0 - 4.209a_0^2 + 7.165a_0^3 - 4.667a_0^4 + 1.093a_0^5$	$0 < a_0 < 1.5$	$\bar{S}_{\phi 1} = 2.5$
Any value	$S_{\phi 2} = 0.0144a_0 + 5.262a_0^2 - 4.177a_0^3 + 1.643a_0^4 - 0.2542a_0^5$		$\bar{S}_{\phi 2} = 1.80$

$$c_\phi = \frac{Gr_0^3}{\omega}\left[C_{\phi 2} + \frac{G_s}{G}\left(\frac{h}{r_0}\right)\left(S_{\phi 2} + \frac{1}{3}\left(\frac{h^2}{r_0^2}\right)S_{x2}\right)\right] \tag{5.8.23}$$

Beredugo and Novak proved that the values k_ϕ, c_ϕ may be approximated by frequency independnet values for all practical purposes by substitution.

$$C_{\phi 1} = \bar{C}_{\phi 1}, \quad C_{\phi 2} = \bar{C}_{\phi 2}, \quad S_{\phi 1} = \bar{S}_{\phi 1}, \quad S_{\phi 2} = \bar{S}_{\phi 2} \quad \text{etc.}$$

The values are as shown in Table 5.8.4.
The frequency independent stiffness and damping value are thus given by

$$k_\phi = Gr_0^3\left[\bar{C}_{\phi 1} + \frac{G_s}{G}\frac{h}{r_0}\left(\bar{S}_{\phi 1} + \frac{h^2}{3r_0^2}\bar{S}_{x1}\right)\right] \quad \text{and}$$

$$c_\phi = \sqrt{\rho G}r_0^4\left[\bar{C}_{\phi 2} + \frac{G_s}{G}\left(\frac{h}{r_0}\right)\left(\bar{S}_{\phi 2} + \frac{1}{3}\left(\frac{h^2}{r_0^2}\right)\bar{S}_{x2}\right)\right] \tag{5.8.24}$$

$$\omega_\phi = \sqrt{\frac{k_\phi}{J\phi}}, \quad c_{cr} = 2\sqrt{k_\phi J_\phi} \quad \text{and} \quad D = c_\phi/c_{cr} \tag{5.8.25}$$

$$\phi(t) = \frac{M_y e^{i\omega t}}{k_\phi\sqrt{\left(1 - r^2\right)^2 + (2Dr)^2}}, \quad \text{where } r = \frac{\omega}{\omega_\phi} \tag{5.8.26}$$

5.8.1.5 Coupled sliding and rocking motion

In this case as shown in Figure 5.8.5, the motion is coupled (translation and rocking) which gives rise to two equations of motion:

$$m\ddot{x}(t) = P(t) - R_x(t) - N_x(t) \quad \text{and} \quad J_\phi\ddot{\phi}(t) = M_y(t) - R_\phi(t) - N_\phi(t) \tag{5.8.27}$$

where,

$$R_x(t) = Gr_0\,(C_{x1} + iC_{x2})\,[x(t) - Z_c\phi(t)]$$

$$\text{and} \quad R_\phi(t) = Gr_0^3(C_{\phi1} + iC_{\phi2})\phi(t) - Gr_0(C_{x1} + iC_{x2})[x(t)Z_c - Z_c^2\phi(t)]; \tag{5.8.28}$$

$$N_x(t) = Gr_0\left(\frac{h}{r_0}\right)(S_{x1} + iS_{x2})\left[x(t) + \left(\frac{h}{2} - Z_c\right)\phi(t)\right];$$

$$N_\phi(t) = Gr_0^3\left\{\left(\frac{h}{r_0}\right)(S_{\phi1} + iS_{\phi2}) + \left[\frac{h^2}{3r_0^2} - \frac{hZ_c}{r_0^2} + \frac{Z_c^2}{r_0^2}\right]\right\}\phi(t)$$
$$+ \frac{1}{r_0}\left(\frac{h}{2r_0} - \frac{Z_c}{r_0}\right)(S_{x1} + iS_{x2})\,x(t) \tag{5.8.29}$$

Substituting the above in equations of motion and writing in matrix notation we have

$$\begin{bmatrix} m_x & 0 \\ 0 & J_\phi \end{bmatrix}\begin{Bmatrix} \ddot{x} \\ \ddot{\phi} \end{Bmatrix} + \begin{bmatrix} c_x & c_{x\phi} \\ c_{x\phi} & c_\phi \end{bmatrix}\begin{Bmatrix} \dot{x} \\ \dot{\phi} \end{Bmatrix} + \begin{bmatrix} k_x & k_{x\phi} \\ k_{x\phi} & k_\phi \end{bmatrix}\begin{Bmatrix} x \\ \phi \end{Bmatrix} = \begin{Bmatrix} P_x \\ M_y \end{Bmatrix} e^{i\omega_m t} \tag{5.8.30}$$

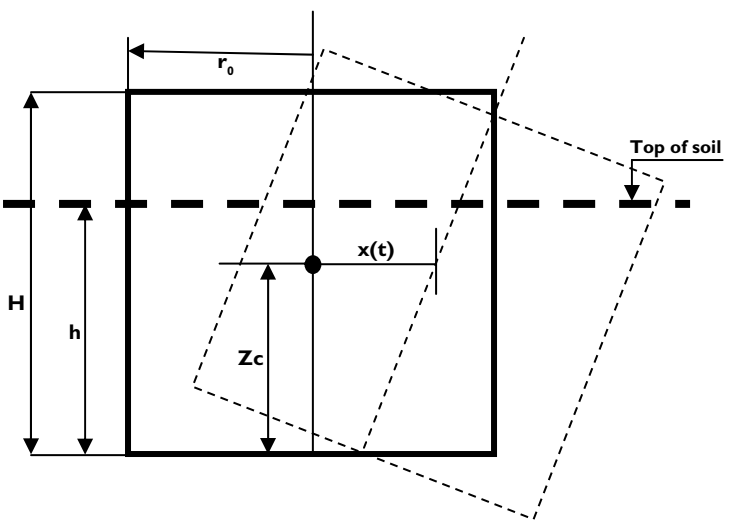


Figure 5.8.5 Coupled rocking and sliding motion of an embedded cylindrical foundation.

where

$$k_x = Gr_0\left(C_{x1} + \frac{G_s}{G}\frac{h}{r_0}S_{x1}\right)$$

$$k_\phi = Gr_0^3\left[C_{\phi 1} + \left(\frac{Z_c}{r_0^2}\right)C_{x1} + \frac{G_s}{G}\left(\frac{h}{r_0}\right)S_{\phi 1} + \left(\frac{G_s}{G}\right)\left(\frac{h}{r_0}\right)\left\{\frac{h^2}{3r_0^2} + \frac{Z_c^2}{r_0^2} - \frac{hZ_c}{r_0^2}\right\}S_{x1}\right]$$

$$k_{x\phi} = -Gr_0\left[Z_cC_{x1} + \left(\frac{G_s}{G}\right)\left(\frac{h}{r_0}\right)\left(Z_c - \frac{h}{2}\right)S_{x1}\right]$$

$$c_x = \sqrt{\rho G}r_0^2\left(C_{x2} + \left(\frac{h}{r_0}\right)\sqrt{\frac{\rho_s}{\rho}\frac{G_s}{G}}S_{x2}\right)$$

$$c_\phi = \sqrt{\rho G}r_0^4\left[C_{\phi 2} + \left(\frac{Z_c}{r_0^2}\right)^2 C_{x2} + \frac{h}{r_0}\sqrt{\frac{\rho_s G_s}{\rho G}}\left\{S_{\phi 2} + \left(\frac{h^2}{3r_0^2} + \frac{Z_c^2}{r_0^2} - \frac{hZ_c}{r_0^2}\right)S_{x2}\right\}\right]$$

$$c_{x\phi} = -\sqrt{\rho G}r_0^2\left[Z_cC_{x2} + \left(\frac{h}{r_0}\right)\sqrt{\frac{\rho_s G_s}{\rho G}}\left(Z_c - \frac{h}{2}\right)S_{x2}\right]$$

For practical analysis as stated earlier $C_{x1} = \bar{C}_{x1}$, $C_{x2} = \bar{C}_{x2}$, $S_{x1} = \bar{S}_{x1}$ etc. can be used values are given earlier in the Table 5.8.4).

Once the stiffness, damping and inertial properties are known standard modal technique may be applied to derive the natural frequencies and the amplitude of the vibration.

5.8.2 Research carried out in India

In India significant researches has been carried out on response of embedded footing.

Almost at the same time Novak and Berdugo (1972) published their paper on dynamic response of embedded foundation Anandakrishnan and Krishanswamy (1973) published a paper on vertical response of embedded foundation.

5.8.2.1 Anandakrishnan and Krishnaswamy's model

The mathematical model proposed by them is as shown in Figure 5.8.6.

Following Lysmer's notation as proposed earlier the equation of motion proposed by them is

$$m\ddot{z} + \left[\frac{3.4r_0^2}{1-\nu}\sqrt{\rho G} + F\right]\dot{z} + \frac{4Gr_0}{1-\nu}z = P(t) \tag{5.8.31}$$

where $F = \left[\frac{1}{2}K_0H^2\rho g\mu_f + C_aH\right]L_p$

K_0 = Coefficient of earth pressure at rest; ρg = Wt density of soil; μ_f = Coefficient of kinematic friction; Ca = Adhesion between the soil and the sides of embedded

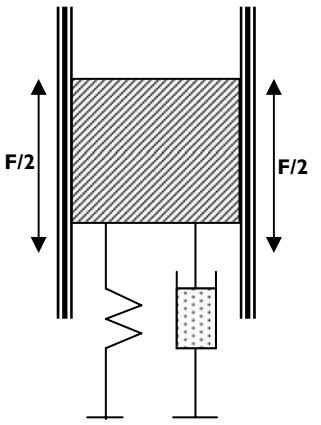


Figure 5.8.6 Mathematical model of Anandakrishnan & Krishnaswamy 1973.

footing usually considered as 1 to 2% of the undrained cohesive strength of the soil and L_p = Perimeter Length of the embedded footing.

Unfortunately the research was not further extended for lateral and rocking mode and neither any comparison available with other established methods like Novak or Wolf.

Sridharan et al. (1981) developed a procedure for vertical vibration of footings in similar line to what was proposed by Anandakrishnan and the results obtained are found to be of similar nature.

5.8.2.2 Vijayavargiya's method

Vijayavargiya (1981) developed a practical procedure for embedded response of foundation for all modes based on Barkan's parameters and a lumped mass model. The mathematical model as proposed is shown in Figure 5.8.7.

Equivalent vertical stiffness of soil

$$K_{ze} = C_u BL + 2C_{\tau av} h\,(L + B) \tag{5.8.32}$$

where, C_u = Coefficient of uniform compression determined at base of foundation;

$C_{\tau av}$ = Average value of coefficient of elastic uniform shear at the ground surface and base of foundation; h = Depth of embedment; B = Width of foundation and L = Length of foundation.

Equation of motion is given by

$$m\ddot{z} + K_{ze} z = P_0 \sin \omega_m t \tag{5.8.33}$$

The amplitude of vibration is given by the expression

$$\delta_z = \frac{\left(\frac{P_0}{K_{ze}}\right) \sin \omega_m t}{1 - r^2} \tag{5.8.34}$$

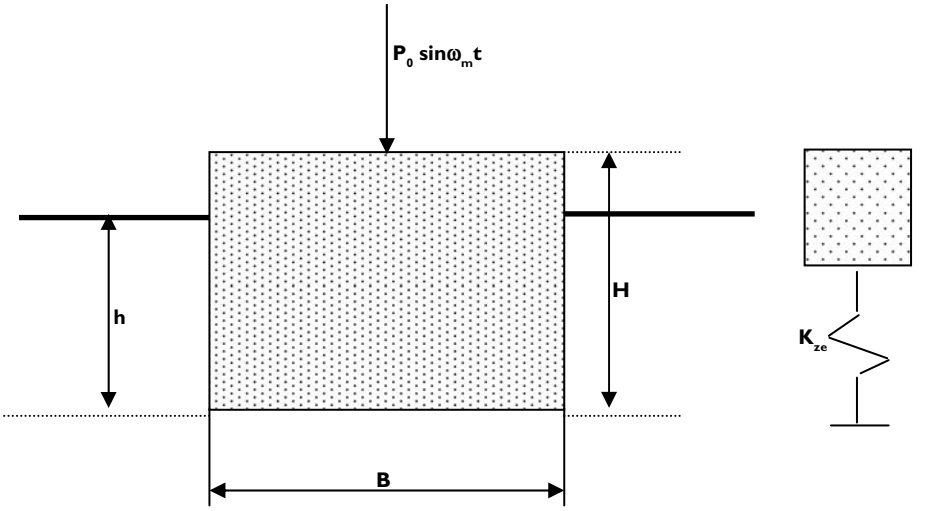


Figure 5.8.7 Model for vertical vibration of Foundation (Vijayavargiya 1981).

where r = ratio of the operating frequency of the machine and the natural frequency of the foundation.

For sliding motion stiffness proposed is as follows

$$K_{xe} = C_{\tau h} BL + 2C_{uav} Bh(L + B) \tag{5.8.35}$$

in which, K_{xe} = equivalent vertical stiffness of soil; C_{uav} = average coefficient of uniform compression at ground level and base of foundation and $C_{\tau h}$ = coefficient of elastic uniform shear at the base of foundation.

Equation of motion is given by

$$m\ddot{x} + K_{xe}x = P_0 \sin \omega_m t \tag{5.8.36}$$

The amplitude of vibration is given by the expression

$$\delta_x = \frac{(P_0/K_{xe}) \sin \omega_m t}{1 - r^2} \tag{5.8.37}$$

Similarly for rocking motion the equivalent rocking stiffness is expressed as

$$K_{\phi e} = C_{\phi h} I - WZ_c + \frac{C_{\phi av} L}{24} \left(16h^3 - 12Hh^2\right) + 2C_{\phi av} I_0 + C_{\tau av} \frac{hLB^2}{2} \tag{5.8.38}$$

where, $C_{\phi h}$ = Coefficient of non uniform compression at base of foundation; $C_{\phi av}$ = average value of non uniform compression at ground level and base of foundation;

Zc = Height of combined c.g of machine + foundation from center of base; W = weight of the foundation; $I = LB^3/12$, $I_0 = Bh^3/3$; $\omega_\phi = \sqrt{K_{\phi e}/J_\phi}$; and J_f = mass moment of inertia of the foundation system.

The rotational amplitude is given by

$$\delta_\phi = \frac{(M_y/K_{\phi e})\sin\omega_m t}{1-r^2} \tag{5.8.39}$$

For coupled sliding and rocking motion the equation of motion is given by

$$\begin{bmatrix} M & 0 \\ 0 & J_\phi \end{bmatrix} \begin{Bmatrix} \ddot{x} \\ \ddot{\phi} \end{Bmatrix} + \begin{bmatrix} K_{xx} & K_{x\phi} \\ K_{\phi x} & K_{\phi\phi} \end{bmatrix} \begin{Bmatrix} x \\ \phi \end{Bmatrix} = \begin{Bmatrix} P_x \\ M_y \end{Bmatrix} \sin\omega_m t \tag{5.8.40}$$

where

$$K_{xx} = C\tau_h BL + 2C_{uav}h(B+L); \quad K_{x\phi} = C_{\phi av}L(h^2 - 2hZ_c) - C_{\tau h}BLZ_c$$

$$K_{\phi\phi} = C_{\phi h}I + C_{\tau h}BLZ_c^2 - WZ_c + 2C_{\psi av}I_y + C_{\tau av}Lh\frac{B^2}{2} + \frac{2}{3}C_{\phi av}[Z_c^3 + (h-Z_c)^3]$$

here

$$K_\psi = 0.75Cu; \quad K_{\phi x} = -\left[C\tau_h BLZ_c + 2C_{uav}Lh\left(Z_c - \frac{h}{3}\right) + 2C_{\tau av}\left(Z_c - \frac{h}{3}\right)Lh\right]$$

and $Iy = \dfrac{hB^3}{12} + \dfrac{BhL^2}{4}$.

Vijayavargiya's method needs to be compared to other established methods to evaluate how they compare in terms of frequency and amplitude. The method however does not take into cognizance damping effect of soil and as such would show infinite amplitude at resonance or very high value near $\omega_m/\omega_n \to 1$. This is however actually not the case in reality for due to presence of damping. The amplitude could be more, but shows a finite value near resonance.

This is surely a limitation of the method for practical use especially in brown field project, where often due to lack of space the foundation size cannot be modified and the rotating equipment is thus allowed to operate at close proximity of the resonant zone taking the advantage of soil damping and controlling the amplitude within acceptable limit.

5.8.2.3 Dasgupta and Rao's model for dynamic response of foundation

Dasgupta and Rao (1976) presented a comprehensive analysis for machine foundation under dynamic loading based on finite element analysis for two dimensional (plane stress and plane strain) axisymmetric and three-dimensional model. This procedure takes into cognizance the silent transmitting boundaries essential to dissipate away the propagating waves to infinity. The details of the approach and the results are discussed elsewhere (Kameswara Rao 1998).

5.8.3 Energy transmitted from a circular area

Miller and Pursey (1955) presented the analysis of a normal stress, applied to a circular area $r \leq a$, and varying harmonically with time. For the far-field where $0 \leq \theta < \pi/2$, the displacements are

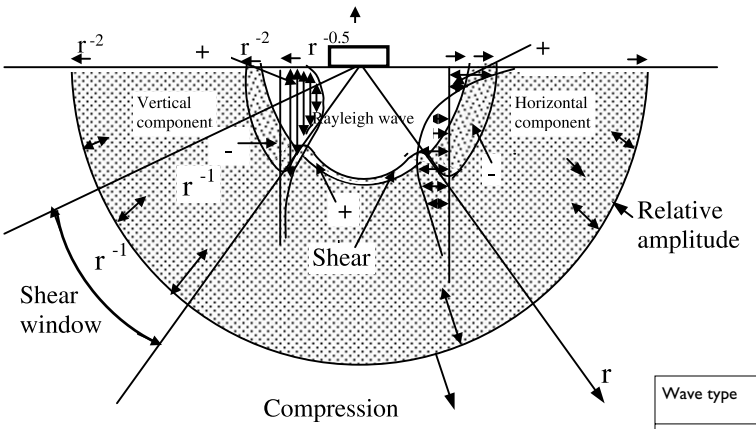
$$u_R = -\frac{a^2}{2G}\frac{e^{-iR}}{R}\frac{\cos(k^2 - 2\sin^2\theta)}{F_0 \sin\theta} \quad \text{and}$$
$$u_\theta = -\frac{ia^2k^2}{2G}\frac{e^{-ikR}}{R}\frac{\sin 2\theta(k^2\sin^2\theta - 1)}{F_0(k\sin\theta)} \tag{5.8.41}$$

The surface wave results are given for $\nu = 1/4$

$$u_r(r,0) = 0.215\frac{a^2 e^{\frac{i\pi}{4}}}{G\sqrt{r}}e^{-1.88ir} \quad \text{and} \quad u_y(r,0) = 0.316\frac{a^2 e^{\frac{i\pi}{4}}}{G\sqrt{r}}e^{-1.88ir} \tag{5.8.42}$$

For $\nu = 1/3$, 0.215, 0.316 and 1.884 are to be replaced by 0.182, 0.286 and 2.145, respectively.

Miller and Pursey computed the partition of energy among the dilatational, shear and the surface waves due to an oscillating normal point force. The variation, shown in Figure 5.8.8, is given by Woods in an informative way. The compressional and shear waves propagate out in hemispherical wavefronts. The spacing of the wavefronts is in accord with their differing velocities. The relative amplitude of particle motion is shown. Also shown are the Rayleigh surface waves, with vertical and horizontal displacement components shown on the leftward- and rightward-propagating parts of the wave. The various powers of r^{-n} ($n = .5,1,2$) give the geometric attenuation of



Wave type	Percentage of Total energy
Rayleigh	67
Shear	26
Compression	07

Figure 5.8.8 Distribution of displacement and energy in dilatation, shear and surface waves from a harmonic normal load on a half-space for $\nu = 0.25$.

the displacement amplitudes with radial distance r. The shear window indicates the portion of the shear wave along which amplitudes are greatest. It has been shown that the Rayleigh wave carries around 67 per cent of the total energy and undergoing more gradual amplitude attenuation.

Based on above it may again be concluded that the most important wave which affects the response of a foundation under earthquake and dynamic loading from a machine it is the Rayleigh wave which has maximum influence.

5.9 FINITE ELEMENT SOLUTION FOR FOUNDATION DYNAMICS

5.9.1 Soil dynamics and finite element analysis

Finite Element Analysis as we know developed as a numerical computational tool for analysis of continuum. Considering the fact that soil medium is a continuum (though often heterogeneous in its properties due to layering) it is but obvious that Finite Element has a significant application in problems related to propagation of waves (be from machine foundation or earthquake) in soil.

However unlike structural analysis a three dimensional analysis of soil or a soil-structure interaction problem is rarely carried out in practice for it becomes significantly cost and schedule prohibitive. In many cases for practical engineering problems a two dimensional analysis would mostly suffice. However unlike structural analysis, problem of dynamic analysis related to soil has some unique problem of its own which needs special attention. While a structure would usually have a finite boundary of its own a soil medium is usually infinite.

For a foundation resting over soil if we try to find out the dynamic response of the footing and have boundary cut off at say 1.5 to 2 times its width (which would be fine for static load case) we may arrive at an answer which could have significant error. The reason for this is that the waves propagating from the foundation would reflect back from such boundary and would induce spurious modes in the foundation resulting in erroneous results[85].

Since the wave propagating in the soil should not reflect back to the foundation the intuitive logic to arrive at a correct model would be to take the boundary away at a sufficient distance so that the waves cannot reflect back. While doing this for a single foundation or a machine foundation does not pose significant problem. However for a comprehensive dynamic soil structure interaction problem where the complete structure is taken into cognizance[86] this could become prohibitively expensive in terms of cost, data input and complex in terms of interpretation.

Above has been a source of many a debate and discussions both in academic and industrial circle undertaking such task of dynamic soil structure interaction.

So what are the options we have to address this issue as mentioned above?

Possible solutions are as follows

- Accept the inevitable and come up with a model with thousands of degrees of freedoms taking the mesh boundary to a significant distance away from the source.

85 This is often termed as the box effect for such analysis.

86 Like reactor building in a Nuclear power Plant or a dam-fluid – soil interaction analysis etc.

- Consider frequency independent spring elements to define the soil properties at the soil-structure boundary[87].
- Use finite element up to a certain depth below the structure and then use special elements to cater to the condition that waves do not reflect back[88].
- Use infinite finite elements a special type of finite element having shape function which decays exponentially to zero as the position vector r approaches infinity.

We will discuss each of the above in some detail below.

5.9.2 Use of structural boundary conditions

If we decide to use static boundary like hinges and rollers like we do in structures, we need to take the boundary sufficiently away from the foundation to give correct response of the footing. *However the question remains – what is this sufficient distance?*

For earthquake analysis the depth is usually taken to bedrock level from which the seismic waves usually propagate[89]. However for lateral direction there are no clear guidelines and one has to possibly proceed with a trial and error to arrive at a solution when two successive runs would nearly give same results it is assumed that the results have converged and boundaries taken are sufficient.

Shown in Figure 5.9.1, are the conceptual steps that may be used to find out the boundary of a soil medium overlying bedrock where progressive increase is made in lateral direction to arrive at a safe distance where chances of wave reflection is greatly minimized.

It can be well inferred from above that depending on the geometry of the structure and soil parameters there could be cases when the soil model (even for a 2D problem) could be significant and cost of analysis could be quite high.

For machine foundation it is not necessary to go upto the bedrock level in vertical direction and the rule of thumb (if at all such 2D FEM model is used) to take the boundary at 1.5 to 2 times the Rayleigh wave length. For lateral direction again a trial and error as discussed earlier to be used.

5.9.3 Use of spring or boundary elements

It is for this use of frequency independent springs and dashpots coupled with structures has remained the most popular and effective technique in design offices to find out the coupled response of soil-structure system. The advantages could be summarized as hereafter.

1 The analysis is surely more economic than using detailed finite element of the soil.

87 By far the most popular model adapted by the structural engineers.
88 Often known as Silent or transmitting boundaries for infinite domain problem.
89 In some cases site would have no bedrock when level at which the shear wave velocity approaches 600 m/sec is usually considered the bedrock level.

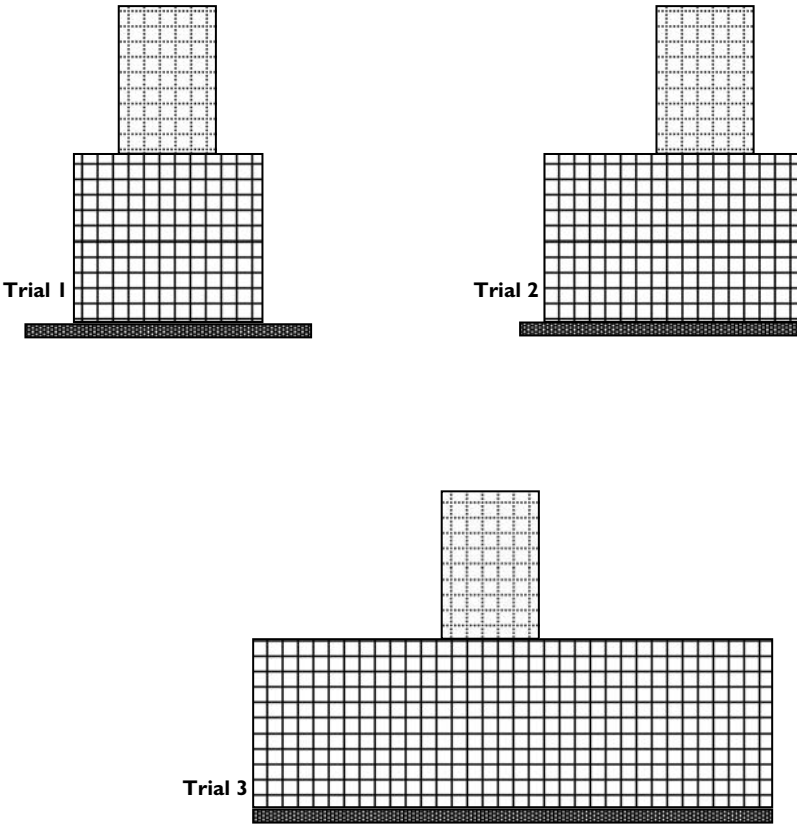


Figure 5.9.1 Trial increment of soil boundary in lateral direction to cater to wave transmittal.

2 In majority of the case we are more interested to know the response of the structure itself due to the presence of the underlying soil and not vice-versa thus spring or the boundary elements adequately serves the purpose in most of the cases.
3 Techniques are available albeit in an approximate way to force the radiation damping in the modal damping matrix thus to cater to the radiation as well as material damping of the system[90].
4 For machine foundations which are usually resting or embedded on ground the method is good enough to provide results which matches well with exact elastodynamic response based on half space theory and usually does not warrant further sophistication in mathematical modeling.

90 Refer Chapter 1 (Vol. 2) on dynamic soil-structure interaction where we have worked out a frame-soil interaction problem considering this effect.

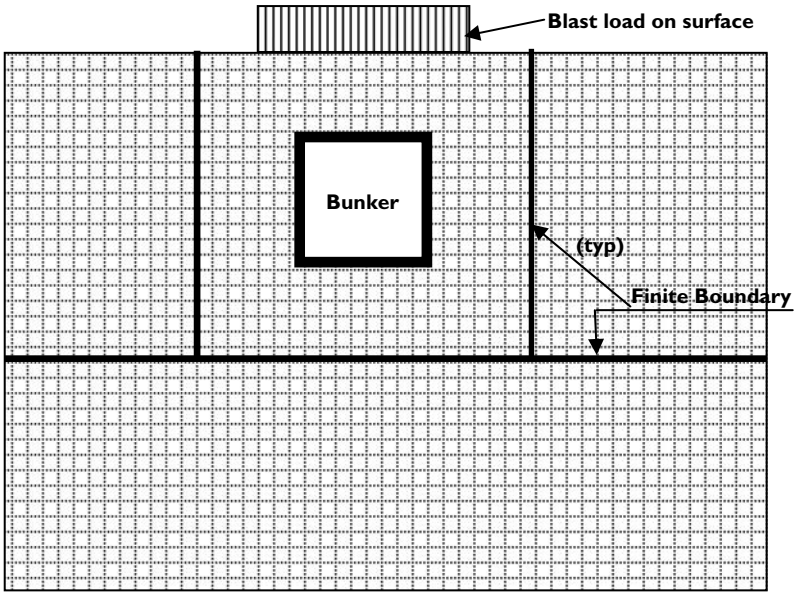


Figure 5.9.2 Underground bunker with blast load on the soil surface.

However it should also be pointed out that in spite of its versatility and simplicity in use it is possibly the most abused method in practice. In most of the cases especially under earthquake the values chosen are not correct and so are the damping values for rarely does the basic characteristics of soil-stiffness degradation and enhancement of damping under high strain is catered to. Engineers are mostly found to blindly assume the shear modulus data given in soil report and adapt them for seismic analysis and arrive at a wrong result. Very few realize that the data furnished in soil report is low strain and may be directly used for machine foundation and not for seismic analysis[91].

5.9.4 Use of transmitting/silent boundaries with finite elements

There are certain types of problem where finite element modeling of soil is inevitable.

As shown in Figure 5.9.2, we show an underground structure whose response needs to be determined under blast load on surface which is transient in nature. In such case trying to model the soil with structural boundary conditions where the waves do not reflect back can make the model significantly large.

In such cases one of the effective methods used is to use finite element model to a certain depth below and around the structure (as shown by dark lines) and then use special absorbing elements which would absorb away the energy from there onwards.

91 This topic is also addressed in detail with worked out problems in Chapter 1 (Vol. 1).

It is obvious that in such case considerable economy in analysis can be achieved as the model size is reduced significantly. We will discuss some of these boundary elements in detail hereafter.

We have shown at the outset of this chapter that when waves propagate through the soil medium which is considered elastic and homogeneous three types of waves are generated in it namely compression or *P* waves, shear or *S* waves and Rayleigh waves which create significant response at the surface. Thus if we have to apply these absorbing boundaries at a finite depth they should be good enough to absorb all three type of waves as mentioned above.

To start with we first describe the standard viscous boundaries which are capable of absorbing the *P* and *S* waves.

5.9.5 Standard viscous and Rayleigh boundary elements

As shown in Figure 5.9.3 is a soil element through which waves are propagating in positive x direction.

The dynamic equilibrium equation of motion as per De Alembert's theory is thus given as

$$-\sigma_{xx} - \rho\frac{\partial^2 u}{\partial t^2} + \sigma_{xx} + \frac{\partial \sigma_{xx}}{\partial x} = 0 \quad \text{or} \rho\frac{\partial^2 u}{\partial t^2} - \frac{\partial \sigma_{xx}}{\partial x} = 0 \tag{5.9.1}$$

Considering $\sigma_{xx} = \lambda\varepsilon_{xx} = \lambda\frac{\partial u}{\partial x}$ we have $\rho\frac{\partial^2 u}{\partial t^2} = \lambda\frac{\partial^2 u}{\partial x^2}$, where λ is the Lame's constant. This gives

$$\frac{\partial^2 u}{\partial t^2} = V_p^2\frac{\partial^2 u}{\partial x^2} \tag{5.9.2}$$

where *Vp* is velocity of the *P* wave propagating through the medium.

Solution to the above partial differential equation of motion is given by

$$u(x,t) = U\left[\sin\left(\omega t - \frac{\omega x}{V_p}\right) + \cos\left(\omega t - \frac{\omega x}{V_p}\right)\right] \tag{5.9.3}$$

where ω = Arbitrary frequency of the harmonic motion.

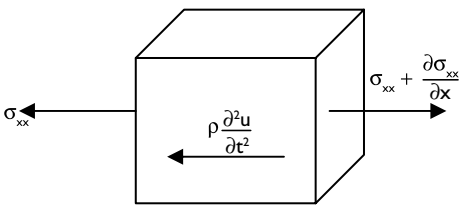


Figure 5.9.3 Wave propagation through a soil element.

Differentiating above with respect to t we have

$$\dot{u}(x,t) = U\omega\left[\cos\left(\omega t - \frac{\omega x}{V_p}\right) - \sin\left(\omega t - \frac{\omega x}{V_p}\right)\right] \tag{5.9.4}$$

Considering $\varepsilon_{xx} = \frac{\partial u}{\partial x} = -\frac{U\omega}{V_p}\left[\cos\left(\omega t - \frac{\omega x}{V_p}\right) - \sin\left(\omega t - \frac{\omega x}{V_p}\right)\right] = -\frac{\dot{u}(x,t)}{V_p}$
Again considering $\sigma_{xx} = \lambda\varepsilon_{xx}$

$$\sigma_{xx} = -\lambda\frac{\dot{u}(x,t)}{V_p} = -\rho V_p^2\frac{\dot{u}(x,t)}{V_p} = -\rho V_p\dot{u}(x,t) \tag{5.9.5}$$

Now, if we multiply this stress by the area of the soil element (say A) we get a force in negative x direction

$$F_x = \sigma_{xx}A = -\rho V_p A\dot{u}(x,t) \tag{5.9.6}$$

Thus we see that F_x is force, which is identical to the force in a simple viscous damper whose value is equal to $\rho v_p A$.

Therefore instead of going to a large distance after the finite depth (modeled by finite element) a boundary condition can be created which will allow the P waves to pass without any reflection and allow the strain energy to radiate away from the source.

In lieu of V_p if we consider V_s (where $V_s = \sqrt{G/\rho}$) it can be proved by same arguments that there exists another set of force given by

$$F_z = -\rho v_s A\dot{w}(z,t) \tag{5.9.7}$$

Instead of modeling to a large depth, the model can now be reduced to a model as shown in Figure 5.9.4.

Above caters to the transmittal of the P and S waves through the idealized viscous dampers while modeling infinite domain by finite boundary. The above viscous boundaries though are valid for P and S waves cannot transmit Rayleigh waves that transmit a major part of the energy.

Lysmer and Kuhlemeyer (1969) proposed a similar expression like standard viscous boundaries for absorption of such Rayleigh waves given by

$$F_z = \alpha_1\rho v_p A\dot{w}(x,t) \quad \text{and} \quad F_x = \alpha_2\rho v_s A\dot{u}(x,t) \tag{5.9.8}$$

where $\alpha_1 = \frac{\eta_R}{S_p}\left[1 - \left(1 - 2S_p^2\right)\frac{\dot{w}(nz)}{u(nz)}\right]$ and $\alpha_2 = \eta_R\left[1 + \frac{\dot{u}(nz)}{w(nz)}\right]$
in which,

w = Displacement in vertical z direction;
u = Displacement in horizontal x direction and

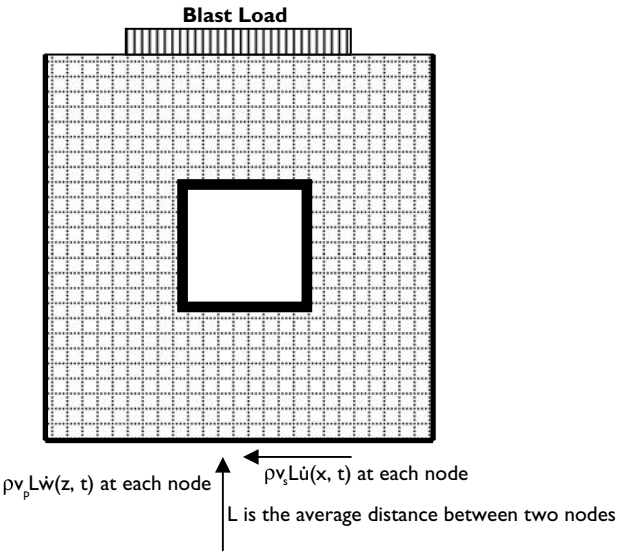


Figure 5.9.4 Underground bunker with viscous dampers at boundary.

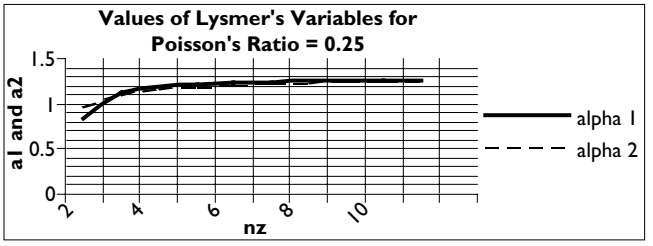


Figure 5.9.5 Values of Lysmer's variables for Poisson's ratio = 0.25.

$n = \frac{\omega}{V_R}, \omega =$ Frequency of the system;
$V_R =$ Velocity of Rayleigh Wave, $Vs =$ Velocity of Shear wave;
$Vp =$ Velocity of compression wave.

$$\eta_R = \frac{V_s}{V_R}, \quad S_p = \frac{V_s}{V_p} = \sqrt{\frac{1-2\nu}{2(1-\nu)}} \tag{5.9.9}$$

For Poisson's Ratio of $\nu = 0.25$ values of α_1 and α_2 are as shown in Figure 5.9.5.

For Poisson's ratio = 0.3, Dasgupta (1976) has given a similar solution wherein the Rayleigh viscous absorbers are expressed as

$$Fz = \alpha_1 \dot{w} \quad \text{and} \quad Fx = \alpha_2 \dot{u} \tag{5.9.10}$$

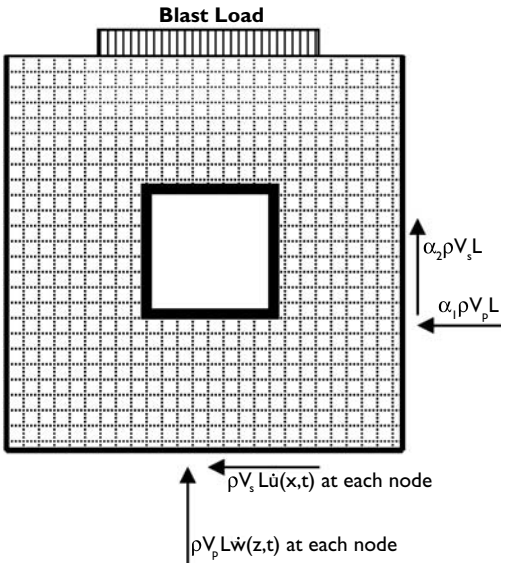


Figure 5.9.6 Underground bunker with Rayleigh and viscous dampers at boundary.

where

$$\alpha_1 = \frac{G}{V_R}\left[\frac{-1.380e^{-0.885nz} + 0.641e^{-0.362nz}}{0.566e^{-0.885nz} - 0.320e^{-0.362nz}}\right] \quad \text{and}$$

$$\alpha_2 = \frac{G}{V_R}\left[\frac{-1.131e^{-0.885nz} - e^{-0.362nz}}{0.566e^{-0.885nz} - e^{-0.362nz}}\right]$$

Based on above the final model for the problem posed reduces to the one shown in Figure 5.9.6.

5.9.6 Paraxial boundaries

These types of Boundaries are improved boundaries over what we derived earlier and can absorb all the three types of waves (*P*, *S*, and *R*).

Considering the wave equation in two dimensions we have

$$\frac{\partial^2 u}{\partial x^2} + \frac{\partial^2 u}{\partial z^2} = \frac{1}{V_s^2}\frac{\partial^2 u}{\partial t^2} \quad \text{where } V_s = \sqrt{\frac{G}{\rho}} \tag{5.9.11}$$

Solution to the above equation in exponential form is given (Cohen and Jennings 1984) by

$$u = e^{[i(\omega t - n_x x - n_z z)]} \tag{5.9.12}$$

Substituting the above in the two dimensional wave equation yields

$$n_x^2 + n_z^2 - \frac{\omega^2}{V_s^2} = 0$$

which can be further expressed as

$$n_x^2 - \frac{\omega^2}{V_s^2}\left[1 - \frac{n_z^2 V_s^2}{\omega^2}\right] = 0$$

$$\text{or} \quad \left[n_x + \tfrac{\omega}{V_s}\sqrt{1 - \left(\tfrac{n_z V_s}{\omega}\right)^2}\right]\left[n_x - \tfrac{\omega}{V_s}\sqrt{1 - \left(\tfrac{n_z V_s}{\omega}\right)^2}\right] = 0 \tag{5.9.13}$$

For outgoing waves as the second term is only valid hence we have

$$n_x = \frac{\omega}{V_s}\sqrt{1 - \left(\frac{n_z V_s}{\omega}\right)^2}$$

Above when expanded to first two terms of Taylor series gives

$$n_x - \frac{\omega}{V_s} + \frac{V_s}{2\omega} n_z^2 = 0 \quad \text{or } n_x \frac{\omega}{V_s} + \frac{n_z^2}{2} - \frac{\omega^2}{V_s^2} = 0$$

The above actually represents a differential equation of the form

$$\frac{1}{V_s}\frac{\partial}{\partial t}\left[\frac{\partial u}{\partial x}\right] - \frac{1}{2}\frac{\partial^2 u}{\partial z^2} + \frac{1}{V_s^2}\frac{\partial^2 u}{\partial t^2} = 0 \tag{5.9.14}$$

The above equation in approximate way permits propagation of all the three type of waves in positive x direction.

If we consider only the first term of the Taylor series only we have

$$n_x - \frac{\omega}{V_s} = 0 \quad \text{or } \frac{\partial u}{\partial x} + \frac{1}{V_s}\frac{\partial u}{\partial t} = 0 \tag{5.9.15}$$

Multiplying each of the term by G we have

$$G\frac{\partial u}{\partial x} + \frac{G}{V_s}\frac{\partial u}{\partial t} = 0 \quad \text{or } \tau_{xz} + \rho V_s \dot{u} = 0 \tag{5.9.16}$$

Thus it is seen paraxial boundaries are nothing but an improved form of standard viscous dampers.

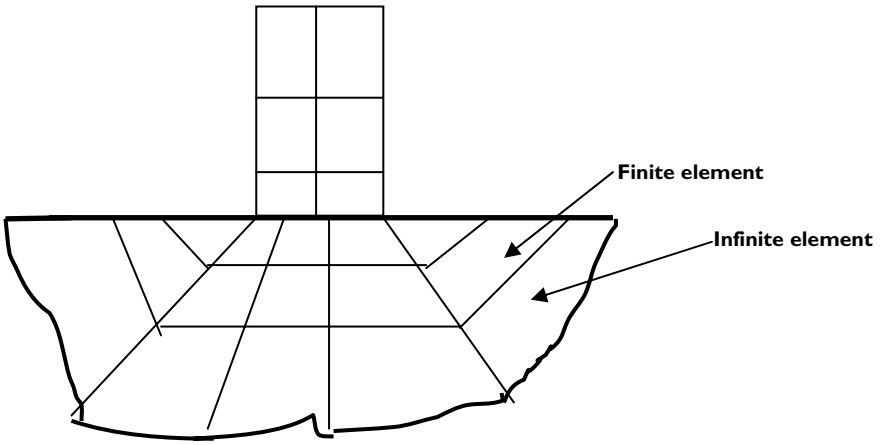


Figure 5.9.7 Structure resting on infinite soil modeled by finite and infinite element.

5.9.7 Infinite finite elements

We will not derive the detailed mathematics involved in such elements for the same has already been done in Chapter 4 (Vol. 1) under Static soil structure interaction. Wherein these elements can be attached to the finite elements at a certain depth wherein it automatically takes care of the propagation of waves to infinity (Figure 5.9.7). This method has been used in many practical problems related to infinite boundary problems (Bettes & Zienkiwicz 1977; Kim & Bang 2000).

One of the major limitations of using the viscous damper is that it cannot be used directly in commonly used commercially available finite element software available in the market.

Either one has to develop his own software or use special purpose program that can cater to this feature.

However Softwares like SASSI (Lysmer et al), FLUSH, ANSYS or SAP 2000 have this feature and may be used for such interaction analysis.

We will not discuss further on this topic here anymore. The detail of modelling and application of the same will be elaborated further with results in the chapter on Numerical and Analytical methods in Civil engineering (Chapter 2 (Vol. 1)) wherein we have dealt with Finite Element Theory and Application in detail pertaining to various discipline in civil engineering.

5.9.8 Epilogue

We had stated at the outset that the topic is still a growing technology and lots of researches need to be carried out to get clear answer on many issues like

- Liquefaction (this we have dealt in the chapter of Earthquake Engineering).
- Three dimensional constitutive model for 3D Finite Element analysis.
- Instrumented observed data from real field.

- Effect of layering of soil and its anisotropic effect.
- Dynamic consolidation etc.

The section basically highlights the theoretical developments which took place in various areas of soil dynamics from continuum mechanics to the present state of art as practiced in the profession.

SUGGESTED FURTHER READING

It is surprising to find that though this is now a very standard topic being offered at post graduate level and gaining design importance in industry books and design guides available (especially in international market) are very limited. We give herein a few available which may referred further to gain more insights.

Structural dynamics

1 Timoshenko, S.P. & Young, D.H. 1964, *Vibration Problems in Engineering*, 3rd edn, Affiliated East-West Press, Pvt. Ltd., New Delhi.
2 Paz, M. 1991, *Structural Dynamics: Theory and Computation*, Van Nostrand-Reinhold, NY.
3 Clough, Ray, W. & Penzien, J. 1975, *Dynamics of Structure,* McGraw-Hill Kogakusha Ltd., Tokyo.
4 Chopra, A.K. 1996, *Dynamics of Structure: Theory and application to Earthquake engineering*, Prentice-Hall of India Pvt. Ltd., New Delhi.
5 Hurty, W.C. & Rubenstein, M.F. 1967, *Dynamics of Structure*, Prentice Hall of India Pvt. Ltd., New Delhi.
6 Craig, R.H. Jr. 1981, *Structural Dynamics: An Introduction to Computer Methods*, John Wiley & Sons, NY.
7 Mukhopadhyay, M. 2002, *Vibration Dynamics and Structural Systems*, Second Edition, Oxford-IBH, New Delhi.
8 Bathe, K.J. 1984, *Finite Element Procedures in Engineering Analysis*, Prentice Hall of India Pvt. Ltd., New Delhi.
9 Meirovitch, L. 1975, *Elements of Vibration Analysis*, McGraw-Hill Book Co. NY.

Advanced topics in structural dynamics

1 Donea, J.P. Editor, 1980, *Advanced Structural Dynamics*, Pergamon, NY.
2 Crandall, S.H., Ed., 1963, *Random Vibration*, Vol. I&II, The MIT Press, Cambridge, Mass.
3 Nigam, N.C. & Narayanan, S. 1994, *Random Vibration Analysis and Application*, Narosa Publication, New Delhi.
4 Lin, Y.K. 1976, *Probabilistic Theory of Structural Dynamics*, McGraw-Hill, NY.

Foundation dynamics

1 Barkan, Dominic D. 1962, *Dynamics of Bases and Foundations*, McGraw-Hill Book Co., NY.

2 Das, B.M. 1983, *Fundamentals of soil dynamics,* Elsevier Science Publishing Co., Amsterdam.
3 Kameswara Rao, N.S.V. 1998, *Vibration Analysis and Foundation Dynamics*, Wheeler Publishing, New Delhi.
4 Kramer, S. 2004, *Geotechnical Earthquake Engineering*, Pearson Education Publication, New Delhi.
5 Major, A. 1980, *Dynamics in Civil Engineering – Analysis and Design*, Vols. I–IV, Akademia Kiado, Budaapest and Collets Holding London.
6 Newmark, N.M. & Rosenblueth, E. 1971, *Fundamentals of Earthquake Engineering*, Prentice-Hall, Englewood Cliffs, N.J.
7 Richart, Jr. F.E., Hall, Jr. J.R., & Woods, R.D. 1970, *Vibrations of Soils and Foundations*, Prentice-Hall, Englewood Cliffs, N.J.
8 Srinivasalu, P. & Vadiyanathan, C.V. 1977, *Handbook of Machine Foundations*, Tata Mcgraw-Hill, New Delhi.
9 Saran, S. 1999, *Soil Dynamics and Machine Foundation*, Galgotia publications Pvt. Ltd., New Delhi.

Advanced topics in foundation dynamics

1 Ayres, Frank Jr., 1962, *Theory and Problems of Matrices*, Schaum, NY.
2 Bathe, K.J. 1973, *Nonlinear Dynamic Analysis of Complex Structures,* Int. J. Earth. Engg. Struc. Dyn., Vol. 1, pp. 241–252.
3 Bathe, K.J. 1990, *Finite Element Procedures in Engineering Analysis*, Prentice Hall of India, New Delhi.
4 Barkan, Dominic D. 1962, *Dynamics of Bases and Foundations*, McGraw-Hill Book Co., NY.
5 Caughey, T.K. 1960, 'ClassicaI Normal Modes in Damped Linear Dynamic Systems', *J. App. Mech*., ASME, Vol. 27, pp. 269–271.
6 Dowrick, D.J. 1987, Earthquake Resistant Design For Engineers and Architects, 2nd edn, John Willey & Sons Inc., NY.
7 Goldstein, H.H., Murray F.J. & Neumann von J, 1959, 'The Jacobi Method of real symmetric matrices', *J. of the Assoc. of the Comp. Machines*, Vol. 6, pp. 59–96.
8 Hurty, W.C. & Rubenstein, M.F. 1967, *Dynamics of Structure*, Prentice-Hall of India Pvt. Ltd., New Delhi.
9 Jacobi, C.G.J. 1846, 'Uber ein leichtes Verfahren die in der Theorie der Sacular-storungen vorkommenden Gelichungen numerisch aufzulosen', *Crelle's Journal,* Vol. 30, pp. 51–94.
10 Newmark, N.M. 1959, 'A method of computation for structural dynamics', *JEMD*, ASCE, Vol. 85, pp. 67–94.
11 Scarborough, J.B. 1958, *Numerical Mathematical Analysis*, 4th edn, John Hopkins Press, Madison.
12 Timoshenko, S.P. & Goodier, J.N. 1970, *Theory of Elasticity*, 3rd edn, McGraw-Hill Kogakusha, Ltd., Tokyo.
13 Timoshenko, S.P. 1956, *Strength of materials*, Vol. 2, 3rd edn, Van Nostrand, NY.
14 Wilkinson, J.H. 1968, 'On the quadratic convergence of the Cyclic Jacobi Process', *Numerische Mathematik,* Vol. 11.
15 Wilson, E.L., Farhoomand, I. & Bathe, K.J. 1973, 'Nonlinear Dynamic analysis of Complex Structures', *Int. J. Earthquake Eng. Struc. Dyn*., Vol. 1, pp. 241–252.

References

1 Abel, J.F. & Popov, E.P. 1968, 'Static and dynamic finite element analysis of sandwich structures', *2nd Conference in Matrix Analysis of Structures*, Wright Patterson Air Force Base, Ohio, USA.
2 Abramowitz, M. & Stegan, I.A. 1964, *Handbook of Mathematical Functions*, Dover, NY.
3 Achenbach, J.D. 1976, *Wave Propagation in Elastic Solid*, North Holland Publication, NY.
4 Adini, A. & Clough, R.W. 1960, 'Analysis of plate bending by Finite Element Method', *Report G-7337*, National Science Foundation, Washington DC.
5 Aki, P. & Richards, P. 1980, *Quantitative Seismology*, University Science Books, USA.
6 Akin, J.E. 1986, *Finite Element Analysis for Undergraduates*, London Academic, London.
7 Anandakrishnan, M. & Krishnaswamy, N.R. 1973, 'Response of Embedded Footings to Vertical Vibrations', *J. Soil Mech. Found. Engg.*, ASCE, Vol. 99, No. 10, pp. 863–883.
8 Archer, J.S. 1963, 'Consistent mass matrix for distributed mass systems', *Journal of Structural Division*, ASCE 89, ST4, pp. 161–178.
9 Arfken, G.B. & Weber, H.J. 2001, *Mathematical Methods for Physics*, 5th edn, Academic Press, NY.
10 Arnold, R.N., Bycroft, G.N. & Warburton, G.B. 1955, 'Forced Vibration of a body on an Infinite Elastic Stratum', *J. Applied Mechanics*, Trans. ASME September, pp. 391–400.
11 Awojobi, A.O. & Grootenhuis, P. 1965, 'Vibration of rigid bodies on semi-infinite elastic media', *Proc. Royal Society*, London, Series A, Vol. 287, pp. 27–63.
12 Ayres, Frank Jr. 1962, *Theory and Problems of Matrices*, Schaum, NY.
13 Baranov, V.A. 1967, 'On the calculation of excited vibrations of an embedded foundation'(In Russian) *Voprosy Dynamiki I Prochnocti*, No. 14, Polytechnical Institute of Riga, pp. 195–209.
14 Barkan, Dominic, D. 1962, *Dynamics of Bases and Foundations*, McGraw-Hill Book Co., NY.
15 Bateman, H. & Pekeris, C.L. 1945, 'Transmission of light from a point source in a medium bounded by diffusely reflecting parallel plane surfaces', *J. Opt. Soc. Amer*, 35, pp. 651–657.
16 Bath, M. 1966, 'Earthquake Seismology', *Earth Science Review*, Vol. 1, Elsevier, Amesterdam, p. 69.
17 Bathe, K.J. 1973, *Nonlinear Dynamic Analysis of Complex Structures*, Int. J. Earth. Engg. Struc. Dyn., Vol. 1, pp. 241–252.
18 Bathe, K.J. & Wilson, E.L. 1976, *Numerical Methods in Finite Element Analysis*, Prentice Hall of India, New Delhi.
19 Bathe, K.J. 1984, *Finite Element Procedures in Engineering Analysis*, Prentice Hall of India, New Delhi.

20 Bathe, K.J. 1990, *Finite Element Procedures in Engineering Analysis*, Prentice Hall of India Pvt. Ltd., New Delhi.
21 Batoz, J.L. Bathe, K.J. & Ho, L. 1980, 'A study of three node triangular plate bending elements', *IJNME*, Vol. 15, pp. 1771–1812.
22 Batoz, J.L. 1982, 'An explicit formulation for an efficient triangular plate bending element', *IJNME*, Vol. 18, pp. 1077–1089.
23 Beer, C. & Meek, J.L. 1981, 'Infinite domain elements', *IJNME*, Vol. 17, pp. 43–53.
24 Bettes, P. 1977, 'Infinite elements', *IJNME*, Vol. 11, pp. 53–64.
25 Bettes, P. & Zienkiwicz, O.C. 1977, 'Diffraction and refraction of surface waves using finite and infinite elements', *IJNME*, 11, 1271–90.
26 Bickford, W.M. 1990, *A First Course in Finite Element Method*, Homewood IL R.D. Irwin.
27 Blume, J.A. 1965, 'Earthquake Ground Motion and Engineering Procedure for Important Installations near Active faults', *Proc. 3rd World Conf. on Earthquake Engg*, Vol. III, New Zealand.
28 Bogner, F.K., Fox, R.L. & Schmit, L.A. 1965, 'The Generation of Inter-element compatible stiffness and mass matrices by use of interpolation formulas', *Proc. Conf. on Matrix Method in Structural Mechanics*, Airforce Institute of Technology, Wright Paterson Air Force Base, Ohio, USA.
29 Bowes, W.H. & Russel, L.T. 1975, *Stress Analysis by the Finite element method for Practicing Engineers*, Lexington Books.
30 Bowles, J.E. 1974, *Analytical and Computer Methods in Foundation Engineering*, McGraw-Hill Book Co., NY.
31 Bowles, J.E. 1988, Foundation Analysis and Design, 4th Edition, McGraw-Hill Book Co. NY.
32 Bullen, K.E. & Bolt, B. 1985, *An introduction to the Theory of seismology*, 4th edn, Cambridge University Press, Cambridge, UK.
33 Bycroft, G.N. 1977, 'Soil-Structure Interaction at High Frequency Factors', *Int. J. Earth. Engg. and Struc. Dyn.*, 5, 235–248.
34 Carey, G.F. & Oden, J.T. 1983, *Finite Element*, Vols. 1 and 2, Prentice-Hall Inc. NJ.
35 Caughey, T.K. 1960, 'Classical normal modes in damped linear dynamic system', *J. App. Mech.*, ASME, Vol. 27, pp. 269–271.
36 Chao, Chi-Chang 1960, 'Dynamic response of an elastic half-space to tangential surface loadings', *J. Applied Mechanics*, Trans. ASME, September, pp. 559–567.
37 Chopra, A.K. 1996, *Dynamics of Structure: Theory and application to Earthquake engineering*, Prentice-Hall of India Pvt. Ltd., New Delhi.
38 Chandruptala, T.R. & Belegundu, A.D. 1997, *Introduction to Finite Elements in Engineering* Prentice-Hall of India Pvt. Ltd., New Delhi.
39 Cheung, Y.K. & Nag, D.K. 1968, 'Plates and beams on elastic foundation', *Geotechnique*, 18(2), pp. 250–260.
40 Chowdhury, I. & Dasgupta, S.P. 2004, 'Computation of Rayleigh Damping coefficient for systems with large degrees of freedom', *Electronic Journal of Geotechnical Engineering* Volume-8.
41 Chowdhury, I. & Dasgupta, S.P. 2007, 'Dynamic Earth Pressure on rigid unyielding walls under earthquake forces', *Indian Geotechnical Journal*, Vol. 37(2), pp. 81–93.
42 Clough, R.W. & Felippa, C.A. 1968, 'A Refined Quadrilateral Element for Plate Bending', *2nd Conference on Matrix Method in Structural Mechanics Wright Paterson Air Force Base*, Ohio.
43 Clough, Ray, W. & Penzien, J. 1975, *Dynamics of Structure*, McGraw-Hill Kogakusha Ltd., Tokyo.

44 Clough, R.W. 1991, 'Original formulation of the Finite Element Method', *Finite Element Analysis and Design*, Vol. 7, pp. 89–101.
45 Clough, R.W. & Wilson, E.L. 1999, 'Early finite element research at Berkeley', Proc. *5th US National. Conf. Comp. Mech*, Boulder, CO., August.
46 Coates, R.C., Coutie, M.G. & Kong, F.K. 1997, *Structural Analysis*, 3rd edn, Chapman & Hall, London.
47 Cohen, M. & Jennings, P.C. 1984, 'Silent Boundary Methods for Transient Analysis', *Computational Methods in Transient Analysis—Computational Methods in Mechanics*, Vol. 1, North Holland, pp. 310–360.
48 Cook, R.D., Malkus, D.S. & Plesha, M.E. 1989, *Concepts and Applications of Finite Element Analysis*, Third Edition, John Wiley and Sons, NY.
49 Courant, R. 1943, 'Variational methods for solution of equilibrium and vibration', *Bull. Am. Math Soc.* Vol. 49, pp. 1–43.
50 Crandall, S.H., ed., 1963, *Random Vibration*, Vols. I&II, The MIT Press, Cambridge, Mass.
51 Craig, R.H. Jr. 1981, *Structural Dynamics: An Introduction to Computer Methods*, John Wiley & Sons, NY.
52 Das, B.M. 1983, *Fundamentals of soil dynamics*, Elsevier Science Publishing Co, Amsterdam.
53 Dasgupta, S.P. 1976, Finite Element Solutions to Some Problems in the Dynamics of Footings, *Ph.D Thesis*, Indian Institute of Technology, Kanpur, India.
54 Dasgupta, S.P. & Kallam, S. 2006 'Vibration of an Elastic Half space under rectangular loading' *Indian Geotechnical Journal*, 36(2), pp. 86–114.
55 Dasgupta, S.P. & Kameswara Rao, N.S.V. 1978, 'Dynamics of rectangular footings by Finite elements', *Journal of GT Division*, ASCE, Vol. 104, 5.
56 Davies, A.J. 1980, *The Finite Element Method—first approach*, Oxford Clarendon.
57 Den Hartog, J.P. 1924, *Mechanical Vibrations*, Dover Publications, NY.
58 Desai, C.S. 1979, *Elementary Finite Element Method* Prentice-Hall, New Jersey.
59 Desai, C.S. & Abel, J. 1972, *Introduction to Finite Element Method*, Van Nostrand Reinhold Company, NY.
60 Donea, J.P. Editor, 1980, *Advanced Structural Dynamics*, Pergamon, NY.
61 Donovan N.C. 1974, 'Earthquake Hazards for Buildings', *Engineering Bulletin* No. 46, Dames and Moore, Los Angeles, pp. 3–20.
62 Dowrick, D.J. 1987, Earthquake Resistant Design For Engineers and Architects, 2nd edn, John Willey & Sons Inc., NY.
63 Dowrick, D.J. 2003, *Earthquake Risk Reduction*, John Wiley & Sons, UK.
64 Esteva, L. & Villerverde, L. 1973, 'Seismic risk design spectra and structural reliability', *Proc. 5th World Conference on Earthquake Engineering Rome (2)*, pp. 2586–96.
65 Fung, Y.C. 1965, *Foundations of Solid Mechanics*, Prentice-Hall, Inc., Englewood Cliffs, NJ.
66 Galileo Galilei 1594, *Della Scienza Mechanica.*
67 Gallagher, R.H. 1975, *Finite Element Analysis Fundamentals*, Prentice-Hall Inc., NJ.
68 Graff, K.F. 1991, *Wave Motion in Elastic Solids*, Dover Publications, NY.
69 Ghali, A. & Neville, A.M. 1997, *Structural Analysis*, F & FN Spon, 4th Edition.
70 Ghali, A. & Bathe, K.J. 1970, 'Analysis of plates in bending, using large finite elements', *IABSE 30/11*, Zurich.
71 Goldstein, H.H., Murray, F.J. & Neumann von, J. 1959, 'The Jacobi Method of real symmetric matrices', *J. of the Assoc. of the Comp. Machines*, Vol. 6, pp. 59–96.
72 Graff, K.F. 1975, *Wave Motions in Elastic Solids*, Claredon Press, Oxford, UK.
73 GTSTRUDL *Theoretical and Users Manual* Georgia University, Atlanta.

74 Gutenberg, B. & Richter, C.F. 1956, 'Earthquake Magnitude, Intensity Energy and Acceleration', *Bull. Seis. Soc. America*, Vol. 46, No. 2, pp. 105–146.
75 Hall, J.R. Jr. 1967, 'Coupled Rocking and Sliding Oscillations of Rigid Circular Footings', *Proc. Int. Symp. On Wave Propagation and Dyn. Properties of Earth Materials*, Albuquerque, NM, Aug.
76 Harr, M.E. 1969, *Foundations of Theoretical Soil Mechanics*, McGraw-Hill Kogakusha Co. Ltd., Tokyo.
77 Holzl Ö hner, U. 1969, 'Schwingungen des elastischen Halbraums bei Erregung auf einer Rechteckfl ä che', Ing. Archiv., 38, pp. 370–79.
78 Hrennikoff, A. 1941, 'Solution of problems in Elasticity by the frame work method', *J. App. Mech.*, Vol. 8, pp. 169–175.
79 Hsieh, T.K. 1962, 'Foundation Vibrations', *Proc. of Inst. of Civil Engineers*, Vol. 22, pp. 211–226.
80 Hughes, T.J.R., Taylor, R.L. & Kanoknukulchai, W. 1977, 'A simple and efficient finite element for plate bending', *IJNME*, Vol. 11, No. 10, pp. 1529–1543.
81 Hughes, T.J.R. 1987, *The Finite Element Method: Linear Static and Dynamic Finite Element Analysis*, Prentice-Hall, Englewood Cliffs, NJ.
82 Hughes, T.J.R. 2000, *The Finite Element Method: Linear Static and Dynamic Finite Element Analysis*, Dover Publishers, NY.
83 Hughes, T.G. 1974, Study in the criminology of Non-conforming element, *B.Sc. Engg. Thesis* University of Wales Swansea.
84 Hurty, W.C. & Rubenstein, M.F. 1967, *Dynamics of Structure*, Prentice Hall of India Pvt. Ltd., New Delhi.
85 Irons, B.M. 1966, 'Numerical Integration application in Stiffness Method', *JAIAA*, Vol. 14, pp. 2035–2037.
86 Irons, B.M. 1970, 'A frontal solution program for finite element analysis', *IJNME*, Vol. 3, pp. 5–32.
87 Irons, B.M. & Razzaque, A. 1972, 'Experience with Patch Test for convergence of Finite Element', *Mathematical foundation of Finite Element*, A. Razzaque ed, Academic Press, NY, pp. 557–587.
88 Irons, B.M. & Ahmad, S. 1980, *Techniques of Finite Elements*, Ellis Horwood, Chichester, UK.
89 Irons, B.M. & Shrive, N. 1980, *Finite Element Primer*, John Wiley & Sons, NY.
90 IS 2950(Part1)—Code of practice for design and construction of raft foundation.
91 IS-456, Indian standard code of practice for design of reinforced concrete structure.
92 Jacobi, C.G.J. 1846, 'Uber ein leichtes Verfahren die in der Theorie der Sacularstorungen vorkommenden Gelichungen numerisch aufzulosen', *Crelle's Journal*, Vol. 30, pp. 51–94.
93 Kameswara Rao, N.S.V. 1998, *Vibration Analysis and Foundation Dynamics*, Wheeler Publishing, New Delhi.
94 Karasudhi, P., Keer, L.M. & Lee, S.L. 1968, 'Vibratory motion of a body on an elastic half plane', *J. Apl. Mech.,Trans. ASME*, December, pp. 697–705.
95 Kardestuncer, H. & Norrie, D.H. ed 1987, *Finite Element Handbook*, McGraw-Hill Inc., NY.
96 Kausel, E. 2005, *Fundamental Solutions in Elastodynamics: A compendium*, MIT, Cambridge Press, Cambridge.
97 Kim Doo Kie & Yun Chung Bang, 2000, 'Time Domain Soil-Structure Analysis in two dimensional medium based on Frequency dependent Infinite Elements', *IJNME*, 47, pp. 1241–1261.
98 Kramer, S. 2004, *Geotechnical Earthquake Engineering*, Pearson Education Publication. New Delhi.

99 Kreyszig, E. 2001, *Advanced Engineering Mathematics*, 8th edn, John Wiley & Sons Inc., NY.
100 Krishnamurthy, E.V. & Sen, S.K. 1989, *Numerical Algorithms: Computations in Science and Engineering*, Affiliated East West Press, Pvt. Ltd., New Delhi.
101 Lamb, H. 1904, 'On propagation of tremors over the Surface of an elastic solid', *Phil. Trans. of Royal Soc.* London, Vol. 203, pp. 1–42.
102 Landau, L.D. & Lifshitz, E.M. 1989, *Theory of Elasticity*, 3rd edn, Pergamon Press, NY.
103 Lin, Y.K. 1976, *Probabilistic Theory of Structural Dynamics*, McGraw-Hill, NY.
104 Livesley, R.K. 1983, *Finite Element an introduction to Engineers*, Cambridge University Press, London.
105 Logan, D.L. 1986, *A First Course on Finite Element Method*, PWS Publishers, Boston, MA.
106 Love, A.E.H. 1944, *A Treatise on Mathematical Theory of Elasticity*, Dover, NY.
107 Luco, J.E. and Westmann, 1971, *Dynamic response of circular footings*, Report. UCLA-ENG-7113, University of California, Los Angeles, USA.
108 Luco, J.E. & Westmann, R.A. 1972, 'Dynamic response of a rigid footing bonded to an elastic half-space', *J. Appl. Mech., Trans. ASME*, 39(2), pp. 527–534.
109 Lysmer, J. 1965, *Vertical Motion of Rigid footings*, Contract Report, No. 3-115, US. Army Engineer WES, Vicksburg, Miss.S. 1–130.
110 Lysmer, J. & Richart, F.E. Jr. 1966, 'Dynamic response of footings to vertical loading', *J. Soil Mech. and Found. Div., Proc. ASCE*, Vol. 92, No. SM1, January, pp. 65–91.
111 Lysmer, J. & Kuhlemeyer, R.L. 1969, 'Finite dynamic model for Infinite Media', *JEMD, ASCE*, Vol. 95, EM6, pp. 859–877.
112 Macguire, R.K. 1974, *Seismic structural response analysis, incorporating peak response regressions on earthquake magnitude and distance*. Research Report No. R74-51, Department of Civil Engineering Massachusetts Institute of Technology.
113 Main, I.G. 1995, *Vibrations and Waves in Physics*, Cambridge University Press, UK.
114 Major, A. 1980, *Dynamics in Civil Engineering—Analysis and Design*, Vols. I–IV, Akademia Kiado, Budaapest and Collets Holding London.
115 Malvern, L.E. 1969, *Introduction to the Mechanics of a Continuous Medium*, Prentice-Hall, Inc., Englewood Cliffs, NJ.
116 Martin, H.C. & Carey, G.F. 1973, *An introduction to Finite Element Analysis*, Theory and Application, McGraw-Hill, NY.
117 McHenry, D. 1943, 'A lattice analogy for the plane stress problem', *J. Inst. of Civil Engineers*, Vol. 21(2).
118 Meek, J.L. 1971, *Matrix Structural Analysis*, McGraw-Hill Kogakusha, Ltd., Tokyo.
119 Meirovitch, L. 1975, *Elements of Vibration Analysis*, McGraw-Hill Book Co. NY.
120 Melosh, R.J. 1963, 'Basis for derivation of matrices for direct stiffness method', *J. AIAA*, pp. 1631–1637.
121 Miller, G.F. & Pursey, H. 1955, 'On the partition of Energy between Elastic Waves in a Semi Infininte Solid', *Proc. Royal Society*, A233, pp. 55–69.
122 Mindlin, R.D. 1936, 'Force at a point in the interior of a semi-infinite Solid', *Physics*, Vol. 7, May, pp. 195–202.
123 Mukhopadhyay, M. 1984, *Matrix, Finite Element, Computer and Structural Analysis*, Oxford & IBH Publishing Company, New Delhi.
124 Mukhopadhyay, M. 2002, *Vibration Dynamics and Structural Systems*, Second Edition, Oxford-IBH, New Delhi.
125 Murthy, V.N.S. 1991, *Soil Mechanics and Foundation Engineering*, Vols. I&II, Sai-Kripa Technical Consultants, Bangalore(India).
126 Nath, B. 1974, *Fundamentals of Finite Elements for Engineers*, Athlone, London.
127 Neuber, H. 1934, Z. Angew. *Math. Mech.*, Vol. 14, p. 203.
128 Neville, A.M. 1981, *Properties of Concrete*, 3rd edn, Pitman, London.

129 Newmark, N.M. 1959, "A method of computation for structural dynamics", *JEMD, ASCE*, Vol. 85, pp. 67–94.
130 Newmark, N.M. & Rosenblueth, E. 1971, *Fundamentals of Earthquake Engineering*, Prentice-Hall, Englewood Cliffs, NJ.
131 Nigam, N.C. & Narayanan, S. 1994, *Random Vibration Analysis and Application*, Narosa Publication, New Delhi.
132 Norrie, D.H. & Vries De, G. 1973, *The Finite Element Method Fundamentals and Applications*, Academic Press, NY.
133 Novak, M. & Beredugo, Y.O. 1972, 'Vertical Vibration of embedded footings', *J. soil Mech, and Found. Div., Proc ASCE*, Vol. 98, No. SM12, December, pp. 1291–1310.
134 Novak, M., Nogami, T. & Aboul-Ella, F. 1978, 'Dynamic soil reaction for plane strain case', *J. Engng. Mech., ASCE*, Vol. 104(4), pp. 953–595.
135 Newmark, N.M. 1959, 'A method of computation for structural dynamics', *JEMD*, ASCE, Vol. 85, pp. 67–94.
136 Oden, J.T. & Reddy, J.N. 1976, *An Introduction to Mathematical Theory of Finite Element,* John Wiley, NY.
137 Papkovitch, P.F. 1932, *Compt. Rend.* Vol. 195, pp. 513 and 754.
138 Parton, V.Z. and Perlin, P.I. 1984, *Mathematical Methods of the Theory of Elasticity*, Vols. I &II, MIR Publisher, Moscow.
139 Paz, M. 1991, *Structural Dynamics: Theory and Computation*, Van Nostrand-Reinhold, NY.
140 Pekeris, C.L. 1955, 'The Seismic Surface Pulse', *Proc. National Academy of Science USA*, Vol. 41, pp. 469–480.
141 Pekeris, C.L. 1955, 'The Seismic Buried Pulse', *Proc. National Academy of Science USA*, Vol. 41, pp. 629–639.
142 Pekeris, C.L. & Lifson, H. 1957, 'Motion of the Surface of a Uniform Elastic Half Space Produced by a Buried Pulse', J. of Acoustical Society of America, Vol. 29(11), pp. 1233–1238.
143 Pian, T.H.H. & Tong, P.A. 1969, 'Basis of methods for solid continua', *IJNME*, Vol. 1, pp. 13–28.
144 Pipes, L.A. and Harvill, L.R. 1970, *Applied Mathematics for Engineers and Physicists*, McGraw- Hill-Kogakusha, Tokyo.
145 Prager, W. & Synge, J.L. 1947, 'Approximation in elasticity based on functional space', *Q.J. App. Math. Soc*, Vol. 5, pp. 241–269.
146 Przemieniecki, J.S. 1968, *Theory of Matrix Structural Analysis*, McGraw-Hill Book Co., NY.
147 Rajasekaran, S. 1983, *Finite Element Analysis in Engineering Practice*, A.H. Wheeler Publication, New Delhi.
148 Rao, S.S. 1980, *The Finite Element method in Engineerin*, Pergamon Press, NY.
149 Razzaque, A. ed., 1972, *Mathematical foundation of Finite Element*, Academic Press, pp. 557–587, NY.
150 Reddy, J.N. 1993, *An introduction to finite element method*, McGraw-Hill, NY.
151 Reissner, E. 1936, 'Staionare axilasymmetriche durch eine schuterende Masse erregte Schwingungen eines homogenen elastischen Halbraumes', *Ingenieur Archiv* (22), December, pp. 381–396.
152 Reissner, E. & Sagoci, H.F. 1944, 'Forced torsional oscillations of an elastic halfspace', *J. of Appl. Physics*, Vol. 15, pp. 652–662.
153 Richart, F.E. Jr. 1962, 'Foundation Vibration', *Trans. ASCE*, Vol. 127, Part 1, pp. 863–898.
154 Richart, Jr. F.E., Hall, Jr. J.R. and Woods, R.D. 1970, *Vibrations of Soils and Foundations*, Prentice-Hall, Englewood Cliffs, NJ.

155 Richter, C.F. 1958, *Elementary Seismology*, W.H. Freeman and Co. Inc., San Francisco.
156 Riley, K.F., Hobson, M.P. & Bence, S.J. 2002, *Mathematical Methods for Physics and Engineering*, Cambridge University Press, UK.
157 Robertson, I.A. 1966, 'Forced vertical vibration of a rigid circular disc on semi-infinite elastic soild', *Proc. Camb. Phil. Soc.*, 62, pp. 547– 553.
158 Salvadori, M.G. & Baron, M.L. 1966, *Numerical Methods in Engineering*, Prentice-Hall of India, Pvt. Ltd., New Delhi.
159 SAP 2000, *Theoretical and Users Manual*, University of California, Berkeley.
160 Saran, S. 1999, *Soil Dynamics and Machine Foundation*, Galgotia publications Pvt. Ltd., New Delhi.
161 Sastry, S.S. 1986, *Numerical Methods for Engineers and Scientists*, Prentice-Hall of India Pvt. Ltd., New Delhi.
162 Scarborough, J.B. 1958, *Numerical Mathematical Analysis*, 4th edn, John Hopkins Press, Madison.
163 Segerlind, L.J. 1984, *Applied Finite Element Analysis*. John Wiley & Sons, NY.
164 Selvadurai, A.P.S. 1979, *Elastic Analysis of Soil Foundation Interaction*, Elsevier, NY.
165 Shames, I.H. 1975, *Introduction to Solid Mechanics*, Prentice-Hall, Englewood Cliffs, NJ.
166 Shames, I.H. & Dym, C.L. 1995, *Energy and Finite Element Method in Structural Mechanics,* New Age International Publishers Ltd., New Delhi.
167 Srinivasalu, P. & Vadiyanathan, C.V. 1977, *Handbook of Machine Foundations*, Tata Mcgraw-Hill, New Delhi.
168 Sridharan, A., Nagendra, M.V. & Chinnaswamy, C. 1981, 'Embedded foundations under vertical vibration', *Journal of Geotechnical Engineering, ASCE*, 107(GT10), pp. 1429–1434.
169 Strang, G.W. & Fix, G.J. 1973, *Analysis of Finite Element Method*, Prentice Hall Inc., NJ.
170 Sung, T.Y. 1953, 'Vibrations in semi infinite solids due to Periodic surface loading', ASTM *Special Technical Publication No. 156*, Symposium on soil dynamics, July, pp. 35–64.
171 Szilard, R. 2004, *Theories and Applications of Plate Analysis: Classical Numerical and Engineering Methods*, John Wiley & Sons, New Jersey.
172 Taylor, R.L., Beresford, P.J. & Wilson, E.L. 1976, 'A Non-conforming Element for Stress Analysis', *IJNME*, Vol. 10.
173 Taig, C. 1961, 'Structural analysis by Matrix displacement method', *English Electric Aviation* Report No. S017.
174 Teng, W.C. 1962, *Foundation Design*, Prentice-Hall of India, Pvt. Ltd., New Delhi.
175 Terzaghi, K. & Peck, R.B. 1967, *Soil Mechanics in Engineering Practice*, John Wiley & Sons, NY.
176 Tong, P. & Rossetos, J.N. 1977, *Finite Element Method Basic Techniques and Implementation,* Cambridge MIT Press.
177 Thomson, W.T. & Kobori, T. 1963, 'Dynamic compliance of rectangular foundations on elastic half space', Journal of applied mechanics, Trans ASME, Vol. 30, pp. 579–584.
178 Timoshenko, S.P. 1956, *Strength of materials*, Vol. 2, 3rd edn., Van Nostrand, NY.
179 Timoshenko, S.P. & Woinowsky-Krieger 1958, *Theory of Plates and Shells*, McGraw-Hill Kogakusha, Ltd., Tokyo.
180 Timoshenko, S.P. and Young, D.H. 1964, *Vibration Problems in Engineering*, 3rd edn, Affiliated East-West Press, Pvt. Ltd., New Delhi.
181 Timoshenko, S.P. & Goodier, J.N. 1970, *Theory of Elasticity*, 3rd edn, McGraw-Hill Kogakusha, Ltd., Tokyo.
182 Tocher, D. 1958, 'Earthquake Energy and Ground Breakage', *Bull. Seis. Soc. Am.*, Vol. 2, No. 2, pp. 147–153.
183 Tocher, J.L. 1962, *Analysis of Plate Bending using Triangular Elements*, *Ph.D Thesis*, University of California, Berkeley.

184 Tschebotarioff, G.P. 1973, *Foundations, Retaining and Earth Structures-The Art of Design and Construction and its Scientific Basis in Soil Mechanics*, 2nd edn, McGraw-Hill, NY.
185 Tse, F.S., Morse, I.E. & Hinkle, R.T. 1968, Mechanical Vibrations, Prentice-Hall of India Pvt. Ltd., New Delhi.
186 Turner, M.J., Clough, R.W., Martin, H.C., & Topp, L.J. 1956, 'Stiffness and deflection analysis of complex structures', *J. Aero. Sci.*, 23(9), pp. 805–823.
187 Veubeke, F.D.B. 1967, 'A Conforming finite element for plate bending', *J. Solids and Structures*, Vol. 4, No. 1, pp. 95–108.
188 Vesic, A.S. 1961, 'Bending of beams resting on isotropic elastic solid', *J. Engg. Mech. Div. ASCE*, Vol. 87, EM2, April, 35–53.
189 von Karman, T. and Biot, M.A. 1940, Mathematical Methods in Engineering, McGraw-Hill Book Co. Inc., NY, pp. 115–119.
190 Weaver, Jr. W. & Gere, J.M. 1986, *Matrix Analysis of Framed Structure*, CBS Publishers & Distributors, Delhi, India.
191 Wilkinson, J.H. 1968, 'On the quadratic convergence of the Cyclic Jacobi Process', *Numerische Mathematik*, Vol. 11.
192 Wilson, E.L., Taylor, R.L., Doherty, W.P. & Ghaboussi, P. 1973, 'Incompatible displacement Models', *Numerical and Computer Methods in Structural Mechanics*, Feneves, J. ed., Academic Press, pp. 43–57.
193 Wilson, E.L., Farhoomand, I. & Bathe, K.J. 1973, 'Nonlinear Dynamic analysis of Complex Structures', *Int. J. Earthquake Eng. Struc. Dyn.*, Vol. 1, pp. 241–252.
194 Wilkinson, J.H. 1968, 'On the quadratic convergence of the Cyclic Jacobi Process', *Numerische Mathematik*, Vol. 11.
195 Zeevart, L. 1983, *Foundation Engineering for Difficult Subsoil Conditions*, Van Nostrand Reinhold Co., NY.
196 Zienkiewicz, O.C. & Cheung, Y.K. 1964, 'The finite element method for the analysis of elastic isotropic and orthotropic slabs', *Proc. Inst. Civ. Eng.*, 28, pp. 471–488.
197 Zienkiewicz, O.C. 1970, *Finite Element Method in Engineering Science*, McGraw-Hill Inc. London.
198 Zienkiewics, O.C. & Morgan, K. 1982, *Finite Elements and Approximations*, Wiley Interscience, NY.
199 Zienkiewics, O.C. & Taylor, R.L. 1991, *The Finite Element Method*, Vols. 1&2 McGraw-Hill Book Co., London.

Subject index

Acceleration 81, 84, 87, 342, 343, 347, 355, 359, 360, 362, 363, 383, 385, 405, 533, 549, 557, 559, 561, 565, 566, 568, 571, 576, 646, 723, 725–728, 732, 734, 737, 725–728, 732, 734, 737, 779, 787, 789
  Peak 359, 385, 723, 726, 728, 737
Amplification 6, 360, 507, 728, 737
Amplitude 353, 359, 360, 363, 367, 373, 374, 379, 448–451, 743, 753, 823, 824, 829, 832
ANSYS 482, 537, 843
Attenuation 377, 727, 834
Autonomous system 404, 415

Base Shear 126
Bearing Capacity 323, 469, 475, 476, 478
Bending moment 119, 121, 128, 150, 153, 323–325
  Lateral Load 122, 123
  Lateral response
  Pile 122–124, 126, 127, 129, 133, 149, 267, 390, 482, 491, 494, 495, 534, 538
Biharmonic equations 147

Chang's Solution 719
Chaos 463
Compatibility 34–37, 60, 65, 92, 93, 169, 225, 236, 656, 692, 705
  Condition 34, 36, 65, 225
  Equations 34, 37, 63
Condensation 214–217, 233, 242, 247, 308, 309, 638
  Dynamic 638
  Static 215–217, 233, 247, 308, 309, 640
Consolidation 130, 136, 139, 479, 480, 502
Constitutive relations 52, 56, 92, 493
Coordinates 10, 32, 33, 40, 44, 49, 58, 79,81, 82, 91, 99, 146, 147, 201, 202, 206, 207, 213, 225, 229, 245, 256, 260, 280, 282, 284, 297, 400, 403–405, 422, 434, 441, 761, 791, 810
  Cartesian 91, 161, 404, 498, 649, 686
  Cylindrical 40, 657, 699, 703, 791
  Spherical 51, 649, 740
Coupled 5, 306, 434, 437, 439, 444, 469, 470, 507, 523, 526, 533, 546, 574, 639, 642, 756, 761, 785, 789, 798, 828, 832, 835
  Motion 434, 761
  Translation and Rotation 437, 439
Coupling 490, 611, 615, 669, 798, 804
  Dynamic 615
  Fluid-structure 533
  Soil-structure 533, 835
Coupling of Soil-Structure 835
Critical Points 393, 397

Damped 349, 350, 356, 362, 367, 370, 380–382, 406, 450, 460, 512, 533
  Critically 512
  Over 349, 512
  Under 512
Damped free vibration 367, 533
Damping 6, 347, 348, 349, 355, 356, 359, 360, 362, 370, 372–374, 377, 378, 382, 404, 423, 449–451, 454, 460, 511–514, 532–545, 549, 550, 552, 555, 560, 568, 574, 575, 577, 582, 731–733, 737, 753, 755–758, 760, 761, 822–825, 827, 829, 832, 836, 837
  Caughey 542, 543
  Critical 349, 370, 512, 513, 533
  Heavy 362
  Modal 6, 540, 836
  Radiation 511, 534, 757, 836
  Rayleigh 535, 536, 545, 577, 582
  Soil 733, 832
  Solid 374
  Velocity squared 373
DEGEBO 741

Differential equations 2, 34, 60, 62, 73, 105, 335, 370, 391, 404, 408, 415, 416, 424–426, 428, 429, 453, 465, 545, 641, 644, 658, 671, 689, 699, 733
Elliptic 130, 132, 142, 406, 456, 711, 712, 721
Hyperbolic 130, 141, 142, 146, 147
Ordinary 105, 119, 157, 335
Partial 34, 73, 335, 641
Dilatation 28, 29, 44, 88, 89, 94, 647, 662, 704, 766, 767, 783, 805, 833
Direction cosines 12, 32, 33, 41, 43, 47, 50, 52, 54–56, 61, 132, 521, 663
Displacement 10, 12, 15, 16, 22, 24, 25, 29, 31, 34, 36, 60, 66, 70, 71–73, 78, 79, 82, 86–88, 91–94, 96, 98, 99, 101, 106, 108–110, 112, 114, 121, 124, 128, 142, 150, 169, 171, 173, 174, 177–179, 182, 185, 187, 188, 194, 198, 201, 204, 210, 212, 215, 219, 222, 223, 225–228, 247, 254, 262, 271–274, 278, 280, 288, 289, 291, 292, 294, 295, 300, 301, 307, 308, 310–312, 322, 324, 325, 329, 338, 339, 342, 347, 355–357, 359, 360, 362, 372, 374–376, 379, 389, 404, 405, 440, 441, 443, 450, 451, 453, 454, 458, 477–479, 484–490, 494, 497, 499, 510, 520, 527, 533, 546, 549–553, 556, 558, 561, 565, 567–569, 571, 573–575, 604, 626, 627, 630, 640, 643, 647, 649, 653, 657, 659, 661, 662, 664–666, 670, 687, 690, 692, 694–696, 698, 699, 701–706, 711–713, 716, 719, 721, 722, 730, 733–737, 739–741, 743–747, 750–752, 754–757, 761, 764–767, 771, 774, 782, 783, 786, 789–791, 793, 793, 795–798, 800, 805–808, 815, 817, 818, 820, 821, 833, 834, 839
Bessel's 641, 658, 685, 687, 700, 733, 769, 787, 801, 805, 821
Bi-harmonic 91
Continuous 10, 80, 114, 124, 674, 687
Dirac's Delta 803
Function 10, 18, 34, 74, 80, 81, 86, 90, 91, 106–116, 124, 130, 132, 136, 137, 141, 158, 168, 173, 174, 178, 179, 182, 184–188, 190–192, 194, 198, 201, 203, 204, 210, 212, 220, 222, 223, 225, 226, 228, 234, 235, 238–245, 247, 249–251, 254, 256, 258, 264, 266, 268, 271–273, 302, 304, 307, 311, 312, 316, 349, 351, 353, 357, 359, 362, 372, 379, 380, 383–386, 389, 392, 404, 407, 408, 412, 413, 415, 416, 421, 422, 424, 426–433, 449, 451, 453, 454, 486, 494, 497–500, 507, 510, 512, 534, 550, 553, 561, 569, 576, 604, 617, 618, 630, 631, 641, 643, 649–651, 653, 656–658, 662, 664, 672, 674–679, 681, 685–687, 690–693, 696, 698–701, 703, 707, 710, 713, 715, 719, 730, 732–734, 736, 740, 741, 743–745, 747–749, 751, 754, 757, 762, 765, 768–770, 783, 785, 787, 790, 791, 793–795, 797, 801, 803–805, 807–809, 811, 812, 814–818, 821, 823, 824, 835
Gamma 734
Hankel 641, 770, 795
Harmonic 90, 91, 351, 359, 454
Heaveside 703
Polynomial 173, 184, 186–188, 194, 210, 220, 222, 241, 242, 247, 249, 494, 497, 498
Shape 108–112, 114, 115, 173, 178, 182, 184–186, 201, 234, 235, 238, 240–245, 249, 251, 256, 258, 264, 266, 268, 273, 311, 312, 316, 499, 630, 631, 736, 835
Transfer 190, 685, 730, 732, 733
Transient 323, 324, 381, 385, 402, 513, 684, 837
Dynamic Shear Modulus 163, 644, 733, 735, 737
Degradation 837
Linear Variation 557, 751
Dynamics 1–7, 85, 102, 165, 169, 171, 214, 335, 505–508, 523, 576, 585, 591, 610, 615, 639–642, 687, 722, 739, 740, 752, 844
Elasto-dynamics 6
Soil dynamics 1, 3, 6, 7, 102, 335, 506, 507, 639, 640, 642, 687, 722, 739, 740
Structural dynamics 3, 5, 6, 165, 169, 214, 505, 576, 585, 591, 615, 640, 642, 752

Earth Pressure 739, 829
At rest 829
Earthquake Analysis 576, 835
Buildings 4, 507
Chimneys 161, 312, 313, 470, 538, 574, 585, 604
Duhamel Integral 381
Geotechnical 3, 7, 9, 102, 640
Time history 737
Eigen value 43, 166, 214, 248, 274, 398, 400, 516, 521–525, 528, 532, 533, 535, 538–540, 545, 574, 584–587, 591, 592, 594–597, 599, 600, 602, 607–610, 612,

615, 617, 618, 622, 623, 631, 634, 637, 638
Economizer 214, 637
Finite Element 264, 574, 585, 612
In dynamics 523
Physics of 313, 521
Test 248, 269, 273, 274
Eigen Value Analysis 521, 523, 525, 528, 584, 612, 623
Free-Free Structure 606
Generalized Jacobi 615, 617–619
Matrix deflation 592, 596, 599, 600, 608, 609, 617
Newton Raphson 166, 579, 587, 588, 594, 597, 615
Ramanujan 589–591
Rayleigh Ritz 107, 110, 602, 604
Standard Jacobi 610, 615
Stodola 166, 599, 600, 609, 617
Vector Transformation 609
Visual inspection 586
Eigen Vector 43, 274, 516, 523–525, 527–529, 542, 577, 581, 582, 594, 595, 599, 600–602, 604, 609, 610, 618, 637
Elastostatics 94
Element stress 288, 295
Energy methods 339
Epicenter 671, 724, 726
Equations of 9, 34, 40, 59, 60, 62, 64, 65, 74, 83, 84, 86, 88, 92, 93, 142, 370, 424, 438, 441, 444, 445, 531,533, 545, 546, 646, 697, 782, 791, 793, 828
Motion 64, 83, 84, 86, 88, 89, 106, 341, 356, 370, 371, 374, 375, 378, 391, 404, 438, 441, 444, 445, 449, 451, 453, 454, 457, 511, 523, 525–527, 529–531, 533, 534, 545–547, 549–552, 567, 573, 575, 583, 585, 639–641, 646–648, 650, 687, 688, 696, 697, 699, 729, 731, 733, 737, 756, 758, 759, 761, 766, 787, 791, 824, 826, 828–832, 838
Estimation of sub-grade modulus 478

FEMA 167
Field Tests 501, 741
Finite difference method 105, 114, 115, 119, 124, 151, 154, 171, 172
application in dynamics 165, 610
backward difference 115
central difference 115, 116, 137, 142, 172, 551, 553, 560, 568, 573, 574, 576
Crank-Nicolson scheme 138
Elliptic equations 130, 142
forward difference 115, 137
Hyperbolic equations 141
initial value problem 106, 163, 392, 467
Lateral load analysis of pile 122, 123
Parabolic equations 136
polar co-ordinate 161, 162, 657, 671, 686, 698, 699, 704, 712
Refined finite difference 157–159, 164
Finite element method (FEM) 5, 105, 167, 168, 170, 171, 177, 306, 470, 502, 585, 623
Basic Philosophy 172, 270
Boundary condition 172, 275, 482, 502, 839
Bubonov-Galerkin Method 310
Constant Strain 168, 182, 183, 188, 227, 270, 271, 275
Constitutional laws 183
Convergence 157, 158, 169, 182, 183, 188, 189, 269, 611, 612, 617
DKT Plate element 252, 253
Dynamic finite element 6
Eight nodded Hexahedral Element 264
Eight-nodded quadrilateral 242, 245
Equilibrium equation 60, 62, 68, 215, 216, 226, 274, 280, 305, 306, 309, 315, 473, 559, 573, 838
Frontal Wave Solution 302, 308
Gauss Quadrature Formula 191
Gaussian elimination 303
Geometric mapping 204
Hermite Polynomials 247
Heuristic type polynomial 247
Hierarchical polynomial 247
Higher order finite elements 234
History 168
Infinite domain problem 495, 496
Infinite finite element 496, 497, 500, 835
Iso-parametric formulation 199, 206, 211, 227, 261, 264, 297, 318, 483
Jacobian matrix 203, 204, 223, 227, 261, 262, 291
Law of convergence 187
LDLT decomposition 304
MCZ-element 255
Natural coordinates 189
Nine nodded Rectangular Element 241
Non-conforming element 189, 220
Non-conforming Elements 189
Numerical integration 191
Plane Stress Analysis 170
Plate element 248, 323, 483, 490
Quadrilateral element 199, 201, 203, 206, 211, 217, 219, 222, 229, 235, 245, 258, 260, 268, 291, 484, 638
Rectangular plate element 254
Refined meshes 151, 220, 577
Rule of polynomial 184

Serendipidity Family 242, 244, 252
Specified support displacement 293
Static Condensation 215–217, 233, 247, 308, 309, 638
Sub-parametric element 210
Super-parametric element 210
Thermal analysis of composite wall 312
Triangular plate element 249
Twenty-nodded hexahedral element 268
Finite grid method 476, 488
FLUSH 843
Focus 9, 102, 168, 301, 315, 320, 407, 469, 505, 671, 718, 723, 724, 727, 742
Forced vibration 362, 367, 378, 460, 461, 463, 527, 684, 745, 781
Foundation/footing 40, 129, 470, 474, 483, 820
Block 437, 574, 805
Circular 40, 741, 743, 744, 750–752, 791, 820
Embedded 820, 823, 824, 829, 830
Frame 323, 471
Impact (*see Hammer*)
Isolated 470, 483
Machine 7, 434, 439, 534, 649, 687, 740, 751, 755, 820, 831, 832, 834–837
Rectangular 761, 781, 805, 807–809, 817, 818
Rigid 437, 507, 740, 744, 746, 750–752, 781, 820
Steel *vs* concrete 2, 67, 70, 269, 374, 577
Strip 494, 765, 781, 785, 790
Turbine (*see frame*) 5, 576
Fourier Integral 676, 677, 693
Complex 677, 693
Trigonometric 676
Fourier Series 671, 675, 676
Complex 674
Trigonometric 672, 676
Free edged plates 159
Frequency 165, 324, 337, 340, 341, 343, 346, 347, 349, 350, 353, 355, 357, 359–364, 367, 369, 373, 374, 379, 380, 385, 386, 424, 434, 435, 443, 445, 446, 448–451, 453, 455, 459–461, 509, 510, 512, 515, 516, 518, 521, 533, 535, 537–540, 543, 575–577, 591, 604, 632, 635, 644, 659, 728–730, 733, 741, 743–748, 751–753, 755–760, 768, 772, 776, 791, 801, 807, 814–819, 821–825, 827, 831, 832, 835, 838, 840
Damped 349, 350, 380, 512
Natural 165, 337, 340, 341, 343, 346, 347, 349, 350, 353, 367, 369, 370, 379, 380, 385, 386, 434, 442, 443, 509, 510, 512, 515, 516, 518, 521, 533, 535, 537, 540, 543, 575, 577, 578, 604, 625, 632, 644, 730, 823, 824, 829, 831
Operating 359, 362, 448, 576, 831
Resonant 353, 354, 359, 360, 362, 367, 448–451, 460, 743, 819, 823
Friction forces 374
Coulomb 374
Dry 374
Fundamental Mode 434, 459, 508, 617, 735, 736

Ground Motion 655, 728, 729, 733
GTSTRUDL 323, 329, 482, 537

Half Space 79, 95, 96, 267, 482, 485, 486, 639, 643, 649, 654–656, 659, 668, 702, 719, 720, 740, 743, 750, 752, 753, 755–759, 762, 765, 766, 781–783, 791, 795–798, 807, 820, 821, 836
Mechanical Analogue 752, 753, 756, 758, 759, 761, 820
Hooke's law 52, 58, 73, 88, 269, 270
Hypo center 724, 726

Instability 146, 428
Lyapunov's 428
IS-456 500
Isotropic elastic bodies 79

Kronecker delta 59

Lagrange's interpolation 238–242
Lagrangian Formulation 545
Lamb's Solution 698, 703, 740
Three Dimension 9, 267, 315, 644–646, 678, 698, 703, 735, 740
Lame's parameter 59, 60, 86, 767
Laplace Equation 130, 147, 159
Linear analysis 391, 737
Liquefaction 639, 640, 843
Loads 9, 79, 198, 215, 267, 325, 328, 335, 402, 435, 470, 475, 490, 493, 624, 791
Condensor 216
Dead 152
Dynamic 9, 79, 323, 324, 335, 469, 687, 741, 744, 752, 764, 810, 832, 834
Harmonic 437, 729, 791
Impulsive 379
Live 152, 434, 517
Seismic 723
Static 6, 9, 332, 469, 765, 834
Thermal 267
Lumped parameter vibration 335

Magnification Factor 353, 364, 367, 505, 765, 819
MASH 728
Mass 4, 5, 39, 69, 80, 83, 106, 163, 165, 169, 171, 267, 315, 323, 335, 336, 338, 339, 341–344, 347, 348, 359, 360, 362–364, 367, 369, 371–373, 375, 379, 383, 385, 390, 392, 434–436, 441–444, 446–449, 451–453, 455, 458–460, 502, 508, 514, 515, 518, 519, 523, 524, 533–535, 543–545, 552, 554, 560, 568, 575, 576, 586, 592, 603, 605, 609, 615, 619, 621, 625, 629–631, 634–639, 646, 701, 720, 733, 736, 737, 741, 751, 752, 754–756, 758–760, 767, 772, 776,781,819, 820, 823, 824, 830, 832
  Distributed/Consistent 629
  Lumped 5, 106, 163, 335, 336, 338, 434, 508, 514, 523, 575, 615, 629–631, 634, 637–639, 752, 830
Matrix analysis 488, 489, 507
Mechanical Impedance 355, 435
Mechanical vibration 5, 6, 335, 508, 639
Meshes 151, 158, 159, 183, 187, 189, 194, 198, 220, 235, 236, 328, 480, 481, 484, 485, 577, 637
Modal Analysis 6, 545, 575, 577
Modal mass 323, 545, 576
Mode shapes 443, 506, 519–521, 577, 580, 582
Modulus 9, 56, 58, 59, 86, 87, 92, 96, 122–124, 126, 127, 163, 165, 206, 221, 229, 296, 323, 449, 451, 475,476, 478–483, 486,487,493, 500,501, 508,517,635,639,644, 548,720, 731, 732, 735, 737, 742, 744, 751, 756, 761, 793, 821, 837
  Bulk 59, 87
  Shear 56, 87, 92, 103, 644, 648, 720, 731, 732, 735, 737, 741, 744, 751, 756, 761, 793, 821, 837
  Sub-grade 122–124, 127, 475, 476, 478–483, 500, 501
  Young's 9, 58, 59, 86, 92, 96, 123, 165, 206, 229, 493, 508, 639
Mohr diagram 44, 45, 47–49
Moment 2, 39, 76, 83,85, 86, 119, 121–124, 126, 128, 150, 152–154, 165, 177, 268, 284, 289, 322–325, 329, 337, 341, 344, 371, 409, 416–418, 437, 442, 452, 469–476, 501, 508, 751, 759, 781, 783, 795, 798, 813, 832
Momentum 3, 83, 85, 86
Multi-degrees freedom 6, 434, 435, 752
NASTRAN 166
Non-harmonic motion 453
Non-linear analysis 735
Numerical Methods 4, 5, 102, 171, 476, 477
  Collocation 111, 112
  Galerkin's 112, 311, 314, 315, 317
  Least Square 113, 758, 771
  Rayleigh-Ritz 107, 110, 604
  Sub-domain 112
  Weighted Residual Methods 110

Orthogonal 28, 29, 31, 43, 58, 524–527, 533, 534, 536, 537, 542, 545, 575, 595, 600, 601, 610, 805
  Properties 527
  Transformation 524, 525, 527, 533, 534, 537, 545, 575
Orthotropic material 55

Paraxial boundary 6, 842
Patch test 248, 258, 269–272, 275
Pekeris's Solution 6, 712, 718, 719
  Buried Pulse 712
  Surface Pulse 748, 712, 718
Phase planes 390
Plasticity Index 91
Poisson's ratio 187, 204, 227, 483, 486, 487, 493, 500, 502, 639, 648, 653, 654, 719, 735, 747, 751, 752, 754, 756, 759, 761, 763, 767, 783, 789, 793, 799, 811, 816, 821, 840
Power absorption 360, 362
Pressure 38, 69, 99, 137, 138, 267, 268, 326, 327, 437, 471, 474, 475, 478, 491, 492, 501, 640, 644, 721, 739, 741, 743, 744, 829
  Dynamic 640, 644, 744
  Non-uniform 437, 475
  Soil/Earth 475, 478, 739, 829
  Uniform 99
Principles of superposition 65
Problem 5–7, 9, 15, 34, 37, 40, 43, 62, 65, 79, 86, 91, 98, 101–103, 105–113, 115, 119, 122, 124, 126, 129, 130, 134–136, 141, 142, 144, 146, 147, 149, 151, 152, 154, 161, 163–167, 169, 170, 172,173, 177, 182, 189–191, 199, 206, 220, 235, 236, 238, 242, 247–250, 259, 273–275, 283, 292, 301, 302, 306–308, 311–313, 315, 316, 319–322, 325, 327–329, 350, 360, 374, 381, 392, 393, 396, 401, 402, 407, 408, 412, 416, 439, 440, 443, 444, 449, 451, 456, 460, 467, 470, 474, 476–478, 481–483, 490–492, 494–498, 500, 502, 503, 505, 506, 516, 521, 523, 533, 535, 537, 539, 553, 561, 568,

574–577, 584, 585, 587, 591, 597, 599, 602, 604, 606, 610, 615–618, 623, 638, 641, 642, 644, 653, 659, 662, 671, 685, 696, 699, 703–705, 723, 740, 745, 746, 765, 766, 774, 781–783, 791, 800, 807, 808, 817, 820, 834, 835, 837, 841, 843
Boundary value 91, 102, 106, 107, 141, 163, 765, 766, 783
Boussinesq 95, 96, 98
Cerruti 96, 101
Initial value 106, 163, 392, 467
Kelvin 94, 98, 101
Mindlin 96, 97
Mixed boundary value 766
Pseudo Static analysis 505

Raft 161, 268, 322, 323, 470, 475–477, 479, 480, 483, 485, 488, 490
Flexible 476
Rigid 475, 476
Rayleigh coefficients 537
Resonance 359, 360, 362, 367, 374, 378, 449–451, 460, 461, 632, 644, 730, 732, 832
Response 102, 323, 337, 340, 345, 349, 351, 353, 354, 355, 359, 360, 362, 364, 368, 377–380, 382, 385, 386, 388–390, 402, 434–436, 439, 441, 447, 449, 460, 463, 486, 505, 507, 513, 514, 540, 549, 574–577, 602, 643, 682, 687, 719, 723, 724, 728, 734, 735, 737, 740, 741, 743–745, 751, 755, 761, 766, 793, 800, 820, 821, 823, 829, 830, 834–838
Steady state 353, 355, 364, 436, 441, 447, 449, 513, 821
Transient 323, 385, 513
Response Spectra 385, 386, 388, 728
Response spectrum 385, 386, 388, 389

Saddle point 397, 398, 420, 426, 429
SAP2000 843
SASSI 843
Scaling Factor 528, 529, 597
Seepage problem 132, 319
Self-excited oscillations 404
SHAKE 728, 733
Single degree of freedom 6, 337, 346, 373, 379, 380, 382, 385, 435, 449, 450, 508, 523, 632, 635, 758, 772
Small deformation 15, 25, 27, 29, 66
Soil-Structure Interaction 4, 5, 306, 470, 471, 474, 477, 482, 507, 533, 642, 745, 791, 834, 843
Dynamic 1, 3, 5, 335, 470, 507, 834
Static 5, 470, 477, 502, 843
Spiral Points 397, 399

Spring 5, 7, 106, 124, 128, 163, 275–277, 292, 301, 323, 335, 336, 339, 342–345, 349, 355, 359, 360, 367, 372, 374, 375, 383, 385, 392, 434, 437, 441, 444, 446, 448, 449, 451–453, 455, 457, 460, 472, 473, 477–483, 485, 488–490, 500, 508, 523, 627, 639, 640, 685, 752, 753, 755, 756, 758, 759, 835, 836
Effect of weight 342
Equivalent 336, 343, 448, 508, 639, 752
In series 347, 627
Nodal 480, 481
Nonlinear 460
Parallel 446
Soil 323, 489, 490
Winkler 124, 477, 482, 483, 488, 500
STAADPRO 167
Stability 72, 73, 390, 405, 407, 408, 410, 413–415, 417, 422, 424–430, 432, 433, 574–576, 612
Asymptotic 422, 425, 426, 428, 433
Autonomous System 415
Lyapunov 408, 412, 413
Numerical 4, 5, 163, 171, 191, 304, 511, 576, 764, 799, 816, 843
Stability of equilibrium 72
State space 404
State speed 405
Stiffness matrix 169, 171–174, 176, 177, 181–184, 187, 189–191, 194, 197–199, 203, 206, 207, 210, 211, 213, 214, 217–220, 222, 225, 226, 228, 229, 231, 233–235, 242, 244, 247, 248, 250, 252–255, 258, 259, 263, 267, 268, 273–276, 278, 282, 283, 285–289, 291, 295–297, 301, 302, 305–310, 312, 318, 322, 487–490, 497, 499, 500, 515, 519, 533–535, 552, 554, 560, 561, 568, 608, 627, 629, 631–633, 635, 638, 736, 737
2D Beam Element 174
2D triangular element 176, 178
4-nodded rectangular element 194, 198
CST element 184, 190, 211, 217
Global 177, 198, 275, 276, 287, 291, 301, 302, 307, 309, 629, 632, 633, 635, 638
Strain 9, 16, 18, 22, 23, 25, 27–29, 31–37, 42, 44, 49–52, 58, 61, 63, 64, 67–75, 77, 79, 86, 87, 89, 91–93, 99, 168, 169, 173, 180, 182, 183, 188, 189, 194, 196–198, 203–205, 212, 221, 223, 226, 227, 246, 248, 251, 253, 256, 258–260, 262, 265, 270, 271, 274, 275, 296, 301, 325, 328, 339, 374, 477, 481, 483, 493–495, 631, 639, 642, 644–647, 649,

656, 666, 667, 689, 722, 733, 735, 737, 820, 832, 837, 839
Energy 67–75, 198, 259, 260, 274, 339, 722, 735, 839
Invariants 33, 44
Normal 24, 25, 27, 29, 30
Octahedral 50
Plane 37, 49, 50, 64, 99, 182, 194, 197, 198, 248, 275, 301, 328, 477, 493, 494, 666, 667, 735, 820, 832
Principal 33, 34, 44, 58
Shear 27–29, 31, 33, 34, 58, 89, 198, 253, 258, 259, 735
Tensor 16, 29, 33, 35, 37, 58, 86, 87
Transformation of 29, 30, 42, 58
Virtual 71
Stress 4, 9, 33, 38, 39, 41–44, 46–52, 54, 55, 58, 63–65, 67, 69, 70, 72–75, 84–86, 90–92, 94, 102, 167–171, 173, 174, 177, 178, 181–183, 188, 189, 198, 199, 206, 213, 220, 225, 229, 248, 250, 268–273, 275, 288, 289, 295, 296, 301, 307, 310, 313, 315, 318, 322, 325, 328, 329, 374, 471, 475, 483, 484, 486, 488, 491, 493, 496, 497, 499, 521, 522, 584, 607, 631, 635, 639, 642, 645–647, 656, 665, 689–691, 700, 703–705, 718, 722, 730, 731, 737, 743, 748, 750, 765–767, 771, 774–776, 779, 782, 783, 791, 793, 807–809, 811, 813, 821, 832, 833, 839
Cauchy 44, 84
Concept of 10, 37, 38
Deviatoric 51, 69
Dynamic 640, 807
Invariants 43
Normal 38, 43, 44, 47, 50, 75, 96, 691, 704, 767, 813, 833
Octahedral 50
Plane 43, 48–50, 63, 64, 72, 169, 170, 177, 178, 181, 182, 206, 213, 229, 248, 271, 275, 301, 307, 493, 494, 521, 522, 832
Principal 33, 43, 44, 48–50, 58, 521, 522, 584
Shear 38, 46, 51, 58, 75, 96, 522, 704, 730, 731, 737, 748, 767, 776, 811, 813
Spherical 47, 51
Sub-harmonic resonance 460

Taylor's improved incompatible quadrilateral 225
Taylor's series 10, 12, 15, 24, 81, 117, 155, 158, 552
Theorem 21, 37, 65, 73, 78, 79, 82, 84, 85, 274, 408, 412, 416, 425, 426, 428–430, 432, 433, 624, 641, 671, 684, 707, 709
Castigliano's 73
Chasle's 21
Maxwell-Betti's 77
Theory of Elasticity 4, 9, 102, 493, 639
Time history analysis (THA) 6, 163, 575, 737
Central Difference 115, 116, 137, 142, 172, 551, 553, 560, 568, 573, 574, 576
Newmark-β 163, 568, 569, 571, 573, 574, 576, 734
Wilson-θ 163, 561, 565, 567, 573, 574, 576, 734
Time period 372, 508, 510, 517, 518, 574–576, 591, 602, 604, 606, 635, 637, 644, 672, 728, 735
Transformation matrix 58, 280–283, 286, 609, 611–614, 616, 617, 619–621, 633
Transforms 426, 523, 525, 533, 594, 641, 671, 677–682, 685–687, 703, 705, 745, 767, 806, 808
Cosine Fourier 678
Fourier 677, 678, 685, 686, 703, 705, 745, 767, 806, 808
Hankel 685, 687
Integral 84, 641, 671, 681
Laplace 679–681
Sine Fourier 678
Three dimension 678

Underground Blast 390, 740

Vibration Isolation 360
Virtual work 70, 71, 497, 499
Viscous boundaries 7, 838, 839

Waves 90, 102, 640–642, 646–649, 652–656, 659–664, 667–669, 671, 689, 700, 703, 713–716, 718, 721–723, 729, 739, 740, 748, 769, 783, 832–835, 837–839, 841–843
Dispersion 308, 657
Love 643, 655–657, 671
P 643, 646, 662, 663, 667–669, 671, 714, 718, 721, 838, 839, 841
Rayleigh 643, 649, 652–654, 659, 671, 687, 689, 719, 721, 749, 795–797, 833–835, 838, 840
Reflection 659–661, 663, 668, 671, 839
Refraction 659, 663
S 90, 643, 646, 648, 656, 662, 667, 668, 714, 716, 718, 721, 838, 839, 841
SH 90, 648, 654–656, 662, 663, 666, 670
SV 90, 648, 662, 663, 668, 669, 714
Wronskian 394, 395

Designed to provide engineers with quick access to current and practical information on the dynamics of structure and foundation, this unique work, consisting of two separately available volumes, serves as a complete reference, especially for those involved with earthquake or dynamic analysis, or the design of machine foundations in the oil, gas, and energy sector.

Whereas the first volume deals with the fundamentals, this volume is dedicated to applications in various civil engineering problems, related to dynamic soil-structure interaction, machine foundation and earthquake engineering. It presents innovative, easy-to-apply and practical solutions to various problems and difficulties a design engineer will encounter. This well-illustrated volume allows quick access to targeted information; it includes a wealth of case studies and also examines geotechnical considerations with regard to dynamic soil-structure interaction.

This book is concentrated on three major application areas:

- Dynamic soil-structure interaction (DSSI),
- The analysis and design of machine foundations, and on
- The analytical and design concepts for earthquake engineering.

This book is intended for academics and professionals in civil and structural engineering involved with earthquake or dynamic analysis or the design of machine foundations. In combination with the **Fundamentals** book (Volume 1), it could be used as course material for advanced university and professional education in Structural Dynamics (Vibration), Soil Dynamics, Analysis and Design of Machined Foundations and Earthquake Engineering.

CRC Press
Taylor & Francis Group
an **informa** business
www.crcpress.com

6000 Broken Sound Parkway, NW
Suite 300, Boca Raton, FL 33487
Schipholweg 107C
2316 XC Leiden, NL
2 Park Square, Milton Park
Abingdon, Oxon OX14 4RN, UK

ISBN-13: 978-0-415-49223-2
9 780415 492232

an **informa** business